*** RMIS View/Print Document Cover Sheet ***

This document was retrieved from the Documentation and Records Management (DRM) ISEARCH System. It is intended for Information only and may not be the most recent or updated version. Contact a Document Service Center (see Hanford Info for locations) if you need additional retrieval information.

Accession #: D196080859

Document #: SD-RTG-SARP-001

Title/Desc:
RTG TRANSPORTATION SYSTEM SARP DOCKET NO 94-6-9904 [VOL I] [SEC 1 OF 4]

Pages: 301

This document was too large to scan as a whole document, therefore it required breaking into smaller sections.

Document number: SD-RTG-SARP-001

Section 1 **of** 4

Title: RADIOISOTOPE THERMOELECTRIC GENERATOR TRANSPORTATION SYSTEM SAFETY ANALYSIS REPORT FOR PACKAGING

Date: 4/18/96 **Revision:** 0

Originator: FERRELL PC
Co: WHC

Recipient:
Co:

References: EDT-613639

APR 18 1996
Sta. 21

ENGINEERING DATA TRANSMITTAL

Page 1 of 1

1. EDT № 613639

2. To: (Receiving Organization)	3. From: (Originating Organization)	4. Related EDT No.:
Distribution	Packaging Engineering	NA
5. Proj./Prog./Dept./Div.:	6. Cog. Engr.:	7. Purchase Order No.:
RTG Packaging/84100/XJ10A	P. C. Ferrell	NA

8. Originator Remarks:

This document is being transmitted to DOE-EM and Lawrence Livermore National Laboratory for final review under Docket No. 94-6-9904. Once the document is determined to be acceptable, DOE-EM will issue a Certificate of Compliance (CoC). This document is cleared for Public Release.

9. Equip./Component No.: NA

10. System/Bldg./Facility: 427

11. Receiver Remarks:

12. Major Assm. Dwg. No.: NA

13. Permit/Permit Application No.: NA

14. Required Response Date: 04/19/96

15. DATA TRANSMITTED

(A) Item No.	(B) Document/Drawing No.	(C) Sheet No.	(D) Rev. No.	(E) Title or Description of Data Transmitted	(F) Approval Designator	(G) Reason for Transmittal	(H) Originator Disposition	(I) Receiver Disposition
1	WHC-SD-RTG-SARP-001	All	0	Radioisotope Thermoelectric Generator Transportation System Safety Analysis Report for Packaging	SQ	1,2	1	1
				Vol 1 + 2				

16. KEY

Approval Designator (F)	Reason for Transmittal (G)	Disposition (H) & (I)
E, S, Q, D or N/A (see WHC-CM-3-5, Sec.12.7)	1. Approval 4. Review 2. Release 5. Post-Review 3. Information 6. Dist. (Receipt Acknow. Required)	1. Approved 4. Reviewed no/comment 2. Approved w/comment 5. Reviewed w/comment 3. Disapproved w/comment 6. Receipt acknowledged

17. SIGNATURE/DISTRIBUTION (See Approval Designator for required signatures)

(G) Reason	(H) Disp.	(J) Name	(K) Signature	(L) Date	(M) MSIN	(J) Name	(K) Signature	(L) Date	(M) MSIN	(G) Reason	(H) Disp.
1	/	Cog.Eng.: PC Ferrell	P.C. Ferrell	4/16/96	G1-11						
1	/	Cog. Mgr.: JG Field		4/17/96	G1-11						
1	/	QA: ME Riste	M.E. Riste	4-16-96	N2-11						
1	/	Safety: DW McNally	D.W. McNally	4-16-96	H6-11						
		Env.									
1	/	DL Becker		4/17/96	G1-11						
1	/	VL Birkland	V.L. Birkland	4/17/96	H6-08						

18. P. C. Ferrell — P.C. Ferrell 4/16/96
Signature of EDT Originator — Date

19. Authorized Representative for Receiving Organization — Date

20. J. G. Field — 4/17/96
Cognizant Manager — Date

21. DOE APPROVAL (if required) Ctrl. No.
[ ] Approved
[ ] Approved w/comments
[ ] Disapproved w/comments

BD-7400-172-2 (04/94) GEF097

BD-7400-172-1

Radioisotope Thermoelectric Generator Transportation System Safety Analysis Report for Packaging

(Volumes I and II)

P. C. Ferrell
Westinghouse Hanford Company, Richland, WA 99352
U.S. Department of Energy Contract DE-AC06-87RL10930

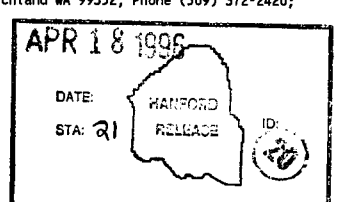
EDT/ECN: 613639 UC: 513
Org Code: 84100 Charge Code: XJ10A
B&R Code: AF7010200 Total Pages: 976

Key Words: RTG, General Purpose Heat Source, Package, Inner Containment Vessel, Outer Containment Vessel, Shielding Criticality

Abstract: This SARP describes the RTG Transportation System Package, a Type B(U) packaging system that is used to transport an RTG or similar payload. The payload, which is included in this SARP, is a generic, enveloping payload that specifically encompasses the General Purpose Heat Source (GPHS) RTG payload. The package consists of two independent containment systems mounted on a shock isolation transport skid and transported within an exclusive-use trailer.

TRADEMARK DISCLAIMER. Reference herein to any specific commercial product, process, or service by trade name, trademark, manufacturer, or otherwise, does not necessarily constitute or imply its endorsement, recommendation, or favoring by the United States Government or any agency thereof or its contractors or subcontractors.

Printed in the United States of America. To obtain copies of this document, contact: WHC/BCS Document Control Services, P.O. Box 1970, Mailstop H6-08, Richland WA 99352, Phone (509) 372-2420; Fax (509) 376-4989.



U. L. Birkland 4/16/96
Release Approval Date

Release Stamp

Approved for Public Release

WHC-SD-RTG-SARP-001
Revision 0
Volume I

Radioisotope Thermoelectric Generator Transportation System Safety Analysis Report for Packaging

Docket No. 94-6-9904

Prepared for the U.S. Department of Energy
Office of Environmental Restoration and
Waste Management



Westinghouse Hanford Company Richland, Washington

Management and Operations Contractor for the
U.S. Department of Energy under Contract DE-AC06-87RL10930

Approved for Public Release

LIST OF EFFECTIVE PAGES

Page	Rev	Comment	Page	Rev	Comment
1-iii - 1-vii	0	TOC	3.6.1-1 - 3.6.1-2	0	
1-viii - 1-ix	0	Acronyms	3.6.2-1 - 3.6.2-30	0	
1-1 - 1-12	0		3.6.3-1 - 3.6.3-4	0	
1.3.0-1	0		3.6.4-1 - 3.6.4-16	0	
1.3.1-1	0		3.6.5-1 - 3.6.5-145	0	
1.3.2-1 - 1.3.2-17	0		3.6.6-1 - 3.6.7-15	0	
1.3.3-1 - 1.3.3-3	0		3.6.7-1 - 3.6.7-19	0	
2-1 - 2-92	0		4-1 - 4-21	0	
2.10.0-1	0		4.5.0-1	0	
2.10.1-1 - 2.10.1-2	0		4.5.1-1	0	
2.10.2-1 - 2.10.2-29	0		4.5.2-1 - 4.5.2-41	0	
2.10.3-1 - 2.10.3-29	0		5-1 - 5-21	0	
2.10.4-1 - 2.10.4-2	0		5.5.0-1	0	
2.10.5-1 - 2.10.5-28	0		5.5.1-1	0	
2.10.6-1 - 2.10.6-5	0		5.5.2-1 - 5.5.2-14	0	
2.10.7-1 - 2.10.7-5	0		5.5.3-1 - 5.5.3-16	0	
2.10.8-1 - 2.10.8-49	0		6-1 - 6-27	0	
2.10.9-1 - 2.10.9-4	0		6.6.0-1	0	
2.10.10-1	0		6.6.1-1	0	
2.10.11-1 - 2.10.11-7	0		6.6.2-1 - 6.6.2-11	0	
2.10.12-1 - 2.10.12-68	0		7-1 - 7-6	0	
2.10.13-1 - 2.10.13-11	0		7.4-1	0	
2.10.14-1 - 2.10.14-2	0		8-1 - 8-12	0	
2.10.15-1 - 2.10.15-120	0		8.3-1	0	
3-1 - 3-54	0		9-1 - 9-12	0	
3.6.0-1	0		9.4-1	0	

CONTENTS

1.0 GENERAL INFORMATION 1-1
1.1 INTRODUCTION 1-1
1.2 PACKAGE DESCRIPTION 1-1
1.2.1 Packaging 1-1
1.2.2 Operational Features 1-6
1.2.3 Contents of Packaging 1-6
1.3 APPENDIX 1.3.0-1
1.3.1 References 1.3.1-1
1.3.2 General Arrangement Drawings 1.3.2-1
1.3.3 GPHS RTG Interface Control Drawing 1.3.3-1

2.0 STRUCTURAL EVALUATION 2-1
2.1 STRUCTURAL DESIGN 2-1
2.1.1 Discussion 2-1
2.1.2 Design Criteria 2-4
2.2 WEIGHTS AND CENTER OF GRAVITY 2-10
2.3 MECHANICAL PROPERTIES OF MATERIALS 2-11
2.4 GENERAL STANDARDS FOR ALL PACKAGES 2-19
2.4.1 Minimum Package Size 2-19
2.4.2 Tamper-Indicating Feature 2-19
2.4.3 Positive Closure 2-19
2.4.4 Chemical and Galvanic Reactions 2-19
2.5 LIFTING AND TIEDOWN STANDARDS FOR ALL PACKAGES 2-20
2.5.1 Lifting Devices 2-20
2.5.2 Tiedown Devices 2-28
2.6 NORMAL CONDITIONS OF TRANSPORT 2-39
2.6.1 Heat 2-40
2.6.2 Cold 2-50
2.6.3 Reduced External Pressure 2-51
2.6.4 Increased External Pressure 2-51
2.6.5 Vibration 2-51
2.6.6 Water Spray 2-52
2.6.7 Free Drop 2-52
2.6.8 Corner Drop 2-53
2.6.9 Compression 2-54
2.6.10 Penetration 2-56
2.7 HYPOTHETICAL ACCIDENT CONDITIONS 2-57
2.7.1 Free Drop 2-57
2.7.2 Puncture 2-61
2.7.3 Thermal 2-64
2.7.4 Immersion 2-82
2.7.5 Immersion--All Packages 2-82
2.7.6 Summary of Damage 2-87
2.8 SPECIAL FORM 2-92
2.9 FUEL RODS 2-92
2.10 APPENDIX 2.10.0-1

CONTENTS (cont'd)

2.10.1 References 2.10.1-1
2.10.2 ICV Two-Dimensional (Axisymmetric) ANSYS Model 2.10.2-1
2.10.3 OCV Head and Fin Model 2.10.3-1
2.10.4 Fin-to-OCV Head Weld Properties ANSYS Model 2.10.4-1
2.10.5 OCV Head ANSYS Model for Tiedown Analysis 2.10.5-1
2.10.6 Elastomer O-ring Performance Test Data 2.10.6-1
2.10.7 Summary of Thermal Load Cases and Results 2.10.7-1
2.10.8 OCV Two-Dimensional (Axisymmetric) ANSYS Model 2.10.8-1
2.10.9 RTG Transportation System Package Certification Test Plan 2.10.9-1
2.10.10 Certification Drop Test Procedure for the RTG Transportation System Package 2.10.10-1
2.10.11 Structural Development Test Program 2.10.11-1
2.10.12 ICV Three-Dimensional ANSYS Model 2.10.12-1
2.10.13 OCV Three-Dimensional ANSYS Model 2.10.13-1
2.10.14 O-ring Seal Compression Measurements 2.10.14-1
2.10.15 Summary of Damage from Certification Testing 2.10.15-1

3.0 THERMAL EVALUATION 3-1
3.1 DISCUSSION 3-1
3.2 SUMMARY OF THERMAL PROPERTIES OF MATERIALS 3-4
3.3 TECHNICAL SPECIFICATIONS OF COMPONENTS 3-9
3.4 THERMAL EVALUATION FOR NORMAL CONDITIONS OF TRANSPORT 3-10
3.4.1 Thermal Model 3-11
3.4.2 Maximum Temperatures 3-21
3.4.3 Minimum Temperatures 3-24
3.4.4 Maximum Internal Pressures 3-24
3.4.5 Maximum Thermal Stresses 3-25
3.4.6 Temperatures For Operational Conditions 3-25
3.4.7 Evaluation of Package Performance for Normal Conditions of Transport 3-30
3.5 HYPOTHETICAL ACCIDENT THERMAL EVALUATION 3-30
3.5.1 Thermal Model 3-31
3.5.2 Package Conditions and Environment 3-35
3.5.3 Package Temperatures 3-45
3.5.4 Maximum Internal Pressures 3-47
3.5.5 Maximum Thermal Stresses 3-54
3.5.6 Evaluation of Package Performance for the Thermal Hypothetical Accident Conditions 3-54
3.6 APPENDIX 3.6.0-1
3.6.1 References 3.6.1-1
3.6.2 Thermal Modeling Details 3.6.2-1

CONTENTS (cont'd)

3.6.3 Performance Of Rigid Polyurethane Foam Under Fire Accident Conditions 3.6.3-1
3.6.4 SINDA Output For Normal Conditions Of Transport 3.6.4-1
3.6.5 SINDA Output For Hypothetical Accident Conditions Of Transport 3.6.5-1
3.6.6 Miscellaneous Calculations 3.6.6-1
3.6.7 Listing of 2-D Computer Model 3.6.7-1

4.0 CONTAINMENT 4-1
4.1 CONTAINMENT BOUNDARY 4-1
4.1.1 Containment Vessel 4-1
4.1.2 Containment Penetrations 4-4
4.1.3 Seals and Welds 4-10
4.1.4 Closure 4-15
4.2 REQUIREMENTS FOR NORMAL CONDITIONS OF TRANSPORT 4-15
4.2.1 Containment of Radioactive Material 4-15
4.2.2 Pressurization of Containment Vessel 4-16
4.2.3 Containment Criterion 4-16
4.3 CONTAINMENT REQUIREMENTS FOR HYPOTHETICAL ACCIDENT CONDITIONS 4-16
4.3.1 Fission Gas Products 4-16
4.3.2 Containment of Radioactive Materials 4-17
4.3.3 Containment Criterion 4-19
4.4 SPECIAL REQUIREMENTS 4-21
4.5 APPENDIX 4.5.0-1
4.5.1 References 4.5.1-1
4.5.2 Teledyne Test Reports HPG5-DST-236 and HPG3-DST-1000 ..... 4.5.2-1

5.0 SHIELDING EVALUATION 5-1
5.1 DISCUSSION AND RESULTS 5-1
5.2 SOURCE SPECIFICATION 5-2
5.3 MODEL SPECIFICATION 5-16
5.3.1 Regulatory Normal Conditions of Transport Model 5-16
5.3.2 Regulatory Hypothetical Accident Condition Model 5-16
5.4 SHIELDING EVALUATION 5-16
5.4.1 Gamma Shielding Analyses 5-21
5.4.2 Neutron Shielding Analyses 5-21
5.4.3 Uncertainties in the Shielding Analysis Models 5-21
5.5 APPENDIX 5.5.0-1
5.5.1 References 5.5.1-1
5.5.2 Gamma Shielding Analyses MCNP Input Files 5.5.2-1
5.5.3 Neutron Shielding Analyses MCNP Input Files 5.5.3-1

CONTENTS (cont'd)

6.0 CRITICALITY EVALUATION 6-1
6.1 DISCUSSION AND RESULTS 6-1
6.2 PACKAGE FUEL LOADING 6-2
6.3 MODEL SPECIFICATION 6-2
6.3.1 Description of Calculational Model 6-2
6.3.2 Package Regional Densities 6-17
6.4 CRITICALITY CALCULATIONS 6-18
6.4.1 Calculational Method 6-18
6.4.2 Fuel/Moderator Loading Optimization 6-18
6.4.3 Criticality Results 6-19
6.5 CRITICAL BENCHMARK EXPERIMENTS 6-22
6.5.1 Benchmark Experiments and Applicability 6-22
6.5.2 Details of Benchmark Calculations 6-22
6.5.3 Results of Benchmark Calculations 6-25
6.6 APPENDIX 6.6.0-1
6.6.1 References 6.6.1-1
6.6.2 MCNP Code Input Listings 6.6.2-1

7.0 OPERATING PROCEDURES 7-1
7.1 PROCEDURES FOR LOADING THE PACKAGE 7-1
7.1.1 General Information 7-1
7.1.2 Opening the Empty Package 7-2
7.1.3 Payload Installation 7-2
7.1.4 Closure of the Inner Containment Vessel (ICV) 7-3
7.1.5 Closure of the Outer Containment Vessel (OCV) 7-3
7.1.6 Installation of the Impact Limiter and Final Preparations for Shipment 7-4
7.2 PROCEDURES FOR UNLOADING THE PACKAGE 7-5
7.2.1 Opening the Package 7-5
7.2.2 Payload Removal 7-6
7.3 PREPARATION OF AN EMPTY PACKAGE FOR TRANSPORT 7-6
7.4 REFERENCES 7.4-1

8.0 ACCEPTANCE TESTS AND MAINTENANCE PROGRAM 8-1
8.1 ACCEPTANCE TESTS 8-1
8.1.1 Visual Inspection 8-1
8.1.2 Structural and Pressure Tests 8-1
8.1.3 Leakage Rate Tests 8-2
8.1.4 Component Tests 8-6
8.1.5 Tests for Shielding Integrity 8-7
8.1.6 Thermal Acceptance Tests 8-7

CONTENTS (cont'd)

8.2 MAINTENANCE PROGRAM 8-7
8.2.1 Structural and Pressure Tests 8-7
8.2.2 Leakage Rate Tests 8-7
8.2.3 Subsystems Maintenance 8-11
8.2.4 Valves, Rupture Discs, and Gaskets on the Containment Vessel 8-12
8.2.5 Shielding 8-12
8.2.6 Thermal 8-12
8.3 REFERENCES 8.3-1

9.0 QUALITY ASSURANCE 9-1
9.1 INTRODUCTION 9-1
9.2 SCOPE 9-1
9.3 QUALITY ASSURANCE PLAN 9-2
9.3.1 Quality Element 1.0, Organization 9-2
9.3.2 Quality Element 2.0, Quality Assurance Program 9-4
9.3.3 Quality Element 3.0, Package Design Control 9-6
9.3.4 Quality Element 4.0, Procurement Document Control 9-6
9.3.5 Quality Element 5.0, Instructions, Procedures, and Drawings 9-7
9.3.6 Quality Element 6.0, Document Control 9-7
9.3.7 Quality Element 7.0, Control of Purchased Material, Equipment and Services 9-7
9.3.8 Quality Element 8.0, Identification and Control of Material, Parts and Components 9-8
9.3.9 Quality Element 9.0, Control of Special Processes 9-8
9.3.10 Quality Element 10.0, Inspection 9-9
9.3.11 Quality Element 11.0, Test Control 9-9
9.3.12 Quality Element 12.0, Control of Measuring and Test Equipment 9-9
9.3.13 Quality Element 13.0, Handling, Storage, and Shipping Control 9-9
9.3.14 Quality Element 14.0, Inspection, Test, and Operating Status 9-10
9.3.15 Quality Element 15.0, Nonconforming Materials, Parts, or Components 9-10
9.3.16 Quality Element 16.0, Corrective Action 9-10
9.3.17 Quality Element 17.0, Quality Assurance Records 9-11
9.3.18 Quality Element 18.0, Audits 9-12
9.4 REFERENCES 9.4-1

LIST OF ACRONYMS

ABS	Acrylonitrile Butadiene Styrene
AISI	American Iron and Steel Institute
AMS	Aerospace Materials Specification
ANSI	American National Standards Institute
ASME B&PV	American Society of Mechanical Engineers Boiler and Pressure Vessel Code
ASTM	American Society for Testing and Materials
BTU	British Thermal Unit
CCW	counterclockwise
CFR	Code of Federal Regulations
CG	Center of Gravity
Ci	Curies
CTA	Certification Test Article
DOE	U.S. Department of Energy
DOT	U.S. Department of Transportation
EAQA	Engineering Applications Quality Assurance
EA&SQA	Engineering Applications and Support Quality Assurance
EB	Electron Beam
ENDF	Evaluated Nuclear Data Files
ETG	Electrically Heated Thermoelectric Generator
GPHS	General Purpose Heat Source
GTAW	Gas Tungsten Arc Weld
HAC	Hypothetical Accident Conditions
HF	Hot Face
IAEA	International Atomic Energy Agency
ICV	Inner Containment Vessel
ID	Inside Diameter
LANL	Los Alamos National Laboratory
MCNP	Monte Carlo Neutron Photon
MNOP	Maximum Normal Operating Pressure
MSLD	Mass Spectrometer Leak Detector
NASA	National Aeronautics and Space Administration
NIST	National Institute for Science and Technology
NCR	Nonconformance Report
NCT	Normal Conditions of Transport
NPT	National Pipe Thread
NRC	Nuclear Regulatory Commission
OCV	Outer Containment Vessel
OD	Outsider Diameter
PC	Personal Computer
PSIA	Pounds per Square Inch Absolute
PSIG	Pounds per Square Inch Gage
PVC	Polyvinyl Chloride
QA	Quality Assurance
QAP	Quality Assurance Program
QAPI	Quality Assurance Plan Index
QAPP	Quality Assurance Program Plan
RFQ	Request For Quote
RTG	Radioisotope Thermoelectric Generator
RTV	Room Temperature Vulcanizing

LIST OF ACRONYMS (cont'd)

SARP	Safety Analysis Report for Packaging
SST	Safe, Secure Transporter
STP	Standard Temperature and Pressure
TGA	Thermogravimetric Analysis
UN	Unified National
UNC	Unified National Course
UNF	Unified National Fine
WHC	Westinghouse Hanford Company

1.0 GENERAL INFORMATION

1.1 INTRODUCTION

The Radioisotope Thermoelectric Generator (RTG) Transportation System Package is a Type B(U) packaging system that is used to transport a RTG or similar payload. The payload, which is included in this Safety Analysis Report for Packaging (SARP), is a generic, enveloping payload that specifically encompasses the General Purpose Heat Source (GPHS) RTG payload. The payload is classified as Fissile Class III and contains sufficient quantities of plutonium to warrant the special requirements of 10 CFR 71.63[1] ("*Special Requirements for Plutonium Shipments*").

The RTG Transportation System Package consists of two independent containment systems. The package is mounted on its own shock-isolation transport skid (for shock and vibration protection of the payloads) and is transported within an exclusive-use trailer. Up to two packages may be shipped within one trailer, depending on payload heatload and plutonium content. For operational protection of the payload, an active cooling system is provided for the package. In accordance with 10 CFR 71.51(b), the cooling system is not required to be active for the RTG Transportation System Package to successfully comply with the activity release limits of 10 CFR 71.51(a). The packaging and its individual components are shown in the General Arrangement Drawings in Appendix 1.3.2. The packaging model name is RTG Package.

1.2 PACKAGE DESCRIPTION

1.2.1 Packaging

The RTG Transportation System Package consists of a packaging (with a removable impact limiter) and a payload. The packaging stands approximately 77 in. high, with a maximum diameter (of the impact limiter) of 70 in. The gross weight of each package, with impact limiter and payload, is approximately 9,600 pounds. Each packaging consists of two separate containment vessels: an inner containment vessel (ICV) and an outer containment vessel (OCV). The containment structures are fabricated from AISI Type 304L stainless steel. Each containment vessel consists of a bell-shaped structure attached to a heavy base with high-strength alloy steel closure bolts. Each bell assembly consists of a cylindrical shell with a standard American Society of Mechanical Engineers (ASME) torispherical head at the top and a bolting flange at the bottom. Leaktight sealing of each level of containment is effected with butyl O-ring seals in a face seal configuration between the bolting flange and base. Each containment vessel uses an inner O-ring for containment and an outer O-ring for leakage rate checking. The major containment boundary components of each vessel are the bell, base, and containment O-ring.

Each containment vessel is equipped with a helium fill (primary vent) port; the ICV also has a secondary vent port. These ports are used to establish a pressurized (19 ± 1 psia) helium atmosphere inside each packaging containment boundary at the time of loading. In addition, each containment vessel is equipped with a leakage rate test port. These test ports, which access the volume between the containment O-ring and the leakage rate test O-ring, verify leak tightness, via helium leakage rate testing, of each level of containment after assembly. All ports are sealed with brass cap screws fitted with butyl Parker Stat-O-Seals®*. Vent ports, which penetrate containment, are leakage rate checked before shipment. Electrical feed-through connectors are

Stat-O-Seal is a registered trademark of the Parker Hannifin Corporation.

used to monitor the RTG payload during transport. To provide the required level of leak tightness, the electrical feed-throughs use D.G. O'Brien Series 107 sealed electrical connector assemblies that are welded into the ICV and OCV base. The containment vessels are designed to withstand all pressure buildups that may occur during normal conditions of transport (NCT) and hypothetical accident conditions (HAC). No pressure relief systems for the containment boundaries are provided.

No neutron absorbing materials other than the packaging steel walls are required for compliance with 10 CFR 71. However, for normal handling purposes, a water-glycol solution is used, in the OCV cooling jacket, that acts as a neutron absorber to reduce worker radiation exposure. Other means of heat dissipation include the following:

- High emissivity surface treatments on the inner and outer surfaces of the ICV and the inner surface of the OCV
- A dimensionally-controlled gap between the ICV and OCV bells
- A helium cover gas within the containment vessel cavities.

The packaging has a removable impact limiter at the bottom end. The impact limiter is comprised of two densities of fire-resistant, polyurethane foam fully encased in a AISI Type 304 stainless steel shell. A sheetmetal thermal shield is incorporated in the impact limiter, adjacent to the bottom of the OCV base. The impact limiter shell is equipped with plastic melt-out plugs for pressure relief if off-gassing of the foam occurs during the HAC fire event. The impact limiter also has drain tubes that drain any potential condensate from the cooling jacket. The impact limiter includes an integral bolting ring and is attached to the base of the OCV with 1-in. diameter high-strength Inconel bolts. The bolt shanks are necked down to 0.805 in. in diameter to allow them to stretch rather than break on impact. The steel shell is painted white to achieve low solar absorptivity.

The payload cavity is approximately 57 in. (maximum height at centerline) by 34 in. in diameter. Each payload has its own shipping rack assembly, which attaches to the base of the ICV. The shipping rack assembly includes a 33-in. diameter AISI Type 304 stainless steel barrier plate, elevated from the ICV base, to segregate any heat-producing elements of the payload from the ICV containment seal and electrical feed-through connector. The shipping rack assembly may also include additional payload support structure, fabricated from AISI Type 304 stainless steel. The shipping rack assembly will remain in place when subjected to the regulatory test requirements of 10 CFR 71.71 and 71.73. Payloads attach through the shipping rack assembly as opposed to directly to it. This arrangement permits the payloads to break free during HAC events without compromising shipping rack assembly retention.

The package is secured to its transport skid with a pair of tiedown straps that pass over the top of the locally-reinforced OCV bell at right angles to one another. Consequently, there are no tiedown devices that are an integral part of the packaging. Lifting the package is accomplished via three OCV fins, which double as lifting lugs. ICV bell lifting is accomplished by a single lift point centered in the ICV head. A personnel barrier is provided at the center of the OCV head to satisfy the exclusive use shipment temperature limitation (180 °F) for accessible surfaces per 10 CFR 71.43(g).

An exploded view of the cask assembly is presented in Figure 1.2.1-1. Additional detail of the two containment vessels is provided in Sections 1.2.1.1 (OCV) and 1.2.1.2 (ICV).

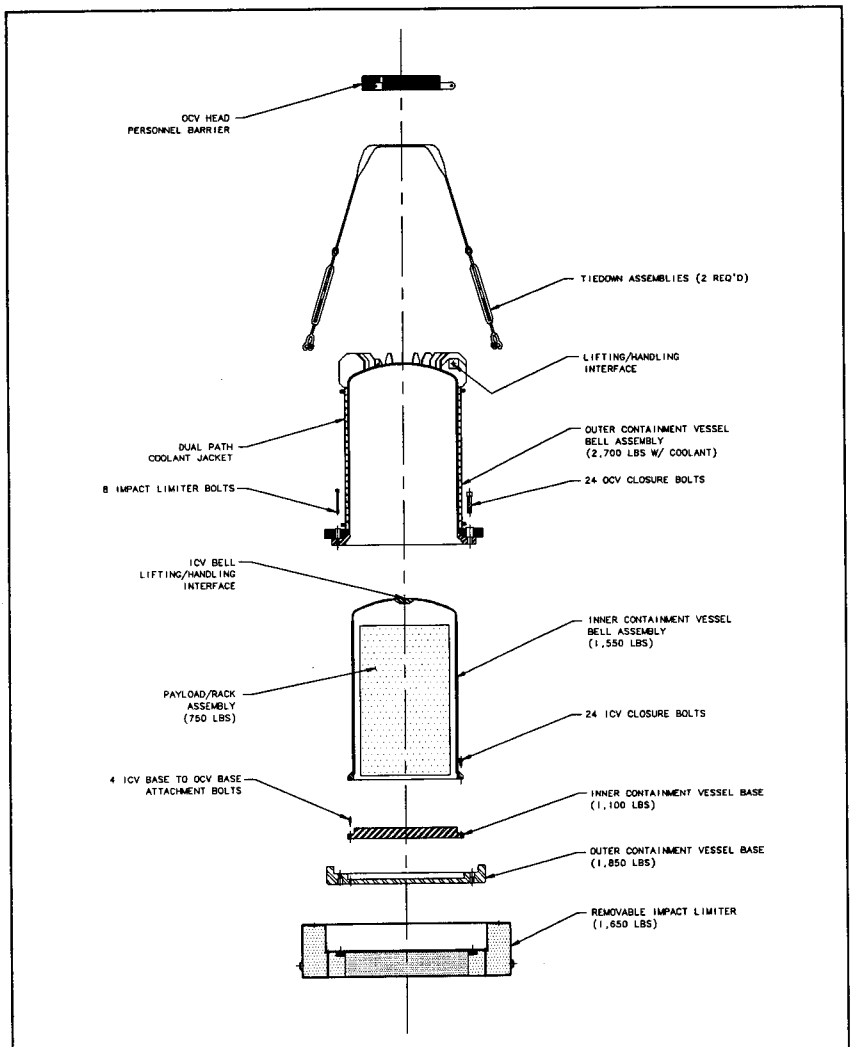


FIGURE 1.2.1-1. RTG Packaging Exploded View.

1.2.1.1 Outer Containment Vessel (OCV). The OCV consists of a AISI Type 304L stainless steel base (53.25 in. O.D., 3.50-in. thickness in the seal area), to which an AISI Type 304L stainless steel bell assembly is attached by 24, 1¼-in., ASTM-A320, Grade L43 bolts (identified as cap screws on the drawings in Appendix 1.3.2). The bell flange fits within a 2.40-in.-deep counterbore in the base, sized to limit motion in an accident so the closure bolts cannot be loaded in direct shear. The seal between the bell flange and the base is achieved by using two concentrically arranged butyl rubber O-ring face seals. The inner containment seal has a nominal diameter of 0.393 in.; the outer test seal has a nominal diameter of 0.275 in. The bell is made of a cylindrical shell, 35.88-in. I.D., welded to an ASME torispherical head, both having a wall thickness of 0.50 in. The head includes 0.25-in. thick doubler strips that locally strengthen the head at the location of the tiedown straps. Twenty-four 0.25-in.-thick fins are attached to the head around the knuckle region, three of which are slightly shorter and have holes for lifting the loaded package. The fins provide a degree of impact cushioning in a top-down impact, as well as some heat rejection capability during transport. The overall height of the OCV, including the fins, is 68 in. Located on the upper side of the bell bolting flange is a thermal shield. The thermal shield is a hollow structure (which is filled with fiberglass insulation to protect the sealing area from HAC fire temperatures) and fabricated from 0.38-in. and 0.25-in. thick AISI Type 304L plate material. Closure and impact limiter bolt heads are accessed through tubes running through the thermal shield.

Located within a recessed hole in the OCV base is the electrical feed-through assembly, which provides a means to continuously monitor the RTG payload during transport. The electrical feed-through assembly consists of a D.G. O'Brien Series 107 electrical connector mounted in an AISI type 316L stainless steel sleeve. This sleeve is welded to the OCV base. From the D.G. O'Brien connector, wiring is routed to a contact housing plate (polyethermide Ultem 1000®**), which is located on the top surface of the OCV base. Because it passes through the containment boundary, the D.G. O'Brien connector and sleeve form part of the boundary. In addition, the gold-plated, carbon steel electrical pins and the glass seals surrounding the pins are part of the OCV containment boundary. Once installed, the electrical feed-through portion of the containment boundary is never broken; therefore, leakage rate testing at the time of shipment is not required.

The only port that passes through the OCV containment boundary is a vent port, located in the base, through which air is evacuated from and helium is backfilled through the annulus between the ICV and OCV. A test port is located between the two O-ring seals for leakage rate testing. Vent and test port plugs are made of brass and sealed using a butyl Parker Stat-O-Seal®. Each plug is protected by a brass cap sealed with a Teflon®*** weather gasket.

Located on the outside of the OCV is a coolant jacket, extending from the top of the thermal shield to the bottom of the fins. It consists of two parallel spiral passages, each having a cross section of 2 in. long by 1 in. in the radial direction. The cooling system uses a 70% water/30% propylene glycol solution, and is designed such that either or both of the cooling paths may be used to protect the package payloads from excessive heat buildup during handling and transportation operations. The coolant jacket incorporates a pressure relief device to preclude an over-pressure condition if a cooling system malfunction occurs. During normal transportation, two redundant chilling systems are connected to the coolant jacket, one to each coolant loop. However, for purposes of the evaluation of compliance with 10 CFR 71.51(b), the coolant jacket is assumed to be drained and dry, with no active cooling in effect, when it is conservative for evaluation purposes.

****** *Ultem-1000* is a registered trademark of General Electric Plastics.

******* *Teflon* is a registered trademark of the E.I. duPont de Nemours Company.

The interior of the OCV bell is painted flat black to enhance radiative heat transfer from the ICV. Eight nonmetallic contact buttons that help protect the paint during handling operations are located near the bottom inside surface of the OCV bell. The exterior of the OCV bell is painted white to achieve low solar absorptivity.

1.2.1.2 Inner Containment Vessel (ICV). The ICV consists of a AISI Type 304L stainless steel base (38.94 in. O.D., 3.47 in. thick), to which an AISI Type 304L stainless steel bell assembly is attached by 24, 3/4-in., ASTM-A540, Grade B23, Class 1 bolts. The seal between the bell flange and the base is achieved by using two concentrically arranged butyl rubber O-ring face seals. The inner seal, which is the containment seal, is a single, 0.275-in. nominal diameter butyl rubber O-ring seal. The test seal is a single, 0.275-in. nominal diameter butyl rubber O-ring seal and is located outboard of the containment seal. The bell is made of a cylindrical shell, 34-in. I.D. and 0.75-in. thick, and an ASME torispherical head that is 0.38-in. thick. At the top center of the head, a 2-in.-thick plate is located, which is drilled and tapped to accept a 0.75-in. swivel lifting eye (not present during transport). The overall ICV assembly height is approximately 62.63 in. Both the inside and outside of the bell are painted flat black to enhance radiative heat transfer. There is a radial gap from 0.03 in. minimum to 0.25 in. maximum between the ICV outside diameter and the OCV inside diameter. The axial gap between the ICV and OCV heads is from 0.06 in. minimum to 0.50 in. maximum. This axial gap is sized to ensure that, under HAC events that load the package in an axial direction, contact will first occur between the two heads rather than between the ICV and OCV flanges. The ICV base fits within a counterbore in the OCV base and is attached by four 1/4-in. bolts. These bolts constrain the two containment vessels to act together during transportation so that more accurate monitoring of the normal shock and vibration response of the RTG payloads can be obtained. The bolts have no regulatory structural significance and will fail at inertia loads well under 10 g's.

Located within a stainless steel mounting receptacle on the ICV base is the ICV electrical feed-through assembly which, together with the OCV electrical feed-through assembly, is used to provide continuous monitoring of the RTG payload. The electrical feed-through assembly consists of a D.G. O'Brien Series 107 electrical connector mounted in an AISI Type 316L stainless steel sleeve that is welded to the AISI Type 304L stainless steel ICV mounting receptacle. An insulating sleeve, used to thermally protect the electrical feed-through assembly, surrounds the mounting receptacle. Below the D.G. O'Brien connector, wiring is routed to a spring loaded plunger mounting plate (polyethermide Ultem 1000®) that interfaces with the OCV contact housing plate. Because it passes through the containment boundary, the D.G. O'Brien connector and stainless steel sleeve form part of the containment boundary. In addition, the gold-plated carbon steel electrical pins and the glass seals surrounding the pins are part of the ICV containment boundary. As with the OCV, the electrical feed-through portion of the containment boundary is never broken.

Two ICV vent ports, which penetrate the ICV containment boundary and are used during the helium purge process, and one ICV seal leakage rate test port, are located in the bell flange. The ports are similar in design to the previously discussed OCV ports. One of the vent ports connects to a 0.38-in.-diameter, stainless steel riser tube that transports the fill gas from the flange to the top of the ICV interior cavity. This tube allows for more uniform helium insertion into the payload cavity and precludes direct helium impingement onto the payload. Vent and test port plugs are made of brass and sealed using a butyl Parker Stat-O-Seal®.

The RTG payloads are attached to the ICV base through a shipping rack assembly for positive restraint during normal shipping and handling operations. The shipping rack assembly attaches directly to the ICV base with four 3/4-10 unified national course (UNC) bolts, and is totally independent of the payload attachment. The shipping rack assembly includes a 33-in.-diameter, 0.38-in.-thick, AISI Type 304 stainless steel barrier plate. The barrier plate will keep any heat-producing debris, which could conceivably result from payload breakup during a HAC free drop,

away from the ICV seal area and electrical feed-through assembly. This, in turn, will ensure that the ICV containment seal and electrical feed-through assembly will never exceed their maximum allowable temperature limits. The lower surface of the barrier plate is insulated for added thermal protection. To further protect the seals from smaller sized debris (if any), a debris shield is located at the internal junction of the ICV bell and base. Although the debris shield is not intended to form a seal, vent ports are designed to access both sides of the shield, thus ensuring the presence of helium adjacent to the containment O-ring during leakage rate checking. Geometric and structural details of the GPHS shipping rack assembly are provided in Appendix 1.3.2.

1.2.2 Operational Features

For normal transportation operations, one or two packages, along with their shock-mounted transport skid(s) and auxiliary cooling systems (if required), are carried in a single, exclusive-use trailer. The transport skids are equipped with channels for removal from the trailer by fork truck. During transport, in addition to direct monitoring of the payloads via the electrical feed-throughs, package coolant temperature may be actively monitored to ensure that payload temperature limits are not exceeded. Additionally, transportation induced shock and vibration may be measured. Passive shock indicators attached to the package(s) would determine if payload acceleration limits have been exceeded during transport. Accelerometers may also be mounted on the package(s) to actively monitor vibrations to ensure that payload operational limits are not exceeded.

Active cooling is provided for the payload by a 70% water/30% propylene glycol mixture circulating through the package OCV cooling jacket. The recirculated coolant is conditioned by two trailer-mounted auxiliary chiller units. Each unit serves one cooling loop, with either cooling loop being capable of protecting the operational integrity of the payload. Thus, the cooling system is completely redundant. For two package shipments, each auxiliary chiller services one cooling loop of each package.

The ICV bell is typically nested within the OCV bell for loading and unloading purposes. That is, the two containment vessel bells are connected via special spacer blocks and lifted or lowered together. This configuration allows active cooling of the entire assembly, including the payload, during loading and unloading operations. Each spacer block used for the nesting operation attaches to the OCV bell using two closure bolt holes and to the ICV bell using one tapped attachment hole (refer to Section G-G of General Arrangement Drawing Number H-9-5003).

For assembly purposes, alignment pins are provided to ensure correct installation of the packaging components (i.e., the ICV and OCV bells with their respective bases, the ICV within the OCV, and the OCV within the impact limiter). The ICV base is attached to the OCV base with four 1/4-in. diameter bolts so that the entire package assembly acts as essentially a rigid body for vibration monitoring purposes.

1.2.3 Contents of Packaging

The payloads to be accommodated by the RTG Transportation System Packaging are typically RTGs. The RTGs use a radioactive heat source (^{238}Pu) to generate electricity. The packaging design is also compatible with other similar payloads that serve only as heat sources. Governing characteristics for a generic, enveloping payload are summarized in Table 1.2.3-1. Limits on selected initial isotopic content for the ^{238}Pu fuel are listed in Table 1.2.3-4. Plutonium-238 initial fuel properties and associated gamma and neutron spectra are provided in Tables 5-3, 5-4, and 5-5 of Section 5.0. Adequacy of the packaging design to accommodate the generic enveloping payload definition is established in the remainder of the SARP.

The GPHS RTG is the specific payload that is the primary driver for the design of the RTG Transportation System Packaging. Consequently, characteristics corresponding to that specific payload are also covered in detail in the remainder of the SARP. General Arrangement Drawing Number H-9-5005, which is included in Appendix 1.3.2, illustrates the GPHS RTG mounted in the RTG Transportation System Package. Interface details for the GPHS RTG are given in interface control drawings, which are also included as Appendix 1.3.3. The key characteristics of the GPHS RTG payload, which directly influence the packaging design, are summarized in Table 1.2.3-2. By comparison with Table 1.2.3-1, it is apparent that the GPHS RTG payload is enveloped by the generic payload definition. The main components of the GPHS RTG are shown in Figure 1.2.3-1.

The GPHS housing is constructed of ASTM Type 2219 aluminum. Excluding the lower end midring and converter support ring assembly hardware used for attachment to the GPHS shipping rack assembly, the GPHS RTG weighs 123.5 pounds. The total weight of the GPHS RTG, including the interface hardware, is 200 pounds.

The GPHS RTG payload is bolted to the ICV base plate via four 3/4-10 UNC by 8-in.-long bolts that pass through both the converter support ring and shipping rack assembly. Because the shipping rack assembly is also attached directly to the ICV base by another payload independent set of bolts, payload attachment bolts can fail in a HAC event without compromising retention of the shipping rack assembly. Although the packaging design basis requires that the shipping rack assembly remains in place, it is conservatively assumed that the GPHS RTG payload can break away from its mounts and the RTG itself can break up during a HAC event.

The GPHS RTG contains plutonium fuel in the form of PuO_2, which is sintered into pellets. Each fuel pellet is a right circular cylinder with rounded edges and a density of 9.6 g/cm^3. The properties for the fuel pellets used in the GPHS RTG are provided in Tables 1.2.3-3 and 1.2.3-4. Each fuel pellet is clad with an iridium shell that contains a vent that allows helium produced during the decay of the ^{238}Pu to escape. The iridium-clad pellets are 1.085 in. long by 1.084 in. in diameter. Two of the clad pellets (also known as fueled clads) are encapsulated in a graphite impact shell and two of these impact shells are enclosed in a reentry member called an aeroshell. The aeroshell arrangement is shown in Figure 1.2.3-2. The aeroshell is designed to survive atmospheric reentry and is the smallest size of heat-generating fragment that could arise from the break-up of the GPHS RTG under a HAC impact. A series of tests were performed to verify the aeroshell's structural integrity[3].

The maximum specified heat-generating capacity of each aeroshell is 250 W (62.5 W per fueled clad, four fueled clads per aeroshell). The GPHS RTG contains 18 aeroshells that are stacked along the axial center line of the RTG. Hence, the maximum GPHS RTG internal heat load is 4,500 W.

TABLE 1.2.3-1. Generic Payload Definition.

Parameter	Enveloping definition
Number of payloads per package	No specific control; limited by maximum allowed heat load, weight, and PuO_2 content per package
Number of packages per trailer	1 or 2; limited by maximum allowed heat load and PuO_2 content per package
Payload weight (w/o shipping rack assembly) per package	525 pound maximum
Heat load per package	4,500 W maximum
Heat load per trailer	5,000 W maximum
Size of heat-producing sources used within the payload	Minimum dimension for smallest possible post-accident, heat-producing source shall be greater than 1 in. (i.e., difference between barrier plate OD and ICV ID)
Maximum PuO_2 content per package	11,304 g; 142,000 Ci
Maximum PuO_2 content per trailer	12,560 g; 157,800 Ci
Maximum neutron emission rate for fueled clad	6000 n/s-g ^{238}Pu
Cooling fins (if any) that protrude from body of payload	Must be structurally bounded by fin representation used for structural certification testing, i.e., • Fin material no stronger than A-36 steel • Fins no thicker than 1/4 in. • Fin corners with included angle no less than 90°
Initial payload internal inert gas charge per package (assumed to communicate with ICV cavity)	Initial charge to consist of a maximum of 0.0135 lb-moles
Gas generation rate from within the payload per package	2.06×10^{-4} cm^3/sec maximum at STP (assumed to communicate with ICV cavity)
Off-gas because of cabling and other payload specific auxiliaries external to the payload housing, per package	No more than the amount possible from complete decomposition of 2 pounds of Silicone rubber
Minimum distance between adjacent packages within the trailer, centerline to centerline	9.5 ft.

TABLE 1.2.3-2. GPHS RTG Payload Definition.

Parameter	GPHS RTG payload definition
Maximum number per package	1
Maximum number per trailer	1
Payload weight (w/o shipping rack assembly) per package	200 pound maximum
Heat output per package	4,500 W maximum
Heat output per trailer	4,500 W maximum
Size of heat-producing sources used within the payload	Minimum dimension for smallest possible postaccident, heat-producing source is 2.091 in. (i.e., minimum dimension of an aeroshell assembly)
Maximum PuO_2 content per package	11,304 g; 142,000 Ci
Maximum PuO_2 content per trailer	11,304 g; 142,000 Ci
Maximum neutron emission rate per package	6,000 n/s-g ^{238}Pu (5.14×10^7 n/s, total)
Maximum fissile material content per package (^{238}Pu, ^{239}Pu and ^{241}Pu)	9,960 g
Cooling fins that protrude from body of payload	• Material is ASTM 2219 aluminum • Fins are 0.015 in. thick at tip, 0.055 in. thick at root • Fins use 90° corners
Initial payload internal inert gas charge per package (assumed to communicate with ICV cavity)	Initial charge to consist of 0.565 ft^3 (16 L) of inert gas at STP, equivalent to 1.57×10^{-3} lb-moles. With this initial charge, payload internal pressure equalizes to 25 psia.
Gas generation rate from within the payload per package	2.06×10^{-3} cm^3/sec maximum at STP (assumed to communicate with ICV cavity)
Off-gas because of cabling and other payload specific auxiliaries external to the payload housing, per package	The dominant components that can off-gas are two, approximately 80-in.-long cable assemblies that include less than one pound of silicone rubber insulation each

GPHS - RTG

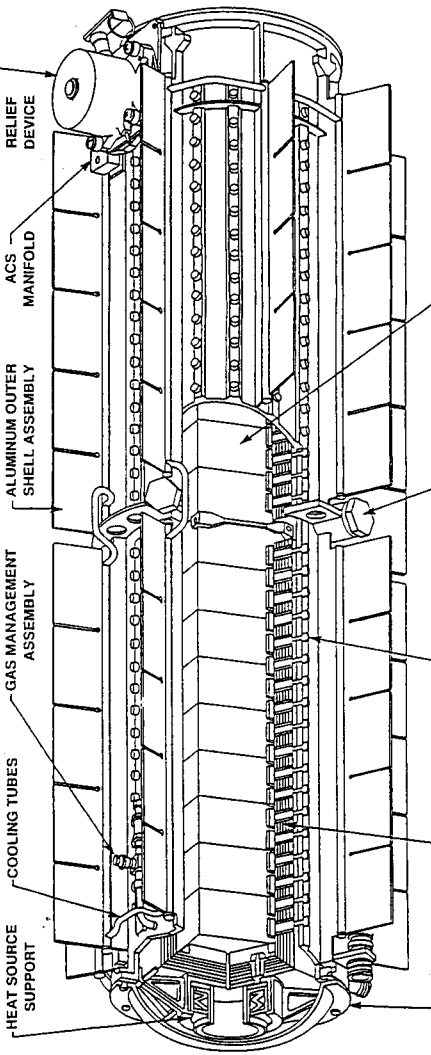


FIGURE 1.2.3-1. GPHS RTG Payload Configuration.

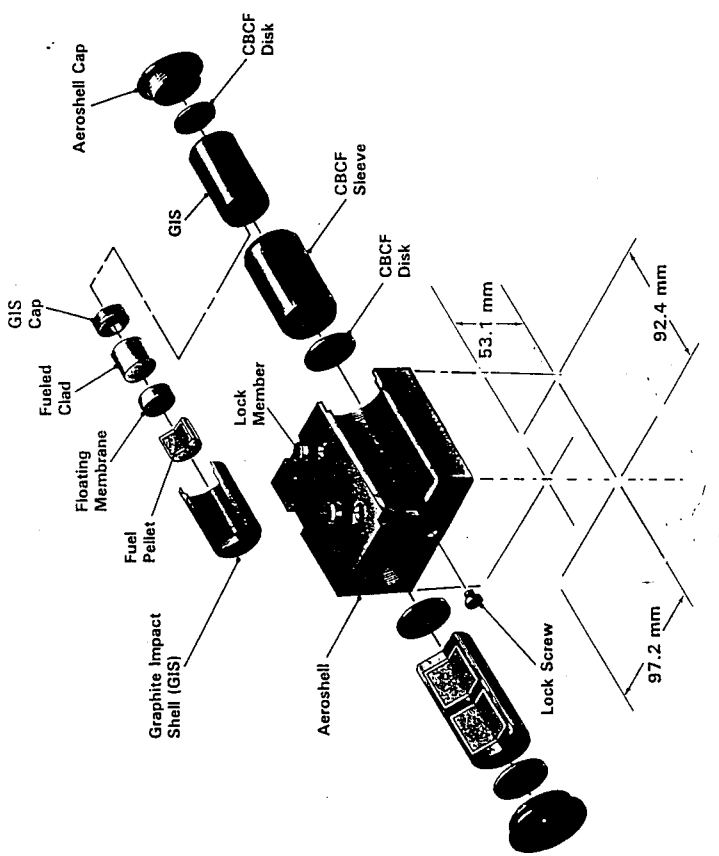


FIGURE 1.2.3-2. GPHS Fuel Arrangement.

BEST COPY AVAILABLE

TABLE 1.2.3-3. Fuel Pellet Properties of the GPHS RTG.

Fuel pellet property (excluding cladding)	GPHS fuel pellet
Diameter (cm)	2.7534
Length (cm)	2.7559
Fuel Volume (cm^3)	16.409
Density (g PuO_2/cm^3)	9.6
Weight (g)	157
Thermal Power (W)	62.5
Activity (Ci)	1,990
Specific Activity (Ci/g)	12.6

TABLE 1.2.3-4. Plutonium Fuel Initial Isotopic Limits for Generic and GPHS Payloads.

^{238}Pu content	80 to 86 mol - % of total plutonium
^{236}Pu content	≤0.0001 mol - % of total plutonium
^{238}Pu content	<20 mol - % of total plutonium
^{16}O content	>99.98 mol - % of total oxygen

1.3 APPENDIX

The following is a list of appendices contained within this section:

1.3.1 References

1.3.2 General Arrangement Drawings

1.3.3 GPHS RTG Interface Control Drawing

1.3.1 References

1. 10 CFR 71, 1993, "Packaging and Transportation of Radioactive Materials," *Code of Federal Regulations*, as amended.

2. DOE, 1988, "Physical Protection of Special Nuclear Material and Vital Equipment," Department of Energy Order 5632.2A, U.S. Department of Energy, Washington, D.C.

3. *General Purpose Heat Source Safety Verification* Programs:

   a. *Edge-on Flyer Plate Test*, LA-10872-MS, March 1987.

   b. *SVT-1 through SVT-6*, LA-10353-MS, June 1985.

   c. *SVT-7 through SVT-10*, LA-10408-MS, September 1985.

   d. *SVT-11 through SVT-12*, LA-10710-MS, May 1986.

   e. *Bullet/Fragment Test Series*, LA-10364-MS, May 1985.

   f. *Explosion Overpressure Test Series*, LA-10697-MS, September 1986.

1.3.2 General Arrangement Drawings

Drawing Number	Title	Number of sheets
H-9-5000	General Notes, RTG Transportation Package	1
H-9-5001	General Assembly and Details, RTG Transportation Package	2
H-9-5002	Assembly and Details, Outer Containment Vessel (OCV), RTG Transportation Package	5
H-9-5003	Assembly and Details, Inner Containment Vessel (ICV), RTG Transportation Package	4
H-9-5004	Assembly and Details, Impact Limiter, RTG Transportation Package	1
H-9-5005	GPHS RTG Shipping Configuration, RTG Transportation Package	2
H-9-5007	RTG OCV Head Personnel Barrier, RTG Transportation Package	1

GENERAL NOTES (UNLESS OTHERWISE SPECIFIED)

1. ALL DIMENSIONS ARE IN INCHES.
2. THREADS PER ANSI B1.1-1982.
3. IDENTIFICATION: PACKAGE SHALL BE IDENTIFIED IN ACCORDANCE WITH THE REQUIREMENTS OF 10 CFR 71.85 (c). ON THE OUTER CONTAINMENT VESSEL COOLANT JACKET WITH A STAINLESS STEEL NAMEPLATE, TACK WELDED.
4. POLYURETHANE FOAM SHALL HAVE NOMINAL DENSITIES AS SPECIFIED IN THE DRAWING DETAILS. INSTALLATION TECHNIQUES, ACCEPTANCE TESTS AND ACCEPTABLE DEVIATIONS IN PROPERTIES ARE SUMMARIZED IN SECTION 8.1.4 OF THE SAFETY ANALYSIS REPORT.
5. PRIOR TO ASSEMBLY, ALL COMPONENTS SHALL BE CLEANED OF CUTTING OILS, MARKING DYES, WELD FLUX, SPATTER, SCALE, GRIME AND ALL OTHER FOREIGN MATERIALS. FINISHED ASSEMBLY AND ALL INTERIOR SURFACES SHALL BE CLEANED.
6. ALL WELDING PROCEDURES AND PERSONNEL SHALL BE QUALIFIED IN ACCORDANCE WITH ASME CODE, SECTION IX. WELD PROCEDURES AND WELDER QUALIFICATIONS SHALL BE AVAILABLE FOR AUDIT OR REVIEW.
7. ALL WELDS SHALL BE VISUALLY EXAMINED IN ACCORDANCE WITH AWS D1.1, SECTION 8.15.1. VISUAL WELD INSPECTORS SHALL BE QUALIFIED PER AWS D1.1.
8. INDICATED WELDS SHALL BE LIQUID PENETRANT INSPECTED ON ROOT AND FINAL PASSES IF A MULTIPASS WELD AND ON THE COMPLETED WELD IF A SINGLE PASS WELD, IN ACCORDANCE WITH ASME CODE, SECTION III, DIVISION 1, SUBSECTION NB, ARTICLE NB-5000, AND SECTION V, ARTICLE 6.
9. INDICATED WELDS SHALL BE RADIOGRAPH INSPECTED IN ACCORDANCE WITH ASME CODE SECTION III, DIVISION 1, SUBSECTION NB, ARTICLE NB-5000 AND SECTION V, ARTICLE 2.
10. ALL CONTAINMENT SHELL JOINTS SHALL BE MADE IN ACCORDANCE WITH ASME CODE, SECTION III, DIVISION 1, SUBSECTION NB, ARTICLE NB-4230.
11. ALL CYLINDRICAL AND CONTAINMENT SHELL FABRICATIONS SHALL COMPLY WITH THE TOLERANCE REQUIREMENTS OF ASME CODE, SECTION III, DIVISION 1, SUBSECTION NE, ARTICLE NE-4220.
12. INNER AND OUTER VESSEL CONTAINMENT BOUNDARIES SHALL BE SUBJECTED TO AN INTERNAL TEST PRESSURE EQUAL TO A MINIMUM OF 150% OF THE MAXIMUM NORMAL OPERATING PRESSURE PER 10CFR 71.85(b).
13. INNER AND OUTER VESSEL CONTAINMENT BOUNDARIES SHALL BE LEAK TESTED TO DEMONSTRATE A LEAKAGE RATE NOT TO EXCEED 1×10^{-7} STANDARD CUBIC CENTIMETERS PER SECOND AIR PER ANSI N14.5-1987.
14. OCV AND ICV LIFTING FEATURES SHALL BE LOAD TESTED TO A MINIMUM OF 150% OF THEIR MAXIMUM WORKING LOAD.
15. PRIOR TO ASSEMBLY, COAT EACH O-RING WITH A THIN FILM OF VACUUM GREASE. SEAL FLANGES MAY ALSO BE COATED WITH A THIN FILM OF VACUUM GREASE AS AN OPTION.
16. BUTYL MATERIAL PER RR0405-70, RANIER RUBBER CO., SEATTLE, WA. OTHER O-RING ACCEPTANCE REQUIREMENTS ARE SUMMARIZED IN SECTION 8.1.4 OF THE SAFETY ANALYSIS REPORT.
17. TAMPER INDICATING DEVICE SHALL BE INSTALLED AT ONE (1) IMPACT LIMITER BOLT LOCATION.
18. FASTENERS SHALL BE INSTALLED FOR ACTUAL PACKAGE USE IN ACCORDANCE WITH THE FOLLOWING:
    a. TORQUE OCV CLOSURE BOLTS (1 1/4-7UNC-2A) TO 270-330 FT-LBS.
    b. TORQUE ICV CLOSURE BOLTS (3/4-10UNC-3A) TO 225-275 FT-LBS.
    c. TORQUE ICV BASE TO OCV BASE BOLTS (1/4-20UNC-3A) TO 110-130 IN-LBS.
    d. TORQUE IMPACT LIMITER BOLTS (1-8UNC-3A) TO 180-220 FT-LBS.
19. VENT AND TEST PORT PLUGS SHALL BE INSTALLED BY TIGHTENING TO A TORQUE OF 100-120 IN-LBS.
20. EACH COOLANT JACKET FLOW LOOP SHALL BE PRESSURE TESTED TO A MINIMUM OF 140 PSIG.
21. THE FOLLOWING LONGITUDINAL CONTAINMENT VESSEL WELDS ARE NOT SHOWN, BUT SHALL BE UTILIZED AND SHALL BE FULL PENETRATION "V" GROOVE PER G/N 6, AND INSPECTED PER G/N 7 & F/N 9 WHEN UTILIZING ASTM A240 MATERIAL.
    a. OCV SHELL
    b. ICV SHELL
22. ANY ADDITIONAL WELDS REQUIRED TO JOIN NON-CONTAINMENT SHELL MATERIALS SHALL BE FULL PENETRATION WELDS PER G/N 6, AND INSPECTED PER G/N 7 & F/N 8.
23. STENCIL USING 1/2 INCH HIGH CHARACTERS WITH A STANDARD INDUSTRIAL ENAMEL PAINT OR MARKING INK.
24. COAT VENT AND TEST PORT PLUG SEALING ELEMENT WITH A THIN COAT OF VACUUM GREASE.
25. INDUSTRIAL GRADE EPOXY COATING, TNEMEC 66-BJ45; COLOR: WHITE.
26. HEAT RESISTANT COATING,CARBOLINE 4674, C900; COLOR: FLAT BLACK. APPLY PER MANUFACTURER'S INSTRUCTIONS.
27. CADMIUM PLATING PER QQ-P-416E, TYPE II, CLASS 2, BAKE OUT ICV CLOSURE BOLT HARDENED WASHERS PER MANUFACTURERS RECOMMENDATIONS.
28. INDICATED WELDS SHALL BE LIQUID PENETRANT INSPECTED ON FINAL PASSES IF A MULTIPASS WELD AND ON THE COMPLETED WELD IF A SINGLE PASS WELD IN ACCORDANCE WITH ASME CODE, SECTION III, DIVISION 1, SUBSECTION NB, ARTICLE NB-5000, AND SECTION V, ARTICLE 6.
29. TRANSITION TAPER (IF REQUIRED) FOR SHELL TO FLANGE OR SHELL TO HEAD WELDS SHALL BE A MINIMUM OF 3-TO-1 IN ACCORDANCE WITH ASME CODE, SECTION III, DIVISION 1, SUBSECTION NB, ARTICLE NB-4230.
30. OPTIONAL MATERIAL: ASTM A-351 CF3.
31. OPTIONAL MATERIAL: ASTM A-312, TYPE 304L.
32. APPLY BLACK PAINT TO ALL ICV BELL INTERNAL AND EXTERNAL SURFACES ABOVE THE 3.0 INCH POINT ON THE OUTSIDE AND ABOVE THE 7.0 INCH POINT ON THE INSIDE.
33. THE ICV AND OCV SHALL BE INITIALLY ASSEMBLED PRIOR TO FIRST USE WITH THE FOLLOWING FASTENER TORQUES:
    a. OCV CLOSURE BOLTS: 1500 FT-LBS.
    b. ICV CLOSURE BOLTS: 300 FT-LBS.
34. FULL PENETRATION OF GTAW WELD SHALL BE VERIFIED BY MACHINING BACK SHOULDER OF SLEEVE. PERFORM VISUAL INSPECTION, THEN LT AND THEN PT.
35. ALL THE RTG PACKAGING CONTAINMENT BOUNDARY WELDS ARE PERFORMED USING ONE OF THE FOLLOWING PROCESSES: SHIELDED METAL ARC (SMAW), GAS TUNGSTEN ARC WELD (GTAW), OR SUBMERGED ARC WELD (SAW).

APR 11 1996
DATE STA. 21 HANFORD RELEASE ID 21

DRAWING TRACEABILITY LIST				REVISIONS									
DWG NO	TITLE	REF NUMBER	TITLE	REV NO	DESCRIPTION	ENGR DATE	CHK DATE	ENGR	CHK
		NEXT USED ON	FND	ITEV									

CADFILE K005000A | CADCODE 005 5.0: AC02:12.0:SS

DRAWN M. RICHARDS	DATE 4-10-96	U.S. DEPARTMENT OF ENERGY Richland Operations Office Westinghouse Hanford Company
ENGR		
DES ENGR PC FERRELL		RTG TRANSPORTATION PACKAGE GENERAL NOTES
APPD FOR IMPLEMENTATION		

SIZE	PLAN NO	HOUSE NO	DWG NO	REV
F	427	5010	H-9-5000	0

SCALE NONE | REF 613635 | SHEET 1 OF 1

H-9-5000

54-8000-027(3/89)

FOR GENERAL NOTES AND FLAG NOTES
SEE DRAWING No. H-9-5000.

DOCUMENT NUMBER, WHC-SD-RTG-SARP-001
PAGE NUMBER, 1.3.2-3
Rev. 0

APR 11 1995

U.S. DEPARTMENT OF ENERGY
Richland Operations Office
Westinghouse Hanford Company

RTG TRANSPORTATION PACKAGE
GENERAL ASSEMBLY AND DETAILS

F 427 5010 H-9-5001 0

ELEVATION

ø70.00

77.00

42.50

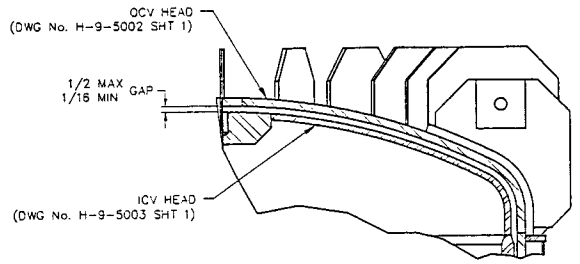
- ICV BELL LIFT POINT (DWG No. H-9-5003 SHT 1)
- OCV HEAD PERSONNEL BARRIER (DWG No. H-9-5007)
- SEE DETAIL-C (SHT 2)
- PERSONNEL BARRIER RETENTION PIN (DWG No. H-9-5007)
- IMPACT FINS/LIFT LUGS (DWG No. H-9-5002 SHT 1)
- DUAL PATH COOLANT JACKET (DWG No. H-9-5002 SHT 4)
- INNER CONTAINMENT VESSEL (ICV) BELL (DWG No. H-9-5003 SHT 1)
- OUTER CONTAINMENT VESSEL (OCV) BELL (DWG No. H-9-5002 SHT 1)
- ICV BASE (DWG No. H-9-5003 SHT 1)
- OCV CLOSURE BOLTS (DWG No. H-9-5003 SHT 3)
- OCV CLOSURE BOLTS (DWG No. H-9-5002 SHT 3)
- THERMAL SHIELD (DWG No. H-9-5002 SHT 1)
- IMPACT LIMITER (DWG No. H-9-5004 SHT 1)
- OCV BASE (DWG No. H-9-5002 SHT 1)
- NAMEPLATE

PLAN

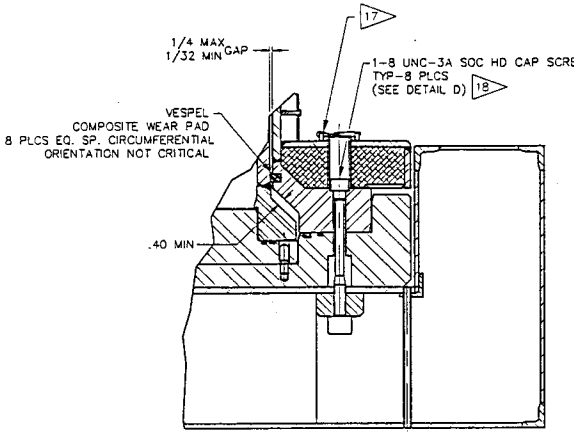
- F (SHT 2)
- A (SHT 2)
- E (SHT 2)
- B (SHT 2)
- DOUBLER PLATES FOR TIEDOWN INTERFACE (DWG No. H-9-5002 SHT 1)
- COOLANT JACKET INLET/OUTLET (DWG No. H-9-5002 SHT 4)
- COOLANT JACKET PRESSURE RELIEF DEVICE (DWG No. H-9-5002 SHT 4)

DWG NO | TITLE | REF NUMBER | REFERENCES | TITLE
DRAWING TRACEABILITY LIST | NEXT USED ON | CADFILE K0050013 | REVISIONS | CASCODE ADS 9.0 4.00.2 12.0-SS

H-9-5001

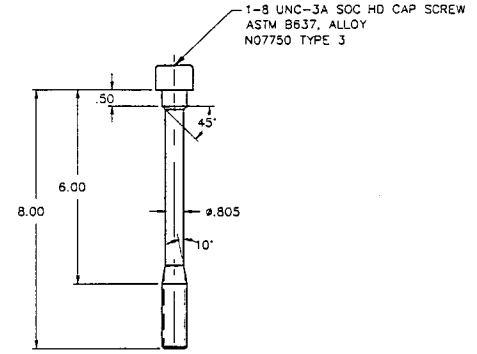


DETAIL-C (SHT 1)



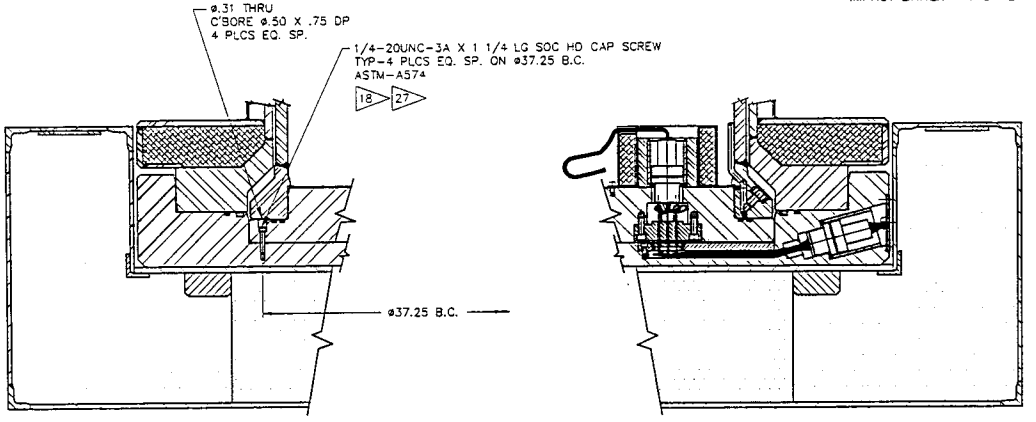
SECTION B-B (SHT 1)

IMPACT LIMITER ATTACHMENT BOLT



DETAIL D

IMPACT LIMITER BOLT

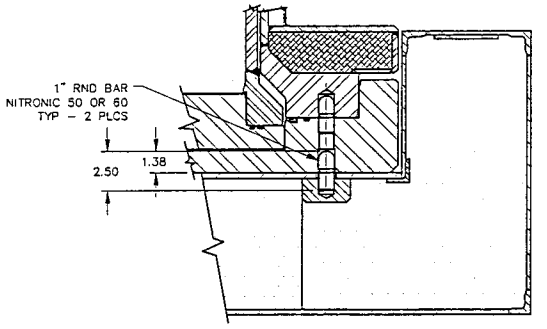


SECTION A-A (SHT 1)

ICV-OCV BASE ATTACHMENT BOLT

SECTION E-E (SHT 1)

FEED-THRU



SECTION F-F (SHT 1)

OCV-IMPACT LIMITER AUGNMENT PIN

FOR GENERAL NOTES AND FLAG NOTES
SEE DRAWING No. H-9-5000.

APR 11 1996

DOCUMENT NUMBER, WHC-SD-RTG-SARP-001
PAGE NUMBER, 1.3.2-4 Rev. 0

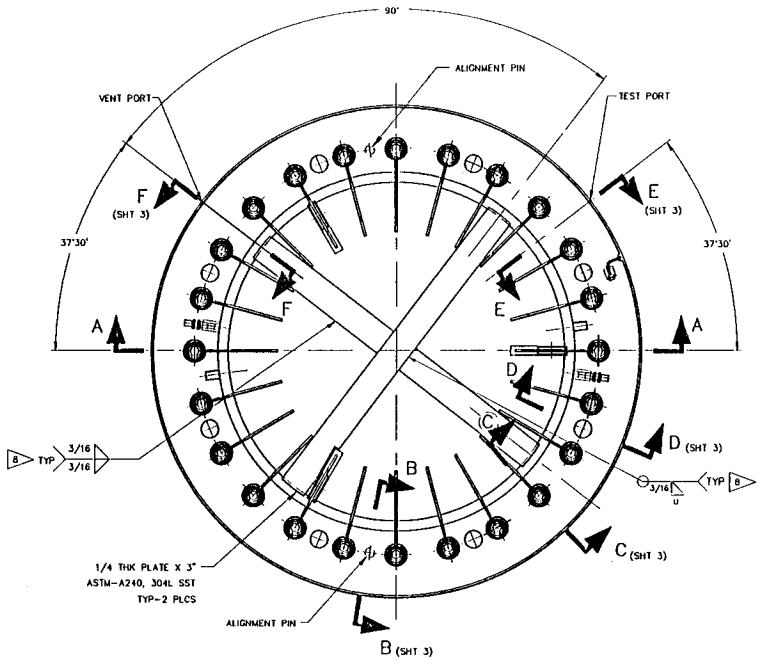
DRAWN N. RICHARDS	4-12-96	U.S. DEPARTMENT OF ENERGY Richland Operations Office Westinghouse Hanford Company	
CHECKED	4/11/96		
ENG APPROVAL	4/11/96	RTG TRANSPORTATION PACKAGE GENERAL ASSEMBLY AND DETAILS	
ENG APPROVAL PC PEARELL	4/11/96		
QA APPROVAL	4/11/96		
OTHER			
OTHER			
OTHER			

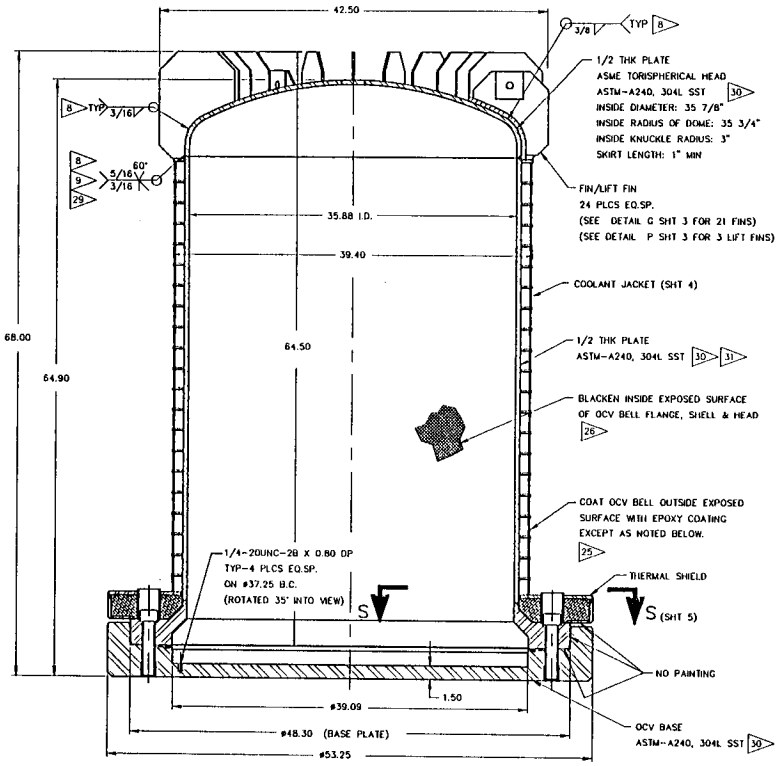
F 427 | 5010 | H-9-5001 | 0

SCALE NONE | SHEET 2

DWG NO / TITLE — DRAWING TRACEABILITY LIST
REF NUMBER / TITLE — REFERENCES
NEXT USED ON / END ITEM
REV / DESCRIPTION / DATE / APPROVALS — REVISIONS
CADFILE K0050018 | CADCODE DOS: 5.0; ACAD: 13.0; SS

SA-6000-027(5/89)





SECTION A-A

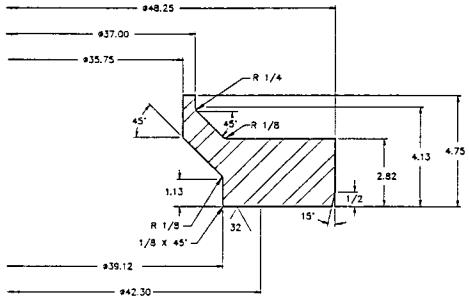
FOR GENERAL NOTES AND FLAG NOTES
SEE DRAWING No. H-9-5000.

DOCUMENT NUMBER, WHC-SD-RTG-SARP-001
PAGE NUMBER, 1.3.2-5

Rev. 0

APR 11 1996
DATE STA. 27
RECEIVED
OSTI
27

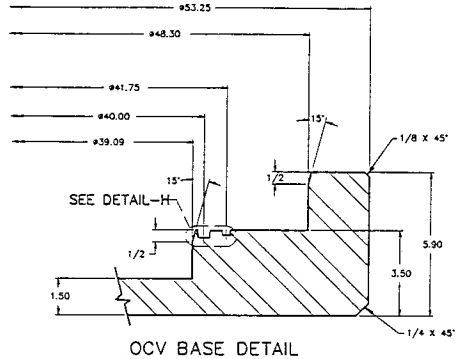
| | | |



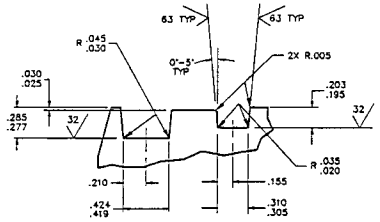
OCV BELL FLANGE DETAIL

MATL: ASTM-A240, 304L SST

30



OCV BASE DETAIL



DETAIL-H

O-RING GROOVES

FOR GENERAL NOTES AND FLAG NOTES
SEE DRAWING No. H-9-5000.

APR 11 1995

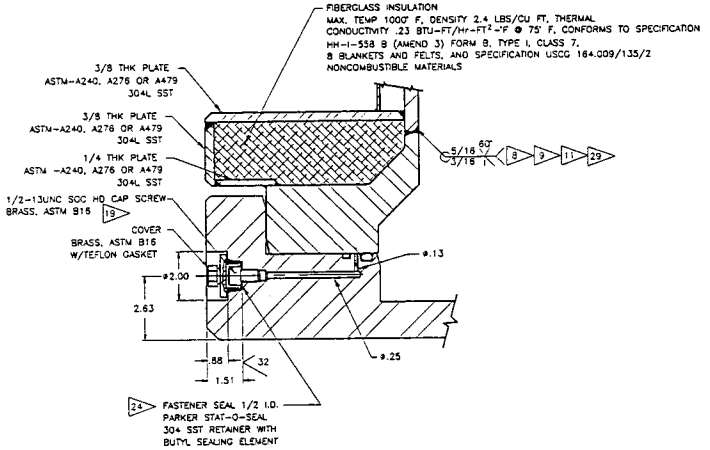
DOCUMENT NUMBER, WHC-SD-RTG-SARP-001
PAGE NUMBER, 1.3.2-6 Rev. 0

Drawn M RICHARDS	Date 4-10-95	U.S. DEPARTMENT OF ENERGY Richland Operations Office Westinghouse Hanford Company	
Designer			
Engr			
Engr PC FERRELL		RTG TRANSP PKG OUTER CONTAINMENT VESSEL (OCV) ASSY AND DET	
QA			
Other			
Other			
Other			
Appd for Publication			
By			
Size F	Dwg No 427	Rev No 5010	Drawing No H-9-5002	Rev 0
Scale NONE	Ref 413635	Sheet 2		

DWG NO	TITLE	REF NUMBER	TITLE
DRAWING TRACEABILITY LIST		REFERENCES	
		NEXT USED ON	END ITEM

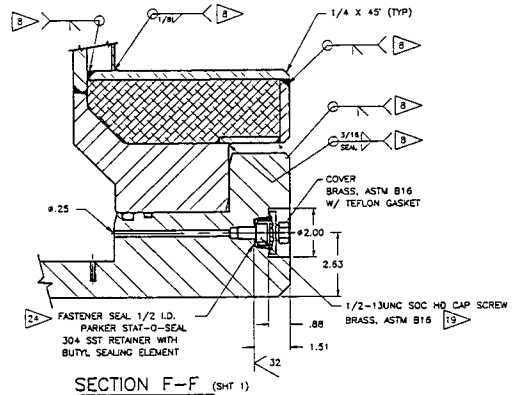
NO	DESCRIPTION	ENGR DATE	QA DATE	APPROVALS OTHER	OTHER
REVISIONS					
CADFILE K0050078		CASCODE 305.6.0 ACD2:12.2:55			

54-6000-027(5/89)



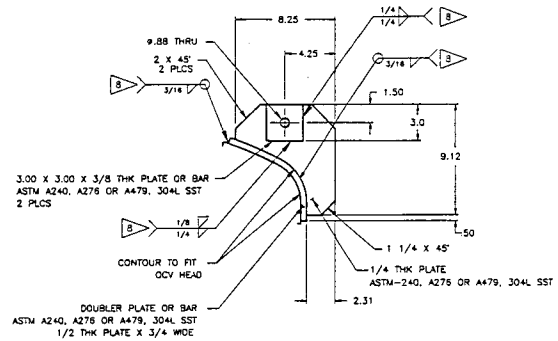
SECTION E-E (SHT 1)

OUTER CONTAINMENT TEST PORT



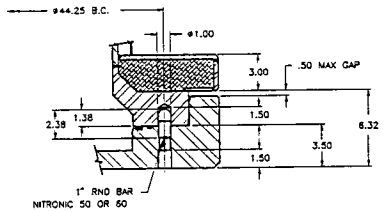
SECTION F-F (SHT 1)

OUTER CONTAINMENT VENT PORT



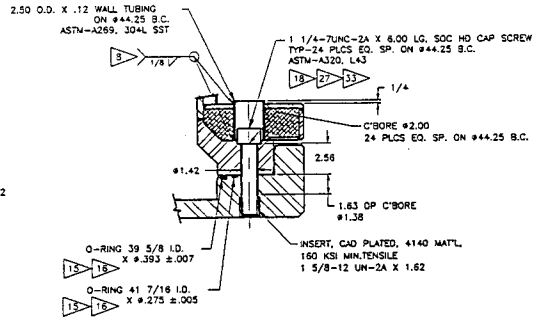
DETAIL-P (SHT 1)

FIN



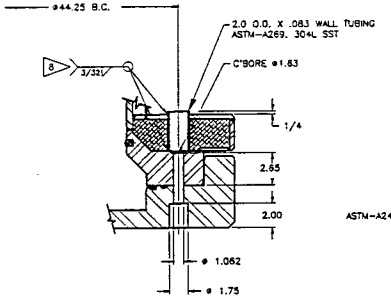
SECTION B-B (SHT 1)

ALIGNMENT PIN TYP-2 PLCS



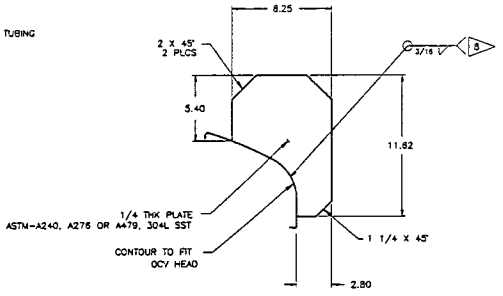
SECTION C-C (SHT 1)

CLOSURE BOLT



SECTION D-D (SHT 1)

IMPACT LIMITER BOLT HOLE TYP-8 PLCS



DETAIL-G (SHT 1)

FIN

FOR GENERAL NOTES AND FLAG NOTES SEE DRAWING No. H-9-5000.

APR 11 1995

DOCUMENT NUMBER, WHC-SD-RTG-SARP-001
PAGE NUMBER, 1.3.2-7 Rev. 0

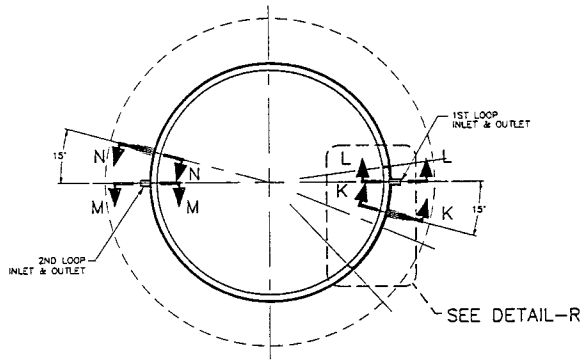
DRAWN M RICHARDS	4-10-95	U.S. DEPARTMENT OF ENERGY Richland Operations Office Westinghouse Hanford Company	
DESIGN	4/11/95	RTG TRANSP PKG OUTER CONTAINMENT VESSEL (OCV) ASSY AND DET	
QA	4/11/95		
CM PC FERRELL	4/11/95		
SAFETY		SIZE F	CAGE NO. 427
ENVIRONMENTAL		DRAWING NO. 5010 H-9-5002	REV 0
OTHER		WEIGHT NONE	SHEET 3

DWG NO / TITLE / DRAWING TRACEABILITY LIST — REF NUMBER / TITLE / REFERENCES — NEXT USED ON / FAD ITEM

REVISIONS — DESCRIPTION — ENGINEERING — QUALITY ASSURANCE — OTHER

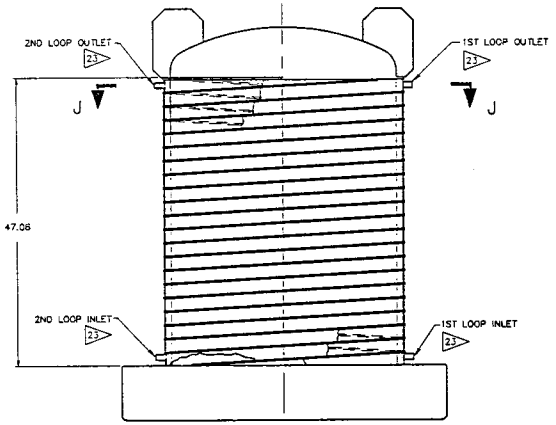
CADFILE K0050020 — CADCODE DOS 5.0: ACD2:12 0:55

54-9000-027(5/89)

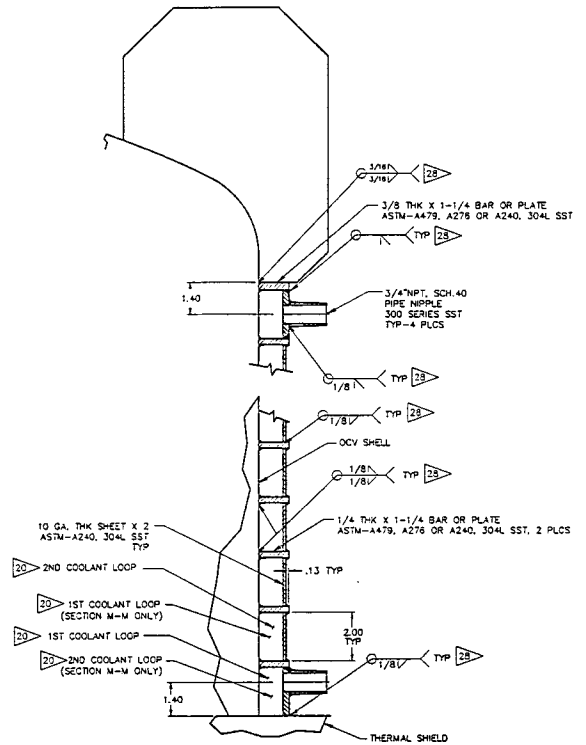


SECTION J-J

(ROTATED 7°30' CW FROM ELEVATION VIEW - SHT 4)

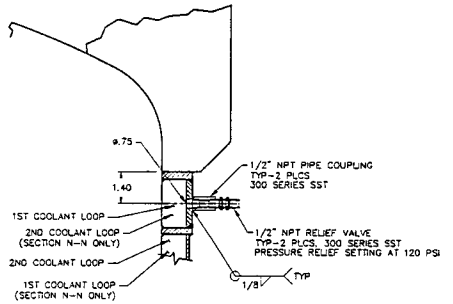


(VIEW ROTATED 7°30' CW FROM ELEVATION VIEW - SHT 4)



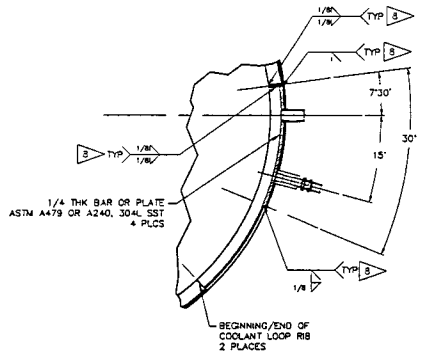
SECTION L-L (AS SHOWN)

SECTION M-M (AS NOTED)



SECTION K-K (AS SHOWN)

SECTION N-N (AS NOTED)



DETAIL-R

FOR GENERAL NOTES AND FLAG NOTES
SEE DRAWING No. H-9-5000.

APR 11 1995

DOCUMENT NUMBER, WHC-SD-RTG-SARP-001
PAGE NUMBER, 1.3.2-8 Rev. 0

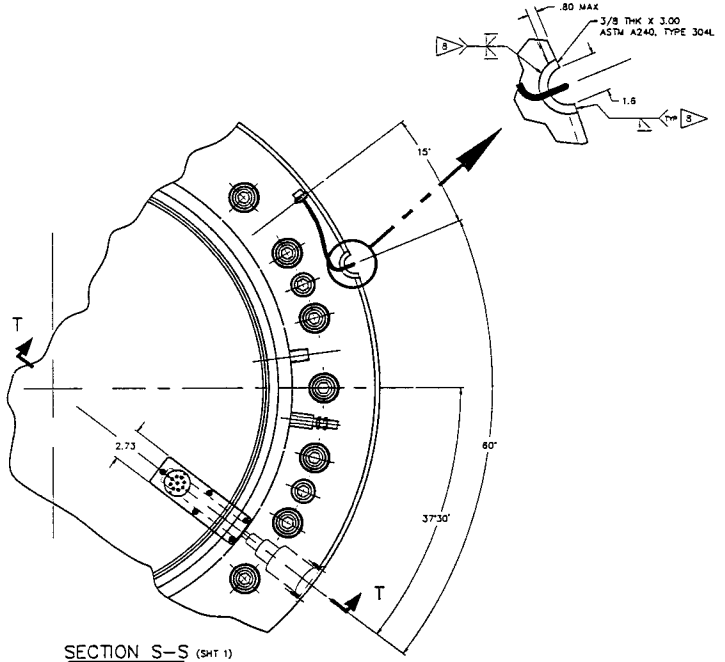
Drawn N RICHARDS	4-10-95	U.S. DEPARTMENT OF ENERGY	
Designed	4/11/95	Richland Operations Office	
Eng Supv	4/11/95	Westinghouse Hanford Company	
Eng Supv PC FERRELL	4/11/95	RTG TRANSP PKG	
Q.A.	4/11/95	OUTER CONTAINMENT VESSEL (OCV) ASSY AND DET	
Others		SIZE F	DRAWING NO H-9-5002 REV 0
Others		SCALE NONE	WT 613635 SHEET 4
Others			

DWG NO	TITLE	REF NUMBER	TITLE
DRAWING TRACEABILITY LIST		REFERENCES	
		NEXT USED ON END ITEM	

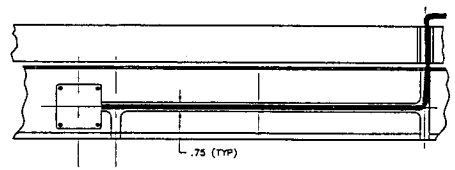
REVISIONS

CAGEFILE KC0050020 *CAGECODE 20S 3 0 4C02 *2 0 SS

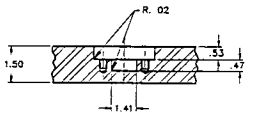
54-6000-027(5/88)



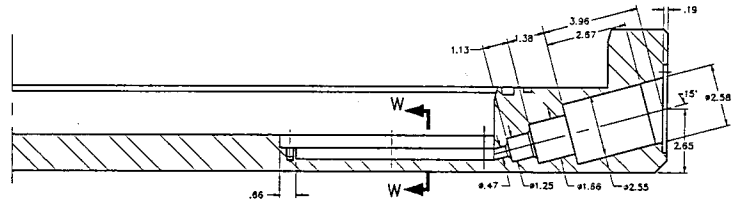
SECTION S–S (SHT 1)



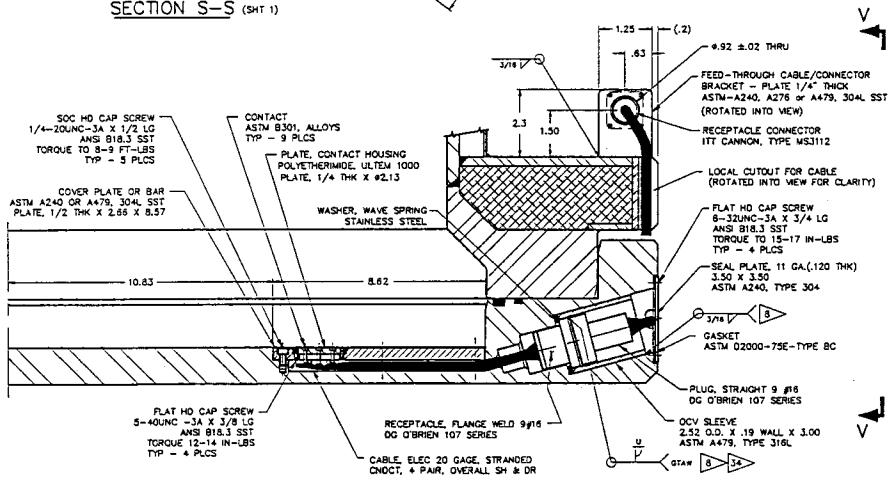
VIEW V–V



SECTION W–W

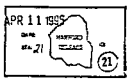


SECTION T–T
(OCV BASE PLATE ONLY, FEED–THROUGH ASSEMBLY REMOVED FOR CLARITY)



SECTION T–T

FOR GENERAL NOTES AND FLAG NOTES SEE DRAWING No. H–9–5000.



DOCUMENT NUMBER, WHC–SD–RTG–SARP–001
PAGE NUMBER, 1.3.2–9 Rev. 0

DRAWING TRACEABILITY LIST			REVISIONS	
DWG NO	TITLE	REF NUMBER / REFERENCES	NEXT USED ON	END ITEM
			CADFILE K0050025	ICACODE 005.6.0:ACD2.12.0:SS

Drawn M RICHARDS	4-10-95	U.S. DEPARTMENT OF ENERGY
Designer P.C. Farrell	4/4/95	Richland Operations Office
Stress		Westinghouse Hanford Company
Stress PC FERRELL	4/4/95	RTG TRANSP PKG
Weights	4/11/95	OUTER CONTAINMENT VESSEL (OCV)
Others		ASSY AND DET
Others		
Others for Information		

SIZE	DWG NO	REV
F	427 5010 H–9–5002	0

SCALE NONE | WT 513635 | SHEET 5

H–9–5002 REV 0

54–6000–027(3/89)

FOR GENERAL NOTES AND FLAG NOTES
SEE DRAWING No. H-9-5000.

DOCUMENT NUMBER, WHC-SD-RTG-SARP-001
PAGE NUMBER, 1.3.2-10

Rev. 0

AP2.11 USE
DATE
STATUS
CLOSED
21

U.S. DEPARTMENT OF ENERGY
Richland Operations Office
Westinghouse Hanford Company

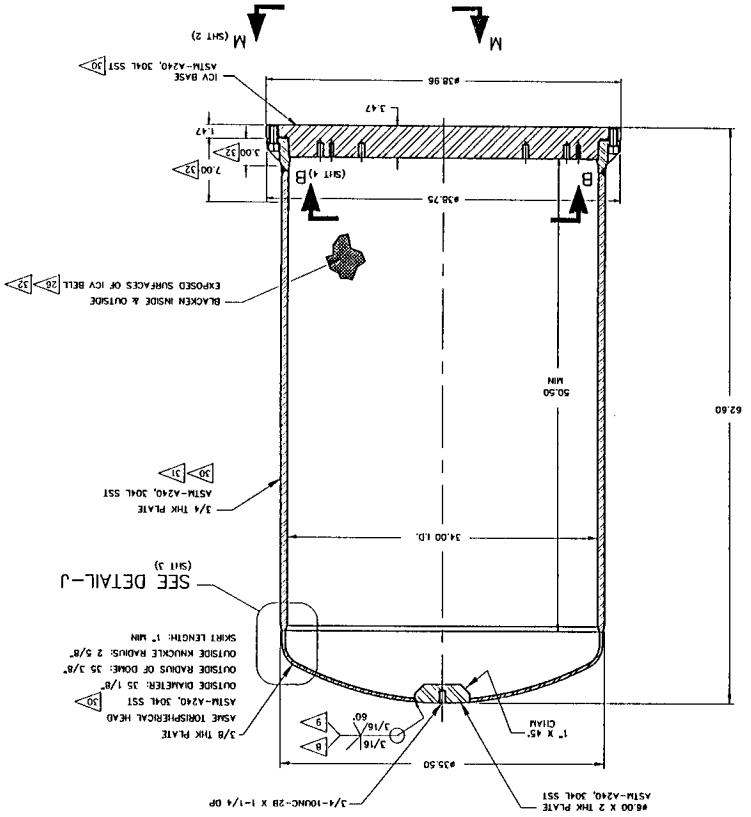
RTG TRANSP PKG
INNER CONTAINMENT VESSEL (ICV)
ASSY AND DET

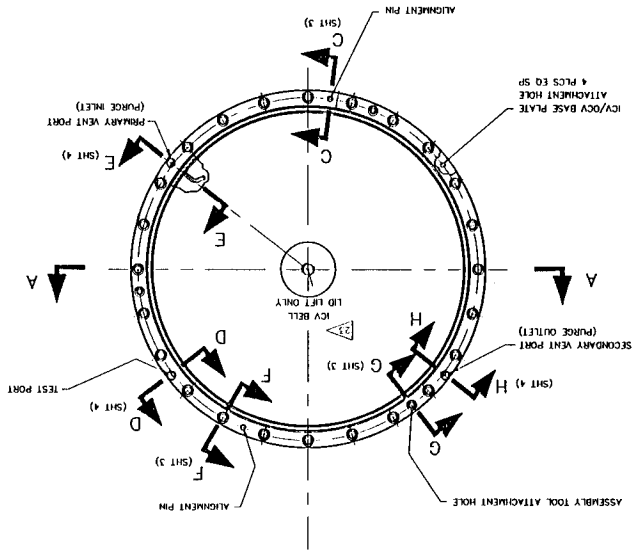
F | 427 | 5010 | H-9-5003 | 0

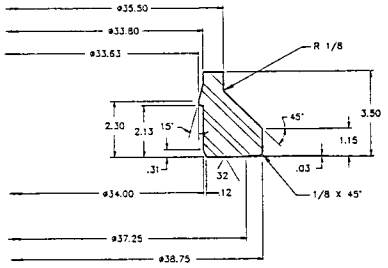
SCALE: NONE

DWG NO	TITLE	REF NUMBER	REVISIONS	DES	CHK	APP
DRAWING TRACEABILITY LIST		NEXT USED ON	CADFILE H095003A			
		REFERENCES				
		TITLE				

SECTION A–A

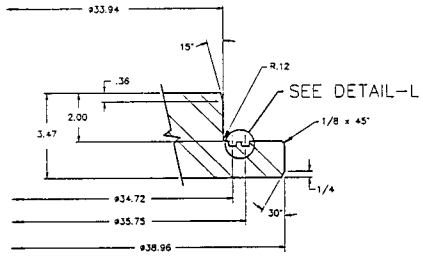




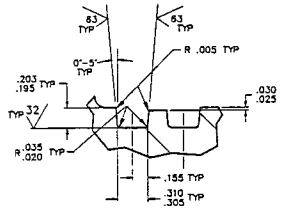


ICV BELL FLANGE DETAIL

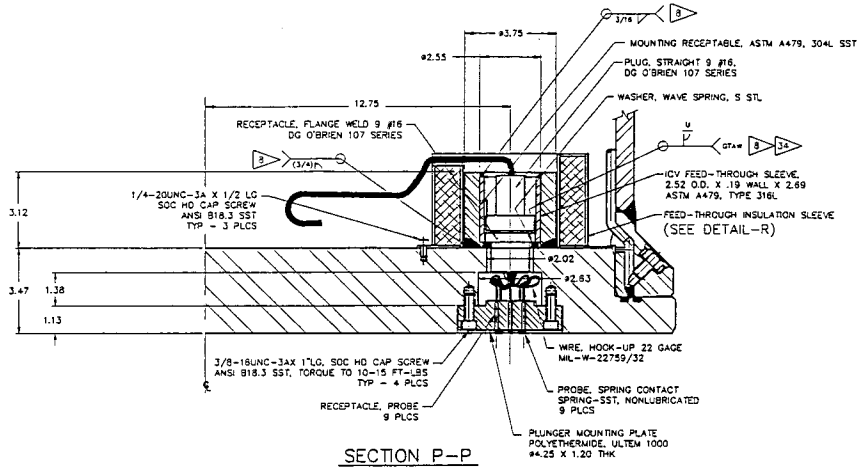
MATL: ASTM-A240, 304L SST (30)



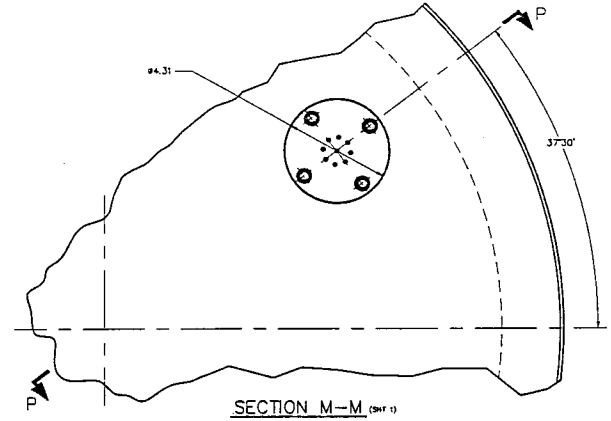
ICV BASE DETAIL



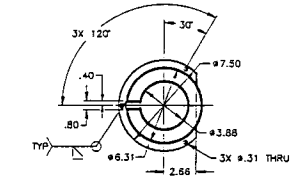
DETAIL-L

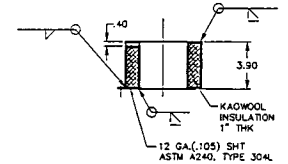


SECTION P-P



SECTION M-M (SHT 1)





DETAIL-R

FEED-THROUGH INSULATION SLEEVE

FOR GENERAL NOTES AND FLAG NOTES SEE DRAWING No. H-9-5000.

APR 11 1996

DOCUMENT NUMBER, WHC-SD-RTG-SARP-001
PAGE NUMBER, 1.3.2-11 Rev. 0

DRAWN M RICHARDS	4-12-96	U.S. DEPARTMENT OF ENERGY Richland Operations Office Westinghouse Hanford Company	
CHECKED PH Powell	4/12/96		
DES AUTH Mike Wilson	4/12/96		
DES CHIEF PC FERRELL		RTG TRANSP PKG INNER CONTAINMENT VESSEL (ICV) ASSY AND DET	
QA Paul Peterson	4/12/96		
OTHER			
OTHER			
APVD FOR IMPLEMENTATION			
PE		SIZE F	FSCM NO 427
		SCALE NONE	DWG NO H-9-5003
			REV 0

DWG NO	TITLE	REF NUMBER	TITLE
DRAWING TRACEABILITY LIST		REFERENCES	
		NEXT USED ON	END ITEM

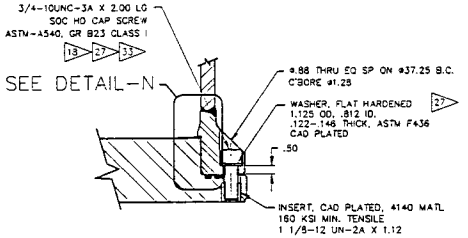
REV NO	DESCRIPTION	REV BY DATE	CHK BY DATE	APVD BY DATE	OTHER	OTHER
REVISIONS						

CADFILE K0050038 | CADCODE DOS: 6.0 ACD: 13.0: SS

SHEET 2

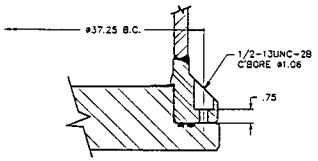
H-9-5003 REV 0

34-6000-027(5/89)



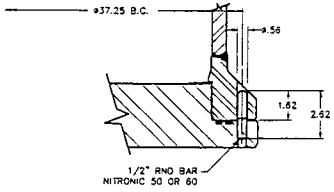
SECTION F-F (SHT 1)

CLOSURE BOLT
TYP-24 PL



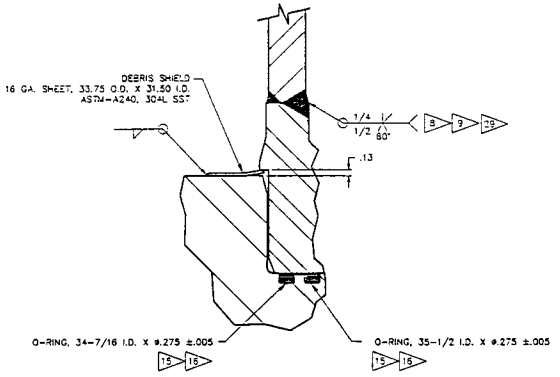
SECTION G-G (SHT 1)

SPACER BLOCK ATTACHMENT HOLE
TYP-3 PLCS



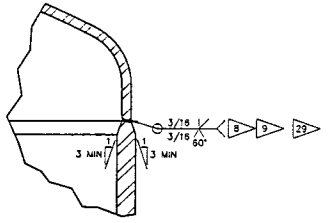
SECTION C-C (SHT 1)

ALIGNMENT PIN
TYP-2 PLCS



DETAIL-N

ICV SEAL AREA



DETAIL-J (SHT 1)

FOR GENERAL NOTES AND FLAG NOTES
SEE DRAWING No. H-9-5000.

APR 11 1995

DOCUMENT NUMBER, WHC-SD-RTG-SARP-001
PAGE NUMBER, 1.3.2-12 Rev. 0

DRAWN M. RICHARDS	DATE 4-10-95	U.S. DEPARTMENT OF ENERGY Richland Operations Office Westinghouse Hanford Company	
CHECKED [illegible]	DATE 4/11/95		
ENGR APPROVAL [illegible]	DATE 4/11/95	RTG TRANSP PKG INNER CONTAINMENT VESSEL (ICV) ASSY AND DET	
ENGR APPROVAL PC FERRELL	DATE 4/11/95		
QA [illegible]	DATE 4/11/95		
OTHER			
OTHER			
OTHER			
APPD FOR NON-CONFORMANCE			

DWG NO.	TITLE	REF NUMBER	TITLE
DRAWING TRACEABILITY LIST		REFERENCES	
		NEXT USED ON	END ITEM

REV NO.	DESCRIPTION	DRAFTING DATE	ENGR DATE	QUALITY DATE	ENGR	QUALITY	OTHER
	REVISIONS			APPROVALS BY/DATE			

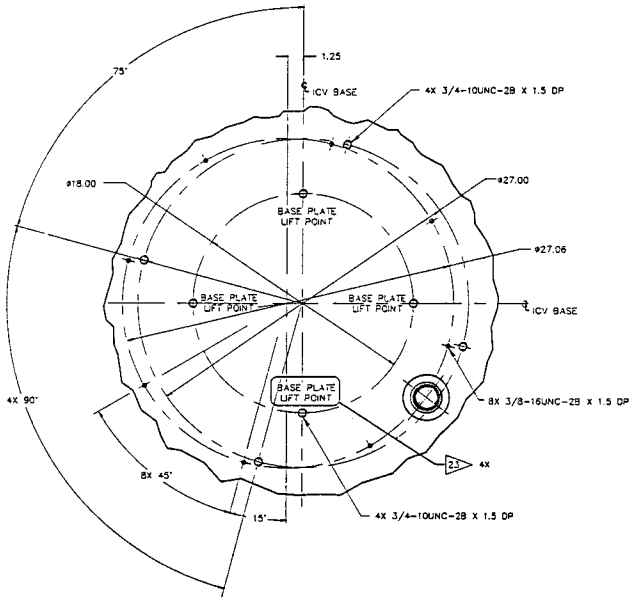
CADFILE K0050030 (CADCODE DOS 5.0: ACAD 12.0: SS

SIZE	CODE IDENT NO	DWG NO	REV NO
F	427	5010 H-9-5003	0

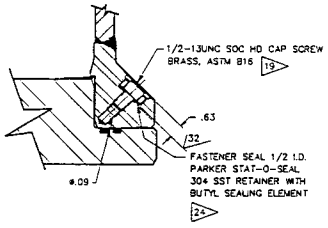
SCALE NONE | WP 913635 | SHEET 3

34-5000-027(5/89)

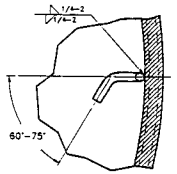
H-9-5003



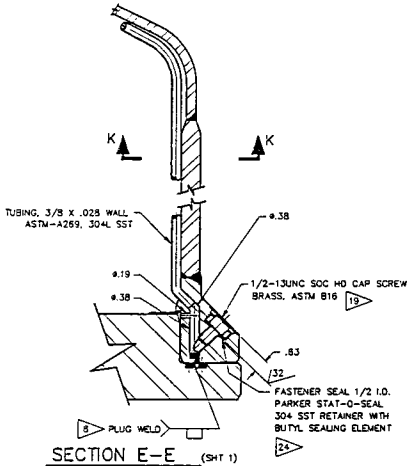
SECTION B-B (SHT 1)
RACK MOUNTING BOLT HOLES



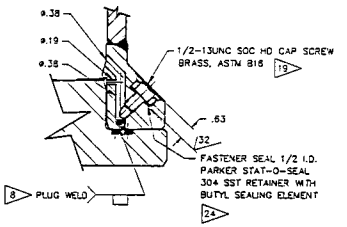
SECTION D-D (SHT 1)
INNER CONTAINMENT TEST PORT



SECTION K-K



SECTION E-E (SHT 1)
INNER CONTAINMENT PRIMARY VENT PORT



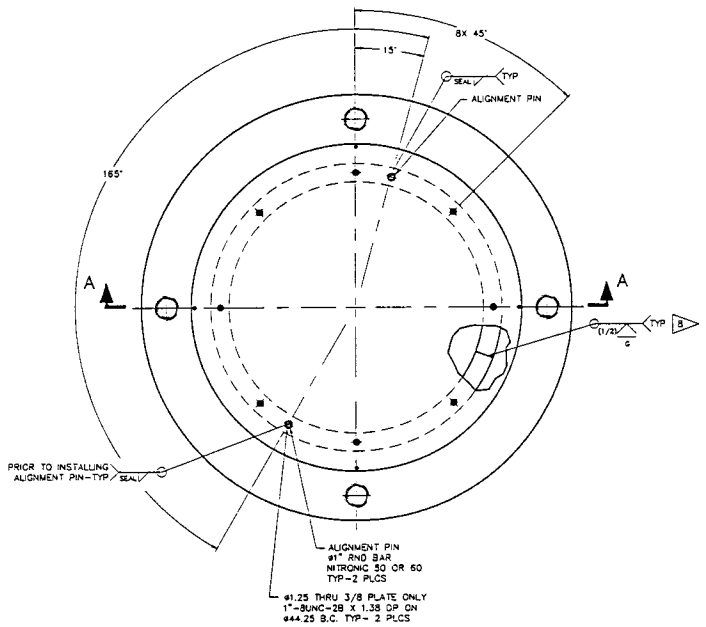
SECTION H-H (SHT 1)
INNER CONTAINMENT SECONDARY VENT PORT

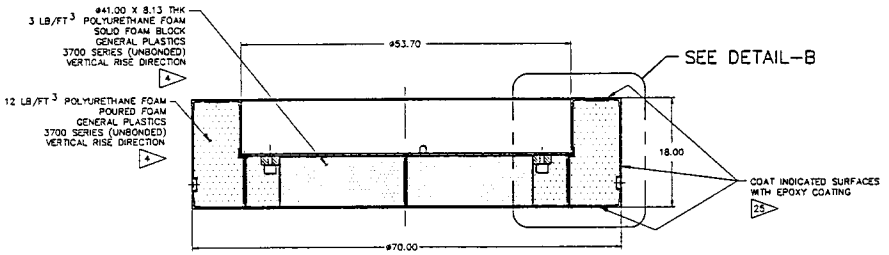
FOR GENERAL NOTES AND FLAG NOTES
SEE DRAWING No. H-9-5000.

APR 11 1995
STA. 21

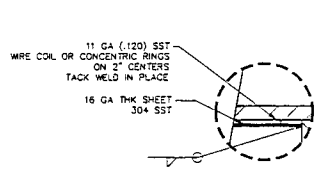
DOCUMENT NUMBER, WHC-SD-RTG-SARP-001
PAGE NUMBER, 1.3.2-13 Rev. 0

| | | |

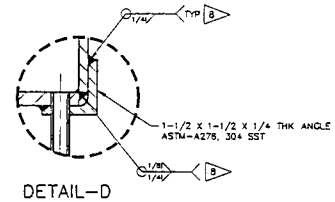




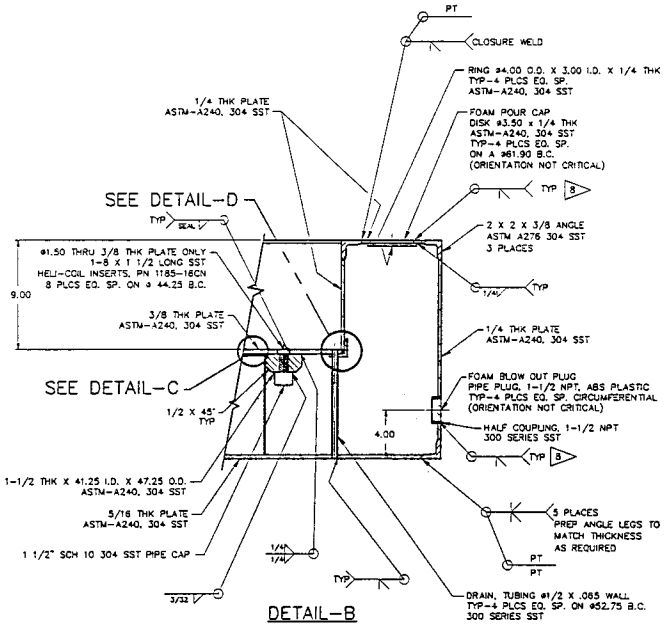
SECTION A-A



DETAIL-C
THERMAL BARRIER

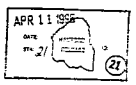


DETAIL-D



DETAIL-B

FOR GENERAL NOTES AND FLAG NOTES
SEE DRAWING No. H-9-5000.



DOCUMENT NUMBER, WHC-SD-RTG-SARP-001
PAGE NUMBER, 1.3.2-14 Rev. 0

DRAWN M RICHARDS	4-10-96	U.S. DEPARTMENT OF ENERGY	
CHECKED PC Powell	4/11/96	Richland Operations Office	
DATE APPROVED 4/11/96		Westinghouse Hanford Company	
ENG MGR PC POWELL	4/11/96	RTG TRANSPORTATION PACKAGE IMPACT LIMITER ASSY AND DET	
OTHER			
OTHER			
OTHER			
DWG FOR IMPLEMENTATION			
OTHER			

DWG NO	TITLE	REF NUMBER	TITLE
DRAWING TRACEABILITY LIST		REFERENCES	
		NEXT USED ON	END ITEM

REVISIONS

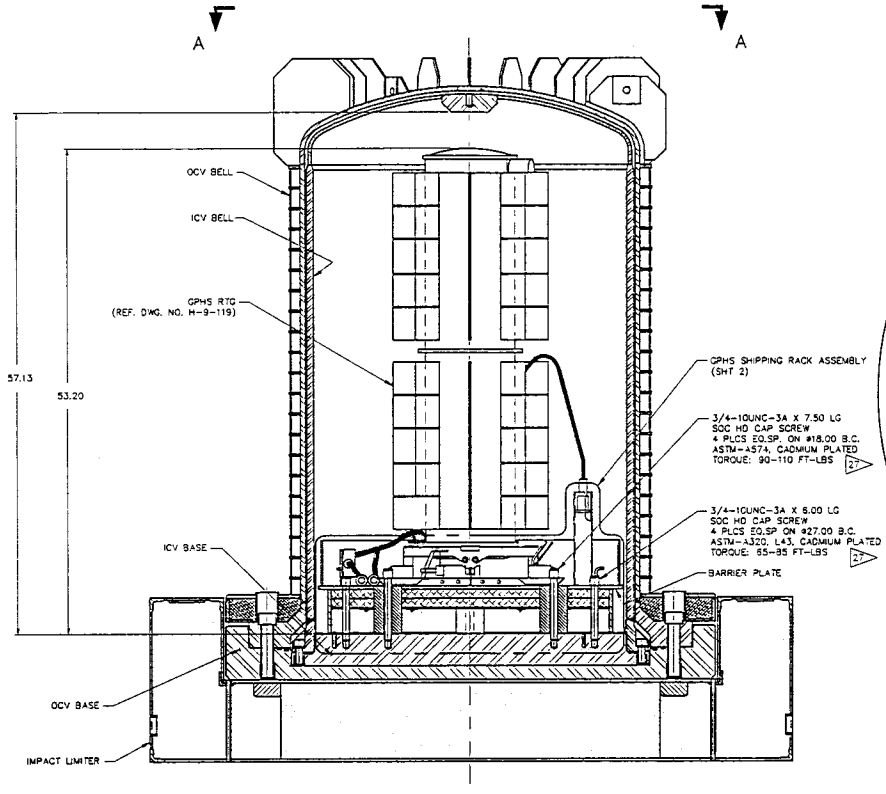
REV	DESCRIPTION	REV DATE	APPROVED BY/DATE

CADFILE K0050044A CADCODE 305 4.2 ACD2.12.0-SS

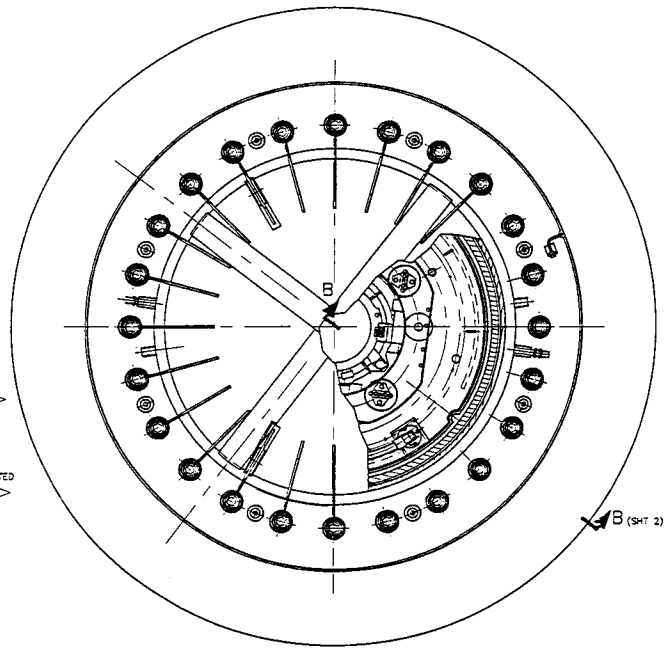
SIZE	FSCM NO	DWG NO	REV
F	427	5010 H-9-5004	0

SCALE NONE WT 513635 SHEET 1 OF 1

5A-6000-027(5/99)



PERSONNEL BARRIER AND TIEDOWN STRAPS REMOVED FOR CLARITY



GPHS RTG SHIPPING CONFIGURATION

VIEW A-A

FOR GENERAL NOTES AND FLAG NOTES
SEE DRAWING No. H-9-5000.

APR 11 1995

DOCUMENT NUMBER, WHC-SD-RTG-SARP-001
PAGE NUMBER, 1.3.2-15 Rev. 0

Drawn M. RICHARDS	4-12-95	U.S. DEPARTMENT OF ENERGY	
Designer		Richland Operations Office	
Engr Approval		Westinghouse Hanford Company	
Cog Engr PC FERRELL		RTG TRANSPORTATION PACKAGE	
QA		GPHS RTG SHIPPING CONFIGURATION	
Others			

DWG NO	TITLE	REF NUMBER	REFERENCES	TITLE
DRAWING TRACEABILITY LIST		NEXT USED ON 2ND ITEM		

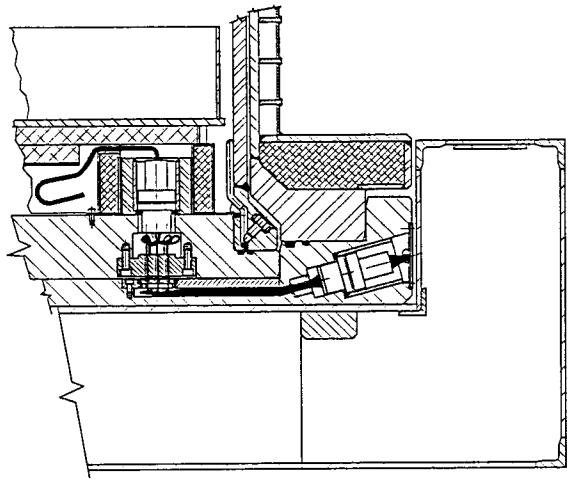
REVISIONS

CADFILE KC05105A | CADCODE DOS: 5.0; ACD2: 12.0; SS

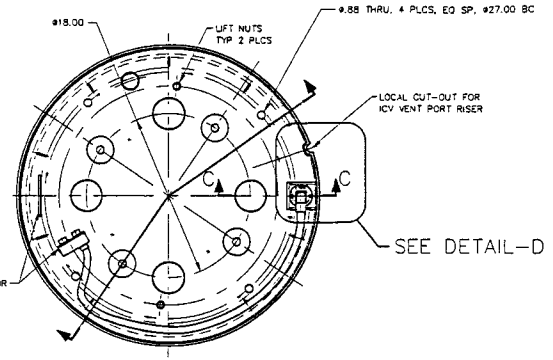
SIZE	PLANT NO	MODEL NO	DWG NO	REV
F	427	5010	H-9-5005	0

SCALE NONE | DRN 51.1635 | SHEET 1 OF 2

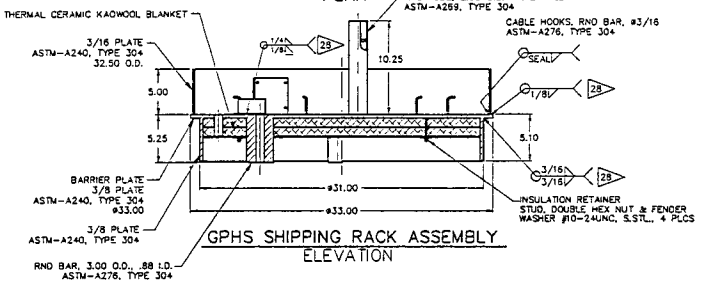
34-6000-027(5/89)



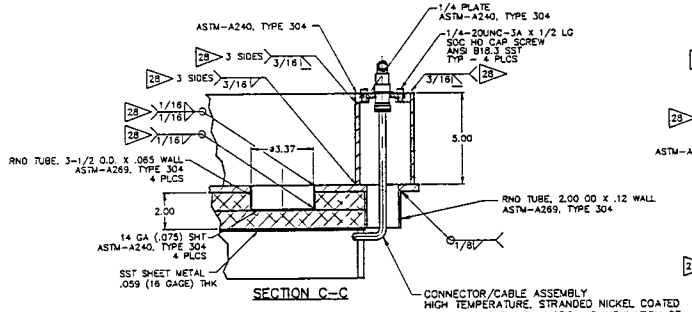
SECTION B–B (SHT 1)



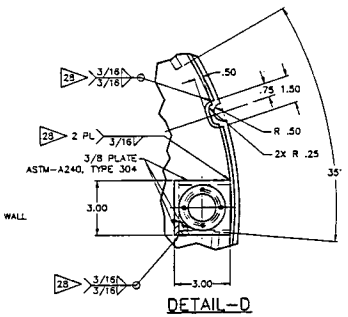
PLAN



GPHS SHIPPING RACK ASSEMBLY
ELEVATION

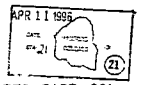


SECTION C–C



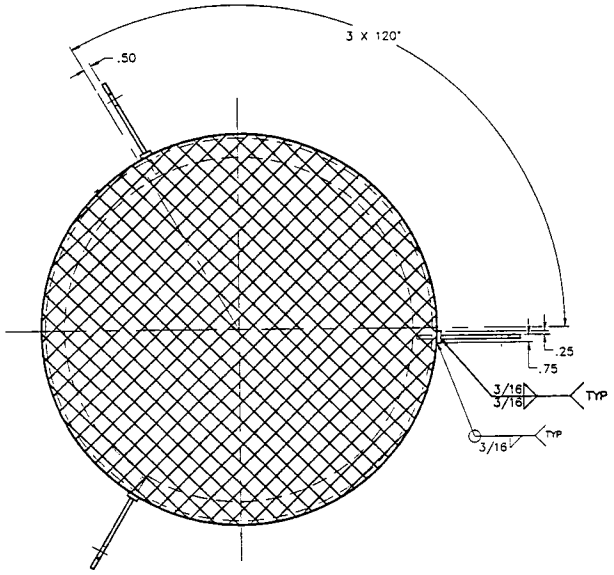
DETAIL–D

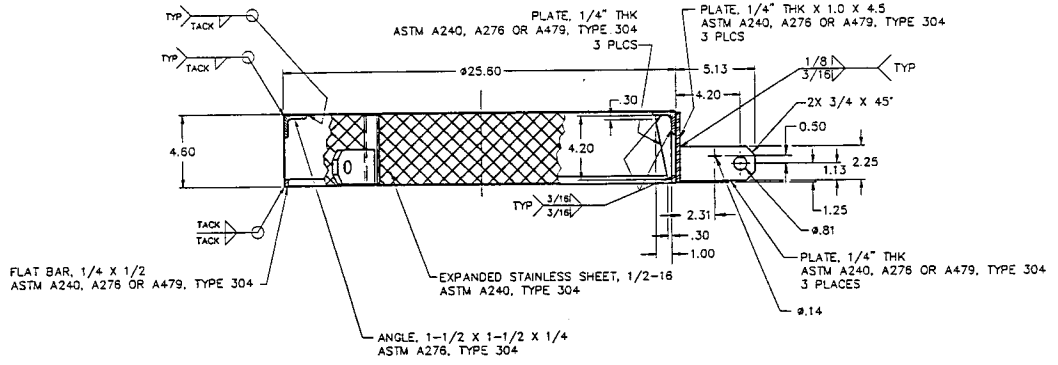
FOR GENERAL NOTES AND FLAG NOTES
SEE DRAWING No. H–9–5000.



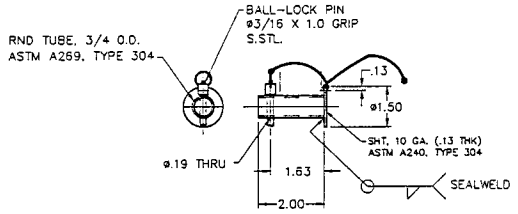
DOCUMENT NUMBER, WHC–SD–RTG–SARP–001
PAGE NUMBER, 1.3.2–16 Rev. 0

| | | |





RTG OCV HEAD PERSONNEL BARRIER



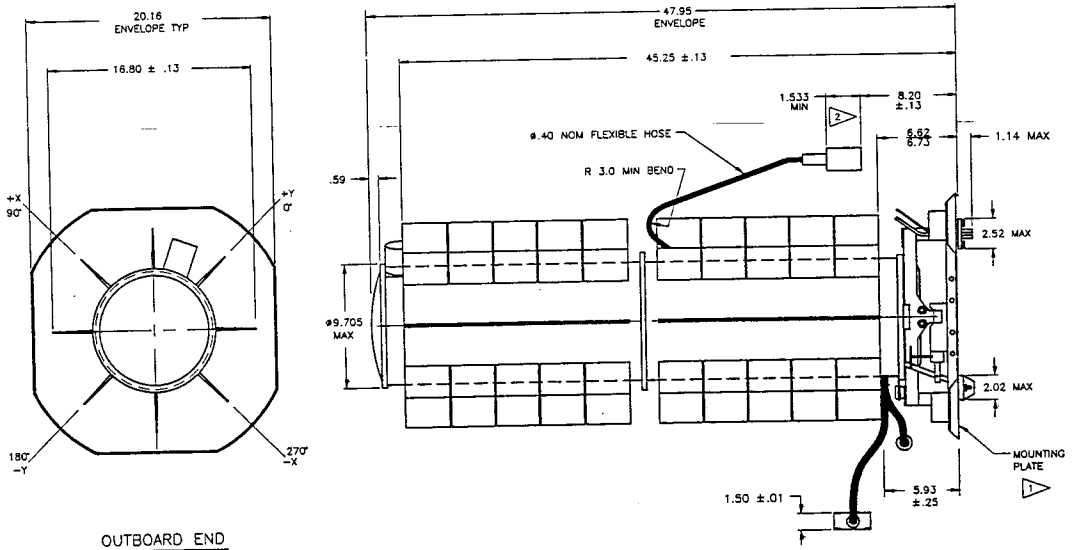
PERSONNEL BARRIER RETENTION PIN

FOR GENERAL NOTES AND FLAG NOTES
SEE DRAWING No. H-9-5000.

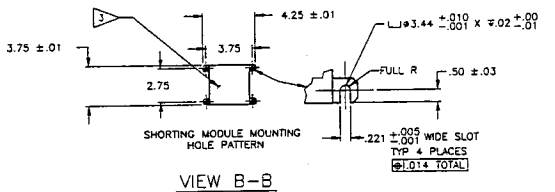
APR 11 1996

DOCUMENT NUMBER, WHC-SD-RTG-SARP-001
PAGE NUMBER, 1.3.2-17 Rev. 0

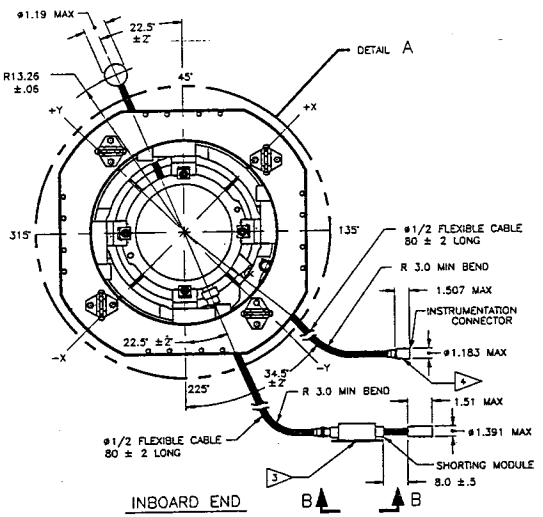
Drawn M RICHARDS	4-10-96	U.S. DEPARTMENT OF ENERGY Richland Operations Office Westinghouse Hanford Company	
Checked R.A. Hall	4/4/96	RTG TRANSPORTATION PACKAGE RTG OCV HEAD PERSONNEL BARRIER	
Date Issued 4/4/96			
Use Over PC FERRELL			
Released [signature]	4/11/96		
Other			
Other			
Other			
Other			
Other Approvals By/Date			
Other			
Other			
Other			
Other



OUTBOARD END



VIEW B-B



INBOARD END

NOTES:

1. GPHS RACK ASSEMBLY INTERFACE
2. GAS CONNECTOR INTERFACE
3. SHORTING MODULE INTERFACE
4. INSTRUMENTATION CONNECTOR INTERFACE

THE TWO CABLES INTERFACE WITH DUMMY CONNECTORS SHOWN ON G.E. DRAWING 47E305551 I.D. #'S MS3115-18-A AND MS3115-14-A.

APR 15 1996

DOCUMENT NUMBER, WHC-SD-RTG-SARP-001
PAGE NUMBER, 1.3.3-2 Rev. 0

DRAWN	TRACY	DATE	4/15/96
ENGINEER		DATE	4/15/96
PROJECT ENGINEER	PC FERNELL	DATE	
QA	N/A		

U.S. DEPARTMENT OF ENERGY
Richland Operations Office
Westinghouse Hanford Company

GPHS
INTERFACE CONTROL DRAWING

F	427	5010	H-9-119

SCALE 1/4 | SIZE D | 913638 | SHEET 1 OF 2

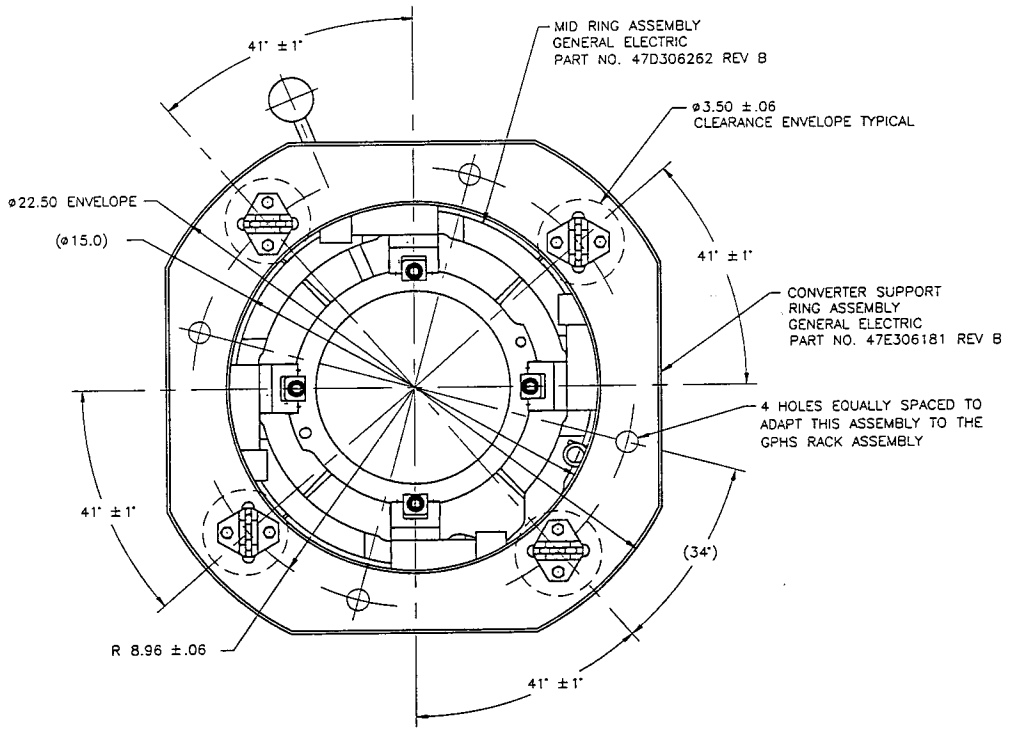
DRAWING TRACEABILITY LIST

DWG NO	TITLE	REF NUMBER	TITLE
		NEXT USED ON	END ITEM

REVISIONS

CADFILE K0001198A | CADCODE DOS:6.00:ACD2:12.0:SS

H-9-119 1 of 2



DETAIL A

APR 15 1996

DOCUMENT NUMBER, WHC-SD-RTG-SARP-001
PAGE NUMBER, 1.3.3-3 Rev. 0

U.S. DEPARTMENT OF ENERGY
Richland Operations Office
Westinghouse Hanford Company

GPHS
INTERFACE CONTROL DRAWING

F 427 5010 H-9-119 0

SIZE 1/2 813638 SHEET 2 OF

H-9-119

DWG NO TITLE
DRAWING TRACEABILITY LIST
REF NUMBER TITLE
REFERENCES
NEXT USED ON END ITEM
REVISIONS
CAGE/LE X0001198 CADCODE 005:8.00:AC02:12.0:SS

1.3.3 GPHS RTG Interface Control Drawing

Drawing Number	Title	Number of sheets
H-9-119	GPHS Interface Control Drawing	2

2.0 STRUCTURAL EVALUATION

This section presents evaluations that demonstrate that the RTG Transportation System Package meets all applicable structural criteria. The package consists of an outer containment vessel (OCV), an inner containment vessel (ICV), an impact limiter, and payloads with associated shipping rack assemblies. Normal conditions of transport (NCT) and hypothetical accident condition (HAC) evaluations, using analytic and experimental techniques, are performed to address 10 CFR 71[1] performance requirements. Analytic demonstration techniques comply with the methodology presented in NRC Regulatory Guide 7.6[2]. With the exception of the free drop event, the NCT events are handled analytically. For the HAC events, fire and immersion are handled analytically, and the other events by a combination of analysis, half-scale development testing, and full-scale certification testing.

Experience with previous packaging designs is taken advantage of to the fullest extent possible. Thus, the temperature dependent physical properties and intumescence* of the polyurethane foam used in the impact limiter are taken from the manufacturer's extensive data base[3]. Nuclear Packaging's TRUPACT-II development program demonstrated the impact absorbing and thermal insulating properties of polyurethane foam. Butyl rubber O-ring performance characteristics have been established by test and are detailed in Appendix 2.10.6. Properties of AISI Type 304L stainless steel, used almost exclusively for packaging structural components, are well documented over a wide range of temperatures in the ASME Boiler and Pressure Vessel (B&PV) Code[6].

A full series of NCT free drop, HAC 30-ft free drop, and HAC 40-in. puncture drop tests were successfully run with the package remaining leaktight (an integrated leakage rate of less than 1.0×10^{-7} scc/sec, air). The test plan is given in Appendix 2.10.9 and the test procedure in Appendix 2.10.10.

2.1 STRUCTURAL DESIGN

2.1.1 Discussion

This packaging will safely transport Radioisotope Thermoelectric Generators (RTG). The RTG payloads provide highly reliable power sources for use in deep space and terrestrial missions. The packaging consists of three major component subassemblies: (1) an OCV, which provides a primary containment boundary, (2) an ICV, which provides a secondary containment boundary, and (3) an impact limiter, which cushions impact under the HAC drop events, as well as providing insulation for the seal area from the HAC fire temperatures. The ICV and OCV assemblies constitute independent containments as required by 10 CFR 71.63 for shipments containing more than 20 curies (Ci) of plutonium.

---

*_Intumescence_ is the property of this family of foams that describes their ability to _increase_ their volume as they melt in the presence of flame, thus filling voids left by punctures or tears in the impact limiter sheathing, and providing reliable thermal insulation, even after damage.

2.1.1.1 Outer Containment Vessel (OCV). The OCV consists of an AISI Type 304L stainless steel base to which a Type 304L stainless steel bell assembly is attached by 24, 1 1/4-in., ASTM A320-L43 alloy steel closure bolts. The closure bolts engage hardened steel inserts that are threaded into the OCV base. The bell flange fits within a counterbore in the base sized to limit motion in an accident so that the attaching bolts cannot be loaded in direct shear. The bell is made of a cylindrical shell welded to an American Society of Mechanical Engineers (ASME) torispherical head, both having a wall thickness of 0.50 in. Twenty-four 0.25-in.-thick energy absorbing fins are attached to the head approximately at the knuckle region. Three of the fins have reinforced holes for lifting the entire package.

The seal between the bell flange and the base is effected by use of two concentrically arranged butyl rubber O-ring face seals. The inner containment seal has a nominal diameter of 0.393 in., and the outer noncontainment test seal has a nominal diameter of 0.275 in. A vent port is located in the base, through which air is evacuated from the annulus between the ICV and OCV and through which helium is backfilled. There is also a noncontainment test port located between the two O-ring seals for leakage rate testing the containment seal. Vent and test port plugs are made of brass and sealed using butyl O-rings. Port covers with Teflon® seals are used outboard of the plugs and provide an enclosure to retain any leakage per 10 CFR 71.43(e). One electrical feed-through connector is located in the base plate. The device consists of a Type 316L stainless steel body, electrical conductor pins, and a glass-sealing material between the body and the pins. The body is firmly held in place in the base plate by a surrounding structure, and is attached to the base plate material with a gas tungsten arc weld. Outside the OCV containment, a removable plug is used to connect the electrical feed-through connector to the recording equipment. Between the ICV and OCV bases, permanent wire connections are used in conjunction with a spring-loaded pin contact assembly to complete the electrical feed-through circuit between the two vessels. See Figure 2.3-1 for a schematic of the electrical feed-through components.

Located on the outside of the OCV cylindrical area is a coolant jacket consisting of two identical, parallel spiral passages. The passages are constructed of Type 304L and are integrally welded to the OCV shell. Two pressure relief valves, one for each coolant loop, are set for 50 psi and will release excessive pressure that may develop in the coolant jacket because of abnormal system operation. During normal transportation operations, two redundant chilling systems will be connected to the coolant jacket, one to each cooling loop. However, for purposes of the evaluation of compliance with 10 FR 71, the coolant jacket will be assumed to be drained and dry with no active cooling in effect. A thermal shield is located between the lower end of the cooling jacket and the OCV flange consisting of a hollow structure with a 3/8-in. thick top plate and filled with insulation. This feature will protect the flange from puncture and the elastomer seals from the fire peak transient temperatures. The interior of the OCV bell is painted flat black to enhance radiative heat transfer from the ICV. The outside of the OCV bell is painted white to achieve low solar absorptivity while retaining a relatively high emissivity.

2.1.1.2 Inner Containment Vessel (ICV). The ICV consists of an AISI Type 304L stainless steel base, to which a Type 304L stainless steel bell is attached by 24, 3/4-in., ASTM A540-B23 alloy steel closure bolts. The closure bolts engage hardened steel inserts that are threaded into the ICV base. The bell is made of a cylindrical shell, with a 0.75-in.-wall thickness, and an ASME torispherical head that is 0.38 inch thick. At the top center of the head is a block which is drilled and tapped to accept a lifting eye. Both the inside and outside of the bell are painted flat black to enhance radiative heat transfer. A radial gap of 1/32 in. minimum and 1/4 in. maximum exists between the ICV outside diameter and the OCV inside diameter. The gap between the ICV and OCV heads is from 1/16 in. minimum to 1/2 in. maximum, and is sized to ensure that under HAC events, contact will first occur between the two heads rather than between the ICV and OCV

flanges. This feature avoids direct loading of the OCV flange by the ICV in a HAC drop. The ICV fits within a counterbore in the OCV base and is located there by two alignment pins and attached by four 1/4-in. diameter, A-574 bolts.

Containment sealing between the bell flange and base is effected by use of two concentrically arranged, 0.275-in. nominal diameter butyl rubber O-ring face seals. As with the OCV, the inner O-ring seal provides the containment boundary and the outer O-ring supports leakage rate testing. Two vent ports through the containment boundary (used during the helium purge process), and one O-ring seal leakage rate test port (noncontainment) are located in the bell flange. Vent and test port plugs are made of brass and sealed using butyl O-rings. One electrical feed-through connector, of identical construction to the corresponding OCV component, is located in the base plate. As with the OCV, the electrical feed-through body is firmly held in place in the base plate by surrounding structure and is attached to the base plate material with a gas tungsten arc weld. Inside the ICV containment, a removable plug is used to connect the electrical feed-through connector to the temperature measuring devices mounted on the payload. See Figure 2.3-1 for a schematic of the electrical feed-through components.

Payload specific shipping rack assemblies are securely fastened to the ICV base using ASTM A320 L43 alloy steel bolts, and are designed to remain in place during a HAC drop event and prevent proximity of payload heat sources to the seal area. The shipping rack assembly for the General Purpose Heat Source (GPHS) RTG is attached using four 6-in.-long, 3/4-in. bolts. The length of these bolts, coupled with limited clearance between the shipping rack assembly and ICV wall, exclude the potential for direct shear forces. The payload is fastened to the ICV base using bolts that pass through the shipping rack assembly, thus payload inertia loads are not transmitted to the shipping rack assembly or its attaching bolts. The payload bolts are allowed to fail in a HAC drop event without compromising the shipping rack assembly-to-base attachment. The GPHS RTG is attached using four 3/4-in., ASTM A-574 bolts. The shipping rack assembly for all payloads includes a 3/8-in.-thick, 33-in. O.D. stainless steel barrier plate. The small, 0.50 in. radial gap between the shipping rack and ICV wall will not allow payload heat sources to relocate below the shipping rack assembly. To further protect the ICV containment seal from smaller size debris, if any, a stainless steel debris shield is located at the internal junction of the ICV bell and base.

2.1.1.3 Impact Limiter. The impact limiter is a AISI Type 304 stainless steel shell, 70 in. in O.D., and 18 in. tall, with a 53.75-in. diameter central pocket on the top, 9 in. deep, into which fits the OCV base. The plate at the bottom of the impact limiter is 0.31 in. thick. The plate forming the bottom of the pocket is 0.38 in. thick. The inner and outer cylindrical walls and top annular section are 0.25 in. thick. All corner joints are reinforced with Type 304 stainless steel angles.

A 1.5-in.-thick bolting ring just beneath the pocket bottom is used to attach the impact limiter to the OCV, and contains threaded holes that have stainless steel Heli-coil inserts. Eight 1-in.-diameter ASTM B637, Alloy N07750 Type 3 bolts, with a shank diameter reduced to 0.805 in. to better absorb energy by stretching, attach the impact limiter to the package. Direct shear in the bolts is precluded by the relatively long bolts and extra hole clearance in the mating OCV base.

The cavity within the impact limiter is filled with rigid polyurethane structural foam of 3 lb/ft^3 and 12 lb/ft^3 densities. For the center portion, out to a diameter of 41 in., 3 lb/ft^3 density is used. A sheet metal thermal shield is incorporated in the structure between the center pocket bottom plate and the foam. For the remainder, 12 lb/ft^3 foam is used. To ensure that structural performance will not vary over time, the foam is not bonded to the shell structure. The foam serves the dual purpose of limiting impact loads from drop and puncture events, and providing thermal insulation during the HAC fire event. Thermal melt out plugs are provided to vent gas that may be produced by the foam during the HAC fire. Drain tubes, which pass through the impact

limiter, are provided to conduct any condensate from the OCV surface to a collection pan located beneath the package.

2.1.1.4 Manufacturing. Standard methods are used to fabricate these components, in accordance with NUREGs CR-3019[7] and CR-3854[8]. All heads are standard ASME torispherical head designs. All vessel bell joints and transitions in thickness, such as from the 0.75-in.-thick ICV wall to the 0.38-in.-thick ICV head, are in accordance with the ASME B&PV Code. All circumferential and longitudinal welds used in the ICV and OCV containment boundary bells are full penetration and radiograph inspected. Certain containment boundary welds, such as those associated with vent port and electrical feed-through penetrations that see little structural loading, are inspected by liquid penetrant, as allowed by NuReg CR-3019. All structurally significant noncontainment welds are liquid penetrant inspected.

Polyurethane foam installation techniques used for the impact limiter are the same as those employed in many other radioactive shipping packagings. These foam installation techniques are discussed in Sections 2.3 and 8.1.4.1.

2.1.2 Design Criteria

The package meets regulatory requirements by a combination of analysis and test. The acceptance criteria for analytic assessments is in accordance with Regulatory Guide 7.6 as supplemented by Section III of the ASME B&PV Code. Load combinations are in accordance with Regulatory Guide 7.8[9]. Full-scale prototypical hardware is also tested by subjecting it to several free drop and puncture orientations. The following post-test acceptance criteria is used:

- A demonstration of leaktight containment boundaries (less than 1×10^{-7} scc/sec leakage rate, air, per ANSI N14.5[6])
- A demonstration that seal area geometry still provides adequate compression on a minimum diameter O-ring seal for all worst-case HAC scenarios, including a subsequent fire.

Package deformations resulting from structural testing must be such that deformed geometry assumptions used in shielding, criticality, and thermal analyses are not invalidated. Furthermore, the shipping rack assembly must remain attached to the ICV base and the impact limiter must remain attached to the OCV. For the NCT 4-ft free drop case, the acceptance criteria selected for the package is that the ability of the package to adequately survive a subsequent HAC sequence (i.e., maintain two leaktight containment boundaries) is not compromised.

2.1.2.1 Allowable Stresses. Mechanical properties of the materials of construction, such as yield strength, S_y, ultimate strength, S_u, and allowable strength, S_m, are listed in Tables 2.3-1 and 2.3-2. All analytical assessments made herein use these properties and the allowable stresses listed below in Table 2.1.2-1.

TABLE 2.1.2-1. Allowable Stress Limits.

Stress category	NCT	HAC
General Primary Membrane Stress Intensity	S_m	Lesser of $2.4S_m$ or $0.7S_u$
Local Primary Membrane Stress Intensity	$1.5S_m$	Lesser of $3.6S_m$ or S_u
Primary Membrane + Bending Stress Intensity	$1.5S_m$	Lesser of $3.6S_m$ or S_u
Range of Primary + Secondary Stress Intensity	$3.0S_m$	Not applicable
Pure Shear Stress	$0.6S_m$	$0.42S_u$
Fastener Membrane Stress	Lesser of $2.0S_m$ or S_y	Lesser of S_y or $0.7S_u$
Fastener Membrane + Bending Stress	Lesser of $3.0S_m$ or S_y	S_y[a]
Bearing Stress	S_y	S_y for seal surfaces, S_u elsewhere
Peak	Per Section 2.1.2.2.2	

[a]Stress limits on the containment fasteners are predicated by containment criteria delineated in Section 4.0, *Containment*, i.e., no yielding allowed for closure bolts used with face seals.

2.1.2.1.1 Lifting. A minimum safety factor of three against yield, consistent with 10 CFR 71.45(a) must be present on any lifting attachment that is a structural part of the package.

2.1.2.1.2 Tiedowns. Under the simultaneous action of the $10g$ longitudinal, $5g$ lateral, and $2g$ vertical body forces, the stresses in the package must not exceed material yield strengths, consistent with 10 CFR 71.45(b). Although this section does not apply to the RTG Transportation System Package, which has no integral tiedown devices as part of the licensed package, tiedown evaluations are conservatively included which consider tiedown interface loads with the package.

2.1.2.1.3 Normal Conditions of Transport and Hypothetical Accident Conditions. Regulatory Guide 7.6 is used in the assessment of the package components for both the NCT and the HAC. A tabulated summary of allowable stresses used for package structures is presented in Table 2.1.2-1. These data are consistent with Regulatory Guide 7.6 and Section NB-3000 and Appendix F of the ASME B&PV Code, Section III.

2.1.2.1.4 Buckling. Using of Regulatory Guide 7.6 design criteria is dependent on linearly elastic structural response. Nonlinear phenomena such as buckling would preclude using Regulatory Guide 7.6 as a basis for evaluating containment structure integrity as determined by theoretical analysis. Buckling assessments are required only under the following conditions:

- Structural evaluation is by theoretical analysis, using Regulatory Guide 7.6 as the design basis
- Applied loadings could potentially produce buckling.

For the RTG Transportation System Package, there are only three structural assessments for

which a buckling analysis would be relevant. The valid load cases are Sections 2.6.4, 2.6.9, and 2.7.5.

To assess the potential for buckling in these load cases, the relevant geometric components of the package containment structure will be evaluated separately. There are two containment boundaries in the package where buckling analysis is appropriate. Those are the bell assemblies of both the ICV and the OCV. Each assembly comprises a cylindrical shell topped with a torispherically dished head.

For the torispherical heads, ASME B&PV Code, Section III, Subsection NE will be applied. For the cylindrical shells, the methodology of ASME B&PV Code Case N-284[10] will be applied.

The four basic steps involved in the application of ASME B&PV Code Case N-284 are summarized below.

1. Theoretical Elastic buckling stresses are determined for hoop and axial compression and in-plane shear loadings using classical theory.

2. Capacity reduction factors are applied that account for the difference between classical theory and predicted instability stresses for fabricated shells.

3. Plasticity reduction factors are applied for those cases where elastically determined buckling stresses are above the proportional limit.

4. Elastic and inelastic buckling checks that employ an appropriate factor of safety and applicable interaction equations are made using worst case applied compressive and in-plane shear stresses.

Consistent with Regulatory Guide 7.6 philosophy, factors of safety corresponding to ASME B&PV Code Level A and D Service conditions are employed for NCT (Section 2.6) and HAC (Section 2.7) loadings, respectively. The applicable factors of safety are 2.0 for NCT and 1.34 for HAC, as specified in ASME B&PV Code Case N-284.

2.1.2.2 Miscellaneous Structural Failure Modes. This subsection addresses the potential structural failure modes of brittle fracture and fatigue. Bolted joint designs are also shown to develop the full strength of the bolt before tearout from the base material.

2.1.2.2.1 Brittle Fracture. All packaging structural components are made from ductile materials. All containment boundary vessels are made from AISI Type 304L stainless steel; the impact limiter shell is made from AISI Type 304 stainless steel. Because Type 304/304L stainless steel does not undergo a ductile-to-brittle transition in the temperature range of interest (down to -40 °F), brittle fracture is precluded. The materials used for bolts in the package (ASTM-A320, Grade 43 for the OCV closure and shipping rack attachment, ASTM-A540, Grade B23 Class 1 for the ICV closure and ASTM B637 Alloy N07750, Type 3 for the impact limiter attachment) are expressly designed for cold-temperature service. Section 5 of NuReg/CR-1815[11] states, *"Bolts are generally not considered as fracture-critical components because multiple load paths exist and because bolted systems are designed to be redundant. In other words, failure of one or more bolts can be tolerated since failure normally does not lead to penetration or rupture of the container."* The nominal factor of safety on the closure bolts is large and will be discussed later. Thus, brittle fracture of packaging components is of no concern.

2.1.2.2.2 Fatigue.

2.1.2.2.2.1 Normal Operating Cycles. Normal operating cycles do not present a fatigue concern for package components. This is because none of the components exhibit significant stress concentrations, and by satisfying the allowable limit for range of primary plus secondary stress intensity for NCT ($3.0S_m$), the allowable fatigue stress limit for the expected number of operating cycles will automatically be satisfied.

The maximum number of operating cycles is conservatively estimated to be 1,000 over a package life span of 20 years, or one complete load/unload cycle about every 7 days. A cycle is defined as the loading of the highest heat payload, arriving at thermal and pressure equilibrium, and unloading, thereby returning to ambient pressure and temperature, without active cooling. In practice, this would never be allowed, because without active cooling the payload would be damaged and would result in a significant economic loss.

From the ASME B&PV Code, Section III, Appendix I, Figure I-9.2.1 (included as Figure 2.1.2-1), and Table I-9.1 of the Code, the fatigue allowable alternating stress intensity amplitude, S_a, for 1,000 cycles is 119,000 psi. When corrected for the ratio of elastic moduli (essentially a temperature correction), the fatigue allowable for the warmest part of the package (conservatively, 350 °F, for the ICV head per Table 2.10.7.1-2 of the temperature summary of Appendix 2.10.7 becomes:

$$S_a = 119{,}000 \left[\frac{26.8(10)^6}{28.3(10)^6}\right] = 112{,}700\ psi$$

The nonfatigue allowable stress intensity range, from the ASME B&PV Code, Section III, Division 1, Subsection NB-3222.2, however, is $3.0S_m$. Interpolating values of S_m from Table 2.3-1 for the temperature of 350 °F above, the resulting allowable stress intensity range is $3.0S_m$ = 48,750 psi. The maximum allowable alternating stress intensity is one-half of this range, or 24,375 psi. Thus, because of the absence of significant stress concentrations, the fatigue allowable alternating stress intensity will not govern the package design.

2.1.2.2.2.2 Normal Vibration Over the Road. Fatigue concerns associated with normal vibration over the road are addressed in Section 2.6.5.

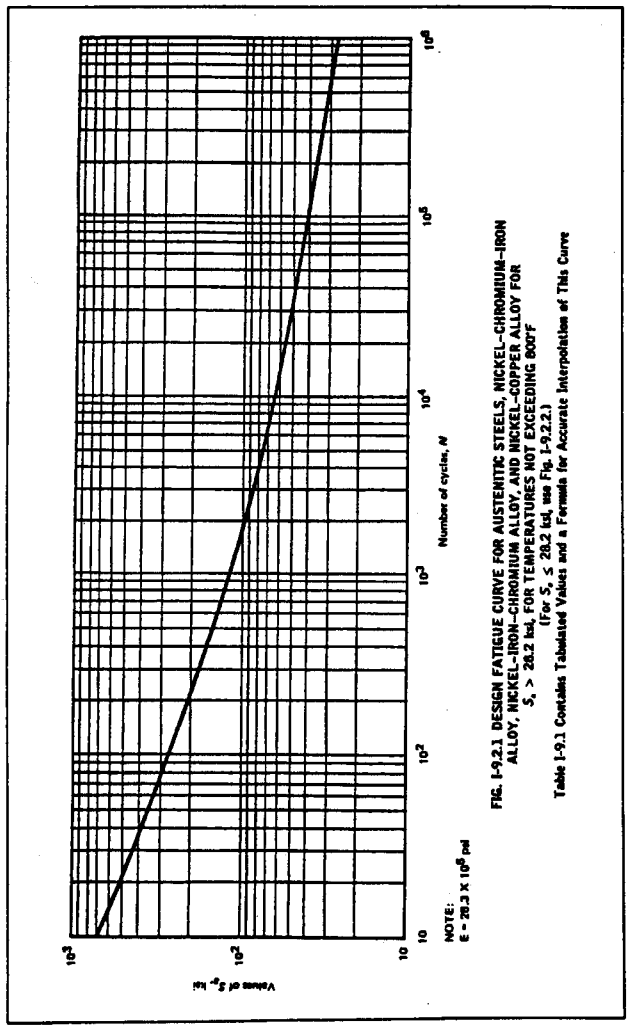


FIGURE 2.1.2-1. ASME B&PV Code, Section III, Appendix I, Figure 1.9.2.1.

2.1.2.2.2.3 Bolt Tearout from Base Material. The bolting materials (ASTM A320 L43 and ASTM A540 Gr B23, Class 1 alloy steel and ASTM B637, Alloy NO7750 Type 3) are inherently stronger than the material into which they thread (ASTM Type 304 or 304L). However, the full strength of the bolt is developed by the engaged length of thread and/or use of replaceable threaded inserts. According to Table 2.1.2-1, the highest allowable stress limit on containment closure bolts is the yield point, S_y. It is also shown that the full tensile yield strength of the ICV and OCV closure bolts is developed by the shear yield strength of the bolt, insert, and base material threads.

Calculations for the shipping rack assembly attachment bolts will be shown as an example. The bolts are 3/4-10 UNC-3A, but class 2A will be conservatively assumed for both internal and external threads. The bolts are 6 in. long, and the shipping rack assembly height is 5.25 in. Therefore, the engaged thread length is 0.75 in. From the article *Strength of Threads* by Raymond Boucher[18], the corresponding ICV base hole threads will have a shear area of 1.7225 in.^{2} per in. of engagement. For a 0.75-in. engagement, the area is 1.2919 in.^{2}. For Type 304L, the base material shear strength will be 60% of the tensile strength, or 0.6 x 70,000 = 42,000 psi. The shear-out load for the threads will be as follows:

$$S \times A = 54{,}260 \ lb$$

Where: S = 42,000 psi
A = 1.2919 in.^{2}

The tensile stress area of the bolt is 0.330 in.^{2}. The tensile strength of the A320 L43 bolting material is 125,000 psi, and the tensile failure load of the bolt is given below.

$$F \times A = 41{,}250 \ lb$$

where: F = 125,000 psi
A = 0.330 in.^{2}

Thus, the bolt ultimate failure load is less than the thread strip-out load, and the full strength of the bolt is therefore developed. Table 2.1.2.2.2.3-1 summarizes the results for the bolts that are important to containment. Closure bolt yield checks utilize the same approach as above, but are based on the tensile yield strength of the particular bolt material. In addition, since the minimum tensile strength of the thread inserts is 160,000 psi, which is essentially at (for ICV) or above (for OCV) the closure bolt material strength, shear-out is governed by bolt strength. Consequently, shear-out calculations for the ICV and OCV closure bolts use bolt external thread shear area and shear strength rather than insert internal thread shear area and shear strength.

The inserts for the ICV and OCV are firmly mounted against a shoulder in the base. The insert outer thread pitch diameters (1-5/8-12 UN for the OCV and 1-1/8-12 UNF for the ICV) are considerably larger than the bolt clearance holes in the base material above the insert, and thus, a margin against strip-out is ensured on the insert external threads. For purposes of determining shear-out force for the impact limiter bolts, the threaded inserts are conservatively ignored.

TABLE 2.1.2.2.2.3-1. Comparison of Bolt Tensile Strength and Pull-out Forces.

Bolt identification	Bolt size & material	Thread shear area per in.	Engaged length (in.)	Bolt tensile failure force (lb)	Thread shear-out force (lb)
Barrier plate attachment (ultimate)	3/4-10 x 6 A320, L43	1.7225[a]	0.75	41,250	54,259
Impact limiter attachment (ultimate)	1-8 x 8.0 B637, Alloy NO7750 Type 3	2.3256[a]	1.47	81,430[c]	143,580
ICV closure (ultimate)	3/4-10 x 2.0 A540, Gr B23 Class 1	1.217[b]	1.02	54,450	122,893
ICV closure (yield)	3/4-10 x 2.0 A540, Gr B23 Class 1	1.217[b]	1.02	49,500	111,721
OCV closure (ultimate)	1¼-7 x 6 A320, L43	2.1098[b]	1.52	119,050	240,517
OCV closure (yield)	1¼-7 x 6 A320, L43	2.1098[b]	1.52	100,002	202,034

[a]Hole internal thread.
[b]Bolt external thread.
[c]Based on 0.805 in. diameter and 160.000 psi minimum ultimate strength for the bolt.

The 1/4-20 UNC bolts that attach the ICV and OCV base plates together and the 3/4-10 UNC bolts that attach the payload to the ICV base are not required to survive a HAC drop. Because the bolt is seen to be the limiting component in all bolted joints, no further reference is made to engaged thread capacity in the Safety Analysis Report for Packaging (SARP).

To ensure full seating between the ICV and OCV closure bolts and threads, a one-time torque value which is in excess of the value specified for normal use will be applied to the bolted joint during the manufacturing process. This will reduce the possibility of closure bolt torque loss in HAC drop and puncture events. For the ICV, this value is 300 ft-lb, and for the OCV, 1,500 ft-lb. The formula governing the relationship between bolt torque and tensile force is introduced in Section 2.6.1.2.1.

2.2 WEIGHTS AND CENTER OF GRAVITY

The weight of the empty package is 8,850 pounds. The maximum weight of the payload, including the shipping rack assembly, is 750 pounds, which includes a margin for possible future increases in payload weight. The component breakdown is given in Table 2.2-1. The reference for center of gravity is the bottom surface of the impact limiter.

TABLE 2.2-1. RTG Transportation System Package Component Weights.

Component	Weight (lb)	CG (in.)
Inner containment vessel bell	1,550	40.8
Inner containment vessel base	1,100	12.1
Outer containment vessel bell (with cooling water)	2,700	37.9
Outer containment vessel base	1,850	10.9
Impact limiter	1,650	7.8
Maximum payload and shipping rack	750	40.0
Maximum payload	525	49.0
Maximum shipping rack	225	19.0

The total weight and center of gravity location used for calculations is 9,600 pounds and 25.2 in. above the bottom surface of the impact limiter. The radial center of gravity is on the package centerline, because of symmetry.

2.3 MECHANICAL PROPERTIES OF MATERIALS

The structural materials used in the package are as follows:

- AISI Type 304L austenitic stainless steel (OCV, ICV containment boundaries)
- AISI Type 304 austenitic stainless steel (impact limiter shell, payload shipping rack assembly)
- ASTM-A320, Grade L43, bolts (heat treated alloy steel), cadmium plated
- ASTM-A540, Grade B23, Class 1 bolts (heat-treated alloy steel), cadmium plated (ICV bolts)
- ASTM-B16 brass (vent and test port plugs)
- D. G. O'Brien electrical feed-through receptacle, 107 Series, part No. 1070019-112 (ICV and OCV electrical feed-through)
- ASTM A479 Type 316L electrical feed-through sleeve
- AISI 4130 hardened thread insert (OCV and ICV), cadmium plated
- ASTM B637, Alloy N07750 Type 3 impact limiter attachment bolts

- AMS7245 stainless steel Heli-coil®** threaded inserts (for impact limiter attachment bolts).

Other nonstructural materials used are as follows:

- 3 lb/ft³ and 12 lb/ft³ polyurethane foam (General Plastics 3700 series)
- Fiberglass insulation in the thermal shield
- Ceramic fiber insulation in the shipping rack assemblies
- Du Pont Vespel®*** (OCV bell alignment pads)
- Butyl O-rings for ICV and OCV containment seals
- Teflon® gaskets (OCV vent and test port plug covers)
- Austenitic stainless steel (coolant jacket pressure relief valves)
- Nitronic 50 or 60 alignment pins (nitrided austenitic stainless steel)
- ABS plastic (impact limiter pressure relief plugs)
- Miscellaneous steel fasteners.

Nonstructural materials associated with the instrumentation feed-through are as follows (see Figure 2.3-1):

- Plug, D. G. O'Brien 107 Series, part No. 1071003-119
- Connector, Deutsch part No. DB050-14-18PX-059
- Polythermide resin, G. E. Plastics Ultem-1000®
- Electrical cable, Belden part No. 85164, including Du Pont Tefzel®**** insulation
- Conductor wire, MIL-W-22759/32, Alpha Wire Corporation
- Rubber gasket, ASTM D2000-75E-Type BC
- Contact pins, ASTM B301, nickel and gold plated
- Contact probe and spring, Interconnect Devices part Nos. R5CR and S5H18.7G
- Electrical feed-through cable, flexible standard nickel-coated copper conductor with an

---

**_Heli-coil_ is a registered trademark of Emhart Fastening Technologies.

***_Vespel_ is a registered trademark of the E.I. dePont de Nemours Company.

****_Tefzel_ is a registered trademark of the E.I. duPont de Nemours Company.

inorganic insulation of mica and glass fiber.

The Packaging General Arrangement Drawings presented in Appendix 1.3.2 identify these materials and their use. The schematic shown in Figure 2.3-1 identifies the locations of the electrical feed-through components.

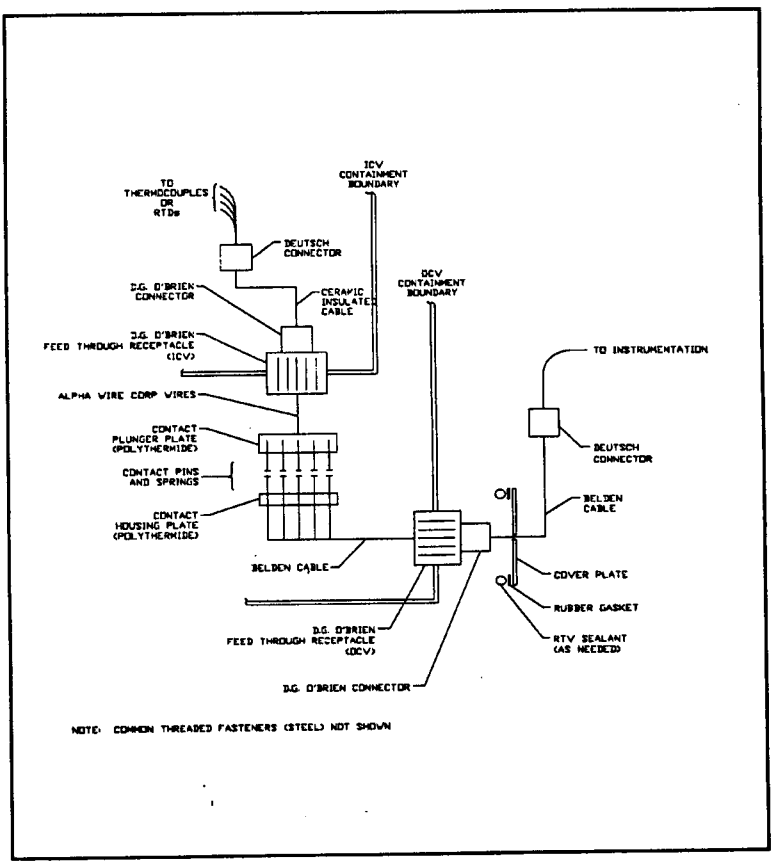


FIGURE 2.3-1. Electrical Feed-through Materials Schematic.

The following tables present the properties of the structural materials used in the package.

The following tables present the properties of the structural materials used in the package. Material properties are linearly interpolated or extrapolated from these values as necessary. For the analysis of the impact limiter shell in Section 2.5.2, material properties for Type 304L are conservatively used in place of properties of Type 304 stainless steel. No properties are given for the materials used for the brass vent and test port plugs or for the electrical feed-through assemblies, since these components are not structurally analyzed. They see only negligible loads, even in the HAC drop and puncture events.

TABLE 2.3-1. Mechanical Properties of AISI Type 304L Stainless Steel.

Steel material specification	Temperature (°F)	Yield[a] strength S_y (ksi)	Ultimate[b] strength S_u (ksi)	Allowable[c] strength S_m (ksi)	Elastic[d] modulus (10^6 psi)	Coefficient[e] of thermal expansion (10^{-6} in/in/°F)
AISI Type 304L (ASTM A240) (ASTM A479) (ASTM A269) (ASTM A312) (ASTM A276)	70	--	--	--	28.3	8.46
	100	25.0	70.0	16.7	--	8.55
	200	21.3	66.2	16.7	27.6	8.79
	300	19.1	60.9	16.7	27.0	9.00
	400	17.5	58.5	15.8	26.5	9.19
	500	16.3	57.8	14.8	25.8	9.37
	600	15.5	57.0	14.0	25.3	9.53
	700	14.9	56.2	13.5	24.8	9.69
	800	14.4	55.5	13.0	24.1	9.82
	900	13.9	53.9	--	23.5	--
	1000	13.3	50.8	--	--	10.3
	1100	12.5	46.9	--	22.1	--
	1200	--	--	--	--	10.4
	1300	10.1	31.4	--	20.5	--

[a]Properties for temperatures through 1000 °F are taken from the ASME B&PV Code, Section II, Part D, Table Y-1; for higher temperatures, values from Ref. 26 are used, reduced by 2,500 psi to provide a smooth transition from the ASME data for lower temperatures.

[b]Properties for temperatures through 1000 °F are taken from the ASME B&PV Code, Section II, Part D, Table U; for higher temperatures, values from Ref. 24 are used.

[c]Properties for temperatures through 800 °F are taken from the ASME B&PV Code, Section II, Part D, Table 2A.

[d]Properties for temperatures through 900 °F are taken from the ASME B&PV Code, Section II, Part D, Table TM-1, Material Group G; for higher temperatures, values from Ref. 26 are used.

[e]Properties for temperatures through 800 °F are taken from the ASME B&PV Code, Section II, Part D, Table TE-1; for higher temperatures, values from Ref. 26 are used. The value shown is mean from 70 °F.

Notes: (1) Values given for S_y, S_u, and S_m at 100 °F apply from -20 to 100 °F.
(2) Stainless Steel Density is 0.29 lb/in^3.
(3) Poisson's Ratio is 0.3.
(4) ASTM A351 CF3 casting material may be used for the containment boundaries as an alternate material because minimum ultimate, yield, and allowable strengths equal or slightly exceed the tabulated values.

TABLE 2.3-2. Mechanical Properties of ASTM-A320, Grade L43, Bolting Material.

Bolting material specification	Temperature (°F)	Yield[a] strength S_y (ksi)	Ultimate[b] strength S_u (ksi)	Allowable[c] strength S_m (ksi)	Elastic[d] modulus (10^6 psi)	Coefficient[e] of thermal expansion (10^{-6}in/in/°F)
ASTM-A320 Grade L43	70	--	--	--	27.8	6.20
	100	105.0	125.0	35.0	--	6.27
	200	99.0	--	33.0	27.1	6.54
	300	95.7	--	31.9	26.7	6.78
	400	91.8	--	30.6	26.1	6.98
	500	88.5	--	29.5	25.7	7.16

[a]ASME B&PV Code, Section II, Part D, Table Y-1.
[b]ASME B&PV Code, Section II, Part D, Table Y-1.
[c]ASME B&PV Code, Section II, Part D, Table 4.
[d]ASME B&PV Code, Section II, Part D, Table TM-1, Material Group B.
[e]ASME B&PV Code, Section II, Part D, Table TE-1, Material Group E. The value shown is mean from 70 °F.

TABLE 2.3-3. Mechanical Properties of ASTM-A540, Grade B23, Class 1, Bolting Material.

Bolting material specification	Temperature (°F)	Yield[a] strength S_y (ksi)	Ultimate[b] strength S_u (ksi)	Allowable[c] strength S_m (ksi)	Elastic[d] modulus (10^6 psi)	Coefficient[e] of thermal expansion (10^{-6}in/in/°F)
ASTM-A540 Grade B23 Class 1	70	--	--	--	27.8	6.20
	100	150.0	165.0	50.0	--	6.27
	200	140.1	--	47.8	27.1	6.54
	300	135.3	--	46.2	26.7	6.78
	400	131.7	--	44.8	26.1	6.98
	500	127.7	--	43.4	25.7	7.16

[a]ASME B&PV Code, Section II, Part D, Table Y-1.
[b]ASME B&PV Code, Section II, Part D, Table Y-1.
[c]ASME B&PV Code, Section II, Part D, Table 4.
[d]ASME B&PV Code, Section II, Part D, Table TM-1, Material Group B.
[e]ASME B&PV Code, Section II, Part D, Table TE-1, Material Group E. The value shown is mean from 70 °F.

The energy-absorbing foam used in the removable impact limiter is a closed-cell polyurethane foam. The nominal densities used are 3 lb/ft^3 for foam located directly beneath the OCV base plate, and 12 lb/ft^3 in the remainder of the impact limiter. This type of material has been used extensively and successfully in transportation packages for a number of years. Examples are Nuclear Packaging's 125-B[13] (NRC Docket 71-9200), 10-142[14] (NRC Docket 71-9208), PAS-1[15] (NRC Docket 71-9184), TRUPACT-II[4] (NRC Docket 71-9218), as well as Chem Nuclear System's 1-13C II[16] (NRC Docket 71-9152).

The polyurethane foam's energy-absorbing characteristics have been amply demonstrated via comprehensive testing programs. Compression testing over a wide range of densities (3 to 25 lb/ft^3) and temperatures (-20 to 300 °F) has been performed. Additionally, the intumescent properties have been verified by fire testing of appropriately encapsulated foam samples[3] (General Plastics Last-A-Foam******).

Detailed stress-strain relationships for the polyurethane foam are not required for analysis, because analytic assessments are not performed for the NCT and HAC free drop or HAC puncture events. However, because package performance is demonstrated by testing, and performance is a function of foam properties, stress-strain characteristics and installation techniques for the foam are carefully controlled. Foam installation consists of the following two steps:

1. The 3 lb/ft^3 nominal density foam is pre-cast as a solid slab and is then placed into the impact limiter.

2. The 12 lb/ft^3 nominal density foam is poured into the impact limiter as a liquid, which then solidifies to fill all voids in the impact limiter not already filled by the 3 lb/ft^3 foam.

The polyurethane foam stress-strain relationships are carefully controlled, regardless of whether the foam is pre-fabricated or poured in situ. For both foams, the direction of rise on curing is controlled to be parallel to the axis of the package. At the time the foam is originally poured, samples are retained and tested to certify foam compressive strength, and stress-strain plots are developed from the test results.

Table 2.3-4 provides the strength data used to judge acceptance of the tested foam samples. Nominally expected compressive strengths for the 3 and 12 lb/ft^3 foams in both parallel and perpendicular to rise directions are presented. The 3 lb/ft^3 foam plays only a minor role in packaging response, and its acceptance is controlled based on room temperature (72 to 78°F) strengths. Recognizing the more significant role played by the 12 lb/ft^3 foam and the strong dependence of polyurethane foam strength on temperature (strength significantly increases with decreasing temperature), acceptance of 12 lb/ft^3 foam is based on strength at worst case temperature extremes. Thus, retained sample testing for 12 lb/ft^3 foam is performed at both cold (-20 to -25 °F) and hot (160 to 165 °F) conditions.

To be acceptable, measured strength for individual samples of 3 lb/ft^3 foam must fall within 15% of the nominal strengths in Table 2.3-4. When averaged, the strength for all samples of 3 lb/ft^3 foam must fall within 10% of tabulated nominals. For the 12 lb/ft^3 foam, acceptance at cold temperatures is based on measured strengths for individual samples being no more than 15% greater than tabulated nominals. The average cold strength for all samples of 12 lb/ft^3 foam must be no more than 10% above nominals. At hot conditions, measured strengths for individual samples of 12 lb/ft^3 foam must be at least 85% of tabulated nominals. The average hot strength for all 12 lb/ft^3 samples must be at least 90% of nominals.

******Last-A-Foam is a registered trademark of the General Plastics Company.

TABLE 2.3-4. Nominal Compressive Strengths of Polyurethane Foam.

	Direction of rise	Parallel			Perpendicular		
	Nominal foam density	3 lb/ft^3	12 lb/ft^3		3 lb/ft^3	12 lb/ft^3	
	Test Temperature	72 to 78 °F	-20 to -25 °F	160 to 165 °F	72 to 78 °F	-20 to -25 °F	160 to 165 °F
Strain	10 %	59	635	327	54	606	331
	40 %	62	803	425	51	785	427
	70 %	97	2,577	1,171	88	2,694	1,260

Figure 2.3-2 graphically presents a comparison of the foam strength used in the Structural Certification Test Article impact limiter (15-1/2 lb/ft^3, perpendicular to rise, 75 °F foam) with the acceptance controls placed on corresponding production limiter foam (12 lb/ft^3, perpendicular to rise, -20 and 160 °F foam). The strength of the foam used in the structures testing was at or above that which would exist in a production unit limiter at cold conditions. Thus, impact accelerations experienced during structures testing clearly envelope those that could ever occur for a production unit. The other temperature extreme is handled by extrapolation and is detailed In Section 2.7.3.1.1.1. For hot conditions, foam strength is assumed to be the average hot strength shown in Figure 2.3-2.

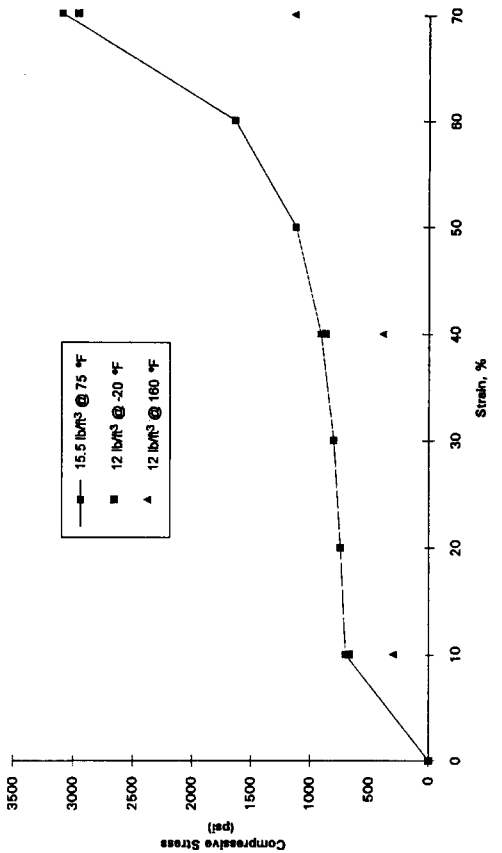


FIGURE 2.3-2. Comparison of Average Foam Strength Properties.

2.4 GENERAL STANDARDS FOR ALL PACKAGES

This section demonstrates that the general standards for all packages are met.

2.4.1 Minimum Package Size

The minimum dimension of the package is 39.4 in. over the OCV coolant jacket outer diameter. Thus, the requirement of 10 CFR 71.43(a) is satisfied.

2.4.2 Tamper-Indicating Feature

A tamper-indicating device is included in the form of a lockwire across one impact limiter attachment bolt tube. Breakage or detachment of this wire will provide evidence of possible unauthorized access to the package because all impact limiter attachment bolts must be removed to gain access to either the OCV cavity or vent port plug.

2.4.3 Positive Closure

The package cannot be opened unintentionally. The OCV bell is attached by 24, 1 1/4-in. closure bolts, and the ICV by 24, 3/4-in. closure bolts. Complete removal of all bolts from a given vessel is necessary before a bell may be removed. Notably, removal of all eight 1.0-in. impact limiter attachment bolts is also required before removal of the OCV bell.

2.4.4 Chemical and Galvanic Reactions

The materials of construction used in the packaging will not have significant reactions with the payload, air, or water. Essentially all of these materials have been used previously in radioactive material packaging without incident.

The payloads are thermoelectric generators using radioisotope fuel in oxide form. These devices are designed to perform many years in space or in terrestrial missions, and contain no liquids and only inert gas. The materials of construction are common structural materials. Thus, no corrosive agents exist in the payloads. Further, these payloads present no source of volatiles that could affect the butyl rubber O-ring containment seals. Therefore, no reaction between the payload and any part of the packaging will occur.

Both packaging containment boundaries are constructed exclusively of AISI Type 304L stainless steel, which is highly corrosion resistant to most environments. The weld material and processes have been selected per the ASME B&PV Code to provide as good or better material properties as the base material, including corrosion resistance. The base material and weld material have about the same electrochemical potential, minimizing any galvanic corrosion that could occur. This material is also not subject to corrosion from the glycol/water coolant mixture used in the OCV coolant jacket. Noncontainment structures such as the shipping rack assemblies and the impact limiter shell are made from AISI Type 304 stainless steels.

The polyurethane foam that is used in the impact limiter has the same chemical makeup relative to corrosion as that which has been successfully used in a number of transportation packages, such as the NuPac 125-B[13] and the CNSI 1-13C II[16]. These and other packagings using this foam have had a long and successful record of performance, demonstrating that the foam does

not cause any adverse conditions on the packaging. The polyurethane foam is a closed cell foam that is low in free halogens. The foam material is sealed with plastic pipe caps inside a dry cavity in the impact limiter. For these reasons, no significant corrosion will occur because of the polyurethane foam.

Brass fittings used in the packaging are corrosion resistant. Brass material is slightly anodic to the stainless steel. Any damage that could occur to the brass is easily detectable because the fittings are all removed and handled each time the packaging is loaded or unloaded.

All threaded fasteners used in the packaging are made from cadmium-plated alloy steel except the impact limiter attachment bolts, which are made of Inconel. The compatibility of cadmium, Inconel and austenitic stainless steels in transport of nuclear materials has been clearly established in previous designs, such as the NuPac 125-B Cask.

Aluminum is used only for the payload and is not a material of packaging construction. Aluminum is only present within the ICV in an atmosphere of dry helium, thus, no possibility of corrosion involving aluminum exists.

2.5 LIFTING AND TIEDOWN STANDARDS FOR ALL PACKAGES

2.5.1 Lifting Devices

The following two types of lifting devices are used on the RTG Transportation System Package:

1. A standard lifting eye, bolted to the top of the ICV, for lifting the ICV bell only. The lifting eye is removed during transport.

2. Three fins provided with holes, on the top of the OCV, for lifting either the OCV bell or the entire licensed package, including the payload. Nonlicensed hardware, such as support skids, will not be lifted with the package.

2.5.1.1 Inner Containment Vessel Bell Lifting

2.5.1.1.1 Lifting Forces. The weight of the ICV bell is 1,550 pounds, but for conservatism, a value of 1,600 pounds will be used in the analysis. The ICV bell lift point is labeled "Lid Lift Only," to preclude lifting anything but the bell.

2.5.1.1.2 Stress Calculations. To determine the lifting adequacy of the ICV bell, four modes of failure will be examined: (1) Torispherical Head Material Yield, (2) Lift Block Weld Shear, (3) Lifting Eye Thread Strip-out, and (4) Lifting Eye Failure.

To ensure that any possible lifting overload does not damage the containment boundary (per 10 CFR 71.45[a]), the design is such that the minimum margin of safety occurs for the lifting eye mounting hole thread strip-out. That is, if the lifting system is overloaded, the lifting eye mounting hole threads will fail before any other component of the package fails. The lifting eye itself will fail before the mounting hole threads, but it is not a part of the licensed package to which this requirement applies.

The temperature of the ICV head, which is applicable to all of the failure modes above, is 338 °F from Appendix 2.10.7, Table 2.10.7.1-2 (thermal node 200). However, a value of 350 °F

will be conservatively used. From Table 2.3-1, S_y = 18,300 psi and S_u = 59,700 psi.

(1) Torispherical Head Material Yield

To determine the stresses in the ICV head, a simple finite element model was used. The model is a two dimensional (2-D) representation of the entire ICV, including base, and is described in Appendix 2.10.2. For the present application, the base elements were excluded, and the lower flange of the bell was restrained. The lifting load of 1,600 pounds was applied upward at the center of the top of the ICV bell. The maximum resultant stress intensity (including bending) was 1,906 psi at the junction between the shell and lifting block, element 153. The margin of safety given below.

$$M.S. = \frac{18{,}300}{3(1{,}906)} - 1 = +2.20$$

To determine the applied load at which the head fails, assume a failure defined as the primary local membrane stress intensity P_L(without bending) exceeding the ultimate strength in tension. For the given loading of 1,600 pounds, the maximum primary local membrane stress intensity is 709 psi, likewise in element 153. The ratio is given below.

$$\frac{FailureLoad}{59{,}700\ psi} = \frac{1{,}600 lb}{709\ psi} \rightarrow FailureLoad = 134{,}725\ lb$$

(2) Lift Block Weld Shear

The ICV lift block has an outside diameter of 6 in., the ICV wall is 0.375 in. thick, and the weld is full penetration. The shear area is $(6.0)(0.375)\pi$ = 7.07 in.^{2}. Assuming full weld properties, the weld shear strengths are as follows:

Shear yield = (0.6)(18,300) = 10,980 psi
Shear ultimate = (0.6)(59,700) = 35,820 psi

The shear stress in the weld is:

$$\frac{1{,}600}{7.07} = 226\ psi$$

The margin of safety is:

$$M.S. = \frac{10{,}980}{3(226)} - 1 = +Large$$

The failure load is the ultimate shear strength times the area, or (7.07)(35,820) = 253,247 pounds.

(3) Lifting Eye Thread Strip-out

The lifting eye will use a 3/4-10UNC-2A thread, with a 1-in. engagement. From the article *Strength of Threads* by Raymond Boucher, the corresponding bolt hole will have a shear area of 1.7225 in.^{2} per in. of engagement. The shear stress in the threads will be:

$$\frac{1,600}{1.7225} = 929 \; psi$$

the margin of safety, using the same shear yield of 10,980 psi is:

$$M.S. = \frac{10,980}{3(929)} - 1 = +2.94$$

The failure load, using the shear ultimate strength, is (35,820)(1.7225) = 61,700 pounds.

(4) Lifting Eye Failure

Although it is not a part of the licensed package, the ICV lifting eye will be treated here because of importance in lifting. The ICV lifting eye will be a swivel eye from American Drill Bushing Co., part No. 23102, with a catalog rating of 7,000 pounds. A factor of safety of five is included in this rating, so that the ultimate failure load will be at least:

$$(5)(7,000) = 35,000 \text{ lb}$$

The margin of safety on ultimate is (using a load multiplication factor of five instead of three):

$$M.S. = \frac{35,000}{5,(1,600)} - 1 = +3.38$$

Thus, each mode of failure has a minimum safety factor in excess of three on yield (or five on ultimate in the case of the ICV lifting eye), and the first element of the licensed package to fail in the event of an overload is the screw thread of the ICV lifting block. The ICV lifting eye itself, however, will fail first before the failure of any packaging component, as shown in the table below.

TABLE 2.5.1.1.2-1. ICV Bell Lifting Failure Mode Hierarchy.

Failure mode	Ultimate failure load (lb)
Eyebolt breakage	35,000
Thread strip-out	61,700
Head failure	134,725
Weld shear	253,247

2.5.1.2 Outer Containment Vessel Lifting

2.5.1.2.1 Lifting Forces. The OCV lifting devices must lift the entire package, including the payload, ICV, OCV, and impact limiter. These components weigh a maximum of 9,600 pounds. Three evenly spaced fins are provided with 0.88-in. diameter holes for attachment of lifting hardware. The area surrounding the lifting hole is reinforced on both sides with 0.38-in.-thick plates. The fins are 0.25-in. thick and are fastened using 3/16-in. fillet welds along both sides to a 0.75-in.-wide, 0.50-in. thick doubler plate, which is in turn fastened using 3/8-in. fillet welds to the OCV head, in a region that spans the knuckle area. The doubler plate protects the OCV head (containment boundary) in the event of a lifting overload, as described in Section 2.5.1.2.2. A lifting cable angle to the horizontal of at least 60° is operationally imposed. The maximum load per cable is:

$$F_{cable} = \frac{9{,}600}{3(sin60°)} = 3{,}695\ lb$$

A value of 3,800 pounds will be conservatively used in all calculations.

2.5.1.2.2 Stress Calculations. The lifting of the OCV will consider three failure modes: (1) Torispherical Head Material Yield, (2) Lift Hole Bearing Yield, and (3) Fin Weld Shear Yield.

To ensure that any possible lifting overload does not damage the containment boundary (per 10 CFR 71.45[a]), the design is such that the minimum margin of safety occurs for the failure of the fin-to-doubler weld. That is, if the lifting system is overloaded, the stronger doubler-to-OCV head weld will remain undamaged, and the weaker fin-to-doubler weld will fail, thus protecting the containment boundary.

From Appendix 2.10.7, Table 2.10.7.1-2, the temperature of the OCV head (no active cooling) in the region of the fin weld (thermal node 304) is 237 °F. A value of 250 °F will be conservatively used. For this temperature, from Table 2.3-1 the yield strength S_y is 20,200 psi, and the ultimate strength S_u is 63,550 psi. The corresponding shear strengths are:

Shear yield = (0.6)(20,200) = 12,120 psi
Shear ultimate = (0.6)(63,550) = 38,130 psi.

From Appendix 2.10.7, Table 2.10.7.1-2, the temperature of the fin near the lifting hole (thermal node 305) is 158 °F. A value of 175 °F will be conservatively used. For this

temperature, from Table 2.3-1 the yield strength S_y is 22,225 psi and the ultimate strength S_u is 67,150 psi.

(1) Torispherical Head Material Yield

The stresses in the OCV torispherical head due to lifting with the lift fins were examined using a finite element model. The model is described in Appendix 2.10.3. Because three lift fins are used, a 1/3 symmetry portion of the OCV bell was modeled, with the lift fin located in the center of the segment. To simplify the model, the doubler plate was not included. Instead, the fin was modeled as directly attached to the OCV head. The action of the doubler plate is to distribute fin lifting loads over a slightly larger area of the OCV head, and thus, to omit the doubler conservatively increased OCV head stress. A lifting cable unit force of 1 pound was applied to the fin at an angle of 60° to the horizontal in the plane of the fin. The resulting maximum stress intensity (including bending) is 1.472 psi per pound of load, or for the maximum lifting cable load of 3,800 pounds, the maximum stress is (1.472)(3,800) = 5,994 psi. For a yield strength of 20,200 psi, the margin of safety is:

$$M.S. = \frac{20{,}200}{3(5{,}994)} - 1 = +0.12$$

To determine the applied load at which the head fails, assume a failure defined as the primary local membrane stress intensity P_L (without bending) exceeding the ultimate strength in tension. From the model, the maximum primary local membrane stress is 0.434 psi per pound of load, or 1,649 psi for the 3,800-pound maximum cable load. Therefore, the ratio:

$$\frac{Failure\ Load}{63{,}550\ psi} = \frac{3{,}800\ lb}{1{,}649\ psi} \rightarrow Failure\ Load = 146{,}446\ lb$$

(2) Lift Hole Bearing Yield

The lifting cable will be attached to the lift fins by means of a shackle (or equivalent) that passes through a 0.88-in. diameter hole in each lift fin. The pin that passes through the hole will be at least 0.75 in. in diameter. Because of the 0.38-in.-thick reinforcements on each side of the 0.25-in.-thick fin, the length of the hole will be 1 in. The bearing area is found from the product of pin diameter and hole length, and for the maximum lifting cable load of 3,800 pounds, the bearing stress is:

$$\frac{3{,}800}{(0.75)(1.0)} = 5{,}067\ psi$$

A conservative approach is to assume the bearing yield is identical to the tensile yield. The yield strength at the temperature of the fin is 22,225 psi, and the margin of safety is:

$$M.S. = \frac{22{,}225}{3(5{,}067)} - 1 = +0.46$$

The failure load for the hole bearing mode of failure can be found from the ratio:

$$\frac{Failure\ Load}{67{,}150\ psi} = \frac{3{,}800\ lb}{5{,}067\ psi} \rightarrow Failure\ Load = 50{,}359\ lb$$

(3) Fin Weld Shear

The fin weld is a 0.188-in. fillet weld on both sides of the fin along the line of contact with the OCV head. Because the fin is loaded in its own plane, the weld is loaded by direct shear and a torsion around its centroid. To determine the area properties of the weld, it was modeled using a finite element analysis program using 24 elements, from which the centroidal position of each element and the element length was obtained. These values were then used to calculate the area, centroid, polar moment of inertia, and other properties necessary for the calculation of weld stress as shown below. These property calculations are treated in Appendix 2.10.4. Table 2.5.1.2.2-1 summarizes the relevant properties and dimensions, with reference to Figure 2.5.1.2.2-1:

TABLE 2.5.1.2.2-1. Fin Weld Physical Properties on Each Side of the Fin.

Property or Dimension	Value	Unit
Weld length	9.48	in.
x-centroid	3.83	in.
y-centroid	4.26	in.
J, Polar Moment of Inertia	64.59	in.^{4} per in. of weld width
c (upper)	4.54	in.
c (lower)	4.76	in.
Θ (upper)	57.53	degrees
Θ (lower)	26.32	degrees
Perpendicular distance	1.83	in.

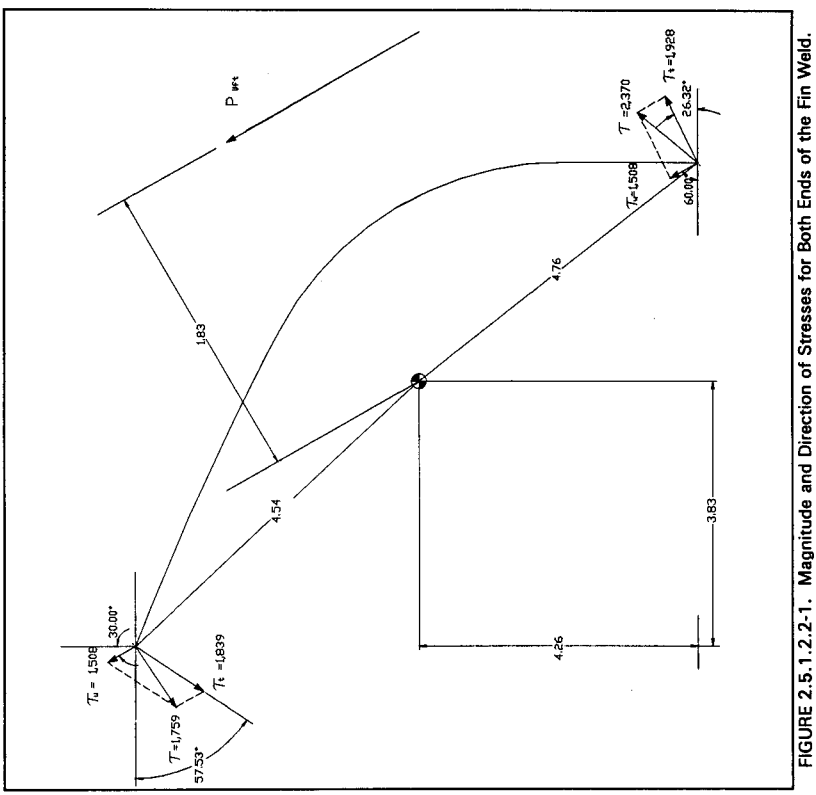


FIGURE 2.5.1.2.2-1. Magnitude and Direction of Stresses for Both Ends of the Fin Weld.

Because the shear area of a fillet weld is 0.707 times the weld leg dimension, the actual area and moment of inertia are as follows:

$$A = (9.48)(2)(0.188)(0.707) = 2.52 \text{ in.}^2$$

$$J = (64.59)(2)(0.188)(0.707) = 17.17 \text{ in.}^4$$

There will be two kinds of shear stress on the weld. One will be a uniform shear because of the cable load directed along the line of action of the cable. The other will be a torsional shear, acting perpendicular to the radius from the centroid. From Table 2.5.1.2.2-1 and Figure 2.5.1.2.2-1 above, the perpendicular distance from the line of action of the cable to the weld centroid is 1.83 in., and the moment, therefore, is:

$$T = (3,800)(1.83) = 6,954 \text{ in.-lb}$$

where 3,800 pounds is the cable load. The torsional shear stress at the upper end is:

$$\tau_t = \frac{Tc}{J} = 1,839 \; psi$$

where: $T = 6,954$ in.-lb
$c = 4.54$ in.
$J = 17.17$ in.^{4}

At the lower end, the torsional shear stress is 1,928 psi, where 4.76 in. is substituted for c in the above equation. The uniform shear stress is:

$$\tau_u = \frac{F}{A} = 1,508 \; psi$$

where: $F = 3,800$ lb
$A = 2.52$ in.^{2}

Figure 2.5.1.2.2-1 shows the magnitude and direction of these stresses for both the upper and lower ends of the weld. Combining by vectorial methods, the resultant stress at the top is 1,759 psi, and 2,370 psi at the bottom. Thus, the maximum stress occurs at the bottom. Using a weld shear yield strength of 12,120 psi, the minimum margin of safety is:

$$M.S. = \frac{12,120}{3(2,370)} - 1 = +0.70$$

Using a weld shear ultimate strength of 38,130 psi, the cable load at which the weld will fail can be found from the following ratio:

$$\frac{Failure\ Load}{38{,}130\ psi} = \frac{3{,}800\ lb}{2{,}370\ psi} \rightarrow Failure\ Load = 61{,}137\ lb$$

Thus, all failure modes have positive margins of safety using a load factor of three. The hole bearing and fin weld ultimate failure loads are comparable in value and will occur well before the torispherical head failure, as shown in Table 2.5.1.2.2-2 below, affording complete protection to the containment boundary.

Table 2.5.1.2.2-2. OCV Lifting Failure Mode Hierarchy.

Failure mode	Ultimate failure load (lb)
Hole bearing	50,354
Fin weld shear	61,137
Head failure	146,446

2.5.2 Tiedown Devices

The RTG transportation system trailer carries up to two packages. Each package will be fastened to a shock and vibration isolated trailer skid. The upper surface of the trailer skid, on which the package (impact limiter) rests, is a platform that is suspended by shock and vibration isolators. A socket is formed on the top of the platform by a ring made from steel bar into which the impact limiter fits, and which serves the purpose of reacting chocking loads. The package is secured to the trailer skid by two flat, 3-in.-wide flexible metal mesh straps, passing over the top of the package at right angles, and attaching to the platform at its diagonal corners. This configuration is shown in Figure 2.5.2-1. Inertial loads are assumed to act through the package center of gravity. The worst case loads will be found from the maximum payload condition, where total weight is 9,600 pounds and center of gravity location is 25.2 in. above the platform.

Because no tiedown devices are a part of the licensed package, the requirements of 10 CFR 71.45 do not apply. However, in the interest of completeness, the interface loads and resulting stresses will be determined. Inertial loads of 10g longitudinal, 5g lateral, and 2g vertically upward will be applied simultaneously. Friction between the package and straps is included in the calculations to show that an assumption of zero for friction is conservative.

2.5.2.1 Tiedown Forces. The geometry of the package strap tiedown is shown in Figures 2.5.2.1-1 and 2.5.2.1-2. The plane of the second figure is parallel to the (longitudinal) direction of motion, thus the straps, which are oriented at 45° to the direction of motion, are represented by their projections onto this plane. As shown in the first figure, the strap makes an angle with the package vertical wall in the plane of the strap. The interface between the straps and the package is modeled by assuming that each strap passes over frictionless pulleys at the top corners, with friction applied at one point in the top center of the package. To find total strap tension, the portion due to each inertia load will be found separately, and finally added.

Let X, Y, and Z represent the 10g, 5g, and 2g inertia forces, respectively. Referring to Figure 2.5.2.1-2, summing moments about point A gives:

$$WXL_1 + 2L_2 \sin 45° \left[-T_x - F + (T_x + F) - (T_x + F) \sin \theta\right] - 2L_3 (T_x + F)\cos \theta = 0$$

or:

$$T_x = \frac{WXL_1}{2\left[L_2(\sin 45°)(\sin \theta) + L_3 (\cos\theta)\right]} - F = 18{,}991 lb$$

where: T_x = strap tension due to the longitudinal load
W = the weight of the package, 9,600 lb
θ = the strap angle to the vertical, 24.5°, see Figure 2.5.2.1-1
F = friction reaction force (F = 0 for maximum strap load)
L_1 = the height of the center of gravity, 25.2 in.
L_2 = a moment arm, 68.35 in., see Figures 2.5.2.1-1 and 2.5.2.1-2
L_3 = a moment arm, found from.

$$L_3 = R_{\substack{impact \\ limiter}} + R_{\substack{knuckle \\ contact}} = 47.97 \text{ in.}$$

where: Radius of impact limiter is 35 in.
Radius to contact of strap on knuckle is 18.35 in., see Figures 2.5.2.1-1 and 2.5.2.1-2.

Because of package symmetry, the same calculation can be used for the lateral direction by substituting the inertia force Y for X, resulting in:

T_y = 9,496 lb

where T_y = strap tension because of the lateral load. Summing forces vertically:

$$WZ = 4T_z(\cos\theta)$$

from which T_z = 5,275 pounds, where W and θ have the same values as before. It is clear that the strap tension forces are maximized by setting the friction force, F, to zero. If this is done, strap forces completely cancel when summed in the horizontal direction. Therefore, horizontal inertia loads are reacted solely by the ring mounted on the skid by the bottom of the impact limiter. The chocking forces are as follows:

H_x = (9,600)X = 96,000 lb

H_y = (9,600)Y = 48,000 lb

where: H_x = the longitudinal chocking load
H_y = the lateral chocking load

Note also that H_z = 0 (no chocking force from vertical inertia load). The total strap load is a linear

sum of T_x, T_y, and T_z, or T_t = 18,991 + 9,496 + 5,275 = 33,762 pounds. The two chocking loads must be combined by vector summation:

$$H_t = \sqrt{(96{,}000)^2 + (48{,}000)^2} = 107{,}331 \text{ lb}$$

For conservatism, the stress calculations on the licensed hardware will be carried out using T = 35,000 pounds and H = 110,000 pounds.

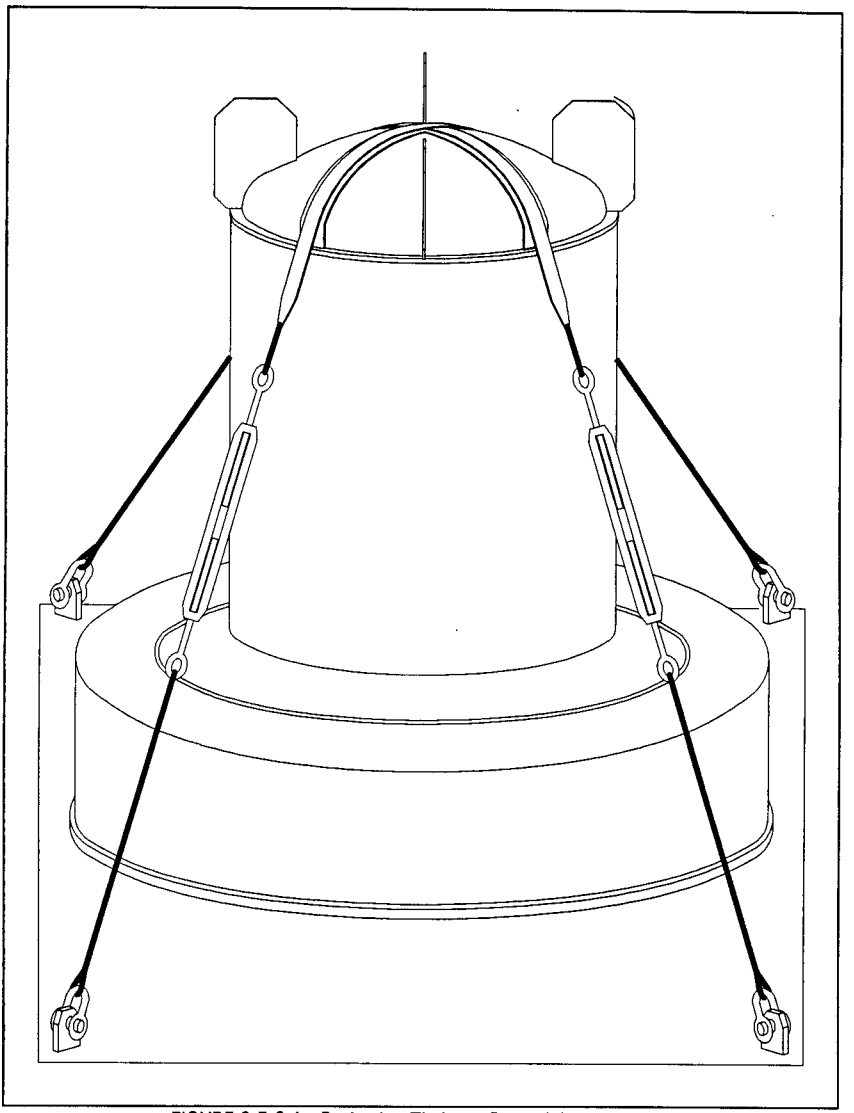


FIGURE 2.5.2-1. Packaging Tiedown General Arrangement.

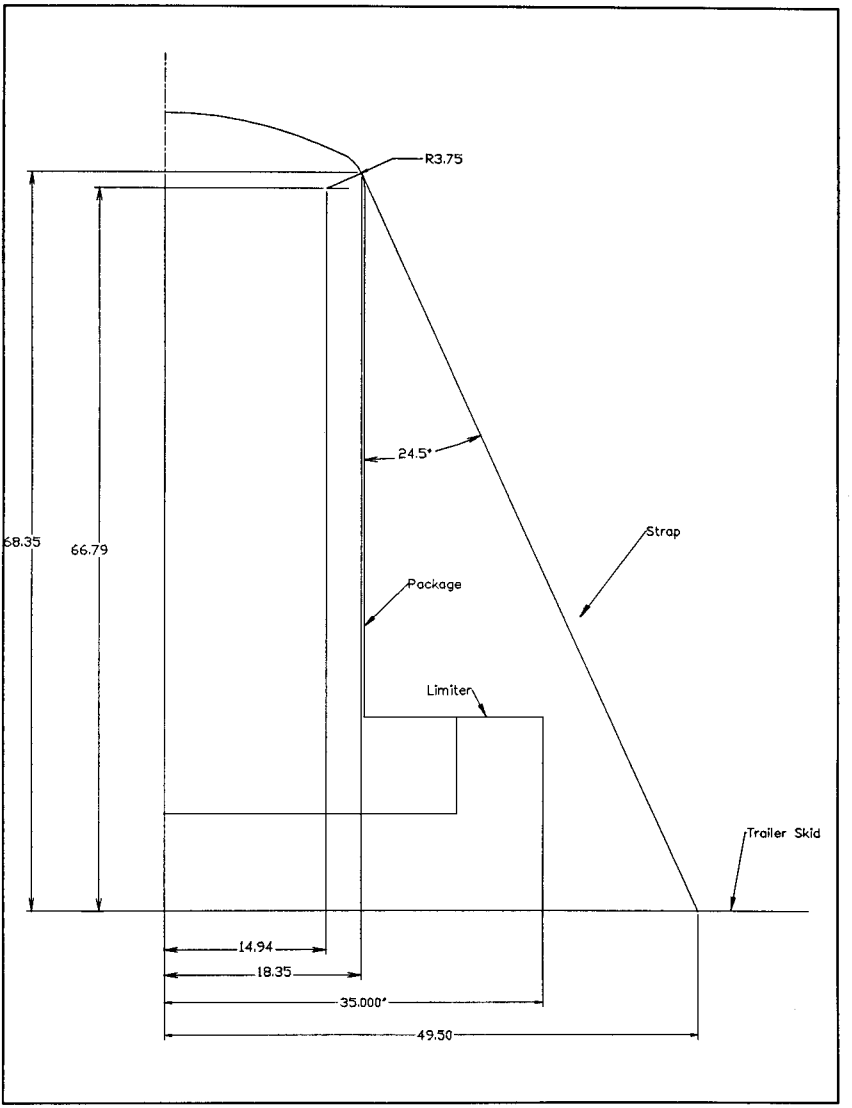


FIGURE 2.5.2.1-1. Package Tiedown Geometric Parameters.

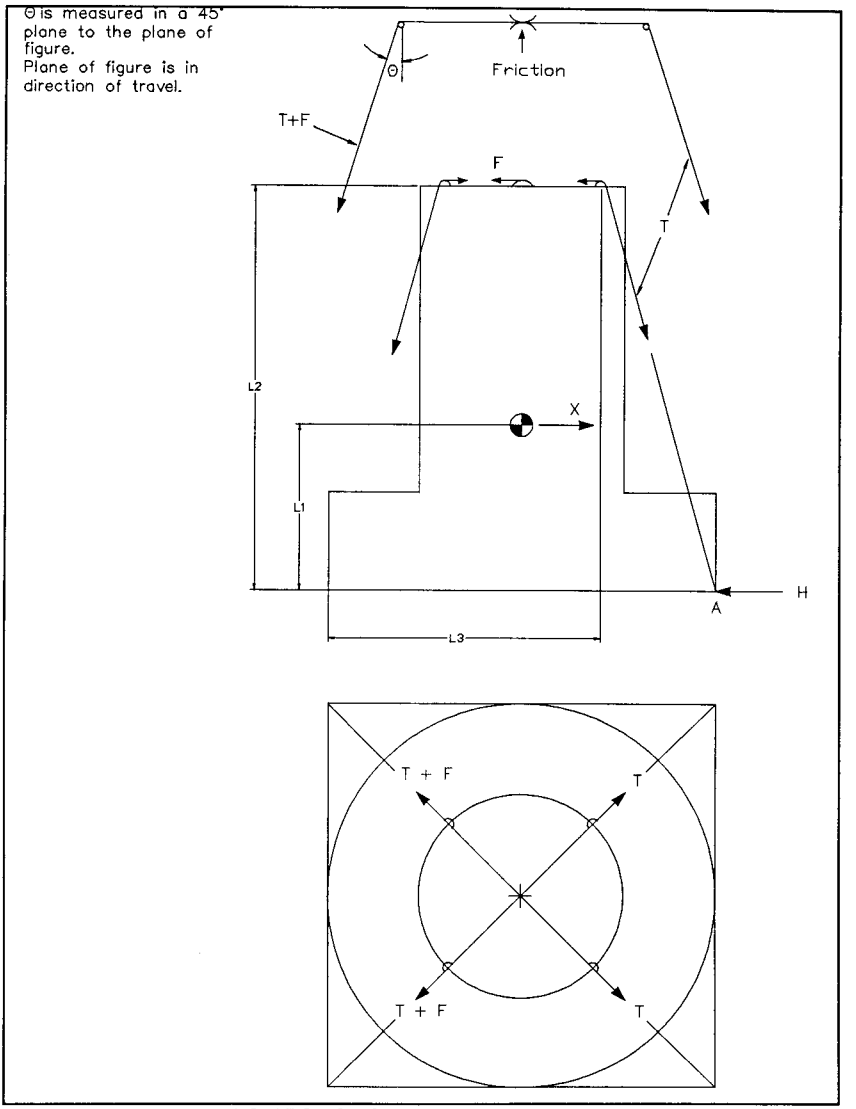


FIGURE 2.5.2.1-2. Package Tiedown Forces.

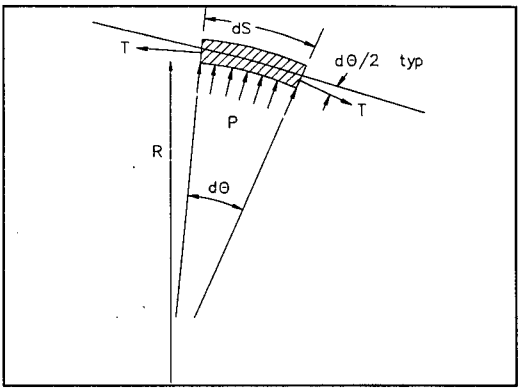


FIGURE 2.5.2.2-1. Tiedown Doubler Differential Segment.

2.5.2.2 Stresses in the Package Due to Tiedown Forces. The two tiedown straps are 3-in.-wide flexible metal straps, and pass over the OCV head, crossing in the middle. Because of a tensile load in the straps, they exert a pressure on the torispherical head that results in stresses in the head and sidewall, as determined from the following considerations.

Figure 2.5.2.2-1 depicts a small segment of strap of length dS, subtending the angle $d\theta$, with a constant radius R. There is a uniform tension in the strap, T, which is reacted by a pressure on the concave side, P. For a strap width, w, the sum of forces in the radial direction gives the following:

$$(Pw)dS = 2T\left[\sin\left[\frac{d\theta}{2}\right]\right]$$

Note that $dS = (R)\,d\theta$ and for small θ:

$$\sin\left[\frac{d\theta}{2}\right] \approx \frac{d\theta}{2}$$

Substituting these values and simplifying:

$$P = \frac{T}{wR}$$

Thus, for constant tension and width, the pressure beneath a strap is inversely proportional to the bend radius. The tiedown strap passes over the following two radii:

1. The 0.50 in. thick torispherical head with 0.25 in. thick doubler, having an outside radius of

36.25 + 0.25 = 36.50 in.

2. The knuckle and doubler, having a combined outside radius of 3.75 in.

The two pressures applied to the package are then (assuming T = 35,000 lb and w = 3.0 in.):

$$P_1 = \frac{T}{wR} = 319.6\ psi$$

where: R = 36.50 in., and:

$$P_2 = \frac{T}{wR} = 3{,}111\ psi$$

where: R = 3.75 in.

A finite element model was constructed of a quarter section of the OCV head, including a portion of the cylindrical side wall, as shown in Figure 2.10.5-1, Appendix 2.10.5. The head thickness was 0.50 in., and a 3-in.-wide doubler plate of 0.25-in. thickness was added to cover the area beneath each strap, starting at the top of the coolant jacket on one side and continuing over to the top of the coolant jacket on the other side. Displacements on the lower edge of the cylindrical sidewall portion were set to zero, and appropriate displacement constraints were used to enforce circumferential symmetry. Details of the model are given in Appendix 2.10.5.

The maximum stress intensity of 19,051 psi occurs in the shell material because of bending, and is located beneath the strap in the knuckle, near the transition to the cylindrical wall. From Appendix 2.10.7, Table 2.10.7.1-2, the temperature of the head in this region (thermal node 304) is 237 °F, but a value of 250 °F will conservatively be used. From Table 2.3-1, the yield strength of AISI Type 304L at this temperature is 20,200 psi. The margin of safety is:

$$M.S. = \frac{20{,}200}{19{,}051} - 1 = +0.06$$

The stresses in the impact limiter due to tiedown forces will be considered under three possible failure modes (referring to Figure 2.5.2.2-2): (1) top plate yield, (2) side wall yield, (3) base plate yield.

For the purposes of this analysis, the impact limiter foam will conservatively be assumed to have negligible properties. The load from the package must be reacted by the 1-in. high bar at the top of the trailer skid that forms a ring around the bottom of the impact limiter. The load path, shown in Figure 2.5.2.2-2, is from the OCV baseplate to the pocket structure into which the OCV fits, then to the impact limiter top plate, through the side walls, into the impact limiter base, and out to the ring. The impact limiter pocket structure, which fits closely around the OCV baseplate, has no appreciable stress. The pocket sidewalls are significantly more flexible than the impact limiter top plate, which will carry the reaction load. Material strength values of Type 304L will be conservatively used in place of the higher Type 304 values.

(1) Impact Limiter Top Plate

An approximation to the stress in the impact limiter top plate may be obtained by considering it as an infinite plate loaded in-plane by the chocking load of 110,000 pounds. In *Theory of Elasticity*[19], Article 42, Equation 75, the following formulations for principal stress are given, for a point directly ahead of the load at the inside radius of a plate loaded in-plane:

$$\sigma_r = -\frac{P(3+\mu)}{(4\pi rt)}$$

$$\sigma_n = \frac{P(1-\mu)}{(4\pi rt)}$$

By substituting the quantities:

μ = 0.3 (Poisson's ratio)
r = 27.125 in.
P = 110,000 lb
t = 0.25-in. thick.

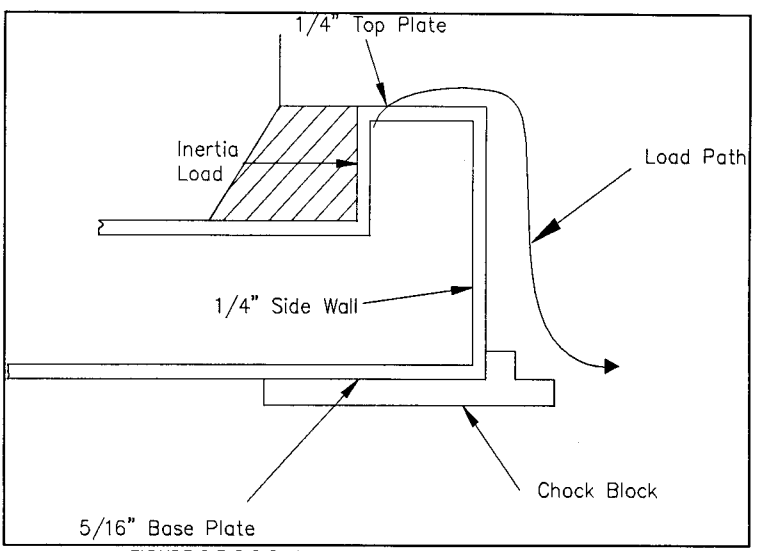


FIGURE 2.5.2.2-2. Tiedown Loading of the Impact Limiter.

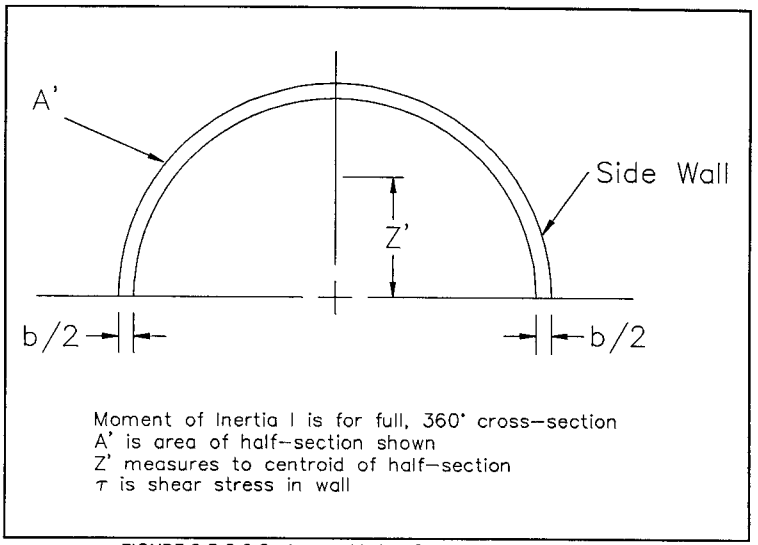


FIGURE 2.5.2.2-3. Impact Limiter Shell Analysis Parameters.

then:

$$\sigma_r = -4{,}259\ psi = \sigma_{min}$$

$$\sigma_n = 904\ psi = \sigma_{max}$$

Stress intensity (SI) equals twice the maximum shear stress, or:

$$SI = 2\tau_{max} = (\sigma_{max} - \sigma_{min}) = 904 - (-4{,}259) = 5{,}163\ psi$$

From Appendix 2.10.7, Table 2.10.7.1-2, the temperature of the top plate (thermal node 406) is 153 °F, but a value of 160 °F will be conservatively used. From Table 2.3-1, the yield strength of AISI Type 304L at this temperature is 22,780 psi. The margin of safety is:

$$M.S. = \frac{22{,}780}{5{,}163} - 1 = +3.41$$

(2) Impact Limiter Side Wall

The shear stress in the side wall per pound of chocking load will be examined. According to Young[20], page 95, Equation 2:

$$\tau = \frac{VA'z'}{Ib}$$

where the dimensional parameters are identified in Figure 2.5.2.2-3.

For the present case, V = 110,000 pounds. The outer diameter of the wall is 70 in., and the thickness is 0.25 in. The moment of inertia is:

$$I = \frac{\pi}{64}\left[(70.0)^4 - (69.5)^4\right] = 33{,}315\ in.^4$$

The parameter b for a hollow section is the sum of two wall thicknesses or the following:

$$b = (2)(0.25) = 0.50$$

The quantity A' is the area of the section on one side of the neutral axis. Therefore:

$$A' = \frac{(0.50)\pi}{4}\left[(70.0)^2 - (69.5)^2\right] = 27.39\ in.^2$$

The quantity z' is the distance from the neutral axis to the centroid of the area A'. Using Table 1, Case 22, of *Roark's Formulas for Stress and Strain* for this case (half of a circular thin ring), z' = 22.20 in. Substituting these values into the above formula for shear stress provide the following:

$$\tau_{max} = \frac{(110{,}000)(27.39)(22.20)}{(33{,}315)(0.50)} = 4{,}015 psi$$

Stress intensity is equal to twice the maximum shear or the following:

$$SI = 2\tau_{max} = (2)(4{,}015) = 8{,}030 \text{ psi}$$

From Appendix 2.10.7, Table 2.10.7.1-2, the temperature of the sidewall (thermal node 408) is 123 °F, but a value of 140 °F will be conservatively used. From Table 2.3-1, the yield strength is 23,520 psi. The margin of safety is:

$$M.S. = \frac{23,520}{8,031} - 1 = +1.93$$

(3) Impact Limiter Base Plate

The impact limiter base plate must bear in-plane against the reaction ring on the trailer skid. Because the plate is 0.31 in. thick and the diameter 70.0 in., the projected area is:

$$A = (70)(0.31) = 21.7 \text{ in.}^2$$

The compressive stress is:

$$\sigma_c = \frac{110,000}{21.7} = 5,069 \text{ psi}$$

A conservative approach is to assume the bearing yield is identical to the tensile yield. From Appendix 2.10.7, Table 2.10.7.1-2, the temperature of the base plate (thermal node 410) is 132 °F, but a value of 140 °F will be conservatively used. From Table 2.3-1, the yield strength is 23,520 psi. The margin of safety is:

$$M.S. = \frac{23,520}{5,069} - 1 = +3.64$$

Thus, all margins relating to tiedown loads are positive.

2.6 NORMAL CONDITIONS OF TRANSPORT

When subjected to Normal Conditions of Transport (NCT), as specified in 10 CFR 71.71, the package meets the performance requirements specified in Subpart E of 10 CFR 71, as documented in the following subsections. With the exception of NCT free drop, the primary proof of performance is via analysis. The NRC Regulatory Guide 7.6 criteria is shown to be met for all analytical evaluations presented in this section. The specific issues of brittle fracture, fatigue, and shear-out of bolted fasteners are analytically addressed in Section 2.1.2.2 and shown not to be limiting for the package. The ability of the butyl O-ring containment seals to remain leaktight at NCT temperature extremes is demonstrated with reference to performance testing, documented in Appendix 2.10.6.

Qualification of the RTG Transportation System Package for the NCT free drop test requirements of 10 CFR 71.71 was accomplished via a comprehensive certification test program. Previously, an engineering development test program using a half-scale prototype model was also undertaken.

Full-scale certification testing demonstrated package effectiveness in meeting all NCT free drop requirements. The certification test program showed that no reduction in effectiveness of the package results from any NCT free drop. Further, the NCT free drop certification test sequence demonstrated that the ability of the package to adequately survive a subsequent HAC free drop and

puncture test sequence was not compromised. Certification testing results show that NCT free drop package deformations are insignificant relative to NCT thermal, shielding, and criticality performance. The NCT free drop testing is discussed in Section 2.6.7.

2.6.1 Heat

The NCT thermal analyses, presented in Section 3.0, provide package component temperatures for several combinations of payload and environment. The principal case examined is the worst case of maximum payload heat load (the GPHS RTG, which generates 4,500 W of thermal power) and insolation, maximum external temperature, and without active cooling. For this principal case, active cooling is not considered, and the coolant jacket is drained of coolant, per 10 CFR 71.51(b). A case involving the maximum heat load and minimum ambient temperature without insolation, and a case where active cooling is present were also examined to establish the entire range of stress states experienced by the package in typical usage. These load cases are summarized in Table 2.6.1-1.

TABLE 2.6.1-1. NCT and Normal Operational Load Combinations.

Condition	Case 1	Case 2	Case 3
Solar	Full solar	No solar	Full solar
Ambient temperature	100 °F	-40 °F	100 °F
Payload	GPHS	GPHS	GPHS
Cooling	No active cooling	No active cooling	Active cooling (both loops)

2.6.1.1 Summary of Temperatures and Pressures. The stress analyses to follow use the temperatures and pressures listed in Appendix 2.10.7 for the cases listed in Table 2.6.1-1. These values result from the thermal analyses described in Section 3.0. The baseline for pressure is the package initial loading configuration, with the chiller providing 40 °F coolant to both loops, 70 °F ambient temperature, and no insolation. For that case, the steady state pressure internal to the ICV is 20 psia; the pressure internal to the ICV/OCV annulus is also 20 psia. These pressures are controlled as described in Sections 8.2.2.2 and 8.2.2.5.

A summary of vessel operational gas temperatures is given in Table 2.6.1.1-1, taken directly from the results given in Section 3.0 and summarized in Appendix 2.10.7, Table 2.10.7.1-5. For purposes of structural analysis, the pressures shown in Table 2.6.1.1-2 have been adjusted from those calculated in Section 3.0 (summarized in Table 2.10.7.1-6) to form a conservatively large net pressure differential for each containment vessel. This is accomplished by rounding applicable internal pressures upward and the external pressures downward. The pressure external to the ICV and internal to the OCV is listed as two different values, even though it must nominally be a single value, because the lower value forms a larger net pressure differential for the ICV, and the higher value forms a larger net pressure differential for the OCV. The ICV internal pressures given in the table have been further adjusted upward to account for other sources of gas pressure described in the next section. The OCV minimum external pressure is 3.5 psia, in anticipation of Section 2.6.3.

For example, Case 1 pressures are determined as follows. From Appendix 2.10.7, Table 2.10.7.1-6, the calculated ICV internal pressure, based on the amount of helium gas placed within the ICV and its temperature, is 24.4 psia. From Section 2.6.1.1.1, the additional pressure is

determined as 5.3 psia, or a sum of 29.7 psia. Then, for conservatism, this value is rounded upward to 30.0 psia, and is listed in Table 2.6.1.1-2. Next, from Appendix 2.10.7, Table 2.10.7.1-6, the calculated OCV internal pressure, based on the amount of helium gas placed within the OCV and its temperature, is 26.3 psia. This value is rounded downward to 20.0 psia to form a conservatively large net differential pressure of 30.0 - 20.0 = 10.0 psid for the ICV, and rounded upward to 30.0 psia to form a conservatively large net differential pressure of 30.0 - 3.5 = 26.5 psid for the OCV. Cases 2 and 3 are handled in a similar manner. For simplicity in the analyses that follow, Case 1 pressure differentials (10 psid for the ICV and 26.5 psid for the OCV) will be used in place of the lower Case 2 and 3 pressure differentials.

TABLE 2.6.1.1-1. Summary of NCT and Normal Operational Internal Gas Temperatures.

Location	Case 1 full solar 100 °F ambient no cooling	Case 2 no solar -40 °F ambient no cooling	Case 3 full solar 100 °F ambient active cooling
ICV Internal Gas Temperature (°F)	354	256	213
OCV Internal Gas Temperature (°F)	285	165	115

TABLE 2.6.1.1-2. Summary of NCT and Normal Operational Internal Gas Pressures.

Location	Case 1 full solar 100 °F ambient no cooling	Case 2 no solar -40 °F ambient no cooling	Case 3 full solar 100 °F ambient active cooling
ICV internal gas pressure (psia)	30	27	26
ICV external gas pressure (psia)	20	19	18
OCV internal gas pressure (psia)	30	24	22
OCV external gas pressure (psia)	3.5	3.5	3.5

2.6.1.1.1 Sources of Pressure. The baseline vessel internal pressures were defined in Section 2.6.1.1. These initial equilibrium pressures will increase or decrease as the gas temperatures change under varying nonoperational (i.e., regulatory) conditions, and such changes are reflected in the pressures listed in Table 2.10.7.1-6. Additionally, there are two potential sources of gas within the ICV which, over time, could possibly cause a slight increase in total pressure: (1) Leakage from the payload initial gas charge and (2) Decay of heat source radionuclides.

The first source, leakage from the payload initial gas charge, could arise because of payload pressure boundary failure, in which case the payload internal gas would escape into the package cavity and increase the ICV pressure. However, as will now be demonstrated, the potential pressure increase is relatively small.

According to Table 1.2.3-2, the amount of gas within the GPHS payload, which could be added to the gas already inside the ICV, is 16 L (0.565 ft^3) at STP. Because one lb-mole of any

gas occupies 359 ft^3 at STP**, the amount of gas within the GPHS is:

$$n = \frac{0.565}{359} = 1.57(10)^{-3}\ lb\text{-}mole$$

The corresponding amount of gas within the generic payload, per Table 1.2.3-1, is 0.0135 lb-mole, which, as the higher value, forms the basis for all further calculations.

The other source of gas that could accumulate over time is the helium resulting from the decay of the radioactive heat source. The maximum helium gas generation rate for all of the radioactive material within the GPHS payload is $2.06(10)^{-4}$ standard cm^3/sec. This may be converted to 0.038 ft^3 in 60 days. Converting to lb-moles is:

$$n = \frac{0.038}{359} = 1.06(10)^{-4}\ lb\text{-}mole$$

This would be added to the gas already in the cavity in 60 days.

The perfect gas law will determine the partial pressure resulting from the two added amounts. To do this requires knowing *V*, the cavity void volume with the payload installed. Because releasing a given amount of gas into a smaller volume will result in a higher pressure, an underestimation of void volume is conservative. Such an estimate can be formed by ignoring the void volume of the torispherical head and the void volume below the shipping rack assembly, and simply subtracting the basic cylindrical volume of the GPHS RTG payload from the remaining volume of the ICV, taking ICV volume from the top of the shipping rack assembly to the top of the cylindrical section:

$$V = \frac{\pi}{4}\left[(34.0)^2\ (51.5\text{-}5.25)\text{-}(9.7)^2\ (47.95)\right] = 38{,}448\ in.^3 = 22.25\ ft^3$$

where:
ICV inner diameter = 34.0 in.
ICV cylindrical length = 51.5 in.
GPHS RTG basic diameter = 9.7 in.
GPHS RTG length = 47.95 in.
Shipping rack assembly height = 5.25 in.

The pressure differential due to the two additional sources now is:

$$p = \frac{(n_1 + n_2)RT}{V} = 5.3\ psia$$

**Standard conditions are 14.7 psia and 32 °F.

where: n_1 = 0.0135(10^{-3}) lb-mole
n_2 = 1.06(10^{-4}) lb-mole
V = 22.25 ft^3
R = 10.74 psia-ft^3/lb-mole-°R
T = 814 °R (354 °F, from Table 2.6.1.1-1).

2.6.1.2 Differential Thermal Expansion. A radial and axial clearance is maintained between the ICV bell and the OCV bell. The variation of this clearance because of differential thermal expansion will now be examined.

Both the radial and axial thermal expansion of each vessel will be dominated by the temperature of the cylindrical walls, which are thermally modeled in each case by four nodes: 210 to 240 in the ICV, and 310 to 340 in the OCV. As shown in Figure 3.4.1-2, nodes 210/310 are located 6.86 in. below the top of the coolant jacket. The corresponding measurements for the other node pairs are: nodes 220/320, 20.58 in.; nodes 230/330, 34.30 in.; and nodes 240/340, 43.66 in. The radial differential thermal expansion between the two vessels is found by subtracting the radial thermal expansion of the OCV from that of the ICV at each of the four elevations discussed above. The residual radial clearance is found by subtracting this result from the initial minimum manufactured clearance. Temperatures are taken from Section 3.6.4. For example, for Case 3, the temperature for node 210 is 151 °F, and for node 310, 64 °F. The outside diameter of the ICV is 35.5 in., and the inside diameter of the OCV is 35.88 in. From Table 2.3-1, the coefficient of thermal expansion for Type 304L at temperatures of 151 °F and 64 °F are 8.67(10^{-6}) in/in/°F and 8.44(10^{-6}) in/in/°F, respectively. The minimum initial radial clearance is 1/32 in. The residual radial clearance therefore, is:

$$RC_{res} = 0.031 - 0.5[35.5(151 - 70)8.67(10^{-6}) - 35.88(64 - 70)8.44(10^{-6})] = 0.018\ in.$$

Residual radial clearances at other locations and for all load cases are presented in Table 2.6.1.2-1.

The axial differential thermal expansion between the two vessels is found by subtracting the axial thermal expansion of the OCV from that of the ICV using the average temperature of the four stations described above. (Average temperature is valid because each node represents about equal lengths of vessel shell.) The residual axial clearance is found by subtracting this result from the initial minimum manufactured clearance. For example, for Case 3, the temperatures of nodes 210 to 240 are 151, 134, 118, and 78 °F, respectively, and the average is 120 °F. The temperatures of nodes 310 to 340 are 64, 59, 54, and 49 °F, respectively, and the average is 56 °F. From Table 2.3-1, the coefficient of thermal expansion for Type 304L at temperatures of 120 °F and 56 °F are 8.60(10^{-6}) in/in/°F and 8.42(10^{-6}) in/in/°F, respectively. The OCV inside height, 62.9 in., may be conservatively used for both vessels. The minimum initial axial clearance is 1/16 in. The residual axial clearance, therefore, is:

$$AC_{res} = 0.062 - 62.9[(120 - 70)8.60(10^{-6}) - (56 - 70)8.42(10^{-6})] = 0.028\ in.$$

Residual axial clearances for all load cases are presented in Table 2.6.1.2-1.

TABLE 2.6.1.2-1. Summary of NCT and Normal Operational Differential Expansions.

Parameter	Case 1 full solar 100 °F ambient, no cooling	Case 2 no solar -40 °F ambient, no cooling	Case 3 full solar 100 °F ambient, active cooling
Residual axial clearance (in.)	0.039	0.036	0.028
Residual radial clearance (in.)			
Elevation 210/310	0.024	0.022	0.018
Elevation 220/320	0.024	0.022	0.020
Elevation 230/330	0.024	0.022	0.021
Elevation 240/340	0.028	0.028	0.027

Thus, a positive clearance is maintained between the ICV and OCV bells under NCT and normal operational conditions. The relative differential thermal expansion between the closure bolts and vessel flanges is treated in the next section.

2.6.1.2.1 Bolt Thermal Expansion. As noted in Section 2.3, the bolting material used for the OCV and ICV containment assembly closure bolts (ASTM-A320, Grade L43 and ASTM-A540, Grade B23, Class 1) has a different coefficient of thermal expansion than the material used for the vessel flanges (AISI Type 304L). As the temperature of the vessels changes from the initial conditions, this leads to variations in bolt pre-load because of different amounts of thermal expansion/contraction in the bolt and in the joint material. Because the expansion coefficient of AISI Type 304L in the joint is greater than that of the bolt, an increase in joint temperature will normally mean an increase in bolt clamping force and bolt stress. A decrease in joint temperature will normally mean a decrease in bolt clamping force and bolt stress. In the analyses to follow, the actual temperatures of the bolt and joint, as calculated in Section 3.0 (and as summarized in Appendix 2.10.7) are used. From Shigley, *Mechanical Engineering Design*[21], the initial pre-load force in the bolts, resulting from assembly torque, is:

$$F_i = \frac{T}{Kd}$$

where: T = bolt torque, in.-lb
K = 0.186, friction toque coefficient for cadmium plated threads[23]
d = nominal bolt diameter, in.

Table 2.6.1.2.1-1 lists the bolt parameters along with pre-load force for the ICV and OCV closure bolts.

TABLE 2.6.1.2.1-1. Closure Bolt Parameters and Pre-load Force.

Location	d (in.)	Stress area (in.^{2})	Length*(in.)	Torque (ft-lb)	Pre-load force (lb)
ICV	0.75	0.3300	1.49	250	21,505
OCV	1.25	0.9524	5.19	300	15,484

*Grip length, defined as the length from the head to the midpoint of the engaged threads.

The finite element models described in the last section (see Appendices 2.10.2 for the ICV and 2.10.8 for the OCV model) include a model of the closure bolts as spars. They are given an initial stretch so that under nominal conditions (zero net pressure and uniform reference temperature of 70 °F) the load in the bolts is equal to the pre-load force values given in the table above. During model postprocessing, the resultant force in the spar is extracted. Because in the 2-D model a single spar must represent all of the bolts, the force in each bolt may be found as:

$$F_b = \frac{2\pi F_s}{n}$$

where: F_b = force in each bolt, lb
F_s = force in model spar, lb/radian
n = number of bolts.

Based on a tensile stress area of A_s, the stress in the bolt is:

$$\sigma_b = \frac{F_b}{A_s}$$

The allowable bolt stress for NCT is $2S_m$, based on the ASME B&PV Code, Section III, Article NB-3232.1, and is found from bolt temperature and Tables 2.3-2 and 2.3-3. The margin of safety is:

$$M.S. = \frac{2S_m}{\sigma_b} - 1$$

The following table summarizes load, stress, temperature, allowable, and margin of safety for the closure vessel bolts for each case in Table 2.6.1-1.

TABLE 2.6.1.2.1-2. Closure Bolt Load, Stress, and Margin of Safety.

Load case	Bolt location	Bolt load (lb)	Bolt stress (psi)	Bolt temp. (°F)[a]	$2S_m$ Allowable (psi)	Margin of safety
1	ICV	23,417	70,961	217	95,056	+0.34
	OCV	23,390	24,559	210	65,780	+1.68
2	ICV	21,445	64,985	70	100,000	+0.54
	OCV	14,833	15,574	61	70,000	+3.49
3	ICV	21,746	65,897	85	100,000	+0.52
	OCV	16,281	17,095	86	70,000	+3.09

[a]The closure bolts were not explicitly modeled in the 2-D NCT thermal analysis. The bolt temperatures listed are those of the respective bolting flanges, i.e., thermal node 250 for the ICV and thermal node 350 for the OCV, and are taken from Tables 2.10.7.1-2, -3, and -4.

According to Reference 23, the preload force may vary by up to ±30% for a given applied torque value. Therefore, Case 1 (the case having the lowest bolt margin of safety) was rerun, using a pre-stretch in the element representing the bolts of 130% of the nominal value. This case represents the maximum possible load in the bolts. The results are shown in Table 2.6.1.2.1-3, where the relatively large margins of safety demonstrate that the bolt stress is still well below yield, even when conservatively accounting for a large scatter in bolt preload force.

TABLE 2.6.1.2.1-3. Closure Bolt Load and Stress Considering Preload Force Variation.

Load case	Bolt location	Bolt load (lb)	Bolt stress (psi)	Bolt temp. (°F)	Yield strength (psi)	Margin of safety on yield
1	ICV	29,656	89,867	217	139,280	0.55
	OCV	27,904	29,299	210	98,670	2.37

Thus, a positive margin of safety is maintained under NCT and normal operational conditions for all closure bolts.

2.6.1.3 Stress Calculations. The axisymmetric finite element models of the ICV and OCV already introduced in Section 2.6.1.2 are used to determine the stress in both containment vessels because of the combined effects of differential thermal expansion and pressure loads. To aid in the classification of stress, the cases of Table 2.6.1-1 are broken down into several load cases as shown in Table 2.6.1.3-1. The internal pressure-only cases (ICV-P and OCV-P) are run to allow primary (pressure) stresses to be considered independently of secondary (thermal) stresses. Classification of stress intensities is per Table NB-3217-1 of the ASME B&PV Code. According to Table NB-3217-1, pressure-induced membrane stresses in the knuckle portion of the torispherical heads are classified as local membrane stresses, and bending stresses in the knuckle are classified as secondary stresses. The cases ICV-A and OCV-A aid in consideration of the total range of stress by including the period during payload assembly operations during which the annulus between the vessels is evacuated before helium backfill.

TABLE 2.6.1.3-1. Containment Vessel Stress Analysis Load Cases.

	Load case No.	Description
ICV cases	ICV-P	10 psi net internal pressure only, uniform 70 °F
	ICV-1	10 psi net internal pressure, case 1[a] temperatures
	ICV-2	10 psi net internal pressure, case 2 temperatures
	ICV-3	10 psi net internal pressure, case 3 temperatures
	ICV-A	20 psi net internal pressure, loading transient temperatures[b]
OCV cases	OCV-P	26.5 psi net internal pressure only, uniform 70 °F
	OCV-1	26.5 psi net internal pressure, case 1 temperatures
	OCV-2	26.5 psi net internal pressure, case 2 temperatures
	OCV-3	26.5 psi net internal pressure, case 3 temperatures
	OCV-A	14.7 psi net ext. pressure, loading transient temperatures[b]

[a]Cases 1, 2, and 3 are defined in Table 2.6.1-1.

[b]Load cases ICV-A and OCV-A correspond to the point during package assembly when the ICV/OCV annulus is evacuated before backfill.

Temperatures for each case are taken from Appendix 2.10.7 and temperature-dependent moduli of elasticity and thermal expansion coefficients are used as given in Section 2.3. Finite element model plots are shown in Figures 2.10.2-1 (ICV) and 2.10.8-1 (OCV). Stress intensity results are summarized in Tables 2.6.1.3-2 and 2.6.1.3-3.

For each load case listed above, the stress location, classification, stress value, allowable, and margin of safety are listed. The minimum margin of safety is +2.93 (case OCV-3). The allowables shown in the tables are based on the design criteria given in Table 2.1.2-1 and properties given in Table 2.3-1.

Membrane and bending stresses, resulting from the pressure-only cases (without thermal effect), are insignificant. The only cases of interest are the combined pressure and thermal cases, where the maximum membrane and bending stress intensity occurs in or near the ICV and OCV head knuckle regions.

TABLE 2.6.1.3-2. Summary of ICV Stress Intensities and Margins of Safety.

Case No.	Stress location	Stress category	Maximum stress intensity (psi)	Allowable stress intensity (psi)[a]	Margin of safety
	Head crown midshell	P_m	1,041 (elem 145)	16,700 (S_m)	> +10
ICV-P	Head Crown, shell surface	$P_L + P_b$	1,955 (elem 145)	25,050 ($1.5S_m$)	> +10
	Knuckle midshell	P_L	1,093 (elem 144)	25,050 ($1.5S_m$)	> +10
	Knuckle shell surface	$P_L + P_b + Q$	2,110 (elem 144)	50,100 ($3.0S_m$)	> +10
ICV-1	Knuckle shell surface	$P_L + P_b + Q$	3,139 (elem 145)	48,750 ($3.0S_m$)	> +10
ICV-2	Knuckle shell surface	$P_L + P_b + Q$	3,535 (elem 145)	50,100 ($3.0S_m$)	> +10
ICV-3	Knuckle shell surface	$P_L + P_b + Q$	2,716 (elem 145)	50,100 ($3.0S_m$)	> +10
ICV-A	Knuckle shell surface	$P_L + P_b + Q$	4,646 (elem 144)	50,100 ($3.0S_m$)	> +10

[a]Allowable stress intensity based on temperatures of applicable stress location, given in Appendix 2.10.7.1. For case ICV-1, the maximum temperature is 338 °F, but 350 °F will be conservatively assumed for all locations. For Cases ICV-2, ICV-3, ICV-A and ICV-P, temperatures are below 300 °F, but 300 °F is conservatively used for all locations.

TABLE 2.6.1.3-3. Summary of OCV Stress Intensities and Margins of Safety.

Case No.	Stress location	Stress category[216]	Maximum stress intensity (psi)	Allowable stress intensity (psi)[a]	Margin of safety
	Head crown midshell	P_m	1,085 (elem 121)	16,700 (S_m)	> +10
OCV-P	Head crown shell surface	$P_L + P_b$	1,667 (elem 122)	25,050 ($1.5S_m$)	> +10
	Knuckle mid-shell	P_L	1,840 (elem 119)	25,050 ($1.5S_m$)	> +10
	Knuckle shell surface	$P_L + P_b + Q$	3,522 (elem 119)	50,100 ($3.0S_m$)	> +10
OCV-1	Knuckle shell surface	$P_L + P_b + Q$	7,585 (elem 116)	50,100 ($3.0S_m$)	+5.61
OCV-2	Knuckle shell surface	$P_L + P_b + Q$	9,002 (elem 116)	50,100 ($3.0S_m$)	+4.57
OCV-3	Knuckle shell surface	$P_L + P_b + Q$	12,733 (elem 117)	50,100 ($3.0S_m$)	+2.93
OCV-A	Knuckle midshell	$P_L + P_b + Q$	7,287 (elem 117)	50,100 ($3.0S_m$)	+5.88

[a]Allowable stress intensity based on temperatures given in Appendix 2.10.7.1. All temperatures are below 300 °F, but 300 °F is conservatively used for all locations.

2.6.1.4 Comparison With Allowable Stresses. As discussed in Section 2.1.2, stress limits are in accordance with Regulatory Guide 7.6, and load combinations are in accordance with Regulatory Guide 7.8. From Table 2.3-1, the S_m value for AISI Type 304L stainless steel used in both vessels is 16,700 psi up to 300 °F, and is 16,250 psi at the conservative maximum of 350 °F. From Table 2.1.2-1, the allowable stress intensity limits under NCT are S_m for general primary membrane stress intensities (P_m), $1.5S_m$ for local primary membrane stress intensities (P_L), $1.5S_m$ for primary membrane (general or local) plus primary bending stress intensities ($P_L + P_b$), and $3.0S_m$ for the range of primary plus secondary stress intensities ($P_L + P_b + Q$). Minimum margins of safety, all of which are positive, are presented in Tables 2.6.1.3-2 and 2.6.1.3-3. Thus, the design criteria are satisfied.

2.6.1.5 Range of Primary Plus Secondary Stress Intensities. Per Regulatory Guide 7.6, Paragraph C.4, the maximum range of primary plus secondary stress intensity under NCT must be less than $3.0S_m$. This limitation on stress intensity range applies to the entire history of NCT loadings, and not just to the stress intensities from each individual load transient. To evaluate the maximum range, examination was made of the various load cases, including both regulatory and worst-case operational, and the maximum stress intensity arising from the worst-case load case was determined. To conservatively bound the maximum stress intensity range, the difference between the worst-case maximum stress intensity and the nominal (70 °F, no stress) condition was doubled, to account for a maximum possible stress reversal.

From Tables 2.6.1.3-2 and 2.6.1.3-3, the worst case is OCV-3, with a stress intensity of 12,733 psi. Doubling this value results in a maximum range for primary and secondary stress

intensity of 25,466 psi. As discussed in Section 2.6.1.4, the value of S_m for AISI Type 304L stainless steel is 16,700 psi for case OCV-3, because the peak temperature is less than 300 °F. The margin of safety for the range of primary plus secondary stress intensity is as follows:

$$M.S. = \frac{3S_m}{\sigma_r} - 1 = +0.97$$

where: S_m = 16,700 psi
σ_r = 25,466 psi.

2.6.2 Cold

The cold NCT consists of exposing the RTG Transportation System Package to a steady-state ambient temperature of -40 °F. Insolation and payload internal decay heat are assumed to be negligible. These conditions will result in a uniform temperature throughout the package of -40 °F.

The effect on the two containment vessels will be negligible. The only containment structural component not comprised of ASTM-A240, Type 304L, stainless steel are the ASTM-A320, Grade L43 OCV closure bolts and the ASTM-A540, Grade B23, Class 1 ICV closure bolts. Both materials have the same coefficient of thermal expansion, which is less than that for the Type 304L structural material. Hence, a reduction in temperature from that at which the closure bolts were installed will result in some loss of pre-load in the closure system. The pre-load loss is easily determined from the two-dimensional, axisymmetric finite element models, assuming a bolt installation temperature of 70 °F.

The ICV model is described in Appendix 2.10.2. No net pressure is assumed for the cold NCT analysis. As previously described in Section 2.6.1.2.1, the closure bolt is modeled as a spar, and for this analysis is given an initial stretch that results in 70% of the pre-load applied to the bolt at assembly, or (0.7) (21,505) = 15,054 (see Table 2.6.1.2.1-1). Then, setting all the temperatures in the model to -40 °F results in a spar load of 58,580 lb/radian, using material properties extrapolated from the values shown in Tables 2.3-1 and 2.3-3. This can be converted into load per closure bolt as before, resulting in:

$$F_b = \frac{2\pi F_s}{n} = 15{,}336\ lb$$

where: F_b = load per bolt, lb
F_s = spar load, 58,580 lb/radian
n = 24 bolts.

Because F_b is positive, a residual closure force will exist in the ICV closure system at -40 °F. This will correspondingly ensure that a residual compression remains on the ICV O-ring seals.

The OCV model is described in Appendix 2.10.8. The bolt preload used is conservatively taken as (0.7)(15,484) = 10,839 lb (see Table 2.6.1.2.1-1). Following the same procedure as for the ICV, the spar load at -40 °F is 16,365 pounds. The conversion to load per closure bolt is given below:

$$F_b = \frac{2\pi F_s}{n} = 4{,}284 \text{ lb}$$

where: F_b = load per bolt, lb
F_s = spar load, 16,365 lb/radian
n = 24 bolts.

Because F_b is positive, a residual closure force will exist in the OCV closure system at -40 °F. This will correspondingly ensure that a residual compression remains on the OCV O-ring seals.

Because all other containment structural components are fabricated from the same material and are at a uniform temperature, differential expansion stresses are not a concern. Brittle fracture concerns are addressed in Section 2.1.2.2.1, and O-ring sealing performance at -40 °F is discussed in Section 4.0.

2.6.3 Reduced External Pressure

The effect of a reduced external pressure of 3.5 psia has been examined in Section 2.6.1 where, in anticipation of this requirement, pressure external to the OCV was set to 3.5 psia. The internal pressure of the OCV was conservatively rounded upward to 30 psia, yielding a conservative net pressure differential of 30 - 3.5 = 26.5 psid (see Section 2.6.1.1). This pressure was used with the most unfavorable temperature conditions, and margins of safety were positive as shown in Table 2.6.1.3-3. Therefore, reduced external pressure is not a concern.

2.6.4 Increased External Pressure

The effect of an increased external pressure of 20 psia is negligible for the RTG Transportation System Package. As discussed in Section 2.6.1.1, the pressure within the OCV was conservatively rounded downward to 18.0 psia, as shown for case 3. The effect of the increased external pressure on the OCV would be a 20.0 - 18.0 = 2.0 psig external pressure. However, the OCV can withstand a full vacuum (zero psia internal, 14.7 psia external pressure), because this load is applied during the process of assembly of the payload into the package, just before helium backfill of the annulus. Margins of safety for that case (Case OCV-A) were shown to be positive in Table 2.6.1.3-3. Therefore, increased external pressure is not a concern.

2.6.5 Vibration

The effects of the vibration normally incident to transportation are shown to be insignificant. To protect the relatively delicate payloads from harmful effects of shock and vibration, the package is mounted on shock isolators having a natural frequency much lower than the lowest natural frequency of any package component, including payloads. For this reason, the package behaves essentially as a rigid body and responds to the vibratory inertia loads in a quasi-static manner. Because these resulting inertia loads are so small, they create no significant level of alternating stress.

2.6.5.1 Vibratory Response Analysis. The RTG Transportation System will consist of a package, as defined in Section 1.0, in addition to an exclusive-use trailer and a shock-isolated skid. To protect the RTG payloads from the effects of over-the-road vibration, the isolated natural frequency of the package and skid will be about 2.5 Hz. Because the lowest natural frequencies of the package components are on the order of 200 Hz, it is possible to treat the package and shock isolation skid as a single degree of freedom, spring-mass system, and inertial response loading may be applied to the package quasi-statically.

Draft ANSI Standard N14.23[22] identifies peak truck trailer vibration inputs. Table 2 of ANSI N14.23 shows peak vibration accelerations of a trailer bed as a function of package and tiedown system natural frequency. For the frequency range 0 to 5 Hz, and conservatively assuming a light package, Table 2 gives peak accelerations (99% level) of $2g$ in the vertical direction, and $0.1g$ in both the lateral and longitudinal directions.

2.6.5.2 Calculation of Alternating Stresses. Section 6.2 of ANSI N14.23 states that the fatigue effects of random vibration can be approximated by using 75% of the constant-amplitude stress. Therefore, the fatigue stress, S_v, on the vessel can be found by applying 75% of the peak acceleration as a constant body force. The vertical acceleration to be applied is given below:

$$2(0.75) = 1.5\ g$$

Because this is virtually identical to the force of gravity itself, and the package is quite rigid, (designed to withstand several hundred g's in impact scenarios), the stresses resulting from this load will be insignificant. A similar conclusion can be reached for the 0.1g lateral and longitudinal loads. A further, significant conservatism is afforded by the fact that, while the values from ANSI N14.23 reflect 3% damping, the isolators used will impart at least 10% damping. This will further reduce the vibrational response of the package.

2.6.6 Water Spray

The materials of construction used for the package are such that the water spray test identified in 10 CFR 71.71(c)(6) will have a negligible effect on the package.

2.6.7 Free Drop

The maximum weight of the RTG Transportation System Package is less than 11,000 pounds. Subpart F of 10 CFR 71 requires a determination of the effect of dropping a package of this weight from a height of 4 ft onto a flat, horizontal, essentially unyielding surface, striking the surface in a position for which maximum damage is expected. Physical testing of a full scale prototype was used to address this 4-ft free drop requirement. Two full-scale prototypes, called certification test articles (CTA-1 and CTA-2), were used during the drop testing program. The first test article (CTA-1) experienced two failures during the first drop test series. The package was subsequently modified and a second test article (CTA-2) was fabricated. All of the 4-ft free drop tests performed on CTA-1 were repeated on CTA-2. Only CTA-1 had active and passive accelerometers. The accelerometer data is included for information only.

The drop orientations for which maximum damage can be assumed are discussed in Appendix 2.10.9.1. These orientations are as follows:

- Bottom-down near-vertical oblique drop
- Bottom-down center of gravity over struck corner
- Side-slapdown drop
- Bottom-down flat end drop
- Top-down flat end drop.

The NCT 4-ft free drops are significant only in the sense that they must not compromise the ability of the package to successfully undergo subsequent 30-ft HAC free drops. Accordingly, for certification testing, each of the above NCT free drops was followed by a HAC free drop impact in the same orientation and impacting at the same initial point of contact.

The results of the NCT free drops on package performance are negligible, particularly in comparison to the results of the HAC free drops. Only CTA-1 was outfitted with active and passive accelerometers as described in Appendix 2.10.15.4.3. Table 2.6.7-1 gives the results for peak acceleration at the c.g. of the package and the status of the passive accelerometers (whether tripped or not) for the NCT free drops that were conducted using CTA-1. Observed containment boundary deformations as a result of the NCT free drops using both CTA-1 and CTA-2 were essentially the same and negligible. The peak acceleration values were less than the corresponding values obtained from the HAC, 30-ft free drops, discussed in Section 2.7.6. More detailed descriptions of the damage for each NCT free drop are recorded, including photographs, in Appendix 2.10.15.

TABLE 2.6.7-1. NCT Free Drop Impact Limiter Deformations and Package Center of Gravity Peak Accelerations for CTA-1.

Drop No.	Description	Impact limiter deformation (in.)	Peak accel. (g)	Passive accel. status		
				200 *g*	300 *g*	400 *g*
1	Near vertical	Negligible	53	No trip	No trip	No trip
2	CG over corner	1.1	69	No trip	No trip	No trip
3	Side-slapdown	1.9	66	No trip	No trip	No trip
4	Bottom down	Negligible	170	Trip	No trip	No trip
5	Top down	Fin damage only	90	No trip	No trip	No trip

With negligible containment boundary deformations and small impact limiter deformations, it is clear that NCT free drops do not substantially reduce the effectiveness of the packaging, either directly as a result of the 4-ft free drops, or indirectly, by compromising the ability of the package to withstand a subsequent HAC sequence. Observed NCT freedrop deformations are modest and completely consistent with NCT thermal shielding and criticality evaluations.

2.6.8 Corner Drop

This test does not apply to the package, because the package weight is in excess of 100 kg (220 pounds) and the materials of construction do not include wood or fiberboard.

2.6.9 Compression

It can be demonstrated that a pressure on the top and bottom of the package equal to five times the package weight produces small stresses. Per 10 CFR 71.71(c)(9), a uniform pressure of the greater of 1.85 psi, or a pressure equivalent to the weight of five packages, shall be applied to the top and bottom of the package. The package weight is 9,600 pounds. The vertically projected area is given below:

$$A = \frac{\pi}{4} D^2 = 1{,}068 \ in.^2$$

where: D = OCV shell outside diameter = 36.88 in.

The pressure created by five packages is:

$$p = \frac{5(9{,}600)}{1{,}068} = 44.9 \ psi$$

This clearly exceeds 1.85 psi and becomes controlling. In the analysis, a conservative value of 50 psi will be used.

Using the same finite element model for the OCV as that used in Section 2.6.1, the stresses in the OCV bell because of the application of 50 psi can be found. The pressure was assumed to be applied uniformly to the OCV torispherical head area, and the bottom of the package is vertically fixed, in order to react the compressive load. Internal pressure is conservatively assumed to be zero. Temperatures from Case 1 are included in the analysis, taken from Section 3.6.4. The maximum local membrane stress intensity is 7,626 psi, classified as P_L because it occurs in the OCV head knuckle area. Similarly, the maximum sum of membrane plus bending stress is 8,331 psi at the same location, but classified as a $P_L + P_b + Q$ (secondary) stress, once again, because of its location in the knuckle. From Tables 2.1.2-1 and 2.3-1, the allowable for P_L is 25,050 psi, and for $P_L + P_b + Q$ the limit is 50,100 psi, for temperatures lower than 300 °F. For the OCV head, the maximum temperature is below 300 °F. The margin of safety on local membrane stress is:

$$M.S. = \frac{25{,}050}{7{,}626} - 1 = +2.28$$

The margin of safety on the sum of local membrane and bending stress in the knuckle is given below:

$$M.S. = \frac{50{,}100}{8{,}331} - 1 = +5.01$$

To confirm structural stability, a buckling analysis is performed on the OCV for the maximum anticipated compression load of (50 psi)(1,068 in.^{2}) = 53,400 pounds. For analysis purposes, the

stiffening effects of the cooling jacket are conservatively ignored. Additionally, an elevated temperature of 350 °F is conservatively assumed. For the basic OCV shell, the axial and hoop compressive stresses associated with the 53,400 pound external load are calculated below:

$$\sigma_\phi = \frac{P}{2\pi Rt} = 934.5 \; psi$$

$$\sigma_\theta = \mu\sigma_\phi = 280.4 \; psi$$

where:
- σ_ϕ = axial compressive stress
- σ_θ = hoop compressive stress (at restrained ends of cylindrical shell)
- R = shell mean radius = 18.19 in.
- t = shell thickness = 0.50 in.
- P = external load = 53,400 lb
- μ = Poisson's ratio = 0.3.

At these low stress magnitudes, resulting plasticity reduction factors from Section 1610 of ASME B&PV Code Case N-284 are equal to unity. Hence, inelastic buckling checks are not required. Consequently, the buckling analysis requires only a determination of theoretical buckling stress values. The results can then be compared to the above actual, calculated stress values, with capacity reduction factors and appropriate factors of safety (FS = 2.0 for NCT) applied. If the theoretical buckling stresses are greater than the adjusted actual stress values, then buckling will not occur.

From Section 1511 of Code Case N-284, the appropriate capacity reduction values are determined to be as follows:

$$\sigma_{\phi L} \; (axial \; compression) = 0.207$$

$$\sigma_{\theta L} \; (hoop \; compression) = 0.800$$

from which adjusted actual stress values can be determined:

$$\sigma_{\phi s} = \frac{\sigma_\phi \times FS}{\sigma_{\phi_L}} = 9{,}029 \; psi$$

$$\sigma_{\theta s} = \frac{\sigma_\theta \times FS}{\sigma_{\theta_L}} = 701 \; psi$$

From Section 1712 of Code Case N-284, the theoretical buckling values for an effective OCV free length of 56 in. are determined to be as follows:

$$\sigma_{\phi L} \text{ (axial compression)} = 444{,}914 \text{ psi}$$

$$\sigma_{\theta L} \text{ (hoop compression)} = 37{,}725 \text{ psi}$$

Comparison of results indicates:

$$M.S. \text{ (axial)} = \frac{444{,}914}{9{,}029} - 1 = +Large$$

$$M.S. \text{ (hoop)} = \frac{37{,}725}{701.0} - 1 = +Large$$

Consequently, buckling of the OCV shell will not occur.

The buckling analysis of the OCV torispherical head follows the procedure outlined in Section 2.7.5 for HAC, except that the 150% increase in allowable stress is not applied. Therefore, an allowable pressure for NCT can be obtained by dividing the value of 140 psig obtained for HAC by the factor of 1.5 as follows:

$$P_a = \frac{140}{1.5} = 93 psi$$

Thus, the margin of safety is:

$$M.S. = \frac{P_a}{P} - 1 = \frac{93}{50} - 1 = +0.86$$

Thus, the margins of safety on buckling are all positive.

2.6.10 Penetration

The 40-in. drop of a 13-pound, spherically headed, 1.25-in.-diameter steel bar is of negligible consequence to the package. This is because the package has been designed to minimize the consequences associated with the much more limiting case of a 40-in. drop of the entire package onto a puncture bar (see Section 2.7.2). The containment boundary is a smooth, curved steel surface, without any fragile features that could be damaged by the bar. The vent and test port plugs and electrical feed-through assemblies are protected by the impact limiter. Some slight denting of the coolant jacket (0.14 in. thick) or the impact limiter (0.25 in. thick) outer shells might possibly occur, but would have no effect on package operation or effectiveness. Thus, no damage of any consequence will result from this test.

2.7 HYPOTHETICAL ACCIDENT CONDITIONS

The RTG Transportation System Package, when subjected to the sequence of HAC events specified in 10 CFR 71.73, must meet the performance requirements specified in Subpart E of 10 CFR 71. With the exception of the Thermal and Immersion tests, the primary proof of performance for HAC is via the use of full-scale testing. These requirements, as specifically related to the objectives of the certification test program, may be summarized as follows:

1. No loss of containment: Leaktightness of both containment boundaries (i.e., less than 1×10^{-7} std cc/sec air) will be maintained throughout the sequence of tests (see Section 4.0). Additionally, no deformations will be induced that would lead to degradation of containment under the subsequent HAC fire event (see Section 2.7.3).

2. Maintenance of adequate biological shielding capability: The ability of the package system to satisfy the post-HAC dose rate criterion of 1,000 mrem/hr at 1-m from the package will not be compromised (see Section 5.0).

3. Maintenance of subcritical payload: No post-test conditions will exist that would result in a transformation of any payload into a supracritical state (see Section 6.0).

For additional details regarding the structural certification testing performed, see Appendix 2.10.9. Results of the certification free drop testing are presented in Appendix 2.10.15 and summarized in Section 2.7.2.3. Analyses are presented where necessary to supplement or expand on the test results. The HAC Thermal and Immersion tests are addressed herein by analysis.

2.7.1 Free Drop

Subpart F of 10 CFR 71 requires that a 30-ft HAC free drop be considered for the RTG Transportation System Package. The free drop is to be onto a flat, horizontal, essentially unyielding surface, and the package is to strike the surface in a position for which maximum damage is expected. The ability of the package to adequately withstand this specified HAC free drop condition is demonstrated by testing a full-scale prototypical package. Section 3.0 of Appendix 2.10.9 presents the configuration details of the Certification Test Articles (CTAs).

As noted in Appendix 2.10.15, two CTAs were used. The first CTA experienced two failures during testing. The package design was subsequently modified and a second CTA was fabricated. All of the 4-ft and 30-ft free drop tests performed on the first CTA (CTA-1) were repeated on the second CTA (CTA-2).

2.7.1.1 Identification of Worst-Case Drop Conditions. For both the NCT and HAC free drops, it is required that the package strike the essentially unyielding surface "in a position for which maximum damage is expected." Because of the relatively high structural strength of the package containment vessels, the possibility of any impact-induced structural deformation being great enough to adversely affect shielding capability and/or criticality control is considered to be negligible. Results of the half-scale developmental free drop testing affirm this conclusion (see Appendix 2.10.11). Therefore, in determining which free drop orientations would satisfy the regulatory "worst damage" requirement, attention was focused predominantly on the issue of containment. A detailed discussion of free drop test rationale is given in Appendix 2.10.9 and is summarized below.

Loss of containment could potentially occur either directly as a result of free drop impact

loading, or indirectly, because of impact-induced damage that might lead to degradation of sealing capability in the subsequent HAC fire event.

For the first case (direct damage), the following possibilities must be considered:

1. Loss of sealing capability because of seal area structural deformations.
Seal area structural deformations might arise from impact forces that could bend the OCV flange and distort the seal area surfaces. HAC free drop orientations in which the impact force must first pass through the OCV flange before being distributed throughout the rest of the package present such a possibility. Variations in free drop orientation entail variations in both impact force and in the extent of the OCV flange that absorbs the force. A center of gravity-over-impacted corner drop represents large impact forces (because no energy is converted to package rotation) and simultaneously represents a case where the total force must pass through a small portion of the OCV flange. Other orientations are also identified that could impart distorting forces to the OCV flange seal areas. One is a bottom-down drop where, because of the stiffness of the impact limiter in this particular orientation, the greatest overall impact forces are expected. However, because the entire OCV flange is essentially evenly loaded, less potential for flange bending is expected. Another is a side-slapdown drop, where even though the impact is directed at the relatively strong edge of the flange, some potential for flange distortion exists.

2. Loss of sealing capability of the electrical feed-through connectors.
The seal between the electrical feed-through body and the electrical pins would be affected primarily by inertia forces along the axis of the pins. The bottom-down drop mentioned above, in which maximum overall impact forces are expected, would subject the electrical feed-through pins to worst-case forces along their axes, since the ICV electrical feed-through orientation is parallel to the drop axis. Impact forces are also applied both perpendicular and oblique to electrical feed-through pin axes in the c.g.-over-corner and side-slapdown drops mentioned above.

3. Rupture of containment.
The only potential for rupture of containment shells in a HAC free drop would arise from payload-vessel interaction. Therefore, a simulated payload was included during free drop testing, which besides properly simulating the weight and c.g. of the worst-case payload, also incorporated conservatively strong, square-cornered fins. Further, the top of the simulated payload that faces the ICV head is an open-ended, 14 in. O.D., 0.50-in.-thick steel pipe. The worst case interaction of payload and ICV head would occur in a top-down drop, because the ICV head is 0.37-in. thick, whereas the ICV sidewall is 0.75-in. thick.

4. Separation of either or both bell assemblies from their respective bases (i.e., closure bolt failure). The only likely HAC free drop orientation that could induce a separation loading on the closure bolts and lead to physical separation of a bell from a base would be a side-slapdown impact. All other impact orientations would have the effect of driving the base onto the bell, or vice versa. This effect is included in the side-slapdown orientation discussed above. Because of flange and baseplate design, no closure bolt shear load is possible in any orientation.

The thermal analysis for the HAC fire event depends on the insulating presence of the impact limiter and shipping rack assembly to protect the containment seals for the duration of the fire. Consequently, the following must also be considered to determine worst-case free drop orientations:

5. Loss of impact limiter.
In a bottom-down, near vertical free drop, separation loads on some of the limiter attachment bolts can occur. The initial impact forces at the outside edge of the limiter, using the near corner of the package as a fulcrum, cause tensile reaction forces on the limiter attachments on the far side of the package. These forces are maximized for a package free drop of 10° from the vertical using a circumferential orientation that places an impact limiter attachment bolt 180° from the point of impact.

6. Excessive impact limiter damage.
Maximum impact limiter deformation can be expected for the c.g. over impacted corner orientation, because considerable "stroke" is required before significant amounts of polyurethane foam are mobilized to absorb the free drop kinetic energy. The same effect would be found in the side-slapdown free drop, though to a somewhat lesser extent, because of energy dissipation in the top end fins. Both cases can be addressed by the free drop orientations discussed above.

7. Separation of payload shipping rack assembly from inner vessel base.
The top-down and side-slapdown free drops impose maximum tensile and shear loads on the shipping rack assembly-to-ICV base attachments and on the payload attachments. These free drops thus demonstrate shipping rack assembly retention.

2.7.1.2 Pressure. In addition to package orientation, test pressures and temperatures must also be selected to complete the definition of the conditions existing at the time of a HAC 30-ft free drop test. The maximum package normal operational internal pressure, conservatively taken to be 30 psia (see Section 2.6.1.1), is insignificant from a structural standpoint (see Tables 2.6.1.3-2, Case ICV-P, and 2.6.1.3-3, Case OCV-P). Therefore, full-scale structural certification testing was performed with the package certification test article (CTA) interior filled with air at the ambient atmospheric pressure.

2.7.1.3 Adjustments for Ambient Temperature. In going from regulatory maximum temperatures (maximum payload heat generation, 100 °F ambient temperature, no active cooling, with solar loading applied) to the regulatory minimum (-20 °F ambient, no payload heat, no solar loading), the strength of the impact limiter increases more rapidly than that of structural components, primarily because of the influence of the polyurethane foam. See Section 2.3 for a discussion on the temperature-dependent nature of the mechanical strength of polyurethane foam.

Thus, maximum structural effects because of impact reaction loading can generally be expected at minimum temperature conditions, where loads will be greatest relative to containment component structural strength. Because of its relatively lower strength at higher temperatures, the impact limiter will undergo the greatest deformations at maximum temperature conditions. Because certification testing was carried out at the prevailing ambient temperature, adjustments were made to conservatively account for the variation in impact limiter reaction loads and deformations over the anticipated operational temperature range.

For the low temperature extreme, at which maximum impact loads were expected, the impact limiter was artificially stiffened to match worst-case production unit impact limiter characteristics at -20 °F. To accomplish this, polyurethane foam at a higher density than the nominal value of 12 lb/ft^3 was used in the impact limiter. As explained in Section 2.3, the mechanical strength of polyurethane foam increases in proportion to its density. As also explained in that section, the mechanical strength of the foam increases in proportion to a decrease in its temperature. It was therefore possible to select a foam density that would be as stiff at ambient (test) temperature as the production unit (12 lb/ft^3) would be at its minimum operational temperature of -20 °F. The substitute density is approximately 15.5 lb/ft^3. A comparison of the

mechanical properties of the two foams is given in Figure 2.3-2. The data for the 15.5 lb/ft^3 test foam is the average strength of the foam actually used in the CTA impact limiter in the perpendicular to rise orientation at room temperature. The corresponding data for production unit foam (from Table 2.3-4) is for high-limit strength, 12 lb/ft^3 density, and -20 °F. Note that this procedure conservatively overestimates impact effects on the containment structures, because the relative strength of the structure is less at the test temperature than it would be at the -20 °F temperature for which impact loads were simulated.

To conservatively account for the effects of increased temperature on impact limiter deformations, a simplified analytical approach is used determine impact limiter response to various temperature conditions. For this analysis, total energy absorption of the impact limiter is divided into the strain energy arising from deformation of the stainless steel outer shell and strain energy arising from deformation of the polyurethane foam. The approach is described in Section 4.1.3.2 of Appendix 2.10.9. This methodology will establish worst case impact limiter deformations that will correspond to the highest environmental and payload temperatures at the time of the HAC free drop.

2.7.1.4 Identification of Specific Drop Tests to be Performed. Based on the above general discussions, five specific HAC 30-ft free drop tests have been selected for inclusion in the certification test program. Although only a single worst case HAC 30-ft drop is required by the Regulations, all five tests will be performed to ensure that the most vulnerable package features are subjected to worst case loads/deformations. The free drop tests were performed in the following order:

1. Bottom-down near-vertical oblique free drop, at 10° from the vertical, with an impact limiter attachment bolt located 180° away from the point of impact. Addresses impact limiter retention.

2. Bottom-down c. g. over impacted corner, with the electrical feed-through oriented at the point of impact (0°). Addresses localized seal area structural deformations, specifically including electrical feed-through location; also impact limiter maximum deflections.

3. Bottom-down flat end free drop. Addresses seal area structural deformations; ICV electrical feed-through connector pins parallel to their axes; maximum overall impact levels.

4. Side-slapdown free drop, with electrical feed-through oriented at 90° from the point of impact. Package axis at 18° to horizontal with fins contacting ground first. Addresses seal area structural deformations; closure bolt rupture; ICV electrical feed-through connector pins, perpendicular to their axes; separation of shipping rack assembly from ICV baseplate and impact limiter damage.

5. Top-down flat end drop. Addresses separation of shipping rack assembly from ICV baseplate; rupture of containment because of interaction with loose payload.

These free drop orientations are shown schematically in Figure 1 of Appendix 2.10.9.2. Rationale for the choice of drop angles for free drop Nos. 1 and 3 is given in Section 4.1 of Appendix 2.10.9.1. These drops will be preceded by the same series of NCT free drops from a height of 4-ft, as described in Section 2.6.7.

2.7.1.5 Summary of Results from Free Drop Tests. The discussion of the results of HAC free drops is combined with that of HAC puncture drops and is presented in Section 2.7.2.3.

2.7.2 Puncture

Subpart F of 10 CFR 71 requires that a 40-in. free drop of the RTG Transportation System Package onto the upper end of a solid, vertical, cylindrical, mild steel (puncture) bar mounted on a horizontal, essentially unyielding surface be considered. The puncture bar must be 6 in. in diameter, with the top surface horizontal and its edge rounded to a radius of not more that 0.25 in. The package must be oriented in a position for which maximum damage is expected, and the length of the puncture bar is to be such that maximum damage will occur. The minimum length of the puncture bar must be 8 in.

The ability of the package to adequately withstand this specified puncture condition was demonstrated by testing two full-scale package CTAs. Before the puncture tests, the CTAs were subjected to the full range of NCT and HAC 4- and 30-ft drops. Puncture tests were typically directed through the center of gravity at the regions of the package damaged by the preceding 30-ft free drops. This is consistent with 10 CFR 71.73(a), which requires that puncture be considered subsequent to the HAC free drop condition.

2.7.2.1 Identification of Worst-Case Puncture Conditions. To properly select a worst-case set of puncture conditions, items that would potentially compromise the integrity of the package must be clearly identified. The primary item to be addressed is the potential for loss of containment. Such a possible failure mode could arise directly, because of the actual puncture bar impact on the containment components, or indirectly, by inducing damage that would compromise the ability of the package containment seals or electrical feed-through connectors to survive the subsequent HAC fire event. Accordingly, the following worst-case possibilities were identified:

1. Loss of sealing capability because of seal area structural deformations.
   Structural deformations in the seal area could arise from puncture impacts on the impact limiter where the puncture bar is aimed at the OCV flange region. Other orientations with potential to cause seal area deformations would be impacts on the side of the OCV wall and on the top of the OCV thermal shield. In each case, direct impact between the puncture bar and the OCV flange is impossible because of the presence of intervening structure, i.e., the impact limiter, the coolant jacket, or the thermal shield. For the worst-case interaction with the impact limiter, the puncture bar should impact directly on previous free drop damage.

2. Loss of sealing capability of the electrical feed-through connectors.
   Loss of sealing capability of the electrical feed-through connectors would be unlikely to occur unless the puncture bar contacted at or near the electrical feed-through connector itself. The ICV electrical feed-through connector is well protected by surrounding structure and is not susceptible to damage from the puncture bar. The electrical feed-through OCV connector is protected by the impact limiter side thickness. As long as the puncture bar cannot penetrate the impact limiter shell, no damage to the electrical feed-through connector can accrue from a puncture event. Prevention of penetration can be demonstrated by a puncture aimed at the side of the impact limiter.

3. Rupture of containment.
   The only portion of the OCV bell not protected by either the fins, the thermal shield, or the cooling jacket is the top of the OCV torispherical head. Therefore, rupture of containment is unlikely. This can be demonstrated by a near vertical, top down puncture drop on the region of the OCV head not covered by doubler plates, and by oblique impact of the bar on the coolant jacket ribs.

4. Separation of either or both bell assemblies from their respective base plates.
   Separation of either or both bell assemblies from their respective base plates is also

considered unlikely to arise because of a puncture event, because no puncture bar impact orientation could produce a significant separation load on the CTA closure bolts. Additionally, puncture impacts entail significantly reduced energy compared to the HAC free drops, and would therefore be much less likely to induce closure separation.

5. Loss of thermal protection.
Loss of thermal protection would occur if the impact limiter was separated from the package. The limiter would be subjected to worst-case pry-off forces in a top-down free drop, where the puncture bar contacts the outer top surface of the impact limiter.

On a smaller scale, loss of thermal protection could occur because of penetration of the puncture bar through the impact limiter in the seal region, thus opening up a thermal path to the seals or electrical feed-through connectors. Deep penetration of the puncture bar could result in tear-out of foam as the package rotates off the bar. Likewise, impingement of the puncture bar onto the thermal shield could render it ineffective in providing a thermal barrier for the HAC fire event.

2.7.2.2 Identification of Puncture Tests to be Specifically Performed. Considering the discussions provided above, eleven specific puncture tests were selected. As noted in Section 2.7.1, two CTAs were used during the course of the package certification testing effort. Nine punctures were performed on CTA-1. For CTA-2, four of these punctures were repeated and two new punctures were performed. The selected puncture orientations are shown schematically in Figure 6 of Appendix 2.10.9.1 and Figure 2 of Appendix 2.10.9.2. Although only a single worst-case, 40-in. drop onto a puncture bar is required by the Regulations, all eleven tests were performed to ensure that the most vulnerable package features are actually subjected to worst-case puncture bar impacts. All puncture drops (except Nos. 7, 8, and 9 for CTA-1 and No. 7 for CTA-2) were performed with the puncture bar oriented toward the package c.g., because this maximized impact damage to the CTA. As with the free drop tests, all puncture tests were performed at the prevailing ambient temperature and without pressure in the containment vessels.

For punctures on the impact limiter, the impacted surface will generally be aligned to be at an angle to the puncture bar. As demonstrated in the half-scale engineering development tests, Appendix 2.10.11, as well as certification testing of the TRUPACT II, NRC Docket 71-9218, this will tend to maximize the potential for rupture of the impact limiter shell, as well as consequent tear-out of foam as the package rotates off the puncture bar.

A summary of planned HAC puncture tests is as follows:

1. Impact on the previous c.g. over impacted corner 30-ft free drop damage. The orientation of the electrical feed-through area also corresponds to this damage. Addresses seal area structural deformations, and loss of thermal protection because of excessive impact limiter damage.

2. Impact on the bottom surface of the impact limiter near the outer edge of the region backed by the lower-density foam. Addresses loss of thermal protection because of excessive impact limiter damage.

3. Side impact on the impact limiter, puncture bar axis directed at the OCV vent port feature. Addresses seal area structural deformations and loss of thermal protection because of excessive impact limiter damage.

4. Impact on the side surface (coolant jacket) of the package, just above OCV thermal shield, oriented to correspond to the electrical feed-through location. Addresses seal

area structural deformations.

5. Oblique impact on the side surface (coolant jacket), package oriented top down with its axis at 45° to the puncture bar axis. Impact point will be 45° CCW from the electrical feed-through location, viewed from finned end. Addresses damage that may occur because of puncture impact on coolant jacket ribs.

6. Top-down, near-vertical, package oriented at 9° to the vertical axis. The impact point is located 225° CCW from the electrical feed-through, viewed from above. This impact point is as close as possible to the center of the OCV head, while not contacting the region that is reinforced by the over-the-top doubler plates. The drop height will be measured from the position of the personnel barrier, but for conservatism, the barrier will not be present. Addresses potential for rupture of the OCV head.

7. Top-down package orientation, impact on the top surface of the impact limiter. Impact point is at 150° CCW from the electrical feed-through, in alignment with an impact limiter attachment bolt. Addresses loss of thermal protection because of loss of impact limiter.

8. Top-down package orientation, impact on the top surface of the thermal shield, with the puncture bar axis at 30° to package axis, aimed at the corner between the thermal shield and the coolant jacket. Initial contact of edge of puncture bar to be 1 in. inboard of the outer edge of the thermal shield, equidistant between two OCV closure bolt tubes. Addresses seal area structural deformations; loss of thermal protection because of thermal shield damage.

9. Top-down package orientation, impact directly on an impact limiter attachment bolt access tube. Addresses potential for distortion of the OCV flange due to the transmission of impact force through the tube.

10. Side impact on impact limiter through the package c.g., edge of puncture bar aligned with the impact limiter lower corner joint weld seam. This will subject the weld to shearing loads since the impact limiter corner angle is somewhat stiffer than the sidewall.

11. Side impact on impact limiter through the package c.g., edge of puncture bar aligned with center of one of the plastic melt plugs. This will subject this weld area to a shearing load and will try to rupture the impact limiter side wall.

More detail concerning certification drop testing is found in Appendix 2.10.9.

2.7.2.3 Results of Free Drop and Puncture Tests. Testing of two full-size certification test articles indicates that the package can withstand the HAC free drop and puncture events. The first acceptance criterion, that of a leaktight condition (1×10^{-7} scc/sec, air or less), was met by the OCV and ICV of the second certification test article (CTA-2). Leakage rate tests performed on both the containment boundary butyl O-ring seals and the remainder of the containment boundary (including the electrical feed-through) after the NCT free drops and HAC free drops and punctures demonstrate that the leaktight criterion was satisfied by both the ICV and OCV.

In addition to leakage rate testing, measurements of compression of the containment O-rings subsequent to the complete test sequence was made (see Appendix 2.10.14). These measurements demonstrated minimal reduction in O-ring compression because of the combination

of all NCT and HAC free drop and HAC puncture events. These measured reductions in compression were added to the calculated reductions in O-ring compression because of thermal distortion. For the worst-case configuration, the maximum measured compression reduction was assumed to occur at the same location as the maximum calculated reduction because of thermal distortion, and the two values were added. For both the ICV and OCV, resultant minimum O-ring compressions did not fall below the minimum value used in qualifying the O-ring material. These material tests (see Appendix 2.10.6) demonstrated the ability of the butyl material used for the containment O-rings (Rainier Rubber compound RR0405-70) to maintain a leaktight seal at lower values of compression and at higher temperatures than are predicted for the HAC fire event. The thermal analysis assumptions regarding the extent of impact limiter deformation and the observed retention of the limiter and shipping rack assembly (that insulate the seal areas) were validated. Thus, leaktight boundaries will be maintained after the sequence of NCT free drops, HAC free drops and punctures, and the HAC fire event.

The second acceptance criterion, maintenance of adequate biological shielding capability (see Section 2.7), is met because the worst case reconfigured and concentrated radioactive material may be placed in contact with the thinnest portion of the containment boundaries (the torispherical heads) without exceeding the applicable limits of 1,000 mrem/hr at a distance of 1-m.

The third acceptance criterion, maintenance of subcritical payload, is also met, because similarly reconfigured and concentrated payload, when optimally moderated, remains in a subcritical condition (see Section 6.0). Both of the latter two acceptance criterion are completely unaffected by any permanent deformations of the package containment boundaries that could result from HAC free drops and punctures.

2.7.3 Thermal

During the HAC event sequence, the package will be exposed to fire conditions as described in 10 CFR 71.73(b)(3). This will increase the temperature and pressure of the gas within the ICV and the gas within the annulus between the ICV and OCV. The most critical stress state will occur at the highest package temperature, because the material allowables will be lowest at that time. The maximum gas pressure will be assumed to coincide with the peak temperatures of the package. This ensures the conservatism of the analysis. Furthermore, the maximum possible amount of decomposition gas from the electrical cable insulation included with the payload will be assumed to be added to the gas already within the ICV. Finally, to ensure the minimum required amount of O-ring seal compression is maintained, the thermal expansion stresses in the closure bolts will be examined to ensure they do not exceed yield as a result of the HAC fire temperatures. Thermal distortions of the adjacent seal surfaces are quantified in Section 4.0, again to ensure that sufficient compression remains for leaktight seals.

2.7.3.1 Summary of Pressures and Temperatures. The stress and deformation analyses in this section use the temperatures listed in Section 3.6.5. Because the 30-ft free drop must precede the fire in the prescribed HAC sequence, the possibility of payload structural failure and release of the heat-producing modules has been considered. A review of payload structural design identified the GPHS RTG as possessing a potential for reconfiguration in certain 30-ft free drop orientations. Analysis of the GPHS RTG by its manufacturer (General Electric) established that the minimum size component containing a heat source that could possibly result from the reconfiguration would be the rectangular aeroshells. These components, which are 97.2 mm by 92.4 mm by 53.1 mm, are designed to withstand atmospheric re-entry. Because the worst-case reconfiguration of the GPHS RTG is conservatively assumed (i.e., release of all aeroshells into the ICV), and because the GPHS RTG represents the highest heat payload, consideration of the other payloads is unnecessary.

2.7.3.1.1 Packaging Temperatures. The temperatures listed result from an analysis where conservative assumptions are used concerning the post-HAC reconfiguration of both the packaging and the GPHS RTG payload. According to 10 CFR 71, post-HAC fire ambient temperature is identical to pre-HAC fire temperature (i.e., either -20 or 100 °F), insolation is zero, and no active cooling is assumed. HAC fire temperatures will be a function of the external package deformation, principally of the impact limiter, and of the reconfiguration of the payload internal to the package.

2.7.3.1.1.1 Packaging External Deformation Effects. The post-HAC free drop packaging reconfiguration of greatest interest will primarily involve deformations to the polyurethane foam-filled impact limiter on the bottom end of the package. This is because the impact limiter acts as a thermal insulator in the seal area during the HAC fire event, and thus provides an additional level of protection for the containment seals. Maximum impact limiter deformations in the vicinity of the closure seal flanges because of 30-ft free drops and subsequent 40-in. puncture bar impacts could be expected to arise from two free drop orientations:

- Bottom-down oblique orientation, with the package center of gravity over the impacted corner (CTA-2 test No. 4).

- Side slapdown impact, defined for the package as the near-simultaneous impact of the top-end fins and the bottom-end impact limiter (CTA-2 test No. 12).

Accordingly, both configurations have been evaluated for thermal response in the HAC fire. The effect of char and void space formation are included as detailed in Appendix 3.6.3. Thermal analysis described in Section 3.5.2 indicates that the highest seal temperatures resulted from side slapdown impact damage. Consequently, all analyses use this package reconfiguration geometry. Further, worst-case impact limiter deformations will arise from initial conditions that produce the highest temperatures for the polyurethane foam in the impact limiter (i.e., foam temperatures arising from maximum payload heat, combined with the maximum regulatory ambient temperature of 100 °F and regulatory solar loading). Determination of worst-case impact limiter deformations that would be expected at maximum foam temperatures was accomplished by analytical modification of the ambient temperature impact results obtained from the certification drop testing. The amount of foam exposed by the puncture bar in CTA-2 Test No. 16 was approximately 12.7 in^2. This area is quite small relative to the area of the impact limiter and, because of the intumescent behavior of the pulyurethane foam material (see Reference 10 of chapter 3), the opening will be effectively closed during the HAC fire event. Using the approach detailed in Section 4.1.3.2 of Appendix 2.10.9, the impact limiter deformations for each of the two orientations above at maximum temperature conditions are calculated as follows.

As discussed in Section 2.7.1.3, the impact limiter foam strength for use in the free drop tests (at ambient temperature) was selected to have a value slightly in excess of the maximum strength of the production unit foam when at a temperature of -20 °F. The measured post-impact deflections of the impact limiter represent minimum values. The corresponding maximum deflections are functions only of the minimum deflections and of the maximum pre-impact foam temperatures. As described above, these pre-impact conditions correspond to maximum payload heat, 100 °F ambient, and regulatory insolation, without active cooling (i.e., Case 1 of Section 2.6.1). These foam temperatures are given in Section 3.6.4. For purposes of calculation, a volume-weighted average temperature will be used. This is conservative for maximum deflection, because the foam that actually crushes is located in the outer portions of the impact limiter, where temperatures are below the average value.

Each nodal temperature in the impact limiter foam region corresponds to an annular volume. The volume-weighted temperature is found by multiplying each nodal temperature by its corresponding annular volume, summing all such products, and dividing the sum by the total foam

volume. Only the stronger, 12 lb/ft³ foam is included, because the 3 lb/ft³ foam is not active in the two orientations of interest defined above. Figure 2.7.3.1.1.1-1 illustrates the correspondence of node number to location in the model, and the dimensions from which each annulus volume can be calculated. For example, the annulus corresponding to thermal node Nos. 431, 432, and 433 has an o.d. of 59.3 in., an i.d. of 54.2 in., and a thickness of 3.04 in. The volume is given below:

$$\frac{\pi}{4}(59.3^2 - 54.2^2)(3.04) = 1382\ in.^3$$

The total volume of 12 lb/ft³ foam is 34,110 in³. Using the method just described, and impact limiter foam temperatures from Section 3.6.4, the maximum pre-impact, volume-weighted temperature of the 12 lb/ft³ foam is 152 °F. A value of 160 °F will be conservatively used. Given the pre-impact maximum foam temperature, it is now possible to determine the foam plateau crush strength. From Table 2.3-4, the lower-limit crush strength at a strain of 25% (the approximate plateau), perpendicular to rise, and at a temperature of 160 °F is 341 psi. (This value represents the minimum for the average of all samples and is equal to 90% of the table values.) From Figure 2.3-2, the plateau strength (also at 25% strain) of the foam used in the CTA was 755 psi.

A. Side Drop Damage

Although the side drop crush deflection of the impact limiter was not uniform over the limiter length, the maximum value will be used over the entire length of the limiter. This conservatively accounts for additional puncture drop damage. From Section 2.7.6 the maximum radial deflection

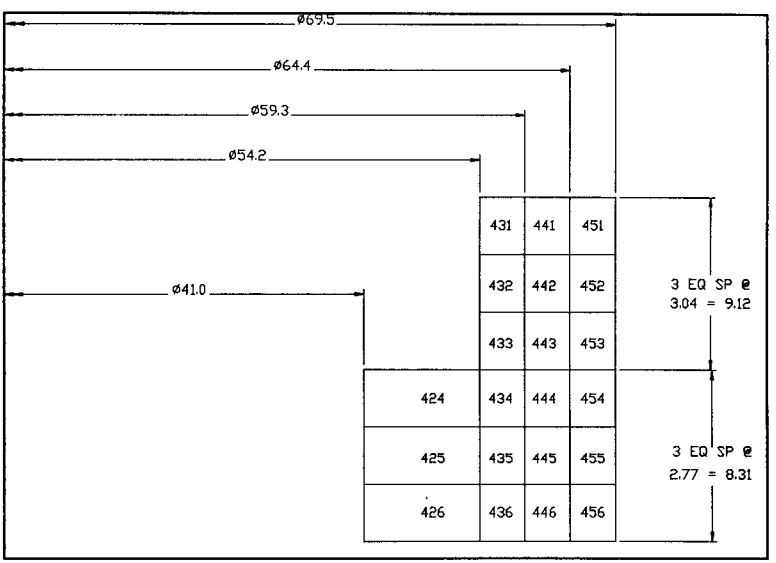


FIGURE 2.7.3.1.1.1-1. Impact Limiter Foam Thermal Node Relationships.

from the fourth HAC-free drop (CTA-2 test No. 12, side-slapdown) was 4 in. This value resulted from the full series of HAC free drop and puncture events. The first step in the modification of this value to reflect maximum temperature is to determine the energy absorbed by the impact limiter shell, from which the average force per unit length of the crumpled impact limiter shell can be derived. The energy absorbed by the impact limiter shell is given below.

W_s = total drop kinetic energy - W_f, where W_f is the energy absorbed by the foam.

W_f is equal to the product of crushed foam volume and foam plateau strength. The crushed volume is given below:

$$V = \ell \left[\frac{1}{2}(R)^2(2\theta - sin2\theta)\right] = 1{,}534 \ in.^3$$

where: ℓ is 17.438 in. (length of foam in impact limiter)
R is 34.75 in. (outside radius of foam in impact limiter)
θ is half the included angle of the impact surface, found from:

$$\theta = cos^{-1}\left[\frac{R - \delta}{R}\right] = 27.76°$$

where: δ is the radial crush deflection, 4 in.

The crush footprint area is given below:

$$A = 2\ell R sin\theta = 564.5 \ in.^2$$

The energy absorbed by the foam is then 1,158,170 in-lb, which is the product of the plateau strength of the test foam of 755 psi and the crushed volume of 1,534 in.^{3} found above. The energy absorbed by the impact limiter shell is given below:

$$W_s = (M)(360+\delta) - W_f = 2.336(10^6) \ in.-lb$$

where: M is package weight, 9,600 lb
δ is 4.0 in.
W_f is 1,158,170 in.-lb.

The average force per unit length of the impact limiter shell is:

$$f = \frac{W_s}{A} = 4{,}138 \ lb/in.$$

This value corresponds to ambient test temperature. It must be adjusted to reflect maximum temperature conditions. From Appendix 2.10.7, Table 2.10.7.1-2, the average temperature of the

active parts of the impact limiter shell (nodes 406, 408, and 410) will be conservatively taken as 150 °F. From Table 2.3-1, the ratio of yield strength of the shell material at 150 °F to the strength at ambient temperature (75 °F) is 0.926, where ASTM Type 304L data is used in place of ASTM Type 304 data. The force per unit length of the impact limiter shell at maximum temperature conditions is given below:

$$f = 0.926(4{,}138) = 3{,}832 \ lb/in.$$

The following equation can now be solved for the radial crush deflection, δ, at maximum temperature conditions:

$$M(360+\delta) = fA(\delta) + sV(\delta)$$

where: M is 9,600 lb
f is 3,832 lb/in.
s is 341 psi (12 lb/ft^3 foam crush strength at maximum temperature conditions)
$A(\delta)$ is footprint area, a function of δ, same as shown above
$V(\delta)$ is crushed volume, a function of δ, same as shown above.

Solving iteratively, the maximum crush deflection, δ, is 5.9 in.

B. C.G. Over Corner Damage

This type of damage results from the c.g. over corner orientation. From Section 2.7.6, the maximum deflection along the line of crush from the second HAC free drop (CTA-2 test No. 5, c.g. over corner) was 5.5 in. This value resulted from the full series of HAC free drop and puncture events. As in the case of radial damage, the force per unit length of impact limiter shell must first be calculated.

The damaged volume in this case is an ungula of a right circular cylinder. Figure 2.7.3.1.1.1-2 shows the definition of the crush, δ, as well as the pertinent angles of the ungula. The volume is found from the following series of calculations:

$$\theta = \cos^{-1}\left[\frac{R - 1.24\delta}{R}\right] = 36.51°$$

$$H = 1.7\delta = 9.35 \ in.$$
$$c = R - 1.24\delta = 27.93 \ in.$$
$$a = R \sin\theta = 20.67 \ in.$$

$$V = \frac{H\left[a(R^2 - \frac{1}{3}a^2) - R^2c\theta\right]}{R - c} = 728 \ in.^3$$

where: θ = half the included angle of the ungula on the impact limiter base

H = the height of the ungula on the outer cylindrical surface
c and a are intermediate parameters
R = impact limiter foam radius, 34.75 in.
V = crushed volume, in.^{3}
δ = 5.5 in.

$$1.7 = \frac{1}{\sin 36^\circ}$$

$$1.24 = \frac{1}{\sin 54^\circ}$$

The footprint area of contact is the upper surface (partial ellipse) of the ungula. It is found from the following:

$$A = \frac{\pi(1.7R^2)}{2} - R\left[(1.7R - 2.1\delta)\left[1 - \left[\frac{1.7R - 2.1\delta}{1.7R}\right]^2\right]^{0.5} + 1.7R\sin^{-1}\left[\frac{1.7R - 2.1\delta}{1.7R}\right]\right] = 325\ in.^2$$

R and δ are as described above. The energy absorbed by the foam is then 549,640 in.-lb, which is the product of the plateau strength of the test foam of 755 psi and the crushed volume of 728 in.^{3} found above. The energy absorbed by the impact limiter shell is given below:

$$W_s = (M)(360 + \delta) - W_f = 2.959(10^6)\ in.\text{-}lb$$

where: M = package weight, 9,600 lb
δ = 5.5 in.
W_f = 549,640 in.-lb

The average force per unit length of the impact limiter shell is given below:

$$f = \frac{W_s}{A} = 9{,}105\ lb/in.$$

As for the side drop damage, this value will be adjusted to reflect a conservative impact limiter shell temperature of 150 °F. The result is 0.926(9,105) = 8,431 lb/in. The following equation can now be solved for the maximum c.g. over corner crush deflection at maximum temperature conditions:

$$M(360 + \delta) = fA(\delta) + sV(\delta)$$

These parameters are as defined above. Solving iteratively, the maximum crush deflection, δ, is 6.1 in.

The radial crush damage represents the most conservative case with respect to seal area

temperatures, and is therefore used for all HAC thermal analyses. The thermal analyses also incorporate thermal shield damage, which is modeled as a 6-in.-diameter impression with a depth equal to one-half of the fiberglass insulation thickness, or 1.3 in., which is conservatively greater than the actual damage described in Section 2.7.6.2.

2.7.3.1.1.2 Payload Reconfiguration Effects. For the post-HAC free drop payload reconfiguration, the worst case will conservatively be taken as release of all 18 aeroshells from a GPHS RTG into the ICV. Though the free drop orientations assumed for worst-case impact limiter damage do not induce the largest impact loadings on the package, it will be conservatively assumed that all aeroshells will be released into the interior of the package independent of free drop orientation. Consequently, worst-case thermal response of the packaging will depend on the post-impact distribution of the aeroshells. This will hinge in turn on the post-impact orientation of the package.

There are only two credible orientations that the package may come to rest on the regulatory flat, essentially unyielding surface, following the HAC free drop and puncture bar tests. These are as follows: (1) upright, resting on the impact limiter, and (2) on its side, resting simultaneously on the side of the impact limiter and the upper end OCV torispherical head/fin assembly. All other orientations would be unstable. Both orientations are evaluated to determine the effect of payload reconfiguration on maximum seal temperature and differential thermal distortion in the seal area. Though an upright package would not normally leave the bottom of the impact limiter exposed to the HAC fire, the entire impact limiter will conservatively be subjected to the HAC fire.

To conservatively estimate the effects of heat transfer from the aeroshells to the package structure, the following assumptions will be made for post-free drop aeroshell distribution:

- For the package bottom-down orientation, the aeroshells will be distributed uniformly around the perimeter of the shipping rack barrier plate, in positions nearest the ICV seal region; this distribution will be referred to as "circumferential."

- With the package on its side, the aeroshells will be distributed axially along one side of the package, extending from the top of the vertical portion of the shipping rack barrier plate to the juncture with the ICV torispherical head; this distribution will be referred to as "axial."

In addition to these two cases, an extremely conservative, unstable post-free drop orientation will be evaluated. Although there is no credible basis for such a case, it will be assumed that all aeroshells will collect in one corner at the lower end of the ICV, and on top of the shipping rack (with some aeroshells in contact with the ICV wall above the shipping rack barrier plate), in as compact a mass as the random orientation of their geometries will allow. Simplified scale model testing indicated that the resulting mass of aeroshells would exhibit an approximately 50% void volume. This distribution will be referred to as "corner (or ungula)." This arbitrary geometric assumption will tend to concentrate the aeroshell heat generation into a minimum volume, thus artificially intensifying the effects of payload reconfiguration on seal temperatures and seal area thermal expansion/distortion.

For additional conservatism, all HAC thermal analysis cases will assume that the GPHS RTG structure has also broken off its mount, and has come to rest in a position that either partially or completely blocks radiative and convective heat transfer from the aeroshells into the interior of the package (depending on final package orientation).

2.7.3.1.1.3 Combined Effects. For even greater conservatism, it will be assumed that the reconfigured payload, the impact limiter damage, and the thermal shield damage will be circumferentially coincident during the HAC fire.

The effects of maximum seal area differential thermal expansion and HAC free drop-induced seal area deformations (if any) will also occur simultaneously at the same location on the containment seal for each containment vessel. This compounding of conservative assumptions will ensure that the worst-case reduction in seal compression during the entire course of the HAC sequence will never result in residual seal compressions less than those confirmed as acceptable by prior testing. See Section 4.3.2 for additional detail.

A summary of thermal HAC load cases is given in Table 2.7.3.1.1.3-1. All load cases combine maximum HAC free drop and puncture damage with the HAC fire event. The HAC load cases evaluated comply with the load combination requirements of 10 CFR 71 and Regulatory Guide 7.8 by imposing minimum and maximum ambient temperature conditions (-20 and 100 °F, respectively) with package temperatures arising from maximum payload heat generation. Zero payload heat generation and minimum ambient temperature result in essentially uniform package component temperatures. The structural and containment effects of this load case are insignificant and are not included in the summary table. The nonregulatory combination of minimum ambient-maximum payload temperatures was also imposed. This latter load case was evaluated because of greater potential for inducing maximum differential thermal expansions in the package components. Consistent with 10 CFR 71, solar loading is ignored before, during, and after the HAC fire.

TABLE 2.7.3.1.1.3-1. Summary of Thermal HAC Load Cases.

Condition	Case 1	Case 2	Case 3	Case 4	Case 5	Case 6
Ambient temperature (°F)	100	-20	100	-20	100	-20
Damaged payload configuration	Circum.	Circum.	Axial	Axial	Corner	Corner
Damaged impact limiter configuration	Side crush	Side crush	Side crush	Side crush	Side crush	Side crush

2.7.3.1.2 Sources of Pressure. Internal pressure arising from the HAC fire has been developed by the perfect gas law, and includes decomposition gas of the electrical cable insulation. As discussed in Section 2.6.1.1.1, the pressure within the ICV under NCT will result from the following:

- The initial charge of helium, 20 psia in each vessel at the time of loading
- Possible leakage from the GPHS RTG initial charge
- Decay of heat source radionuclides.

The resulting pressure was calculated to be 29.7 psia at the no-coolant condition gas temperature of 354 °F. The potential off-gas from the thermal decomposition of the GPHS RTG payload electrical cable insulation under the HAC fire must be added to this pressure. Electrical cable offgas was not added under NCT because the cable is "baked out" before use.

The GPHS RTG payload electrical cable insulation is a silicone rubber, containing silicon, oxygen, and hydrogen. The decomposition products will be inert silicon dioxide and hydrogen gas,

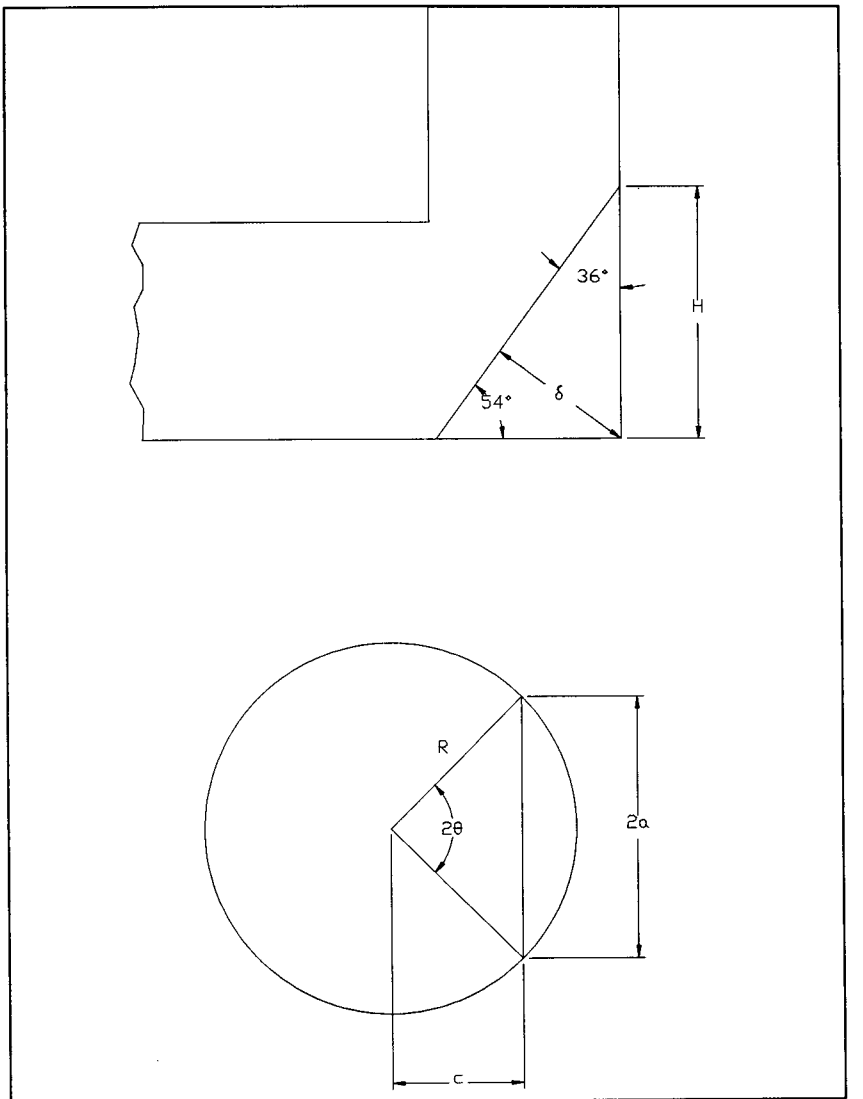


FIGURE 2.7.3.1.1.1-2. Impact Limiter Crush Relationships.

H_2. Each of the two 80.0-in.-long electrical cables contains one pound of rubber for a total of two pounds, all of which is assumed to decompose. The basic building block of the compound will be a monomer consisting of one silicon atom, one oxygen, and two hydrogen. The weight of one lb-mole of the monomer can be found from the following breakdown:

1 x 28 = 28 lb of silicon (Si) per lb-mole of monomer
1 x 16 = 16 lb of oxygen (O) per lb-mole of monomer
2 x 1 = 2 lb of hydrogen (H) per lb-mole of monomer

This gives a sum of 28 + 16 + 2 = 46 lb per lb-mole of monomer. Because there are 2 pounds of rubber, there are:

$$\frac{2}{46} = 0.043 \textit{ lb-mole of rubber present in the ICV}$$

Because it takes 2 lb-moles of hydrogen to make one lb-mole of H_2, there is one lb-mole of H_2 per lb-mole of rubber, or the following:

1 x 0.043 = 0.043 lb-mole of H_2 gas that will be released in the worst case. From Appendix 2.10.7, Table 2.10.7.2-2, HAC case 5, the maximum ICV gas temperature from the worst-case reconfiguration assumption is 840 °F. From the perfect gas law, the pressure of the added gas is given below:

$$p = \frac{nRT}{V} = 27.0 \textit{ psia}$$

where: n = 0.043 lb-mole
R = 10.74 psia-ft^3/lb-mole-°R
T = 840 + 460 = 1300°R
V = 22.25 ft^3 from Section 2.6.1.1.1.

In Section 2.6.1.1, the existing gas in the ICV under NCT had a pressure of 29.7 psia at a temperature of 354 °F. When raised to a temperature of 840 °F, the pressure can be found from the ratio of absolute temperatures to be as follows:

$$p_{HAC} = p_{NCT} \frac{(840+460)}{(354+460)} = 47.4 \textit{ psia}$$

where: p_{HAC} = the HAC ICV partial pressure
p_{NCT} = the NCT ICV pressure, 29.7 psia.

The total pressure within the ICV during the HAC event is the sum of the pressure of the pre-existing gas and the off-gas:

p_{tot} = 47.4 + 27.0 = 74.4 psia.

In Section 2.6.1.1, the gas in the OCV under NCT had a pressure of 26.3 psia at 285 °F. When raised to 852 °F (OCV internal gas temperature for HAC case 5, Table 2.10.7.2-2), the OCV pressure can be found from the ratio of absolute temperatures to be as follows:

$$p_{HAC} = p_{NCT} \frac{(852 + 460)}{(285 + 460)} = 46.3 \; psia$$

where: p_{HAC} is the HAC OCV pressure
p_{NCT} is the NCT OCV pressure, 26.3 psia

Off-gassing is not a concern in the OCV, because no component generates gas during the HAC fire. Pressure external to the OCV is atmospheric ambient, or 14.7 psia. A summary of HAC load cases and resulting maximum containment vessel gas temperatures is presented in Table 2.7.3.1.2-1. Corresponding vessel pressures are summarized in Table 2.7.3.1.2-2.

For conservatism, the maximum pressure differentials of the ICV and OCV, augmented by 10%, will be used to evaluate each vessel in all HAC load cases. For the ICV, this will be (74.4 - 46.3)(1.1) = 30.9 psid, and for the OCV this will be (46.3 - 14.7)(1.1) = 34.8 psid.

TABLE 2.7.3.1.2-1. Summary of HAC Containment Vessel Gas Temperatures.

Condition	Case 1	Case 2	Case 3	Case 4	Case 5	Case 6
Ambient temperature (°F)	100	-20	100	-20	100	-20
Damaged payload configuration	Circum.	Circum.	Axial	Axial	Corner	Corner
ICV internal gas temperature (°F)	836	779	747	684	840	782
OCV internal gas temperature (°F)	849	796	851	798	852	799

TABLE 2.7.3.1.2-2. Summary of HAC Containment Vessel Pressures.

Condition	Case 1	Case 2	Case 3	Case 4	Case 5	Case 6
ICV internal gas pressure (psia)	74.3	72.2	71.0	68.7	74.1	72.3
OCV internal gas pressure (psia)	46.2	44.3	46.3	44.4	46.3	44.4
ICV external gas pressure (psia)	46.2	44.3	46.3	44.4	46.3	44.4
OCV external gas pressure (psia)	14.7	14.7	14.7	14.7	14.7	14.7

2.7.3.2 Thermal Expansion. The containment vessel HAC relative differential expansion analysis is similar to that for the NCT, which was covered in Section 2.6.1.2. Much of that section is repeated here, with appropriate substitutions reflecting any differences between the NCT and HAC cases.

A radial and axial clearance is maintained between both the ICV and OCV bell during the HAC fire event, and thus, no vessel loading because of relative differential thermal expansion will occur. This is because the OCV reaches higher temperatures and expands away from the ICV. When a steady state condition has been reached after the HAC fire, however, the relative

temperature difference is reversed, and the ICV becomes the warmer of the two vessels. Because, after the top-down HAC free drop, the heads of the two vessels are likely to be in contact, the fact that the OCV is cooler than the ICV indicates an axial interference will exist between the vessels. However, the interference is small, as will now be demonstrated. Further, because the interference occurs in the center of the heads, little force is transferred to the vessel walls or seal areas.

Both the radial and axial thermal expansion of each vessel will be dominated by the temperature of the cylindrical walls, which are thermally modeled in each case by four nodes: 210 to 240 in the ICV, and 310 to 340 in the OCV. As shown in Figure 3.4.1-2, nodes 210 and 310 are located 6.86 in. below the top of the coolant jacket. The corresponding measurements for the other node pairs are as follows: nodes 220 and 320, 20.58 in.; nodes 230 and 330, 34.30 in.; and nodes 240 and 340, 43.66 in. A third dimension is added by the inclusion of four circumferential segments, A through D, each having identical nodal geometric relationships. The radial differential thermal expansion between the two vessels is found by subtracting the radial thermal expansion of the OCV from that of the ICV at each of the four elevations discussed above. The residual radial clearance is found by subtracting this result from the initial minimum manufactured clearance. The single temperature value corresponding to each elevation is a weighted average of the temperatures from each circumferential segment, using temperatures from Section 3.6.5. The weighting factor is based on the size of the angular segments, as given in Table 2.7.3.2-1.

TABLE 2.7.3.2-1. Segment Weighting Factors.

	HAC cases 1, 2, 5, and 6		HAC cases 3 and 4	
Segment	Included angle (°)	Factor	Included angle (°)	Factor
A	22.5	0.125	15	0.083
B	45	0.250	30	0.167
C	67.5	0.375	90	0.500
D	45	0.250	45	0.250

For example, for HAC case 6 (ungula rubble configuration, -20 °F ambient, post-HAC fire steady state), the segment sizes are (see Figure 3.5.2-3): 22.5°, 45°, 67.5°, and 45° for segments A through D, respectively. The half-symmetry total angle is 180°. The segment A weighting factor is therefore 22.5/180 = 0.125. The other three weighting factors for segments B, C, and D are 0.25, 0.375, and 0.25, respectively. From Section 3.6.5, the temperatures of segments A through D at the node 240 (ICV) elevation are 443, 337, 165, and 153 °F, respectively. The weighted average temperature is given below:

$$T_{ave} = 0.125(443) + 0.25(337) + 0.375(165) + 0.25(153) = 240\ °F \qquad \text{(ICV)}$$

The corresponding temperatures for the OCV at node 340 elevation are 307, 236, 129, and 123 °F. The weighted average temperature for the OCV is given below:

$$T_{ave} = 0.125(307) + 0.25(236) + 0.375(129) + 0.25(123) = 177\ °F \qquad \text{(OCV)}$$

From Table 2.3-1, the coefficient of thermal expansion for Type 304L at temperatures of

240 °F and 177 °F are $8.87(10^{-6})$ and $8.73(10^{-6})$ in/in/°F, respectively. The nominal outside diameter of the ICV is 35.5 in., and the nominal inside diameter of the OCV is 35.88 in. The minimum initial manufactured radial clearance is 1/32 in. The residual radial clearance is given below:

$$RC_{res} = 0.031 - 0.5[35.5(240 - 70)8.87(10^{-6}) - 35.88(177 - 70)8.73(10^{-6})] = 0.021 \ in.$$

Residual radial clearances at other locations and for all HAC load cases are presented in Table 2.7.3.2-3.

The axial thermal differential expansion between the two vessels is found by subtracting the axial thermal expansion of the OCV from that of the ICV using the average temperature of the four stations together with the four segments described above. The average of the four stations in one segment is a straight average, and the average of the four segments uses weighted inputs as described above. For example, for HAC case 6 (same post-HAC fire steady state condition as above), the temperatures and resulting averages are given in Table 2.7.3.2-2.

TABLE 2.7.3.2-2. HAC Case 6 (Post-HAC Fire Steady State) Temperature Averages, °F.

ICV segments					OCV segments				
Nodes	A	B	C	D	Nodes	A	B	C	D
210	195	192	191	188	310	149	146	145	142
220	222	208	193	187	320	174	162	148	143
230	341	272	171	178	330	275	218	132	132
240	443	337	165	153	340	307	236	129	123
Segment averages	300	252	180	177	Segment averages	226	191	139	135
Weighting factor	0.125	0.25	0.375	0.25	Weighting factor	0.125	0.25	0.375	0.25
Overall ICV average temperature				212	Overall OCV average temperature				162

From Table 2.3-1, the coefficient of thermal expansion for Type 304L at 212 and 162 °F are $8.81(10^{-6})$ and $8.70(10^{-6})$ in./in./°F, respectively. The OCV inside height of 62.9 in. may be conservatively used as a length for both vessels. The minimum initial axial manufactured clearance is 1/16 in. The maximum potential axial interference is given below:

$$AC_{res} = 0.0 - 62.9[(212 - 70)8.81(10^{-6}) - (162 - 70)8.70(10^{-6})] = -0.029 \ in.$$

Residual axial clearances for all HAC load cases are presented in Table 2.7.3.2-3.

TABLE 2.7.3.2-3. Summary of HAC Differential Expansions.

Condition	Case 1	Case 2	Case 3	Case 4	Case 5	Case 6
Residual axial clearance (in.)	-0.025	-0.028	-0.016	-0.018	-0.025	-0.029
Residual radial clearance (in.)						
Elevation 210 and 310	0.025	0.024	0.026	0.025	0.025	0.024
Elevation 220 and 320	0.025	0.024	0.026	0.025	0.025	0.024
Elevation 230 and 330	0.024	0.023	0.025	0.024	0.024	0.023
Elevation 240 and 340	0.021	0.021	0.030	0.030	0.022	0.021

The worst-case radial condition is a clearance reduction of 32% (HAC case 6, elevation 240 and 340), and the worst case axial condition is a clearance reduction of 47% (also HAC case 6).

The HAC bolt differential expansion and stress analysis is very similar to that for the NCT. Much of that section is repeated here, with appropriate substitutions reflecting any differences between the NCT and HAC cases. The differential thermal stress values were determined from the ANSYS finite element models of the ICV and OCV presented in Appendices 2.10.12 and 2.10.8 respectively. Because of the potential for payload reconfiguration and subsequent nonaxisymmetric thermal loading, the ICV was modeled as a half-symmetry three-dimensional (3-D) representation. A 2-D OCV model is considered adequate for the HAC cases primarily because the controlling thermal condition for the OCV is radiation from the HAC fire, which is assumed to be totally engulfing and constitutes a uniform radiative input of relatively large magnitude. In addition, unlike the ICV, the OCV does not have concentrated heat sources applied directly to its interior. As further confirmation of the adequacy of an axisymmetric model, a 3-D model of the OCV was made for the segment of the OCV where the impact limiter damage and damaged payload coincide, and where flange distortion is greatest. As detailed in Appendix 2.10.13, the 2-D representation is conservative for both the OCV closure bolt load and flange distortion. For each HAC case of Table 2.7.3.1.1.3-1, temperatures from the thermal analysis of Section 3.6.5 are applied to the structural finite element models, allowing the determination of thermal stress and distortion. In each HAC case, distortions are referenced to room temperature (70 °F), and the pressure established in Section 2.7.3.1.2 is included.

As noted in Section 2.3 the bolting material used for the containment assembly closure bolts (ASTM-A320, Grade L43 or ASTM A540, Grade B23, Class 1) has a different coefficient of thermal expansion than the material used for the vessel flanges (Type 304L). As the temperature of the vessels changes from the initial conditions, this leads to variations in closure bolt pre-load because of different amounts of thermal expansion/contraction in both the bolt and flange material. Because the expansion coefficient of Type 304L in the flange is greater than that of the closure bolt, an increase in flange material temperature will normally mean an increase in closure bolt clamping force and stress. A decrease in flange material temperature will normally mean a decrease in closure bolt clamping force and stress. In the analyses to follow, the actual temperatures of the closure bolts and flanges, as listed in Section 3.6.5 are used. The initial pre-load force in the closure bolts, because of assembly torque, is given below:

$$F_i = \frac{T}{Kd}$$

where: T = closure bolt torque, in.-lb
K = 0.186, friction torque coefficient for cadmium plated threads[23]
d = nominal closure bolt diameter, in.

Table 2.7.3.2-4 lists the closure bolt parameters along with pre-load force for the ICV and OCV closure bolts.

TABLE 2.7.3.2-4. Closure Bolt Parameters and Pre-load Force.

Location	d (in.)	Stress area (in.^{2})	Length[a] (in.)	Torque (ft-lb)	Pre-load force (lb)
ICV	0.75	0.3300	1.49	250	21,505
OCV	1.25	0.9524	5.19	300	15,484

[a]Grip length, defined as the length from the head to the midpoint of the threads.

The finite element models of the containment assemblies described in Appendices 2.10.12 and 2.10.8 include a model of the closure bolts as spars. They are given an initial stretch such that under nominal conditions (zero net pressure and uniform temperature) the load in the closure bolts is equal to the pre-load force values given in Table 2.7.3.2-4. During model post-processing, the resultant force in the spar is extracted. For the OCV, 2-D model, a single spar must represent all of the closure bolts. In this case, the force in each closure bolt is found from the following:

$$F_b = \frac{2\pi F_s}{n}$$

where: F_b = the individual closure bolt force, lb
F_s = the spar load, lb/radian
n = the number of closure bolts.

For the ICV 3-D model, the closure bolts are modeled individually, and their force may be directly extracted. In both cases, the stress in each closure bolt is given below:

$$\sigma_b = = \frac{F_b}{A_s}$$

where: F_b = closure bolt force, lb
A_s = stress area of closure bolt, in.^{2}

The margin of safety is:

$$M.S. = \frac{S_{all}}{\sigma_b} - 1$$

The allowable stress, S_{all}, for HAC is the lesser of S_y or $0.7S_u$, based on the ASME B&PV Code, Section III, Appendix F-1335.1, and is found from closure bolt temperature and Table 2.3-2. Table 2.7.3.2-5 summarizes load, stress, temperature, allowable, and margin of safety for the closure bolts for each HAC case in Table 2.7.3.1.1.3-1. As can be seen in Table 2.7.3.2-5, a positive margin of safety is maintained during HAC events for all closure bolts. Seal area distortions are addressed in Section 4.3.2 and are shown to remain within the limits necessary to ensure leaktight containment boundaries.

TABLE 2.7.3.2-5. Closure Bolt Load, Stress and Margin of Safety.

Case number	Bolt location	Bolt load (lb)	Bolt stress (psi)	Bolt temperature (°F)*	Allowable bolt stress (psi)	Margin of safety
1	ICV	23,956	72,594	252	115,500	+0.59
	OCV	66,911	70,255	342	87,500	+0.25
2	ICV	22,588	68,448	154	115,500	+0.69
	OCV	70,987	74,535	242	87,500	+0.17
3	ICV	24,635	74,652	264	115,500	+0.55
	OCV	66,856	70,197	368	87,500	+0.25
4	ICV	23,201	70,306	159	115,500	+0.64
	OCV	70,880	74,423	273	87,500	+0.18
5	ICV	23,995	72,712	257	115,500	+0.59
	OCV	68,730	72,165	343	87,500	+0.21
6	ICV	22,572	68,400	156	115,500	+0.69
	OCV	72,655	76,286	243	87,500	+0.15

*Because the ICV thermal model did not specifically include closure bolts, the closure bolt temperature for structural purposes is conservatively taken as the temperature of the ICV flange (thermal node 250) at the warmest circumferential location. The OCV closure bolts were explicitly modeled, and their temperatures listed above correspond to the warmer of thermal node 353 (shank portion of bolt) or thermal node 355 (thread portion of bolt), again at the warmest circumferential location. The transient location is the time at which peak wall temperature occurs: 30 minutes after the start of the HAC fire for the OCV and 40 minutes for the ICV.

According to Reference 23, the preload force may vary by up to ±30% for a given applied torque value. Therefore, the cases having the lowest bolt margin of safety (Case 3 for the ICV and Case 6 for the OCV) were rerun, using a pre-stretch in the elements representing the bolts of 130% of the nominal value. This represents the maximum possible load in the bolts. The results are shown in Table 2.7.3.2-6, where the relatively large margins of safety demonstrate that the bolt stress is still well below yield, even when accounting for a large scatter in the bolt preload force.

Table 2.7.3.2-6. Closure Bolt Load and Stress Considering Preload Force Variation (HAC)

Load case (HAC)	Bolt location	Bolt load (lb)	Bolt stress (psi)	Bolt temp. (°F)	Yield strength (psi)	Margin of safety on yield
3	ICV	30,886	93,594	264	137,028	+0.46
6	OCV	68,740	72,176	243	97,581	+0.35

2.7.3.3 Stress Calculations. Allowable stress limits for HAC events are available from Table 2.1.2-1 and are based on ASME B&PV Code, Appendix F (Service Level D) limits. Per that table, closure bolt stresses and primary stresses in the vessel structures resulting from the HAC thermal event must be determined and shown to remain within stated allowable limits. As indicated by Table 2.1.2-1, there are no limits applicable for secondary stresses resulting from HAC events. Consequently, thermally induced secondary stresses do not need to be quantified.

The closure bolt thermal distortion stresses (including pre-load and pressure effects) have been calculated in the preceding section and were shown to remain within allowable limits. The remainder of this section, therefore, focuses on vessel primary stresses, i.e., those resulting from worst case internal pressures occurring during the HAC thermal event.

The finite element model results for internal pressure only (NCT load cases ICV-P and OCV-P from Section 2.6.1.3) will be scaled to derive the primary stress under HAC events. These two NCT load cases used 10 psid internal pressure and 26.5 psid internal pressure, respectively, and thus, the results for the HAC maximum pressure is found by scaling the ratios of the HAC pressure differentials developed in Section 2.7.3.1.2:

$$\frac{30.9}{10.0} = 3.09 \textit{ for the ICV}$$

and,

$$\frac{34.8}{26.5} = 1.313 \textit{ for the OCV}$$

Tables 2.7.3.3-1 and 2.7.3.3-2 summarize the stress results for membrane and membrane plus bending stress for the ICV and OCV. The worst-case containment boundary temperatures correspond to HAC case 3. The peak ICV is 1190 °F at thermal node 210, and the peak OCV is 1249 °F at thermal node 304. Temperatures are taken from Section 3.6.5 and are conservatively rounded up to 1200 °F for the ICV and to 1300 °F for the OCV.

TABLE 2.7.3.3-1. Summary of ICV Stress Intensities and Margins of Safety.

Case No.	Stress location	Stress category	Maximum stress intensity (psi)	Temp. (°F)	Allowable stress intensity (psi)	Margin of safety
ICV-P	Head crown midshell	P_m	3,217 (elem 145)	1,200	27,405 ($0.7S_u$)	+7.52
	Head crown shell surface	$P_L + P_b$	6,041 (elem 145)	1,200	39,150 (S_u)	+5.48
	Knuckle midshell	P_L	3,377 (elem 144)	1,200	39,150 (S_u)	> +10

TABLE 2.7.3.3-2. Summary of OCV Stress Intensities and Margins of Safety.

Case No.	Stress location	Stress category	Maximum stress intensity (psi)	Temp. (°F)	Allowable stress intensity (psi)	Margin of safety
OCV-P	Head crown midshell	P_m	1,425 (elem 121)	1,300	21,980 ($0.7S_u$)	> +10
	Head crown shell surface	$P_L + P_b$	2,189 (elem 122)	1,300	31,400 (S_u)	> +10
	Knuckle midshell	P_L	2,416 (elem 119)	1,300	31,400 (S_u)	> +10

2.7.3.4 Comparison with Allowable Stresses. As discussed in Section 2.1.2 stress limits are in accordance with Regulatory Guide 7.6, and load combinations are in accordance with Regulatory Guide 7.8. From Table 2.1.2-1, for HAC, the allowable stress intensity for primary membrane stress is the lesser of $2.4S_m$ or $0.7S_u$. For both vessels, the value of $0.7S_u$ is the lesser, and is listed as the allowable stress intensity at temperature for P_m in the tables above. From Table 2.1.2-1, the allowable stress intensity for both primary membrane plus bending stress ($P_L + P_b$) and local primary membrane stress (P_L) is the lesser of $3.6S_m$ or S_u. For both vessels, S_u is the lesser, and is listed as the allowable stress at temperature for ($P_L + P_b$) and P_L in the tables above. For both vessels, the critical stress locations are in the head, where temperatures are the greatest. Minimum margins of safety are presented in the last column of Tables 2.7.3.3-1 and 2.7.3.3-2, and all margins of safety are positive. Thus, the design criteria are satisfied.

Closure bolt, bell flange, and base responses to the HAC thermal event have also been studied to ensure that the leaktight capability of the ICV and OCV containment O-rings is not compromised. Closure bolt stresses were addressed in Section 2.7.3.2. Section 4.3.2 addresses maximum seal area distortions and residual compressions for the ICV and OCV containment O-rings. Figures 2.10.12-12 and 2.10.8-13 present worst-case stress intensities in the vicinity of the O-rings for the ICV and OCV. Based on the following observations relating to those analyses, it is concluded that the HAC thermal event will not compromise the leaktight capability of the O-rings. First, the closure bolts remain elastic for all potential worst-case HAC thermal events (see Section 2.7.3.2). This ensures that a positive clamping force will always exist between mating bell flanges and bases. Second, O-ring seal area distortions and corresponding residual compressions for containment O-rings remain within the limits necessary to ensure O-ring leaktight performance (see Section 4.3.2). Third, although there are no limits placed on HAC secondary

stresses (see Section 2.7.3.3), a review of Figures 2.10.8-13 and 2.10.12-12 indicate that secondary stresses caused by the HAC thermal event remain within corresponding NCT allowable limits.

2.7.4 Immersion

The criticality evaluation presented in Section 6.0 assumes optimum hydrogenous moderation of the contents. Thus, the effects and consequences of water in-leakage are conservatively addressed.

2.7.5 Immersion -- all Packages

For the RTG Transportation System Package, the effect of immersing an undamaged specimen in 50 ft of water is equivalent to imposing an external pressure of 21 psig on the OCV. Although the effect of immersion on package temperatures is expected to be equivalent to that of active cooling of the package, the component temperatures used are conservatively taken from NCT case 1 of Table 2.6.1-1, which lists maximum regulatory temperatures.

Initial acceptance tests will give assurance that the OCV will withstand the 21 psig HAC external pressure. Specifically, the Fabrication Verification Leak Test subjects the OCV boundary to a full internal vacuum, or the equivalent of a 14.7 psig external pressure. A 14.7 psig external pressure can therefore be considered to be a minimum acceptable condition for external pressure as confirmed by testing. Per ASME B&PV Code Case N-284, the factor of safety for NCT is 2.0, whereas for HAC the applicable factor of safety is 1.34. This difference in factors of safety implies that, for HAC, an acceptable external pressure would be a minimum of (14.7)(2.0/1.34) = 21.9 psig.

To confirm structural stability, buckling analyses are performed on the relevant structural containment components of both the OCV and ICV. The results of these analyses, which demonstrate large margins of safety, indicate that buckling will not occur.

The immersion pressure differential is formed by conservatively assuming an internal pressure of zero, and therefore, a pressure of 21 psid is applied externally to both vessel cylindrical shells. The ICV cylindrical shell has a smaller diameter, shorter length and a greater wall thickness than that of the OCV. Therefore, it will be less vulnerable to structural instability than the shell of the OCV, and an indication of structural stability in the OCV shell automatically implies structural stability in the ICV shell under the same applied external pressure loading and at the same temperature.

The OCV shell is assumed to be 350 °F, which is conservatively higher than the temperature for both the ICV and OCV shells, considering the maximum wall temperature from Table 2.10.7.1-2 of Appendix 2.10.7. For the basic OCV shell, the hoop and axial compressive stresses associated with the 21 psig external pressure are calculated below:

$$\sigma_\phi = \frac{PR}{2t} = 382.0\ psi$$

$$\sigma_\theta = \frac{PR}{t} = 764.0\ psi$$

where: σ_θ = hoop compressive stress
σ_ϕ = axial compressive stress
P = external pressure = 21 psig
R = shell mean radius = 18.19 in.
t = shell thickness = 0.50 in.

Resulting plasticity reduction factors from Section 1610 of ASME B&PV Code Case N-284 are equal to unity. Hence, inelastic buckling checks are not required. Consequently, all that the buckling analysis entails is determination of theoretical buckling stress values. The results can then be compared to the above actual, calculated stress values, with capacity reduction factors and appropriate factors of safety (FS = 1.34 for HAC) applied. If the theoretical buckling stresses are greater than the adjusted actual stress values, then buckling will not occur.

From Section 1511 of Code Case N-284, the appropriate capacity reduction values are determined to be as follows:

$\alpha_{\phi L}$ (axial compression) = 0.207

$\alpha_{\theta L}$ (hoop compression) = 0.800

Adjusted actual stress values are determined as follows:

$$\sigma_{\phi a} = \frac{\sigma_\phi \times FS}{\alpha_{\phi L}} = 2{,}472.9\ psi$$

$$\sigma_{\theta a} = \frac{\sigma_\theta \times FS}{\alpha_{\theta L}} = 1{,}279.7\ psi$$

where: $\sigma_{\phi a}$ = adjusted axial compressive stress

$\sigma_{\theta a}$ = adjusted hoop compressive stress.

From Section 1712 of Code Case N-284, the theoretical buckling values for an effective OCV shell free length of 56 in. are determined to be as follows:

$\sigma_{\phi cL}$ (axial compression) = 444,914 psi

$\sigma_{\theta cL}$ (hoop compression) = 37,725 psi

Comparison of results indicates the following:

$$M.S.\ (axial\ compression) = \frac{444{,}914}{2{,}159.8} - 1 = +\ Large$$

$$M.S.\ (hoop\ compression) = \frac{37{,}725}{1{,}279.7} - 1 = +\ Large$$

Consequently, buckling of the OCV shell will not occur.

The buckling analysis of the torispherical heads is based on the ASME B&PV Code, Section III, Subsection NE, Paragraph NE-3133.4(e). This section applies for Design Condition and level A and B loadings. Because the pressure loading due to immersion can be classified as Level D, the allowable buckling stress and, therefore, the allowable pressure, can be increased by 150% per Paragraph NE-3222.2. The basic calculational procedure is outlined below:

1. Calculate factor A using the following formula:

$$A = \frac{0.125}{(R/T)}$$

where: R = crown inside radius
T = head thickness

2. Read value of factor B from Figure 2.7.5-1
(Figure VII-1102-4 of the above-referenced Code section)

3. Calculate the maximum allowable pressure, P_a, using the following formula:

The dimensions for the ICV and OCV heads are summarized in Table 2.7.5-1.

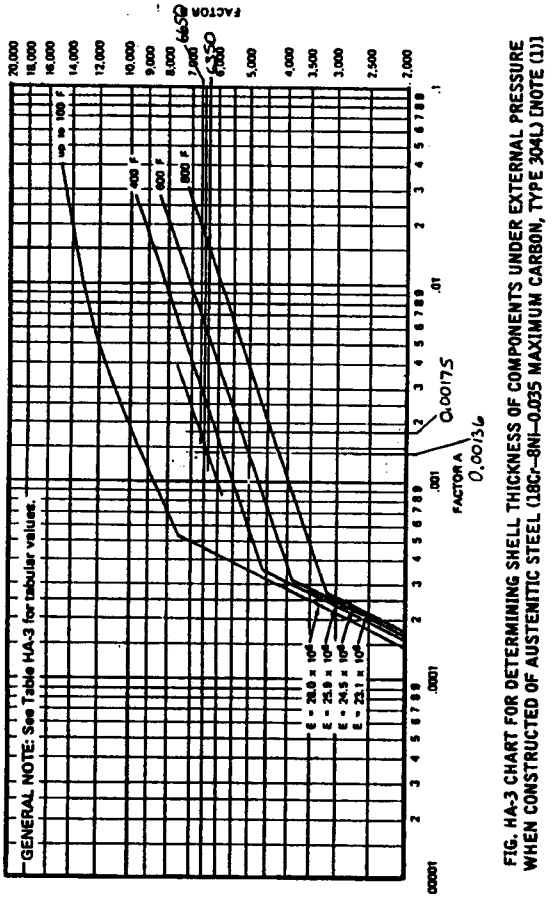


FIGURE 2.7.5-1. ASME B&PV Code, Section III, Part D, Figure HA-3.

$$P_a = \frac{1.50B}{(R/T)}$$

TABLE 2.7.5-1. Torispherical Head Geometric Parameters.

Vessel	Inside radius (in.)	Thickness (in.)	R/T
ICV	35.00	0.38	92.10
OCV	35.75	0.50	71.50

The allowable pressure for the ICV torispherical head will now be calculated per the procedure outlined above.

1. $A = \frac{0.125}{(R/T)} = \frac{0.125}{92.10} = 0.00136$

or

2. B = 6,350 (see Figure 2.7.5-1)

Note: The ICV maximum head temperature is taken as 350 °F (conservatively in excess of the value given for thermal node 200 from Table 2.10.7.1-2, Appendix 2.10.7). The corresponding value for "B" is interpolated between temperature curves labeled "400 °F" and "up to 100 °F."

3. $P_a = \frac{1.50B}{(R/T)} = \frac{(1.50)(6,350)}{92.10} = 103.4\ psi$

Thus, the margin of safety for the ICV torispherical head is given below:

$$M.S. = \frac{P_a}{P} - 1 = \frac{103.4}{21.0} - 1 = +3.92$$

Following the same procedure for the OCV head yields the following results:

1. A = 0.00175

2. B = 6,650

The OCV maximum head temperature is taken as 350 °F (conservatively in excess of the value given for thermal node 300 from Table 2.10.7.1-2, Appendix 2.10.7). The corresponding value for B is interpolated between temperature curves labeled "400 °F" and "up to 100 °F."

3. P_a = 140 psi

The margin of safety for the OCV torispherical head is given below:

The margins of safety on buckling are all positive.

$$M.S. = \frac{P_a}{P} - 1 = \frac{140.0}{21.0} - 1 = +5.67$$

2.7.6 Summary of Damage

Two full-scale prototypes of the package were subjected to a series of NCT 4-ft free drops, HAC 30-ft free drops, and HAC 40-in. puncture drops. The two drop test series are described in Appendix 2.10.9 and summarized in Sections 2.7.1 and 2.7.2. A description of the first and second Certification Test Articles (CTA-1 and CTA-2), the simulated payload, and the drop pad, and details of test results, are given in Appendix 2.10.15. Subsequent to all tests, the CTA was leak-tight, having an integrated leakage rate of less than $1(10^{-7})$ scc/sec, air, for both ICV and OCV. The following paragraphs summarize the results of the drop testing.

2.7.6.1 Summary of Free Drop Damage. A series of five free drops was performed from a height of 4 ft followed by the same series from 30 ft. As a result of problems encountered during the first certification test series (which used CTA-1), a new certification test article, designated CTA-2, was fabricated. All of the 4-ft and 30-ft free drops were repeated with CTA-2 and these results are summarized in the following paragraphs. The results of the 4-ft drops (corresponding to NCT) are described in Section 2.6.7. In general, the only criteria for the 4-ft free drops is that the damage not compromise the ability of the package to survive subsequent 30-ft free drops. This was true in each case. The package deformations resulting from the 30-ft free drops were scaled-up versions of the damage resulting from 4-ft free drops, and subsequent to all testing (including punctures), the success criteria of Section 2.7 were satisfied as follows:

1. Containment was maintained. The second certification test consisted of a series of four sets of tests as described in Appendix 2.10.15. After each set of tests, the OCV and ICV O-ring seals were leakage rate tested and no detectable leakage was found. At the end of all of the drop tests, the entire OCV and ICV containment boundaries (sum of the leakage rates for the seals and for the structural boundary) were leakage rate tested. The final containment boundary leakage rate of the CTA-2 vessels was 4.35 (10^{-9}) scc/sec (air) for the OCV and 8.3 (10^{-9}) scc/sec (air) for the ICV, which are less than the maximum leakage rate for a definition of leak tightness of 1 (10^{-7}) scc/sec (air).*** Additionally, the deformations in the seal area of each vessel were below levels which would, when added to thermal distortions resulting from the HAC fire event, compromise the ability of the seals to maintain leak tight containment. The evaluation of seal area distortions and the relationship to containment is discussed in Section 4.3.2.

2. Biological shielding was maintained, as demonstrated by the relatively small overall deformations of CTA-2, and the extremely conservative assumptions made in the shielding analysis of Section 5.0.

3. A subcritical payload was maintained, as demonstrated by the relatively small overall deformations of CTA-2, and the extremely conservative assumptions made in the criticality analysis of Section 6.0.

*** The leakage rates measured by the mass spectrometer leak detector were in terms of helium and were 1.13×10^{-8} scc/sec for the OCV and 2.15×10^{-8} scc/sec for the ICV, and were converted to a leak rate of air by dividing the helium rate by 2.6.

Specific results of HAC free drop testing follows. After each HAC free drop, the OCV closure bolts exhibited average residual torques that varied from 223 to 252 ft-lb. Drops are identified in Section 2.7.1.4. Photographs are presented in Appendix 2.10.15.

1. The bottom-down, near-vertical free drop (CTA-2 test No. 2) was intended to demonstrate impact limiter retention by developing a large separation moment between the impact limiter and the package body. The angle of impact with the ground and the circumferential orientation of the package to the impact point was designed to maximize limiter attachment bolt forces. External limiter deformations were small. The result of this free drop was complete retention of the limiter with no visible change in position on the package body. Two of the eight impact limiter attachment bolt torques, however, fell to negligible or zero values. This is considered acceptable, since the purpose of the attachment bolts is to retain the position of the impact limiter, which was achieved. Examination of the attachment bolts subsequent to testing showed small amounts of deformation and stretching (<0.025 in.), particularly in the "necked down" region of the bolt shank. This feature was included specifically to enhance the bolts ability to absorb energy without failure.

2. The bottom-down, c.g. over corner free drop (CTA-2 test No. 5) caused the impact limiter corner to crush 5.5 inches, which extrapolates to 6.1 in. in the warm foam condition (this calculation is carried out in Section 2.7.3.1.1.1(B). Because the original distance of foam along the line of crush is 11 in., the localized maximum uniaxial foam strain, in the worst case, would be 6.1/11 = 55%. This is acceptable and demonstrates the ability of the impact limiter to protect the package from bottoming-out when all of the free drop energy is directed at the impact limiters weakest corner.

3. The side-slapdown free drop (CTA-2 test No. 12) was oriented to impart the maximum impact to the side of the impact limiter and the package baseplate region. It caused the impact limiter to crush radially inward a distance of 4 in. at the top of the impact limiter, tapering down to a negligible amount at the bottom of the impact limiter. This was extrapolated to a value of 5.9 in. in the warm foam condition, conservatively assuming the same maximum deformation at both the top and bottom of the impact limiter. (This calculation is carried out in Section 2.7.3.1.1.1(A). Because the original distance of foam along a radius is 7.65 in., the localized maximum uniaxial foam strain, in the worst case, would be 5.9/7.65 = 77%.

   This is acceptable and demonstrates the ability of the impact limiter to protect the package from bottoming-out in severe slapdown conditions.

   The package also sustained damage in a region at the top of the coolant jacket due to primary impact. The top rib of the coolant jacket was deformed radially inward 1.25 in., which included some OCV and ICV sidewall deformation. This is acceptable because the OCV boundary remained leaktight.

4. The bottom end down free drop (CTA-2 test No. 8) had the potential for producing the highest impact decelerations. Impact limiter deformations were negligible as this drop caused a flattening of the previous deformations that protruded from the bottom of the impact limiter.

5. The top end down free drop (CTA-2 test No. 13) demonstrated the ability of the top end of the package to absorb the full impact energy of the free drop. The fins deformed until the top of the OCV head contacted the impact surface. The final diameter of the resulting flat on the top end was approximately 15 in.

2.7.6.2 Summary of Puncture Damage. A series of eleven puncture drops was performed from a height of 40 in. As noted in Section 2.7.6, two certification test articles (CTA-1 and CTA-2) were used during certification testing of the package. Nine puncture drops were performed on CTA-1. Six puncture drops were performed on CTA-2; four were repeated from the first test and two new puncture drops were added. The effect of the puncture damage on the acceptance criteria of Section 2.7 has already been included in the discussion in Section 2.7.6.1. Specific results of HAC puncture damage follows. The puncture drops are identified in Section 2.7.2.2. Photographs are presented in Appendix 2.10.15.

1. The first puncture (CTA-2 test No. 3) demonstrated that the puncture bar, contacting the impact limiter in the most unfavorable orientation, could not dislodge the impact limiter from the package. The package was oriented top end down, and the 80-in.-long puncture bar was used. Contact occurred on the top surface of the impact limiter, near its outside edge. The circumferential position, as viewed from the top of the CTA, was 75° cw from the electrical feed-through, adjacent to impact limiter attachment bolt No. 7. (This was the only impact limiter attachment bolt that exhibited no residual torque.) Because of the package orientation, the puncture bar did not align with the package c.g. The resulting dent was only 0.3 in. deep, and no evidence of overall impact limiter movement relative to the package was noted.

2. The second puncture (CTA-2 test No. 6) was directly on the damage created by the c.g. over bottom limiter corner free drop. The puncture bar, therefore, contacted the impact limiter through the CTA-2 c.g. This puncture drop demonstrated that a puncture on previously compacted foam would neither penetrate the impact limiter shell nor compromise the integrity of the seal area, through which the line of force traveled. The puncture bar did not penetrate the impact limiter shell and the depth of indentation was 1.7 in.

3. The third puncture (CTA-2 test No. 9) demonstrated that a puncture on the side of the impact limiter at the lower corner joint weld seam would not rupture the weld. The puncture dent depth, measured from the side of the impact limiter, was approximately 3.5 in. No evidence of incipient ripping of the impact limiter shell was noted.

4. The fourth puncture (CTA-2 test No. 14) demonstrated the ability of the OCV sidewall and coolant jacket to absorb the entire drop energy without rupture, buckling, or deleterious deformations in the seal area. The CTA-2 was placed horizontally over the puncture bar at the c.g. The dent depth (measured from the outer diameter of the coolant jacket ribs) was 1 in. The ICV sidewall deformed approximately 0.37 in.

5. The fifth puncture (CTA-2 test No. 15) showed that the package torispherical heads could absorb the entire drop energy without rupture, buckling, or penetration. The CTA-2 was oriented at 9° from the vertical so that the puncture bar would just contact the unreinforced area of the OCV head. The drop height was 45 in., which was the distance between the OCV head and the puncture bar. The drop height was increased to simulate the presence of the OCV head personnel barrier. The resulting dent was 1-1/4 in. deep, with a similar depth in the ICV head.

6. The sixth puncture (CTA-2 test No. 16) showed that the puncture would only rupture a small amount of the impact limiter side wall when the impact was directed at the plastic melt plug. The melt plug holder weld failed and allowed the impact limiter shell to tear, exposing about 12.7 sq. in. of foam. The effect of this amount of exposed foam is insignificant and is evaluated in Section 3.6.2.4 of Appendix 3.6.2, Chapter 3.0.

7. The second puncture (CTA-1 test No. 12) demonstrated that the bottom impact limiter shell

could prevent penetration of the puncture bar, even under the unfavorable shearing conditions set up by impacting the impact limiter on the low-density foam, but just adjacent to the high-density foam. Further, the corner of the puncture bar contacted the impact limiter shell at an angle. Initial impact was 20 in. from the impact limiter center, or within 1 in. of the junction between the high- and low-density foams. Because the line of force was through the c.g., all of the drop energy was available for deformation. The resulting dent was 2.5 in. deep, and no evidence of incipient ripping of the impact limiter shell was noted.

8. The third puncture performed on CTA-1 (CTA-1 test No. 13) demonstrated that a puncture on the impact limiter side shell adjacent to virgin high-density foam would not penetrate the shell. Also, because the line of force was directed through one of the OCV vent ports to the c.g., this puncture demonstrated that the vent ports located in the OCV base were not vulnerable to punctures. The puncture dent depth, measured from the side of the impact limiter, was 3 in. No evidence of incipient ripping of the impact limiter shell was noted.

9. The fifth puncture performed on CTA-1 (CTA-1 test No. 15) demonstrated the ability of the OCV sidewall and coolant jacket to absorb an oblique impact with the puncture bar, and to prove that the coolant jacket ribs, if ripped off, could not cause a breach of the OCV sidewall. The puncture bar contacted the package at an angle of 45° and aligned with the c.g. The maximum depth of the resulting dent (measured from the outer diameter of the coolant jacket ribs) was 1.5 in., with some deformation of the OCV sidewall. The ICV sidewall deformed 0.22 in.

10. The eighth puncture performed on CTA-1 (CTA-1 test No. 18) demonstrated that oblique impact of the OCV thermal shield with the puncture bar would not cause deformations in excess of those assumed in the thermal analysis. The long puncture bar was again used, and contacted the top of the OCV thermal shield 1 in. inboard from its outside edge. The package was oriented at 30° from the vertical. The resulting dent was just under 1.3 in. deep at its center, and of lesser depth elsewhere. For the analysis, a more conservative dent of 6 in. in diameter with a uniform depth of 1.3 in. was assumed.

11. The ninth puncture performed on CTA-1 (CTA-1 test No. 19) showed that direct impact on an impact limiter bolt access tube could not impart deleterious deformations to the OCV bolting flange. The package was oriented with axis vertical, and centered on an impact limiter bolt access tube. The 80-in.-long puncture bar was used. Portions of two adjacent OCV closure bolt access tubes were also impacted. Also, one of the coolant jacket nipples was crushed by secondary impact with the puncture bar.

2.7.6.3 Electrical Feed-through. The electrical feed-through located in the OCV and ICV remained leaktight after the full series of free drop and puncture events. (The electrical feed-throughs were leakage rate tested as a part of the vessel boundaries.) Because the OCV electrical feed-through is mounted at an orientation that is nearly perpendicular to that of the ICV electrical feed-through, it was possible to test the electrical feed-through structurally at several orientations to the principal impact load. In other words, the electrical feed-through pins were tested under conditions of peak impact load in orientations parallel to their axes, normal to their axes, and at several orientations in between. Further, it was demonstrated that the puncture bar could not penetrate the impact limiter shell or cause direct or indirect damage to the electrical feed-through devices.

2.7.6.4 Payload Interaction and Payload Rack Performance. During both the drop test series, the simulated payload interacted structurally with the ICV and the shipping rack assembly. The simulated payload broke free as the four payload attachment bolts pulled through the payload base. This allowed the payload to strike the inside of the ICV wall and head. Two of the payload fins crushed down to the rigid payload body. Three other fins were also damaged. The simulated

payload fins were of a stronger design and made from a stronger material than any of the actual payload fins. Interaction also occurred between the top of the simulated payload and the ICV head. The end of the main structural member of the simulated payload (a 14 in. o.d., 0.5 in. wall thickness steel pipe) struck the ICV lifting block, leaving a dent in the pipe that was 4.5 in. long and 0.5 in. deep. The ability of the ICV to withstand interaction forces with a loose, worst-case payload in a 30 ft HAC drop is thus demonstrated.

Damage to the shipping rack assembly was negligible. The shipping rack assembly barrier plate was deformed slightly (less than 1/16 in.) due to the loose simulated payload. The rack remained substantially in place without contacting the ICV wall. The ceramic fiber insulation located beneath the barrier plate also remained in place. The insulated sleeve that surrounds the ICV electrical feed-through mounting receptacle sustained no damage.

Because prototypical attachment bolts were used, the simulated payload was capable of applying the maximum amount of force to the mounting interface, which is the shipping rack assembly. These interface loads consisted of compression (toward the ICV baseplate) and traction in the plane of the shipping rack assembly barrier plate. Tension loads were not applied, because the simulated payload attachment bolts pass through the shipping rack assembly and attach directly to the ICV baseplate. The ability of the shipping rack assembly to protect the closure seals and electrical feed-through devices both structurally and thermally was thus demonstrated.

2.7.6.5 Measurements

2.7.6.5.1 Closure Bolt Removal Torque. None of the OCV or ICV closure bolts suffered a loss of pre-load because of the testing. A complete record of residual torques due to the entire series of free drop and puncture events for CTA-2 is given in Appendix 2.10.15.4.4. Before any drop testing, a study using CTA-2 demonstrated that removal torque could be as low as 50% of the assembly torque. With that test in mind, it is noted that the minimum removal torque after the full series of tests was well over 50% of the original application torque for both the OCV and ICV closure bolts.

The average OCV closure bolt removal torques varied from a low of 223 ft-lb to a high of 252 ft-lb. The assembly torque was 300 ft-lb. It is noted that several OCV closure bolts exhibited a removal torque of the full value of 300 ft-lb. The average ICV closure bolt removal torques varied from a low of 178 ft-lb to a high of 208 ft-lb. The assembly torque was 250 ft-lb. Measurements before and after the test series indicated there was no change in length in either the ICV or OCV closure bolts.

2.7.6.5.2 Seal Area Measurements. To perform properly, the containment vessel closure seals are dependent, in part, upon sufficient compression. Compression of the seals is a direct function of the space that the seal is forced (by surrounding metal) to occupy. During drop testing, permanent deformations of the flanges near the seals could change the relationship of the flanges to each other and thus change the seal compression. These measurements are discussed in greater detail in Appendix 2.10.14.

The maximum change in seal compression was a decrease of 0.005 in. for the OCV containment (0.393 nominal diameter) O-ring seal, and 0.001 in. for the ICV containment (0.275 nominal diameter) O-ring seal. These values are used in the analysis of containment in Section 4.3.2.

2.7.6.6 Measured Accelerations. During the first series of free drop tests, CTA-1 was instrumented with active and passive accelerometers. Details regarding placement and instrumentation parameters are given in the test procedure, Appendix 2.10.15. Passive

accelerometers were clustered as near as possible to the c.g. on one side of the CTA-1, and consisted of omni-directional trip indicators of 200, 300, and 400 g capacity. The active accelerometers were of the piezoresistive type, with a capacity of ± 750 g. The raw signals were recorded on analog tape and digitally filtered at 300Hz. This filtering frequency preserved a small degree of "ringing", which affords confidence that the full height of the original impact pulse is not lost. Thus, listed peaks are somewhat conservative. In cases of redundant measurements, the maximum reading is shown.

TABLE 2.7.6.8-1. Accelerometer Measurements (CTA-1).

	Active Accelerometer Peak Measurements		Passive Accelerometer Status		
Test No.	c.g. acceleration (*g*s)	Angular acceleration (rad/sec²)	200 *g*	300 *g*	400 *g*
6	275	2.26	Trip	Trip	Trip
7	269	Negligible	Trip	No trip	No trip
8	296	2.78	Trip	Trip	Trip
9	260	Negligible	Trip	Trip	Trip
10	240	Negligible	Trip	Trip	No trip

2.8 SPECIAL FORM

This section does not apply, because special form is not claimed.

2.9 FUEL RODS

This section does not apply, because fuel rods will not be shipped in this package.

2.10 APPENDIX

The following is a list of appendices contained within this section:

2.10.1 References

2.10.2 ICV Two-Dimensional (Axisymmetric) ANSYS Model

2.10.3 OCV Head and Fin ANSYS Model for Lifting Analysis

2.10.4 OCV Fin-to-Head Weld Properties ANSYS Model for Lifting Analysis

2.10.5 OCV Head ANSYS Model for Tiedown Analysis

2.10.6 Elastomer O-ring Performance Test Data

2.10.7 Summary of Thermal Load Cases and Results

2.10.8 OCV Two-Dimensional (Axisymmetric) ANSYS Model

2.10.9 RTG Transportation System Package Certification Test Plan

2.10.10 Certification Drop Test Procedure for the RTG Package

2.10.11 Half-Scale Structural Development Test Report

2.10.12 ICV Three-Dimensional ANSYS Model

2.10.13 OCV Three-Dimensional ANSYS Model

2.10.14 O-Ring Seal Compression Measurements

2.10.15 Summary of Damage from Certification Testing

2.10.1 References

1. 10 CFR 71, 1993, "Packaging and Transportation of Radioactive Materials," *Code of Federal Regulations*, as amended.

2. Regulatory Guide (Reg Guide) 7.6, 1978, *Design Criteria for the Structural Analysis of Shipping Cask Containment Vessels*, Rev. 1.

3. "*General Plastics Last-A-Foam® FR-3700 for Crash & Fire Protection of Nuclear Material Shipping Containers*," 1992, General Plastics Manufacturing Co., Tacoma, Washington.

4. "*Safety Analysis Report for the TRUPACT-II Shipping Package*," NRC Docket Number 71-7218, Nuclear Packaging, Inc., Federal Way, Washington.

5. American Society of Mechanical Engineers (ASME) Boiler and Pressure Vessel (B&PV) Code.

6. ANSI, 1987, *American National Standard for Radioactive Materials--Leakage Tests on Packages for Shipment* ANSI Standard N14.5, American National Standards Institute, New York, New York.

7. NUREG CR-3019, 1985, *Recommended Welding Criteria for Use in the Fabrication of Shipping Containers for Radioactive Material*.

8. NUREG CR-3854, 1985, *Fabrication Criteria for Shipping Containers*.

9. Regulatory Guide (Reg Guide) 7.8, 1989, *Load Combinations for the Structural Analysis of Shipping Casks for Radioactive Material*, Rev. 1.

10. ASME B&PV Code Case N-284, 1980, *Metal Containment Shell Buckling Design Methods*, Section III, Division 1, Class MC.

11. NUREG/CR-1815, 1981, *Recommendations for Protecting Against Failure by Brittle Fracture in Ferritic Steel Shipping Containers Up to Four Inches Thick*.

12. ASME B&PV Code Case N-47-23, Class 1 Components in Elevated Temperature Service.

13. *Safety Analysis Report for the NuPac 125-B Fuel Shipping Cask*, NRC Docket No. 71-9200, Nuclear Packaging, Inc., Federal Way, Washington.

14. *Safety Analysis Report for the NuPac 10-142 Shipping Cask*, NRC Docket No. 71-9208, Nuclear Packaging, Inc., Federal Way, Washington.

15. *Safety Analysis Report for the NuPac PAS-1 Shipping Cask*, NRC Docket No. 71-9184, Nuclear Packaging, Inc., Federal Way, Washington.

16. *Safety Analysis Report for the CNSI 1-13C II Shipping Cask*, NRC Docket No. 71-9152, Chem-Nuclear Systems, Inc., Columbia, South Carolina.

17. *Parker O-Ring Handbook*, ORD 5700, Parker Seal O-Ring Division, Lexington, Kentucky.

18. Boucher, R., 1961, "Strength of Threads," *Product Engineering*, 1961.

19. Timoshenko, S., and J., Goodier, *Theory of Elasticity*, 3rd Edition, McGraw-Hill, New York, New York.

20. Young, W. C., *Roark's Formulas for Stress and Strain*, 6th Edition, McGraw-Hill, New York, New York.

21. Shigley, J. E., and L. D., Mitchell, *Mechanical Engineering Design*, 4th Edition, McGraw-Hill, New York, New York.

22. ANSI, 1980, *Design Basis for Resistance to Shock and Vibration of Radioactive Material Packages Greater Than One Ton in Truck Transport*, Standard N-14.23, American National Standards Institute, New York, New York.

23. Bickford, J., *An Introduction to the Design and Behavior of Bolted Joints*, Marcel Dekker, New York, New York.

24. Baily, B., *STRAIN, A Computerized Database Program*, Lawrence Livermore National Laboratory.

25. Steele, J. M., *Applied Finite Element Modeling*, Marcel Dekker, New York, New York.

2.10.2 ICV Two-Dimensional (Axisymmetric) ANSYS Model

2.10.2.1 Description. The 2-D ICV model is an axisymmetric finite element model of the entire ICV. It consists of a base and a bell, connected by a bolt element and a gap element. It is used to evaluate containment vessel stresses and closure bolt stresses under NCT. (The model used for HAC is 3-D and is described in Appendix 2.10.12.) The applied loading takes the form of internal gas pressure, nodal temperatures, and initial closure bolt pre-load. The model is used for the ICV analysis cases given in Table 2.6.1.3-1, as well as the ICV bell lifting analysis of Section 2.5.1.1.2. The model layout is shown in Figure 2.10.2-1.

2.10.2.2 Construction. The model consists of four element types:

1. To model the ICV containment boundary, isoparametric 2-D elements are used for both the 3.47-in.-thick base and ICV flange. This element type is also used in the ICV bell wall, with a quantity of four through the wall thickness, up to a height of 11.725 in. above the datum (the bottom of the base).

2. For the remainder of the ICV bell, axisymmetric shells, located at the section midplane, are used. The shell thicknesses are 0.75 in. in the wall, 0.375 in. in the torispherical head, and in the area of the lifting block, 2 in. To join shell and isoparametric elements, an embedded shell element is used, having 1/10th of the bending stiffness of the adjacent shell element. See Reference 25, Chapter 9.

3. A single 2-D spar (element 156, nodes 52 and 104) was used to represent all of the closure bolts. The property of closure bolt area was entered on a per-radian basis by first multiplying the equivalent area of each bolt by the total bolt quantity (24) and then dividing by 2π. Since the threads extend all the way to the bolt head, the closure bolt area is based on the minimum thread area and is equal to 0.330 $in.^2$ per bolt. The bolt element was given an initial strain to achieve the desired closure bolt pre-load force at 70 °F in the absence of other loads (per Table 2.6.1.2.1-1).

4. A gap is used between the ICV base and flange at the closure bolt location to react to the bolt loads. Because this coincides with a step machined in the flange lower surface, no other gap elements were necessary.

Node and element plots of key portions of the model are given in Figures 2.10.2-2 through 2.10.2-7. An interpreted ANSYS input listing is given in Table 2.10.2-1.

2.10.2.3 Material Properties. The modulus of elasticity and coefficient of thermal expansion varied with temperature according to the data in Tables 2.3-1 and 2.3-2. Poisson's ratio is 0.3.

2.10.2.4 Constraints. The bottom center node of the ICV base was fixed in all coordinate directions, but the rest of the base was allowed to deflect as determined by the loading. The top center of the ICV was restrained in a radial direction to ensure axisymmetry. The hoop direction of all nodes was restrained. The top center node was also restrained from rotation about the hoop axis.

2.10.2.5 Applied Loading. All ICV surfaces subject to internal pressure had a constant pressure applied. Nodal temperature loading was applied using temperatures resulting from thermal model output. Because there were fewer thermal model nodes than structural model nodes, interpolation of thermal model temperatures was required. Temperatures in the ICV base were set as follows: nodes 1 to 20 used the average of thermal nodes 260 and 261; nodes 21 to 30 used the average of thermal nodes 262 and 263; and nodes 31 to 58 used the average of thermal nodes 264, 265,

and 266. The ICV flange temperature was set using thermal node 250. In the wall region above the ICV flange, the temperatures of structural nodes that corresponded exactly in location to the thermal model counterparts were set directly; the temperatures of structural nodes that fell in between thermal nodes were established using linear interpolation. Because the closure bolt was not modeled thermally, in the structural model it took the temperatures of the ICV flange and base at its attachment nodes. The reference temperature was 70 °F.

The ICV base and closure bolts were not used in the lifting analysis. The lower flange nodes (96 to 101) were fixed in the axial direction, and a vertical force of 1,600 pounds was applied to the center of the ICV head. For lifting, nodal temperatures corresponding to NCT case 1 were used. No pressure loading was used.

2.10.2.6 Results. Worst-case ICV lifting stress intensity occurs in the head and is shown in Figure 2.10.2.8. The worst-case containment boundary stresses occur for NCT case ICV-2 (see Section 2.6.1.3) and are shown in Figure 2.10.2-9 through 2.10.2-11. The worst-case ICV flange stress intensity is for NCT case ICV-1 and is shown in Figure 2.10.2-12.

APPENDIX 2.10.2
REVISED ANSYS COMPUTER OUTPUT

```
STATIC ANALYSIS (KAN= 0)

LINEAR ANALYSIS - NO NON-LINEAR PROPERTIES

REFERENCE TEMPERATURE=     70.000 (TREF)
UNIFORM TEMPERATURE  =    -40.000 (TUNIF)

*****ANALYSIS OPTIONS (KAY VALUES) (IF ANY) *****

NO STATIC INTERPOLATION/EXTRAPOLATION (KAY(3)=0)

SMALL DEFLECTION SOLUTION (KAY(6)=0)

NO STRESS STIFFENING (KAY(8)=0)

USE INITIAL-STIFFNESS NEWTON-RAPHSON SOLUTION PROCEDURE  (KAY(9)=3)

IN-CORE WAVE-FRONT EQUATION SOLVER (KAY(10)=0)

LIST ELEMENT TYPES FROM  1 TO 20 BY 1

NO. STIF          KEYOPT VALUES          INOPR
 1   42   0  0  1   0  0  0   0  0  0   0  ISOPAR. STRESS SOLID, 2-D
 2   51   0  0  0   0  0  0   0  0  0   0  PLASTIC AXISYM. CONIC SHELL
 3    1   0  0  0   0  0  0   0  0  0   0  SPAR, 2-D
 4   12   0  0  0   0  0  0   0  0  0   0  INTERFACE ELEM. 2-D

LIST ALL REAL SETS

 REAL CONSTANT SET   1  ITEMS   1 TO   6
  0.75000      0.00000E+00  0.00000E+00  0.00000E+00  0.00000E+00  0.00000E+00

 REAL CONSTANT SET   2  ITEMS   1 TO   6
  0.37500      0.00000E+00  0.00000E+00  0.00000E+00  0.00000E+00  0.00000E+00

 REAL CONSTANT SET   3  ITEMS   1 TO   6
   1.2600      0.26810E-02  0.00000E+00  0.00000E+00  0.00000E+00  0.00000E+00

 REAL CONSTANT SET   4  ITEMS   1 TO   6
  0.00000E+00  0.95500E+09  0.00000E+00  0.00000E+00  0.00000E+00  0.00000E+00

 REAL CONSTANT SET   5  ITEMS   1 TO   6
   2.0000      0.00000E+00  0.00000E+00  0.00000E+00  0.00000E+00  0.00000E+00

 REAL CONSTANT SET   6  ITEMS   1 TO   6
  0.34800      0.00000E+00  0.00000E+00  0.00000E+00  0.00000E+00  0.00000E+00
LIST ALL COORDINATE SYSTEMS

    SYSTEM TYPE                    CENTER              PARAMETERS    SING KEYS
 0  0 (CARTESIAN)          0.000      0.000      0.000   0.000  0.000  0  0
 1  1 (CYLINDRICAL)        0.000      0.000      0.000   1.000  0.000  0  0
 2  2 (SPHERICAL)          0.000      0.000      0.000   1.000  1.000  0  0
11  1 (CYLINDRICAL)        0.000     27.220      0.000   1.000  1.000  0  0
12  1 (CYLINDRICAL)       14.940     56.370      0.000   1.000  1.000  0  0

SYSTEM              ORIENTATION VECTORS (X,Y,Z)
    0      1.00  0.00  0.00    0.00  1.00  0.00    0.00  0.00  1.00
    1      1.00  0.00  0.00    0.00  1.00  0.00    0.00  0.00  1.00
    2      1.00  0.00  0.00    0.00  1.00  0.00    0.00  0.00  1.00
   11      1.00  0.00  0.00    0.00  1.00  0.00    0.00  0.00  1.00
   12      1.00  0.00  0.00    0.00  1.00  0.00    0.00  0.00  1.00
CSYS TYPE    XC          YC          ZC          THXY      THYZ      THXZ
 11    1 0.00000E+00  27.220     0.00000E+00     0.000     0.000     0.000
 12    1  14.940      56.370     0.00000E+00     0.000     0.000     0.000

LIST ALL SELECTED ELEMENTS.   (LIST NODES)

  ELEM MAT TYP REL ESYS         NODES
```

1	1	1	1	0	1	6	7	2
2	1	1	1	0	2	7	8	3
3	1	1	1	0	3	8	9	4
4	1	1	1	0	4	9	10	5
5	1	1	1	0	6	11	12	7
6	1	1	1	0	7	12	13	8
7	1	1	1	0	8	13	14	9
8	1	1	1	0	9	14	15	10
9	1	1	1	0	11	16	17	12
10	1	1	1	0	12	17	18	13
11	1	1	1	0	13	18	19	14
12	1	1	1	0	14	19	20	15
13	1	1	1	0	16	21	22	17
14	1	1	1	0	17	22	23	18
15	1	1	1	0	18	23	24	19
16	1	1	1	0	19	24	25	20
17	1	1	1	0	21	26	27	22
18	1	1	1	0	22	27	28	23
19	1	1	1	0	23	28	29	24
20	1	1	1	0	24	29	30	25

ELEM	MAT	TYP	REL	ESYS	NODES			
21	1	1	1	0	26	31	32	27
22	1	1	1	0	27	32	33	28
23	1	1	1	0	28	33	34	29
24	1	1	1	0	29	34	35	30
25	1	1	1	0	31	36	37	32
26	1	1	1	0	32	37	38	33
27	1	1	1	0	33	38	39	34
28	1	1	1	0	34	39	40	35
29	1	1	1	0	36	41	42	37
30	1	1	1	0	37	42	43	38
31	1	1	1	0	41	46	47	42
32	1	1	1	0	42	47	48	43
33	1	1	1	0	46	51	52	47
34	1	1	1	0	47	52	53	48
35	1	1	1	0	51	56	57	52
36	1	1	1	0	52	57	58	53
37	1	1	1	0	96	97	102	101
38	1	1	1	0	97	98	103	102
39	1	1	1	0	98	99	104	103
40	1	1	1	0	99	100	105	104

ELEM	MAT	TYP	REL	ESYS	NODES			
41	1	1	1	0	101	102	107	106
42	1	1	1	0	102	103	108	107
43	1	1	1	0	103	104	109	108
44	1	1	1	0	104	105	110	109
45	1	1	1	0	106	107	112	111
46	1	1	1	0	107	108	113	112
47	1	1	1	0	108	109	114	113
48	1	1	1	0	109	110	115	114
49	1	1	1	0	111	112	117	116
50	1	1	1	0	112	113	118	117
51	1	1	1	0	113	114	119	118
52	1	1	1	0	114	115	120	119
53	1	1	1	0	116	117	122	121
54	1	1	1	0	117	118	123	122
55	1	1	1	0	118	119	124	123
56	1	1	1	0	119	120	125	124
57	1	1	1	0	121	122	127	126
58	1	1	1	0	122	123	128	127
59	1	1	1	0	123	124	129	128
60	1	1	1	0	124	125	130	129

ELEM	MAT	TYP	REL	ESYS	NODES			
61	1	1	1	0	126	127	132	131
62	1	1	1	0	127	128	133	132
63	1	1	1	0	128	129	134	133
64	1	1	1	0	129	130	135	134
65	1	1	1	0	131	132	137	136

66	1	1	1	0	132	133	138	137
67	1	1	1	0	133	134	139	138
68	1	1	1	0	134	135	140	139
69	1	1	1	0	136	137	142	141
70	1	1	1	0	137	138	143	142
71	1	1	1	0	138	139	144	143
72	1	1	1	0	139	140	145	144
73	1	1	1	0	141	142	147	146
74	1	1	1	0	142	143	148	147
75	1	1	1	0	143	144	149	148
76	1	1	1	0	144	145	150	149
77	1	1	1	0	146	147	152	151
78	1	1	1	0	147	148	153	152
79	1	1	1	0	148	149	154	153
80	1	1	1	0	149	150	155	154

ELEM	MAT	TYP	REL	ESYS	NODES			
81	1	1	1	0	151	152	157	156
82	1	1	1	0	152	153	158	157
83	1	1	1	0	153	154	159	158
84	1	1	1	0	154	155	160	159
85	1	1	1	0	156	157	162	161
86	1	1	1	0	157	158	163	162
87	1	1	1	0	158	159	164	163
88	1	1	1	0	159	160	165	164
89	1	1	1	0	161	162	167	166
90	1	1	1	0	162	163	168	167
91	1	1	1	0	163	164	169	168
92	1	1	1	0	164	165	170	169
93	1	1	1	0	166	167	172	171
94	1	1	1	0	167	168	173	172
95	1	1	1	0	168	169	174	173
96	1	1	1	0	169	170	175	174
97	1	1	1	0	171	172	177	176
98	1	1	1	0	172	173	178	177
99	1	1	1	0	173	174	179	178
100	1	1	1	0	174	175	180	179

ELEM	MAT	TYP	REL	ESYS	NODES			
101	1	1	1	0	95	121	126	126
102	1	2	6	0	173	178		
103	1	2	1	0	178	201		
104	1	2	1	0	201	202		
105	1	2	1	0	202	203		
106	1	2	1	0	203	204		
107	1	2	1	0	204	205		
108	1	2	1	0	205	206		
109	1	2	1	0	206	207		
110	1	2	1	0	207	208		
111	1	2	1	0	208	209		
112	1	2	1	0	209	210		
113	1	2	1	0	210	211		
114	1	2	1	0	211	212		
115	1	2	1	0	212	213		
116	1	2	1	0	213	214		
117	1	2	1	0	214	215		
118	1	2	1	0	215	216		
119	1	2	1	0	216	217		
120	1	2	1	0	217	218		

ELEM	MAT	TYP	REL	ESYS	NODES	
121	1	2	1	0	218	219
122	1	2	1	0	219	220
123	1	2	1	0	220	221
124	1	2	1	0	221	222
125	1	2	1	0	222	223
126	1	2	1	0	223	224
127	1	2	1	0	224	225
128	1	2	1	0	225	226
129	1	2	1	0	226	227
130	1	2	1	0	227	228

131	1	2	1	0	228	229
132	1	2	1	0	229	230
133	1	2	1	0	230	231
134	1	2	1	0	231	232
135	1	2	1	0	232	233
136	1	2	1	0	233	234
137	1	2	1	0	234	235
138	1	2	1	0	235	236
139	1	2	2	0	236	237
140	1	2	2	0	237	238

ELEM	MAT	TYP	REL	ESYS	NODES	
141	1	2	2	0	238	239
142	1	2	2	0	239	240
143	1	2	2	0	240	241
144	1	2	2	0	241	242
145	1	2	2	0	242	243
146	1	2	2	0	243	244
147	1	2	2	0	244	245
148	1	2	2	0	245	246
149	1	2	2	0	246	247
150	1	2	2	0	247	248
151	1	2	2	0	248	249
152	1	2	2	0	249	250
153	1	2	2	0	250	251
154	1	2	5	0	251	252
155	1	2	5	0	252	253
156	2	3	3	0	52	104
157	2	4	4	0	43	97
158	2	4	4	0	53	99

LIST ALL SELECTED NODE DSYS= 0

NODE	X	Y	Z	THXY	THYZ	THXZ
1	0.00000E+00	0.00000E+00	0.00000E+00	0.00	0.00	0.00
2	0.00000E+00	0.86750	0.00000E+00	0.00	0.00	0.00
3	0.00000E+00	1.7350	0.00000E+00	0.00	0.00	0.00
4	0.00000E+00	2.6025	0.00000E+00	0.00	0.00	0.00
5	0.00000E+00	3.4700	0.00000E+00	0.00	0.00	0.00
6	3.5000	0.00000E+00	0.00000E+00	0.00	0.00	0.00
7	3.5000	0.86750	0.00000E+00	0.00	0.00	0.00
8	3.5000	1.7350	0.00000E+00	0.00	0.00	0.00
9	3.5000	2.6025	0.00000E+00	0.00	0.00	0.00
10	3.5000	3.4700	0.00000E+00	0.00	0.00	0.00
11	7.0000	0.00000E+00	0.00000E+00	0.00	0.00	0.00
12	7.0000	0.86750	0.00000E+00	0.00	0.00	0.00
13	7.0000	1.7350	0.00000E+00	0.00	0.00	0.00
14	7.0000	2.6025	0.00000E+00	0.00	0.00	0.00
15	7.0000	3.4700	0.00000E+00	0.00	0.00	0.00
16	9.8750	0.00000E+00	0.00000E+00	0.00	0.00	0.00
17	9.8750	0.86750	0.00000E+00	0.00	0.00	0.00
18	9.8750	1.7350	0.00000E+00	0.00	0.00	0.00
19	9.8750	2.6025	0.00000E+00	0.00	0.00	0.00
20	9.8750	3.4700	0.00000E+00	0.00	0.00	0.00

NODE	X	Y	Z	THXY	THYZ	THXZ
21	12.750	0.00000E+00	0.00000E+00	0.00	0.00	0.00
22	12.750	0.86750	0.00000E+00	0.00	0.00	0.00
23	12.750	1.7350	0.00000E+00	0.00	0.00	0.00
24	12.750	2.6025	0.00000E+00	0.00	0.00	0.00
25	12.750	3.4700	0.00000E+00	0.00	0.00	0.00
26	14.325	0.00000E+00	0.00000E+00	0.00	0.00	0.00
27	14.325	0.86750	0.00000E+00	0.00	0.00	0.00
28	14.325	1.7350	0.00000E+00	0.00	0.00	0.00
29	14.325	2.6025	0.00000E+00	0.00	0.00	0.00
30	14.325	3.4700	0.00000E+00	0.00	0.00	0.00
31	15.900	0.00000E+00	0.00000E+00	0.00	0.00	0.00
32	15.900	0.86750	0.00000E+00	0.00	0.00	0.00
33	15.900	1.7350	0.00000E+00	0.00	0.00	0.00
34	15.900	2.6025	0.00000E+00	0.00	0.00	0.00
35	15.900	3.4700	0.00000E+00	0.00	0.00	0.00
36	16.970	0.00000E+00	0.00000E+00	0.00	0.00	0.00

37	16.970	0.86750	0.00000E+00	0.00	0.00	0.00
38	16.970	1.4700	0.00000E+00	0.00	0.00	0.00
39	16.970	2.6025	0.00000E+00	0.00	0.00	0.00
40	16.970	3.4700	0.00000E+00	0.00	0.00	0.00

NODE	X	Y	Z	THXY	THYZ	THXZ
41	17.360	0.00000E+00	0.00000E+00	0.00	0.00	0.00
42	17.360	0.86750	0.00000E+00	0.00	0.00	0.00
43	17.360	1.4700	0.00000E+00	0.00	0.00	0.00
46	17.875	0.00000E+00	0.00000E+00	0.00	0.00	0.00
47	17.875	0.86750	0.00000E+00	0.00	0.00	0.00
48	17.875	1.4700	0.00000E+00	0.00	0.00	0.00
51	18.625	0.00000E+00	0.00000E+00	0.00	0.00	0.00
52	18.625	0.58000	0.00000E+00	0.00	0.00	0.00
53	18.625	1.4700	0.00000E+00	0.00	0.00	0.00
56	19.480	0.00000E+00	0.00000E+00	0.00	0.00	0.00
57	19.480	0.58000	0.00000E+00	0.00	0.00	0.00
58	19.480	1.4700	0.00000E+00	0.00	0.00	0.00
95	16.815	3.6000	0.00000E+00	0.00	0.00	0.00
96	17.000	1.4700	0.00000E+00	0.00	0.00	0.00
97	17.360	1.4700	0.00000E+00	0.00	0.00	0.00
98	17.875	1.4700	0.00000E+00	0.00	0.00	0.00
99	18.625	1.4700	0.00000E+00	0.00	0.00	0.00
100	19.375	1.4700	0.00000E+00	0.00	0.00	0.00
101	17.000	2.0700	0.00000E+00	0.00	0.00	0.00
102	17.360	2.0700	0.00000E+00	0.00	0.00	0.00

NODE	X	Y	Z	THXY	THYZ	THXZ
103	17.875	2.0700	0.00000E+00	0.00	0.00	0.00
104	18.625	2.0700	0.00000E+00	0.00	0.00	0.00
105	19.375	2.0700	0.00000E+00	0.00	0.00	0.00
106	17.000	2.6200	0.00000E+00	0.00	0.00	0.00
107	17.594	2.6200	0.00000E+00	0.00	0.00	0.00
108	18.188	2.6200	0.00000E+00	0.00	0.00	0.00
109	18.781	2.6200	0.00000E+00	0.00	0.00	0.00
110	19.375	2.6200	0.00000E+00	0.00	0.00	0.00
111	17.000	2.9467	0.00000E+00	0.00	0.00	0.00
112	17.458	3.0004	0.00000E+00	0.00	0.00	0.00
113	17.917	3.0542	0.00000E+00	0.00	0.00	0.00
114	18.375	3.1079	0.00000E+00	0.00	0.00	0.00
115	18.833	3.1617	0.00000E+00	0.00	0.00	0.00
116	17.000	3.2733	0.00000E+00	0.00	0.00	0.00
117	17.323	3.3808	0.00000E+00	0.00	0.00	0.00
118	17.646	3.4883	0.00000E+00	0.00	0.00	0.00
119	17.969	3.5958	0.00000E+00	0.00	0.00	0.00
120	18.292	3.7033	0.00000E+00	0.00	0.00	0.00
121	17.000	3.6000	0.00000E+00	0.00	0.00	0.00
122	17.188	3.7613	0.00000E+00	0.00	0.00	0.00

NODE	X	Y	Z	THXY	THYZ	THXZ
123	17.375	3.9225	0.00000E+00	0.00	0.00	0.00
124	17.563	4.0838	0.00000E+00	0.00	0.00	0.00
125	17.750	4.2450	0.00000E+00	0.00	0.00	0.00
126	16.815	3.7700	0.00000E+00	0.00	0.00	0.00
127	17.049	3.9869	0.00000E+00	0.00	0.00	0.00
128	17.283	4.2038	0.00000E+00	0.00	0.00	0.00
129	17.516	4.4206	0.00000E+00	0.00	0.00	0.00
130	17.750	4.6375	0.00000E+00	0.00	0.00	0.00
131	17.000	4.4600	0.00000E+00	0.00	0.00	0.00
132	17.188	4.6025	0.00000E+00	0.00	0.00	0.00
133	17.375	4.7450	0.00000E+00	0.00	0.00	0.00
134	17.563	4.8875	0.00000E+00	0.00	0.00	0.00
135	17.750	5.0300	0.00000E+00	0.00	0.00	0.00
136	17.000	5.0150	0.00000E+00	0.00	0.00	0.00
137	17.188	5.1100	0.00000E+00	0.00	0.00	0.00
138	17.375	5.2050	0.00000E+00	0.00	0.00	0.00
139	17.563	5.3000	0.00000E+00	0.00	0.00	0.00
140	17.750	5.3950	0.00000E+00	0.00	0.00	0.00
141	17.000	5.5700	0.00000E+00	0.00	0.00	0.00
142	17.188	5.6175	0.00000E+00	0.00	0.00	0.00

NODE	X	Y	Z	THXY	THYZ	THXZ
143	17.375	5.6650	0.00000E+00	0.00	0.00	0.00
144	17.563	5.7125	0.00000E+00	0.00	0.00	0.00

145	17.750	5.7600	0.00000E+00	0.00	0.00	0.00
146	17.000	6.1250	0.00000E+00	0.00	0.00	0.00
147	17.188	6.1250	0.00000E+00	0.00	0.00	0.00
148	17.375	6.1250	0.00000E+00	0.00	0.00	0.00
149	17.563	6.1250	0.00000E+00	0.00	0.00	0.00
150	17.750	6.1250	0.00000E+00	0.00	0.00	0.00
151	17.000	7.0583	0.00000E+00	0.00	0.00	0.00
152	17.188	7.0583	0.00000E+00	0.00	0.00	0.00
153	17.375	7.0583	0.00000E+00	0.00	0.00	0.00
154	17.563	7.0583	0.00000E+00	0.00	0.00	0.00
155	17.750	7.0583	0.00000E+00	0.00	0.00	0.00
156	17.000	7.9917	0.00000E+00	0.00	0.00	0.00
157	17.188	7.9917	0.00000E+00	0.00	0.00	0.00
158	17.375	7.9917	0.00000E+00	0.00	0.00	0.00
159	17.563	7.9917	0.00000E+00	0.00	0.00	0.00
160	17.750	7.9917	0.00000E+00	0.00	0.00	0.00
161	17.000	8.9250	0.00000E+00	0.00	0.00	0.00
162	17.188	8.9250	0.00000E+00	0.00	0.00	0.00

NODE	X	Y	Z	THXY	THYZ	THXZ
163	17.375	8.9250	0.00000E+00	0.00	0.00	0.00
164	17.563	8.9250	0.00000E+00	0.00	0.00	0.00
165	17.750	8.9250	0.00000E+00	0.00	0.00	0.00
166	17.000	9.8583	0.00000E+00	0.00	0.00	0.00
167	17.188	9.8583	0.00000E+00	0.00	0.00	0.00
168	17.375	9.8583	0.00000E+00	0.00	0.00	0.00
169	17.563	9.8583	0.00000E+00	0.00	0.00	0.00
170	17.750	9.8583	0.00000E+00	0.00	0.00	0.00
171	17.000	10.792	0.00000E+00	0.00	0.00	0.00
172	17.188	10.792	0.00000E+00	0.00	0.00	0.00
173	17.375	10.792	0.00000E+00	0.00	0.00	0.00
174	17.563	10.792	0.00000E+00	0.00	0.00	0.00
175	17.750	10.792	0.00000E+00	0.00	0.00	0.00
176	17.000	11.725	0.00000E+00	0.00	0.00	0.00
177	17.188	11.725	0.00000E+00	0.00	0.00	0.00
178	17.375	11.725	0.00000E+00	0.00	0.00	0.00
179	17.563	11.725	0.00000E+00	0.00	0.00	0.00
180	17.750	11.725	0.00000E+00	0.00	0.00	0.00
201	17.375	12.689	0.00000E+00	0.00	0.00	0.00
202	17.375	13.654	0.00000E+00	0.00	0.00	0.00

NODE	X	Y	Z	THXY	THYZ	THXZ
203	17.375	14.619	0.00000E+00	0.00	0.00	0.00
204	17.375	15.583	0.00000E+00	0.00	0.00	0.00
205	17.375	16.548	0.00000E+00	0.00	0.00	0.00
206	17.375	17.512	0.00000E+00	0.00	0.00	0.00
207	17.375	18.477	0.00000E+00	0.00	0.00	0.00
208	17.375	19.441	0.00000E+00	0.00	0.00	0.00
209	17.375	20.406	0.00000E+00	0.00	0.00	0.00
210	17.375	21.370	0.00000E+00	0.00	0.00	0.00
211	17.375	22.710	0.00000E+00	0.00	0.00	0.00
212	17.375	24.050	0.00000E+00	0.00	0.00	0.00
213	17.375	25.390	0.00000E+00	0.00	0.00	0.00
214	17.375	26.730	0.00000E+00	0.00	0.00	0.00
215	17.375	28.070	0.00000E+00	0.00	0.00	0.00
216	17.375	29.410	0.00000E+00	0.00	0.00	0.00
217	17.375	30.750	0.00000E+00	0.00	0.00	0.00
218	17.375	32.090	0.00000E+00	0.00	0.00	0.00
219	17.375	33.430	0.00000E+00	0.00	0.00	0.00
220	17.375	34.770	0.00000E+00	0.00	0.00	0.00
221	17.375	36.110	0.00000E+00	0.00	0.00	0.00
222	17.375	37.450	0.00000E+00	0.00	0.00	0.00

NODE	X	Y	Z	THXY	THYZ	THXZ
223	17.375	38.790	0.00000E+00	0.00	0.00	0.00
224	17.375	40.130	0.00000E+00	0.00	0.00	0.00
225	17.375	41.470	0.00000E+00	0.00	0.00	0.00
226	17.375	42.810	0.00000E+00	0.00	0.00	0.00
227	17.375	44.150	0.00000E+00	0.00	0.00	0.00
228	17.375	45.490	0.00000E+00	0.00	0.00	0.00
229	17.375	46.830	0.00000E+00	0.00	0.00	0.00
230	17.375	48.170	0.00000E+00	0.00	0.00	0.00
231	17.375	49.137	0.00000E+00	0.00	0.00	0.00
232	17.375	50.103	0.00000E+00	0.00	0.00	0.00

233	17.375	51.070	0.00000E+00	0.00	0.00	0.00
234	17.375	52.037	0.00000E+00	0.00	0.00	0.00
235	17.375	53.003	0.00000E+00	0.00	0.00	0.00
236	17.375	53.970	0.00000E+00	0.00	0.00	0.00
237	17.375	55.170	0.00000E+00	0.00	0.00	0.00
238	17.377	56.370	0.00000E+00	0.00	0.00	0.00
239	17.319	56.900	0.00000E+00	0.00	0.00	0.00
240	17.146	57.405	0.00000E+00	0.00	0.00	0.00
241	16.868	57.860	0.00000E+00	0.00	0.00	0.00
242	16.498	58.244	0.00000E+00	0.00	0.00	0.00

NODE	X	Y	Z	THXY	THYZ	THXZ
243	16.052	58.538	0.00000E+00	0.00	0.00	0.00
244	14.551	59.263	0.00000E+00	0.00	0.00	0.00
245	13.018	59.915	0.00000E+00	0.00	0.00	0.00
246	11.455	60.495	0.00000E+00	0.00	0.00	0.00
247	9.8666	60.999	0.00000E+00	0.00	0.00	0.00
248	8.2561	61.428	0.00000E+00	0.00	0.00	0.00
249	6.6272	61.780	0.00000E+00	0.00	0.00	0.00
250	4.9834	62.055	0.00000E+00	0.00	0.00	0.00
251	3.3284	62.251	0.00000E+00	0.00	0.00	0.00
252	1.6661	62.369	0.00000E+00	0.00	0.00	0.00
253	0.13711E-09	62.408	0.00000E+00	0.00	0.00	0.00

```
LIST ALL MATERIALS  PROPERTY= ALL

PROPERTY TABLE NUXY  MAT=   1  NUM. POINTS=  2
    TEMPERATURE      DATA     TEMPERATURE      DATA
     -9999.0      0.30000       9999.0      0.30000

PROPERTY TABLE EX    MAT=   1  NUM. POINTS= 15
    TEMPERATURE      DATA     TEMPERATURE      DATA
      -40.000     0.28900E+08  70.000      0.28300E+08
       100.00     0.28100E+08  200.00      0.27600E+08
       300.00     0.27000E+08  400.00      0.26500E+08
       500.00     0.25800E+08  600.00      0.25300E+08
       700.00     0.24800E+08  800.00      0.24100E+08
       900.00     0.23500E+08  1000.0      0.22500E+08
       1100.0     0.22100E+08  1200.0      0.21300E+08
       1300.0     0.20500E+08

PROPERTY TABLE ALPX  MAT=   1  NUM. POINTS= 15
    TEMPERATURE      DATA     TEMPERATURE      DATA
      -40.000     0.81300E-05  70.000      0.84600E-05
       100.00     0.85500E-05  200.00      0.87900E-05
       300.00     0.90000E-05  400.00      0.91900E-05
       500.00     0.93700E-05  600.00      0.95300E-05
       700.00     0.96900E-05  800.00      0.98200E-05
       900.00     0.10060E-04  1000.0      0.10300E-04
       1100.0     0.10350E-04  1200.0      0.10400E-04
       1300.0     0.10450E-04

PROPERTY TABLE EX    MAT=   2  NUM. POINTS=  7
    TEMPERATURE      DATA     TEMPERATURE      DATA
      -40.000     0.28400E+08  70.000      0.27800E+08
       100.00     0.27600E+08  200.00      0.27100E+08
       300.00     0.26700E+08  400.00      0.26100E+08
       500.00     0.25700E+08

PROPERTY TABLE ALPX  MAT=   2  NUM. POINTS=  7
    TEMPERATURE      DATA     TEMPERATURE      DATA
      -40.000     0.59400E-05  70.000      0.62000E-05
       100.00     0.62700E-05  200.00      0.65400E-05
       300.00     0.67800E-05  400.00      0.69800E-05
       500.00     0.71600E-05
TIME= 0.00000E+00  NITTER=     -5
KTEMP-  LSTP=     -1  ITER=     0

UNIFORM TEMPERATURE=   -40.000  (TREF=    70.000)
 BOUNDARY CONDITIONS STEPPED DUE TO STATIC CONVERGENCE OPTION
PLASTIC CONVERG. CRITERION=      0.0100
CREEP OPTIMUM. CRITERION=      0.1000
LARGE DEFL. CONVERG. CRITERION=    0.001000
DISPLACEMENT LIMIT= 0.00000E+00
```

```
NPRINT= 99900   NPOST=     5   REACTION PRINT FREQ= 99900
 DISP. POST DATA FREQ=     5  REACT. POST DATA FREQ=     5

 ELEMENT PRINT AND POST DATA FREQUENCIES
  TYPE  STIFF  STRESS  FORCE   STRESS   DATA  FORCE
        NO.    PRINT  PRINT    DATA    LEVEL  DATA
     1    42  99900  99900       5      3     5
     2    51  99900  99900       5      3     5
     3     1  99900  99900       5      3     5
     4    12  99900  99900       5      3     5

LOADS INPUT FILE= 26     LOADS OUTPUT FILE= 23

ALL ANALYSIS DATA WILL BE WRITTEN ONTO FILE27

LIST DISPLACEMENTS FOR ALL SELECTED NODES

 NODE  LABEL     DISP            CDISP
    1 UZ     0.000000000E+00 0.000000000E+00
    2 UZ     0.000000000E+00 0.000000000E+00
    3 UZ     0.000000000E+00 0.000000000E+00
    4 UZ     0.000000000E+00 0.000000000E+00
    5 UZ     0.000000000E+00 0.000000000E+00
    6 UZ     0.000000000E+00 0.000000000E+00
    7 UZ     0.000000000E+00 0.000000000E+00
    8 UZ     0.000000000E+00 0.000000000E+00
    9 UZ     0.000000000E+00 0.000000000E+00
   10 UZ     0.000000000E+00 0.000000000E+00
   11 UZ     0.000000000E+00 0.000000000E+00
   12 UZ     0.000000000E+00 0.000000000E+00
   13 UZ     0.000000000E+00 0.000000000E+00
   14 UZ     0.000000000E+00 0.000000000E+00
   15 UZ     0.000000000E+00 0.000000000E+00
   16 UZ     0.000000000E+00 0.000000000E+00
   17 UZ     0.000000000E+00 0.000000000E+00
   18 UZ     0.000000000E+00 0.000000000E+00
   19 UZ     0.000000000E+00 0.000000000E+00
   20 UZ     0.000000000E+00 0.000000000E+00

 NODE  LABEL     DISP            CDISP
   21 UZ     0.000000000E+00 0.000000000E+00
   22 UZ     0.000000000E+00 0.000000000E+00
   23 UZ     0.000000000E+00 0.000000000E+00
   24 UZ     0.000000000E+00 0.000000000E+00
   25 UZ     0.000000000E+00 0.000000000E+00
   26 UZ     0.000000000E+00 0.000000000E+00
   27 UZ     0.000000000E+00 0.000000000E+00
   28 UZ     0.000000000E+00 0.000000000E+00
   29 UZ     0.000000000E+00 0.000000000E+00
   30 UZ     0.000000000E+00 0.000000000E+00
   31 UZ     0.000000000E+00 0.000000000E+00
   32 UZ     0.000000000E+00 0.000000000E+00
   33 UZ     0.000000000E+00 0.000000000E+00
   34 UZ     0.000000000E+00 0.000000000E+00
   35 UZ     0.000000000E+00 0.000000000E+00
   36 UZ     0.000000000E+00 0.000000000E+00
   37 UZ     0.000000000E+00 0.000000000E+00
   38 UZ     0.000000000E+00 0.000000000E+00
   39 UZ     0.000000000E+00 0.000000000E+00
   40 UZ     0.000000000E+00 0.000000000E+00

 NODE  LABEL     DISP            CDISP
   41 UZ     0.000000000E+00 0.000000000E+00
   42 UZ     0.000000000E+00 0.000000000E+00
   43 UZ     0.000000000E+00 0.000000000E+00
   46 UZ     0.000000000E+00 0.000000000E+00
   47 UZ     0.000000000E+00 0.000000000E+00
   48 UZ     0.000000000E+00 0.000000000E+00
   51 UZ     0.000000000E+00 0.000000000E+00
   52 UZ     0.000000000E+00 0.000000000E+00
   53 UZ     0.000000000E+00 0.000000000E+00
   56 UZ     0.000000000E+00 0.000000000E+00
   57 UZ     0.000000000E+00 0.000000000E+00
   58 UZ     0.000000000E+00 0.000000000E+00
```

95	UZ	0.000000000E+00	0.000000000E+00
96	UZ	0.000000000E+00	0.000000000E+00
97	UZ	0.000000000E+00	0.000000000E+00
98	UZ	0.000000000E+00	0.000000000E+00
99	UZ	0.000000000E+00	0.000000000E+00
100	UZ	0.000000000E+00	0.000000000E+00
101	UZ	0.000000000E+00	0.000000000E+00
102	UZ	0.000000000E+00	0.000000000E+00

NODE	LABEL	DISP	CDISP
103	UZ	0.000000000E+00	0.000000000E+00
104	UZ	0.000000000E+00	0.000000000E+00
105	UZ	0.000000000E+00	0.000000000E+00
106	UZ	0.000000000E+00	0.000000000E+00
107	UZ	0.000000000E+00	0.000000000E+00
108	UZ	0.000000000E+00	0.000000000E+00
109	UZ	0.000000000E+00	0.000000000E+00
110	UZ	0.000000000E+00	0.000000000E+00
111	UZ	0.000000000E+00	0.000000000E+00
112	UZ	0.000000000E+00	0.000000000E+00
113	UZ	0.000000000E+00	0.000000000E+00
114	UZ	0.000000000E+00	0.000000000E+00
115	UZ	0.000000000E+00	0.000000000E+00
116	UZ	0.000000000E+00	0.000000000E+00
117	UZ	0.000000000E+00	0.000000000E+00
118	UZ	0.000000000E+00	0.000000000E+00
119	UZ	0.000000000E+00	0.000000000E+00
120	UZ	0.000000000E+00	0.000000000E+00
121	UZ	0.000000000E+00	0.000000000E+00
122	UZ	0.000000000E+00	0.000000000E+00

NODE	LABEL	DISP	CDISP
123	UZ	0.000000000E+00	0.000000000E+00
124	UZ	0.000000000E+00	0.000000000E+00
125	UZ	0.000000000E+00	0.000000000E+00
126	UZ	0.000000000E+00	0.000000000E+00
127	UZ	0.000000000E+00	0.000000000E+00
128	UZ	0.000000000E+00	0.000000000E+00
129	UZ	0.000000000E+00	0.000000000E+00
130	UZ	0.000000000E+00	0.000000000E+00
131	UZ	0.000000000E+00	0.000000000E+00
132	UZ	0.000000000E+00	0.000000000E+00
133	UZ	0.000000000E+00	0.000000000E+00
134	UZ	0.000000000E+00	0.000000000E+00
135	UZ	0.000000000E+00	0.000000000E+00
136	UZ	0.000000000E+00	0.000000000E+00
137	UZ	0.000000000E+00	0.000000000E+00
138	UZ	0.000000000E+00	0.000000000E+00
139	UZ	0.000000000E+00	0.000000000E+00
140	UZ	0.000000000E+00	0.000000000E+00
141	UZ	0.000000000E+00	0.000000000E+00
142	UZ	0.000000000E+00	0.000000000E+00

NODE	LABEL	DISP	CDISP
143	UZ	0.000000000E+00	0.000000000E+00
144	UZ	0.000000000E+00	0.000000000E+00
145	UZ	0.000000000E+00	0.000000000E+00
146	UZ	0.000000000E+00	0.000000000E+00
147	UZ	0.000000000E+00	0.000000000E+00
148	UZ	0.000000000E+00	0.000000000E+00
149	UZ	0.000000000E+00	0.000000000E+00
150	UZ	0.000000000E+00	0.000000000E+00
151	UZ	0.000000000E+00	0.000000000E+00
152	UZ	0.000000000E+00	0.000000000E+00
153	UZ	0.000000000E+00	0.000000000E+00
154	UZ	0.000000000E+00	0.000000000E+00
155	UZ	0.000000000E+00	0.000000000E+00
156	UZ	0.000000000E+00	0.000000000E+00
157	UZ	0.000000000E+00	0.000000000E+00
158	UZ	0.000000000E+00	0.000000000E+00
159	UZ	0.000000000E+00	0.000000000E+00
160	UZ	0.000000000E+00	0.000000000E+00
161	UZ	0.000000000E+00	0.000000000E+00
162	UZ	0.000000000E+00	0.000000000E+00

NODE	LABEL	DISP	CDISP
163	UZ	0.000000000E+00	0.000000000E+00
164	UZ	0.000000000E+00	0.000000000E+00
165	UZ	0.000000000E+00	0.000000000E+00
166	UZ	0.000000000E+00	0.000000000E+00
167	UZ	0.000000000E+00	0.000000000E+00
168	UZ	0.000000000E+00	0.000000000E+00
169	UZ	0.000000000E+00	0.000000000E+00
170	UZ	0.000000000E+00	0.000000000E+00
171	UZ	0.000000000E+00	0.000000000E+00
172	UZ	0.000000000E+00	0.000000000E+00
173	UZ	0.000000000E+00	0.000000000E+00
174	UZ	0.000000000E+00	0.000000000E+00
175	UZ	0.000000000E+00	0.000000000E+00
176	UZ	0.000000000E+00	0.000000000E+00
177	UZ	0.000000000E+00	0.000000000E+00
178	UZ	0.000000000E+00	0.000000000E+00
179	UZ	0.000000000E+00	0.000000000E+00
180	UZ	0.000000000E+00	0.000000000E+00
201	UZ	0.000000000E+00	0.000000000E+00
202	UZ	0.000000000E+00	0.000000000E+00

NODE	LABEL	DISP	CDISP
203	UZ	0.000000000E+00	0.000000000E+00
204	UZ	0.000000000E+00	0.000000000E+00
205	UZ	0.000000000E+00	0.000000000E+00
206	UZ	0.000000000E+00	0.000000000E+00
207	UZ	0.000000000E+00	0.000000000E+00
208	UZ	0.000000000E+00	0.000000000E+00
209	UZ	0.000000000E+00	0.000000000E+00
210	UZ	0.000000000E+00	0.000000000E+00
211	UZ	0.000000000E+00	0.000000000E+00
212	UZ	0.000000000E+00	0.000000000E+00
213	UZ	0.000000000E+00	0.000000000E+00
214	UZ	0.000000000E+00	0.000000000E+00
215	UZ	0.000000000E+00	0.000000000E+00
216	UZ	0.000000000E+00	0.000000000E+00
217	UZ	0.000000000E+00	0.000000000E+00
218	UZ	0.000000000E+00	0.000000000E+00
219	UZ	0.000000000E+00	0.000000000E+00
220	UZ	0.000000000E+00	0.000000000E+00
221	UZ	0.000000000E+00	0.000000000E+00
222	UZ	0.000000000E+00	0.000000000E+00

NODE	LABEL	DISP	CDISP
223	UZ	0.000000000E+00	0.000000000E+00
224	UZ	0.000000000E+00	0.000000000E+00
225	UZ	0.000000000E+00	0.000000000E+00
226	UZ	0.000000000E+00	0.000000000E+00
227	UZ	0.000000000E+00	0.000000000E+00
228	UZ	0.000000000E+00	0.000000000E+00
229	UZ	0.000000000E+00	0.000000000E+00
230	UZ	0.000000000E+00	0.000000000E+00
231	UZ	0.000000000E+00	0.000000000E+00
232	UZ	0.000000000E+00	0.000000000E+00
233	UZ	0.000000000E+00	0.000000000E+00
234	UZ	0.000000000E+00	0.000000000E+00
235	UZ	0.000000000E+00	0.000000000E+00
236	UZ	0.000000000E+00	0.000000000E+00
237	UZ	0.000000000E+00	0.000000000E+00
238	UZ	0.000000000E+00	0.000000000E+00
239	UZ	0.000000000E+00	0.000000000E+00
240	UZ	0.000000000E+00	0.000000000E+00
241	UZ	0.000000000E+00	0.000000000E+00
242	UZ	0.000000000E+00	0.000000000E+00

NODE	LABEL	DISP	CDISP
243	UZ	0.000000000E+00	0.000000000E+00
244	UZ	0.000000000E+00	0.000000000E+00
245	UZ	0.000000000E+00	0.000000000E+00
246	UZ	0.000000000E+00	0.000000000E+00
247	UZ	0.000000000E+00	0.000000000E+00
248	UZ	0.000000000E+00	0.000000000E+00

249	UZ	0.000000000E+00	0.000000000E+00
250	UZ	0.000000000E+00	0.000000000E+00
251	UZ	0.000000000E+00	0.000000000E+00
252	UZ	0.000000000E+00	0.000000000E+00
253	UZ	0.000000000E+00	0.000000000E+00
1	UX	0.000000000E+00	0.000000000E+00
5	UX	0.000000000E+00	0.000000000E+00
253	UX	0.000000000E+00	0.000000000E+00
1	UY	0.000000000E+00	0.000000000E+00
253	ROTZ	0.000000000E+00	0.000000000E+00

LIST ELEMENT PRESSURES FOR ALL SELECTED ELEMENTS

ELEM	FACE	VALUE(S)		FACE NODES	
4	3	10.0000000	0.000000000E+00	10	5
8	3	10.0000000	0.000000000E+00	15	10
12	3	10.0000000	0.000000000E+00	20	15
16	3	10.0000000	0.000000000E+00	25	20
20	3	10.0000000	0.000000000E+00	30	25
24	3	10.0000000	0.000000000E+00	35	30
28	3	10.0000000	0.000000000E+00	40	35
27	2	10.0000000	0.000000000E+00	38	39
28	2	10.0000000	0.000000000E+00	39	40
30	3	10.0000000	0.000000000E+00	43	38
37	1	10.0000000	0.000000000E+00	96	97
37	4	10.0000000	0.000000000E+00	101	96
41	4	10.0000000	0.000000000E+00	106	101
45	4	10.0000000	0.000000000E+00	111	106
49	4	10.0000000	0.000000000E+00	116	111
53	4	10.0000000	0.000000000E+00	121	116
101	1	10.0000000	0.000000000E+00	95	121
101	4	10.0000000	0.000000000E+00	126	95
61	4	10.0000000	0.000000000E+00	131	126
65	4	10.0000000	0.000000000E+00	136	131

ELEM	FACE	VALUE(S)		FACE NODES	
69	4	10.0000000	0.000000000E+00	141	136
73	4	10.0000000	0.000000000E+00	146	141
77	4	10.0000000	0.000000000E+00	151	146
81	4	10.0000000	0.000000000E+00	156	151
85	4	10.0000000	0.000000000E+00	161	156
89	4	10.0000000	0.000000000E+00	166	161
93	4	10.0000000	0.000000000E+00	171	166
97	4	10.0000000	0.000000000E+00	176	171
103	1	10.0000000	0.000000000E+00	178	201
104	1	10.0000000	0.000000000E+00	201	202
105	1	10.0000000	0.000000000E+00	202	203
106	1	10.0000000	0.000000000E+00	203	204
107	1	10.0000000	0.000000000E+00	204	205
108	1	10.0000000	0.000000000E+00	205	206
109	1	10.0000000	0.000000000E+00	206	207
110	1	10.0000000	0.000000000E+00	207	208
111	1	10.0000000	0.000000000E+00	208	209
112	1	10.0000000	0.000000000E+00	209	210
113	1	10.0000000	0.000000000E+00	210	211
114	1	10.0000000	0.000000000E+00	211	212

ELEM	FACE	VALUE(S)		FACE NODES	
115	1	10.0000000	0.000000000E+00	212	213
116	1	10.0000000	0.000000000E+00	213	214
117	1	10.0000000	0.000000000E+00	214	215
118	1	10.0000000	0.000000000E+00	215	216
119	1	10.0000000	0.000000000E+00	216	217
120	1	10.0000000	0.000000000E+00	217	218
121	1	10.0000000	0.000000000E+00	218	219
122	1	10.0000000	0.000000000E+00	219	220
123	1	10.0000000	0.000000000E+00	220	221
124	1	10.0000000	0.000000000E+00	221	222
125	1	10.0000000	0.000000000E+00	222	223
126	1	10.0000000	0.000000000E+00	223	224
127	1	10.0000000	0.000000000E+00	224	225
128	1	10.0000000	0.000000000E+00	225	226
129	1	10.0000000	0.000000000E+00	226	227
130	1	10.0000000	0.000000000E+00	227	228

131	1	10.0000000	0.000000000E+00	228	229
132	1	10.0000000	0.000000000E+00	229	230
133	1	10.0000000	0.000000000E+00	230	231
134	1	10.0000000	0.000000000E+00	231	232

ELEM	FACE	VALUE(S)		FACE NODES	
135	1	10.0000000	0.000000000E+00	232	233
136	1	10.0000000	0.000000000E+00	233	234
137	1	10.0000000	0.000000000E+00	234	235
138	1	10.0000000	0.000000000E+00	235	236
139	1	10.0000000	0.000000000E+00	236	237
140	1	10.0000000	0.000000000E+00	237	238
141	1	10.0000000	0.000000000E+00	238	239
142	1	10.0000000	0.000000000E+00	239	240
143	1	10.0000000	0.000000000E+00	240	241
144	1	10.0000000	0.000000000E+00	241	242
145	1	10.0000000	0.000000000E+00	242	243
146	1	10.0000000	0.000000000E+00	243	244
147	1	10.0000000	0.000000000E+00	244	245
148	1	10.0000000	0.000000000E+00	245	246
149	1	10.0000000	0.000000000E+00	246	247
150	1	10.0000000	0.000000000E+00	247	248
151	1	10.0000000	0.000000000E+00	248	249
152	1	10.0000000	0.000000000E+00	249	250
153	1	10.0000000	0.000000000E+00	250	251
154	1	10.0000000	0.000000000E+00	251	252

ELEM	FACE	VALUE(S)		FACE NODES	
155	1	10.0000000	0.000000000E+00	252	253

LIST ELEMENT CONVECTIONS FOR ALL SELECTED ELEMENTS

LIST TEMPERATURES FOR ALL SELECTED NODES

NODE	TEMPERATURE	FLUENCE
1	221.59	0.00000E+00
2	221.59	0.00000E+00
3	221.59	0.00000E+00
4	221.59	0.00000E+00
5	221.59	0.00000E+00
6	221.59	0.00000E+00
7	221.59	0.00000E+00
8	221.59	0.00000E+00
9	221.59	0.00000E+00
10	221.59	0.00000E+00
11	221.59	0.00000E+00
12	221.59	0.00000E+00
13	221.59	0.00000E+00
14	221.59	0.00000E+00
15	221.59	0.00000E+00
16	221.59	0.00000E+00
17	221.59	0.00000E+00
18	221.59	0.00000E+00
19	221.59	0.00000E+00
20	221.59	0.00000E+00

NODE	TEMPERATURE	FLUENCE
21	220.44	0.00000E+00
22	220.44	0.00000E+00
23	220.44	0.00000E+00
24	220.44	0.00000E+00
25	220.44	0.00000E+00
26	220.44	0.00000E+00
27	220.44	0.00000E+00
28	220.44	0.00000E+00
29	220.44	0.00000E+00
30	220.44	0.00000E+00
31	218.20	0.00000E+00
32	218.20	0.00000E+00
33	218.20	0.00000E+00
34	218.20	0.00000E+00
35	218.20	0.00000E+00
36	218.20	0.00000E+00
37	218.20	0.00000E+00

38	218.20	0.00000E+00
39	218.20	0.00000E+00
40	218.20	0.00000E+00

NODE	TEMPERATURE	FLUENCE
41	218.20	0.00000E+00
42	218.20	0.00000E+00
43	218.20	0.00000E+00
46	218.20	0.00000E+00
47	218.20	0.00000E+00
48	218.20	0.00000E+00
51	218.20	0.00000E+00
52	218.20	0.00000E+00
53	218.20	0.00000E+00
56	218.20	0.00000E+00
57	218.20	0.00000E+00
58	218.20	0.00000E+00
95	218.91	0.00000E+00
96	218.91	0.00000E+00
97	218.91	0.00000E+00
98	218.91	0.00000E+00
99	218.91	0.00000E+00
100	218.91	0.00000E+00
101	218.91	0.00000E+00
102	218.91	0.00000E+00

NODE	TEMPERATURE	FLUENCE
103	218.91	0.00000E+00
104	218.91	0.00000E+00
105	218.91	0.00000E+00
106	218.91	0.00000E+00
107	218.91	0.00000E+00
108	218.91	0.00000E+00
109	218.91	0.00000E+00
110	218.91	0.00000E+00
111	218.91	0.00000E+00
112	218.91	0.00000E+00
113	218.91	0.00000E+00
114	218.91	0.00000E+00
115	218.91	0.00000E+00
116	218.91	0.00000E+00
117	218.91	0.00000E+00
118	218.91	0.00000E+00
119	218.91	0.00000E+00
120	218.91	0.00000E+00
121	218.91	0.00000E+00
122	218.91	0.00000E+00

NODE	TEMPERATURE	FLUENCE
123	218.91	0.00000E+00
124	218.91	0.00000E+00
125	218.91	0.00000E+00
126	221.22	0.00000E+00
127	221.22	0.00000E+00
128	221.22	0.00000E+00
129	221.22	0.00000E+00
130	221.22	0.00000E+00
131	223.52	0.00000E+00
132	223.52	0.00000E+00
133	223.52	0.00000E+00
134	223.52	0.00000E+00
135	223.52	0.00000E+00
136	225.83	0.00000E+00
137	225.83	0.00000E+00
138	225.83	0.00000E+00
139	225.83	0.00000E+00
140	225.83	0.00000E+00
141	228.13	0.00000E+00
142	228.13	0.00000E+00

NODE	TEMPERATURE	FLUENCE
143	228.13	0.00000E+00
144	228.13	0.00000E+00
145	228.13	0.00000E+00

146	230.44	0.00000E+00
147	230.44	0.00000E+00
148	230.44	0.00000E+00
149	230.44	0.00000E+00
150	230.44	0.00000E+00
151	234.03	0.00000E+00
152	234.03	0.00000E+00
153	234.03	0.00000E+00
154	234.03	0.00000E+00
155	234.03	0.00000E+00
156	237.61	0.00000E+00
157	237.61	0.00000E+00
158	237.61	0.00000E+00
159	237.61	0.00000E+00
160	237.61	0.00000E+00
161	241.20	0.00000E+00
162	241.20	0.00000E+00

NODE	TEMPERATURE	FLUENCE
163	241.20	0.00000E+00
164	241.20	0.00000E+00
165	241.20	0.00000E+00
166	244.78	0.00000E+00
167	244.78	0.00000E+00
168	244.78	0.00000E+00
169	244.78	0.00000E+00
170	244.78	0.00000E+00
171	248.37	0.00000E+00
172	248.37	0.00000E+00
173	248.37	0.00000E+00
174	248.37	0.00000E+00
175	248.37	0.00000E+00
176	251.95	0.00000E+00
177	251.95	0.00000E+00
178	251.95	0.00000E+00
179	251.95	0.00000E+00
180	251.95	0.00000E+00
201	256.35	0.00000E+00
202	260.74	0.00000E+00

NODE	TEMPERATURE	FLUENCE
203	265.14	0.00000E+00
204	269.54	0.00000E+00
205	273.93	0.00000E+00
206	278.33	0.00000E+00
207	282.73	0.00000E+00
208	287.13	0.00000E+00
209	291.52	0.00000E+00
210	295.92	0.00000E+00
211	299.28	0.00000E+00
212	302.63	0.00000E+00
213	305.99	0.00000E+00
214	309.34	0.00000E+00
215	312.70	0.00000E+00
216	316.05	0.00000E+00
217	319.41	0.00000E+00
218	322.76	0.00000E+00
219	326.12	0.00000E+00
220	329.47	0.00000E+00
221	329.56	0.00000E+00
222	329.66	0.00000E+00

NODE	TEMPERATURE	FLUENCE
223	329.75	0.00000E+00
224	329.85	0.00000E+00
225	329.94	0.00000E+00
226	330.04	0.00000E+00
227	330.13	0.00000E+00
228	330.23	0.00000E+00
229	330.32	0.00000E+00
230	330.42	0.00000E+00
231	328.66	0.00000E+00
232	326.90	0.00000E+00
233	325.15	0.00000E+00

234	323.39	0.00000E+00
235	321.63	0.00000E+00
236	319.87	0.00000E+00
237	318.12	0.00000E+00
238	316.36	0.00000E+00
239	314.60	0.00000E+00
240	312.84	0.00000E+00
241	311.09	0.00000E+00
242	309.33	0.00000E+00

NODE	TEMPERATURE	FLUENCE
243	307.57	0.00000E+00
244	312.70	0.00000E+00
245	317.82	0.00000E+00
246	322.95	0.00000E+00
247	328.08	0.00000E+00
248	333.20	0.00000E+00
249	338.33	0.00000E+00
250	338.33	0.00000E+00
251	338.33	0.00000E+00
252	338.33	0.00000E+00
253	338.33	0.00000E+00

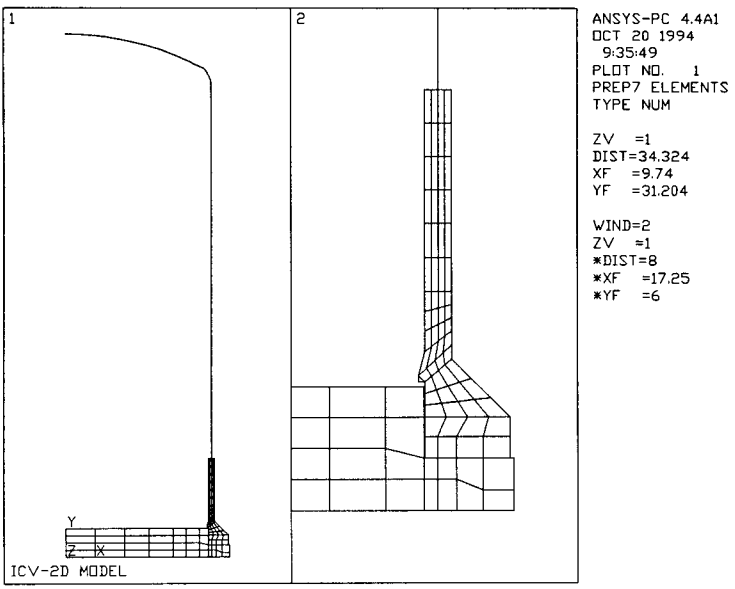


FIGURE 2.10.2-1.

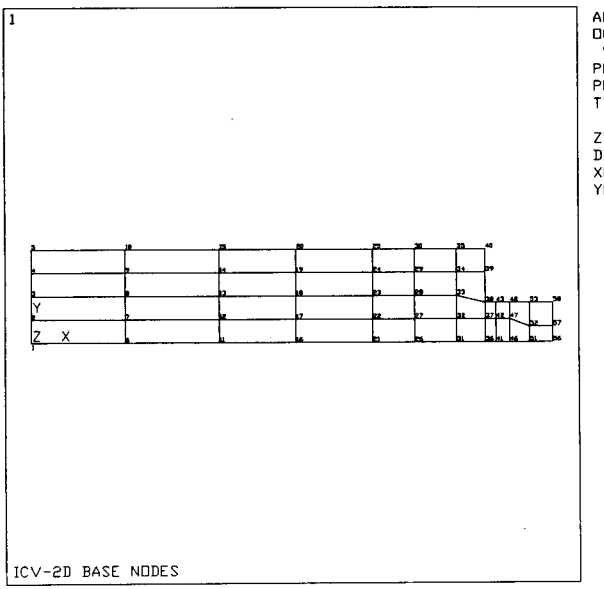


FIGURE 2.10.2-2.

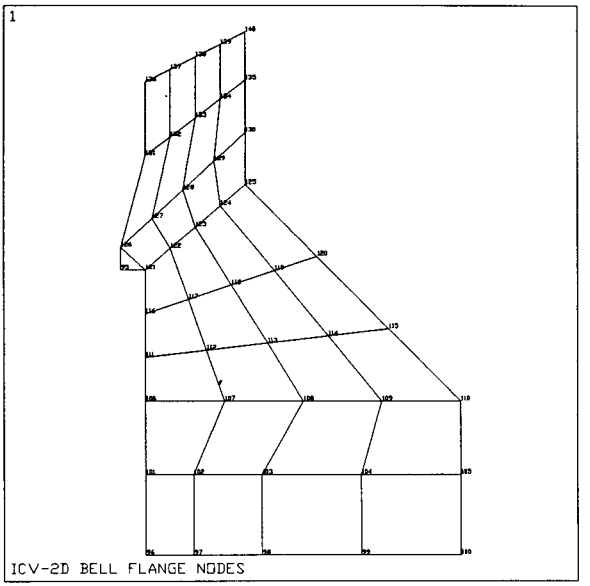


FIGURE 2.10.2-3.

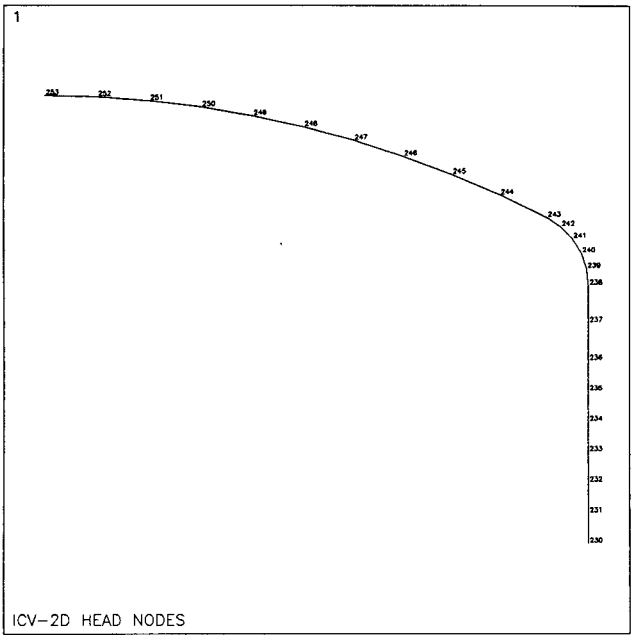


FIGURE 2.10.2-4.

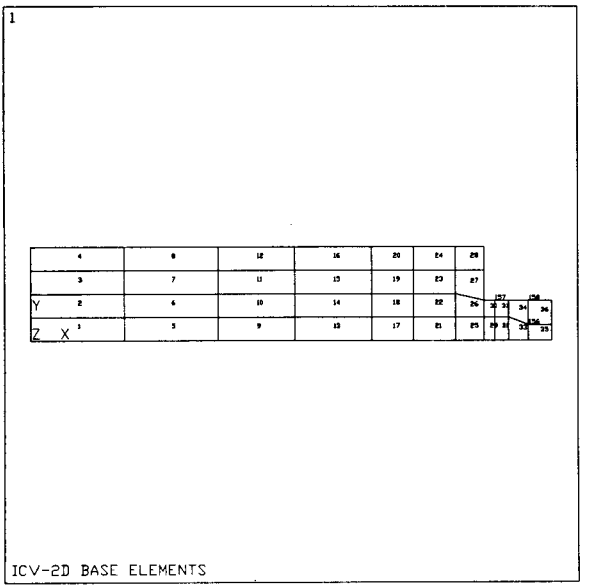


FIGURE 2.10.2-5.

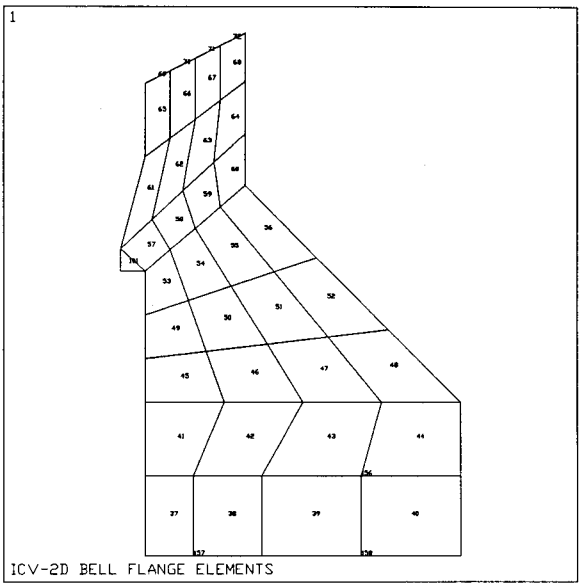


FIGURE 2.10.2-6.

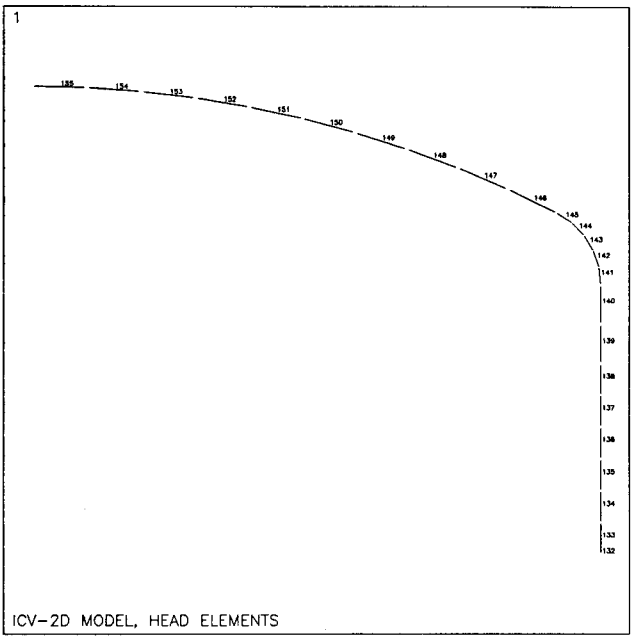


FIGURE 2.10.2-7.

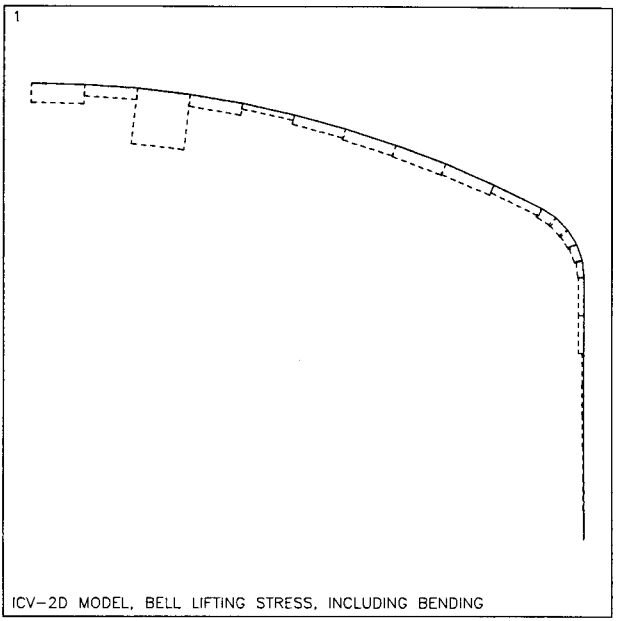


FIGURE 2.10.2-8.

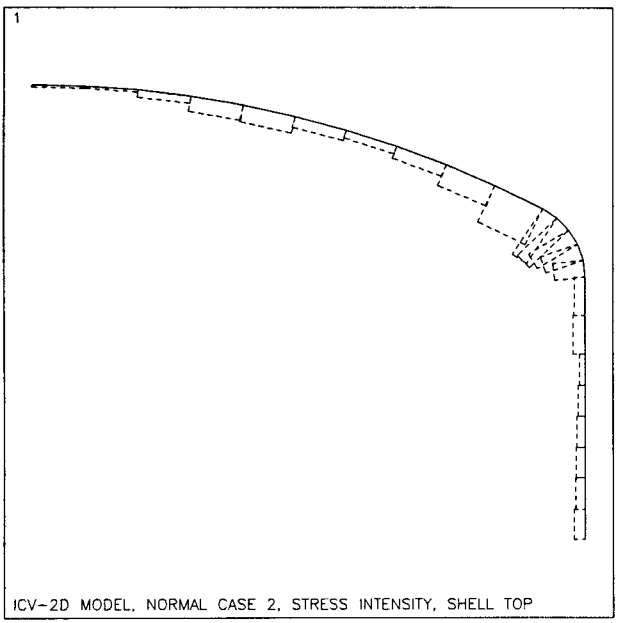


FIGURE 2.10.2-9.

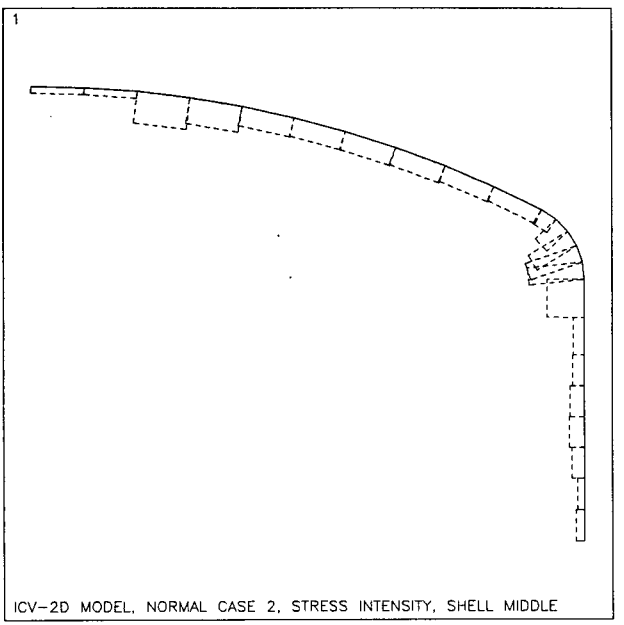


FIGURE 2.10.2-10.

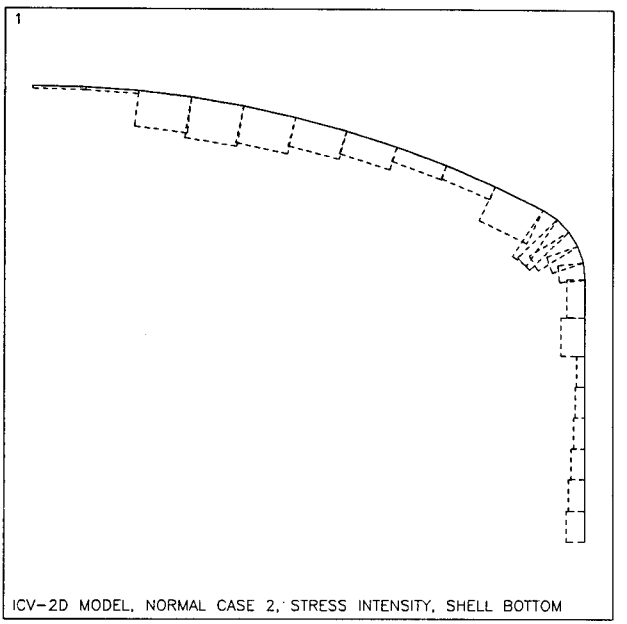


FIGURE 2.10.2-11.

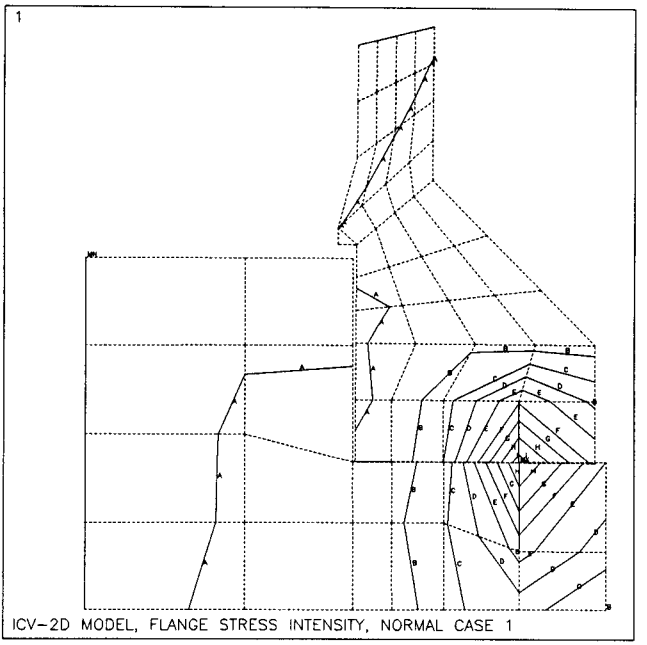


FIGURE 2.10.2-12.

2.10.3 OCV Head and Fin Model

2.10.3.1 Description. The OCV head and fin model is a 3-D finite element model of a one-third symmetry segment of the upper portion of the OCV, used to evaluate lifting stresses in the OCV head. Other stresses related to lifting the package using the OCV fins are evaluated in Section 2.5.1.2. The extent of the model is 120° with a single lifting fin in the center. To simplify the model, the doubler plate between the fin and the OCV head was not modeled. Instead, the fin was modeled as directly attached to the OCV head. The action of the doubler plate is to distribute fin-lifting loads over a slightly larger area of the OCV head, and thus, to omit the doubler plate conservatively increased OCV head stress. The fin is therefore connected at a right angle directly to the OCV head. The lower edge of the model ends in the OCV wall a short distance above the OCV flange, because flange details are irrelevant to this analysis. The coolant jacket is also not modeled for the same reason. The lifting load is applied directly to a node located at the fin hole center, and the fin hole itself is not modeled. Bearing stress at the lift hole and stresses in the fin weld are analyzed using classical methods in Section 2.5.1.2. The weld properties are found with the aid of a small finite element model documented in Appendix 2.10.4. The model layout is shown in Figure 2.10.3-1.

2.10.3.2 Construction. The model is constructed of quadrilateral shell elements of two thicknesses: 0.50 in. for the OCV wall, and 0.25 in. for the fin. The fin hole reinforcement is conservatively ignored. The model extends from its lower edge just above the OCV flange up to the center of the top of the OCV head. The highest row of nodes is actually located at a small radius from the center to simplify modeling. No stress or strain discontinuities occur. Node and element plots of key portions of the model are given in Figures 2.10.3-2 through 2.10.3-6. An interpreted ANSYS input listing is given in Table 2.10.3-1.

2.10.3.3 Material Properties. A modulus of elasticity of $27.18(10)^6$ psi was used, corresponding to 270 °F, which represents overall head temperature. Poisson's ratio was 0.3.

2.10.3.4 Constraints. Nodes along the cut edges were constrained in the one linear and two rotational degrees of freedom required to ensure symmetry of the model. The nodes along the bottom were fixed in all six degrees of freedom, as appropriate to the lifting case. This edge was far enough away from the area of interest around the fin that constraint details were relatively unimportant.

2.10.3.5 Applied Loading. Two loads were applied to the fin in its own plane at the location of the fin hole center, node 756. Their vector sum was a unit load along the line of action of the cable, which is at 60° to the horizontal. Pressure internal to the OCV was not used. Nodal temperatures were not used.

2.10.3.6 Results. A plot of maximum stress intensity in the OCV head is shown in Figures 2.10.3-7 and 2.10.3-8, and for the OCV wall bottom in Figure 2.10.3-9. The full value of stress is found by multiplying the stress result shown here with the cable load, as detailed in Section 2.5.1.2.

TABLE 2.10.3-1. Interpreted ANSYS Input Listing.

```
STATIC ANALYSIS (KAN= 0)

LINEAR ANALYSIS - NO NON-LINEAR PROPERTIES

REFERENCE TEMPERATURE=      0.000 (TREF)
UNIFORM TEMPERATURE  =      0.000 (TUNIF)

*****ANALYSIS OPTIONS (KAY VALUES) (IF ANY) *****

NO STATIC INTERPOLATION/EXTRAPOLATION (KAY(3)=0)

SMALL DEFLECTION SOLUTION (KAY(6)=0)

NO STRESS STIFFENING (KAY(8)=0)

USE LINEAR SOLUTION PROCEDURE  (KAY(9)=0)

IN-CORE WAVE-FRONT EQUATION SOLVER (KAY(10)=0)

LIST ELEMENT TYPES FROM  1 TO 20 BY 1

NO. STIF         KEYOPT VALUES         INOPR
 1   63   0  0  0   0  0  0   0  0  0   0  QUAD. FLAT SHELL

LIST ALL REAL SETS

 REAL CONSTANT SET   1  ITEMS   1 TO  18
  0.50000      0.00000E+00  0.00000E+00  0.00000E+00  0.00000E+00  0.00000E+00
  0.00000E+00  0.00000E+00  0.00000E+00  0.00000E+00  0.00000E+00  0.00000E+00
  0.00000E+00  0.00000E+00  0.00000E+00  0.00000E+00  0.00000E+00  0.00000E+00

 REAL CONSTANT SET   2  ITEMS   1 TO  18
  0.25000      0.00000E+00  0.00000E+00  0.00000E+00  0.00000E+00  0.00000E+00
  0.00000E+00  0.00000E+00  0.00000E+00  0.00000E+00  0.00000E+00  0.00000E+00
  0.00000E+00  0.00000E+00  0.00000E+00  0.00000E+00  0.00000E+00  0.00000E+00
LIST ALL COORDINATE SYSTEMS

    SYSTEM TYPE                      CENTER              PARAMETERS    SING KEYS
 0  0 (CARTESIAN)          0.000      0.000      0.000    0.000  0.000   0  0
 1  1 (CYLINDRICAL)        0.000      0.000      0.000    1.000  0.000   0  0
 2  2 (SPHERICAL)          0.000      0.000      0.000    1.000  1.000   0  0
11  1 (CYLINDRICAL)        0.000     25.150      0.000    1.000  1.000   0  0
12  1 (CYLINDRICAL)       14.940     54.290      0.000    1.000  1.000   0  0
13  1 (CYLINDRICAL)        0.000      0.000      0.000    1.000  1.000   0  0

SYSTEM              ORIENTATION VECTORS (X,Y,Z)
    0      1.00  0.00  0.00    0.00  1.00  0.00    0.00  0.00  1.00
    1      1.00  0.00  0.00    0.00  1.00  0.00    0.00  0.00  1.00
    2      1.00  0.00  0.00    0.00  1.00  0.00    0.00  0.00  1.00
   11      1.00  0.00  0.00    0.00  1.00  0.00    0.00  0.00  1.00
   12      1.00  0.00  0.00    0.00  1.00  0.00    0.00  0.00  1.00
   13      1.00  0.00  0.00    0.00  0.00 -1.00    0.00  1.00  0.00
CSYS TYPE     XC            YC            ZC          THXY      THYZ      THXZ
 11    1 0.00000E+00  25.150       0.00000E+00       0.000     0.000     0.000
 12    1  14.940      54.290       0.00000E+00       0.000     0.000     0.000
 13    1 0.00000E+00 0.00000E+00 0.00000E+00       0.000     0.000   -90.000

LIST   ALL   SELECTED KEYPOINTS.   DSYS=   0

   PT.              X,Y,Z LOCATION                    NODE  ELEM  ESIZE
    1    18.1900      53.3800      0.000000E+00        221     0
    2    18.1900      54.2900      0.000000E+00        220     0
    3    16.4200      57.1800      0.000000E+00        214     0
    4    13.0000      58.7200      0.000000E+00        211     0
    5    13.0000      60.5000      0.000000E+00        444     0
    6    15.0000      62.5000      0.000000E+00        448     0
    7    19.2500      62.5000      0.000000E+00        450     0
    8    21.2500      60.5000      0.000000E+00        454     0
    9    21.2500      54.6300      0.000000E+00        456     0
   10    20.0000      53.3800      0.000000E+00        462     0
   11    14.9400      54.6300      0.000000E+00          0     0
```

LIST ALL SELECTED LINE SEGMENTS.

SEG.NO.	KEYPT	DIRECTION			DIV	SPACING	NODES/ELEM	
1	1	0.0000	-1.0000	0.0000	1	1.0000	-1	-1
	2	0.0000	1.0000	0.0000			0	0
2	3	-0.8903	0.4554	0.0000	6	1.0000	215	219
	2	0.0011	-1.0000	0.0000			0	0
3	4	-0.9320	0.3625	0.0000	3	1.0000	212	213
	3	0.8892	-0.4575	0.0000			0	0
4	4	0.0000	-1.0000	0.0000	4	1.0000	445	447
	5	0.0000	1.0000	0.0000			0	0
5	5	-0.7071	-0.7071	0.0000	2	1.0000	449	449
	6	0.7071	0.7071	0.0000			0	0
6	6	-1.0000	0.0000	0.0000	4	1.0000	451	453
	7	1.0000	0.0000	0.0000			0	0
7	7	-0.7071	0.7071	0.0000	2	1.0000	455	455
	8	0.7071	-0.7071	0.0000			0	0
8	8	0.0000	1.0000	0.0000	6	1.0000	457	461
	9	0.0000	-1.0000	0.0000			0	0
9	9	0.7071	0.7071	0.0000	2	1.0000	463	463
	10	-0.7071	-0.7071	0.0000			0	0
10	10	1.0000	0.0000	0.0000	2	1.0000	464	464
	1	-1.0000	0.0000	0.0000			0	0

LIST ALL SELECTED AREAS.

NO.	KEYPOINTS/LINE SEG.				NODES		ELEMENTS		MAT	REL	TYP	ESYS
1	-	-	-	-	465	510	301	368	1	2	1	0
	1	2	3	4								
	5	6	7	8								
	9	10										

LIST ALL SELECTED ELEMENTS. (LIST NODES)

ELEM	MAT	TYP	REL	ESYS	NODES			
1	1	1	1	0	2	3	43	42
2	1	1	1	0	3	4	44	43
3	1	1	1	0	4	5	45	44
4	1	1	1	0	5	6	46	45
5	1	1	1	0	6	7	47	46
6	1	1	1	0	7	8	48	47
7	1	1	1	0	8	9	49	48
8	1	1	1	0	9	10	50	49
9	1	1	1	0	10	11	51	50
10	1	1	1	0	11	12	52	51
11	1	1	1	0	12	13	53	52
12	1	1	1	0	13	14	54	53
13	1	1	1	0	14	15	55	54
14	1	1	1	0	15	16	56	55
15	1	1	1	0	16	17	57	56
16	1	1	1	0	17	18	58	57
17	1	1	1	0	18	19	59	58
18	1	1	1	0	19	20	60	59
19	1	1	1	0	20	21	61	60
20	1	1	1	0	21	22	62	61

ELEM	MAT	TYP	REL	ESYS	NODES			
21	1	1	1	0	22	23	63	62
22	1	1	1	0	23	24	64	63
23	1	1	1	0	24	25	65	64
24	1	1	1	0	25	26	66	65
25	1	1	1	0	26	27	67	66
26	1	1	1	0	27	28	68	67
27	1	1	1	0	28	29	69	68
28	1	1	1	0	29	30	70	69
29	1	1	1	0	30	31	71	70
30	1	1	1	0	31	32	72	71
31	1	1	1	0	42	43	83	82
32	1	1	1	0	43	44	84	83
33	1	1	1	0	44	45	85	84
34	1	1	1	0	45	46	86	85
35	1	1	1	0	46	47	87	86
36	1	1	1	0	47	48	88	87
37	1	1	1	0	48	49	89	88
38	1	1	1	0	49	50	90	89

39	1	1	1	0	50	51	91	90
40	1	1	1	0	51	52	92	91

ELEM	MAT	TYP	REL	ESYS	NODES			
41	1	1	1	0	52	53	93	92
42	1	1	1	0	53	54	94	93
43	1	1	1	0	54	55	95	94
44	1	1	1	0	55	56	96	95
45	1	1	1	0	56	57	97	96
46	1	1	1	0	57	58	98	97
47	1	1	1	0	58	59	99	98
48	1	1	1	0	59	60	100	99
49	1	1	1	0	60	61	101	100
50	1	1	1	0	61	62	102	101
51	1	1	1	0	62	63	103	102
52	1	1	1	0	63	64	104	103
53	1	1	1	0	64	65	105	104
54	1	1	1	0	65	66	106	105
55	1	1	1	0	66	67	107	106
56	1	1	1	0	67	68	108	107
57	1	1	1	0	68	69	109	108
58	1	1	1	0	69	70	110	109
59	1	1	1	0	70	71	111	110
60	1	1	1	0	71	72	112	111

ELEM	MAT	TYP	REL	ESYS	NODES			
61	1	1	1	0	82	83	123	122
62	1	1	1	0	83	84	124	123
63	1	1	1	0	84	85	125	124
64	1	1	1	0	85	86	126	125
65	1	1	1	0	86	87	127	126
66	1	1	1	0	87	88	128	127
67	1	1	1	0	88	89	129	128
68	1	1	1	0	89	90	130	129
69	1	1	1	0	90	91	131	130
70	1	1	1	0	91	92	132	131
71	1	1	1	0	92	93	133	132
72	1	1	1	0	93	94	134	133
73	1	1	1	0	94	95	135	134
74	1	1	1	0	95	96	136	135
75	1	1	1	0	96	97	137	136
76	1	1	1	0	97	98	138	137
77	1	1	1	0	98	99	139	138
78	1	1	1	0	99	100	140	139
79	1	1	1	0	100	101	141	140
80	1	1	1	0	101	102	142	141

ELEM	MAT	TYP	REL	ESYS	NODES			
81	1	1	1	0	102	103	143	142
82	1	1	1	0	103	104	144	143
83	1	1	1	0	104	105	145	144
84	1	1	1	0	105	106	146	145
85	1	1	1	0	106	107	147	146
86	1	1	1	0	107	108	148	147
87	1	1	1	0	108	109	149	148
88	1	1	1	0	109	110	150	149
89	1	1	1	0	110	111	151	150
90	1	1	1	0	111	112	152	151
91	1	1	1	0	122	123	163	162
92	1	1	1	0	123	124	164	163
93	1	1	1	0	124	125	165	164
94	1	1	1	0	125	126	166	165
95	1	1	1	0	126	127	167	166
96	1	1	1	0	127	128	168	167
97	1	1	1	0	128	129	169	168
98	1	1	1	0	129	130	170	169
99	1	1	1	0	130	131	171	170
100	1	1	1	0	131	132	172	171

ELEM	MAT	TYP	REL	ESYS	NODES			
101	1	1	1	0	132	133	173	172
102	1	1	1	0	133	134	174	173

103	1	1	1	0	134	135	175	174
104	1	1	1	0	135	136	176	175
105	1	1	1	0	136	137	177	176
106	1	1	1	0	137	138	178	177
107	1	1	1	0	138	139	179	178
108	1	1	1	0	139	140	180	179
109	1	1	1	0	140	141	181	180
110	1	1	1	0	141	142	182	181
111	1	1	1	0	142	143	183	182
112	1	1	1	0	143	144	184	183
113	1	1	1	0	144	145	185	184
114	1	1	1	0	145	146	186	185
115	1	1	1	0	146	147	187	186
116	1	1	1	0	147	148	188	187
117	1	1	1	0	148	149	189	188
118	1	1	1	0	149	150	190	189
119	1	1	1	0	150	151	191	190
120	1	1	1	0	151	152	192	191

ELEM	MAT	TYP	REL	ESYS	NODES			
121	1	1	1	0	162	163	203	202
122	1	1	1	0	163	164	204	203
123	1	1	1	0	164	165	205	204
124	1	1	1	0	165	166	206	205
125	1	1	1	0	166	167	207	206
126	1	1	1	0	167	168	208	207
127	1	1	1	0	168	169	209	208
128	1	1	1	0	169	170	210	209
129	1	1	1	0	170	171	211	210
130	1	1	1	0	171	172	212	211
131	1	1	1	0	172	173	213	212
132	1	1	1	0	173	174	214	213
133	1	1	1	0	174	175	215	214
134	1	1	1	0	175	176	216	215
135	1	1	1	0	176	177	217	216
136	1	1	1	0	177	178	218	217
137	1	1	1	0	178	179	219	218
138	1	1	1	0	179	180	220	219
139	1	1	1	0	180	181	221	220
140	1	1	1	0	181	182	222	221

ELEM	MAT	TYP	REL	ESYS	NODES			
141	1	1	1	0	182	183	223	222
142	1	1	1	0	183	184	224	223
143	1	1	1	0	184	185	225	224
144	1	1	1	0	185	186	226	225
145	1	1	1	0	186	187	227	226
146	1	1	1	0	187	188	228	227
147	1	1	1	0	188	189	229	228
148	1	1	1	0	189	190	230	229
149	1	1	1	0	190	191	231	230
150	1	1	1	0	191	192	232	231
151	1	1	1	0	202	203	243	242
152	1	1	1	0	203	204	244	243
153	1	1	1	0	204	205	245	244
154	1	1	1	0	205	206	246	245
155	1	1	1	0	206	207	247	246
156	1	1	1	0	207	208	248	247
157	1	1	1	0	208	209	249	248
158	1	1	1	0	209	210	250	249
159	1	1	1	0	210	211	251	250
160	1	1	1	0	211	212	252	251

ELEM	MAT	TYP	REL	ESYS	NODES			
161	1	1	1	0	212	213	253	252
162	1	1	1	0	213	214	254	253
163	1	1	1	0	214	215	255	254
164	1	1	1	0	215	216	256	255
165	1	1	1	0	216	217	257	256
166	1	1	1	0	217	218	258	257
167	1	1	1	0	218	219	259	258
168	1	1	1	0	219	220	260	259
169	1	1	1	0	220	221	261	260

170	1	1	1	0	221	222	262	261
171	1	1	1	0	222	223	263	262
172	1	1	1	0	223	224	264	263
173	1	1	1	0	224	225	265	264
174	1	1	1	0	225	226	266	265
175	1	1	1	0	226	227	267	266
176	1	1	1	0	227	228	268	267
177	1	1	1	0	228	229	269	268
178	1	1	1	0	229	230	270	269
179	1	1	1	0	230	231	271	270
180	1	1	1	0	231	232	272	271

ELEM	MAT	TYP	REL	ESYS	NODES			
181	1	1	1	0	242	243	283	282
182	1	1	1	0	243	244	284	283
183	1	1	1	0	244	245	285	284
184	1	1	1	0	245	246	286	285
185	1	1	1	0	246	247	287	286
186	1	1	1	0	247	248	288	287
187	1	1	1	0	248	249	289	288
188	1	1	1	0	249	250	290	289
189	1	1	1	0	250	251	291	290
190	1	1	1	0	251	252	292	291
191	1	1	1	0	252	253	293	292
192	1	1	1	0	253	254	294	293
193	1	1	1	0	254	255	295	294
194	1	1	1	0	255	256	296	295
195	1	1	1	0	256	257	297	296
196	1	1	1	0	257	258	298	297
197	1	1	1	0	258	259	299	298
198	1	1	1	0	259	260	300	299
199	1	1	1	0	260	261	301	300
200	1	1	1	0	261	262	302	301

ELEM	MAT	TYP	REL	ESYS	NODES			
201	1	1	1	0	262	263	303	302
202	1	1	1	0	263	264	304	303
203	1	1	1	0	264	265	305	304
204	1	1	1	0	265	266	306	305
205	1	1	1	0	266	267	307	306
206	1	1	1	0	267	268	308	307
207	1	1	1	0	268	269	309	308
208	1	1	1	0	269	270	310	309
209	1	1	1	0	270	271	311	310
210	1	1	1	0	271	272	312	311
211	1	1	1	0	282	283	323	322
212	1	1	1	0	283	284	324	323
213	1	1	1	0	284	285	325	324
214	1	1	1	0	285	286	326	325
215	1	1	1	0	286	287	327	326
216	1	1	1	0	287	288	328	327
217	1	1	1	0	288	289	329	328
218	1	1	1	0	289	290	330	329
219	1	1	1	0	290	291	331	330
220	1	1	1	0	291	292	332	331

ELEM	MAT	TYP	REL	ESYS	NODES			
221	1	1	1	0	292	293	333	332
222	1	1	1	0	293	294	334	333
223	1	1	1	0	294	295	335	334
224	1	1	1	0	295	296	336	335
225	1	1	1	0	296	297	337	336
226	1	1	1	0	297	298	338	337
227	1	1	1	0	298	299	339	338
228	1	1	1	0	299	300	340	339
229	1	1	1	0	300	301	341	340
230	1	1	1	0	301	302	342	341
231	1	1	1	0	302	303	343	342
232	1	1	1	0	303	304	344	343
233	1	1	1	0	304	305	345	344
234	1	1	1	0	305	306	346	345
235	1	1	1	0	306	307	347	346
236	1	1	1	0	307	308	348	347

237	1	1	1	0	308	309	349	348
238	1	1	1	0	309	310	350	349
239	1	1	1	0	310	311	351	350
240	1	1	1	0	311	312	352	351

ELEM	MAT	TYP	REL	ESYS	NODES			
241	1	1	1	0	322	323	363	362
242	1	1	1	0	323	324	364	363
243	1	1	1	0	324	325	365	364
244	1	1	1	0	325	326	366	365
245	1	1	1	0	326	327	367	366
246	1	1	1	0	327	328	368	367
247	1	1	1	0	328	329	369	368
248	1	1	1	0	329	330	370	369
249	1	1	1	0	330	331	371	370
250	1	1	1	0	331	332	372	371
251	1	1	1	0	332	333	373	372
252	1	1	1	0	333	334	374	373
253	1	1	1	0	334	335	375	374
254	1	1	1	0	335	336	376	375
255	1	1	1	0	336	337	377	376
256	1	1	1	0	337	338	378	377
257	1	1	1	0	338	339	379	378
258	1	1	1	0	339	340	380	379
259	1	1	1	0	340	341	381	380
260	1	1	1	0	341	342	382	381

ELEM	MAT	TYP	REL	ESYS	NODES			
261	1	1	1	0	342	343	383	382
262	1	1	1	0	343	344	384	383
263	1	1	1	0	344	345	385	384
264	1	1	1	0	345	346	386	385
265	1	1	1	0	346	347	387	386
266	1	1	1	0	347	348	388	387
267	1	1	1	0	348	349	389	388
268	1	1	1	0	349	350	390	389
269	1	1	1	0	350	351	391	390
270	1	1	1	0	351	352	392	391
271	1	1	1	0	362	363	403	402
272	1	1	1	0	363	364	404	403
273	1	1	1	0	364	365	405	404
274	1	1	1	0	365	366	406	405
275	1	1	1	0	366	367	407	406
276	1	1	1	0	367	368	408	407
277	1	1	1	0	368	369	409	408
278	1	1	1	0	369	370	410	409
279	1	1	1	0	370	371	411	410
280	1	1	1	0	371	372	412	411

ELEM	MAT	TYP	REL	ESYS	NODES			
281	1	1	1	0	372	373	413	412
282	1	1	1	0	373	374	414	413
283	1	1	1	0	374	375	415	414
284	1	1	1	0	375	376	416	415
285	1	1	1	0	376	377	417	416
286	1	1	1	0	377	378	418	417
287	1	1	1	0	378	379	419	418
288	1	1	1	0	379	380	420	419
289	1	1	1	0	380	381	421	420
290	1	1	1	0	381	382	422	421
291	1	1	1	0	382	383	423	422
292	1	1	1	0	383	384	424	423
293	1	1	1	0	384	385	425	424
294	1	1	1	0	385	386	426	425
295	1	1	1	0	386	387	427	426
296	1	1	1	0	387	388	428	427
297	1	1	1	0	388	389	429	428
298	1	1	1	0	389	390	430	429
299	1	1	1	0	390	391	431	430
300	1	1	1	0	391	392	432	431

ELEM	MAT	TYP	REL	ESYS	NODES			
301	1	1	2	0	211	445	474	212
302	1	1	2	0	445	446	475	474
303	1	1	2	0	446	447	476	475
304	1	1	2	0	447	444	449	476
305	1	1	2	0	474	475	473	212
306	1	1	2	0	475	495	473	473
307	1	1	2	0	475	476	491	495
308	1	1	2	0	212	473	472	213
309	1	1	2	0	476	449	488	491
310	1	1	2	0	449	448	451	488
311	1	1	2	0	473	495	504	472
312	1	1	2	0	213	472	471	214
313	1	1	2	0	495	496	504	504
314	1	1	2	0	495	491	492	496
315	1	1	2	0	472	504	509	471
316	1	1	2	0	491	488	489	492
317	1	1	2	0	214	471	470	215
318	1	1	2	0	488	451	452	489
319	1	1	2	0	504	496	497	509
320	1	1	2	0	471	509	510	470

ELEM	MAT	TYP	REL	ESYS	NODES			
321	1	1	2	0	215	470	469	216
322	1	1	2	0	496	492	493	497
323	1	1	2	0	216	469	468	217
324	1	1	2	0	492	489	490	493
325	1	1	2	0	509	497	498	510
326	1	1	2	0	470	510	506	469
327	1	1	2	0	217	468	467	218
328	1	1	2	0	489	452	453	490
329	1	1	2	0	218	467	466	219
330	1	1	2	0	220	219	466	465
331	1	1	2	0	221	220	465	464
332	1	1	2	0	469	506	507	468
333	1	1	2	0	498	505	510	510
334	1	1	2	0	505	506	510	510
335	1	1	2	0	497	494	498	498
336	1	1	2	0	468	507	508	467
337	1	1	2	0	508	466	467	467
338	1	1	2	0	487	464	465	465
339	1	1	2	0	465	466	500	487
340	1	1	2	0	497	493	477	494

ELEM	MAT	TYP	REL	ESYS	NODES			
341	1	1	2	0	493	490	477	477
342	1	1	2	0	498	494	502	505
343	1	1	2	0	506	505	502	503
344	1	1	2	0	490	453	477	477
345	1	1	2	0	486	464	487	487
346	1	1	2	0	466	508	499	500
347	1	1	2	0	506	503	501	507
348	1	1	2	0	507	501	499	508
349	1	1	2	0	486	462	464	464
350	1	1	2	0	487	500	485	486
351	1	1	2	0	499	485	500	500
352	1	1	2	0	486	485	463	462
353	1	1	2	0	494	479	480	502
354	1	1	2	0	453	450	455	477
355	1	1	2	0	502	480	481	503
356	1	1	2	0	503	481	482	501
357	1	1	2	0	499	501	482	483
358	1	1	2	0	499	483	484	485
359	1	1	2	0	494	477	478	479
360	1	1	2	0	485	484	456	463

ELEM	MAT	TYP	REL	ESYS	NODES			
361	1	1	2	0	484	483	461	456
362	1	1	2	0	483	482	460	461
363	1	1	2	0	477	455	454	478
364	1	1	2	0	482	481	459	460
365	1	1	2	0	481	480	458	459

366	1	1	2	0	478	457	479	479
367	1	1	2	0	480	479	457	458
368	1	1	2	0	478	454	457	457

LIST ALL SELECTED NODE DSYS= 0

NODE	X	Y	Z	THXY	THYZ	THXZ
2	0.66486	61.125	1.1516	-90.00	-30.00	90.00
3	1.3288	61.052	2.3016	-90.00	-30.00	90.00
4	1.9910	60.929	3.4484	-90.00	-30.00	90.00
5	2.6504	60.758	4.5906	-90.00	-30.00	90.00
6	3.3062	60.538	5.7265	-90.00	-30.00	90.00
7	3.9575	60.269	6.8546	-90.00	-30.00	90.00
8	4.6034	59.953	7.9733	-90.00	-30.00	90.00
9	5.2430	59.589	9.0811	-90.00	-30.00	90.00
10	5.8754	59.178	10.177	-90.00	-30.00	90.00
11	6.4999	58.721	11.258	-90.00	-30.00	90.00
12	7.0790	58.249	12.261	-90.00	-30.00	90.00
13	7.6496	57.737	13.250	-90.00	-30.00	90.00
14	8.2110	57.186	14.222	-90.00	-30.00	90.00
15	8.4619	56.868	14.657	-90.00	-30.00	90.00
16	8.6797	56.463	15.034	-90.00	-30.00	90.00
17	8.8570	55.987	15.341	-90.00	-30.00	90.00
18	8.9879	55.453	15.568	-90.00	-30.00	90.00
19	9.0681	54.881	15.706	-90.00	-30.00	90.00
20	9.0950	54.290	15.753	-90.00	-30.00	90.00
21	9.0950	53.380	15.753	-90.00	-30.00	90.00

NODE	X	Y	Z	THXY	THYZ	THXZ
22	9.0950	52.212	15.753	-90.00	-30.00	90.00
23	9.0950	50.871	15.753	-90.00	-30.00	90.00
24	9.0950	49.330	15.753	-90.00	-30.00	90.00
25	9.0950	47.560	15.753	-90.00	-30.00	90.00
26	9.0950	45.527	15.753	-90.00	-30.00	90.00
27	9.0950	43.192	15.753	-90.00	-30.00	90.00
28	9.0950	40.509	15.753	-90.00	-30.00	90.00
29	9.0950	37.427	15.753	-90.00	-30.00	90.00
30	9.0950	33.887	15.753	-90.00	-30.00	90.00
31	9.0950	29.821	15.753	-90.00	-30.00	90.00
32	9.0950	25.150	15.753	-90.00	-30.00	90.00
42	0.94026	61.125	0.94026	0.00	0.00	0.00
43	1.8792	61.052	1.8792	0.00	0.00	0.00
44	2.8156	60.929	2.8156	0.00	0.00	0.00
45	3.7482	60.758	3.7482	0.00	0.00	0.00
46	4.6756	60.538	4.6756	0.00	0.00	0.00
47	5.5967	60.269	5.5967	0.00	0.00	0.00
48	6.5101	59.953	6.5101	0.00	0.00	0.00
49	7.4147	59.589	7.4147	0.00	0.00	0.00
50	8.3091	59.178	8.3091	0.00	0.00	0.00

NODE	X	Y	Z	THXY	THYZ	THXZ
51	9.1922	58.721	9.1922	0.00	0.00	0.00
52	10.011	58.249	10.011	0.00	0.00	0.00
53	10.818	57.737	10.818	0.00	0.00	0.00
54	11.612	57.186	11.612	0.00	0.00	0.00
55	11.967	56.868	11.967	0.00	0.00	0.00
56	12.275	56.463	12.275	0.00	0.00	0.00
57	12.526	55.987	12.526	0.00	0.00	0.00
58	12.711	55.453	12.711	0.00	0.00	0.00
59	12.824	54.881	12.824	0.00	0.00	0.00
60	12.862	54.290	12.862	0.00	0.00	0.00
61	12.862	53.380	12.862	0.00	0.00	0.00
62	12.862	52.212	12.862	0.00	0.00	0.00
63	12.862	50.871	12.862	0.00	0.00	0.00
64	12.862	49.330	12.862	0.00	0.00	0.00
65	12.862	47.560	12.862	0.00	0.00	0.00
66	12.862	45.527	12.862	0.00	0.00	0.00
67	12.862	43.192	12.862	0.00	0.00	0.00
68	12.862	40.509	12.862	0.00	0.00	0.00
69	12.862	37.427	12.862	0.00	0.00	0.00
70	12.862	33.887	12.862	0.00	0.00	0.00

NODE	X	Y	Z	THXY	THYZ	THXZ
71	12.862	29.821	12.862	0.00	0.00	0.00
72	12.862	25.150	12.862	0.00	0.00	0.00

82	1.1516	61.125	0.66486	0.00	0.00	0.00
83	2.3016	61.052	1.3288	0.00	0.00	0.00
84	3.4484	60.929	1.9910	0.00	0.00	0.00
85	4.5906	60.758	2.6504	0.00	0.00	0.00
86	5.7265	60.538	3.3062	0.00	0.00	0.00
87	6.8546	60.269	3.9575	0.00	0.00	0.00
88	7.9733	59.953	4.6034	0.00	0.00	0.00
89	9.0811	59.589	5.2430	0.00	0.00	0.00
90	10.177	59.178	5.8754	0.00	0.00	0.00
91	11.258	58.721	6.4999	0.00	0.00	0.00
92	12.261	58.249	7.0790	0.00	0.00	0.00
93	13.250	57.737	7.6496	0.00	0.00	0.00
94	14.222	57.186	8.2110	0.00	0.00	0.00
95	14.657	56.868	8.4619	0.00	0.00	0.00
96	15.034	56.463	8.6797	0.00	0.00	0.00
97	15.341	55.987	8.8570	0.00	0.00	0.00
98	15.568	55.453	8.9879	0.00	0.00	0.00
99	15.706	54.881	9.0681	0.00	0.00	0.00

NODE	X	Y	Z	THXY	THYZ	THXZ
100	15.753	54.290	9.0950	0.00	0.00	0.00
101	15.753	53.380	9.0950	0.00	0.00	0.00
102	15.753	52.212	9.0950	0.00	0.00	0.00
103	15.753	50.871	9.0950	0.00	0.00	0.00
104	15.753	49.330	9.0950	0.00	0.00	0.00
105	15.753	47.560	9.0950	0.00	0.00	0.00
106	15.753	45.527	9.0950	0.00	0.00	0.00
107	15.753	43.192	9.0950	0.00	0.00	0.00
108	15.753	40.509	9.0950	0.00	0.00	0.00
109	15.753	37.427	9.0950	0.00	0.00	0.00
110	15.753	33.887	9.0950	0.00	0.00	0.00
111	15.753	29.821	9.0950	0.00	0.00	0.00
112	15.753	25.150	9.0950	0.00	0.00	0.00
122	1.2495	61.125	0.45479	0.00	0.00	0.00
123	2.4974	61.052	0.90896	0.00	0.00	0.00
124	3.7418	60.929	1.3619	0.00	0.00	0.00
125	4.9811	60.758	1.8130	0.00	0.00	0.00
126	6.2136	60.538	2.2616	0.00	0.00	0.00
127	7.4376	60.269	2.7071	0.00	0.00	0.00
128	8.6515	59.953	3.1489	0.00	0.00	0.00

NODE	X	Y	Z	THXY	THYZ	THXZ
129	9.8536	59.589	3.5864	0.00	0.00	0.00
130	11.042	59.178	4.0190	0.00	0.00	0.00
131	12.216	58.721	4.4462	0.00	0.00	0.00
132	13.304	58.249	4.8423	0.00	0.00	0.00
133	14.377	57.737	5.2326	0.00	0.00	0.00
134	15.432	57.186	5.6167	0.00	0.00	0.00
135	15.903	56.868	5.7883	0.00	0.00	0.00
136	16.312	56.463	5.9373	0.00	0.00	0.00
137	16.646	55.987	6.0585	0.00	0.00	0.00
138	16.892	55.453	6.1481	0.00	0.00	0.00
139	17.043	54.881	6.2030	0.00	0.00	0.00
140	17.093	54.290	6.2213	0.00	0.00	0.00
141	17.093	53.380	6.2213	0.00	0.00	0.00
142	17.093	52.212	6.2213	0.00	0.00	0.00
143	17.093	50.871	6.2213	0.00	0.00	0.00
144	17.093	49.330	6.2213	0.00	0.00	0.00
145	17.093	47.560	6.2213	0.00	0.00	0.00
146	17.093	45.527	6.2213	0.00	0.00	0.00
147	17.093	43.192	6.2213	0.00	0.00	0.00
148	17.093	40.509	6.2213	0.00	0.00	0.00

NODE	X	Y	Z	THXY	THYZ	THXZ
149	17.093	37.427	6.2213	0.00	0.00	0.00
150	17.093	33.887	6.2213	0.00	0.00	0.00
151	17.093	29.821	6.2213	0.00	0.00	0.00
152	17.093	25.150	6.2213	0.00	0.00	0.00
162	1.3095	61.125	0.23090	0.00	0.00	0.00
163	2.6173	61.052	0.46149	0.00	0.00	0.00
164	3.9214	60.929	0.69145	0.00	0.00	0.00
165	5.2202	60.758	0.92047	0.00	0.00	0.00
166	6.5119	60.538	1.1482	0.00	0.00	0.00
167	7.7947	60.269	1.3744	0.00	0.00	0.00
168	9.0669	59.953	1.5987	0.00	0.00	0.00
169	10.327	59.589	1.8209	0.00	0.00	0.00

170	11.572	59.178	2.0405	0.00	0.00	0.00
171	12.802	58.721	2.2574	0.00	0.00	0.00
172	13.943	58.249	2.4585	0.00	0.00	0.00
173	15.067	57.737	2.6567	0.00	0.00	0.00
174	16.172	57.186	2.8516	0.00	0.00	0.00
175	16.667	56.868	2.9388	0.00	0.00	0.00
176	17.096	56.463	3.0144	0.00	0.00	0.00
177	17.445	55.987	3.0760	0.00	0.00	0.00

NODE	X	Y	Z	THXY	THYZ	THXZ
178	17.703	55.453	3.1215	0.00	0.00	0.00
179	17.861	54.881	3.1493	0.00	0.00	0.00
180	17.914	54.290	3.1587	0.00	0.00	0.00
181	17.914	53.380	3.1587	0.00	0.00	0.00
182	17.914	52.212	3.1587	0.00	0.00	0.00
183	17.914	50.871	3.1587	0.00	0.00	0.00
184	17.914	49.330	3.1587	0.00	0.00	0.00
185	17.914	47.560	3.1587	0.00	0.00	0.00
186	17.914	45.527	3.1587	0.00	0.00	0.00
187	17.914	43.192	3.1587	0.00	0.00	0.00
188	17.914	40.509	3.1587	0.00	0.00	0.00
189	17.914	37.427	3.1587	0.00	0.00	0.00
190	17.914	33.887	3.1587	0.00	0.00	0.00
191	17.914	29.821	3.1587	0.00	0.00	0.00
192	17.914	25.150	3.1587	0.00	0.00	0.00
202	1.3297	61.125	0.23818E-09	0.00	0.00	0.00
203	2.6576	61.052	0.23789E-09	0.00	0.00	0.00
204	3.9819	60.929	0.23741E-09	0.00	0.00	0.00
205	5.3008	60.758	0.23674E-09	0.00	0.00	0.00
206	6.6124	60.538	0.23588E-09	0.00	0.00	0.00

NODE	X	Y	Z	THXY	THYZ	THXZ
207	7.9150	60.269	0.23484E-09	0.00	0.00	0.00
208	9.2067	59.953	0.23361E-09	0.00	0.00	0.00
209	10.486	59.589	0.23219E-09	0.00	0.00	0.00
210	11.751	59.178	0.23059E-09	0.00	0.00	0.00
211	13.000	58.721	0.22880E-09	0.00	0.00	0.00
212	14.158	58.249	0.22697E-09	0.00	0.00	0.00
213	15.299	57.737	0.22497E-09	0.00	0.00	0.00
214	16.422	57.186	0.22282E-09	0.00	0.00	0.00
215	16.924	56.868	0.22158E-09	0.00	0.00	0.00
216	17.359	56.463	0.22001E-09	0.00	0.00	0.00
217	17.714	55.987	0.21815E-09	0.00	0.00	0.00
218	17.976	55.453	0.21607E-09	0.00	0.00	0.00
219	18.136	54.881	0.21384E-09	0.00	0.00	0.00
220	18.190	54.290	0.21154E-09	0.00	0.00	0.00
221	18.190	53.380	0.20799E-09	0.00	0.00	0.00
222	18.190	52.212	0.20344E-09	0.00	0.00	0.00
223	18.190	50.871	0.19822E-09	0.00	0.00	0.00
224	18.190	49.330	0.19221E-09	0.00	0.00	0.00
225	18.190	47.560	0.18532E-09	0.00	0.00	0.00
226	18.190	45.527	0.17739E-09	0.00	0.00	0.00

NODE	X	Y	Z	THXY	THYZ	THXZ
227	18.190	43.192	0.16829E-09	0.00	0.00	0.00
228	18.190	40.509	0.15784E-09	0.00	0.00	0.00
229	18.190	37.427	0.14583E-09	0.00	0.00	0.00
230	18.190	33.887	0.13204E-09	0.00	0.00	0.00
231	18.190	29.821	0.11619E-09	0.00	0.00	0.00
232	18.190	25.150	0.97995E-10	0.00	0.00	0.00
242	1.3095	61.125	-0.23090	0.00	0.00	0.00
243	2.6173	61.052	-0.46149	0.00	0.00	0.00
244	3.9214	60.929	-0.69145	0.00	0.00	0.00
245	5.2202	60.758	-0.92047	0.00	0.00	0.00
246	6.5119	60.538	-1.1482	0.00	0.00	0.00
247	7.7947	60.269	-1.3744	0.00	0.00	0.00
248	9.0669	59.953	-1.5987	0.00	0.00	0.00
249	10.327	59.589	-1.8209	0.00	0.00	0.00
250	11.572	59.178	-2.0405	0.00	0.00	0.00
251	12.802	58.721	-2.2574	0.00	0.00	0.00
252	13.943	58.249	-2.4585	0.00	0.00	0.00
253	15.067	57.737	-2.6567	0.00	0.00	0.00
254	16.172	57.186	-2.8516	0.00	0.00	0.00
255	16.667	56.868	-2.9388	0.00	0.00	0.00

NODE	X	Y	Z	THXY	THYZ	THXZ
256	17.096	56.463	-3.0144	0.00	0.00	0.00
257	17.445	55.987	-3.0760	0.00	0.00	0.00
258	17.703	55.453	-3.1215	0.00	0.00	0.00
259	17.861	54.881	-3.1493	0.00	0.00	0.00
260	17.914	54.290	-3.1587	0.00	0.00	0.00
261	17.914	53.380	-3.1587	0.00	0.00	0.00
262	17.914	52.212	-3.1587	0.00	0.00	0.00
263	17.914	50.871	-3.1587	0.00	0.00	0.00
264	17.914	49.330	-3.1587	0.00	0.00	0.00
265	17.914	47.560	-3.1587	0.00	0.00	0.00
266	17.914	45.527	-3.1587	0.00	0.00	0.00
267	17.914	43.192	-3.1587	0.00	0.00	0.00
268	17.914	40.509	-3.1587	0.00	0.00	0.00
269	17.914	37.427	-3.1587	0.00	0.00	0.00
270	17.914	33.887	-3.1587	0.00	0.00	0.00
271	17.914	29.821	-3.1587	0.00	0.00	0.00
272	17.914	25.150	-3.1587	0.00	0.00	0.00
282	1.2495	61.125	-0.45479	0.00	0.00	0.00
283	2.4974	61.052	-0.90896	0.00	0.00	0.00
284	3.7418	60.929	-1.3619	0.00	0.00	0.00

NODE	X	Y	Z	THXY	THYZ	THXZ
285	4.9811	60.758	-1.8130	0.00	0.00	0.00
286	6.2136	60.538	-2.2616	0.00	0.00	0.00
287	7.4376	60.269	-2.7071	0.00	0.00	0.00
288	8.6515	59.953	-3.1489	0.00	0.00	0.00
289	9.8536	59.589	-3.5864	0.00	0.00	0.00
290	11.042	59.178	-4.0190	0.00	0.00	0.00
291	12.216	58.721	-4.4462	0.00	0.00	0.00
292	13.304	58.249	-4.8423	0.00	0.00	0.00
293	14.377	57.737	-5.2326	0.00	0.00	0.00
294	15.432	57.186	-5.6167	0.00	0.00	0.00
295	15.903	56.868	-5.7883	0.00	0.00	0.00
296	16.312	56.463	-5.9373	0.00	0.00	0.00
297	16.646	55.987	-6.0585	0.00	0.00	0.00
298	16.892	55.453	-6.1481	0.00	0.00	0.00
299	17.043	54.881	-6.2030	0.00	0.00	0.00
300	17.093	54.290	-6.2213	0.00	0.00	0.00
301	17.093	53.380	-6.2213	0.00	0.00	0.00
302	17.093	52.212	-6.2213	0.00	0.00	0.00
303	17.093	50.871	-6.2213	0.00	0.00	0.00
304	17.093	49.330	-6.2213	0.00	0.00	0.00

NODE	X	Y	Z	THXY	THYZ	THXZ
305	17.093	47.560	-6.2213	0.00	0.00	0.00
306	17.093	45.527	-6.2213	0.00	0.00	0.00
307	17.093	43.192	-6.2213	0.00	0.00	0.00
308	17.093	40.509	-6.2213	0.00	0.00	0.00
309	17.093	37.427	-6.2213	0.00	0.00	0.00
310	17.093	33.887	-6.2213	0.00	0.00	0.00
311	17.093	29.821	-6.2213	0.00	0.00	0.00
312	17.093	25.150	-6.2213	0.00	0.00	0.00
322	1.1516	61.125	-0.66486	0.00	0.00	0.00
323	2.3016	61.052	-1.3288	0.00	0.00	0.00
324	3.4484	60.929	-1.9910	0.00	0.00	0.00
325	4.5906	60.758	-2.6504	0.00	0.00	0.00
326	5.7265	60.538	-3.3062	0.00	0.00	0.00
327	6.8546	60.269	-3.9575	0.00	0.00	0.00
328	7.9733	59.953	-4.6034	0.00	0.00	0.00
329	9.0811	59.589	-5.2430	0.00	0.00	0.00
330	10.177	59.178	-5.8754	0.00	0.00	0.00
331	11.258	58.721	-6.4999	0.00	0.00	0.00
332	12.261	58.249	-7.0790	0.00	0.00	0.00
333	13.250	57.737	-7.6496	0.00	0.00	0.00

NODE	X	Y	Z	THXY	THYZ	THXZ
334	14.222	57.186	-8.2110	0.00	0.00	0.00
335	14.657	56.868	-8.4619	0.00	0.00	0.00
336	15.034	56.463	-8.6797	0.00	0.00	0.00
337	15.341	55.987	-8.8570	0.00	0.00	0.00
338	15.568	55.453	-8.9879	0.00	0.00	0.00
339	15.706	54.881	-9.0681	0.00	0.00	0.00
340	15.753	54.290	-9.0950	0.00	0.00	0.00
341	15.753	53.380	-9.0950	0.00	0.00	0.00
342	15.753	52.212	-9.0950	0.00	0.00	0.00

343	15.753	50.871	-9.0950	0.00	0.00	0.00
344	15.753	49.330	-9.0950	0.00	0.00	0.00
345	15.753	47.560	-9.0950	0.00	0.00	0.00
346	15.753	45.527	-9.0950	0.00	0.00	0.00
347	15.753	43.192	-9.0950	0.00	0.00	0.00
348	15.753	40.509	-9.0950	0.00	0.00	0.00
349	15.753	37.427	-9.0950	0.00	0.00	0.00
350	15.753	33.887	-9.0950	0.00	0.00	0.00
351	15.753	29.821	-9.0950	0.00	0.00	0.00
352	15.753	25.150	-9.0950	0.00	0.00	0.00
362	0.94026	61.125	-0.94026	0.00	0.00	0.00

NODE	X	Y	Z	THXY	THYZ	THXZ
363	1.8792	61.052	-1.8792	0.00	0.00	0.00
364	2.8156	60.929	-2.8156	0.00	0.00	0.00
365	3.7482	60.758	-3.7482	0.00	0.00	0.00
366	4.6756	60.538	-4.6756	0.00	0.00	0.00
367	5.5967	60.269	-5.5967	0.00	0.00	0.00
368	6.5101	59.953	-6.5101	0.00	0.00	0.00
369	7.4147	59.589	-7.4147	0.00	0.00	0.00
370	8.3091	59.178	-8.3091	0.00	0.00	0.00
371	9.1922	58.721	-9.1922	0.00	0.00	0.00
372	10.011	58.249	-10.011	0.00	0.00	0.00
373	10.818	57.737	-10.818	0.00	0.00	0.00
374	11.612	57.186	-11.612	0.00	0.00	0.00
375	11.967	56.868	-11.967	0.00	0.00	0.00
376	12.275	56.463	-12.275	0.00	0.00	0.00
377	12.526	55.987	-12.526	0.00	0.00	0.00
378	12.711	55.453	-12.711	0.00	0.00	0.00
379	12.824	54.881	-12.824	0.00	0.00	0.00
380	12.862	54.290	-12.862	0.00	0.00	0.00
381	12.862	53.380	-12.862	0.00	0.00	0.00
382	12.862	52.212	-12.862	0.00	0.00	0.00

NODE	X	Y	Z	THXY	THYZ	THXZ
383	12.862	50.871	-12.862	0.00	0.00	0.00
384	12.862	49.330	-12.862	0.00	0.00	0.00
385	12.862	47.560	-12.862	0.00	0.00	0.00
386	12.862	45.527	-12.862	0.00	0.00	0.00
387	12.862	43.192	-12.862	0.00	0.00	0.00
388	12.862	40.509	-12.862	0.00	0.00	0.00
389	12.862	37.427	-12.862	0.00	0.00	0.00
390	12.862	33.887	-12.862	0.00	0.00	0.00
391	12.862	29.821	-12.862	0.00	0.00	0.00
392	12.862	25.150	-12.862	0.00	0.00	0.00
402	0.66486	61.125	-1.1516	90.00	-30.00	-90.00
403	1.3288	61.052	-2.3016	90.00	-30.00	-90.00
404	1.9910	60.929	-3.4484	90.00	-30.00	-90.00
405	2.6504	60.758	-4.5906	90.00	-30.00	-90.00
406	3.3062	60.538	-5.7265	90.00	-30.00	-90.00
407	3.9575	60.269	-6.8546	90.00	-30.00	-90.00
408	4.6034	59.953	-7.9733	90.00	-30.00	-90.00
409	5.2430	59.589	-9.0811	90.00	-30.00	-90.00
410	5.8754	59.178	-10.177	90.00	-30.00	-90.00
411	6.4999	58.721	-11.258	90.00	-30.00	-90.00

NODE	X	Y	Z	THXY	THYZ	THXZ
412	7.0790	58.249	-12.261	90.00	-30.00	-90.00
413	7.6496	57.737	-13.250	90.00	-30.00	-90.00
414	8.2110	57.186	-14.222	90.00	-30.00	-90.00
415	8.4619	56.868	-14.657	90.00	-30.00	-90.00
416	8.6797	56.463	-15.034	90.00	-30.00	-90.00
417	8.8570	55.987	-15.341	90.00	-30.00	-90.00
418	8.9879	55.453	-15.568	90.00	-30.00	-90.00
419	9.0681	54.881	-15.706	90.00	-30.00	-90.00
420	9.0950	54.290	-15.753	90.00	-30.00	-90.00
421	9.0950	53.380	-15.753	90.00	-30.00	-90.00
422	9.0950	52.212	-15.753	90.00	-30.00	-90.00
423	9.0950	50.871	-15.753	90.00	-30.00	-90.00
424	9.0950	49.330	-15.753	90.00	-30.00	-90.00
425	9.0950	47.560	-15.753	90.00	-30.00	-90.00
426	9.0950	45.527	-15.753	90.00	-30.00	-90.00
427	9.0950	43.192	-15.753	90.00	-30.00	-90.00
428	9.0950	40.509	-15.753	90.00	-30.00	-90.00
429	9.0950	37.427	-15.753	90.00	-30.00	-90.00

430	9.0950	33.887	-15.753	90.00	-30.00	-90.00
431	9.0950	29.821	-15.753	90.00	-30.00	-90.00

NODE	X	Y	Z	THXY	THYZ	THXZ
432	9.0950	25.150	-15.753	90.00	-30.00	-90.00
444	13.000	60.500	0.00000E+00	0.00	0.00	0.00
445	13.000	59.165	0.00000E+00	0.00	0.00	0.00
446	13.000	59.610	0.00000E+00	0.00	0.00	0.00
447	13.000	60.055	0.00000E+00	0.00	0.00	0.00
448	15.000	62.500	0.00000E+00	0.00	0.00	0.00
449	14.000	61.500	0.00000E+00	0.00	0.00	0.00
450	19.250	62.500	0.00000E+00	0.00	0.00	0.00
451	16.063	62.500	0.00000E+00	0.00	0.00	0.00
452	17.125	62.500	0.00000E+00	0.00	0.00	0.00
453	18.188	62.500	0.00000E+00	0.00	0.00	0.00
454	21.250	60.500	0.00000E+00	0.00	0.00	0.00
455	20.250	61.500	0.00000E+00	0.00	0.00	0.00
456	21.250	54.630	0.00000E+00	0.00	0.00	0.00
457	21.250	59.522	0.00000E+00	0.00	0.00	0.00
458	21.250	58.543	0.00000E+00	0.00	0.00	0.00
459	21.250	57.565	0.00000E+00	0.00	0.00	0.00
460	21.250	56.587	0.00000E+00	0.00	0.00	0.00
461	21.250	55.608	0.00000E+00	0.00	0.00	0.00
462	20.000	53.380	0.00000E+00	0.00	0.00	0.00

NODE	X	Y	Z	THXY	THYZ	THXZ
463	20.625	54.005	0.00000E+00	0.00	0.00	0.00
464	19.095	53.380	0.00000E+00	0.00	0.00	0.00
465	18.766	54.273	0.00000E+00	0.00	0.00	0.00
466	18.752	55.001	0.00000E+00	0.00	0.00	0.00
467	18.452	55.684	0.00000E+00	0.00	0.00	0.00
468	18.119	56.263	0.00000E+00	0.00	0.00	0.00
469	17.805	56.862	0.00000E+00	0.00	0.00	0.00
470	17.297	57.433	0.00000E+00	0.00	0.00	0.00
471	16.610	57.939	0.00000E+00	0.00	0.00	0.00
472	15.744	58.421	0.00000E+00	0.00	0.00	0.00
473	14.802	58.909	0.00000E+00	0.00	0.00	0.00
474	13.820	59.045	0.00000E+00	0.00	0.00	0.00
475	14.134	59.615	0.00000E+00	0.00	0.00	0.00
476	14.103	60.377	0.00000E+00	0.00	0.00	0.00
477	19.267	60.768	0.00000E+00	0.00	0.00	0.00
478	20.429	60.215	0.00000E+00	0.00	0.00	0.00
479	20.036	59.500	0.00000E+00	0.00	0.00	0.00
480	20.158	58.504	0.00000E+00	0.00	0.00	0.00
481	20.266	57.540	0.00000E+00	0.00	0.00	0.00
482	20.354	56.551	0.00000E+00	0.00	0.00	0.00

NODE	X	Y	Z	THXY	THYZ	THXZ
483	20.445	55.620	0.00000E+00	0.00	0.00	0.00
484	20.523	54.876	0.00000E+00	0.00	0.00	0.00
485	19.939	54.592	0.00000E+00	0.00	0.00	0.00
486	19.649	54.011	0.00000E+00	0.00	0.00	0.00
487	19.236	54.255	0.00000E+00	0.00	0.00	0.00
488	15.701	61.446	0.00000E+00	0.00	0.00	0.00
489	17.000	61.000	0.00000E+00	0.00	0.00	0.00
490	17.933	61.279	0.00000E+00	0.00	0.00	0.00
491	15.499	60.461	0.00000E+00	0.00	0.00	0.00
492	16.812	60.438	0.00000E+00	0.00	0.00	0.00
493	17.935	60.305	0.00000E+00	0.00	0.00	0.00
494	18.799	59.415	0.00000E+00	0.00	0.00	0.00
495	15.478	59.576	0.00000E+00	0.00	0.00	0.00
496	16.671	59.587	0.00000E+00	0.00	0.00	0.00
497	17.697	59.483	0.00000E+00	0.00	0.00	0.00
498	18.078	58.787	0.00000E+00	0.00	0.00	0.00
499	19.634	55.500	0.00000E+00	0.00	0.00	0.00
500	19.334	54.799	0.00000E+00	0.00	0.00	0.00
501	19.520	56.495	0.00000E+00	0.00	0.00	0.00
502	19.185	58.422	0.00000E+00	0.00	0.00	0.00

NODE	X	Y	Z	THXY	THYZ	THXZ
503	19.357	57.480	0.00000E+00	0.00	0.00	0.00
504	16.154	58.977	0.00000E+00	0.00	0.00	0.00
505	18.471	58.258	0.00000E+00	0.00	0.00	0.00
506	18.451	57.341	0.00000E+00	0.00	0.00	0.00
507	18.755	56.366	0.00000E+00	0.00	0.00	0.00
508	19.013	55.617	0.00000E+00	0.00	0.00	0.00

```
   509    17.068      58.708     0.00000E+00    0.00    0.00    0.00
   510    17.785      58.052     0.00000E+00    0.00    0.00    0.00

LIST ALL MATERIALS  PROPERTY= ALL

PROPERTY TABLE EX    MAT=   1  NUM. POINTS=  2
    TEMPERATURE      DATA    TEMPERATURE      DATA
     -9999.0     0.27180E+08  9999.0     0.27180E+08

PROPERTY TABLE NUXY  MAT=   1  NUM. POINTS=  2
    TEMPERATURE      DATA    TEMPERATURE      DATA
      -9999.0      0.30000      9999.0      0.30000
TIME= 0.00000E+00  NITTER=      1

UNIFORM TEMPERATURE=      0.000  (TREF=      0.000)
PLASTIC CONVERG. CRITERION=       0.0100
CREEP OPTIMUM. CRITERION=        0.1000
LARGE DEFL. CONVERG. CRITERION=     0.001000
DISPLACEMENT LIMIT= 0.00000E+00

NPRINT= 99900   NPOST=      1   REACTION PRINT FREQ= 99900
 DISP. POST DATA FREQ=      1  REACT. POST DATA FREQ=      1

 ELEMENT PRINT AND POST DATA FREQUENCIES
  TYPE  STIFF  STRESS  FORCE   STRESS   DATA  FORCE
          NO.   PRINT  PRINT    DATA    LEVEL  DATA
    1     63  99900  99900       1       3      1

LOADS INPUT FILE= 26     LOADS OUTPUT FILE= 23

ALL ANALYSIS DATA WILL BE WRITTEN ONTO FILE27

LIST DISPLACEMENTS FOR ALL SELECTED NODES

 NODE  LABEL     DISP            CDISP
   32  UX    0.000000000E+00 0.000000000E+00
  432  ROTX  0.000000000E+00 0.000000000E+00
   32  UZ    0.000000000E+00 0.000000000E+00
  432  UY    0.000000000E+00 0.000000000E+00
   32  ROTY  0.000000000E+00 0.000000000E+00
  431  ROTX  0.000000000E+00 0.000000000E+00
   72  UX    0.000000000E+00 0.000000000E+00
   72  UY    0.000000000E+00 0.000000000E+00
   72  UZ    0.000000000E+00 0.000000000E+00
   72  ROTX  0.000000000E+00 0.000000000E+00
   72  ROTY  0.000000000E+00 0.000000000E+00
   72  ROTZ  0.000000000E+00 0.000000000E+00
  112  UX    0.000000000E+00 0.000000000E+00
  112  UY    0.000000000E+00 0.000000000E+00
  112  UZ    0.000000000E+00 0.000000000E+00
  112  ROTX  0.000000000E+00 0.000000000E+00
  112  ROTY  0.000000000E+00 0.000000000E+00
  112  ROTZ  0.000000000E+00 0.000000000E+00
  152  UX    0.000000000E+00 0.000000000E+00
  152  UY    0.000000000E+00 0.000000000E+00

 NODE  LABEL     DISP            CDISP
  152  UZ    0.000000000E+00 0.000000000E+00
  152  ROTX  0.000000000E+00 0.000000000E+00
  152  ROTY  0.000000000E+00 0.000000000E+00
  152  ROTZ  0.000000000E+00 0.000000000E+00
  192  UX    0.000000000E+00 0.000000000E+00
  192  UY    0.000000000E+00 0.000000000E+00
  192  UZ    0.000000000E+00 0.000000000E+00
  192  ROTX  0.000000000E+00 0.000000000E+00
  192  ROTY  0.000000000E+00 0.000000000E+00
  192  ROTZ  0.000000000E+00 0.000000000E+00
  232  UX    0.000000000E+00 0.000000000E+00
  232  UY    0.000000000E+00 0.000000000E+00
  232  UZ    0.000000000E+00 0.000000000E+00
  232  ROTX  0.000000000E+00 0.000000000E+00
  232  ROTY  0.000000000E+00 0.000000000E+00
  232  ROTZ  0.000000000E+00 0.000000000E+00
  272  UX    0.000000000E+00 0.000000000E+00
  272  UY    0.000000000E+00 0.000000000E+00
```

272	UZ	0.000000000E+00	0.000000000E+00
272	ROTX	0.000000000E+00	0.000000000E+00

NODE	LABEL	DISP	CDISP
272	ROTY	0.000000000E+00	0.000000000E+00
272	ROTZ	0.000000000E+00	0.000000000E+00
312	UX	0.000000000E+00	0.000000000E+00
312	UY	0.000000000E+00	0.000000000E+00
312	UZ	0.000000000E+00	0.000000000E+00
312	ROTX	0.000000000E+00	0.000000000E+00
312	ROTY	0.000000000E+00	0.000000000E+00
312	ROTZ	0.000000000E+00	0.000000000E+00
352	UX	0.000000000E+00	0.000000000E+00
352	UY	0.000000000E+00	0.000000000E+00
352	UZ	0.000000000E+00	0.000000000E+00
352	ROTX	0.000000000E+00	0.000000000E+00
352	ROTY	0.000000000E+00	0.000000000E+00
352	ROTZ	0.000000000E+00	0.000000000E+00
392	UX	0.000000000E+00	0.000000000E+00
392	UY	0.000000000E+00	0.000000000E+00
392	UZ	0.000000000E+00	0.000000000E+00
392	ROTX	0.000000000E+00	0.000000000E+00
392	ROTY	0.000000000E+00	0.000000000E+00
392	ROTZ	0.000000000E+00	0.000000000E+00

NODE	LABEL	DISP	CDISP
432	UX	0.000000000E+00	0.000000000E+00
432	ROTY	0.000000000E+00	0.000000000E+00
432	UZ	0.000000000E+00	0.000000000E+00
431	UY	0.000000000E+00	0.000000000E+00
2	UY	0.000000000E+00	0.000000000E+00
3	UY	0.000000000E+00	0.000000000E+00
4	UY	0.000000000E+00	0.000000000E+00
5	UY	0.000000000E+00	0.000000000E+00
6	UY	0.000000000E+00	0.000000000E+00
7	UY	0.000000000E+00	0.000000000E+00
8	UY	0.000000000E+00	0.000000000E+00
9	UY	0.000000000E+00	0.000000000E+00
10	UY	0.000000000E+00	0.000000000E+00
11	UY	0.000000000E+00	0.000000000E+00
12	UY	0.000000000E+00	0.000000000E+00
13	UY	0.000000000E+00	0.000000000E+00
14	UY	0.000000000E+00	0.000000000E+00
15	UY	0.000000000E+00	0.000000000E+00
16	UY	0.000000000E+00	0.000000000E+00
17	UY	0.000000000E+00	0.000000000E+00

NODE	LABEL	DISP	CDISP
18	UY	0.000000000E+00	0.000000000E+00
19	UY	0.000000000E+00	0.000000000E+00
20	UY	0.000000000E+00	0.000000000E+00
21	UY	0.000000000E+00	0.000000000E+00
22	UY	0.000000000E+00	0.000000000E+00
23	UY	0.000000000E+00	0.000000000E+00
24	UY	0.000000000E+00	0.000000000E+00
25	UY	0.000000000E+00	0.000000000E+00
26	UY	0.000000000E+00	0.000000000E+00
27	UY	0.000000000E+00	0.000000000E+00
28	UY	0.000000000E+00	0.000000000E+00
29	UY	0.000000000E+00	0.000000000E+00
30	UY	0.000000000E+00	0.000000000E+00
31	UY	0.000000000E+00	0.000000000E+00
32	UY	0.000000000E+00	0.000000000E+00
402	UY	0.000000000E+00	0.000000000E+00
403	UY	0.000000000E+00	0.000000000E+00
404	UY	0.000000000E+00	0.000000000E+00
405	UY	0.000000000E+00	0.000000000E+00
406	UY	0.000000000E+00	0.000000000E+00

NODE	LABEL	DISP	CDISP
407	UY	0.000000000E+00	0.000000000E+00
408	UY	0.000000000E+00	0.000000000E+00
409	UY	0.000000000E+00	0.000000000E+00
410	UY	0.000000000E+00	0.000000000E+00
411	UY	0.000000000E+00	0.000000000E+00
412	UY	0.000000000E+00	0.000000000E+00

413	UY	0.000000000E+00	0.000000000E+00
414	UY	0.000000000E+00	0.000000000E+00
415	UY	0.000000000E+00	0.000000000E+00
416	UY	0.000000000E+00	0.000000000E+00
417	UY	0.000000000E+00	0.000000000E+00
418	UY	0.000000000E+00	0.000000000E+00
419	UY	0.000000000E+00	0.000000000E+00
420	UY	0.000000000E+00	0.000000000E+00
421	UY	0.000000000E+00	0.000000000E+00
422	UY	0.000000000E+00	0.000000000E+00
423	UY	0.000000000E+00	0.000000000E+00
424	UY	0.000000000E+00	0.000000000E+00
425	UY	0.000000000E+00	0.000000000E+00
426	UY	0.000000000E+00	0.000000000E+00

NODE	LABEL	DISP	CDISP
427	UY	0.000000000E+00	0.000000000E+00
428	UY	0.000000000E+00	0.000000000E+00
429	UY	0.000000000E+00	0.000000000E+00
430	UY	0.000000000E+00	0.000000000E+00
2	ROTX	0.000000000E+00	0.000000000E+00
3	ROTX	0.000000000E+00	0.000000000E+00
4	ROTX	0.000000000E+00	0.000000000E+00
5	ROTX	0.000000000E+00	0.000000000E+00
6	ROTX	0.000000000E+00	0.000000000E+00
7	ROTX	0.000000000E+00	0.000000000E+00
8	ROTX	0.000000000E+00	0.000000000E+00
9	ROTX	0.000000000E+00	0.000000000E+00
10	ROTX	0.000000000E+00	0.000000000E+00
11	ROTX	0.000000000E+00	0.000000000E+00
12	ROTX	0.000000000E+00	0.000000000E+00
13	ROTX	0.000000000E+00	0.000000000E+00
14	ROTX	0.000000000E+00	0.000000000E+00
15	ROTX	0.000000000E+00	0.000000000E+00
16	ROTX	0.000000000E+00	0.000000000E+00
17	ROTX	0.000000000E+00	0.000000000E+00

NODE	LABEL	DISP	CDISP
18	ROTX	0.000000000E+00	0.000000000E+00
19	ROTX	0.000000000E+00	0.000000000E+00
20	ROTX	0.000000000E+00	0.000000000E+00
21	ROTX	0.000000000E+00	0.000000000E+00
22	ROTX	0.000000000E+00	0.000000000E+00
23	ROTX	0.000000000E+00	0.000000000E+00
24	ROTX	0.000000000E+00	0.000000000E+00
25	ROTX	0.000000000E+00	0.000000000E+00
26	ROTX	0.000000000E+00	0.000000000E+00
27	ROTX	0.000000000E+00	0.000000000E+00
28	ROTX	0.000000000E+00	0.000000000E+00
29	ROTX	0.000000000E+00	0.000000000E+00
30	ROTX	0.000000000E+00	0.000000000E+00
31	ROTX	0.000000000E+00	0.000000000E+00
32	ROTX	0.000000000E+00	0.000000000E+00
402	ROTX	0.000000000E+00	0.000000000E+00
403	ROTX	0.000000000E+00	0.000000000E+00
404	ROTX	0.000000000E+00	0.000000000E+00
405	ROTX	0.000000000E+00	0.000000000E+00
406	ROTX	0.000000000E+00	0.000000000E+00

NODE	LABEL	DISP	CDISP
407	ROTX	0.000000000E+00	0.000000000E+00
408	ROTX	0.000000000E+00	0.000000000E+00
409	ROTX	0.000000000E+00	0.000000000E+00
410	ROTX	0.000000000E+00	0.000000000E+00
411	ROTX	0.000000000E+00	0.000000000E+00
412	ROTX	0.000000000E+00	0.000000000E+00
413	ROTX	0.000000000E+00	0.000000000E+00
414	ROTX	0.000000000E+00	0.000000000E+00
415	ROTX	0.000000000E+00	0.000000000E+00
416	ROTX	0.000000000E+00	0.000000000E+00
417	ROTX	0.000000000E+00	0.000000000E+00
418	ROTX	0.000000000E+00	0.000000000E+00
419	ROTX	0.000000000E+00	0.000000000E+00
420	ROTX	0.000000000E+00	0.000000000E+00
421	ROTX	0.000000000E+00	0.000000000E+00
422	ROTX	0.000000000E+00	0.000000000E+00

423	ROTX	0.000000000E+00	0.000000000E+00
424	ROTX	0.000000000E+00	0.000000000E+00
425	ROTX	0.000000000E+00	0.000000000E+00
426	ROTX	0.000000000E+00	0.000000000E+00

NODE	LABEL	DISP	CDISP
427	ROTX	0.000000000E+00	0.000000000E+00
428	ROTX	0.000000000E+00	0.000000000E+00
429	ROTX	0.000000000E+00	0.000000000E+00
430	ROTX	0.000000000E+00	0.000000000E+00
2	ROTZ	0.000000000E+00	0.000000000E+00
3	ROTZ	0.000000000E+00	0.000000000E+00
4	ROTZ	0.000000000E+00	0.000000000E+00
5	ROTZ	0.000000000E+00	0.000000000E+00
6	ROTZ	0.000000000E+00	0.000000000E+00
7	ROTZ	0.000000000E+00	0.000000000E+00
8	ROTZ	0.000000000E+00	0.000000000E+00
9	ROTZ	0.000000000E+00	0.000000000E+00
10	ROTZ	0.000000000E+00	0.000000000E+00
11	ROTZ	0.000000000E+00	0.000000000E+00
12	ROTZ	0.000000000E+00	0.000000000E+00
13	ROTZ	0.000000000E+00	0.000000000E+00
14	ROTZ	0.000000000E+00	0.000000000E+00
15	ROTZ	0.000000000E+00	0.000000000E+00
16	ROTZ	0.000000000E+00	0.000000000E+00
17	ROTZ	0.000000000E+00	0.000000000E+00

NODE	LABEL	DISP	CDISP
18	ROTZ	0.000000000E+00	0.000000000E+00
19	ROTZ	0.000000000E+00	0.000000000E+00
20	ROTZ	0.000000000E+00	0.000000000E+00
21	ROTZ	0.000000000E+00	0.000000000E+00
22	ROTZ	0.000000000E+00	0.000000000E+00
23	ROTZ	0.000000000E+00	0.000000000E+00
24	ROTZ	0.000000000E+00	0.000000000E+00
25	ROTZ	0.000000000E+00	0.000000000E+00
26	ROTZ	0.000000000E+00	0.000000000E+00
27	ROTZ	0.000000000E+00	0.000000000E+00
28	ROTZ	0.000000000E+00	0.000000000E+00
29	ROTZ	0.000000000E+00	0.000000000E+00
30	ROTZ	0.000000000E+00	0.000000000E+00
31	ROTZ	0.000000000E+00	0.000000000E+00
32	ROTZ	0.000000000E+00	0.000000000E+00
402	ROTZ	0.000000000E+00	0.000000000E+00
403	ROTZ	0.000000000E+00	0.000000000E+00
404	ROTZ	0.000000000E+00	0.000000000E+00
405	ROTZ	0.000000000E+00	0.000000000E+00
406	ROTZ	0.000000000E+00	0.000000000E+00

NODE	LABEL	DISP	CDISP
407	ROTZ	0.000000000E+00	0.000000000E+00
408	ROTZ	0.000000000E+00	0.000000000E+00
409	ROTZ	0.000000000E+00	0.000000000E+00
410	ROTZ	0.000000000E+00	0.000000000E+00
411	ROTZ	0.000000000E+00	0.000000000E+00
412	ROTZ	0.000000000E+00	0.000000000E+00
413	ROTZ	0.000000000E+00	0.000000000E+00
414	ROTZ	0.000000000E+00	0.000000000E+00
415	ROTZ	0.000000000E+00	0.000000000E+00
416	ROTZ	0.000000000E+00	0.000000000E+00
417	ROTZ	0.000000000E+00	0.000000000E+00
418	ROTZ	0.000000000E+00	0.000000000E+00
419	ROTZ	0.000000000E+00	0.000000000E+00
420	ROTZ	0.000000000E+00	0.000000000E+00
421	ROTZ	0.000000000E+00	0.000000000E+00
422	ROTZ	0.000000000E+00	0.000000000E+00
423	ROTZ	0.000000000E+00	0.000000000E+00
424	ROTZ	0.000000000E+00	0.000000000E+00
425	ROTZ	0.000000000E+00	0.000000000E+00
426	ROTZ	0.000000000E+00	0.000000000E+00

NODE	LABEL	DISP	CDISP
427	ROTZ	0.000000000E+00	0.000000000E+00
428	ROTZ	0.000000000E+00	0.000000000E+00
429	ROTZ	0.000000000E+00	0.000000000E+00
430	ROTZ	0.000000000E+00	0.000000000E+00

```
   431 ROTZ  0.000000000E+00 0.000000000E+00
   432 ROTZ  0.000000000E+00 0.000000000E+00
 LIST FORCES FOR ALL SELECTED NODES

  NODE  LABEL      FORCE          CFORCE
   489 FY      0.866000000    0.000000000E+00
   489 FX     -0.500000000    0.000000000E+00
```

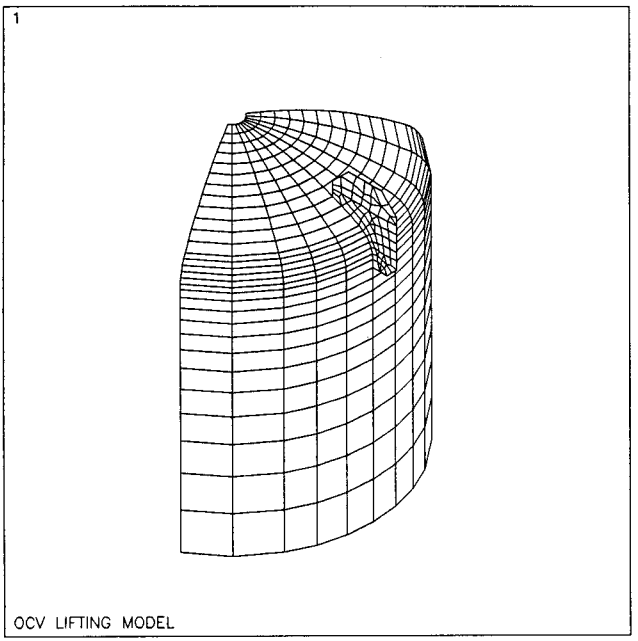


FIGURE 2.10.3-1.

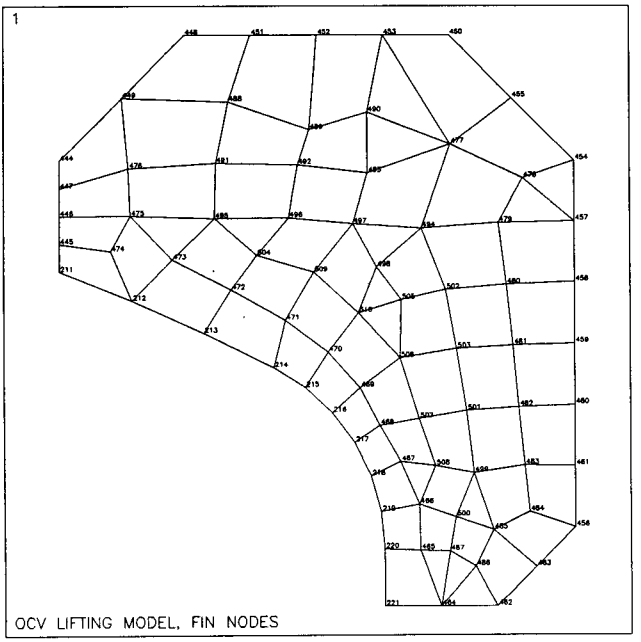


FIGURE 2.10.3-2.

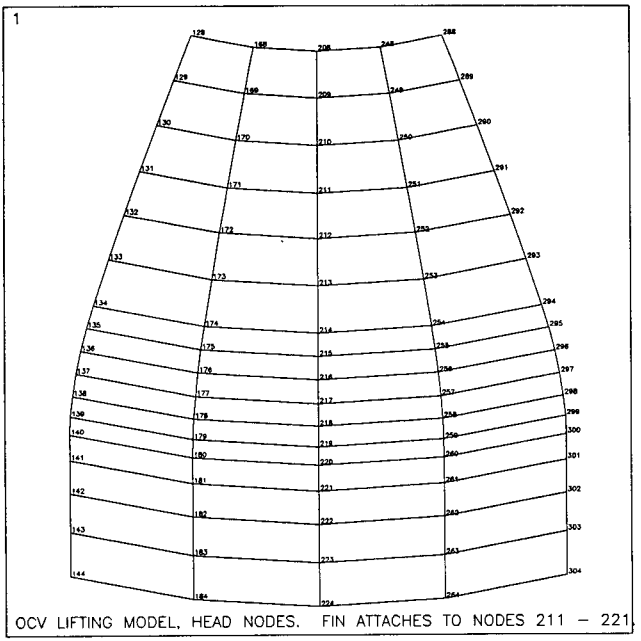


FIGURE 2.10.3-3.

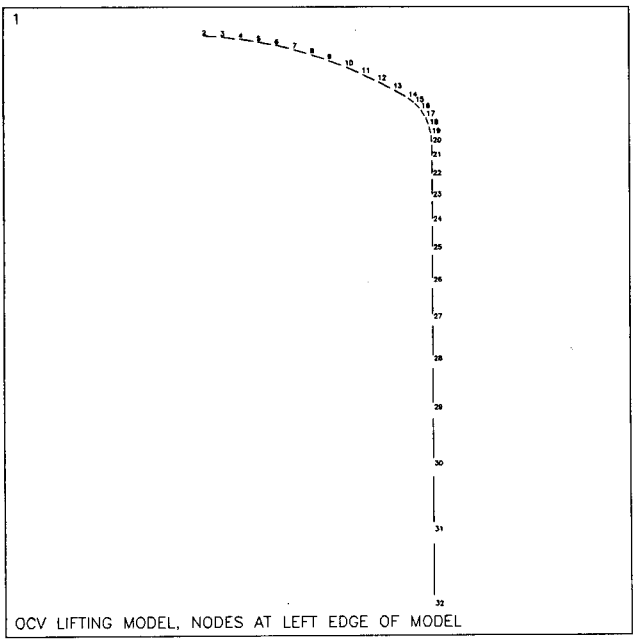


FIGURE 2.10.3-4.

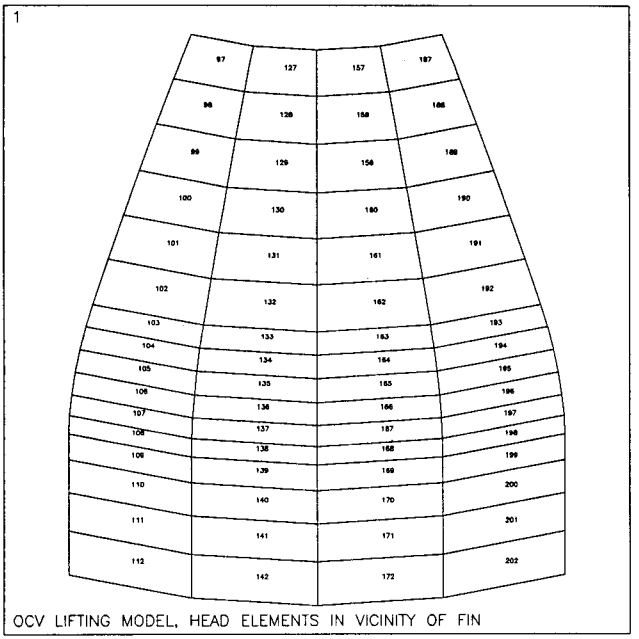


FIGURE 2.10.3-5.

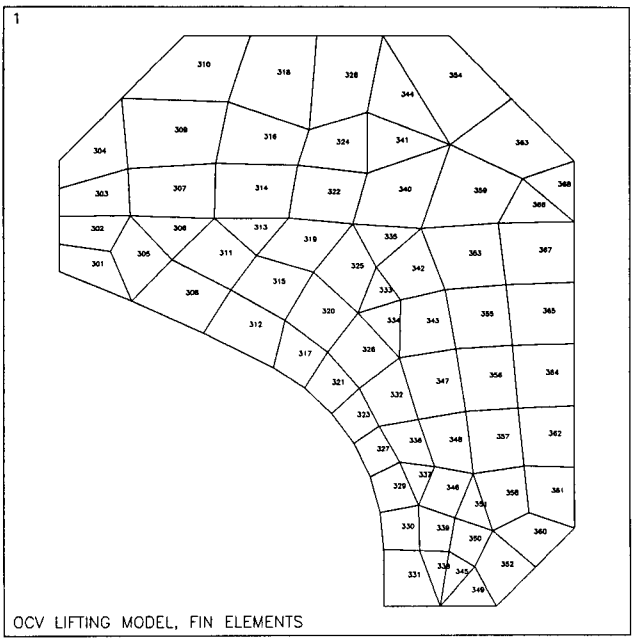


FIGURE 2.10.3-6.

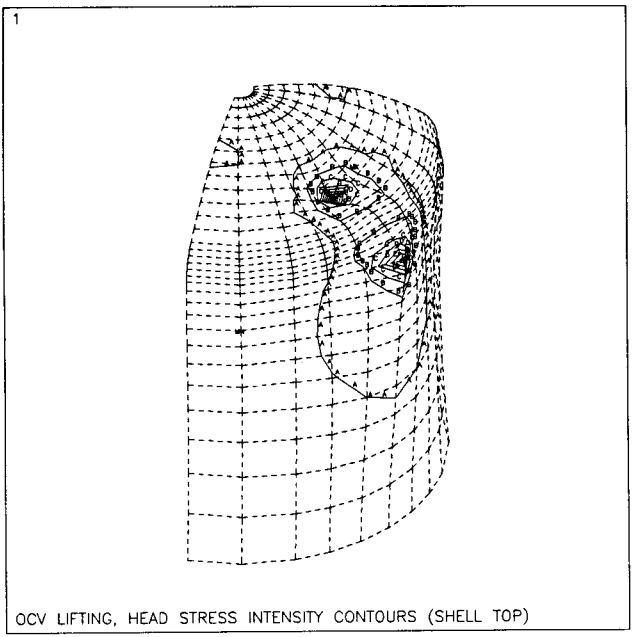


FIGURE 2.10.3-7.

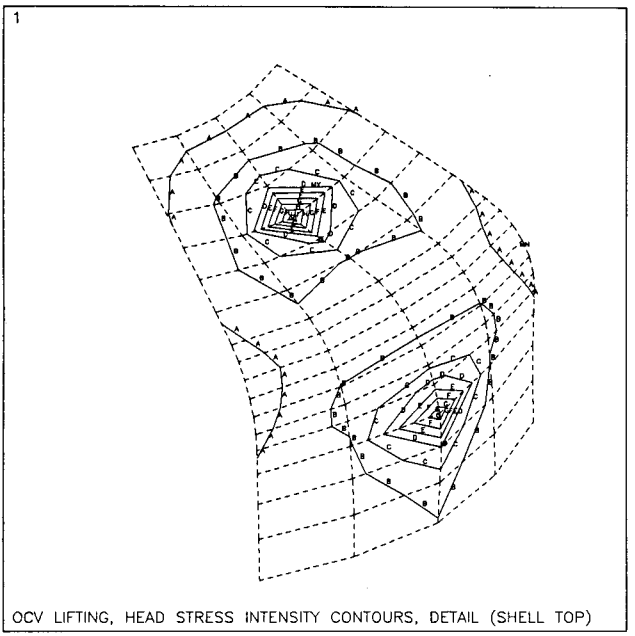


FIGURE 2.10.3-8.

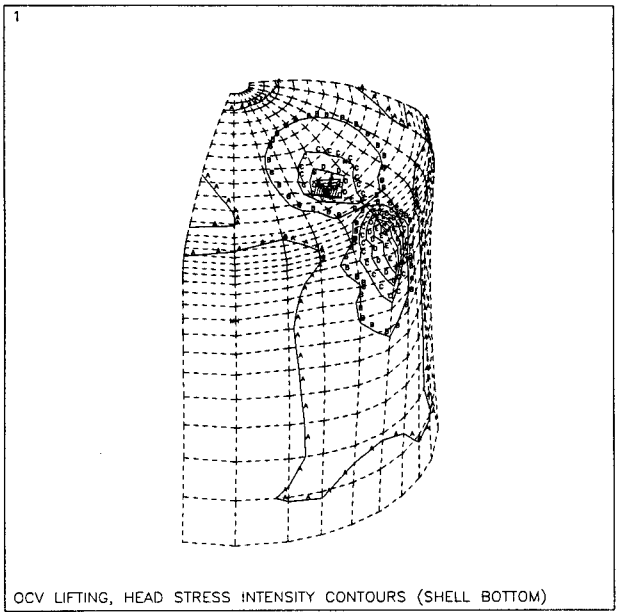


FIGURE 2.10.3-9.

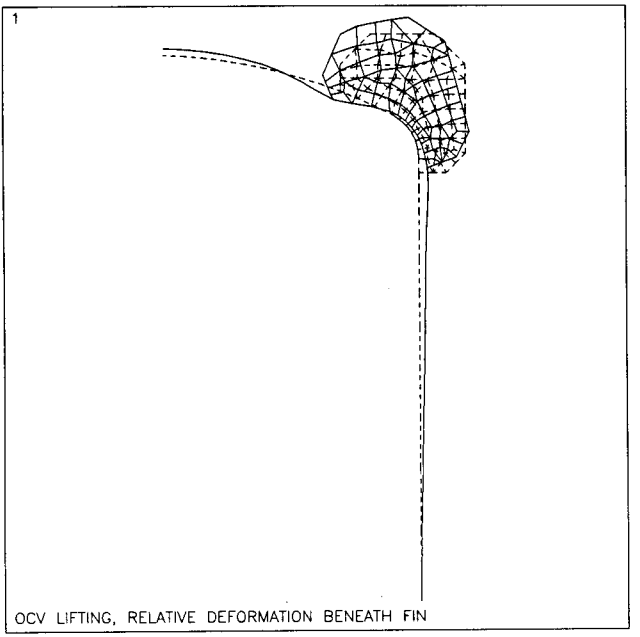


FIGURE 2.10.3-10.

2.10.4 Fin-to-OCV Head Weld Properties ANSYS Model

2.10.4.1 Description

This 3-D model of the fin-to-OCV head weld is used only to determine the centroid and moment of inertia of the weld for use in weld stress calculations. It is modeled as a strip of 24 elements along the contour of the OCV head. Centroidal locations of the centers of each element relative to the global origin and length of each element were used in a spreadsheet to arrive at the overall centroid and length of the weld. The spreadsheet also calculated other parameters necessary to the calculation of maximum weld stress: the distances from the weld centroid to the extreme ends of the weld, the moment arm from the line of action of the lifting force to the weld centroid, and the angles to the horizontal of the maximum weld stresses. These parameters are summarized in Table 2.5.1.2.2-1 and illustrated in Figure 2.5.1.2.2-1.

2.10.4.2 Construction. Two rows of 25 nodes were used to model the fin-to-OCV head weld from bottom to top, with each row separated by a nominal distance to form quadrilateral elements. The finite element output consisted of element centroidal locations and element area. The element length along the weld was found by dividing the element area by width. A plot of node locations is given in Figure 2.10.4-1.

2.10.4.3 Material Properties. Not used.

2.10.4.4 Constraints. All nodes completely constrained.

2.10.4.5 Applied Loads. None.

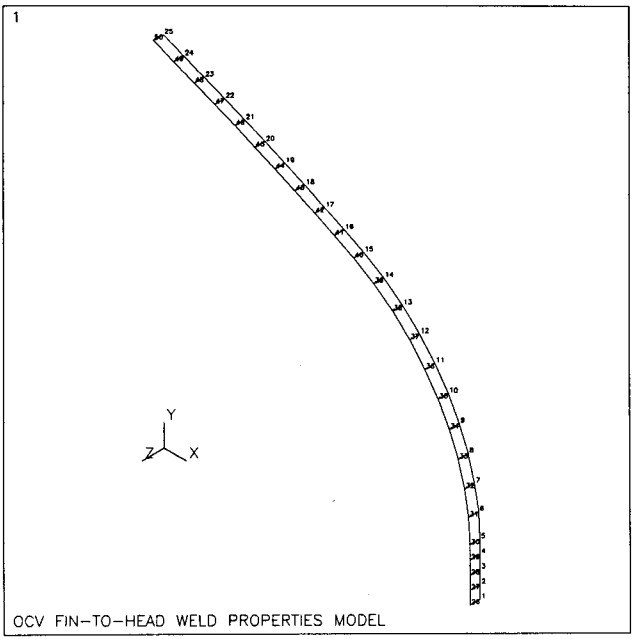


FIGURE 2.10.4-1.

2.10.5 OCV Head ANSYS Model for Tiedown Analysis

2.10.5.1 Description. The OCV head tiedown model is a 3-D model of a one-quarter symmetry segment of the upper portion of the OCV used to evaluate tiedown stresses in the OCV head. The extent of the model is 90° with a 3-in.-wide, 0.25-in.-thick doubler plate extending from the center of the head, over the knuckle radius, and to the top of the water jacket. The lower edge of the model ends in the wall a short distance above the OCV flange, because flange details are irrelevant to this analysis. The water jacket and fins are also not modeled, as they have little effect on tiedown induced head stress. The model layout is shown in Figure 2.10.5-1.

2.10.5.2 Construction. The model is constructed of quadrilateral shell elements of two thicknesses: 0.5 in. for the OCV wall and 0.75 in. (equal to the sum of the head and doubler thicknesses) in the area of the doubler strip. The doubler strip is bounded by nodes 489, 264, 361 (at the top center), 276, and 502. A model node plot is given in Figure 2.10.5-2 and an element plot in Figure 2.10.5-3. An interpreted ANSYS input listing is given in Table 2.10.5-1.

2.10.5.3 Material Properties. A modulus of elasticity of $27.18(10)^6$ psi was used, corresponding to 270 °F, which represents overall head temperature. Poisson's ratio was 0.3.

2.10.5.4 Constraints. Nodes along the cut edges were constrained in the one linear and two rotational degrees of freedom required to ensure symmetry of the model. The node at the exact top center of the OCV head was restrained to have no radial displacement. The nodes along the bottom were fixed in all six degrees of freedom, as appropriate to the tiedown case. This edge was far enough away from the area of interest (the knuckle) that constraint details were relatively unimportant.

2.10.5.5 Applied Loading. Pressure loading was applied to the top surface of the doubler plate to simulate the load from the tiedown strap. As discussed in Section 2.5.2.2, two pressures were used to model the tiedown strap loads. Besides tiedown strap tension, the magnitude of pressure also depended on the radius of the body beneath the strap. Therefore, one value of pressure (319.6 psi) was applied from the OCV head center down to the top of the knuckle (edge defined by nodes 265, 273, 274, and 275), and the second value of pressure (3,111 psi) was applied in the knuckle region down to the point where the strap leaves the OCV surface (defined by nodes 201, 202, 203, and 196). Pressure internal to the OCV was conservatively ignored. Nodal temperatures were not used.

2.10.5.6 Results. Stress intensity because of applied strap loads are shown in Figures 2.10.5-4 through 2.10.5-6.

TABLE 2.10.5-1. Interpreted ANSYS Input Listing.

```
STATIC ANALYSIS (KAN= 0)

LINEAR ANALYSIS - NO NON-LINEAR PROPERTIES

REFERENCE TEMPERATURE=      0.000 (TREF)
UNIFORM TEMPERATURE  =      0.000 (TUNIF)

*****ANALYSIS OPTIONS (KAY VALUES) (IF ANY) *****

NO STATIC INTERPOLATION/EXTRAPOLATION (KAY(3)=0)

SMALL DEFLECTION SOLUTION (KAY(6)=0)

NO STRESS STIFFENING (KAY(8)=0)

USE LINEAR SOLUTION PROCEDURE  (KAY(9)=0)

IN-CORE WAVE-FRONT EQUATION SOLVER (KAY(10)=0)

LIST ELEMENT TYPES FROM  1 TO 20 BY 1

NO. STIF          KEYOPT VALUES          INOPR
 1   63    0  0  0   0  0  0   0  0  0   0  QUAD. FLAT SHELL

LIST ALL REAL SETS

 REAL CONSTANT SET   1  ITEMS   1 TO  18
  0.50000       0.00000E+00  0.00000E+00  0.00000E+00  0.00000E+00  0.00000E+00
  0.00000E+00   0.00000E+00  0.00000E+00  0.00000E+00  0.00000E+00  0.00000E+00
  0.00000E+00   0.00000E+00  0.00000E+00  0.00000E+00  0.00000E+00  0.00000E+00

 REAL CONSTANT SET   2  ITEMS   1 TO  18
  0.25000       0.00000E+00  0.00000E+00  0.00000E+00  0.00000E+00  0.00000E+00
  0.00000E+00   0.00000E+00  0.00000E+00  0.00000E+00  0.00000E+00  0.00000E+00
  0.00000E+00   0.00000E+00  0.00000E+00  0.00000E+00  0.00000E+00  0.00000E+00

 REAL CONSTANT SET   3  ITEMS   1 TO  18
  0.75000       0.00000E+00  0.00000E+00  0.00000E+00  0.00000E+00  0.00000E+00
  0.00000E+00   0.00000E+00  0.00000E+00  0.00000E+00  0.00000E+00  0.00000E+00
  0.00000E+00   0.00000E+00  0.00000E+00  0.00000E+00  0.00000E+00  0.00000E+00
LIST ALL COORDINATE SYSTEMS

    SYSTEM TYPE                    CENTER              PARAMETERS    SING KEYS
 0  0 (CARTESIAN)          0.000     0.000     0.000     0.000  0.000   0  0
 1  1 (CYLINDRICAL)        0.000     0.000     0.000     1.000  0.000   0  0
 2  2 (SPHERICAL)          0.000     0.000     0.000     1.000  1.000   0  0
11  1 (CYLINDRICAL)        0.000     0.000     0.000     1.000  1.000   0  0
12  1 (CYLINDRICAL)       14.910    29.270     0.000     1.000  1.000   0  0
13  3 (TOROIDAL)           0.000    29.150     0.000    14.940  1.000   0  0
14  3 (TOROIDAL)           0.000    29.270     0.000    14.910  1.000   0  0

SYSTEM              ORIENTATION VECTORS (X,Y,Z)
    0     1.00  0.00  0.00    0.00  1.00  0.00    0.00  0.00  1.00
    1     1.00  0.00  0.00    0.00  1.00  0.00    0.00  0.00  1.00
    2     1.00  0.00  0.00    0.00  1.00  0.00    0.00  0.00  1.00
   11     1.00  0.00  0.00    0.00  0.00 -1.00    0.00  1.00  0.00
   12     1.00  0.00  0.00    0.00  1.00  0.00    0.00  0.00  1.00
   13     1.00  0.00  0.00    0.00  0.00 -1.00    0.00  1.00  0.00
   14     1.00  0.00  0.00    0.00  0.00 -1.00    0.00  1.00  0.00
CSYS TYPE     XC              YC              ZC            THXY      THYZ      THXZ
 11    1 0.00000E+00 0.00000E+00 0.00000E+00    0.000     0.000   -90.000
 12    1  14.910       29.270      0.00000E+00    0.000     0.000     0.000
 13    3 0.00000E+00  29.150      0.00000E+00    0.000     0.000   -90.000
 14    3 0.00000E+00  29.270      0.00000E+00    0.000     0.000   -90.000

LIST   ALL   SELECTED KEYPOINTS.   DSYS=   0

   PT.              X,Y,Z LOCATION                    NODE  ELEM  ESIZE
    5    18.1900       29.2700      0.000000E+00       515     0
LIST ALL SELECTED LINE SEGMENTS.
```

SEG.NO.	KEYPT	DIRECTION			DIV	SPACING	NODES/ELEM	
23	28	0.9983	-0.0587	0.0000	3	1.0000	362	363
	2	-1.0000	0.0000	0.0000			0	0
27	2	0.0000	0.0000	1.0000	3	1.0000	364	365
	19	0.0000	-0.0587	-0.9983			0	0
48	31	-0.7065	0.0418	0.7064	8	1.0000	266	272
	32	0.6309	-0.4516	-0.6309			0	0
49	32	0.6398	0.0000	0.7685	3	1.0000	274	275
	36	-0.7685	0.0000	-0.6398			0	0
50	37	-0.7064	0.0418	0.7065	8	1.0000	277	283
	36	0.6309	-0.4516	-0.6309			0	0
51	31	0.0004	0.0294	0.9996	3	1.0000	284	285
	37	-0.9996	0.0294	-0.0004			0	0
52	31	0.9983	-0.0587	0.0000	3	1.0000	362	363
	38	-1.0000	0.0000	0.0000			0	0
53	38	0.0000	0.0000	1.0000	3	1.0000	364	365
	37	0.0000	-0.0587	-0.9983			0	0
54	32	-0.6316	0.4499	0.6315	3	1.0000	369	370
	39	0.2972	-0.9074	-0.2971			0	0
55	39	0.6457	0.0000	0.7636	3	1.0000	202	203
	40	-0.7636	0.0000	-0.6457			0	0

SEG.NO.	KEYPT	DIRECTION			DIV	SPACING	NODES/ELEM	
56	36	-0.6315	0.4499	0.6316	3	1.0000	371	372
	40	0.2971	-0.9074	-0.2972			0	0
57	41	-0.7065	0.0418	0.7064	8	1.0000	266	272
	42	0.6309	-0.4516	-0.6309			0	0
58	42	0.6398	0.0000	0.7685	3	1.0000	274	275
	43	-0.7685	0.0000	-0.6398			0	0
59	44	-0.7064	0.0418	0.7065	8	1.0000	277	283
	43	0.6309	-0.4516	-0.6309			0	0
60	41	0.0004	0.0294	0.9996	3	1.0000	284	285
	44	-0.9996	0.0294	-0.0004			0	0
61	41	0.9983	-0.0587	0.0000	3	1.0000	362	363
	45	-1.0000	0.0000	0.0000			0	0
62	45	0.0000	0.0000	1.0000	3	1.0000	364	365
	44	0.0000	-0.0587	-0.9983			0	0
63	42	-0.6316	0.4499	0.6315	3	1.0000	369	370
	46	0.2972	-0.9074	-0.2971			0	0
64	46	0.6457	0.0000	0.7636	3	1.0000	202	203
	47	-0.7636	0.0000	-0.6457			0	0
65	43	-0.6315	0.4499	0.6316	3	1.0000	371	372
	47	0.2971	-0.9074	-0.2972			0	0

SEG.NO.	KEYPT	DIRECTION			DIV	SPACING	NODES/ELEM	
66	48	-0.0115	-0.9998	-0.0136	2	1.0000	521	521
	49	-0.3078	0.9084	0.2830			0	0
67	50	-0.7630	0.0000	-0.6464	3	1.0000	503	504
	48	0.6464	0.0000	0.7630			0	0
68	50	0.0136	-0.9998	0.0115	2	1.0000	526	526
	51	-0.2830	0.9084	0.3078			0	0
69	49	0.6457	0.0000	0.7636	3	1.0000	202	203
	51	-0.7636	0.0000	-0.6457			0	0

LIST NO.	ALL KEYPOINTS/LINE SEG.				NODES		ELEMENTS		MAT	REL	TYP	ESYS
1	17	34	35	27	505	514	472	489	1	1	1	0
	38	39	40	43								
2	4	5	17	33	522	525	490	499	1	1	1	0
	3	44	45	36								
3	33	17	27	26	527	528	500	505	1	1	1	0
	45	43	46	35								
4	26	27	9	8	535	538	506	515	1	1	1	0
	46	47	11	37								
5	11	12	13	14	0	0	0	0	0	0	0	0
	13	14	15	16								
6	21	22	23	24	0	0	0	0	0	0	0	0
	17	18	19	20								
7	28	29	20	19	286	299	228	251	1	1	1	0
	21	31	26	32								
8	3	28	29	29	310	328	252	282	1	1	1	0
	24	21	0	25								
9	7	20	19	19	341	360	283	314	1	1	1	0
	29	26	0	30								

10	2	2	28	19	366	368	315	321	1	1	1	0
	0	23	32	27								

NO.	KEYPOINTS/LINE SEG.				NODES		ELEMENTS		MAT	REL	TYP	ESYS
11	29	33	26	20	373	376	322	330	1	1	1	0
	33	35	34	31								
12	3	4	33	29	379	386	331	345	1	1	1	0
	2	36	33	25								
13	20	26	8	7	389	396	346	360	1	1	1	0
	34	37	10	29								
14	-	-	-	-	558	655	516	648	1	1	1	0
	4	8	12	47								
	40	39	38	44								

LIST ALL SELECTED ELEMENTS. (LIST NODES)

ELEM	MAT	TYP	REL	ESYS	NODES			
228	1	1	3	0	286	284	264	266
229	1	1	3	0	287	286	266	267
230	1	1	3	0	288	287	267	268
231	1	1	3	0	289	288	268	269
232	1	1	3	0	290	289	269	270
233	1	1	3	0	291	290	270	271
234	1	1	3	0	292	291	271	272
235	1	1	3	0	274	292	272	265
236	1	1	3	0	293	285	284	286
237	1	1	3	0	294	293	286	287
238	1	1	3	0	295	294	287	288
239	1	1	3	0	296	295	288	289
240	1	1	3	0	297	296	289	290
241	1	1	3	0	298	297	290	291
242	1	1	3	0	299	298	291	292
243	1	1	3	0	275	299	292	274
244	1	1	3	0	277	276	285	293
245	1	1	3	0	278	277	293	294
246	1	1	3	0	279	278	294	295
247	1	1	3	0	280	279	295	296

ELEM	MAT	TYP	REL	ESYS	NODES			
248	1	1	3	0	281	280	296	297
249	1	1	3	0	282	281	297	298
250	1	1	3	0	283	282	298	299
251	1	1	3	0	273	283	299	275
252	1	1	1	0	305	264	266	266
253	1	1	1	0	302	303	312	311
254	1	1	1	0	303	304	313	312
255	1	1	1	0	301	302	311	310
256	1	1	1	0	300	301	310	309
257	1	1	1	0	304	305	314	313
258	1	1	1	0	305	266	267	314
259	1	1	1	0	326	312	313	313
260	1	1	1	0	312	326	323	311
261	1	1	1	0	314	267	328	313
262	1	1	1	0	313	328	325	326
263	1	1	1	0	323	320	311	311
264	1	1	1	0	311	320	317	310
265	1	1	1	0	310	317	308	309
266	1	1	1	0	267	327	328	328
267	1	1	1	0	326	325	322	323

ELEM	MAT	TYP	REL	ESYS	NODES			
268	1	1	1	0	327	325	328	328
269	1	1	1	0	267	268	327	327
270	1	1	1	0	323	322	319	320
271	1	1	1	0	327	324	325	325
272	1	1	1	0	320	319	316	317
273	1	1	1	0	325	324	321	322
274	1	1	1	0	327	268	269	324
275	1	1	1	0	317	316	307	308
276	1	1	1	0	322	321	318	319
277	1	1	1	0	324	269	270	321
278	1	1	1	0	319	318	315	316

279	1	1	1	0	321	270	271	318
280	1	1	1	0	316	315	306	307
281	1	1	1	0	318	271	272	315
282	1	1	1	0	315	272	265	306
283	1	1	1	0	331	332	343	342
284	1	1	1	0	332	333	344	343
285	1	1	1	0	331	342	341	330
286	1	1	1	0	333	273	283	344
287	1	1	1	0	330	341	340	329

ELEM	MAT	TYP	REL	ESYS	NODES			
288	1	1	1	0	342	343	352	351
289	1	1	1	0	343	344	345	352
290	1	1	1	0	342	351	350	341
291	1	1	1	0	344	283	282	345
292	1	1	1	0	341	350	339	340
293	1	1	1	0	351	352	355	354
294	1	1	1	0	352	345	346	355
295	1	1	1	0	351	354	353	350
296	1	1	1	0	345	282	281	346
297	1	1	1	0	350	353	338	339
298	1	1	1	0	355	359	357	354
299	1	1	1	0	355	346	347	359
300	1	1	1	0	354	357	356	353
301	1	1	1	0	346	281	280	347
302	1	1	1	0	353	356	337	338
303	1	1	1	0	357	359	360	360
304	1	1	1	0	356	357	360	360
305	1	1	1	0	359	347	348	360
306	1	1	1	0	358	356	360	360
307	1	1	1	0	347	280	279	348

ELEM	MAT	TYP	REL	ESYS	NODES			
308	1	1	1	0	356	358	336	337
309	1	1	1	0	360	348	349	358
310	1	1	1	0	348	279	278	349
311	1	1	1	0	358	349	335	336
312	1	1	1	0	334	335	349	349
313	1	1	1	0	349	278	277	334
314	1	1	1	0	277	276	334	334
315	1	1	3	0	361	363	366	364
316	1	1	3	0	364	366	368	365
317	1	1	3	0	363	362	367	366
318	1	1	3	0	368	366	367	367
319	1	1	3	0	365	368	285	276
320	1	1	3	0	362	264	284	367
321	1	1	3	0	368	367	284	285
322	1	1	3	0	373	274	265	369
323	1	1	3	0	374	373	369	370
324	1	1	3	0	202	374	370	201
325	1	1	3	0	375	275	274	373
326	1	1	3	0	376	375	373	374
327	1	1	3	0	203	376	374	202

ELEM	MAT	TYP	REL	ESYS	NODES			
328	1	1	3	0	371	273	275	375
329	1	1	3	0	372	371	375	376
330	1	1	3	0	196	372	376	203
331	1	1	1	0	379	309	300	377
332	1	1	1	0	380	379	377	378
333	1	1	1	0	204	380	378	182
334	1	1	1	0	381	308	309	379
335	1	1	1	0	382	381	379	380
336	1	1	1	0	205	382	380	204
337	1	1	1	0	383	307	308	381
338	1	1	1	0	384	383	381	382
339	1	1	1	0	206	384	382	205
340	1	1	1	0	385	306	307	383
341	1	1	1	0	386	385	383	384
342	1	1	1	0	207	386	384	206
343	1	1	1	0	369	265	306	385

344	1	1	1	0	370	369	385	386
345	1	1	1	0	201	370	386	207
346	1	1	1	0	389	333	273	371
347	1	1	1	0	390	389	371	372

ELEM	MAT	TYP	REL	ESYS	NODES			
348	1	1	1	0	197	390	372	196
349	1	1	1	0	391	332	333	389
350	1	1	1	0	392	391	389	390
351	1	1	1	0	198	392	390	197
352	1	1	1	0	393	331	332	391
353	1	1	1	0	394	393	391	392
354	1	1	1	0	199	394	392	198
355	1	1	1	0	395	330	331	393
356	1	1	1	0	396	395	393	394
357	1	1	1	0	200	396	394	199
358	1	1	1	0	387	329	330	395
359	1	1	1	0	388	387	395	396
360	1	1	1	0	194	388	396	200
472	1	1	3	0	505	504	487	489
473	1	1	1	0	506	505	489	490
474	1	1	1	0	507	506	490	491
475	1	1	1	0	508	507	491	492
476	1	1	1	0	509	508	492	493
477	1	1	1	0	495	509	493	488
478	1	1	3	0	510	503	504	505

ELEM	MAT	TYP	REL	ESYS	NODES			
479	1	1	1	0	511	510	505	506
480	1	1	1	0	512	511	506	507
481	1	1	1	0	513	512	507	508
482	1	1	1	0	514	513	508	509
483	1	1	1	0	496	514	509	495
484	1	1	3	0	502	497	503	510
485	1	1	1	0	501	502	510	511
486	1	1	1	0	500	501	511	512
487	1	1	1	0	499	500	512	513
488	1	1	1	0	498	499	513	514
489	1	1	1	0	494	498	514	496
490	1	1	1	0	522	204	182	516
491	1	1	1	0	517	522	516	515
492	1	1	1	0	523	205	204	522
493	1	1	1	0	518	523	522	517
494	1	1	1	0	524	206	205	523
495	1	1	1	0	519	524	523	518
496	1	1	1	0	525	207	206	524
497	1	1	1	0	520	525	524	519
498	1	1	1	0	521	201	207	525

ELEM	MAT	TYP	REL	ESYS	NODES			
499	1	1	1	0	487	521	525	520
500	1	1	3	0	527	202	201	521
501	1	1	3	0	504	527	521	487
502	1	1	3	0	528	203	202	527
503	1	1	3	0	503	528	527	504
504	1	1	3	0	526	196	203	528
505	1	1	3	0	497	526	528	503
506	1	1	1	0	535	197	196	526
507	1	1	1	0	530	535	526	497
508	1	1	1	0	536	198	197	535
509	1	1	1	0	531	536	535	530
510	1	1	1	0	537	199	198	536
511	1	1	1	0	532	537	536	531
512	1	1	1	0	538	200	199	537
513	1	1	1	0	533	538	537	532
514	1	1	1	0	534	194	200	538
515	1	1	1	0	529	534	538	533
516	1	1	1	0	550	551	582	581
517	1	1	1	0	549	550	581	580
518	1	1	1	0	551	552	563	582

ELEM	MAT	TYP	REL	ESYS	NODES			
519	1	1	1	0	548	549	580	579
520	1	1	1	0	547	548	579	578
521	1	1	1	0	546	547	578	562
522	1	1	1	0	552	545	557	563
523	1	1	1	0	539	546	562	544
524	1	1	1	0	579	580	643	643
525	1	1	1	0	581	582	638	640
526	1	1	1	0	581	640	641	580
527	1	1	1	0	582	563	637	638
528	1	1	1	0	580	642	643	643
529	1	1	1	0	580	641	642	642
530	1	1	1	0	578	579	634	633
531	1	1	1	0	579	643	644	644
532	1	1	1	0	578	633	604	562
533	1	1	1	0	579	644	645	634
534	1	1	1	0	563	564	637	637
535	1	1	1	0	627	641	640	640
536	1	1	1	0	563	557	556	564
537	1	1	1	0	625	640	638	638
538	1	1	1	0	643	642	630	631

ELEM	MAT	TYP	REL	ESYS	NODES			
539	1	1	1	0	643	631	632	644
540	1	1	1	0	544	562	561	543
541	1	1	1	0	642	641	629	630
542	1	1	1	0	637	639	638	638
543	1	1	1	0	626	627	640	640
544	1	1	1	0	627	628	641	641
545	1	1	1	0	625	626	640	640
546	1	1	1	0	628	629	641	641
547	1	1	1	0	644	632	622	645
548	1	1	1	0	624	625	638	638
549	1	1	1	0	634	636	635	633
550	1	1	1	0	634	645	646	636
551	1	1	1	0	638	639	608	624
552	1	1	1	0	637	564	607	639
553	1	1	1	0	622	646	645	645
554	1	1	1	0	631	630	618	619
555	1	1	1	0	627	615	616	628
556	1	1	1	0	627	626	614	615
557	1	1	1	0	630	629	617	618
558	1	1	1	0	631	619	620	632

ELEM	MAT	TYP	REL	ESYS	NODES			
559	1	1	1	0	629	628	616	617
560	1	1	1	0	562	604	603	561
561	1	1	1	0	626	625	613	614
562	1	1	1	0	632	620	621	622
563	1	1	1	0	633	635	623	604
564	1	1	1	0	639	607	608	608
565	1	1	1	0	625	624	612	613
566	1	1	1	0	636	646	647	647
567	1	1	1	0	622	621	594	646
568	1	1	1	0	636	647	653	635
569	1	1	1	0	616	615	601	573
570	1	1	1	0	624	608	606	612
571	1	1	1	0	616	573	494	617
572	1	1	1	0	615	614	611	601
573	1	1	1	0	618	617	494	496
574	1	1	1	0	619	618	496	495
575	1	1	1	0	619	495	488	620
576	1	1	1	0	646	594	592	647
577	1	1	1	0	620	488	593	621
578	1	1	1	0	621	593	594	594

ELEM	MAT	TYP	REL	ESYS	NODES			
579	1	1	1	0	614	613	610	611
580	1	1	1	0	608	607	605	606
581	1	1	1	0	635	653	652	623

582	1	1	1	0	564	565	605	607
583	1	1	1	0	564	556	555	565
584	1	1	1	0	594	593	591	592
585	1	1	1	0	647	648	654	653
586	1	1	1	0	543	561	560	542
587	1	1	1	0	603	560	561	561
588	1	1	1	0	604	623	602	603
589	1	1	1	0	611	600	601	601
590	1	1	1	0	613	612	609	610
591	1	1	1	0	652	653	654	654
592	1	1	1	0	601	600	572	573
593	1	1	1	0	647	592	590	648
594	1	1	1	0	593	488	493	591
595	1	1	1	0	573	572	498	494
596	1	1	1	0	652	654	655	655
597	1	1	1	0	611	599	600	600
598	1	1	1	0	654	648	649	655

ELEM	MAT	TYP	REL	ESYS	NODES			
599	1	1	1	0	612	606	596	609
600	1	1	1	0	592	591	589	590
601	1	1	1	0	611	610	598	599
602	1	1	1	0	650	652	655	655
603	1	1	1	0	600	599	571	572
604	1	1	1	0	648	590	588	649
605	1	1	1	0	649	650	655	655
606	1	1	1	0	623	652	651	602
607	1	1	1	0	591	493	492	589
608	1	1	1	0	606	605	595	596
609	1	1	1	0	572	571	499	498
610	1	1	1	0	610	609	597	598
611	1	1	1	0	651	652	650	650
612	1	1	1	0	603	602	559	560
613	1	1	1	0	590	589	587	588
614	1	1	1	0	605	565	566	595
615	1	1	1	0	599	598	570	571
616	1	1	1	0	649	588	586	650
617	1	1	1	0	565	555	554	566
618	1	1	1	0	586	651	650	650

ELEM	MAT	TYP	REL	ESYS	NODES			
619	1	1	1	0	560	559	541	542
620	1	1	1	0	589	492	491	587
621	1	1	1	0	571	570	500	499
622	1	1	1	0	609	596	584	597
623	1	1	1	0	598	597	569	570
624	1	1	1	0	588	587	585	586
625	1	1	1	0	651	576	602	602
626	1	1	1	0	596	595	583	584
627	1	1	1	0	602	576	577	559
628	1	1	1	0	570	569	501	500
629	1	1	1	0	587	491	490	585
630	1	1	1	0	651	586	575	576
631	1	1	1	0	595	566	567	583
632	1	1	1	0	597	584	568	569
633	1	1	1	0	586	585	574	575
634	1	1	1	0	566	554	553	567
635	1	1	1	0	559	558	540	541
636	1	1	1	0	569	568	502	501
637	1	1	1	0	585	490	489	574
638	1	1	1	0	559	577	517	558

ELEM	MAT	TYP	REL	ESYS	NODES			
639	1	1	1	0	584	583	532	531
640	1	1	1	0	576	575	519	518
641	1	1	1	0	576	518	517	577
642	1	1	1	0	584	531	530	568
643	1	1	1	0	583	567	533	532
644	1	1	1	0	575	574	520	519
645	1	1	1	0	567	553	529	533
646	1	1	1	0	558	517	515	540

647	1	1	1	0	568	530	497	502
648	1	1	1	0	574	489	487	520

LIST ALL SELECTED NODE DSYS= 0

NODE	X	Y	Z	THXY	THYZ	THXZ
182	17.894	30.505	0.52817E-11	0.00	-90.00	0.00
194	0.18914E-09	30.505	-17.894	90.00	0.00	-90.00
196	11.547	30.505	-13.670	90.00	-40.19	-90.00
197	9.5221	30.505	-15.150	90.00	-32.15	-90.00
198	7.3103	30.505	-16.332	90.00	-24.11	-90.00
199	4.9548	30.505	-17.194	90.00	-16.08	-90.00
200	2.5020	30.505	-17.718	90.00	-8.04	-90.00
201	13.670	30.505	-11.547	90.00	-49.81	-90.00
202	13.002	30.505	-12.294	90.00	-46.60	-90.00
203	12.294	30.505	-13.002	90.00	-43.40	-90.00
204	17.718	30.505	-2.5020	90.00	-81.96	-90.00
205	17.194	30.505	-4.9548	90.00	-73.92	-90.00
206	16.332	30.505	-7.3103	90.00	-65.89	-90.00
207	15.150	30.505	-9.5221	90.00	-57.85	-90.00
264	2.1135	35.938	0.00000E+00	0.00	-90.00	0.00
265	12.626	32.042	-10.501	90.00	-50.25	-90.00
266	3.4704	35.807	-1.3567	90.00	-68.65	-90.00
267	4.8203	35.573	-2.7065	90.00	-60.69	-90.00
268	6.1595	35.238	-4.0456	90.00	-56.70	-90.00
269	7.4841	34.802	-5.3700	90.00	-54.34	-90.00

NODE	X	Y	Z	THXY	THYZ	THXZ
270	8.7903	34.266	-6.6761	90.00	-52.78	-90.00
271	10.075	33.632	-7.9601	90.00	-51.69	-90.00
272	11.333	32.903	-9.2183	90.00	-50.87	-90.00
273	10.501	32.042	-12.626	90.00	-39.75	-90.00
274	11.962	32.042	-11.252	90.00	-46.75	-90.00
275	11.252	32.042	-11.962	90.00	-43.25	-90.00
276	0.14003E-09	35.938	-2.1135	90.00	0.00	-90.00
277	1.3567	35.807	-3.4704	90.00	-21.35	-90.00
278	2.7065	35.573	-4.8203	90.00	-29.31	-90.00
279	4.0456	35.238	-6.1595	90.00	-33.30	-90.00
280	5.3700	34.802	-7.4841	90.00	-35.66	-90.00
281	6.6761	34.266	-8.7903	90.00	-37.22	-90.00
282	7.9601	33.632	-10.075	90.00	-38.31	-90.00
283	9.2183	32.903	-11.333	90.00	-39.13	-90.00
284	1.8315	35.938	-1.0572	90.00	-60.00	-90.00
285	1.0572	35.938	-1.8315	90.00	-30.00	-90.00
286	3.1400	35.784	-2.3749	90.00	-52.90	-90.00
287	4.4404	35.535	-3.6842	90.00	-50.32	-90.00
288	5.7295	35.190	-4.9821	90.00	-48.99	-90.00
289	7.0043	34.752	-6.2656	90.00	-48.19	-90.00

NODE	X	Y	Z	THXY	THYZ	THXZ
290	8.2618	34.220	-7.5316	90.00	-47.65	-90.00
291	9.4990	33.597	-8.7771	90.00	-47.26	-90.00
292	10.713	32.882	-9.9991	90.00	-46.97	-90.00
293	2.3749	35.784	-3.1400	90.00	-37.10	-90.00
294	3.6842	35.535	-4.4404	90.00	-39.68	-90.00
295	4.9821	35.190	-5.7295	90.00	-41.01	-90.00
296	6.2656	34.752	-7.0043	90.00	-41.81	-90.00
297	7.5316	34.220	-8.2618	90.00	-42.35	-90.00
298	8.7771	33.597	-9.4990	90.00	-42.74	-90.00
299	9.9991	32.882	-10.713	90.00	-43.03	-90.00
300	16.422	32.042	0.11270E-10	0.00	-90.00	0.00
301	14.097	33.125	-0.31917E-08	0.00	-90.00	0.00
302	11.789	34.015	-0.50703E-08	0.00	-90.00	0.00
303	9.4254	34.744	-0.56583E-08	0.00	-90.00	0.00
304	7.0174	35.309	-0.49850E-08	0.00	-90.00	0.00
305	4.5762	35.708	-0.30854E-08	0.00	-90.00	0.00
306	13.957	32.042	-8.6535	90.00	-58.20	-90.00
307	15.020	32.042	-6.6400	90.00	-66.15	-90.00
308	15.794	32.042	-4.4991	90.00	-74.10	-90.00
309	16.264	32.042	-2.2715	90.00	-82.05	-90.00

NODE	X	Y	Z	THXY	THYZ	THXZ
310	14.047	33.086	-2.0034	90.00	-81.88	-90.00
311	11.850	33.945	-1.8316	90.00	-81.21	-90.00
312	9.5695	34.672	-1.5130	90.00	-81.02	-90.00
313	7.3243	35.210	-1.6212	90.00	-77.52	-90.00
314	5.4043	35.564	-1.4205	90.00	-75.27	-90.00
315	12.394	32.949	-7.5315	90.00	-58.71	-90.00
316	13.260	32.967	-5.7762	90.00	-66.46	-90.00
317	13.823	33.006	-3.9428	90.00	-74.08	-90.00
318	10.948	33.676	-6.4852	90.00	-59.36	-90.00
319	11.663	33.690	-4.9922	90.00	-66.83	-90.00
320	12.165	33.694	-3.5653	90.00	-73.67	-90.00
321	9.5141	34.289	-5.4520	90.00	-60.19	-90.00
322	10.070	34.304	-4.2234	90.00	-67.25	-90.00
323	10.479	34.313	-2.9634	90.00	-74.21	-90.00
324	8.2107	34.747	-4.6055	90.00	-60.71	-90.00
325	8.4340	34.821	-3.5135	90.00	-67.38	-90.00
326	8.8410	34.803	-2.5667	90.00	-73.81	-90.00
327	7.1453	35.085	-3.7399	90.00	-62.37	-90.00
328	6.8809	35.224	-2.8142	90.00	-67.76	-90.00
329	0.63990E-10	32.042	-16.422	90.00	0.00	-90.00

NODE	X	Y	Z	THXY	THYZ	THXZ
330	2.2715	32.042	-16.264	90.00	-7.95	-90.00
331	4.4991	32.042	-15.794	90.00	-15.90	-90.00
332	6.6400	32.042	-15.020	90.00	-23.85	-90.00
333	8.6535	32.042	-13.957	90.00	-31.80	-90.00
334	0.26780E-08	35.781	-3.9621	90.00	0.00	-90.00
335	0.46958E-08	35.530	-5.8002	90.00	0.00	-90.00
336	0.60948E-08	35.184	-7.6229	90.00	0.00	-90.00
337	0.67696E-08	34.744	-9.4254	90.00	0.00	-90.00
338	0.66162E-08	34.213	-11.203	90.00	0.00	-90.00
339	0.55332E-08	33.590	-12.950	90.00	0.00	-90.00
340	0.34222E-08	32.878	-14.664	90.00	0.00	-90.00
341	2.0721	32.927	-14.405	90.00	-8.19	-90.00
342	4.0607	32.928	-13.973	90.00	-16.20	-90.00
343	5.9052	32.922	-13.314	90.00	-23.92	-90.00
344	7.6153	32.925	-12.408	90.00	-31.54	-90.00
345	6.6173	33.622	-11.035	90.00	-30.95	-90.00
346	5.5505	34.216	-9.7190	90.00	-29.73	-90.00
347	4.3939	34.708	-8.4892	90.00	-27.37	-90.00
348	3.0210	35.121	-7.3087	90.00	-22.46	-90.00
349	1.4693	35.511	-5.7302	90.00	-14.38	-90.00

NODE	X	Y	Z	THXY	THYZ	THXZ
350	1.8904	33.639	-12.682	90.00	-8.48	-90.00
351	3.6464	33.628	-12.324	90.00	-16.48	-90.00
352	5.2182	33.610	-11.795	90.00	-23.87	-90.00
353	1.6658	34.236	-11.006	90.00	-8.61	-90.00
354	3.1601	34.216	-10.736	90.00	-16.40	-90.00
355	4.5601	34.148	-10.446	90.00	-23.58	-90.00
356	1.5375	34.719	-9.3941	90.00	-9.29	-90.00
357	2.6604	34.595	-9.5970	90.00	-15.49	-90.00
358	1.4387	35.140	-7.6869	90.00	-10.60	-90.00
359	3.6206	34.565	-9.3892	90.00	-21.09	-90.00
360	2.5402	34.855	-8.6423	90.00	-16.38	-90.00
361	0.14027E-09	36.000	0.00000E+00	0.00	-90.00	0.00
362	1.4094	35.972	0.00000E+00	0.00	-90.00	0.00
363	0.70486	35.993	0.00000E+00	0.00	-90.00	0.00
364	0.38936E-09	35.993	-0.70486	90.00	0.00	-90.00
365	0.14017E-09	35.972	-1.4094	90.00	0.00	-90.00
366	0.61482	35.990	-0.60311	90.00	-45.55	-90.00
367	1.1990	35.973	-0.68776	90.00	-60.16	-90.00
368	0.70412	35.974	-1.1793	90.00	-30.84	-90.00
369	12.990	31.710	-10.876	90.00	-50.06	-90.00

NODE	X	Y	Z	THXY	THYZ	THXZ
370	13.351	31.215	-11.236	90.00	-49.92	-90.00
371	10.876	31.710	-12.990	90.00	-39.94	-90.00
372	11.236	31.215	-13.351	90.00	-40.08	-90.00
373	12.308	31.731	-11.603	90.00	-46.69	-90.00
374	12.681	31.225	-11.975	90.00	-46.64	-90.00
375	11.603	31.731	-12.308	90.00	-43.31	-90.00
376	11.975	31.225	-12.681	90.00	-43.36	-90.00

377	16.942	31.710	0.99754E-11	0.00	-90.00	0.00
378	17.450	31.215	0.80443E-11	0.00	-90.00	0.00
379	16.776	31.712	-2.3513	90.00	-82.02	-90.00
380	17.278	31.217	-2.4310	90.00	-81.99	-90.00
381	16.286	31.713	-4.6584	90.00	-74.04	-90.00
382	16.769	31.218	-4.8158	90.00	-73.98	-90.00
383	15.480	31.713	-6.8764	90.00	-66.05	-90.00
384	15.933	31.218	-7.1079	90.00	-65.96	-90.00
385	14.374	31.712	-8.9623	90.00	-58.06	-90.00
386	14.787	31.217	-9.2620	90.00	-57.94	-90.00
387	0.18942E-09	31.710	-16.942	90.00	0.00	-90.00
388	0.18938E-09	31.215	-17.450	90.00	0.00	-90.00
389	8.9623	31.712	-14.374	90.00	-31.94	-90.00

NODE	X	Y	Z	THXY	THYZ	THXZ
390	9.2620	31.217	-14.787	90.00	-32.06	-90.00
391	6.8764	31.713	-15.480	90.00	-23.95	-90.00
392	7.1079	31.218	-15.933	90.00	-24.04	-90.00
393	4.6584	31.713	-16.286	90.00	-15.96	-90.00
394	4.8158	31.218	-16.769	90.00	-16.02	-90.00
395	2.3513	31.712	-16.776	90.00	-7.98	-90.00
396	2.4310	31.217	-17.278	90.00	-8.01	-90.00
487	13.880	29.150	-11.757	90.00	-49.73	-90.00
488	13.880	23.000	-11.757	90.00	-49.73	-90.00
489	13.880	27.630	-11.757	90.00	-49.73	-90.00
490	13.880	27.180	-11.757	90.00	-49.73	-90.00
491	13.880	26.135	-11.757	90.00	-49.73	-90.00
492	13.880	25.090	-11.757	90.00	-49.73	-90.00
493	13.880	24.045	-11.757	90.00	-49.73	-90.00
494	11.757	23.000	-13.880	90.00	-40.27	-90.00
495	13.211	23.000	-12.503	90.00	-46.58	-90.00
496	12.503	23.000	-13.211	90.00	-43.42	-90.00
497	11.757	29.150	-13.880	90.00	-40.27	-90.00
498	11.757	24.045	-13.880	90.00	-40.27	-90.00
499	11.757	25.090	-13.880	90.00	-40.27	-90.00

NODE	X	Y	Z	THXY	THYZ	THXZ
500	11.757	26.135	-13.880	90.00	-40.27	-90.00
501	11.757	27.180	-13.880	90.00	-40.27	-90.00
502	11.757	27.630	-13.880	90.00	-40.27	-90.00
503	12.503	29.150	-13.211	90.00	-43.42	-90.00
504	13.211	29.150	-12.503	90.00	-46.58	-90.00
505	13.212	27.630	-12.504	90.00	-46.58	-90.00
506	13.212	27.180	-12.503	90.00	-46.58	-90.00
507	13.212	26.135	-12.503	90.00	-46.58	-90.00
508	13.212	25.090	-12.503	90.00	-46.58	-90.00
509	13.212	24.045	-12.503	90.00	-46.58	-90.00
510	12.504	27.630	-13.212	90.00	-43.42	-90.00
511	12.503	27.180	-13.212	90.00	-43.42	-90.00
512	12.503	26.135	-13.212	90.00	-43.42	-90.00
513	12.503	25.090	-13.212	90.00	-43.42	-90.00
514	12.503	24.045	-13.212	90.00	-43.42	-90.00
515	18.190	29.150	0.22102E-16	0.00	-90.00	0.00
516	18.086	29.964	0.31731E-11	0.00	-90.00	0.00
517	18.011	29.150	-2.5484	90.00	-81.95	-90.00
518	17.476	29.150	-5.0465	90.00	-73.89	-90.00
519	16.597	29.150	-7.4451	90.00	-65.84	-90.00

NODE	X	Y	Z	THXY	THYZ	THXZ
520	15.390	29.150	-9.6968	90.00	-57.79	-90.00
521	13.809	29.964	-11.681	90.00	-49.77	-90.00
522	17.908	29.965	-2.5309	90.00	-81.96	-90.00
523	17.378	29.965	-5.0126	90.00	-73.91	-90.00
524	16.505	29.965	-7.3959	90.00	-65.86	-90.00
525	15.307	29.965	-9.6333	90.00	-57.82	-90.00
526	11.681	29.964	-13.809	90.00	-40.23	-90.00
527	13.139	29.964	-12.429	90.00	-46.59	-90.00
528	12.429	29.964	-13.139	90.00	-43.41	-90.00
529	0.18493E-09	29.150	-18.190	90.00	0.00	-90.00
530	9.6968	29.150	-15.390	90.00	-32.21	-90.00
531	7.4451	29.150	-16.597	90.00	-24.16	-90.00
532	5.0465	29.150	-17.476	90.00	-16.11	-90.00
533	2.5484	29.150	-18.011	90.00	-8.05	-90.00
534	0.18708E-09	29.964	-18.086	90.00	0.00	-90.00

535	9.6333	29.965	-15.307	90.00	-32.18	-90.00
536	7.3959	29.965	-16.505	90.00	-24.14	-90.00
537	5.0126	29.965	-17.378	90.00	-16.09	-90.00
538	2.5309	29.965	-17.908	90.00	-8.04	-90.00
539	18.190	15.000	0.00000E+00	0.00	-90.00	0.00

NODE	X	Y	Z	THXY	THYZ	THXZ
540	18.190	27.989	0.00000E+00	0.00	-90.00	0.00
541	18.190	26.393	0.00000E+00	0.00	-90.00	0.00
542	18.190	24.405	0.00000E+00	0.00	-90.00	0.00
543	18.190	21.928	0.00000E+00	0.00	-90.00	0.00
544	18.190	18.843	0.00000E+00	0.00	-90.00	0.00
545	0.12932E-09	15.000	-18.190	90.00	0.00	-90.00
546	17.844	15.000	-3.5496	90.00	-78.75	-90.00
547	16.810	15.000	-6.9627	90.00	-67.50	-90.00
548	15.126	15.000	-10.107	90.00	-56.25	-90.00
549	12.862	15.000	-12.862	90.00	-45.00	-90.00
550	10.107	15.000	-15.126	90.00	-33.75	-90.00
551	6.9627	15.000	-16.810	90.00	-22.50	-90.00
552	3.5496	15.000	-17.844	90.00	-11.25	-90.00
553	0.17994E-09	27.989	-18.190	90.00	0.00	-90.00
554	0.17372E-09	26.393	-18.190	90.00	0.00	-90.00
555	0.16597E-09	24.405	-18.190	90.00	0.00	-90.00
556	0.15632E-09	21.928	-18.190	90.00	0.00	-90.00
557	0.14430E-09	18.843	-18.190	90.00	0.00	-90.00
558	18.117	27.675	-1.6285	90.00	-84.86	-90.00
559	18.057	25.977	-2.2001	90.00	-83.05	-90.00

NODE	X	Y	Z	THXY	THYZ	THXZ
560	18.096	24.117	-1.8489	90.00	-84.17	-90.00
561	18.044	21.959	-2.3008	90.00	-82.73	-90.00
562	17.839	18.828	-3.5570	90.00	-78.72	-90.00
563	3.5429	18.511	-17.842	90.00	-11.23	-90.00
564	2.6998	21.603	-17.989	90.00	-8.54	-90.00
565	2.1188	23.984	-18.066	90.00	-6.69	-90.00
566	2.1142	25.906	-18.067	90.00	-6.67	-90.00
567	2.2975	27.657	-18.045	90.00	-7.26	-90.00
568	9.8850	27.765	-15.270	90.00	-32.92	-90.00
569	10.259	26.543	-15.021	90.00	-34.33	-90.00
570	10.611	25.564	-14.774	90.00	-35.69	-90.00
571	10.842	24.722	-14.606	90.00	-36.59	-90.00
572	10.946	23.846	-14.528	90.00	-37.00	-90.00
573	10.944	22.878	-14.529	90.00	-36.99	-90.00
574	15.233	27.846	-9.9412	90.00	-56.87	-90.00
575	16.440	27.336	-7.7859	90.00	-64.66	-90.00
576	17.437	27.113	-5.1794	90.00	-73.46	-90.00
577	17.906	27.384	-3.2044	90.00	-79.85	-90.00
578	16.746	18.081	-7.1036	90.00	-67.01	-90.00
579	14.945	18.290	-10.370	90.00	-55.24	-90.00

NODE	X	Y	Z	THXY	THYZ	THXZ
580	12.429	17.987	-13.282	90.00	-43.10	-90.00
581	9.7361	17.556	-15.365	90.00	-32.36	-90.00
582	6.8977	17.701	-16.832	90.00	-22.28	-90.00
583	4.6756	27.331	-17.579	90.00	-14.89	-90.00
584	7.4251	26.988	-16.606	90.00	-24.09	-90.00
585	15.006	26.599	-10.281	90.00	-55.58	-90.00
586	15.952	25.732	-8.7421	90.00	-61.28	-90.00
587	14.769	25.551	-10.618	90.00	-54.29	-90.00
588	15.509	24.838	-9.5052	90.00	-58.50	-90.00
589	14.567	24.601	-10.894	90.00	-53.21	-90.00
590	15.203	24.027	-9.9868	90.00	-56.70	-90.00
591	14.395	23.681	-11.120	90.00	-52.31	-90.00
592	14.917	23.183	-10.410	90.00	-55.09	-90.00
593	14.231	22.901	-11.330	90.00	-51.48	-90.00
594	14.587	22.461	-10.868	90.00	-53.31	-90.00
595	4.2096	25.517	-17.696	90.00	-13.38	-90.00
596	6.1957	24.925	-17.103	90.00	-19.91	-90.00
597	8.7852	25.557	-15.928	90.00	-28.88	-90.00
598	9.5502	24.756	-15.482	90.00	-31.67	-90.00
599	10.044	24.205	-15.166	90.00	-33.51	-90.00

NODE	X	Y	Z	THXY	THYZ	THXZ
600	10.283	23.641	-15.005	90.00	-34.42	-90.00
601	10.195	22.802	-15.064	90.00	-34.09	-90.00
602	17.597	24.748	-4.6084	90.00	-75.32	-90.00
603	17.844	23.436	-3.5303	90.00	-78.81	-90.00
604	17.506	21.628	-4.9430	90.00	-74.23	-90.00
605	3.9691	23.720	-17.752	90.00	-12.60	-90.00
606	5.6618	23.302	-17.287	90.00	-18.13	-90.00
607	4.1893	22.215	-17.701	90.00	-13.31	-90.00
608	5.5029	22.037	-17.338	90.00	-17.61	-90.00
609	7.6659	24.226	-16.496	90.00	-24.92	-90.00
610	8.7393	23.598	-15.953	90.00	-28.71	-90.00
611	9.5408	23.173	-15.487	90.00	-31.63	-90.00
612	7.0340	22.770	-16.775	90.00	-22.75	-90.00
613	8.2022	22.306	-16.236	90.00	-26.80	-90.00
614	9.1713	22.020	-15.709	90.00	-30.28	-90.00
615	10.086	21.866	-15.138	90.00	-33.67	-90.00
616	10.950	21.889	-14.525	90.00	-37.01	-90.00
617	11.766	21.928	-13.872	90.00	-40.30	-90.00
618	12.521	21.936	-13.195	90.00	-43.50	-90.00
619	13.195	21.932	-12.521	90.00	-46.50	-90.00

NODE	X	Y	Z	THXY	THYZ	THXZ
620	13.806	22.010	-11.844	90.00	-49.37	-90.00
621	14.183	22.290	-11.389	90.00	-51.24	-90.00
622	14.310	21.631	-11.229	90.00	-51.88	-90.00
623	17.092	22.992	-6.2236	90.00	-69.99	-90.00
624	6.6492	21.575	-16.931	90.00	-21.44	-90.00
625	7.9961	21.057	-16.338	90.00	-26.08	-90.00
626	9.1344	21.008	-15.730	90.00	-30.14	-90.00
627	10.098	20.803	-15.130	90.00	-33.72	-90.00
628	11.038	21.032	-14.458	90.00	-37.36	-90.00
629	11.757	20.972	-13.880	90.00	-40.27	-90.00
630	12.531	20.870	-13.186	90.00	-43.54	-90.00
631	13.283	20.851	-12.428	90.00	-46.91	-90.00
632	13.930	20.946	-11.698	90.00	-49.98	-90.00
633	16.651	20.433	-7.3236	90.00	-66.26	-90.00
634	15.591	20.257	-9.3701	90.00	-58.99	-90.00
635	16.471	21.942	-7.7197	90.00	-64.89	-90.00
636	15.733	21.512	-9.1296	90.00	-59.87	-90.00
637	4.7010	20.269	-17.572	90.00	-14.98	-90.00
638	6.7079	20.005	-16.908	90.00	-21.64	-90.00
639	5.1199	21.194	-17.455	90.00	-16.35	-90.00

NODE	X	Y	Z	THXY	THYZ	THXZ
640	9.3031	19.712	-15.631	90.00	-30.76	-90.00
641	11.283	19.922	-14.268	90.00	-38.34	-90.00
642	12.496	19.832	-13.219	90.00	-43.39	-90.00
643	13.470	19.642	-12.224	90.00	-47.78	-90.00
644	14.267	19.958	-11.284	90.00	-51.66	-90.00
645	14.700	20.701	-10.714	90.00	-53.91	-90.00
646	14.990	21.731	-10.305	90.00	-55.49	-90.00
647	15.556	22.612	-9.4275	90.00	-58.78	-90.00
648	15.777	23.543	-9.0533	90.00	-60.15	-90.00
649	16.016	24.128	-8.6240	90.00	-61.70	-90.00
650	16.328	24.572	-8.0165	90.00	-63.85	-90.00
651	16.857	25.317	-6.8366	90.00	-67.92	-90.00
652	16.621	23.718	-7.3902	90.00	-66.03	-90.00
653	16.245	22.800	-8.1843	90.00	-63.26	-90.00
654	16.180	23.326	-8.3114	90.00	-62.81	-90.00
655	16.268	23.725	-8.1385	90.00	-63.42	-90.00

```
LIST ALL MATERIALS  PROPERTY= ALL

PROPERTY TABLE EX     MAT=    1  NUM. POINTS=  2
    TEMPERATURE       DATA     TEMPERATURE       DATA
      -9999.0      0.27180E+08  9999.0       0.27180E+08
TIME= 0.00000E+00  NITTER=       1

UNIFORM TEMPERATURE=      0.000  (TREF=      0.000)
PLASTIC CONVERG. CRITERION=       0.0100
CREEP OPTIMUM. CRITERION=       0.1000
LARGE DEFL. CONVERG. CRITERION=     0.001000
DISPLACEMENT LIMIT= 0.00000E+00
```

```
NPRINT= 99900   NPOST=     1   REACTION PRINT FREQ= 99900
 DISP. POST DATA FREQ=     1  REACT. POST DATA FREQ=     1

 ELEMENT PRINT AND POST DATA FREQUENCIES
  TYPE  STIFF  STRESS  FORCE   STRESS   DATA  FORCE
        NO.   PRINT  PRINT    DATA    LEVEL  DATA
    1    63  99900  99900       1       3     1

LOADS INPUT FILE= 26     LOADS OUTPUT FILE= 23

ALL ANALYSIS DATA WILL BE WRITTEN ONTO FILE27

LIST DISPLACEMENTS FOR ALL SELECTED NODES

 NODE  LABEL     DISP            CDISP
   182 UY    0.000000000E+00 0.000000000E+00
   264 UY    0.000000000E+00 0.000000000E+00
   300 UY    0.000000000E+00 0.000000000E+00
   301 UY    0.000000000E+00 0.000000000E+00
   302 UY    0.000000000E+00 0.000000000E+00
   303 UY    0.000000000E+00 0.000000000E+00
   304 UY    0.000000000E+00 0.000000000E+00
   305 UY    0.000000000E+00 0.000000000E+00
   544 ROTZ  0.000000000E+00 0.000000000E+00
   362 UY    0.000000000E+00 0.000000000E+00
   363 UY    0.000000000E+00 0.000000000E+00
   377 UY    0.000000000E+00 0.000000000E+00
   378 UY    0.000000000E+00 0.000000000E+00
   515 UY    0.000000000E+00 0.000000000E+00
   516 UY    0.000000000E+00 0.000000000E+00
   557 ROTZ  0.000000000E+00 0.000000000E+00
   540 UY    0.000000000E+00 0.000000000E+00
   541 UY    0.000000000E+00 0.000000000E+00
   542 UY    0.000000000E+00 0.000000000E+00
   543 UY    0.000000000E+00 0.000000000E+00

 NODE  LABEL     DISP            CDISP
   544 UY    0.000000000E+00 0.000000000E+00
   182 ROTX  0.000000000E+00 0.000000000E+00
   264 ROTX  0.000000000E+00 0.000000000E+00
   300 ROTX  0.000000000E+00 0.000000000E+00
   301 ROTX  0.000000000E+00 0.000000000E+00
   302 ROTX  0.000000000E+00 0.000000000E+00
   303 ROTX  0.000000000E+00 0.000000000E+00
   304 ROTX  0.000000000E+00 0.000000000E+00
   305 ROTX  0.000000000E+00 0.000000000E+00
   557 UY    0.000000000E+00 0.000000000E+00
   362 ROTX  0.000000000E+00 0.000000000E+00
   363 ROTX  0.000000000E+00 0.000000000E+00
   377 ROTX  0.000000000E+00 0.000000000E+00
   378 ROTX  0.000000000E+00 0.000000000E+00
   515 ROTX  0.000000000E+00 0.000000000E+00
   516 ROTX  0.000000000E+00 0.000000000E+00
   556 ROTZ  0.000000000E+00 0.000000000E+00
   540 ROTX  0.000000000E+00 0.000000000E+00
   541 ROTX  0.000000000E+00 0.000000000E+00
   542 ROTX  0.000000000E+00 0.000000000E+00

 NODE  LABEL     DISP            CDISP
   543 ROTX  0.000000000E+00 0.000000000E+00
   544 ROTX  0.000000000E+00 0.000000000E+00
   182 ROTZ  0.000000000E+00 0.000000000E+00
   264 ROTZ  0.000000000E+00 0.000000000E+00
   300 ROTZ  0.000000000E+00 0.000000000E+00
   301 ROTZ  0.000000000E+00 0.000000000E+00
   302 ROTZ  0.000000000E+00 0.000000000E+00
   303 ROTZ  0.000000000E+00 0.000000000E+00
   304 ROTZ  0.000000000E+00 0.000000000E+00
   305 ROTZ  0.000000000E+00 0.000000000E+00
   557 ROTX  0.000000000E+00 0.000000000E+00
   362 ROTZ  0.000000000E+00 0.000000000E+00
   363 ROTZ  0.000000000E+00 0.000000000E+00
   377 ROTZ  0.000000000E+00 0.000000000E+00
   378 ROTZ  0.000000000E+00 0.000000000E+00
```

515	ROTZ	0.000000000E+00	0.000000000E+00
516	ROTZ	0.000000000E+00	0.000000000E+00
555	ROTZ	0.000000000E+00	0.000000000E+00
540	ROTZ	0.000000000E+00	0.000000000E+00
541	ROTZ	0.000000000E+00	0.000000000E+00

NODE	LABEL	DISP	CDISP
542	ROTZ	0.000000000E+00	0.000000000E+00
543	ROTZ	0.000000000E+00	0.000000000E+00
194	UY	0.000000000E+00	0.000000000E+00
276	UY	0.000000000E+00	0.000000000E+00
329	UY	0.000000000E+00	0.000000000E+00
334	UY	0.000000000E+00	0.000000000E+00
335	UY	0.000000000E+00	0.000000000E+00
336	UY	0.000000000E+00	0.000000000E+00
337	UY	0.000000000E+00	0.000000000E+00
338	UY	0.000000000E+00	0.000000000E+00
339	UY	0.000000000E+00	0.000000000E+00
340	UY	0.000000000E+00	0.000000000E+00
361	UY	0.000000000E+00	0.000000000E+00
364	UY	0.000000000E+00	0.000000000E+00
365	UY	0.000000000E+00	0.000000000E+00
387	UY	0.000000000E+00	0.000000000E+00
388	UY	0.000000000E+00	0.000000000E+00
529	UY	0.000000000E+00	0.000000000E+00
534	UY	0.000000000E+00	0.000000000E+00
554	ROTZ	0.000000000E+00	0.000000000E+00

NODE	LABEL	DISP	CDISP
553	UY	0.000000000E+00	0.000000000E+00
554	UY	0.000000000E+00	0.000000000E+00
555	UY	0.000000000E+00	0.000000000E+00
556	UY	0.000000000E+00	0.000000000E+00
194	ROTX	0.000000000E+00	0.000000000E+00
276	ROTX	0.000000000E+00	0.000000000E+00
329	ROTX	0.000000000E+00	0.000000000E+00
334	ROTX	0.000000000E+00	0.000000000E+00
335	ROTX	0.000000000E+00	0.000000000E+00
336	ROTX	0.000000000E+00	0.000000000E+00
337	ROTX	0.000000000E+00	0.000000000E+00
338	ROTX	0.000000000E+00	0.000000000E+00
339	ROTX	0.000000000E+00	0.000000000E+00
340	ROTX	0.000000000E+00	0.000000000E+00
361	ROTX	0.000000000E+00	0.000000000E+00
364	ROTX	0.000000000E+00	0.000000000E+00
365	ROTX	0.000000000E+00	0.000000000E+00
387	ROTX	0.000000000E+00	0.000000000E+00
388	ROTX	0.000000000E+00	0.000000000E+00
529	ROTX	0.000000000E+00	0.000000000E+00

NODE	LABEL	DISP	CDISP
534	ROTX	0.000000000E+00	0.000000000E+00
553	ROTZ	0.000000000E+00	0.000000000E+00
553	ROTX	0.000000000E+00	0.000000000E+00
554	ROTX	0.000000000E+00	0.000000000E+00
555	ROTX	0.000000000E+00	0.000000000E+00
556	ROTX	0.000000000E+00	0.000000000E+00
194	ROTZ	0.000000000E+00	0.000000000E+00
276	ROTZ	0.000000000E+00	0.000000000E+00
329	ROTZ	0.000000000E+00	0.000000000E+00
334	ROTZ	0.000000000E+00	0.000000000E+00
335	ROTZ	0.000000000E+00	0.000000000E+00
336	ROTZ	0.000000000E+00	0.000000000E+00
337	ROTZ	0.000000000E+00	0.000000000E+00
338	ROTZ	0.000000000E+00	0.000000000E+00
339	ROTZ	0.000000000E+00	0.000000000E+00
340	ROTZ	0.000000000E+00	0.000000000E+00
361	ROTZ	0.000000000E+00	0.000000000E+00
364	ROTZ	0.000000000E+00	0.000000000E+00
365	ROTZ	0.000000000E+00	0.000000000E+00
387	ROTZ	0.000000000E+00	0.000000000E+00

NODE	LABEL	DISP	CDISP
388	ROTZ	0.000000000E+00	0.000000000E+00
529	ROTZ	0.000000000E+00	0.000000000E+00
534	ROTZ	0.000000000E+00	0.000000000E+00
539	UX	0.000000000E+00	0.000000000E+00
539	UY	0.000000000E+00	0.000000000E+00
539	UZ	0.000000000E+00	0.000000000E+00
539	ROTX	0.000000000E+00	0.000000000E+00
539	ROTY	0.000000000E+00	0.000000000E+00
539	ROTZ	0.000000000E+00	0.000000000E+00
545	UX	0.000000000E+00	0.000000000E+00
545	UY	0.000000000E+00	0.000000000E+00
545	UZ	0.000000000E+00	0.000000000E+00
545	ROTX	0.000000000E+00	0.000000000E+00
545	ROTY	0.000000000E+00	0.000000000E+00
545	ROTZ	0.000000000E+00	0.000000000E+00
546	UX	0.000000000E+00	0.000000000E+00
546	UY	0.000000000E+00	0.000000000E+00
546	UZ	0.000000000E+00	0.000000000E+00
546	ROTX	0.000000000E+00	0.000000000E+00
546	ROTY	0.000000000E+00	0.000000000E+00

NODE	LABEL	DISP	CDISP
546	ROTZ	0.000000000E+00	0.000000000E+00
547	UX	0.000000000E+00	0.000000000E+00
547	UY	0.000000000E+00	0.000000000E+00
547	UZ	0.000000000E+00	0.000000000E+00
547	ROTX	0.000000000E+00	0.000000000E+00
547	ROTY	0.000000000E+00	0.000000000E+00
547	ROTZ	0.000000000E+00	0.000000000E+00
548	UX	0.000000000E+00	0.000000000E+00
548	UY	0.000000000E+00	0.000000000E+00
548	UZ	0.000000000E+00	0.000000000E+00
548	ROTX	0.000000000E+00	0.000000000E+00
548	ROTY	0.000000000E+00	0.000000000E+00
548	ROTZ	0.000000000E+00	0.000000000E+00
549	UX	0.000000000E+00	0.000000000E+00
549	UY	0.000000000E+00	0.000000000E+00
549	UZ	0.000000000E+00	0.000000000E+00
549	ROTX	0.000000000E+00	0.000000000E+00
549	ROTY	0.000000000E+00	0.000000000E+00
549	ROTZ	0.000000000E+00	0.000000000E+00
550	UX	0.000000000E+00	0.000000000E+00

NODE	LABEL	DISP	CDISP
550	UY	0.000000000E+00	0.000000000E+00
550	UZ	0.000000000E+00	0.000000000E+00
550	ROTX	0.000000000E+00	0.000000000E+00
550	ROTY	0.000000000E+00	0.000000000E+00
550	ROTZ	0.000000000E+00	0.000000000E+00
551	UX	0.000000000E+00	0.000000000E+00
551	UY	0.000000000E+00	0.000000000E+00
551	UZ	0.000000000E+00	0.000000000E+00
551	ROTX	0.000000000E+00	0.000000000E+00
551	ROTY	0.000000000E+00	0.000000000E+00
551	ROTZ	0.000000000E+00	0.000000000E+00
552	UX	0.000000000E+00	0.000000000E+00
552	UY	0.000000000E+00	0.000000000E+00
552	UZ	0.000000000E+00	0.000000000E+00
552	ROTX	0.000000000E+00	0.000000000E+00
552	ROTY	0.000000000E+00	0.000000000E+00
552	ROTZ	0.000000000E+00	0.000000000E+00
361	UX	0.000000000E+00	0.000000000E+00

LIST ELEMENT PRESSURES FOR ALL SELECTED ELEMENTS

ELEM	FACE	VALUE(S)		FACE NODES			
283	1	0.000000000E+00	0.000000000E+00	331	332	343	342
284	1	0.000000000E+00	0.000000000E+00	332	333	344	343
285	1	0.000000000E+00	0.000000000E+00	331	342	341	330
286	1	0.000000000E+00	0.000000000E+00	333	273	283	344
287	1	0.000000000E+00	0.000000000E+00	330	341	340	329
288	1	0.000000000E+00	0.000000000E+00	342	343	352	351
289	1	0.000000000E+00	0.000000000E+00	343	344	345	352

290	1	0.000000000E+00	0.000000000E+00	342	351	350	341
291	1	0.000000000E+00	0.000000000E+00	344	283	282	345
292	1	0.000000000E+00	0.000000000E+00	341	350	339	340
293	1	0.000000000E+00	0.000000000E+00	351	352	355	354
294	1	0.000000000E+00	0.000000000E+00	352	345	346	355
295	1	0.000000000E+00	0.000000000E+00	351	354	353	350
296	1	0.000000000E+00	0.000000000E+00	345	282	281	346
297	1	0.000000000E+00	0.000000000E+00	350	353	338	339
298	1	0.000000000E+00	0.000000000E+00	355	359	357	354
299	1	0.000000000E+00	0.000000000E+00	355	346	347	359
300	1	0.000000000E+00	0.000000000E+00	354	357	356	353
301	1	0.000000000E+00	0.000000000E+00	346	281	280	347
302	1	0.000000000E+00	0.000000000E+00	353	356	337	338

ELEM	FACE	VALUE(S)		FACE NODES			
303	1	0.000000000E+00	0.000000000E+00	357	359	360	360
304	1	0.000000000E+00	0.000000000E+00	356	357	360	360
305	1	0.000000000E+00	0.000000000E+00	359	347	348	360
306	1	0.000000000E+00	0.000000000E+00	358	356	360	360
307	1	0.000000000E+00	0.000000000E+00	347	280	279	348
308	1	0.000000000E+00	0.000000000E+00	356	358	336	337
309	1	0.000000000E+00	0.000000000E+00	360	348	349	358
310	1	0.000000000E+00	0.000000000E+00	348	279	278	349
311	1	0.000000000E+00	0.000000000E+00	358	349	335	336
312	1	0.000000000E+00	0.000000000E+00	334	335	349	349
313	1	0.000000000E+00	0.000000000E+00	349	278	277	334
314	1	0.000000000E+00	0.000000000E+00	277	276	334	334
506	1	0.000000000E+00	0.000000000E+00	535	197	196	526
507	1	0.000000000E+00	0.000000000E+00	530	535	526	497
508	1	0.000000000E+00	0.000000000E+00	536	198	197	535
509	1	0.000000000E+00	0.000000000E+00	531	536	535	530
510	1	0.000000000E+00	0.000000000E+00	537	199	198	536
511	1	0.000000000E+00	0.000000000E+00	532	537	536	531
512	1	0.000000000E+00	0.000000000E+00	538	200	199	537
513	1	0.000000000E+00	0.000000000E+00	533	538	537	532

ELEM	FACE	VALUE(S)		FACE NODES			
514	1	0.000000000E+00	0.000000000E+00	534	194	200	538
515	1	0.000000000E+00	0.000000000E+00	529	534	538	533
315	1	0.000000000E+00	0.000000000E+00	361	363	366	364
316	1	0.000000000E+00	0.000000000E+00	364	366	368	365
317	1	0.000000000E+00	0.000000000E+00	363	362	367	366
318	1	0.000000000E+00	0.000000000E+00	368	366	367	367
319	1	0.000000000E+00	0.000000000E+00	365	368	285	276
320	1	0.000000000E+00	0.000000000E+00	362	264	284	367
321	1	0.000000000E+00	0.000000000E+00	368	367	284	285
472	1	0.000000000E+00	0.000000000E+00	505	504	487	489
473	1	0.000000000E+00	0.000000000E+00	506	505	489	490
474	1	0.000000000E+00	0.000000000E+00	507	506	490	491
475	1	0.000000000E+00	0.000000000E+00	508	507	491	492
476	1	0.000000000E+00	0.000000000E+00	509	508	492	493
477	1	0.000000000E+00	0.000000000E+00	495	509	493	488
478	1	0.000000000E+00	0.000000000E+00	510	503	504	505
479	1	0.000000000E+00	0.000000000E+00	511	510	505	506
480	1	0.000000000E+00	0.000000000E+00	512	511	506	507
481	1	0.000000000E+00	0.000000000E+00	513	512	507	508
482	1	0.000000000E+00	0.000000000E+00	514	513	508	509

ELEM	FACE	VALUE(S)		FACE NODES			
483	1	0.000000000E+00	0.000000000E+00	496	514	509	495
484	1	0.000000000E+00	0.000000000E+00	502	497	503	510
485	1	0.000000000E+00	0.000000000E+00	501	502	510	511
486	1	0.000000000E+00	0.000000000E+00	500	501	511	512
487	1	0.000000000E+00	0.000000000E+00	499	500	512	513
488	1	0.000000000E+00	0.000000000E+00	498	499	513	514
489	1	0.000000000E+00	0.000000000E+00	494	498	514	496
490	1	0.000000000E+00	0.000000000E+00	522	204	182	516
491	1	0.000000000E+00	0.000000000E+00	517	522	516	515
492	1	0.000000000E+00	0.000000000E+00	523	205	204	522
493	1	0.000000000E+00	0.000000000E+00	518	523	522	517
494	1	0.000000000E+00	0.000000000E+00	524	206	205	523
495	1	0.000000000E+00	0.000000000E+00	519	524	523	518
496	1	0.000000000E+00	0.000000000E+00	525	207	206	524
497	1	0.000000000E+00	0.000000000E+00	520	525	524	519

498	1	0.000000000E+00	0.000000000E+00	521	201	207	525
499	1	0.000000000E+00	0.000000000E+00	487	521	525	520
500	1	0.000000000E+00	0.000000000E+00	527	202	201	521
501	1	0.000000000E+00	0.000000000E+00	504	527	521	487
502	1	0.000000000E+00	0.000000000E+00	528	203	202	527

ELEM	FACE	VALUE(S)		FACE NODES			
503	1	0.000000000E+00	0.000000000E+00	503	528	527	504
504	1	0.000000000E+00	0.000000000E+00	526	196	203	528
505	1	0.000000000E+00	0.000000000E+00	497	526	528	503
228	1	0.000000000E+00	0.000000000E+00	286	284	264	266
229	1	0.000000000E+00	0.000000000E+00	287	286	266	267
230	1	0.000000000E+00	0.000000000E+00	288	287	267	268
231	1	0.000000000E+00	0.000000000E+00	289	288	268	269
232	1	0.000000000E+00	0.000000000E+00	290	289	269	270
233	1	0.000000000E+00	0.000000000E+00	291	290	270	271
234	1	0.000000000E+00	0.000000000E+00	292	291	271	272
235	1	0.000000000E+00	0.000000000E+00	274	292	272	265
236	1	0.000000000E+00	0.000000000E+00	293	285	284	286
237	1	0.000000000E+00	0.000000000E+00	294	293	286	287
238	1	0.000000000E+00	0.000000000E+00	295	294	287	288
239	1	0.000000000E+00	0.000000000E+00	296	295	288	289
240	1	0.000000000E+00	0.000000000E+00	297	296	289	290
241	1	0.000000000E+00	0.000000000E+00	298	297	290	291
242	1	0.000000000E+00	0.000000000E+00	299	298	291	292
243	1	0.000000000E+00	0.000000000E+00	275	299	292	274
244	1	0.000000000E+00	0.000000000E+00	277	276	285	293

ELEM	FACE	VALUE(S)		FACE NODES			
245	1	0.000000000E+00	0.000000000E+00	278	277	293	294
246	1	0.000000000E+00	0.000000000E+00	279	278	294	295
247	1	0.000000000E+00	0.000000000E+00	280	279	295	296
248	1	0.000000000E+00	0.000000000E+00	281	280	296	297
249	1	0.000000000E+00	0.000000000E+00	282	281	297	298
250	1	0.000000000E+00	0.000000000E+00	283	282	298	299
251	1	0.000000000E+00	0.000000000E+00	273	283	299	275
252	1	0.000000000E+00	0.000000000E+00	305	264	266	266
253	1	0.000000000E+00	0.000000000E+00	302	303	312	311
254	1	0.000000000E+00	0.000000000E+00	303	304	313	312
255	1	0.000000000E+00	0.000000000E+00	301	302	311	310
256	1	0.000000000E+00	0.000000000E+00	300	301	310	309
257	1	0.000000000E+00	0.000000000E+00	304	305	314	313
258	1	0.000000000E+00	0.000000000E+00	305	266	267	314
259	1	0.000000000E+00	0.000000000E+00	326	312	313	313
260	1	0.000000000E+00	0.000000000E+00	312	326	323	311
261	1	0.000000000E+00	0.000000000E+00	314	267	328	313
262	1	0.000000000E+00	0.000000000E+00	313	328	325	326
263	1	0.000000000E+00	0.000000000E+00	323	320	311	311
264	1	0.000000000E+00	0.000000000E+00	311	320	317	310

ELEM	FACE	VALUE(S)		FACE NODES			
265	1	0.000000000E+00	0.000000000E+00	310	317	308	309
266	1	0.000000000E+00	0.000000000E+00	267	327	328	328
267	1	0.000000000E+00	0.000000000E+00	326	325	322	323
268	1	0.000000000E+00	0.000000000E+00	327	325	328	328
269	1	0.000000000E+00	0.000000000E+00	267	268	327	327
270	1	0.000000000E+00	0.000000000E+00	323	322	319	320
271	1	0.000000000E+00	0.000000000E+00	327	324	325	325
272	1	0.000000000E+00	0.000000000E+00	320	319	316	317
273	1	0.000000000E+00	0.000000000E+00	325	324	321	322
274	1	0.000000000E+00	0.000000000E+00	327	268	269	324
275	1	0.000000000E+00	0.000000000E+00	317	316	307	308
276	1	0.000000000E+00	0.000000000E+00	322	321	318	319
277	1	0.000000000E+00	0.000000000E+00	324	269	270	321
278	1	0.000000000E+00	0.000000000E+00	319	318	315	316
279	1	0.000000000E+00	0.000000000E+00	321	270	271	318
280	1	0.000000000E+00	0.000000000E+00	316	315	306	307
281	1	0.000000000E+00	0.000000000E+00	318	271	272	315
282	1	0.000000000E+00	0.000000000E+00	315	272	265	306
322	1	0.000000000E+00	0.000000000E+00	373	274	265	369
323	1	0.000000000E+00	0.000000000E+00	374	373	369	370

ELEM	FACE	VALUE($)		FACE NODES			
324	1	0.000000000E+00	0.000000000E+00	202	374	370	201
325	1	0.000000000E+00	0.000000000E+00	375	275	274	373
326	1	0.000000000E+00	0.000000000E+00	376	375	373	374
327	1	0.000000000E+00	0.000000000E+00	203	376	374	202
328	1	0.000000000E+00	0.000000000E+00	371	273	275	375
329	1	0.000000000E+00	0.000000000E+00	372	371	375	376
330	1	0.000000000E+00	0.000000000E+00	196	372	376	203
331	1	0.000000000E+00	0.000000000E+00	379	309	300	377
332	1	0.000000000E+00	0.000000000E+00	380	379	377	378
333	1	0.000000000E+00	0.000000000E+00	204	380	378	182
334	1	0.000000000E+00	0.000000000E+00	381	308	309	379
335	1	0.000000000E+00	0.000000000E+00	382	381	379	380
336	1	0.000000000E+00	0.000000000E+00	205	382	380	204
337	1	0.000000000E+00	0.000000000E+00	383	307	308	381
338	1	0.000000000E+00	0.000000000E+00	384	383	381	382
339	1	0.000000000E+00	0.000000000E+00	206	384	382	205
340	1	0.000000000E+00	0.000000000E+00	385	306	307	383
341	1	0.000000000E+00	0.000000000E+00	386	385	383	384
342	1	0.000000000E+00	0.000000000E+00	207	386	384	206
343	1	0.000000000E+00	0.000000000E+00	369	265	306	385

ELEM	FACE	VALUE($)		FACE NODES			
344	1	0.000000000E+00	0.000000000E+00	370	369	385	386
345	1	0.000000000E+00	0.000000000E+00	201	370	386	207
346	1	0.000000000E+00	0.000000000E+00	389	333	273	371
347	1	0.000000000E+00	0.000000000E+00	390	389	371	372
348	1	0.000000000E+00	0.000000000E+00	197	390	372	196
349	1	0.000000000E+00	0.000000000E+00	391	332	333	389
350	1	0.000000000E+00	0.000000000E+00	392	391	389	390
351	1	0.000000000E+00	0.000000000E+00	198	392	390	197
352	1	0.000000000E+00	0.000000000E+00	393	331	332	391
353	1	0.000000000E+00	0.000000000E+00	394	393	391	392
354	1	0.000000000E+00	0.000000000E+00	199	394	392	198
355	1	0.000000000E+00	0.000000000E+00	395	330	331	393
356	1	0.000000000E+00	0.000000000E+00	396	395	393	394
357	1	0.000000000E+00	0.000000000E+00	200	396	394	199
358	1	0.000000000E+00	0.000000000E+00	387	329	330	395
359	1	0.000000000E+00	0.000000000E+00	388	387	395	396
360	1	0.000000000E+00	0.000000000E+00	194	388	396	200
516	1	0.000000000E+00	0.000000000E+00	550	551	582	581
517	1	0.000000000E+00	0.000000000E+00	549	550	581	580
518	1	0.000000000E+00	0.000000000E+00	551	552	563	582

ELEM	FACE	VALUE($)		FACE NODES			
519	1	0.000000000E+00	0.000000000E+00	548	549	580	579
520	1	0.000000000E+00	0.000000000E+00	547	548	579	578
521	1	0.000000000E+00	0.000000000E+00	546	547	578	562
522	1	0.000000000E+00	0.000000000E+00	552	545	557	563
523	1	0.000000000E+00	0.000000000E+00	539	546	562	544
524	1	0.000000000E+00	0.000000000E+00	579	580	643	643
525	1	0.000000000E+00	0.000000000E+00	581	582	638	640
526	1	0.000000000E+00	0.000000000E+00	581	640	641	580
527	1	0.000000000E+00	0.000000000E+00	582	563	637	638
528	1	0.000000000E+00	0.000000000E+00	580	642	643	643
529	1	0.000000000E+00	0.000000000E+00	580	641	642	642
530	1	0.000000000E+00	0.000000000E+00	578	579	634	633
531	1	0.000000000E+00	0.000000000E+00	579	643	644	644
532	1	0.000000000E+00	0.000000000E+00	578	633	604	562
533	1	0.000000000E+00	0.000000000E+00	579	644	645	634
534	1	0.000000000E+00	0.000000000E+00	563	564	637	637
535	1	0.000000000E+00	0.000000000E+00	627	641	640	640
536	1	0.000000000E+00	0.000000000E+00	563	557	556	564
537	1	0.000000000E+00	0.000000000E+00	625	640	638	638
538	1	0.000000000E+00	0.000000000E+00	643	642	630	631

ELEM	FACE	VALUE($)		FACE NODES			
539	1	0.000000000E+00	0.000000000E+00	643	631	632	644
540	1	0.000000000E+00	0.000000000E+00	544	562	561	543
541	1	0.000000000E+00	0.000000000E+00	642	641	629	630
542	1	0.000000000E+00	0.000000000E+00	637	639	638	638
543	1	0.000000000E+00	0.000000000E+00	626	627	640	640
544	1	0.000000000E+00	0.000000000E+00	627	628	641	641
545	1	0.000000000E+00	0.000000000E+00	625	626	640	640

546	1	0.000000000E+00	0.000000000E+00	628	629	641	641
547	1	0.000000000E+00	0.000000000E+00	644	632	622	645
548	1	0.000000000E+00	0.000000000E+00	624	625	638	638
549	1	0.000000000E+00	0.000000000E+00	634	636	635	633
550	1	0.000000000E+00	0.000000000E+00	634	645	646	636
551	1	0.000000000E+00	0.000000000E+00	638	639	608	624
552	1	0.000000000E+00	0.000000000E+00	637	564	607	639
553	1	0.000000000E+00	0.000000000E+00	622	646	645	645
554	1	0.000000000E+00	0.000000000E+00	631	630	618	619
555	1	0.000000000E+00	0.000000000E+00	627	615	616	628
556	1	0.000000000E+00	0.000000000E+00	627	626	614	615
557	1	0.000000000E+00	0.000000000E+00	630	629	617	618
558	1	0.000000000E+00	0.000000000E+00	631	619	620	632

ELEM	FACE	VALUE(S)		FACE NODES			
559	1	0.000000000E+00	0.000000000E+00	629	628	616	617
560	1	0.000000000E+00	0.000000000E+00	562	604	603	561
561	1	0.000000000E+00	0.000000000E+00	626	625	613	614
562	1	0.000000000E+00	0.000000000E+00	632	620	621	622
563	1	0.000000000E+00	0.000000000E+00	633	635	623	604
564	1	0.000000000E+00	0.000000000E+00	639	607	608	608
565	1	0.000000000E+00	0.000000000E+00	625	624	612	613
566	1	0.000000000E+00	0.000000000E+00	636	646	647	647
567	1	0.000000000E+00	0.000000000E+00	622	621	594	646
568	1	0.000000000E+00	0.000000000E+00	636	647	653	635
569	1	0.000000000E+00	0.000000000E+00	616	615	601	573
570	1	0.000000000E+00	0.000000000E+00	624	608	606	612
571	1	0.000000000E+00	0.000000000E+00	616	573	494	617
572	1	0.000000000E+00	0.000000000E+00	615	614	611	601
573	1	0.000000000E+00	0.000000000E+00	618	617	494	496
574	1	0.000000000E+00	0.000000000E+00	619	618	496	495
575	1	0.000000000E+00	0.000000000E+00	619	495	488	620
576	1	0.000000000E+00	0.000000000E+00	646	594	592	647
577	1	0.000000000E+00	0.000000000E+00	620	488	593	621
578	1	0.000000000E+00	0.000000000E+00	621	593	594	594

ELEM	FACE	VALUE(S)		FACE NODES			
579	1	0.000000000E+00	0.000000000E+00	614	613	610	611
580	1	0.000000000E+00	0.000000000E+00	608	607	605	606
581	1	0.000000000E+00	0.000000000E+00	635	653	652	623
582	1	0.000000000E+00	0.000000000E+00	564	565	605	607
583	1	0.000000000E+00	0.000000000E+00	564	556	555	565
584	1	0.000000000E+00	0.000000000E+00	594	593	591	592
585	1	0.000000000E+00	0.000000000E+00	647	648	654	653
586	1	0.000000000E+00	0.000000000E+00	543	561	560	542
587	1	0.000000000E+00	0.000000000E+00	603	560	561	561
588	1	0.000000000E+00	0.000000000E+00	604	623	602	603
589	1	0.000000000E+00	0.000000000E+00	611	600	601	601
590	1	0.000000000E+00	0.000000000E+00	613	612	609	610
591	1	0.000000000E+00	0.000000000E+00	652	653	654	654
592	1	0.000000000E+00	0.000000000E+00	601	600	572	573
593	1	0.000000000E+00	0.000000000E+00	647	592	590	648
594	1	0.000000000E+00	0.000000000E+00	593	488	493	591
595	1	0.000000000E+00	0.000000000E+00	573	572	498	494
596	1	0.000000000E+00	0.000000000E+00	652	654	655	655
597	1	0.000000000E+00	0.000000000E+00	611	599	600	600
598	1	0.000000000E+00	0.000000000E+00	654	648	649	655

ELEM	FACE	VALUE(S)		FACE NODES			
599	1	0.000000000E+00	0.000000000E+00	612	606	596	609
600	1	0.000000000E+00	0.000000000E+00	592	591	589	590
601	1	0.000000000E+00	0.000000000E+00	611	610	598	599
602	1	0.000000000E+00	0.000000000E+00	650	652	655	655
603	1	0.000000000E+00	0.000000000E+00	600	599	571	572
604	1	0.000000000E+00	0.000000000E+00	648	590	588	649
605	1	0.000000000E+00	0.000000000E+00	649	650	655	655
606	1	0.000000000E+00	0.000000000E+00	623	652	651	602
607	1	0.000000000E+00	0.000000000E+00	591	493	492	589
608	1	0.000000000E+00	0.000000000E+00	606	605	595	596
609	1	0.000000000E+00	0.000000000E+00	572	571	499	498
610	1	0.000000000E+00	0.000000000E+00	610	609	597	598
611	1	0.000000000E+00	0.000000000E+00	651	652	650	650
612	1	0.000000000E+00	0.000000000E+00	603	602	559	560
613	1	0.000000000E+00	0.000000000E+00	590	589	587	588

614	1	0.000000000E+00	0.000000000E+00	605	565	566	595
615	1	0.000000000E+00	0.000000000E+00	599	598	570	571
616	1	0.000000000E+00	0.000000000E+00	649	588	586	650
617	1	0.000000000E+00	0.000000000E+00	565	555	554	566
618	1	0.000000000E+00	0.000000000E+00	586	651	650	650

ELEM	FACE	VALUE(S)		FACE NODES			
619	1	0.000000000E+00	0.000000000E+00	560	559	541	542
620	1	0.000000000E+00	0.000000000E+00	589	492	491	587
621	1	0.000000000E+00	0.000000000E+00	571	570	500	499
622	1	0.000000000E+00	0.000000000E+00	609	596	584	597
623	1	0.000000000E+00	0.000000000E+00	598	597	569	570
624	1	0.000000000E+00	0.000000000E+00	588	587	585	586
625	1	0.000000000E+00	0.000000000E+00	651	576	602	602
626	1	0.000000000E+00	0.000000000E+00	596	595	583	584
627	1	0.000000000E+00	0.000000000E+00	602	576	577	559
628	1	0.000000000E+00	0.000000000E+00	570	569	501	500
629	1	0.000000000E+00	0.000000000E+00	587	491	490	585
630	1	0.000000000E+00	0.000000000E+00	651	586	575	576
631	1	0.000000000E+00	0.000000000E+00	595	566	567	583
632	1	0.000000000E+00	0.000000000E+00	597	584	568	569
633	1	0.000000000E+00	0.000000000E+00	586	585	574	575
634	1	0.000000000E+00	0.000000000E+00	566	554	553	567
635	1	0.000000000E+00	0.000000000E+00	559	558	540	541
636	1	0.000000000E+00	0.000000000E+00	569	568	502	501
637	1	0.000000000E+00	0.000000000E+00	585	490	489	574
638	1	0.000000000E+00	0.000000000E+00	559	577	517	558

ELEM	FACE	VALUE(S)		FACE NODES			
639	1	0.000000000E+00	0.000000000E+00	584	583	532	531
640	1	0.000000000E+00	0.000000000E+00	576	575	519	518
641	1	0.000000000E+00	0.000000000E+00	576	518	517	577
642	1	0.000000000E+00	0.000000000E+00	584	531	530	568
643	1	0.000000000E+00	0.000000000E+00	583	567	533	532
644	1	0.000000000E+00	0.000000000E+00	575	574	520	519
645	1	0.000000000E+00	0.000000000E+00	567	553	529	533
646	1	0.000000000E+00	0.000000000E+00	558	517	515	540
647	1	0.000000000E+00	0.000000000E+00	568	530	497	502
648	1	0.000000000E+00	0.000000000E+00	574	489	487	520
228	2	319.633248	0.000000000E+00	286	284	264	266
229	2	319.633248	0.000000000E+00	287	286	266	267
230	2	319.633248	0.000000000E+00	288	287	267	268
231	2	319.633248	0.000000000E+00	289	288	268	269
232	2	319.633248	0.000000000E+00	290	289	269	270
233	2	319.633248	0.000000000E+00	291	290	270	271
234	2	319.633248	0.000000000E+00	292	291	271	272
235	2	319.633248	0.000000000E+00	274	292	272	265
236	2	319.633248	0.000000000E+00	293	285	284	286
237	2	319.633248	0.000000000E+00	294	293	286	287

ELEM	FACE	VALUE(S)		FACE NODES			
238	2	319.633248	0.000000000E+00	295	294	287	288
239	2	319.633248	0.000000000E+00	296	295	288	289
240	2	319.633248	0.000000000E+00	297	296	289	290
241	2	319.633248	0.000000000E+00	298	297	290	291
242	2	319.633248	0.000000000E+00	299	298	291	292
243	2	319.633248	0.000000000E+00	275	299	292	274
244	2	319.633248	0.000000000E+00	277	276	285	293
245	2	319.633248	0.000000000E+00	278	277	293	294
246	2	319.633248	0.000000000E+00	279	278	294	295
247	2	319.633248	0.000000000E+00	280	279	295	296
248	2	319.633248	0.000000000E+00	281	280	296	297
249	2	319.633248	0.000000000E+00	282	281	297	298
250	2	319.633248	0.000000000E+00	283	282	298	299
251	2	319.633248	0.000000000E+00	273	283	299	275
315	2	319.633248	0.000000000E+00	361	363	366	364
316	2	319.633248	0.000000000E+00	364	366	368	365
317	2	319.633248	0.000000000E+00	363	362	367	366
318	2	319.633248	0.000000000E+00	368	366	367	367
319	2	319.633248	0.000000000E+00	365	368	285	276
320	2	319.633248	0.000000000E+00	362	264	284	367

ELEM	FACE	VALUE($)		FACE NODES			
321	2	319.633248	0.000000000E+00	368	367	284	285
322	2	3111.13115	0.000000000E+00	373	274	265	369
323	2	3111.13115	0.000000000E+00	374	373	369	370
324	2	3111.13115	0.000000000E+00	202	374	370	201
325	2	3111.13115	0.000000000E+00	375	275	274	373
326	2	3111.13115	0.000000000E+00	376	375	373	374
327	2	3111.13115	0.000000000E+00	203	376	374	202
328	2	3111.13115	0.000000000E+00	371	273	275	375
329	2	3111.13115	0.000000000E+00	372	371	375	376
330	2	3111.13115	0.000000000E+00	196	372	376	203

LIST ELEMENT CONVECTIONS FOR ALL SELECTED ELEMENTS

LIST SOLID MODEL BOUNDARY CONDITIONS (LABEL = APSF)
ON ALL SELECTED AREAS

AREA	PRESSURE	SLKCN	SLDIR	SLZERO	SLOPE
1	0.000E+00	0	0	0.000E+00	0.000E+00
2	0.000E+00	0	0	0.000E+00	0.000E+00
3	0.000E+00	0	0	0.000E+00	0.000E+00
4	0.000E+00	0	0	0.000E+00	0.000E+00
7	0.000E+00	0	0	0.000E+00	0.000E+00
8	0.000E+00	0	0	0.000E+00	0.000E+00
9	0.000E+00	0	0	0.000E+00	0.000E+00
10	0.000E+00	0	0	0.000E+00	0.000E+00
11	0.000E+00	0	0	0.000E+00	0.000E+00
12	0.000E+00	0	0	0.000E+00	0.000E+00
13	0.000E+00	0	0	0.000E+00	0.000E+00
14	0.000E+00	0	0	0.000E+00	0.000E+00

LIST SOLID MODEL BOUNDARY CONDITIONS (LABEL = ACVS)
ON ALL SELECTED AREAS

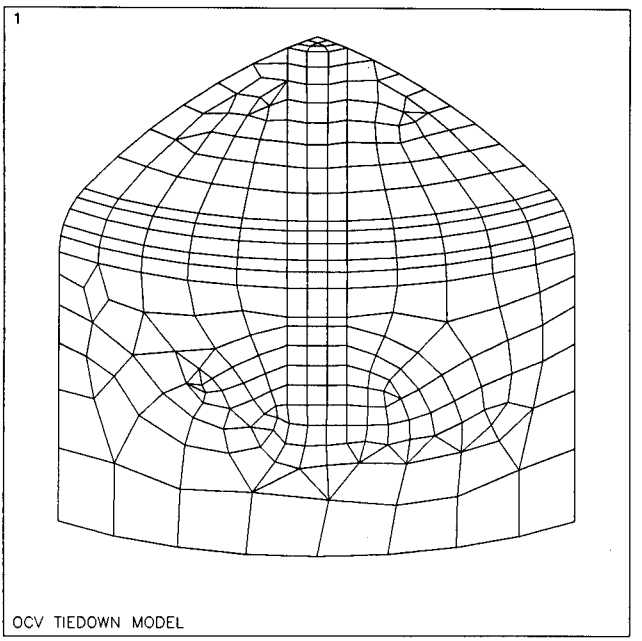


FIGURE 2.10.5-1.

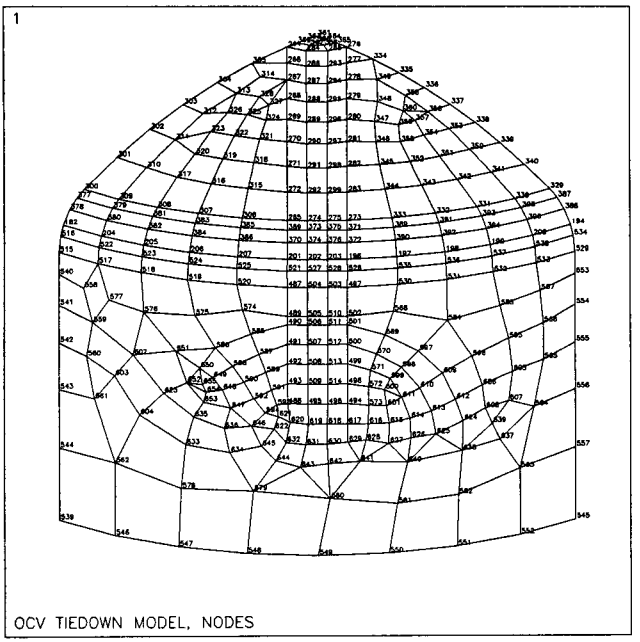


FIGURE 2.10.5-2.

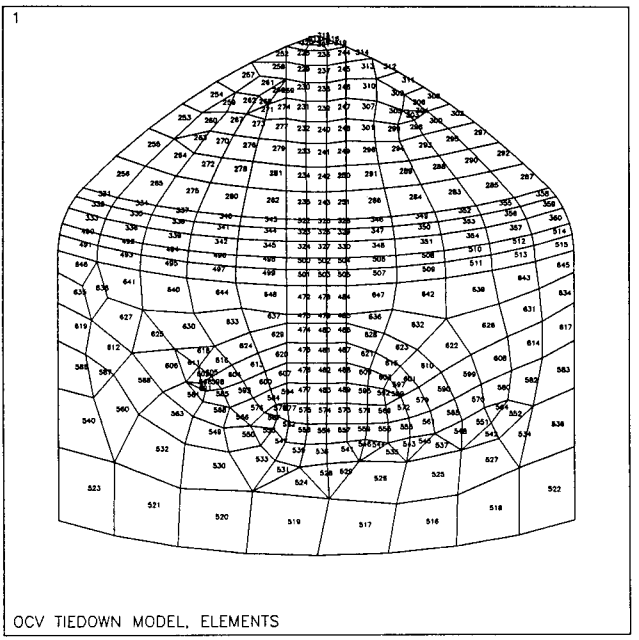


FIGURE 2.10.5-3.

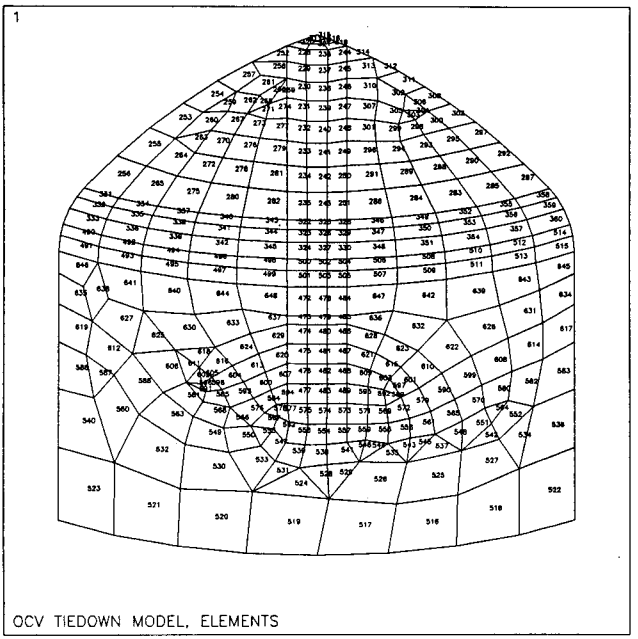


FIGURE 2.10.5-4.

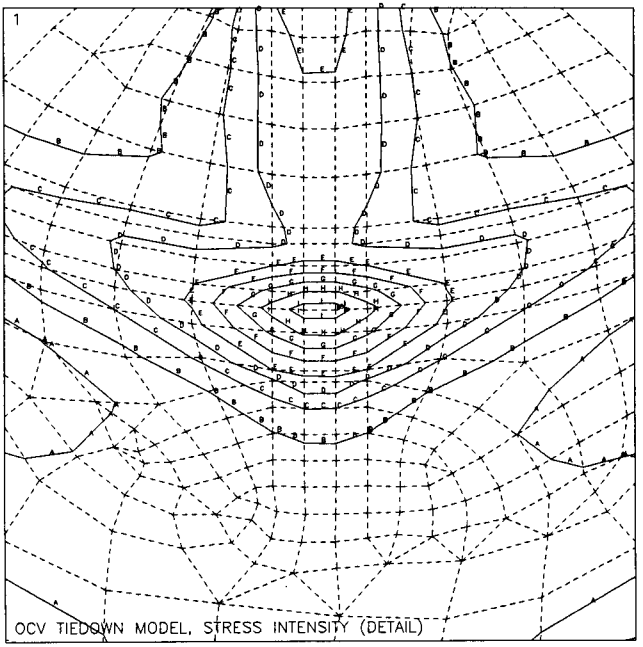


FIGURE 2.10.5-5.

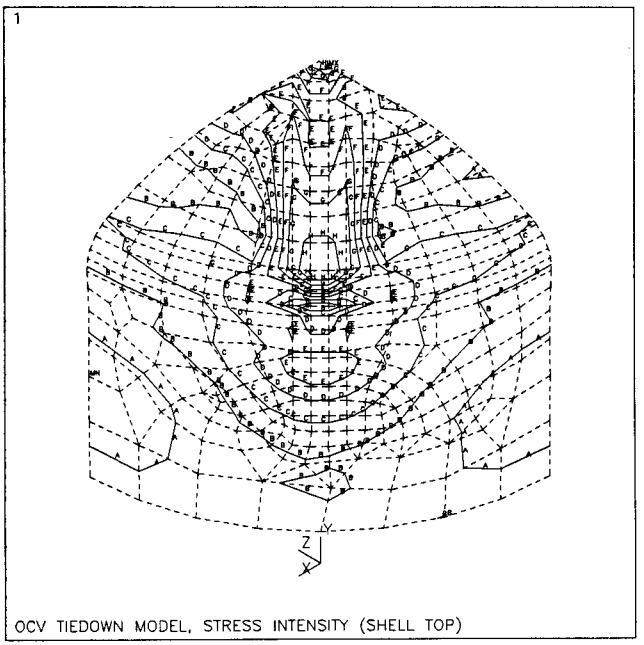


FIGURE 2.10.5-6.

2.10.6 Elastomer O-ring Performance Test Data

Radioisotope Thermoelectric Generator Transportation System Packaging O-Ring Material Thermal Validation Test Report

1.0 INTRODUCTION

The Radioisotope Thermoelectric Generator (RTG) Transportation System packaging uses elastomeric O-rings for the primary containment boundary seals. These O-rings are required to maintain leaktight containment (i.e., part of an integrated leakage rate of less than 1.0×10^{-7} scc/sec, air) under normal conditions of transport (NCT) and hypothetical accident conditions (HAC), as set forth in 10 CFR 71. (The foregoing definition of the term "leaktight" is assumed in the balance of this report.) The tests described herein were performed to demonstrate the ability of the elastomer material to perform adequately under the conditions of compression, temperature, and time at temperature that are predicted to occur in the RTG packaging under both NCT and HAC.

2.0 PURPOSE

These tests were performed to demonstrate the ability of the elastomer material to provide a leaktight seal under specific conditions of compression, temperature, and time at temperature. The material used in the tests, Butyl compound RR0405-70, manufactured by Rainier Rubber of Seattle, Washington, is identical to that used in the full-scale packaging seals.

3.0 TEST DESCRIPTION

Sample O-rings made of the subject Butyl material were tested in a test fixture constructed to test four different compressions during one sequence. The fixture consists of an inner plate with three concentric O-ring grooves of different depths on each side. Each side is then assembled by bolting a circular plate on each side with shims between each side plate and the inner plate sized to give the desired compression on the O-rings (see 4.1, Discussion of Compression Ranges). The outer O-rings have a higher compression and the center O-rings are in place to allow the inner/outer O-rings to be tested. The center O-rings have a considerably higher compression (21%) to assure sealing under all conditions. All O-rings had a nominal cross-section diameter of 0.275 in. Leakage rate testing was performed on the spaces between the outer/center and inner/center O-rings via ports through the outer plates. The fixture was placed within an environmental test chamber and brought to uniform temperatures for specified times. The test consisted of an initial low temperature segment at -40 °F, followed by a 380 °F segment for 24 hours, then continuing at 350 °F for 144 hours, followed by a final low-temperature segment at -20 °F. Upon initial assembly and the end of each low-temperature segment, the O-rings were tested for leaktight conditions using standard helium mass spectrometer leakage rate testing equipment. At the end of each high-temperature segment, a vacuum test was performed using the mass spectrometer to achieve a pressure low enough to perform a test (less than 0.2 mbar). Details are given in the following section.

4.0 TEST PARAMETERS

This section will discuss the calculation of O-ring specimen compression in the fixture, followed by test temperature/time specifications.

4.1 DISCUSSION OF COMPRESSION RANGES

With the O-rings installed in the accommodation grooves of the center plate, the compression condition is a function of the space available for the cross-section to occupy. This space is controlled by the depth of the groove and the shims installed. Shims are installed inboard and outboard of the three concentric grooves between each of eight bolts on each side.

The test fixture is shown on Packaging Technology, Inc. (PacTec) drawing D-AA-314. The fixture dimensions are listed in Table 4.1-1.

Table 4.1-1. Test Fixture Dimensions.

Feature	Dimension (in.) left side*	Dimension (in.) right side*
Outer O-ring groove depth (x)	.2053	.2075
Center O-ring groove depth (y)	.175	.175
Inner O-ring groove depth (z)	.200	.2033
Shim thickness (t) L, R (t)	.044	.031
Average outer O-ring cross-section (Dmo)	.2770	.2776
Average center O-ring cross-section (Dmc)	.2772	.2773
Average inner O-ring cross-section (Dmi)	.2773	.2774

* Left and right sides are delineated by the installation into the environmental chamber viewed facing the unit door.

The values of compression in the test fixture will now be calculated. The space available for the O-ring to occupy is equal to the sum of the groove depth plus the shim thickness, or (x), (y) or (Z) to (t).

The compression of the outer O-ring is then

$$C_j = \frac{D_{moj} - [x + t_j]}{D_{moj}} \qquad j = \text{Left, Right}$$

for the left side, outer O-ring:

X_{left} = .2053

Dmo(left) = .2770

t_{left} = .044

$$C_{left(outer)} = \frac{.2770 - (.2053 + .044)}{.2770}$$

= .10 (10%)

Using the same method as described above, the compression values for a completely full test fixture are listed in Table 4.1-2.

Table 4.1-2. Compression Values (%).

Location	Left	Right
Outer	10%	14%
Center	21%	21%
Inner	12%	15.5%

4.2 TEST CONDITIONS

Before being subjected to test conditions, the fixture was assembled with the proper O-ring and the center and outer seals. (The inner O-rings were not available at this time.) This pair of specimens, at compressions of 10% (left side) and 14% (right side) was tested at the temperatures and time durations shown in Table 4.2-1.

Table 4.2-1. Temperature/Time Segment Test Parameters.

Test Segment	Temperature (°F)	Time duration (hr)	Test Type
Initial assembly	Ambient	Immediate upon assembly	Helium
Low-temperature (1)	-40	Immediate upon stabilization	Helium
High-temperature (1)	380	24	High vacuum*
High-temperature (2)	350	144	High vacuum*
Low-temperature (2)	-20	Immediate upon stabilization	Helium

*Less than 0.2 mbar.

5.0 EQUIPMENT

5.1 TEST HARDWARE AND EQUIPMENT

The fixture used for the O-ring testing is shown in PacTec drawing D-AA-314. The test was conducted in an environmental test chamber capable of accommodating the fixture, cooling it to -40 °F, and warming it to 380 °F. Helium-based leakage rate test equipment with a minimum sensitivity of 2×10^{-9} scc/sec. was used to establish O-ring leakage rates at temperatures throughout the test range.

5.2 TEST SPECIMEN

The O-ring test specimens were made from Rainier Rubber Butyl compound RR0405-70. The O-ring cross-sectional diameter was nominally 0.275 in. The cross-sectional diameter was measured in 4 quadrants before and after testing. Each O-ring test specimen contained at least one production-quality splice. Actual dimensions for each O-ring test specimen are given in Table 4.1-1. As inner O-rings were not available at the time of the test, only outer O-rings (10% and 14% compression) were installed.

5.3 LEAKAGE MEASUREMENT

Leakage rate test equipment, equipment operational calibration, and connection to the test fixture was the responsibility of Nondestructive Examination (NDE) technicians. Leakage rate tests were performed in accordance with WHC-CM-4-38, Nondestructive Examination Procedures, NDT-LT-6000, Appendix A and the Helium Mass Spectrometer Test - Tracer Probe and Hood Techniques method described in the American Society of Mechanical Engineers (ASME) Boiler and Pressure Vessel Code, Section V, Article 10, Appendix V.

5.4 TEMPERATURE MEASUREMENT

Temperature measurement data was recorded and printed using a six-thermocouple data logger system.

5.5 HEATING AND COOLING

An electric resistance, heated oven was used for heating and cooling the test fixture. Bottled CO_2 gas was used for the cooling function.

6.0 RESULTS

Detailed test results are provided in Reference 1. The test results are summarized in Table 6-1. The specimens were leakage rate tested against an acceptance criteria of 1×10^{-7} scc/sec (air). All O-ring tests were satisfactory and the O-rings did not show any sign of failure over the entire test sequence.

Table 6-1. Summary of Test Results.

O-ring	Compression (%)	Test Temperature	Leaktight per criteria?
Left (outer)	10	-40 °F then 380 °F for 8 hr. then 350 °F for 144 hr. then -20 °F	Yes
Right (outer)	14		Yes

Subsequent to testing, minor changes in durometer were noted, and the O-rings took a compression set, as shown by the post-test cross-sectional diameter measurements of Table 6-2. These changes had no apparent effect on the ability of the O-ring to maintain leaktight integrity for

the range of temperatures and durations tested.

Table 6-2. O-ring Specimen Measurement Data.

O-ring Location	Measurement Sequence B: before test A: after test	Cross-sectional Diameter Axial Direction (in.)	O-ring Inside Diameter (in.)	Hardness (durometer)
Left (outer)	B	.2770	12.96	57
Left (outer)	A	.2380	12.71	66
Right (outer)	B	.2776	12.96	56
Right (outer)	A	.2500	12.70	64

7.0 CONCLUSIONS

The Butyl O-ring material to be used in the RTG Transportation System Packaging has been demonstrated to be satisfactory at compression values as low as 10% and at the temperatures and durations listed in Table 6-1, including pre-test segments at -40 °F, and post-test segments at -20 °F.

8.0 REFERENCES

1. *Radioisotope Thermoelectric Generator Transportation System Packaging O-ring Material Thermal Validation Test Report for Face Seal Test Fixture*, WHC-SD-RTG-TRP-010.

2.10.7 Summary of Thermal Load Cases and Results

This appendix summarizes key temperature results from Sections 3.6.4 and 3.6.5 for use in Chapter 2.0 and 4.0. Nodes are identified in Figures 3.4.1-2, details A through D.

2.10.7.1 Normal Conditions of Transport.

TABLE 2.10.7.1-1. Regulatory NCT and Operational Conditions Load Cases.

Condition	Case 1	Case 2	Case 3
Solar	Full solar	No solar	Full solar
Ambient temperature	100 °F	-40 °F	100 °F
Payload	Maximum heat	Maximum heat	Maximum heat
Cooling	No active cooling	No active cooling	Active cooling (both loops)

TABLE 2.10.7.1-2. Regulatory Normal Conditions of Transport Load Case 1 Results.

Package component	Model node number	Temperature °F
Ambient air	1	100
OCV top	300 / 304	267 / 237
Coolant jacket	326	238
OCV sidewall	320	284
OCV base	360	220
ICV top	200 / 204	338 / 308
ICV sidewall	220	329
ICV base	261	222
OCV main seals	350	210
ICV main seals	250	219
OCV fin	305	158
Impact limiter shell	406 / 408 / 410	153 / 123 / 132
Impact limiter foam	421 / 455	203 / 128

TABLE 2.10.7.1-3. Regulatory Normal Conditions of Transport Load Case 2 Results.

Package component	Model node number	Temperature °F
Ambient air	1	-40
OCV top	300 / 304	148 / 105
Coolant jacket	326	115
OCV sidewall	320	165
OCV base	360	74
ICV top	200 / 204	245 / 203
ICV sidewall	220	220
ICV base	261	76
OCV main seals	350	61
ICV main seals	250	73
ICV fin	305	12
Impact limiter shell	406 / 408 / 410	-13 / -34 / -23
Impact limiter foam	421 / 455	55 / -28

TABLE 2.10.7.1-4. Operational Conditions Load Case 3 Results.

Package component	Model node number	Temperature °F
Ambient air	1	100
Coolant fluid	901	40
OCV top	300 / 304	222 / 178
Coolant jacket	326	48
OCV sidewall	320	59
OCV base	360	87
ICV top	200 / 204	275 / 231
ICV sidewall	220	134
ICV base	261	87
OCV main seals	350	85
ICV main seals	250	83
OCV fin	305	135
Impact limiter shell	406 / 408 / 410	122 / 119 / 116
Impact limiter foam	421 / 455	91 / 117

TABLE 2.10.7.1-5. Summary of NCT Gas Temperatures.

Condition	Case 1 full solar 100 °F ambient no cooling	Case 2 no solar -40 °F ambient no cooling	Case 3 full solar 100 °F ambient active cooling
ICV internal gas temperature (°F)	354	256	213
OCV internal gas temperature (°F)	285	165	115

TABLE 2.10.7.1-6. Summary of NCT Gas Pressures (excluding payload gas generation).

Condition	Case 1 full solar 100 °F ambient no cooling	Case 2 no solar -40 °F ambient no cooling	Case 3 full solar 100 °F ambient active cooling
ICV internal gas temperature (psia)	24.4	21.5	20.2
OCV internal gas temperature (psia)	26.3	22.1	20.3

2.10.7.2 Hypothetical Accident Conditions.

TABLE 2.10.7.2-1. Load Cases for the Hypothetical Accident Condition Analyses.

Case	Pre-hypothetical accident conditions	Post-hypothetical accident conditions
1	a. Undamaged payload, 4,500 W maximum decay heat load. b. Undamaged package, upright position, adiabatic bottom conditions. c. Cooling jacket drained d. Steady state conditions with 100 °F still air; no solar.	a. Circumferential distribution of heat-source modules on barrier plate, 4,500 W total. b. Side drop impact limiter damage; package upright, all surfaces exposed to ambient. c. Cooling jacket drained. d. 1475 °F fire for 30 minutes, followed by ambient air at 100 °F; no solar during and after fire.
2	Same as load case No. 1 except: d. Steady state conditions with -20 °F still air; no solar.	Same as load case No. 1 except: d. 1475 °F fire for 30 minutes, followed by ambient air at -20 °F; no solar during and after fire.
3	Same as load case No. 1.	Same as load case No. 1, except: a. Axial distribution of heat-source modules along ICV wall above rubble dam; 4,500 W total b. Side drop impact limiter damage; package on its side, all surfaces exposed.
4	Same as load case No. 2.	Same as load case No. 3, except: d. 1475 °F fire for 30 minutes, followed by ambient air at -20 °F; no solar during and after fire.
5	Same as load case No. 1.	Same as load case No. 1, except: a. Ungula shaped rubble pile of heat source modules on barrier plate; 4,500 W total. b. Side drop impact limiter damage; package at 45° angle of repose, all surfaces exposed.
6	Same as load case No. 2.	Same as load case No. 5, except: d. 1475 °F fire for 30 minutes, followed by ambient air at -20 °F; no solar during and after fire.

TABLE 2.10.7.2-2. Summary of HAC Peak Temperatures.

Condition	Case 1	Case 2	Case 3	Case 4	Case 5	Case 6
ICV internal gas temperature (°F)	836	779	747	684	840	782
OCV internal gas temperature (°F)	849	796	851	798	852	799

TABLE 2.10.7.2-3. Summary of HAC Pressures (excluding gas generation).

Condition	Case 1	Case 2	Case 3	Case 4	Case 5	Case 6
ICV internal gas pressure (psia)	38.9	37.2	36.2	34.3	39.0	37.3
OCV internal gas pressure (psia)	46.2	44.3	46.2	44.4	46.3	44.4

2.10.8 OCV Two-Dimensional (Axisymmetric) ANSYS Model

2.10.8.1 Description. The 2-D, OCV model is an axisymmetric finite element model of the entire OCV. It consists of a base and a bell, connected by a bolt element and flange interface gap elements. It is used to evaluate containment vessel stresses and closure bolt stresses under NCT and closure bolt stresses and residual O-ring compression under HAC. Further use of the model is made to determine stresses in the torispherical head under NCT compression loads. The containment bell, the bolting flange, the thermal shield, and the coolant jacket are fully modeled. The fins, which are only significant to lifting analyses, are not modeled. The tiedown strap doublers, which are only significant to the tiedown analysis, are also not included. The applied loading takes the form of internal gas pressure, nodal temperatures, and initial closure bolt pre-load. Certain node locations were chosen to coincide with the nodes found in the SINDA thermal models described in Section 3. The relative displacement of two coincident nodes, one belonging to the OCV base structure and one to the bell at the location of the containment O-ring, are used to determine the change in O-ring compression because of the applied conditions. The model layout is shown in Figure 2.10.8-1. The model is used for the OCV analysis for the NCT load cases given in Table 2.6.1.3-1, the HAC load cases given in Table 2.7.3.1.1.3-1, and the compression analysis of Section 2.6.9.

2.10.8.2 Construction. The model consists of five element types:

1. To model the containment boundary near the OCV flange, 2-D isoparametric elements are used. This element type is used to a distance of 5.50 in. above the bottom of the OCV flange (this level corresponds to the top of the thermal shield). The entire OCV base is also modeled with this element type.

2. For the remainder of the containment vessel, for the thermal shield, and for the coolant jacket, axisymmetric shells are used, located at the section midplane. To join shell and isoparametric elements, embedded elements are used, having 1/10th the bending stiffness of the adjacent shell elements (see Reference 25, Chapter 9). The containment shell elements are 0.50 in. thick, the thermal shield contains elements of 0.25 and 0.375 in. in thickness, and the coolant jacket contains elements of 0.135 and 0.25 in. in thickness.

3. A single 2-D spar (element 100, nodes 15 and 120) was used to represent all of the closure bolts. The property of bolt area was entered on a per-radian basis. It was calculated by first multiplying the standard area of each closure bolt by the total bolt quantity (24) and then dividing by 2π. The standard area of each bolt was a length-weighted average of shank area and thread area and is equal to 1.10 $in.^2$. The bolt element was also given an initial strain to achieve the desired closure bolt pre-load force at 70 °F, in the absence of other applied loads, per Table 2.6.1.2.1-1.

4. A single 2-D beam (element 101) was used to represent the closure bolt access tubes. The properties of tube area and moment of inertia were entered on a per-radian basis. They were calculated by first multiplying the standard area and moment of inertia of each tube by the total tube quantity (24) and then dividing by 2π. To accomplish moment transfer between the beam element and the 2-D isoparametric elements of the flange, an embedded element, having 1/10th of the area and moment of inertia of the tube element, was used.

5. Four gaps are used between the OCV base and OCV flange (located at flange nodes 1, 11, 16, 21, and 26) to react the closure bolt loads and to model the propensity of the OCV flange to pivot about its outside edge because of thermal distortion.

Model node and element plots of key portions of the model are given in Figures 2.10.8-2

through 2.10.8-7. An interpreted ANSYS input listing is given in Table 2.10.8-1.

2.10.8.3 Material Properties. The modulus of elasticity and coefficient of thermal expansion varied with temperature according to the data in Tables 2.3-1 and 2.3-2. Poisson's ratio was 0.3.

2.10.8.4 Constraints. The bottom center node of the OCV base was fixed in all coordinate directions. In addition, one other node at the OCV base center and the node at the center of the OCV head were fixed in the radial direction, and all nodes are fixed in the hoop direction, consistent with axisymmetry. The top center node was also restrained from rotation about the hoop axis. For the compression analysis, the lower edge of the OCV flange is fixed in the axial direction.

2.10.8.5 Applied Loading. All surfaces subject to internal pressure had a constant pressure applied. Nodal temperature loading was applied using temperatures resulting from NCT thermal model output. Because there were fewer thermal model nodes than structural model nodes, interpolation of NCT thermal model temperatures was required. Temperatures in the OCV base were set as follows: nodes 155 to 162 are set to thermal node 360; nodes 149 and 150 are set to thermal node 362; nodes 143 and 144 are set to thermal node 364; nodes 119 to 140 and 163 are set to the average of thermal nodes 366 and 367; and nodes 101 to 118 are set to the average of thermal nodes 368 and 369. The rectangular portion of the OCV flange used thermal nodes 350, 352, 354, and 356, and the angled portion used thermal node 344. The thermal shield used thermal nodes 345 to 347. The closure bolt temperature was set using thermal model node 353 for the upper shank and node 355 for the lower threads. In the region above the OCV flange where shell elements were used, the temperatures of structural nodes that corresponded exactly to the thermal model counterparts were set directly, and the temperatures of structural nodes which fell in between thermal nodes were established using linear interpolation. The reference was 70 °F.

For the compression load case, the applied loading was 50 psi on the torispherical head and knuckle, using temperatures from NCT case 1, and no internal pressure.

2.10.8.6 Results. A plot of stress intensity corresponding to the analysis described in Section 2.6.9 is shown in Figure 2.10.8-8. Worst-case containment boundary stresses for NCT loadings (see Section 2.6.1.3) are shown in Figures 2.10.8-9 through 2.10.8-11, and a corresponding plot of stress intensity in the OCV flange is shown in Figure 2.10.8-12. A plot of worst-case OCV flange stress intensity for HAC loadings is shown in Figure 2.10.8-13. Closure bolt stress results are given in Sections 2.6.1.2.1 and 2.7.3.2. Relative thermal distortion of the containment O-ring seal area is discussed in Section 4.3.2.

2.10.8.7 Refined Model. A refined version of the model was also developed, and is shown in Figure 2.10.8-14. The refinement occurs in the flange-to-base interface region, where the number of gap elements is increased from four to 17. The position of the outermost gap, at the flange pry point, is unchanged. The increased density of gaps serves the purpose of more accurately calculating the bolt loads and the thermal distortion at the containment O-ring in the worst-case HAC fire event. Gap elements have a zero (or negligible) stiffness when open, and a stiffness when closed that represents the "bearing" of the surfaces in contact. In the HAC fire event, the OCV bell flange rotates a small amount by pivoting about the pry point at the outside edge of the flange, loading the closure bolts. The prying force creates a contact stress in the flange and base material that causes the pry point to increase to an area. The area extends until the prying load can be supported without exceeding the yield strength of the material. This is accomplished in the modeling process by decreasing the closed stiffness of the interface gap elements such that the flange and base portions of the model "pass through" each other under load, allowing more gap elements to come in contact, and thus modeling the actual contact area. A plot of the distorted

model under HAC fire conditions is shown in Figure 2.10.8-15. The area in contact is calculated based on the number of gaps in contact. The model was run, using decreased gap stiffness values, until the sum of closed gap forces (the prying force) could be supported on the contact area (located in between the closed gaps) without exceeding the yield strength of 304L at a conservative temperature of 160 °F. The use of yield strength conservatively ignores strain hardening. The overall effect of this refinement is to increase conservatively the opening between the flange and base at the containment O-ring, thus decreasing seal compression. To increase conservatism further in the analysis of seal opening, a run was made using only 70% of the nominal bolt preload force. An additional run was made focusing on maximum bolt load, using 130% of nominal bolt preload force.

Other aspects of the refined model are identical to those described in Sections 2.10.8.1 through 2.10.8.6 above. An interpreted ANSYS input listing is given in Table 2.10.8-2.

TABLE 2.10.8-1. Interpreted ANSYS Input Listing.

```
STATIC ANALYSIS (KAN= 0)

LINEAR ANALYSIS - NO NON-LINEAR PROPERTIES

REFERENCE TEMPERATURE=    70.000 (TREF)
UNIFORM TEMPERATURE  =   -40.000 (TUNIF)

*****ANALYSIS OPTIONS (KAY VALUES) (IF ANY) *****

NO STATIC INTERPOLATION/EXTRAPOLATION (KAY(3)=0)

SMALL DEFLECTION SOLUTION (KAY(6)=0)

NO STRESS STIFFENING (KAY(8)=0)

USE INITIAL-STIFFNESS NEWTON-RAPHSON SOLUTION PROCEDURE  (KAY(9)=3)

IN-CORE WAVE-FRONT EQUATION SOLVER (KAY(10)=0)

LIST ELEMENT TYPES FROM  1 TO 20 BY 1

NO. STIF          KEYOPT VALUES          INOPR
 1   42   0  0  1   0  0  0   0  0  0   0  ISOPAR. STRESS SOLID, 2-D
 2   51   0  0  0   0  0  0   0  0  0   0  PLASTIC AXISYM. CONIC SHELL
 3    1   0  0  0   0  0  0   0  0  0   0  SPAR, 2-D
 4    3   0  0  0   0  0  0   0  0  0   0  ELASTIC BEAM, 2-D
 5   12   0  0  0   0  0  0   0  0  0   0  INTERFACE ELEM. 2-D

LIST ALL REAL SETS

 REAL CONSTANT SET   2  ITEMS   1 TO   6
  0.50000       0.00000E+00  0.00000E+00  0.00000E+00  0.00000E+00  0.00000E+00

 REAL CONSTANT SET   3  ITEMS   1 TO   6
    4.2020      0.56140E-03  0.00000E+00  0.00000E+00  0.00000E+00  0.00000E+00

 REAL CONSTANT SET   4  ITEMS   1 TO   6
    3.4260       2.4330       2.5000       2.0000       0.00000E+00  0.00000E+00

 REAL CONSTANT SET   5  ITEMS   1 TO   6
  0.00000E+00  0.19100E+10  0.00000E+00  0.00000E+00  0.00000E+00  0.00000E+00

 REAL CONSTANT SET  21  ITEMS   1 TO   6
  0.37500       0.00000E+00  0.00000E+00  0.00000E+00  0.00000E+00  0.00000E+00

 REAL CONSTANT SET  22  ITEMS   1 TO   6
  0.25000       0.00000E+00  0.00000E+00  0.00000E+00  0.00000E+00  0.00000E+00

 REAL CONSTANT SET  23  ITEMS   1 TO   6
  0.13500       0.00000E+00  0.00000E+00  0.00000E+00  0.00000E+00  0.00000E+00

 REAL CONSTANT SET  24  ITEMS   1 TO   6
  0.23200       0.00000E+00  0.00000E+00  0.00000E+00  0.00000E+00  0.00000E+00

 REAL CONSTANT SET  25  ITEMS   1 TO   6
  0.34260       0.24330       0.25000       2.0000       0.00000E+00  0.00000E+00

 REAL CONSTANT SET  26  ITEMS   1 TO   6
  0.11600       0.00000E+00  0.00000E+00  0.00000E+00  0.00000E+00  0.00000E+00
LIST ALL COORDINATE SYSTEMS

    SYSTEM TYPE                      CENTER                PARAMETERS    SING KEYS
 0  0 (CARTESIAN)          0.000       0.000       0.000    0.000  0.000   0  0
 1  1 (CYLINDRICAL)        0.000       0.000       0.000    1.000  0.000   0  0
 2  2 (SPHERICAL)          0.000       0.000       0.000    1.000  1.000   0  0
11  1 (CYLINDRICAL)        0.000      25.150       0.000    1.000  1.000   0  0
12  1 (CYLINDRICAL)       14.940      54.290       0.000    1.000  1.000   0  0
```

SYSTEM	ORIENTATION VECTORS (X,Y,Z)								
0	1.00	0.00	0.00	0.00	1.00	0.00	0.00	0.00	1.00
1	1.00	0.00	0.00	0.00	1.00	0.00	0.00	0.00	1.00
2	1.00	0.00	0.00	0.00	1.00	0.00	0.00	0.00	1.00
11	1.00	0.00	0.00	0.00	1.00	0.00	0.00	0.00	1.00
12	1.00	0.00	0.00	0.00	1.00	0.00	0.00	0.00	1.00

CSYS	TYPE	XC	YC	ZC	THXY	THYZ	THXZ
11	1	0.00000E+00	25.150	0.00000E+00	0.000	0.000	0.000
12	1	14.940	54.290	0.00000E+00	0.000	0.000	0.000

LIST ALL SELECTED ELEMENTS. (LIST NODES)

ELEM	MAT	TYP	REL	ESYS	NODES			
1	1	1	1	0	1	2	7	6
2	1	1	1	0	2	3	8	7
3	1	1	1	0	3	4	9	8
4	1	1	1	0	4	5	10	9
5	1	1	1	0	6	7	12	11
6	1	1	1	0	7	8	13	12
7	1	1	1	0	8	9	14	13
8	1	1	1	0	9	10	15	14
9	1	1	1	0	11	12	17	16
10	1	1	1	0	12	13	18	17
11	1	1	1	0	13	14	19	18
12	1	1	1	0	14	15	20	19
13	1	1	1	0	16	17	22	21
14	1	1	1	0	17	18	23	22
15	1	1	1	0	18	19	24	23
16	1	1	1	0	19	20	25	24
17	1	1	1	0	26	21	22	22
18	1	1	1	0	22	23	28	27
19	1	1	1	0	23	24	29	28
20	1	1	1	0	24	25	30	29

ELEM	MAT	TYP	REL	ESYS	NODES			
21	1	1	1	0	27	28	33	32
22	1	1	1	0	28	29	34	33
23	1	1	1	0	29	30	35	34
24	1	1	1	0	33	34	39	38
25	1	1	1	0	34	35	40	39
26	1	1	1	0	32	33	38	38
27	1	1	1	0	38	39	43	42
28	1	1	1	0	39	40	44	43
29	1	1	1	0	42	43	46	45
30	1	1	1	0	43	44	47	46
31	1	1	1	0	45	46	49	48
32	1	1	1	0	46	47	50	49
33	1	1	1	0	101	102	109	108
34	1	1	1	0	102	103	110	109
35	1	1	1	0	103	104	111	110
36	1	1	1	0	104	105	112	111
37	1	1	1	0	105	106	113	112
38	1	1	1	0	106	107	114	113
39	1	1	1	0	108	109	116	115
40	1	1	1	0	109	110	117	116

ELEM	MAT	TYP	REL	ESYS	NODES			
41	1	1	1	0	110	111	118	117
42	1	1	1	0	111	112	119	118
43	1	1	1	0	112	113	120	119
44	1	1	1	0	113	114	121	120
45	1	1	1	0	115	116	123	122
46	1	1	1	0	116	117	124	123
47	1	1	1	0	117	118	125	124
51	1	1	1	0	122	123	130	129
52	1	1	1	0	123	124	131	130
53	1	1	1	0	124	125	132	131
54	1	1	1	0	125	126	133	132
57	1	1	1	0	129	130	137	136
58	1	1	1	0	130	131	138	137
59	1	1	1	0	131	132	139	138

60	1	1	1	0	132	133	140	139
63	1	1	1	0	136	137	144	143
64	1	1	1	0	137	138	145	144
65	1	1	1	0	138	139	146	145
66	1	1	1	0	139	140	147	146
69	1	1	1	0	143	144	151	150

ELEM	MAT	TYP	REL	ESYS	NODES			
70	1	1	1	0	144	145	152	151
75	1	1	1	0	150	151	158	157
76	1	1	1	0	151	152	159	158
81	1	1	1	0	157	158	165	164
82	1	1	1	0	158	159	166	165
87	1	1	1	0	164	165	172	171
88	1	1	1	0	165	166	173	172
93	1	1	1	0	125	118	178	126
94	1	1	1	0	118	119	178	178
95	1	2	2	0	49	53		
96	1	2	2	0	53	55		
97	1	2	2	0	55	57		
98	1	2	2	0	57	59		
99	1	2	2	0	59	61		
100	1	2	2	0	61	63		
101	1	2	2	0	63	65		
102	1	2	2	0	65	67		
103	1	2	2	0	67	69		
104	1	2	2	0	69	71		
105	1	2	2	0	71	73		

ELEM	MAT	TYP	REL	ESYS	NODES	
106	1	2	2	0	73	75
107	1	2	2	0	75	77
108	1	2	2	0	77	79
109	1	2	2	0	79	81
110	1	2	2	0	81	83
111	1	2	2	0	83	85
112	1	2	2	0	85	87
113	1	2	2	0	87	89
114	1	2	2	0	89	91
115	1	2	2	0	91	93
116	1	2	2	0	93	180
117	1	2	2	0	180	181
118	1	2	2	0	181	182
119	1	2	2	0	182	183
120	1	2	2	0	183	184
121	1	2	2	0	184	185
122	1	2	2	0	185	186
123	1	2	2	0	186	187
124	1	2	2	0	187	188
125	1	2	22	0	53	54

ELEM	MAT	TYP	REL	ESYS	NODES	
126	1	2	22	0	55	56
127	1	2	22	0	57	58
128	1	2	22	0	59	60
129	1	2	22	0	61	62
130	1	2	22	0	63	64
131	1	2	22	0	65	66
132	1	2	22	0	67	68
133	1	2	22	0	69	70
134	1	2	22	0	71	72
135	1	2	22	0	73	74
136	1	2	22	0	75	76
137	1	2	22	0	77	78
138	1	2	22	0	79	80
139	1	2	22	0	81	82
140	1	2	22	0	83	84
141	1	2	22	0	85	86
142	1	2	22	0	87	88
143	1	2	22	0	89	90

144	1	2	22	0	91	92
145	1	2	21	0	93	94

ELEM	MAT	TYP	REL	ESYS	NODES	
146	1	2	23	0	41	54
147	1	2	23	0	54	56
148	1	2	23	0	56	58
149	1	2	23	0	58	60
150	1	2	23	0	60	62
151	1	2	23	0	62	64
152	1	2	23	0	64	66
153	1	2	23	0	66	68
154	1	2	23	0	68	70
155	1	2	23	0	70	72
156	1	2	23	0	72	74
157	1	2	23	0	74	76
158	1	2	23	0	76	78
159	1	2	23	0	78	80
160	1	2	23	0	80	82
161	1	2	23	0	82	84
162	1	2	23	0	84	86
163	1	2	23	0	86	88
164	1	2	23	0	88	90
165	1	2	23	0	90	92

ELEM	MAT	TYP	REL	ESYS	NODES	
166	1	2	23	0	92	94
167	1	2	21	0	49	41
168	1	2	21	0	41	31
169	1	2	21	0	31	36
170	1	2	21	0	36	37
171	1	2	22	0	5	37
172	1	2	24	0	46	49
173	1	2	26	0	10	5
174	1	4	4	0	15	31
175	1	4	25	0	14	15
176	2	3	3	0	124	15
177	2	5	5	0	140	21
178	2	5	5	0	133	16
179	2	5	5	0	126	11
180	2	5	5	0	178	1

LIST ALL SELECTED NODE DSYS= 0

NODE	X	Y	Z	THXY	THYZ	THXZ
1	23.991	0.00000E+00	0.00000E+00	0.00	0.00	0.00
2	24.125	0.50000	0.00000E+00	0.00	0.00	0.00
3	24.125	1.4100	0.00000E+00	0.00	0.00	0.00
4	24.125	2.1150	0.00000E+00	0.00	0.00	0.00
5	24.125	2.8200	0.00000E+00	0.00	0.00	0.00
6	23.125	0.00000E+00	0.00000E+00	0.00	0.00	0.00
7	23.125	0.70500	0.00000E+00	0.00	0.00	0.00
8	23.125	1.4100	0.00000E+00	0.00	0.00	0.00
9	23.125	2.1150	0.00000E+00	0.00	0.00	0.00
10	23.125	2.8200	0.00000E+00	0.00	0.00	0.00
11	22.125	0.00000E+00	0.00000E+00	0.00	0.00	0.00
12	22.125	0.70500	0.00000E+00	0.00	0.00	0.00
13	22.125	1.4100	0.00000E+00	0.00	0.00	0.00
14	22.125	2.1150	0.00000E+00	0.00	0.00	0.00
15	22.125	2.8200	0.00000E+00	0.00	0.00	0.00
16	20.875	0.00000E+00	0.00000E+00	0.00	0.00	0.00
17	20.875	0.70500	0.00000E+00	0.00	0.00	0.00
18	20.875	1.4100	0.00000E+00	0.00	0.00	0.00
19	20.875	2.1150	0.00000E+00	0.00	0.00	0.00
20	20.875	2.8200	0.00000E+00	0.00	0.00	0.00

NODE	X	Y	Z	THXY	THYZ	THXZ
21	20.000	0.00000E+00	0.00000E+00	0.00	0.00	0.00
22	19.560	1.1300	0.00000E+00	0.00	0.00	0.00
23	19.643	1.6933	0.00000E+00	0.00	0.00	0.00
24	19.727	2.2567	0.00000E+00	0.00	0.00	0.00

25	19.810	2.8200	0.00000E+00	0.00	0.00	0.00
26	19.560	0.00000E+00	0.00000E+00	0.00	0.00	0.00
27	18.718	1.9725	0.00000E+00	0.00	0.00	0.00
28	18.936	2.4006	0.00000E+00	0.00	0.00	0.00
29	19.155	2.8286	0.00000E+00	0.00	0.00	0.00
30	19.373	3.2567	0.00000E+00	0.00	0.00	0.00
31	22.125	5.6320	0.00000E+00	0.00	0.00	0.00
32	17.875	2.8150	0.00000E+00	0.00	0.00	0.00
33	18.229	3.1078	0.00000E+00	0.00	0.00	0.00
34	18.583	3.4006	0.00000E+00	0.00	0.00	0.00
35	18.937	3.6933	0.00000E+00	0.00	0.00	0.00
36	26.438	5.6320	0.00000E+00	0.00	0.00	0.00
37	26.438	2.8200	0.00000E+00	0.00	0.00	0.00
38	17.875	3.5050	0.00000E+00	0.00	0.00	0.00
39	18.188	3.8175	0.00000E+00	0.00	0.00	0.00
40	18.500	4.1300	0.00000E+00	0.00	0.00	0.00

NODE	X	Y	Z	THXY	THYZ	THXZ
41	19.508	5.6320	0.00000E+00	0.00	0.00	0.00
42	17.875	4.7500	0.00000E+00	0.00	0.00	0.00
43	18.188	4.7500	0.00000E+00	0.00	0.00	0.00
44	18.500	4.7500	0.00000E+00	0.00	0.00	0.00
45	17.940	4.9450	0.00000E+00	0.00	0.00	0.00
46	18.190	4.9450	0.00000E+00	0.00	0.00	0.00
47	18.440	4.9450	0.00000E+00	0.00	0.00	0.00
48	17.940	5.6320	0.00000E+00	0.00	0.00	0.00
49	18.190	5.6320	0.00000E+00	0.00	0.00	0.00
50	18.440	5.6320	0.00000E+00	0.00	0.00	0.00
53	18.190	7.7920	0.00000E+00	0.00	0.00	0.00
54	19.508	7.7920	0.00000E+00	0.00	0.00	0.00
55	18.190	10.042	0.00000E+00	0.00	0.00	0.00
56	19.508	10.042	0.00000E+00	0.00	0.00	0.00
57	18.190	12.292	0.00000E+00	0.00	0.00	0.00
58	19.508	12.292	0.00000E+00	0.00	0.00	0.00
59	18.190	14.542	0.00000E+00	0.00	0.00	0.00
60	19.508	14.542	0.00000E+00	0.00	0.00	0.00
61	18.190	16.792	0.00000E+00	0.00	0.00	0.00
62	19.508	16.792	0.00000E+00	0.00	0.00	0.00

NODE	X	Y	Z	THXY	THYZ	THXZ
63	18.190	19.042	0.00000E+00	0.00	0.00	0.00
64	19.508	19.042	0.00000E+00	0.00	0.00	0.00
65	18.190	21.292	0.00000E+00	0.00	0.00	0.00
66	19.508	21.292	0.00000E+00	0.00	0.00	0.00
67	18.190	23.542	0.00000E+00	0.00	0.00	0.00
68	19.508	23.542	0.00000E+00	0.00	0.00	0.00
69	18.190	25.792	0.00000E+00	0.00	0.00	0.00
70	19.508	25.792	0.00000E+00	0.00	0.00	0.00
71	18.190	28.042	0.00000E+00	0.00	0.00	0.00
72	19.508	28.042	0.00000E+00	0.00	0.00	0.00
73	18.190	30.292	0.00000E+00	0.00	0.00	0.00
74	19.508	30.292	0.00000E+00	0.00	0.00	0.00
75	18.190	32.542	0.00000E+00	0.00	0.00	0.00
76	19.508	32.542	0.00000E+00	0.00	0.00	0.00
77	18.190	34.792	0.00000E+00	0.00	0.00	0.00
78	19.508	34.792	0.00000E+00	0.00	0.00	0.00
79	18.190	37.042	0.00000E+00	0.00	0.00	0.00
80	19.508	37.042	0.00000E+00	0.00	0.00	0.00
81	18.190	39.292	0.00000E+00	0.00	0.00	0.00
82	19.508	39.292	0.00000E+00	0.00	0.00	0.00

NODE	X	Y	Z	THXY	THYZ	THXZ
83	18.190	41.542	0.00000E+00	0.00	0.00	0.00
84	19.508	41.542	0.00000E+00	0.00	0.00	0.00
85	18.190	43.792	0.00000E+00	0.00	0.00	0.00
86	19.508	43.792	0.00000E+00	0.00	0.00	0.00
87	18.190	46.042	0.00000E+00	0.00	0.00	0.00
88	19.508	46.042	0.00000E+00	0.00	0.00	0.00
89	18.190	48.292	0.00000E+00	0.00	0.00	0.00
90	19.508	48.292	0.00000E+00	0.00	0.00	0.00
91	18.190	50.542	0.00000E+00	0.00	0.00	0.00
92	19.508	50.542	0.00000E+00	0.00	0.00	0.00
93	18.190	52.700	0.00000E+00	0.00	0.00	0.00
94	19.508	52.700	0.00000E+00	0.00	0.00	0.00

101	26.625	-3.5000	0.00000E+00	0.00	0.00	0.00
102	26.625	-2.7500	0.00000E+00	0.00	0.00	0.00
103	26.625	-2.0000	0.00000E+00	0.00	0.00	0.00
104	26.625	-1.0000	0.00000E+00	0.00	0.00	0.00
105	26.625	0.00000E+00	0.00000E+00	0.00	0.00	0.00
106	26.625	1.2500	0.00000E+00	0.00	0.00	0.00
107	26.625	2.4300	0.00000E+00	0.00	0.00	0.00
108	25.387	-3.5000	0.00000E+00	0.00	0.00	0.00

NODE	X	Y	Z	THXY	THYZ	THXZ
109	25.387	-2.7500	0.00000E+00	0.00	0.00	0.00
110	25.387	-2.0000	0.00000E+00	0.00	0.00	0.00
111	25.387	-1.0000	0.00000E+00	0.00	0.00	0.00
112	25.387	0.00000E+00	0.00000E+00	0.00	0.00	0.00
113	25.387	1.2500	0.00000E+00	0.00	0.00	0.00
114	25.387	2.4300	0.00000E+00	0.00	0.00	0.00
115	24.150	-3.5000	0.00000E+00	0.00	0.00	0.00
116	24.150	-2.7500	0.00000E+00	0.00	0.00	0.00
117	24.150	-2.0000	0.00000E+00	0.00	0.00	0.00
118	24.150	-1.0000	0.00000E+00	0.00	0.00	0.00
119	24.150	0.00000E+00	0.00000E+00	0.00	0.00	0.00
120	24.150	1.2500	0.00000E+00	0.00	0.00	0.00
121	24.150	2.4300	0.00000E+00	0.00	0.00	0.00
122	22.125	-3.5000	0.00000E+00	0.00	0.00	0.00
123	22.125	-3.0000	0.00000E+00	0.00	0.00	0.00
124	22.125	-2.3700	0.00000E+00	0.00	0.00	0.00
125	22.125	-1.0000	0.00000E+00	0.00	0.00	0.00
126	22.125	0.00000E+00	0.00000E+00	0.00	0.00	0.00
129	20.875	-3.5000	0.00000E+00	0.00	0.00	0.00
130	20.875	-2.7500	0.00000E+00	0.00	0.00	0.00

NODE	X	Y	Z	THXY	THYZ	THXZ
131	20.875	-2.0000	0.00000E+00	0.00	0.00	0.00
132	20.875	-1.0000	0.00000E+00	0.00	0.00	0.00
133	20.875	0.00000E+00	0.00000E+00	0.00	0.00	0.00
136	20.000	-3.5000	0.00000E+00	0.00	0.00	0.00
137	20.000	-2.7500	0.00000E+00	0.00	0.00	0.00
138	20.000	-2.0000	0.00000E+00	0.00	0.00	0.00
139	20.000	-1.0000	0.00000E+00	0.00	0.00	0.00
140	20.000	0.00000E+00	0.00000E+00	0.00	0.00	0.00
143	19.545	-3.5000	0.00000E+00	0.00	0.00	0.00
144	19.545	-2.7500	0.00000E+00	0.00	0.00	0.00
145	19.545	-2.0000	0.00000E+00	0.00	0.00	0.00
146	19.545	-1.0000	0.00000E+00	0.00	0.00	0.00
147	19.545	0.00000E+00	0.00000E+00	0.00	0.00	0.00
150	14.659	-3.5000	0.00000E+00	0.00	0.00	0.00
151	14.659	-2.7500	0.00000E+00	0.00	0.00	0.00
152	14.659	-2.0000	0.00000E+00	0.00	0.00	0.00
157	9.7726	-3.5000	0.00000E+00	0.00	0.00	0.00
158	9.7726	-2.7500	0.00000E+00	0.00	0.00	0.00
159	9.7726	-2.0000	0.00000E+00	0.00	0.00	0.00
164	4.8864	-3.5000	0.00000E+00	0.00	0.00	0.00

NODE	X	Y	Z	THXY	THYZ	THXZ
165	4.8864	-2.7500	0.00000E+00	0.00	0.00	0.00
166	4.8864	-2.0000	0.00000E+00	0.00	0.00	0.00
171	0.20000E-03	-3.5000	0.00000E+00	0.00	0.00	0.00
172	0.20000E-03	-2.7500	0.00000E+00	0.00	0.00	0.00
173	0.20000E-03	-2.0000	0.00000E+00	0.00	0.00	0.00
178	23.991	0.00000E+00	0.00000E+00	0.00	0.00	0.00
180	18.190	54.290	0.00000E+00	0.00	0.00	0.00
181	18.069	55.170	0.00000E+00	0.00	0.00	0.00
182	17.713	55.985	0.00000E+00	0.00	0.00	0.00
183	17.150	56.673	0.00000E+00	0.00	0.00	0.00
184	16.423	57.182	0.00000E+00	0.00	0.00	0.00
185	12.523	58.899	0.00000E+00	0.00	0.00	0.00
186	8.4475	60.143	0.00000E+00	0.00	0.00	0.00
187	4.2537	60.897	0.00000E+00	0.00	0.00	0.00
188	0.14027E-09	61.150	0.00000E+00	0.00	0.00	0.00

LIST ALL MATERIALS PROPERTY= ALL

```
PROPERTY TABLE NUXY  MAT=   1  NUM. POINTS=  2
    TEMPERATURE      DATA    TEMPERATURE      DATA
     -9999.0      0.30000      9999.0      0.30000

PROPERTY TABLE EX    MAT=   1  NUM. POINTS= 15
    TEMPERATURE      DATA    TEMPERATURE      DATA
      -40.000     0.28900E+08  70.000      0.28300E+08
      100.00      0.28100E+08  200.00      0.27600E+08
      300.00      0.27000E+08  400.00      0.26500E+08
      500.00      0.25800E+08  600.00      0.25300E+08
      700.00      0.24800E+08  800.00      0.24100E+08
      900.00      0.23500E+08  1000.0      0.22500E+08
      1100.0      0.22100E+08  1200.0      0.21300E+08
      1300.0      0.20500E+08

PROPERTY TABLE ALPX  MAT=   1  NUM. POINTS= 15
    TEMPERATURE      DATA    TEMPERATURE      DATA
      -40.000     0.81300E-05  70.000      0.84600E-05
      100.00      0.85500E-05  200.00      0.87900E-05
      300.00      0.90000E-05  400.00      0.91900E-05
      500.00      0.93700E-05  600.00      0.95300E-05
      700.00      0.96900E-05  800.00      0.98200E-05
      900.00      0.10060E-04  1000.0      0.10300E-04
      1100.0      0.10350E-04  1200.0      0.10400E-04
      1300.0      0.10450E-04

PROPERTY TABLE EX    MAT=   2  NUM. POINTS=  7
    TEMPERATURE      DATA    TEMPERATURE      DATA
      -40.000     0.28400E+08  70.000      0.27800E+08
      100.00      0.27600E+08  200.00      0.27100E+08
      300.00      0.26700E+08  400.00      0.26100E+08
      500.00      0.25700E+08

PROPERTY TABLE ALPX  MAT=   2  NUM. POINTS=  7
    TEMPERATURE      DATA    TEMPERATURE      DATA
      -40.000     0.59400E-05  70.000      0.62000E-05
      100.00      0.62700E-05  200.00      0.65400E-05
      300.00      0.67800E-05  400.00      0.69800E-05
      500.00      0.71600E-05
TIME= 0.00000E+00  NITTER=     -5
KTEMP-  LSTP=    -1  ITER=      0

UNIFORM TEMPERATURE=   -40.000  (TREF=    70.000)
 BOUNDARY CONDITIONS STEPPED DUE TO STATIC CONVERGENCE OPTION
PLASTIC CONVERG. CRITERION=       0.0100
CREEP OPTIMUM. CRITERION=        0.1000
LARGE DEFL. CONVERG. CRITERION=    0.001000
DISPLACEMENT LIMIT= 0.00000E+00

NPRINT= 99900   NPOST=     5   REACTION PRINT FREQ= 99900
 DISP. POST DATA FREQ=     5  REACT. POST DATA FREQ=     5

 ELEMENT PRINT AND POST DATA FREQUENCIES
  TYPE  STIFF  STRESS  FORCE   STRESS   DATA  FORCE
         NO.   PRINT  PRINT    DATA    LEVEL  DATA
    1     42  99900  99900       5       3      5
    2     51  99900  99900       5       3      5
    3      1  99900  99900       5       3      5
    4      3  99900  99900       5       3      5
    5     12  99900  99900       5       3      5

LOADS INPUT FILE= 26     LOADS OUTPUT FILE= 23

ALL ANALYSIS DATA WILL BE WRITTEN ONTO FILE27

LIST DISPLACEMENTS FOR ALL SELECTED NODES

 NODE  LABEL      DISP              CDISP
    1 UZ     0.000000000E+00 0.000000000E+00
    2 UZ     0.000000000E+00 0.000000000E+00
    3 UZ     0.000000000E+00 0.000000000E+00
    4 UZ     0.000000000E+00 0.000000000E+00
    5 UZ     0.000000000E+00 0.000000000E+00
    6 UZ     0.000000000E+00 0.000000000E+00
```

7	UZ	0.000000000E+00	0.000000000E+00
8	UZ	0.000000000E+00	0.000000000E+00
9	UZ	0.000000000E+00	0.000000000E+00
10	UZ	0.000000000E+00	0.000000000E+00
11	UZ	0.000000000E+00	0.000000000E+00
12	UZ	0.000000000E+00	0.000000000E+00
13	UZ	0.000000000E+00	0.000000000E+00
14	UZ	0.000000000E+00	0.000000000E+00
15	UZ	0.000000000E+00	0.000000000E+00
16	UZ	0.000000000E+00	0.000000000E+00
17	UZ	0.000000000E+00	0.000000000E+00
18	UZ	0.000000000E+00	0.000000000E+00
19	UZ	0.000000000E+00	0.000000000E+00
20	UZ	0.000000000E+00	0.000000000E+00

NODE	LABEL	DISP	CDISP
21	UZ	0.000000000E+00	0.000000000E+00
22	UZ	0.000000000E+00	0.000000000E+00
23	UZ	0.000000000E+00	0.000000000E+00
24	UZ	0.000000000E+00	0.000000000E+00
25	UZ	0.000000000E+00	0.000000000E+00
26	UZ	0.000000000E+00	0.000000000E+00
27	UZ	0.000000000E+00	0.000000000E+00
28	UZ	0.000000000E+00	0.000000000E+00
29	UZ	0.000000000E+00	0.000000000E+00
30	UZ	0.000000000E+00	0.000000000E+00
31	UZ	0.000000000E+00	0.000000000E+00
32	UZ	0.000000000E+00	0.000000000E+00
33	UZ	0.000000000E+00	0.000000000E+00
34	UZ	0.000000000E+00	0.000000000E+00
35	UZ	0.000000000E+00	0.000000000E+00
36	UZ	0.000000000E+00	0.000000000E+00
37	UZ	0.000000000E+00	0.000000000E+00
38	UZ	0.000000000E+00	0.000000000E+00
39	UZ	0.000000000E+00	0.000000000E+00
40	UZ	0.000000000E+00	0.000000000E+00

NODE	LABEL	DISP	CDISP
41	UZ	0.000000000E+00	0.000000000E+00
42	UZ	0.000000000E+00	0.000000000E+00
43	UZ	0.000000000E+00	0.000000000E+00
44	UZ	0.000000000E+00	0.000000000E+00
45	UZ	0.000000000E+00	0.000000000E+00
46	UZ	0.000000000E+00	0.000000000E+00
47	UZ	0.000000000E+00	0.000000000E+00
48	UZ	0.000000000E+00	0.000000000E+00
49	UZ	0.000000000E+00	0.000000000E+00
50	UZ	0.000000000E+00	0.000000000E+00
53	UZ	0.000000000E+00	0.000000000E+00
54	UZ	0.000000000E+00	0.000000000E+00
55	UZ	0.000000000E+00	0.000000000E+00
56	UZ	0.000000000E+00	0.000000000E+00
57	UZ	0.000000000E+00	0.000000000E+00
58	UZ	0.000000000E+00	0.000000000E+00
59	UZ	0.000000000E+00	0.000000000E+00
60	UZ	0.000000000E+00	0.000000000E+00
61	UZ	0.000000000E+00	0.000000000E+00
62	UZ	0.000000000E+00	0.000000000E+00

NODE	LABEL	DISP	CDISP
63	UZ	0.000000000E+00	0.000000000E+00
64	UZ	0.000000000E+00	0.000000000E+00
65	UZ	0.000000000E+00	0.000000000E+00
66	UZ	0.000000000E+00	0.000000000E+00
67	UZ	0.000000000E+00	0.000000000E+00
68	UZ	0.000000000E+00	0.000000000E+00
69	UZ	0.000000000E+00	0.000000000E+00
70	UZ	0.000000000E+00	0.000000000E+00
71	UZ	0.000000000E+00	0.000000000E+00
72	UZ	0.000000000E+00	0.000000000E+00
73	UZ	0.000000000E+00	0.000000000E+00
74	UZ	0.000000000E+00	0.000000000E+00
75	UZ	0.000000000E+00	0.000000000E+00
76	UZ	0.000000000E+00	0.000000000E+00

77	UZ	0.000000000E+00	0.000000000E+00
78	UZ	0.000000000E+00	0.000000000E+00
79	UZ	0.000000000E+00	0.000000000E+00
80	UZ	0.000000000E+00	0.000000000E+00
81	UZ	0.000000000E+00	0.000000000E+00
82	UZ	0.000000000E+00	0.000000000E+00

NODE	LABEL	DISP	CDISP
83	UZ	0.000000000E+00	0.000000000E+00
84	UZ	0.000000000E+00	0.000000000E+00
85	UZ	0.000000000E+00	0.000000000E+00
86	UZ	0.000000000E+00	0.000000000E+00
87	UZ	0.000000000E+00	0.000000000E+00
88	UZ	0.000000000E+00	0.000000000E+00
89	UZ	0.000000000E+00	0.000000000E+00
90	UZ	0.000000000E+00	0.000000000E+00
91	UZ	0.000000000E+00	0.000000000E+00
92	UZ	0.000000000E+00	0.000000000E+00
93	UZ	0.000000000E+00	0.000000000E+00
94	UZ	0.000000000E+00	0.000000000E+00
101	UZ	0.000000000E+00	0.000000000E+00
102	UZ	0.000000000E+00	0.000000000E+00
103	UZ	0.000000000E+00	0.000000000E+00
104	UZ	0.000000000E+00	0.000000000E+00
105	UZ	0.000000000E+00	0.000000000E+00
106	UZ	0.000000000E+00	0.000000000E+00
107	UZ	0.000000000E+00	0.000000000E+00
108	UZ	0.000000000E+00	0.000000000E+00

NODE	LABEL	DISP	CDISP
109	UZ	0.000000000E+00	0.000000000E+00
110	UZ	0.000000000E+00	0.000000000E+00
111	UZ	0.000000000E+00	0.000000000E+00
112	UZ	0.000000000E+00	0.000000000E+00
113	UZ	0.000000000E+00	0.000000000E+00
114	UZ	0.000000000E+00	0.000000000E+00
115	UZ	0.000000000E+00	0.000000000E+00
116	UZ	0.000000000E+00	0.000000000E+00
117	UZ	0.000000000E+00	0.000000000E+00
118	UZ	0.000000000E+00	0.000000000E+00
119	UZ	0.000000000E+00	0.000000000E+00
120	UZ	0.000000000E+00	0.000000000E+00
121	UZ	0.000000000E+00	0.000000000E+00
122	UZ	0.000000000E+00	0.000000000E+00
123	UZ	0.000000000E+00	0.000000000E+00
124	UZ	0.000000000E+00	0.000000000E+00
125	UZ	0.000000000E+00	0.000000000E+00
126	UZ	0.000000000E+00	0.000000000E+00
129	UZ	0.000000000E+00	0.000000000E+00
130	UZ	0.000000000E+00	0.000000000E+00

NODE	LABEL	DISP	CDISP
131	UZ	0.000000000E+00	0.000000000E+00
132	UZ	0.000000000E+00	0.000000000E+00
133	UZ	0.000000000E+00	0.000000000E+00
136	UZ	0.000000000E+00	0.000000000E+00
137	UZ	0.000000000E+00	0.000000000E+00
138	UZ	0.000000000E+00	0.000000000E+00
139	UZ	0.000000000E+00	0.000000000E+00
140	UZ	0.000000000E+00	0.000000000E+00
143	UZ	0.000000000E+00	0.000000000E+00
144	UZ	0.000000000E+00	0.000000000E+00
145	UZ	0.000000000E+00	0.000000000E+00
146	UZ	0.000000000E+00	0.000000000E+00
147	UZ	0.000000000E+00	0.000000000E+00
150	UZ	0.000000000E+00	0.000000000E+00
151	UZ	0.000000000E+00	0.000000000E+00
152	UZ	0.000000000E+00	0.000000000E+00
157	UZ	0.000000000E+00	0.000000000E+00
158	UZ	0.000000000E+00	0.000000000E+00
159	UZ	0.000000000E+00	0.000000000E+00
164	UZ	0.000000000E+00	0.000000000E+00

NODE	LABEL	DISP	CDISP
165	UZ	0.000000000E+00	0.000000000E+00
166	UZ	0.000000000E+00	0.000000000E+00
171	UZ	0.000000000E+00	0.000000000E+00
172	UZ	0.000000000E+00	0.000000000E+00
173	UZ	0.000000000E+00	0.000000000E+00
178	UZ	0.000000000E+00	0.000000000E+00
180	UZ	0.000000000E+00	0.000000000E+00
181	UZ	0.000000000E+00	0.000000000E+00
182	UZ	0.000000000E+00	0.000000000E+00
183	UZ	0.000000000E+00	0.000000000E+00
184	UZ	0.000000000E+00	0.000000000E+00
185	UZ	0.000000000E+00	0.000000000E+00
186	UZ	0.000000000E+00	0.000000000E+00
187	UZ	0.000000000E+00	0.000000000E+00
188	UZ	0.000000000E+00	0.000000000E+00
171	UX	0.000000000E+00	0.000000000E+00
172	UX	0.000000000E+00	0.000000000E+00
173	UX	0.000000000E+00	0.000000000E+00
188	UX	0.000000000E+00	0.000000000E+00
188	ROTZ	0.000000000E+00	0.000000000E+00

NODE	LABEL	DISP	CDISP
171	UY	0.000000000E+00	0.000000000E+00

LIST ELEMENT PRESSURES FOR ALL SELECTED ELEMENTS

ELEM	FACE	VALUE(S)		FACE NODES	
95	1	26.5000000	0.000000000E+00	49	53
96	1	26.5000000	0.000000000E+00	53	55
97	1	26.5000000	0.000000000E+00	55	57
98	1	26.5000000	0.000000000E+00	57	59
99	1	26.5000000	0.000000000E+00	59	61
100	1	26.5000000	0.000000000E+00	61	63
101	1	26.5000000	0.000000000E+00	63	65
102	1	26.5000000	0.000000000E+00	65	67
103	1	26.5000000	0.000000000E+00	67	69
104	1	26.5000000	0.000000000E+00	69	71
105	1	26.5000000	0.000000000E+00	71	73
106	1	26.5000000	0.000000000E+00	73	75
107	1	26.5000000	0.000000000E+00	75	77
108	1	26.5000000	0.000000000E+00	77	79
109	1	26.5000000	0.000000000E+00	79	81
110	1	26.5000000	0.000000000E+00	81	83
111	1	26.5000000	0.000000000E+00	83	85
112	1	26.5000000	0.000000000E+00	85	87
113	1	26.5000000	0.000000000E+00	87	89
114	1	26.5000000	0.000000000E+00	89	91

ELEM	FACE	VALUE(S)		FACE NODES	
115	1	26.5000000	0.000000000E+00	91	93
116	1	26.5000000	0.000000000E+00	93	180
117	1	26.5000000	0.000000000E+00	180	181
118	1	26.5000000	0.000000000E+00	181	182
119	1	26.5000000	0.000000000E+00	182	183
120	1	26.5000000	0.000000000E+00	183	184
121	1	26.5000000	0.000000000E+00	184	185
122	1	26.5000000	0.000000000E+00	185	186
123	1	26.5000000	0.000000000E+00	186	187
124	1	26.5000000	0.000000000E+00	187	188
65	3	26.5000000	0.000000000E+00	146	145
66	3	26.5000000	0.000000000E+00	147	146
70	2	26.5000000	0.000000000E+00	145	152
76	2	26.5000000	0.000000000E+00	152	159
82	2	26.5000000	0.000000000E+00	159	166
88	2	26.5000000	0.000000000E+00	166	173
17	4	26.5000000	0.000000000E+00	22	26
18	4	26.5000000	0.000000000E+00	27	22
21	4	26.5000000	0.000000000E+00	32	27
26	4	26.5000000	0.000000000E+00	38	32

ELEM	FACE	VALUE(S)		FACE NODES	
27	4	26.5000000	0.000000000E+00	42	38
29	4	26.5000000	0.000000000E+00	45	42
31	4	26.5000000	0.000000000E+00	48	45

LIST ELEMENT CONVECTIONS FOR ALL SELECTED ELEMENTS

LIST ELEMENT TEMPERATURES FOR ALL SELECTED ELEMENTS

ELEMENT	TEMPERATURES			
176	207.990000	210.160000	0.000000000E+00	0.000000000E+00
	0.000000000E+00	0.000000000E+00	0.000000000E+00	0.000000000E+00
	0.000000000E+00	0.000000000E+00		

LIST TEMPERATURES FOR ALL SELECTED NODES

NODE	TEMPERATURE	FLUENCE
1	209.30	0.00000E+00
2	209.30	0.00000E+00
3	208.94	0.00000E+00
4	208.59	0.00000E+00
5	208.59	0.00000E+00
6	209.30	0.00000E+00
7	209.30	0.00000E+00
8	208.94	0.00000E+00
9	208.59	0.00000E+00
10	208.59	0.00000E+00
11	209.30	0.00000E+00
12	209.30	0.00000E+00
13	208.94	0.00000E+00
14	208.59	0.00000E+00
15	208.59	0.00000E+00
16	209.80	0.00000E+00
17	209.80	0.00000E+00
18	209.69	0.00000E+00
19	209.57	0.00000E+00
20	209.57	0.00000E+00

NODE	TEMPERATURE	FLUENCE
21	209.80	0.00000E+00
22	209.80	0.00000E+00
23	209.69	0.00000E+00
24	209.57	0.00000E+00
25	209.57	0.00000E+00
26	209.80	0.00000E+00
27	212.54	0.00000E+00
28	212.54	0.00000E+00
29	212.54	0.00000E+00
30	212.54	0.00000E+00
31	182.85	0.00000E+00
32	212.54	0.00000E+00
33	212.54	0.00000E+00
34	212.54	0.00000E+00
35	212.54	0.00000E+00
36	190.09	0.00000E+00
37	201.61	0.00000E+00
38	212.54	0.00000E+00
39	212.54	0.00000E+00
40	212.54	0.00000E+00

NODE	TEMPERATURE	FLUENCE
41	213.14	0.00000E+00
42	220.96	0.00000E+00
43	220.96	0.00000E+00
44	220.96	0.00000E+00
45	220.96	0.00000E+00
46	220.96	0.00000E+00
47	220.96	0.00000E+00
48	220.96	0.00000E+00
49	220.96	0.00000E+00
50	220.96	0.00000E+00
53	228.16	0.00000E+00
54	213.14	0.00000E+00
55	235.37	0.00000E+00
56	213.14	0.00000E+00

57	239.33	0.00000E+00
58	214.38	0.00000E+00
59	243.29	0.00000E+00
60	215.61	0.00000E+00
61	247.24	0.00000E+00
62	216.85	0.00000E+00

NODE	TEMPERATURE	FLUENCE
63	251.20	0.00000E+00
64	218.09	0.00000E+00
65	256.68	0.00000E+00
66	222.85	0.00000E+00
67	262.16	0.00000E+00
68	227.62	0.00000E+00
69	267.64	0.00000E+00
70	232.38	0.00000E+00
71	273.11	0.00000E+00
72	237.14	0.00000E+00
73	278.59	0.00000E+00
74	241.91	0.00000E+00
75	284.07	0.00000E+00
76	246.67	0.00000E+00
77	284.03	0.00000E+00
78	246.59	0.00000E+00
79	283.99	0.00000E+00
80	246.51	0.00000E+00
81	283.96	0.00000E+00
82	246.43	0.00000E+00

NODE	TEMPERATURE	FLUENCE
83	283.92	0.00000E+00
84	246.36	0.00000E+00
85	283.88	0.00000E+00
86	246.28	0.00000E+00
87	283.84	0.00000E+00
88	246.20	0.00000E+00
89	283.80	0.00000E+00
90	246.12	0.00000E+00
91	283.76	0.00000E+00
92	246.04	0.00000E+00
93	283.72	0.00000E+00
94	245.96	0.00000E+00
101	208.89	0.00000E+00
102	208.89	0.00000E+00
103	208.89	0.00000E+00
104	208.89	0.00000E+00
105	208.89	0.00000E+00
106	208.89	0.00000E+00
107	208.89	0.00000E+00
108	208.89	0.00000E+00

NODE	TEMPERATURE	FLUENCE
109	208.89	0.00000E+00
110	208.89	0.00000E+00
111	208.89	0.00000E+00
112	208.89	0.00000E+00
113	208.89	0.00000E+00
114	208.89	0.00000E+00
115	208.89	0.00000E+00
116	208.89	0.00000E+00
117	208.89	0.00000E+00
118	208.89	0.00000E+00
119	208.89	0.00000E+00
120	208.89	0.00000E+00
121	208.89	0.00000E+00
122	210.29	0.00000E+00
123	210.29	0.00000E+00
124	210.29	0.00000E+00
125	210.29	0.00000E+00
126	210.29	0.00000E+00
129	210.29	0.00000E+00
130	210.29	0.00000E+00

NODE	TEMPERATURE	FLUENCE
131	210.29	0.00000E+00
132	210.29	0.00000E+00
133	210.29	0.00000E+00
136	210.29	0.00000E+00
137	210.29	0.00000E+00
138	210.29	0.00000E+00
139	210.29	0.00000E+00
140	210.29	0.00000E+00
143	210.29	0.00000E+00
144	210.29	0.00000E+00
145	210.29	0.00000E+00
146	210.29	0.00000E+00
147	210.29	0.00000E+00
150	215.78	0.00000E+00
151	215.78	0.00000E+00
152	215.78	0.00000E+00
157	218.74	0.00000E+00
158	218.74	0.00000E+00
159	218.74	0.00000E+00
164	220.18	0.00000E+00

NODE	TEMPERATURE	FLUENCE
165	220.18	0.00000E+00
166	220.18	0.00000E+00
171	220.18	0.00000E+00
172	220.18	0.00000E+00
173	220.18	0.00000E+00
178	208.89	0.00000E+00
180	236.61	0.00000E+00
181	236.61	0.00000E+00
182	236.61	0.00000E+00
183	236.61	0.00000E+00
184	236.61	0.00000E+00
185	252.03	0.00000E+00
186	267.45	0.00000E+00
187	267.45	0.00000E+00
188	267.45	0.00000E+00

TABLE 2.10.8.2. Refined ANSYS Input Listing.

```
STATIC ANALYSIS (KAN= 0)

LINEAR ANALYSIS - NO NON-LINEAR PROPERTIES

REFERENCE TEMPERATURE=    70.000 (TREF)
UNIFORM TEMPERATURE  =    70.000 (TUNIF)

*****ANALYSIS OPTIONS (KAY VALUES) (IF ANY) *****

NO STATIC INTERPOLATION/EXTRAPOLATION (KAY(3)=0)

SMALL DEFLECTION SOLUTION (KAY(6)=0)

NO STRESS STIFFENING (KAY(8)=0)

USE INITIAL-STIFFNESS NEWTON-RAPHSON SOLUTION PROCEDURE  (KAY(9)=3)

IN-CORE WAVE-FRONT EQUATION SOLVER (KAY(10)=0)

LIST ELEMENT TYPES FROM  1 TO 20 BY 1

NO. STIF         KEYOPT VALUES         INOPR
 1   42   0  0  1   0  0  0   0  0  0   0  ISOPAR. STRESS SOLID, 2-D
 2   51   0  0  0   0  0  0   0  0  0   0  PLASTIC AXISYM. CONIC SHELL
 3    1   0  0  0   0  0  0   0  0  0   0  SPAR, 2-D
 4    3   0  0  0   0  0  0   0  0  0   0  ELASTIC BEAM, 2-D
 5   12   0  0  0   0  0  0   0  0  0   0  INTERFACE ELEM. 2-D
 6   42   0  0  1   0  0  0   0  0  0   0  ISOPAR. STRESS SOLID, 2-D

LIST ALL REAL SETS

 REAL CONSTANT SET   2  ITEMS   1 TO   6
  0.50000      0.00000E+00  0.00000E+00  0.00000E+00  0.00000E+00  0.00000E+00

 REAL CONSTANT SET   3  ITEMS   1 TO   6
   4.2020      0.39080E-03  0.00000E+00  0.00000E+00  0.00000E+00  0.00000E+00

 REAL CONSTANT SET   4  ITEMS   1 TO   6
   3.4260       2.4330       2.5000       2.0000      0.00000E+00  0.00000E+00

 REAL CONSTANT SET   5  ITEMS   1 TO   6
 0.00000E+00  0.49000E+10  0.00000E+00  0.00000E+00  0.00000E+00  0.00000E+00

 REAL CONSTANT SET   6  ITEMS   1 TO   6
 0.00000E+00  0.25000E+08  0.00000E+00  0.00000E+00  0.00000E+00  0.00000E+00

 REAL CONSTANT SET  21  ITEMS   1 TO   6
  0.37500      0.00000E+00  0.00000E+00  0.00000E+00  0.00000E+00  0.00000E+00

 REAL CONSTANT SET  22  ITEMS   1 TO   6
  0.25000      0.00000E+00  0.00000E+00  0.00000E+00  0.00000E+00  0.00000E+00

 REAL CONSTANT SET  23  ITEMS   1 TO   6
  0.13500      0.00000E+00  0.00000E+00  0.00000E+00  0.00000E+00  0.00000E+00

 REAL CONSTANT SET  24  ITEMS   1 TO   6
  0.23200      0.00000E+00  0.00000E+00  0.00000E+00  0.00000E+00  0.00000E+00

 REAL CONSTANT SET  25  ITEMS   1 TO   6
  0.34260      0.24330      0.25000       2.0000      0.00000E+00  0.00000E+00

 REAL CONSTANT SET  26  ITEMS   1 TO   6
  0.11600      0.00000E+00  0.00000E+00  0.00000E+00  0.00000E+00  0.00000E+00
LIST ALL COORDINATE SYSTEMS

    SYSTEM TYPE                    CENTER              PARAMETERS    SING KEYS
 0  0 (CARTESIAN)          0.000    0.000    0.000    0.000   0.000   0  0
 1  1 (CYLINDRICAL)        0.000    0.000    0.000    1.000   0.000   0  0
 2  2 (SPHERICAL)          0.000    0.000    0.000    1.000   1.000   0  0
11  1 (CYLINDRICAL)        0.000   25.150    0.000    1.000   1.000   0  0
```

```
12  1 (CYLINDRICAL)      14.940      54.290       0.000      1.000    1.000    0  0

SYSTEM              ORIENTATION VECTORS (X,Y,Z)
    0      1.00  0.00  0.00   0.00  1.00  0.00   0.00  0.00  1.00
    1      1.00  0.00  0.00   0.00  1.00  0.00   0.00  0.00  1.00
    2      1.00  0.00  0.00   0.00  1.00  0.00   0.00  0.00  1.00
   11      1.00  0.00  0.00   0.00  1.00  0.00   0.00  0.00  1.00
   12      1.00  0.00  0.00   0.00  1.00  0.00   0.00  0.00  1.00
CSYS TYPE      XC          YC          ZC          THXY      THYZ      THXZ
 11     1 0.00000E+00   25.150      0.00000E+00    0.000     0.000     0.000
 12     1  14.940       54.290      0.00000E+00    0.000     0.000     0.000

LIST ALL SELECTED ELEMENTS.   (LIST NODES)

  ELEM MAT TYP REL ESYS          NODES

     3   1   1   1    0        3     4     9     8
     4   1   1   1    0        4     5    10     9
     7   1   1   1    0        8     9    14    13
     8   1   1   1    0        9    10    15    14
    11   1   1   1    0       13    14    19    18
    12   1   1   1    0       14    15    20    19
    15   1   1   1    0       18    19    24    23
    16   1   1   1    0       19    20    25    24
    18   1   1   1    0       22    23    28    27
    19   1   1   1    0       23    24    29    28
    20   1   1   1    0       24    25    30    29
    21   1   1   1    0       27    28    33    32
    22   1   1   1    0       28    29    34    33
    23   1   1   1    0       29    30    35    34
    24   1   1   1    0       33    34    39    38
    25   1   1   1    0       34    35    40    39
    26   1   1   1    0       32    33    38    38
    27   1   1   1    0       38    39    43    42
    28   1   1   1    0       39    40    44    43
    29   1   1   1    0       42    43    46    45

  ELEM MAT TYP REL ESYS          NODES

    30   1   1   1    0       43    44    47    46
    31   1   1   1    0       45    46    49    48
    32   1   1   1    0       46    47    50    49
    33   1   6   1    0      101   102   109   108
    34   1   6   1    0      102   103   110   109
    35   1   6   1    0      103   104   111   110
    36   1   6   1    0      104   105   112   111
    37   1   6   1    0      105   106   113   112
    38   1   6   1    0      106   107   114   113
    39   1   6   1    0      108   109   116   115
    40   1   6   1    0      109   110   117   116
    41   1   6   1    0      110   111   118   117
    43   1   6   1    0      112   113   120   119
    44   1   6   1    0      113   114   121   120
    51   1   6   1    0      122   123   130   129
    52   1   6   1    0      123   124   131   130
    57   1   6   1    0      129   130   137   136
    58   1   6   1    0      130   131   138   137
    63   1   6   1    0      136   137   144   143
    64   1   6   1    0      137   138   145   144

  ELEM MAT TYP REL ESYS          NODES

    69   1   6   1    0      143   144   151   150
    70   1   6   1    0      144   145   152   151
    75   1   6   1    0      150   151   158   157
    76   1   6   1    0      151   152   159   158
    81   1   6   1    0      157   158   165   164
    82   1   6   1    0      158   159   166   165
    87   1   6   1    0      164   165   172   171
    88   1   6   1    0      165   166   173   172
    95   1   2   2    0       49    53
    96   1   2   2    0       53    55
    97   1   2   2    0       55    57
    98   1   2   2    0       57    59
```

99	1	2	2	0	59	61
100	1	2	2	0	61	63
101	1	2	2	0	63	65
102	1	2	2	0	65	67
103	1	2	2	0	67	69
104	1	2	2	0	69	71
105	1	2	2	0	71	73
106	1	2	2	0	73	75

ELEM	MAT	TYP	REL	ESYS	NODES	
107	1	2	2	0	75	77
108	1	2	2	0	77	79
109	1	2	2	0	79	81
110	1	2	2	0	81	83
111	1	2	2	0	83	85
112	1	2	2	0	85	87
113	1	2	2	0	87	89
114	1	2	2	0	89	91
115	1	2	2	0	91	93
116	1	2	2	0	93	180
117	1	2	2	0	180	181
118	1	2	2	0	181	182
119	1	2	2	0	182	183
120	1	2	2	0	183	184
121	1	2	2	0	184	185
122	1	2	2	0	185	186
123	1	2	2	0	186	187
124	1	2	2	0	187	188
125	1	2	22	0	53	54
126	1	2	22	0	55	56

ELEM	MAT	TYP	REL	ESYS	NODES	
127	1	2	22	0	57	58
128	1	2	22	0	59	60
129	1	2	22	0	61	62
130	1	2	22	0	63	64
131	1	2	22	0	65	66
132	1	2	22	0	67	68
133	1	2	22	0	69	70
134	1	2	22	0	71	72
135	1	2	22	0	73	74
136	1	2	22	0	75	76
137	1	2	22	0	77	78
138	1	2	22	0	79	80
139	1	2	22	0	81	82
140	1	2	22	0	83	84
141	1	2	22	0	85	86
142	1	2	22	0	87	88
143	1	2	22	0	89	90
144	1	2	22	0	91	92
145	1	2	21	0	93	94
146	1	2	23	0	41	54

ELEM	MAT	TYP	REL	ESYS	NODES	
147	1	2	23	0	54	56
148	1	2	23	0	56	58
149	1	2	23	0	58	60
150	1	2	23	0	60	62
151	1	2	23	0	62	64
152	1	2	23	0	64	66
153	1	2	23	0	66	68
154	1	2	23	0	68	70
155	1	2	23	0	70	72
156	1	2	23	0	72	74
157	1	2	23	0	74	76
158	1	2	23	0	76	78
159	1	2	23	0	78	80
160	1	2	23	0	80	82
161	1	2	23	0	82	84
162	1	2	23	0	84	86
163	1	2	23	0	86	88

164	1	2	23	0	88	90		
165	1	2	23	0	90	92		
166	1	2	23	0	92	94		

ELEM	MAT	TYP	REL	ESYS	NODES			
167	1	2	21	0	49	41		
168	1	2	21	0	41	31		
169	1	2	21	0	31	36		
170	1	2	21	0	36	37		
171	1	2	22	0	5	37		
172	1	2	24	0	46	49		
173	1	2	26	0	10	5		
174	1	4	4	0	15	31		
175	1	4	25	0	14	15		
176	2	3	3	0	124	15		
177	1	1	1	0	201	221	222	202
178	1	1	1	0	202	222	223	203
179	1	1	1	0	203	223	224	204
180	1	1	1	0	204	224	225	205
181	1	1	1	0	205	225	226	206
182	1	1	1	0	206	226	227	207
183	1	1	1	0	207	227	228	208
184	1	1	1	0	208	228	229	209
185	1	1	1	0	209	229	230	210
186	1	1	1	0	210	230	231	211

ELEM	MAT	TYP	REL	ESYS	NODES			
187	1	1	1	0	211	231	232	212
188	1	1	1	0	212	232	233	213
189	1	1	1	0	213	233	234	214
190	1	1	1	0	214	234	235	215
191	1	1	1	0	215	235	236	216
192	1	1	1	0	216	236	237	217
193	1	1	1	0	221	241	222	222
194	1	1	1	0	222	241	242	242
195	1	1	1	0	222	242	223	223
196	1	1	1	0	223	242	224	224
197	1	1	1	0	224	242	243	243
198	1	1	1	0	224	243	225	225
199	1	1	1	0	225	243	226	226
200	1	1	1	0	226	243	244	244
201	1	1	1	0	226	244	227	227
202	1	1	1	0	227	244	228	228
203	1	1	1	0	228	244	245	245
204	1	1	1	0	228	245	229	229
205	1	1	1	0	229	245	230	230
206	1	1	1	0	230	245	246	246

ELEM	MAT	TYP	REL	ESYS	NODES			
207	1	1	1	0	230	246	231	231
208	1	1	1	0	231	246	232	232
209	1	1	1	0	232	246	247	247
210	1	1	1	0	232	247	233	233
211	1	1	1	0	233	247	234	234
212	1	1	1	0	234	247	248	248
213	1	1	1	0	234	248	235	235
214	1	1	1	0	235	248	236	236
215	1	1	1	0	236	248	22	22
216	1	1	1	0	236	22	237	237
217	1	1	1	0	241	3	242	242
218	1	1	1	0	242	3	8	8
219	1	1	1	0	242	8	243	243
220	1	1	1	0	243	8	244	244
221	1	1	1	0	244	8	13	13
222	1	1	1	0	244	13	245	245
223	1	1	1	0	245	13	246	246
224	1	1	1	0	246	13	18	18
225	1	1	1	0	246	18	247	247
226	1	1	1	0	247	18	248	248

ELEM	MAT	TYP	REL	ESYS	NODES

227	1	1	1	0	248	18	23	22
228	1	6	1	0	301	302	322	321
229	1	6	1	0	302	303	323	322
230	1	6	1	0	303	304	324	323
231	1	6	1	0	304	305	325	324
232	1	6	1	0	305	306	326	325
233	1	6	1	0	306	307	327	326
234	1	6	1	0	307	308	328	327
235	1	6	1	0	308	309	329	328
236	1	6	1	0	309	310	330	329
237	1	6	1	0	310	311	331	330
238	1	6	1	0	311	312	332	331
239	1	6	1	0	312	313	333	332
240	1	6	1	0	313	314	334	333
241	1	6	1	0	314	315	335	334
242	1	6	1	0	315	316	336	335
243	1	6	1	0	316	317	337	336
244	1	6	1	0	321	301	119	119
245	1	6	1	0	321	341	322	322
246	1	6	1	0	322	341	342	342

ELEM	MAT	TYP	REL	ESYS	NODES			
247	1	6	1	0	322	342	323	323
248	1	6	1	0	323	342	324	324
249	1	6	1	0	324	342	343	343
250	1	6	1	0	324	343	325	325
251	1	6	1	0	325	343	326	326
252	1	6	1	0	326	343	344	344
253	1	6	1	0	326	344	327	327
254	1	6	1	0	327	344	328	328
255	1	6	1	0	328	344	345	345
256	1	6	1	0	328	345	329	329
257	1	6	1	0	329	345	330	330
258	1	6	1	0	330	345	346	346
259	1	6	1	0	330	346	331	331
260	1	6	1	0	331	346	332	332
261	1	6	1	0	332	346	347	347
262	1	6	1	0	332	347	333	333
263	1	6	1	0	347	333	334	334
264	1	6	1	0	347	334	335	348
265	1	6	1	0	348	335	336	336
266	1	6	1	0	348	336	337	349

ELEM	MAT	TYP	REL	ESYS	NODES			
267	1	6	1	0	341	111	321	321
268	1	6	1	0	321	111	112	112
269	1	6	1	0	321	112	119	119
270	1	6	1	0	117	341	342	342
271	1	6	1	0	117	342	343	352
272	1	6	1	0	352	343	344	124
273	1	6	1	0	124	344	345	345
274	1	6	1	0	124	345	346	346
275	1	6	1	0	124	346	131	131
276	1	6	1	0	131	346	347	347
277	1	6	1	0	131	347	348	138
278	1	6	1	0	138	348	349	145
279	1	6	1	0	116	117	352	351
280	1	6	1	0	115	116	351	350
281	1	6	1	0	351	352	124	123
282	1	6	1	0	350	351	123	122
283	2	5	6	0	301	201		
284	2	5	6	0	302	202		
285	2	5	6	0	303	203		
286	2	5	6	0	304	204		

ELEM	MAT	TYP	REL	ESYS	NODES	
287	2	5	6	0	305	205
288	2	5	6	0	306	206
289	2	5	6	0	307	207
290	2	5	6	0	308	208

291	2	5	6	0	309	209
292	2	5	6	0	310	210
293	2	5	6	0	311	211
294	2	5	6	0	312	212
295	2	5	6	0	313	213
296	2	5	6	0	314	214
297	2	5	6	0	315	215
298	2	5	6	0	316	216
299	2	5	6	0	317	217

LIST ALL SELECTED NODE DSYS= 0

NODE	X	Y	Z	THXY	THYZ	THXZ
3	24.125	1.4100	0.00000E+00	0.00	0.00	0.00
4	24.125	2.1150	0.00000E+00	0.00	0.00	0.00
5	24.125	2.8200	0.00000E+00	0.00	0.00	0.00
8	23.125	1.4100	0.00000E+00	0.00	0.00	0.00
9	23.125	2.1150	0.00000E+00	0.00	0.00	0.00
10	23.125	2.8200	0.00000E+00	0.00	0.00	0.00
13	22.125	1.4100	0.00000E+00	0.00	0.00	0.00
14	22.125	2.1150	0.00000E+00	0.00	0.00	0.00
15	22.125	2.8200	0.00000E+00	0.00	0.00	0.00
18	20.875	1.4100	0.00000E+00	0.00	0.00	0.00
19	20.875	2.1150	0.00000E+00	0.00	0.00	0.00
20	20.875	2.8200	0.00000E+00	0.00	0.00	0.00
22	19.560	1.1300	0.00000E+00	0.00	0.00	0.00
23	19.643	1.6933	0.00000E+00	0.00	0.00	0.00
24	19.727	2.2567	0.00000E+00	0.00	0.00	0.00
25	19.810	2.8200	0.00000E+00	0.00	0.00	0.00
27	18.718	1.9725	0.00000E+00	0.00	0.00	0.00
28	18.936	2.4006	0.00000E+00	0.00	0.00	0.00
29	19.155	2.8286	0.00000E+00	0.00	0.00	0.00
30	19.373	3.2567	0.00000E+00	0.00	0.00	0.00

NODE	X	Y	Z	THXY	THYZ	THXZ
31	22.125	5.6320	0.00000E+00	0.00	0.00	0.00
32	17.875	2.8150	0.00000E+00	0.00	0.00	0.00
33	18.229	3.1078	0.00000E+00	0.00	0.00	0.00
34	18.583	3.4006	0.00000E+00	0.00	0.00	0.00
35	18.937	3.6933	0.00000E+00	0.00	0.00	0.00
36	26.438	5.6320	0.00000E+00	0.00	0.00	0.00
37	26.438	2.8200	0.00000E+00	0.00	0.00	0.00
38	17.875	3.5050	0.00000E+00	0.00	0.00	0.00
39	18.188	3.8175	0.00000E+00	0.00	0.00	0.00
40	18.500	4.1300	0.00000E+00	0.00	0.00	0.00
41	19.508	5.6320	0.00000E+00	0.00	0.00	0.00
42	17.875	4.7500	0.00000E+00	0.00	0.00	0.00
43	18.188	4.7500	0.00000E+00	0.00	0.00	0.00
44	18.500	4.7500	0.00000E+00	0.00	0.00	0.00
45	17.940	4.9450	0.00000E+00	0.00	0.00	0.00
46	18.190	4.9450	0.00000E+00	0.00	0.00	0.00
47	18.440	4.9450	0.00000E+00	0.00	0.00	0.00
48	17.940	5.6320	0.00000E+00	0.00	0.00	0.00
49	18.190	5.6320	0.00000E+00	0.00	0.00	0.00
50	18.440	5.6320	0.00000E+00	0.00	0.00	0.00

NODE	X	Y	Z	THXY	THYZ	THXZ
53	18.190	7.7920	0.00000E+00	0.00	0.00	0.00
54	19.508	7.7920	0.00000E+00	0.00	0.00	0.00
55	18.190	10.042	0.00000E+00	0.00	0.00	0.00
56	19.508	10.042	0.00000E+00	0.00	0.00	0.00
57	18.190	12.292	0.00000E+00	0.00	0.00	0.00
58	19.508	12.292	0.00000E+00	0.00	0.00	0.00
59	18.190	14.542	0.00000E+00	0.00	0.00	0.00
60	19.508	14.542	0.00000E+00	0.00	0.00	0.00
61	18.190	16.792	0.00000E+00	0.00	0.00	0.00
62	19.508	16.792	0.00000E+00	0.00	0.00	0.00
63	18.190	19.042	0.00000E+00	0.00	0.00	0.00
64	19.508	19.042	0.00000E+00	0.00	0.00	0.00
65	18.190	21.292	0.00000E+00	0.00	0.00	0.00
66	19.508	21.292	0.00000E+00	0.00	0.00	0.00
67	18.190	23.542	0.00000E+00	0.00	0.00	0.00
68	19.508	23.542	0.00000E+00	0.00	0.00	0.00

69	18.190	25.792	0.00000E+00	0.00	0.00	0.00
70	19.508	25.792	0.00000E+00	0.00	0.00	0.00
71	18.190	28.042	0.00000E+00	0.00	0.00	0.00
72	19.508	28.042	0.00000E+00	0.00	0.00	0.00

NODE	X	Y	Z	THXY	THYZ	THXZ
73	18.190	30.292	0.00000E+00	0.00	0.00	0.00
74	19.508	30.292	0.00000E+00	0.00	0.00	0.00
75	18.190	32.542	0.00000E+00	0.00	0.00	0.00
76	19.508	32.542	0.00000E+00	0.00	0.00	0.00
77	18.190	34.792	0.00000E+00	0.00	0.00	0.00
78	19.508	34.792	0.00000E+00	0.00	0.00	0.00
79	18.190	37.042	0.00000E+00	0.00	0.00	0.00
80	19.508	37.042	0.00000E+00	0.00	0.00	0.00
81	18.190	39.292	0.00000E+00	0.00	0.00	0.00
82	19.508	39.292	0.00000E+00	0.00	0.00	0.00
83	18.190	41.542	0.00000E+00	0.00	0.00	0.00
84	19.508	41.542	0.00000E+00	0.00	0.00	0.00
85	18.190	43.792	0.00000E+00	0.00	0.00	0.00
86	19.508	43.792	0.00000E+00	0.00	0.00	0.00
87	18.190	46.042	0.00000E+00	0.00	0.00	0.00
88	19.508	46.042	0.00000E+00	0.00	0.00	0.00
89	18.190	48.292	0.00000E+00	0.00	0.00	0.00
90	19.508	48.292	0.00000E+00	0.00	0.00	0.00
91	18.190	50.542	0.00000E+00	0.00	0.00	0.00
92	19.508	50.542	0.00000E+00	0.00	0.00	0.00

NODE	X	Y	Z	THXY	THYZ	THXZ
93	18.190	52.700	0.00000E+00	0.00	0.00	0.00
94	19.508	52.700	0.00000E+00	0.00	0.00	0.00
101	26.625	-3.5000	0.00000E+00	0.00	0.00	0.00
102	26.625	-2.7500	0.00000E+00	0.00	0.00	0.00
103	26.625	-2.0000	0.00000E+00	0.00	0.00	0.00
104	26.625	-1.0000	0.00000E+00	0.00	0.00	0.00
105	26.625	0.00000E+00	0.00000E+00	0.00	0.00	0.00
106	26.625	1.2500	0.00000E+00	0.00	0.00	0.00
107	26.625	2.4300	0.00000E+00	0.00	0.00	0.00
108	25.387	-3.5000	0.00000E+00	0.00	0.00	0.00
109	25.387	-2.7500	0.00000E+00	0.00	0.00	0.00
110	25.387	-2.0000	0.00000E+00	0.00	0.00	0.00
111	25.387	-1.0000	0.00000E+00	0.00	0.00	0.00
112	25.387	0.00000E+00	0.00000E+00	0.00	0.00	0.00
113	25.387	1.2500	0.00000E+00	0.00	0.00	0.00
114	25.387	2.4300	0.00000E+00	0.00	0.00	0.00
115	24.150	-3.5000	0.00000E+00	0.00	0.00	0.00
116	24.150	-2.7500	0.00000E+00	0.00	0.00	0.00
117	24.150	-2.0000	0.00000E+00	0.00	0.00	0.00
118	24.150	-1.0000	0.00000E+00	0.00	0.00	0.00

NODE	X	Y	Z	THXY	THYZ	THXZ
119	24.150	0.00000E+00	0.00000E+00	0.00	0.00	0.00
120	24.150	1.2500	0.00000E+00	0.00	0.00	0.00
121	24.150	2.4300	0.00000E+00	0.00	0.00	0.00
122	22.125	-3.5000	0.00000E+00	0.00	0.00	0.00
123	22.125	-3.0000	0.00000E+00	0.00	0.00	0.00
124	22.125	-2.3700	0.00000E+00	0.00	0.00	0.00
129	20.875	-3.5000	0.00000E+00	0.00	0.00	0.00
130	20.875	-2.7500	0.00000E+00	0.00	0.00	0.00
131	20.875	-2.0000	0.00000E+00	0.00	0.00	0.00
136	20.000	-3.5000	0.00000E+00	0.00	0.00	0.00
137	20.000	-2.7500	0.00000E+00	0.00	0.00	0.00
138	20.000	-2.0000	0.00000E+00	0.00	0.00	0.00
143	19.545	-3.5000	0.00000E+00	0.00	0.00	0.00
144	19.545	-2.7500	0.00000E+00	0.00	0.00	0.00
145	19.545	-2.0000	0.00000E+00	0.00	0.00	0.00
150	14.659	-3.5000	0.00000E+00	0.00	0.00	0.00
151	14.659	-2.7500	0.00000E+00	0.00	0.00	0.00
152	14.659	-2.0000	0.00000E+00	0.00	0.00	0.00
157	9.7726	-3.5000	0.00000E+00	0.00	0.00	0.00
158	9.7726	-2.7500	0.00000E+00	0.00	0.00	0.00

NODE	X	Y	Z	THXY	THYZ	THXZ
159	9.7726	-2.0000	0.00000E+00	0.00	0.00	0.00
164	4.8864	-3.5000	0.00000E+00	0.00	0.00	0.00

165	4.8864	-2.7500	0.00000E+00	0.00	0.00	0.00
166	4.8864	-2.0000	0.00000E+00	0.00	0.00	0.00
171	0.20000E-03	-3.5000	0.00000E+00	0.00	0.00	0.00
172	0.20000E-03	-2.7500	0.00000E+00	0.00	0.00	0.00
173	0.20000E-03	-2.0000	0.00000E+00	0.00	0.00	0.00
180	18.190	54.290	0.00000E+00	0.00	0.00	0.00
181	18.069	55.170	0.00000E+00	0.00	0.00	0.00
182	17.713	55.985	0.00000E+00	0.00	0.00	0.00
183	17.150	56.673	0.00000E+00	0.00	0.00	0.00
184	16.423	57.182	0.00000E+00	0.00	0.00	0.00
185	12.523	58.899	0.00000E+00	0.00	0.00	0.00
186	8.4475	60.143	0.00000E+00	0.00	0.00	0.00
187	4.2537	60.897	0.00000E+00	0.00	0.00	0.00
188	0.14027E-09	61.150	0.00000E+00	0.00	0.00	0.00
201	23.991	0.00000E+00	0.00000E+00	0.00	0.00	0.00
202	23.808	0.00000E+00	0.00000E+00	0.00	0.00	0.00
203	23.625	0.00000E+00	0.00000E+00	0.00	0.00	0.00
204	23.375	0.00000E+00	0.00000E+00	0.00	0.00	0.00

NODE	X	Y	Z	THXY	THYZ	THXZ
205	23.125	0.00000E+00	0.00000E+00	0.00	0.00	0.00
206	22.875	0.00000E+00	0.00000E+00	0.00	0.00	0.00
207	22.625	0.00000E+00	0.00000E+00	0.00	0.00	0.00
208	22.375	0.00000E+00	0.00000E+00	0.00	0.00	0.00
209	22.125	0.00000E+00	0.00000E+00	0.00	0.00	0.00
210	21.813	0.00000E+00	0.00000E+00	0.00	0.00	0.00
211	21.500	0.00000E+00	0.00000E+00	0.00	0.00	0.00
212	21.188	0.00000E+00	0.00000E+00	0.00	0.00	0.00
213	20.875	0.00000E+00	0.00000E+00	0.00	0.00	0.00
214	20.546	0.00000E+00	0.00000E+00	0.00	0.00	0.00
215	20.218	0.00000E+00	0.00000E+00	0.00	0.00	0.00
216	20.000	0.00000E+00	0.00000E+00	0.00	0.00	0.00
217	19.560	0.00000E+00	0.00000E+00	0.00	0.00	0.00
221	24.058	0.25000	0.00000E+00	0.00	0.00	0.00
222	23.825	0.27575	0.00000E+00	0.00	0.00	0.00
223	23.592	0.30150	0.00000E+00	0.00	0.00	0.00
224	23.358	0.32725	0.00000E+00	0.00	0.00	0.00
225	23.125	0.35300	0.00000E+00	0.00	0.00	0.00
226	22.875	0.35300	0.00000E+00	0.00	0.00	0.00
227	22.625	0.35300	0.00000E+00	0.00	0.00	0.00

NODE	X	Y	Z	THXY	THYZ	THXZ
228	22.375	0.35300	0.00000E+00	0.00	0.00	0.00
229	22.125	0.35300	0.00000E+00	0.00	0.00	0.00
230	21.813	0.35300	0.00000E+00	0.00	0.00	0.00
231	21.500	0.35300	0.00000E+00	0.00	0.00	0.00
232	21.188	0.35300	0.00000E+00	0.00	0.00	0.00
233	20.875	0.35300	0.00000E+00	0.00	0.00	0.00
234	20.546	0.40600	0.00000E+00	0.00	0.00	0.00
235	20.218	0.45900	0.00000E+00	0.00	0.00	0.00
236	19.889	0.51200	0.00000E+00	0.00	0.00	0.00
237	19.560	0.56500	0.00000E+00	0.00	0.00	0.00
241	24.125	0.50000	0.00000E+00	0.00	0.00	0.00
242	23.625	0.60250	0.00000E+00	0.00	0.00	0.00
243	23.125	0.70500	0.00000E+00	0.00	0.00	0.00
244	22.625	0.70500	0.00000E+00	0.00	0.00	0.00
245	22.125	0.70500	0.00000E+00	0.00	0.00	0.00
246	21.500	0.70500	0.00000E+00	0.00	0.00	0.00
247	20.875	0.70500	0.00000E+00	0.00	0.00	0.00
248	20.218	0.91750	0.00000E+00	0.00	0.00	0.00
301	23.991	0.00000E+00	0.00000E+00	0.00	0.00	0.00
302	23.808	0.00000E+00	0.00000E+00	0.00	0.00	0.00

NODE	X	Y	Z	THXY	THYZ	THXZ
303	23.625	0.00000E+00	0.00000E+00	0.00	0.00	0.00
304	23.375	0.00000E+00	0.00000E+00	0.00	0.00	0.00
305	23.125	0.00000E+00	0.00000E+00	0.00	0.00	0.00
306	22.875	0.00000E+00	0.00000E+00	0.00	0.00	0.00
307	22.625	0.00000E+00	0.00000E+00	0.00	0.00	0.00
308	22.375	0.00000E+00	0.00000E+00	0.00	0.00	0.00
309	22.125	0.00000E+00	0.00000E+00	0.00	0.00	0.00
310	21.813	0.00000E+00	0.00000E+00	0.00	0.00	0.00
311	21.500	0.00000E+00	0.00000E+00	0.00	0.00	0.00
312	21.188	0.00000E+00	0.00000E+00	0.00	0.00	0.00

313	20.875	0.00000E+00	0.00000E+00	0.00	0.00	0.00
314	20.546	0.00000E+00	0.00000E+00	0.00	0.00	0.00
315	20.218	0.00000E+00	0.00000E+00	0.00	0.00	0.00
316	20.000	0.00000E+00	0.00000E+00	0.00	0.00	0.00
317	19.560	0.00000E+00	0.00000E+00	0.00	0.00	0.00
321	24.150	-0.50000	0.00000E+00	0.00	0.00	0.00
322	23.808	-0.50000	0.00000E+00	0.00	0.00	0.00
323	23.625	-0.50000	0.00000E+00	0.00	0.00	0.00
324	23.375	-0.50000	0.00000E+00	0.00	0.00	0.00
325	23.125	-0.50000	0.00000E+00	0.00	0.00	0.00

NODE	X	Y	Z	THXY	THYZ	THXZ
326	22.875	-0.50000	0.00000E+00	0.00	0.00	0.00
327	22.625	-0.50000	0.00000E+00	0.00	0.00	0.00
328	22.375	-0.50000	0.00000E+00	0.00	0.00	0.00
329	22.125	-0.50000	0.00000E+00	0.00	0.00	0.00
330	21.813	-0.50000	0.00000E+00	0.00	0.00	0.00
331	21.500	-0.50000	0.00000E+00	0.00	0.00	0.00
332	21.188	-0.50000	0.00000E+00	0.00	0.00	0.00
333	20.875	-0.50000	0.00000E+00	0.00	0.00	0.00
334	20.546	-0.50000	0.00000E+00	0.00	0.00	0.00
335	20.218	-0.50000	0.00000E+00	0.00	0.00	0.00
336	20.000	-0.50000	0.00000E+00	0.00	0.00	0.00
337	19.545	-0.50000	0.00000E+00	0.00	0.00	0.00
341	24.150	-1.0000	0.00000E+00	0.00	0.00	0.00
342	23.638	-1.0000	0.00000E+00	0.00	0.00	0.00
343	23.125	-1.0000	0.00000E+00	0.00	0.00	0.00
344	22.625	-1.0000	0.00000E+00	0.00	0.00	0.00
345	22.125	-1.0000	0.00000E+00	0.00	0.00	0.00
346	21.500	-1.0000	0.00000E+00	0.00	0.00	0.00
347	20.875	-1.0000	0.00000E+00	0.00	0.00	0.00
348	20.000	-1.0000	0.00000E+00	0.00	0.00	0.00

NODE	X	Y	Z	THXY	THYZ	THXZ
349	19.545	-1.0000	0.00000E+00	0.00	0.00	0.00
350	23.137	-3.5000	0.00000E+00	0.00	0.00	0.00
351	23.137	-2.8750	0.00000E+00	0.00	0.00	0.00
352	23.137	-2.1850	0.00000E+00	0.00	0.00	0.00

LIST ALL MATERIALS PROPERTY= ALL

PROPERTY TABLE NUXY MAT= 1 NUM. POINTS= 2

TEMPERATURE	DATA	TEMPERATURE	DATA
-9999.0	0.30000	9999.0	0.30000

PROPERTY TABLE EX MAT= 1 NUM. POINTS= 15

TEMPERATURE	DATA	TEMPERATURE	DATA
-40.000	0.28900E+08	70.000	0.28300E+08
100.00	0.28100E+08	200.00	0.27600E+08
300.00	0.27000E+08	400.00	0.26500E+08
500.00	0.25800E+08	600.00	0.25300E+08
700.00	0.24800E+08	800.00	0.24100E+08
900.00	0.23500E+08	1000.0	0.22500E+08
1100.0	0.22100E+08	1200.0	0.21300E+08
1300.0	0.20500E+08		

PROPERTY TABLE ALPX MAT= 1 NUM. POINTS= 15

TEMPERATURE	DATA	TEMPERATURE	DATA
-40.000	0.81300E-05	70.000	0.84600E-05
100.00	0.85500E-05	200.00	0.87900E-05
300.00	0.90000E-05	400.00	0.91900E-05
500.00	0.93700E-05	600.00	0.95300E-05
700.00	0.96900E-05	800.00	0.98200E-05
900.00	0.10060E-04	1000.0	0.10300E-04
1100.0	0.10350E-04	1200.0	0.10400E-04
1300.0	0.10450E-04		

PROPERTY TABLE EX MAT= 2 NUM. POINTS= 7

TEMPERATURE	DATA	TEMPERATURE	DATA
-40.000	0.28400E+08	70.000	0.27800E+08
100.00	0.27600E+08	200.00	0.27100E+08
300.00	0.26700E+08	400.00	0.26100E+08
500.00	0.25700E+08		

```
PROPERTY TABLE ALPX  MAT=   2  NUM. POINTS=  7
    TEMPERATURE      DATA    TEMPERATURE      DATA
     -40.000      0.59400E-05  70.000      0.62000E-05
      100.00      0.62700E-05  200.00      0.65400E-05
      300.00      0.67800E-05  400.00      0.69800E-05
      500.00      0.71600E-05
TIME= 0.00000E+00  NITTER=    -10
KTEMP-  LSTP=    -1  ITER=     0

UNIFORM TEMPERATURE=    70.000  (TREF=    70.000)
 BOUNDARY CONDITIONS STEPPED DUE TO STATIC CONVERGENCE OPTION
PLASTIC CONVERG. CRITERION=       0.0100
CREEP OPTIMUM. CRITERION=         0.1000
LARGE DEFL. CONVERG. CRITERION=    0.001000
DISPLACEMENT LIMIT= 0.00000E+00

NPRINT= 99900   NPOST=    10   REACTION PRINT FREQ= 99900
 DISP. POST DATA FREQ=    10  REACT. POST DATA FREQ=    10

 ELEMENT PRINT AND POST DATA FREQUENCIES
  TYPE  STIFF  STRESS  FORCE   STRESS   DATA  FORCE
         NO.   PRINT  PRINT    DATA    LEVEL  DATA
    1     42  99900  99900      10       3     10
    2     51  99900  99900      10       3     10
    3      1  99900  99900      10       3     10
    4      3  99900  99900      10       3     10
    5     12  99900  99900      10       3     10
    6     42  99900  99900      10       3     10

LOADS INPUT FILE= 26     LOADS OUTPUT FILE= 23

ALL ANALYSIS DATA WILL BE WRITTEN ONTO FILE27

LIST DISPLACEMENTS FOR ALL SELECTED NODES

 NODE  LABEL     DISP           CDISP
    3 UZ     0.000000000E+00 0.000000000E+00
    4 UZ     0.000000000E+00 0.000000000E+00
    5 UZ     0.000000000E+00 0.000000000E+00
    8 UZ     0.000000000E+00 0.000000000E+00
    9 UZ     0.000000000E+00 0.000000000E+00
   10 UZ     0.000000000E+00 0.000000000E+00
   13 UZ     0.000000000E+00 0.000000000E+00
   14 UZ     0.000000000E+00 0.000000000E+00
   15 UZ     0.000000000E+00 0.000000000E+00
   18 UZ     0.000000000E+00 0.000000000E+00
   19 UZ     0.000000000E+00 0.000000000E+00
   20 UZ     0.000000000E+00 0.000000000E+00
   22 UZ     0.000000000E+00 0.000000000E+00
   23 UZ     0.000000000E+00 0.000000000E+00
   24 UZ     0.000000000E+00 0.000000000E+00
   25 UZ     0.000000000E+00 0.000000000E+00
   27 UZ     0.000000000E+00 0.000000000E+00
   28 UZ     0.000000000E+00 0.000000000E+00
   29 UZ     0.000000000E+00 0.000000000E+00
   30 UZ     0.000000000E+00 0.000000000E+00

 NODE  LABEL     DISP           CDISP
   31 UZ     0.000000000E+00 0.000000000E+00
   32 UZ     0.000000000E+00 0.000000000E+00
   33 UZ     0.000000000E+00 0.000000000E+00
   34 UZ     0.000000000E+00 0.000000000E+00
   35 UZ     0.000000000E+00 0.000000000E+00
   36 UZ     0.000000000E+00 0.000000000E+00
   37 UZ     0.000000000E+00 0.000000000E+00
   38 UZ     0.000000000E+00 0.000000000E+00
   39 UZ     0.000000000E+00 0.000000000E+00
   40 UZ     0.000000000E+00 0.000000000E+00
   41 UZ     0.000000000E+00 0.000000000E+00
   42 UZ     0.000000000E+00 0.000000000E+00
   43 UZ     0.000000000E+00 0.000000000E+00
   44 UZ     0.000000000E+00 0.000000000E+00
   45 UZ     0.000000000E+00 0.000000000E+00
   46 UZ     0.000000000E+00 0.000000000E+00
```

47	UZ	0.000000000E+00	0.000000000E+00
48	UZ	0.000000000E+00	0.000000000E+00
49	UZ	0.000000000E+00	0.000000000E+00
50	UZ	0.000000000E+00	0.000000000E+00

NODE	LABEL	DISP	CDISP
53	UZ	0.000000000E+00	0.000000000E+00
54	UZ	0.000000000E+00	0.000000000E+00
55	UZ	0.000000000E+00	0.000000000E+00
56	UZ	0.000000000E+00	0.000000000E+00
57	UZ	0.000000000E+00	0.000000000E+00
58	UZ	0.000000000E+00	0.000000000E+00
59	UZ	0.000000000E+00	0.000000000E+00
60	UZ	0.000000000E+00	0.000000000E+00
61	UZ	0.000000000E+00	0.000000000E+00
62	UZ	0.000000000E+00	0.000000000E+00
63	UZ	0.000000000E+00	0.000000000E+00
64	UZ	0.000000000E+00	0.000000000E+00
65	UZ	0.000000000E+00	0.000000000E+00
66	UZ	0.000000000E+00	0.000000000E+00
67	UZ	0.000000000E+00	0.000000000E+00
68	UZ	0.000000000E+00	0.000000000E+00
69	UZ	0.000000000E+00	0.000000000E+00
70	UZ	0.000000000E+00	0.000000000E+00
71	UZ	0.000000000E+00	0.000000000E+00
72	UZ	0.000000000E+00	0.000000000E+00

NODE	LABEL	DISP	CDISP
73	UZ	0.000000000E+00	0.000000000E+00
74	UZ	0.000000000E+00	0.000000000E+00
75	UZ	0.000000000E+00	0.000000000E+00
76	UZ	0.000000000E+00	0.000000000E+00
77	UZ	0.000000000E+00	0.000000000E+00
78	UZ	0.000000000E+00	0.000000000E+00
79	UZ	0.000000000E+00	0.000000000E+00
80	UZ	0.000000000E+00	0.000000000E+00
81	UZ	0.000000000E+00	0.000000000E+00
82	UZ	0.000000000E+00	0.000000000E+00
83	UZ	0.000000000E+00	0.000000000E+00
84	UZ	0.000000000E+00	0.000000000E+00
85	UZ	0.000000000E+00	0.000000000E+00
86	UZ	0.000000000E+00	0.000000000E+00
87	UZ	0.000000000E+00	0.000000000E+00
88	UZ	0.000000000E+00	0.000000000E+00
89	UZ	0.000000000E+00	0.000000000E+00
90	UZ	0.000000000E+00	0.000000000E+00
91	UZ	0.000000000E+00	0.000000000E+00
92	UZ	0.000000000E+00	0.000000000E+00

NODE	LABEL	DISP	CDISP
93	UZ	0.000000000E+00	0.000000000E+00
94	UZ	0.000000000E+00	0.000000000E+00
101	UZ	0.000000000E+00	0.000000000E+00
102	UZ	0.000000000E+00	0.000000000E+00
103	UZ	0.000000000E+00	0.000000000E+00
104	UZ	0.000000000E+00	0.000000000E+00
105	UZ	0.000000000E+00	0.000000000E+00
106	UZ	0.000000000E+00	0.000000000E+00
107	UZ	0.000000000E+00	0.000000000E+00
108	UZ	0.000000000E+00	0.000000000E+00
109	UZ	0.000000000E+00	0.000000000E+00
110	UZ	0.000000000E+00	0.000000000E+00
111	UZ	0.000000000E+00	0.000000000E+00
112	UZ	0.000000000E+00	0.000000000E+00
113	UZ	0.000000000E+00	0.000000000E+00
114	UZ	0.000000000E+00	0.000000000E+00
115	UZ	0.000000000E+00	0.000000000E+00
116	UZ	0.000000000E+00	0.000000000E+00
117	UZ	0.000000000E+00	0.000000000E+00
118	UZ	0.000000000E+00	0.000000000E+00

NODE	LABEL	DISP	CDISP
119	UZ	0.000000000E+00	0.000000000E+00
120	UZ	0.000000000E+00	0.000000000E+00

121	UZ	0.000000000E+00	0.000000000E+00
122	UZ	0.000000000E+00	0.000000000E+00
123	UZ	0.000000000E+00	0.000000000E+00
124	UZ	0.000000000E+00	0.000000000E+00
129	UZ	0.000000000E+00	0.000000000E+00
130	UZ	0.000000000E+00	0.000000000E+00
131	UZ	0.000000000E+00	0.000000000E+00
136	UZ	0.000000000E+00	0.000000000E+00
137	UZ	0.000000000E+00	0.000000000E+00
138	UZ	0.000000000E+00	0.000000000E+00
143	UZ	0.000000000E+00	0.000000000E+00
144	UZ	0.000000000E+00	0.000000000E+00
145	UZ	0.000000000E+00	0.000000000E+00
150	UZ	0.000000000E+00	0.000000000E+00
151	UZ	0.000000000E+00	0.000000000E+00
152	UZ	0.000000000E+00	0.000000000E+00
157	UZ	0.000000000E+00	0.000000000E+00
158	UZ	0.000000000E+00	0.000000000E+00

NODE	LABEL	DISP	CDISP
159	UZ	0.000000000E+00	0.000000000E+00
164	UZ	0.000000000E+00	0.000000000E+00
165	UZ	0.000000000E+00	0.000000000E+00
166	UZ	0.000000000E+00	0.000000000E+00
171	UZ	0.000000000E+00	0.000000000E+00
172	UZ	0.000000000E+00	0.000000000E+00
173	UZ	0.000000000E+00	0.000000000E+00
180	UZ	0.000000000E+00	0.000000000E+00
181	UZ	0.000000000E+00	0.000000000E+00
182	UZ	0.000000000E+00	0.000000000E+00
183	UZ	0.000000000E+00	0.000000000E+00
184	UZ	0.000000000E+00	0.000000000E+00
185	UZ	0.000000000E+00	0.000000000E+00
186	UZ	0.000000000E+00	0.000000000E+00
187	UZ	0.000000000E+00	0.000000000E+00
188	UZ	0.000000000E+00	0.000000000E+00
201	UZ	0.000000000E+00	0.000000000E+00
202	UZ	0.000000000E+00	0.000000000E+00
203	UZ	0.000000000E+00	0.000000000E+00
204	UZ	0.000000000E+00	0.000000000E+00

NODE	LABEL	DISP	CDISP
205	UZ	0.000000000E+00	0.000000000E+00
206	UZ	0.000000000E+00	0.000000000E+00
207	UZ	0.000000000E+00	0.000000000E+00
208	UZ	0.000000000E+00	0.000000000E+00
209	UZ	0.000000000E+00	0.000000000E+00
210	UZ	0.000000000E+00	0.000000000E+00
211	UZ	0.000000000E+00	0.000000000E+00
212	UZ	0.000000000E+00	0.000000000E+00
213	UZ	0.000000000E+00	0.000000000E+00
214	UZ	0.000000000E+00	0.000000000E+00
215	UZ	0.000000000E+00	0.000000000E+00
216	UZ	0.000000000E+00	0.000000000E+00
217	UZ	0.000000000E+00	0.000000000E+00
221	UZ	0.000000000E+00	0.000000000E+00
222	UZ	0.000000000E+00	0.000000000E+00
223	UZ	0.000000000E+00	0.000000000E+00
224	UZ	0.000000000E+00	0.000000000E+00
225	UZ	0.000000000E+00	0.000000000E+00
226	UZ	0.000000000E+00	0.000000000E+00
227	UZ	0.000000000E+00	0.000000000E+00

NODE	LABEL	DISP	CDISP
228	UZ	0.000000000E+00	0.000000000E+00
229	UZ	0.000000000E+00	0.000000000E+00
230	UZ	0.000000000E+00	0.000000000E+00
231	UZ	0.000000000E+00	0.000000000E+00
232	UZ	0.000000000E+00	0.000000000E+00
233	UZ	0.000000000E+00	0.000000000E+00
234	UZ	0.000000000E+00	0.000000000E+00
235	UZ	0.000000000E+00	0.000000000E+00
236	UZ	0.000000000E+00	0.000000000E+00
237	UZ	0.000000000E+00	0.000000000E+00

241	UZ	0.000000000E+00	0.000000000E+00
242	UZ	0.000000000E+00	0.000000000E+00
243	UZ	0.000000000E+00	0.000000000E+00
244	UZ	0.000000000E+00	0.000000000E+00
245	UZ	0.000000000E+00	0.000000000E+00
246	UZ	0.000000000E+00	0.000000000E+00
247	UZ	0.000000000E+00	0.000000000E+00
248	UZ	0.000000000E+00	0.000000000E+00
301	UZ	0.000000000E+00	0.000000000E+00
302	UZ	0.000000000E+00	0.000000000E+00

NODE	LABEL	DISP	CDISP
303	UZ	0.000000000E+00	0.000000000E+00
304	UZ	0.000000000E+00	0.000000000E+00
305	UZ	0.000000000E+00	0.000000000E+00
306	UZ	0.000000000E+00	0.000000000E+00
307	UZ	0.000000000E+00	0.000000000E+00
308	UZ	0.000000000E+00	0.000000000E+00
309	UZ	0.000000000E+00	0.000000000E+00
310	UZ	0.000000000E+00	0.000000000E+00
311	UZ	0.000000000E+00	0.000000000E+00
312	UZ	0.000000000E+00	0.000000000E+00
313	UZ	0.000000000E+00	0.000000000E+00
314	UZ	0.000000000E+00	0.000000000E+00
315	UZ	0.000000000E+00	0.000000000E+00
316	UZ	0.000000000E+00	0.000000000E+00
317	UZ	0.000000000E+00	0.000000000E+00
321	UZ	0.000000000E+00	0.000000000E+00
322	UZ	0.000000000E+00	0.000000000E+00
323	UZ	0.000000000E+00	0.000000000E+00
324	UZ	0.000000000E+00	0.000000000E+00
325	UZ	0.000000000E+00	0.000000000E+00

NODE	LABEL	DISP	CDISP
326	UZ	0.000000000E+00	0.000000000E+00
327	UZ	0.000000000E+00	0.000000000E+00
328	UZ	0.000000000E+00	0.000000000E+00
329	UZ	0.000000000E+00	0.000000000E+00
330	UZ	0.000000000E+00	0.000000000E+00
331	UZ	0.000000000E+00	0.000000000E+00
332	UZ	0.000000000E+00	0.000000000E+00
333	UZ	0.000000000E+00	0.000000000E+00
334	UZ	0.000000000E+00	0.000000000E+00
335	UZ	0.000000000E+00	0.000000000E+00
336	UZ	0.000000000E+00	0.000000000E+00
337	UZ	0.000000000E+00	0.000000000E+00
341	UZ	0.000000000E+00	0.000000000E+00
342	UZ	0.000000000E+00	0.000000000E+00
343	UZ	0.000000000E+00	0.000000000E+00
344	UZ	0.000000000E+00	0.000000000E+00
345	UZ	0.000000000E+00	0.000000000E+00
346	UZ	0.000000000E+00	0.000000000E+00
347	UZ	0.000000000E+00	0.000000000E+00
348	UZ	0.000000000E+00	0.000000000E+00

NODE	LABEL	DISP	CDISP
349	UZ	0.000000000E+00	0.000000000E+00
350	UZ	0.000000000E+00	0.000000000E+00
351	UZ	0.000000000E+00	0.000000000E+00
352	UZ	0.000000000E+00	0.000000000E+00
171	UX	0.000000000E+00	0.000000000E+00
172	UX	0.000000000E+00	0.000000000E+00
173	UX	0.000000000E+00	0.000000000E+00
188	UX	0.000000000E+00	0.000000000E+00
188	ROTZ	0.000000000E+00	0.000000000E+00
171	UY	0.000000000E+00	0.000000000E+00

LIST ELEMENT PRESSURES FOR ALL SELECTED ELEMENTS

ELEM	FACE	VALUE($)		FACE NODES	
95	1	34.7998000	0.000000000E+00	49	53
96	1	34.7998000	0.000000000E+00	53	55
97	1	34.7998000	0.000000000E+00	55	57
98	1	34.7998000	0.000000000E+00	57	59

99	1	34.7998000	0.000000000E+00	59	61
100	1	34.7998000	0.000000000E+00	61	63
101	1	34.7998000	0.000000000E+00	63	65
102	1	34.7998000	0.000000000E+00	65	67
103	1	34.7998000	0.000000000E+00	67	69
104	1	34.7998000	0.000000000E+00	69	71
105	1	34.7998000	0.000000000E+00	71	73
106	1	34.7998000	0.000000000E+00	73	75
107	1	34.7998000	0.000000000E+00	75	77
108	1	34.7998000	0.000000000E+00	77	79
109	1	34.7998000	0.000000000E+00	79	81
110	1	34.7998000	0.000000000E+00	81	83
111	1	34.7998000	0.000000000E+00	83	85
112	1	34.7998000	0.000000000E+00	85	87
113	1	34.7998000	0.000000000E+00	87	89
114	1	34.7998000	0.000000000E+00	89	91

ELEM	FACE	VALUE(S)		FACE NODES	
115	1	34.7998000	0.000000000E+00	91	93
116	1	34.7998000	0.000000000E+00	93	180
117	1	34.7998000	0.000000000E+00	180	181
118	1	34.7998000	0.000000000E+00	181	182
119	1	34.7998000	0.000000000E+00	182	183
120	1	34.7998000	0.000000000E+00	183	184
121	1	34.7998000	0.000000000E+00	184	185
122	1	34.7998000	0.000000000E+00	185	186
123	1	34.7998000	0.000000000E+00	186	187
124	1	34.7998000	0.000000000E+00	187	188
70	2	34.7998000	0.000000000E+00	145	152
76	2	34.7998000	0.000000000E+00	152	159
82	2	34.7998000	0.000000000E+00	159	166
88	2	34.7998000	0.000000000E+00	166	173
278	3	34.7998000	0.000000000E+00	349	145
266	3	34.7998000	0.000000000E+00	337	349
243	2	34.7998000	0.000000000E+00	317	337
192	3	34.7998000	0.000000000E+00	237	217
216	2	34.7998000	0.000000000E+00	22	237
18	4	34.7998000	0.000000000E+00	27	22

ELEM	FACE	VALUE(S)		FACE NODES	
21	4	34.7998000	0.000000000E+00	32	27
26	4	34.7998000	0.000000000E+00	38	32
27	4	34.7998000	0.000000000E+00	42	38
29	4	34.7998000	0.000000000E+00	45	42
31	4	34.7998000	0.000000000E+00	48	45
192	4	34.7998000	0.000000000E+00	217	216
243	1	34.7998000	0.000000000E+00	316	317

LIST ELEMENT CONVECTIONS FOR ALL SELECTED ELEMENTS

LIST TEMPERATURES FOR ALL SELECTED NODES

NODE	TEMPERATURE	FLUENCE
3	180.28	0.00000E+00
4	203.81	0.00000E+00
5	203.81	0.00000E+00
8	180.28	0.00000E+00
9	203.81	0.00000E+00
10	203.81	0.00000E+00
13	180.28	0.00000E+00
14	203.81	0.00000E+00
15	203.81	0.00000E+00
18	174.06	0.00000E+00
19	194.77	0.00000E+00
20	194.77	0.00000E+00
22	153.35	0.00000E+00
23	174.06	0.00000E+00
24	194.77	0.00000E+00
25	194.77	0.00000E+00
27	243.17	0.00000E+00
28	243.17	0.00000E+00
29	243.17	0.00000E+00
30	243.17	0.00000E+00

NODE	TEMPERATURE	FLUENCE
31	1250.5	0.00000E+00
32	243.17	0.00000E+00
33	243.17	0.00000E+00
34	243.17	0.00000E+00
35	243.17	0.00000E+00
36	907.05	0.00000E+00
37	455.98	0.00000E+00
38	243.17	0.00000E+00
39	243.17	0.00000E+00
40	243.17	0.00000E+00
41	772.95	0.00000E+00
42	538.16	0.00000E+00
43	538.16	0.00000E+00
44	538.16	0.00000E+00
45	538.16	0.00000E+00
46	538.16	0.00000E+00
47	538.16	0.00000E+00
48	538.16	0.00000E+00
49	538.16	0.00000E+00
50	538.16	0.00000E+00

NODE	TEMPERATURE	FLUENCE
53	710.35	0.00000E+00
54	772.95	0.00000E+00
55	882.55	0.00000E+00
56	772.95	0.00000E+00
57	882.60	0.00000E+00
58	877.56	0.00000E+00
59	882.65	0.00000E+00
60	982.17	0.00000E+00
61	882.69	0.00000E+00
62	1086.8	0.00000E+00
63	882.74	0.00000E+00
64	1191.4	0.00000E+00
65	884.31	0.00000E+00
66	1195.0	0.00000E+00
67	885.88	0.00000E+00
68	1198.5	0.00000E+00
69	887.45	0.00000E+00
70	1202.1	0.00000E+00
71	889.02	0.00000E+00
72	1205.7	0.00000E+00

NODE	TEMPERATURE	FLUENCE
73	890.59	0.00000E+00
74	1209.2	0.00000E+00
75	892.16	0.00000E+00
76	1212.8	0.00000E+00
77	893.73	0.00000E+00
78	1213.8	0.00000E+00
79	895.30	0.00000E+00
80	1214.8	0.00000E+00
81	896.87	0.00000E+00
82	1215.7	0.00000E+00
83	898.44	0.00000E+00
84	1216.7	0.00000E+00
85	900.01	0.00000E+00
86	1217.7	0.00000E+00
87	901.58	0.00000E+00
88	1218.7	0.00000E+00
89	903.15	0.00000E+00
90	1219.7	0.00000E+00
91	904.72	0.00000E+00
92	1220.7	0.00000E+00

NODE	TEMPERATURE	FLUENCE
93	906.29	0.00000E+00
94	1221.6	0.00000E+00
101	144.81	0.00000E+00
102	144.81	0.00000E+00
103	144.81	0.00000E+00
104	144.81	0.00000E+00
105	144.81	0.00000E+00

106	144.81	0.00000E+00
107	144.81	0.00000E+00
108	144.81	0.00000E+00
109	144.81	0.00000E+00
110	144.81	0.00000E+00
111	144.81	0.00000E+00
112	144.81	0.00000E+00
113	144.81	0.00000E+00
114	144.81	0.00000E+00
115	144.81	0.00000E+00
116	144.81	0.00000E+00
117	144.81	0.00000E+00
118	144.81	0.00000E+00

NODE	TEMPERATURE	FLUENCE
119	144.81	0.00000E+00
120	144.81	0.00000E+00
121	144.81	0.00000E+00
122	111.08	0.00000E+00
123	111.08	0.00000E+00
124	111.08	0.00000E+00
129	111.08	0.00000E+00
130	111.08	0.00000E+00
131	111.08	0.00000E+00
136	111.08	0.00000E+00
137	111.08	0.00000E+00
138	111.08	0.00000E+00
143	111.08	0.00000E+00
144	111.08	0.00000E+00
145	111.08	0.00000E+00
150	93.893	0.00000E+00
151	93.893	0.00000E+00
152	93.893	0.00000E+00
157	94.837	0.00000E+00
158	94.837	0.00000E+00

NODE	TEMPERATURE	FLUENCE
159	94.837	0.00000E+00
164	95.051	0.00000E+00
165	95.051	0.00000E+00
166	95.051	0.00000E+00
171	95.051	0.00000E+00
172	95.051	0.00000E+00
173	95.051	0.00000E+00
180	1219.1	0.00000E+00
181	1219.1	0.00000E+00
182	1219.1	0.00000E+00
183	1219.1	0.00000E+00
184	1219.1	0.00000E+00
185	1215.0	0.00000E+00
186	1210.9	0.00000E+00
187	1210.9	0.00000E+00
188	1210.9	0.00000E+00
201	156.76	0.00000E+00
202	156.76	0.00000E+00
203	156.76	0.00000E+00
204	156.76	0.00000E+00

NODE	TEMPERATURE	FLUENCE
205	156.76	0.00000E+00
206	156.76	0.00000E+00
207	156.76	0.00000E+00
208	156.76	0.00000E+00
209	156.76	0.00000E+00
210	153.35	0.00000E+00
211	153.35	0.00000E+00
212	153.35	0.00000E+00
213	153.35	0.00000E+00
214	153.35	0.00000E+00
215	153.35	0.00000E+00
216	153.35	0.00000E+00
217	153.35	0.00000E+00
221	156.76	0.00000E+00
222	156.76	0.00000E+00

223	156.76	0.00000E+00
224	156.76	0.00000E+00
225	156.76	0.00000E+00
226	156.76	0.00000E+00
227	156.76	0.00000E+00

NODE	TEMPERATURE	FLUENCE
228	156.76	0.00000E+00
229	156.76	0.00000E+00
230	153.35	0.00000E+00
231	153.35	0.00000E+00
232	153.35	0.00000E+00
233	153.35	0.00000E+00
234	153.35	0.00000E+00
235	153.35	0.00000E+00
236	153.35	0.00000E+00
237	153.35	0.00000E+00
241	156.76	0.00000E+00
242	156.76	0.00000E+00
243	156.76	0.00000E+00
244	156.76	0.00000E+00
245	156.76	0.00000E+00
246	153.35	0.00000E+00
247	153.35	0.00000E+00
248	153.35	0.00000E+00
301	111.08	0.00000E+00
302	111.08	0.00000E+00

NODE	TEMPERATURE	FLUENCE
303	111.08	0.00000E+00
304	111.08	0.00000E+00
305	111.08	0.00000E+00
306	111.08	0.00000E+00
307	111.08	0.00000E+00
308	111.08	0.00000E+00
309	111.08	0.00000E+00
310	111.08	0.00000E+00
311	111.08	0.00000E+00
312	111.08	0.00000E+00
313	111.08	0.00000E+00
314	111.08	0.00000E+00
315	111.08	0.00000E+00
316	111.08	0.00000E+00
317	111.08	0.00000E+00
321	111.08	0.00000E+00
322	111.08	0.00000E+00
323	111.08	0.00000E+00
324	111.08	0.00000E+00
325	111.08	0.00000E+00

NODE	TEMPERATURE	FLUENCE
326	111.08	0.00000E+00
327	111.08	0.00000E+00
328	111.08	0.00000E+00
329	111.08	0.00000E+00
330	111.08	0.00000E+00
331	111.08	0.00000E+00
332	111.08	0.00000E+00
333	111.08	0.00000E+00
334	111.08	0.00000E+00
335	111.08	0.00000E+00
336	111.08	0.00000E+00
337	111.08	0.00000E+00
341	111.08	0.00000E+00
342	111.08	0.00000E+00
343	111.08	0.00000E+00
344	111.08	0.00000E+00
345	111.08	0.00000E+00
346	111.08	0.00000E+00
347	111.08	0.00000E+00
348	111.08	0.00000E+00

NODE	TEMPERATURE	FLUENCE
349	111.08	0.00000E+00

350	111.08	0.00000E+00
351	111.08	0.00000E+00
352	111.08	0.00000E+00

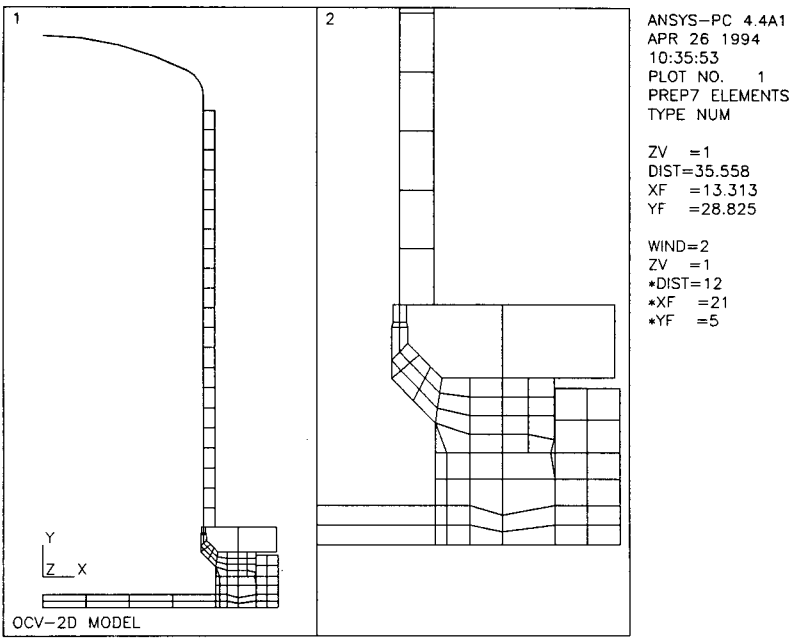


FIGURE 2.10.8-1.

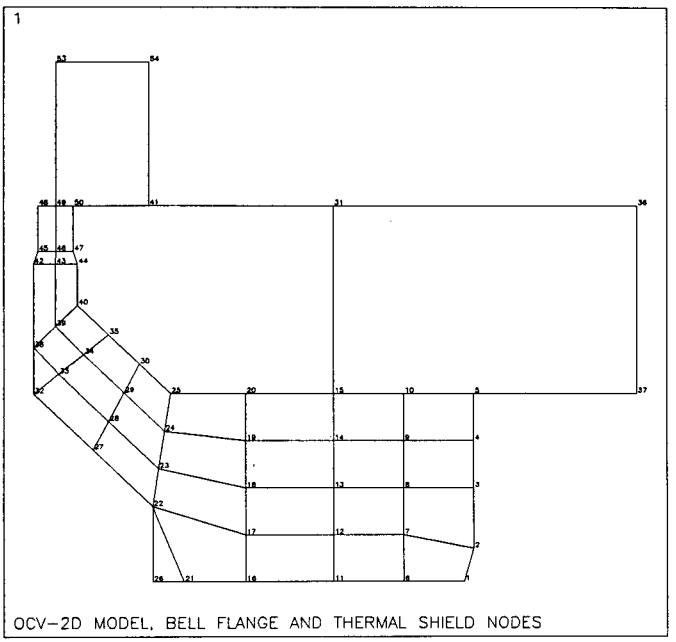


FIGURE 2.10.8-2.

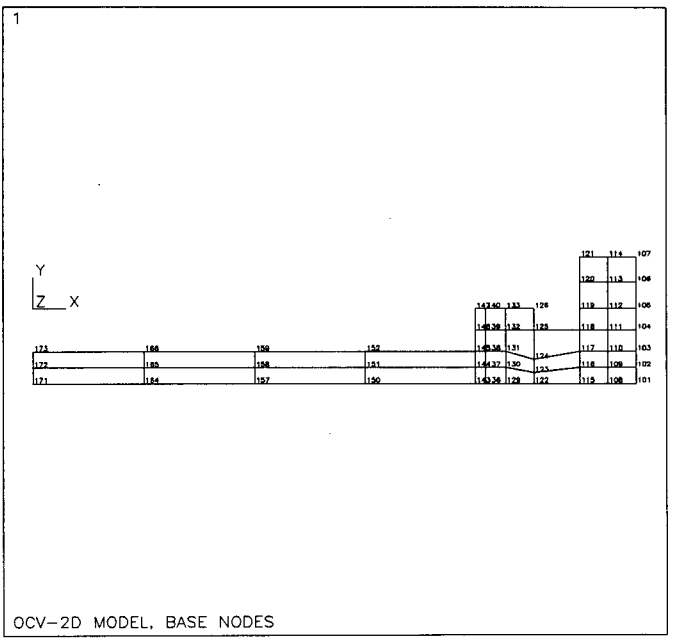


FIGURE 2.10.8-3.

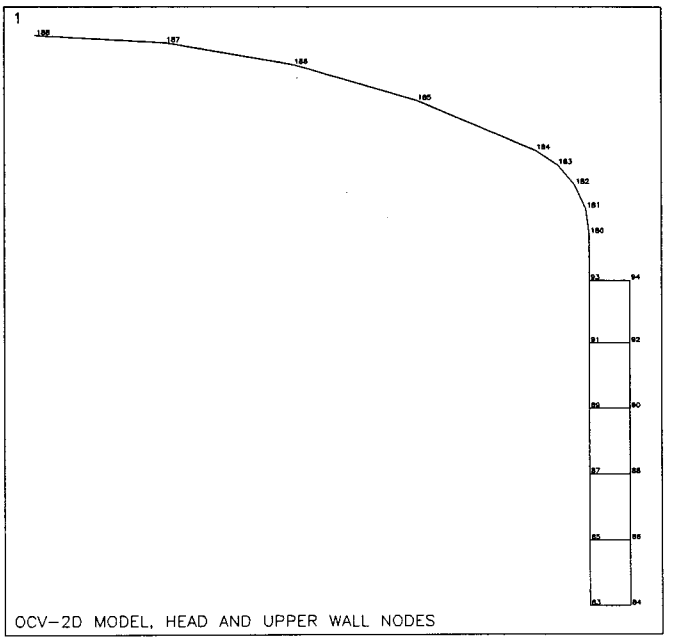


FIGURE 2.10.8-4.

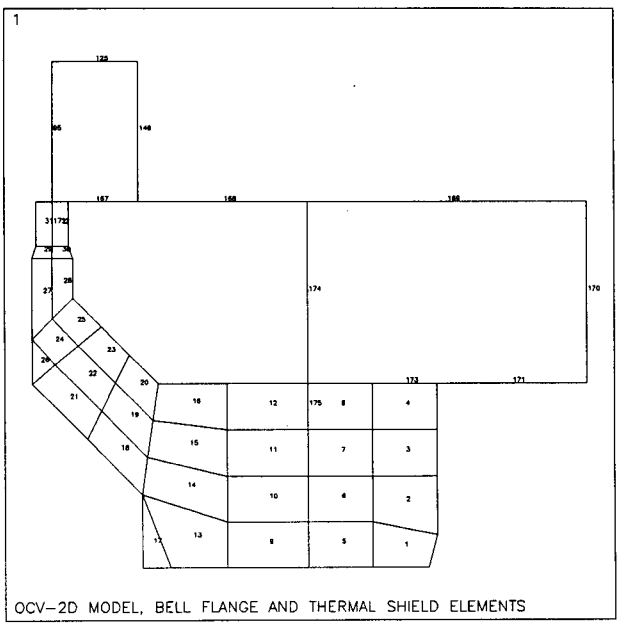


FIGURE 2.10.8-5.

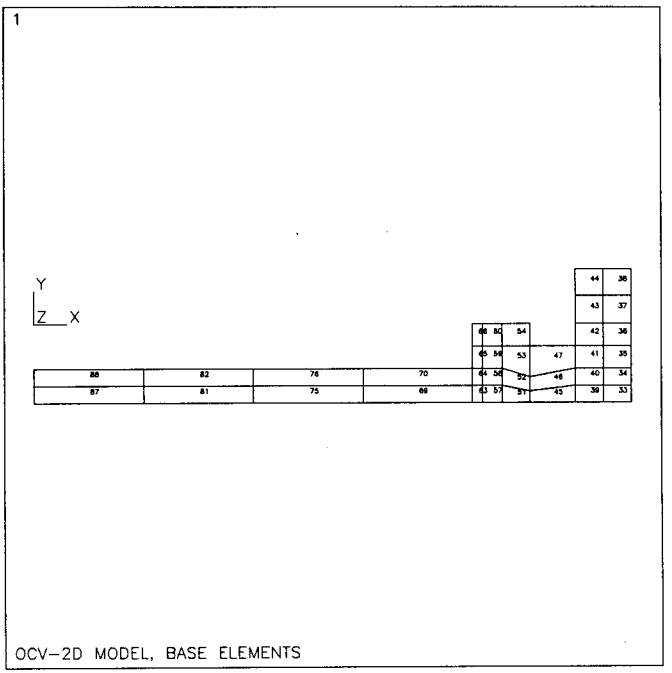


FIGURE 2.10.8-6.

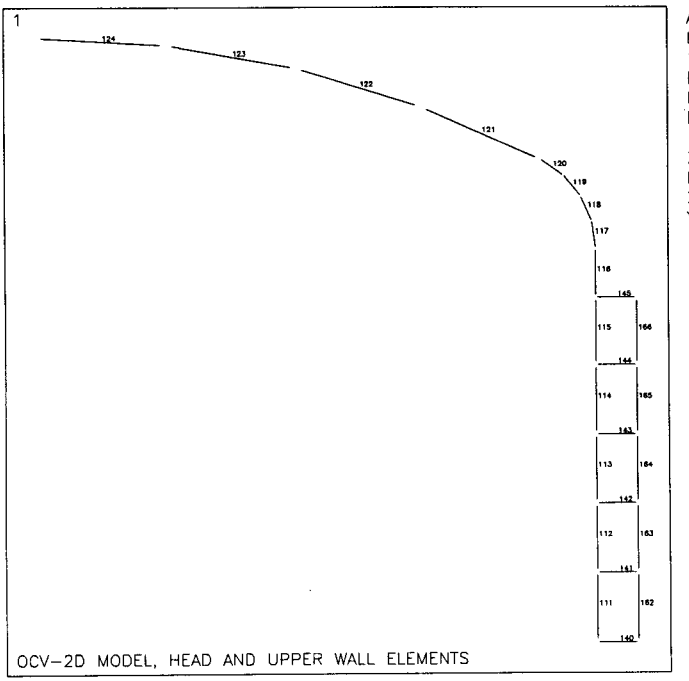


FIGURE 2.10.8-7.

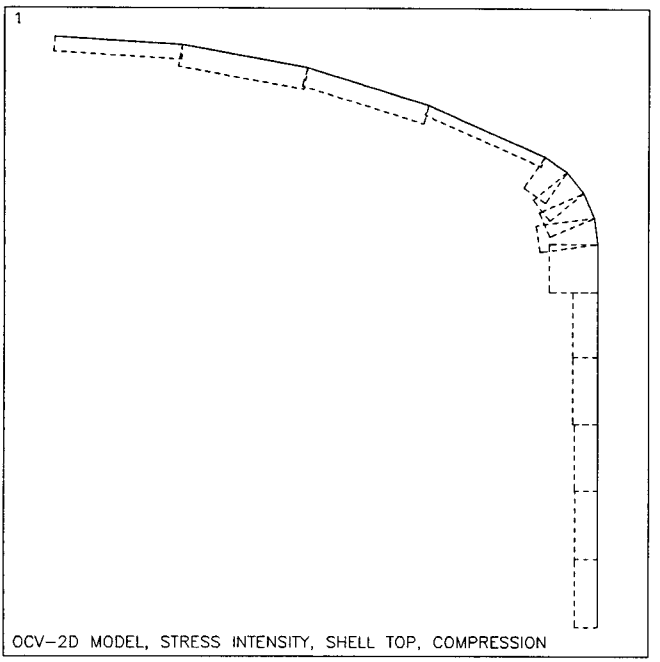


FIGURE 2.10.8-8.

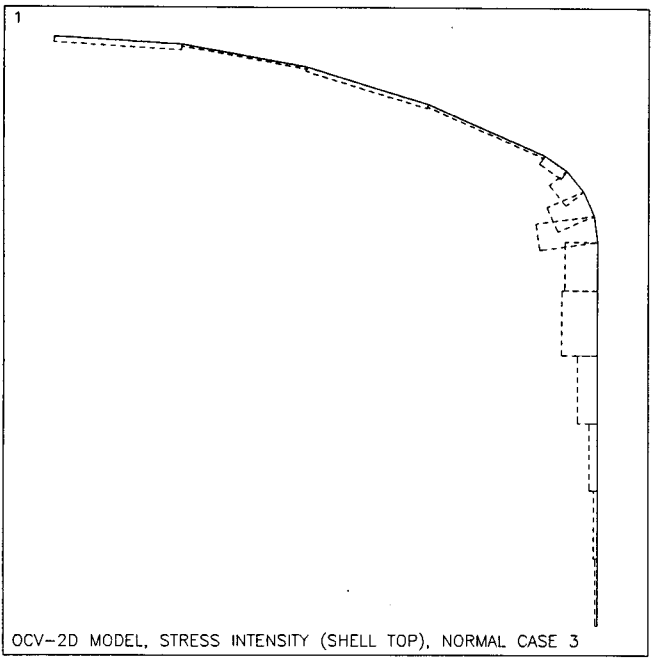


FIGURE 2.10.8-9.

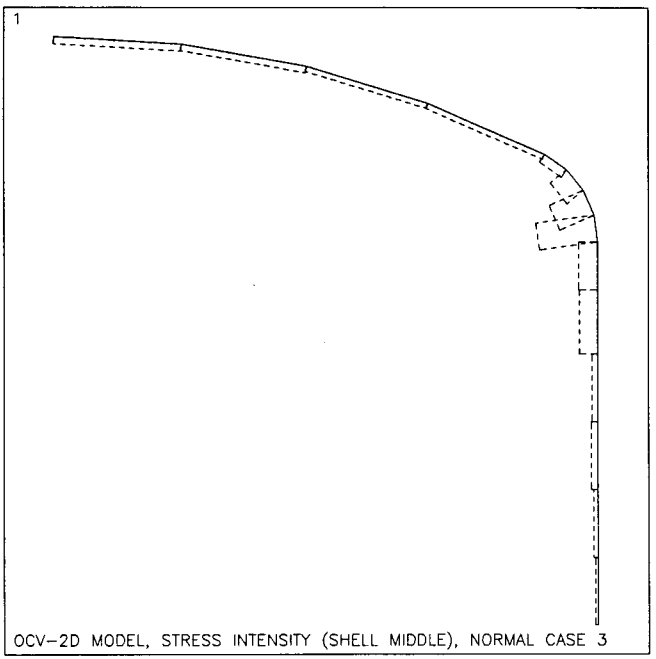


FIGURE 2.10.8-10.

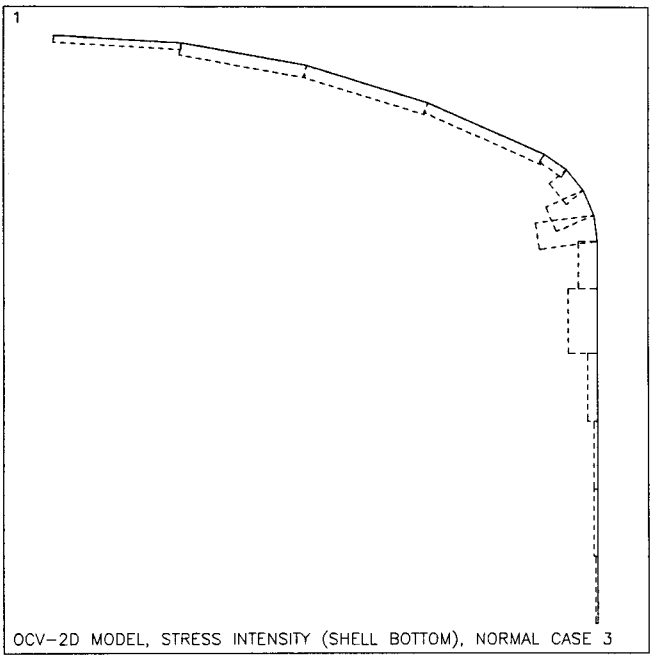


FIGURE 2.10.8-11.

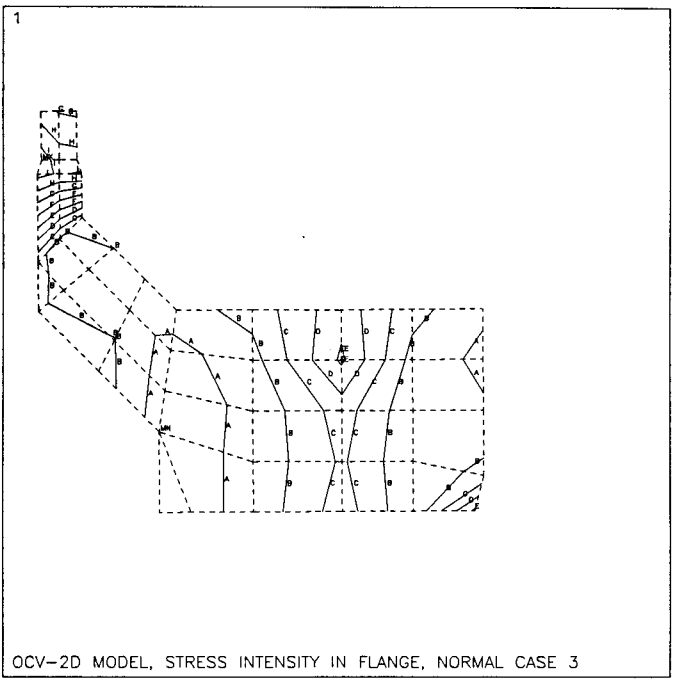


FIGURE 2.10.8-12.

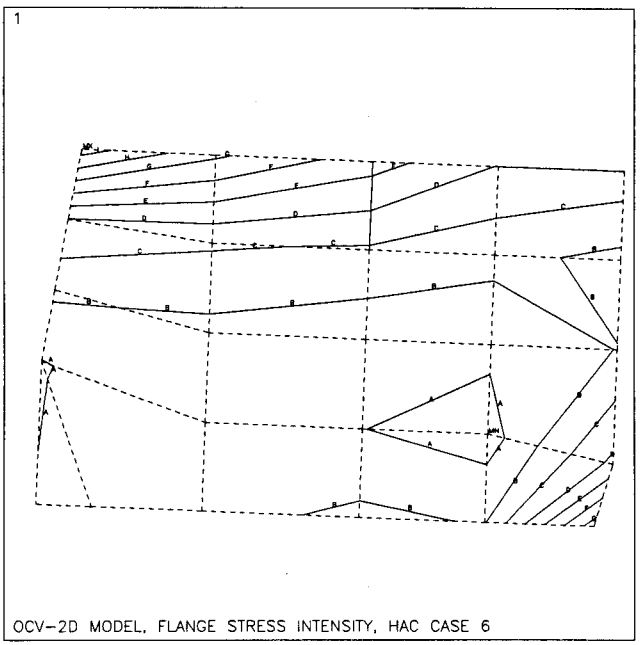


FIGURE 2.10.8-13.

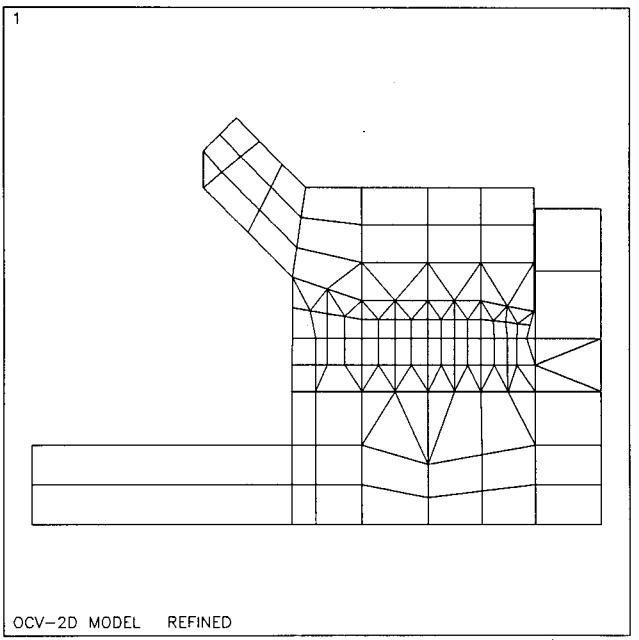


FIGURE 2.10.8-14.

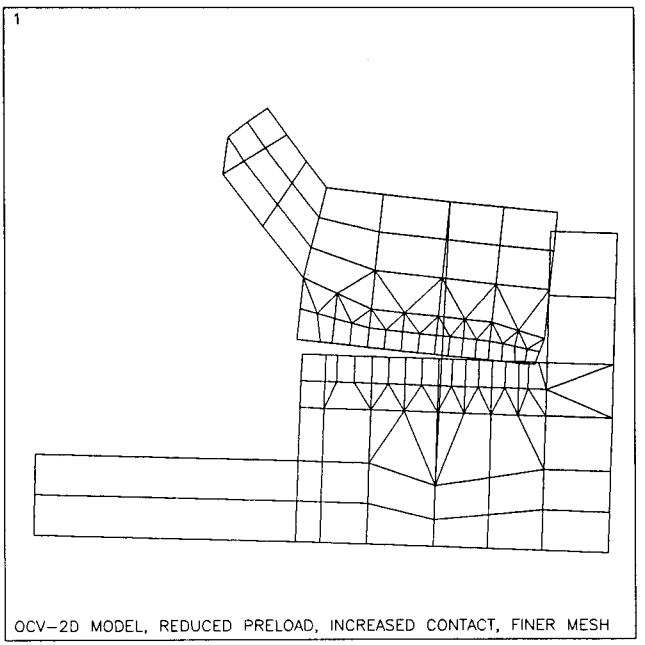


FIGURE 2.10.8-15.

2.10.9 RTG Transportation System Package Certification Test Plan

2.10.9.1 First Certification Test Series. The RTG Transportation System Certification Test Plan for the first certification test series is included in its entirety in document WHC-SD-RTG-TP-009. The first certification test article (CTA-1) was used during this drop test series.

2.10.9.2 Second Certification Test Series. The RTG Transportation System Certification Test Plan for the second certification test series is included in its entirety in document WHC-SD-RTG-TP-018, Rev. 1. The second certification test article (CTA-2) was used during this drop test series.

2.10.9.3 Simulated Payload. Attached are a fabrication drawing of the simulated payload configuration (Figure 2.10.9.3-3) and sketches of the simulated payload and the GPHS payload within the package (Figures 2.10.9.3-1 and 2.10.9.3-2, respectively). For visual comparison purposes, superimposed on the GPHS payload is an outline of the simulated payload. The cg marks on each figure indicate the cg of the payload (without rack). The following weight and center of gravity information table is provided as additional information to aid in the comparison of simulated and real payloads.

Table 2.10.9.3-1. Simulated Payload Comparisons.

Payload	Payload shipping rack weight (lb)	Payload weight w/o shipping rack (lb)	Total weight of payload plus shipping rack (lb)	Height of payload cg above barrier plate (in.)	Height of payload plus rack cg above ICV base plate (in.)
Simulated	225	570	795	26.9	24.5
GPHS	225	200	425	17.5	13.4

As shown, the weight of the simulated payload conservatively envelopes the weight of the GPHS RTG payload. With a packaging weight and cg (excluding payload and shipping rack) of 8,850 pounds and 9.98 in. above the ICV base plate per Table 2.2-1, the overall cg of the package only varies by 1.05 in. between the simulated and GPHS payload configurations (11.18 and 10.14 in. above ICV base plate, respectively). This slight cg variation has negligible effect on package response to HAC free drop and puncture events.

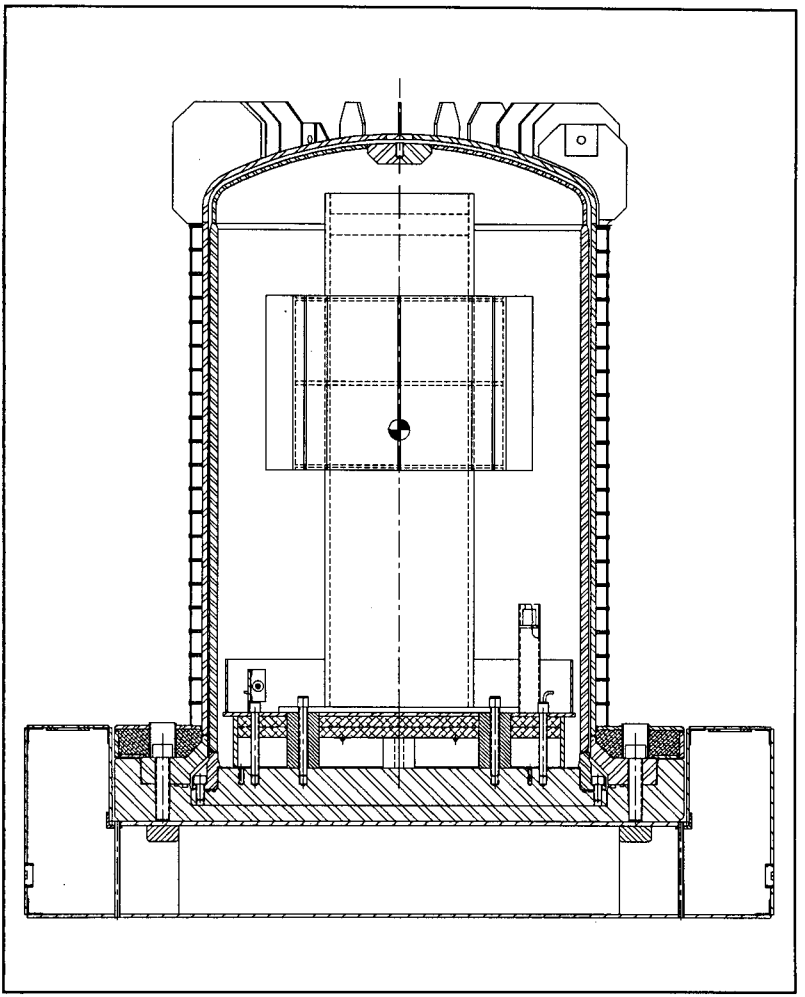


FIGURE 2.10.9.3-1. Simulated Payload Within the RTG Shipping Package.

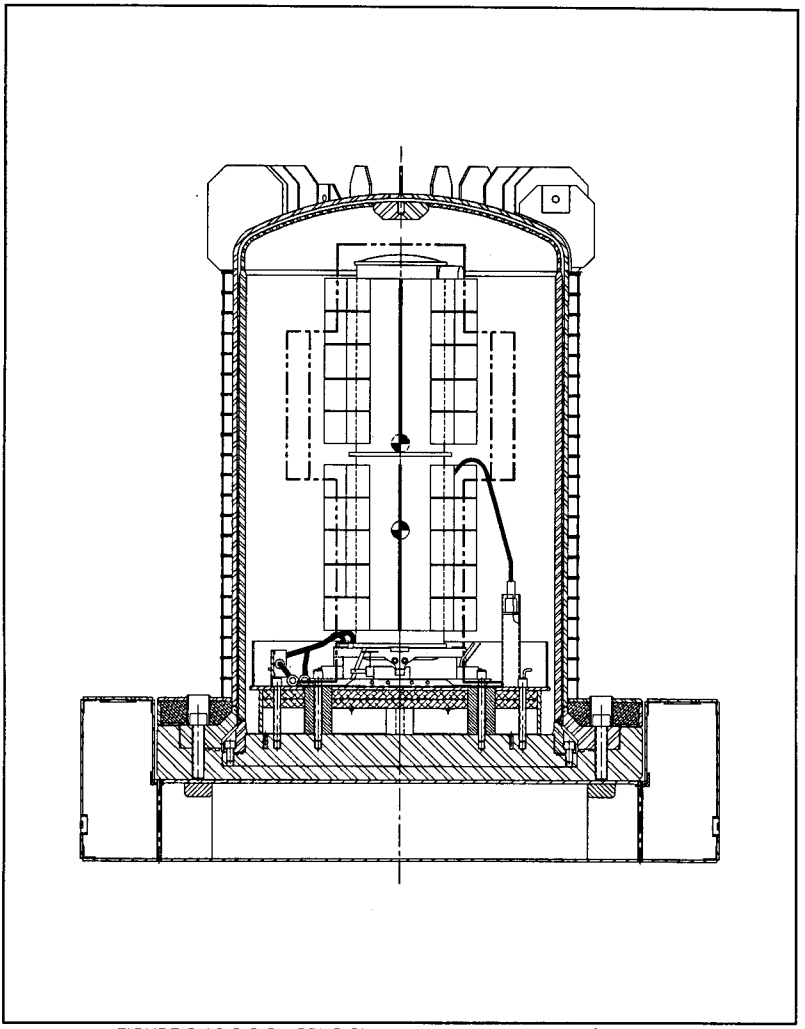


FIGURE 2.10.9.3-2. GPHS/Simulated Payload Within RTG Package.

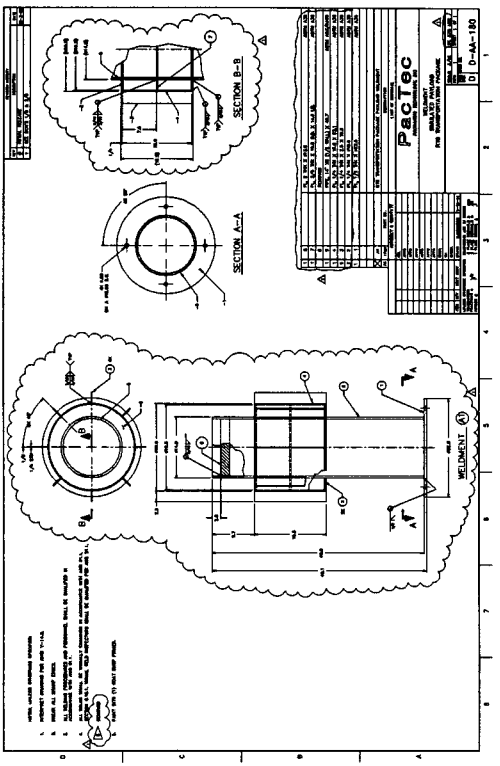


FIGURE 2.10.9.3-3.

BEST COPY AVAILABLE

2.10.10 Certification Drop Test Procedure for the RTG Transportation System Package

The test procedure for Drop Testing of the RTG Transportation System Package Prototype is included in its entirety in document WHC-SD-RTG-TC-003 for CTA-1 and WHC-SD-RTG-TC-015, Rev. 1 for CTA-2.

2.10.11 Structural Development Test Program

As a part of the design process, structural design development testing was performed in February 1992.

2.10.11.1 Test Objectives.

2.10.11.1.1 Primary. (1) To confirm impact limiter design (dimensions, materials, attachments), or to guide design refinements, as necessary. (2) To confirm OCV head fin design, or to guide design refinements, as necessary.

2.10.11.1.2 Secondary. (1) To investigate OCV seal area response (establish amount of permanent deformations at sealing surfaces or in closure bolts, if any.)

2.10.11.2 Test Hardware. A half-scale simulation of the package was used in the test program (see Figure 2.10.11.2-1). Components related to test objectives were duplicated to a degree of accuracy considered appropriate for purposes of design concept verification. For instance, components related to primary objectives (impact limiter and OCV head fins) were scaled precisely. Secondary objective components (OCV seal flange and base plate, and closure bolts) were scaled with accuracy sufficient to allow a broad determination of overall structural response.

2.10.11.2.1 Impact Limiter. The impact limiter geometry was precisely scaled. The primary impact absorption material was polyurethane foam. The density of the foam directly beneath the OCV was 3 lb/ft^3, with the remainder being 12 lb/ft^3. The impact limiter outer shell incorporated 11 gage (0.12 in. thick) carbon steel sheet metal on one half-segment, and 13 gage (0.09-in. thickness) carbon steel sheet metal on the other half-segment. These gages were intended to conservatively scale 1/4 in. and 3/16 in. thick plate, respectively. Testing was conducted on both half segments in order to gauge the effects of shell thickness on impact limiter response.

Eight 3/8-in. diameter impact limiter attachment bolts were used to represent the 3/4-in. diameter bolts of the actual package. This was somewhat conservative, because the scaled-up tensile stress area of the 3/8-in. diameter bolts is 4×0.0775 $in.^2 = 0.310$ $in.^2$, which is less than the 0.334 $in.^2$ tensile stress area of a standard 3/4 in. diameter bolt. The half-scale impact limiter attachment bolts were torqued to 150 in-lb, resulting in an equivalent pre-load on a stress basis to the actual anticipated full-scale impact limiter bolt pre-load of 100 ft-lb.

2.10.11.2.2 Outer Containment Vessel. The OCV components, particularly in the seal area, were closely simulated to allow a determination of seal response to the regulatory test events. The OCV flange and base plate geometries in the seal region were accurately scaled, except that actual O-ring seal grooves were not incorporated. The vessel bell was also accurately represented, except that the cooling jacket was not included (its weight was lumped into the scale payload mass). The OCV head thickness was 3/8 in., whereas the actual full-scale thickness will be 1/2 in. This conservatively simulated the combined OCV and ICV head thicknesses: $1/2 \times (1/2 + 3/8) = 7/16$ in., where the full-scale ICV head thickness is 3/8 in.

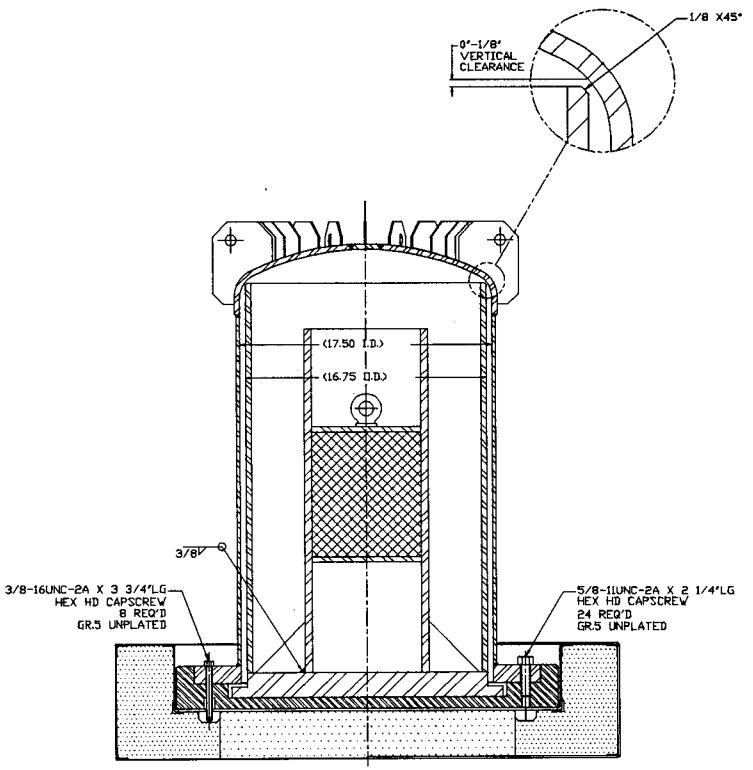


FIGURE 2.10.11.2-1. RTG Half Scale Test Article.

The OCV head fins were precisely scaled. The only difference was that all 24 of the half-scale fins had 3/4-in. diameter holes in them (to simulate shackle holes for lifting purposes), whereas the actual package will have 3/4-in. diameter lifting holes in only three of its fins.

Twenty-four, 5/8-in. diameter OCV closure bolts were used to represent the 1-1/4 in. diameter closure bolts of the actual package. This was somewhat conservative, since the scaled-up tensile stress area of the 5/8-in. diameter bolts is 4 x 0.226 $in.^2$ = 0.904 $in.^2$, which is less than the 0.969 $in.^2$ tensile stress area of a standard 1 1/4 inch diameter bolt. The half-scale closure bolts were torqued to 300 in-lb, resulting in an equivalent pre-load on a stress basis to two-thirds of the actual anticipated full-scale OCV closure bolt pre-load of 300 ft-lb.

The OCV thermal shield was not simulated on the half-scale test article. Because the thermal shield acts to stiffen the OCV flange, its absence tended to conservatively maximize any deformation effects that might occur in the OCV seal region. The overall geometry of the OCV flange, as well as the offset of the OCV wall from the closure bolt circle, were only roughly approximated.

2.10.11.2.3 Inner Containment Vessel. The ICV geometry was approximated with a simple welded plate and shell assembly. This structure was intended to simulate the response of an actual ICV relative to the OCV for the regulatory test events. Accordingly, the ICV base plate was positioned within the OCV base plate in the same manner as will occur in the actual package. Clearance between the top of the ICV head and the OCV head and between the sides of the ICV and OCV was adjusted to allow realistic relative impacts between the ICV and OCV. The ICV base plate and bell thicknesses were both scaled exactly.

2.10.11.2.4 Other Features. The total weight of the half-scale test package assembly, including simulated payload, was 1,170 pounds, which represents a full-scale weight of 8 x 1,170 pounds = 9,360 pounds. The center of gravity of the assembly was 11.5 in. from the base of the impact limiter, representing a full-scale distance of 2 x 11.5 in. = 23 in.

The payload assumed was the maximum-weight RTG, equal to 620 pounds, including shipping rack. Additionally, package weight not directly simulated on the half-scale model (e.g., the cooling jacket) was lumped into the payload weight. The overall package weight and c.g. was obtained by a segment of steel pipe, welded vertically to the ICV base plate, and partially filled with lead ballast.

The OCV and ICV half-scale test assemblies were both fabricated of carbon steel, instead of the stainless steel that will be used on the actual package. This was conservative, particularly for puncture tests, because carbon steel is less ductile than stainless steel, and would tend to rupture or tear more readily than would actual package materials.

For each drop test, three passive accelerometers were installed on the half-scale test article at the elevation of the c.g. These accelerometers indicated impact accelerations of 200*g*, 300*g*, and 400*g*, corresponding to full-scale values of 100*g*, 150*g*, and 200*g*, respectively.

2.10.11.3 Test Sequence. All testing was done at the prevailing ambient temperature, which was generally around 60 °F. The development test program consisted of two separate phases, an initial phase, and a follow-up phase. Generally, the follow-up phase incorporated design refinements in the half-scale test package that arose from knowledge gained from the test results of the initial phase.

2.10.11.3.1 Initial Phase. The first round of half-scale structural development testing consisted of the following tests:

- Six NCT free drops of 4 ft
- Five HAC free drops of 30 ft
- Six HAC puncture drops of 40 in.

Drop orientations ranged from flat end drops to flat side drops (defined for the RTG Transportation System Package as simultaneous impact on the OCV head fins and the impact limiter) and several orientations in between. Drop orientations were selected on the following bases:

- To maximize impact loading and consequent structural deformations, particularly in the OCV seal region
- To maximize separation loading on the OCV closure bolts and the impact limiter attachment bolts
- To maximize impact limiter deflections to ensure that sufficient crush depth will be available to preclude "bottoming out" on the package structure beneath the impact limiter, as well as to provide a residual thermal barrier against the HAC fire event
- To maximize HAC puncture bar damage to the impact limiter to ensure no loss of thermal barrier integrity.

Each HAC free drop impact occurred at the same point of impact and at the same orientation as a prior NCT free drop impact. This ensures that no NCT drop compromises the ability of the package to sustain a similarly-oriented HAC drop at the same impact location.

2.10.11.3.2 Follow-Up Phase. The follow-up testing was conducted to address specific issues unearthed during the initial phase of testing. This phase consisted of the following tests:

- One HAC free drop of 30 ft
- Five HAC puncture drops of 40 in.

Particular issues covered by the additional testing (see Section 2.10.11.4 below) included the following:

- Evaluate impact limiter outer bottom shell modification to reduce puncture bar penetration
- Evaluate impact limiter attachment bolt modification to preclude bolt breakage
- Evaluate effects of lubrication on closure and impact limiter attachment bolt pre-load retention.

Specifically, the carbon steel bottom plate of the impact limiter was replaced with 11 gage stainless steel to improve puncture resistance. Also, the impact limiter attachment bolts were "necked down" in the unthreaded shaft region to allow greater straining (energy absorption) during impact events and prevent fracture. Finally, all bolts (OCV closure and impact limiter attachment) were lubricated before installation to reduce torsional stress and induce more axial (pre-load) strain in the bolts.

2.10.11.4 Significant Results of Initial Test Phase.

2.10.11.4.1 Normal Conditions of Transport 4-Foot Free Drops.

1. Deformations were limited to OCV head fins and impact limiter; no permanent deformation was visually detected in the OCV seal region.

2. The impact limiter was retained for all drops, and no foam was exposed.

3. Positive residual torques existed for all bolts (OCV closure and impact limiter attachment) at the conclusion of the NCT free drops.

4. Accelerations were limited to 300*g* (150*g* full scale) for all NCT free drops.

5. Accelerations were less than 200*g* (100*g* full scale) for NCT side drops.

2.10.11.4.2 Hypothetical Accident Condition 30-Foot Free Drops.

1. All significant deformations were limited to OCV head fins and impact limiter.

2. The impact limiter was retained for all drops, and no foam was exposed.

3. For the near-vertical drop (10° angle), three impact limiter attachment bolts broke; no other drop orientations resulted in broken bolts.

4. Positive residual torques existed for all bolts (OCV closure and impact limiter attachment) at the conclusion of all other HAC free drops.

5. A minimum residual impact limiter foam thickness of about 2 in. (4 in. in full scale) remained after all HAC free drops (c.g. over corner and side drop resulted in the greatest impact limiter deformations); this is considered sufficient for protection against the HAC fire event.

6. Insignificant permanent deformation occurred in the OCV seal region (see Section 2.10.11.6).

7. Accelerations exceeded 400*g* (200*g* full scale) for all except the top end drop (consistent with 300*g* design basis assumed for actual package).

8. Acceleration was between 300 and 400*g* (150 and 200*g* full scale) for the top end drop.

2.10.11.4.3 Hypothetical Accident Condition 40-In. Puncture Drops.

1. Containment vessels were not punctured; modest (<1 in. deep), fully acceptable local deformation occurred on OCV bell after direct impact of puncture bar.

2. Impact limiter bottom plate (both thicknesses) ruptured, and "bottoming out" of puncture bar on OCV base plate occurred.

3. Impact limiter 11-gauge cylindrical sidewall exhibited minor, fully acceptable, crescent-shaped tear.

4. For the side puncture drop, one OCV closure bolt (the one nearest the impact point) lost all pre-load; adjacent closure bolts retained pre-load torques of more than 250 in-lb (of the initial 300 in-lb pre-load torque).

5. Positive residual torques existed for all bolts (OCV closure and impact limiter attachment) at the conclusion of all other HAC puncture drops.

6. Maximum acceleration was less than 200*g* (100*g* full scale) for all puncture tests.

2.10.11.5 Significant Results of Follow-Up Test Phase

2.10.11.5.1 Hypothetical Accident Condition 30 Foot Free Drops.

1. Repetition of the near-vertical HAC free drop, with modified impact limiter attachment bolts installed, resulted in bolt stretch (and loss of all pre-load on one attachment bolt), but no breakage; design refinement is considered successful.

2. Minimum residual pre-load on all OCV closure bolts was greater than for previous similar drop, probably because of lubrication of bolts.

3. Accelerations exceeded 400*g* (200*g* full scale).

2.10.11.5.2 Hypothetical Accident Condition 40-In. Puncture Drops.

1. Modified impact limiter bottom shell reduced puncture bar penetration, but did not preclude it entirely; resulting puncture damage was considered minor from a HAC fire barrier standpoint, because of the intumescent character of the foam.

2. No accelerometers tripped for any of the follow-up HAC puncture tests.

2.10.11.6 Conclusions. In general, the structural development test program was considered to be very successful. The basic structural design being used has been sound. Both the removable foam impact limiter and particularly the OCV head fins performed well in reducing impact loads. No significant deformations were observed that would lead to loss of containment, excessive loss of shielding, or which would preclude acceptable package performance in a subsequent HAC fire event.

As a result of the developmental testing, the following design refinements have been made to the RTG Transportation System Package:

1. Use of stainless steel instead of carbon steel for the impact limiter shell

2. Use of 1/4-in. thick plate on the top and outer cylindrical side surfaces, and 5/16-in. thick plate on the bottom surface of the impact limiter

3. Addition of 2 in. of height to the impact limiter (7 in. increased to 9 in.)

4. "Necking down" impact limiter attachment bolts

5. Minor OCV base plate design change to allow for longer effective length on OCV closure bolts

6. Cadmium plating of all bolts

7. Incorporate thermal barrier interior to limiter, adjacent to OCV base.

Items 1 and 2 will improve impact limiter puncture resistance, and item 3 will increase the residual foam depth after HAC impact. Although performance in these categories was deemed adequate subsequent to the follow-up testing, these design refinements will provide an additional comfort margin in the design.

Item 4 results in improved impact limiter attachment bolt performance, as discussed in Section 2.10.11.3.2. Item 5 allows greater axial stretch of the OCV closure bolts under pre-load, providing more margin against an excessive loss of pre-load during handling and operation. Item 6 will provide permanent lubrication for all bolts; again, the result will be improved retention of initial pre-load.

Item 7 is a backup thermal feature that may not be ultimately retained. The decision will be based on the results of the full-scale certification puncture tests.

*** RMIS View/Print Document Cover Sheet ***

This document was retrieved from the Documentation and Records Management (DRM) ISEARCH System. It is intended for Information only and may not be the most recent or updated version. Contact a Document Service Center (see Hanford Info for locations) if you need additional retrieval information.

Accession #: D196080875

Document #: SD-RTG-SARP-001

Title/Desc:
RTG TRANSPORTATION SYSTEM SARP DOCKET NO 94-6-9904 [VOL I] [SEC 2 OF 4]

Pages: 203

This document was too large to scan as a whole document, therefore it required breaking into smaller sections.

Document number: SD-RTG-SARP-001

Section 2 **of** 4

Title: RADIOISOTOPE THERMOELECTRIC GENERATOR TRANSPORTATION SYSTEM SAFETY ANALYSIS REPORT FOR PACKAGING

Date: 4/18/96 **Revision:** 0

Originator: FERRELL PC
Co: WHC

Recipient:
Co:

References: EDT-613639

2.10.12 ICV Three-Dimensional ANSYS Model

2.10.12.1 Description. The 3-D ICV finite element model employs half symmetry to address nonaxisymmetric RTG heat-producing debris potentially resulting from the HAC 30-ft free drop. It consists of a base and a bell, connected by bolt elements and gap elements. The plane of symmetry bisects an arc between two closure bolts. Impact limiter damage and heat-producing debris are both conservatively assumed to be centered on the plane of symmetry, halfway between two closure bolts.

The model helps evaluate closure bolt stresses and O-ring residual compression for the ICV under HAC. (The model used for NCT is 2-D and is described in Appendix 2.10.2.) The applied loading takes the form of internal gas pressure, nodal temperatures, and initial closure bolt pre-load. Certain node locations were chosen to coincide with the nodes found in the SINDA thermal models described in Section 3.0. The relative displacement of two coincident nodes, one belonging to the ICV base structure and one to the ICV bell at the inside diameter of the ICV flange, are used with linear extrapolation to determine the change in O-ring compression from the applied conditions. The model is used for ICV analysis for the HAC load cases given in Table 2.7.3.1.1.3-1. The model layout is shown in Figure 2.10.12-1.

2.10.12.2 Construction. The model consists of four element types:

1. To model the region around the ICV flange and base, 3-D isoparametric solid elements were used. The nodal pattern was repeated in the circumferential direction every 15° of arc, incrementing node numbers by 30 each time.

2. For the center of the ICV base and for the ICV wall and head, quadrilateral shell elements were used. In the ICV base, the thickness was 3.47 in., in the ICV wall, 0.75 in., and in the ICV head, 0.375 in. (The lifting block was not modeled because it was located far from regions of interest.) To join shell and isoparametric elements, embedded elements are used, having 1/10th the bending stiffness of the adjacent shell elements (see Reference 25, Chapter 9).

3. A 3-D spar element was used to model each closure bolt. The half-symmetry model used had 13 closure bolts with a pre-load force corresponding to a torque of 250 ft-lb. The bolt element was given an initial strain to achieve the desired closure bolt pre-load force at 70 °F, without other applied loads.

4. Gap elements were used between nodes 25 and 403 (and at every corresponding location circumferentially) for a total of 13 between the ICV base and flange. Every such gap corresponds to a closure bolt location. Because the bolt/gap radial location coincides with a step machined in the flange lower surface, no other gap elements on the contact face proved to be necessary. Three additional gaps are also used in the radial direction at 0°, 90°, and 180° to locate the ICV bell horizontally with respect to the ICV base. These gaps have a small "open stiffness" for model stability and a nominal gap size of 0.03 in., which is the nominal centered radial clearance between the ICV bell I.D. and the ICV base O.D.

Node and element plots of key portions of the model are given in Figures 2.10.12-2 through 2.10.12-11. An interpreted ANSYS input listing is given in Table 2.10.12-1.

2.10.12.3 Material Properties. The modulus of elasticity and coefficient of thermal expansion varied with temperature according to the data in Tables 2.3-1 and 2.3-2. Poisson's ratio is 0.3.

2.10.12.4 Constraints. The node at the center of the ICV base is fixed in all six degrees of

freedom, but the rest of the ICV base was allowed to deflect as determined by the applied loading. Nodes along the cut edges were constrained in the one linear and two rotational degrees of freedom required to ensure symmetry of the model.

2.10.12.5 Applied Loading. All ICV surfaces subject to internal pressure had a constant pressure applied. Nodal temperature loading was applied using temperatures resulting from the 3-D thermal model output for each HAC configuration assumption. Each HAC thermal model was composed of six segments: one centered on 0°, one centered on 180°, and four segments in between (two on each side). The centers of the HAC thermal model segments corresponded (with one exception) to a circumferential location of nodes in the structural model. (In one case, the center of a HAC thermal model segment fell on 101.25°, but a location of 105° was assumed in the structural model.) Circumferential interpolation was used to set the nodal temperatures of structural locations that fell in between the centers of the HAC thermal model segments. Some interpolation was also used within each circumferential location to fully define the temperatures of the structural model. Because the closure bolts were not modeled thermally in the structural model, it took the temperatures of the ICV flange and base at its attachment nodes. The reference was 70 °F.

2.10.12.6 Results. A plot of ICV flange stress intensity for the HAC event analysis is given in Figure 2.10.12-12. Other results are given in Sections 2.7.3.2 and 4.3.2.

APPENDIX 2.10.12
REVISED ANSYS INPUT LISTING

```
STATIC ANALYSIS (KAN= 0)

LINEAR ANALYSIS - NO NON-LINEAR PROPERTIES

REFERENCE TEMPERATURE=     70.000 (TREF)
UNIFORM TEMPERATURE  =     70.000 (TUNIF)

*****ANALYSIS OPTIONS (KAY VALUES) (IF ANY) *****

NO STATIC INTERPOLATION/EXTRAPOLATION (KAY(3)=0)

SMALL DEFLECTION SOLUTION (KAY(6)=0)

NO STRESS STIFFENING (KAY(8)=0)

USE INITIAL-STIFFNESS NEWTON-RAPHSON SOLUTION PROCEDURE  (KAY(9)=3)

IN-CORE WAVE-FRONT EQUATION SOLVER (KAY(10)=0)

LIST ELEMENT TYPES FROM  1 TO 20 BY 1

NO. STIF          KEYOPT VALUES          INOPR
 2   63   0  0  0   0  0  0   0  0  0    0  QUAD. FLAT SHELL
 3    8   0  0  0   0  0  0   0  0  0    0  SPAR, 3-D
 4   52   0  0  1   0  0  0   0  0  0    0  INTERFACE ELEM. 3-D
 5   45   0  0  0   0  0  0   0  0  0    0  ISOPAR. STRESS SOLID, 3-D
 6   63   0  0  0   0  0  0   0  0  0    0  QUAD. FLAT SHELL
 7   45   0  0  0   0  0  0   0  0  0    0  ISOPAR. STRESS SOLID, 3-D
 8   63   0  0  0   0  0  0   0  0  0    0  QUAD. FLAT SHELL
 9   63   0  0  0   0  0  0   0  0  0    0  QUAD. FLAT SHELL

LIST ALL REAL SETS

 REAL CONSTANT SET   2  ITEMS    1 TO  18
  0.75000      0.00000E+00  0.00000E+00  0.00000E+00  0.00000E+00  0.00000E+00
  0.00000E+00  0.00000E+00  0.00000E+00  0.00000E+00  0.00000E+00  0.00000E+00
  0.00000E+00  0.00000E+00  0.00000E+00  0.00000E+00  0.00000E+00  0.00000E+00

 REAL CONSTANT SET   3  ITEMS    1 TO  18
  0.33000      0.26324E-02  0.00000E+00  0.00000E+00  0.00000E+00  0.00000E+00
  0.00000E+00  0.00000E+00  0.00000E+00  0.00000E+00  0.00000E+00  0.00000E+00
  0.00000E+00  0.00000E+00  0.00000E+00  0.00000E+00  0.00000E+00  0.00000E+00

 REAL CONSTANT SET   4  ITEMS    1 TO  18
  0.16500      0.26324E-02  0.00000E+00  0.00000E+00  0.00000E+00  0.00000E+00
  0.00000E+00  0.00000E+00  0.00000E+00  0.00000E+00  0.00000E+00  0.00000E+00
  0.00000E+00  0.00000E+00  0.00000E+00  0.00000E+00  0.00000E+00  0.00000E+00

 REAL CONSTANT SET  21  ITEMS    1 TO  18
  0.37500      0.00000E+00  0.00000E+00  0.00000E+00  0.00000E+00  0.00000E+00
  0.00000E+00  0.00000E+00  0.00000E+00  0.00000E+00  0.00000E+00  0.00000E+00
  0.00000E+00  0.00000E+00  0.00000E+00  0.00000E+00  0.00000E+00  0.00000E+00

 REAL CONSTANT SET  22  ITEMS    1 TO  18
  0.34800      0.00000E+00  0.00000E+00  0.00000E+00  0.00000E+00  0.00000E+00
  0.00000E+00  0.00000E+00  0.00000E+00  0.00000E+00  0.00000E+00  0.00000E+00
  0.00000E+00  0.00000E+00  0.00000E+00  0.00000E+00  0.00000E+00  0.00000E+00

 REAL CONSTANT SET  23  ITEMS    1 TO  18
  3.4700       0.00000E+00  0.00000E+00  0.00000E+00  0.00000E+00  0.00000E+00
  0.00000E+00  0.00000E+00  0.00000E+00  0.00000E+00  0.00000E+00  0.00000E+00
  0.00000E+00  0.00000E+00  0.00000E+00  0.00000E+00  0.00000E+00  0.00000E+00

 REAL CONSTANT SET  24  ITEMS    1 TO  18
  1.6250       0.00000E+00  0.00000E+00  0.00000E+00  0.00000E+00  0.00000E+00
  0.00000E+00  0.00000E+00  0.00000E+00  0.00000E+00  0.00000E+00  0.00000E+00
  0.00000E+00  0.00000E+00  0.00000E+00  0.00000E+00  0.00000E+00  0.00000E+00

 REAL CONSTANT SET  41  ITEMS    1 TO  18
  0.50000E+10 -0.20000E-09  0.00000E+00  0.00000E+00  0.00000E+00  0.00000E+00
```

```
  0.00000E+00  0.00000E+00  0.00000E+00  0.00000E+00  0.00000E+00  0.00000E+00
  0.00000E+00  0.00000E+00  0.00000E+00  0.00000E+00  0.00000E+00  0.00000E+00

 REAL CONSTANT SET  42  ITEMS    1 TO  18
  0.25000E+10 -0.20000E-09  0.00000E+00  0.00000E+00  0.00000E+00  0.00000E+00
  0.00000E+00  0.00000E+00  0.00000E+00  0.00000E+00  0.00000E+00  0.00000E+00
  0.00000E+00  0.00000E+00  0.00000E+00  0.00000E+00  0.00000E+00  0.00000E+00

 REAL CONSTANT SET  43  ITEMS    1 TO  18
  0.50000E+10  0.30000E-01  0.00000E+00  0.00000E+00  0.00000E+00  0.00000E+00
  0.00000E+00  0.00000E+00  0.00000E+00  0.00000E+00  0.00000E+00  0.00000E+00
  0.00000E+00  0.00000E+00  0.00000E+00  0.00000E+00  0.00000E+00  0.00000E+00

 REAL CONSTANT SET  44  ITEMS    1 TO  18
  0.25000E+10  0.30000E-01  0.00000E+00  0.00000E+00  0.00000E+00  0.00000E+00
  0.00000E+00  0.00000E+00  0.00000E+00  0.00000E+00  0.00000E+00  0.00000E+00
  0.00000E+00  0.00000E+00  0.00000E+00  0.00000E+00  0.00000E+00  0.00000E+00
LIST ALL COORDINATE SYSTEMS

    SYSTEM TYPE                      CENTER                PARAMETERS    SING KEYS
 0  0 (CARTESIAN)          0.000      0.000      0.000      0.000  0.000   0  0
 1  1 (CYLINDRICAL)        0.000      0.000      0.000      1.000  0.000   0  0
 2  2 (SPHERICAL)          0.000      0.000      0.000      1.000  1.000   0  0
11  1 (CYLINDRICAL)        0.000      0.000      0.000      1.000  1.000   0  0
12  1 (CYLINDRICAL)        0.000     27.252      0.000      1.000  1.000   0  0
13  1 (CYLINDRICAL)       14.937     56.397      0.000      1.000  1.000   0  0
15  1 (CYLINDRICAL)        0.016      0.000      0.000      1.000  1.000   0  0

SYSTEM          ORIENTATION VECTORS (X,Y,Z)
    0      1.00  0.00  0.00    0.00  1.00  0.00    0.00  0.00  1.00
    1      1.00  0.00  0.00    0.00  1.00  0.00    0.00  0.00  1.00
    2      1.00  0.00  0.00    0.00  1.00  0.00    0.00  0.00  1.00
   11      1.00  0.00  0.00    0.00  0.00 -1.00    0.00  1.00  0.00
   12      1.00  0.00  0.00    0.00  1.00  0.00    0.00  0.00  1.00
   13      1.00  0.00  0.00    0.00  1.00  0.00    0.00  0.00  1.00
   15      1.00  0.00  0.00    0.00  0.00 -1.00    0.00  1.00  0.00
CSYS TYPE     XC           YC           ZC          THXY      THYZ      THXZ
 11    1 0.00000E+00 0.00000E+00 0.00000E+00     0.000     0.000   -90.000
 12    1 0.00000E+00  27.252      0.00000E+00     0.000     0.000     0.000
 13    1  14.937       56.397      0.00000E+00     0.000     0.000     0.000
 15    1 0.16000E-01 0.00000E+00 0.00000E+00     0.000     0.000   -90.000

LIST ALL SELECTED ELEMENTS.   (LIST NODES)

  ELEM MAT TYP REL ESYS        NODES

     1   1   6  23    0     391   151   181   390
     2   1   6  23    0     390   181   211   396
     3   1   6  23    0     392   121   151   391
     4   1   6  23    0     396   211   241   397
     5   1   6  23    0     121   122   152   151
     6   1   6  23    0     151   152   182   181
     7   1   6  23    0     181   182   212   211
     8   1   6  23    0     211   212   242   241
     9   1   6  23    0     393    91   121   392
    10   1   6  23    0      91    92   122   121
    11   1   6  23    0     397   241   271   398
    12   1   6  23    0     241   242   272   271
    13   1   6  23    0      92    93   123   122
    14   1   6  23    0     122   123   153   152
    15   1   6  23    0     152   153   183   182
    16   1   6  23    0     182   183   213   212
    17   1   6  23    0     212   213   243   242
    18   1   6  23    0     242   243   273   272
    19   1   6  23    0     394    61    91   393
    20   1   6  23    0      61    62    92    91

  ELEM MAT TYP REL ESYS        NODES

    21   1   6  23    0      62    63    93    92
    22   1   6  23    0     398   271   301   399
    23   1   6  23    0     271   272   302   301
    24   1   6  23    0     272   273   303   302
    25   1   6  24    0      63    71   101    93
```

26	1	6	24	0	93	101	131	123				
27	1	6	24	0	123	131	161	153				
28	1	6	24	0	153	161	191	183				
29	1	6	24	0	183	191	221	213				
30	1	6	24	0	213	221	251	243				
31	1	6	24	0	243	251	281	273				
32	1	6	24	0	273	281	311	303				
33	1	5	1	0	63	71	72	67	93	101	102	97
34	1	5	1	0	93	101	102	97	123	131	132	127
35	1	5	1	0	123	131	132	127	153	161	162	157
36	1	5	1	0	153	161	162	157	183	191	192	187
37	1	5	1	0	183	191	192	187	213	221	222	217
38	1	5	1	0	213	221	222	217	243	251	252	247
39	1	5	1	0	243	251	252	247	273	281	282	277
40	1	5	1	0	273	281	282	277	303	311	312	307

ELEM	MAT	TYP	REL	ESYS	NODES							
41	1	5	1	0	65	70	71	63	95	100	101	93
42	1	5	1	0	95	100	101	93	125	130	131	123
43	1	5	1	0	125	130	131	123	155	160	161	153
44	1	5	1	0	155	160	161	153	185	190	191	183
45	1	5	1	0	185	190	191	183	215	220	221	213
46	1	5	1	0	215	220	221	213	245	250	251	243
47	1	5	1	0	245	250	251	243	275	280	281	273
48	1	5	1	0	275	280	281	273	305	310	311	303
49	1	6	23	0	395	31	61	394				
50	1	6	23	0	31	32	62	61				
51	1	6	23	0	32	33	63	62				
52	1	6	24	0	33	41	71	63				
53	1	6	23	0	399	301	331	400				
54	1	6	23	0	301	302	332	331				
55	1	6	23	0	302	303	333	332				
56	1	6	24	0	303	311	341	333				
57	1	5	1	0	303	311	312	307	333	341	342	337
58	1	5	1	0	305	310	311	303	335	340	341	333
59	1	5	1	0	33	41	42	37	63	71	72	67
60	1	5	1	0	35	40	41	33	65	70	71	63

ELEM	MAT	TYP	REL	ESYS	NODES							
61	1	5	1	0	37	42	43	38	67	72	73	68
62	1	5	1	0	67	72	73	68	97	102	103	98
63	1	5	1	0	97	102	103	98	127	132	133	128
64	1	5	1	0	127	132	133	128	157	162	163	158
65	1	5	1	0	157	162	163	158	187	192	193	188
66	1	5	1	0	187	192	193	188	217	222	223	218
67	1	5	1	0	217	222	223	218	247	252	253	248
68	1	5	1	0	247	252	253	248	277	282	283	278
69	1	5	1	0	277	282	283	278	307	312	313	308
70	1	5	1	0	307	312	313	308	337	342	343	338
71	1	5	1	0	42	48	49	43	72	78	79	73
72	1	5	1	0	72	78	79	73	102	108	109	103
73	1	5	1	0	102	108	109	103	132	138	139	133
74	1	5	1	0	132	138	139	133	162	168	169	163
75	1	5	1	0	162	168	169	163	192	198	199	193
76	1	5	1	0	192	198	199	193	222	228	229	223
77	1	5	1	0	222	228	229	223	252	258	259	253
78	1	5	1	0	252	258	259	253	282	288	289	283
79	1	5	1	0	282	288	289	283	312	318	319	313
80	1	5	1	0	312	318	319	313	342	348	349	343

ELEM	MAT	TYP	REL	ESYS	NODES							
81	1	5	1	0	311	317	318	312	341	347	348	342
82	1	5	1	0	281	287	288	282	311	317	318	312
83	1	5	1	0	251	257	258	252	281	287	288	282
84	1	5	1	0	221	227	228	222	251	257	258	252
85	1	5	1	0	191	197	198	192	221	227	228	222
86	1	5	1	0	161	167	168	162	191	197	198	192
87	1	5	1	0	131	137	138	132	161	167	168	162
88	1	5	1	0	101	107	108	102	131	137	138	132
89	1	5	1	0	71	77	78	72	101	107	108	102
90	1	5	1	0	41	47	48	42	71	77	78	72

91	1	5	1	0	41	46	47	47	71	76	77	77
92	1	5	1	0	71	76	77	77	101	106	107	107
93	1	5	1	0	101	106	107	107	131	136	137	137
94	1	5	1	0	131	136	137	137	161	166	167	167
95	1	5	1	0	161	166	167	167	191	196	197	197
96	1	5	1	0	191	196	197	197	221	226	227	227
97	1	5	1	0	221	226	227	227	251	256	257	257
98	1	5	1	0	251	256	257	257	281	286	287	287
99	1	5	1	0	281	286	287	287	311	316	317	317
100	1	5	1	0	311	316	317	317	341	346	347	347

ELEM	MAT	TYP	REL	ESYS	NODES							
101	1	5	1	0	40	45	46	41	70	75	76	71
102	1	5	1	0	70	75	76	71	100	105	106	101
103	1	5	1	0	100	105	106	101	130	135	136	131
104	1	5	1	0	130	135	136	131	160	165	166	161
105	1	5	1	0	160	165	166	161	190	195	196	191
106	1	5	1	0	190	195	196	191	220	225	226	221
107	1	5	1	0	220	225	226	221	250	255	256	251
108	1	5	1	0	250	255	256	251	280	285	286	281
109	1	5	1	0	280	285	286	281	310	315	316	311
110	1	5	1	0	310	315	316	311	340	345	346	341
111	1	5	1	0	34	39	40	35	64	69	70	65
112	1	5	1	0	64	69	70	65	94	99	100	95
113	1	5	1	0	94	99	100	95	124	129	130	125
114	1	5	1	0	124	129	130	125	154	159	160	155
115	1	5	1	0	154	159	160	155	184	189	190	185
116	1	5	1	0	184	189	190	185	214	219	220	215
117	1	5	1	0	214	219	220	215	244	249	250	245
118	1	5	1	0	244	249	250	245	274	279	280	275
119	1	5	1	0	274	279	280	275	304	309	310	305
120	1	5	1	0	304	309	310	305	334	339	340	335

ELEM	MAT	TYP	REL	ESYS	NODES							
121	1	5	1	0	39	44	45	40	69	74	75	70
122	1	5	1	0	69	74	75	70	99	104	105	100
123	1	5	1	0	99	104	105	100	129	134	135	130
124	1	5	1	0	129	134	135	130	159	164	165	160
125	1	5	1	0	159	164	165	160	189	194	195	190
126	1	5	1	0	189	194	195	190	219	224	225	220
127	1	5	1	0	219	224	225	220	249	254	255	250
128	1	5	1	0	249	254	255	250	279	284	285	280
129	1	5	1	0	279	284	285	280	309	314	315	310
130	1	5	1	0	309	314	315	310	339	344	345	340
131	1	6	23	0	395	1	31	31				
132	1	6	23	0	1	2	32	31				
133	1	6	23	0	2	3	33	32				
134	1	6	23	0	400	331	361	361				
135	1	6	23	0	331	332	362	361				
136	1	6	23	0	332	333	363	362				
137	1	6	24	0	3	11	41	33				
138	1	6	24	0	333	341	371	363				
139	1	5	1	0	342	348	349	343	372	378	379	373
140	1	5	1	0	337	342	343	338	367	372	373	368

ELEM	MAT	TYP	REL	ESYS	NODES							
141	1	5	1	0	333	341	342	337	363	371	372	367
142	1	5	1	0	341	347	348	342	371	377	378	372
143	1	5	1	0	341	346	347	347	371	376	377	377
144	1	5	1	0	335	340	341	333	365	370	371	363
145	1	5	1	0	334	339	340	335	364	369	370	365
146	1	5	1	0	340	345	346	341	370	375	376	371
147	1	5	1	0	339	344	345	340	369	374	375	370
148	1	5	1	0	12	18	19	13	42	48	49	43
149	1	5	1	0	7	12	13	8	37	42	43	38
150	1	5	1	0	3	11	12	7	33	41	42	37
151	1	5	1	0	11	17	18	12	41	47	48	42
152	1	5	1	0	11	16	17	17	41	46	47	47
153	1	5	1	0	5	10	11	3	35	40	41	33
154	1	5	1	0	4	9	10	5	34	39	40	35
155	1	5	1	0	10	15	16	11	40	45	46	41

156	1	5	1	0	9	14	15	10	39	44	45	40
157	1	5	1	0	14	20	21	15	44	50	51	45
158	1	5	1	0	15	21	22	16	45	51	52	46
159	1	5	1	0	44	50	51	45	74	80	81	75
160	1	5	1	0	45	51	52	46	75	81	82	76

ELEM	MAT	TYP	REL	ESYS	NODES							
161	1	5	1	0	74	80	81	75	104	110	111	105
162	1	5	1	0	75	81	82	76	105	111	112	106
163	1	5	1	0	104	110	111	105	134	140	141	135
164	1	5	1	0	105	111	112	106	135	141	142	136
165	1	5	1	0	134	140	141	135	164	170	171	165
166	1	5	1	0	135	141	142	136	165	171	172	166
167	1	5	1	0	164	170	171	165	194	200	201	195
168	1	5	1	0	165	171	172	166	195	201	202	196
169	1	5	1	0	194	200	201	195	224	230	231	225
170	1	5	1	0	195	201	202	196	225	231	232	226
171	1	5	1	0	224	230	231	225	254	260	261	255
172	1	5	1	0	225	231	232	226	255	261	262	256
173	1	5	1	0	254	260	261	255	284	290	291	285
174	1	5	1	0	255	261	262	256	285	291	292	286
175	1	5	1	0	284	290	291	285	314	320	321	315
176	1	5	1	0	285	291	292	286	315	321	322	316
177	1	5	1	0	314	320	321	315	344	350	351	345
178	1	5	1	0	315	321	322	316	345	351	352	346
179	1	5	1	0	344	350	351	345	374	380	381	375
180	1	5	1	0	345	351	352	346	375	381	382	376

ELEM	MAT	TYP	REL	ESYS	NODES							
181	1	5	1	0	20	23	24	21	50	53	54	51
182	1	5	1	0	21	24	25	22	51	54	55	52
183	1	5	1	0	50	53	54	51	80	83	84	81
184	1	5	1	0	51	54	55	52	81	84	85	82
185	1	5	1	0	80	83	84	81	110	113	114	111
186	1	5	1	0	81	84	85	82	111	114	115	112
187	1	5	1	0	110	113	114	111	140	143	144	141
188	1	5	1	0	111	114	115	112	141	144	145	142
189	1	5	1	0	140	143	144	141	170	173	174	171
190	1	5	1	0	141	144	145	142	171	174	175	172
191	1	5	1	0	170	173	174	171	200	203	204	201
192	1	5	1	0	171	174	175	172	201	204	205	202
193	1	5	1	0	200	203	204	201	230	233	234	231
194	1	5	1	0	201	204	205	202	231	234	235	232
195	1	5	1	0	230	233	234	231	260	263	264	261
196	1	5	1	0	231	234	235	232	261	264	265	262
197	1	5	1	0	260	263	264	261	290	293	294	291
198	1	5	1	0	261	264	265	262	291	294	295	292
199	1	5	1	0	290	293	294	291	320	323	324	321
200	1	5	1	0	291	294	295	292	321	324	325	322

ELEM	MAT	TYP	REL	ESYS	NODES							
201	1	5	1	0	320	323	324	321	350	353	354	351
202	1	5	1	0	321	324	325	322	351	354	355	352
203	1	5	1	0	350	353	354	351	380	383	384	381
204	1	5	1	0	351	354	355	352	381	384	385	382
205	2	4	41	0	55	433						
206	2	4	41	0	355	733						
207	2	4	41	0	115	493						
208	2	4	41	0	175	553						
209	2	4	41	0	235	613						
210	2	4	41	0	295	673						
211	2	3	3	0	54	437						
212	2	3	3	0	354	737						
213	2	3	3	0	114	497						
214	2	3	3	0	174	557						
215	2	3	3	0	234	617						
216	2	3	3	0	294	677						
217	1	5	1	0	23	26	27	24	53	56	57	54
218	1	5	1	0	24	27	28	25	54	57	58	55
219	1	5	1	0	53	56	57	54	83	86	87	84
220	1	5	1	0	54	57	58	55	84	87	88	85

ELEM	MAT	TYP	REL	ESYS	NODES							
221	1	5	1	0	83	86	87	84	113	116	117	114
222	1	5	1	0	84	87	88	85	114	117	118	115
223	1	5	1	0	113	116	117	114	143	146	147	144
224	1	5	1	0	114	117	118	115	144	147	148	145
225	1	5	1	0	143	146	147	144	173	176	177	174
226	1	5	1	0	144	147	148	145	174	177	178	175
227	1	5	1	0	173	176	177	174	203	206	207	204
228	1	5	1	0	174	177	178	175	204	207	208	205
229	1	5	1	0	203	206	207	204	233	236	237	234
230	1	5	1	0	204	207	208	205	234	237	238	235
231	1	5	1	0	233	236	237	234	263	266	267	264
232	1	5	1	0	234	237	238	235	264	267	268	265
233	1	5	1	0	263	266	267	264	293	296	297	294
234	1	5	1	0	264	267	268	265	294	297	298	295
235	1	5	1	0	293	296	297	294	323	326	327	324
236	1	5	1	0	294	297	298	295	324	327	328	325
237	1	5	1	0	323	326	327	324	353	356	357	354
238	1	5	1	0	324	327	328	325	354	357	358	355
239	1	5	1	0	353	356	357	354	383	386	387	384
240	1	5	1	0	354	357	358	355	384	387	388	385

ELEM	MAT	TYP	REL	ESYS	NODES							
241	1	7	1	0	403	404	408	407	433	434	438	437
242	1	7	1	0	402	403	407	406	432	433	437	436
243	1	7	1	0	407	408	412	411	437	438	442	441
244	1	7	1	0	406	407	411	410	436	437	441	440
245	1	7	1	0	433	434	438	437	463	464	468	467
246	1	7	1	0	463	464	468	467	493	494	498	497
247	1	7	1	0	432	433	437	436	462	463	467	466
248	1	7	1	0	462	463	467	466	492	493	497	496
249	1	7	1	0	437	438	442	441	467	468	472	471
250	1	7	1	0	436	437	441	440	466	467	471	470
251	1	7	1	0	467	468	472	471	497	498	502	501
252	1	7	1	0	466	467	471	470	496	497	501	500
253	1	7	1	0	493	494	498	497	523	524	528	527
254	1	7	1	0	523	524	528	527	553	554	558	557
255	1	7	1	0	492	493	497	496	522	523	527	526
256	1	7	1	0	522	523	527	526	552	553	557	556
257	1	7	1	0	497	498	502	501	527	528	532	531
258	1	7	1	0	496	497	501	500	526	527	531	530
259	1	7	1	0	527	528	532	531	557	558	562	561
260	1	7	1	0	526	527	531	530	556	557	561	560

ELEM	MAT	TYP	REL	ESYS	NODES							
261	1	7	1	0	553	554	558	557	583	584	588	587
262	1	7	1	0	583	584	588	587	613	614	618	617
263	1	7	1	0	552	553	557	556	582	583	587	586
264	1	7	1	0	582	583	587	586	612	613	617	616
265	1	7	1	0	557	558	562	561	587	588	592	591
266	1	7	1	0	556	557	561	560	586	587	591	590
267	1	7	1	0	587	588	592	591	617	618	622	621
268	1	7	1	0	586	587	591	590	616	617	621	620
269	1	7	1	0	613	614	618	617	643	644	648	647
270	1	7	1	0	643	644	648	647	673	674	678	677
271	1	7	1	0	612	613	617	616	642	643	647	646
272	1	7	1	0	642	643	647	646	672	673	677	676
273	1	7	1	0	617	618	622	621	647	648	652	651
274	1	7	1	0	616	617	621	620	646	647	651	650
275	1	7	1	0	647	648	652	651	677	678	682	681
276	1	7	1	0	646	647	651	650	676	677	681	680
277	1	7	1	0	673	674	678	677	703	704	708	707
278	1	7	1	0	703	704	708	707	733	734	738	737
279	1	7	1	0	672	673	677	676	702	703	707	706
280	1	7	1	0	702	703	707	706	732	733	737	736

ELEM	MAT	TYP	REL	ESYS	NODES							
281	1	7	1	0	677	678	682	681	707	708	712	711
282	1	7	1	0	676	677	681	680	706	707	711	710

283	1	7	1	0	707	708	712	711	737	738	742	741
284	1	7	1	0	706	707	711	710	736	737	741	740
285	1	7	1	0	733	734	738	737	763	764	768	767
286	1	7	1	0	732	733	737	736	762	763	767	766
287	1	7	1	0	737	738	742	741	767	768	772	771
288	1	7	1	0	736	737	741	740	766	767	771	770
289	1	7	1	0	401	402	406	405	431	432	436	435
290	1	7	1	0	431	432	436	435	461	462	466	465
291	1	7	1	0	405	406	410	409	435	436	440	439
292	1	7	1	0	435	436	440	439	465	466	470	469
293	1	7	1	0	461	462	466	465	491	492	496	495
294	1	7	1	0	465	466	470	469	495	496	500	499
295	1	7	1	0	491	492	496	495	521	522	526	525
296	1	7	1	0	495	496	500	499	525	526	530	529
297	1	7	1	0	521	522	526	525	551	552	556	555
298	1	7	1	0	525	526	530	529	555	556	560	559
299	1	7	1	0	551	552	556	555	581	582	586	585
300	1	7	1	0	555	556	560	559	585	586	590	589

ELEM	MAT	TYP	REL	ESYS	NODES							
301	1	7	1	0	581	582	586	585	611	612	616	615
302	1	7	1	0	585	586	590	589	615	616	620	619
303	1	7	1	0	611	612	616	615	641	642	646	645
304	1	7	1	0	615	616	620	619	645	646	650	649
305	1	7	1	0	641	642	646	645	671	672	676	675
306	1	7	1	0	645	646	650	649	675	676	680	679
307	1	7	1	0	671	672	676	675	701	702	706	705
308	1	7	1	0	675	676	680	679	705	706	710	709
309	1	7	1	0	701	702	706	705	731	732	736	735
310	1	7	1	0	731	732	736	735	761	762	766	765
311	1	7	1	0	705	706	710	709	735	736	740	739
312	1	7	1	0	735	736	740	739	765	766	770	769
313	1	7	1	0	411	412	416	415	441	442	446	445
314	1	7	1	0	410	411	415	414	440	441	445	444
315	1	7	1	0	409	410	414	413	439	440	444	443
316	1	7	1	0	441	442	446	445	471	472	476	475
317	1	7	1	0	440	441	445	444	470	471	475	474
318	1	7	1	0	439	440	444	443	469	470	474	473
319	1	7	1	0	471	472	476	475	501	502	506	505
320	1	7	1	0	470	471	475	474	500	501	505	504

ELEM	MAT	TYP	REL	ESYS	NODES							
321	1	7	1	0	469	470	474	473	499	500	504	503
322	1	7	1	0	501	502	506	505	531	532	536	535
323	1	7	1	0	500	501	505	504	530	531	535	534
324	1	7	1	0	499	500	504	503	529	530	534	533
325	1	7	1	0	531	532	536	535	561	562	566	565
326	1	7	1	0	530	531	535	534	560	561	565	564
327	1	7	1	0	529	530	534	533	559	560	564	563
328	1	7	1	0	561	562	566	565	591	592	596	595
329	1	7	1	0	560	561	565	564	590	591	595	594
330	1	7	1	0	559	560	564	563	589	590	594	593
331	1	7	1	0	591	592	596	595	621	622	626	625
332	1	7	1	0	590	591	595	594	620	621	625	624
333	1	7	1	0	589	590	594	593	619	620	624	623
334	1	7	1	0	621	622	626	625	651	652	656	655
335	1	7	1	0	620	621	625	624	650	651	655	654
336	1	7	1	0	619	620	624	623	649	650	654	653
337	1	7	1	0	651	652	656	655	681	682	686	685
338	1	7	1	0	650	651	655	654	680	681	685	684
339	1	7	1	0	649	650	654	653	679	680	684	683
340	1	7	1	0	681	682	686	685	711	712	716	715

ELEM	MAT	TYP	REL	ESYS	NODES							
341	1	7	1	0	680	681	685	684	710	711	715	714
342	1	7	1	0	679	680	684	683	709	710	714	713
343	1	7	1	0	711	712	716	715	741	742	746	745
344	1	7	1	0	741	742	746	745	771	772	776	775
345	1	7	1	0	710	711	715	714	740	741	745	744
346	1	7	1	0	740	741	745	744	770	771	775	774
347	1	7	1	0	709	710	714	713	739	740	744	743

348	1	7	1	0	739	740	744	743	769	770	774	773
349	1	7	1	0	415	416	420	419	445	446	450	449
350	1	7	1	0	414	415	419	418	444	445	449	448
351	1	7	1	0	413	414	418	417	443	444	448	447
352	1	7	1	0	445	446	450	449	475	476	480	479
353	1	7	1	0	444	445	449	448	474	475	479	478
354	1	7	1	0	443	444	448	447	473	474	478	477
355	1	7	1	0	475	476	480	479	505	506	510	509
356	1	7	1	0	474	475	479	478	504	505	509	508
357	1	7	1	0	473	474	478	477	503	504	508	507
358	1	7	1	0	505	506	510	509	535	536	540	539
359	1	7	1	0	504	505	509	508	534	535	539	538
360	1	7	1	0	503	504	508	507	533	534	538	537

ELEM	MAT	TYP	REL	ESYS	NODES							
361	1	7	1	0	535	536	540	539	565	566	570	569
362	1	7	1	0	534	535	539	538	564	565	569	568
363	1	7	1	0	533	534	538	537	563	564	568	567
364	1	7	1	0	565	566	570	569	595	596	600	599
365	1	7	1	0	564	565	569	568	594	595	599	598
366	1	7	1	0	563	564	568	567	593	594	598	597
367	1	7	1	0	595	596	600	599	625	626	630	629
368	1	7	1	0	594	595	599	598	624	625	629	628
369	1	7	1	0	593	594	598	597	623	624	628	627
370	1	7	1	0	625	626	630	629	655	656	660	659
371	1	7	1	0	624	625	629	628	654	655	659	658
372	1	7	1	0	623	624	628	627	653	654	658	657
373	1	7	1	0	655	656	660	659	685	686	690	689
374	1	7	1	0	654	655	659	658	684	685	689	688
375	1	7	1	0	653	654	658	657	683	684	688	687
376	1	7	1	0	685	686	690	689	715	716	720	719
377	1	7	1	0	684	685	689	688	714	715	719	718
378	1	7	1	0	683	684	688	687	713	714	718	717
379	1	7	1	0	715	716	720	719	745	746	750	749
380	1	7	1	0	745	746	750	749	775	776	780	779

ELEM	MAT	TYP	REL	ESYS	NODES							
381	1	7	1	0	714	715	719	718	744	745	749	748
382	1	7	1	0	744	745	749	748	774	775	779	778
383	1	7	1	0	713	714	718	717	743	744	748	747
384	1	7	1	0	743	744	748	747	773	774	778	777
385	1	8	22	0	748	778	784	754				
386	1	8	22	0	718	748	754	724				
387	1	8	22	0	688	718	724	694				
388	1	8	22	0	658	688	694	664				
389	1	8	22	0	628	658	664	634				
390	1	8	22	0	598	628	634	604				
391	1	8	22	0	568	598	604	574				
392	1	8	22	0	538	568	574	544				
393	1	8	22	0	508	538	544	514				
394	1	8	22	0	478	508	514	484				
395	1	8	22	0	448	478	484	454				
396	1	8	22	0	418	448	454	424				
397	1	7	1	0	749	750	756	755	779	780	786	785
398	1	7	1	0	748	749	755	754	778	779	785	784
399	1	7	1	0	719	720	726	725	749	750	756	755
400	1	7	1	0	718	719	725	724	748	749	755	754

ELEM	MAT	TYP	REL	ESYS	NODES							
401	1	7	1	0	689	690	696	695	719	720	726	725
402	1	7	1	0	688	689	695	694	718	719	725	724
403	1	7	1	0	659	660	666	665	689	690	696	695
404	1	7	1	0	658	659	665	664	688	689	695	694
405	1	7	1	0	629	630	636	635	659	660	666	665
406	1	7	1	0	628	629	635	634	658	659	665	664
407	1	7	1	0	599	600	606	605	629	630	636	635
408	1	7	1	0	598	599	605	604	628	629	635	634
409	1	7	1	0	569	570	576	575	599	600	606	605
410	1	7	1	0	568	569	575	574	598	599	605	604
411	1	7	1	0	539	540	546	545	569	570	576	575
412	1	7	1	0	538	539	545	544	568	569	575	574

413	1	7	1	0	509	510	516	515	539	540	546	545
414	1	7	1	0	508	509	515	514	538	539	545	544
415	1	7	1	0	479	480	486	485	509	510	516	515
416	1	7	1	0	478	479	485	484	508	509	515	514
417	1	7	1	0	449	450	456	455	479	480	486	485
418	1	7	1	0	419	420	426	425	449	450	456	455
419	1	7	1	0	418	419	425	424	448	449	455	454
420	1	7	1	0	448	449	455	454	478	479	485	484

ELEM	MAT	TYP	REL	ESYS	NODES							
421	1	7	1	0	417	418	424	423	447	448	454	453
422	1	7	1	0	421	417	423	422	451	447	453	452
423	1	7	1	0	447	448	454	453	477	478	484	483
424	1	7	1	0	451	447	453	452	481	477	483	482
425	1	7	1	0	477	478	484	483	507	508	514	513
426	1	7	1	0	481	477	483	482	511	507	513	512
427	1	7	1	0	507	508	514	513	537	538	544	543
428	1	7	1	0	511	507	513	512	541	537	543	542
429	1	7	1	0	537	538	544	543	567	568	574	573
430	1	7	1	0	541	537	543	542	571	567	573	572
431	1	7	1	0	567	568	574	573	597	598	604	603
432	1	7	1	0	571	567	573	572	601	597	603	602
433	1	7	1	0	597	598	604	603	627	628	634	633
434	1	7	1	0	601	597	603	602	631	627	633	632
435	1	7	1	0	627	628	634	633	657	658	664	663
436	1	7	1	0	631	627	633	632	661	657	663	662
437	1	7	1	0	657	658	664	663	687	688	694	693
438	1	7	1	0	661	657	663	662	691	687	693	692
439	1	7	1	0	687	688	694	693	717	718	724	723
440	1	7	1	0	691	687	693	692	721	717	723	722

ELEM	MAT	TYP	REL	ESYS	NODES							
441	1	7	1	0	717	718	724	723	747	748	754	753
442	1	7	1	0	721	717	723	722	751	747	753	752
443	1	7	1	0	751	747	753	752	781	777	783	782
444	1	7	1	0	747	748	754	753	777	778	784	783
445	1	2	2	0	754	784	1161	1131				
446	1	2	2	0	424	454	831	801				
447	1	2	2	0	454	484	861	831				
448	1	2	2	0	724	754	1131	1101				
449	1	2	2	0	484	514	891	861				
450	1	2	2	0	694	724	1101	1071				
451	1	2	2	0	514	544	921	891				
452	1	2	2	0	544	574	951	921				
453	1	2	2	0	574	604	981	951				
454	1	2	2	0	604	634	1011	981				
455	1	2	2	0	634	664	1041	1011				
456	1	2	2	0	664	694	1071	1041				
457	1	2	2	0	801	831	832	802				
458	1	2	2	0	831	861	862	832				
459	1	2	2	0	802	832	833	803				
460	1	2	2	0	832	862	863	833				

ELEM	MAT	TYP	REL	ESYS	NODES			
461	1	2	2	0	861	891	892	862
462	1	2	2	0	862	892	893	863
463	1	2	2	0	803	833	834	804
464	1	2	2	0	833	863	864	834
465	1	2	2	0	863	893	894	864
466	1	2	2	0	891	921	922	892
467	1	2	2	0	892	922	923	893
468	1	2	2	0	893	923	924	894
469	1	2	2	0	804	834	835	805
470	1	2	2	0	834	864	865	835
471	1	2	2	0	864	894	895	865
472	1	2	2	0	894	924	925	895
473	1	2	2	0	805	835	836	806
474	1	2	2	0	835	865	866	836
475	1	2	2	0	865	895	896	866
476	1	2	2	0	895	925	926	896
477	1	2	2	0	921	951	952	922

478	1	2	2	0	922	952	953	923
479	1	2	2	0	923	953	954	924
480	1	2	2	0	924	954	955	925

ELEM	MAT	TYP	REL	ESYS	NODES			
481	1	2	2	0	925	955	956	926
482	1	2	2	0	806	836	837	807
483	1	2	2	0	836	866	867	837
484	1	2	2	0	866	896	897	867
485	1	2	2	0	896	926	927	897
486	1	2	2	0	926	956	957	927
487	1	2	2	0	951	981	982	952
488	1	2	2	0	952	982	983	953
489	1	2	2	0	953	983	984	954
490	1	2	2	0	954	984	985	955
491	1	2	2	0	955	985	986	956
492	1	2	2	0	956	986	987	957
493	1	2	2	0	981	1011	1012	982
494	1	2	2	0	982	1012	1013	983
495	1	2	2	0	983	1013	1014	984
496	1	2	2	0	984	1014	1015	985
497	1	2	2	0	985	1015	1016	986
498	1	2	2	0	986	1016	1017	987
499	1	2	2	0	1016	1046	1047	1017
500	1	2	2	0	1015	1045	1046	1016

ELEM	MAT	TYP	REL	ESYS	NODES			
501	1	2	2	0	1014	1044	1045	1015
502	1	2	2	0	1013	1043	1044	1014
503	1	2	2	0	1012	1042	1043	1013
504	1	2	2	0	1011	1041	1042	1012
505	1	2	2	0	1046	1076	1077	1047
506	1	2	2	0	1045	1075	1076	1046
507	1	2	2	0	1044	1074	1075	1045
508	1	2	2	0	1043	1073	1074	1044
509	1	2	2	0	1042	1072	1073	1043
510	1	2	2	0	1041	1071	1072	1042
511	1	2	2	0	1076	1106	1107	1077
512	1	2	2	0	1075	1105	1106	1076
513	1	2	2	0	1074	1104	1105	1075
514	1	2	2	0	1073	1103	1104	1074
515	1	2	2	0	1072	1102	1103	1073
516	1	2	2	0	1071	1101	1102	1072
517	1	2	2	0	1106	1136	1137	1107
518	1	2	2	0	1105	1135	1136	1106
519	1	2	2	0	1104	1134	1135	1105
520	1	2	2	0	1103	1133	1134	1104

ELEM	MAT	TYP	REL	ESYS	NODES			
521	1	2	2	0	1102	1132	1133	1103
522	1	2	2	0	1101	1131	1132	1102
523	1	2	2	0	1136	1166	1167	1137
524	1	2	2	0	1135	1165	1166	1136
525	1	2	2	0	1134	1164	1165	1135
526	1	2	2	0	1133	1163	1164	1134
527	1	2	2	0	1132	1162	1163	1133
528	1	2	2	0	1131	1161	1162	1132
637	2	4	41	0	325	703		
638	2	4	41	0	265	643		
639	2	4	41	0	205	583		
640	2	4	41	0	145	523		
641	2	4	41	0	85	463		
642	2	4	42	0	385	763		
643	2	4	42	0	25	403		
668	2	4	44	0	17	405		
669	2	4	44	0	377	765		
670	2	4	43	0	197	585		
671	1	2	2	0	807	837	838	808
672	1	2	2	0	808	838	839	809

ELEM	MAT	TYP	REL	ESYS	NODES

673	1	9	21	0	809	839	840	810
674	1	9	21	0	810	840	841	811
675	1	9	21	0	811	841	842	812
676	1	9	21	0	812	842	843	813
677	1	9	21	0	813	843	844	814
678	1	9	21	0	814	844	845	815
679	1	9	21	0	815	845	846	816
680	1	9	21	0	816	846	847	817
681	1	2	2	0	837	867	868	838
682	1	2	2	0	838	868	869	839
683	1	9	21	0	839	869	870	840
684	1	9	21	0	840	870	871	841
685	1	9	21	0	841	871	872	842
686	1	9	21	0	842	872	873	843
687	1	9	21	0	843	873	874	844
688	1	9	21	0	844	874	875	845
689	1	9	21	0	845	875	876	846
690	1	9	21	0	846	876	877	847
691	1	2	2	0	867	897	898	868
692	1	2	2	0	868	898	899	869

ELEM	MAT	TYP	REL	ESYS	NODES			
693	1	9	21	0	869	899	900	870
694	1	9	21	0	870	900	901	871
695	1	9	21	0	871	901	902	872
696	1	9	21	0	872	902	903	873
697	1	9	21	0	873	903	904	874
698	1	9	21	0	874	904	905	875
699	1	9	21	0	875	905	906	876
700	1	9	21	0	876	906	907	877
701	1	2	2	0	897	927	928	898
702	1	2	2	0	898	928	929	899
703	1	9	21	0	899	929	930	900
704	1	9	21	0	900	930	931	901
705	1	9	21	0	901	931	932	902
706	1	9	21	0	902	932	933	903
707	1	9	21	0	903	933	934	904
708	1	9	21	0	904	934	935	905
709	1	9	21	0	905	935	936	906
710	1	9	21	0	906	936	937	907
711	1	2	2	0	927	957	958	928
712	1	2	2	0	928	958	959	929

ELEM	MAT	TYP	REL	ESYS	NODES			
713	1	9	21	0	929	959	960	930
714	1	9	21	0	930	960	961	931
715	1	9	21	0	931	961	962	932
716	1	9	21	0	932	962	963	933
717	1	9	21	0	933	963	964	934
718	1	9	21	0	934	964	965	935
719	1	9	21	0	935	965	966	936
720	1	9	21	0	936	966	967	937
721	1	2	2	0	957	987	988	958
722	1	2	2	0	958	988	989	959
723	1	9	21	0	959	989	990	960
724	1	9	21	0	960	990	991	961
725	1	9	21	0	961	991	992	962
726	1	9	21	0	962	992	993	963
727	1	9	21	0	963	993	994	964
728	1	9	21	0	964	994	995	965
729	1	9	21	0	965	995	996	966
730	1	9	21	0	966	996	997	967
731	1	2	2	0	987	1017	1018	988
732	1	2	2	0	988	1018	1019	989

ELEM	MAT	TYP	REL	ESYS	NODES			
733	1	9	21	0	989	1019	1020	990
734	1	9	21	0	990	1020	1021	991
735	1	9	21	0	991	1021	1022	992
736	1	9	21	0	992	1022	1023	993

737	1	9	21	0	993	1023	1024	994
738	1	9	21	0	994	1024	1025	995
739	1	9	21	0	995	1025	1026	996
740	1	9	21	0	996	1026	1027	997
741	1	2	2	0	1017	1047	1048	1018
742	1	2	2	0	1018	1048	1049	1019
743	1	9	21	0	1019	1049	1050	1020
744	1	9	21	0	1020	1050	1051	1021
745	1	9	21	0	1021	1051	1052	1022
746	1	9	21	0	1022	1052	1053	1023
747	1	9	21	0	1023	1053	1054	1024
748	1	9	21	0	1024	1054	1055	1025
749	1	9	21	0	1025	1055	1056	1026
750	1	9	21	0	1026	1056	1057	1027
751	1	2	2	0	1047	1077	1078	1048
752	1	2	2	0	1048	1078	1079	1049

ELEM	MAT	TYP	REL	ESYS	NODES			
753	1	9	21	0	1049	1079	1080	1050
754	1	9	21	0	1050	1080	1081	1051
755	1	9	21	0	1051	1081	1082	1052
756	1	9	21	0	1052	1082	1083	1053
757	1	9	21	0	1053	1083	1084	1054
758	1	9	21	0	1054	1084	1085	1055
759	1	9	21	0	1055	1085	1086	1056
760	1	9	21	0	1056	1086	1087	1057
761	1	2	2	0	1077	1107	1108	1078
762	1	2	2	0	1078	1108	1109	1079
763	1	9	21	0	1079	1109	1110	1080
764	1	9	21	0	1080	1110	1111	1081
765	1	9	21	0	1081	1111	1112	1082
766	1	9	21	0	1082	1112	1113	1083
767	1	9	21	0	1083	1113	1114	1084
768	1	9	21	0	1084	1114	1115	1085
769	1	9	21	0	1085	1115	1116	1086
770	1	9	21	0	1086	1116	1117	1087
771	1	2	2	0	1107	1137	1138	1108
772	1	2	2	0	1108	1138	1139	1109

ELEM	MAT	TYP	REL	ESYS	NODES			
773	1	9	21	0	1109	1139	1140	1110
774	1	9	21	0	1110	1140	1141	1111
775	1	9	21	0	1111	1141	1142	1112
776	1	9	21	0	1112	1142	1143	1113
777	1	9	21	0	1113	1143	1144	1114
778	1	9	21	0	1114	1144	1145	1115
779	1	9	21	0	1115	1145	1146	1116
780	1	9	21	0	1116	1146	1147	1117
781	1	2	2	0	1137	1167	1168	1138
782	1	2	2	0	1138	1168	1169	1139
783	1	9	21	0	1139	1169	1170	1140
784	1	9	21	0	1140	1170	1171	1141
785	1	9	21	0	1141	1171	1172	1142
786	1	9	21	0	1142	1172	1173	1143
787	1	9	21	0	1143	1173	1174	1144
788	1	9	21	0	1144	1174	1175	1145
789	1	9	21	0	1145	1175	1176	1146
790	1	9	21	0	1146	1176	1177	1147
791	1	9	21	0	817	847	818	818
792	1	9	21	0	847	877	818	818

ELEM	MAT	TYP	REL	ESYS	NODES			
793	1	9	21	0	877	907	818	818
794	1	9	21	0	907	937	818	818
795	1	9	21	0	937	967	818	818
796	1	9	21	0	967	997	818	818
797	1	9	21	0	997	1027	818	818
798	1	9	21	0	1027	1057	818	818
799	1	9	21	0	1057	1087	818	818
800	1	9	21	0	1087	1117	818	818
801	1	9	21	0	1117	1147	818	818

802	1	9	21	0	1147	1177	818	818
803	2	3	3	0	84	467		
804	2	3	3	0	144	527		
805	2	3	3	0	204	587		
806	2	3	3	0	264	647		
807	2	3	3	0	324	707		
808	2	3	4	0	24	407		
809	2	3	4	0	384	767		

LIST ALL SELECTED NODE DSYS= 0

NODE	X	Y	Z	THXY	THYZ	THXZ
1	6.0000	1.7350	0.67604E-11	0.00	0.00	0.00
2	9.3750	1.7350	0.67604E-11	0.00	0.00	0.00
3	12.750	1.7350	0.67604E-11	0.00	0.00	0.00
4	12.750	0.00000E+00	0.10000E-29	0.00	0.00	0.00
5	12.750	0.84500	0.32925E-11	0.00	0.00	0.00
7	12.750	2.5950	0.10111E-10	0.00	0.00	0.00
8	12.750	3.4700	0.13521E-10	0.00	0.00	0.00
9	15.900	0.00000E+00	0.10000E-29	0.00	0.00	0.00
10	15.900	0.84500	0.32925E-11	0.00	0.00	0.00
11	15.900	1.7350	0.67604E-11	0.00	0.00	0.00
12	15.900	2.5950	0.10111E-10	0.00	0.00	0.00
13	15.900	3.4700	0.13521E-10	0.00	0.00	0.00
14	16.970	0.00000E+00	0.00000E+00	0.00	0.00	0.00
15	16.970	0.84500	0.32925E-11	0.00	0.00	0.00
16	16.970	1.4700	0.57279E-11	0.00	0.00	0.00
17	16.970	2.0700	0.80658E-11	0.00	0.00	0.00
18	16.970	2.6200	0.10209E-10	0.00	0.00	0.00
19	16.970	3.4700	0.13521E-10	0.00	0.00	0.00
20	17.813	0.00000E+00	0.00000E+00	0.00	0.00	0.00
21	17.813	0.84500	0.32925E-11	0.00	0.00	0.00

NODE	X	Y	Z	THXY	THYZ	THXZ
22	17.813	1.4700	0.57279E-11	0.00	0.00	0.00
23	18.625	0.00000E+00	0.00000E+00	0.00	0.00	0.00
24	18.625	0.58000	0.22600E-11	0.00	0.00	0.00
25	18.625	1.4690	0.57240E-11	0.00	0.00	0.00
26	19.470	0.00000E+00	0.10000E-29	0.00	0.00	0.00
27	19.470	0.58000	0.22600E-11	0.00	0.00	0.00
28	19.470	1.4700	0.57279E-11	0.00	0.00	0.00
31	5.7956	1.7350	-1.5529	0.00	0.00	0.00
32	9.0556	1.7350	-2.4264	0.00	0.00	0.00
33	12.316	1.7350	-3.2999	0.00	0.00	0.00
34	12.316	0.12858E-10	-3.2999	0.00	0.00	0.00
35	12.316	0.84500	-3.2999	0.00	0.00	0.00
37	12.316	2.5950	-3.2999	0.00	0.00	0.00
38	12.316	3.4700	-3.2999	0.00	0.00	0.00
39	15.358	0.16035E-10	-4.1152	0.00	0.00	0.00
40	15.358	0.84500	-4.1152	0.00	0.00	0.00
41	15.358	1.7350	-4.1152	0.00	0.00	0.00
42	15.358	2.5950	-4.1152	0.00	0.00	0.00
43	15.358	3.4700	-4.1152	0.00	0.00	0.00
44	16.392	0.17114E-10	-4.3922	0.00	0.00	0.00

NODE	X	Y	Z	THXY	THYZ	THXZ
45	16.392	0.84500	-4.3922	0.00	0.00	0.00
46	16.392	1.4700	-4.3922	0.00	0.00	0.00
47	16.392	2.0700	-4.3922	0.00	0.00	0.00
48	16.392	2.6200	-4.3922	0.00	0.00	0.00
49	16.392	3.4700	-4.3922	0.00	0.00	0.00
50	17.206	0.17964E-10	-4.6103	0.00	0.00	0.00
51	17.206	0.84500	-4.6103	0.00	0.00	0.00
52	17.206	1.4700	-4.6103	0.00	0.00	0.00
53	17.990	0.18783E-10	-4.8205	0.00	0.00	0.00
54	17.990	0.58000	-4.8205	0.00	0.00	0.00
55	17.990	1.4690	-4.8205	0.00	0.00	0.00
56	18.807	0.19635E-10	-5.0392	0.00	0.00	0.00
57	18.807	0.58000	-5.0392	0.00	0.00	0.00
58	18.807	1.4700	-5.0392	0.00	0.00	0.00
61	5.1962	1.7350	-3.0000	0.00	0.00	0.00
62	8.1190	1.7350	-4.6875	0.00	0.00	0.00
63	11.042	1.7350	-6.3750	0.00	0.00	0.00

64	11.042	0.24840E-10	-6.3750	0.00	0.00	0.00
65	11.042	0.84500	-6.3750	0.00	0.00	0.00
67	11.042	2.5950	-6.3750	0.00	0.00	0.00
NODE	X	Y	Z	THXY	THYZ	THXZ
68	11.042	3.4700	-6.3750	0.00	0.00	0.00
69	13.770	0.30977E-10	-7.9500	0.00	0.00	0.00
70	13.770	0.84500	-7.9500	0.00	0.00	0.00
71	13.770	1.7350	-7.9500	0.00	0.00	0.00
72	13.770	2.5950	-7.9500	0.00	0.00	0.00
73	13.770	3.4700	-7.9500	0.00	0.00	0.00
74	14.696	0.33062E-10	-8.4850	0.00	0.00	0.00
75	14.696	0.84500	-8.4850	0.00	0.00	0.00
76	14.696	1.4700	-8.4850	0.00	0.00	0.00
77	14.696	2.0700	-8.4850	0.00	0.00	0.00
78	14.696	2.6200	-8.4850	0.00	0.00	0.00
79	14.696	3.4700	-8.4850	0.00	0.00	0.00
80	15.427	0.34704E-10	-8.9065	0.00	0.00	0.00
81	15.427	0.84500	-8.9065	0.00	0.00	0.00
82	15.427	1.4700	-8.9065	0.00	0.00	0.00
83	16.130	0.36286E-10	-9.3125	0.00	0.00	0.00
84	16.130	0.58000	-9.3125	0.00	0.00	0.00
85	16.130	1.4690	-9.3125	0.00	0.00	0.00
86	16.862	0.37932E-10	-9.7350	0.00	0.00	0.00
87	16.862	0.58000	-9.7350	0.00	0.00	0.00
NODE	X	Y	Z	THXY	THYZ	THXZ
88	16.862	1.4700	-9.7350	0.00	0.00	0.00
91	4.2426	1.7350	-4.2426	0.00	0.00	0.00
92	6.6291	1.7350	-6.6291	0.00	0.00	0.00
93	9.0156	1.7350	-9.0156	0.00	0.00	0.00
94	9.0156	0.35129E-10	-9.0156	0.00	0.00	0.00
95	9.0156	0.84500	-9.0156	0.00	0.00	0.00
97	9.0156	2.5950	-9.0156	0.00	0.00	0.00
98	9.0156	3.4700	-9.0156	0.00	0.00	0.00
99	11.243	0.43808E-10	-11.243	0.00	0.00	0.00
100	11.243	0.84500	-11.243	0.00	0.00	0.00
101	11.243	1.7350	-11.243	0.00	0.00	0.00
102	11.243	2.5950	-11.243	0.00	0.00	0.00
103	11.243	3.4700	-11.243	0.00	0.00	0.00
104	12.000	0.46756E-10	-12.000	0.00	0.00	0.00
105	12.000	0.84500	-12.000	0.00	0.00	0.00
106	12.000	1.4700	-12.000	0.00	0.00	0.00
107	12.000	2.0700	-12.000	0.00	0.00	0.00
108	12.000	2.6200	-12.000	0.00	0.00	0.00
109	12.000	3.4700	-12.000	0.00	0.00	0.00
110	12.596	0.49079E-10	-12.596	0.00	0.00	0.00
NODE	X	Y	Z	THXY	THYZ	THXZ
111	12.596	0.84500	-12.596	0.00	0.00	0.00
112	12.596	1.4700	-12.596	0.00	0.00	0.00
113	13.170	0.51316E-10	-13.170	0.00	0.00	0.00
114	13.170	0.58000	-13.170	0.00	0.00	0.00
115	13.170	1.4690	-13.170	0.00	0.00	0.00
116	13.767	0.53645E-10	-13.767	0.00	0.00	0.00
117	13.767	0.58000	-13.767	0.00	0.00	0.00
118	13.767	1.4700	-13.767	0.00	0.00	0.00
121	3.0000	1.7350	-5.1962	0.00	0.00	0.00
122	4.6875	1.7350	-8.1190	0.00	0.00	0.00
123	6.3750	1.7350	-11.042	0.00	0.00	0.00
124	6.3750	0.43024E-10	-11.042	0.00	0.00	0.00
125	6.3750	0.84500	-11.042	0.00	0.00	0.00
127	6.3750	2.5950	-11.042	0.00	0.00	0.00
128	6.3750	3.4700	-11.042	0.00	0.00	0.00
129	7.9500	0.53654E-10	-13.770	0.00	0.00	0.00
130	7.9500	0.84500	-13.770	0.00	0.00	0.00
131	7.9500	1.7350	-13.770	0.00	0.00	0.00
132	7.9500	2.5950	-13.770	0.00	0.00	0.00
133	7.9500	3.4700	-13.770	0.00	0.00	0.00
NODE	X	Y	Z	THXY	THYZ	THXZ
134	8.4850	0.57265E-10	-14.696	0.00	0.00	0.00
135	8.4850	0.84500	-14.696	0.00	0.00	0.00
136	8.4850	1.4700	-14.696	0.00	0.00	0.00

137	8.4850	2.0700	-14.696	0.00	0.00	0.00
138	8.4850	2.6200	-14.696	0.00	0.00	0.00
139	8.4850	3.4700	-14.696	0.00	0.00	0.00
140	8.9065	0.60109E-10	-15.427	0.00	0.00	0.00
141	8.9065	0.84500	-15.427	0.00	0.00	0.00
142	8.9065	1.4700	-15.427	0.00	0.00	0.00
143	9.3125	0.62849E-10	-16.130	0.00	0.00	0.00
144	9.3125	0.58000	-16.130	0.00	0.00	0.00
145	9.3125	1.4690	-16.130	0.00	0.00	0.00
146	9.7350	0.65701E-10	-16.862	0.00	0.00	0.00
147	9.7350	0.58000	-16.862	0.00	0.00	0.00
148	9.7350	1.4700	-16.862	0.00	0.00	0.00
151	1.5529	1.7350	-5.7956	0.00	0.00	0.00
152	2.4264	1.7350	-9.0556	0.00	0.00	0.00
153	3.2999	1.7350	-12.316	0.00	0.00	0.00
154	3.2999	0.47988E-10	-12.316	0.00	0.00	0.00
155	3.2999	0.84500	-12.316	0.00	0.00	0.00

NODE	X	Y	Z	THXY	THYZ	THXZ
157	3.2999	2.5950	-12.316	0.00	0.00	0.00
158	3.2999	3.4700	-12.316	0.00	0.00	0.00
159	4.1152	0.59843E-10	-15.358	0.00	0.00	0.00
160	4.1152	0.84500	-15.358	0.00	0.00	0.00
161	4.1152	1.7350	-15.358	0.00	0.00	0.00
162	4.1152	2.5950	-15.358	0.00	0.00	0.00
163	4.1152	3.4700	-15.358	0.00	0.00	0.00
164	4.3922	0.63870E-10	-16.392	0.00	0.00	0.00
165	4.3922	0.84500	-16.392	0.00	0.00	0.00
166	4.3922	1.4700	-16.392	0.00	0.00	0.00
167	4.3922	2.0700	-16.392	0.00	0.00	0.00
168	4.3922	2.6200	-16.392	0.00	0.00	0.00
169	4.3922	3.4700	-16.392	0.00	0.00	0.00
170	4.6103	0.67043E-10	-17.206	0.00	0.00	0.00
171	4.6103	0.84500	-17.206	0.00	0.00	0.00
172	4.6103	1.4700	-17.206	0.00	0.00	0.00
173	4.8205	0.70099E-10	-17.990	0.00	0.00	0.00
174	4.8205	0.58000	-17.990	0.00	0.00	0.00
175	4.8205	1.4690	-17.990	0.00	0.00	0.00
176	5.0392	0.73280E-10	-18.807	0.00	0.00	0.00

NODE	X	Y	Z	THXY	THYZ	THXZ
177	5.0392	0.58000	-18.807	0.00	0.00	0.00
178	5.0392	1.4700	-18.807	0.00	0.00	0.00
181	0.23379E-10	1.7350	-6.0000	0.00	0.00	0.00
182	0.36530E-10	1.7350	-9.3750	0.00	0.00	0.00
183	0.49680E-10	1.7350	-12.750	0.00	0.00	0.00
184	0.49680E-10	0.49680E-10	-12.750	0.00	0.00	0.00
185	0.49680E-10	0.84500	-12.750	0.00	0.00	0.00
187	0.49680E-10	2.5950	-12.750	0.00	0.00	0.00
188	0.49680E-10	3.4700	-12.750	0.00	0.00	0.00
189	0.61954E-10	0.61954E-10	-15.900	0.00	0.00	0.00
190	0.61954E-10	0.84500	-15.900	0.00	0.00	0.00
191	0.61954E-10	1.7350	-15.900	0.00	0.00	0.00
192	0.61954E-10	2.5950	-15.900	0.00	0.00	0.00
193	0.61954E-10	3.4700	-15.900	0.00	0.00	0.00
194	0.66124E-10	0.66124E-10	-16.970	0.00	0.00	0.00
195	0.66124E-10	0.84500	-16.970	0.00	0.00	0.00
196	0.66124E-10	1.4700	-16.970	0.00	0.00	0.00
197	0.66124E-10	2.0700	-16.970	0.00	0.00	0.00
198	0.66124E-10	2.6200	-16.970	0.00	0.00	0.00
199	0.66124E-10	3.4700	-16.970	0.00	0.00	0.00

NODE	X	Y	Z	THXY	THYZ	THXZ
200	0.69408E-10	0.69408E-10	-17.813	0.00	0.00	0.00
201	0.69408E-10	0.84500	-17.813	0.00	0.00	0.00
202	0.69408E-10	1.4700	-17.813	0.00	0.00	0.00
203	0.72572E-10	0.72572E-10	-18.625	0.00	0.00	0.00
204	0.72572E-10	0.58000	-18.625	0.00	0.00	0.00
205	0.72572E-10	1.4690	-18.625	0.00	0.00	0.00
206	0.75865E-10	0.75865E-10	-19.470	0.00	0.00	0.00
207	0.75865E-10	0.58000	-19.470	0.00	0.00	0.00
208	0.75865E-10	1.4700	-19.470	0.00	0.00	0.00
211	-1.5529	1.7350	-5.7956	0.00	0.00	0.00
212	-2.4264	1.7350	-9.0556	0.00	0.00	0.00

213	-3.2999	1.7350	-12.316	0.00	0.00	0.00
214	-3.2999	0.47988E-10	-12.316	0.00	0.00	0.00
215	-3.2999	0.84500	-12.316	0.00	0.00	0.00
217	-3.2999	2.5950	-12.316	0.00	0.00	0.00
218	-3.2999	3.4700	-12.316	0.00	0.00	0.00
219	-4.1152	0.59843E-10	-15.358	0.00	0.00	0.00
220	-4.1152	0.84500	-15.358	0.00	0.00	0.00
221	-4.1152	1.7350	-15.358	0.00	0.00	0.00
222	-4.1152	2.5950	-15.358	0.00	0.00	0.00

NODE	X	Y	Z	THXY	THYZ	THXZ
223	-4.1152	3.4700	-15.358	0.00	0.00	0.00
224	-4.3922	0.63870E-10	-16.392	0.00	0.00	0.00
225	-4.3922	0.84500	-16.392	0.00	0.00	0.00
226	-4.3922	1.4700	-16.392	0.00	0.00	0.00
227	-4.3922	2.0700	-16.392	0.00	0.00	0.00
228	-4.3922	2.6200	-16.392	0.00	0.00	0.00
229	-4.3922	3.4700	-16.392	0.00	0.00	0.00
230	-4.6103	0.67043E-10	-17.206	0.00	0.00	0.00
231	-4.6103	0.84500	-17.206	0.00	0.00	0.00
232	-4.6103	1.4700	-17.206	0.00	0.00	0.00
233	-4.8205	0.70099E-10	-17.990	0.00	0.00	0.00
234	-4.8205	0.58000	-17.990	0.00	0.00	0.00
235	-4.8205	1.4690	-17.990	0.00	0.00	0.00
236	-5.0392	0.73280E-10	-18.807	0.00	0.00	0.00
237	-5.0392	0.58000	-18.807	0.00	0.00	0.00
238	-5.0392	1.4700	-18.807	0.00	0.00	0.00
241	-3.0000	1.7350	-5.1962	0.00	0.00	0.00
242	-4.6875	1.7350	-8.1190	0.00	0.00	0.00
243	-6.3750	1.7350	-11.042	0.00	0.00	0.00
244	-6.3750	0.43024E-10	-11.042	0.00	0.00	0.00

NODE	X	Y	Z	THXY	THYZ	THXZ
245	-6.3750	0.84500	-11.042	0.00	0.00	0.00
247	-6.3750	2.5950	-11.042	0.00	0.00	0.00
248	-6.3750	3.4700	-11.042	0.00	0.00	0.00
249	-7.9500	0.53654E-10	-13.770	0.00	0.00	0.00
250	-7.9500	0.84500	-13.770	0.00	0.00	0.00
251	-7.9500	1.7350	-13.770	0.00	0.00	0.00
252	-7.9500	2.5950	-13.770	0.00	0.00	0.00
253	-7.9500	3.4700	-13.770	0.00	0.00	0.00
254	-8.4850	0.57265E-10	-14.696	0.00	0.00	0.00
255	-8.4850	0.84500	-14.696	0.00	0.00	0.00
256	-8.4850	1.4700	-14.696	0.00	0.00	0.00
257	-8.4850	2.0700	-14.696	0.00	0.00	0.00
258	-8.4850	2.6200	-14.696	0.00	0.00	0.00
259	-8.4850	3.4700	-14.696	0.00	0.00	0.00
260	-8.9065	0.60109E-10	-15.427	0.00	0.00	0.00
261	-8.9065	0.84500	-15.427	0.00	0.00	0.00
262	-8.9065	1.4700	-15.427	0.00	0.00	0.00
263	-9.3125	0.62849E-10	-16.130	0.00	0.00	0.00
264	-9.3125	0.58000	-16.130	0.00	0.00	0.00
265	-9.3125	1.4690	-16.130	0.00	0.00	0.00

NODE	X	Y	Z	THXY	THYZ	THXZ
266	-9.7350	0.65701E-10	-16.862	0.00	0.00	0.00
267	-9.7350	0.58000	-16.862	0.00	0.00	0.00
268	-9.7350	1.4700	-16.862	0.00	0.00	0.00
271	-4.2426	1.7350	-4.2426	0.00	0.00	0.00
272	-6.6291	1.7350	-6.6291	0.00	0.00	0.00
273	-9.0156	1.7350	-9.0156	0.00	0.00	0.00
274	-9.0156	0.35129E-10	-9.0156	0.00	0.00	0.00
275	-9.0156	0.84500	-9.0156	0.00	0.00	0.00
277	-9.0156	2.5950	-9.0156	0.00	0.00	0.00
278	-9.0156	3.4700	-9.0156	0.00	0.00	0.00
279	-11.243	0.43808E-10	-11.243	0.00	0.00	0.00
280	-11.243	0.84500	-11.243	0.00	0.00	0.00
281	-11.243	1.7350	-11.243	0.00	0.00	0.00
282	-11.243	2.5950	-11.243	0.00	0.00	0.00
283	-11.243	3.4700	-11.243	0.00	0.00	0.00
284	-12.000	0.46756E-10	-12.000	0.00	0.00	0.00
285	-12.000	0.84500	-12.000	0.00	0.00	0.00
286	-12.000	1.4700	-12.000	0.00	0.00	0.00
287	-12.000	2.0700	-12.000	0.00	0.00	0.00

288	-12.000	2.6200	-12.000	0.00	0.00	0.00

NODE	X	Y	Z	THXY	THYZ	THXZ
289	-12.000	3.4700	-12.000	0.00	0.00	0.00
290	-12.596	0.49079E-10	-12.596	0.00	0.00	0.00
291	-12.596	0.84500	-12.596	0.00	0.00	0.00
292	-12.596	1.4700	-12.596	0.00	0.00	0.00
293	-13.170	0.51316E-10	-13.170	0.00	0.00	0.00
294	-13.170	0.58000	-13.170	0.00	0.00	0.00
295	-13.170	1.4690	-13.170	0.00	0.00	0.00
296	-13.767	0.53645E-10	-13.767	0.00	0.00	0.00
297	-13.767	0.58000	-13.767	0.00	0.00	0.00
298	-13.767	1.4700	-13.767	0.00	0.00	0.00
301	-5.1962	1.7350	-3.0000	0.00	0.00	0.00
302	-8.1190	1.7350	-4.6875	0.00	0.00	0.00
303	-11.042	1.7350	-6.3750	0.00	0.00	0.00
304	-11.042	0.24840E-10	-6.3750	0.00	0.00	0.00
305	-11.042	0.84500	-6.3750	0.00	0.00	0.00
307	-11.042	2.5950	-6.3750	0.00	0.00	0.00
308	-11.042	3.4700	-6.3750	0.00	0.00	0.00
309	-13.770	0.30977E-10	-7.9500	0.00	0.00	0.00
310	-13.770	0.84500	-7.9500	0.00	0.00	0.00
311	-13.770	1.7350	-7.9500	0.00	0.00	0.00

NODE	X	Y	Z	THXY	THYZ	THXZ
312	-13.770	2.5950	-7.9500	0.00	0.00	0.00
313	-13.770	3.4700	-7.9500	0.00	0.00	0.00
314	-14.696	0.33062E-10	-8.4850	0.00	0.00	0.00
315	-14.696	0.84500	-8.4850	0.00	0.00	0.00
316	-14.696	1.4700	-8.4850	0.00	0.00	0.00
317	-14.696	2.0700	-8.4850	0.00	0.00	0.00
318	-14.696	2.6200	-8.4850	0.00	0.00	0.00
319	-14.696	3.4700	-8.4850	0.00	0.00	0.00
320	-15.427	0.34704E-10	-8.9065	0.00	0.00	0.00
321	-15.427	0.84500	-8.9065	0.00	0.00	0.00
322	-15.427	1.4700	-8.9065	0.00	0.00	0.00
323	-16.130	0.36286E-10	-9.3125	0.00	0.00	0.00
324	-16.130	0.58000	-9.3125	0.00	0.00	0.00
325	-16.130	1.4690	-9.3125	0.00	0.00	0.00
326	-16.862	0.37932E-10	-9.7350	0.00	0.00	0.00
327	-16.862	0.58000	-9.7350	0.00	0.00	0.00
328	-16.862	1.4700	-9.7350	0.00	0.00	0.00
331	-5.7956	1.7350	-1.5529	0.00	0.00	0.00
332	-9.0556	1.7350	-2.4264	0.00	0.00	0.00
333	-12.316	1.7350	-3.2999	0.00	0.00	0.00

NODE	X	Y	Z	THXY	THYZ	THXZ
334	-12.316	0.12858E-10	-3.2999	0.00	0.00	0.00
335	-12.316	0.84500	-3.2999	0.00	0.00	0.00
337	-12.316	2.5950	-3.2999	0.00	0.00	0.00
338	-12.316	3.4700	-3.2999	0.00	0.00	0.00
339	-15.358	0.16035E-10	-4.1152	0.00	0.00	0.00
340	-15.358	0.84500	-4.1152	0.00	0.00	0.00
341	-15.358	1.7350	-4.1152	0.00	0.00	0.00
342	-15.358	2.5950	-4.1152	0.00	0.00	0.00
343	-15.358	3.4700	-4.1152	0.00	0.00	0.00
344	-16.392	0.17114E-10	-4.3922	0.00	0.00	0.00
345	-16.392	0.84500	-4.3922	0.00	0.00	0.00
346	-16.392	1.4700	-4.3922	0.00	0.00	0.00
347	-16.392	2.0700	-4.3922	0.00	0.00	0.00
348	-16.392	2.6200	-4.3922	0.00	0.00	0.00
349	-16.392	3.4700	-4.3922	0.00	0.00	0.00
350	-17.206	0.17964E-10	-4.6103	0.00	0.00	0.00
351	-17.206	0.84500	-4.6103	0.00	0.00	0.00
352	-17.206	1.4700	-4.6103	0.00	0.00	0.00
353	-17.990	0.18783E-10	-4.8205	0.00	0.00	0.00
354	-17.990	0.58000	-4.8205	0.00	0.00	0.00

NODE	X	Y	Z	THXY	THYZ	THXZ
355	-17.990	1.4690	-4.8205	0.00	0.00	0.00
356	-18.807	0.19635E-10	-5.0392	0.00	0.00	0.00
357	-18.807	0.58000	-5.0392	0.00	0.00	0.00
358	-18.807	1.4700	-5.0392	0.00	0.00	0.00
361	-6.0000	1.7350	-0.10512E-07	0.00	0.00	0.00

362	-9.3750	1.7350	-0.16429E-07	0.00	0.00	0.00
363	-12.750	1.7350	-0.22346E-07	0.00	0.00	0.00
364	-12.750	0.87096E-19	0.10000E-29	0.00	0.00	0.00
365	-12.750	0.84500	-0.22349E-07	0.00	0.00	0.00
367	-12.750	2.5950	-0.22342E-07	0.00	0.00	0.00
368	-12.750	3.4700	-0.22339E-07	0.00	0.00	0.00
369	-15.900	0.10861E-18	0.10000E-29	0.00	0.00	0.00
370	-15.900	0.84500	-0.27871E-07	0.00	0.00	0.00
371	-15.900	1.7350	-0.27868E-07	0.00	0.00	0.00
372	-15.900	2.5950	-0.27865E-07	0.00	0.00	0.00
373	-15.900	3.4700	-0.27861E-07	0.00	0.00	0.00
374	-16.970	0.11592E-18	-0.29750E-07	0.00	0.00	0.00
375	-16.970	0.84500	-0.29747E-07	0.00	0.00	0.00
376	-16.970	1.4700	-0.29745E-07	0.00	0.00	0.00
377	-16.970	2.0700	-0.29742E-07	0.00	0.00	0.00

NODE	X	Y	Z	THXY	THYZ	THXZ
378	-16.970	2.6200	-0.29740E-07	0.00	0.00	0.00
379	-16.970	3.4700	-0.29737E-07	0.00	0.00	0.00
380	-17.813	0.12168E-18	-0.31228E-07	0.00	0.00	0.00
381	-17.813	0.84500	-0.31225E-07	0.00	0.00	0.00
382	-17.813	1.4700	-0.31223E-07	0.00	0.00	0.00
383	-18.625	0.12723E-18	-0.32652E-07	0.00	0.00	0.00
384	-18.625	0.58000	-0.32650E-07	0.00	0.00	0.00
385	-18.625	1.4690	-0.32646E-07	0.00	0.00	0.00
386	-19.470	0.13300E-18	0.10000E-29	0.00	0.00	0.00
387	-19.470	0.58000	-0.34131E-07	0.00	0.00	0.00
388	-19.470	1.4700	-0.34128E-07	0.00	0.00	0.00
390	0.00000E+00	1.7350	0.67604E-11	0.00	0.00	0.00
391	1.0000	1.7350	0.67604E-11	0.00	0.00	0.00
392	2.0000	1.7350	0.67604E-11	0.00	0.00	0.00
393	3.0000	1.7350	0.67604E-11	0.00	0.00	0.00
394	4.0000	1.7350	0.67604E-11	0.00	0.00	0.00
395	5.0000	1.7350	0.67604E-11	0.00	0.00	0.00
396	-1.0000	1.7350	-0.17464E-08	0.00	0.00	0.00
397	-2.0000	1.7350	-0.34995E-08	0.00	0.00	0.00
398	-3.0000	1.7350	-0.52526E-08	0.00	0.00	0.00

NODE	X	Y	Z	THXY	THYZ	THXZ
399	-4.0000	1.7350	-0.70057E-08	0.00	0.00	0.00
400	-5.0000	1.7350	-0.87589E-08	0.00	0.00	0.00
401	17.000	1.4700	0.57279E-11	0.00	0.00	0.00
402	17.813	1.4700	0.57279E-11	0.00	0.00	0.00
403	18.625	1.4700	0.57279E-11	0.00	0.00	0.00
404	19.375	1.4700	0.57279E-11	0.00	0.00	0.00
405	17.000	2.0700	0.80658E-11	0.00	0.00	0.00
406	17.813	2.0700	0.80658E-11	0.00	0.00	0.00
407	18.625	2.0700	0.80658E-11	0.00	0.00	0.00
408	19.375	2.0700	0.80658E-11	0.00	0.00	0.00
409	17.000	2.6200	0.10209E-10	0.00	0.00	0.00
410	17.813	2.6200	0.10209E-10	0.00	0.00	0.00
411	18.625	2.6200	0.10209E-10	0.00	0.00	0.00
412	19.375	2.6200	0.10209E-10	0.00	0.00	0.00
413	17.000	3.0450	0.11865E-10	0.00	0.00	0.00
414	17.531	3.1742	0.12368E-10	0.00	0.00	0.00
415	18.063	3.3033	0.12871E-10	0.00	0.00	0.00
416	18.563	3.4325	0.13375E-10	0.00	0.00	0.00
417	17.000	3.4700	0.13521E-10	0.00	0.00	0.00
418	17.250	3.7283	0.14527E-10	0.00	0.00	0.00

NODE	X	Y	Z	THXY	THYZ	THXZ
419	17.500	3.9867	0.15534E-10	0.00	0.00	0.00
420	17.750	4.2450	0.16541E-10	0.00	0.00	0.00
421	16.855	3.4700	0.13521E-10	0.00	0.00	0.00
422	17.000	4.8200	0.18781E-10	0.00	0.00	0.00
423	17.188	4.8200	0.18781E-10	0.00	0.00	0.00
424	17.375	4.8200	0.18781E-10	0.00	0.00	0.00
425	17.562	4.8200	0.18781E-10	0.00	0.00	0.00
426	17.750	4.8200	0.18781E-10	0.00	0.00	0.00
431	16.421	1.4700	-4.3999	0.00	0.00	0.00
432	17.206	1.4700	-4.6102	0.00	0.00	0.00
433	17.990	1.4700	-4.8205	0.00	0.00	0.00
434	18.715	1.4700	-5.0146	0.00	0.00	0.00
435	16.421	2.0700	-4.3999	0.00	0.00	0.00

436	17.206	2.0700	-4.6102	0.00	0.00	0.00
437	17.990	2.0700	-4.8205	0.00	0.00	0.00
438	18.715	2.0700	-5.0146	0.00	0.00	0.00
439	16.421	2.6200	-4.3999	0.00	0.00	0.00
440	17.206	2.6200	-4.6102	0.00	0.00	0.00
441	17.990	2.6200	-4.8205	0.00	0.00	0.00
442	18.715	2.6200	-5.0146	0.00	0.00	0.00

NODE	X	Y	Z	THXY	THYZ	THXZ
443	16.421	3.0450	-4.3999	0.00	0.00	0.00
444	16.934	3.1742	-4.5374	0.00	0.00	0.00
445	17.447	3.3033	-4.6749	0.00	0.00	0.00
446	17.930	3.4325	-4.8043	0.00	0.00	0.00
447	16.421	3.4700	-4.3999	0.00	0.00	0.00
448	16.662	3.7283	-4.4646	0.00	0.00	0.00
449	16.904	3.9867	-4.5293	0.00	0.00	0.00
450	17.145	4.2450	-4.5940	0.00	0.00	0.00
451	16.281	3.4700	-4.3624	0.00	0.00	0.00
452	16.421	4.8200	-4.3999	0.00	0.00	0.00
453	16.602	4.8200	-4.4485	0.00	0.00	0.00
454	16.783	4.8200	-4.4970	0.00	0.00	0.00
455	16.964	4.8200	-4.5455	0.00	0.00	0.00
456	17.145	4.8200	-4.5940	0.00	0.00	0.00
461	14.722	1.4700	-8.5000	0.00	0.00	0.00
462	15.426	1.4700	-8.9062	0.00	0.00	0.00
463	16.130	1.4700	-9.3125	0.00	0.00	0.00
464	16.779	1.4700	-9.6875	0.00	0.00	0.00
465	14.722	2.0700	-8.5000	0.00	0.00	0.00
466	15.426	2.0700	-8.9062	0.00	0.00	0.00

NODE	X	Y	Z	THXY	THYZ	THXZ
467	16.130	2.0700	-9.3125	0.00	0.00	0.00
468	16.779	2.0700	-9.6875	0.00	0.00	0.00
469	14.722	2.6200	-8.5000	0.00	0.00	0.00
470	15.426	2.6200	-8.9062	0.00	0.00	0.00
471	16.130	2.6200	-9.3125	0.00	0.00	0.00
472	16.779	2.6200	-9.6875	0.00	0.00	0.00
473	14.722	3.0450	-8.5000	0.00	0.00	0.00
474	15.183	3.1742	-8.7656	0.00	0.00	0.00
475	15.643	3.3033	-9.0312	0.00	0.00	0.00
476	16.076	3.4325	-9.2812	0.00	0.00	0.00
477	14.722	3.4700	-8.5000	0.00	0.00	0.00
478	14.939	3.7283	-8.6250	0.00	0.00	0.00
479	15.155	3.9867	-8.7500	0.00	0.00	0.00
480	15.372	4.2450	-8.8750	0.00	0.00	0.00
481	14.597	3.4700	-8.4275	0.00	0.00	0.00
482	14.722	4.8200	-8.5000	0.00	0.00	0.00
483	14.885	4.8200	-8.5937	0.00	0.00	0.00
484	15.047	4.8200	-8.6875	0.00	0.00	0.00
485	15.210	4.8200	-8.7812	0.00	0.00	0.00
486	15.372	4.8200	-8.8750	0.00	0.00	0.00

NODE	X	Y	Z	THXY	THYZ	THXZ
491	12.021	1.4700	-12.021	0.00	0.00	0.00
492	12.595	1.4700	-12.595	0.00	0.00	0.00
493	13.170	1.4700	-13.170	0.00	0.00	0.00
494	13.700	1.4700	-13.700	0.00	0.00	0.00
495	12.021	2.0700	-12.021	0.00	0.00	0.00
496	12.595	2.0700	-12.595	0.00	0.00	0.00
497	13.170	2.0700	-13.170	0.00	0.00	0.00
498	13.700	2.0700	-13.700	0.00	0.00	0.00
499	12.021	2.6200	-12.021	0.00	0.00	0.00
500	12.595	2.6200	-12.595	0.00	0.00	0.00
501	13.170	2.6200	-13.170	0.00	0.00	0.00
502	13.700	2.6200	-13.700	0.00	0.00	0.00
503	12.021	3.0450	-12.021	0.00	0.00	0.00
504	12.396	3.1742	-12.396	0.00	0.00	0.00
505	12.772	3.3033	-12.772	0.00	0.00	0.00
506	13.126	3.4325	-13.126	0.00	0.00	0.00
507	12.021	3.4700	-12.021	0.00	0.00	0.00
508	12.198	3.7283	-12.198	0.00	0.00	0.00
509	12.374	3.9867	-12.374	0.00	0.00	0.00
510	12.551	4.2450	-12.551	0.00	0.00	0.00

NODE	X	Y	Z	THXY	THYZ	THXZ
511	11.918	3.4700	-11.918	0.00	0.00	0.00
512	12.021	4.8200	-12.021	0.00	0.00	0.00
513	12.153	4.8200	-12.153	0.00	0.00	0.00
514	12.286	4.8200	-12.286	0.00	0.00	0.00
515	12.419	4.8200	-12.419	0.00	0.00	0.00
516	12.551	4.8200	-12.551	0.00	0.00	0.00
521	8.5000	1.4700	-14.722	0.00	0.00	0.00
522	8.9063	1.4700	-15.426	0.00	0.00	0.00
523	9.3125	1.4700	-16.130	0.00	0.00	0.00
524	9.6875	1.4700	-16.779	0.00	0.00	0.00
525	8.5000	2.0700	-14.722	0.00	0.00	0.00
526	8.9063	2.0700	-15.426	0.00	0.00	0.00
527	9.3125	2.0700	-16.130	0.00	0.00	0.00
528	9.6875	2.0700	-16.779	0.00	0.00	0.00
529	8.5000	2.6200	-14.722	0.00	0.00	0.00
530	8.9063	2.6200	-15.426	0.00	0.00	0.00
531	9.3125	2.6200	-16.130	0.00	0.00	0.00
532	9.6875	2.6200	-16.779	0.00	0.00	0.00
533	8.5000	3.0450	-14.722	0.00	0.00	0.00
534	8.7656	3.1742	-15.183	0.00	0.00	0.00

NODE	X	Y	Z	THXY	THYZ	THXZ
535	9.0313	3.3033	-15.643	0.00	0.00	0.00
536	9.2813	3.4325	-16.076	0.00	0.00	0.00
537	8.5000	3.4700	-14.722	0.00	0.00	0.00
538	8.6250	3.7283	-14.939	0.00	0.00	0.00
539	8.7500	3.9867	-15.155	0.00	0.00	0.00
540	8.8750	4.2450	-15.372	0.00	0.00	0.00
541	8.4275	3.4700	-14.597	0.00	0.00	0.00
542	8.5000	4.8200	-14.722	0.00	0.00	0.00
543	8.5938	4.8200	-14.885	0.00	0.00	0.00
544	8.6875	4.8200	-15.047	0.00	0.00	0.00
545	8.7813	4.8200	-15.210	0.00	0.00	0.00
546	8.8750	4.8200	-15.372	0.00	0.00	0.00
551	4.3999	1.4700	-16.421	0.00	0.00	0.00
552	4.6102	1.4700	-17.206	0.00	0.00	0.00
553	4.8205	1.4700	-17.990	0.00	0.00	0.00
554	5.0146	1.4700	-18.715	0.00	0.00	0.00
555	4.3999	2.0700	-16.421	0.00	0.00	0.00
556	4.6102	2.0700	-17.206	0.00	0.00	0.00
557	4.8205	2.0700	-17.990	0.00	0.00	0.00
558	5.0146	2.0700	-18.715	0.00	0.00	0.00

NODE	X	Y	Z	THXY	THYZ	THXZ
559	4.3999	2.6200	-16.421	0.00	0.00	0.00
560	4.6102	2.6200	-17.206	0.00	0.00	0.00
561	4.8205	2.6200	-17.990	0.00	0.00	0.00
562	5.0146	2.6200	-18.715	0.00	0.00	0.00
563	4.3999	3.0450	-16.421	0.00	0.00	0.00
564	4.5374	3.1742	-16.934	0.00	0.00	0.00
565	4.6749	3.3033	-17.447	0.00	0.00	0.00
566	4.8043	3.4325	-17.930	0.00	0.00	0.00
567	4.3999	3.4700	-16.421	0.00	0.00	0.00
568	4.4646	3.7283	-16.662	0.00	0.00	0.00
569	4.5293	3.9867	-16.904	0.00	0.00	0.00
570	4.5940	4.2450	-17.145	0.00	0.00	0.00
571	4.3624	3.4700	-16.281	0.00	0.00	0.00
572	4.3999	4.8200	-16.421	0.00	0.00	0.00
573	4.4485	4.8200	-16.602	0.00	0.00	0.00
574	4.4970	4.8200	-16.783	0.00	0.00	0.00
575	4.5455	4.8200	-16.964	0.00	0.00	0.00
576	4.5940	4.8200	-17.145	0.00	0.00	0.00
581	0.66240E-10	1.4700	-17.000	0.00	0.00	0.00
582	0.69406E-10	1.4700	-17.812	0.00	0.00	0.00

NODE	X	Y	Z	THXY	THYZ	THXZ
583	0.72572E-10	1.4700	-18.625	0.00	0.00	0.00
584	0.75495E-10	1.4700	-19.375	0.00	0.00	0.00
585	0.66240E-10	2.0700	-17.000	0.00	0.00	0.00
586	0.69406E-10	2.0700	-17.812	0.00	0.00	0.00
587	0.72572E-10	2.0700	-18.625	0.00	0.00	0.00
588	0.75495E-10	2.0700	-19.375	0.00	0.00	0.00
589	0.66240E-10	2.6200	-17.000	0.00	0.00	0.00

590	0.69406E-10	2.6200	-17.812	0.00	0.00	0.00
591	0.72572E-10	2.6200	-18.625	0.00	0.00	0.00
592	0.75495E-10	2.6200	-19.375	0.00	0.00	0.00
593	0.66240E-10	3.0450	-17.000	0.00	0.00	0.00
594	0.68311E-10	3.1742	-17.531	0.00	0.00	0.00
595	0.70381E-10	3.3033	-18.062	0.00	0.00	0.00
596	0.72329E-10	3.4325	-18.562	0.00	0.00	0.00
597	0.66240E-10	3.4700	-17.000	0.00	0.00	0.00
598	0.67215E-10	3.7283	-17.250	0.00	0.00	0.00
599	0.68189E-10	3.9867	-17.500	0.00	0.00	0.00
600	0.69163E-10	4.2450	-17.750	0.00	0.00	0.00
601	0.65676E-10	3.4700	-16.855	0.00	0.00	0.00
602	0.66240E-10	4.8200	-17.000	0.00	0.00	0.00

NODE	X	Y	Z	THXY	THYZ	THXZ
603	0.66971E-10	4.8200	-17.188	0.00	0.00	0.00
604	0.67702E-10	4.8200	-17.375	0.00	0.00	0.00
605	0.68432E-10	4.8200	-17.563	0.00	0.00	0.00
606	0.69163E-10	4.8200	-17.750	0.00	0.00	0.00
611	-4.3999	1.4700	-16.421	0.00	0.00	0.00
612	-4.6102	1.4700	-17.206	0.00	0.00	0.00
613	-4.8205	1.4700	-17.990	0.00	0.00	0.00
614	-5.0146	1.4700	-18.715	0.00	0.00	0.00
615	-4.3999	2.0700	-16.421	0.00	0.00	0.00
616	-4.6102	2.0700	-17.206	0.00	0.00	0.00
617	-4.8205	2.0700	-17.990	0.00	0.00	0.00
618	-5.0146	2.0700	-18.715	0.00	0.00	0.00
619	-4.3999	2.6200	-16.421	0.00	0.00	0.00
620	-4.6102	2.6200	-17.206	0.00	0.00	0.00
621	-4.8205	2.6200	-17.990	0.00	0.00	0.00
622	-5.0146	2.6200	-18.715	0.00	0.00	0.00
623	-4.3999	3.0450	-16.421	0.00	0.00	0.00
624	-4.5374	3.1742	-16.934	0.00	0.00	0.00
625	-4.6749	3.3033	-17.447	0.00	0.00	0.00
626	-4.8043	3.4325	-17.930	0.00	0.00	0.00

NODE	X	Y	Z	THXY	THYZ	THXZ
627	-4.3999	3.4700	-16.421	0.00	0.00	0.00
628	-4.4646	3.7283	-16.662	0.00	0.00	0.00
629	-4.5293	3.9867	-16.904	0.00	0.00	0.00
630	-4.5940	4.2450	-17.145	0.00	0.00	0.00
631	-4.3624	3.4700	-16.281	0.00	0.00	0.00
632	-4.3999	4.8200	-16.421	0.00	0.00	0.00
633	-4.4485	4.8200	-16.602	0.00	0.00	0.00
634	-4.4970	4.8200	-16.783	0.00	0.00	0.00
635	-4.5455	4.8200	-16.964	0.00	0.00	0.00
636	-4.5940	4.8200	-17.145	0.00	0.00	0.00
641	-8.5000	1.4700	-14.722	0.00	0.00	0.00
642	-8.9062	1.4700	-15.426	0.00	0.00	0.00
643	-9.3125	1.4700	-16.130	0.00	0.00	0.00
644	-9.6875	1.4700	-16.779	0.00	0.00	0.00
645	-8.5000	2.0700	-14.722	0.00	0.00	0.00
646	-8.9062	2.0700	-15.426	0.00	0.00	0.00
647	-9.3125	2.0700	-16.130	0.00	0.00	0.00
648	-9.6875	2.0700	-16.779	0.00	0.00	0.00
649	-8.5000	2.6200	-14.722	0.00	0.00	0.00
650	-8.9062	2.6200	-15.426	0.00	0.00	0.00

NODE	X	Y	Z	THXY	THYZ	THXZ
651	-9.3125	2.6200	-16.130	0.00	0.00	0.00
652	-9.6875	2.6200	-16.779	0.00	0.00	0.00
653	-8.5000	3.0450	-14.722	0.00	0.00	0.00
654	-8.7656	3.1742	-15.183	0.00	0.00	0.00
655	-9.0312	3.3033	-15.643	0.00	0.00	0.00
656	-9.2812	3.4325	-16.076	0.00	0.00	0.00
657	-8.5000	3.4700	-14.722	0:00	0.00	0.00
658	-8.6250	3.7283	-14.939	0.00	0.00	0.00
659	-8.7500	3.9867	-15.155	0.00	0.00	0.00
660	-8.8750	4.2450	-15.372	0.00	0.00	0.00
661	-8.4275	3.4700	-14.597	0.00	0.00	0.00
662	-8.5000	4.8200	-14.722	0.00	0.00	0.00
663	-8.5937	4.8200	-14.885	0.00	0.00	0.00
664	-8.6875	4.8200	-15.047	0.00	0.00	0.00
665	-8.7812	4.8200	-15.210	0.00	0.00	0.00

666	-8.8750	4.8200	-15.372	0.00	0.00	0.00
671	-12.021	1.4700	-12.021	0.00	0.00	0.00
672	-12.595	1.4700	-12.595	0.00	0.00	0.00
673	-13.170	1.4700	-13.170	0.00	0.00	0.00
674	-13.700	1.4700	-13.700	0.00	0.00	0.00
NODE	X	Y	Z	THXY	THYZ	THXZ
675	-12.021	2.0700	-12.021	0.00	0.00	0.00
676	-12.595	2.0700	-12.595	0.00	0.00	0.00
677	-13.170	2.0700	-13.170	0.00	0.00	0.00
678	-13.700	2.0700	-13.700	0.00	0.00	0.00
679	-12.021	2.6200	-12.021	0.00	0.00	0.00
680	-12.595	2.6200	-12.595	0.00	0.00	0.00
681	-13.170	2.6200	-13.170	0.00	0.00	0.00
682	-13.700	2.6200	-13.700	0.00	0.00	0.00
683	-12.021	3.0450	-12.021	0.00	0.00	0.00
684	-12.396	3.1742	-12.396	0.00	0.00	0.00
685	-12.772	3.3033	-12.772	0.00	0.00	0.00
686	-13.126	3.4325	-13.126	0.00	0.00	0.00
687	-12.021	3.4700	-12.021	0.00	0.00	0.00
688	-12.198	3.7283	-12.198	0.00	0.00	0.00
689	-12.374	3.9867	-12.374	0.00	0.00	0.00
690	-12.551	4.2450	-12.551	0.00	0.00	0.00
691	-11.918	3.4700	-11.918	0.00	0.00	0.00
692	-12.021	4.8200	-12.021	0.00	0.00	0.00
693	-12.153	4.8200	-12.153	0.00	0.00	0.00
694	-12.286	4.8200	-12.286	0.00	0.00	0.00
NODE	X	Y	Z	THXY	THYZ	THXZ
695	-12.419	4.8200	-12.419	0.00	0.00	0.00
696	-12.551	4.8200	-12.551	0.00	0.00	0.00
701	-14.722	1.4700	-8.5000	0.00	0.00	0.00
702	-15.426	1.4700	-8.9063	0.00	0.00	0.00
703	-16.130	1.4700	-9.3125	0.00	0.00	0.00
704	-16.779	1.4700	-9.6875	0.00	0.00	0.00
705	-14.722	2.0700	-8.5000	0.00	0.00	0.00
706	-15.426	2.0700	-8.9063	0.00	0.00	0.00
707	-16.130	2.0700	-9.3125	0.00	0.00	0.00
708	-16.779	2.0700	-9.6875	0.00	0.00	0.00
709	-14.722	2.6200	-8.5000	0.00	0.00	0.00
710	-15.426	2.6200	-8.9063	0.00	0.00	0.00
711	-16.130	2.6200	-9.3125	0.00	0.00	0.00
712	-16.779	2.6200	-9.6875	0.00	0.00	0.00
713	-14.722	3.0450	-8.5000	0.00	0.00	0.00
714	-15.183	3.1742	-8.7656	0.00	0.00	0.00
715	-15.643	3.3033	-9.0313	0.00	0.00	0.00
716	-16.076	3.4325	-9.2813	0.00	0.00	0.00
717	-14.722	3.4700	-8.5000	0.00	0.00	0.00
718	-14.939	3.7283	-8.6250	0.00	0.00	0.00
NODE	X	Y	Z	THXY	THYZ	THXZ
719	-15.155	3.9867	-8.7500	0.00	0.00	0.00
720	-15.372	4.2450	-8.8750	0.00	0.00	0.00
721	-14.597	3.4700	-8.4275	0.00	0.00	0.00
722	-14.722	4.8200	-8.5000	0.00	0.00	0.00
723	-14.885	4.8200	-8.5938	0.00	0.00	0.00
724	-15.047	4.8200	-8.6875	0.00	0.00	0.00
725	-15.210	4.8200	-8.7813	0.00	0.00	0.00
726	-15.372	4.8200	-8.8750	0.00	0.00	0.00
731	-16.421	1.4700	-4.3999	0.00	0.00	0.00
732	-17.206	1.4700	-4.6102	0.00	0.00	0.00
733	-17.990	1.4700	-4.8205	0.00	0.00	0.00
734	-18.715	1.4700	-5.0146	0.00	0.00	0.00
735	-16.421	2.0700	-4.3999	0.00	0.00	0.00
736	-17.206	2.0700	-4.6102	0.00	0.00	0.00
737	-17.990	2.0700	-4.8205	0.00	0.00	0.00
738	-18.715	2.0700	-5.0146	0.00	0.00	0.00
739	-16.421	2.6200	-4.3999	0.00	0.00	0.00
740	-17.206	2.6200	-4.6102	0.00	0.00	0.00
741	-17.990	2.6200	-4.8205	0.00	0.00	0.00
742	-18.715	2.6200	-5.0146	0.00	0.00	0.00
NODE	X	Y	Z	THXY	THYZ	THXZ
743	-16.421	3.0450	-4.3999	0.00	0.00	0.00

744	-16.934	3.1742	-4.5374	0.00	0.00	0.00
745	-17.447	3.3033	-4.6749	0.00	0.00	0.00
746	-17.930	3.4325	-4.8043	0.00	0.00	0.00
747	-16.421	3.4700	-4.3999	0.00	0.00	0.00
748	-16.662	3.7283	-4.4646	0.00	0.00	0.00
749	-16.904	3.9867	-4.5293	0.00	0.00	0.00
750	-17.145	4.2450	-4.5940	0.00	0.00	0.00
751	-16.281	3.4700	-4.3624	0.00	0.00	0.00
752	-16.421	4.8200	-4.3999	0.00	0.00	0.00
753	-16.602	4.8200	-4.4485	0.00	0.00	0.00
754	-16.783	4.8200	-4.4970	0.00	0.00	0.00
755	-16.964	4.8200	-4.5455	0.00	0.00	0.00
756	-17.145	4.8200	-4.5940	0.00	0.00	0.00
761	-17.000	1.4700	-0.29797E-07	0.00	0.00	0.00
762	-17.813	1.4700	-0.31222E-07	0.00	0.00	0.00
763	-18.625	1.4700	-0.32646E-07	0.00	0.00	0.00
764	-19.375	1.4700	-0.33961E-07	0.00	0.00	0.00
765	-17.000	2.0700	-0.29795E-07	0.00	0.00	0.00
766	-17.813	2.0700	-0.31219E-07	0.00	0.00	0.00

NODE	X	Y	Z	THXY	THYZ	THXZ
767	-18.625	2.0700	-0.32644E-07	0.00	0.00	0.00
768	-19.375	2.0700	-0.33959E-07	0.00	0.00	0.00
769	-17.000	2.6200	-0.29793E-07	0.00	0.00	0.00
770	-17.813	2.6200	-0.31217E-07	0.00	0.00	0.00
771	-18.625	2.6200	-0.32642E-07	0.00	0.00	0.00
772	-19.375	2.6200	-0.33957E-07	0.00	0.00	0.00
773	-17.000	3.0450	-0.29791E-07	0.00	0.00	0.00
774	-17.531	3.1742	-0.30722E-07	0.00	0.00	0.00
775	-18.063	3.3033	-0.31653E-07	0.00	0.00	0.00
776	-18.563	3.4325	-0.32529E-07	0.00	0.00	0.00
777	-17.000	3.4700	-0.29790E-07	0.00	0.00	0.00
778	-17.250	3.7283	-0.30227E-07	0.00	0.00	0.00
779	-17.500	3.9867	-0.30664E-07	0.00	0.00	0.00
780	-17.750	4.2450	-0.31101E-07	0.00	0.00	0.00
781	-16.855	3.4700	-0.29535E-07	0.00	0.00	0.00
782	-17.000	4.8200	-0.29784E-07	0.00	0.00	0.00
783	-17.188	4.8200	-0.30113E-07	0.00	0.00	0.00
784	-17.375	4.8200	-0.30442E-07	0.00	0.00	0.00
785	-17.562	4.8200	-0.30770E-07	0.00	0.00	0.00
786	-17.750	4.8200	-0.31099E-07	0.00	0.00	0.00

NODE	X	Y	Z	THXY	THYZ	THXZ
801	17.375	6.0950	0.23749E-10	0.00	0.00	0.00
802	17.375	8.8950	0.34659E-10	0.00	0.00	0.00
803	17.375	11.695	0.45570E-10	0.00	0.00	0.00
804	17.375	16.532	0.64419E-10	0.00	0.00	0.00
805	17.375	21.370	0.83268E-10	0.00	0.00	0.00
806	17.375	34.770	0.13548E-09	0.00	0.00	0.00
807	17.375	48.170	0.18769E-09	0.00	0.00	0.00
808	17.375	52.270	0.20367E-09	0.00	0.00	0.00
809	17.375	56.370	0.21965E-09	0.00	0.00	0.00
810	17.283	57.030	0.22222E-09	0.00	0.00	0.00
811	17.016	57.640	0.22459E-09	0.00	0.00	0.00
812	16.595	58.155	0.22660E-09	0.00	0.00	0.00
813	16.049	58.537	0.22809E-09	0.00	0.00	0.00
814	13.015	59.914	0.23346E-09	0.00	0.00	0.00
815	9.8650	60.999	0.23768E-09	0.00	0.00	0.00
816	6.6262	61.780	0.24073E-09	0.00	0.00	0.00
817	3.3280	62.252	0.24257E-09	0.00	0.00	0.00
818	0.00000E+00	62.410	0.24318E-09	0.00	0.00	0.00
831	16.783	6.0950	-4.4970	0.00	0.00	0.00
832	16.783	8.8950	-4.4970	0.00	0.00	0.00

NODE	X	Y	Z	THXY	THYZ	THXZ
833	16.783	11.695	-4.4970	0.00	0.00	0.00
834	16.783	16.532	-4.4970	0.00	0.00	0.00
835	16.783	21.370	-4.4970	0.00	0.00	0.00
836	16.783	34.770	-4.4970	0.00	0.00	0.00
837	16.783	48.170	-4.4970	0.00	0.00	0.00
838	16.783	52.270	-4.4970	0.00	0.00	0.00
839	16.783	56.370	-4.4970	0.00	0.00	0.00
840	16.694	57.030	-4.4732	0.00	0.00	0.00
841	16.437	57.640	-4.4042	0.00	0.00	0.00

842	16.029	58.155	-4.2950	0.00	0.00	0.00
843	15.502	58.537	-4.1538	0.00	0.00	0.00
844	12.572	59.914	-3.3686	0.00	0.00	0.00
845	9.5289	60.999	-2.5533	0.00	0.00	0.00
846	6.4005	61.780	-1.7150	0.00	0.00	0.00
847	3.2146	62.252	-0.86136	0.00	0.00	0.00
861	15.047	6.0950	-8.6875	0.00	0.00	0.00
862	15.047	8.8950	-8.6875	0.00	0.00	0.00
863	15.047	11.695	-8.6875	0.00	0.00	0.00
864	15.047	16.532	-8.6875	0.00	0.00	0.00
865	15.047	21.370	-8.6875	0.00	0.00	0.00

NODE	X	Y	Z	THXY	THYZ	THXZ
866	15.047	34.770	-8.6875	0.00	0.00	0.00
867	15.047	48.170	-8.6875	0.00	0.00	0.00
868	15.047	52.270	-8.6875	0.00	0.00	0.00
869	15.047	56.370	-8.6875	0.00	0.00	0.00
870	14.968	57.030	-8.6416	0.00	0.00	0.00
871	14.737	57.640	-8.5082	0.00	0.00	0.00
872	14.371	58.155	-8.2973	0.00	0.00	0.00
873	13.899	58.537	-8.0245	0.00	0.00	0.00
874	11.272	59.914	-6.5077	0.00	0.00	0.00
875	8.5434	60.999	-4.9325	0.00	0.00	0.00
876	5.7385	61.780	-3.3131	0.00	0.00	0.00
877	2.8822	62.252	-1.6640	0.00	0.00	0.00
891	12.286	6.0950	-12.286	0.00	0.00	0.00
892	12.286	8.8950	-12.286	0.00	0.00	0.00
893	12.286	11.695	-12.286	0.00	0.00	0.00
894	12.286	16.532	-12.286	0.00	0.00	0.00
895	12.286	21.370	-12.286	0.00	0.00	0.00
896	12.286	34.770	-12.286	0.00	0.00	0.00
897	12.286	48.170	-12.286	0.00	0.00	0.00
898	12.286	52.270	-12.286	0.00	0.00	0.00

NODE	X	Y	Z	THXY	THYZ	THXZ
899	12.286	56.370	-12.286	0.00	0.00	0.00
900	12.221	57.030	-12.221	0.00	0.00	0.00
901	12.032	57.640	-12.032	0.00	0.00	0.00
902	11.734	58.155	-11.734	0.00	0.00	0.00
903	11.348	58.537	-11.348	0.00	0.00	0.00
904	9.2032	59.914	-9.2032	0.00	0.00	0.00
905	6.9756	60.999	-6.9756	0.00	0.00	0.00
906	4.6855	61.780	-4.6855	0.00	0.00	0.00
907	2.3533	62.252	-2.3533	0.00	0.00	0.00
921	8.6875	6.0950	-15.047	0.00	0.00	0.00
922	8.6875	8.8950	-15.047	0.00	0.00	0.00
923	8.6875	11.695	-15.047	0.00	0.00	0.00
924	8.6875	16.533	-15.047	0.00	0.00	0.00
925	8.6875	21.370	-15.047	0.00	0.00	0.00
926	8.6875	34.770	-15.047	0.00	0.00	0.00
927	8.6875	48.170	-15.047	0.00	0.00	0.00
928	8.6875	52.270	-15.047	0.00	0.00	0.00
929	8.6875	56.370	-15.047	0.00	0.00	0.00
930	8.6416	57.030	-14.968	0.00	0.00	0.00
931	8.5082	57.640	-14.737	0.00	0.00	0.00

NODE	X	Y	Z	THXY	THYZ	THXZ
932	8.2973	58.155	-14.371	0.00	0.00	0.00
933	8.0245	58.537	-13.899	0.00	0.00	0.00
934	6.5077	59.914	-11.272	0.00	0.00	0.00
935	4.9325	60.999	-8.5434	0.00	0.00	0.00
936	3.3131	61.780	-5.7385	0.00	0.00	0.00
937	1.6640	62.252	-2.8822	0.00	0.00	0.00
951	4.4970	6.0950	-16.783	0.00	0.00	0.00
952	4.4970	8.8950	-16.783	0.00	0.00	0.00
953	4.4970	11.695	-16.783	0.00	0.00	0.00
954	4.4970	16.533	-16.783	0.00	0.00	0.00
955	4.4970	21.370	-16.783	0.00	0.00	0.00
956	4.4970	34.770	-16.783	0.00	0.00	0.00
957	4.4970	48.170	-16.783	0.00	0.00	0.00
958	4.4970	52.270	-16.783	0.00	0.00	0.00
959	4.4970	56.370	-16.783	0.00	0.00	0.00
960	4.4732	57.030	-16.694	0.00	0.00	0.00
961	4.4042	57.640	-16.437	0.00	0.00	0.00

962	4.2950	58.155	-16.029	0.00	0.00	0.00
963	4.1538	58.537	-15.502	0.00	0.00	0.00
964	3.3686	59.914	-12.572	0.00	0.00	0.00

NODE	X	Y	Z	THXY	THYZ	THXZ
965	2.5533	60.999	-9.5289	0.00	0.00	0.00
966	1.7150	61.780	-6.4005	0.00	0.00	0.00
967	0.86136	62.252	-3.2146	0.00	0.00	0.00
981	0.67702E-10	6.0950	-17.375	0.00	0.00	0.00
982	0.67702E-10	8.8950	-17.375	0.00	0.00	0.00
983	0.67702E-10	11.695	-17.375	0.00	0.00	0.00
984	0.67702E-10	16.533	-17.375	0.00	0.00	0.00
985	0.67702E-10	21.370	-17.375	0.00	0.00	0.00
986	0.67702E-10	34.770	-17.375	0.00	0.00	0.00
987	0.67702E-10	48.170	-17.375	0.00	0.00	0.00
988	0.67702E-10	52.270	-17.375	0.00	0.00	0.00
989	0.67702E-10	56.370	-17.375	0.00	0.00	0.00
990	0.67344E-10	57.030	-17.283	0.00	0.00	0.00
991	0.66305E-10	57.640	-17.016	0.00	0.00	0.00
992	0.64661E-10	58.155	-16.595	0.00	0.00	0.00
993	0.62535E-10	58.537	-16.049	0.00	0.00	0.00
994	0.50714E-10	59.914	-13.015	0.00	0.00	0.00
995	0.38439E-10	60.999	-9.8650	0.00	0.00	0.00
996	0.25819E-10	61.780	-6.6262	0.00	0.00	0.00
997	0.12968E-10	62.252	-3.3280	0.00	0.00	0.00

NODE	X	Y	Z	THXY	THYZ	THXZ
1011	-4.4970	6.0950	-16.783	0.00	0.00	0.00
1012	-4.4970	8.8950	-16.783	0.00	0.00	0.00
1013	-4.4970	11.695	-16.783	0.00	0.00	0.00
1014	-4.4970	16.533	-16.783	0.00	0.00	0.00
1015	-4.4970	21.370	-16.783	0.00	0.00	0.00
1016	-4.4970	34.770	-16.783	0.00	0.00	0.00
1017	-4.4970	48.170	-16.783	0.00	0.00	0.00
1018	-4.4970	52.270	-16.783	0.00	0.00	0.00
1019	-4.4970	56.370	-16.783	0.00	0.00	0.00
1020	-4.4732	57.030	-16.694	0.00	0.00	0.00
1021	-4.4042	57.640	-16.437	0.00	0.00	0.00
1022	-4.2950	58.155	-16.029	0.00	0.00	0.00
1023	-4.1538	58.537	-15.502	0.00	0.00	0.00
1024	-3.3686	59.914	-12.572	0.00	0.00	0.00
1025	-2.5533	60.999	-9.5289	0.00	0.00	0.00
1026	-1.7150	61.780	-6.4005	0.00	0.00	0.00
1027	-0.86136	62.252	-3.2146	0.00	0.00	0.00
1041	-8.6875	6.0950	-15.047	0.00	0.00	0.00
1042	-8.6875	8.8950	-15.047	0.00	0.00	0.00
1043	-8.6875	11.695	-15.047	0.00	0.00	0.00

NODE	X	Y	Z	THXY	THYZ	THXZ
1044	-8.6875	16.533	-15.047	0.00	0.00	0.00
1045	-8.6875	21.370	-15.047	0.00	0.00	0.00
1046	-8.6875	34.770	-15.047	0.00	0.00	0.00
1047	-8.6875	48.170	-15.047	0.00	0.00	0.00
1048	-8.6875	52.270	-15.047	0.00	0.00	0.00
1049	-8.6875	56.370	-15.047	0.00	0.00	0.00
1050	-8.6416	57.030	-14.968	0.00	0.00	0.00
1051	-8.5082	57.640	-14.737	0.00	0.00	0.00
1052	-8.2973	58.155	-14.371	0.00	0.00	0.00
1053	-8.0245	58.537	-13.899	0.00	0.00	0.00
1054	-6.5077	59.914	-11.272	0.00	0.00	0.00
1055	-4.9325	60.999	-8.5434	0.00	0.00	0.00
1056	-3.3131	61.780	-5.7385	0.00	0.00	0.00
1057	-1.6640	62.252	-2.8822	0.00	0.00	0.00
1071	-12.286	6.0950	-12.286	0.00	0.00	0.00
1072	-12.286	8.8950	-12.286	0.00	0.00	0.00
1073	-12.286	11.695	-12.286	0.00	0.00	0.00
1074	-12.286	16.532	-12.286	0.00	0.00	0.00
1075	-12.286	21.370	-12.286	0.00	0.00	0.00
1076	-12.286	34.770	-12.286	0.00	0.00	0.00

NODE	X	Y	Z	THXY	THYZ	THXZ
1077	-12.286	48.170	-12.286	0.00	0.00	0.00
1078	-12.286	52.270	-12.286	0.00	0.00	0.00
1079	-12.286	56.370	-12.286	0.00	0.00	0.00

1080	-12.221	57.030	-12.221	0.00	0.00	0.00
1081	-12.032	57.640	-12.032	0.00	0.00	0.00
1082	-11.734	58.155	-11.734	0.00	0.00	0.00
1083	-11.348	58.537	-11.348	0.00	0.00	0.00
1084	-9.2032	59.914	-9.2032	0.00	0.00	0.00
1085	-6.9756	60.999	-6.9756	0.00	0.00	0.00
1086	-4.6855	61.780	-4.6855	0.00	0.00	0.00
1087	-2.3533	62.252	-2.3533	0.00	0.00	0.00
1101	-15.047	6.0950	-8.6875	0.00	0.00	0.00
1102	-15.047	8.8950	-8.6875	0.00	0.00	0.00
1103	-15.047	11.695	-8.6875	0.00	0.00	0.00
1104	-15.047	16.532	-8.6875	0.00	0.00	0.00
1105	-15.047	21.370	-8.6875	0.00	0.00	0.00
1106	-15.047	34.770	-8.6875	0.00	0.00	0.00
1107	-15.047	48.170	-8.6875	0.00	0.00	0.00
1108	-15.047	52.270	-8.6875	0.00	0.00	0.00
1109	-15.047	56.370	-8.6875	0.00	0.00	0.00

NODE	X	Y	Z	THXY	THYZ	THXZ
1110	-14.968	57.030	-8.6416	0.00	0.00	0.00
1111	-14.737	57.640	-8.5082	0.00	0.00	0.00
1112	-14.371	58.155	-8.2973	0.00	0.00	0.00
1113	-13.899	58.537	-8.0245	0.00	0.00	0.00
1114	-11.272	59.914	-6.5077	0.00	0.00	0.00
1115	-8.5434	60.999	-4.9325	0.00	0.00	0.00
1116	-5.7385	61.780	-3.3131	0.00	0.00	0.00
1117	-2.8822	62.252	-1.6640	0.00	0.00	0.00
1131	-16.783	6.0950	-4.4970	0.00	0.00	0.00
1132	-16.783	8.8950	-4.4970	0.00	0.00	0.00
1133	-16.783	11.695	-4.4970	0.00	0.00	0.00
1134	-16.783	16.532	-4.4970	0.00	0.00	0.00
1135	-16.783	21.370	-4.4970	0.00	0.00	0.00
1136	-16.783	34.770	-4.4970	0.00	0.00	0.00
1137	-16.783	48.170	-4.4970	0.00	0.00	0.00
1138	-16.783	52.270	-4.4970	0.00	0.00	0.00
1139	-16.783	56.370	-4.4970	0.00	0.00	0.00
1140	-16.694	57.030	-4.4732	0.00	0.00	0.00
1141	-16.437	57.640	-4.4042	0.00	0.00	0.00
1142	-16.029	58.155	-4.2950	0.00	0.00	0.00

NODE	X	Y	Z	THXY	THYZ	THXZ
1143	-15.502	58.537	-4.1538	0.00	0.00	0.00
1144	-12.572	59.914	-3.3686	0.00	0.00	0.00
1145	-9.5289	60.999	-2.5533	0.00	0.00	0.00
1146	-6.4005	61.780	-1.7150	0.00	0.00	0.00
1147	-3.2146	62.252	-0.86136	0.00	0.00	0.00
1161	-17.375	6.0950	-0.30437E-07	0.00	0.00	0.00
1162	-17.375	8.8950	-0.30426E-07	0.00	0.00	0.00
1163	-17.375	11.695	-0.30415E-07	0.00	0.00	0.00
1164	-17.375	16.532	-0.30396E-07	0.00	0.00	0.00
1165	-17.375	21.370	-0.30377E-07	0.00	0.00	0.00
1166	-17.375	34.770	-0.30325E-07	0.00	0.00	0.00
1167	-17.375	48.170	-0.30273E-07	0.00	0.00	0.00
1168	-17.375	52.270	-0.30257E-07	0.00	0.00	0.00
1169	-17.375	56.370	-0.30241E-07	0.00	0.00	0.00
1170	-17.283	57.030	-0.30077E-07	0.00	0.00	0.00
1171	-17.016	57.640	-0.29607E-07	0.00	0.00	0.00
1172	-16.595	58.155	-0.28866E-07	0.00	0.00	0.00
1173	-16.049	58.537	-0.27908E-07	0.00	0.00	0.00
1174	-13.015	59.914	-0.22584E-07	0.00	0.00	0.00
1175	-9.8650	60.999	-0.17057E-07	0.00	0.00	0.00

NODE	X	Y	Z	THXY	THYZ	THXZ
1176	-6.6262	61.780	-0.11376E-07	0.00	0.00	0.00
1177	-3.3280	62.252	-0.55919E-08	0.00	0.00	0.00

LIST ALL MATERIALS PROPERTY= ALL

PROPERTY TABLE NUXY MAT= 1 NUM. POINTS= 2

TEMPERATURE	DATA	TEMPERATURE	DATA
-9999.0	0.30000	9999.0	0.30000

PROPERTY TABLE EX MAT= 1 NUM. POINTS= 15

TEMPERATURE	DATA	TEMPERATURE	DATA

```
     -40.000     0.28900E+08  70.000     0.28300E+08
      100.00     0.28100E+08  200.00     0.27600E+08
      300.00     0.27000E+08  400.00     0.26500E+08
      500.00     0.25800E+08  600.00     0.25300E+08
      700.00     0.24800E+08  800.00     0.24100E+08
      900.00     0.23500E+08  1000.0     0.22500E+08
      1100.0     0.22100E+08  1200.0     0.21300E+08
      1300.0     0.20500E+08

PROPERTY TABLE ALPX  MAT=   1  NUM. POINTS= 15
    TEMPERATURE      DATA    TEMPERATURE      DATA
     -40.000     0.81300E-05  70.000     0.84600E-05
      100.00     0.85500E-05  200.00     0.87900E-05
      300.00     0.90000E-05  400.00     0.91900E-05
      500.00     0.93700E-05  600.00     0.95300E-05
      700.00     0.96900E-05  800.00     0.98200E-05
      900.00     0.10060E-04  1000.0     0.10300E-04
      1100.0     0.10350E-04  1200.0     0.10400E-04
      1300.0     0.10450E-04

PROPERTY TABLE EX    MAT=   2  NUM. POINTS=  7
    TEMPERATURE      DATA    TEMPERATURE      DATA
     -40.000     0.28400E+08  70.000     0.27800E+08
      100.00     0.27600E+08  200.00     0.27100E+08
      300.00     0.26700E+08  400.00     0.26100E+08
      500.00     0.25700E+08

PROPERTY TABLE ALPX  MAT=   2  NUM. POINTS=  7
    TEMPERATURE      DATA    TEMPERATURE      DATA
     -40.000     0.59400E-05  70.000     0.62000E-05
      100.00     0.62700E-05  200.00     0.65400E-05
      300.00     0.67800E-05  400.00     0.69800E-05
      500.00     0.71600E-05

LIST ALL COUPLED SETS
TIME= 0.00000E+00  NITTER=     -5
KTEMP-  LSTP=    -1  ITER=      0

UNIFORM TEMPERATURE=    70.000  (TREF=    70.000)

PRINT REACTION FORCES WITH NO ELEMENT FORCES (KRF=2)
 BOUNDARY CONDITIONS STEPPED DUE TO STATIC CONVERGENCE OPTION
PLASTIC CONVERG. CRITERION=      0.0100
CREEP OPTIMUM. CRITERION=       0.1000
LARGE DEFL. CONVERG. CRITERION=    0.001000
DISPLACEMENT LIMIT= 0.00000E+00

NPRINT= 99900   NPOST=     5   REACTION PRINT FREQ= 99900
 DISP. POST DATA FREQ=     5  REACT. POST DATA FREQ=     5

 ELEMENT PRINT AND POST DATA FREQUENCIES
  TYPE  STIFF  STRESS  FORCE   STRESS   DATA  FORCE
          NO.   PRINT  PRINT    DATA   LEVEL  DATA
     2     63  99900  99900       5      3     5
     3      8  99900  99900       5      3     5
     4     52  99900  99900       5      3     5
     5     45  99900  99900       5      3     5
     6     63  99900  99900       5      3     5
     7     45  99900  99900       5      3     5
     8     63  99900  99900       5      3     5
     9     63  99900  99900       5      3     5

LOADS INPUT FILE= 26     LOADS OUTPUT FILE= 23

ALL ANALYSIS DATA WILL BE WRITTEN ONTO FILE27

LIST DISPLACEMENTS FOR ALL SELECTED NODES

 NODE  LABEL     DISP            CDISP
  1177 ROTX  0.000000000E+00 0.000000000E+00
  1177 UZ    0.000000000E+00 0.000000000E+00
  1176 ROTX  0.000000000E+00 0.000000000E+00
  1176 UZ    0.000000000E+00 0.000000000E+00
  1175 ROTX  0.000000000E+00 0.000000000E+00
```

1175	UZ	0.000000000E+00	0.000000000E+00
1174	ROTX	0.000000000E+00	0.000000000E+00
1174	UZ	0.000000000E+00	0.000000000E+00
1173	ROTX	0.000000000E+00	0.000000000E+00
1173	UZ	0.000000000E+00	0.000000000E+00
1172	ROTX	0.000000000E+00	0.000000000E+00
1172	UZ	0.000000000E+00	0.000000000E+00
1171	ROTX	0.000000000E+00	0.000000000E+00
1171	UZ	0.000000000E+00	0.000000000E+00
1170	ROTX	0.000000000E+00	0.000000000E+00
1170	UZ	0.000000000E+00	0.000000000E+00
1169	ROTX	0.000000000E+00	0.000000000E+00
1169	UZ	0.000000000E+00	0.000000000E+00
1168	ROTX	0.000000000E+00	0.000000000E+00
1168	UZ	0.000000000E+00	0.000000000E+00

NODE	LABEL	DISP	CDISP
1167	ROTX	0.000000000E+00	0.000000000E+00
1167	UZ	0.000000000E+00	0.000000000E+00
1166	ROTX	0.000000000E+00	0.000000000E+00
1166	UZ	0.000000000E+00	0.000000000E+00
1165	ROTX	0.000000000E+00	0.000000000E+00
1165	UZ	0.000000000E+00	0.000000000E+00
1164	ROTX	0.000000000E+00	0.000000000E+00
1164	UZ	0.000000000E+00	0.000000000E+00
1163	ROTX	0.000000000E+00	0.000000000E+00
1163	UZ	0.000000000E+00	0.000000000E+00
1162	ROTX	0.000000000E+00	0.000000000E+00
1162	UZ	0.000000000E+00	0.000000000E+00
1161	ROTX	0.000000000E+00	0.000000000E+00
1161	UZ	0.000000000E+00	0.000000000E+00
390	ROTZ	0.000000000E+00	0.000000000E+00
818	ROTX	0.000000000E+00	0.000000000E+00
818	UZ	0.000000000E+00	0.000000000E+00
390	UY	0.000000000E+00	0.000000000E+00
390	UX	0.000000000E+00	0.000000000E+00
817	ROTX	0.000000000E+00	0.000000000E+00

NODE	LABEL	DISP	CDISP
816	ROTX	0.000000000E+00	0.000000000E+00
815	ROTX	0.000000000E+00	0.000000000E+00
814	ROTX	0.000000000E+00	0.000000000E+00
813	ROTX	0.000000000E+00	0.000000000E+00
812	ROTX	0.000000000E+00	0.000000000E+00
811	ROTX	0.000000000E+00	0.000000000E+00
810	ROTX	0.000000000E+00	0.000000000E+00
809	ROTX	0.000000000E+00	0.000000000E+00
808	ROTX	0.000000000E+00	0.000000000E+00
807	ROTX	0.000000000E+00	0.000000000E+00
806	ROTX	0.000000000E+00	0.000000000E+00
805	ROTX	0.000000000E+00	0.000000000E+00
804	ROTX	0.000000000E+00	0.000000000E+00
803	ROTX	0.000000000E+00	0.000000000E+00
802	ROTX	0.000000000E+00	0.000000000E+00
801	ROTX	0.000000000E+00	0.000000000E+00
786	ROTX	0.000000000E+00	0.000000000E+00
785	ROTX	0.000000000E+00	0.000000000E+00
784	ROTX	0.000000000E+00	0.000000000E+00
783	ROTX	0.000000000E+00	0.000000000E+00

NODE	LABEL	DISP	CDISP
782	ROTX	0.000000000E+00	0.000000000E+00
781	ROTX	0.000000000E+00	0.000000000E+00
780	ROTX	0.000000000E+00	0.000000000E+00
779	ROTX	0.000000000E+00	0.000000000E+00
778	ROTX	0.000000000E+00	0.000000000E+00
777	ROTX	0.000000000E+00	0.000000000E+00
776	ROTX	0.000000000E+00	0.000000000E+00
775	ROTX	0.000000000E+00	0.000000000E+00
774	ROTX	0.000000000E+00	0.000000000E+00
773	ROTX	0.000000000E+00	0.000000000E+00
772	ROTX	0.000000000E+00	0.000000000E+00
771	ROTX	0.000000000E+00	0.000000000E+00
770	ROTX	0.000000000E+00	0.000000000E+00

769	ROTX	0.000000000E+00	0.000000000E+00
768	ROTX	0.000000000E+00	0.000000000E+00
767	ROTX	0.000000000E+00	0.000000000E+00
766	ROTX	0.000000000E+00	0.000000000E+00
765	ROTX	0.000000000E+00	0.000000000E+00
764	ROTX	0.000000000E+00	0.000000000E+00
763	ROTX	0.000000000E+00	0.000000000E+00

NODE	LABEL	DISP	CDISP
762	ROTX	0.000000000E+00	0.000000000E+00
761	ROTX	0.000000000E+00	0.000000000E+00
426	ROTX	0.000000000E+00	0.000000000E+00
425	ROTX	0.000000000E+00	0.000000000E+00
424	ROTX	0.000000000E+00	0.000000000E+00
423	ROTX	0.000000000E+00	0.000000000E+00
422	ROTX	0.000000000E+00	0.000000000E+00
421	ROTX	0.000000000E+00	0.000000000E+00
420	ROTX	0.000000000E+00	0.000000000E+00
419	ROTX	0.000000000E+00	0.000000000E+00
418	ROTX	0.000000000E+00	0.000000000E+00
417	ROTX	0.000000000E+00	0.000000000E+00
416	ROTX	0.000000000E+00	0.000000000E+00
415	ROTX	0.000000000E+00	0.000000000E+00
414	ROTX	0.000000000E+00	0.000000000E+00
413	ROTX	0.000000000E+00	0.000000000E+00
412	ROTX	0.000000000E+00	0.000000000E+00
411	ROTX	0.000000000E+00	0.000000000E+00
410	ROTX	0.000000000E+00	0.000000000E+00
409	ROTX	0.000000000E+00	0.000000000E+00

NODE	LABEL	DISP	CDISP
408	ROTX	0.000000000E+00	0.000000000E+00
407	ROTX	0.000000000E+00	0.000000000E+00
406	ROTX	0.000000000E+00	0.000000000E+00
405	ROTX	0.000000000E+00	0.000000000E+00
404	ROTX	0.000000000E+00	0.000000000E+00
403	ROTX	0.000000000E+00	0.000000000E+00
402	ROTX	0.000000000E+00	0.000000000E+00
401	ROTX	0.000000000E+00	0.000000000E+00
400	ROTX	0.000000000E+00	0.000000000E+00
399	ROTX	0.000000000E+00	0.000000000E+00
398	ROTX	0.000000000E+00	0.000000000E+00
397	ROTX	0.000000000E+00	0.000000000E+00
396	ROTX	0.000000000E+00	0.000000000E+00
395	ROTX	0.000000000E+00	0.000000000E+00
394	ROTX	0.000000000E+00	0.000000000E+00
393	ROTX	0.000000000E+00	0.000000000E+00
392	ROTX	0.000000000E+00	0.000000000E+00
391	ROTX	0.000000000E+00	0.000000000E+00
390	ROTX	0.000000000E+00	0.000000000E+00
388	ROTX	0.000000000E+00	0.000000000E+00

NODE	LABEL	DISP	CDISP
387	ROTX	0.000000000E+00	0.000000000E+00
386	ROTX	0.000000000E+00	0.000000000E+00
385	ROTX	0.000000000E+00	0.000000000E+00
384	ROTX	0.000000000E+00	0.000000000E+00
383	ROTX	0.000000000E+00	0.000000000E+00
382	ROTX	0.000000000E+00	0.000000000E+00
381	ROTX	0.000000000E+00	0.000000000E+00
380	ROTX	0.000000000E+00	0.000000000E+00
379	ROTX	0.000000000E+00	0.000000000E+00
378	ROTX	0.000000000E+00	0.000000000E+00
377	ROTX	0.000000000E+00	0.000000000E+00
376	ROTX	0.000000000E+00	0.000000000E+00
375	ROTX	0.000000000E+00	0.000000000E+00
817	UZ	0.000000000E+00	0.000000000E+00
816	UZ	0.000000000E+00	0.000000000E+00
815	UZ	0.000000000E+00	0.000000000E+00
814	UZ	0.000000000E+00	0.000000000E+00
813	UZ	0.000000000E+00	0.000000000E+00
812	UZ	0.000000000E+00	0.000000000E+00
811	UZ	0.000000000E+00	0.000000000E+00

NODE	LABEL	DISP	CDISP
810	UZ	0.000000000E+00	0.000000000E+00
809	UZ	0.000000000E+00	0.000000000E+00
808	UZ	0.000000000E+00	0.000000000E+00
807	UZ	0.000000000E+00	0.000000000E+00
806	UZ	0.000000000E+00	0.000000000E+00
805	UZ	0.000000000E+00	0.000000000E+00
804	UZ	0.000000000E+00	0.000000000E+00
803	UZ	0.000000000E+00	0.000000000E+00
802	UZ	0.000000000E+00	0.000000000E+00
801	UZ	0.000000000E+00	0.000000000E+00
786	UZ	0.000000000E+00	0.000000000E+00
785	UZ	0.000000000E+00	0.000000000E+00
784	UZ	0.000000000E+00	0.000000000E+00
783	UZ	0.000000000E+00	0.000000000E+00
782	UZ	0.000000000E+00	0.000000000E+00
781	UZ	0.000000000E+00	0.000000000E+00
780	UZ	0.000000000E+00	0.000000000E+00
779	UZ	0.000000000E+00	0.000000000E+00
778	UZ	0.000000000E+00	0.000000000E+00
777	UZ	0.000000000E+00	0.000000000E+00

NODE	LABEL	DISP	CDISP
776	UZ	0.000000000E+00	0.000000000E+00
775	UZ	0.000000000E+00	0.000000000E+00
774	UZ	0.000000000E+00	0.000000000E+00
773	UZ	0.000000000E+00	0.000000000E+00
772	UZ	0.000000000E+00	0.000000000E+00
771	UZ	0.000000000E+00	0.000000000E+00
770	UZ	0.000000000E+00	0.000000000E+00
769	UZ	0.000000000E+00	0.000000000E+00
768	UZ	0.000000000E+00	0.000000000E+00
767	UZ	0.000000000E+00	0.000000000E+00
766	UZ	0.000000000E+00	0.000000000E+00
765	UZ	0.000000000E+00	0.000000000E+00
764	UZ	0.000000000E+00	0.000000000E+00
763	UZ	0.000000000E+00	0.000000000E+00
762	UZ	0.000000000E+00	0.000000000E+00
761	UZ	0.000000000E+00	0.000000000E+00
426	UZ	0.000000000E+00	0.000000000E+00
425	UZ	0.000000000E+00	0.000000000E+00
424	UZ	0.000000000E+00	0.000000000E+00
423	UZ	0.000000000E+00	0.000000000E+00

NODE	LABEL	DISP	CDISP
422	UZ	0.000000000E+00	0.000000000E+00
421	UZ	0.000000000E+00	0.000000000E+00
420	UZ	0.000000000E+00	0.000000000E+00
419	UZ	0.000000000E+00	0.000000000E+00
418	UZ	0.000000000E+00	0.000000000E+00
417	UZ	0.000000000E+00	0.000000000E+00
416	UZ	0.000000000E+00	0.000000000E+00
374	ROTX	0.000000000E+00	0.000000000E+00
415	UZ	0.000000000E+00	0.000000000E+00
414	UZ	0.000000000E+00	0.000000000E+00
413	UZ	0.000000000E+00	0.000000000E+00
412	UZ	0.000000000E+00	0.000000000E+00
411	UZ	0.000000000E+00	0.000000000E+00
410	UZ	0.000000000E+00	0.000000000E+00
409	UZ	0.000000000E+00	0.000000000E+00
408	UZ	0.000000000E+00	0.000000000E+00
407	UZ	0.000000000E+00	0.000000000E+00
406	UZ	0.000000000E+00	0.000000000E+00
405	UZ	0.000000000E+00	0.000000000E+00
404	UZ	0.000000000E+00	0.000000000E+00

NODE	LABEL	DISP	CDISP
403	UZ	0.000000000E+00	0.000000000E+00
402	UZ	0.000000000E+00	0.000000000E+00
401	UZ	0.000000000E+00	0.000000000E+00
400	UZ	0.000000000E+00	0.000000000E+00
399	UZ	0.000000000E+00	0.000000000E+00
398	UZ	0.000000000E+00	0.000000000E+00
397	UZ	0.000000000E+00	0.000000000E+00

396	UZ	0.000000000E+00	0.000000000E+00
395	UZ	0.000000000E+00	0.000000000E+00
394	UZ	0.000000000E+00	0.000000000E+00
393	UZ	0.000000000E+00	0.000000000E+00
392	UZ	0.000000000E+00	0.000000000E+00
391	UZ	0.000000000E+00	0.000000000E+00
390	UZ	0.000000000E+00	0.000000000E+00
388	UZ	0.000000000E+00	0.000000000E+00
387	UZ	0.000000000E+00	0.000000000E+00
386	UZ	0.000000000E+00	0.000000000E+00
385	UZ	0.000000000E+00	0.000000000E+00
384	UZ	0.000000000E+00	0.000000000E+00
383	UZ	0.000000000E+00	0.000000000E+00

NODE	LABEL	DISP	CDISP
382	UZ	0.000000000E+00	0.000000000E+00
381	UZ	0.000000000E+00	0.000000000E+00
380	UZ	0.000000000E+00	0.000000000E+00
379	UZ	0.000000000E+00	0.000000000E+00
378	UZ	0.000000000E+00	0.000000000E+00
377	UZ	0.000000000E+00	0.000000000E+00
376	UZ	0.000000000E+00	0.000000000E+00
375	UZ	0.000000000E+00	0.000000000E+00
374	UZ	0.000000000E+00	0.000000000E+00
373	UZ	0.000000000E+00	0.000000000E+00
372	UZ	0.000000000E+00	0.000000000E+00
371	UZ	0.000000000E+00	0.000000000E+00
370	UZ	0.000000000E+00	0.000000000E+00
369	UZ	0.000000000E+00	0.000000000E+00
368	UZ	0.000000000E+00	0.000000000E+00
367	UZ	0.000000000E+00	0.000000000E+00
365	UZ	0.000000000E+00	0.000000000E+00
364	UZ	0.000000000E+00	0.000000000E+00
363	UZ	0.000000000E+00	0.000000000E+00
362	UZ	0.000000000E+00	0.000000000E+00

NODE	LABEL	DISP	CDISP
361	UZ	0.000000000E+00	0.000000000E+00
28	UZ	0.000000000E+00	0.000000000E+00
27	UZ	0.000000000E+00	0.000000000E+00
26	UZ	0.000000000E+00	0.000000000E+00
25	UZ	0.000000000E+00	0.000000000E+00
24	UZ	0.000000000E+00	0.000000000E+00
23	UZ	0.000000000E+00	0.000000000E+00
22	UZ	0.000000000E+00	0.000000000E+00
21	UZ	0.000000000E+00	0.000000000E+00
20	UZ	0.000000000E+00	0.000000000E+00
19	UZ	0.000000000E+00	0.000000000E+00
18	UZ	0.000000000E+00	0.000000000E+00
17	UZ	0.000000000E+00	0.000000000E+00
16	UZ	0.000000000E+00	0.000000000E+00
15	UZ	0.000000000E+00	0.000000000E+00
14	UZ	0.000000000E+00	0.000000000E+00
13	UZ	0.000000000E+00	0.000000000E+00
12	UZ	0.000000000E+00	0.000000000E+00
11	UZ	0.000000000E+00	0.000000000E+00
10	UZ	0.000000000E+00	0.000000000E+00

NODE	LABEL	DISP	CDISP
9	UZ	0.000000000E+00	0.000000000E+00
8	UZ	0.000000000E+00	0.000000000E+00
7	UZ	0.000000000E+00	0.000000000E+00
5	UZ	0.000000000E+00	0.000000000E+00
4	UZ	0.000000000E+00	0.000000000E+00
3	UZ	0.000000000E+00	0.000000000E+00
373	ROTX	0.000000000E+00	0.000000000E+00
372	ROTX	0.000000000E+00	0.000000000E+00
371	ROTX	0.000000000E+00	0.000000000E+00
370	ROTX	0.000000000E+00	0.000000000E+00
369	ROTX	0.000000000E+00	0.000000000E+00
368	ROTX	0.000000000E+00	0.000000000E+00
367	ROTX	0.000000000E+00	0.000000000E+00
365	ROTX	0.000000000E+00	0.000000000E+00
364	ROTX	0.000000000E+00	0.000000000E+00

363	ROTX	0.000000000E+00	0.000000000E+00
362	ROTX	0.000000000E+00	0.000000000E+00
361	ROTX	0.000000000E+00	0.000000000E+00
28	ROTX	0.000000000E+00	0.000000000E+00
27	ROTX	0.000000000E+00	0.000000000E+00

NODE	LABEL	DISP	CDISP
26	ROTX	0.000000000E+00	0.000000000E+00
25	ROTX	0.000000000E+00	0.000000000E+00
24	ROTX	0.000000000E+00	0.000000000E+00
23	ROTX	0.000000000E+00	0.000000000E+00
22	ROTX	0.000000000E+00	0.000000000E+00
21	ROTX	0.000000000E+00	0.000000000E+00
20	ROTX	0.000000000E+00	0.000000000E+00
19	ROTX	0.000000000E+00	0.000000000E+00
18	ROTX	0.000000000E+00	0.000000000E+00
17	ROTX	0.000000000E+00	0.000000000E+00
16	ROTX	0.000000000E+00	0.000000000E+00
15	ROTX	0.000000000E+00	0.000000000E+00
14	ROTX	0.000000000E+00	0.000000000E+00
13	ROTX	0.000000000E+00	0.000000000E+00
12	ROTX	0.000000000E+00	0.000000000E+00
11	ROTX	0.000000000E+00	0.000000000E+00
10	ROTX	0.000000000E+00	0.000000000E+00
9	ROTX	0.000000000E+00	0.000000000E+00
8	ROTX	0.000000000E+00	0.000000000E+00
7	ROTX	0.000000000E+00	0.000000000E+00

NODE	LABEL	DISP	CDISP
5	ROTX	0.000000000E+00	0.000000000E+00
4	ROTX	0.000000000E+00	0.000000000E+00
3	ROTX	0.000000000E+00	0.000000000E+00
1	UZ	0.000000000E+00	0.000000000E+00
2	UZ	0.000000000E+00	0.000000000E+00
1	ROTX	0.000000000E+00	0.000000000E+00
2	ROTX	0.000000000E+00	0.000000000E+00
1	ROTY	0.000000000E+00	0.000000000E+00
2	ROTY	0.000000000E+00	0.000000000E+00
3	ROTY	0.000000000E+00	0.000000000E+00
4	ROTY	0.000000000E+00	0.000000000E+00
5	ROTY	0.000000000E+00	0.000000000E+00
7	ROTY	0.000000000E+00	0.000000000E+00
8	ROTY	0.000000000E+00	0.000000000E+00
9	ROTY	0.000000000E+00	0.000000000E+00
10	ROTY	0.000000000E+00	0.000000000E+00
11	ROTY	0.000000000E+00	0.000000000E+00
12	ROTY	0.000000000E+00	0.000000000E+00
13	ROTY	0.000000000E+00	0.000000000E+00
14	ROTY	0.000000000E+00	0.000000000E+00

NODE	LABEL	DISP	CDISP
15	ROTY	0.000000000E+00	0.000000000E+00
16	ROTY	0.000000000E+00	0.000000000E+00
17	ROTY	0.000000000E+00	0.000000000E+00
18	ROTY	0.000000000E+00	0.000000000E+00
19	ROTY	0.000000000E+00	0.000000000E+00
20	ROTY	0.000000000E+00	0.000000000E+00
21	ROTY	0.000000000E+00	0.000000000E+00
22	ROTY	0.000000000E+00	0.000000000E+00
23	ROTY	0.000000000E+00	0.000000000E+00
24	ROTY	0.000000000E+00	0.000000000E+00
25	ROTY	0.000000000E+00	0.000000000E+00
26	ROTY	0.000000000E+00	0.000000000E+00
27	ROTY	0.000000000E+00	0.000000000E+00
28	ROTY	0.000000000E+00	0.000000000E+00
361	ROTY	0.000000000E+00	0.000000000E+00
362	ROTY	0.000000000E+00	0.000000000E+00
363	ROTY	0.000000000E+00	0.000000000E+00
364	ROTY	0.000000000E+00	0.000000000E+00
365	ROTY	0.000000000E+00	0.000000000E+00
367	ROTY	0.000000000E+00	0.000000000E+00

NODE	LABEL	DISP	CDISP
368	ROTY	0.000000000E+00	0.000000000E+00

369	ROTY	0.000000000E+00	0.000000000E+00
370	ROTY	0.000000000E+00	0.000000000E+00
371	ROTY	0.000000000E+00	0.000000000E+00
372	ROTY	0.000000000E+00	0.000000000E+00
373	ROTY	0.000000000E+00	0.000000000E+00
374	ROTY	0.000000000E+00	0.000000000E+00
375	ROTY	0.000000000E+00	0.000000000E+00
376	ROTY	0.000000000E+00	0.000000000E+00
377	ROTY	0.000000000E+00	0.000000000E+00
378	ROTY	0.000000000E+00	0.000000000E+00
379	ROTY	0.000000000E+00	0.000000000E+00
380	ROTY	0.000000000E+00	0.000000000E+00
381	ROTY	0.000000000E+00	0.000000000E+00
382	ROTY	0.000000000E+00	0.000000000E+00
383	ROTY	0.000000000E+00	0.000000000E+00
384	ROTY	0.000000000E+00	0.000000000E+00
385	ROTY	0.000000000E+00	0.000000000E+00
386	ROTY	0.000000000E+00	0.000000000E+00
387	ROTY	0.000000000E+00	0.000000000E+00

NODE	LABEL	DISP	CDISP
388	ROTY	0.000000000E+00	0.000000000E+00
390	ROTY	0.000000000E+00	0.000000000E+00
391	ROTY	0.000000000E+00	0.000000000E+00
392	ROTY	0.000000000E+00	0.000000000E+00
393	ROTY	0.000000000E+00	0.000000000E+00
394	ROTY	0.000000000E+00	0.000000000E+00
395	ROTY	0.000000000E+00	0.000000000E+00
396	ROTY	0.000000000E+00	0.000000000E+00
397	ROTY	0.000000000E+00	0.000000000E+00
398	ROTY	0.000000000E+00	0.000000000E+00
399	ROTY	0.000000000E+00	0.000000000E+00
400	ROTY	0.000000000E+00	0.000000000E+00
401	ROTY	0.000000000E+00	0.000000000E+00
402	ROTY	0.000000000E+00	0.000000000E+00
403	ROTY	0.000000000E+00	0.000000000E+00
404	ROTY	0.000000000E+00	0.000000000E+00
405	ROTY	0.000000000E+00	0.000000000E+00
406	ROTY	0.000000000E+00	0.000000000E+00
407	ROTY	0.000000000E+00	0.000000000E+00
408	ROTY	0.000000000E+00	0.000000000E+00

NODE	LABEL	DISP	CDISP
409	ROTY	0.000000000E+00	0.000000000E+00
410	ROTY	0.000000000E+00	0.000000000E+00
411	ROTY	0.000000000E+00	0.000000000E+00
412	ROTY	0.000000000E+00	0.000000000E+00
413	ROTY	0.000000000E+00	0.000000000E+00
414	ROTY	0.000000000E+00	0.000000000E+00
415	ROTY	0.000000000E+00	0.000000000E+00
416	ROTY	0.000000000E+00	0.000000000E+00
417	ROTY	0.000000000E+00	0.000000000E+00
418	ROTY	0.000000000E+00	0.000000000E+00
419	ROTY	0.000000000E+00	0.000000000E+00
420	ROTY	0.000000000E+00	0.000000000E+00
421	ROTY	0.000000000E+00	0.000000000E+00
422	ROTY	0.000000000E+00	0.000000000E+00
423	ROTY	0.000000000E+00	0.000000000E+00
424	ROTY	0.000000000E+00	0.000000000E+00
425	ROTY	0.000000000E+00	0.000000000E+00
426	ROTY	0.000000000E+00	0.000000000E+00
761	ROTY	0.000000000E+00	0.000000000E+00
762	ROTY	0.000000000E+00	0.000000000E+00

NODE	LABEL	DISP	CDISP
763	ROTY	0.000000000E+00	0.000000000E+00
764	ROTY	0.000000000E+00	0.000000000E+00
765	ROTY	0.000000000E+00	0.000000000E+00
766	ROTY	0.000000000E+00	0.000000000E+00
767	ROTY	0.000000000E+00	0.000000000E+00
768	ROTY	0.000000000E+00	0.000000000E+00
769	ROTY	0.000000000E+00	0.000000000E+00
770	ROTY	0.000000000E+00	0.000000000E+00
771	ROTY	0.000000000E+00	0.000000000E+00

772	ROTY	0.000000000E+00	0.000000000E+00
773	ROTY	0.000000000E+00	0.000000000E+00
774	ROTY	0.000000000E+00	0.000000000E+00
775	ROTY	0.000000000E+00	0.000000000E+00
776	ROTY	0.000000000E+00	0.000000000E+00
777	ROTY	0.000000000E+00	0.000000000E+00
778	ROTY	0.000000000E+00	0.000000000E+00
779	ROTY	0.000000000E+00	0.000000000E+00
780	ROTY	0.000000000E+00	0.000000000E+00
781	ROTY	0.000000000E+00	0.000000000E+00
782	ROTY	0.000000000E+00	0.000000000E+00

NODE	LABEL	DISP	CDISP
783	ROTY	0.000000000E+00	0.000000000E+00
784	ROTY	0.000000000E+00	0.000000000E+00
785	ROTY	0.000000000E+00	0.000000000E+00
786	ROTY	0.000000000E+00	0.000000000E+00
801	ROTY	0.000000000E+00	0.000000000E+00
802	ROTY	0.000000000E+00	0.000000000E+00
803	ROTY	0.000000000E+00	0.000000000E+00
804	ROTY	0.000000000E+00	0.000000000E+00
805	ROTY	0.000000000E+00	0.000000000E+00
806	ROTY	0.000000000E+00	0.000000000E+00
807	ROTY	0.000000000E+00	0.000000000E+00
808	ROTY	0.000000000E+00	0.000000000E+00
809	ROTY	0.000000000E+00	0.000000000E+00
810	ROTY	0.000000000E+00	0.000000000E+00
811	ROTY	0.000000000E+00	0.000000000E+00
812	ROTY	0.000000000E+00	0.000000000E+00
813	ROTY	0.000000000E+00	0.000000000E+00
814	ROTY	0.000000000E+00	0.000000000E+00
815	ROTY	0.000000000E+00	0.000000000E+00
816	ROTY	0.000000000E+00	0.000000000E+00

NODE	LABEL	DISP	CDISP
817	ROTY	0.000000000E+00	0.000000000E+00
818	ROTY	0.000000000E+00	0.000000000E+00
1161	ROTY	0.000000000E+00	0.000000000E+00
1162	ROTY	0.000000000E+00	0.000000000E+00
1163	ROTY	0.000000000E+00	0.000000000E+00
1164	ROTY	0.000000000E+00	0.000000000E+00
1165	ROTY	0.000000000E+00	0.000000000E+00
1166	ROTY	0.000000000E+00	0.000000000E+00
1167	ROTY	0.000000000E+00	0.000000000E+00
1168	ROTY	0.000000000E+00	0.000000000E+00
1169	ROTY	0.000000000E+00	0.000000000E+00
1170	ROTY	0.000000000E+00	0.000000000E+00
1171	ROTY	0.000000000E+00	0.000000000E+00
1172	ROTY	0.000000000E+00	0.000000000E+00
1173	ROTY	0.000000000E+00	0.000000000E+00
1174	ROTY	0.000000000E+00	0.000000000E+00
1175	ROTY	0.000000000E+00	0.000000000E+00
1176	ROTY	0.000000000E+00	0.000000000E+00
1177	ROTY	0.000000000E+00	0.000000000E+00

LIST ELEMENT PRESSURES FOR ALL SELECTED ELEMENTS

ELEM	FACE	VALUE(S)		FACE NODES			
443	2	30.8999605	0.000000000E+00	747	751	781	777
442	2	30.8999605	0.000000000E+00	717	721	751	747
440	2	30.8999605	0.000000000E+00	687	691	721	717
438	2	30.8999605	0.000000000E+00	657	661	691	687
436	2	30.8999605	0.000000000E+00	627	631	661	657
434	2	30.8999605	0.000000000E+00	597	601	631	627
432	2	30.8999605	0.000000000E+00	567	571	601	597
430	2	30.8999605	0.000000000E+00	537	541	571	567
428	2	30.8999605	0.000000000E+00	507	511	541	537
426	2	30.8999605	0.000000000E+00	477	481	511	507
424	2	30.8999605	0.000000000E+00	447	451	481	477
422	2	30.8999605	0.000000000E+00	417	421	451	447
445	1	30.8999605	0.000000000E+00	754	784	1161	1131
446	1	30.8999605	0.000000000E+00	424	454	831	801
447	1	30.8999605	0.000000000E+00	454	484	861	831
448	1	30.8999605	0.000000000E+00	724	754	1131	1101

449	1	30.8999605	0.000000000E+00	484	514	891	861
450	1	30.8999605	0.000000000E+00	694	724	1101	1071
451	1	30.8999605	0.000000000E+00	514	544	921	891
452	1	30.8999605	0.000000000E+00	544	574	951	921

ELEM	FACE	VALUE(S)		FACE NODES			
453	1	30.8999605	0.000000000E+00	574	604	981	951
454	1	30.8999605	0.000000000E+00	604	634	1011	981
455	1	30.8999605	0.000000000E+00	634	664	1041	1011
456	1	30.8999605	0.000000000E+00	664	694	1071	1041
457	1	30.8999605	0.000000000E+00	801	831	832	802
458	1	30.8999605	0.000000000E+00	831	861	862	832
459	1	30.8999605	0.000000000E+00	802	832	833	803
460	1	30.8999605	0.000000000E+00	832	862	863	833
461	1	30.8999605	0.000000000E+00	861	891	892	862
462	1	30.8999605	0.000000000E+00	862	892	893	863
463	1	30.8999605	0.000000000E+00	803	833	834	804
464	1	30.8999605	0.000000000E+00	833	863	864	834
465	1	30.8999605	0.000000000E+00	863	893	894	864
466	1	30.8999605	0.000000000E+00	891	921	922	892
467	1	30.8999605	0.000000000E+00	892	922	923	893
468	1	30.8999605	0.000000000E+00	893	923	924	894
469	1	30.8999605	0.000000000E+00	804	834	835	805
470	1	30.8999605	0.000000000E+00	834	864	865	835
471	1	30.8999605	0.000000000E+00	864	894	895	865
472	1	30.8999605	0.000000000E+00	894	924	925	895

ELEM	FACE	VALUE(S)		FACE NODES			
473	1	30.8999605	0.000000000E+00	805	835	836	806
474	1	30.8999605	0.000000000E+00	835	865	866	836
475	1	30.8999605	0.000000000E+00	865	895	896	866
476	1	30.8999605	0.000000000E+00	895	925	926	896
477	1	30.8999605	0.000000000E+00	921	951	952	922
478	1	30.8999605	0.000000000E+00	922	952	953	923
479	1	30.8999605	0.000000000E+00	923	953	954	924
480	1	30.8999605	0.000000000E+00	924	954	955	925
481	1	30.8999605	0.000000000E+00	925	955	956	926
482	1	30.8999605	0.000000000E+00	806	836	837	807
483	1	30.8999605	0.000000000E+00	836	866	867	837
484	1	30.8999605	0.000000000E+00	866	896	897	867
485	1	30.8999605	0.000000000E+00	896	926	927	897
486	1	30.8999605	0.000000000E+00	926	956	957	927
487	1	30.8999605	0.000000000E+00	951	981	982	952
488	1	30.8999605	0.000000000E+00	952	982	983	953
489	1	30.8999605	0.000000000E+00	953	983	984	954
490	1	30.8999605	0.000000000E+00	954	984	985	955
491	1	30.8999605	0.000000000E+00	955	985	986	956
492	1	30.8999605	0.000000000E+00	956	986	987	957

ELEM	FACE	VALUE(S)		FACE NODES			
493	1	30.8999605	0.000000000E+00	981	1011	1012	982
494	1	30.8999605	0.000000000E+00	982	1012	1013	983
495	1	30.8999605	0.000000000E+00	983	1013	1014	984
496	1	30.8999605	0.000000000E+00	984	1014	1015	985
497	1	30.8999605	0.000000000E+00	985	1015	1016	986
498	1	30.8999605	0.000000000E+00	986	1016	1017	987
499	1	30.8999605	0.000000000E+00	1016	1046	1047	1017
500	1	30.8999605	0.000000000E+00	1015	1045	1046	1016
501	1	30.8999605	0.000000000E+00	1014	1044	1045	1015
502	1	30.8999605	0.000000000E+00	1013	1043	1044	1014
503	1	30.8999605	0.000000000E+00	1012	1042	1043	1013
504	1	30.8999605	0.000000000E+00	1011	1041	1042	1012
505	1	30.8999605	0.000000000E+00	1046	1076	1077	1047
506	1	30.8999605	0.000000000E+00	1045	1075	1076	1046
507	1	30.8999605	0.000000000E+00	1044	1074	1075	1045
508	1	30.8999605	0.000000000E+00	1043	1073	1074	1044
509	1	30.8999605	0.000000000E+00	1042	1072	1073	1043
510	1	30.8999605	0.000000000E+00	1041	1071	1072	1042
511	1	30.8999605	0.000000000E+00	1076	1106	1107	1077
512	1	30.8999605	0.000000000E+00	1075	1105	1106	1076

ELEM	FACE	VALUE(S)		FACE NODES			
513	1	30.8999605	0.000000000E+00	1074	1104	1105	1075
514	1	30.8999605	0.000000000E+00	1073	1103	1104	1074

515	1	30.8999605	0.000000000E+00	1072	1102	1103	1073
516	1	30.8999605	0.000000000E+00	1071	1101	1102	1072
517	1	30.8999605	0.000000000E+00	1106	1136	1137	1107
518	1	30.8999605	0.000000000E+00	1105	1135	1136	1106
519	1	30.8999605	0.000000000E+00	1104	1134	1135	1105
520	1	30.8999605	0.000000000E+00	1103	1133	1134	1104
521	1	30.8999605	0.000000000E+00	1102	1132	1133	1103
522	1	30.8999605	0.000000000E+00	1101	1131	1132	1102
523	1	30.8999605	0.000000000E+00	1136	1166	1167	1137
524	1	30.8999605	0.000000000E+00	1135	1165	1166	1136
525	1	30.8999605	0.000000000E+00	1134	1164	1165	1135
526	1	30.8999605	0.000000000E+00	1133	1163	1164	1134
527	1	30.8999605	0.000000000E+00	1132	1162	1163	1133
528	1	30.8999605	0.000000000E+00	1131	1161	1162	1132
802	1	30.8999605	0.000000000E+00	1147	1177	818	818
801	1	30.8999605	0.000000000E+00	1117	1147	818	818
800	1	30.8999605	0.000000000E+00	1087	1117	818	818
799	1	30.8999605	0.000000000E+00	1057	1087	818	818

ELEM	FACE	VALUE(S)		FACE NODES			
798	1	30.8999605	0.000000000E+00	1027	1057	818	818
797	1	30.8999605	0.000000000E+00	997	1027	818	818
796	1	30.8999605	0.000000000E+00	967	997	818	818
795	1	30.8999605	0.000000000E+00	937	967	818	818
794	1	30.8999605	0.000000000E+00	907	937	818	818
793	1	30.8999605	0.000000000E+00	877	907	818	818
792	1	30.8999605	0.000000000E+00	847	877	818	818
791	1	30.8999605	0.000000000E+00	817	847	818	818
790	1	30.8999605	0.000000000E+00	1146	1176	1177	1147
789	1	30.8999605	0.000000000E+00	1145	1175	1176	1146
788	1	30.8999605	0.000000000E+00	1144	1174	1175	1145
787	1	30.8999605	0.000000000E+00	1143	1173	1174	1144
786	1	30.8999605	0.000000000E+00	1142	1172	1173	1143
785	1	30.8999605	0.000000000E+00	1141	1171	1172	1142
784	1	30.8999605	0.000000000E+00	1140	1170	1171	1141
783	1	30.8999605	0.000000000E+00	1139	1169	1170	1140
782	1	30.8999605	0.000000000E+00	1138	1168	1169	1139
781	1	30.8999605	0.000000000E+00	1137	1167	1168	1138
780	1	30.8999605	0.000000000E+00	1116	1146	1147	1117
779	1	30.8999605	0.000000000E+00	1115	1145	1146	1116

ELEM	FACE	VALUE(S)		FACE NODES			
778	1	30.8999605	0.000000000E+00	1114	1144	1145	1115
777	1	30.8999605	0.000000000E+00	1113	1143	1144	1114
776	1	30.8999605	0.000000000E+00	1112	1142	1143	1113
775	1	30.8999605	0.000000000E+00	1111	1141	1142	1112
774	1	30.8999605	0.000000000E+00	1110	1140	1141	1111
773	1	30.8999605	0.000000000E+00	1109	1139	1140	1110
772	1	30.8999605	0.000000000E+00	1108	1138	1139	1109
771	1	30.8999605	0.000000000E+00	1107	1137	1138	1108
770	1	30.8999605	0.000000000E+00	1086	1116	1117	1087
769	1	30.8999605	0.000000000E+00	1085	1115	1116	1086
768	1	30.8999605	0.000000000E+00	1084	1114	1115	1085
767	1	30.8999605	0.000000000E+00	1083	1113	1114	1084
766	1	30.8999605	0.000000000E+00	1082	1112	1113	1083
765	1	30.8999605	0.000000000E+00	1081	1111	1112	1082
764	1	30.8999605	0.000000000E+00	1080	1110	1111	1081
763	1	30.8999605	0.000000000E+00	1079	1109	1110	1080
762	1	30.8999605	0.000000000E+00	1078	1108	1109	1079
761	1	30.8999605	0.000000000E+00	1077	1107	1108	1078
760	1	30.8999605	0.000000000E+00	1056	1086	1087	1057
759	1	30.8999605	0.000000000E+00	1055	1085	1086	1056

ELEM	FACE	VALUE(S)		FACE NODES			
758	1	30.8999605	0.000000000E+00	1054	1084	1085	1055
757	1	30.8999605	0.000000000E+00	1053	1083	1084	1054
756	1	30.8999605	0.000000000E+00	1052	1082	1083	1053
755	1	30.8999605	0.000000000E+00	1051	1081	1082	1052
754	1	30.8999605	0.000000000E+00	1050	1080	1081	1051
753	1	30.8999605	0.000000000E+00	1049	1079	1080	1050
752	1	30.8999605	0.000000000E+00	1048	1078	1079	1049
751	1	30.8999605	0.000000000E+00	1047	1077	1078	1048
750	1	30.8999605	0.000000000E+00	1026	1056	1057	1027
749	1	30.8999605	0.000000000E+00	1025	1055	1056	1026

748	1	30.8999605	0.000000000E+00	1024	1054	1055	1025
747	1	30.8999605	0.000000000E+00	1023	1053	1054	1024
746	1	30.8999605	0.000000000E+00	1022	1052	1053	1023
745	1	30.8999605	0.000000000E+00	1021	1051	1052	1022
744	1	30.8999605	0.000000000E+00	1020	1050	1051	1021
743	1	30.8999605	0.000000000E+00	1019	1049	1050	1020
742	1	30.8999605	0.000000000E+00	1018	1048	1049	1019
741	1	30.8999605	0.000000000E+00	1017	1047	1048	1018
740	1	30.8999605	0.000000000E+00	996	1026	1027	997
739	1	30.8999605	0.000000000E+00	995	1025	1026	996

ELEM	FACE	VALUE(S)		FACE NODES			
738	1	30.8999605	0.000000000E+00	994	1024	1025	995
737	1	30.8999605	0.000000000E+00	993	1023	1024	994
736	1	30.8999605	0.000000000E+00	992	1022	1023	993
735	1	30.8999605	0.000000000E+00	991	1021	1022	992
734	1	30.8999605	0.000000000E+00	990	1020	1021	991
733	1	30.8999605	0.000000000E+00	989	1019	1020	990
732	1	30.8999605	0.000000000E+00	988	1018	1019	989
731	1	30.8999605	0.000000000E+00	987	1017	1018	988
730	1	30.8999605	0.000000000E+00	966	996	997	967
729	1	30.8999605	0.000000000E+00	965	995	996	966
728	1	30.8999605	0.000000000E+00	964	994	995	965
727	1	30.8999605	0.000000000E+00	963	993	994	964
726	1	30.8999605	0.000000000E+00	962	992	993	963
725	1	30.8999605	0.000000000E+00	961	991	992	962
724	1	30.8999605	0.000000000E+00	960	990	991	961
723	1	30.8999605	0.000000000E+00	959	989	990	960
722	1	30.8999605	0.000000000E+00	958	988	989	959
721	1	30.8999605	0.000000000E+00	957	987	988	958
720	1	30.8999605	0.000000000E+00	936	966	967	937
719	1	30.8999605	0.000000000E+00	935	965	966	936

ELEM	FACE	VALUE(S)		FACE NODES			
718	1	30.8999605	0.000000000E+00	934	964	965	935
717	1	30.8999605	0.000000000E+00	933	963	964	934
716	1	30.8999605	0.000000000E+00	932	962	963	933
715	1	30.8999605	0.000000000E+00	931	961	962	932
714	1	30.8999605	0.000000000E+00	930	960	961	931
713	1	30.8999605	0.000000000E+00	929	959	960	930
712	1	30.8999605	0.000000000E+00	928	958	959	929
711	1	30.8999605	0.000000000E+00	927	957	958	928
710	1	30.8999605	0.000000000E+00	906	936	937	907
709	1	30.8999605	0.000000000E+00	905	935	936	906
708	1	30.8999605	0.000000000E+00	904	934	935	905
707	1	30.8999605	0.000000000E+00	903	933	934	904
706	1	30.8999605	0.000000000E+00	902	932	933	903
705	1	30.8999605	0.000000000E+00	901	931	932	902
704	1	30.8999605	0.000000000E+00	900	930	931	901
703	1	30.8999605	0.000000000E+00	899	929	930	900
702	1	30.8999605	0.000000000E+00	898	928	929	899
701	1	30.8999605	0.000000000E+00	897	927	928	898
700	1	30.8999605	0.000000000E+00	876	906	907	877
699	1	30.8999605	0.000000000E+00	875	905	906	876

ELEM	FACE	VALUE(S)		FACE NODES			
698	1	30.8999605	0.000000000E+00	874	904	905	875
697	1	30.8999605	0.000000000E+00	873	903	904	874
696	1	30.8999605	0.000000000E+00	872	902	903	873
695	1	30.8999605	0.000000000E+00	871	901	902	872
694	1	30.8999605	0.000000000E+00	870	900	901	871
693	1	30.8999605	0.000000000E+00	869	899	900	870
692	1	30.8999605	0.000000000E+00	868	898	899	869
691	1	30.8999605	0.000000000E+00	867	897	898	868
690	1	30.8999605	0.000000000E+00	846	876	877	847
689	1	30.8999605	0.000000000E+00	845	875	876	846
688	1	30.8999605	0.000000000E+00	844	874	875	845
687	1	30.8999605	0.000000000E+00	843	873	874	844
686	1	30.8999605	0.000000000E+00	842	872	873	843
685	1	30.8999605	0.000000000E+00	841	871	872	842
684	1	30.8999605	0.000000000E+00	840	870	871	841
683	1	30.8999605	0.000000000E+00	839	869	870	840
682	1	30.8999605	0.000000000E+00	838	868	869	839
681	1	30.8999605	0.000000000E+00	837	867	868	838

680	1	30.8999605	0.000000000E+00	816	846	847	817
679	1	30.8999605	0.000000000E+00	815	845	846	816

ELEM	FACE	VALUE($)		FACE NODES			
678	1	30.8999605	0.000000000E+00	814	844	845	815
677	1	30.8999605	0.000000000E+00	813	843	844	814
676	1	30.8999605	0.000000000E+00	812	842	843	813
675	1	30.8999605	0.000000000E+00	811	841	842	812
674	1	30.8999605	0.000000000E+00	810	840	841	811
673	1	30.8999605	0.000000000E+00	809	839	840	810
672	1	30.8999605	0.000000000E+00	808	838	839	809
671	1	30.8999605	0.000000000E+00	807	837	838	808
1	2	30.8999605	0.000000000E+00	391	151	181	390
2	2	30.8999605	0.000000000E+00	390	181	211	396
3	2	30.8999605	0.000000000E+00	392	121	151	391
4	2	30.8999605	0.000000000E+00	396	211	241	397
5	2	30.8999605	0.000000000E+00	121	122	152	151
6	2	30.8999605	0.000000000E+00	151	152	182	181
7	2	30.8999605	0.000000000E+00	181	182	212	211
8	2	30.8999605	0.000000000E+00	211	212	242	241
9	2	30.8999605	0.000000000E+00	393	91	121	392
10	2	30.8999605	0.000000000E+00	91	92	122	121
11	2	30.8999605	0.000000000E+00	397	241	271	398
12	2	30.8999605	0.000000000E+00	241	242	272	271

ELEM	FACE	VALUE($)		FACE NODES			
13	2	30.8999605	0.000000000E+00	92	93	123	122
14	2	30.8999605	0.000000000E+00	122	123	153	152
15	2	30.8999605	0.000000000E+00	152	153	183	182
16	2	30.8999605	0.000000000E+00	182	183	213	212
17	2	30.8999605	0.000000000E+00	212	213	243	242
18	2	30.8999605	0.000000000E+00	242	243	273	272
19	2	30.8999605	0.000000000E+00	394	61	91	393
20	2	30.8999605	0.000000000E+00	61	62	92	91
21	2	30.8999605	0.000000000E+00	62	63	93	92
22	2	30.8999605	0.000000000E+00	398	271	301	399
23	2	30.8999605	0.000000000E+00	271	272	302	301
24	2	30.8999605	0.000000000E+00	272	273	303	302
49	2	30.8999605	0.000000000E+00	395	31	61	394
50	2	30.8999605	0.000000000E+00	31	32	62	61
51	2	30.8999605	0.000000000E+00	32	33	63	62
53	2	30.8999605	0.000000000E+00	399	301	331	400
54	2	30.8999605	0.000000000E+00	301	302	332	331
55	2	30.8999605	0.000000000E+00	302	303	333	332
131	2	30.8999605	0.000000000E+00	395	1	31	31
132	2	30.8999605	0.000000000E+00	1	2	32	31

ELEM	FACE	VALUE($)		FACE NODES			
133	2	30.8999605	0.000000000E+00	2	3	33	32
134	2	30.8999605	0.000000000E+00	400	331	361	361
135	2	30.8999605	0.000000000E+00	331	332	362	361
136	2	30.8999605	0.000000000E+00	332	333	363	362
61	4	30.8999605	0.000000000E+00	38	43	73	68
62	4	30.8999605	0.000000000E+00	68	73	103	98
63	4	30.8999605	0.000000000E+00	98	103	133	128
64	4	30.8999605	0.000000000E+00	128	133	163	158
65	4	30.8999605	0.000000000E+00	158	163	193	188
66	4	30.8999605	0.000000000E+00	188	193	223	218
67	4	30.8999605	0.000000000E+00	218	223	253	248
68	4	30.8999605	0.000000000E+00	248	253	283	278
69	4	30.8999605	0.000000000E+00	278	283	313	308
70	4	30.8999605	0.000000000E+00	308	313	343	338
71	4	30.8999605	0.000000000E+00	43	49	79	73
72	4	30.8999605	0.000000000E+00	73	79	109	103
73	4	30.8999605	0.000000000E+00	103	109	139	133
74	4	30.8999605	0.000000000E+00	133	139	169	163
75	4	30.8999605	0.000000000E+00	163	169	199	193
76	4	30.8999605	0.000000000E+00	193	199	229	223

ELEM	FACE	VALUE($)		FACE NODES			
77	4	30.8999605	0.000000000E+00	223	229	259	253
78	4	30.8999605	0.000000000E+00	253	259	289	283
79	4	30.8999605	0.000000000E+00	283	289	319	313
80	4	30.8999605	0.000000000E+00	313	319	349	343

139	4	30.8999605	0.000000000E+00	343	349	379	373
140	4	30.8999605	0.000000000E+00	338	343	373	368
148	4	30.8999605	0.000000000E+00	13	19	49	43
149	4	30.8999605	0.000000000E+00	8	13	43	38
71	3	30.8999605	0.000000000E+00	49	48	78	79
72	3	30.8999605	0.000000000E+00	79	78	108	109
73	3	30.8999605	0.000000000E+00	109	108	138	139
74	3	30.8999605	0.000000000E+00	139	138	168	169
75	3	30.8999605	0.000000000E+00	169	168	198	199
76	3	30.8999605	0.000000000E+00	199	198	228	229
77	3	30.8999605	0.000000000E+00	229	228	258	259
78	3	30.8999605	0.000000000E+00	259	258	288	289
79	3	30.8999605	0.000000000E+00	289	288	318	319
80	3	30.8999605	0.000000000E+00	319	318	348	349
443	5	30.8999605	0.000000000E+00	751	752	782	781
442	5	30.8999605	0.000000000E+00	721	722	752	751

ELEM	FACE	VALUE($)		FACE NODES			
440	5	30.8999605	0.000000000E+00	691	692	722	721
438	5	30.8999605	0.000000000E+00	661	662	692	691
436	5	30.8999605	0.000000000E+00	631	632	662	661
434	5	30.8999605	0.000000000E+00	601	602	632	631
432	5	30.8999605	0.000000000E+00	571	572	602	601
430	5	30.8999605	0.000000000E+00	541	542	572	571
428	5	30.8999605	0.000000000E+00	511	512	542	541
426	5	30.8999605	0.000000000E+00	481	482	512	511
139	3	30.8999605	0.000000000E+00	349	348	378	379
424	5	30.8999605	0.000000000E+00	451	452	482	481
148	3	30.8999605	0.000000000E+00	19	18	48	49
422	5	30.8999605	0.000000000E+00	421	422	452	451
315	5	30.8999605	0.000000000E+00	409	413	443	439
318	5	30.8999605	0.000000000E+00	439	443	473	469
321	5	30.8999605	0.000000000E+00	469	473	503	499
324	5	30.8999605	0.000000000E+00	499	503	533	529
327	5	30.8999605	0.000000000E+00	529	533	563	559
330	5	30.8999605	0.000000000E+00	559	563	593	589
333	5	30.8999605	0.000000000E+00	589	593	623	619
336	5	30.8999605	0.000000000E+00	619	623	653	649

ELEM	FACE	VALUE($)		FACE NODES			
339	5	30.8999605	0.000000000E+00	649	653	683	679
342	5	30.8999605	0.000000000E+00	679	683	713	709
347	5	30.8999605	0.000000000E+00	709	713	743	739
348	5	30.8999605	0.000000000E+00	739	743	773	769
351	5	30.8999605	0.000000000E+00	413	417	447	443
354	5	30.8999605	0.000000000E+00	443	447	477	473
357	5	30.8999605	0.000000000E+00	473	477	507	503
360	5	30.8999605	0.000000000E+00	503	507	537	533
363	5	30.8999605	0.000000000E+00	533	537	567	563
366	5	30.8999605	0.000000000E+00	563	567	597	593
369	5	30.8999605	0.000000000E+00	593	597	627	623
372	5	30.8999605	0.000000000E+00	623	627	657	653
375	5	30.8999605	0.000000000E+00	653	657	687	683
378	5	30.8999605	0.000000000E+00	683	687	717	713
383	5	30.8999605	0.000000000E+00	713	717	747	743
384	5	30.8999605	0.000000000E+00	743	747	777	773
289	5	30.8999908	0.000000000E+00	401	405	435	431
290	5	30.8999908	0.000000000E+00	431	435	465	461
291	5	30.8999908	0.000000000E+00	405	409	439	435
292	5	30.8999908	0.000000000E+00	435	439	469	465

ELEM	FACE	VALUE($)		FACE NODES			
293	5	30.8999908	0.000000000E+00	461	465	495	491
294	5	30.8999908	0.000000000E+00	465	469	499	495
295	5	30.8999908	0.000000000E+00	491	495	525	521
296	5	30.8999908	0.000000000E+00	495	499	529	525
297	5	30.8999908	0.000000000E+00	521	525	555	551
298	5	30.8999908	0.000000000E+00	525	529	559	555
299	5	30.8999908	0.000000000E+00	551	555	585	581
300	5	30.8999908	0.000000000E+00	555	559	589	585
301	5	30.8999908	0.000000000E+00	581	585	615	611
302	5	30.8999908	0.000000000E+00	585	589	619	615
303	5	30.8999908	0.000000000E+00	611	615	645	641
304	5	30.8999908	0.000000000E+00	615	619	649	645

305	5	30.8999908	0.000000000E+00	641	645	675	671
306	5	30.8999908	0.000000000E+00	645	649	679	675
307	5	30.8999908	0.000000000E+00	671	675	705	701
308	5	30.8999908	0.000000000E+00	675	679	709	705
309	5	30.8999908	0.000000000E+00	701	705	735	731
310	5	30.8999908	0.000000000E+00	731	735	765	761
311	5	30.8999908	0.000000000E+00	705	709	739	735
312	5	30.8999908	0.000000000E+00	735	739	769	765

ELEM	FACE	VALUE(S)		FACE NODES			
81	3	30.8999908	0.000000000E+00	318	317	347	348
82	3	30.8999908	0.000000000E+00	288	287	317	318
83	3	30.8999908	0.000000000E+00	258	257	287	288
84	3	30.8999908	0.000000000E+00	228	227	257	258
85	3	30.8999908	0.000000000E+00	198	197	227	228
86	3	30.8999908	0.000000000E+00	168	167	197	198
87	3	30.8999908	0.000000000E+00	138	137	167	168
88	3	30.8999908	0.000000000E+00	108	107	137	138
89	3	30.8999908	0.000000000E+00	78	77	107	108
90	3	30.8999908	0.000000000E+00	48	47	77	78
91	3	30.8999908	0.000000000E+00	47	46	76	77
92	3	30.8999908	0.000000000E+00	77	76	106	107
93	3	30.8999908	0.000000000E+00	107	106	136	137
94	3	30.8999908	0.000000000E+00	137	136	166	167
95	3	30.8999908	0.000000000E+00	167	166	196	197
96	3	30.8999908	0.000000000E+00	197	196	226	227
97	3	30.8999908	0.000000000E+00	227	226	256	257
98	3	30.8999908	0.000000000E+00	257	256	286	287
99	3	30.8999908	0.000000000E+00	287	286	316	317
100	3	30.8999908	0.000000000E+00	317	316	346	347

ELEM	FACE	VALUE(S)		FACE NODES			
142	3	30.8999908	0.000000000E+00	348	347	377	378
143	3	30.8999908	0.000000000E+00	347	346	376	377
151	3	30.8999908	0.000000000E+00	18	17	47	48
152	3	30.8999908	0.000000000E+00	17	16	46	47

LIST ELEMENT CONVECTIONS FOR ALL SELECTED ELEMENTS

LIST TEMPERATURES FOR ALL SELECTED NODES

NODE	TEMPERATURE	FLUENCE
1	206.84	0.00000E+00
2	210.48	0.00000E+00
3	214.11	0.00000E+00
4	214.11	0.00000E+00
5	214.11	0.00000E+00
7	214.11	0.00000E+00
8	214.11	0.00000E+00
9	220.42	0.00000E+00
10	220.42	0.00000E+00
11	220.42	0.00000E+00
12	220.42	0.00000E+00
13	220.42	0.00000E+00
14	220.42	0.00000E+00
15	220.42	0.00000E+00
16	220.42	0.00000E+00
17	220.42	0.00000E+00
18	220.42	0.00000E+00
19	220.42	0.00000E+00
20	220.42	0.00000E+00
21	220.42	0.00000E+00

NODE	TEMPERATURE	FLUENCE
22	220.42	0.00000E+00
23	220.42	0.00000E+00
24	220.42	0.00000E+00
25	220.42	0.00000E+00
26	220.42	0.00000E+00
27	220.42	0.00000E+00
28	220.42	0.00000E+00
31	206.56	0.00000E+00
32	209.50	0.00000E+00
33	212.44	0.00000E+00

34	212.44	0.00000E+00
35	212.44	0.00000E+00
37	212.44	0.00000E+00
38	212.44	0.00000E+00
39	219.57	0.00000E+00
40	219.57	0.00000E+00
41	219.57	0.00000E+00
42	219.57	0.00000E+00
43	219.57	0.00000E+00
44	219.57	0.00000E+00

NODE	TEMPERATURE	FLUENCE
45	219.57	0.00000E+00
46	219.57	0.00000E+00
47	219.57	0.00000E+00
48	219.57	0.00000E+00
49	219.57	0.00000E+00
50	219.57	0.00000E+00
51	219.57	0.00000E+00
52	219.57	0.00000E+00
53	219.57	0.00000E+00
54	219.57	0.00000E+00
55	219.57	0.00000E+00
56	219.57	0.00000E+00
57	219.57	0.00000E+00
58	219.57	0.00000E+00
61	206.28	0.00000E+00
62	208.52	0.00000E+00
63	210.77	0.00000E+00
64	210.77	0.00000E+00
65	210.77	0.00000E+00
67	210.77	0.00000E+00

NODE	TEMPERATURE	FLUENCE
68	210.77	0.00000E+00
69	218.71	0.00000E+00
70	218.71	0.00000E+00
71	218.71	0.00000E+00
72	218.71	0.00000E+00
73	218.71	0.00000E+00
74	218.71	0.00000E+00
75	218.71	0.00000E+00
76	218.71	0.00000E+00
77	218.71	0.00000E+00
78	218.71	0.00000E+00
79	218.71	0.00000E+00
80	218.71	0.00000E+00
81	218.71	0.00000E+00
82	218.71	0.00000E+00
83	218.71	0.00000E+00
84	218.71	0.00000E+00
85	218.71	0.00000E+00
86	218.71	0.00000E+00
87	218.71	0.00000E+00

NODE	TEMPERATURE	FLUENCE
88	218.71	0.00000E+00
91	205.99	0.00000E+00
92	207.55	0.00000E+00
93	209.10	0.00000E+00
94	209.10	0.00000E+00
95	209.10	0.00000E+00
97	209.10	0.00000E+00
98	209.10	0.00000E+00
99	217.85	0.00000E+00
100	217.85	0.00000E+00
101	217.85	0.00000E+00
102	217.85	0.00000E+00
103	217.85	0.00000E+00
104	217.85	0.00000E+00
105	217.85	0.00000E+00
106	217.85	0.00000E+00
107	217.85	0.00000E+00
108	217.85	0.00000E+00

109	217.85	0.00000E+00
110	217.85	0.00000E+00

NODE	TEMPERATURE	FLUENCE
111	217.85	0.00000E+00
112	217.85	0.00000E+00
113	217.85	0.00000E+00
114	217.85	0.00000E+00
115	217.85	0.00000E+00
116	217.85	0.00000E+00
117	217.85	0.00000E+00
118	217.85	0.00000E+00
121	205.95	0.00000E+00
122	207.49	0.00000E+00
123	209.04	0.00000E+00
124	209.04	0.00000E+00
125	209.04	0.00000E+00
127	209.04	0.00000E+00
128	209.04	0.00000E+00
129	217.81	0.00000E+00
130	217.81	0.00000E+00
131	217.81	0.00000E+00
132	217.81	0.00000E+00
133	217.81	0.00000E+00

NODE	TEMPERATURE	FLUENCE
134	217.81	0.00000E+00
135	217.81	0.00000E+00
136	217.81	0.00000E+00
137	217.81	0.00000E+00
138	217.81	0.00000E+00
139	217.81	0.00000E+00
140	217.81	0.00000E+00
141	217.81	0.00000E+00
142	217.81	0.00000E+00
143	217.81	0.00000E+00
144	217.81	0.00000E+00
145	217.81	0.00000E+00
146	217.81	0.00000E+00
147	217.81	0.00000E+00
148	217.81	0.00000E+00
151	205.91	0.00000E+00
152	207.44	0.00000E+00
153	208.98	0.00000E+00
154	208.98	0.00000E+00
155	208.98	0.00000E+00

NODE	TEMPERATURE	FLUENCE
157	208.98	0.00000E+00
158	208.98	0.00000E+00
159	217.76	0.00000E+00
160	217.76	0.00000E+00
161	217.76	0.00000E+00
162	217.76	0.00000E+00
163	217.76	0.00000E+00
164	217.76	0.00000E+00
165	217.76	0.00000E+00
166	217.76	0.00000E+00
167	217.76	0.00000E+00
168	217.76	0.00000E+00
169	217.76	0.00000E+00
170	217.76	0.00000E+00
171	217.76	0.00000E+00
172	217.76	0.00000E+00
173	217.76	0.00000E+00
174	217.76	0.00000E+00
175	217.76	0.00000E+00
176	217.76	0.00000E+00

NODE	TEMPERATURE	FLUENCE
177	217.76	0.00000E+00
178	217.76	0.00000E+00
181	205.86	0.00000E+00
182	207.39	0.00000E+00

183	208.92	0.00000E+00
184	208.92	0.00000E+00
185	208.92	0.00000E+00
187	208.92	0.00000E+00
188	208.92	0.00000E+00
189	217.72	0.00000E+00
190	217.72	0.00000E+00
191	217.72	0.00000E+00
192	217.72	0.00000E+00
193	217.72	0.00000E+00
194	217.72	0.00000E+00
195	217.72	0.00000E+00
196	217.72	0.00000E+00
197	217.72	0.00000E+00
198	217.72	0.00000E+00
199	217.72	0.00000E+00

NODE	TEMPERATURE	FLUENCE
200	217.72	0.00000E+00
201	217.72	0.00000E+00
202	217.72	0.00000E+00
203	217.72	0.00000E+00
204	217.72	0.00000E+00
205	217.72	0.00000E+00
206	217.72	0.00000E+00
207	217.72	0.00000E+00
208	217.72	0.00000E+00
211	205.82	0.00000E+00
212	207.34	0.00000E+00
213	208.87	0.00000E+00
214	208.87	0.00000E+00
215	208.87	0.00000E+00
217	208.87	0.00000E+00
218	208.87	0.00000E+00
219	217.67	0.00000E+00
220	217.67	0.00000E+00
221	217.67	0.00000E+00
222	217.67	0.00000E+00

NODE	TEMPERATURE	FLUENCE
223	217.67	0.00000E+00
224	217.67	0.00000E+00
225	217.67	0.00000E+00
226	217.67	0.00000E+00
227	217.67	0.00000E+00
228	217.67	0.00000E+00
229	217.67	0.00000E+00
230	217.67	0.00000E+00
231	217.67	0.00000E+00
232	217.67	0.00000E+00
233	217.67	0.00000E+00
234	217.67	0.00000E+00
235	217.67	0.00000E+00
236	217.67	0.00000E+00
237	217.67	0.00000E+00
238	217.67	0.00000E+00
241	205.81	0.00000E+00
242	207.33	0.00000E+00
243	208.86	0.00000E+00
244	208.86	0.00000E+00

NODE	TEMPERATURE	FLUENCE
245	208.86	0.00000E+00
247	208.86	0.00000E+00
248	208.86	0.00000E+00
249	217.67	0.00000E+00
250	217.67	0.00000E+00
251	217.67	0.00000E+00
252	217.67	0.00000E+00
253	217.67	0.00000E+00
254	217.67	0.00000E+00
255	217.67	0.00000E+00
256	217.67	0.00000E+00
257	217.67	0.00000E+00

258	217.67	0.00000E+00
259	217.67	0.00000E+00
260	217.67	0.00000E+00
261	217.67	0.00000E+00
262	217.67	0.00000E+00
263	217.67	0.00000E+00
264	217.67	0.00000E+00
265	217.67	0.00000E+00

NODE	TEMPERATURE	FLUENCE
266	217.67	0.00000E+00
267	217.67	0.00000E+00
268	217.67	0.00000E+00
271	205.81	0.00000E+00
272	207.33	0.00000E+00
273	208.85	0.00000E+00
274	208.85	0.00000E+00
275	208.85	0.00000E+00
277	208.85	0.00000E+00
278	208.85	0.00000E+00
279	217.67	0.00000E+00
280	217.67	0.00000E+00
281	217.67	0.00000E+00
282	217.67	0.00000E+00
283	217.67	0.00000E+00
284	217.67	0.00000E+00
285	217.67	0.00000E+00
286	217.67	0.00000E+00
287	217.67	0.00000E+00
288	217.67	0.00000E+00

NODE	TEMPERATURE	FLUENCE
289	217.67	0.00000E+00
290	217.67	0.00000E+00
291	217.67	0.00000E+00
292	217.67	0.00000E+00
293	217.67	0.00000E+00
294	217.67	0.00000E+00
295	217.67	0.00000E+00
296	217.67	0.00000E+00
297	217.67	0.00000E+00
298	217.67	0.00000E+00
301	205.80	0.00000E+00
302	207.32	0.00000E+00
303	208.84	0.00000E+00
304	208.84	0.00000E+00
305	208.84	0.00000E+00
307	208.84	0.00000E+00
308	208.84	0.00000E+00
309	217.67	0.00000E+00
310	217.67	0.00000E+00
311	217.67	0.00000E+00

NODE	TEMPERATURE	FLUENCE
312	217.67	0.00000E+00
313	217.67	0.00000E+00
314	217.67	0.00000E+00
315	217.67	0.00000E+00
316	217.67	0.00000E+00
317	217.67	0.00000E+00
318	217.67	0.00000E+00
319	217.67	0.00000E+00
320	217.67	0.00000E+00
321	217.67	0.00000E+00
322	217.67	0.00000E+00
323	217.67	0.00000E+00
324	217.67	0.00000E+00
325	217.67	0.00000E+00
326	217.67	0.00000E+00
327	217.67	0.00000E+00
328	217.67	0.00000E+00
331	205.79	0.00000E+00
332	207.31	0.00000E+00
333	208.83	0.00000E+00

NODE	TEMPERATURE	FLUENCE
334	208.83	0.00000E+00
335	208.83	0.00000E+00
337	208.83	0.00000E+00
338	208.83	0.00000E+00
339	217.67	0.00000E+00
340	217.67	0.00000E+00
341	217.67	0.00000E+00
342	217.67	0.00000E+00
343	217.67	0.00000E+00
344	217.67	0.00000E+00
345	217.67	0.00000E+00
346	217.67	0.00000E+00
347	217.67	0.00000E+00
348	217.67	0.00000E+00
349	217.67	0.00000E+00
350	217.67	0.00000E+00
351	217.67	0.00000E+00
352	217.67	0.00000E+00
353	217.67	0.00000E+00
354	217.67	0.00000E+00

NODE	TEMPERATURE	FLUENCE
355	217.67	0.00000E+00
356	217.67	0.00000E+00
357	217.67	0.00000E+00
358	217.67	0.00000E+00
361	205.79	0.00000E+00
362	207.30	0.00000E+00
363	208.82	0.00000E+00
364	208.82	0.00000E+00
365	208.82	0.00000E+00
367	208.82	0.00000E+00
368	208.82	0.00000E+00
369	217.67	0.00000E+00
370	217.67	0.00000E+00
371	217.67	0.00000E+00
372	217.67	0.00000E+00
373	217.67	0.00000E+00
374	217.67	0.00000E+00
375	217.67	0.00000E+00
376	217.67	0.00000E+00
377	217.67	0.00000E+00

NODE	TEMPERATURE	FLUENCE
378	217.67	0.00000E+00
379	217.67	0.00000E+00
380	217.67	0.00000E+00
381	217.67	0.00000E+00
382	217.67	0.00000E+00
383	217.67	0.00000E+00
384	217.67	0.00000E+00
385	217.67	0.00000E+00
386	217.67	0.00000E+00
387	217.67	0.00000E+00
388	217.67	0.00000E+00
390	206.31	0.00000E+00
391	206.31	0.00000E+00
392	206.31	0.00000E+00
393	206.31	0.00000E+00
394	206.31	0.00000E+00
395	206.31	0.00000E+00
396	206.31	0.00000E+00
397	206.31	0.00000E+00
398	206.31	0.00000E+00

NODE	TEMPERATURE	FLUENCE
399	206.31	0.00000E+00
400	206.31	0.00000E+00
401	251.76	0.00000E+00
402	251.76	0.00000E+00
403	251.76	0.00000E+00
404	251.76	0.00000E+00

405	251.76	0.00000E+00
406	251.76	0.00000E+00
407	251.76	0.00000E+00
408	251.76	0.00000E+00
409	251.76	0.00000E+00
410	251.76	0.00000E+00
411	251.76	0.00000E+00
412	251.76	0.00000E+00
413	251.76	0.00000E+00
414	251.76	0.00000E+00
415	251.76	0.00000E+00
416	251.76	0.00000E+00
417	251.76	0.00000E+00
418	251.76	0.00000E+00

NODE	TEMPERATURE	FLUENCE
419	251.76	0.00000E+00
420	251.76	0.00000E+00
421	251.76	0.00000E+00
422	345.70	0.00000E+00
423	345.70	0.00000E+00
424	345.70	0.00000E+00
425	345.70	0.00000E+00
426	345.70	0.00000E+00
431	251.30	0.00000E+00
432	251.30	0.00000E+00
433	251.30	0.00000E+00
434	251.30	0.00000E+00
435	251.30	0.00000E+00
436	251.30	0.00000E+00
437	251.30	0.00000E+00
438	251.30	0.00000E+00
439	251.30	0.00000E+00
440	251.30	0.00000E+00
441	251.30	0.00000E+00
442	251.30	0.00000E+00

NODE	TEMPERATURE	FLUENCE
443	251.30	0.00000E+00
444	251.30	0.00000E+00
445	251.30	0.00000E+00
446	251.30	0.00000E+00
447	251.30	0.00000E+00
448	251.30	0.00000E+00
449	251.30	0.00000E+00
450	251.30	0.00000E+00
451	251.30	0.00000E+00
452	346.61	0.00000E+00
453	346.61	0.00000E+00
454	346.61	0.00000E+00
455	346.61	0.00000E+00
456	346.61	0.00000E+00
461	250.84	0.00000E+00
462	250.84	0.00000E+00
463	250.84	0.00000E+00
464	250.84	0.00000E+00
465	250.84	0.00000E+00
466	250.84	0.00000E+00

NODE	TEMPERATURE	FLUENCE
467	250.84	0.00000E+00
468	250.84	0.00000E+00
469	250.84	0.00000E+00
470	250.84	0.00000E+00
471	250.84	0.00000E+00
472	250.84	0.00000E+00
473	250.84	0.00000E+00
474	250.84	0.00000E+00
475	250.84	0.00000E+00
476	250.84	0.00000E+00
477	250.84	0.00000E+00
478	250.84	0.00000E+00
479	250.84	0.00000E+00
480	250.84	0.00000E+00

481	250.84	0.00000E+00
482	347.52	0.00000E+00
483	347.52	0.00000E+00
484	347.52	0.00000E+00
485	347.52	0.00000E+00
486	347.52	0.00000E+00

NODE	TEMPERATURE	FLUENCE
491	250.38	0.00000E+00
492	250.38	0.00000E+00
493	250.38	0.00000E+00
494	250.38	0.00000E+00
495	250.38	0.00000E+00
496	250.38	0.00000E+00
497	250.38	0.00000E+00
498	250.38	0.00000E+00
499	250.38	0.00000E+00
500	250.38	0.00000E+00
501	250.38	0.00000E+00
502	250.38	0.00000E+00
503	250.38	0.00000E+00
504	250.38	0.00000E+00
505	250.38	0.00000E+00
506	250.38	0.00000E+00
507	250.38	0.00000E+00
508	250.38	0.00000E+00
509	250.38	0.00000E+00
510	250.38	0.00000E+00

NODE	TEMPERATURE	FLUENCE
511	250.38	0.00000E+00
512	348.43	0.00000E+00
513	348.43	0.00000E+00
514	348.43	0.00000E+00
515	348.43	0.00000E+00
516	348.43	0.00000E+00
521	250.32	0.00000E+00
522	250.32	0.00000E+00
523	250.32	0.00000E+00
524	250.32	0.00000E+00
525	250.32	0.00000E+00
526	250.32	0.00000E+00
527	250.32	0.00000E+00
528	250.32	0.00000E+00
529	250.32	0.00000E+00
530	250.32	0.00000E+00
531	250.32	0.00000E+00
532	250.32	0.00000E+00
533	250.32	0.00000E+00
534	250.32	0.00000E+00

NODE	TEMPERATURE	FLUENCE
535	250.32	0.00000E+00
536	250.32	0.00000E+00
537	250.32	0.00000E+00
538	250.32	0.00000E+00
539	250.32	0.00000E+00
540	250.32	0.00000E+00
541	250.32	0.00000E+00
542	348.28	0.00000E+00
543	348.28	0.00000E+00
544	348.28	0.00000E+00
545	348.28	0.00000E+00
546	348.28	0.00000E+00
551	250.27	0.00000E+00
552	250.27	0.00000E+00
553	250.27	0.00000E+00
554	250.27	0.00000E+00
555	250.27	0.00000E+00
556	250.27	0.00000E+00
557	250.27	0.00000E+00
558	250.27	0.00000E+00

NODE	TEMPERATURE	FLUENCE

559	250.27	0.00000E+00
560	250.27	0.00000E+00
561	250.27	0.00000E+00
562	250.27	0.00000E+00
563	250.27	0.00000E+00
564	250.27	0.00000E+00
565	250.27	0.00000E+00
566	250.27	0.00000E+00
567	250.27	0.00000E+00
568	250.27	0.00000E+00
569	250.27	0.00000E+00
570	250.27	0.00000E+00
571	250.27	0.00000E+00
572	348.13	0.00000E+00
573	348.13	0.00000E+00
574	348.13	0.00000E+00
575	348.13	0.00000E+00
576	348.13	0.00000E+00
581	250.21	0.00000E+00
582	250.21	0.00000E+00

NODE	TEMPERATURE	FLUENCE
583	250.21	0.00000E+00
584	250.21	0.00000E+00
585	250.21	0.00000E+00
586	250.21	0.00000E+00
587	250.21	0.00000E+00
588	250.21	0.00000E+00
589	250.21	0.00000E+00
590	250.21	0.00000E+00
591	250.21	0.00000E+00
592	250.21	0.00000E+00
593	250.21	0.00000E+00
594	250.21	0.00000E+00
595	250.21	0.00000E+00
596	250.21	0.00000E+00
597	250.21	0.00000E+00
598	250.21	0.00000E+00
599	250.21	0.00000E+00
600	250.21	0.00000E+00
601	250.21	0.00000E+00
602	347.98	0.00000E+00

NODE	TEMPERATURE	FLUENCE
603	347.98	0.00000E+00
604	347.98	0.00000E+00
605	347.98	0.00000E+00
606	347.98	0.00000E+00
611	250.15	0.00000E+00
612	250.15	0.00000E+00
613	250.15	0.00000E+00
614	250.15	0.00000E+00
615	250.15	0.00000E+00
616	250.15	0.00000E+00
617	250.15	0.00000E+00
618	250.15	0.00000E+00
619	250.15	0.00000E+00
620	250.15	0.00000E+00
621	250.15	0.00000E+00
622	250.15	0.00000E+00
623	250.15	0.00000E+00
624	250.15	0.00000E+00
625	250.15	0.00000E+00
626	250.15	0.00000E+00

NODE	TEMPERATURE	FLUENCE
627	250.15	0.00000E+00
628	250.15	0.00000E+00
629	250.15	0.00000E+00
630	250.15	0.00000E+00
631	250.15	0.00000E+00
632	347.83	0.00000E+00
633	347.83	0.00000E+00
634	347.83	0.00000E+00

635	347.83	0.00000E+00
636	347.83	0.00000E+00
641	250.16	0.00000E+00
642	250.16	0.00000E+00
643	250.16	0.00000E+00
644	250.16	0.00000E+00
645	250.16	0.00000E+00
646	250.16	0.00000E+00
647	250.16	0.00000E+00
648	250.16	0.00000E+00
649	250.16	0.00000E+00
650	250.16	0.00000E+00

NODE	TEMPERATURE	FLUENCE
651	250.16	0.00000E+00
652	250.16	0.00000E+00
653	250.16	0.00000E+00
654	250.16	0.00000E+00
655	250.16	0.00000E+00
656	250.16	0.00000E+00
657	250.16	0.00000E+00
658	250.16	0.00000E+00
659	250.16	0.00000E+00
660	250.16	0.00000E+00
661	250.16	0.00000E+00
662	347.88	0.00000E+00
663	347.88	0.00000E+00
664	347.88	0.00000E+00
665	347.88	0.00000E+00
666	347.88	0.00000E+00
671	250.17	0.00000E+00
672	250.17	0.00000E+00
673	250.17	0.00000E+00
674	250.17	0.00000E+00

NODE	TEMPERATURE	FLUENCE
675	250.17	0.00000E+00
676	250.17	0.00000E+00
677	250.17	0.00000E+00
678	250.17	0.00000E+00
679	250.17	0.00000E+00
680	250.17	0.00000E+00
681	250.17	0.00000E+00
682	250.17	0.00000E+00
683	250.17	0.00000E+00
684	250.17	0.00000E+00
685	250.17	0.00000E+00
686	250.17	0.00000E+00
687	250.17	0.00000E+00
688	250.17	0.00000E+00
689	250.17	0.00000E+00
690	250.17	0.00000E+00
691	250.17	0.00000E+00
692	347.93	0.00000E+00
693	347.93	0.00000E+00
694	347.93	0.00000E+00

NODE	TEMPERATURE	FLUENCE
695	347.93	0.00000E+00
696	347.93	0.00000E+00
701	250.19	0.00000E+00
702	250.19	0.00000E+00
703	250.19	0.00000E+00
704	250.19	0.00000E+00
705	250.19	0.00000E+00
706	250.19	0.00000E+00
707	250.19	0.00000E+00
708	250.19	0.00000E+00
709	250.19	0.00000E+00
710	250.19	0.00000E+00
711	250.19	0.00000E+00
712	250.19	0.00000E+00
713	250.19	0.00000E+00
714	250.19	0.00000E+00

715	250.19	0.00000E+00
716	250.19	0.00000E+00
717	250.19	0.00000E+00
718	250.19	0.00000E+00

NODE	TEMPERATURE	FLUENCE
719	250.19	0.00000E+00
720	250.19	0.00000E+00
721	250.19	0.00000E+00
722	347.98	0.00000E+00
723	347.98	0.00000E+00
724	347.98	0.00000E+00
725	347.98	0.00000E+00
726	347.98	0.00000E+00
731	250.20	0.00000E+00
732	250.20	0.00000E+00
733	250.20	0.00000E+00
734	250.20	0.00000E+00
735	250.20	0.00000E+00
736	250.20	0.00000E+00
737	250.20	0.00000E+00
738	250.20	0.00000E+00
739	250.20	0.00000E+00
740	250.20	0.00000E+00
741	250.20	0.00000E+00
742	250.20	0.00000E+00

NODE	TEMPERATURE	FLUENCE
743	250.20	0.00000E+00
744	250.20	0.00000E+00
745	250.20	0.00000E+00
746	250.20	0.00000E+00
747	250.20	0.00000E+00
748	250.20	0.00000E+00
749	250.20	0.00000E+00
750	250.20	0.00000E+00
751	250.20	0.00000E+00
752	348.03	0.00000E+00
753	348.03	0.00000E+00
754	348.03	0.00000E+00
755	348.03	0.00000E+00
756	348.03	0.00000E+00
761	250.21	0.00000E+00
762	250.21	0.00000E+00
763	250.21	0.00000E+00
764	250.21	0.00000E+00
765	250.21	0.00000E+00
766	250.21	0.00000E+00

NODE	TEMPERATURE	FLUENCE
767	250.21	0.00000E+00
768	250.21	0.00000E+00
769	250.21	0.00000E+00
770	250.21	0.00000E+00
771	250.21	0.00000E+00
772	250.21	0.00000E+00
773	250.21	0.00000E+00
774	250.21	0.00000E+00
775	250.21	0.00000E+00
776	250.21	0.00000E+00
777	250.21	0.00000E+00
778	250.21	0.00000E+00
779	250.21	0.00000E+00
780	250.21	0.00000E+00
781	250.21	0.00000E+00
782	348.09	0.00000E+00
783	348.09	0.00000E+00
784	348.09	0.00000E+00
785	348.09	0.00000E+00
786	348.09	0.00000E+00

NODE	TEMPERATURE	FLUENCE
801	439.65	0.00000E+00
802	571.63	0.00000E+00

803	703.60	0.00000E+00
804	734.41	0.00000E+00
805	765.22	0.00000E+00
806	793.93	0.00000E+00
807	812.97	0.00000E+00
808	812.97	0.00000E+00
809	992.32	0.00000E+00
810	992.32	0.00000E+00
811	992.32	0.00000E+00
812	992.32	0.00000E+00
813	992.32	0.00000E+00
814	992.32	0.00000E+00
815	997.75	0.00000E+00
816	997.75	0.00000E+00
817	997.75	0.00000E+00
818	997.75	0.00000E+00
831	441.92	0.00000E+00
832	573.06	0.00000E+00

NODE	TEMPERATURE	FLUENCE
833	704.20	0.00000E+00
834	735.61	0.00000E+00
835	767.01	0.00000E+00
836	794.43	0.00000E+00
837	813.31	0.00000E+00
838	813.31	0.00000E+00
839	992.26	0.00000E+00
840	992.26	0.00000E+00
841	992.26	0.00000E+00
842	992.26	0.00000E+00
843	992.26	0.00000E+00
844	992.26	0.00000E+00
845	997.45	0.00000E+00
846	997.45	0.00000E+00
847	997.45	0.00000E+00
861	444.20	0.00000E+00
862	574.50	0.00000E+00
863	704.81	0.00000E+00
864	736.80	0.00000E+00
865	768.80	0.00000E+00

NODE	TEMPERATURE	FLUENCE
866	794.94	0.00000E+00
867	813.64	0.00000E+00
868	813.64	0.00000E+00
869	992.19	0.00000E+00
870	992.19	0.00000E+00
871	992.19	0.00000E+00
872	992.19	0.00000E+00
873	992.19	0.00000E+00
874	992.19	0.00000E+00
875	997.15	0.00000E+00
876	997.15	0.00000E+00
877	997.15	0.00000E+00
891	446.47	0.00000E+00
892	575.94	0.00000E+00
893	705.41	0.00000E+00
894	738.00	0.00000E+00
895	770.59	0.00000E+00
896	795.44	0.00000E+00
897	813.98	0.00000E+00
898	813.98	0.00000E+00

NODE	TEMPERATURE	FLUENCE
899	992.13	0.00000E+00
900	992.13	0.00000E+00
901	992.13	0.00000E+00
902	992.13	0.00000E+00
903	992.13	0.00000E+00
904	992.13	0.00000E+00
905	996.85	0.00000E+00
906	996.85	0.00000E+00
907	996.85	0.00000E+00
921	446.23	0.00000E+00

922	575.36	0.00000E+00
923	704.49	0.00000E+00
924	735.36	0.00000E+00
925	766.24	0.00000E+00
926	796.21	0.00000E+00
927	816.40	0.00000E+00
928	816.40	0.00000E+00
929	983.28	0.00000E+00
930	983.28	0.00000E+00
931	983.28	0.00000E+00

NODE	TEMPERATURE	FLUENCE
932	983.28	0.00000E+00
933	983.28	0.00000E+00
934	983.28	0.00000E+00
935	991.51	0.00000E+00
936	991.51	0.00000E+00
937	991.51	0.00000E+00
951	445.99	0.00000E+00
952	574.78	0.00000E+00
953	703.57	0.00000E+00
954	732.73	0.00000E+00
955	761.88	0.00000E+00
956	796.97	0.00000E+00
957	818.82	0.00000E+00
958	818.82	0.00000E+00
959	974.43	0.00000E+00
960	974.43	0.00000E+00
961	974.43	0.00000E+00
962	974.43	0.00000E+00
963	974.43	0.00000E+00
964	974.43	0.00000E+00

NODE	TEMPERATURE	FLUENCE
965	986.16	0.00000E+00
966	986.16	0.00000E+00
967	986.16	0.00000E+00
981	445.74	0.00000E+00
982	574.20	0.00000E+00
983	702.65	0.00000E+00
984	730.09	0.00000E+00
985	757.53	0.00000E+00
986	797.74	0.00000E+00
987	821.23	0.00000E+00
988	821.23	0.00000E+00
989	965.59	0.00000E+00
990	965.59	0.00000E+00
991	965.59	0.00000E+00
992	965.59	0.00000E+00
993	965.59	0.00000E+00
994	965.59	0.00000E+00
995	980.82	0.00000E+00
996	980.82	0.00000E+00
997	980.82	0.00000E+00

NODE	TEMPERATURE	FLUENCE
1011	445.50	0.00000E+00
1012	573.61	0.00000E+00
1013	701.73	0.00000E+00
1014	727.45	0.00000E+00
1015	753.17	0.00000E+00
1016	798.50	0.00000E+00
1017	823.65	0.00000E+00
1018	823.65	0.00000E+00
1019	956.74	0.00000E+00
1020	956.74	0.00000E+00
1021	956.74	0.00000E+00
1022	956.74	0.00000E+00
1023	956.74	0.00000E+00
1024	956.74	0.00000E+00
1025	975.48	0.00000E+00
1026	975.48	0.00000E+00
1027	975.48	0.00000E+00
1041	445.59	0.00000E+00

1042	573.85	0.00000E+00
1043	702.11	0.00000E+00

NODE	TEMPERATURE	FLUENCE
1044	728.58	0.00000E+00
1045	755.04	0.00000E+00
1046	798.74	0.00000E+00
1047	823.93	0.00000E+00
1048	823.93	0.00000E+00
1049	956.91	0.00000E+00
1050	956.91	0.00000E+00
1051	956.91	0.00000E+00
1052	956.91	0.00000E+00
1053	956.91	0.00000E+00
1054	956.91	0.00000E+00
1055	975.47	0.00000E+00
1056	975.47	0.00000E+00
1057	975.47	0.00000E+00
1071	445.68	0.00000E+00
1072	574.09	0.00000E+00
1073	702.49	0.00000E+00
1074	729.70	0.00000E+00
1075	756.91	0.00000E+00
1076	798.98	0.00000E+00

NODE	TEMPERATURE	FLUENCE
1077	824.21	0.00000E+00
1078	824.21	0.00000E+00
1079	957.07	0.00000E+00
1080	957.07	0.00000E+00
1081	957.07	0.00000E+00
1082	957.07	0.00000E+00
1083	957.07	0.00000E+00
1084	957.07	0.00000E+00
1085	975.46	0.00000E+00
1086	975.46	0.00000E+00
1087	975.46	0.00000E+00
1101	445.78	0.00000E+00
1102	574.32	0.00000E+00
1103	702.87	0.00000E+00
1104	730.83	0.00000E+00
1105	758.79	0.00000E+00
1106	799.23	0.00000E+00
1107	824.48	0.00000E+00
1108	824.48	0.00000E+00
1109	957.24	0.00000E+00

NODE	TEMPERATURE	FLUENCE
1110	957.24	0.00000E+00
1111	957.24	0.00000E+00
1112	957.24	0.00000E+00
1113	957.24	0.00000E+00
1114	957.24	0.00000E+00
1115	975.46	0.00000E+00
1116	975.46	0.00000E+00
1117	975.46	0.00000E+00
1131	445.87	0.00000E+00
1132	574.56	0.00000E+00
1133	703.25	0.00000E+00
1134	731.95	0.00000E+00
1135	760.66	0.00000E+00
1136	799.47	0.00000E+00
1137	824.76	0.00000E+00
1138	824.76	0.00000E+00
1139	957.40	0.00000E+00
1140	957.40	0.00000E+00
1141	957.40	0.00000E+00
1142	957.40	0.00000E+00

NODE	TEMPERATURE	FLUENCE
1143	957.40	0.00000E+00
1144	957.40	0.00000E+00
1145	975.45	0.00000E+00
1146	975.45	0.00000E+00

1147	975.45	0.00000E+00
1161	445.96	0.00000E+00
1162	574.79	0.00000E+00
1163	703.63	0.00000E+00
1164	733.08	0.00000E+00
1165	762.53	0.00000E+00
1166	799.71	0.00000E+00
1167	825.04	0.00000E+00
1168	825.04	0.00000E+00
1169	957.57	0.00000E+00
1170	957.57	0.00000E+00
1171	957.57	0.00000E+00
1172	957.57	0.00000E+00
1173	957.57	0.00000E+00
1174	957.57	0.00000E+00
1175	975.44	0.00000E+00

NODE	TEMPERATURE	FLUENCE
1176	975.44	0.00000E+00
1177	975.44	0.00000E+00

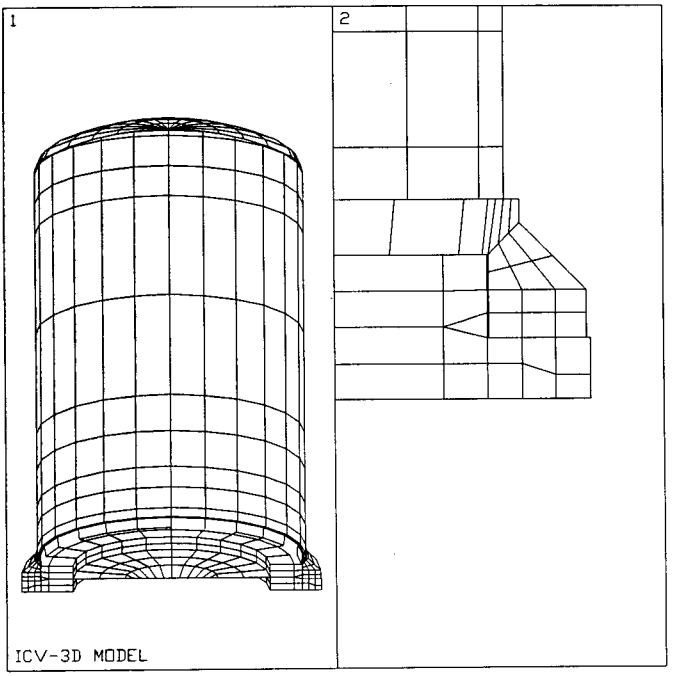


FIGURE 2.10.12-1.

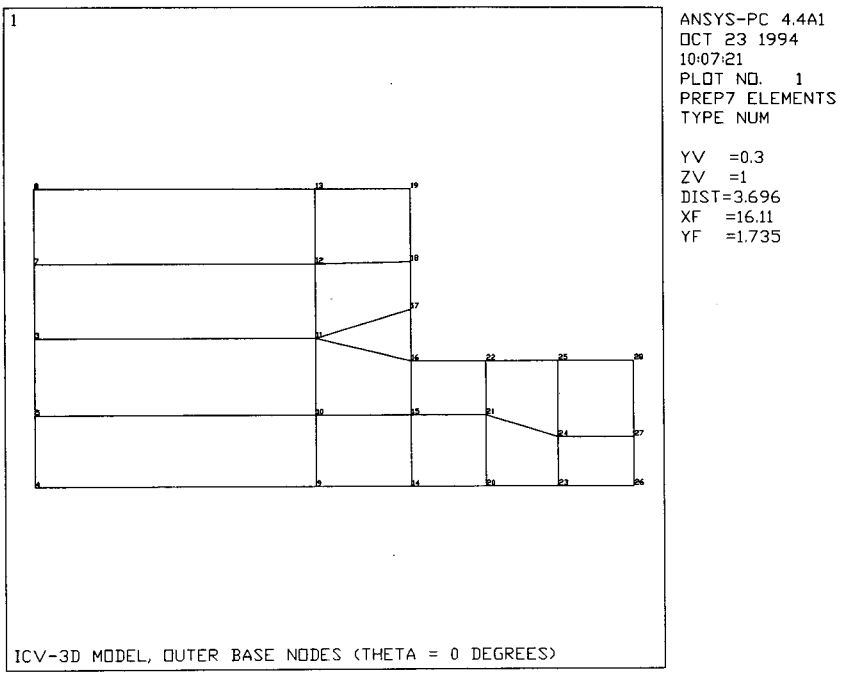


FIGURE 2.10.12-2.

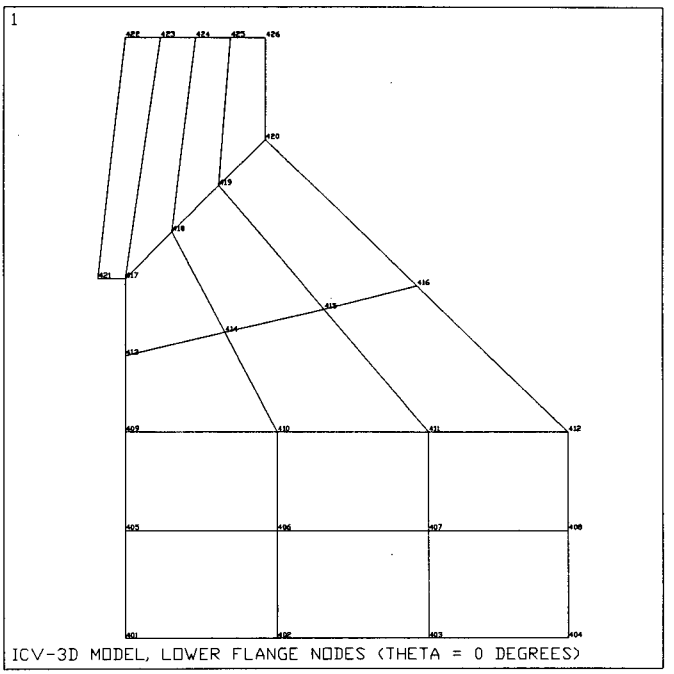


FIGURE 2.10.12-3.

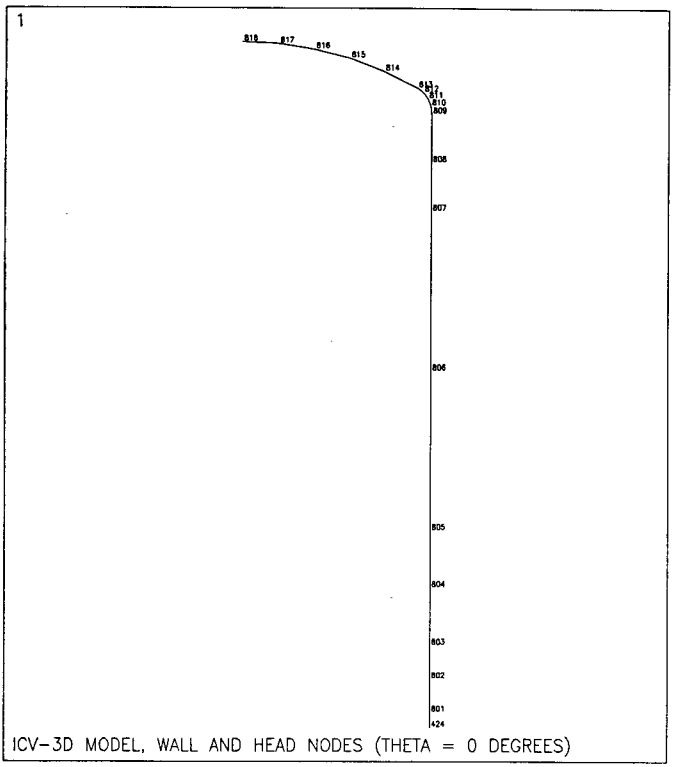


FIGURE 2.10.12-4.

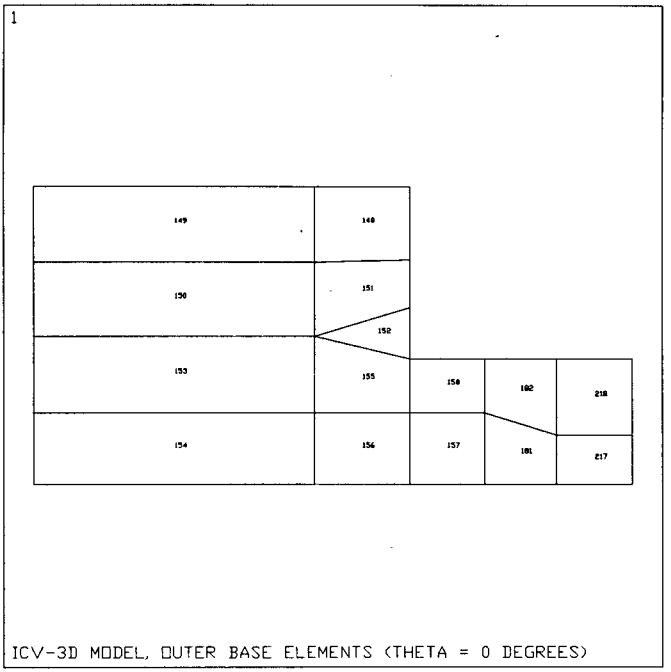


FIGURE 2.10.12-5.

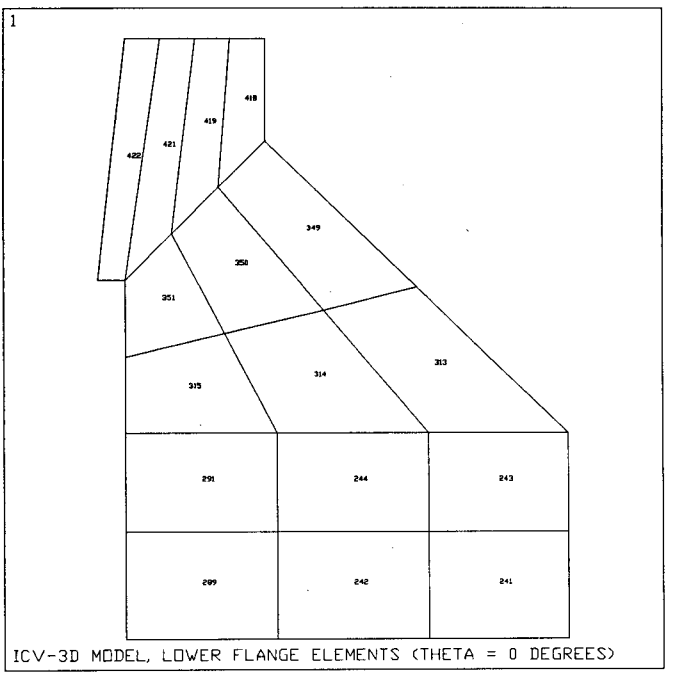


FIGURE 2.10.12-6.

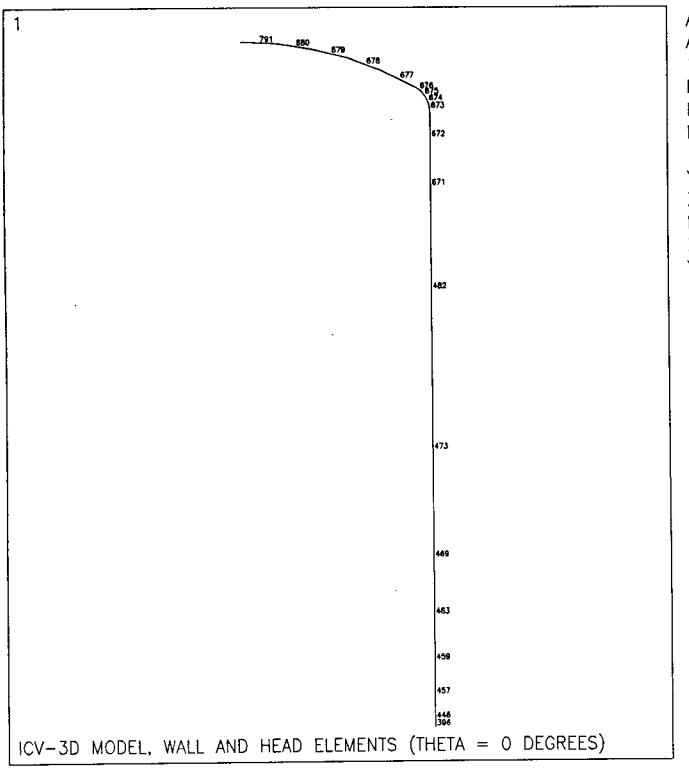


FIGURE 2.10.12-7.

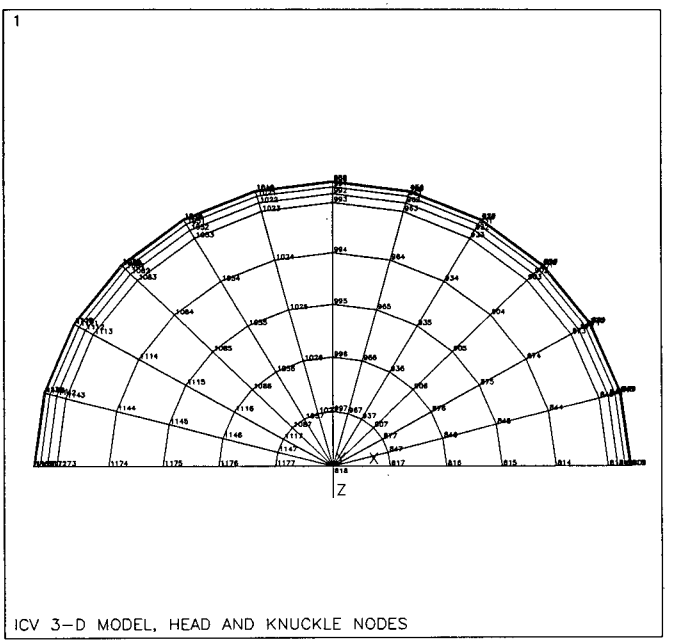


FIGURE 2.10.12-8.

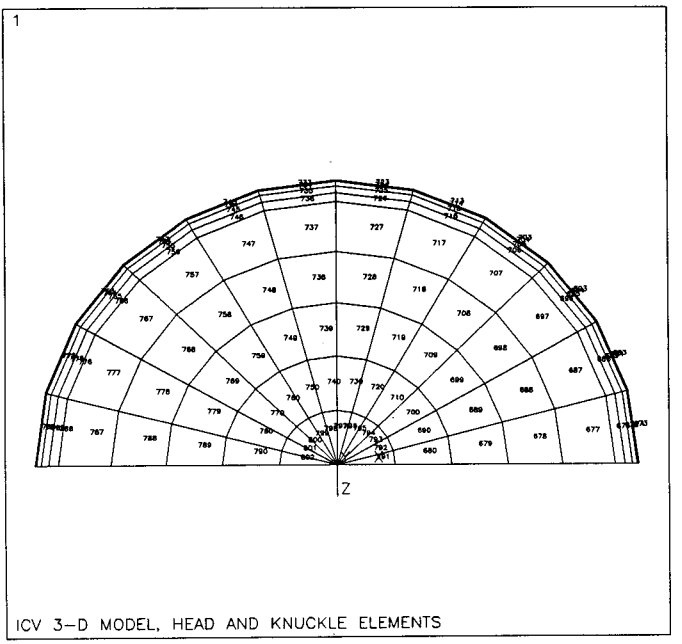


FIGURE 2.10.12-9.

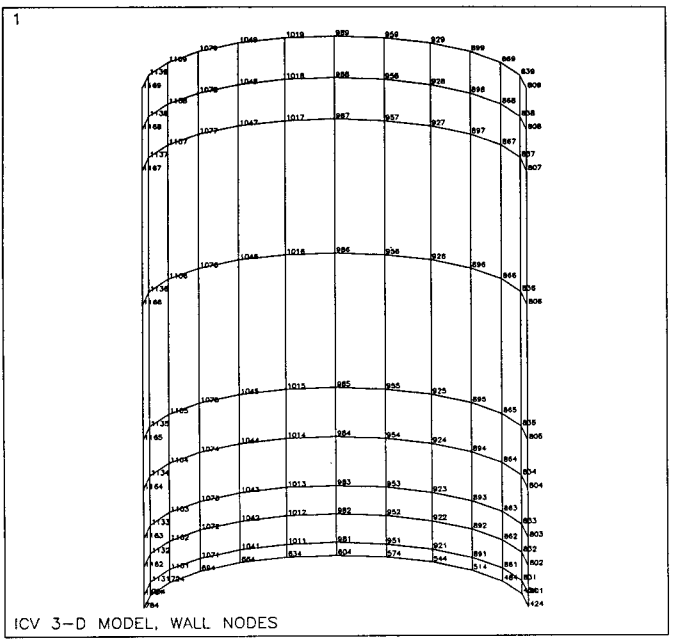


FIGURE 2.10.12-10.

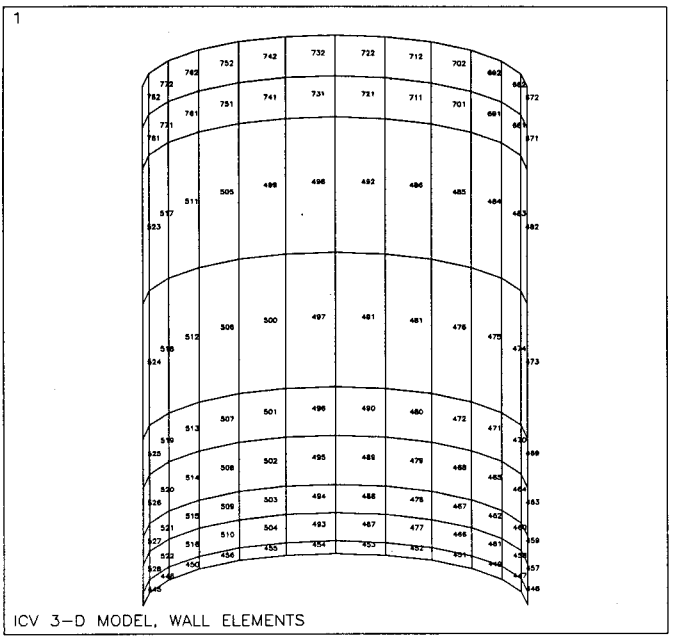


FIGURE 2.10.12-11.

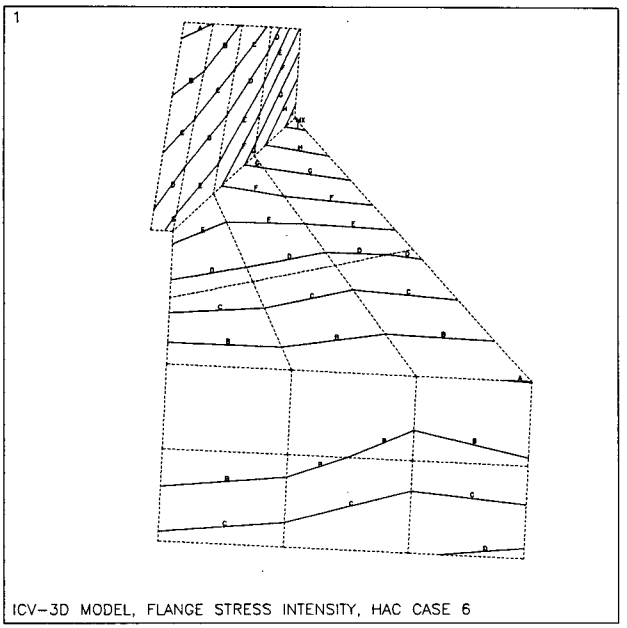


FIGURE 2.10.12-12.

2.10.13 OCV Three-Dimensional ANSYS Model

A 3-D model of the OCV was developed to validate the use of a 2-D OCV model (see Section 2.10.8) for evaluation of HAC events. The primary issue to be investigated was the significance of circumferential variations of temperature caused by payload reconfiguration. A secondary issue, the nonsymmetry introduced in the OCV base because of the electrical feed-through penetration, was also addressed by the 3-D model. By comparing results obtained from the 3-D model with those obtained from a corresponding 2-D model, use of the 2-D OCV model for evaluation of HAC events is justified.

2.10.13.1 Description. The 3-D OCV model is a partial representation of the OCV. It includes a 30° segment of the OCV assembly, including base, flange, wall, thermal shield, coolant jacket, and the two closure bolts contained within the segment. This segment begins at the point of maximum heat load (where impact limiter side impact damage coincides with the axial distribution of the damaged payload), and ends at the angular location where the circumferential temperature gradient is essentially zero (about 30° from the maximum heat location). In this manner, the segment can be treated as an isolated structure for both thermal and structural purposes. The OCV head is not modeled; the OCV wall and thermal shield terminate at an elevation of 38.13 in. from the bottom of the OCV base. This geometry was chosen because the axial temperature gradients become essentially zero at this location, and that it is sufficiently far removed from the seal area that distortion effects above this point will have an insignificant effect on OCV containment.

The electrical feed-through geometry was inserted into the finite element model to evaluate its effects on thermal distortion in the containment seal area. The cutout for the electrical feed-through plug was modeled as a 2.58-in. constant diameter cylindrical void, extending horizontally from the outside diameter of the OCV base to a point directly under the containment seal, at a distance of 0.18 in. below the sealing surface. This approximation is conservative because the electrical feed-through cutout maximum diameter of 2.58 in. actually extends for a length of only 3.96 in., and not all the way to the OCV containment seal location. The remaining electrical feed-through cutout has smaller diameters. Also, the actual electrical feed-through cutout is drilled at an angle into the OCV base, taking the cutout location much further below the containment seal location than is used in the ANSYS model.

The electrical feed-through contact plate cutout was modeled as a 8.62 in. long by 2.73 in. wide by 1.00 in. deep rectangular void in the upper surface of the inside portion of the OCV base (the portion where the ICV base contacts the OCV base). This approximation is conservative because the actual contact plate cutout is 1.00 in. deep only over a 7.96 in. long by 1.41 in. wide area, and the remainder of the contact plate cutout is only 0.53 in. deep. No actual electrical feed-through components were included in the ANSYS model, because their structural effects would be negligible. The finite element model (applicable to both the thermal and structural analyses) is shown in Figures 2.10.13-1 through 2.10.13-3.

The detailed OCV analysis consisted of the following four parts.

1. A SINDA finite difference transient thermal evaluation, using a detailed 3-D OCV model, as documented in Section 3.6.2.4.

2. An ANSYS finite element equivalent static thermal evaluation, using SINDA results and a partial 3-D OCV model, as explained above. Using ANSYS, the SINDA results were expanded into the finer mesh finite element model to obtain a more accurate temperature distribution at the OCV seal location and in the area of the electrical feed-through components.

3. An ANSYS 3-D finite element static structural evaluation, using the refined temperature distribution, along with maximum OCV internal pressure, to evaluate the effects of pressure and thermal distortion in the OCV seal area.

4. A corresponding ANSYS 2-D axisymmetric finite element static structural evaluation using temperatures at the hottest circumferential position from the 3-D thermal model along with maximum OCV internal pressure. Model construction is detailed in Section 2.10.8.

2.10.13.2 Construction. For both the ANSYS 3-D thermal and structural models, the same basic types of finite elements were used.

1. The base, flange, and shell portions of the OCV were modeled with 20-node quadratic, isoparametric brick elements. On surfaces where contact elements were applied (i.e., between the OCV flange and base sealing surfaces), the midside nodes of the brick elements were removed to allow accurate representation of the force-deflection characteristics of the contact elements used in the structural model. Additionally, midside nodes were removed from brick element edges that were normal to the closure bolt elements and in direct contact with bolt attachment nodes to linearize bolt interactions with these elements.

2. The OCV thermal shield and coolant jacket were modeled with 4-node linear shell elements for the thermal analysis. For the structural analysis, these elements were converted to 8-node quadratic elements. Reduced-strength shell elements were embedded in the brick elements at the interfaces of bricks and shells to carry rotational displacements between the two types of elements in the structural analysis.

3. Line elements (conducting rods for the thermal model and spar elements for the structural model) were used to represent the closure bolts. The structural closure bolt elements were pre-loaded by applying the appropriate prestrain to achieve a 14,500-pound OCV closure bolt pre-load. This prestrain was applied before any thermal or pressure loadings were imposed on the structural model.

4. For the structural model, 5-node, 3-D surface contact elements were used to accurately simulate contact or separation of the OCV flange and base sealing surfaces under the influence of all applied loadings.

2.10.13.3 Material Properties. The thermal conductivity of the OCV stainless steel structural elements and alloy steel closure bolts varied as a function of temperature according to the data in Table 3.2-1 of Section 3. The modulus of elasticity and coefficient of thermal expansion varied with temperature according to Tables 2.3-1 and 2.3-2. Poisson's ratio was 0.3.

2.10.13.4 Boundary Conditions. A representative thermal loading corresponding to HAC load case 3 was used for evaluation. This particular case was selected because it provides a relatively large temperature difference between the OCV shell and flange, a significant circumferential temperature gradient, and relatively high OCV O-ring seal temperatures.

2.10.13.4.1 Thermal Model. The worst-case temperatures and temperature gradients in and around the OCV containment seal area occur at the period of time corresponding to the end of the HAC fire event (i.e., 30 minutes from the start of the event). Therefore, thermal conditions occurring at this time were evaluated to determine worst-case OCV containment seal temperatures and seal area distortions.

At all boundaries (external surfaces) of the ANSYS thermal model, except the 0 and 30° surfaces (which were assumed to be symmetry surfaces, and therefore adiabatic), external heat

fluxes from the SINDA model were applied as surface loads. Because each surface node of the SINDA model represents a discrete area, the flux values were divided by the appropriate areas, and the resulting flux densities were imposed directly on the equivalent surface areas of the ANSYS model. Because the SINDA results were derived from a transient analysis, an instantaneous heat flux imbalance was incurred, because of material specific heat effects (heat lost in raising material temperatures). To account for this effect in the ANSYS static analysis, these heat losses were modeled as heat sinks in the model interior. Each interior SINDA node represents a specific volume of material. Therefore, for the ANSYS evaluation, the internal heat loss at each SINDA node was divided by the corresponding volume, and the result was directly applied over the equivalent volume of the finite element model as a volumetric heat sink. In this manner, a static heat flux balance was achieved over the domain of the finite element model. To the interior of this domain were added temperatures derived at interior nodes of the SINDA model. In areas of high heat flux, additional ANSYS initial nodal temperatures were derived by linear interpolation of SINDA internal and external node temperatures. The resulting ANSYS model was then run in a static thermal analysis to accurately determine the remainder of the finite element model nodal temperature values. These temperatures were then transposed into the ANSYS structural model as loads for the structural thermal distortion analysis.

2.10.13.4.2 Structural Model. The thermal analysis nodal temperatures, as described in the above section, along with a representative internal pressure loading of 39.7 psia, were applied to the ANSYS structural model. A reference of 70 °F was used to derive thermal distortion effects. The 0 and 30° surfaces were assumed to be symmetry boundaries, and appropriate displacement constraints were applied accordingly. Additionally, to achieve static stability, a single axial zero-displacement constraint was applied at the center of the bottom surface of the finite element model base.

Resulting closure bolt loads and distortions (sealing surface separation) at the location of the OCV containment seal were determined for comparison with the corresponding 2-D model of the OCV.

2.10.13.5 Analysis Results and Comparison with 2-D ANSYS Model. Both 3-D and 2-D models were run using representative inputs as discussed above. Results of the 3-D thermal analysis, in the form of temperature contours, are shown in Figures 2.10.13-4 through 2.10.13-6.

Results of the 3-D structural analysis indicate the maximum relative displacement between OCV flange and base seal surfaces at the location of the OCV containment seal is 0.022 in., and is essentially constant around the circumference of the 30° model segment. The results also indicate that the presence of the electrical feed-through in the OCV base is of little significance. In general, this is because OCV flange twist is the dominant displacement mode that affects seal compression. OCV base distortions, in contrast, are relatively small. The OCV seal area distortion pattern (with displacements scaled by a factor of 25) is shown in Figure 2.10.13-7. The maximum closure bolt load was 48,795 pounds. Results from the corresponding 2-D model were a relative displacement

between flange and base at the containment seal location of 0.019 in., and a closure bolt load of 42,938 pounds. The good agreement of results between 3-D and 2-D models justifies use of the 2-D model for the OCV.

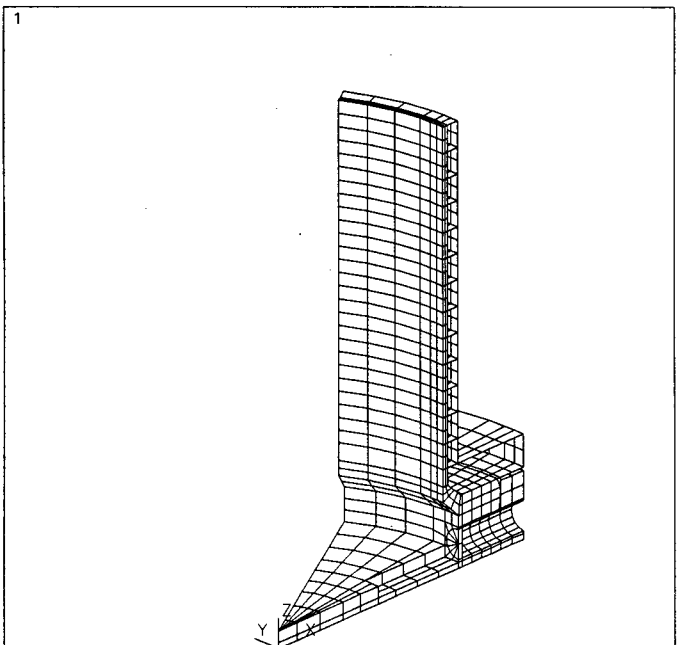


FIGURE 2.10.13-1.

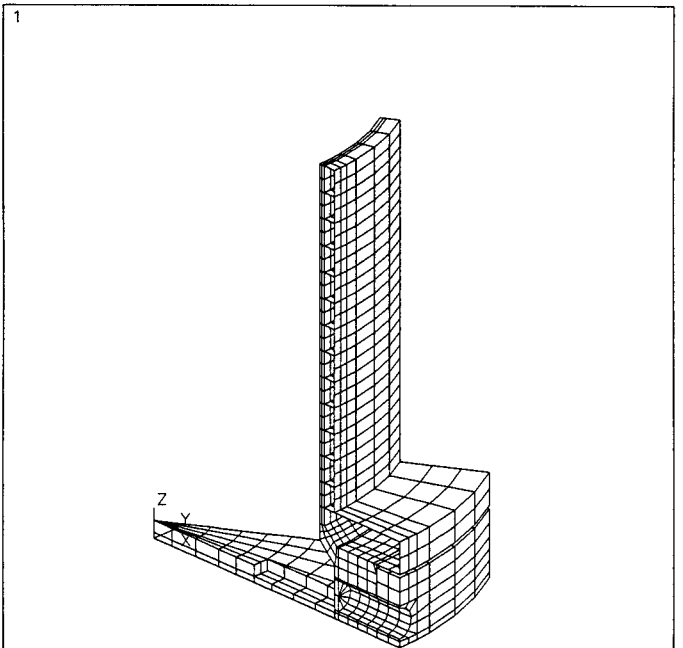


FIGURE 2.10.13-2.

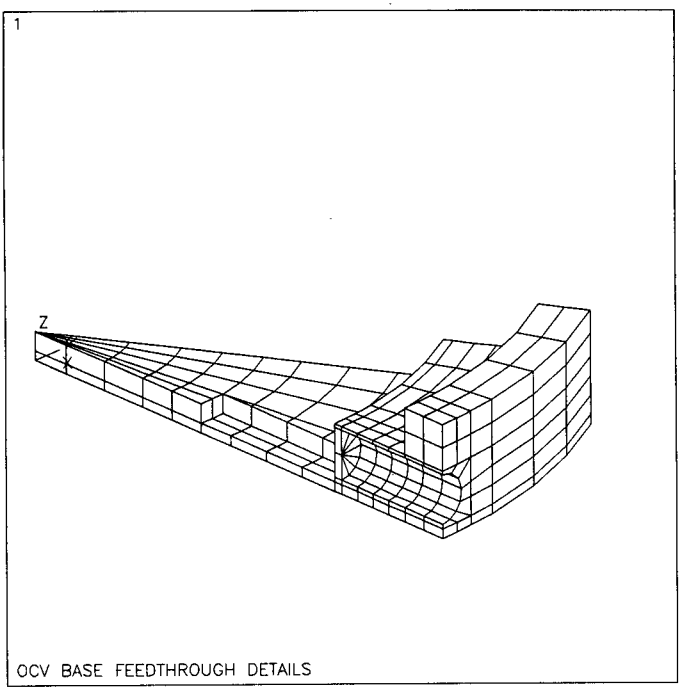


FIGURE 2.10.13-3.

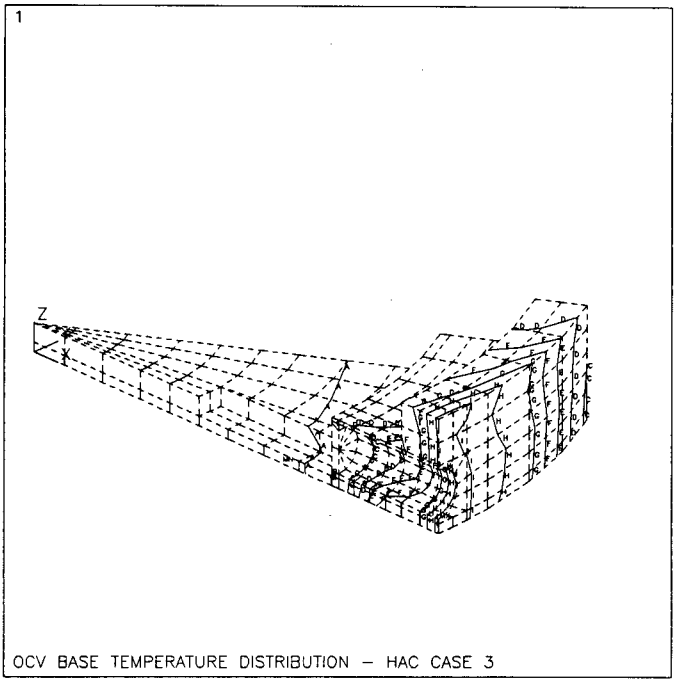


FIGURE 2.10.13-4.

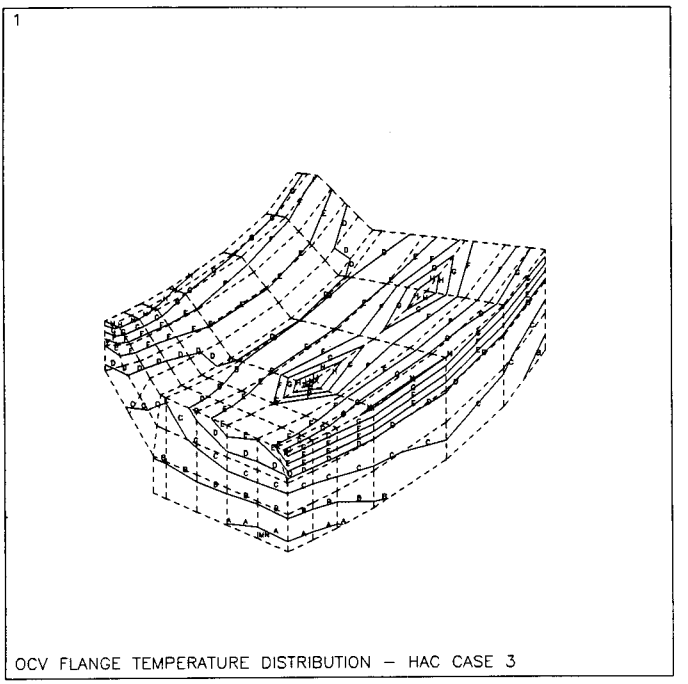


FIGURE 2.10.13-5.

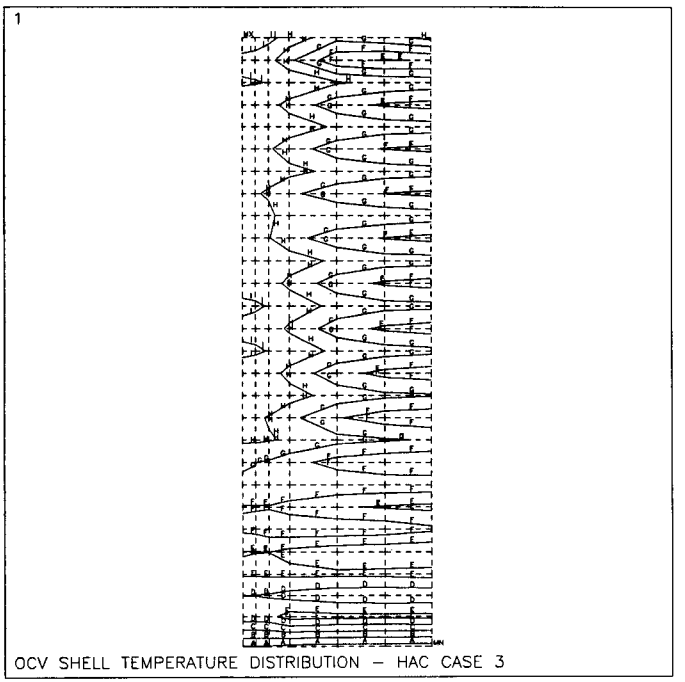


FIGURE 2.10.13-6.

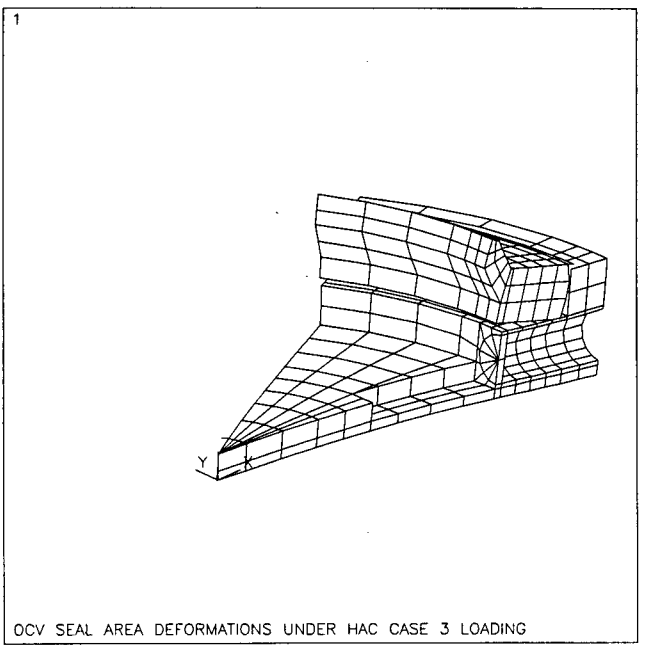


FIGURE 2.10.13-7.

2.10.14 O-ring Seal Compression Measurements

The RTG Transportation System Package uses elastomeric, face-type O-rings as containment seals. The ability of these O-ring seals to function is dependent on the degree of compression afforded by the containment seal area mating surfaces. In the HAC fire event, thermal distortions of the mating surfaces can cause a reduction in O-ring compression. To demonstrate that the combined effects of the HAC 30-ft. free drop, the 40-in. puncture drop, and the HAC fire event do not reduce the O-ring compression below acceptable levels, the compression O-ring reduction due to drop event-related flange distortion is summed with the calculated O-ring compression reduction due to HAC fire event thermal distortion. For this reason, an evaluation of drop event flange distortion and potential reduction in O-ring compression must be made. These calculations are more fully discussed in Section 4.0. Data was collected before and after the entire drop event series.

The O-ring compression is directly related to the axial dimension of the space it is forced to occupy. This axial dimension is created by the relative positions of the bottom of the O-ring groove in the vessel base and the flat bell flange. Nominally, the dimension is simply equal to the O-ring groove depth, as long as the flange is tightly mated to the base. Reduction of O-ring compression can only occur from relative distortion between the groove bottom and the flange surface. The method described below focuses on the space available for the O-ring to occupy. Measurements were taken in accordance with PacTec procedure TP-004, and are recorded on data sheets contained in Appendix 2.10.15.5.

The direct compression method preserves a record of the space available for the O-ring seal to occupy by assembling a soft metal replica of the elastomer O-ring into the O-ring groove. The replica had an initial dimension larger than the groove depth (but not necessarily equal to the O-ring). Subsequent to assembly into the groove, it had a dimension equal to the space available for the O-ring to occupy plus an insignificant amount of elastic springback (less than 2% of its diameter). The elastic springback was present in equal amounts in both pre- and post-test measurements, and thus, had no effect on net measurements. The O-ring replicas were common copper tubing. Nominal 1/4-in. tubing was used for both of the closure seal grooves on the ICV, and nominal 1/4- and 5/16-in. tubing was used to measure the small and large O-ring grooves, respectively, of the OCV. The replicas were of one piece, with a small gap (about 1 to 2 in.) where the ends met. The gap was placed midway between two measurement points. Measurements were made in eight locations on each replica for each of the four O-ring grooves. One measurement was taken at the circumferential position of the electrical feed-through and the others were evenly spaced at 45° increments. Thus, a total of 16 measurements were taken to record the state of compression of each of the closure O-ring seals in the ICV and OCV. Because these measurements were taken before and after testing, a grand total of 128 measurements were made. Table 2.10.14-1 gives the copper tubing crushed height measurements in the pre-test and post-test condition for the ICV, and Table 2.10.14-2 is for the OCV. The column labeled "Change" is the difference in space available for the O-ring to occupy brought about by the drop testing. A positive result indicates an increase in space available, that is, a decrease in O-ring compression.

When tightening the closure bolts to crush the tubing, a star pattern (alternating sides of the OCV) was used. For the pre-drop measurements, full nominal closure bolt torques were used. For post-drop measurements, each bolt was carefully tightened (in 25% increments) to the residual torque value that was measured when the package was disassembled after leakage rate testing.

TABLE 2.10.14-1. ICV Containment O-ring Groove Direct Compression Measurements (in.).

	Inner groove (1/4 in.)			Outer groove (1/4 in.)		
Angular position	Pre-test	Post-test	Change	Pre-test	Post-test	Change
Feed-thru	0.204	0.205	0.001	0.201	0.213	0.012
45	0.204	0.203	-0.001	0.201	0.207	0.006
90	0.204	0.203	-0.001	0.200	0.208	0.008
135	0.203	0.203	0.0	0.200	0.208	0.008
180	0.204	0.205	0.001	0.202	0.210	0.008
225	0.204	0.204	0.0	0.201	0.208	0.007
270	0.204	0.203	-0.001	0.201	0.208	0.007
315	0.204	0.203	-0.001	0.201	0.208	0.007

TABLE 2.10.14-2. OCV Containment O-ring Groove Direct Compression Measurements (in.) Base.

	Inner groove (5/16 in.)			Outer groove (1/4 in.)		
Angular position	Pre-test	Post-test	Change	Pre-test	Post-test	Change
Feed-thru	0.282	0.287	0.005	0.207	0.213	0.006
45	0.282	0.283	0.001	0.207	0.207	0.0
90	0.282	0.282	0.0	0.207	0.208	0.001
135	0.282	0.283	0.001	0.207	0.208	0.001
180	0.282	0.284	0.002	0.207	0.210	0.003
225	0.282	0.282	0.0	0.207	0.208	0.001
270	0.282	0.283	0.001	0.207	0.208	0.001
315	0.282	0.283	0.001	0.207	0.208	0.001

The negative change values (a decrease in space available) in the tables above do not exceed -0.001, and can be attributed to measurement error.

From Table 2.10.14-1, the maximum change in compression of the containment O-ring seal (the inner location) is a reduction of 0.001 in. for the ICV. From Table 2.10.14-2, the corresponding value for the OCV is a reduction of 0.005 in. This data is used further in Section 4.3.2.

2.10.15 Summary of Damage from Certification Testing

2.10.15.1 Introduction. This section provides detailed information regarding the Certification Testing of the RTG Transportation System Package. Two full-scale prototypes of the package were used during the drop test program. The first certification test article (CTA-1) experienced two failures during the first drop test series. The package design was subsequently modified and a second certification test article (CTA-2) was fabricated. All of the 4-ft and 30-ft free drop tests that were performed on CTA-1 were repeated for CTA-2. During the first drop test series, CTA-1 was subjected to nine puncture tests. For the second drop test series, four of these puncture tests were repeated and two additional puncture tests were performed on CTA-2.

The first drop test series is described in Test Plan WHC-SD-RTG-TP-009 and the second drop test series is described in Test Plan WHC-SD-RTG-TP-018. The first drop test series was performed in accordance with Test Procedure WHC-SD-RTG-TP-003 and the second drop test series was performed using Test Procedure WHC-SD-RTG-TC-015. The drop testing was performed to the requirements of 10 CFR 71. The HAC fire was evaluated by analysis as shown in Chapter 3.0.

The CTA-2 unit was fabricated in accordance with the drawings contained in Section 1.3.2, with any differences noted in Section 2.10.15.2.1 below. The differences between CTA-1 and CTA-2 are listed below in Section 2.10.15.2.2. The RTG payload mass, center of gravity, and potential for inflicting damage on the interior of the ICV was simulated in the drop testing as described in Section 2.10.15.2.3. The test pad puncture bars are described in Section 2.10.15.3. It is noted that only CTA-1 had accelerometer instrumentation attached during the drop testing.

The test data included for CTA-1 consists of accelerometer output for the NCT and HAC free drops and damage results from puncture tests CTA-1 Test No. 12, No. 13, No. 15, No. 18 and No. 19. The accelerometer data is included for information only. The results of the above listed CTA-1 puncture tests are included because these tests were not repeated during the second drop test series.

The test data included in this appendix consists of helium leakage rate results, closure bolt torques, accelerometer output (CTA-1 only), completed test data sheets, impact deformations, and a written and photographic record of damage. Seal area measurements are presented in Appendix 2.10.14. A brief explanation of the data is included where needed. A complete summary and discussion of the data is given in Section 2.7.6. Results that are pertinent to NCT are summarized in Section 2.6.7.

2.10.15.2 Test Article. Two full-sized prototypes of the package were fabricated for use as CTAs. This section identifies any differences between CTA-1 and CTA-2, and between CTA-2 and the General Arrangement drawings provided in Section 1.3.2. Unless a specific exception is stated herein, CTA-2 fully complied with the General Arrangement drawings of Section 1.3.2.

2.10.15.2.1 Itemized Differences Between CTA-2 and General Arrangement Drawings. Differences between CTA-2 and the drawings presented in Section 1.3.2 fall into two broad categories:

- Items related specifically to certification testing, such as special vent ports
- Items that were not needed for certification testing, such as paint or coolant.

Each difference is detailed below. In each case, it is demonstrated that the difference had no material effect on the outcome of the certification tests.

1. Measurement Tool Mounting Tabs. Small, 1-in. square, 1/4-in.-thick tabs made of 304L stainless steel were welded to the CTA-2 coolant jacket outer surface in each of four quadrants. One quadrant was located at the electrical feed-through, and the others were at 90° intervals. Three tabs were used in each quadrant to assist in temporarily fastening a measurement reference tool to CTA-2. The tool was used to obtain measurements of impact limiter deformation after each drop test. The tabs did not significantly alter the weight or c.g of CTA-2 and were not directly involved in any free drop or puncture drop events.

2. Impact Limiter Shell Hole. A single, 5/16-in.-diameter hole was drilled into the center of the bottom plate of the CTA-2 impact limiter. The hole was used in conjunction with a measuring rod, used to determine impact limiter deformations. The hole had no influence on any CTA-2 response.

3. Adjustment of Foam Density in Impact Limiter. The density of the nominally 12 lb/in.^{3} foam was adjusted upward to approximately 15.5 lb/in.^{3} to simulate cold (-20 °F) conditions. This adjustment was made to allow ambient temperature certification testing and is fully described in Section 2.7.1.3.

4. Added Leak Test Ports. One seal test port was added to both the ICV and OCV to aid in establishing the dwell time for helium leakage rate testing. The construction of each port is fully prototypical, i.e., is identical to the standard seal test ports shown in the General Arrangement drawings. The location of each added seal test port is 180° opposite the standard seal test port for each vessel.

5. Added Vent Ports. Three port holes, sealed by 1/4-in. NPT pipe plugs, were added to CTA-2: two on the OCV and one on the ICV. The purpose of the ports was to allow the introduction of helium into the vessels (and its subsequent removal) during the certification test leakage rate testing procedure, without the necessity of disturbing the prototypic vent port seals. The ICV port was located in the 2-in. thick lifting block at the top of the bell, and the OCV ports were located just above the top of the coolant jacket. The added ports were not directly involved in any free drop or puncture drop events.

6. Striping. CTA-2 featured tape and paint stripes to aid in drop testing.

7. Nameplate. A nameplate was not present on CTA-2. This omission had no effect on any CTA-2 response.

8. Tamper-Indicating Seal. An impact limiter bolt tamper-indicating seal was not present on CTA-2. This omission had no effect on any CTA-2 response.

9. Paint. Paint was not present on CTA-2. This included the black paint normally used for interior bell surfaces and the white paint normally used for exterior surfaces. This omission had no effect on any CTA-2 response.

10. Electrical Feed-through, Spring-loaded Electrical Pins. The spring-loaded pins that complete the electrical connection between the ICV and OCV for the electrical feed-through were not present on CTA-2. When compressed, they exert only a few ounces of force and have no structural significance. This omission had no effect on any CTA-2 response.

11. Coolant. Coolant was not present in the CTA-2 coolant passages. The passages were essentially dry and contained air. The normal quantity of coolant weighs approximately 180 lb, and therefore its absence had a negligible effect on CTA-2 mass and c.g. The structural significance of coolant is also small. The absence of coolant would cause slightly greater (more conservative) deformations of the OCV vessel wall from puncture events.

12. Personnel Barrier. The personnel barrier was in place for all of the CTA-2 free drops. After the 30-ft top down drop (CTA-2 Test No. 13), the thin expanded metal screen on top of the personnel barrier was removed. In puncture drop No. 15, the distance to the puncture pin was conservatively measured as though the personnel barrier was undamaged and the screen was present. This amounted to a top-down puncture drop distance of approximately 45 in. instead of 40 in. and is therefore conservative.

13. Electrical Feed-through Receptacle-to-Sleeve Weld. This weld was an electron beam (EB) weld on CTA-2, but will be a Gas Tungsten Arc Weld (GTAW) for production units. The GTAW will be stronger and less subject to microfissures than the EB weld, and therefore the use of the EB weld in the certification tests was conservative. Further information on this weld is provided in Reference 6 of Chapter 4.

14. Instrumentation Cables. Cables were connected to each electrical feed-through, which terminated in the respective bracket-mounted connectors. Wiring was not used, however, from the ICV connector to the simulated payload, or from the OCV connector to external instrumentation. The absence of these secondary wires had no effect on any CTA-2 response.

15. Small holes, which penetrated approximately 2 in. into the foam, were placed in the four plastic melt-out plugs in the impact limiter, to facilitate temperature measurement of the foam. There was no effect on any CTA-2 response.

16. OCV coolant jacket and thermal shield weld inspections. The CTA-2 OCV coolant jacket and thermal shield welds were not dye-penetrant inspected. Also, the CTA-2 OCV coolant jacket channels were not pressure tested. These welds are not part of the OCV containment boundary and the inspections were considered to be unnecessary for drop testing. The elimination of these requirements had no effect on any CTA-2 response.

17. The CTA-2 unit used cadmium-plated ICV closure bolt washers for certification drop tests Nos. 1 through 9. The remaining drop tests (Nos. 10 through 16) used the non-cadmium-plated washers. See Section 2.10.15.4.6.

18. The impact limiter guide tubes were not welded to the top of the OCV flange for the CTA-2 unit. The tubes were only welded to the OCV flange thermal shield.

19. The CTA-2 impact limiter attachment holes did not use the bottom cap.

In summary, several minor differences existed between CTA-2 and the General Arrangement drawings. None of these differences, however, had any significant effect on the response of CTA-2 to drop or puncture events.

2.10.15.2.2 Itemized Differences Between CTA-1 and CTA-2. As mentioned in Section 2.10.15.1, CTA-1 experienced two failures and a new certification test article (CTA-2) was fabricated. The main differences between the two test articles were the hardware changes that were made to CTA-2 to correct the failures experienced by CTA-1. The differences between CTA-1 and CTA-2 are listed below.

1. Accelerometer Mounting Blocks and Protective Covers. Mounting blocks for active and passive accelerometers were added to the outside of CTA-1. There were three active accelerometer mounting blocks and one mounting plate used to attach a bank of three passive accelerometers. The mounting blocks were made of 304L stainless steel, and had threaded holes for mounting of the accelerometers. The mounting blocks were welded to the coolant

jacket ribs with at least four 1/8-in. fillet welds to provide a rigid connection to CTA-1. To obtain access to the ribs, a short (approx. 6-in.-long) section of the outer coolant jacket shell was removed in each case. Two mounting blocks were located at the approximate axial location of the CTA-1 center of gravity, one at 90° and the other at 270° CCW from the location of the electrical feed-through. The third was located 30 in. above the center of gravity, at 270° CCW of the electrical feed-through. The mounting plate for the bank of passive accelerometers was located approximately 260° CCW from the electrical feed-through at the c.g., and was welded firmly to the outer exposed edges of the coolant jacket ribs. Protective covers, made of 304L, were fastened using 1/4-in. cap screws to small mounting plates welded to the coolant jacket ribs. There were a total of three covers. These items did not significantly alter the weight or c.g. of CTA-1. Further, they were located in areas of CTA-1 not subject to either free drop or puncture drop damage, and did not impart or alter package stresses.

2. Added vent ports. One additional hole, sealed by a 1/4-in. NPT pipe plug, was added to the CTA-2 OCV. The purpose of the port was to allow the introduction of helium into the vessels (and its subsequent removal) during the certification test leakage rate testing procedure, without the necessity of disturbing the prototypic vent port seals. The additional OCV port was located just above the top of the coolant jacket and 180° from the other port that is in the same location as the CTA-1 OCV port. The added port was not directly involved in any free drop or puncture drop events.

3. Personnel Barrier. The screen (expanded metal) that forms the sides of the barrier was placed outside the barrier framework, not inside as on CTA-1. This difference had no effect on any CTA-2 response.

4. Wear Pads. The wear pads mounted in the CTA-1 OCV flange were made of Kevlar®/Nylon, instead of Vespel®, as was used on CTA-2. The purpose of the pads is to protect the black heat transfer paint on the vessel bells when installing the OCV bell, and they play no structural role. Therefore, this substitution had no effect on any CTA-2 response.

5. Impact Limiter Alignment Pins. The CTA-1 impact limiter contained two extra threaded mounting holes for the alignment pins (because of initial mislocation of the holes). CTA-2 did not contain these extra holes.

6. Payload Shipping Rack Underside Insulation. During normal use of the package, small tufts of Kaowool insulation (located beneath the payload shipping rack) could become loose and hamper helium leak testing. To prevent this, a 16-gauge-thick sheet of 304 stainless steel was used to enclose it on CTA-2, as shown on drawing H-9-5005 in Appendix 1.3.2. This 16-gauge sheet was not used on CTA-1.

7. ICV Bolting System. The redesign consists of an increase in bolt quantity from 12 for CTA-1 to 24 for CTA-2; a change in bolt material to ASTM A540 Class 1; the use of hardened steel thread inserts (identical in material and design to those used in the CTA-1 OCV); the use of hardened steel washers under the bolt heads; and an increase in bolt installation torque, from 100 ft-lb to 250 ft-lb.

   The 24 bolt holes used in the CTA-2 ICV are equally spaced, and the design details of the flange hole and counterbore are identical to the CTA-1 ICV 12-bolt design. The hardened thread inserts are mounted from beneath the ICV baseplate. The bolt diameter remains the same, but bolt length increased by 1/8 in. to account for the added washer thickness. The bottoms of the bolt, insert, and baseplate are approximately flush.

8. Impact Limiter Corner Joints. The original CTA-1 design consisted of a simple corner joint,

joined by a fillet weld and reinforced by angle shapes. The new CTA-2 design consists of a single angle-shape corner piece, full-penetration butt welded on the ends of its legs to the limiter shells. The thickness of the new corner material is equal to the sum of the thicknesses of the CTA-1 impact limiter shell material and reinforcing angle shape.

9. Impact Limiter Attachment Bolts. The diameter of the impact limiter attachment bolts was increased from 3/4 in. (CTA-1) to 1 in. (CTA-2). The bolt length was increased from 7.5 to 8.0 in. The diameter of the central length of the CTA-2 impact limiter attachment bolts is 0.805 in. versus 0.55 in. for CTA-1. For CTA-2, the bolt material was changed to ASTM B637, Alloy NO7750 Type 3. The bolt access tube size for CTA-2 was changed to 2.00-in. diameter by 0.083-in. wall. Bolt torque was increased to 200 from 100 ft-lb. The thread size and depth of engagement in the CTA-2 impact limiter bolting ring were increased to accommodate the larger bolts and Heli-coil thread inserts were installed. The CTA-1 impact limiter bolt ring did not have through holes or caps.

10. OCV Coolant Jacket and Thermal Shield Weld Inspections. The CTA-2 OCV coolant jacket and thermal shield welds were not dye-penetrant inspected. Also, the CTA-2 OCV coolant jacket was not pressure tested. These welds are not a part of the OCV containment boundary and the inspections were considered to be unnecessary for drop testing. The inspection and pressure tests were performed on CTA-1.

2.10.15.2.3 Payload Representation. Simulated payload weight and c.g. location was designed to simulate a maximum weight, maximum c.g. height payload including a maximum weight payload shipping rack. The combined weight and c.g. of the simulated payload with shipping rack was 795 pounds and 24.5 in. above the ICV base plate, respectively. The simulated payload alone weighed 570 pounds and had a c.g. 26.9 in. above its lower mounting surface. The height of the simulated payload c.g. corresponded to within about 1 in. of the height of the c.g. of the maximum weight payload. Fin position relative to payload c.g. was also closely simulated as further discussed below. The total weight of the minimum weight payload and shipping rack is approximately 425 pounds. Because the difference was only 370 pounds, or 3.9% of the total RTG Transportation Package weight, any difference in behavior due to a minimum weight payload can be neglected. The CTA-2 c.g. was also negligibly affected.

The simulated payload consisted of a cylindrical, reinforced steel container, mounted on a 14-in. diameter, 1/2-in. wall thickness steel pipe, which was in turn mounted on a 1/2-in.-thick bolting plate. To simulate the fins present on the actual payloads, eight 1/4-in.-thick steel fins were located radially around the steel container. The top corners of the fins were located 39.4 in. above the top of the shipping rack barrier plate, which corresponded to the position of the top corners of the fins of the heaviest payload. The simulated fins were stronger and had sharper corners than the actual RTG fins, which are made from aluminum, have generally lower buckling strengths, and have chamfered corners. The simulated fins and the open end design of the 14-in. pipe conservatively modeled any damage that could accrue from interaction with an actual payload in a drop. Figure 2.10.9.1-1 shows the simulated payload mounted within the ICV. Section 2.10.9.1 contains more information on the simulated payload. The simulated payload was mounted to the ICV baseplate in a manner identical to an actual payload.

It can be concluded that the simulated payload conservatively models the action of an actual payload in NCT and HAC drop and puncture events.

2.10.15.2.4 Initial Conditions.

CTA-1 Configuration
The first certification test article (CTA-1) was tested in July, 1994 and was similar to the second

certification test article (CTA-2) as previously discussed in Section 2.10.15.2.2. The CTA-1 unit experienced two failures that led to a subsequent redesign of the package and fabrication of a second certification test article (CTA-2). The same prototypical shipping rack and simulated payload were used in both CTA-1 and CTA-2.

CTA-2 Configuration
The CTA-2 consisted of a prototypical package, constructed according to the General Arrangement drawings (see Section 1.3.2), with exceptions and differences as outlined in Section 2.10.15.2.1 above. A prototypical payload shipping rack and a simulated payload were installed as discussed in Section 2.10.15.2.2 above. Before testing, the package containment seals and containment boundaries were subjected to helium leakage rate testing in accordance with the procedure described in document WHC-SD-RTG-TC-015.

Temperature
The CTA-2 impact limiter foam strength was selected to simulate the strength of the production foam at a temperature of -20 °F, assuming the temperature at the time of the certification tests would be approximately 75 °F. A permissible variation in CTA-2 foam temperature of ±15 °F was selected to ensure that cold conditions were adequately simulated. At the time of each drop test, foam temperatures were measured by a thermometer inserted through a hole in the plastic burn out plugs, approximately 2 in. deep into the foam.

Weight
The weight of the completely assembled CTA-2, including impact limiter and simulated payload, was 9,380 pounds. This is only 2.3% below the value of 9,600 pounds used in calculations and had no significant effect on any CTA-2 response. The weight of the completely assembled CTA-1 was 9,350 pounds.

2.10.15.3 Test Facilities. The test pad is located in the 300 Area of the Hanford Site. It is constructed of ASTM C 150, Type II cemented aggregate, having dimensions of 13 ft 6 in. by 18 ft 6 in. by 70 in. thick. The concrete foundation monolith is encased with #6 steel reinforcing bar on 6-in. centers and was poured on soil compacted to 95% of maximum density. It is topped by a steel plate 125 in. by 70 in. by 8-1/2 in. thick. The weight of the impact test pad, including the steel plate, is estimated at 110 short tons. This weight is far in excess of the minimum factor of ten times the dropped weight of approximately 5 tons.

The puncture bars were designed to be in compliance with the requirements of 10 CFR 71.73(c)(2). A short (24-in.) bar was used for all puncture drop tests except CTA-1 tests Nos. 17 through 19 and CTA-2 test No. 3, where a long (80-in.) puncture bar was used. The puncture bars were firmly welded at the lower end to a 2-in.-thick mounting plate, and fastened to a 2-in.-thick mounting pad using 1-3/4-in.-diameter bolts. The mounting pad was firmly welded to the test pad. Figures 2.10.15.3-1 and 2.10.15.3-2 show photographs of the puncture bars.

2.10.15.4 Test Results. The following sections provide details of the results of free drop and puncture testing. The tests using CTA-1 were conducted from July 25 to 27, 1994, in the 300 Area of the Hanford Site. The tests using CTA-2 were conducted in November, 1995 at the same location.

2.10.15.4.1 Drop Test Sequence. The second certification test series, which used CTA-2, consisted of a series of four sets of tests as described in document WHC-SD-RTG-TP-018. Each set of tests included as a minimum a 4-ft free drop, a 30-ft free drop and a 40-in. puncture test. The first set consisted of CTA-2 tests Nos. 1, 2 and 3; the second set consisted of CTA-2 tests Nos. 4, 5 and 6; the third set consisted of CTA-2 tests Nos. 7, 8 and 9; and the fourth set consisted of CTA-2 tests Nos. 10 through 16. Damage caused by each of these tests is described in Section 2.10.15.4.3.

After the first test set was completed, the OCV containment O-ring seal was leakage rate tested, the OCV closure bolt removal torques were recorded, and the OCV was removed. The ICV containment O-ring seal was leakage rate tested and the ICV closure bolt retention torques were checked. The OCV was then reinstalled and the O-ring seal was leakage rate tested. This series of inspections was also performed after the second test set.

At the conclusion of the third test set, the OCV containment seal O-ring was leakage rate tested, the OCV closure bolt removal torques were measured, and the ICV containment seal O-ring was leakage rate tested. The ICV closure bolt removal torques were measured and the ICV was disassembled. All interaction between the simulated payload and ICV was noted. The CTA-2 unit was then reassembled and during the assembly process the ICV and OCV O-ring seals and the ICV and OCV entire containment boundaries were leakage rate tested.

At the conclusion of the fourth and final set of tests, all closure bolt removal torques were checked and the OCV and ICV O-ring seals and containment boundaries were leakage rate tested. All test data recorded for the second certification test series is included on the data sheets at the end of this appendix.

The first certification test series, using CTA-1, consisted of one sequential and continuous set of 19 drops. This test series included five 4-ft free drops followed by five 30-ft free drops, which were in turn followed by nine 40-in. puncture tests. During the testing, the impact limiter corner weld failed, exposing an unacceptable amount of foam. Also, at the conclusion of the testing, the ICV bolts were found to be loose. Both of these anomalies were considered to be failures. The package design was subsequently modified and a second certification test article (CTA-2) was fabricated. All of the 4-ft and 30-ft free drops from the first certification drop test series were repeated for the second certification drop test series. Four of the nine puncture tests performed during the first drop test series were repeated during the second drop test series and two new puncture tests were added. The five puncture tests that were not repeated are included in this appendix for completeness. The location of those puncture tests and resultant damage to the package are independent of the design changes that occurred between CTA-1 and CTA-2. Also included for completeness is the accelerometer data that was obtained during the first test series.

2.10.15.4.2 Helium Leakage Rate Test Results. After completing the first and second sets of free drop and puncture tests, CTA-2 was leakage rate tested in accordance with the procedure outlined in document WHC-SD-RTG-TC-017, Rev. 1. After completing the third set of free drop and puncture tests, CTA-2 was leakage rate tested in accordance with the procedures outlined in documents WHC-SD-RTG-TC-016, Rev. 1 and WHC-SD-RTG-TC-017, Rev. 1. After completing the fourth and final set of free drop and puncture tests, CTA-2 was leakage rate tested in accordance with procedure WHC-SD-RTG-016, Rev. 1.

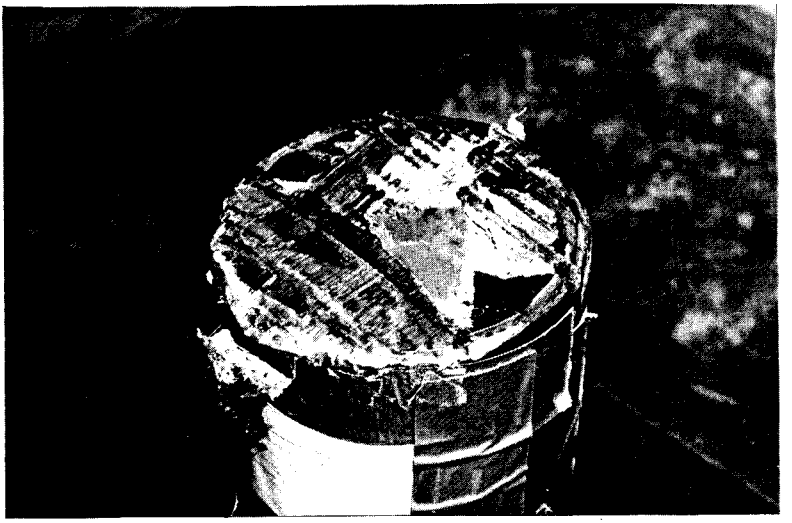


FIGURE 2.10.15.3-1. Short (24-in.) Puncture Bar.

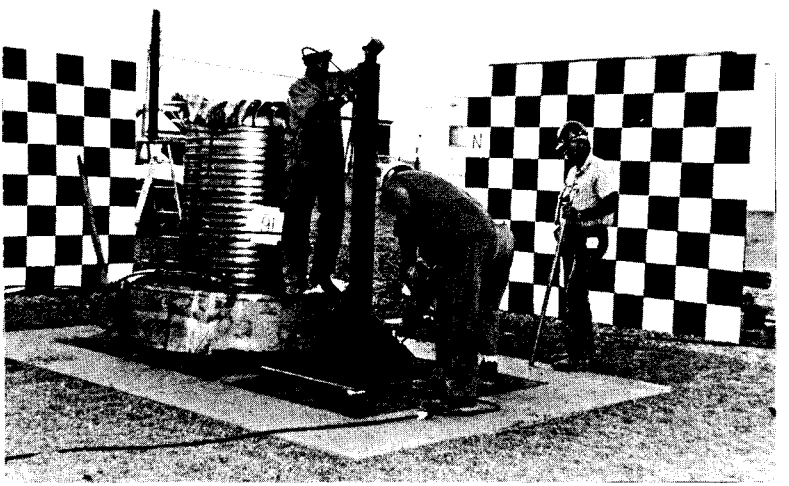


FIGURE 2.10.15.3-2. Long (80-in.) Puncture Bar.

BEST COPY AVAILABLE

Measured leakage rates (as air) for each set of drop tests are given in Tables 2.10.15.4.2-1 through 2.10.15.4.2-4 below. Note that the original leakage rate test data is for helium, the medium used in the testing. The rate for air is calculated by dividing the rate for helium by a factor of 2.6. The Westinghouse NDE Leak Test Procedure and Test Reports are attached to the end of this section.

TABLE 2.10.15.4.2-1. Containment Vessel Leakage Rate Test Results, After First Set of Drop Tests.

Test location	Leakage rate, scc/sec (Air)	
	OCV	ICV
Primary closure O-ring seal	No detectable rate	No detectable rate
Containment boundary	Not applicable	Not applicable
Primary vent port	No detectable rate	No detectable rate
Secondary vent port	Not applicable	No detectable rate
Total vessel	Not applicable	Not applicable

TABLE 2.10.15.4.2-2. Containment Vessel Leakage Rate Test Results, After Second Set of Drop Tests.

Test location	Leakage rate, scc/sec (Air)	
	OCV	ICV
Primary closure O-ring seal	No detectable rate	No detectable rate
Containment boundary	Not applicable	Not applicable
Primary vent port	No detectable rate	No detectable rate
Secondary vent port	Not applicable	No detectable rate
Total vessel	Not applicable	Not applicable

TABLE 2.10.15.4.2-3. Containment Vessel Leakage Rate Test Results, After Third Set of Drop Tests.

Test location	Leakage rate, scc/sec (Air)	
	OCV	ICV
Primary closure O-ring seal	No detectable rate	No detectable rate
Containment boundary	$5.5(10^{-8})$	$7.5(10^{-8})$
Primary vent port	$3.8(10^{-10})$	No detectable rate
Secondary vent port	Not applicable	No detectable rate
Total vessel	$5.5(10^{-8})$	$7.5(10^{-8})$

TABLE 2.10.15.4.2-4. Containment Vessel Leakage Rate Test Results, After Fourth Set of Drop Tests.

Test location	Leakage rate, scc/sec (Air)	
	OCV	ICV
Primary closure O-ring seal	No detectable rate	No detectable rate
Containment boundary	$4.35(10^{-8})$	$8.3(10^{-8})$
Primary vent port	No detectable rate	No detectable rate
Secondary vent port	Not applicable	No detectable rate
Total vessel	$4.35(10^{-8})$	$8.3(10^{-8})$

The criterion for a leaktight condition is a leakage rate of $1.0(10^{-7})$ scc/sec of air. Thus, both levels of containment are leaktight, in satisfaction of the requirements of 10 CFR 71.

2.10.15.4.3 Localized Deformation Results and Photographs. Descriptions of the damage sustained by CTA-2 caused by each free drop and puncture event, including photographs, are given below. Actual data sheets used at the drop site to record damage are given in Section 2.10.15.5. Descriptions and photographs of the damage sustained by CTA-1 from the puncture events is also included. Drop orientations are fully described in Appendix 2.10.9.

CTA-2 first set of drop tests.

CTA-2 Test No. 1. The CTA-2 was oriented bottom-down at 10° from the vertical and the drop height was 4 ft. A small amount of damage to the impact limiter was caused by this drop. The most notable damage was a very slight bulge on the side of the impact limiter. See Figures 2.10.15.4.3-1 and 2.10.15.4.3-2.

CTA-2 Test No. 2. The CTA-2 was oriented bottom-down at 10° from the vertical and the drop height was 30 ft. As with the 4-ft version of this drop, the initial point of impact was located at 75° clockwise (CW) (when viewed from above) from the electrical feed-through. The damage to the impact limiter was similar to that incurred during the 4-ft drop, but of a greater magnitude. See Figures 2.10.15.4.3-3 and 2.10.15.4.3-4.

CTA-2 Test No. 3. This was a 40-in. puncture test with the CTA-2 oriented top-down and the point of impact was located on the outer top surface of the impact limiter. The impact circumferential location was next to the loosest impact limiter bolt (Bolt #7), which was 75° CW (when viewed from above) from the electrical feed-through location. The long (80-in.) puncture bar was used. The resulting dent was 5/16 in. deep and there was no evidence of any movement of the impact limiter relative to the test article. See Figure 2.10.15.4.3-5.

At the conclusion of the first set of drop tests using the CTA-2 unit, the following inspections/leakage rate tests were performed.

- Impact limiter bolt removal torques and lengths
- OCV containment O-ring seal leakage rate test
- OCV closure bolt removal torques and lengths
- ICV containment O-ring seal leakage rate test

. ICV closure bolt retention torques.

The data sheets for each of these operations are included at the end of this appendix. In summary, one impact limiter bolt stretched approximately 0.023 in., the OCV closure bolts did not lose any torque and did not stretch, the OCV and ICV containment O-rings were leaktight, and the ICV closure bolt torque values were higher than the retention check torque of 78 ft-lb.

Once these inspections were completed, the ICV closure bolts were retorqued to their original pre-test value, the ICV containment O-ring seal was leakage rate tested, the OCV was reassembled, the OCV containment O-ring seal was leakage rate tested, and the impact limiter was reinstalled using new attachment bolts. It was noted that the torque wrench did not move when the pre-test torque was applied to the ICV closure bolts. This was a good indication that the bolts had retained all of their pre-test torque values.

CTA-2 second set of drop tests.

CTA-2 Test No. 4. This was a bottom-down, c.g.-over-corner, 4-ft free drop. The CTA-2 was oriented so that the impact was directed at the electrical feed-through. This drop produced an oval-shaped damaged area that was approximately 2 ft long. No cracking of the impact limiter corner joints was observed. See Figures 2.10.15.4.3-6 and 2.10.15.4.3-7.

CTA-2 Test No. 5. This was a repeat of CTA-2 Test No. 4 except the drop height was 30 ft. The eye-shaped damage area was 42 in. long and 18 in. wide and caused a total crush depth of 5.5 in. The impact limiter corner joint welds remained intact and did not crack. See Figures 2.10.15.4.3-8 and 2.10.15.4.3-9.

CTA-2 Test No. 6. This was a 40-in. puncture test directed at the damage created by the c.g.-over-bottom impact limiter corner free drops (CTA-2 Tests No. 4 and No. 5). The impact with the puncture bar caused a localized 10-in.-wide-by-1.7-in.-deep indentation on the bottom surface of the impact limiter. No welds were cracked and the impact limiter outer shell material was not ruptured. See Figures 2.10.15.4.3-10 and 2.10.15.4.3-11.

At the conclusion of the second set of drop tests using the CTA-2 unit, the inspection/leakage rate tests that were performed after the first set of CTA-2 drop tests were repeated. The data sheets for these operations are included at the end of this appendix. In summary, no impact limiter bolts broke, no significant movement of the impact limiter relative to the OCV base occurred, the OCV closure bolts did not lose any torque and did not stretch, the OCV and ICV containment O-rings were leaktight, and the ICV closure bolt torque values were higher than the retention check torque of 78 ft-lb.

Once the inspections were completed, the same reassembly procedure as performed after the first set of tests was completed. New impact limiter attachment bolts were installed.

CTA-2 third set of drop tests.

CTA-2 Test No. 7. This was a 4-ft, bottom-down, flat-on-end free drop. This drop caused only slight changes to the previous damage done to the impact limiter. See Figure 2.10.15.4.3-12.

CTA-2 Test No. 8. This was a repeat of CTA-2 Test No. 7 except the drop height was 30 ft. This drop caused a flattening of the previous deformations that protruded from the bottom of the impact limiter. See Figures 2.10.15.4.3-13 and 2.10.15.4.3-14.

CTA-2 Test No. 9. This was a 40-in. puncture test with the edge of the puncture bar directed at the weld between the impact limiter side shell and the lower corner joint. The point of impact was located 75° CW (when viewed from above) from the electrical feed-through and was directed through the CTA-2 c.g. The resulting localized deformation was approximately 3.5 in. deep. There were no indications of cracking or any other weld failure. Also, the impact limiter sidewall was not breached. See Figure 2.10.15.4.3-15.

At the conclusion of the third set of drop tests on the CTA-2 unit, the entire test article was disassembled and inspected. The OCV and ICV closure bolt removal torques and lengths were recorded, the OCV and ICV containment O-ring seals were leakage rate tested, and the OCV and ICV entire containment boundaries were leakage rate tested. The data obtained from these operations is included at the end of this appendix. In summary, no impact limiter bolts broke, no significant movement of the impact limiter relavent to the OCV base occurred, the OCV and ICV closure bolts retained all of their pre-test torque, and the OCV and ICV O-ring seals were leaktight. The OCV and ICV structural (non-O-ring) containment boundaries were also leaktight (5.5×10^{-8}/scc/sec, air and 7.5×10^{-8}/scc/sec, air respectively).

It was noted that the majority of the ICV closure bolt washers were fractured. The fractured washers did not cause the ICV closure bolts to loosen. The significance of the fractured washers is discussed in Section 2.10.15.4.7. New ICV closure bolt washers were installed prior to the last set of drop tests. New ICV and OCV containment O-ring seals were also installed.

CTA-2 fourth set of drop tests. The fourth and final set of drop tests using the CTA-2 unit consisted of seven separate tests as listed below.

CTA-2 Test No. 10. This was a 4-ft, side-slap-down free drop. The point of impact was 90° CCW from the electrical feed-through when viewed from above the CTA-2. The CTA-2 axis was oriented at 18° from the horizontal and the fins contacted the drop pad first. Three fins were distorted but there was no other contact with the top of the test article. The side of the impact limiter was flattened slightly. No impact limiter welds cracked or showed any other sign of failure. See Figures 2.10.15.4.3-16 and 2.10.15.4.3-17.

CTA-2 Test No. 11. This was a 4-ft, top-end-down, flat-on-end free drop. This drop resulted in a uniform flattening of the CTA-2 fins. The personnel shield was only slightly damaged and still intact. See Figure 2.10.15.4.3-18.

CTA-2 Test No. 12. This was a repeat of CTA-2 Test No. 10, except the drop height was 30 ft. As with the 4-ft version of this drop, the primary impact was at the top of the test article. The impact caused minor cracking of the fin and upper coolant jacket welds that were directly beneath the point of impact. The damage to the impact limiter was a flat area 32 in. long at the top that tapered to negligible damage at the bottom. The depth of crush was 4.0 in. radially inward at the top of the impact limiter and a negligible amount at the bottom. See Figures 2.10.15.4.3-19 and 2.10.15.4.3-20.

CTA-2 Test No. 13. This was a 30-ft, top-end-down, flat-on-end free drop. The fins and personnel barrier collapsed until the OCV head contacted the drop test pad. See Figures 2.10.15.4.3-21 and 2.10.15.4.3-22. The top cover screen on the personnel barrier was removed after this test.

CTA-2 Test No. 14. This was a 40-in. puncture test with the puncture bar normal to the OCV sidewall through the CTA-2 c.g. The test article was oriented with the electrical feed-through down. The resulting dent depth in the coolant jacket was slightly under 1 in. The ICV sidewall had a dent 3/8 in. in depth. See Figures 2.10.15.4.3-23 and 2.10.15.4.3-24.

CTA-2 Test No. 15. The CTA-2 was oriented top-down at 9° from vertical so that the puncture bar would contact the unreinforced area of the OCV head. The drop height between the puncture bar and the OCV head was 45 in. to simulate conservatively a 40-in. puncture drop onto the personnel barrier screen. The OCV head dent depth was approximately 1-1/4 in. See Figure 2.10.15.4.3-25.

CTA-2 Test No. 16. This was a 40-in. puncture test that was directed at the center line of one of the impact limiter plastic melt plugs. The puncture bar was directed through the CTA-2 c.g. and 120° CW from the electrical feed-through location. The impact caused the upper weld around the plastic melt plug holder to fail, which in turn allowed the sidewall of the impact limiter to rip open a small amount. The opening in the impact limiter sidewall was approximately 8-3/4 in. long and varied in width from 0 to 1-1/4 in. The total amount of exposed impact limiter foam was estimated to be 12.7 in^2. See Figure 2.10.15.4.3-26. This small amount of exposed foam has no effect on the package's ability to withstand the HAC fire (see Section 3.5).

CTA-1 puncture tests. As noted in Section 2.10.15.1, five of the nine puncture tests performed on the CTA-1 unit were not repeated during the second certification test series, which used the CTA-2 unit. For completeness, the results of these five CTA-1 puncture tests are included below.

CTA-1 Test No. 12. The 40-in. puncture was performed on the bottom of the impact limiter, through the CTA-1 c.g., and located on the low-density foam next to the joint with the high-density foam. The initial impact was 20 in. from the impact limiter center, with the corner of the puncture bar contacting first. The resulting dent was 2-1/2 in. deep, with a surrounding damage area 15 in. in diameter. The puncture bar did not penetrate the impact limiter shell, and there were no signs of impending rupture in the damaged area. There was also a smaller, secondary impact. See Figures 2.10.15.4.3-27 and 2.10.15.4.3-28.

CTA-1 Test No. 13. This 40-in. puncture was directed through the CTA-1 c.g. onto the impact limiter side shell, in line with the OCV vent port. The resulting dent was 3 in. deep, with a surrounding damage area 15 in. in diameter. The puncture bar did not penetrate the impact limiter shell, and there were no signs of impending rupture in the damaged area. Further, the OCV vent port was leaktight after testing. See Figures 2.10.15.4.3-29 and 2.10.15.4.3-30.

CTA-1 Test No. 15. This 40-in. puncture using CTA-1 was similar to CTA-2 Test No. 14, except with the puncture bar at an oblique (45°) angle to the OCV surface. The puncture bar contacted the coolant jacket at 45° CCW from the electrical feed-through, directed through the CTA-1 c.g. The maximum dent depth was 1-1/2 in. The ICV sidewall had a dent 0.22 in. in depth. The coolant jacket ribs were heavily damaged, but no damage (other than inward deformation) occurred to the OCV sidewall. See Figures 2.10.15.4.3-31 and 2.10.15.4.3-32.

CTA-1 Test No. 18. This 40-in. puncture was directed at the thermal shield of the OCV. The 80-in.-long puncture bar was used, and contacted the top of the thermal shield 1 in. inboard from its outside edge and 30° CCW from the electrical feed-through. The CTA-1 was oriented at 30° from the vertical. The resulting dent was 1-1/4 in. deep at its center and of lesser depth elsewhere. The surrounding damaged area in the thermal shield was 7 in. wide. Some damage was inflicted on the adjacent portion of the coolant jacket. Also, the upper relief valve nipple was crushed by secondary impact with the puncture bar. See Figures 2.10.15.4.3-33 and 2.10.15.4.3-34.

CTA-1 Test No. 19. The last puncture using CTA-1 was directed at an impact limiter bolt

access tube. The CTA-1 was oriented vertically, and the puncture bar contacted the bolt access tube located 330° CCW from the electrical feed-through. The 80-in.-long puncture bar was used. Portions of two adjacent OCV closure bolt access tubes were also impacted. The closure bolt access tubes buckled from the impact. The maximum deformation of the thermal shield was 3/4 in. Also, one of the coolant jacket nipples was crushed by secondary impact with the puncture bar. See Figures 2.10.15.4.3-35 and 2.10.15.4.3-36.

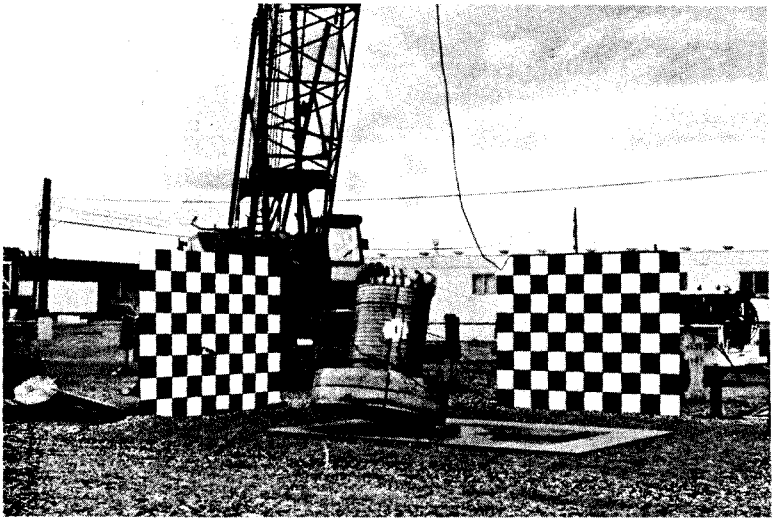


FIGURE 2.10.15.4.3-1. CTA-2 Drop No. 1, 4-ft, 10° from Vertical.

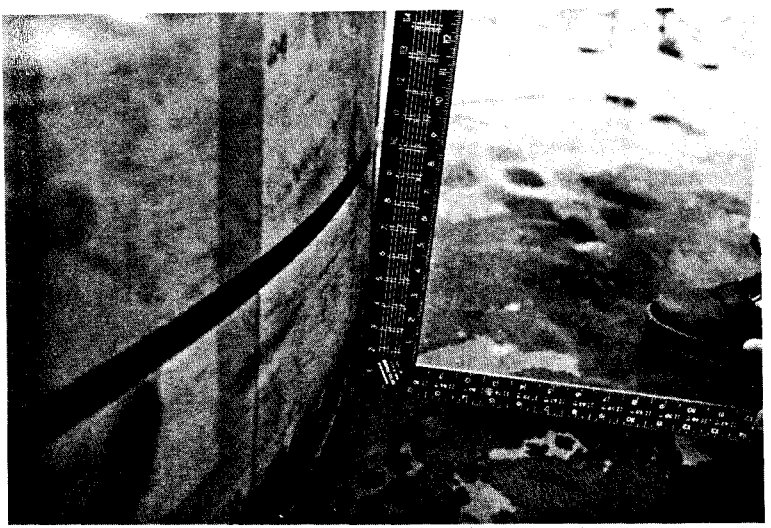


FIGURE 2.10.15.4.3-2. CTA-2 Drop No. 1, 4-ft, 10° from Vertical. Side View of Drop Damage.

BEST COPY AVAILABLE

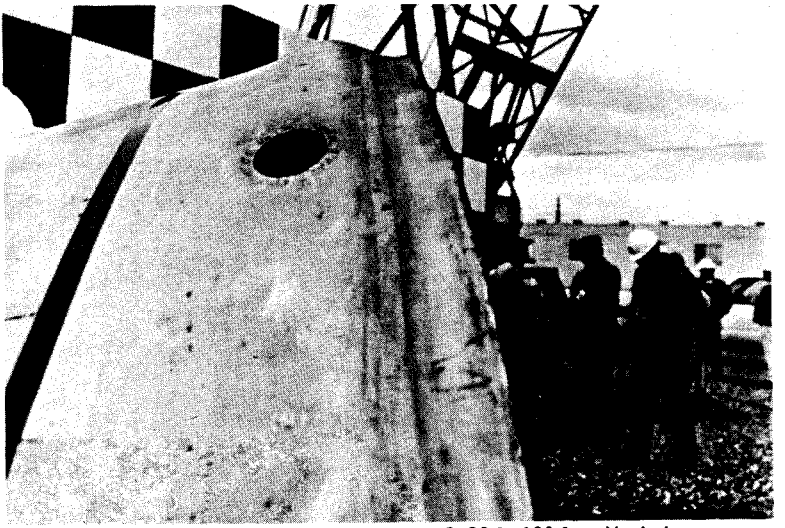


FIGURE 2.10.15.4.3-3. CTA-2 Drop No. 2, 30-ft, 10° from Vertical.

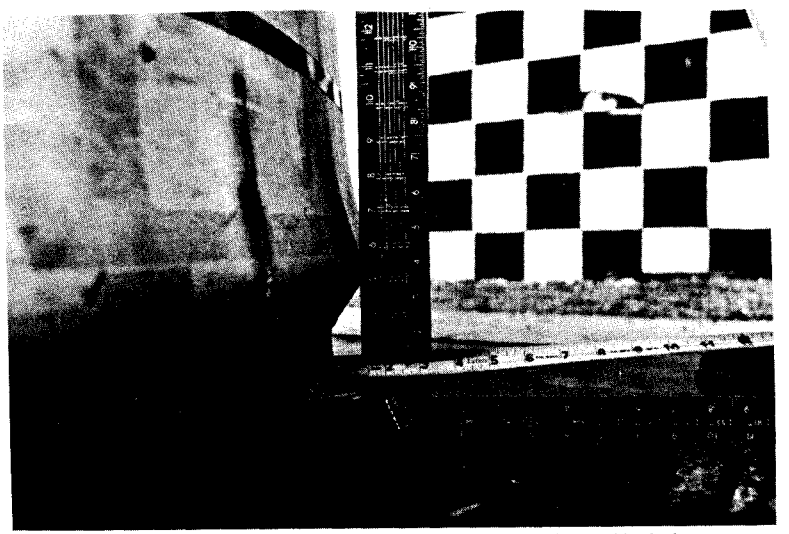


FIGURE 2.10.15.4.3-4. CTA-2 Drop No. 2, 30-ft, 10° from Vertical.

BEST COPY AVAILABLE



FIGURE 2.10.15.4.3-5. CTA-2 Drop No. 3, 40-in. Puncture, Top-down on Impact Limiter Edge.

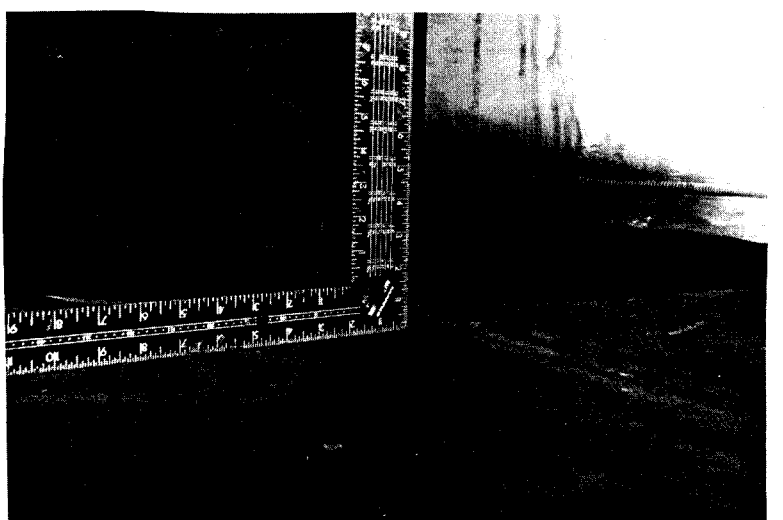


FIGURE 2.10.15.4.3-6. CTA-2 Drop No. 4, 4-ft, C.G. over Impact Limiter Bottom Corner.

BEST COPY AVAILABLE

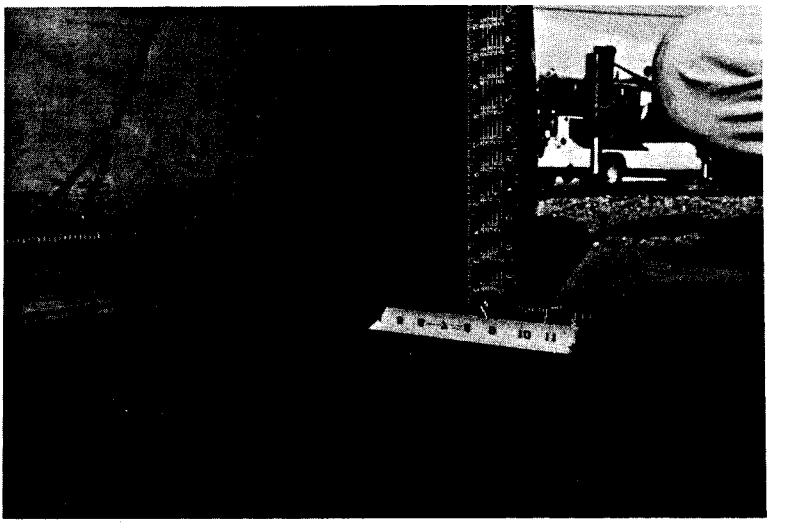


FIGURE 2.10.15.4.3-7. CTA-2 Drop No. 4, 4-ft, C.G. over Impact Limiter Bottom Corner.

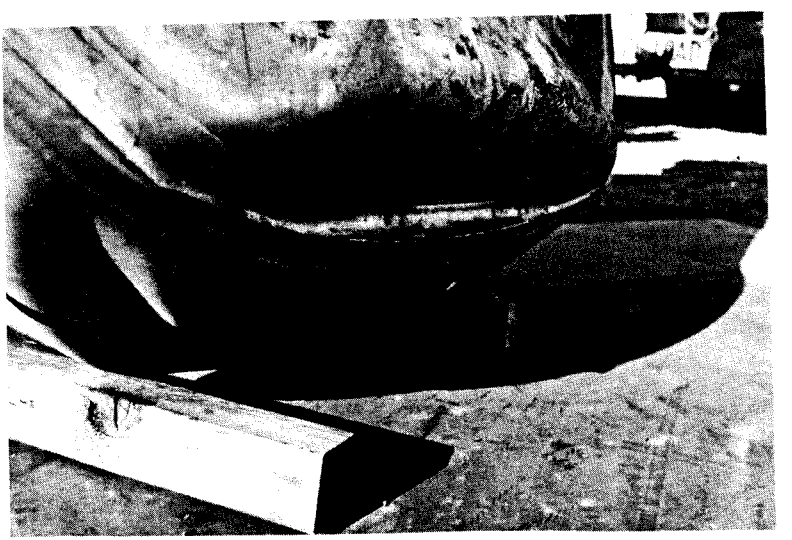


FIGURE 2.10.15.4.3-8. CTA -2 Drop No. 5, 30-ft, C.G. over Impact Limiter Bottom Corner.

BEST COPY AVAILABLE

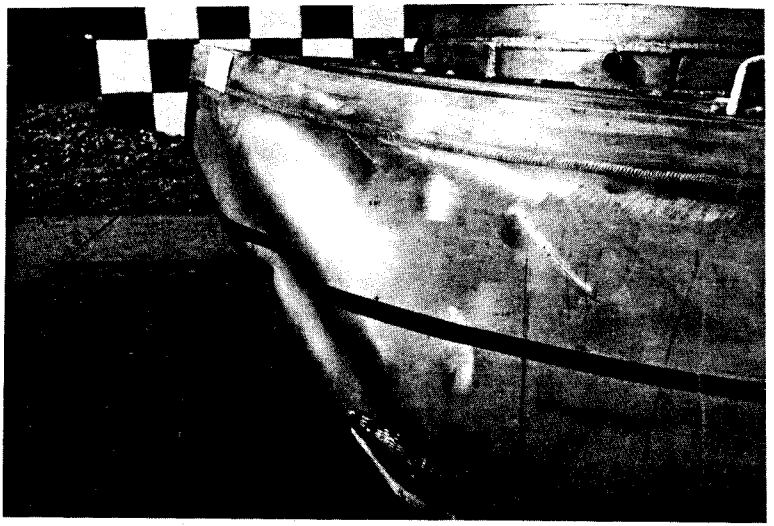


FIGURE 2.10.15.4.3-9. CTA-2 Drop No. 5, 30-ft, C.G. over Impact Limiter Bottom Corner.

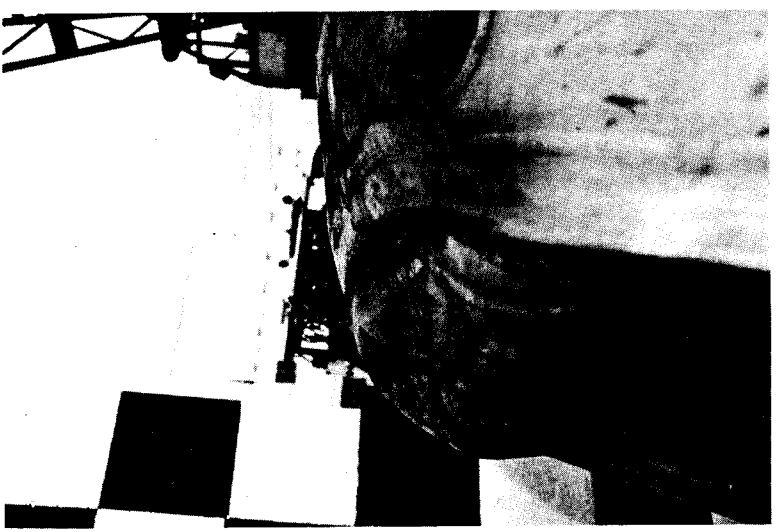


FIGURE 2.10.15.4.3-10. CTA-2 Drop No. 6, 40-in. Puncture on Previous C.G.-over-corner Damage.

BEST COPY AVAILABLE

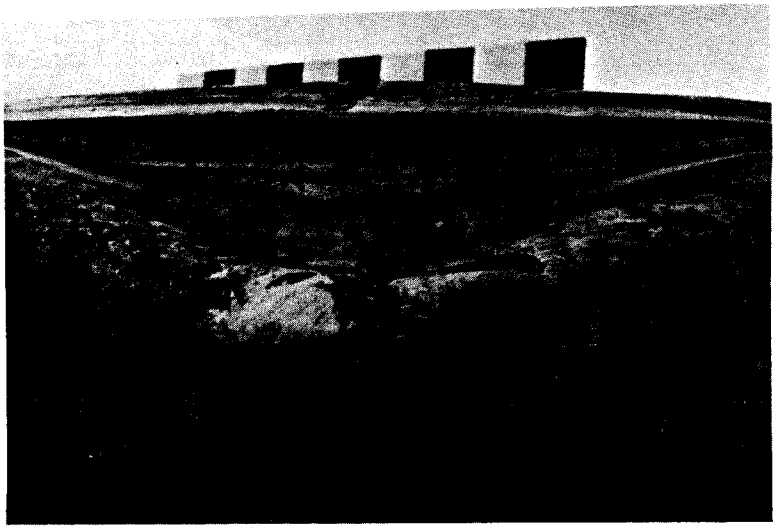


FIGURE 2.10.15.4.3-11. CTA-2 Drop No. 6, 40-in. Puncture on Previous C.G.-over-corner Damage.

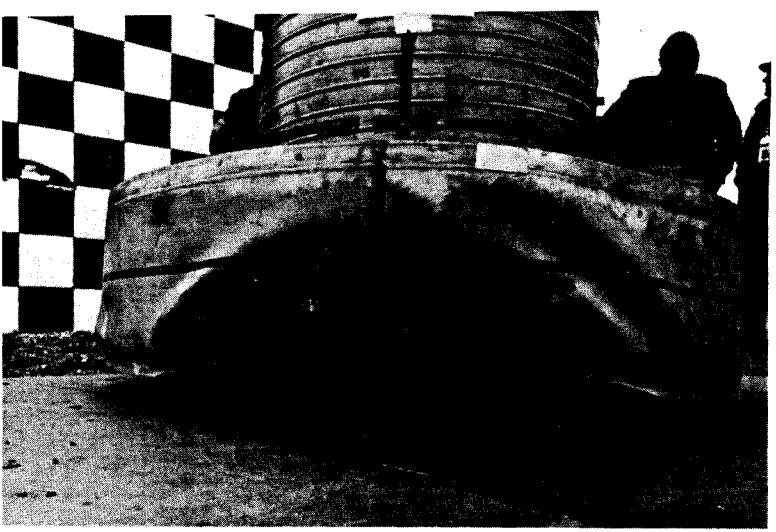


FIGURE 2.10.15.4.3-12. CTA-2 Drop No. 7, 4-ft, Bottom End Down.

BEST COPY AVAILABLE

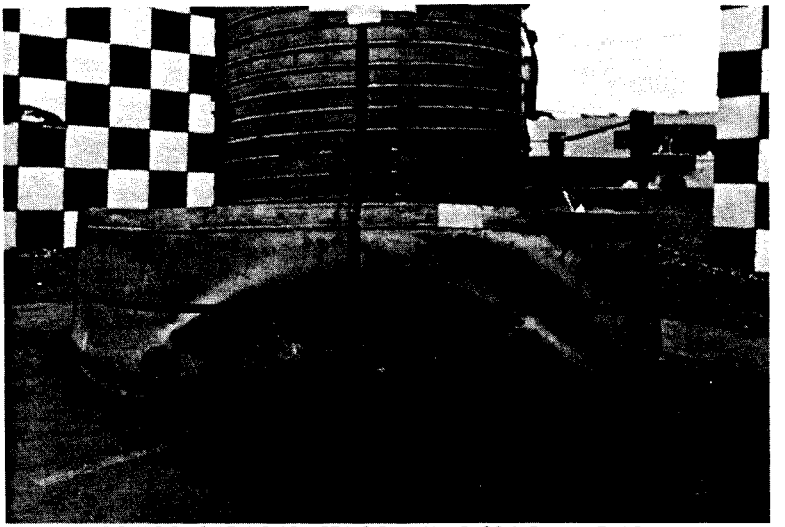


FIGURE 2.10.15.4.3-13. CTA-2 Drop No. 8, 30-ft Bottom End Drop.

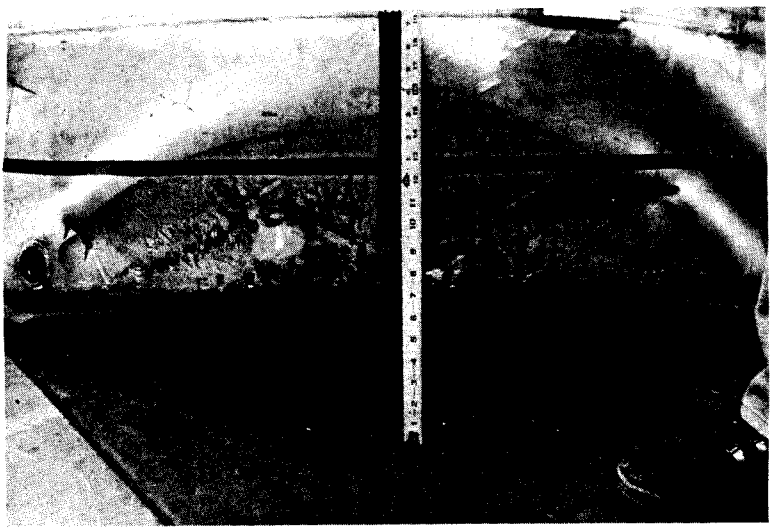


FIGURE 2.10.15.4.3-14. CTA-2 Drop No. 8, 30-ft, Bottom End Drop.

BEST COPY AVAILABLE

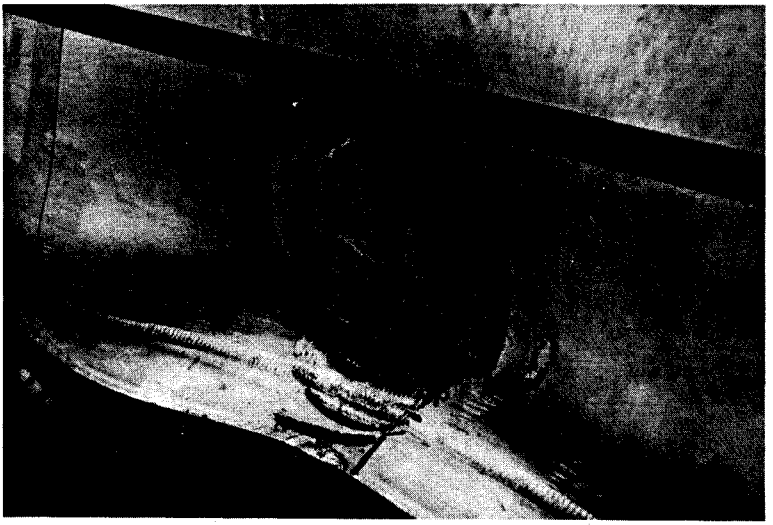


FIGURE 2.10.15.4.3-15. CTA-2 Drop No. 9, 40-in. Puncture at Impact Limiter Lower Corner Weld.

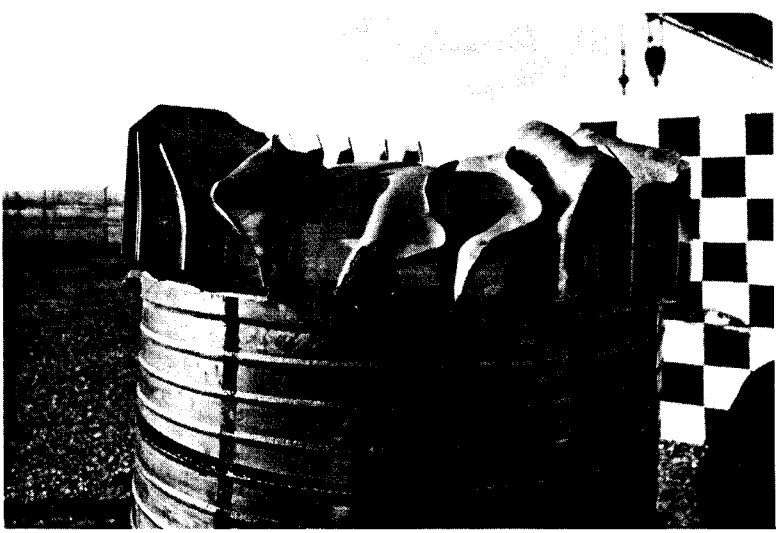


FIGURE 2.10.15.4.3-16. CTA-2 Drop No. 10, 4-ft, Side Slapdown, Showing View of Primary Impact.

BEST COPY AVAILABLE

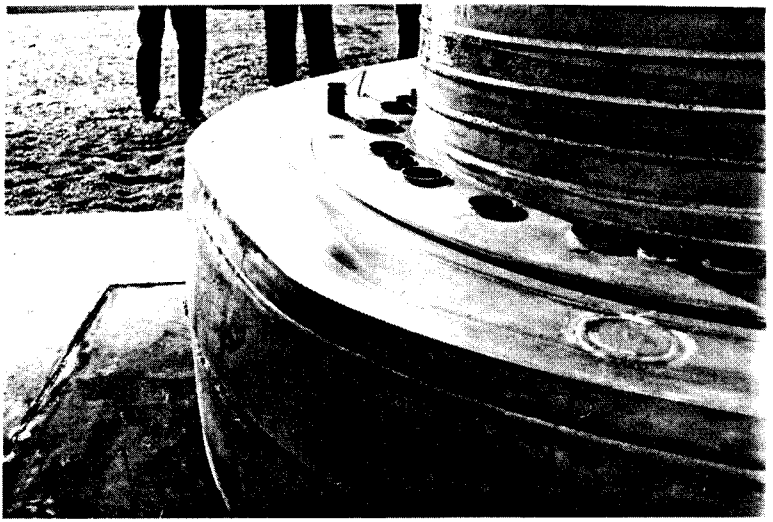


FIGURE 2.10.15.4.3-17. CTA-2 Drop No. 10, 4-ft, Side Slapdown, Showing View of Secondary Impact.

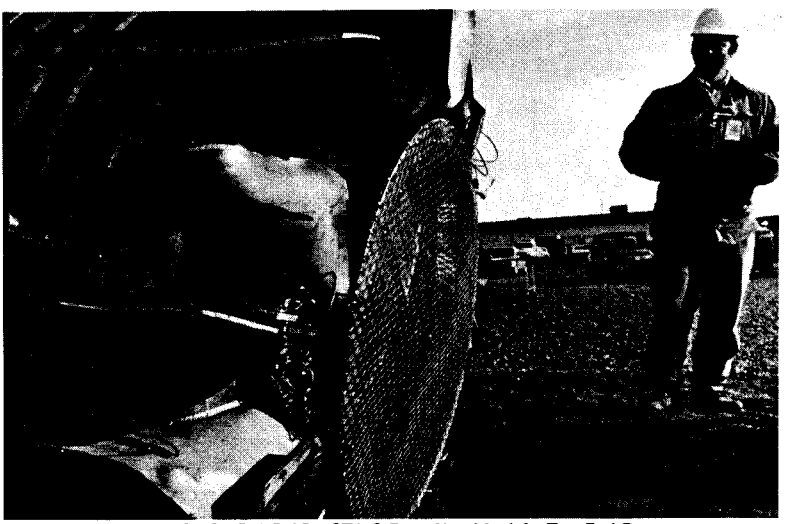


FIGURE 2.10.15.4.3-18. CTA-2 Drop No. 11, 4-ft, Top End Down.

BEST COPY AVAILABLE

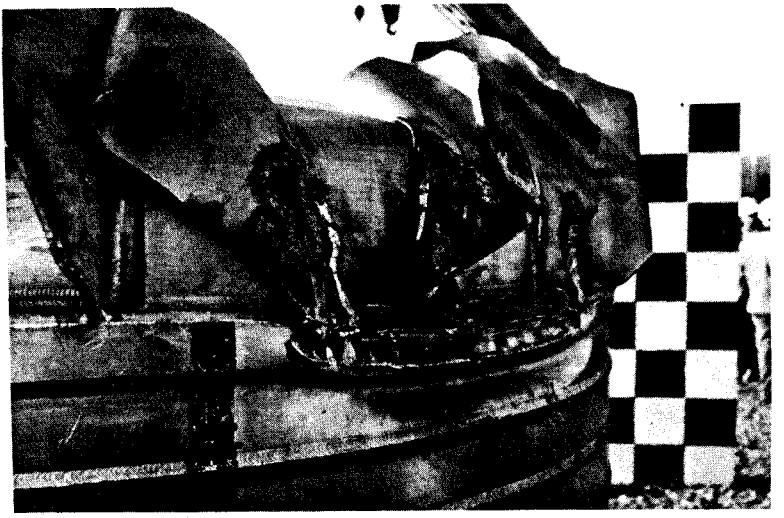


FIGURE 2.10.15.4.3-19. CTA-2 Drop No. 12, 30-ft, Side Slapdown, Showing View of Primary Impact.

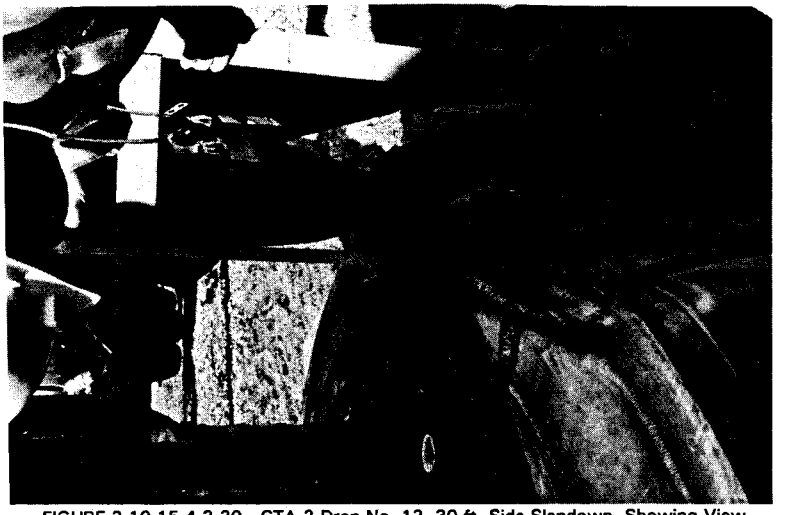


FIGURE 2.10.15.4.3-20. CTA-2 Drop No. 12, 30-ft, Side Slapdown, Showing View of Secondary Impact.

BEST COPY AVAILABLE

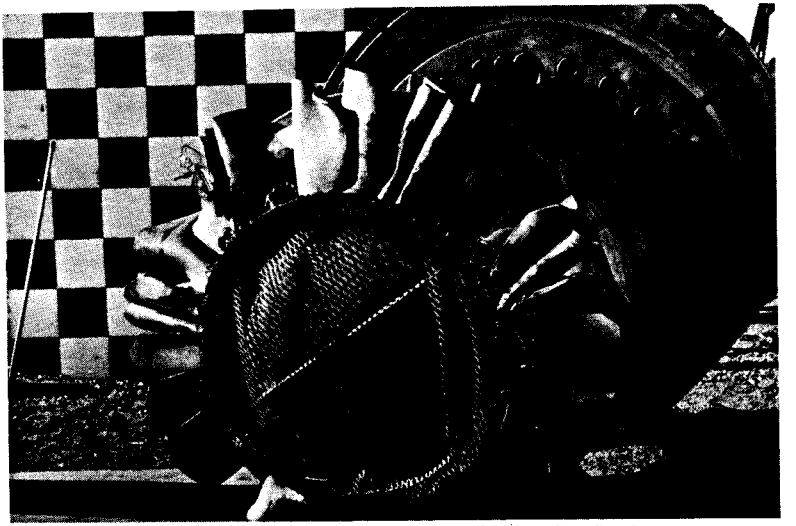


FIGURE 2.10.15.4.3-21. CTA-2 Test No. 13, 30-ft, Top End Down.

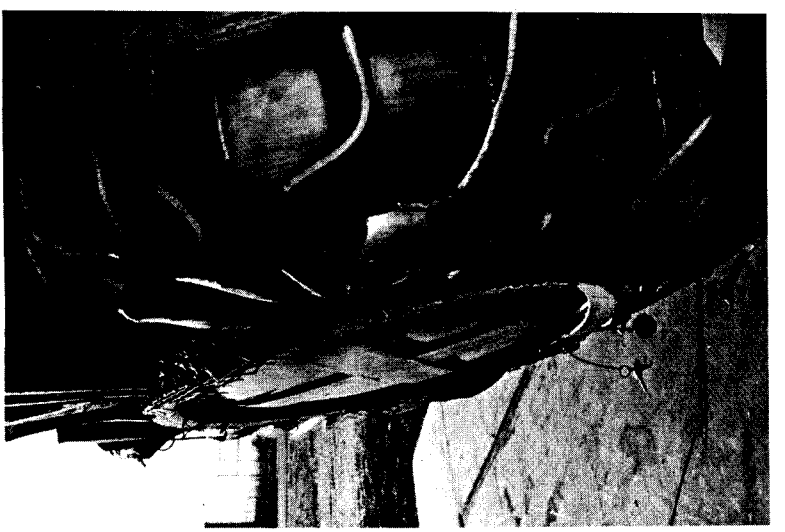


FIGURE 2.10.15.4.3-22. CTA-2 Test No. 13, 30-ft, Top End Down.

BEST COPY AVAILABLE



FIGURE 2.10.15.4.3-23. CTA-2 Test No. 14, 40-in. Puncture on Side of Package Through C.G.

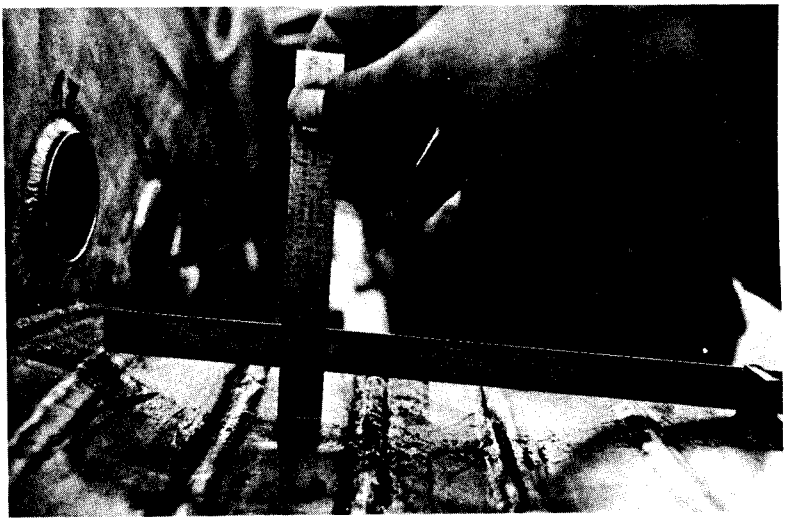


FIGURE 2.10.15.4.3-24. CTA-2 Test No. 14, 40-in. Puncture Showing Closeup of Damage.

BEST COPY AVAILABLE



FIGURE 2.10.15.4.3-25. CTA-2 Test No. 15, 40-in. Puncture, Top End Down.



FIGURE 2.10.15.4.3-26. CTA-2 Test No. 16, 40-in. Puncture Directed at Impact Limiter Melt Plug.

BEST COPY AVAILABLE

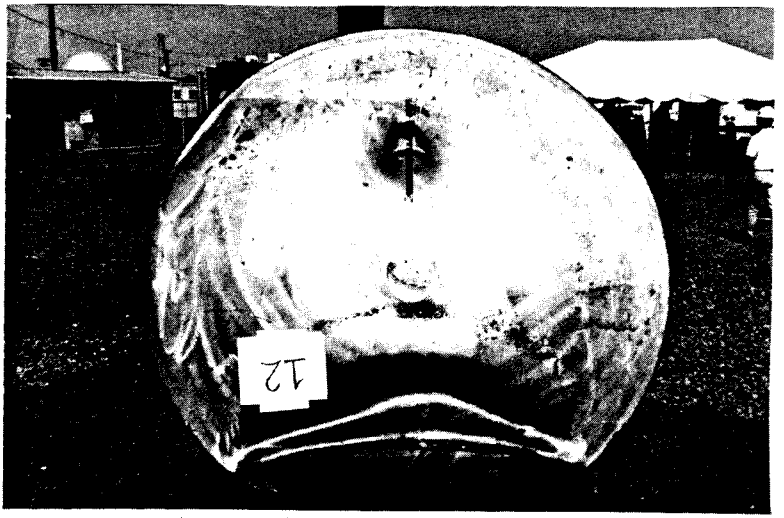


FIGURE 2.10.15.4.3-27. CTA-1 Test No. 12, 40-in. Puncture, C.G. over Foam Transition.

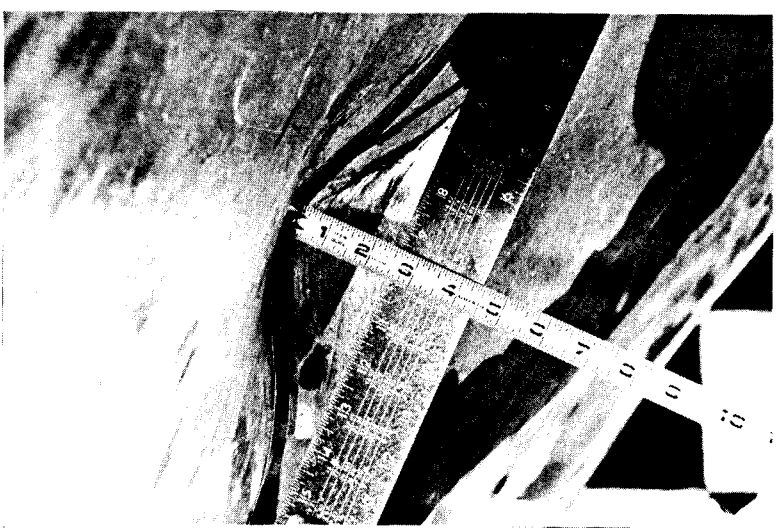


FIGURE 2.10.15.4.3-28. CTA-1 Test No. 12, 40-in. Puncture Showing Closeup of Damage.

BEST COPY AVAILABLE

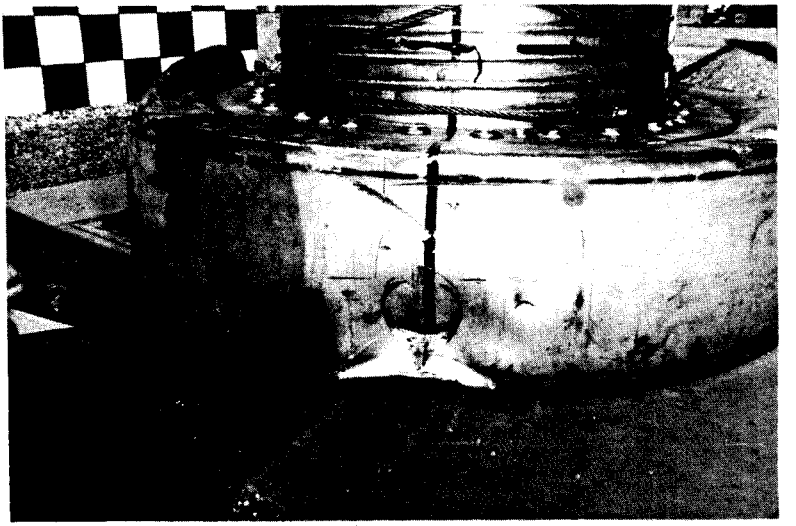


FIGURE 2.10.15.4.3-29. CTA-1 Test No. 13, 40-in. Puncture on Side of Limiter, C.G. over Seal Test Port.

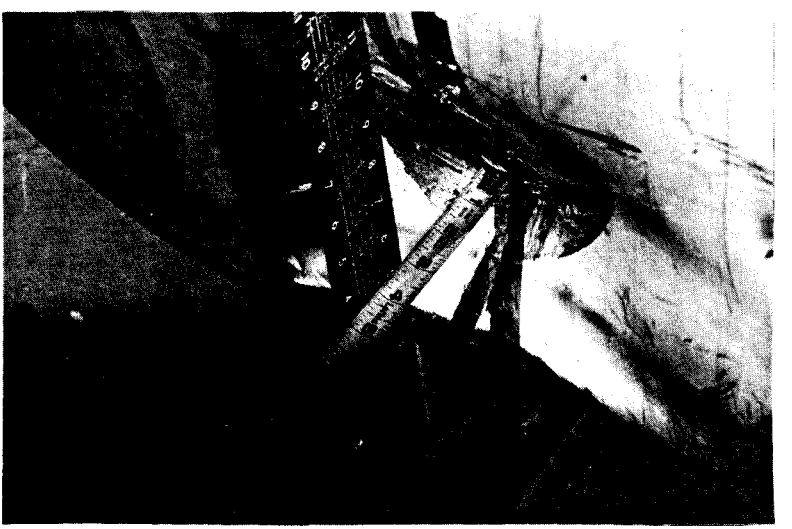


FIGURE 2.10.15.4.3-30. CTA-1 Test No. 13, 40-in. Puncture Showing Closeup of Damage.

BEST COPY AVAILABLE

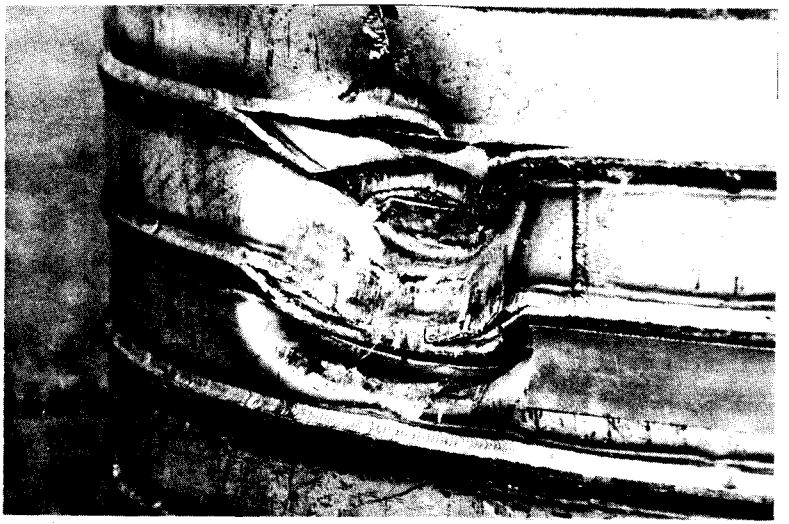


FIGURE 2.10.15.4.3-31. CTA-1 Test No. 15, 40-in. Puncture Oblique to Package Side Through C.G.

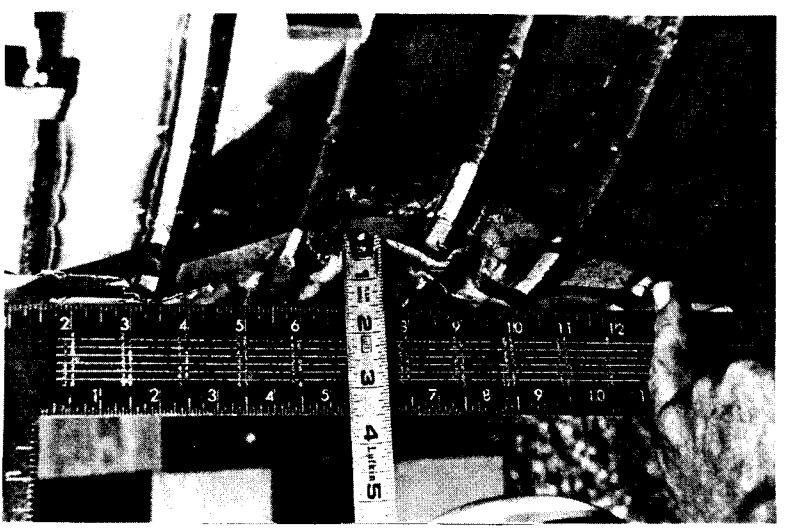


FIGURE 2.10.15.4.3-32. CTA-1 Test No. 15, 40-in. Puncture Showing Closeup of Damage. Note: Picture was rotated CCW.

BEST COPY AVAILABLE

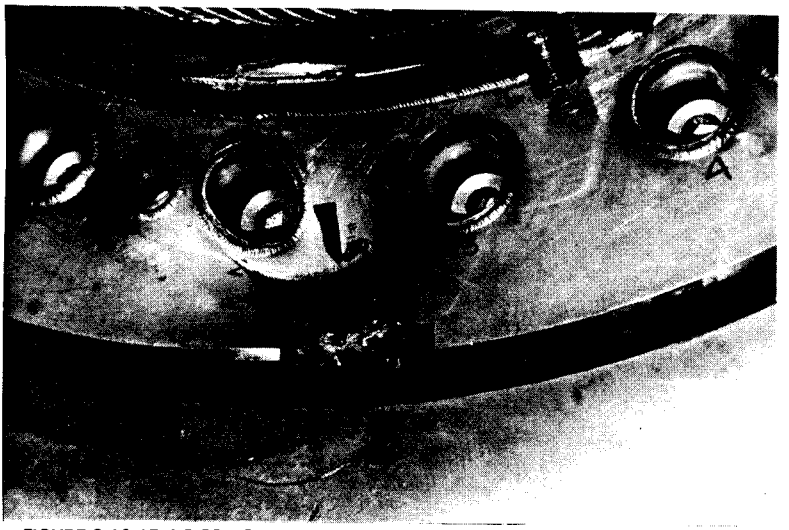


FIGURE 2.10.15.4.3-33. CTA-1 Test No. 18, 40-in. Puncture, Top End Down, Oblique on Top of Thermal Shield.

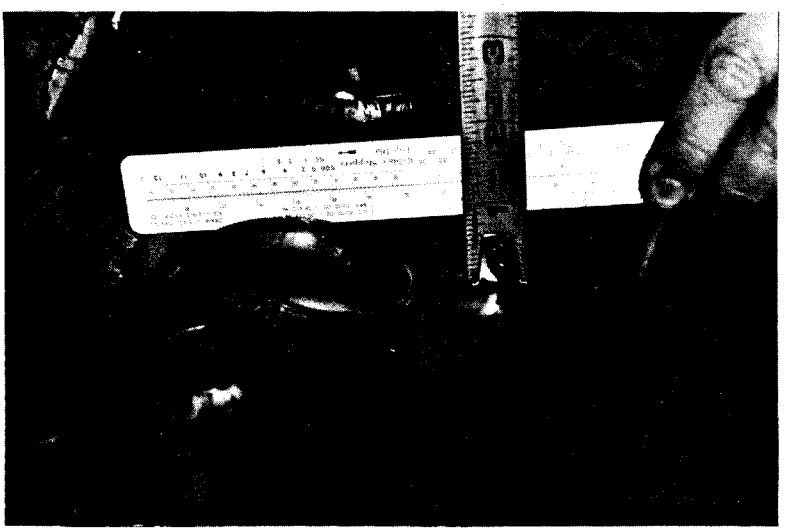


FIGURE 2.10.15.4.3-34. CTA-1 Test No. 18, 40-in. Puncture, Showing Closeup of Damage.

BEST COPY AVAILABLE

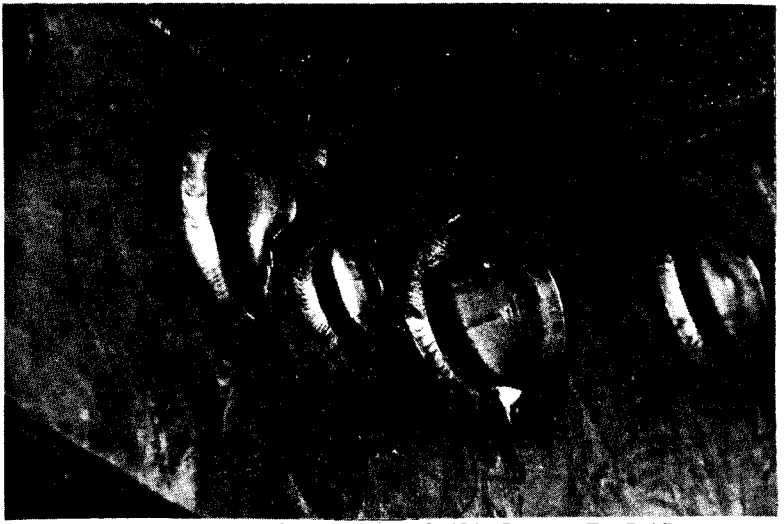


FIGURE 2.10.15.4.3-35. CTA-1 Test No. 19, 40-in. Puncture, Top End Down, Vertical on Impact Limiter Bolt Tube.

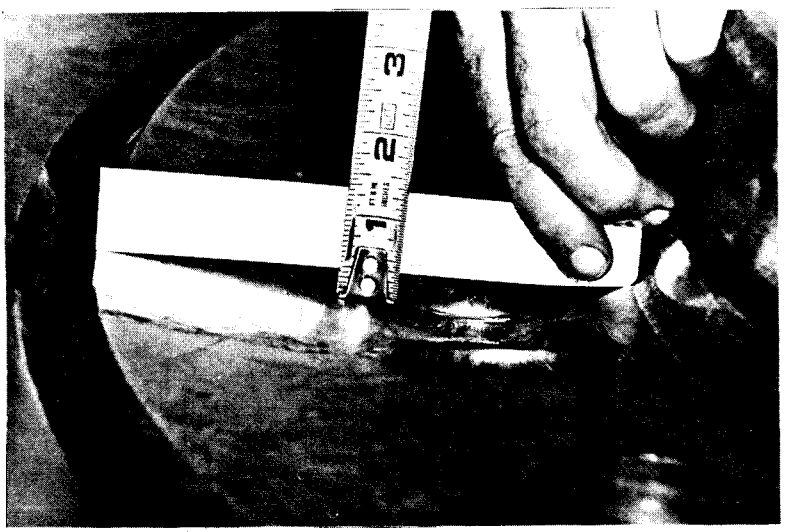


FIGURE 2.10.15.4.3-36. CTA-1 Test No. 19, 40-in. Puncture Showing Closeup of Damage.

BEST COPY AVAILABLE

2.10.15.4.4 Accelerometer Results. During the first certification drop test series, CTA-1 was instrumented with active and passive accelerometers. (CTA-1 was not instrumented for the puncture drops.) Accelerometer instrumentation was not used during the second certification test series, which used CTA-2. For completeness, the instrumentation set-up, filtering, and data reduction from the first certification test series are given in the sections below.

2.10.15.4.4.1 System Configuration and Data Acquisition. Because of the compact shape of the RTG package, the rigid body impact at the center of gravity of the package was the parameter of primary interest. For this reason, most of the transducers (and passive indicators) were located at or near the c.g. of CTA-1. A triaxial set of accelerometers was also located at 30 in. above the c.g. to measure package rotations.

Active accelerometers were mounted as shown in Figure 2.10.15.4.4.1-1. There were nine channels of data from three triaxial sets. The axes of measurement, relative to CTA-1, were axial, radial, and circumferential. Set "a" was located at the height of the c.g. (25.2 in. from the bottom of the impact limiter) and 270° CCW (viewed from above) from the electrical feed-through. Set "c" was mounted 30 in. directly above set "a". Set "b" was located at the height of the c.g., at 90° CCW from the electrical feed-through. Each set was secured to a mounting block using four 1/4-in.-diameter cap screws. Each mounting block consisted of a solid piece of 304L stainless steel, welded to two coolant jacket ribs using at least four 1/8-in. fillet welds, as shown in Figure 2.10.15.4.4.1-2 and -5. Signals from "a" and "c" were fed to a common junction block, from which they were carried by a single cable to the data acquisition equipment. Signals from "b" were carried by a separate cable. Transducers were protected from secondary damage or falling rigging with 3/16-in.-thick steel covers.

The transducers were made by Endevco®*, and were of the piezoresistive type with ±750 g capacity, including dc capability. The flat portion of the response is 0 - 2000 Hz, ±100 Hz, with a resonance of 25 kHz and 0.5% of critical damping. Accuracy was 1% of full scale, or 7.5 g.

Passive accelerometers (Impact-o-graph®**, manufactured by Chatsworth Data Corporation) were mounted as shown in Figures 2.10.15.4.4.1-3 and 2.10.15.4.4.1-6. They consisted of trip-level indicators of ball-and-spring construction. A bank of three passive accelerometers having trip levels of 200, 300, and 400 g was mounted at approximately 260° CCW of the electrical feed-through, with the middle (300 g) passive accelerometer at the c.g. height, in close proximity to active accelerometer set "a".

Active accelerometer signals were carried to signal conditioning equipment, and recorded on analog tape using a tape recorder having a frequency response well in excess of 2 kHz. Subsequent to the drop event, the data was filtered using a Cauer Elliptic analog filter. Then the data was digitized in a Tektronix 2630 analyzer using a sampling frequency of 2.56 times the filter cutoff frequency, and downloaded to a laptop PC running Tektronix software for display. Figure 2.10.15.4.4.1-4 shows the schematic of the instrumentation, indicating an option to input raw data to the Tektronix 2630.

---

*_Endevco_ is a registered trademark of Meggitt Aerospace/Endevco Corporation Division.

**_Impact-o-graph_ is a registered trademark of the Chatsworth Data Corporation.

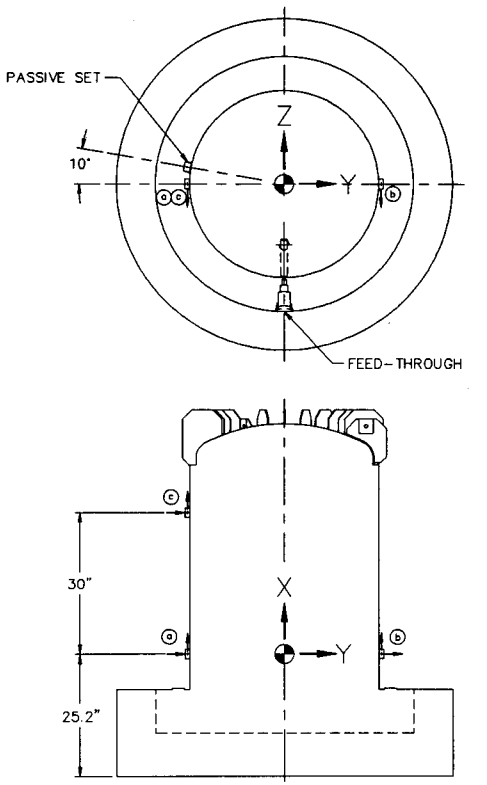


FIGURE 2.10.15.4.4.1-1. Accelerometer Mounting.

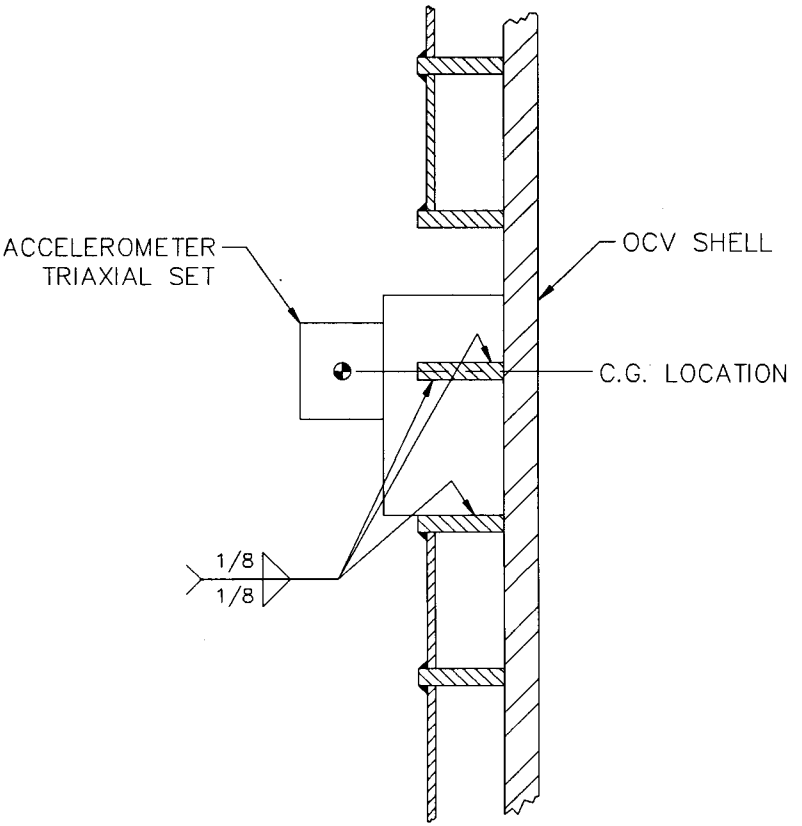


FIGURE 2.10.15.4.4.1-2. Active Accelerometer Mounting Block Details.

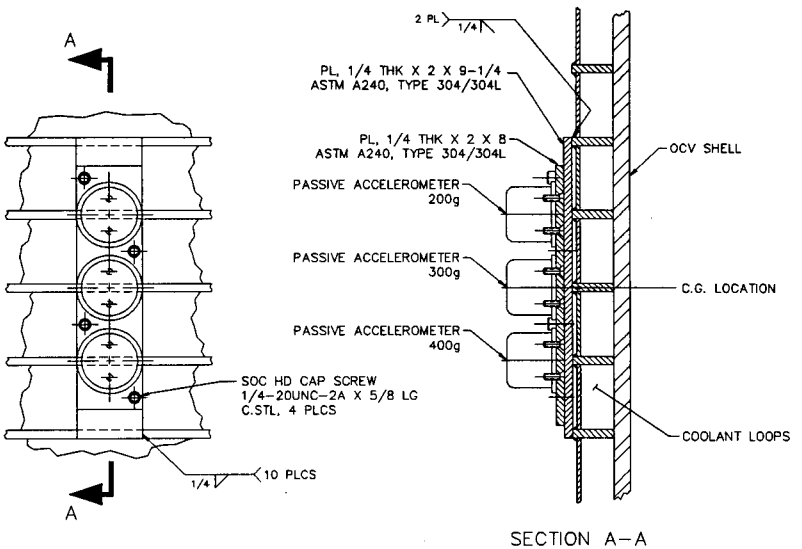


FIGURE 2.10.15.4.4.1-3. Passive Accelerometer Mounting Details.

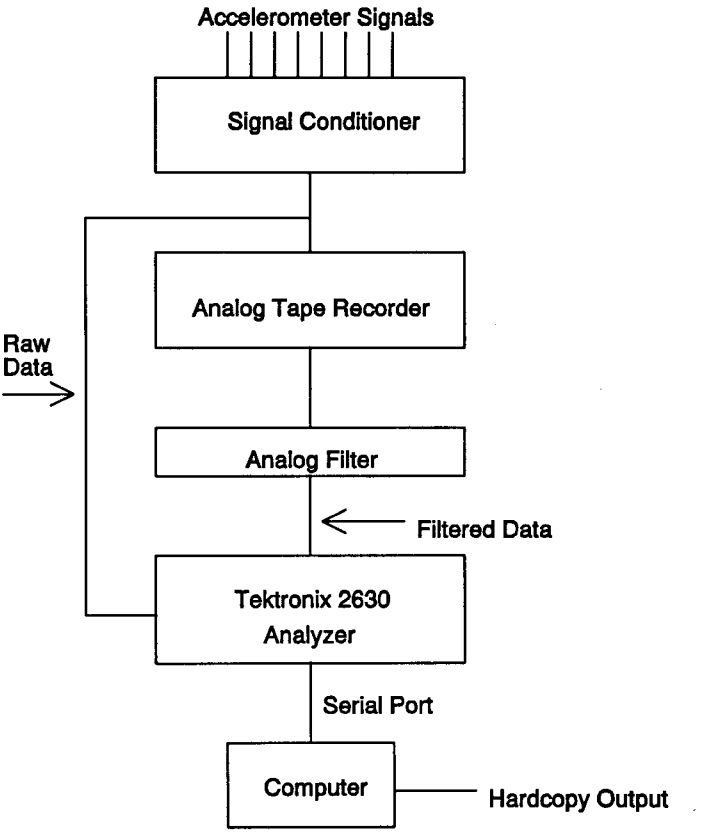


FIGURE 2.10.15.4.4.1-4. Data Acquisition System Schematic.

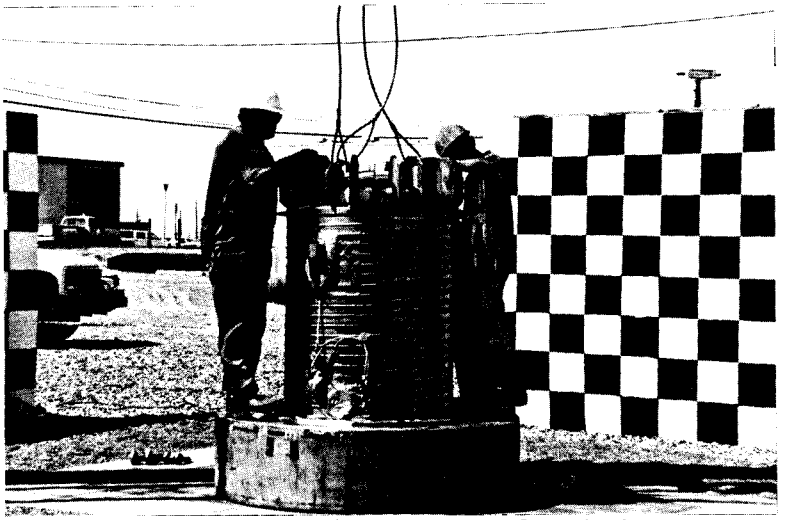


FIGURE 2.10.15.4.4.1-5. Package Before Testing. Shows Accelerometer Locations "a" (lower) and "c" (upper).

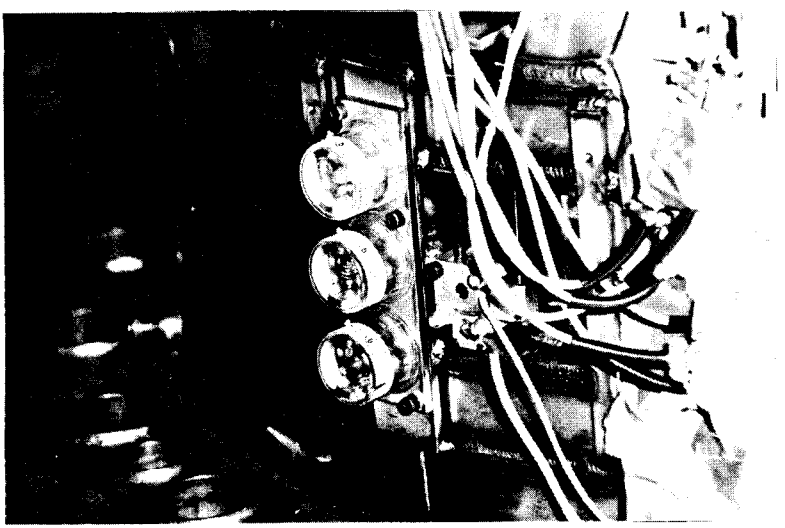


FIGURE 2.10.15.4.4.1-6. Accelerometer Mounting, Showing the Three Passive Accelerometers on the Left and Active Accelerometer Position "a" to the Right.

BEST COPY AVAILABLE

2.10.15.4.4.2 Filtering. The data was filtered using a low pass filter with a cutoff frequency of 300 Hz. This cutoff frequency was chosen to eliminate vibratory responses from the transducer signals, while preserving the entire value of the rigid-body impact. The pulse length of the impacts were approximately 20 ms and greater, and therefore the maximum equivalent pulse "frequency" would be 1/(2x0.02) = 25 Hz or less. This was far below the filter frequency of 300 Hz and demonstrates that there was no risk of loss of the rigid body signal. Inspection of the filtered time histories shows that the use of even lower cutoff frequencies could be justified. A study was done to evaluate the effect of filter frequency on peak impact level. The location "a"-axial signal from the second 30-ft free drop (CTA-1 test No. 7, 30-ft, c.g. over corner) was filtered at various levels, with the results as shown in Table 2.10.15.4.4.2-1 below. The results change little for cutoff frequencies in the range of 100 to 200 Hz.

TABLE 2.10.15.4.4.2-1 Effect of Cutoff Frequency.

Cutoff Freq., Hz	Peak Impact, g
Unfiltered	160
500	95
300	77
200	67
100	61

Before performing the free drop tests, modal testing was performed by striking the CTA with a small weight in numerous locations. The results were post-processed to form frequency response spectra of CTA-1. The lowest response of significance was approximately 950 Hz.

2.10.15.4.4.3 Accelerometer Reduced Data. For each free drop in the NCT and HAC test series, a filtered time history of each accelerometer signal was prepared. From the time history, a peak value was extracted and entered into Table 2.10.15.4.4.3-1 (NCT) and Table 2.10.15.4.4.3-2 (HAC). Calculations are shown in the tables to determine resultant impacts in cases where the drop axis was not parallel to an accelerometer axis. It was found that in most cases in which the accelerometer axis was normal to the impact of CTA-1, the resultant signal was dominated by ringing, which appears as oscillation at approximately the filter frequency, with an essentially zero or insignificant average value. These cases are not needed to determine c.g. impacts and are indicated in the tables as dominated by ringing (DR). In other cases, no data exists because of transducer failure, and these cases are indicated in the tables as no data (ND). The maximum value for the drop is indicated by bold type. The data is identified by location and direction, as shown in the matrix below. Passive accelerometer results for CTA-1 are given in Table 2.10.15.4.3-3.

	Loc. a	Loc. b	Loc. c
Axial	a_x	b_x	c_x
Radial	a_y	b_y	c_y
Circumf	a_z	b_z	c_z

Figures 2.10.15.4.4.3-1 to 2.10.15.4.4.3-14 show the time histories for the important signals listed in Table 2.10.15.4.4.3-2, filtered at 300 Hz (the HAC results).

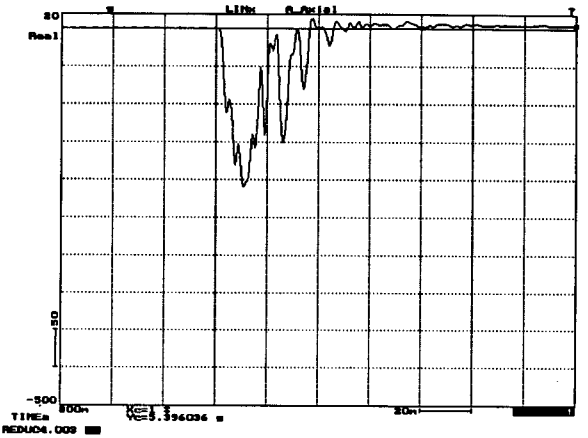


Figure 2.10.15.4.4.3-1. Test No. 6, 30-ft, Bottom Down, Near Vertical, A-Axial Accelerometer Time History.

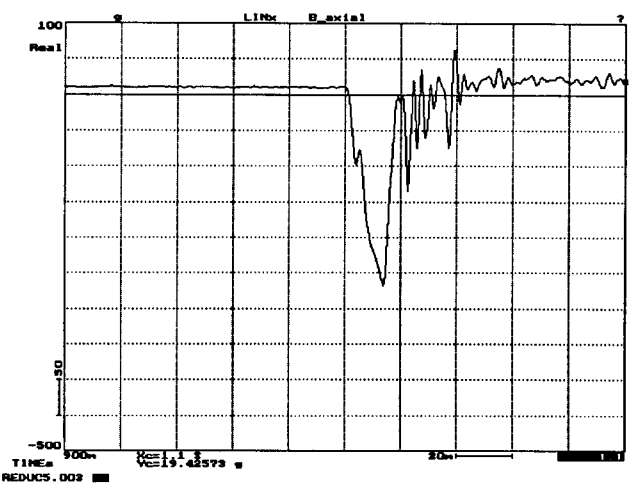


Figure 2.10.15.4.4.3-2. Test No. 6, 30-ft, Bottom Down, Near Vertical, B-Axial Accelerometer Time History.

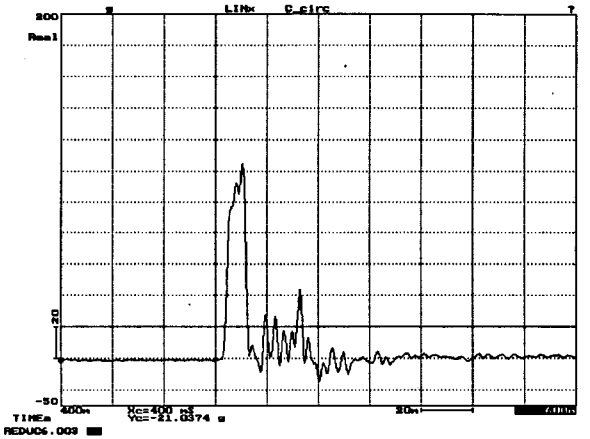


Figure 2.10.15.4.4.3-3. Test No. 6, 30-ft, Bottom Down, Near Vertical, C-Circumferential Accelerometer Time History.

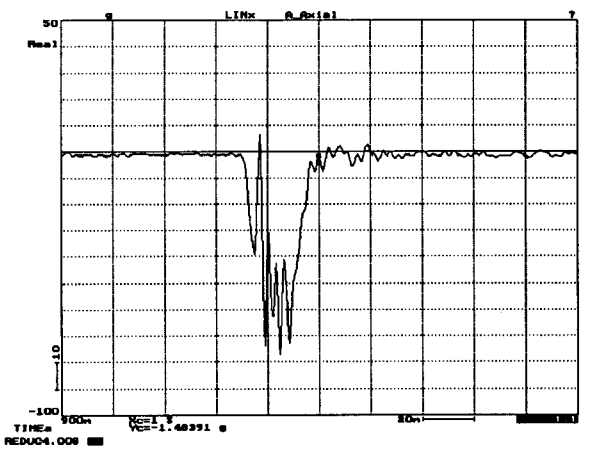


Figure 2.10.15.4.4.3-4. Test No. 7, 30-ft, C.G. over Corner, A-Axial Accelerometer Time History.

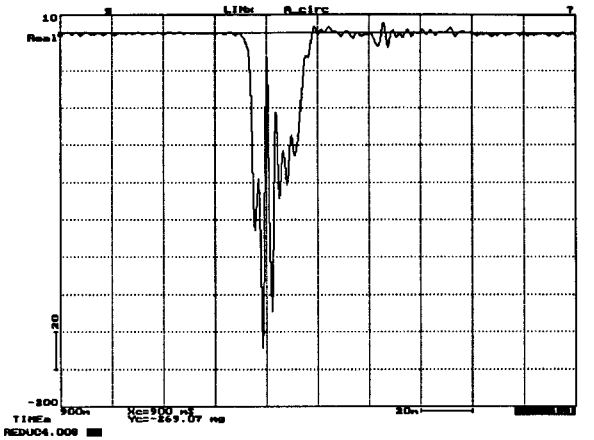


Figure 2.10.15.4.4.3-5. Test No. 7, 30-ft, C.G. over Corner, A-Circumferential Accelerometer Time History.

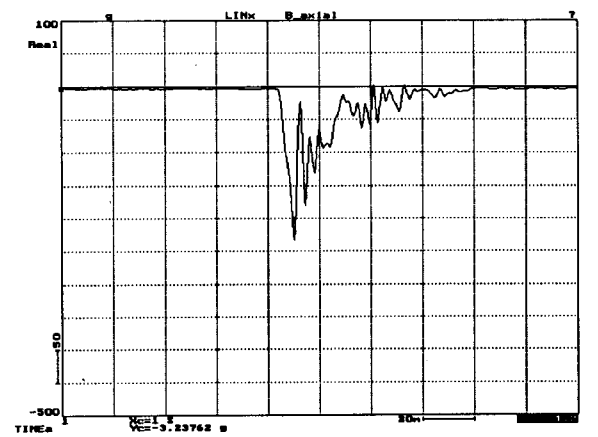


Figure 2.10.15.4.4.3-6. Test No. 7, 30-ft, C.G. over Corner, B-Axial Accelerometer Time History.

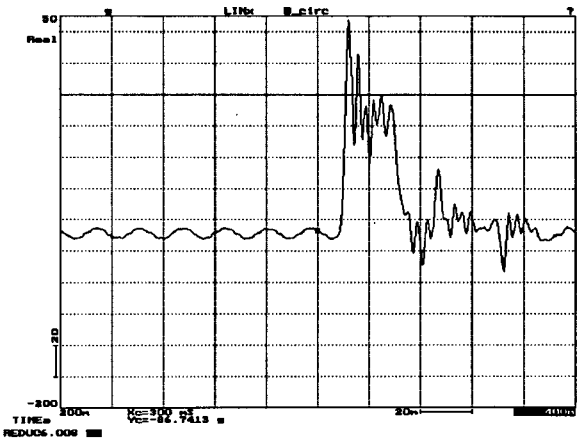


Figure 2.10.15.4.4.3-7. Test No. 7, 30-ft, C.G. over Corner, B-Circumferential Accelerometer Time History.

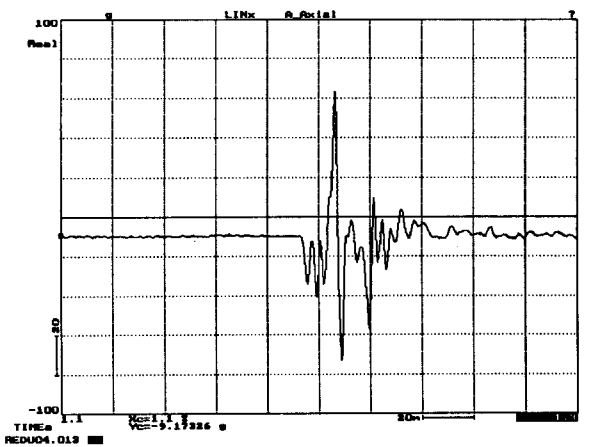


Figure 2.10.15.4.4.3-8. Test No. 8, 30-ft, Side Slapdown, A-Axial Accelerometer Time History.

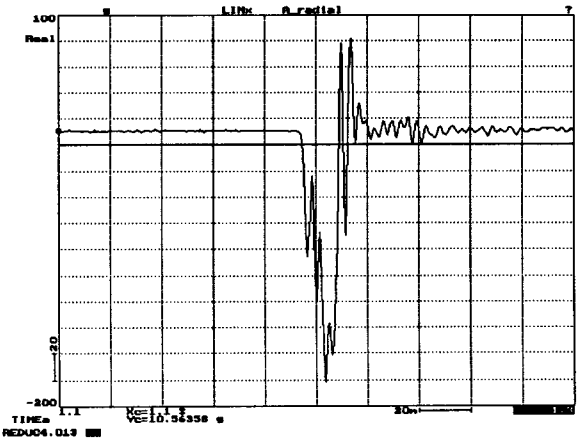


Figure 2.10.15.4.4.3-9. Test No. 8, 30-ft, Side Slapdown, A-Radial Accelerometer Time History.

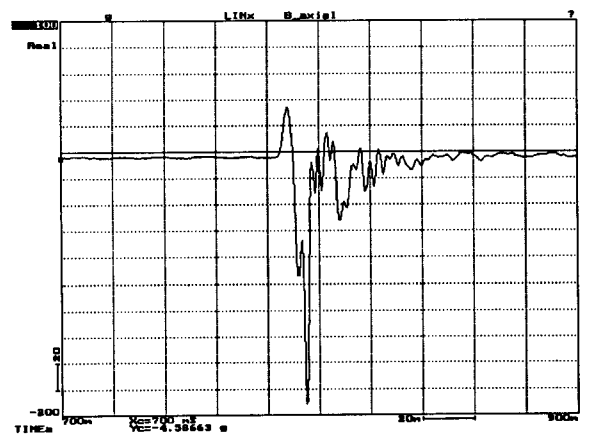


Figure 2.10.15.4.4.3-10. Test No. 8, 30-ft, Side Slapdown, B-Axial Accelerometer Time History.

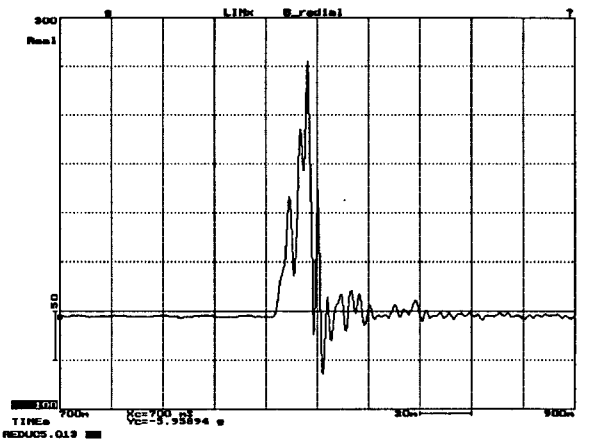


Figure 2.10.15.4.4.3-11. Test No. 8, 30-ft, Side Slapdown, B-Radial Accelerometer Time History.

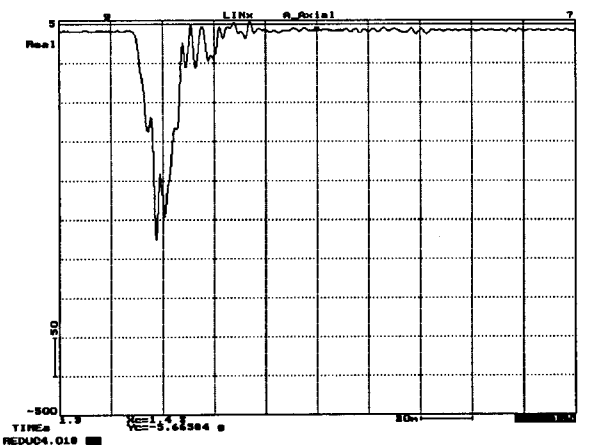


Figure 2.10.15.4.4.3-12. Test No. 9, 30-ft, Flat on Bottom, A-Axial Accelerometer Time History.

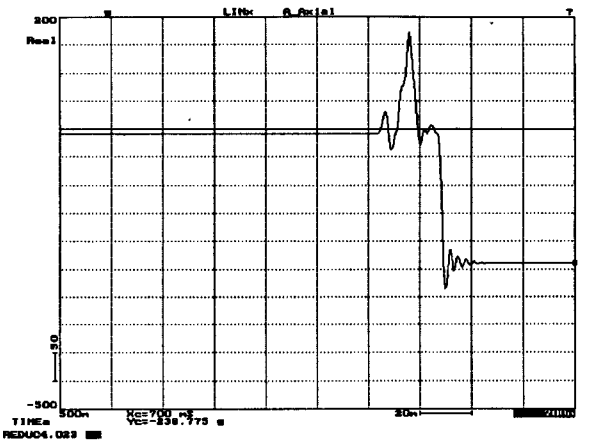


Figure 2.10.15.4.4.3-13. Test No. 10, 30-ft, Flat on Bottom, A-Axial Accelerometer Time History.

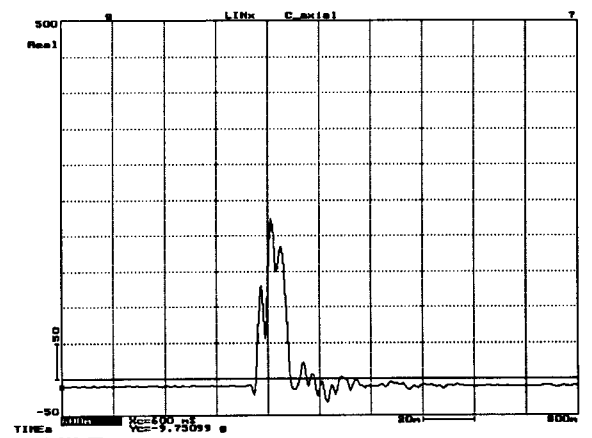


Figure 2.10.15.4.4.3-14. Test No. 10, 30-ft, Flat on Bottom, C-Axial Accelerometer Time History.

TABLE 2.10.15.4.4.3-1. NCT Accelerometer Results (CTA-1).

Test	a_x	a_y	a_z	b_x	b_y	b_z	c_x	c_y	c_z
data:	50 g	DR[1]	15 g	53 g	DR	ND[2]	ND	ND	ND
1	c.g accel.			c.g accel.			angular		
	$(a_x^2 + a_z^2)^{.5}$ = 52 g			$(b_x^2 + b_z^2)^{.5}$ = 53 g			$(a_z - c_z)/30$ = ND		
data:	28 g	DR	63 g	23 g	DR	16 g	52 g	27 g	57 g
2	c.g accel.			c.g accel.					
	$(a_x^2 + a_z^2)^{.5}$ = 69 g			$(b_x^2 + b_z^2)^{.5}$ = 28 g					
data:	20 g	42 g	DR	28 g	61 g	DR	17 g	33 g	10 g
	axial net = AN = $(a_x + b_x)/2$ = 24 g								
3	c.g accel.			c.g accel.			angular		
	$(AN^2 + a_y^2)^{.5}$ = 48 g			$(AN^2 + b_y^2)^{.5}$ = 66 g			$(a_y - c_y)/30$ = 0.3 rad/sec^2		
data:	130 g	DR	20 g	170 g	DR	DR	138 g	DR	64 g
4	c.g accel.			c.g accel.					
	a_x = 130 g			b_x = 170 g					
data:	90 g	DR	17 g	88 g	DR	102 g	61 g	DR	DR
5	c.g accel.			c.g accel.					
	a_x = 90 g			b_x = 88 g					

[1] Dominated by ringing.
[2] No Data.

TABLE 2.10.15.4.4.3-2. HAC Accelerometer Results(CTA-1).

Test	a_x	a_y	a_z	b_x	b_y	b_z	c_x	c_y	c_z
data:	210 g	DR[3]	ND[4]	275 g	DR	ND	ND	DR	125 g
6	c.g accel.			c.g accel.			angular		
Note 1	$(a_x^2 + a_z^2)^{.5}$ = 210 g			$(b_x^2 + b_z^2)^{.5}$ = 275 g			$c_z/(25.2+30)$ = 2.26 rad/sec^2		
data:	77 g	DR	168 g	230 g	121 g	140 g	102 g	ND	84 g
7	c.g accel.			c.g accel.					
	$(a_x^2 + a_z^2)^{.5}$ = 185 g			$(b_x^2 + b_z^2)^{.5}$ = 269 g					
data:	73 g	191 g	48 g	188 g	265 g	DR	DR	ND	DR
	axial net = AN = $(a_x + b_x)/2$ = 131 g								
8	c.g accel.			c.g accel.			angular		
Note 2	$(AN^2 + a_y^2)^{.5}$ = 232 g			$(AN^2 + b_y^2)^{.5}$ = 296 g			$(a_x - b_x)/41.4$ = 2.78 rad/sec^2		
data:	260 g	ND	131 g	ND	ND	DR	ND	DR	DR
9	c.g accel.			c.g accel.					
	a_x = 260 g			b_x = ND					
data:	180 g	ND	75 g	ND	ND	ND	240 g	ND	49 g
10	c.g accel.			c.g accel.			c.g accel.		
	a_x = 180 g			b_x = ND			c_x = 240 g		

Notes:

1. No circumferential (z-direction) readings were available from either location "a" or "b". However, since the package impact angle was only 10° from the vertical, the contribution of the missing directions is small. Further, the angular acceleration is found from the circumferential reading at "c" and the distance from "c" to the pivot point on the impact pad.

2. The angular acceleration is found from the difference between the axial signals at "a" and "b" divided by the distance between them, or 41.4 in. (For the side-slapdown drop, "a" is located on the top of CTA-1, and "b" is located on the bottom.)

3. Dominated by ringing.

4. No data.

TABLE 2.10.15.4.4.3-3. Passive Accelerometer Results (CTA-1).

Test No.	200 g	300 g	400 g
1	No trip	No trip	No trip
2	No trip	No trip	No trip
3	No trip	No trip	No trip
4	Trip	No trip	No trip
5	No trip	No trip	No trip
6	Trip	Trip	Trip
7	Trip	No trip	No trip
8	Trip	Trip	Trip
9	Trip	Trip	Trip
10	Trip	Trip	No trip

2.10.15.4.5 Bolt Residual Torque and Length Measurements. As described in Section 2.10.15.4.1, CTA-2 was subjected to four sets of drop tests. At the end of both the first and second set, the OCV closure bolt removal torques and ICV closure bolt retention check torques were recorded. These torque measurements are listed in Tables 2.10.15.4.5-1 to -4. The lengths of the OCV closure bolts are also included. At the end of both the third and fourth set of drop tests, the OCV closure bolt removal torques and ICV closure bolt removal torques were recorded. The pre- and post-test lengths of all of these bolts were also measured. These torque values and length measurements are included in Tables 2.10.15.4.5-5 to -8.

A study done prior to drop testing showed that bolt removal torque can be as low as 50% of tightening torque. From reviewing data in the tables, it can be concluded that the OCV and ICV closure bolts did not experience any significant loss of torque. The OCV and ICV closure bolt length measurements indicated that no permanent deformation occurred.

Most of the impact limiter attachment bolts were bent during the drop testing and accurate post-test length measurements were difficult to obtain. The impact limiter attachment bolt measurements are given in Tables 2.10.15.4.5-9 and -10.

TABLE 2.10.15.4.5-1. OCV Closure Bolt Removal Torque and Length Measurements After First Set of Drop Tests.

Bolt No.	Removal torque, ft-lb	Pre-test len., in.	Post-test len., in.	Change, in.	Bolt No.	Removal torque, ft-lb	Pre-test len., in.	Post-test len., in.	Change, in.
1	210	5.9730	5.9731	+0.0001	13	235	5.9604	5.9605	+0.0001
2	220	5.9564	5.9566	+0.0002	14	238	5.9703	5.9703	0.0
3	222	5.9654	5.9654	0.0	15	220	5.9698	5.9702	+0.0004
4	198	5.9740	5.9742	+0.0002	16	230	5.9631	5.9633	+0.0002
5	220	5.9619	5.9623	+0.0004	17	235	5.9674	5.9676	+0.0002
6	220	5.9760	5.9764	+0.0004	18	240	5.9661	5.9659	-0.0002
7	230	5.9803	5.9803	0.0	19	280	5.9578	5.9581	+0.0003
8	210	6.0336	6.0336	0.0	20	245	5.9665	5.9661	-0.0004
9	205	5.9762	5.9762	0.0	21	260	5.9547	5.9548	+0.0001
10	190	5.9682	5.9682	0.0	22	230	5.9539	5.9540	+0.0001
11	175	5.9666	5.9667	+0.0001	23	240	5.9730	5.9727	-0.0003
12	190	5.9749	5.9740	-0.0009	24	200	5.9692	5.9691	-0.0001

TABLE 2.10.15.4.5-2. ICV Closure Bolt Retention Torque Check After First Set of Drop Tests.

Bolt #	Torque, ft-lb	Bolt #	Torque, ft-lb
1	>78	13	>78
2	>78	14	>78
3	>78	15	>78
4	>78	16	>78
5	>78	17	>78
6	>78	18	>78
7	>78	19	>78
8	>78	20	>78
9	>78	21	>78
10	>78	22	>78
11	>78	23	>78
12	>78	24	>78

TABLE 2.10.15.4.5-3. OCV Closure Bolt Retention Torque Check After Second Set of Drop Tests.

Bolt No.	Removal torque, ft-lb	Pre-test len., in.	Post-test len., in.	Change, in.	Bolt No.	Removal torque, ft-lb	Pre-test len., in.	Post-test len., in.	Change, in.
1	150	5.9730	5.9728	-0.0002	13	230	5.9604	5.9603	-0.0001
2	190	5.9564	5.9566	+0.0002	14	225	5.9703	5.9700	-0.0003
3	200	5.9654	5.9650	-0.0004	15	230	5.9698	5.9694	-0.0004
4	200	5.9740	5.9738	-0.0002	16	250	5.9631	5.9631	0.0
5	230	5.9619	5.9619	0.0	17	275	5.9674	5.9671	-0.0003
6	300	5.9760	5.9761	+0.0001	18	320	5.9661	5.9658	-0.0003
7	280	5.9803	5.9801	-0.0002	19	330	5.9578	5.9581	+0.0003
8	270	6.0336	6.0337	+0.0001	20	340	5.9665	5.9662	-0.0003
9	225	5.9762	5.9756	-0.0006	21	265	5.9547	5.9549	+0.0002
10	225	5.9682	5.9682	0.0	22	240	5.9539	5.9539	0.0
11	195	5.9666	5.9663	-0.0003	23	260	5.9730	5.9722	-0.0008
12	220	5.9749	5.9746	-0.0003	24	230	5.9692	5.9691	-0.0001

TABLE 2.10.15.4.5-4. ICV Closure Bolt Retention Torque Check After Second Set of Drop Tests.

Bolt #	Torque, ft-lb	Bolt #	Torque, ft-lb
1	>78	13	>78
2	>78	14	>78
3	>78	15	>78
4	>78	16	>78
5	>78	17	>78
6	>78	18	>78
7	>78	19	>78
8	>78	20	>78
9	>78	21	>78
10	>78	22	>78
11	>78	23	>78
12	>78	24	>78

TABLE 2.10.15.4.5-5. OCV Closure Bolt Removal Torque and Length Measurement After Third Set of Drop Tests.

Bolt No.	Removal torque, ft-lb	Pre-test len., in.	Post-test len., in.	Change, in.	Bolt No.	Removal torque, ft-lb	Pre-test len., in.	Post-test len., in.	Change, in.
1	180	5.9730	5.9731	+0.0001	13	260	5.9604	5.9604	0.0
2	230	5.9564	5.9567	+0.0003	14	275	5.9703	5.9702	-0.0001
3	310	5.9654	5.9653	-0.0001	15	270	5.9698	5.9700	+0.0002
4	300	5.9740	5.9739	-0.0001	16	280	5.9631	5.9633	+0.0002
5	290	5.9619	5.9621	+0.0002	17	280	5.9674	5.9677	+0.0003
6	255	5.9760	5.9763	+0.0003	18	260	5.9661	5.9661	0.0
7	235	5.9803	5.9805	+0.0002	19	270	5.9578	5.9579	+0.0001
8	240	6.0336	6.0336	0.0	20	230	5.9665	5.9664	-0.0001
9	250	5.9762	5.9761	-0.0001	21	270	5.9547	5.9549	+0.0002
10	255	5.9682	5.9681	-0.0001	22	250	5.9539	5.9536	-0.0003
11	210	5.9666	5.9666	0.0	23	200	5.9730	5.9723	-0.0007
12	240	5.9749	5.9747	-0.0002	24	200	5.9692	5.9690	-0.0002

TABLE 2.10.15.4.5-6. ICV Closure Bolt Removal Torque and Length Measurements After Third Set of Drop Tests.

Bolt No.	Removal torque, ft-lb	Pre-test len., in.	Post-test len., in.	Change, in.	Bolt No.	Removal torque, ft-lb	Pre-test len., in.	Post-test len., in.	Change, in.
1	180	1.9580	1.9582	+0.0002	13	185	1.9490	1.9492	+0.0002
2	135	1.9624	1.9626	+0.0002	14	175	1.9698	1.9699	+0.0001
3	190	1.9675	1.9674	-0.0001	15	185	1.9554	1.9555	+0.0001
4	180	1.9711	1.9711	0.0	16	170	1.9644	1.9646	+0.0002
5	150	1.9687	1.9687	0.0	17	180	1.9594	1.9595	+0.0001
6	190	1.9670	1.9669	-0.0001	18	180	1.9602	1.9602	0.0
7	185	1.9694	1.9693	-0.0001	19	180	1.9692	1.9690	-0.0002
8	190	1.9561	1.9559	-0.0002	20	180	1.9687	1.9687	0.0
9	175	1.9643	1.9643	0.0	21	180	1.9580	1.9580	0.0
10	190	1.9726	1.9729	+0.0003	22	185	1.9641	1.9639	-0.0002
11	190	1.9614	1.9615	+0.0001	23	187	1.9616	1.9616	0.0
12	165	1.9557	1.9557	0.0	24	170	1.9595	1.9592	-0.0003

TABLE 2.10.15.4.5-7. OCV Closure Bolt Removal Torque and Length Measurements After Fourth Set of Drop Tests.

Bolt No.	Removal torque, ft-lb	Pre-test len., in.	Post-test len., in.	Change, in.	Bolt No.	Removal torque, ft-lb	Pre-test len., in.	Post-test len., in.	Change, in.
1	225	5.9730	5.9734	+0.0004	13	250	5.9604	5.9610	+0.0006
2	240	5.9564	5.9568	+0.0004	14	260	5.9703	5.9706	+0.0003
3	250	5.9654	5.9658	+0.0004	15	230	5.9698	5.9701	+0.0003
4	240	5.9740	5.9741	+0.0001	16	250	5.9631	5.9636	+0.0005
5	265	5.9619	5.9622	+0.0003	17	260	5.9674	5.9678	+0.0004
6	260	5.9760	5.9764	+0.0004	18	265	5.9661	5.9665	+0.0004
7	255	5.9803	5.9802	-0.0001	19	280	5.9578	5.9580	+0.0002
8	265	6.0336	6.0339	+0.0003	20	240	5.9665	5.9665	0.0
9	240	5.9762	5.9764	+0.0002	21	260	5.9547	5.9550	+0.0003
10	280	5.9682	5.9683	+0.0001	22	265	5.9539	5.9540	+0.0001
11	260	5.9666	5.9667	+0.0001	23	280	5.9730	5.9727	-0.0003
12	210	5.9749	5.9754	+0.0005	24	215	5.9692	5.9692	0.0

TABLE 2.10.15.4.5-8. ICV Closure Bolt Removal Torque and Length Measurements After Fourth Set of Drop Tests.

Bolt No.	Removal torque, ft-lb	Pre-test len., in.	Post-test len., in.	Change, in.	Bolt No.	Removal torque, ft-lb	Pre-test len., in.	Post-test len., in.	Change, in.
1	215	1.9580	1.9586	+0.0006	13	230	1.9490	1.9491	+0.0001
2	210	1.9624	1.9626	+0.0002	14	220	1.9698	1.9699	+0.0001
3	210	1.9675	1.9672	-0.0003	15	200	1.9554	1.9552	-0.0002
4	220	1.9711	1.9714	+0.0003	16	215	1.9644	1.9644	0.0
5	230	1.9687	1.9685	-0.0002	17	220	1.9594	1.9598	+0.0004
6	225	1.9670	1.9669	-0.0001	18	210	1.9602	1.9601	-0.0001
7	220	1.9694	1.9690	-0.0004	19	220	1.9692	1.9691	-0.0001
8	200	1.9561	1.9567	+0.0006	20	200	1.9687	1.9689	+0.0002
9	200	1.9643	1.9646	+0.0003	21	175	1.9580	1.9582	+0.0002
10	190	1.9726	1.9729	+0.0003	22	200	1.9641	1.9641	0.0
11	215	1.9614	1.9616	+0.0002	23	175	1.9616	1.9616	0.0
12	190	1.9557	1.9555	-0.0002	24	200	1.9595	1.9601	+0.0006

TABLE 2.10.15.4.5-9. Impact Limiter Attachment Bolt Length Measurements After First and Second Sets of Drop Tests.

Bolt #	Pre-test len., in.	Post-test len., in.	Bolt #	Pre-test len., in.	Post-test len., in.
1	9.00	8.9897	9	8.9911	8.9904
2	9.00	9.0068	10	8.9910	8.9954
3	9.00	9.0231	11	8.9950	8.9888
4	9.00	8.9999	12	8.9963	9.0004
5	9.00	8.9796	13	8.9884	8.9839*
6	9.00	9.0053	14	8.9835	8.9932
7	9.00	9.0140	15	8.9848	8.9878
8	9.00	8.9967	16	8.9914	8.9933

* Bolt severely bent, precluding accurate post-test measurement.

The first set of drop tests used bolts 1 through 8. The second set of drops used new bolts numbered 9 through 16.

TABLE 2.10.15.4.5-10. Impact Limiter Attachment Bolt Length Measurements After Third and Fourth Sets of Drop Tests.

Bolt #	Pre-test len., in.	Post-test len., in.	Bolt #	Pre-test len., in.	Post-test len., in.
17	8.9920	8.9931	17	8.9931	9.0039
18	8.9841	8.9878	18	8.9878	9.0065
19	8.9914	8.9895	19	8.9895	8.9996
20	8.9905	8.9904	20	8.9904	9.0035
21	8.9944	8.9951	21	8.9951	9.0102
22	8.9868	8.9895	22	8.9895	8.9969
23	8.9891	8.9901	23	8.9901	8.9941
24	8.9913	8.9924	24	8.9924	8.9982

The same impact limiter bolts were used for all of these drop tests.

2.10.15.4.6 Payload Interaction and Shipping Rack Condition. During the drop test series, the simulated payload interacted structurally with the ICV and the shipping rack assembly. The simulated payload broke free in that all four payload attaching bolt heads pulled through the payload base. This allowed the payload to strike the inside of the ICV wall and head. Two payload fins were struck direct-on and buckled up to the sturdy payload body. Three other payload fins were involved to a lesser extent (see Figure 2.10.15.4.6-1). Further, interaction with the ICV lifting block also occurred, in that the end of the 14-in. o.d., 1/2-in.-thick wall pipe of the simulated payload impacted the lifting block. As shown in Figure 2.10.15.4.6-2, the impact produced a dent

in the end of the pipe approximately 4.5 in. long and 0.5 in. deep. Figures 2.10.15.4.6-1 and -2 show the damage to the simulated payload that occurred during the first drop test series, which used CTA-1. The damage to the simulated payload during the second drop test series was very similar.

Damage to the shipping rack assembly was negligible. The shipping rack assembly top plate (the barrier plate) was deformed approximately 1/16 in. by contact with the loose payload. All four of the shipping rack assembly attachment bolts were still tight. There was no observable damage to the shipping rack assembly attachment bolts and the shipping rack remained substantially in its initial position. The simulated payload attachment bolts demonstrated some deformation, consistent with separation of the payload. The underside insulation was in place.

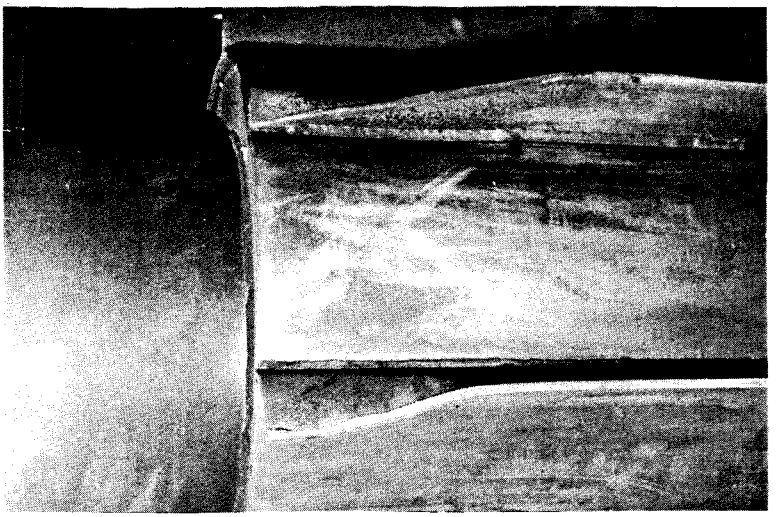


FIGURE 2.10.15.4.6-1. Simulated Payload Damage to Fins.
Note: Picture was rotated CCW.

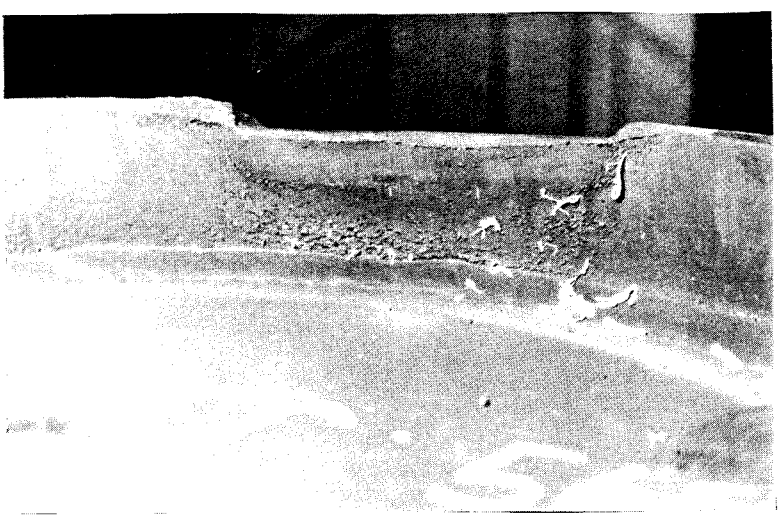


FIGURE 2.10.15.4.6-2. Simulated Payload Top End Damage.

BEST COPY AVAILABLE

2.10.15.4.7 Anomalies. The following test anomaly was noted.

As indicated in Section 2.10.15.4.1, the ICV closure bolts were not removed until after the third set of drop tests (CTA-2 Test Nos. 1 through 9) was completed. After removal of the ICV closure bolts, it was noted that most of the ICV closure bolt washers were fractured. The fracturing can best be described as fine, hairline cracks that extend radially through the washers in one or more locations. In general, the washers remained intact and were not broken into small pieces. Only one washer fell into two parts during disassembly of the ICV. From the data sheets, it is noted that the fractured washers did not result in any loss of torque in the ICV closure bolts. Further, even if broken, the washers are effectively trapped by the ICV bell flange closure bolt counterbore. The washers are high-strength flat washers that meet the requirements of ASTM F436. The washers are purchased from a commercial vender and then the OD is machined down to drawing specifications. After machining, the washers are cadmium plated. During the search for possible causes for the fracturing, it was determined the washers were not baked out after the cadmium plating process. This could result in a potential for hydrogen embrittlement and subsequent fracturing of the washers.

Prior to performing the last set of drop tests (CTA-2 Test Nos. 10 through 16), new washers were fabricated and installed. These washers were not cadmium plated. After completion of the drop testing, the ICV was disassembled and the ICV closure bolt washers were inspected and found to be free of any fractures. For the production packagings, the washers will be properly baked-out to ensure there is no potential for hydrogen embrittlement.

2.10.15.5 Certification Test Data Sheets.

Test Set 1: Drop Test Nos. 1, 2, and 3

Data Sheet A from WHC-SD-RTG-TC-015, Rev. 1
Data Sheets, B, C, D, and E1 from WHC-SD-RTG-TC-017, Rev. 1
NDE Leak Test Procedure and Test Report

DATA SHEET A

Impact Limiter Measurements -- Pretest Reference Only

Obtain all measurements (in) in four quadrants, with quadrant No. 1 centered on feed-through (quadrants measured CCW looking down on package top).

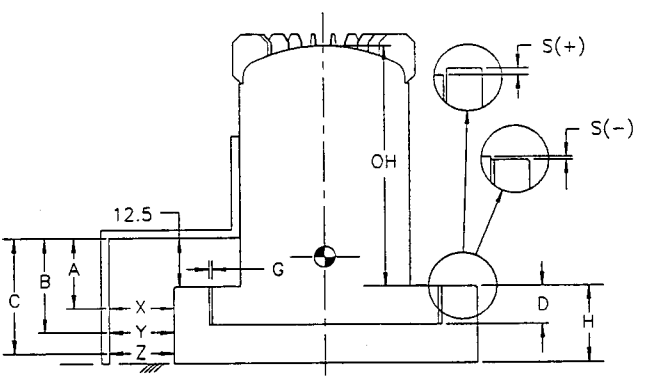
Quadrant	X (±0.13)	Y (±0.13)	Z (±0.13)	H (±0.13)	D (±0.13)	G (±0.06)	S (±0.06)
1	4	3 7/8	4	17 15/16	9	1/4	- 7/16
2	4 1/16	3 7/8	3 7/8	17 15/16	9	1/4	- 7/16
3	3 3/4	3 3/8	4	17 1/2	8 15/16	3/8	- 19/32
4	3 15/16	3 3/4	3 3/4	17 7/8	9	3/8	- 7/16

Thickness near center using 5/16" hole (T, ±0.13): 8 5/8 IN.

Height (OH) of OCV from top of thermal shield to top of OCV head, excluding fins (±0.25): 56 1/16

The 12.5 dimension shown below is a reference dimension to the top of the OCV flange thermal shield.

A = 14.5 ±0.25 in.
B = 21.5 ±0.25 in.
C = 28.5 ±0.25 in.



Test Engineer — Date: 11/1/95 — QA Representative — Date: 11/8/95

DATA SHEET A

Drop Test No. 1, NCT 4-ft Drop, Near Vertical

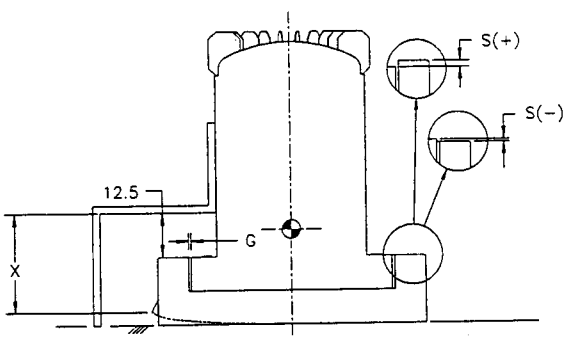
Ambient Temperature: 18 °C Impact Limiter Foam Temperature: 22 °C

Damage Measurements: (See sketch below)

Quadrant	X (±0.13)	G (±0.06)	S (±0.06)
1			
2			
3			
4			

Due to high winds these measurements were not taken

The 12.5 dimension shown below is a reference dimension to the top of the OCV flange thermal shield.



Test Engineer

11/08/95
Date

QA Representative

11/8/95
Date

DATA SHEET A

Drop Test No. 1, NCT 4-ft Drop, Near Vertical

Sketch of Damage and Notes:

Torque checking impact limitter bolts

#1	85 ft lb	broke loose
2	80 + ft lb	
3	60 ft lb	
4	75 ft lb	
5	∅ ft lb	loose
6	30 ft lb	
7	88 ft-lb	tight (reached max)
8	∅ ft-lb	loose

D/S Quintero 11/08/95
Test Engineer Date

M E Bond 11/8/95
QA Representative Date

DATA SHEET A

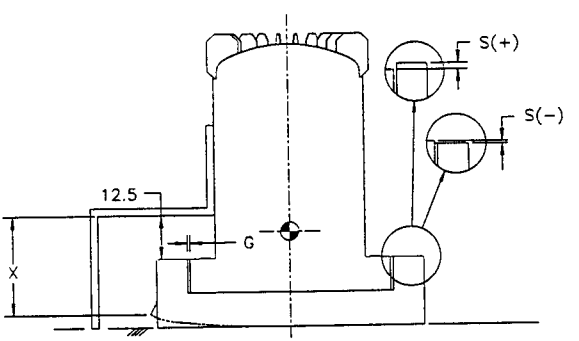
Drop Test No. 2, HAC 30-ft Drop, Near Vertical

Ambient Temperature: 18 °C Impact Limiter Foam Temperature: 22 °C

Damage Measurements: (See sketch below)

Quadrant	X (±0.13)	G (±0.06)	S (±0.06)
1	30 3/4	9/32	- 18/32
2	30 3/4	6/32	- 13/32
3	29 3/8	9/32	- 19/32
4	30 1/4	12/32	- 23/32
Impact Point			

The 12.5 dimension shown below is a reference dimension to the top of the OCV flange thermal shield.



Test Engineer 11/08/95 Date

QA Representative 11/8/95 Date

DATA SHEET A

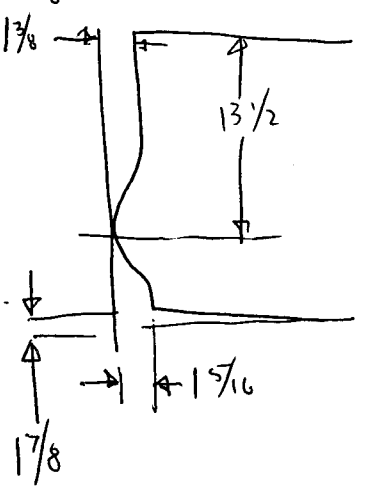
Drop Test No. 2, HAC 30-ft Drop, Near Vertical

Sketch of Damage and Notes:

Torque checking

Impact Limiter bolts

#1	88 ft-lb	(reached max)
2	50 ft-lb	
3	37 ft-lb	
4	65 ft-lb	
5	88 ft-lb	(reached max)
6	30 ft-lb	
7	ø ft-lb	(loose)
8	15 ft-lb	



At impact point

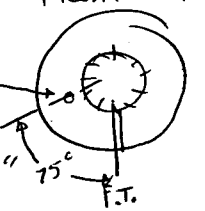
Test Engineer — Date 11/15/95

QA Representative — Date 11/8/95

Depth of dent 5/16"



VIEW LOOKING FROM TOP



DATA SHEET A

Drop Test No. 3, HAC Puncture

Drop on #7 bolt

S-distance at point of impact = -27/32"

(see page 58)

Impact limiter bolt residual torque
(remove OCV/ICV from impact limiter)

Bolt #	Residual Torque
1	200 ft-lb
2	70
3	50
4	65
5	190
6	0
7	0
8	0

D. L. Crutchfield — Test Engineer — 11/08/96 — Date

B. J. Hess — QA Representative — 11/08/96 — Date

DATA SHEET B

Record of OCV closure residual bolt torque performed after completion of interim drop tests. Bolts are numbered CCW, viewed from the top of the Test Article, starting with the first bolt CCW from the feed-through.

OCV Bolts:

Loosen each bolt in turn just sufficient to establish the residual preload, followed by retorquing to the torque level equal to the installation torque, starting with Bolt No. 1, crossing the bell to Bolt No. 13, proceeding to Bolt No. 2 and across to Bolt No. 14, proceed to Bolt No. 24 and across to Bolt No. 12. The balance of the pattern is: 3-15, 23-11, 4-16, 22-10, 5-17, 21-9, 6-18, 20-8, 7-19.

OCV Closure Bolts Residual Preload			
Bolt #	Torque, ft-lb	Bolt #	Torque, ft-lb
1	210	13	235
2	220	14	238
3	222	15	220
4	198	16	230
5	220	17	235
6	220	18	240
7	230	19	280
8	210	20	245
9	205	21	260
10	190	22	230
11	175	23	240
12	190	24	200

Avg → 223

TORQUE WRENCH S/N 584-88-01-CC CAL EXP 9/29/96

Test Engineer 11/08/95 Date

QA Representative 11/8/95 Date

OFFICIAL COPY

DATA SHEET C

Record of ICV closure bolt relative position in relation to the ICV flange after removal of OCV bell.Bolts are numbered CCW, viewed from the top of the Test Article, starting with the first bolt CCW from the electrical feed-through.

ICV Closure Bolts Relative Angular Position			
Bolt #	Position	Bolt #	Position
1	✓OK	13	✓OK
2		14	
3		15	
4		16	
5		17	
6		18	
7		19	
8		20	
9		21	
10		22	
11		23	
12	✓OK	24	✓OK

Test Engineer 11/08/95 Date

QA Representative 11/8/95 Date

OFFICIAL COPY

DATA SHEET D

Record of ICV retention bolt torque performed after completion of interim drop tests and after removal of OCV bell. Bolts are numbered CCW, viewed from the top of the Test Article, starting with the first bolt CCW from the electrical feed-through. Apply loosening torque of one-half the average residual torque established in assembly (see WHC 1995a), starting with Bolt No. 1, crossing the bell to Bolt No. 13, proceeding to Bolt No. 2 and across to Bolt No. 14, proceed to Bolt No. 24 and across to Bolt No. 12. The balance of the pattern is: 3-15, 23-11, 4-16, 22-10, 5-17, 21-9, 6-18, 20-8, 7-19. If bolt loosens below this torque, record the loosening torque and proceed to the next bolt.

Average residual torque from initial assembly 156 ft-lb. ($\frac{1}{2} \Rightarrow$ 78 ft-lb)
(Check in loosening direction to 1/2 this value)

ICV Closure Bolts

Retention Torque Check*

Bolt #	Torque, ft-lb	Bolt #	Torque, ft-lb
1	OK	13	OK
2		14	
3		15	
4		16	
5		17	
6		18	
7		19	
8		20	
9		21	
10		22	
11		23	
12	OK	24	OK

TORQUE WRENCH S/N 950-88-01-06 CAL EXP 10/20/96

*Record ✓OK if half the initial assembly torque is met; record loosening torque if bolt loosens.

Test Engineer 11/08/95 Date QA Representative 11/8/95 Date

OFFICIAL COPY

DATA SHEET E1

Record of RTG Certification Test Article OCV and impact limiter bolt length performed after interim drop tests. Bolts are numbered CCW, viewed from the top of the Test Article, starting with the first bolt CCW from the electrical feed-through.

OCV Closure Bolts			
Bolt no.	Length (in.)	Bolt no.	Length (in.)
1	5.9731	13	5.9605
2	5.9566	14	5.9703
3	5.9654	15	5.9702
4	5.9742	16	5.9633
5	5.9623	17	5.9676
6	5.9764	18	5.9659
7	5.9803	19	5.9581
8	6.0336	20	5.9661
9	5.9762	21	5.9548
10	5.9682	22	5.9540
11	5.9667	23	5.9727
12	5.9740	24	5.9691

Impact Limiter Bolts	
Bolt no.	Length (in.)
1	8.9897
2	9.0068
3	9.0231
4	8.9959
5	8.9796
6	9.0053
7	9.0140
8	8.9967

11/07/95
Test Engineer Date

11-15-95
QA Representative Date

OFFICIAL COPY

Westinghouse Hanford Company

NDE LEAK TEST PROCEDURE AND TEST REPORT

NON DESTRUCTIVE EXAMINATION
306 BLDG., 300 AREA - TEL. 376-5401

Job No. 95-8

Requestor	Company	Project/System/Work Package/Traveler No.
Henry S. Averette	PacTec	Helium Leak Test of Radioisotope Thermoelectric Generator (RTG) After Drop Tests #1-#3 on Certification Test Article #CTA-2, per WHC-SD-RTG-TC-017, Rev. 1

MSIN	Bldg.	Area
G2-02	MO-916	1100

Acceptance Std.	Section	Para.	Date	Dwg. No.	NCR	Cleaning
Leakage Rate < 2.6 x 10 -7 atm.cm3/sec Helium				H-4-302118 H-4-112301	[X] NA	Alcohol

TEST CONDITIONS

- Temperature: Amb. Device ID: _____ [X] NA
- Barometric Pressure: _____ [X] NA
- Test Pressure: ~~^~~ =1 Atm.(14.7psia) [ ] NA
- Gas: UHP Helium [ ] NA
- Concentration: >90% [ ] NA
- Other: _____ [X] NA
- Bubble Solution: _____ [X] NA
- Batch No.: _____
- Gage 1 584-31-04-: 007 [ ] NA
- Range: 0 to 50 psia
- Calib. Exp.: March 9, 1996
- Gage 2 584-31-04-: _____ [X] NA
- Range: _____
- Calib. Exp.: _____
- Relief Valve: _____ [X] NA

TEST EQUIPMENT [ ] NA

- Manufacturer: L/H "UL-100+", #2
- Ident. No.: S/n896-38 (WC48869)
- Fine Range: 1.0×10^{-11} Atmcc/sec/Div [ ] NA
- Std. No. 584-40-03-: 018
- Std. Leak: 1.6×10^{-8} Atmcc/sec
- Calib. Exp.: July 7, 1996
- ~~Medium Range~~ SYSTEM SEALS: 1.8×10^{-11} Atmcc/sec/Div [ ] NA
- Std. No. 584-40-03-: 006
- Std. Leak: 1.3×10^{-7} Atmcc/sec
- Calib. Exp.: July 7, 1996
- Gross Range: x 10 Atmcc/sec/Div [X] NA
- Std. No. 584-40-03-: _____
- Std. Leak: x 10 Atmcc/sec
- Calib. Exp.: _____

WHC PROCEDURE NO. [ ] NA

- [X] NDT-LT-6000 Rev. 3
- Appendix A Rev. 2
- [ ] Special Tech. No.: _____

WORK INST. [X] NA

- [ ] NDT-LT-601 Rev.: _____
- [ ] Other: _____

SYSTEM SENSITIVITY

- [ ] Same as MSLD Calib. or:
- Fine Range: 1.8×10^{-11} Atmcc/sec/Div
- Med. Range: x 10 Atmcc/sec/Div
- Gross Range: x 10 Atmcc/sec/Div

TEST TIME

STAT-O-SEALS + Primary O-RINGS =
He Response Time: IMMEDIATE [ ] NA
He Accum. Time: TEST DURATION [ ] NA
~~Secondary~~ STAT-O-SEALS = 3 min
~~Secondary~~ O-RINGS = 10 min. [ ] NA

Weld No., Part No., or Serial No.	Acc.	Rej.	No Rel. Ind.	Comments	
				OUTER CONTAINMENT VESSEL (OCV) LEAK RATE TESTS:	
"V" Port Stat-O-Seal	X		X	No Detectable Leakage	(Per Step #5.2)
"T" Port Prim.O-Ring	X		X	No Detectable Leakage	(Per Step #5.3)
				INNER CONTAINMENT VESSEL (ICV) LEAK RATE TESTS:	
"P" Port Stat-O-Seal	X		X	No Detectable Leakage	(Per Step #6.2)
"S" Port Stat-O-Seal	X		X	No Detectable Leakage	(Per Step #6.3)
"T" Port Prim.O-Ring	X		X	No Detectable Leakage	(Per Step #6.4)
				OUTER CONTAINMENT VESSEL (OCV) LEAK RATE TESTS: ASSEMBLY	
"V" Port Stat-O-Seal	X		X	No Detectable Leakage	(Per Step #7.2)
"T" Port Prim.O-Ring	X		X	No Detectable Leakage	(Per Step #7.3)

Technique Pre Approval [V] NA — LT Level/Date

Technician	Level	Interpreted by	LT Level II	Reviewed by
W.H.Nelson W D Nelson	I			OFFICIAL COPY
B.J.Sewart B Sewart	II	B.J.Sewart B Sewart	II	John K Kuo
Date of Examination: Nov. 8, 1995		Date: Nov. 8, 1995		Date: 11-14-95

2.10.15-69

A-6000-494 (01/94)

Test Set 2: Drop Test Nos. 4, 5, and 6

Data Sheet A from WHC-SD-RTG-TC-015, Rev. 1
Data Sheets B, C, D, and E1 from WHC-SD-RTG-TC-017, Rev. 1
NDE Leak Test Procedure and Test Report

DATA SHEET A

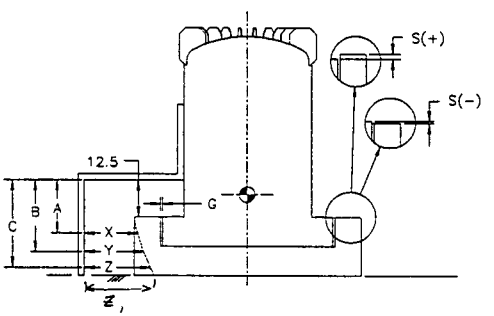
Drop Test No. 4, NCT 4-ft Drop, c.g. Over Bottom Corner

Ambient Temperature: 10°C Impact Limiter Foam Temperature: 26°C

The 12.5 dimension shown below is a reference dimension to the top of the OCV flange thermal shield.

Damage Measurements: (See sketch below)

Quadrant	S (±0.06)	G (±0.06)
1	- 18/32	6/32
2	- 12/32	3/32
3	- 20/32	12/32
4	- 25/32	14/32



$Z_1 = \cancel{220}\ 12.5''$

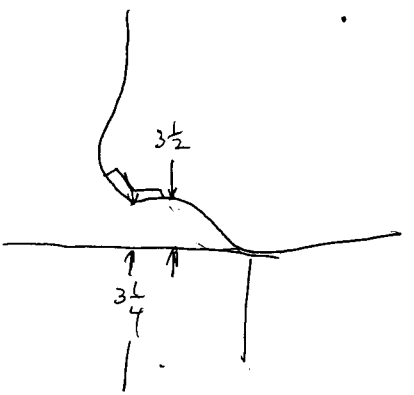
A (±0.25)	B (±0.25)	C (±0.25)	X (±0.25)	Y (±0.25)	Z (±0.25)
22	27	30	3 7/8	3 5/8	5 3/8

Test Engineer Date 11/9/95 QA Representative Date 11/16/95

DATA SHEET A

Drop Test No. 4, NCT 4-ft Drop, c.g. Over Bottom Corner

Sketch of Damage and Notes:



Test Engineer 11/9/95 Date QA Representative N/A Date

DATA SHEET A

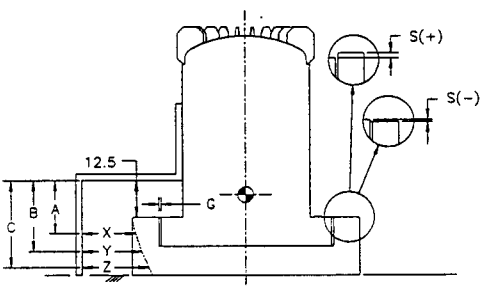
Drop Test No. 5, HAC 30-ft Drop, c.g. Over Bottom Corner

Ambient Temperature: 10 °C Impact Limiter Foam Temperature: 22 °C

The 12.5 dimension shown below is a reference dimension to the top of the OCV flange thermal shield.

Damage Measurements: (See sketch below)

Quadrant	S (±0.06)	G (±0.06)
1	- 14/32	3/32
2	- 12/32	6/32
3	- 20/32	1/2
4	- 21/32	12/32



A (±0.25)	B (±0.25)	C (±0.25)	X (±0.25)	Y (±0.25)	Z (±0.25)
22 3/4	26 3/4	30 1/4	6.0	8.3	10.5

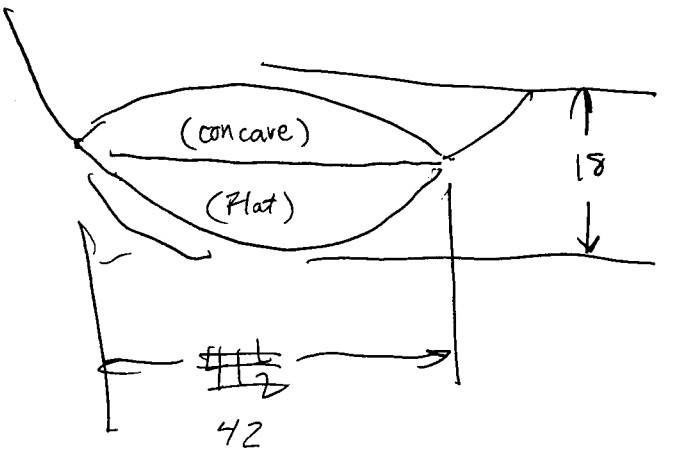
Test Engineer 11/09/95 Date

QA Representative 11/9/95 Date

DATA SHEET A

Drop Test No. 5, HAC 30-ft Drop, c.g. Over Bottom Corner

Sketch of Damage and Notes:



Test Engineer — Date 11/6/95

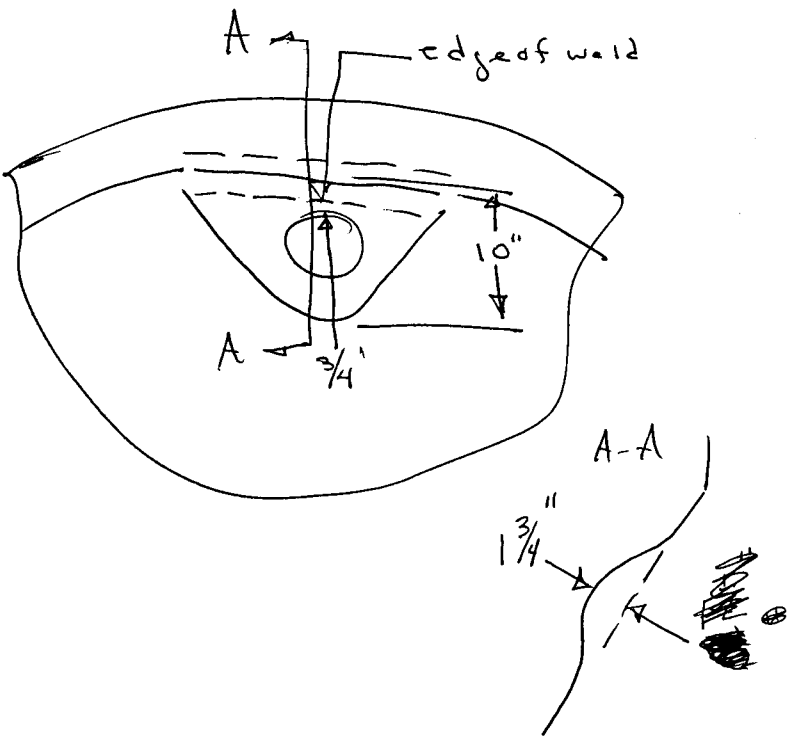
QA Representative — Date 11/6/95

DATA SHEET A

Drop Test No. 6, HAC Puncture

Impact Limiter Foam Temp. = 20°C
Ambient Temp. = 10°C

Post Test
18°C - Limiter
10°C - Ambient



Test Engineer 11/09/95 Date
QA Representative 11/9/95 Date

DATA SHEET B

Record of OCV closure residual bolt torque performed after completion of interim drop tests. Bolts are numbered CCW, viewed from the top of the Test Article, starting with the first bolt CCW from the feed-through.

OCV Bolts:

Loosen each bolt in turn just sufficient to establish the residual preload, followed by retorquing to the torque level equal to the installation torque, starting with Bolt No. 1, crossing the bell to Bolt No. 13, proceeding to Bolt No. 2 and across to Bolt No. 14, proceed to Bolt No. 24 and across to Bolt No. 12. The balance of the pattern is: 3-15, 23-11, 4-16, 22-10, 5-17, 21-9, 6-18, 20-8, 7-19.

OCV Closure Bolts

Residual Preload

Bolt #	Torque, ft-lb	Bolt #	Torque, ft-lb	
1	150	13	230	
2	190	14	225	
3	200	15	230	
4	200	16	250	
5	230	17	275	
6	300	18	(320)	300 (MAX)
7	280	19	(330)	300 (MAX)
8	270	20	(340)	300 (MAX)
9	225	21	265	
10	225	22	240	
11	195	23	260	
12	220	24	230	

AVERAGE → 241

Test Engineer 11/09/95 Date

QA Representative 11/09/95 Date

OFFICIAL COPY

DATA SHEET C

Record of ICV closure bolt relative position in relation to the ICV flange after removal of OCV bell.Bolts are numbered CCW, viewed from the top of the Test Article, starting with the first bolt CCW from the electrical feed-through.

ICV Closure Bolts

Relative Angular Position

Bolt #	Position	Bolt #	Position
1	✓OK	13	✓OK
2		14	
3		15	
4		16	
5		17	
6		18	
7		19	
8		20	
9		21	
10		22	
11		23	
12	✓OK	24	✓OK

D. L. Hunter 11/09/95
Test Engineer Date

B. O. Hay 11/09/95
QA Representative Date

OFFICIAL COPY

DATA SHEET D

Record of ICV retention bolt torque performed after completion of interim drop tests and after removal of OCV bell. Bolts are numbered CCW, viewed from the top of the Test Article, starting with the first bolt CCW from the electrical feed-through. Apply loosening torque of one-half the average residual torque established in assembly (see WHC 1995a), starting with Bolt No. 1, crossing the bell to Bolt No. 13, proceeding to Bolt No 2 and across to Bolt No. 14, proceed to Bolt No. 24 and across to Bolt No. 12. The balance of the pattern is: 3-15, 23-11, 4-16, 22-10, 5-17, 21-9, 6-18, 20-8, 7-19. If bolt loosens below this torque, record the loosening torque and proceed to the next bolt.

Average residual torque from initial assembly 156 ft-lb. ($\frac{1}{2} \Rightarrow 78$ ft-lb)
(Check in loosening direction to 1/2 this value)

ICV Closure Bolts Retention Torque Check*			
Bolt #	Torque, ft-lb	Bolt #	Torque, ft-lb
1	OK	13	OK
2	OK	14	OK
3	OK	15	OK
4	OK	16	OK
5	OK	17	OK
6	OK	18	OK
7	OK	19	OK
8	OK	20	OK
9	OK	21	OK
10	OK	22	OK
11	OK	23	OK
12	OK	24	OK

*Record OK if half the initial assembly torque is met; record loosening torque if bolt loosens.

Test Engineer 11/09/95 Date
QA Representative 11/09/95 Date

OFFICIAL COPY

DATA SHEET E1

Record of RTG Certification Test Article OCV and impact limiter bolt length performed after interim drop tests. Bolts are numbered CCW, viewed from the top of the Test Article, starting with the first bolt CCW from the electrical feed-through.

OCV Closure Bolts			
Bolt no.	Length (in.)	Bolt no.	Length (in.)
1	5.9728	13	5.9603
2	5.9566	14	5.9700
3	5.9650	15	5.9694
4	5.9738	16	5.9631
5	5.9619	17	5.9671
6	5.9761	18	5.9658
7	5.9801	19	5.9581
8	6.0337	20	5.9662
9	5.9756	21	5.9549
10	5.9682	22	5.9539
11	5.9663	23	5.9722
12	5.9746	24	5.9691

Impact Limiter Bolts	
Bolt no.	Length (in.)
9	8.9911 / 8.9904
10	8.9910 / 8.9954
11	8.9950 / 8.9888
12	8.9963 / 9.0004
13	8.9884 / 8.9839 *
14	8.9835 / 8.9932
15	8.9848 / 8.9878
16	8.9914 / 8.9933

	BEFORE TEST / AFTER TEST

*SEVERELY BENT

Impact Limiter Before

D. A. Quilter 11/08/95
Test Engineer Date

Roger W. Tuley 12-04-95
QA Representative Date

D. A. Quilter 11/09/95
OCV after Impact Limiter After Test

M+TE QC 11083

OFFICIAL COPY

Westinghouse Hanford Company

NDE LEAK TEST PROCEDURE AND TEST REPORT UL-100

NON DESTRUCTIVE EXAMINATION
306 BLDG., 300 AREA - TEL. 376-5401

Job No. 95-8

Requestor	Company	Project/System/Work Package/Traveler No.
A. AVERETTE	PACTEC	INTERIM DISASSEMBLY & REASSEMBLY OF THE RADIOISOTOPIC THERMOELECTRIC GENERATOR, SECOND CERTIFICATION, TEST ARTICLE CTA-2. DROP TEST 4,5,6 PER WHC-SD-RTG-TC-017 R/1

MSIN	Bldg.	Area
G2-02	MO-916	1100

Acceptance Std.	Section	Para.	Date	NA
LEAK RATE= <2.6 X 10-7 Atm cc/sec. HELIUM				

Dwg. No. NA
H-4-302118
H-4-112301

TEST CONDITIONS

- Temperature AMB. Device ID ____ NA [X]
- Barometric Pressure AMB. NA [ ]
- Test Pressure 1 ATM. NA [ ]
- Gas HELIUM NA [ ]
- Concentration APPROX. 100% NA [ ]
- Other ____ NA [X]
- Bubble Solution ____ NA [X]
- Batch No. ____
- Gage 1 584-31-04- 007 NA [ ]
- Range 0 TO 50 PSIA
- Calib. Exp. 3-9-96
- Gage 2 584-31-04- ____ NA [X]
- Range ____
- Calib. Exp. ____
- Relief Valve ____ NA [X]

TEST EQUIPMENT NA [ ]

- Manufacturer L/H UL 100 PLUS
- Ident. No. WC48896
- Mach. Sen. 1 X 10-11 Atm/cc/sec/Div
- Std. No. 584-40-03- 018
- Std. Leak 1.6 X 10-8 Atm/cc/sec
- Calib. Exp. 7-7-96

SYSTEM SENSITIVITY NA [ ]

- Same as MSLD Calib. or:
- Sensitivity 2.3 X 10-11 Atm/cc/sec/Div
- Std. No. 584-40-03-006
- Std. Leak 1.3 X 10-7 Atm/cc/sec
- Calib. Exp. 7-7-96

ADDITIONAL STD. NA [X]

- Sensitivity ____ Atm/cc/sec/Div
- Std. No. ____
- Std. Leak ____ Atm/cc/sec
- Calib. Exp. ____

NCR NA [X] | Cleaning NA [X]

WHC PROCEDURE NO. NA [ ]

- NDT-LT-6000 Rev. 3 [X]
- Appendix A Rev. 2
- Special Tech. No. ____ [ ]
- Work Inst. ____ [ ]

TEST TIME

- He Response Time IMMEDIATE NA [ ]
- He Accum. Time ____ NA [X]
- Soak Time ____ NA [X]
- Additional Times
- TEST TIME 2 MIN. NA [ ]

Weld No., Part No., or Serial No.	Acc.	Rej.	No Rel. Ind.	Comments
				OUTER CONTAINMENT VESSEL (OVC) LEAK RATE TESTS
"V" PORT STAT-O-SEAL	X		X	NO DETECTABLE LEAKS (PER STEP #7.2)
"T" PORT PRIM.O-RING	X		X	NO DETECTABLE LEAKS (PER STEP #7.3)
				INNER CONTAINMENT VESSEL (IVC) LEAK RATE TESTS
"P" PORT STAT-O-SEAL	X		X	NO DETECTABLE LEAKS (PER STEP #6.2)
"S" PORT STAT-O-SEAL	X		X	NO DETECTABLE LEAKS (PER STEP #6.3)
"T" PORT PRIM.O-RING	X		X	NO DETECTABLE LEAKS (PER STEP #6.4)

Technique Pre Approval NA [ ] | LT Level/Date

OFFICIAL COPY

Technician	Level	Interpreted by	LT Level II	Reviewed by
W. NELSON	I	B. L. HOPKINS	II	
Date of Examination: 11-09-95		Date: 11-09-95		Date: 11-13-95

2.10.15-80

A-6001-492 (11/94)

Westinghouse Hanford Company

NDE LEAK TEST PROCEDURE AND TEST REPORT UL-100

NON DESTRUCTIVE EXAMINATION
306 BLDG., 300 AREA - TEL. 376-5401

Job No. 95-8

Requestor	Company	Project/System/Work Package/Traveler No.
Jary S. Averette	PacTec	Helium Leak Test of Radioisotope Thermoelectric Generator (RTG) After Drop Tests #4-#6 on Certification Test Article #CTA-2, per WHC-SD-RTG-TC-017, Rev.1

MSIN	Bldg.	Area
G2-02	MO-916	1100

Acceptance Std.	Section	Para.	Date	NA
WHC-SD-RTG-TC-017 (Rev.1) Leakage Rate < 2.6 x 10 -7 atm.cc3/sec Helium		Para. 4.0	10/95	☐

Dwg. No. ☐ NA
H-4-302118
H-4-112301

TEST CONDITIONS

- Temperature: Amb. Device ID: ____ ☒ NA
- Barometric Pressure: ____ ☒ NA
- Test Pressure: ~~A~~ =1 Atm.(14.7psia) ☐ NA
- Gas: UHP Helium ☐ NA
- Concentration: >90% ☐ NA
- Other: ____ ☒ NA
- Bubble Solution: ____ ☒ NA
- Batch No.: ____
- Gage 1 584-31-04- 007 ☐ NA
  - Range: 0 to 50 psia
  - Calib. Exp.: March 9, 1996
- Gage 2 584-31-04- ____ ☒ NA
  - Range: ____
  - Calib. Exp.: ____
- Relief Valve: ____ ☒ NA

TEST EQUIPMENT ☐ NA

- Manufacturer: L/H "UL-100+", #2
- Ident. No.: S/n896-38 (WC48869)
- Mach. Sen.: 9.47 x 10 -12 Atm/cc/sec/Div
- Std. No. 584-40-03- 018
- Std. Leak: 1.6 x 10 -8 Atm/cc/sec
- Calib. Exp.: July 7, 1996

SYSTEM SENSITIVITY ☐ NA

☐ Same as MSLD Calib. or:

- Sensitivity: 1.70 x 10 -11 Atm/cc/sec/Div
- Std. No.: 584-40-03-006
- Std. Leak: 1.3 x 10 -7 Atm/cc/sec
- Calib. Exp.: July 7, 1996

ADDITIONAL STD. ☒ NA

- Sensitivity: ____ Atm/cc/sec/Div
- Std. No.: ____
- Std. Leak: ____ Atm/cc/sec
- Calib. Exp.: ____

NCR ☒ NA

Cleaning ☐ NA: Alcohol

WHC PROCEDURE NO. ☐ NA

- ☒ NDT-LT-6000 Rev. 3
- Appendix A Rev. 2
- ☐ Special Tech. No. ____
- ☐ Work Inst. ____

TEST TIME

- He Response Time: STAT-O-SEAL + PRIMARY O-RING IMMEDIATE ☐ NA
- He Accum. Time: ____ ☒ NA
- Soak Time: ____ ☒ NA
- Additional Times: "TEST DURATION" STAT-O-SEAL = 3 MIN. PRIMARY O-RING = 10 MIN. ☐ NA

Weld No., Part No., or Serial No.	Acc.	Rej.	No Rel. Ind.	Comments
				OUTER CONTAINMENT VESSEL (OCV) LEAK RATE TESTS:
"V" Port Stat-O-Seal	X		X	No Detectable Leakage (Per Step #5.2)
"T" Port Prim.O-Ring	X		X	No Detectable Leakage (Per Step #5.3)
				Note: For results of the remaining leak tests, Steps
				#6.2, 6.3, 6.4, 7.2 and 7.3, see B.L.Hopkins report
				dated November 10, 1995.

Technique Pre Approval ☒ NA — LT Level/Date

OFFICIAL COPY

Technician	Level	Interpreted by	LT Level II	Reviewed by
W.H.Nelson W.H.Nelson	I	B.J.Sewart B.J.Sewart	II	
B.J.Sewart B.J.Sewart	II			
Date of Examination: Nov. 9, 1995		Date: Nov. 9, 1995		Date: 11-14-95 2.10.15-81

Test Set 3: Drop Test Nos. 7, 8, and 9

Data Sheet A from WHC-SD-RTG-TC-015, Rev. 1
Data Sheets A, B, C1, and C2 from WHC-SD-RTG-TC-016, Rev. 1
NDE Leak Test Procedure and Test Report

DATA SHEET A

Drop Test No. 7, NCT 4-ft Drop, Bottom End

Ambient Temperature: 0°C Impact Limiter Foam Temperature: 24°C

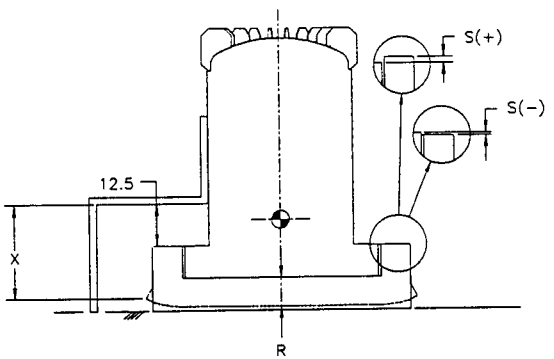
The 12.5 dimension shown below is a reference dimension to the top of the OCV flange thermal shield.

Damage Measurements: (See sketch below)

Quadrant	X (±0.13)	S (±0.06)
1		
2		
3		
4		

R = _____ ±0.13

THESE DIMENSIONS / Data
were not taken ~~HSA~~ 11/10/95
B.Q. Hung 11/10/95



Test Engineer _____ Date _____ QA Representative _____ Date _____

DATA SHEET A

Drop Test No. 7, NCT 4-ft Drop, Bottom End

Sketch of Damage and Notes:

Insufficient damage to record
See 30 ft drop test (Drop Test No. 8)

Test Engineer 11/20/95 Date QA Representative 11/30/95 Date

DATA SHEET A

Drop Test No. 8, HAC 30-ft Drop, Bottom End

Ambient Temperature: 2°C Impact Limiter Foam Temperature: 20°C

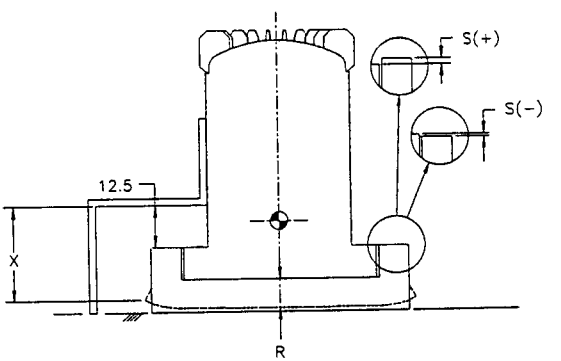
The 12.5 dimension shown below is a reference dimension to the top of the OCV flange thermal shield.

Damage Measurements: (See sketch below)

Quadrant	X (±0.13)	S (±0.06)
1	28 1/8	- 7/16
2	30 7/8	- 3/8
3	29 3/4	- 1/2
4	29 11/16	- 1/2

R = * ±0.13

x1 - distance taken at corner of angle (previously indented due to other drops)



* NOT TAKEN DUE TO DISTORTION OF LOWER PLATE

APPROXIMATE DEPTH OF FOAM ~8"

Test Engineer 11/10/95 Date

QA Representative 11/10/95 Date

DATA SHEET A

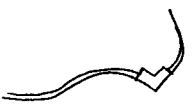
Drop Test No. 8, HAC 30-ft Drop, Bottom End

Sketch of Damage and Notes:

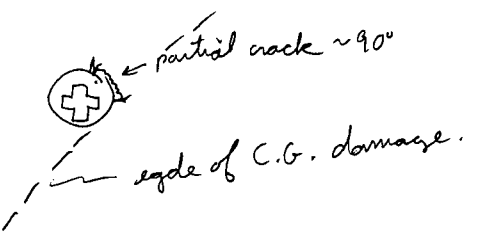
1. Small bulge or pooch most of the way around the package



2. C.G. end corner damage now looks like it did after C.G. 4-ft drop:



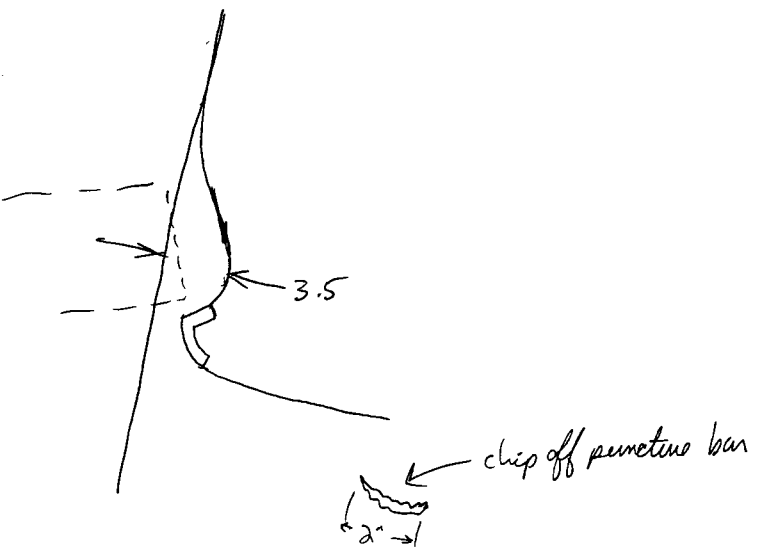
3. Small crack in weld around one melt out plug



Test Engineer — Date: 11/10/95 — QA Representative — Date: 11/10/95

DATA SHEET A

Drop Test No. 9, HAC Puncture



No weld distress.

Test Engineer — 11/10/95 Date

QA Representative — 11/10/95 Date

DATA SHEET A

Record of residual OCV closure and Impact Limiter pre-load bolt torque performed after completion of drop tests. Bolts are numbered CCW, viewed from the top of the Test Article, starting with the first bolt CCW from the feed-through.

OCV Bolts:
Loosen each bolt in turn just sufficient to establish the residual preload, followed by retorquing to the torque level equal to the installation torque multiplied by the ratio of the disassembly residual preload to the assembly residual preload (See WHC-SD-TC-014, Data Sheet A) or the disassembly preload torque, whichever is less, starting with Bolt 1, crossing the bell to Bolt 13, proceeding to Bolt 2 and across to Bolt 14, proceed to Bolt 24 and across to Bolt 12. The balance of the pattern is: 3-15, 23-11, 4-16, 22-10, 5-17, 21-9, 6-18, 20-8, 7-19.

Impact Limiter Bolts:
In a similar manner, loosen each bolt, starting with Bolt 1, crossing the bell to Bolt 5, proceeding to Bolt 2 and across to Bolt 6, proceed to Bolt 8 and across to Bolt 4, then to Bolt 3 and to Bolt 7.

OCV Closure Bolts Residual Preload			
Bolt #	Torque, ft-lb	Bolt #	Torque, ft-lb
1	180	13	260
2	230	14	275
3	(310)	15	270
4	300	16	280
5	290	17	280
6	255	18	260
7	235	19	270
8	240	20	230
9	250	21	270
10	255	22	250
11	210	23	200
12	240	24	200

MAX 300 Called 4/24/96

584-88-01-002 Called 4/24/96

AVE 250

Impact Limiter Bolts Residual Preload	
Bolt #	Torque, ft-lb
1	85
2	90
3	165
4	50
5	30
6	35
7	Loose
8	20

584-88-01-002 CAC exp 4-24-96

Test Engineer 11/10/95 Date

QA Representative 11/10/95 Date

OFFICIAL COPY
2.10.15-88

DATA SHEET B

Record of ICV residual pre-load bolt torque performed after completion of drop tests and after removal of OCV bell. Bolts are numbered CCW, viewed from the top of the Test Article, starting with the first bolt CCW from the electrical feed-through. Loosen each bolt in turn just sufficient to establish the residual preload, followed by retorquing to the torque level equal to the installation torque multiplied by the ratio of the disassembly residual preload to the assembly residual preload (See WHC-SD-TC-014, Data Sheet B) or the disassembly preload torque, whichever is less, starting with Bolt 1, crossing the bell to Bolt 13, proceeding to Bolt 2 and across to Bolt 14, proceed to Bolt 24 and across to Bolt 12. The balance of the pattern is: ✓3-15, ✓23-11, ✓4-16, ✓22-10, ✓5-17, ✓21-9, ✓6-18, ✓20-8, ✓7-19.

ICV Closure Bolts Residual Preload			
Bolt #	Torque, ft-lb	Bolt #	Torque, ft-lb
1	180	13	185
2	135	14	175
3	190	15	185
4	180	16	170
5	150	17	180
6	190	18	180
7	185	19	180
8	190	20	180
9	175	21	180
10	190	22	185
11	190	23	187
12	165	24	170

AVE = 178 FT-LB

584-88-01-002 ENG EXP 9-29-96

D. L. Curtis 11/10/95
Test Engineer Date

QA Representative 11/10/95
Date

OFFICIAL COPY

DATA SHEET C1

Record of RTG Certification Test Article bolt length performed after drop tests. Bolts are numbered CCW, viewed from the top of the Test Article, starting with the first bolt CCW from the electrical feed-through.

NEW BOLTS TEST 7, 8, 9

OCV Closure Bolts			
Bolt #	Length (in.)	Bolt #	Length (in.)
1	5.9731	13	5.9604
2	5.9567	14	5.9702
3	5.9653	15	5.9700
4	5.9739	16	5.9633
5	5.9621	17	5.9677
6	5.9763	18	5.9661
7	5.9805	19	5.9579
8	6.0336	20	5.9664
9	5.9761	21	5.9549
10	5.9681	22	5.9536
11	5.9666	23	5.9723
12	5.9747	24	5.9690

Note: these measurements apply to "before tests" for tests 10 → up

Impact Limiter Bolts		
Bolt #	Length (in.)	
X17	8.9920 ~~8.9931~~	8.9931
X18	8.9841 ~~8.9842~~	8.9878
X19	8.9914 ~~8.9896~~	8.9895
X20	8.9905 8.9904	
X21	8.9944 8.9951	
X22	8.9868 8.9895	8.9901
X23	8.9891 8.9881	0.00
X24	8.9913 8.9924	0.00
		8.9924

Bolt #	Before Test	After Test

Note: the "after" measurement apply to "before testing" for tests 10 → up

Impact Limiter Bolts Before Tests

D. L. Quilt 11/9/95
Test Engineer Date

Ray W. Tuller 11-15-95
QA Representative Date

After Tests 7, 8, 9

D. L. Quilt 11/9/95

OFFICIAL COPY

DATA SHEET C2

ICV Closure Bolts			
Bolt #	Length (in.)	Bolt #	Length (in.)
1	1.9582	13	1.9492
2	1.9626	14	1.9699
3	1.9674	15	1.9555
4	1.9711	16	1.9646
5	1.9687	17	1.9595
6	1.9669	18	1.9602
7	1.9693	19	1.9690
8	1.9559	20	1.9687
9	1.9643	21	1.9580
10	1.9729	22	1.9639
11	1.9615	23	1.9616
12	1.9557	24	1.9592

Note: These measurements apply to "before test" for tests 10 → up

Test Engineer 11/14/95 Date

QA Representative 11-15-95 Date

OFFICIAL COPY
2.10.15-91

Westinghouse Hanford Company

NDE LEAK TEST PROCEDURE AND TEST REPORT UL-100

NON DESTRUCTIVE EXAMINATION
306 BLDG., 300 AREA - TEL. 376-5401

Job No. 95-8

Requestor	Company	Project/System/Work Package/Traveler No.
A. AVERETTE	PACTEC	INTERIM DISASSEMBLY & REASSEMBLY OF THE RADIOISOTOPIC THERMOELECTRIC GENERATOR, SECOND CERTIFICATION, TEST ARTICLE CTA-2. DROP TEST 7,8,9 PER WHC-SD-RTG-TC-017 R/1

MSIN	Bldg.	Area
G2-02	MO-916	1100

Acceptance Std.	Section	Para.	Date	NA
LEAK RATE= <2.6 X 10-7 Atm cc/sec. HELIUM				☐

Dwg. No. ☐ NA
H-4-302118
H-4-112301

TEST CONDITIONS

Temperature	AMB. Device ID	☒ NA
Barometric Pressure	AMB.	☐ NA
Test Pressure	1 ATM.	☐ NA
Gas	HELIUM	☐ NA
Concentration	APPROX. 100%	☐ NA
Other		☒ NA
Bubble Solution		☒ NA
Batch No.		
Gage 1 584-31-04-	007	☐ NA
Range	0 TO 50 PSIA	
Calib. Exp.	3-9-96	
Gage 2 584-31-04-		☒ NA
Range		
Calib. Exp.		
Relief Valve		☒ NA

TEST EQUIPMENT ☐ NA

Manufacturer	L/H UL 100 PLUS	
Ident. No.	WC48896	
Mach. Sen.	1 X 10-11	Atm/cc/sec/Div
Std. No. 584-40-03-	018	
Std. Leak	1.6 X 10-8	Atm/cc/sec
Calib. Exp.	7-7-96	

SYSTEM SENSITIVITY ☐ NA
☐ Same as MSLD Calib. or:

Sensitivity	1.6 X 10-11	Atm/cc/sec/Div
Std. No.	584-40-03-006	
Std. Leak	1.3 X 10-7	Atm/cc/sec
Calib. Exp.	7-7-96	

ADDITIONAL STD. ☒ NA

Sensitivity		Atm/cc/sec/Div
Std. No.		
Std. Leak		Atm/cc/sec
Calib. Exp.		

NCR ☒ NA

Cleaning ☒ NA

WHC PROCEDURE NO. ☐ NA
☒ NDT-LT-6000 Rev. 3
Appendix A Rev. 2
☐ Special Tech. No.
☐ Work Inst.

TEST TIME

He Response Time	IMMEDIATE ☐ NA
He Accum. Time	☒ NA
Soak Time	☒ NA
Additional Times	TEST TIME 2 MIN. ☐ NA

Weld No., Part No., or Serial No.	Acc.	Rej.	No Rel. Ind.	Comments
				OUTER CONTAINMENT VESSEL (OVC) LEAK RATE TESTS
"V" PORT STAT-O-SEAL	X			LEAK RATE = 1.0 X 10 -9 ATM CC/SEC. (PER STEP #6.4)
"T" PORT PRIM.O-RING	X		X	NO DETECTABLE LEAKS (PER STEP #6.5)
				INNER CONTAINMENT VESSEL (IVC) LEAK RATE TESTS
"P" PORT STAT-O-SEAL	X		X	NO DETECTABLE LEAKS (PER STEP #7.2)
"S" PORT STAT-O-SEAL	X		X	NO DETECTABLE LEAKS (PER STEP #7.3)
"T" PORT PRIM.O-RING	X		X	NO DETECTABLE LEAKS (PER STEP #7.4)

Technique Pre Approval ☑ NA — LT Level/Date

Technician	Level	Interpreted by	LT Level II	Reviewed by
W.H. NELSON	I	B. L. HOPKINS	II	R E Layne
		J.K. KEVE	III	
Date of Examination		Date		Date
11-10-95		11-10-95		11/21/95 2.10.15-92

Westinghouse Hanford Company

NDE LEAK TEST PROCEDURE AND TEST REPORT UL-100

NON DESTRUCTIVE EXAMINATION
306 BLDG., 300 AREA - TEL. 376-5401

Job No. 95-8

Requestor	Company	Project/System/Work Package/Traveler No.
Mary S. Averette	PacTec	Helium Leak Test of Radioisotope Thermoelectric Generator (RTG) After Drop Tests #7-#9 on Certification Test Article #CTA-2, per WHC-SD-RTG-TC-016, Rev.1

Bldg.	Area
272-02	MO-916	1100

Acceptance Std.	Section	Para.	Date	NA
WHC-SD-RTG-TC-016, Rev.1 Leakage Rate < 2.6 x 10 -7 atm.cm3/sec Helium		Para. 5.0	10/95	

Dwg. No. NA: H-4-302118, H-4-112301

TEST CONDITIONS

Temperature	Amb. Device ID	X NA
Barometric Pressure		X NA
Test Pressure	4 =1 Atm.(14.7psia)	NA
Gas	UHP Helium	NA
Concentration	> 90%	NA
Other		X NA
Bubble Solution		X NA
Batch No.		
Gage 1 584-31-04-	007	NA
Range	0 to 50 psia	
Calib. Exp.	March 9, 1996	
Gage 2 584-31-04-		X NA
Range		
Calib. Exp.		
Relief Valve		X NA

TEST EQUIPMENT NA

Manufacturer	L/H "UL-100+", #2
Ident. No.	s/n896-38 (WC48869)
Mach. Sen.	1.07 x 10 -11 Atm/cc/sec/Div
Std. No. 584-40-03-	018
Std. Leak	1.6 x 10 -8 Atm/cc/sec
Calib. Exp.	July 7, 1996

SYSTEM SENSITIVITY NA
Same as MSLD Calib. or:

Sensitivity	2.36 x 10 -10 Atm/cc/sec/Div
Std. No.	584-40-03-006
Std. Leak	1.3 x 10 -7 Atm/cc/sec
Calib. Exp.	July 7, 1996

ADDITIONAL STD. X NA

Sensitivity	Atm/cc/sec/Div
Std. No.	
Std. Leak	Atm/cc/sec
Calib. Exp.	

NCR X NA

Cleaning NA: Alcohol

WHC PROCEDURE NO. NA
X NDT-LT-6000 Rev. 3
Appendix A Rev. 2
Special Tech. No.
Work Inst.

TEST TIME ICV STRUCTURE TEST
He Response Time = 3 MIN. NA
He Accum. Time X NA
Soak Time X NA
Additional Times : "TEST DURATION" = 30 MIN NA

Weld No., Part No., or Serial No.	Acc.	Rej.	No Rel. Ind.	Comments
				INNER CONTAINMENT VESSEL (ICV) LEAK RATE TESTS:
ICV Structure	X			Leak Rate=1.96 x 10 -7 atm.cm3/sec Helium (Per Step #7.6)
				Note: For results of the remaining leak tests, Steps
				#6.2, 6.4, 6.5, 7.2, 7.3 and 7.4, see B.L.Hopkins report
				dated November 10, 1995.

Technique Pre Approval: LT Level/Date: NA

OFFICIAL COPY

Tested by	Level	Interpreted by	LT Level II	Reviewed by
W.H.Nelson	I			
B.J.Sewart	II	B.J.Sewart	II	
Date of Examination: Nov.13, 1995		Date: Nov.13, 1995		Date: 11-14-95

2.10.15-93

A-6001-492 (11/94)

Westinghouse Hanford Company

NDE LEAK TEST PROCEDURE AND TEST REPORT UL-100

NON DESTRUCTIVE EXAMINATION
306 BLDG., 300 AREA - TEL. 376-5401

Job No. 95-8

Requestor	Company	Project/System/Work Package/Traveler No.
...ry S. Averette	PacTec	Helium Leak Test of Radioisotope Thermoelectric Generator (RTG) After Drop Tests #7-#9 on Certification Test Article #CTA-2, per WHC-SD-RTG-TC-014, Rev.1

MSIN	Bldg.	Area
G2-02	MO-916	1100

Acceptance Std.	Section	Para.	Date	NA
WHC-SD-RTG-TC-014, Rev.1		Para.5.0	10/95	
Leakage Rate < 2.6 x 10 -7 atm.cm3/sec. Helium				

Dwg. No. NA: H-4-302118, H-4-112301

TEST CONDITIONS

- Temperature Amb. Device ID ____ [X] NA
- Barometric Pressure ____ [X] NA
- Test Pressure =1 Atm.(14.7psia) [ ] NA
- Gas UHP Helium [ ] NA
- Concentration >90% [ ] NA
- Other ____ [X] NA
- Bubble Solution ____ [X] NA
- Batch No. ____
- Gage 1 584-31-04- 007 [ ] NA
  - Range 0 to 50 psia
  - Calib. Exp. March 9, 1996
- Gage 2 584-31-04- ____ [X] NA
  - Range ____
  - Calib. Exp. ____
- Relief Valve ____ [X] NA

TEST EQUIPMENT [ ] NA

- Manufacturer L/H "UL-100+", #2
- Ident. No. s/n896-38 (WC48869)
- Mach. Sen. 9.47 x 10 -12 Atm/cc/sec/Div
- Std. No. 584-40-03- 018
- Std. Leak 1.6.x 10 -8 Atm/cc/sec
- Calib. Exp. July 7, 1996

SYSTEM SENSITIVITY [ ] NA

[ ] Same as MSLD Calib. or:

- Sensitivity 1.26 x 10 -11 Atm/cc/sec/Div
- Std. No. 584-40-03-006
- Std. Leak 1.3 x 10 -7 Atm/cc/sec
- Calib. Exp. July 7, 1996

ADDITIONAL STD. [X] NA

- Sensitivity ____ Atm/cc/sec/Div
- Std. No. ____
- Std. Leak ____ Atm/cc/sec
- Calib. Exp. ____

NCR [X] NA

Cleaning [ ] NA: Alcohol

WHC PROCEDURE NO. [ ] NA

- [X] NDT-LT-6000 Rev. 3
- Appendix A Rev. 2
- [ ] Special Tech. No. ____
- [ ] Work Inst. ____

TEST TIME

STAT-O-SEAL + PRIMARY O-RING

- He Response Time: IMMEDIATE [ ] NA
- He Accum. Time ____ [X] NA
- Soak Time ____ [X] NA
- Additional Times: "TEST DURATION"
  - STAT-O-SEAL = 3 min. [ ] NA
  - PRIMARY O-RING = 10 min.

Weld No., Part No., or Serial No.	Acc.	Rej.	No Rel. Ind.	Comments
				INNER CONTAINMENT VESSEL (ICV) LEAK RATE TESTS:
"P" Port Stat-O-Seal	X		X	No Detectable Leakage (Per Step #6.4)
"S" Port Stat-O-Seal	X		X	No Detectable Leakage (Per Step #6.5)
"T" Port Prim.O-Ring	X		X	No Detectable Leakage (Per Step #6.6)
				OUTER CONTAINMENT VESSEL (OCV) LEAK RATE TESTS:
"V" Port Stat-O-Seal	X		X	No Detectable Leakage (Per Step #7.4)
"T" Port Prim.O-Ring	X		X	No Detectable Leakage (Per Step #7.5)

Technique Pre Approval [X] NA — LT Level/Date

Technician	Level	Interpreted by	LT Level II	Reviewed by
W.H.Nelson	I			
B.J.Sewart	II	B.J.Sewart	II	
Date of Examination: Nov.14, 1995		Date: Nov.14, 1995		Date: 11-15-95 2.10.15-94

Westinghouse Hanford Company

NDE LEAK TEST PROCEDURE AND TEST REPORT UL-100

NON DESTRUCTIVE EXAMINATION
306 BLDG., 300 AREA - TEL. 376-5401

Job No. 95-8

Requestor: ,ry S. Averette — Company: PacTec

Project/System/Work Package/Traveler No.: Helium Leak Test of Radioisotope Thermoelectric Generator (RTG) After Drop Tests #7-#9 on Certification Test Article #CTA-2, per WHC-SD-RTG-TC-016, Rev.1

MSIN	Bldg.	Area
G2-02	MO-916	1100

Acceptance Std.	Section	Para.	Date	NA
WHC-SD-RTG-TC-016 (Rev.1) Leakage Rate < 2.6 x 10 -7 atm.cm3/sec. Helium		Para. 5.0	10/95	☐

Dwg. No. ☐ NA: H-4-302118, H-4-112301

TEST CONDITIONS

- Temperature: Amb. Device ID: ____ ☒ NA
- Barometric Pressure: ____ ☒ NA
- Test Pressure: =1 Atm.(14.7psia) ☐ NA
- Gas: UHP Helium ☐ NA
- Concentration: >90% ☐ NA
- Other: ____ ☒ NA
- Bubble Solution: ____ ☒ NA
- Batch No.: ____
- Gage 1 584-31-04- 007 ☐ NA
- Range: 0 to 50 psia
- Calib. Exp.: March 9, 1996
- 2 584-31-04- ____ ☒ NA
- Range: ____
- Calib. Exp.: ____
- Relief Valve: ____ ☒ NA

TEST EQUIPMENT ☐ NA

- Manufacturer: L/H "UL-100+", #2
- Ident. No.: S/n896-38 (WC48869)
- Mach. Sen.: 9.47 x 10 -12 Atm/cc/sec/Div
- Std. No. 584-40-03- 018
- Std. Leak: 1.6 x 10 -8 Atm/cc/sec
- Calib. Exp.: July 7, 1996

SYSTEM SENSITIVITY ☐ NA

☐ Same as MSLD Calib. or:

- Sensitivity: 8.13 x 10 -11 Atm/cc/sec/Div
- Std. No.: 584-40-03-006
- Std. Leak: 1.3 x 10 -7 Atm/cc/sec
- Calib. Exp.: July 7, 1996

ADDITIONAL STD. ☒ NA

- Sensitivity: ____ Atm/cc/sec/Div
- Std. No.: ____
- Std. Leak: ____ Atm/cc/sec
- Calib. Exp.: ____

NCR ☒ NA

Cleaning ☐ NA: Alcohol

WHC PROCEDURE NO. ☐ NA

- ☒ NDT-LT-6000 Rev. 3
- Appendix A Rev. 2
- ☐ Special Tech. No. ____
- ☐ Work Inst. ____

TEST TIME

- He Response Time = 4 MINUTES ☐ NA
- He Accum. Time ____ ☒ NA
- Soak Time ____ ☒ NA
- Additional Times: "TEST DURATION" OCV STRUCTURE = 30 MINUTES ☐ NA

Weld No., Part No., or Serial No.	Acc.	Rej.	No Rel. Ind.	Comments
				OUTER CONTAINMENT VESSEL (OCV) LEAK RATE TESTS:
OCV Structure	X			Leak Rate=1.42 x 10 -7 atm.cm3/sec.Helium (Per Step #6.2)
				Note: This is the last OCV Structure leak rate test done
				prior to reassembly of package per WHC-SD-RTG-TC-014.

Technique Pre Approval ☒ NA — LT Level/Date

Technician	Level	Interpreted by	LT Level II	Reviewed by
W.H.Nelson	I	B.J.Sewart	II	
B.J.Sewart	II			
Date of Examination: Nov.14, 1995		Date: 11/15/95		Date: 11-15-95 2.10.15-95

Test Set 4: Drop Test Nos. 10, 11, 12, 13, 14, 15, and 16

Data Sheet A from WHC-SD-RTG-TC-015, Rev. 1
Data Sheets A, B, C1, and C2 from WHC-SD-RTG-TC-016, Rev. 1
NDE Leak Test Procedure and Test Report

DATA SHEET A

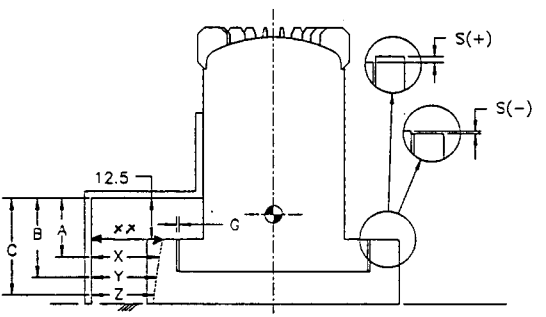
Drop Test No. 10, NCT 4-ft Drop, Side Slapdown

Ambient Temperature: 4°C Impact Limiter Foam Temperature: 28°C

The 12.5 dimension shown below is a reference dimension to the top of the OCV flange thermal shield.

Damage Measurements: (See sketch below)

Quadrant	S (±0.06)	G (±0.06)
1	- 6/10	12/32
2	- 11/32	1/16
3	- 17/32	6/32
4	- 14/32	12/32



XX = 5 5/8

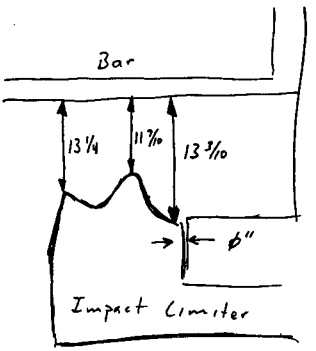
A (±0.25)	B (±0.25)	C (±0.25)	X (±0.25)	Y (±0.25)	Z (±0.25)
14 3/8	22.0	30 1/8	5 1/4	4 1/8	4 1/4

Test Engineer 11/20/95 Date QA Representative 11/20/95 Date

DATA SHEET A

Drop Test No. 10, NCT 4-ft Drop, Side Slapdown

Sketch of Damage and Notes:



Test Engineer — Date 11/20/96

QA Representative — Date 11/20/96

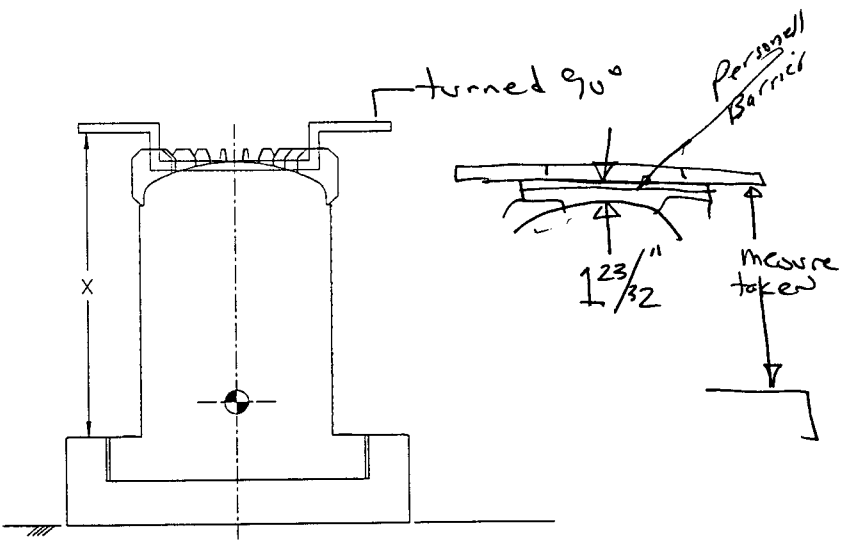
DATA SHEET A

Drop Test No. 11, NCT 4-ft Drop, Top End

Ambient Temperature: 7 °C Impact Limiter Foam Temperature: N/A

Damage Measurements: (See sketch below)

Quadrant	X (±0.13)
1	57 3/4
2	57 1/2
3	58 1/2
4	58



Test Engineer Date 11/19/96 QA Representative Date 11/20/96

DATA SHEET A

Drop Test No. 11, NCT 4-ft Drop, Top End

Sketch of Damage and Notes:

SEE PHOTOS OF DROP
EVEN FLATTENING OF FINS

D. L. Quito 11/20/95
Test Engineer Date

M E Rud 11/20/95
QA Representative Date

DATA SHEET A

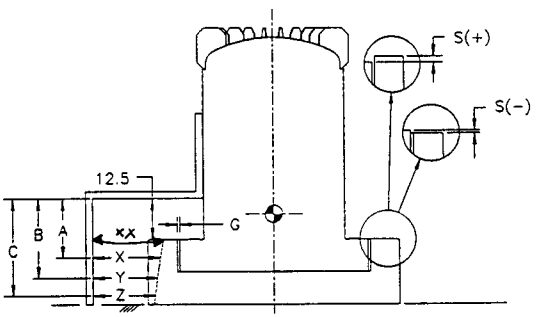
Drop Test No. 12, HAC 30-ft Drop, Side Slapdown

Ambient Temperature: 11°C Impact Limiter Foam Temperature: 28°C

The 12.5 dimension shown below is a reference dimension to the top of the OCV flange thermal shield.

Damage Measurements: (See sketch below)

Quadrant	S (±0.06)	G (±0.06)
1	-18/32	11/32
2	-16/32	1/16
3	-21/32	12/32
4	-14/32	10/32



XX = 7 8/10"

A (±0.25)	B (±0.25)	C (±0.25)	X (±0.25)	Y (±0.25)	Z (±0.25)
14 3/8"	22.0"	30 1/8"	7 3/4	5 3/4	4 7/8

Test Engineer 11/2/95 Date QA Representative 11/2/95 Date

DATA SHEET A

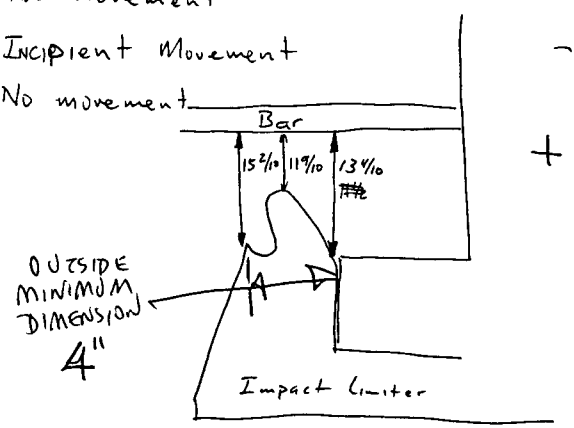
Drop Test No. 12, HAC 30-ft Drop, Side Slapdown

Sketch of Damage and Notes:

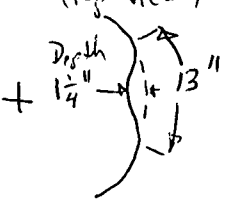
Impact Limiter Bolts

TORQUE WRENCH
SN - 584-88-01-002
CAL EXP 9/29/96

1 - No movement
2 - Incipient Movement
3 - Loose
4 - Loose
5 - No Movement
6 - No Movement
7 - Incipient Movement
8 - No movement



Coolant Jacket at top of cask (top view)



D. L. Reith — Test Engineer — 11/20/95 — Date

M E Kurt — QA Representative — 11/20/95 — Date

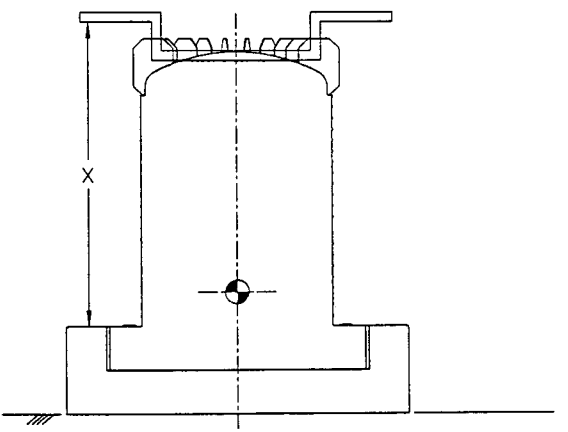
DATA SHEET A

Drop Test No. 13, HAC 30-ft Drop, Top End

Ambient Temperature: 16 °C Impact Limiter Foam Temperature: N/A 25 °C

Damage Measurements: (See sketch below)

Quadrant	X (±0.13)
1	60 1/4
2	~~60 3/16~~ 58 7/8
3	60 3/16
4	61 9/16



Test Engineer 11/20/95 Date QA Representative 11/20/95 Date

DATA SHEET A

Drop Test No. 13, HAC 30-ft Drop, Top End

Sketch of Damage and Notes:

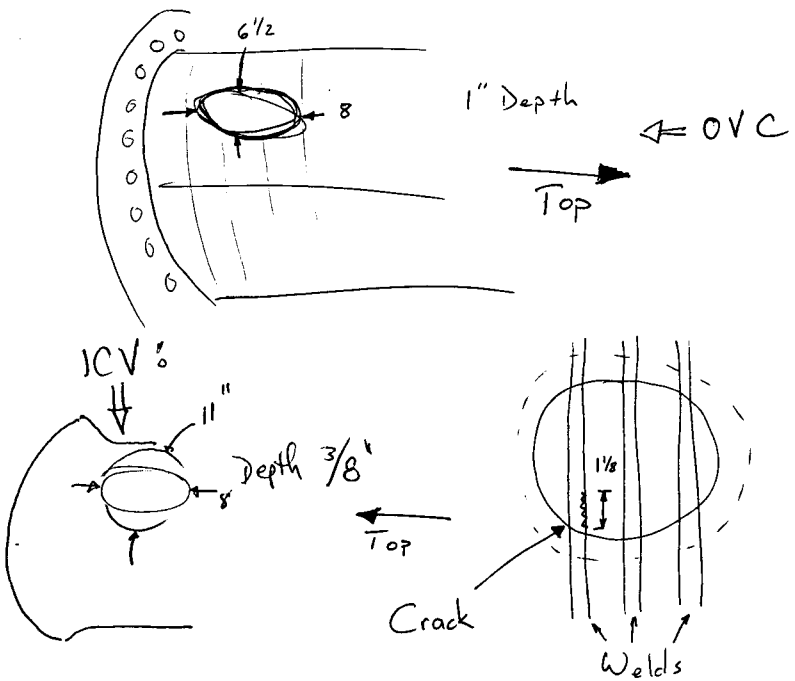
SEE PHOTOS

T. S. Smith 11/20/95
Test Engineer Date

QA Representative 11/20/95
Date

DATA SHEET A

Drop Test No. 14, HAC Puncture AMBIENT TEMP 10°C
FOAM TEMP AFTER TEST 23°C



Test Engineer — Date 11/20/95

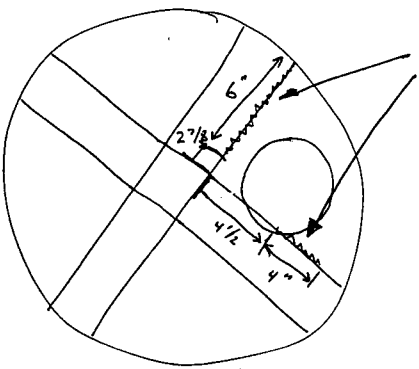
QA Representative — Date 11/20/95

DATA SHEET A

Drop Test No. 15, HAC Puncture

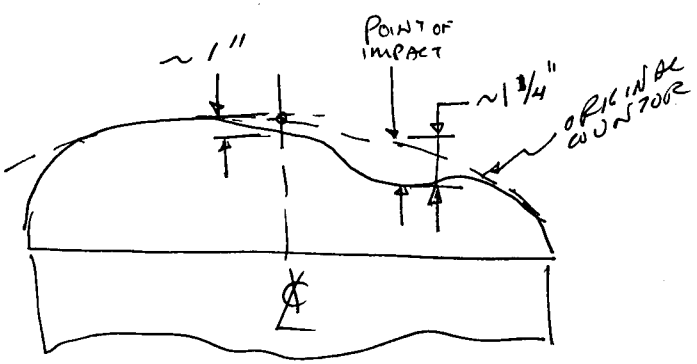
Impact Limiter Foam Temp = 25°C

Ambient Temp = ~~10°C~~ 8°C 15:15 MCR



Cracks through Center of weld

1 1/4" Depth



Test Engineer — Date — QA Representative — Date

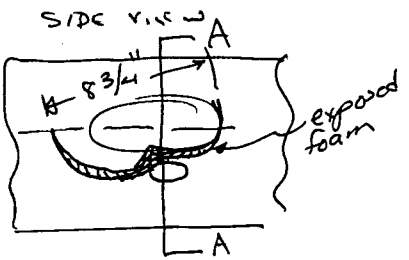
DATA SHEET A

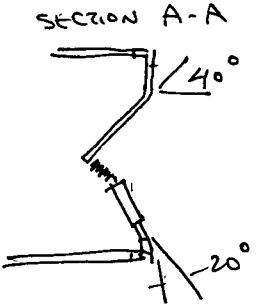
Drop Test No. 16, HAC Puncture

Impact Limiter Foam Temp = 20°C

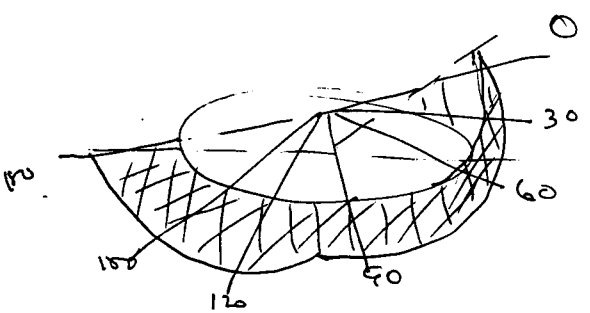
Ambient Temp = 8°C

SIDE WALL OF IMPACT LIMITER CRACKED.





exposed foam (projected dimension)



	FOAM EXP. IN.
0	0
30	7/8"
60	1"
90	1 1/4"
120	1"
150	3/4"
180	0

Test Engineer — Date 11/2/95

QA Representative — Date 11/20/95

DATA SHEET A

Record of residual OCV closure and Impact Limiter pre-load bolt torque performed after completion of drop tests. Bolts are numbered CCW, viewed from the top of the Test Article, starting with the first bolt CCW from the feed-through.

OCV Bolts:
Loosen each bolt in turn just sufficient to establish the residual preload, followed by retorquing to the torque level equal to the installation torque multiplied by the ratio of the disassembly residual preload to the assembly residual preload (See WHC-SD-TC-014, Data Sheet A) or the disassembly preload torque, whichever is less, starting with Bolt 1, crossing the bell to Bolt 13, proceeding to Bolt 2 and across to Bolt 14, proceed to Bolt 24 and across to Bolt 12. The balance of the pattern is: 3-15, 23-11, 4-16, 22-10, 5-17, 21-9, 6-18, 20-8, 7-19.

Impact Limiter Bolts:
In a similar manner, loosen each bolt, starting with Bolt 1, crossing the bell to Bolt 5, proceeding to Bolt 2 and across to Bolt 6, proceed to Bolt 8 and across to Bolt 4, then to Bolt 3 and to Bolt 7.

OCV Closure Bolts Residual Preload			
Bolt #	Torque, ft-lb	Bolt #	Torque, ft-lb
1	225	13	250
2	240	14	260
3	250	15	230
4	240	16	250
5	265	17	260
6	260	18	265
7	255	19	280
8	265	20	240
9	240	21	260
10	280	22	265
11	260	23	280
12	240	24	215

AVERAGE = 252 ft-lb

TORQUE WRENCH 584-88-01-002 CAL EXP 9/29/96

Impact Limiter Bolts Residual Preload	
Bolt #	Torque, ft-lb
1	112
2	LOOSE
3	LOOSE
4	LOOSE
5	80
6	82
7	35
8	62

TORQUE WRENCH 950-88-01-068 CAL EXP 10-20-96

MSR 11/20/95 1827

Test Engineer 11/4/95 Date

QA Representative 11/21/95 Date

OFFICIAL COPY

DATA SHEET B

Record of ICV residual pre-load bolt torque performed after completion of drop tests and after removal of OCV bell. Bolts are numbered CCW, viewed from the top of the Test Article, starting with the first bolt CCW from the electrical feed-through. Loosen each bolt in turn just sufficient to establish the residual preload, followed by retorquing to the torque level equal to the installation torque multiplied by the ratio of the disassembly residual preload to the assembly residual preload (See WHC-SD-TC-014, Data Sheet B) or the disassembly preload torque, whichever is less, starting with Bolt 1, crossing the bell to Bolt 13, proceeding to Bolt 2 and across to Bolt 14, proceed to Bolt 24 and across to Bolt 12. The balance of the pattern is: ✓3-15, ✓23-11, ✓4-16, ✓22-10, ✓5-17, ✓21-9, ✓6-18, ✓20-8, ✓7-19.

ICV Closure Bolts Residual Preload			
Bolt #	Torque, ft-lb	Bolt #	Torque, ft-lb
1	215	13	230
2	210	14	220
3	210	15	200
4	220	16	215
5	230	17	220
6	225	18	210
7	220	19	220
8	200	20	200
9	200	21	175
10	190	22	200
11	215	23	175
12	190	24	200

Lines on bolts were apparently in line with lines on ICV counterbore

TORQUE WRENCH 584-88-01-002 CAL EXP 9/29/96

AVERAGE = 208 FT-LB

D.A. Smith 11/29/95
Test Engineer Date

M.E. Kirkbride 11/29/95
QA Representative Date

OFFICIAL COPY

DATA SHEET C1

Record of RTG Certification Test Article bolt length performed after drop tests. Bolts are numbered CCW, viewed from the top of the Test Article, starting with the first bolt CCW from the electrical feed-through.

OCV Closure Bolts			
Bolt #	Length (in.)	Bolt #	Length (in.)
1	5.9734	13	5.9610
2	5.9568	14	5.9706
3	5.9658	15	5.9701
4	5.9741	16	5.9636
5	5.9622	17	5.9678
6	5.9764	18	5.9665
7	~~5.9802~~ ~~5.9682~~	19	5.9580
8	6.0339	20	5.9665
9	5.9764	21	5.9550
10	5.9683	22	5.9540
11	5.9667	23	5.9727
12	5.9754	24	5.9692

Impact Limiter Bolts	
Bolt #	Length (in.)
1	9.0039
2	9.0065
3	8.9996
4	9.0035
5	9.0102
6	8.9969
7	8.9941
8	8.9982

D. S. Arnold 12/04/95
Test Engineer Date

Ryan Colley 12-04-95
QA Representative Date
M&TE QC 11083

OFFICIAL COPY

DATA SHEET C2

ICV Closure Bolts			
Bolt #	Length (in.)	Bolt #	Length (in.)
1	1.9586	13	1.9491
2	1.9626	14	1.9699
3	1.9672	15	1.9552
4	1.9714	16	1.9644
5	1.9685	17	1.9598
6	1.9669	18	1.9601
7	1.9690	19	1.9691
8	1.9567	20	1.9689
9	1.9646	21	1.9582
10	1.9729	22	1.9641
11	1.9616	23	1.9616
12	1.9555	24	1.9601

D. A. Quick 12/04/98
Test Engineer Date

Frank W. Talley 12-04-98
QA Representative Date
MATE QC 11083

OFFICIAL COPY
2.10.15-111

Westinghouse Hanford Company

NDE LEAK TEST PROCEDURE AND TEST REPORT UL-100

NON DESTRUCTIVE EXAMINATION
306 BLDG., 300 AREA - TEL. 376-5401

Job No. 95-8

Requestor	Company	Project/System/Work Package/Traveler No.
Mary S. Averette	PacTec	Helium Leak Test of Radioisotope Thermoelectric Generator (RTG) After Drop Test #10-#16 on Certification Test Article #CTA-2, per WHC-SD-RTG-TC-016, Rev.1

MSIN	Bldg.	Area
G2-02	MO-916	1100

Acceptance Std.	Section	Para.	Date	NA
WHC-SD-RTG-TC-016, Rev.1 Leakage Rate < 2.6 x 10 -7 atm.cm3/sec Helium		Para. 5.0	10/95	

Dwg. No. NA
H-4-302118
H-4-112301

TEST CONDITIONS

- Temperature: Amb. Device ID: ____ [X] NA
- Barometric Pressure: ____ [X] NA
- Test Pressure: =1 Atm.(14.7psia) [ ] NA
- Gas: UHP Helium [ ] NA
- Concentration: >90% [ ] NA
- Other: ____ [X] NA
- Bubble Solution: ____ [X] NA
- Batch No.: ____
- Gage 1 584-31-04- 007 [ ] NA
- Range: 0 to 50 psia
- Calib. Exp.: March 9, 1996
- Gage 2 584-31-04- ____ [X] NA
- Range: ____
- Calib. Exp.: ____
- Relief Valve: ____ [X] NA

TEST EQUIPMENT [ ] NA

- Manufacturer: L/H "UL-100+", #2
- Ident. No.: s/n896-38 (WC48869)
- Mach. Sen.: 1.04 x 10 -11 Atm/cc/sec/Div
- Std. No. 584-40-03-: 018
- Std. Leak: 1.6 x 10 -8 Atm/cc/sec
- Calib. Exp.: July 7, 1996

SYSTEM SENSITIVITY [ ] NA

- [ ] Same as MSLD Calib. or:
- Sensitivity: 1.48 x 10 -11 Atm/cc/sec/Div
- Std. No.: 584-40-03-006
- Std. Leak: 1.3 x 10 -7 Atm/cc/sec
- Calib. Exp.: July 7, 1996

ADDITIONAL STD. [X] NA

- Sensitivity: ____ Atm/cc/sec/Div
- Std. No.: ____
- Std. Leak: ____ Atm/cc/sec
- Calib. Exp.: ____

NCR [X] NA

Cleaning [ ] NA: Alcohol

WHC PROCEDURE NO. [ ] NA

- [X] NDT-LT-6000 Rev. 3
- Appendix A Rev. 2
- [ ] Special Tech. No. ____
- [ ] Work Inst. ____

TEST TIME

OCV STRUCTURE = 4 MINUTES
STAT-O-SEAL & PRIMARY O-RING =
He Response Time: IMMEDIATE [ ] NA

He Accum. Time: ____ [X] NA

Soak Time: ____ [X] NA

Additional Times: "TEST DURATION"
STAT-O-SEAL = 3 MINUTES
PRIMARY O-RING = 5 MINUTES
STRUCTURE = 25 MINUTES [ ] NA

Weld No., Part No., or Serial No.	Acc.	Rej.	No Rel. Ind.	Comments
				OUTER CONTAINMENT VESSEL (OCV) LEAK RATE TESTS:
OCV Structure	X			Leak Rate = 1.13 x 10 -8 atm.cm3/sec. (Per Step #6.2)
"V" Port Stat-O-Seal	X		X	No Detectable Leakage (Per Step #6.4)
"T" Port Prim.O-Ring	X		X	No Detectable Leakage (Per Step #6.5)
Total OCV Leak Rate:	X			Sum of 6.2, 6.4, and 6.5 = 1.13 x 10 -8 atm.cm3/sec.

Technique Pre Approval [X] NA — LT Level/Date

Technician	Level	Interpreted by	LT Level II	Reviewed by
W.H.Nelson	I	B.J.Sewart	II	
B.J.Sewart	II			
Date of Examination: Nov.21, 1995		Date: Nov.21, 1995		Date: 11-28-95

Westinghouse Hanford Company

NDE LEAK TEST PROCEDURE AND TEST REPORT UL-100

NON DESTRUCTIVE EXAMINATION
306 BLDG., 300 AREA - TEL. 376-5401

Job No. 95-8

Requestor	Company	Project/System/Work Package/Traveler No.
[illegible]y S. Averette	PacTec	Helium Leak Test of Radioisotope Thermoelectric Generator (RTG) After Drop Test #10-#16 on Certification Test Article #CTA-2, per WHC-SD-RTG-TC-016, Rev. 1

MSIN	Bldg.	Area
G2-02	MO-916	1100

Acceptance Std.	Section	Para.	Date	NA	Dwg. No.	NA
WHC-SD-RTG-TC-016, Rev. 1 Leakage Rate < 2.6 x 10 -7 atm.cc3/sec Helium		Para. 5.0	10/95	☐	H-4-302118 H-4-112301	☐

TEST CONDITIONS

- Temperature Amb. Device ID _____ ☒ NA
- Barometric Pressure _____ ☒ NA
- Test Pressure △=1 Atm.(14.7psia) ☐ NA
- Gas UHP Helium ☐ NA
- Concentration >90% ☐ NA
- Other _____ ☒ NA
- Bubble Solution _____ ☒ NA
- Batch No. _____
- Gage 1 584-31-04- 007 ☐ NA
- Range 0 to 50 psia
- Calib. Exp. March 9, 1996
- 584-31-04- _____ ☒ NA
- Range _____
- Calib. Exp. _____
- Relief Valve _____ ☒ NA

TEST EQUIPMENT ☐ NA

- Manufacturer L/H "UL-100+", #2
- Ident. No. s/n896-38 (WC48869)
- Mach. Sen. 1.13 x 10 -11 Atm/cc/sec/Div
- Std. No. 584-40-03- 017
- Std. Leak 1.8 x 10 -8 Atm/cc/sec
- Calib. Exp. July 7, 1996

SYSTEM SENSITIVITY ☐ NA

☐ Same as MSLD Calib. or:

- Sensitivity 1.67 x 10 -11 Atm/cc/sec/Div
- Std. No. 584-40-03-006
- Std. Leak 1.3 x 10 -7 Atm/cc/sec
- Calib. Exp. July 7, 1996

ADDITIONAL STD. ☒ NA

- Sensitivity _____ Atm/cc/sec/Div
- Std. No. _____
- Std. Leak _____ Atm/cc/sec
- Calib. Exp. _____

NCR ☒ NA

Cleaning ☐ NA: Alcohol

WHC PROCEDURE NO. ☐ NA

- ☒ NDT-LT-6000 Rev. 3
- Appendix A Rev. 2
- ☐ Special Tech. No. _____
- ☐ Work Inst. _____

TEST TIME
STAT-O-SEAL + PRIMARY O-RING

- He Response Time = IMMEDIATE ☐ NA
- He Accum. Time _____ ☒ NA
- Soak Time _____ ☒ NA
- Additional Times: "TEST DURATION"
  STAT-O-SEAL = 3min.
  PRIMARY O-RING = 5min. ☐ NA

Weld No., Part No., or Serial No.	Acc.	Rej.	No Rel. Ind.	Comments
				Inner Containment Vessel (ICV) Leak Rate Tests:
"P" Port Stat-O-Seal	X		X	No Detectable Leakage (Per Step #7.2)
"S" Port Stat-O-Seal	X		X	No Detectable Leakage (Per Step #7.3)
"T" Port Prim.O-Ring	X		X	No Detectable Leakage (Per Step #7.4)

Technique Pre Approval ☒ NA — LT Level/Date

Technician	Level	Interpreted by	LT Level II	Reviewed by
W.H.Nelson	I			
B.J.Sewart	II	B.J.Sewart	II	
Date of Examination: Nov.29,1995		Date: Nov.29,1995		Date: 12-18-95

2.10.15-113

A-6001-492 (11/94)

Westinghouse Hanford Company

NDE LEAK TEST PROCEDURE AND TEST REPORT UL-100

NON DESTRUCTIVE EXAMINATION
306 BLDG., 300 AREA - TEL. 376-5401

Job No. 95-8

Requestor	Company	Project/System/Work Package/Traveler No.
Gary S. Averette	PacTec	Helium Leak Test of Radioisotope Thermoelectric Generator (RTG) After Drop Test #10-#16 on Certification Test Article #CTA-2, per WHC-SD-RTG-TC-016, Rev. 1

MSIN	Bldg.	Area
G2-02	MO-916	1100

Acceptance Std.	Section	Para.	Date	NA
WHC-SD-RTG-TC-016, Rev. 1 Leakage Rate < 2.6 x 10 -7 atm.cm3/sec Helium		Para 5.0	10/95	☐

Dwg. No. ☐ NA: H-4-302118, H-4-112301

TEST CONDITIONS

Temperature	Amb. Device ID	☒ NA
Barometric Pressure		☒ NA
Test Pressure	Δ =1Atm.(14.7psia)	☐ NA
Gas	UHP Helium	☐ NA
Concentration	>90%	☐ NA
Other		☒ NA
Bubble Solution		☒ NA
Batch No.		
Gage 1 584-31-04-	007	☐ NA
Range	0 to 50 psia	
Calib. Exp.	March 9, 1996	
Gage 2 584-31-04-		☒ NA
Range		
Calib. Exp.		
Relief Valve		☒ NA

TEST EQUIPMENT ☐ NA

Manufacturer	L/H "UL-100+", #2
Ident. No.	s/n896-38 (WC48869)
Mach. Sen.	1.51 x 10 -11 Atm/cc/sec/Div
Std. No. 584-40-03-	017
Std. Leak	1.8 x 10 -8 Atm/cc/sec
Calib. Exp.	July 7, 1996

SYSTEM SENSITIVITY ☐ NA
☐ Same as MSLD Calib. or:

Sensitivity	2.15 x 10 -10 Atm/cc/sec/Div
Std. No.	002-40-03-010 ← Borrowed From WHC Standards Lab
Std. Leak	3.44 x 10 -7 Atm/cc/sec
Calib. Exp.	April 22, 1996

ADDITIONAL STD. ☒ NA

Sensitivity	Atm/cc/sec/Div
Std. No.	
Std. Leak	Atm/cc/sec
Calib. Exp.	

NCR ☒ NA

Cleaning ☐ NA: Alcohol

WHC PROCEDURE NO. ☐ NA
☒ NDT-LT-6000 Rev. 3
Appendix A Rev. 2
☐ Special Tech. No.
☐ Work Inst.

TEST TIME ICV Structure:

He Response Time	4 min. ☐ NA
He Accum. Time	☒ NA
Soak Time	☒ NA
Additional Times : TEST DURATION:	25 mins. ☐ NA

Weld No., Part No., or Serial No.	Acc.	Rej.	No Rel. Ind.	Comments
				Inner Containment Vessel (ICV) Leak Rate Tests:
ICV Structure	X			Leak Rate = 2.15 x 10 -8 atm.cm3/sec (Per Step #7.6)

Technique Pre Approval ☒ NA — LT Level/Date

Technicians	Level	Interpreted by	LT Level II	Reviewed by
W.H.Nelson	I	B.J.Sewart	II	
B.J.Sewart	II			
Date of Examination: Dec. 1, 1995		Date: Dec. 1, 1995		Date: 12-18-95

2.10.15-114

A-6001-492 (11/94)

Data Sheets from Copper Tube Test
(Seal Area Measurement Data Sheets)

Seal Area Measurement Data Sheet

CTA-2

Direct Compression Method, Section 4.1. (Method #1, primary)

Measurement (circle one): (**Pre-Test**) **Post-Test**

TUBING MEASUREMENTS (inch)								
	ICV				OCV*			
	INNER (¼-inch)		OUTER (¼-inch)		5/16 (3/8-inch) INNER		OUTER (¼-inch)	
Angular Position	Before Comp.	After Comp.	Before Comp.	After Comp.	Before Comp.	After Comp.	Before Comp.	After Comp.
Feed-through	.253	.204	.253	.201	.316	.282	.250	.207
45°	.252	.204	.253	.201	.316	.282	.250	.207
90°	.253	.204	.253	.200	.316	.282	.250	.207
135°	.252	.203	.252	.200	.316	.282	.250	.207
180°	.253	.204	.252	.202	.316	.282	.250	.207
225°	.253	.204	.252	.201	.316	.282	.250	.207
270°	.252	.204	.253	.201	.316	.282	.250	.207
315°	.253	.204	.253	.201	.316	.282	.250	.207

Comments: * NOTE: OCV BASE FROM CTA-1 UNIT WAS REUSED FOR CTA-2 UNIT. THESE MEASUREMENTS ARE PRIOR TO REFURBISHMENT OF BASE PLATE.

9-20-95

Data by Phil Nevs (IDEAL 1) Date 9/20/95

Seal Area Measurement Data Sheet (con't)

CTA-2

Direct Compression Method, Section 4.1. (Method #1, primary)

Measurement (circle one): (**Pre-Test**) **Post-Test**

Closure Bolt Torque Values Utilized

(Bolt #1 is first bolt CCW from feed-through location)

ICV	
Bolt #	Torque ft-lb
1	250
2	↓
3	↓
4	↓
5	↓
6	↓
7	↓
8	↓
9	↓
10	↓
11	↓
12	↓

OCV			
Bolt #	Torque ft-lb	Bolt #	Torque ft-lb
1	300	13	300
2	↓	14	↓
3	↓	15	↓
4	↓	16	↓
5	↓	17	↓
6	↓	18	↓
7	↓	19	↓
8	↓	20	↓
9	↓	21	↓
10	↓	22	↓
11	↓	23	↓
12	↓	24	↓

IDCAL 1 9-20-95

Data by Phil Nors

Date 9/20/95

CTA-2
AFTER I.C. BOLT REMACHINING

Seal Area Measurement Data Sheet

Direct Compression Method, Section 4.1. (Method #1, primary)

Measurement (circle one): **Pre-Test** **Post-Test**

TUBING MEASUREMENTS (inch)								
	ICV				OCV*			
	INNER (¼-inch)		OUTER (¼-inch)		5/16 PWN INNER (~~3/8~~-inch)		OUTER (¼-inch)	
Angular Position	Before Comp.	After Comp.	Before Comp.	After Comp.	Before Comp.	After Comp.	Before Comp.	After Comp.
Feed-through					.315	.282	.250	.208
45°					.316	.282	.249	.207
90°					.315	.282	.250	.208
135°					.316	.283	.251	.208
180°					.316	.283	.250	.208
225°					.316	.282	.251	.207
270°					.316	.282	.250	.208
315°					.316	.282	.251	.207

Comments:

MEASURED CCW FROM FEED-THROUGH

* THESE MEASUREMENTS ARE AFTER REFURBISHMENT OF CTA-1 BASE PLATE FOR USE AS CTA-2 BASEPLATE.

COPY

IDEAL 1

Data by Andrew Burns

AB

Date 10/27/95

Seal Area Measurement Data Sheet

Direct Compression Method, Section 4.1. (Method #1, primary)

Measurement (circle one): **Pre-Test** **Post-Test**

TUBING MEASUREMENTS (inch)								
	ICV				OCV			
	INNER (¼-inch)		OUTER (¼-inch)		INNER (3/8-inch)		OUTER (¼-inch)	
Angular Position	Before Comp.	After Comp.	Before Comp.	After Comp.	Before Comp.	After Comp.	Before Comp.	After Comp.
Feed-through	.253	.205	.252	.202	.314	.287	.252	.213
45°	.252	.203	.252	.201	.314	.283	.251	.207
90°	.253	.203	.251	.201	.314	.282	.251	.208
135°	.253	.203	.251	.201	.314	.283	.251	.208
180°	.253	.205	.251	.2025	.314	.284	.250	.210
225°	.253	.204	.251	.2015	.313	.282	.252	.208
270°	.253	.203	.251	.201	.313	.283	.252	.208
315°	.253	.203	.251	.201	.313	.283	.252	.208

Comments:

OCV VARIANCE: INNER .005
OUTER .006

ICV VARIANCE: INNER .002
OUTER .001 (~0)

Data by D. L. Crutts

Date OCV: 11/22/95
ICV 12/05/95

Seal Area Measurement Data Sheet (con't)

Direct Compression Method, Section 4.1. (Method #1, primary)

Measurement (circle one): **Pre-Test** **Post-Test**

Closure Bolt Torque Values Utilized

(Bolt #1 is first bolt CCW from feed-through location)

ICV	
Bolt #	Torque ft-lb
1	
2	
3	
4	
5	
6	
7	
8	
9	
10	
11	
12	

OCV			
Bolt #	Torque ft-lb	Bolt #	Torque ft-lb
1	225	13	250
2	240	14	260
3	250	15	230
4	240	16	250
5	265	17	260
6	260	18	265
7	255	19	280
8	265	20	240
9	240	21	260
10	280	22	265
11	260	23	280
12	210	24	215

Data by _____ Date 11/22/95

*** RMIS View/Print Document Cover Sheet ***

This document was retrieved from the Documentation and Records Management (DRM) ISEARCH System. It is intended for Information only and may not be the most recent or updated version. Contact a Document Service Center (see Hanford Info for locations) if you need additional retrieval information.

Accession #: D196080883

Document #: SD-RTG-SARP-001

Title/Desc:
RTG TRANSPORTATION SYSTEM SARP DOCKET NO 94-6-9904 [VOL II] [SEC 3 OF 4]

Pages: 289

This document was too large to scan as a whole document, therefore it required breaking into smaller sections.

Document number: SD-RTG-SARP-001

Section 3 **of** 4

Title: RADIOISOTOPE THERMOELECTRIC GENERATOR TRANSPORTATION SYSTEM SAFETY ANALYSIS REPORT FOR PACKAGING

Date: 4/18/96 **Revision:** 0

Originator: FERRELL PC
Co: WHC

Recipient:
Co:

References: EDT-613639

WHC-SD-RTG-SARP-001
Revision 0
Volume II

Radioisotope Thermoelectric Generator Transportation System Safety Analysis Report for Packaging

Docket No. 94-6-9904

Prepared for the U.S. Department of Energy
Office of Environmental Restoration and
Waste Management

Westinghouse
Hanford Company Richland, Washington

Management and Operations Contractor for the
U.S. Department of Energy under Contract DE-AC06-87RL10930

Approved for Public Release

3.0 THERMAL EVALUATION

This chapter describes the principal thermal aspects and performance of the Radioisotope Thermoelectric Generator (RTG) Transportation System Package. The following evaluation demonstrates the compliance per 10 CFR 71 (Reference 1). See Section 1.0 for a detailed description of the RTG Transportation System Package and its key features.

3.1 DISCUSSION

The RTG Transportation System Package is designed to safely transport a variety of RTG payloads. The maximum decay heat load of 4,500 W occurs with a payload consisting of one General Purpose Heat Source (GPHS) RTG. The results for the GPHS RTG will thermally encompass all other potential payloads. The minimum thermal decay heat is assumed to be zero.

Each RTG is a functioning device with an extremely high replacement cost. As such, while the primary purpose of the package design is to provide a Type B packaging meeting the 10 CFR 71 regulatory requirements for safety, the package design must also maintain the RTGs below their thermal limits during the normal operational conditions for load, unload, and transportation. To accomplish this dual purpose, an active cooling system is used to control the boundary conditions on the package's external surface and, thereby, maintain the various RTGs within their respective thermal limits. The cooling system is not required to be active for the RTG Transportation System Package to successfully comply with 10 CFR 71.

The RTG Transportation System Package consists of a double-containment packaging and payload. The remote chillers, interconnecting hoses, associated controls, and power systems needed to provide the active cooling are not considered part of the RTG Transportation System Package and, thus, are not addressed by this Safety Analysis Report for Packaging (SARP). The packaging consists of two separate containment vessels: an inner containment vessel (ICV) and an outer containment vessel (OCV). Each containment vessel consists of a bell assembly and a heavy base. The bell assembly is made of a cylindrical shell with an integral standard American Society of Mechanical Engineers (ASME) torispherical head at the top and a bolt flange at the bottom. The bell assembly is attached to the base with high-strength alloy steel closure bolts. The containment structures are fabricated from AISI Type 304L stainless steel.

The OCV bell assembly incorporates an integral cooling jacket on its outer surface. The cooling jacket provides two equal and independent cooling loops that can be used separately or together to provide the required cooling. The loops are formed by spiral wrapping 0.25 by 1.25 in. Type 304L stainless steel bar stock on 2.25-in. centers around the OCV bell and then welding a 10 gauge (0.135-in.) Type 304L stainless steel cover sheet between the bars to form 1 by 2 in. coolant flow channels. Full length welds at all joints will not only provide a leak-tight environment, but also maximizes the heat transfer through the jacket if coolant fluid is lost. Conversely, the relatively thin shell of the coolant jacket acts as a radiation shield, reducing OCV heating during the hypothetical accident condition (HAC) fire transient from that which would occur with a bare OCV bell.

The bolt flange is protected from pin puncture damage and the HAC fire ambient temperatures by a 3/8-in.-thick thermal shield. The cavity within the thermal shield is filled with 2.4 lb/ft^3 fiberglass insulation to limit conduction, convection, and radiation heat transfer within the cavity. Plugs or caps for the OCV bolt access tubes are not used for reasons of convenience and because the thermal analysis shows they are unnecessary.

A water/propylene glycol solution is used as the cooling medium. The choice of coolant

fluid is based on the possibility of ambient temperatures below the freezing point of water during operation or storage of the package and the desire for a nontoxic solution. In the absence of freezing temperatures, pure water can also be used. The 70%/30%, by volume, mixture of water and propylene glycol provides burst protection down to -60 °F.

The removable impact limiter is fabricated of two densities of fire resistant, polyurethane foam encased in a 0.25 in. or thicker Type 304 stainless steel shell. The center section (41 in.) of the limiter uses a solid block of 3 lb/ft^3 FR-3700 polyurethane foam. The remaining portion of the limiter uses 12 lb/ft^3 poured-in-place FR-3700 polyurethane foam. A sheetmetal thermal shield is incorporated in the center section of the impact limiter, adjacent to the bottom of the OCV base. This thermal shield provides backup thermal protection over the area of the OCV base plate covered by the low density foam. Plastic melt-out plugs provide pressure relief if foam outgassing occurs during the HAC fire event. The relatively thick steel shell of the limiter prevents the puncture pin from tearing the shell and penetrating the foam.

Most of the design aspects of the RTG Transportation System Packaging are set by nonthermal considerations. A combination of shielding, structural, weight, and operational considerations set the overall size of the packaging, the wall thicknesses for the ICV and OCV, and all the stainless steel construction. Even the thickness of the fluid passages in the cooling jacket is set by neutron absorption considerations and not by thermal requirements. Despite this, many of these design aspects work to the thermal advantage of the package. The heavy base plates, OCV flange thickness, and ICV/OCV bell thickness provide a significant thermal mass to absorb the heat fluxes generated during the HAC fire. The relatively low thermal conductivity of Type 304L stainless steel restricts the axial flow of heat to the seal areas of the package. The thin outer shell of the cooling jacket and the air gap created by the flow passages acts as a thermal radiation shield and insulator during the HAC fire.

The design features specifically added to enhance the thermal performance of the package under both normal operation and regulatory normal conditions of transport (NCT) are as follows:

- An external cooling jacket
- High emissivity surface treatments
- Control of the gap dimension between the ICV and OCV
- Use of a helium blanket gas within the ICV and OCV cavities
- RTG payload shipping rack assembly with integral barrier plate
- Seal area insulation.

Although the OCV external cooling jacket was specifically added for normal operation conditions, its desirable effects for regulatory conditions have already been addressed. A high temperature coating (Carboline 4674 black paint) yielding a normal emittance of 0.875 is used on the inner and outer surfaces of the ICV and on the inner surface of the OCV. The coatings enhance the heat transfer performance of the package, especially between the RTG and ICV. The coating is purposely omitted from the lower 7 in. of the ICV inner wall, the ICV/OCV base plates, and the shipping rack to minimize the heat transfer to the seal region of the package. An emittance of 0.48 is assumed for these areas.

The interior surfaces of the cooling jacket are also not coated because these enclosed surfaces cannot be maintained once the package is assembled, and analysis shows enhanced emittance is not required in this area. The exterior surface of the OCV and impact limiter are coated with a two-part white epoxy paint. This surface treatment provides a long wave radiation emittance of 0.80 or greater, while limiting solar radiation absorptivity to 0.25 or less.

The third special design feature used to enhance thermal performance is dimensional control of the ICV-to-OCV gap. By manufacturing the ICV and OCV bells as a nested pair, the inter-vessel

gap is controlled to 1/4 in. maximum at the sides and 1/2 in. maximum between the torispherical heads. These controlled dimensions provide a definitive basis for determining the temperature rise between the bells.

Using helium as the blanket gas within the ICV and OCV cavities increases the convective heat transfer rates within the package over that possible with other inert blanket gases. Although the thermal analysis assumes a pure helium gas, analytical calculations showed no significant temperature sensitivity for gas mixtures down to 95% helium and 5% air. Development and operational tests have shown helium gas purity of 95% or greater is easily achievable using the proposed operating procedures. The target pressure for helium gas within the ICV and ICV/OCV cavities is 19 $\pm$1 psia. This pressure will be established when the payload is loaded into the packaging. Once the packaging is loaded there is no active control of the cavity pressures, instead the pressure will vary according to the ideal gas law. For analysis purposes, the ambient condition at the time of RTG loading is assumed to be 70 °F with no solar insolation.

Each RTG payload has its own shipping rack assembly that is attached to the ICV base plate. The shipping rack assemblies incorporate a stainless steel barrier plate structure; its purpose is to maintain a positive separation between the RTG heat sources and the ICV/OCV seal areas under all circumstances. The 0.5-in. radial gap between the shipping rack assembly O.D. and the ICV I.D. is less than the smallest portion of a HAC impact reconfigured RTG heat source. The rectangular GPHS aeroshell is the smallest size heat-producing fragment that could potentially arise from the breakup of an RTG under a HAC impact. The smallest dimension of the aeroshell is 2.09 in. Consequently, even if an accident during transportation results in severe RTG damage and subsequent spilling of the heat sources within ICV cavity, no heat generating material will be permitted to reach the seal area.

The final design feature added to the package to enhance its thermal performance is thermal insulation at critical locations. These locations are the underside of the shipping rack assembly, the electrical feed-through connector on the ICV base, the OCV base plate, and the OCV seal flange. Heat transfer via radiation and convection between the ICV base plate/seal area and the underside of the shipping rack assembly is restricted by using a 2-in.-thick blanket of "Kaowool"* ceramic fiber insulation. Kaowool* insulation is also used to isolate the electrical feed-through connector housing on the ICV base plate from the hot gas in the ICV cavity.

Additional lower end insulation in the form of an impact limiter protects the ICV/OCV seals from the high external temperatures that arise during the HAC fire. The impact limiter is filled with a combination of 3 and 12 lb/ft^3 rigid polyurethane foam. The structural attachments for the impact limiter prevent it from being torn from the package during the pre-HAC free drops and puncture bar drops. Additional information regarding the performance of the impact limiter in the free drops and HAC fire transient is presented in Appendices 2.10.11 and 3.6.3.

The bolt flange on the OCV is protected from direct exposure to high external temperatures by a thermal shield enclosure fabricated of 0.375-in.-thick stainless steel and filled with fiberglass insulation. The wall thickness prevents a puncture bar impact from penetrating the shield and/or collapsing the shield onto the bolt flange. The thermal shield is shown on Drawing H-9-5002, sheet 3, Appendix 1.3.2. This drawing illustrates the 3/8-inch plate material used for the top and outer plates that enclose approximately 2.6 inches of fiberglass insulation.

The thermal evaluation of the RTG Transportation System Package is conducted using a variety of two- and three-dimensional (2-D and 3-D, respectively) analysis and full-scale test models. Data from the test models confirm that the package design will maintain the various RTGs

Kaowool is a registered trademark of the Babcock & Wilcox Company.

within their temperature limits during the normal operational conditions (i.e., with the chillers operating) for load, unload, and transportation. In addition to thermally qualifying the package for the nonregulatory aspects transportation, the test data validates the analytical thermal models of the package and its inherent heat transfer mechanisms.

Qualification of the package for regulatory aspects of transportation is accomplished analytically. The following sections, appendices, and references detail the basis for the analytical models, tests used to validate the models, and the analysis results for regulatory conditions. The analysis uses conservative assumptions for such nondefinitive parameters as RTG reconfiguration, impact limiter damage, and foam properties during the HAC fire. The results of the analyses demonstrate that the package meets all of the 10 CFR 71 requirements for Type B packaging.

3.2 SUMMARY OF THERMAL PROPERTIES OF MATERIALS

The RTG Transportation System Package is fabricated primarily of Type 304L and Type 304 stainless steel, rigid polyurethane foam, and minor amounts of miscellaneous materials. The shell of the GPHS RTG, the maximum heat payload, is fabricated primarily of 2219 aluminum. Each of the 18 GPHS modules used in the RTG are fabricated of four PuO_2 fuel pellets within iridium shells which, in turn, are mounted within a carbon-carbon composite housing called an "aeroshell." Of the total heat source module weight, 55% is in the fueled capsules and 45% is in the aeroshell. The individual components of the heat source modules are not modeled. Instead, a composite thermal mass of 14.2 Btu/°F is used for all 18 heat source modules, based on data provided by the manufacturer of the GPHS RTG.

The void spaces within the package are filled with helium gas to a purity of 95% or greater and to a pressure of 19 ± 1 psia at the time of package assembly. Air surrounds and fills all package voids outside the OCV containment boundary. The coolant passages are assumed to be drained, dried, and filled with air for all regulatory conditions. For normal operational conditions, with the chillers operating, the coolant passages are assumed to be filled with a coolant mixture of 30% propylene glycol and 70% water, by volume.

The thermal properties of the principal materials used in the fabrication of the packaging and GPHS RTG payload are listed in Tables 3.2-1 through 3.2-5. Where significant, the properties are presented as a function of temperature.

TABLE 3.2-1. Thermal Conductivity Curve Fits.

$k = C_0 + C_1 \cdot T + C_2 \cdot T^2$; Btu-In/Hr-Ft^2-°F, T = Temperature (°F)				
Material	C_0	C_1	C_2	Notes and remarks
Type 304 and 304L stainless steel	91.346	7.1499E-2	-3.9267E-6	Reference 4 and 6
ASTM A320 bolts	303.50	-4.5162E-2	-9.2092E-6	Reference 27
2219-T6 aluminum	804.70	0.5831	-2.2709E-4	Reference 4; same for -T87
Polyurethane foam • 12 lb/ft^3 • 3 lb/ft^3	 0.278 0.181	 0 0	 0 0	Reference 10
30% propylene glycol /70% water solution	2.7816	5.6033E-3	-1.2953E-5	Reference 16
Helium	0.9412	1.2361E-3	-5.1711E-8	Reference 8
Air	0.1574	2.6254E-4	-3.2429E-8	Reference 2 and 3
Fiberglass insulation	0.2217	1.6504E-4	8.9412E-7	References 28 and 29
Kaowool® ceramic insulation	0.1893	3.5879E-4	2.5900E-7	Reference 26

TABLE 3.2-2. Material Density.

Material	Density, Lbm/in.^{3}	Notes and remarks
Type 304 and 304L stainless steel	0.29	Reference 20
ASTM A320 bolts	0.283	Reference 20
2219-T6 aluminum	0.103	Reference 20; same for -T87
30% propylene glycol and 70% water solution	0.0374 at 40 °F	Reference 16; computed as a function of temperature
Kaowool® ceramic insulation	0.00463	Reference 26
Fiberglass insulation	0.00139	Reference 29
Helium	4.8322E-6 at 200 °F and 14.7 psia	Reference 3; computed from ideal gas law
Air	4.1087E-5 at 100 °F and 14.7 psia	Reference 3; computed from ideal gas law

TABLE 3.2-3. Specific Heat Curve Fits.

$c_p = C_o + C_1 * T + C_2 * T^2$; Btu/Lbm-°F, T = Temperature (°F)				
Material	C_o	C_1	C_3	Notes and remarks
Type 304 & 304L stainless steel	0.1155	3.3294E-5	1.1252E-9	Reference 9
ASTM A320 bolts	0.1116	1.3016E-5	3.8778E-8	Reference 27
2219-T6 aluminum	0.1986	8.05729E-5	-2.1537E-8	Reference 4; same for -T87
FR-3700 polyurethane foam • 12 lb/ft³ • 3 lb/ft³	 0.30 0.30	 0 0	 0 0	Reference 10
30% propylene glycol and 70% water solution	0.8968	3.6607E-4	-1.7342E-8	Reference 16
Helium	1.2404	0	0	Reference 7
Air	0.2362	2.7871E-5	-2.2971E-9	Reference 2 and 3
Fiberglass insulation	0.20	0	0	Reference 28
Kaowool® ceramic insulation	0.20	0	0	Reference 28
Fuel source modules (18)	14.2 Btu/°F	--	--	Reference 21

TABLE 3.2-4. Viscosity Curve Fits.

$\mu = C_o + C_1 * T + C_2 * T^2$; Lbm/Hr-Ft, T = Temperature (°F)				
Material	C_o	C_1	C_3	Notes and remarks
30% Propylene Glycol /70% Water Solution	1.5601	-1.1492E-2	2.1454E-5	Reference 16; fit on $\log_{10}$ of viscosity value
Helium	4.4557E-2	5.3443E-5	-4.2091E-9	Reference 9
Air	4.0234E-2	5.8419E-5	-8.5246E-9	Reference 2 and 3

TABLE 3.2-5. Surface Emittance.

Surface/Surface Treatment	Surface Emittance	Solar Absorptivity	Remarks
OCV dome & shell interior - as rolled 304L, abrasive blasted, heat-resistant coating	0.875, 0.54 w/o coating	N/A	See Note 1
OCV flange, bottom surface - 304L machined to 32μ in/in	0.3	N/A	See Note 2
OCV dome exterior & jacket exterior - as rolled 304L, brush-off blast, acid etch, Tnemec** epoxy paint	0.8	0.25	See Note 3
OCV shell exterior below coolant jacket - as rolled 304L	0.3	N/A	See Note 4
ICV dome & shell interior above 7" point & exterior above 3" point - as rolled 304L, abrasive blasted, heat-resistant coating	0.875, 0.54 w/o coating	N/A	See Note 1
ICV shell interior below 7" point, exterior below 3" point, & flange - machine finished 304L	0.30	N/A	See Note 2
ICV base & OCV base - machine finished 304L	0.30	N/A	See Note 2
Shipping rack barrier plate - machine finished 304	0.30	N/A	See Note 2
Shipping rack barrier plate, upper ring - as rolled 304	0.48	N/A	See Note 5
Shipping rack support legs - as rolled 304	0.48	N/A	See Note 5
Shipping rack barrier plate, lower ring - as rolled 304	0.48	N/A	See Note 5
Coolant jacket 1/4"x1" bars - as rolled 304L	0.48	N/A	See Note 5
Coolant jacket cover interior - as rolled 304L	0.48	N/A	See Note 5
Impact limiter shell exterior - as rolled 304, Tnemec® epoxy paint	0.8	0.25	See Note 3
2219-T6 aluminum with coating	0.91	N/A	See Note 6
Heat source aeroshell (graphite)	0.5	N/A	See Note 7

**Tnemic is a registered trademark of the Tnemic Company, Incorporated.

Notes: (1) References 22 and 32 indicates an emissivity range of 0.83 to 0.90 for the Carboline®*** 4674, C900 black heat-resistant coating. Reference 34 emissivity testing on 18 samples of Type 304 stainless steel indicates an emissivity value of 0.54 for the 'white metal blast' surface treatment that exists prior to the application of the Carboline® coating. Figure 360, Reference 24 indicates an emissivity of 0.6 to 0.8 for grit-blasted Type 310 stainless steel. Conclusion is to use an emissivity of 0.875 when the Carboline® coating is present and 0.54 when the coating is not present.

(2) Figure 361, Curves 128 and 132, Reference 24 indicates an emissivity of 0.135 to 0.175 at 1000 °F for mechanically finished Type 304 stainless steel, measured in helium gas. The average value of 0.15 for this condition was doubled to 0.30 to account for long-term oxidization, etc.

(3) Page 8, Reference 15 gives emissivity values of 0.89 or greater for white paints. Similar values are presented in Table 347, Reference 35. During the HAC event, the Tnemec Series 66 epoxy paint is expected to 'craze', flake off, and expose the underlying stainless steel surfaces. While the brush-off blast treatment of the stainless steel used in preparation for the epoxy paint is expected to yield an emissivity of 0.40 (per Reference 34 for 'commercial sand blast' condition), a minimum emissivity of 0.80 is to be used for all HAC conditions in accordance with the Reference 1 requirements. Therefore, a value of 0.80 provides a conservative estimate for NCT conditions and meets the Reference 1 requirements for HAC conditions.

(4) Reference 34 emissivity testing on 18 samples of Type 304 stainless steel indicates an emissivity value of 0.25 to 0.28 for the 'as-received' condition. Table 148, Reference 35 provides values of 0.44 at 420 °F and 0.36 at 914 °F for a light silvery, rough surface. An emissivity value of 0.30 provides an accurate representation of the actual conditions for the OCV shell surface.

(5) Same references as Note 4; however, since these surfaces are light silvery in color and rough, an emissivity value of 0.48 is used.

(6) Emissivity set by manufacturer of GPHS RTG. See Reference 21.

(7) Reference 18 provides emissivity values of 0.49 at 500 °F and 0.54 at 2500 °F. Table 78, Reference 35 provides emissivity values of 0.49 at 500 °F, 0.54 at 1000 °F, and 0.64 at 2000 °F. A value of 0.50 is used since it provides a conservative estimate of the temperature of the heat source aeroshells and the package temperatures in the vicinity of the aeroshells.

The solar absorptivity value of 0.25 used for the Tnemec® Series 66 white epoxy paint is appropriate, given the referenced measured values, the fact the package will be shipped in a vented, enclosed trailer, and because the International Atomic Energy Agency (IAEA) guidelines recognize the validity of using coatings to reduce the heat flux caused by insolation.

***_Carboline_ is a registered trademark of the Carboline Company.

3.3 TECHNICAL SPECIFICATIONS OF COMPONENTS

The materials used in the RTG Transportation System Package that are considered temperature sensitive are the Butyl O-ring seals, the polyurethane foam used in the impact limiter, the pressure relief valves used in the coolant jacket, the instrumentation electrical feed-through connector assemblies, and the Carboline® and Tnemec® coatings.

The Butyl O-ring seals (Rainier rubber compound No. RR-0405-70) have a working temperature range of -40 to 350 °F. Exposure to temperatures in excess of 350 °F is allowable for limited time periods. Developmental test data (see Appendix 2.10.6) has shown that the Butyl seals have a peak temperature rating of 400 °F for time periods of eight hours or less. Seal temperatures between 400 and 350 °F are allowed for time periods that vary as a function of temperature. See SARP Section 4.1.3.1.2 for the time versus temperature capability of the Butyl seals.

The rigid polyurethane foam used in the impact limiter has a working temperature range of -40 to 300 °F. While the foam's compressive strength diminishes rapidly with increasing temperature, temperature excursions within this range will not permanently degrade its properties. The foam begins to break down and outgas at temperatures above 400 °F. This thermal breakdown and outgassing accelerates at temperatures between 500 and 750 °F, levels off between 750 and 1000 °F, and then accelerates again until 1500 °F. The foam will have been reduced to a relatively stable char at temperatures beyond 1500 °F. No definitive high temperature data exists for the foam. For this reason, a conservative approach based on fire test results was used to simulate the foam's response to the HAC fire. Further discussion of the thermal properties of the foam under fire transient conditions is provided in Section 3.5.1, Appendix 3.6.3, and Reference 10.

Outgassing from the polyurethane foam during a HAC fire could produce relatively large volumes of gas within the impact limiter. To prevent an excessive buildup of pressure within its shell, the impact limiter is fitted with four PVC plugs located at 90° intervals around the outer circumference of the shell. During any potential HAC fire, the plugs will burn/melt before any significant charring of the foam. Because the center 3 lb/ft^3 foam disk is not directly poured in the impact limiter shell, it does not bond with the shell walls. Hence, adequate gas communication paths will exist to the PVC plugs.

The cooling jacket on the OCV of the package is protected from overpressurization by relief valves on each coolant channel. The valves prevent a pressure buildup within the coolant channels if a coolant system malfunctions. The 1/2-in. valves are fabricated of 300 series stainless steel and have a pre-set cracking pressure of 50 psi. The relief valves have a temperature rating of 375 °F. These performance limits affect the operational mode only. Failure of the relief valves from either impact damage or the HAC fire will not affect the containment boundaries of the package. The valves will not puncture the OCV if struck during impact.

The temperature-sensitive components of the electrical feed-through assembly is the D.G. O'Brien Series 107 connectors. The temperature rating for the electrical feed-through connector assembly is 475 °F. The basis for the temperature rating is provided in Appendix 4.5.2.

The Carboline® high emissivity coating has a continuous temperature rating of 750 °F and a noncontinuous rating of 1000 °F. The required inspection and maintenance of the coating before individual shipments is addressed in Chapter 8 of the SARP. These O&M procedures require corrective action whenever damaged coating exceeds 5% of any one-square-foot area or 2% of the total area. Since the total loss of the heat-resistant coating over 5% of any given one-square-foot area is equivalent to a reduction in the average emittance over the one-square-foot area of 2%, no impact on package temperatures will occur before the heat-resistant coating is repaired.

The heat-resistant coating is protected from wear and tear during normal transport operations (i.e., loading and unloading procedures) by eight Vespel® wear pads mounted near the OCV flange. These wear pads are illustrated in the Section B-B detail on Sheet 2 of Drawing H-9-5001. The wear pads maintain the alignment between the ICV and the OCV shells during package assembly and disassembly, thereby preventing inadvertent hard contact between the ICV and the OCV. During the Reference 14 qualification tests, the package was assembled and disassembled approximately 40 times. Throughout the tests, the coating remained in excellent condition with only a slight dulling of the finish on the outer surface of the ICV shell where these pads had made contact.

The Tnemec® Series 66 epoxy coating has a continuous temperature rating of 250 °F and a maximum rating of 275 °F. During the HAC fire, the Tnemec® coating is expected to craze and flake off.

The remaining materials used in the fabrication of the packaging have significantly higher temperature capabilities. The Type 304L stainless steel used in the ICV and OCV containment vessels and bases has a melting point of 2600 °F. The Type 304 stainless steel used for shipping racks and the shell of the impact limiter has a similar melting point. The Kaowool® and fiberglass insulations have maximum temperature ratings of 2300 °F and 1000 °F, respectively.

The 1000 °F rating for mineral fiber insulation is set primarily by the loss of structural strength within the individual fibers. The material (Owens Corning TIW type II) will begin to soften at 1200 °F and becomes liquidus at a temperature of 1700 °F. Since the surfaces surrounding the fiberglass insulation do not exceed 1250 °F during the HAC fire event and only exceed 1000 °F for less than an hour, the thermal capability of the fiberglass insulation is consistent with its use in this application.

The shell and fins of the GPHS RTG payload is constructed of 2219-T6 and 2219-T87 aluminum. These materials have a melting point of approximately 1100 °F. The graphite, PuO_2, and the other materials used in the fabrication of the RTG and have a temperature capability between 1100 °F and 6000 °F.

3.4 THERMAL EVALUATION FOR NORMAL CONDITIONS OF TRANSPORT

This section presents the thermal analyses for the normal conditions of transport (NCT). Because of the dual requirements of the package to provide regulatory safety and to protect the RTGs from excessive operational temperatures, the evaluation of thermal performance for NCT is divided into two categories. The first category covers the regulatory NCT as defined in 10 CFR 71, while the second category involves the normal operational conditions expected in day-to-day operation and transport of the package with the cooling system active. The objectives and ground rules are different for each category.

Evaluation of the thermal performance for compliance with the 10 CFR 71.43(g) and 71.71 is conducted to ensure the safety of the packaging for the transportation of radioactive materials. The health and functionality of the RTGs is immaterial for the purposes of compliance with 10 CFR 71. Instead, the temperature distribution within the RTG is important only in establishing the heat flux on the various ICV surfaces. Load cases 1 and 2 evaluate the maximum package temperatures and NCT differential thermal expansions, respectively. Load cases 4 and 5 provide steady-state package temperatures used as pre-accident conditions for the HAC fire presented in Section 3.5.

In contrast, evaluation for normal operational conditions (i.e., with active cooling) ensures that the package design will maintain the RTG payloads within their respective thermal limits, as

well as meeting all regulatory requirements. Although the evaluation covered the full range of expected conditions to be imposed by the load, unload, and transport procedures for the GPHS RTG, only three cases (i.e., cases 3, 6, and 7) are presented in this section. The resultant package temperatures encompass those seen by the other conditions and payloads.

Load case 3 represents the normal operational condition assuming the maximum heat load payload, 100 °F ambient temperature, regulatory solar loading, and active cooling. The conditions for active cooling is assumed to be a flowrate of 4.5 gal/minute in each cooling channel and a coolant inlet temperature of 40 °F. The expected coolant temperature rise will be 5 °F or less. Because the package will be shaded by its transport trailer, the resultant temperatures encompass those expected with the package loaded in an enclosed and vented trailer. Load case 6 evaluates compliance of the package per 10 CFR 71.43(g). Load case 7 illustrates package temperatures and pressures when the GPHS RTG is loaded into the packaging within a climate-controlled facility.

In addition to these seven NCT load cases, a loading/unloading transient case was evaluated to determine the maximum differential thermal expansion in the package during these procedures. Section 2.6.1 provides the results of this evaluation. This information helps establish the entire range of stress in the package. Thermal analysis output for when the ICV sidewall reaches its maximum temperature during the load transient is presented in Section 3.6.4.

TABLE 3.4-1. Table of Normal Conditions of Transport Load Combinations.

Load combination/condition	Solar	Ambient temp. (°F)	Payload	Cooling status
Case 1	Yes	100	GPHS	No active cooling[a]
Case 2	No	-40	GPHS	No active cooling
Case 3	Yes	100	GPHS	Active cooling[b]
Case 4	No	100	GPHS	No active cooling
Case 5	No	-20	GPHS	No active cooling
Case 6	No	100	GPHS	Active cooling
Case 7	No	70	GPHS	Active cooling

[a]"No Active Cooling" defined as coolant channels drained and filled with air.
[b]"Active Cooling" defined as coolant flowrate of 4.5 gal/minute per channel with an inlet temperature of 40 °F.

3.4.1 Thermal Model

Evaluation of the thermal performance for the package under NCT is accomplished using an analytical model. The results of physical model testing confirm the validity of the analytical model. The analytical model is described in Section 3.4.1.1; the test models are described in Section 3.4.1.2.

3.4.1.1 Analytical Model. Four categories of analytical thermal models were developed to analyze the performance of the RTG Transportation System Package for the NCT events. These models are (1) those used to represent the thermal characteristics of the RTG payload, (2) the thermal model of the basic packaging, (3) thermal models of the interface between the undamaged RTG payload

and the packaging, and (4) models used to analyze package configurations for regulatory conditions. All of the analytical thermal models developed used the SINDA '85/Fluint thermal analysis program[30]. SINDA is a finite differencing program developed by NASA's Johnson Space Center.

3.4.1.1.1 RTG Thermal Models. As stated previously, the GPHS RTG is used as the basis for the analysis presented herein. The analytical thermal model developed for the GPHS RTG payload is defined in a separate configuration controlled document. This model has been approved by the manufacturer of the RTG as being a valid thermal model of the undamaged RTG. Model changes can only be made via formal change procedures.

For the sake of brevity, the details of the model are not discussed in this document. Instead, the reader is directed to the Reference 21 payload model document for these details.

Figures 3.4.1-1a and 3.4.1-1b present the layout of the 57 nodes used to thermally model the GPHS RTG. The model provides a 2-D model of the RTG heat source modules and a quasi 3-D model of the outer shell and fins. Symmetry conditions are used to account for other sections of the RTG not specifically modeled. The level of model resolution is set by the need for operational temperature predictions and not by regulatory analysis. Full details of the model are provided in Reference 21.

3.4.1.1.2 Packaging Thermal Model. The thermal analysis of the undamaged RTG Transportation System Packaging is conducted with a 2-D, axisymmetric model. The model uses 124 nodes along 15 axial stations to represent components or portions of components for the packaging. The thermal properties (i.e., specific heat, thermal conductivity, and convective and radiative heat transfer coefficients) are computed as a function of the associated temperatures.

Figure 3.4.1-2 illustrates the distribution of the thermal model nodes for the packaging. See Appendix 3.6.2.1 for specific details about the model. Nodes 200 to 266 represent the inner vessel bell, seal area, and base plate. Nodes 300 to 369 represent similar components in the OCV. The independent loops in the cooling jacket are modeled separately using 15 nodes at three axial stations (i.e., nodes 311, 312, 313, 315, 316, ... 321, ... 335, 336). Detail A illustrates the typical node placement for the thermal model of the coolant jacket. Nodes 311, 312, 321, 322, 331, and 332 represent the coolant fluid in the channels. The odd coolant node numbers represent one coolant loop and the even node numbers represent the second coolant loop. This approach permits simulating the failure of one or both of the cooling loops. The coolant fluid is assumed to be a 70% water/30% propylene glycol mixture by volume. For the regulatory analysis, which assumes the coolant channels to be drained, the thermal properties of the coolant nodes are replaced by those appropriate for air. The coolant is assumed to enter the coolant channels at 40 °F and at a flow rate of 4.5 gallons per minute per channel. The temperature rise is less than 5 °F, assuming both coolant loops are operating.

Details B and C of Figure 3.4.1-2 illustrate node placement at the OCV closure bolts and impact limiter attachment bolts, respectively. The only difference is the node placement and numbering for the two types of attachment bolts.

Detail D of Figure 3.4.1-2 illustrates six of the seven nodes used to model heat transfer within the electrical feed-through connector assembly that extends above the ICV base plate. The seventh node that is not shown is an arithmetic node that represents the mean gas temperature in the electrical feed-through connector cavity. Because of their recessed placement, the thermal mass of the surrounding material, and the limited heat flux in these regions, no specific modeling is made of the electrical feed-through connector assemblies in the ICV and OCV base plates. Instead, the temperatures for these components are assumed to be encompassed by the temperatures of the surrounding base plate material (i.e., node 264 for the ICV electrical feed-through and node

368 for the OCV electrical feed-through).

The temperature of the OCV electrical feed-through connector is assumed to be equivalent to that of node No. 367.

The impact limiter is simulated with a 2-D thermal model using 33 nodes (node 401, the thermal barrier, is not shown). This quantity provides resolution of the temperature through the foam for both structural and thermal calculations. The impact limiter is assumed to rest on an adiabatic surface. This assumption provides a conservative estimate of the package temperatures for NCT events.

The RTG shipping rack assembly is modeled with 21 nodes. Figure 3.4.1-2 illustrates the location of the eight primary shipping rack assembly nodes. The remaining 13 nodes are arithmetic nodes that ease the calculation of the heat transfer in and around this geometrically complex assembly. Heat transfer via conduction, convection, and radiation are addressed for the interfaces between the shipping rack assembly and the various RTG/ICV surfaces.

Based on the O&M requirements presented in Chapter 8 for the heat-resistant coating, the results from the Reference 14 tests that showed little or no degradation of the coating despite the package being assembled and disassembled approximately 40 times, and analysis showing that no surface exceeded 750 °F for NCT, it is concluded that no loss of the Carboline heat-resistant coating will occur for any NCT event.

The basis for the calculation of thermal capacitance at each node and for heat transfer via conduction, convection, and radiation between the model nodes is presented in Appendix 3.6.2.

3.4.1.1.3 RTG-to-ICV Thermal Interface Model. The heat transfer between the GPHS RTG and the ICV occurs by a combination of radiation, convection, and conduction. The complexity of the heat transfer modes depended on the geometries involved, the interaction of the shipping rack assembly, and the heat paths internal to the RTG. Therefore, a third category of thermal model was developed to define the thermal relationship between the nodes used in the RTG model and the nodes used in the packaging model.

The following paragraphs provide a brief overview of the modeling approach used for the GPHS RTG. Further details of the GPHS RTG-to-ICV thermal interface model are provided in Appendix 3.6.2.

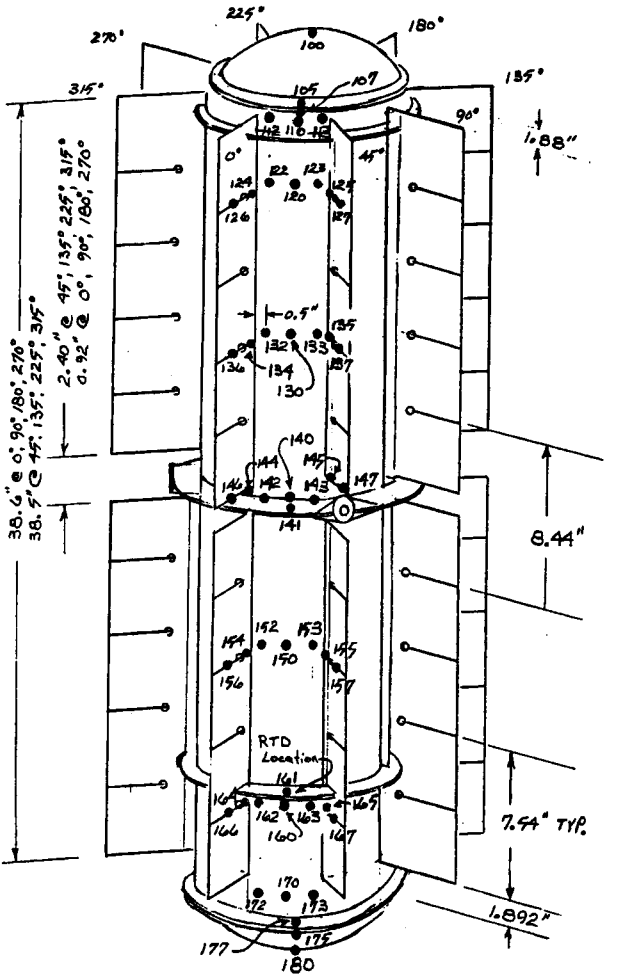


FIGURE 3.4.1-1a. GPHS RTG Thermal Model Nodes (Exterior Shell Nodes).

BEST COPY AVAILABLE

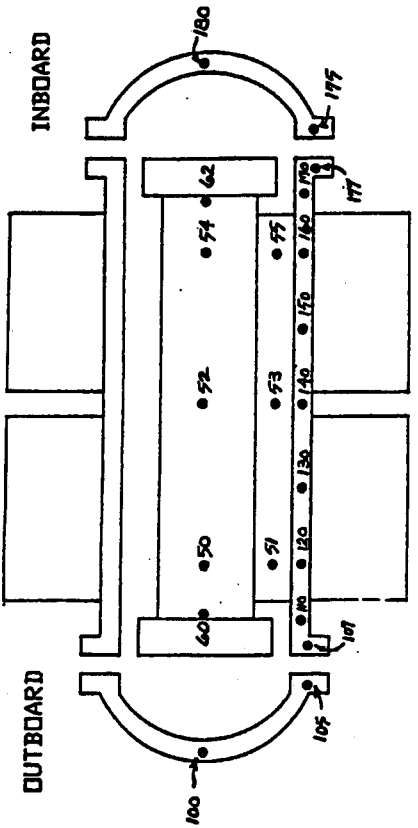


FIGURE 3.4.1-1b. GPHS RTG Thermal Model Nodes (Interior Nodes).

BEST COPY AVAILABLE

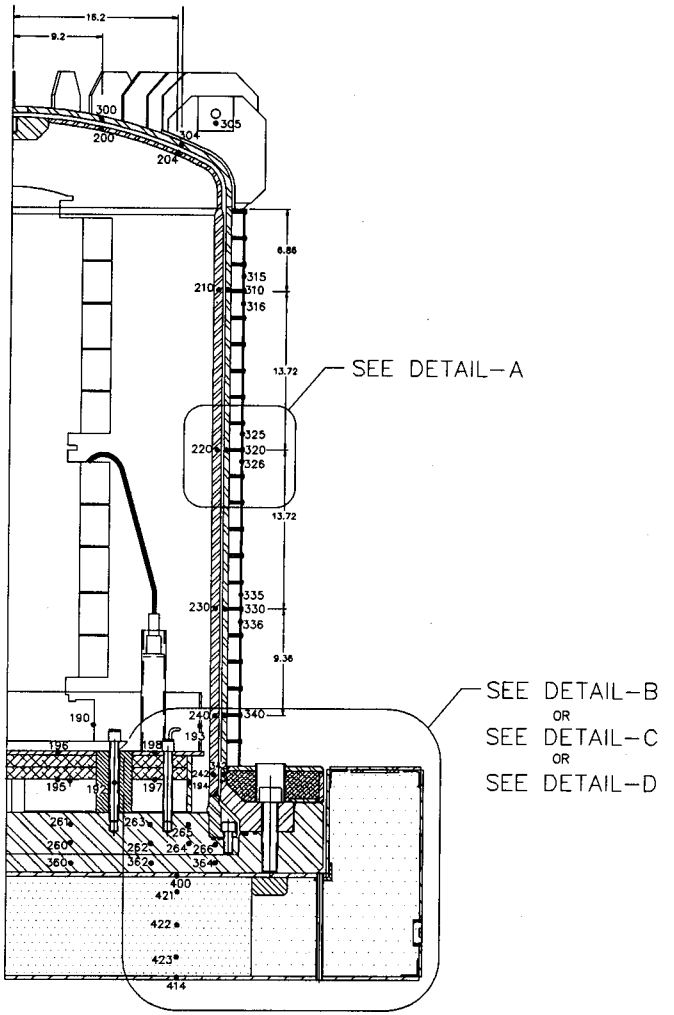
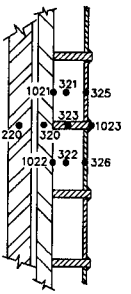
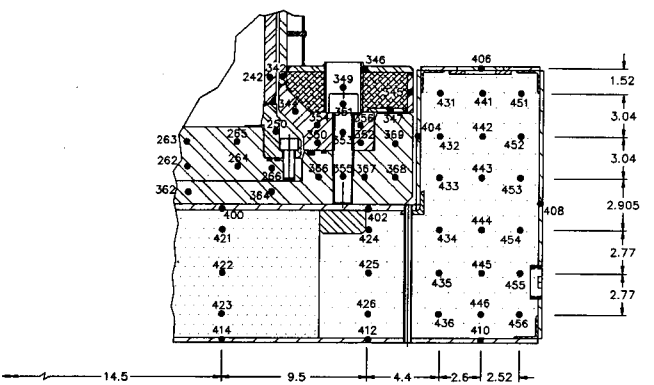


FIGURE 3.4.1-2. RTG Transportation System Package Thermal Model (details).



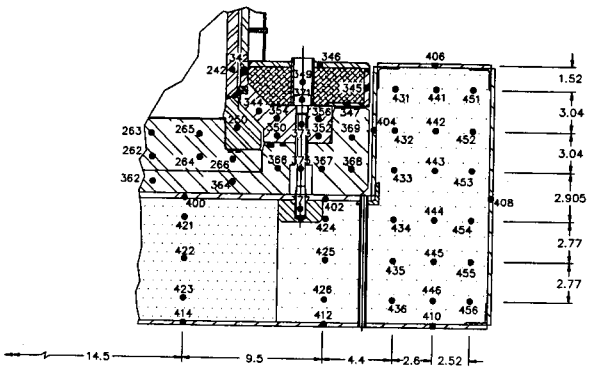
DETAIL–A



DETAIL–B

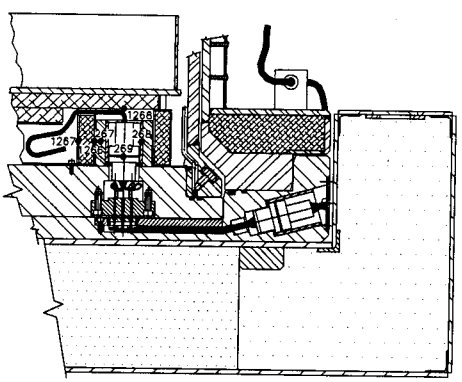
CLOSURE BOLTS ATTACHMENT

FIGURE 3.4.1-2. RTG Transportation System Package Thermal Model (details).



DETAIL–C

IMPACT LIMITER ATTACHMENT BOLT



DETAIL–D

FEED THROUGH

FIGURE 3.4.1-2. RTG Transportation System Packaging Thermal Model (details).

The convection coefficients for the GPHS RTG-to-ICV heat transfer are computed using equation 22 from Khan and Kumar[11]. This correlation was developed for the case of convective heat transfer across a vertical annuli with a constant heat flux on the inner wall. The area of the inner and outer annuli walls is not explicitly entered, but are implied by a characteristic length parameter that is a combination of the ratio of diameters and gap dimension. As such, the coefficients predicted by the correlation require adjustment to account for the fact that the GPHS RTG is a finned cylinder. The general applicability of the Khan and Kumar correlation to the specific geometry of the GPHS RTG and the method used to adjust the correlation was the subject of a thermal development test using a simulator of the GPHS RTG. The test results show that the Khan and Kumar correlation is applicable to the GPHS RTG/ICV geometry and that it can provide an accurate prediction of the convective coefficients. The Reference 12 test report presents a detailed discussion of the test setup, results, and the adjustment procedure used to apply the correlation to this payload. The validity of the adjusted correlation developed under the Reference 12 report was confirmed by qualification testing documented in the Reference 14 report.

Because a significant fraction of the heat transfer between the GPHS RTG and the ICV is via radiation, the shape factors between the various surfaces were determined by computer analysis using the University of Washington's VIEW[31] program. The computed shape factors were validated using results from the GPHS development tests (see Section 3.4.1.2).

3.4.1.1.4 Package Models For Regulatory Conditions. The final category of thermal model developed for this analysis is that used to predict the package response under the regulatory normal conditions of transport specified 10 CFR 71. These models were similar to those used for the normal operational conditions. The primary model modifications involved the assumptions that the chillers are inoperative and that the coolant fluid has been drained or boiled out. As such, the forced fluid conductors in the cooling jacket are replaced with radiation and convection across a dry coolant channel. This modification is appropriate because analysis shows that the steady-state coolant temperatures will exceed the boiling point for the regulatory, inoperative chiller conditions. The package's cooling jacket incorporates pressure relief valves that will relieve pressure should the coolant system malfunction.

Package damage resulting from the NCT free drop tests was minor and would not affect the thermal performance of the package.

3.4.1.2 Test Model. In addition to the analytical models, developmental and qualification test models of the packaging were built to qualify the package design as capable of maintaining the RTGs within their temperature limits and to validate the analytical models. The developmental tests examined the basic heat transfer mechanisms that occur within the ICV cavity during the transport of an undamaged RTG. Included were steady-state results for radiative heat transfer only (i.e., with the ICV cavity evacuated of all gases), combined radiation/convection heat transfer with an air-filled ICV cavity, and combined radiation/convection heat transfer with a helium-filled ICV cavity. The effects on convective heat transfer caused by increasing the helium gas pressure and tilting the package were also examined.

The developmental test model consisted of an ICV bell and base plate, support stand assembly, and a simulator of the GPHS RTG. The OCV bell and base plate and the impact limiter were not modeled for this test. Instead, a cooling jacket was placed directly on the ICV bell, and the coolant temperatures adjusted to simulate the temperature rise across the ICV-OCV gap. Carbon steel was used for the ICV bell and base plate, while the GPHS RTG simulator was fabricated of 6061-T6 aluminum. The various differences in geometry and material were accounted for in the analytical model used to analyze the test results. The thermal

developmental test model was designed to replicate only the geometry of the ICV/RTG interface

used in the calculation of the radiation view-factors and the convective heat transfer coefficients. The developmental test did not address the heat transfer modes between the ICV and OCV or between the OCV and the external environment because these heat transfer modes are well defined and could be modeled analytically using established equations.

The development test results validated the procedures used to calculate the radiation and convection heat transfer conductances between the various nodes on the RTG thermal model and the nodes on the package thermal model. Reference 12 describes the test setup, procedures, conditions, results, and data analysis.

The thermal qualification tests built on the validation of the analytical modeling approach begun by the development tests by removing the majority of the hardware differences between the test and actual articles. The test article was a full-scale representation of the RTG Transportation System Package. The ICV and OCV bells were built to the production drawings. The RTGs were simulated with electrically heated hardware (ETG) built to production drawings and specifications. The shipping rack assembly was built to specifications with two main exceptions. First, the shipping rack included a center hole to allow instrumentation and power cables to pass through. Second, the electrical feed-through instrumentation hardware (see Figure 3.4.1-2, Detail D) was not present.

Only the base plates and impact limiter were built as simplified replicas of the actual articles. This approach was taken for a combination of fabrication ease, cost savings, and the need for numerous instrumentation leads to pass through the base plate.

Instead of separate stainless steel base plates for the ICV and OCV, the test article for the thermal qualification tests used a single carbon steel base plate with integral seal flange areas for both vessels. The impact limiter was simulated using 9 lb/ft^3 polyethylene foam instead of the 12 lb/ft^3 polyurethane foam. The simulated impact limiter was dimensionally correct, but did not have a stainless steel shell. Both test component designs had a negligible effect on the test results because of their similarity to the actual components and the low heat flux to the lower end of the package under normal operational conditions. Polyethylene foam has a thermal conductivity of 0.40 Btu-in/ft^2-°F-hr at 70°F, versus 0.28 Btu-in/ft^2-°F-hr for polyurethane foam at the same temperature.

The thermal qualification tests covered prototypic procedures for loading, unloading, and transporting the RTGs. A limited number of off-design operational conditions were also covered by the tests. No regulatory conditions were tested because of potential damage to the ETG test hardware that these conditions could cause. However, results from the thermal qualification tests further validated the analytical models used to simulate the RTG payload within the package under both operational and regulatory conditions.

Reference 13 defines the test hardware, test procedures, and test conditions used in the thermal qualification tests. Reference 14 documents the test data reduction and correlation with analytic predictions. Figures 3.4.1-3 and 3.4.1-4 present typical benchmark results between the thermal model used for the SARP and the thermal qualification test data. Figure 3.4.1-3 illustrates the comparison between test data and analytical model predictions for package steady-state temperatures under simulated normal operational conditions (i.e., cooling system active) with a GPHS RTG payload. The figure shows an excellent agreement between test and predicted temperatures for all but thermocouple locations TC-10, TC-182, and TC-180.

Thermocouple TC-10 was located at the center of the ICV torispherical head. The closest thermal model node to TC-10 is 200, but the temperature at this node represents the mean temperature of a 26-in. diameter section of the dome. Because of the high temperature gradients in this region, the predicted temperature at node 200 would be lower than that measured by

TC-10. This fact is borne out by the good agreement with TC-9, which is located closer to the geometric mean point on the ICV dome area represented by node 200. The mismatch at TC-180 and TC-182 locations occurs at a section of test hardware (i.e., electric power inlet spool piece) that was not directly modeled by the RTG thermal model and does not exist on the real article. The suspected cause is an underestimation of the heat leakage through the interior ETG insulation where the power cables enter the body of the ETG test article. No adjustment was made to the SARP thermal model for the mismatch at the TC-180 and TC-182 locations because the spool piece is not present on the actual RTG.

Figure 3.4.1-4 presents a comparison between model predictions and test data for the prototypic loading of the GPHS RTG into the packaging. The illustrated transient temperatures represent key thermocouple locations on the GPHS ETG and the packaging. Similar results were seen for the other thermocouple locations. The analytical model provides a close, but conservative estimate of the resulting package and RTG transient temperatures. In conclusion, the thermal qualification tests validate the thermal model for both steady-state and transient calculations of an undamaged packaging and payload.

3.4.2 Maximum Temperatures

NCT thermal load case No. 1 evaluated the maximum temperatures in the package under the 10 CFR 71.71(c) conditions for heat. According to the referenced regulatory condition, the analysis assumes an ambient air temperature of 100 °F and insolation. The total insolation over a 12-hour period on the package is given in Table 3.4.2-1. The hourly average of the table data is the appropriate insolation value to use because the high thermal mass of the package ensures that it will not respond to short-term variations in insolation. A precise modeling of the data in Table 3.4.2-1 calls for a cyclic step function of insolation for 12 hours (daylight) followed by 12 hours of no insolation (nighttime) until steady periodic behavior is established. However, this analysis used the simple, but more conservative approach of assuming a uniform heat flux equal to the hourly average (based on 12 hours) of the table values in a steady-state analysis.

TABLE 3.4.2-1. Insolation Data.

Form and location of surface	Total insolation for a 12-hour period (g cal/cm^2)
Flat surfaces transported horizontally:	
• Base	None
• Other surfaces	800
Flat surfaces not transported horizontally	200
Curved surfaces	400

The amount of solar energy absorbed by the package is calculated as the product of the hourly insolation value times the solar absorption factor for the package surface in question. Because the entire exterior surface of the package is coated with a white, two-part epoxy paint, the appropriate solar absorption factor is 0.25. With the exception of the base of the impact limiter, the full-surface area is used to determine the total solar insolation heat flux on the package's individual surfaces. Shading of one package surface on another surface is assumed to not occur.

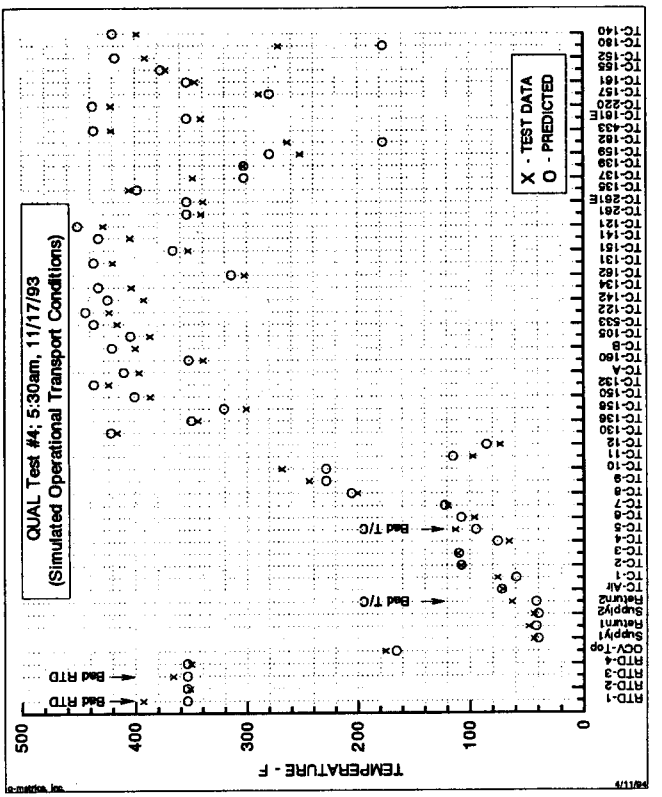


FIGURE 3.4.1-3. Thermal Model Benchmark With Steady-State Test Data.

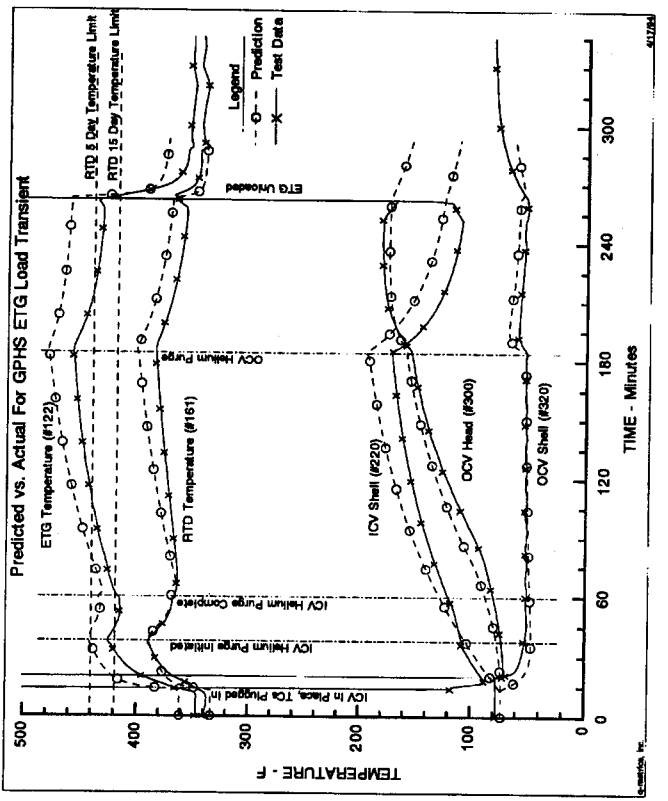


FIGURE 3.4.1-4. Thermal Model Benchmark With Transient Test Data.

Additional assumptions for NCT thermal load case No. 1 include an undamaged payload and packaging, a maximum decay heat load of 4,500 W, and an inactive cooling system with the cooling jacket drained.

Figure 3.4.2-1 presents the maximum package temperatures expected under regulatory NCT. All temperatures are within component allowables.

Figure 3.4.2-2 illustrates the package temperature distribution for the same conditions as above, except without solar insolation. This load case is used as one of the pre-accident conditions for the HAC fire transients presented in Section 3.5.

3.4.3 Minimum Temperatures

The package minimum temperatures are evaluated for two categories of regulatory NCT: worst case differential thermal expansion and minimum component temperatures.

The NCT thermal load case No. 2 helped determine the maximum differential thermal expansion in the seal areas. This load case assumes an undamaged payload and packaging, the maximum decay heat payload of 4,500 W, and that the cooling system is inactive and the cooling jacket is drained. The environmental conditions are those of the 10 CFR 71.71(c) conditions for cold: -40 °F still air and no solar loading.

Figure 3.4.2-3 presents the package temperature distribution for NCT load case No. 2. All temperatures are within component allowables.

Figure 3.4.2-4 illustrates the temperature distribution in the package for NCT load case No. 5. This temperature is used as one of the two pre-accident conditions for the HAC fire presented in Section 3.5.

Package component compatibility with the minimum temperatures expected was determined assuming no solar loading, no active cooling, minimum heat load payload, and either -20 °F (dynamic conditions) or -40 °F (static conditions) ambient temperature. No specific analysis was made for these conditions. Instead, it is assumed that the package temperature distribution will be uniform and equal to the ambient temperature. All package components are capable of operating at temperatures down to -40 °F.

3.4.4 Maximum Internal Pressures

Table 3.4.4-1 presents the gas temperatures and pressures within the ICV and OCV. The gas pressures are estimated using the ideal gas law. The base pressures and temperatures used in the calculations are set by the steady-state condition for NCT load case 7 (see Table 3.4-1). The analysis assumes worst case initial pressures at the time of RTG loading into the packaging (i.e., 19 psia base pressure + 1 psi tolerance = 20 psia). Other sources of pressure rise within the ICV/OCV, and their contribution to the final pressure level are addressed in Section 2.6.1.

TABLE 3.4.4-1. Maximum ICV/OCV Pressures and Temperatures For Normal Conditions of Transport.

Load case/condition	ICV pressure (psia)	ICV gas temp. (°F)	OCV pressure (psia)	OCV gas temp. (°F)
Case 1	24.4	354	26.3	285
Case 2	21.5	256	22.1	165
Case 3	20.2	213	20.3	115
Case 4	24.1	342	25.8	271
Case 5	21.9	269	22.6	181
Case 6	20.1	210	20.1	111
Case 7	20.0	207	20.0	107

3.4.5 Maximum Thermal Stresses

The results from finite element analyses of the ICV and OCV for NCT load cases 1, 2, and 3 are presented in Section 2.6.1. These are the governing cases for stresses because they result in the worst case combination of temperatures and temperature gradients. All margins of safety are positive and the design criteria of Regulatory Guide 7.6 are satisfied. See Section 2.6.1.3 for specific details and further discussion.

3.4.6 Temperatures For Operational Conditions

The NCT thermal load case No. 3 evaluated the package temperature distributions with the mechanical cooling system active, regulatory solar insolation, and the maximum heat payload. The resultant temperatures encompass those seen by a shaded package loaded in a vented trailer that is exposed to 100 °F ambient temperature and regulatory solar insolation.

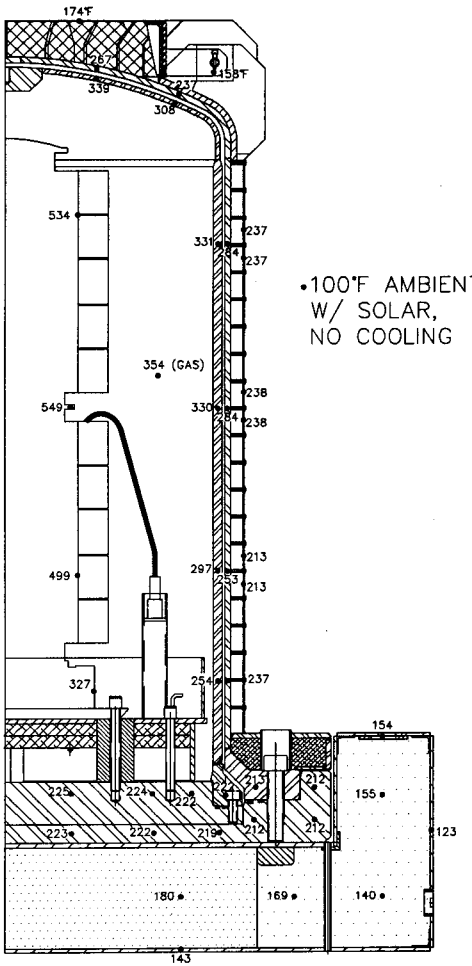


FIGURE 3.4.2-1. Maximum RTG Transportation System Package Temperatures For NCT Load Case No. 1

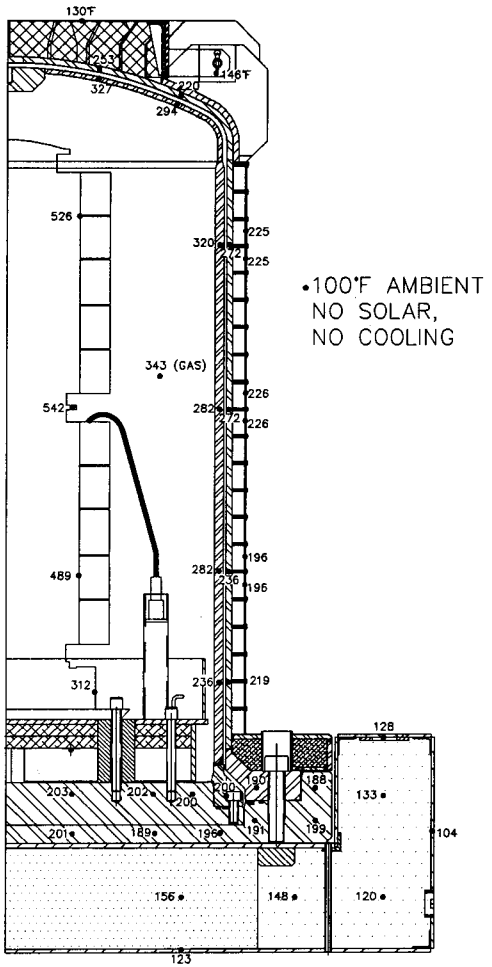


FIGURE 3.4.2-2. RTG Transportation System Package Temperature Distribution For NCT Load Case No. 4.

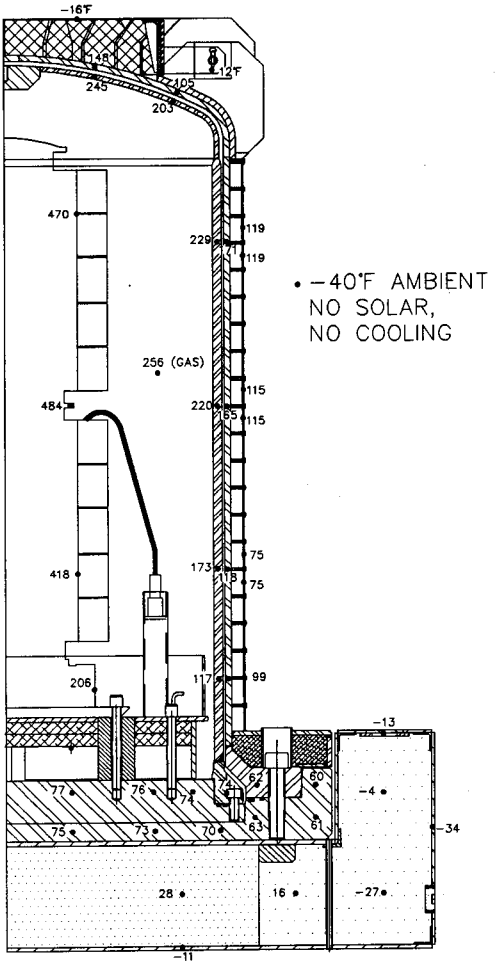


FIGURE 3.4.2-3. Minimum RTG Transportation System Package Temperature For NCT Load Case No. 2.

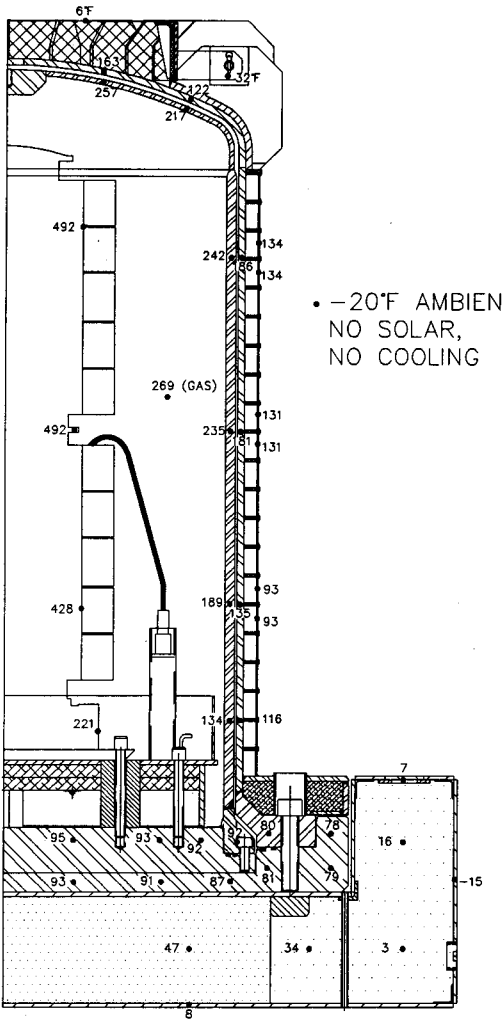


FIGURE 3.4.2-4. RTG Transportation System Package Temperature Distribution for NCT Load Case No. 5.

This load case illustrates the maximum package temperatures seen with active cooling. These temperature levels are the maximums expected during package transport, except in the remote possibility where multiple and independent failures deactivate the cooling system. As such, this load case also illustrates the additional thermal conservatism imposed by the regulatory requirement of starting the package at steady-state under NCT before imposing the HAC fire.

Figure 3.4.6-1 illustrates the temperature distribution for NCT load case No. 3. In general, the ICV sidewall temperatures run 180 °F cooler with active cooling than without cooling for the same ambient temperatures. Package base plate and seal temperatures are approximately 130 °F cooler, while head temperatures are 60 °F cooler.

Figures 3.4.6-2 and 3.4.6-3 illustrate package temperatures without solar for 100 and 70 °F ambient air conditions, respectively (i.e., NCT load cases 6 and 7). Figure 3.4.6-2 confirms compliance with the 10 CFR 71.43(g) requirement that no accessible surface exceed 180 °F. Figure 3.4.6-3 illustrates the temperature distribution after loading the RTG in the packaging. All subsequent calculation of internal ICV and OCV gas pressures are keyed to this temperature distribution.

3.4.7 Evaluation of Package Performance for Normal Conditions of Transport

Through analysis and physical testing, the RTG Transportation System Package is shown to meet the thermal requirements of 10 CFR 71.71. Based on Sections 3.4.2 and 3.3, all components will remain within their working temperature range. The maximum temperature reached in the OCV is 268 °F, while the ICV reaches a maximum temperature of 339 °F. The ICV and OCV seal temperatures are 222 °F and 213 °F, respectively. The electrical feed-through connector remains below 226 °F for NCT, while a maximum temperature of 206 °F is reached in the impact foam adjacent to the OCV base plate. The RTG payload shell remains below 550 °F.

The minimum temperature from Section 3.4.3 for any package component is taken as -40 °F for static conditions and -20 °F for dynamic conditions.

3.5 HYPOTHETICAL ACCIDENT THERMAL EVALUATION

This section presents the thermal analysis of the RTG Transportation System Package for the HAC fire specified in 10 CFR 71.73(c)(3). The thermal performance of the package is evaluated analytically using a 3-D thermal model. The thermal model is based on the NCT model with modifications made to simulate the damage sustained from the HAC 30-ft free drops and the HAC 40-in. puncture drops. The results from a series of drop tests conducted on the Certification Test Article are presented in Sections 2.7.6 and 2.10.15. Analysis of the expected thermal impact associated with the package damage noted after each of the drop tests is presented in Section 3.6.2.4. The initial temperature distribution in the package before the HAC fire is taken from the steady-state conditions with the worst case ambient temperature, no insolation, and no active cooling.

To determine the effect of the HAC fire, the package is exposed to a convective and radiative heat flux based on still, ambient air at 1475 °F and with an emissivity of 0.90. The HAC fire is assumed to last for 30 minutes, after which time the thermal boundary is returned to the original ambient temperature. The thermal transient analysis is continued for a sufficient time to determine the maximum values for all package components, concluding with a post-HAC fire steady-state analysis

3.5.1 Thermal Model

3.5.1.1 Analytical Model. The analytical model for the regulatory NCT is used as the basis for the HAC fire model. The primary modification made for HAC fire evaluation was to create a 3-D model to permit simulation of asymmetric damage caused by the HAC free drop. The 3-D model was created using a SINDA program feature that allows a series of thermal submodels to be combined into one large thermal model. Each of these submodels can be independently scaled and modified as necessary to represent their contribution to the overall thermal model. For this application, the 2-D package models described for the undamaged case were used to represent axial and radial heat transfer within the individual subsegments making up the 3-D model of the package. Circumferential conductors are used to complete the 3-D model by providing thermal communication between the various 2-D model subsegments.

In general, heat transfer within each 2-D submodel is modeled using the same axisymmetric regulatory model data for thermal capacitance, conductance, and radiation as defined in Sections 3.4.1.1 and 3.6.2. Each value for conductance and capacitance is scaled according to the subtended angle represented by the associated submodel. Where appropriate, the individual 2-D submodels are modified to simulate changes in heat transfer modes and/or values because of damage and package orientation caused by the regulatory drops. The specific model changes are described in Appendix 3.6.2.4.

The 3-D HAC fire thermal model uses four 2-D submodels to represent one-half of the package. Symmetry conditions are assumed for the temperatures in the other half of the package. One of the submodel segments represents the damaged section of the package, while the other three segments provide circumferential temperature resolution within the package components. Sections 3.5.2 and 3.6.2.4 describe the type and extent of package damage assumed.

Additional model modifications for the HAC fire included the 10 CFR 71.73(c)(3) requirements for a package external surface absorptivity of 0.8 or greater and exposure of the entire package (including the impact limiter bottom) to the HAC fire.

3.5.1.2 Test Model. No thermal testing for the HAC fire was performed for the RTG Transportation System Package as an entire assembly. However, performance tests were conducted for the polyurethane foam used in the impact limiter, the Butyl seals, and the electrical feed-through connectors. The test results are documented in Appendix 3.6.3, 2.10.6, and 4.5.2, respectively. Briefly, these tests demonstrated the following major findings:

Polyurethane Foam

- Below 400 °F, the variation in foam thermal properties with temperature are slight and reversible. As such, fixed values for specific heat and thermal conductivity are appropriate.
- Irreversible thermal degradation of the foam begins at temperatures above 400 °F. The degradation is accompanied by vigorous outgassing that removes a significant amount of heat through mass transport processes.

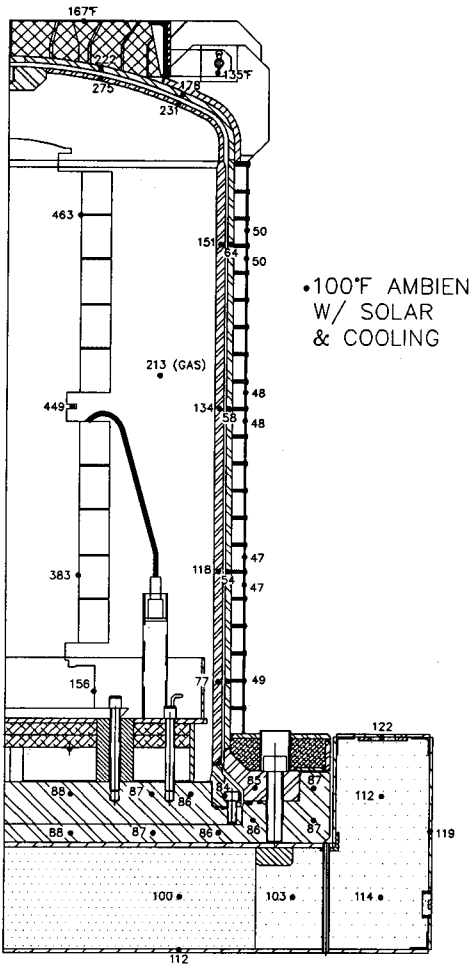


FIGURE 3.4.6-1. RTG Transportation System Package Temperature Distribution For NCT Load Case No. 3.

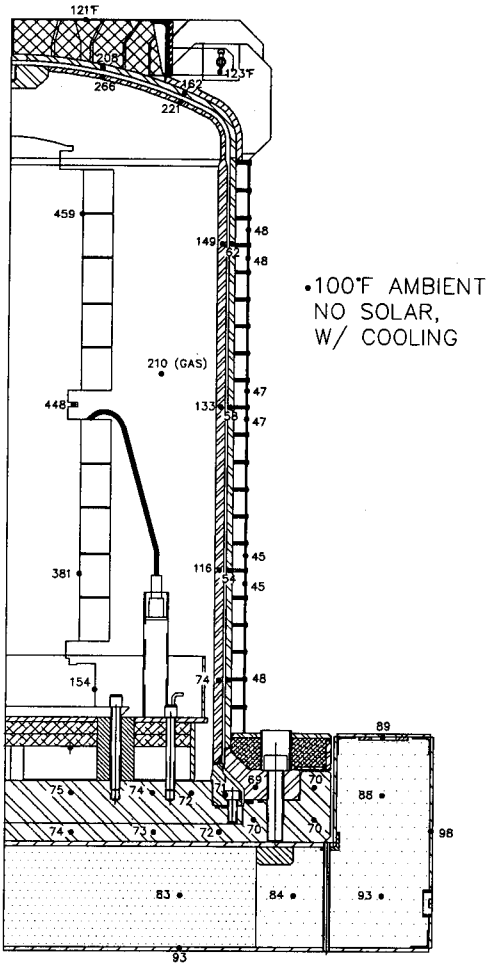


FIGURE 3.4.6-2. RTG Transportation System Package Temperature Distribution For NCT Load Case No. 6.

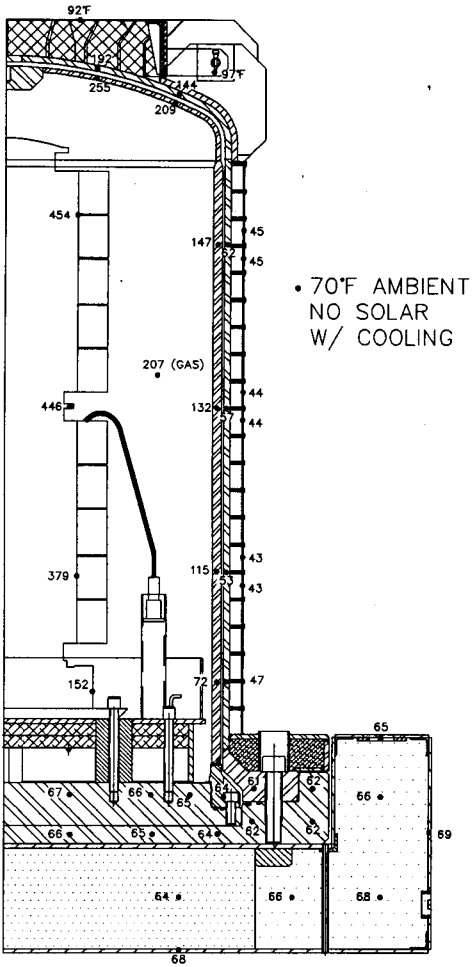


FIGURE 3.4.6-3. RTG Transportation System Package Temperature Distribution For NCT Load Case No. 7.

- A rigid char layer is formed as the thermal degradation continues . In the absence of direct exposure to the flame, the char layer will be the same or slightly thicker than the original foam depth. This char layer provides radiative shielding to the underlying foam material.

- Where a layer of undisturbed 12 lb/ft^3 foam in excess of 3 in. or a layer of 3 lb/ft^3 foam in excess of 8.5 in. exists before the initiation of the fire, little or no thermal response will be seen on the backside of the foam because of the fire event.

O-ring Seal Tests

The butyl O-ring containment seals have successfully demonstrated leaktight behavior at a temperature as high as 380 °F over short durations (24 hours) and 350 °F over extended periods (6 days). The complete details of the time-temperature testing of the O-ring seals is provided in Appendix 2.10.6. Butyl O-ring containment seals exhibiting time-history characteristics below those identified in Appendix 2.10.6 are considered satisfactory for maintenance of leaktight containment in the package.

3.5.2 Package Conditions and Environment

Several combinations of HAC free and puncture drops were evaluated to determine the worst case thermal damage to the package. Details of the analysis and the tests used to support the damage evaluations are presented in Sections 2.7 and 2.10.15. Section 3.6.2.4 summarizes the thermal analysis associated with the damaged package.

Briefly, the finding of these analyses and tests is that the most thermally sensitive post-impact package reconfiguration will result from either (1) a bottom-down c.g. over corner impact orientation, or (2) a side slapdown impact, defined for the package as the near-simultaneous impact of the top-end fins and the bottom-end impact limiter. The impact limiter damage for each of these impact scenarios is illustrated in Figures 3.5.2-1 and 3.5.2-2, respectively. Thermal evaluation of the above potential package reconfigurations showed that the side slapdown impact poses the most conservative case for the thermally sensitive package seals. As such, this drop orientation serves as the basis for all of the HAC fire transients. In addition, the center of the side slap down impact damage is assumed to be aligned with the electrical feed-through.

Based on drop tests and analysis (see Sections 2.7 and 3.6.2.4), the side slapdown impact will crush the top of the impact limiter to about 25% of its original side thickness at the centerline of the damage. The lower end of the impact limiter will sustain essentially no damage. The circumferential extent of the damage to the top of the impact limiter will extend over a 67° arc. Figures 3.5.2-2 and 3.5.2-3 illustrate how the impact limiter damage is modeled analytically. Segment A of the 3-D model assumes the foam thickness to be reduced by 50% over the full height and subtended angle of the segment. Impact limiter damage beyond the angle subtended by segment A is assumed to be encompassed by the conservative assumption that the first 2.5 in. of foam ablates away at the initiation of the HAC fire (see Appendix 3.6.3 for more discussion of this assumption).

In addition to damaging the impact limiter, the side slapdown impact will cause localize damage to the impact fins at the OCV torispherical head and the top 4 in. of the coolant jacket. The damage will consist of buckling and/or bending of two or three fins onto the OCV head and potential contact between the ICV and OCV shells over a 2-in. high by 13-in. wide area. The fin damage will tend to lower the heat transfer with the exterior environment, while the possible ICV/OCV contact will tend to raise the local ICV temperature during the fire and lower the ICV temperatures after the fire. The nature and extent of the damage will not have a significant effect

on the heat transfer characteristics in this area and was not specifically addressed by the analytical thermal model for the HAC fire event.

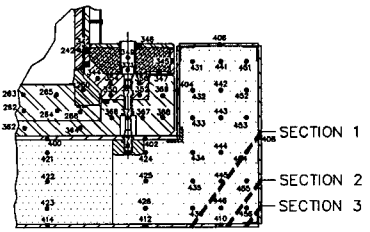
Beyond the damage described above, no significant damage will occur to the package because of the HAC free drops. Puncture bar damage will be limited and highly localized. The structural strength of the impact limiter shell is sufficient to limit puncture bar damage to relatively minor indentations of the shell. Tearing of the shell, with subsequent penetration and gouging of the underlying foam will not occur. Puncture bar impact to the OCV head will produce localized indentation with associated contact between the ICV and OCV heads over a 7-in. diameter area. Puncture bar impact to the cooling jacket will produce localized collapsing of the cooling jacket thickness and, possibly, localized indentation of the OCV and ICV shells. Any subsequent contact between the ICV and OCV will tend to raise the local peak temperature for the ICV during the fire, but lower the local ICV temperature following the fire.

Finally, puncture bar impact to the OCV thermal shield at the bolt flange will result in only minor damage. Because of the location of the surface and the package center of gravity, the impact will be a glancing blow. Damage will be limited to crescent-shaped indentation of the OCV thermal shield, but no penetration. At its greatest depth, the OCV thermal shield will be collapsed to 1/2 its original height above the bolt flange.

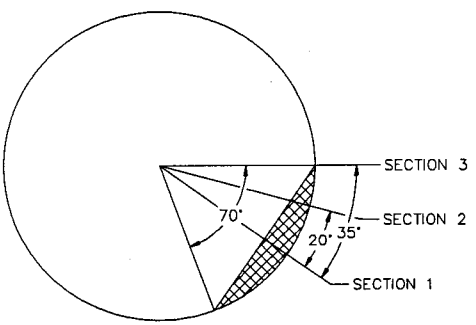
Of the various potential puncture bar damage described above, only the potential for damage to the OCV bolt flange thermal shield is considered significant enough to warrant modeling. The potential damage is conservatively modeled by locating the damaged area adjacent to the impact limiter damage (i.e., Segment A, Figure 3.5.2-3) and by assuming the shield to be collapsed to 1/2 its original height over a 6-in. diameter area (the puncture bar). The density and conductance of the fiberglass insulation underlying the damaged area is increased to account for the collapse of the OCV thermal shield.

The damage analysis indicates that a side slapdown impact will cause the GPHS RTG payload to break away from its shipping rack mounts. For conservatism, it is also assumed that the shell of the GPHS RTG payload is ruptured in the impact and that all 18 GPHS heat-source modules (aeroshells) spill out. The aeroshells, which are the outer housing of each heat source module, measure 92.4 by 97.2 by 53.1 mm. The aeroshells are the smallest heat-producing fragment of the RTG that will occur because of the HAC free drop.

Following the side slapdown impact, the package is envisioned as coming to rest in one of only two credible orientations: upright (resting on the impact limiter's bottom) or on its side. In the first post-HAC orientation, the 18 aeroshells are assumed to be distributed uniformly around the outer circumference of the package shipping rack assembly (i.e., nearest the ICV containment seal). The shell of the GPHS RTG payload is assumed to have broken off from its stand and to be canted at an angle within the ICV. Figure 3.5.2-4 illustrates the configuration for this HAC case.

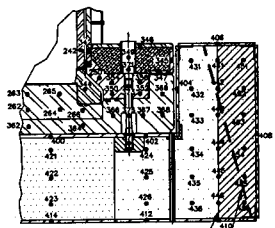


EXTENT OF CRUSH
IN DAMAGED AREA



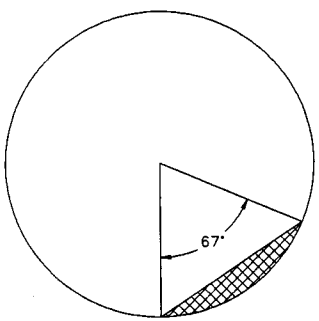
CIRCUMFERENTIAL EXTENT OF DAMMAGE

FIGURE 3.5.2-1. Impact Limiter Damage With C.G.-Over-Corner Drop.



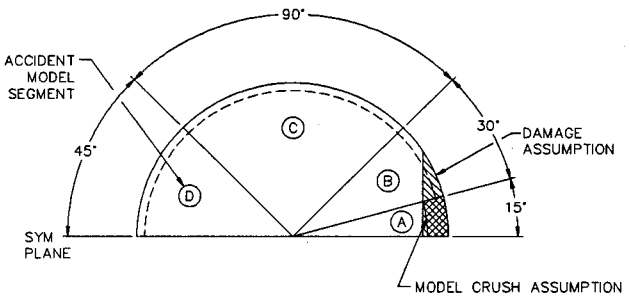
CRUSH LINE ⊕ CENTERLINE OF DAMAGE FOR ANALYTICAL MODEL

EXTRAPOLATED CRUSH LINE ⊕ CENTERLINE OF DAMAGE FROM TEST DATA

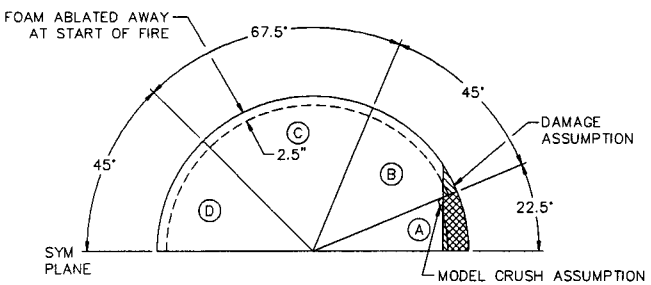


CIRCUMFERENTIAL EXTENT OF DAMAGE

FIGURE 3.5.2-2. Impact Limiter Damage With Side Slapdown Drop.



A. MODEL USED FOR CASES 3 & 4
(AXIAL RUBBLE CONFIGURATION)



B. MODEL USED FOR CASES 1 & 2, 5 & 6
(CIRCUMFERENTIAL AND UNGULA RUBBLE CONFIGURATION)

FIGURE 3.5.2-3. Impact Limiter Modeling Assumptions.

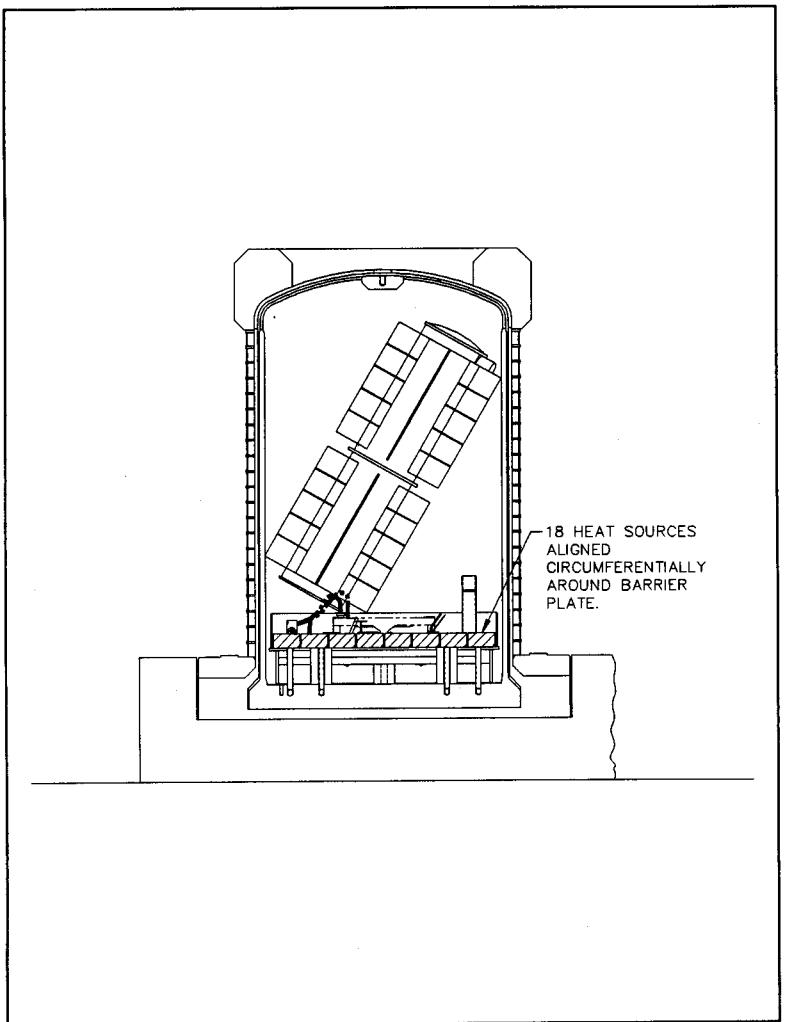


FIGURE 3.5.2-4. Post-HAC Free Drop Package Orientation For Circumferential Heat Source Alignment.

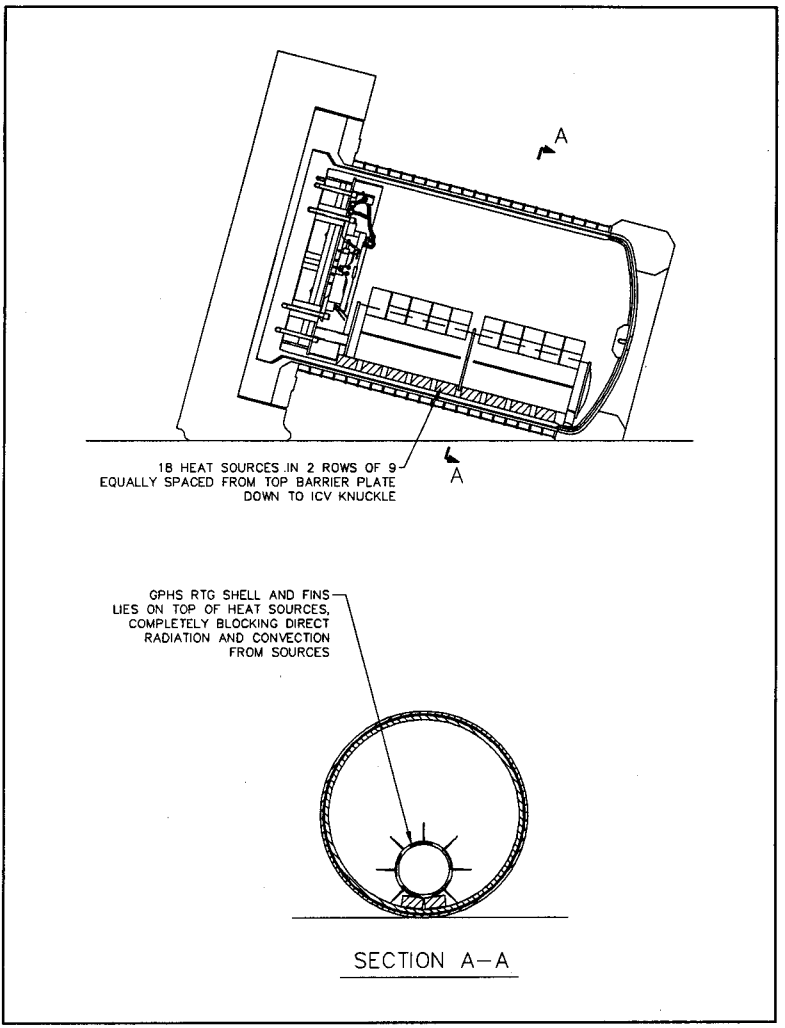


FIGURE 3.5.2-5. Post-HAC Free Drop Package Orientation For Axial Heat Source Alignment.

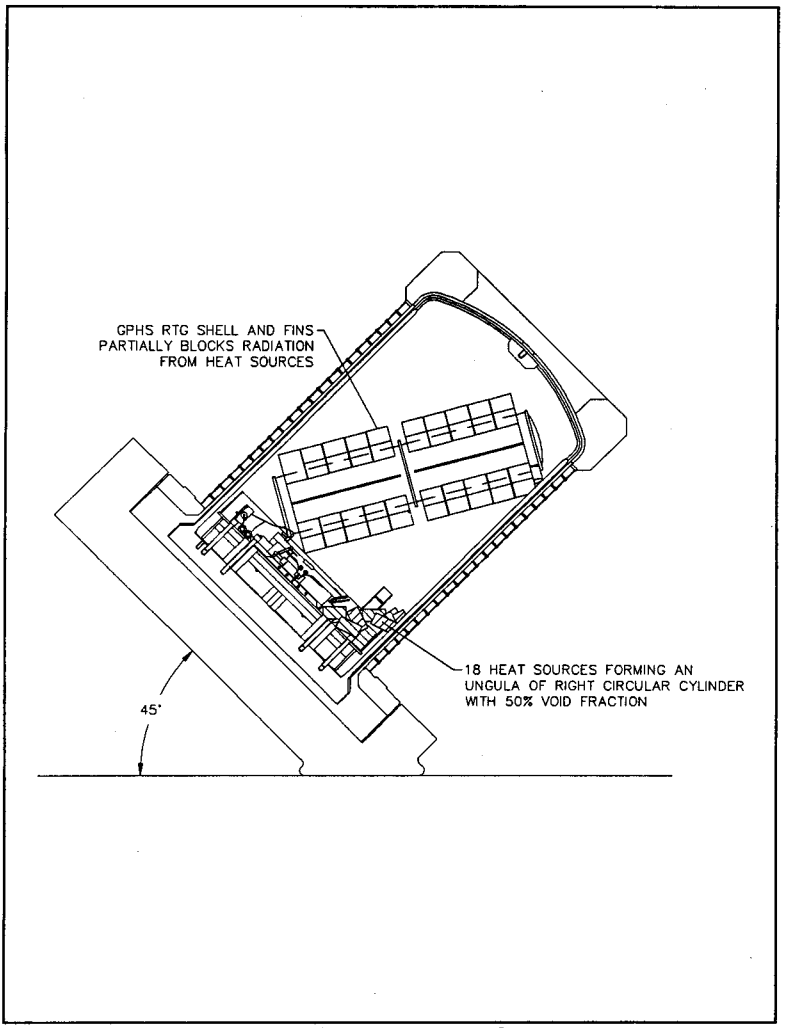


FIGURE 3.5.2-6. Post-HAC Free Drop Package Orientation For Ungula Heat Source Alignment.

For conservatism, the RTG shell is canted in the direction of the impact limiter damage, where it shields the underlying aeroshells from direct radiation interchange with the inside surfaces of the ICV. Convection from the aeroshells is not significantly affected by the position of the RTG shell.

In the second post-HAC package orientation, the 18 GPHS aeroshells are assumed to come to rest in an axial alignment on the ICV wall. The assumed alignment has two modules arranged side by side, starting at the top of the shipping rack assembly and extending to the ICV torispherical head. For conservatism, the centerline of the aeroshells and the package side drop damage are assumed to be aligned. The shell of the GPHS RTG is assumed to end up lying directly on top of the aeroshells, blocking direct convection and radiation interchange between the aeroshells and the interior of the ICV cavity. Figure 3.5.2-5 illustrates the assumed alignment of the package, RTG shell, and aeroshells for this post-HAC free drop condition.

In addition to these credible post-HAC package/payload configurations, an extremely conservative configuration is evaluated wherein the package somehow ends up on its bottom corner, at a 45° orientation relative to the flat, unyielding regulatory impact surface. In this statically unstable post-HAC drop orientation, the 18 aeroshells are assumed to come to rest in an ungula-shaped rubble pile. For further conservatism, the rubble pile is assumed to be on the side of the shipping rack assembly barrier plate adjacent to side drop damage area of the package. Based on analysis and simple experiments, the rubble pile is assumed to have a 50% void fraction and to subtend a 135° arc. The RTG shell is assumed to have come to rest canted at an angle across the rubble pile. This orientation of the RTG shell is assumed to block the underlying aeroshells from direct radiation interchange with the inside surfaces of the ICV. Convection from the aeroshells is assumed to not be significantly affected by the position of the RTG shell. Figure 3.5.2-6 illustrates the assumed alignment of the package, RTG shell, and aeroshells for this post-drop condition.

All of the HAC fire transients begin with the undamaged package at steady-state with the chillers inoperative and the cooling jacket drained, no solar insolation, and an ambient temperature of either 100 or -20 °F. The temperature of the various package components, the shell of the RTG, and the aeroshells are initialized at the temperatures established by the NCT model. Specifically, the convective and radiation heat transfer links for the undamaged payload are used to determine the temperature of each modeled component just prior to the HAC accident sequence occurring. By this means the temperatures presented for NCT load case 4 (i.e., 100 °F, no solar, no active cooling) or NCT load case 5 (i.e., -20 °F, no solar, no active cooling) are used to initialize the equivalent components of the re-configured payload and the packaging prior to beginning the HAC transient. Since the HAC impact/puncture damage and payload reconfiguration is assumed to occur immediately before the start of the HAC fire event, the initial temperatures will be the same as for the associated NCT condition. Following the HAC damage and payload reconfiguration, the HAC model with its revised method of calculating the convective and radiative heat transfer is used to determine the subsequent changes in component temperatures.

Although portions of the ICV/OCV surfaces coated with the Carboline high emissivity coating will briefly exceed the coating's peak temperature rating of 1000 °F, it is assumed to remain intact throughout the HAC fire. This assumption maximizes the heat input to the package during the HAC fire. The Tnemec epoxy paint and primer used on the package exterior will lose its adhesion to the package surfaces during the HAC fire, flake off, and expose the stainless steel surfaces to the HAC fire environment. Although this action will tend to reduce the package surface absorptivity from 0.8 to 0.48, the regulatory value of 0.8 is used to account for sooting.

Six HAC fire load cases are used in the evaluation of the damaged package/payload configurations. Table 3.5.2-1 summarizes the pre- and post-HAC state assumed for each HAC load case. Section 2.7.3.1.1.2 provides additional details and background discussion on each HAC load case. The results of each analysis is presented in the following sections.

TABLE 3.5.2-1. Load Cases For The Hypothetical Accident Condition Analysis.

Load case	Pre-accident conditions	Post-accident conditions
1	a. Undamaged payload, 4,500 W maximum decay heat load b. Undamaged package; upright position, adiabatic bottom conditions c. Cooling jacket drained d. Steady-state conditions with 100 °F still air; no solar	a. Circumferential distribution of heat source modules on barrier plate, 4,500 W total. b. Side drop impact limiter damage; package upright, all surfaces exposed to ambient. c. Cooling jacket drained. d. 1475 °F fire for 30 minutes, followed by ambient air at 100 °F; no solar during and after fire.
2	Same as load case No. 1 except: d. Steady-state conditions with -20 °F still air; no solar	Same as load case No. 1 except: d. 1475 °F fire for 30 minutes, followed by ambient air at -20 °F; no solar during and after fire.
3	Same as load case No. 1	Same as load case No. 1 except: a. Axial distribution of heat source modules along ICV wall above rubble dam; 4,500 W total. b. Side drop impact limiter damage; package on its side, all surfaces exposed.
4	Same as load case No. 2	Same as load case No. 3 except: d. 1475 °F fire for 30 minutes, followed by ambient air at -20 °F; no solar during and after fire.
5	Same as load case No. 1	Same as load case No. 1 except: a. Ungula shaped rubble pile of heat source modules on shipping rack; 4,500 W total. b. Side drop impact limiter damage; package at 45° angle of repose, all surfaces exposed.
6	Same as load case No. 2	Same as load case No. 5 except: d. 1475 °F fire for 30 minutes, followed by ambient air at -20 °F; no solar during and after fire.

3.5.3 Package Temperatures

The HAC load case Nos. 1 and 2 evaluate the transient thermal response of the first post-HAC package configuration per 10 CFR 71.73(c)(3). Steady-state package temperature distributions with 100 and -20 °F ambient air, respectively, are used as the initial starting conditions for the HAC fire.

Figures 3.5.3-1 and 3.5.3-2 illustrate the transient temperature response for the circumferential heat source distribution thermal load cases. The plotted package temperatures are taken from the 3-D model segment centered on the area of the side drop damage (i.e., model segment A, Figure 3.5.2-3). Temperatures at the other circumferential locations are equal to or less than those shown in the figures. The peak ICV and OCV temperatures occur at or just after the end of the HAC fire. The figures provide the peak ICV/OCV temperatures noted during the HAC fire. The maximum temperature of the helium gas internal to the OCV and ICV noted during the HAC fire are 848 and 836 °F, respectively. Thermal protection within the package and temperature stratification within the ICV cavity prevents these relatively hot gas temperatures from affecting the package containment seals.

All of the predicted package temperatures for HAC load case Nos. 1 and 2 remain within the thermal limits of the associated component. The containment seal temperatures reach maximums (see Figures 3.5.3-1 and 3.5.3-2) that are below the temperature limits of the Butyl elastomer material. The peak electrical feed-through connector temperature of 332 °F is substantially less than its 475 °F temperature rating.

The HAC load case Nos. 3 and 4 evaluate the thermal response for the second post-HAC package configuration per 10 CFR 71.73(c)(3). Figure 3.5.3-3 illustrates the transient temperature response for the HAC load case No. 3 damage configuration (i.e., axial heat source distribution and the package on its side) with initial package steady-state temperatures for 100 °F ambient and no solar loading. Figure 3.5.3-4 illustrates the same configuration except with an initial steady-state for -20 °F. Again, the representative package temperatures illustrated are taken from the 3-D model segment A.

Representative peak ICV/OCV temperatures reached during the HAC fire are noted on the figures. The maximum helium gas temperatures internal to the OCV and ICV during the HAC fire are 851 and 747 °F, respectively. The elevated temperatures seen for the ICV and OCV walls for model segment A are because the aeroshells lying directly on the ICV wall under this damage configuration. However, all package component temperatures will remain within their associated working limits. The peak Butyl O-ring seal and electrical feed-through connector temperatures of 325 and 314 °F, respectively, are within the limits of both components.

The HAC load case Nos. 5 and 6 evaluate the worst case post-HAC configuration for the package containment seal temperatures. Figures 3.5.3-5 and 3.5.3-6 illustrate the transient temperature response for these conservative damage configurations (i.e., the aeroshells piled into a single ungula-shaped rubble pile and the package at a 45° angle). The conservatism of these load cases is increased by the basic analysis criteria applied to all HAC load cases; that is, that the package has suffered a double failure in the active cooling system, and the failure has existed long enough for the package to reach steady-state temperatures. If either of these conditions do not exist, the subsequent peak package temperatures reached during the HAC fire will be less than those shown in the figures. Again, the plotted package temperatures are taken from the 3-D model segment A which is centered on the rubble pile and the HAC side drop damage area.

As expected, the transient results for HAC load case No. 5 produces the worst case containment seal temperatures. Although the peak ICV containment seal temperature of 360 °F exceeds the steady-state capability for Butyl, the seal temperature returns to below 350 °F within

15 hours. As such, the time duration versus temperature curve is below the tested temperature capability of the Butyl seal material. The peak electrical feed-through connector temperature of 377 °F is nearly 100 °F below its temperature capability. Likewise, all other predicted package temperatures remain within the associated thermal limits.

The maximum helium gas temperatures internal to the OCV and ICV during either the HAC load case Nos. 5 and 6 HAC fire are 852 and 840 °F, respectively.

Because the Carboline® heat-resistant coating has a continuous rating of 750 °F and a non-continuous rating of 1000 °F and because the temperature of some portions of the OCV and ICV is predicted to exceed 1000 °F during portions of each HAC fire event, it is possible that the coating may fail in these areas. The exact nature of any coating failure that may occur is uncertain since those portions of the ICV and OCV that exceed the non-continuous temperature limit for the coating do so for less than 30 minutes (except for HAC load cases 3 and 4 in which the heat source modules are aligned on the ICV sidewall) and the peak temperature seen will be less than 1250 °F. It is possible that, given the brief period involved and the limited temperature excursion above the non-continuous temperature limit, the coating would remain essentially intact. Assuming a complete loss of the coating, however, the surface emittance would revert to that of the underlying stainless steel. Based on the near-white surface blast preparation used for the application of the heat resistant coating, the appropriate surface emittance is set at 0.54.

A review of the results for the six HAC load cases showed that each case resulted in temperatures at the OCV and ICV dished heads that exceed 1000 °F. With the exception of HAC load cases 3 and 4, all other ICV and OCV surfaces that are treated with the Carboline coating remain below 1000 °F. With HAC load cases 3 and 4, the ICV sidewall at thermal model segment 'A' reaches temperatures of 1200 °F during the HAC event and steady-state temperatures of 950+ °F after the fire. The OCV sidewall temperatures at the same location run about 100 °F cooler.

These elevated temperatures occur because these load cases assume that the re-configured heat source modules end up axially aligned on the ICV sidewall. The ICV and OCV sidewall temperatures at locations a short distance from the heat source modules do not exceed the 1000 °F non-continuous temperature limit of the coating and are well below the coating's 750 °F continuous temperature limit by the time the package reaches steady-state after the HAC fire.

The potential effect on the thermal response of the package due to the loss of the Carboline® coatng was investigated using HAC load case 5. The load case was selected for this analysis because it had resulted in the highest ICV/OCV seal temperatures. The re-analysis of HAC load case 5 was conducted under the assumption that the heat-resistant coating fails for any surface that exceed 1000 °F during the fire. Based on the temperatures seen under the original analysis, only the heads of the ICV and OCV are expected to experience a loss of coating due to excessive temperature. The re-analysis shows that the peak temperature at the OCV head would increase by less than 25 °F, while the peak ICV head temperature would be reduced by approximately 90 °F. This occurs because of the reduction in radiative heat transfer between the ICV and OCV heads during the HAC fire event. The coating failure did not increase the peak ICV seal temperatures, but is predicted to increase the steady-state ICV seal temperature following the HAC fire event by 5 °F. No change to the OCV seal temperature is noted.

The loss of coating on both the ICV and OCV domes simultaneously with the loss of coating below the heat source modules (i.e., HAC load cases 3 and 4) was considered but not specifically analyzed. Instead, the results for this scenario would be encompassed by those for HAC load case 5 because both would experience similar temperature variations at the domes, because HAC load cases 3 and 4 yield lower seal temperatures, and because the extent of the loss of coating on the ICV sidewall would be limited to the immediate vicinity of the heat sources. The general effect of a

loss of coating below the heat source modules will be to increase the heat source temperature, causing an increased heat transfer to the rest of the ICV cavity and a slight decrease in the temperature of the ICV wall directly below the heat sources. Metal temperatures would still remain within their allowables, with little to no change in the predicted differential expansion.

3.5.4 Maximum Internal Pressures

Table 3.5.4-1 presents the maximum gas temperatures and pressures within the ICV and OCV for the HAC fire. The gas pressures are estimated using the ideal gas law and the computed temperatures of the various ICV/OCV thermal model nodes. The pressure calculation does not include the contribution to pressure rise from material outgassing. Outgassing was neglected for these calculations because the timing of material outgassing is difficult to determine and because the effect of the outgas constituents on the thermal conductivity of the blanket gas will be negligible. The sources of and contribution to pressure rise by material outgassing within the ICV/OCV are addressed in Section 2.7.3.1.2.

The base pressures and temperatures used in the calculations are set by the steady-state condition for NCT load case No. 7 (see Table 3.4-1). The analysis assumes the worst case initial pressures at the time of RTG loading into the packaging (i.e., 19 psia base pressure + 1 psi tolerance = 20 psia). Estimates of the maximum ICV/OCV internal pressure are provided for the six HAC fire load cases. See Table 3.5.2-1 for a definition of each load case.

TABLE 3.5.4-1. Maximum ICV/OCV Gas Pressures and Temperatures For HAC.

Load case/condition	ICV pressure	ICV gas temp. (°F)	OCV pressure	OCV gas temp. (°F)
Case 1	38.9 psia	836	46.2 psia	849
Case 2	37.2 psia	779	44.3 psia	796
Case 3	36.2 psia	747	46.2 psia	851
Case 4	34.3 psia	684	44.4 psia	798
Case 5	39.0 psia	840	46.3 psia	852
Case 6	37.3 psia	782	44.4 psia	799

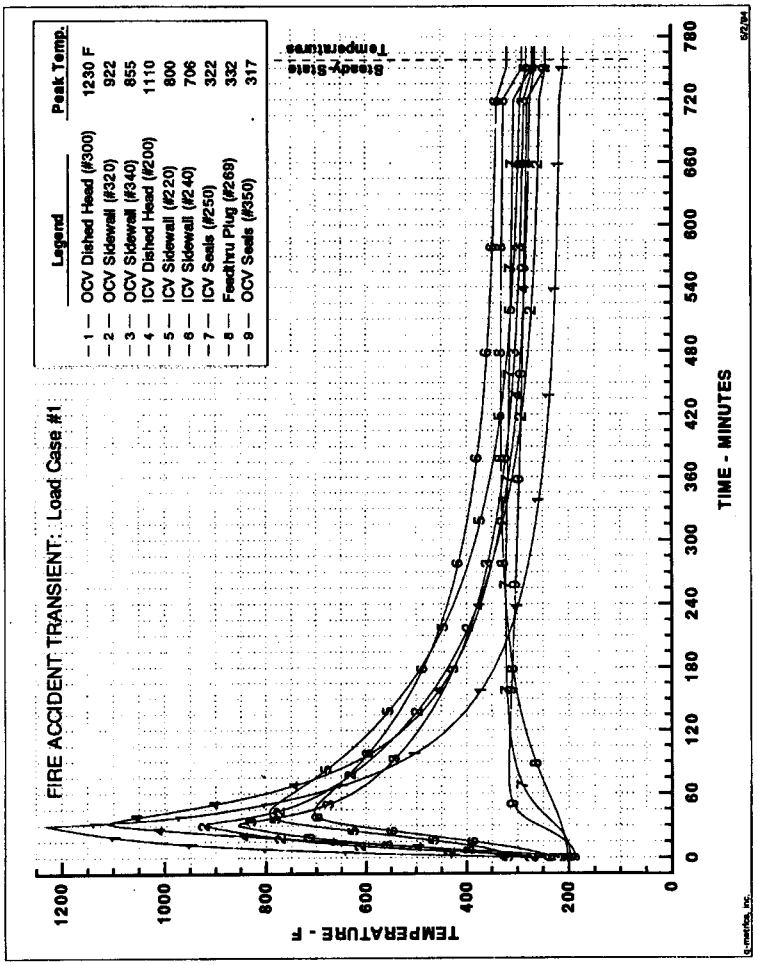


FIGURE 3.5.3-1. HAC Fire Transient For Load Case No. 1.

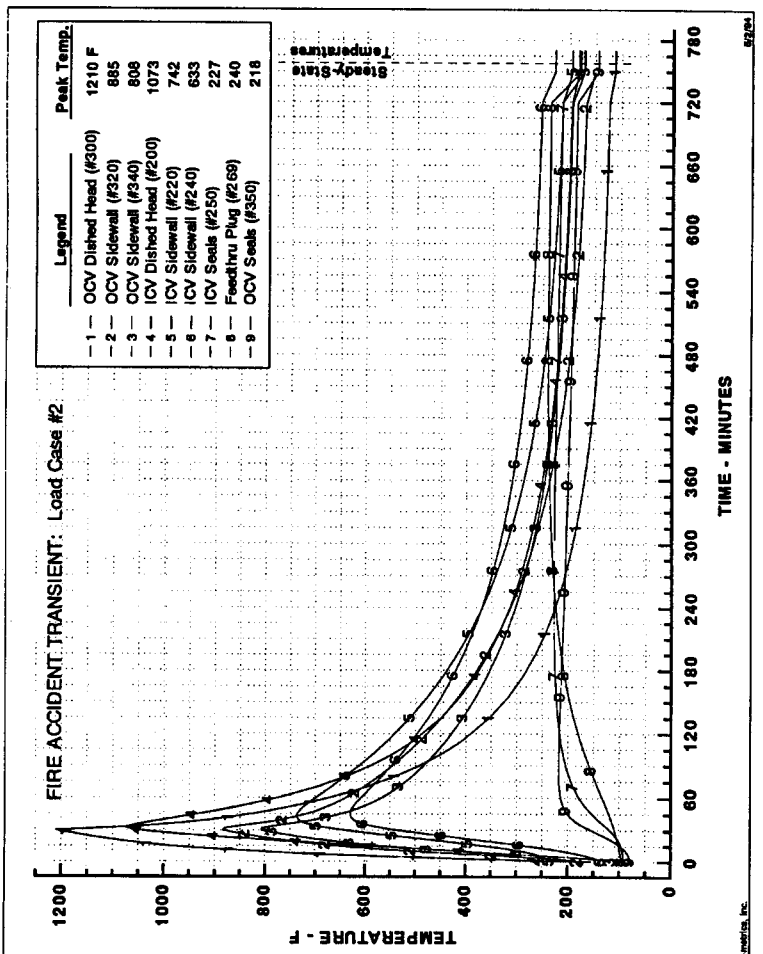


FIGURE 3.5.3-2. HAC Fire Transient For Load Case No. 2.

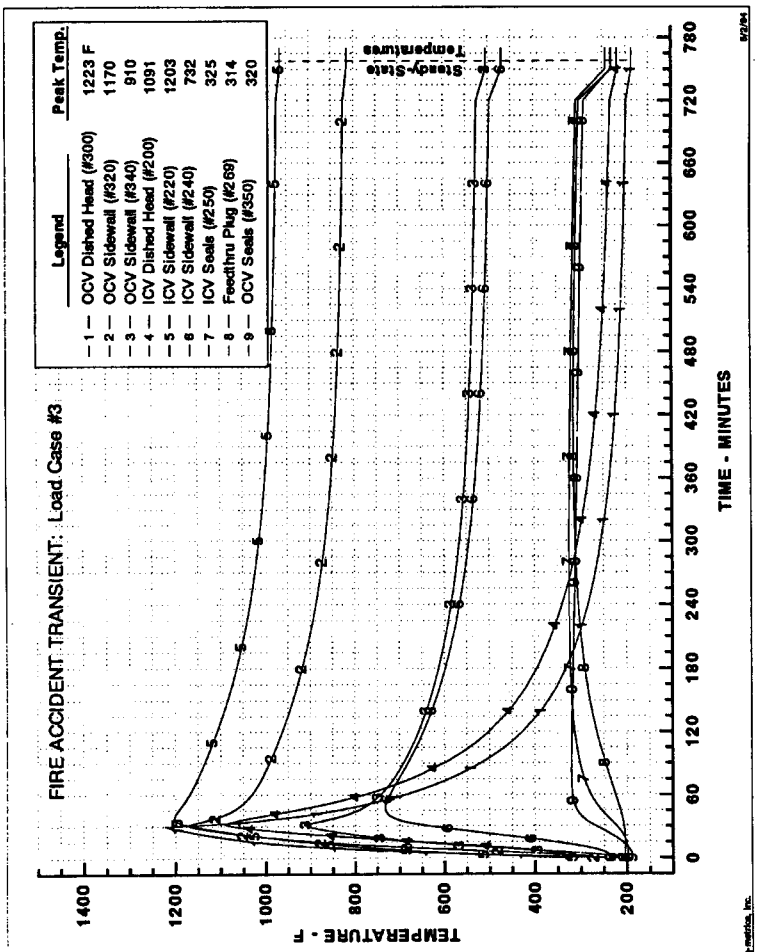


FIGURE 3.5.3-3. HAC Fire Transient For Load Case No. 3.

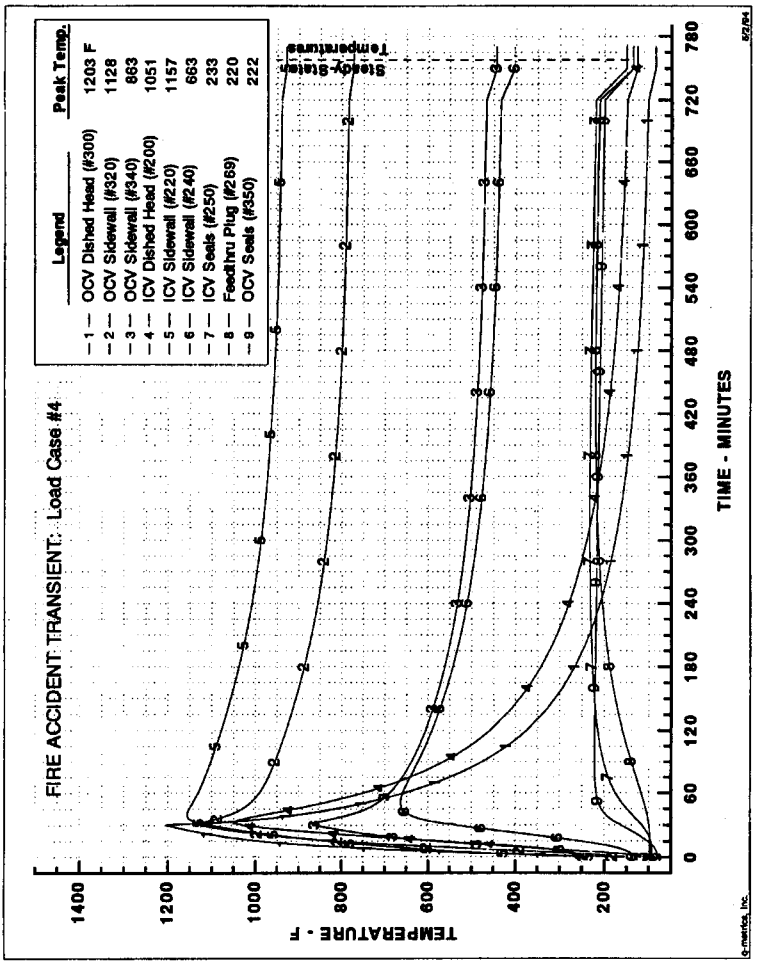


FIGURE 3.5.3-4. HAC Fire Transient For Load Case No. 4.

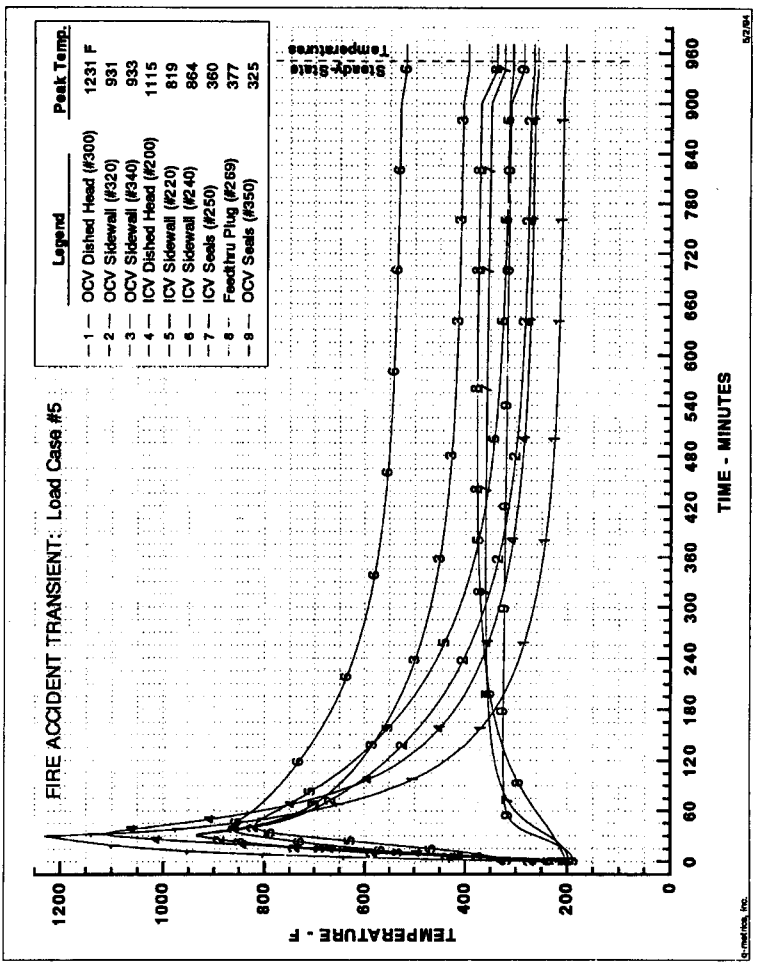


FIGURE 3.5.3-5. HAC Fire Transient For Load Case No. 5.

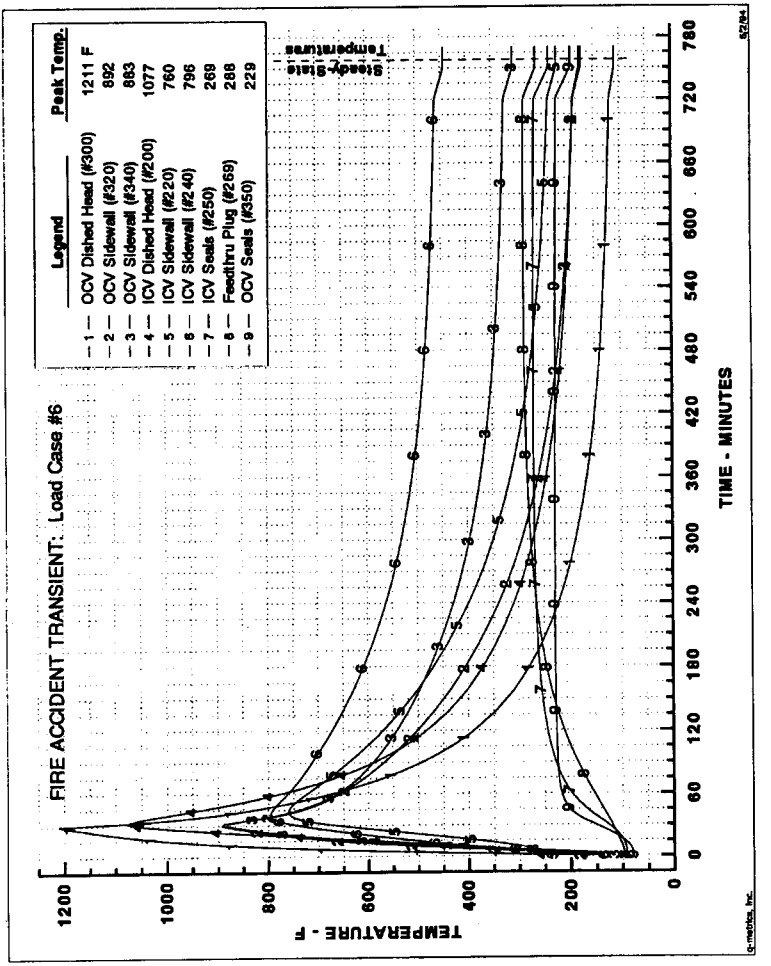


FIGURE 3.5.3-6. HAC Fire Transient For Load Case No. 6.

3.5.5 Maximum Thermal Stresses

The results from finite element analyses of the ICV and OCV are presented in Section 2.7.3.3. The analysis shows that all margins of safety are positive and that the design criteria of Regulatory Guide 7.6 are satisfied.

3.5.6 Evaluation of Package Performance for the Thermal Hypothetical Accident Conditions

Analysis is used to evaluate the thermal performance of the RTG Transportation System Package for the HAC fire event. The analysis is backed up by test data, which validates the basic heat transfer modeling of the package, and conservative assumptions that supposes the worst case combination of parameters. Results of the analysis shows that the package design meets the requirements of 10 CFR 71 regulatory conditions for transport.

The peak containment seal temperatures seen for all six HAC load cases are below the time versus temperature operating curve for the Butyl elastomer O-ring seal material. In fact, the 350 °F steady-state temperature limit for Butyl is exceeded in only one of the six HAC load cases evaluated. The peak seal temperature of 360 °F seen for HAC load case No. 5 is 40 °F below the maximum temperature rating for Butyl, while the transient temperature response is well within the time versus temperature limits of the Butyl.

The electrical feed-through connector remains 100 °F or more below its 475 °F temperature rating for all six HAC load cases. Although the analysis assumes large portions of the impact limiter foam are lost because of outgassing/ablation during the HAC fire, the impact limiter is expected to survive the HAC fire essentially intact.

All other package materials remain within their respective temperature limits.

3.6 APPENDIX

The following is a list of appendices contained within this section:

3.6.1 References
3.6.2 Thermal Modeling Details
3.6.3 Performance of Rigid Polyurethane Foam Under Fire Accident Conditions
3.6.4 SINDA Output for Normal Conditions of Transport
3.6.5 SINDA Output for Hypothetical Accident Conditions
3.6.6 Miscellaneous Calculations
3.6.7 Listing of 2-D Computer Model

3.6.1 References

1. 10 CFR 71, 1993, "Packaging and Transportation of Radioactive Material," *Code of Federal Regulations*, Washington, D.C.

2. *Handbook of Heat Transfer Fundamentals*, 2nd Edition, Rohsenow, Hartnett, & Ganic, McGraw-Hill Publishers.

3. Kreith, F., *Principles of Heat Transfer*, 3rd Edition, Frank Kreith, Harper & Row Publishers.

4. *Metallic Materials and Elements for Aerospace Vehicle Structures*, 1986, Military Handbook, Vol. 1, MIL-HDBK-5E.

5. *Specific Heat-Metallic Elements and Alloys*, TPRC Data Series, Vol. 3, Purdue University.

6. *Thermal Conductivity-Metallic Elements and Alloys*, TPRC Data Series, Vol. 1, Purdue University.

7. *Specific Heat-Nonmetallic Liquids and Gases*, TPRC Data Series, Vol. 6, Purdue University.

8. *Thermal Conductivity-Nonmetallic Liquids and Gases*, TPRC Data Series, Vol. 3, Purdue University.

9. *Viscosity*, TPRC Data Series, Vol. 11, Purdue University.

10. *LAST-A-FOAM FR-3700 for Crash & Fire Protection of Nuclear Material Shipping Containers*, General Plastics Manufacturing Company, P.O. Box 9097, Tacoma, Washington.

11. Khan, J. and Kumar, R., 1989, *Natural Convection In Vertical Annuli: A Numerical Study For Constant Heat Flux On The Inner Wall*, ASME'S Journal of Heat Transfer, pp. 909-915, Washington, D.C.

12. *RTG/DIPS/LWRHU Package Transportation System Thermal Design Development Test*, 1992, Rev. 0; prepared for Westinghouse Hanford Company by Packaging Technology, Inc.

13. *Thermal Qualification Test Plan*, 1992, Rev. 2, Packaging Technology, Inc., Document ED-92-005, Tacoma, Washington.

14. *Thermal Qualification Test Report*, 1994, Rev. 1, Packaging Technology, Inc., Document ED-94-009, Tacoma, Washington.

15. *General Electric Heat Transfer Data Book*, 1961, Section 515.5, Properties of Solids: Emissivity, pp. 515.5-8; listed solar absorptivity values for white paint varies from 0.12 to 0.26; emissivity at 750 °F varies from 0.53 to 0.84; emissivity values at 125 °F varies from 0.90 to 0.95.

16. *Engineering and Operating Guide For DOWFROST Heat Transfer Fluids*, The Dow Chemical Company, Midland, Michigan.

17. SARP, 1987, *Safety Analysis Report for Packaging*, Vol. 1, TES-32130-056, Teledyne Energy Systems, pp. 3-4.

18. *General Electric Heat Transfer Data Book--Section 515.5, Properties of Solids: Emissivity*, 1961.

19. Guyer, E. C., 1989, *Handbook of Applied Thermal Design*, McGraw-Hill Publishers.

20. *Materials Engineering*, Penton Publishing, Inc. Cleveland, Ohio.

21. *GPHS RTG Thermal Model*, 1992, Rev. 2, Packaging Technology, Inc., Document ED-91-001, Bellevue, Washington.

22. *Carboline 4674 Product Brochure*, The Carboline Company, St. Louis, Missouri.

23. Siegel, R., and Howell, J., 1992, *Thermal Radiation Heat Transfer*, Hemisphere Publishing Co., Washington, D.C.

24. *Thermal Radiative Properties-Metallic Elements and Alloys*, TPRC Data Series, Vol. 7, Purdue University.

25. Song, S., Yovanovich, M., and Nho, K., 1992, *Thermal Gap Conductance: Effects of Gas Pressure and Mechanical Load*, AIAA's Journal of Thermophysics and Heat Transfer, January-March pp. 62-68, New York, New York.

26. *Kaowool Blanket Product Literature*, Morgan Thermal Ceramics Company.

27. Brandes, E. A., 1983, *Smithells Metals Reference Book*, 6th Edition, Butterworths Publishing Co., London.

28. *Thermal and Water Vapor Tramsmission Data*, 1993, Table 13, Chapter 22, American "Handbook of Fundamentals," Society of Heating, Refrigerating and Air-Conditioning Engineers, Inc.

29. *Fiberglass Insulation Blanket Product Literature*, McMaster-Carr Company.

30. SINDA '85/FLUINT, 1987, *Systems Improved Numerical Differencing Analyzer and Fluid Integrator*, Version 2.1, Prepared for NASA, Johnson Spacecraft Center, Contract NAS9-17448, Prepared by Martin Marietta Corporation, Denver Aerospace.

31. Emery, A., 1991, VIEW--A Radiation Viewfactor Calculation Program, 1991, Version 5.6.9, NASA Grant NAG-1-41, University of Washington, Seattle, Washington.

32. WHC, 1994, *Radioisotope Thermoelectric Generator Transportation System--Carboline 4674-C900 Paint Emissivity Test Report*, WHC-SD-RTG-TRP-005, Westinghouse Hanford Company, Richland, Washington.

33. Lage, J., Lim, J., and Bejan, A., 1992, *Natural Convection With Radiation in a Cavity With Open Top End*, in "ASME's Journal of Heat Transfer," Vol. 114, pp. 479-486, Washington, D.C.

34. Coordination Sheet R. C. Frank and W. L. Plagemann to S. Goetsch, *Emissivity Testing of Metal Specimens*, testing accomplished by Boeing Analytical Engineering for Nuclear Packaging, Inc.

35. Gubareff, G. G., Janssen, J. E., and Torborg, R. H., 1960, *Thermal Radiation Properties Survey*, Honeywell Research Center, Minneapolis, Minnesota.

3.6.2 Thermal Modeling Details

3.6.2.1 Undamaged Package Thermal Model With Operating Chillers. The undamaged RTG Transportation System Package is modeled using a 2-D, axisymmetric thermal model. The model uses 124 nodes along 15 axial stations to represent components or portions of components for the package. The thermal properties (i.e., specific heat, thermal conductivity, and convective and radiative heat transfer coefficients) are computed as a function of the associated temperatures whenever the variation with temperature is significant.

The thermal capacitance, conductance, and radiation values associated with each node in the package model are presented in Tables 3.6.2.1-1, 3.6.2.1-2, and 3.6.2.1-3, respectively. Each table was created using Microsoft's *EXCEL*® spreadsheet program. As such, the value under the heading Specific Heat Multiplier was automatically calculated based on the data presented in the preceding columns. Where appropriate, these table columns describe the element shape, material, material property, and the pertinent dimensional data used to determine the thermal model values at each node in the thermal model. The terms and equations used in each table are defined in the Nomenclature list in Section 3.6.2.5. Tables 3.6.2.1-4 and 3.6.2.1-5 present the thermal capacitance and conductance calculations for the RTG shipping rack assembly.

The thermal capacitance for each node in the GPHS RTG thermal model is presented in Table 3.6.2.1-6. The location of the nodes is shown in Figure 3.4.1-1. See Reference 21 for a full description of the model.

Because the SINDA thermal analyzer program is a finite-differencing program, the calculated temperatures for each model node actually represents the volumetric mean temperature of the particular component (or portion there of) that the node represents. The reader is advised to study model node layout in Figure 3.4.1-2 and the dimensional data in Table 3.6.2.1-1 to determine the physical location of each node in the model and what portion of the package that it represents.

The following paragraphs describe the assumed heat transfer modes across each boundary of the package. The description is ordered from the outside environment inward.

Heat transfer between the exterior environment and the package outer surface is assumed to occur via convection and radiation. Natural or 'free' convection heat transfer coefficients for the vertical surfaces are calculated as a function of Rayleigh number using the flat plate correlations given in equations 39 to 42 from Chapter 6 of Reference 2. Natural convection correlations for horizontal surfaces are obtained from equations 21, 22, and 23 from Chapter 7 of Reference 3. The calculated free convection coefficient for the OCV bolt tubes and the bolt heads contained within were reduced to account for the fact that the recessed nature of these surfaces and the narrow width of the tubes will restrict the convective heat transfer coefficient below that obtained for a "free" surface. As such, the computed "free" convection coefficient for node 349 was reduced by 50%, while those for nodes 351 and 371 were reduced to 25% of the values computed for a "free" surface.

These correction factors were selected to provide a conservative estimate of the peak closure bolt and access tube temperatures. The actual reduction factors will vary from about 20% when the ambient air temperature is below that of the closure bolts or access tubes (i.e., NCT or following the HAC fire event) to almost 100% when the ambient temperature is above that of the bolts or access tubes (i.e., during the HAC fire event). The 20% reduction factor is based on the work presented in Reference 33 for natural convection in a cavity with an open top end as

---

®*Excel* is a registered trademark of the Microsoft Corporation.

The 100% reduction factor is based on the fact that with "still" air, as specified by 10 CFR 71, there will be no driving force to transport the warm air above the tubes down and into the relatively cold access tube cavities.

Forced convection coefficients for the coolant flow within the OCV coolant jacket are computed using a combination of correlations taken from Table 4.7 of Reference 19 and equations 7, 43 to 44, and 57 from Chapter 7 of Reference 2. The actual equation used depends on the computed Reynold's number for the flow. The hydraulic diameter of the coolant passages is 1.33 in. Coolant flow within each coolant loop is assumed to be 4.5 g/m. Although the chiller system could provide lower coolant temperatures, a 40 °F coolant inlet temperature is used as the lowest available temperature for design purposes because it provides adequate temperature margin for the GPHS RTG, and it will avoid potential problems with frost buildup on the coolant jacket. Condensate, should it form, is collected, drained away, and retained in a storage tank in the transportation trailer. Although condensation will increase the load on the chiller, it will have a negligible effect on package temperatures assuming the chiller is sufficiently sized to handle the added load that condensation will place on it.

TABLE 3.6.2.1-1 THERMAL CAPACITANCE VALUES FOR RTG TRANSPORT THERMAL MODEL

NODE	ELEMENT	MEDIUM	DENSITY	GEOMETRIC DATA X1	X2	X3	SPEC. HEAT MULTIPLIER	REMARKS
200	CYLINDER	S.Stl 304L	0.29	0	13	0.375	71.06255	ICV Torispherical Head + 13.324# For Plug
204a	CYLINDER	S.Stl 304L	0.29	13	17.5625	0.375	47.83991	ICV Torispherical Head; Outer Portion
204b	CYLINDER	S.Stl 304L	0.29	17.1875	17.5625	2.563	30.42864	ICV Torispherical Head; Vertical Portion
210/220/230	CYLINDER	S.Stl 304L	0.29	17	17.75	13.72	325.77523	ICV Shell
238	SPECIAL		0	0			0.00000	Arithmetic Node 2.75 Inches Above Rubble Dam
240	CYLINDER	S.Stl 304L	0.29	17	17.75	5	118.72275	ICV Shell
242	CYLINDER	S.Stl 304L	0.29	17	17.75	5.25	124.65889	ICV Shell & Portion of Flange Above Base Plate
250	CYLINDER	S.Stl 304L	0.29	17	19.375	1.6293	143.97909	ICV Flange; Equivalent Thickness Used
261	CYLINDER	S.Stl 304L	0.29	0	10	1.72	156.70264	ICV Base Plate; Inner Portion
263	CYLINDER	S.Stl 304L	0.29	10	15	1.72	195.87830	ICV Base Plate
265	CYLINDER	S.Stl 304L	0.29	15	16.97	1.72	98.69273	ICV Base Plate @ Seals
260	CYLINDER	S.Stl 304L	0.29	0	10	1.75	159.43583	ICV Base Plate; Inner Portion
262	CYLINDER	S.Stl 304L	0.29	10	15	1.75	199.29478	ICV Base Plate
264	CYLINDER	S.Stl 304L	0.29	15	16.97	1.75	100.41412	ICV Base Plate @ Seals
266	CYLINDER	S.Stl 304L	0.29	16.97	19.48	1.47	122.52831	ICV Base Plate @ Bolt Flange
287	CYLINDER	S.Stl 304L	0.29	1.275	1.875	3.12	5.37235	Feed Thru Housing
288	CYLINDER	S.Stl 304L	0.29	1.072	1.28	2.688	1.07365	Feed Thru Plug Sleeve
289	SPECIAL	O'Brien Plug	0.5	1			0.50000	Feed Thru Plug
1286	SPECIAL	S.Stl 304L	0	1.94	2.045	3.9	0.00000	Arithmetic Node At Inside of Feedthru Insulation
1287	SPECIAL	S.Stl 304L	0	3.05	3.155	3.9	0.00000	Arithmetic Node At Outside of Feedthru Insulation
1288	SPECIAL	S.Stl 304L	0	0	3.155	0	0.00000	Arith. Node At Underside of Barrier Plate Insulation
1289	SPECIAL	Helium	0	0	1.072	3.25	0.00000	Arithmetic Gas Node Within Feedthru Cavity
300	CYLINDER	S.Stl 304L	0.29	0	13	0.5	99.26473	OCV Torispherical Head + 22.28# For Strapping
301	SPECIAL	S.Stl 304	0.29				29.20000	40% Mesh Personnel Barrier; Calculated Value
304a	CYLINDER	S.Stl 304L	0.29	13	17.94	0.5	89.54499	OCV Torispherical Head + 19.92# For Strapping
304b	CYLINDER	S.Stl 304L	0.29	17.94	18.44	2.441	40.45278	OCV Torispherical Head; Vertical Portion
305	PARALLEL	S.Stl 304L	0.29	8.25	8.2324	8	118.17610	24 Fins; Equivalent Height & Thickness Used
310/320/330	CYLINDER	S.Stl 304L	0.29	17.94	18.44	13.72	227.37080	OCV Shell
340	CYLINDER	S.Stl 304L	0.29	17.94	18.44	5	82.86108	OCV Shell
341	SPECIAL		0	0			0.00000	Arithmetic Node At Joint w/ Thermal Shield
342	CYLINDER	S.Stl 304L	0.29	17.94	18.44	4.25	70.43192	OCV Shell
343	CYLINDER	Fiberglass Insul.	0.00139	19	26.25	2.5	3.10147	Minus 0.48 Lbs For Bolt Access Tube Cutouts
344	PARALLEL	S.Stl 304L	0.29	1.7	1.2	119.38	70.82521	OCV Flange Angled Section
345	CYLINDER	S.Stl 304L	0.29	26.25	26.625	2.625	47.41970	OCV Seal Thermal Shield

See Nomenclature List For Definition Of Terms & Equations Used In This Table Subtotal Wt. = 3886.900574 FILE: PTSFILTM.007; p1/3 04/28/94

TABLE 3.6.2.1-1 THERMAL CAPACITANCE VALUES FOR RTG TRANSPORT THERMAL MODEL (Continued)

NODE	ELEMENT	MEDIUM	DENSITY	GEOMETRIC DATA X1	X2	X3	SPEC. HEAT MULTIPLIER	REMARKS
346	CYLINDER	S.Stl 304L	0.29	18.44	26.625	0.375	126.01934	OCV Seal Thermal Shield
347	CYLINDER	S.Stl 304L	0.29	23.75	26.25	0.25	28.47068	OCV Seal Thermal Shield
349a	CYLINDER	S.Stl 304L	0.29	1.13	1.25	78	20.29554	24 Access Tubes, Base Plate; Equiv. Length
349b	CYLINDER	S.Stl 304L	0.29	0.75	0.88	26	4.66172	8 Access Tubes, Impact Limiter; Equiv. Length
350	CYLINDER	S.Stl 304L	0.29	19.56	22.125	1.13	110.07622	OCV Flange Seals
352	CYLINDER	S.Stl 304L	0.29	22.125	24.125	1.13	95.22874	OCV Flange
354	CYLINDER	S.Stl 304L	0.29	19.56	22.125	1.69	164.62726	OCV Flange
356	CYLINDER	S.Stl 304L	0.29	22.125	24.125	1.69	142.42175	OCV Flange
351	SPECIAL	ASTM A320	0.29	3			20.88000	OCV Cap Head Screws (24 Total); Head Portion
353	CYLINDER	ASTM A320	0.29	0	0.625	2.69	22.97584	OCV Cap Head Screws (24 Total)
355	CYLINDER	ASTM A320	0.29	0	0.625	3.31	28.27139	OCV Cap Head Screws (24 Total); Thread End
357	SPECIAL		0	0			0.00000	Arithmetic Node Between Nodes 354 & 356
358	SPECIAL		0	0			0.00000	Arithmetic Node At Base Of OCV Bolt Heads
359	SPECIAL		0	0			0.00000	Arithmetic Node Between Nodes 350 & 352
360	CYLINDER	S.Stl 304L	0.29	0	10	1.5	136.65928	OCV Base Plate; Inner Portion
362	CYLINDER	S.Stl 304L	0.29	10	15	1.5	170.82410	OCV Base Plate
364	CYLINDER	S.Stl 304L	0.29	15	19.545	1.5	214.56467	OCV Base Plate; Below ICV Seals
366	CYLINDER	S.Stl 304L	0.29	19.545	22.125	3.5	342.81445	OCV Base Plate; Portion @ Seals
367	CYLINDER	S.Stl 304L	0.29	22.125	24.15	3.5	298.90466	OCV Base Plate; Portion @ Seals
368	CYLINDER	S.Stl 304L	0.29	24.15	26.625	3.5	400.72003	OCV Base Plate; Edge
369	CYLINDER	S.Stl 304L	0.29	24.15	26.625	2.43	278.21419	OCV Base Plate; Edge
371	SPECIAL	ASTM A320	0.29	0.75			1.74000	OCV Cap Head Screws (8 Total); Head Portion
373	CYLINDER	ASTM A320	0.29	0	0.28	2.82	1.61140	OCV Cap Head Screws (8 Total); Shank Portion
375	CYLINDER	ASTM A320	0.29	0	0.28	3.5	1.99996	OCV Cap Head Screws (8 Total); Shank Portion
377	CYLINDER	ASTM A320	0.29	0	0.35	1.37	1.22319	OCV Cap Head Screws (8 Total); Thread End
379	SPECIAL		0	0			0.00000	Arithmetic Node At I.D. Of OCV Base Bolt Holes
311/321	CYLINDER	Water/Glycol	0.03611	18.44	19.44	6.1	26.21303	Coolant Fluid In 1x2" Spiral Wrapped Channels
312/322	CYLINDER	Water/Glycol	0.03611	18.44	19.44	6.1	26.21303	Coolant Fluid In 1x2" Spiral Wrapped Channels
313/323	CYLINDER	S.Stl 304L	0.29	18.44	19.7	1.52	66.54918	Bar SST; 1/4"x1.26"
315/325	CYLINDER	S.Stl 304L	0.29	19.44	19.575	6.1	29.27137	Cover Shell Over Primary Channel
316/326	CYLINDER	S.Stl 304L	0.29	19.44	19.575	6.1	29.27137	Cover Shell Over Secondary Channel

See Nomenclature List For Definition Of Terms & Equations Used In This Table — Subtotal Wt. = 8855.040946 — FILE: PTSFILTM.007; p2/3 — 04/28/94

TABLE 3.6.2.1-1 THERMAL CAPACITANCE VALUES FOR RTG TRANSPORT THERMAL MODEL (Concluded)

NODE	ELEMENT	MEDIUM	DENSITY	GEOMETRIC DATA X1	X2	X3	SPEC. HEAT MULTIPLIER	REMARKS
331/332	CYLINDER	Water/Glycol	0.03611	18.44	19.44	8.78	37.72957	Coolant Fluid In 1x2" Spiral Wrapped Channels
333	CYLINDER	S.Std 304L	0.29	18.44	19.7	2.2	96.32118	Bar SST: 1/4"x1.26"
335/336	CYLINDER	S.Std 304L	0.29	19.44	19.575	8.78	42.13158	Cover Shell Over Primary & Secondary Channel
337	SPECIAL		0	0			0.00000	Arithmetic Node Between Nodes 341 & 346
1013/1023	SPECIAL		0	0			0.00000	Arithmetic Node At End Of Nodes 313 & 323
1033	SPECIAL		0	0			0.00000	Arithmetic Node At End Of Node 333
1011/1012	SPECIAL		0	0			0.00000	Arithmetic Node At Surface Of Node 310
1021/1022	SPECIAL		0	0			0.00000	Arithmetic Node At Surface Of Node 320
1031/1032	SPECIAL		0	0			0.00000	Arithmetic Node At Surface Of Node 330
1041/1042	SPECIAL		0	0			0.00000	Arithmetic Node At Surface Of Node 340
1043/1044	SPECIAL		0	0			0.00000	Arithmetic Node At Surface Of Node 342
1346	SPECIAL		0	0			0.00000	Arithmetic Node At Junction Between 346 & 345
400	CYLINDER	S.Std 304	0.29	0	20.5	0.375	143.57766	Impact Limiter Base Plate
401	CYLINDER	S.Std 304	0.29	0	20.5	0.0598	22.89585	Internal Thermal Shield - Impact Limiter
402	CYLINDER	S.Std 304	0.29	20.5	26.875	0.375	284.80309	Base Plate + 181.42 Lbs For Bolting Ring
407	SPECIAL		0	0			0.00000	Arithmetic Node At Impact Limiter Bolt Ring
404	CYLINDER	S.Std 304	0.29	26.875	27.125	8.88	142.60810	Impact Limiter Shell + 33.39 Lbs For Angle Iron
406	CYLINDER	S.Std 304	0.29	27.125	34.75	0.25	147.30904	Impact Limiter Shell + 39.85 Lbs For Angle Iron
408	CYLINDER	S.Std 304	0.29	34.75	35	17.5	300.35622	Impact Limiter Shell + 22.34 Lbs For Angle Iron
410	CYLINDER	S.Std 304	0.29	26.875	34.75	0.3125	138.16734	Impact Limiter Shell
412	CYLINDER	S.Std 304	0.29	20.5	26.875	0.3125	85.98591	Impact Limiter Shell
414	CYLINDER	S.Std 304	0.29	0	20.5	0.3125	119.64805	Impact Limiter Shell
421/422/423	CYLINDER	3# Foam	0.00173611	0	20.5	2.77	6.34914	3# Impact Limiter Foam (Solid Block)
424/425/426	CYLINDER	12# Foam	0.00694444	20.5	27.125	2.77	19.06724	12# Impact Limiter Foam
431 to 433	CYLINDER	12# Foam	0.00694444	27.125	29.75	3.04	9.90174	12# Impact Limiter Foam
434 to 436	CYLINDER	12# Foam	0.00694444	27.125	29.75	2.77	9.02231	12# Impact Limiter Foam
441 to 443	CYLINDER	12# Foam	0.00694444	29.75	32.25	3.04	10.27998	12# Impact Limiter Foam
444 to 446	CYLINDER	12# Foam	0.00694444	29.75	32.25	2.77	9.36896	12# Impact Limiter Foam
451 to 453	CYLINDER	12# Foam	0.00694444	32.25	34.75	3.04	11.10901	12# Impact Limiter Foam
454 to 456	CYLINDER	12# Foam	0.00694444	32.25	34.75	2.77	10.12236	12# Impact Limiter Foam
Misc. Components Not Specifically Modelled							25.10000	Mass Value Used Only For Weight Balance Only

See Nomenclature List For Definition Of Terms & Equations Used In This Table — Total Wt. = 6776.991864 — FILE: PTSRLTM.007; p3/3 — 04/26/94

TABLE 3.6.2.1-2 THERMAL CONDUCTANCE VALUES FOR RTG TRANSPORT THERMAL MODEL

NODE 1	NODE 2	ELEMENT	MEDIUM	GEOMETRIC DATA X1	X2	X3	CONDUCTOR MULTIPLIER	REMARKS
200	204	CYLINDER	S. Stl 304L	9.2	16.2	0.375	0.028919	
204	Pt. A	CYLINDER	S. Stl 304L	16.2	17.375	0.375	0.233679	
Pt. A	Pt. B	CIRCLE	S. Stl 304L	17.1875	17.5625	2.563	0.110924	Conductance 204 to 210 = K-SStl/[1/0.233679 +
Pt. B	210	CIRCLE	S. Stl 304L	17	17.75	6.86	0.082886	1/0.110924 + 1/0.082886] = 0.039433xK-SStl
210	220	CIRCLE	S. Stl 304L	17	17.75	13.72	0.041443	
220	230	CIRCLE	S. Stl 304L	17	17.75	13.72	0.041443	
230	238	CIRCLE	S. Stl 304L	17	17.75	4.11	0.138344	
238	240	CIRCLE	S. Stl 304L	17	17.75	5.25	0.108304	
240	242	CIRCLE	S. Stl 304L	17	17.75	5.125	0.110945	
242	Pt. C	CIRCLE	S. Stl 304L	17	17.75	2.625	0.216606	Conductance 242 To 250 = K-SStl/[1/0.216606
Pt. C	250	CIRCLE	S. Stl 304L	17	17.8125	0.915	0.674411	+ 1/0.674411] = 0.163950 x K-SStl
261	263	CYLINDER	S. Stl 304L	7	12.75	1.72	0.125161	
263	265	CYLINDER	S. Stl 304L	12.75	16	1.72	0.330529	
260	262	CYLINDER	S. Stl 304L	7	12.75	1.75	0.127344	
262	264	CYLINDER	S. Stl 304L	12.75	16	1.75	0.336284	
264	266	CYLINDER	S. Stl 304L	16	16.25	1.47	0.487480	
261	260	CIRCLE	S. Stl 304L	0	10	1.735	1.257442	
263	262	CIRCLE	S. Stl 304L	10	15	1.735	1.571802	
265	264	CIRCLE	S. Stl 304L	15	16.97	1.735	0.791948	
267	263	CIRCLE	S. Stl 304L	1.275	1.875	1.99	0.020720	
267	*	CIRCLE	S. Stl 304L	1.275	1.875	1.31	0.031476	Conductance 267 To 268 = K-SStl/[1/0.031476
*	*	CYLINDER	S. Stl 304L	1.166	1.575	0.1875	0.027209	+ 1/0.027209 + 1/0.007117]
*	268	CIRCLE	S. Stl 304L	1.072	1.26	1.344	0.007117	= 0.004784 x K-SStl
267	268	CYLINDER	Helium	1.26	1.275	2.688	9.810562	
268	*	CIRCLE	S. Stl 304L	1.072	1.26	1.344	0.007117	Conductance 268 To 269 = K-SStl/[1/0.007117
*	269	CYLINDER	S. Stl 304L	0.75	1.072	0.25	0.030538	+ 1/1.030538] = 0.005772 x K-SStl
263	269	CYLINDER	Helium	0.8	1.01	0.965	0.180640	
265	250	CYLINDER	SStl 304L	16	16.25	1.72	0.570385	This Conductor To Be In Series w/ Next One
265	250	CYLINDER	Helium Gap	16.97	17	1.72	42.490320	
264	250	CYLINDER	SStl 304L	16	16.25	0.28	0.092853	This Conductor To Be In Series w/ Next One
264	250	CYLINDER	Helium Gap	16.97	17	0.28	8.917029	
266	250	CIRCLE	S. Stl 304L	17	19.375	1.65	1.142273	This Conductor In Series w/ Next Two
266	250	SPECIAL	Contact	311			311.000000	113 Sq-in x 2.75 Btu/Hr-F-Sq.-In (two O-rings)
266	250	CIRCLE	Helium Gap	16.625	19.255	0.03	17.354681	

See Nomenclature List For Definition Of The Terms & Equations Used In These Calculations

FILE: PTSFILTC.007; p1/8 04/28/94

TABLE 3.6.2.1-2 THERMAL CONDUCTANCE VALUES FOR RTG TRANSPORT THERMAL MODEL (Continued)

NODE 1	NODE 2	ELEMENT	MEDIUM	GEOMETRIC DATA X1	X2	X3	CONDUCTOR MULTIPLIER	REMARKS
300	304	CYLINDER	S. Stl 304L	9.2	16.6	0.5	0.036965	
304	*	CYLINDER	S. Stl 304L	16.6	16.19	0.5	0.238513	Conductance 304 To 310 = K-SStl/[1/0.238513
*	310	CIRCLE	S. Stl 304L	17.94	18.44	9.301	0.042667	+ 1/0.042667] = 0.036193 x K-SStl
304	*	RECTANGLE	S. Stl 304L	0.5	5.44	1	0.906667	Multiplied by 48 For 24 Fins & 2 Paths/Fin
*	305	RECTANGLE	S. Stl 304L	9	6	2	0.125000	Twenty-four 0.25-Inch Thick Fins
310	320	CIRCLE	S. Stl 304L	17.94	18.44	13.72	0.028925	
320	330	CIRCLE	S. Stl 304L	17.94	18.44	13.72	0.028925	
330	340	CIRCLE	S. Stl 304L	17.94	18.44	9.36	0.042398	
340	341	CIRCLE	S. Stl 304L	17.94	18.44	4	0.099211	
341	337	CYLINDER	S. Stl 304L	18.19	18.94	0.375	0.404970	
337	346	CYLINDER	S. Stl 304L	18.94	22.9	0.375	0.066181	
341	342	CIRCLE	S. Stl 304L	17.94	18.44	0.625	0.624951	
342	*	CIRCLE	S. Stl 304L	17.94	18.44	1.5	0.264563	This Conductor To Be In Series W/ Next
*	344	CYLINDER	S. Stl 304L	18.19	19.04	1.7	1.624183	
344	354	CYLINDER	S. Stl 304L	19.04	20.88	1.69	0.799354	
354	356	CYLINDER	S. Stl 304L	20.88	23.15	1.69	0.428709	Multiplied by 80% for bolt hole allowance
350	352	CYLINDER	S. Stl 304L	20.88	23.15	1.13	0.286652	Multiplied by 80% for bolt hole allowance
354	350	CIRCLE	S. Stl 304L	19.56	22.125	1.41	1.654381	
356	352	CIRCLE	S. Stl 304L	22.125	24.125	1.41	1.431232	
346	1346	CYLINDER	S. Stl 304L	22.9	26.4375	0.375	0.113908	Conductance 346 To 345 = K-SStl/[1/0.113908
1346	345	CIRCLE	S. Stl 304L	26.25	26.625	1.5	0.288388	+ 1/0.288388] = 0.081856 x K-SStl
345	*	CIRCLE	S. Stl 304L	26.25	26.625	1.1875	0.364280	This Conductor To Be In Series W/ Next
*	347	CYLINDER	S. Stl 304L	25	26.4375	0.25	0.196113	
347	*	CYLINDER	S. Stl 304L	23.94	25	0.25	0.251778	This Conductor To Be In Series W/ Next
*	358	CIRCLE	S. Stl 304L	23.75	24.125	0.5	0.783353	
346	*	RECTANGLE	S. Stl 304L	8.125	0.375	0.9	0.023510	Conductance 346-349 = 32*K-S.Stl/[1/0.023510
*	349	CIRCLE	S. Stl 304L	1.125	1.25	1.1875	0.005454	* 2 paths) + 1/0.005454)] = 0.156388xK-S.Stl
349	358	CIRCLE	S. Stl 304L	1.125	1.25	1.625	0.127543	Multiplied By 32 Tubes For Conservative Total
351	358	SPECIAL	Contact	96.6			96.600000	1.15 Sq-In x 3.5 Btu/Hr-F-Sq-In x 24 Bolts
358	357	CIRCLE	S. Stl 304L	0.7075	1.5	0.845	1.445375	Multiplied By 32 Tubes For Total
351	353	CIRCLE	Carbon Steel	0	0.625	1.75	0.116211	Multiplied by 24 bolts for total
353	355	CIRCLE	Carbon Steel	0	0.5477	3	0.052366	Multiplied by 24 bolts; reduced for threads

See Nomenclature List For Definition Of The Terms & Equations Used In These Calculations

RLE: PTSRLTC.007; p2/8 04/28/94

TABLE 3.6.2.1-2 THERMAL CONDUCTANCE VALUES FOR RTG TRANSPORT THERMAL MODEL (Continued)

NODE 1	NODE 2	ELEMENT	MEDIUM	GEOMETRIC DATA X1	X2	X3	CONDUCTOR MULTIPLIER	REMARKS
353	*	CYLINDER	Air	0.625	0.7075	1.43	12.077918	This conductor to be in series w/ next. Each
*	357	CYLINDER	S. Std 304L	0.45	0.88	1.43	2.232816	are multiplied by 24 bolts for total conductance.
353	*	CYLINDER	Air	0.625	0.7075	1.13	9.544089	This conductor to be in series w/ next. Each
*	359	CYLINDER	S. Stl 304L	0.45	0.88	1.13	1.764393	are multiplied by 24 bolts for total conductance.
357	354/356	CYLINDER	S. Std 304L	0.88	1.25	1.56	2.327258	Multiplied by 12 for 24 bolts & 1/2 each way
359	350/352	CYLINDER	S. Std 304L	0.88	1.25	1.13	1.685771	Multiplied by 12 for 24 bolts & 1/2 each way
355	379	SPECIAL	Keensert	14.11		1.57	338.640000	Multiplied by 24 for 24 bolts
355	*	CYLINDER	Air	0.625	0.69	1.87	19.792404	This conductor to be in series w/ next. Each
*	379	CYLINDER	S. Std 304L	0.45	0.88	1.87	2.919837	are multiplied by 24 bolts for total conductance.
379	366/367	CYLINDER	S. Std 304L	0.88	1.25	3.5	5.221414	Multiplied by 12 for 24 bolts & 1/2 each way
371	368	SPECIAL	Contact	12.9			12.900000	0.46 Sq-in x 3.5 Btu/Hr-F-Sq-in x 8 Bolts
371	373	CIRCLE	Carbon Steel	0	0.275	1.72	0.007674	Multiplied by 8 bolts for total
373	375	CIRCLE	Carbon Steel	0	0.275	3.095	0.004265	Multiplied by 8 bolts for total
375	377	CIRCLE	Carbon Steel	0	0.275	2.5	0.006280	Multiplied by 8 bolts for total
373	*	CYLINDER	Air	0.275	0.405	1.52	1.370597	This conductor to be in series w/ next. Each
*	367	CYLINDER	S. Std 304L	0.2	0.88	1.52	0.358112	are multiplied by 8 bolts for total conductance.
373	*	CYLINDER	Air	0.275	0.405	1.13	1.018931	This conductor to be in series w/ next. Each
*	359	CYLINDER	S. Std 304L	0.2	0.88	1.13	0.266228	are multiplied by 8 bolts for total conductance.
375	*	CYLINDER	Air	0.275	0.602	3.5	1.559351	This conductor to be in series w/ next. Each
*	379	CYLINDER	S. Std 304L	0.2	0.88	3.5	0.824600	are multiplied by 8 bolts for total conductance.
377	403	SPECIAL	Threaded Joint	3.1		1.5	24.800000	Multiplied by 8 bolts for total
360	362	CYLINDER	S. Stl 304L	7	12.75	1.5	0.109152	
362	364	CYLINDER	S. Stl 304L	12.75	17.4	1.5	0.210491	
364	366	CYLINDER	S. Stl 304L	17.4	20.9	1.5	0.357105	
366	367	CYLINDER	S. Stl 304L	20.9	23.16	3.5	0.892404	Multiplied By 80% For Bolt Hole Allowance
367	368	CYLINDER	S. Stl 304L	23.16	25.4	3.5	1.854161	
368	369	CIRCLE	S. Stl 304L	24.15	26.625	2.95	0.929374	
366	*	CIRCLE	S. Stl 304L	19.545	22.125	2.315	1.013184	This Conductor To Be In Series w/ Next
*	350	SPECIAL	Contact	670.5			670.50	243.8 Sq-in x 2.75 Btu/Hr-F-Sq.-in (less O-rings)
367	*	CIRCLE	S. Stl 304L	22.125	24.12	2.25	0.894586	This Conductor To Be In Series w/ Next
*	352	SPECIAL	Contact	579.7			579.70	289.8 Sq-in x 2.0 Btu/Hr-F-Sq.-in

See Nomenclature List For Definition Of The Terms & Equations Used In These Calculations

FILE: PTSFILTC.007; p3/8 04/28/94

TABLE 3.6.2.1-2 THERMAL CONDUCTANCE VALUES FOR RTG TRANSPORT THERMAL MODEL (Continued)

NODE 1	NODE 2	ELEMENT	MEDIUM	GEOMETRIC DATA X1	X2	X3	CONDUCTOR MULTIPLIER	REMARKS
356	*	CYLINDER	S. Std 304L	23.15	25.42	1.3	0.606396	This Conductor To Be In Series w/ Next
*	369	CYLINDER	Air	24.125	24.15	1.3	54.766245	
352	*	CYLINDER	S. Std 304L	23.15	25.42	1.13	0.527098	This Conductor To Be In Series w/ Next
*	369	CYLINDER	Air	24.125	24.15	1.13	47.604506	
311/312	1011/1012	CONVECTIVE	Water/Glycol	2	353.4	1.3333	4.906333	Hydraulic Diameter = 1.3333 Inches
1011/1012	*	CYLINDER	S. Std 304L	18.19	18.44	6.1	19.498777	This Conductor To Be In Series W/ Next
*	310	CIRCLE	S. Std 304L	17.94	18.44	0.5625	4.303555	3.05 ohennels/loop x 2 paths per ohennel
313	*	CYLINDER	S. Std 304L	18.19	18.94	1.52	1.641480	This Conductor To Be In Series W/ Next
*	310	CIRCLE	S. Std 304L	17.94	18.44	0.5625	8.607111	Multiplied By 12.2 For 6.1 Bars & 2 Paths/ Bar
	Repeat The Above 5 Conductors For Stations 320 And 330; Multiply By 0.364 For Station 340 & 0.076 For Station 342							
1013	315/316	CIRCLE	S. Std 304L	19.44	19.575	0.5625	1.246121	Multiplied By 6.1 For 6.1 Bars & 1 Path Per Bar
313	1013	CYLINDER	S. Std 304L	18.94	19.6375	1.52	1.833891	
311/312	315/316	CONVECTIVE	Water/Glycol	2	372.5	1.3333	5.173611	Hydraulic Diameter = 1.3333 Inches
311/312	313	CONVECTIVE	Water/Glycol	1	725.9	1.3333	5.040972	Hydraulic Diameter = 1.3333 Inches
	Repeat The Above 4 Conductors For Stations 320; Multiply By 1.44 For Station 330							
332	337	CONVECTIVE	Water/Glycol	1	119	1.3333	0.826389	Hydraulic Diameter = 1.3333 Inches
901/902	331/332	SPECIAL	Water/Glycol	40	5 GPM	0.80 fps	40	One-way; Multiply By Density x Cp For Coolant
331/332	321/322	SPECIAL	Water/Glycol	40	5 GPM	0.80 fps	40	One-way; Multiply By Density x Cp For Coolant
321/322	311/312	SPECIAL	Water/Glycol	40	5 GPM	0.80 fps	40	One-way; Multiply By Density x Cp For Coolant
342	343	CYLINDER	Fiberglass Insul.	18.44	22.9	2.625	0.526780	
343	346	CIRCLE	Fiberglass Insul.	18.44	26.245	1.3125	5.797259	
343	345	CYLINDER	Fiberglass Insul.	22.9	26.245	2.375	0.760065	
343	354	CIRCLE	Fiberglass Insul.	19.56	22.125	1.3125	1.777278	
343	356	CIRCLE	Fiberglass Insul.	22.125	24.125	1.3125	1.537552	
343	349	CYLINDER	Fiberglass Insul.	1.25	2	2.625	7.798219	Multiplied By 32 Tubes For Total
369	*	CIRCLE	S. Std 304L	24.15	26.625	1.2	2.284711	This Conductor To Be In Series w/ Next
*	1347	CIRCLE	Air	24.3	26.5	0.25	9.752900	
356	*	CYLINDER	S. Std 304L	23.15	24.125	1.69	1.787473	This Conductor To Be In Series w/ Next
*	1347	CYLINDER	Air	24.125	26.5	0.5	0.393590	

See Nomenclature List For Definition Of The Terms & Equations Used In These Calculations

FILE: PTSFILTC.007; p4/6 04/26/94

TABLE 3.6.2.1-2 THERMAL CONDUCTANCE VALUES FOR RTG TRANSPORT THERMAL MODEL (Continued)

NODE 1	NODE 2	ELEMENT	MEDIUM	GEOMETRIC DATA X1	X2	X3	CONDUCTOR MULTIPLIER	REMARKS
347	1347	CIRCLE	Air	24.15	28.825	0.25	10.968613	
404	1347	CYLINDER	Air	25.5	26.85	0.5	0.422906	
400	402	CYLINDER	S. Std 304	14.5	24	0.375	0.032471	
403	402	RECTANGLE	S. Std 304	3	1.5	4.34	0.115207	Multiplied By 16 For 8 Bolts & 2 Paths Per Bolt
402	*	CYLINDER	S. Std 304	24	27	0.375	0.138920	
*	404	CIRCLE	S. Std 304	26.85	27.1	4.6875	0.062774	
404	*	CIRCLE	S. Std 304	26.85	27.1	4.6875	0.062774	
*	406	CYLINDER	S. Std 304	27	31	0.25	0.078960	
406	*	CYLINDER	S. Std 304	31	34.875	0.25	0.092614	
*	408	CIRCLE	S. Std 304	34.75	35	8.875	0.042865	
408	*	CIRCLE	S. Std 304	34.75	35	8.875	0.042865	
*	410	CYLINDER	S. Std 304	31	34.875	0.3125	0.115787	
410	412	CYLINDER	S. Std 304	24	31	0.3125	0.053277	
412	414	CYLINDER	S. Std 304	14.5	24	0.3125	0.027059	
400	401	CIRCLE	Air	0	20.625	0.0625	148.489340	Conductance To Thermal Shield
401	421	CIRCLE	3# Foam	0	20.625	1.385	6.700783	
421/422	422/423	CIRCLE	3# Foam	0	20.625	2.77	3.350391	
423	414	CIRCLE	3# Foam	0	20.625	1.385	6.700783	
402	424	CIRCLE	12# Foam	20.625	27.1	1.385	4.667695	
424/425	425/426	CIRCLE	12# Foam	20.625	27.1	2.77	2.433847	
426	412	CIRCLE	12# Foam	20.625	27.1	1.385	4.667695	
421/422/423	424/425/426	CYLINDER	12# Foam	14.5	24	2.77	0.239855	
406	431	CIRCLE	12# Foam	27.1	29.75	1.52	2.162321	
431/432	432/433	CIRCLE	12# Foam	27.1	29.75	3.04	1.081160	
433	434	CIRCLE	12# Foam	27.1	29.75	2.905	1.131404	
434/435	435/436	CIRCLE	12# Foam	27.1	29.75	2.77	1.186544	
436	410	CIRCLE	12# Foam	27.1	29.75	1.385	2.373089	
404	431/432/433	CYLINDER	12# Foam	27.1	28.4	3.04	2.830943	
424/425/426	434/435/436	CYLINDER	12# Foam	24	28.4	2.77	0.717996	
406	441	CIRCLE	12# Foam	29.75	32.25	1.52	2.224721	
441/442	442/443	CIRCLE	12# Foam	29.75	32.25	3.04	1.112360	
443	444	CIRCLE	12# Foam	29.75	32.25	2.905	1.164054	
444/445	445/446	CIRCLE	12# Foam	29.75	32.25	2.77	1.220786	

See Nomenclature List For Definition Of The Terms & Equations Used In These Calculations

FILE: PTSFILTC.007; p5/6 04/26/94

TABLE 3.6.2.1-2 THERMAL CONDUCTANCE VALUES FOR RTG TRANSPORT THERMAL MODEL (Continued)

				GEOMETRIC DATA			CONDUCTOR	
NODE 1	NODE 2	ELEMENT	MEDIUM	X1	X2	X3	MULTIPLIER	REMARKS
446	410	CIRCLE	12# Foam	29.75	32.25	1.385	2.441571	
431/432/433	441/442/443	CYLINDER	12# Foam	28.4	31	3.04	1.514246	
434/435/436	444/445/446	CYLINDER	12# Foam	28.4	31	2.77	1.379757	
406	451	CIRCLE	12# Foam	32.25	34.75	1.52	2.404134	
451/452	452/453	CIRCLE	12# Foam	32.25	34.75	3.04	1.202067	
453	454	CIRCLE	12# Foam	32.25	34.75	2.905	1.257929	
454/455	455/456	CIRCLE	12# Foam	32.25	34.75	2.77	1.319236	
458	410	CIRCLE	12# Foam	32.25	34.75	1.385	2.638472	
441/442/443	451/452/453	CYLINDER	12# Foam	31	33.52	3.04	1.697203	
444/445/446	454/455/456	CYLINDER	12# Foam	31	33.52	2.77	1.546465	
451/452/453	408	CYLINDER	12# Foam	33.52	34.75	3.04	3.680771	
454/455/458	408	CYLINDER	12# Foam	33.52	34.75	2.77	3.353860	
200	300	CIRCLE	Helium	0	13	0.5	7.374016	Head Gap Ranges From 1/8 to 1/2 Inches
204	304	CIRCLE	Helium	13	17.5625	0.5	6.084279	Head Gap Ranges From 1/8 to 1/2 Inches
204	304	CYLINDER	Helium	17.5625	18	2.441	4.3286	
210/220/230	310/320/330	CYLINDER	Helium	17.75	18	13.72	42.80263	Gap Ranges From 1/16 to 1/4 Inches
240	340	CYLINDER	Helium	17.75	18	5	15.598628	Gap Ranges From 1/16 to 1/4 Inches
242	342	CYLINDER	Helium	17.75	18	4.25	13.258832	Gap Ranges From 1/16 to 1/4 Inches
250	344	RECTANGLE	Helium	2.25	117	0.35	6.223214	
250	350/388	CYLINDER	Helium	19.375	19.56	0.5	2.295739	
280	360	CIRCLE	SStl 304L	0	10	1.625	1.342561	This Conductor To Be In Series W/ Next
280	360	SPECIAL	Contact + SStl 304	62.83			62.830	314.2 Sq-In x 0.2 Btu/Hr-F-Sq.-In
282	362	CIRCLE	SStl 304L	10	15	1.625	1.678201	This Conductor To Be In Series W/ Next
282	362	SPECIAL	Contact + SStl 304	78.54			78.540	392.7 Sq-In x 0.2 Btu/Hr-F-Sq.-In
284	364	CIRCLE	SStl 304L	15	16.97	1.625	0.845557	This Conductor To Be In Series W/ Next
284	364	SPECIAL	Contact + SStl 304	39.6			39.600	197.8 Sq-In x 0.2 Btu/Hr-F-Sq.-In
286	364	CIRCLE	SStl 304L	16.97	19.48	1.625	1.228302	This Conductor To Be In Series W/ Next
286	364	SPECIAL	Contact + SStl 304	57.5		1.625	57.500	287.4 Sq-In x 0.2 Btu/Hr-F-Sq.-In

See Nomenclature List For Definition Of The Terms & Equations Used In These Calculations

FILE: PTSFRLTC.007; p8/8 04/28/94

TABLE 3.6.2.1-2 THERMAL CONDUCTANCE VALUES FOR RTG TRANSPORT THERMAL MODEL (Continued)

NODE 1	NODE 2	ELEMENT	MEDIUM	GEOMETRIC DATA X1	X2	X3	CONDUCTOR MULTIPLIER	REMARKS
266	366	CYLINDER	SStl 304L	18.25	20.9	1.47	0.473071	This Conductor To Be In Series W/ Next
266	366	CYLINDER	Helium	19.48	19.5025	1.47	55.563787	
360	400	CIRCLE	SStl 304L	0	10	0.75	2.908882	This Conductor To Be In Series W/ Next
360	400	CIRCLE	Air	0	10	0.05	43.633231	
362	400	CIRCLE	SStl 304L	10	15	0.75	3.636103	This Conductor To Be In Series W/ Next
362	400	CIRCLE	Air	10	15	0.05	54.541539	
364	400	CIRCLE	SStl 304L	15	19.545	0.75	4.587149	This Conductor To Be In Series W/ Next
364	400	CIRCLE	Air	15	19.545	0.05	68.507238	
366	402	CIRCLE	SStl 304L	19.545	22.125	1.75	1.340271	This Conductor To Be In Series W/ Next
366	402	SPECIAL	Contact	161.6			161.600	202 Sq-in x 0.8 Btu/Hr-F-Sq.-In (Ring Only)
367	402	CIRCLE	SStl 304L	22.125	24.15	1.75	1.16821	This Conductor To Be In Series W/ Next
367	402	SPECIAL	Contact	172.8			172.800	216 Sq-in x 0.8 Btu/Hr-F-Sq.-In (Ring Only)
368	402	CIRCLE	SStl 304L	24.15	26.625	1.75	1.566659	This Conductor To Be In Series W/ Next
368	402	CIRCLE	Air	24.15	26.625	0.05	54.833064	
368	404	CYLINDER	SStl 304L	25.4	26.625	3.5	3.242286	This Conductor To Be In Series W/ Next
368	404	CYLINDER	Air	26.625	26.85	3.5	18.147881	
369	404	CYLINDER	SStl 304L	25.4	26.625	2.43	2.251072	This Conductor To Be In Series W/ Next
369	404	CYLINDER	Air	26.625	26.85	2.43	12.599676	
345	404	CIRCLE	Air	26.625	26.85	2.57	0.102138	

See Nomenclature List For Definition Of The Terms & Equations Used In These Calculations

FILE: PTSRLTC.007; p7/8 04/28/94

TABLE 3.6.2.1-2 THERMAL CONDUCTANCE VALUES FOR RTG TRANSPORT THERMAL MODEL (Concluded)

NODE 1	NODE 2	ELEMENT	MEDIUM	GEOMETRIC DATA X1	X2	X3	CONDUCTOR MULTIPLIER	REMARKS
300	Ambient	CONVECTIVE	Air	530.93	1	26	3.687014	Use horiz. plate correlation; Reduce by 25%
301	Ambient	CONVECTIVE	Air	530	1	0.1	3.680556	Use vertical plate correlation
304	Ambient	CONVECTIVE	Air	762.99	1	26	5.298542	Use horizontal plate correlation
305	Ambient	CONVECTIVE	Air	3169	1	12	22.006944	Use vertical plate correlation
315/316	Ambient	CONVECTIVE	Air	2	375.1	48	5.209722	Use vertical plate correlation
325/326	Ambient	CONVECTIVE	Air	2	375.1	35	5.209722	Use vertical plate correlation
335/336	Ambient	CONVECTIVE	Air	2	539.85	21	7.497917	Use vertical plate correlation
1013	Ambient	CONVECTIVE	Air	0.5	750.26	48	2.605069	Use vertical plate correlation
1023	Ambient	CONVECTIVE	Air	0.5	750.26	32	2.605069	Use vertical plate correlation
1033	Ambient	CONVECTIVE	Air	0.5	1079.88	18	3.749583	Use vertical plate correlation
348	Ambient	CONVECTIVE	Air	885.98	1	35	6.152639	Use horizontal plate correlation (w/o area for tubes)
349	Ambient	CONVECTIVE	Air	676	1	2	4.708333	Use vertical correlation; reduce by 50%
351	Ambient	CONVECTIVE	Air	99	1	1.875	0.687500	Use horizontal correlation; reduced by 75%
371	Ambient	CONVECTIVE	Air	12	1	1.125	0.083333	Use horizontal correlation; reduced by 75%
1346	Ambient	CONVECTIVE	Air	0.46	167.3	0.5	0.534431	Use vertical plate correlation
406	Ambient	CONVECTIVE	Air	1541	1	35	10.701389	Use horizontal plate correlation
408	Ambient	CONVECTIVE	Air	3958	1	16	27.486111	Use vertical plate correlation
	The Following Conductors Are Used Only For The Fire Accident							
410	Ambient	CONVECTIVE	Air	1529	1	35	10.618056	Use vertical plate correlation
412	Ambient	CONVECTIVE	Air	928	1	36	6.444444	Use vertical plate correlation
414	Ambient	CONVECTIVE	Air	1336	1	36	9.277778	Use vertical plate correlation
	The Following Conductors Are Used Only For Drained Or Zero-Flow Coolant Jacket Conditions							
1011/1012	311/312	CYLINDER	Air/Coolant	18.44	18.94	6.1	9.948569	
	Repeat Above Conductor For Stations 320 & 330							
1041/1042	331/332	CYLINDER	Air/Coolant	18.44	18.94	2.222	3.623888	
1043/1044	331/332	CYLINDER	Air/Coolant	18.44	18.94	0.462	0.753482	
313	311/312	RECTANGLE	Air/Coolant	1	725.9	1	5.040972	
315/316	311/312	CYLINDER	Air/Coolant	18.94	18.44	6.1	10.214747	
	Repeat Above Conductors For Stations 320; Multiply By 1.44 For Station 330							
337	332	RECTANGLE	Air/Coolant	1	119	1	0.826389	

See Nomenclature List For Definition Of The Terms & Equations Used In These Calculations

FILE: PTSRLTC.007; p8/8 04/26/94

TABLE 3.6.2.1-3 RADIATION INTERCHANGE VALUES FOR RTG TRANSPORT THERMAL MODEL

NODE 1	NODE 2	EMISS-1	EMISS-2	VIEW FACTOR	AREA1	AREA2	RADIATION FACTOR	REMARKS
250	265	0.3	0.3	1	189.7	189.5	0.23237	
250	264	0.3	0.3	1	29.91	29.85	0.03662	
250	266	0.3	0.3	1	89.54	89.54	0.10973	
265	242	0.3	0.3	0.4248	153.2	520.7	0.19797	
199	242	0.48	0.9	0.4248	100.5	520.7	0.20178	
193	240	0.48	0.9	1	510.509	635.544	1.63179	
194	242	0.48	0.3	0.7386	460.16	560.77	0.73428	
194	265	0.48	0.3	0.1307	460.16	153.2	0.20298	
194	199	0.48	0.48	0.1307	460.16	100.5	0.23334	
194	263	0.48	0.3	0.367	273.2	392.7	0.34930	
194	197	0.48	0.8	0.367	273.2	593.8	0.48360	
192	261	0.48	0.3	0.186	108.4	314.16	0.10362	
192	263	0.48	0.3	0.186	108.4	392.7	0.10597	
192	195	0.48	0.8	0.186	108.4	113.1	0.11237	
192	197	0.48	0.8	0.186	108.4	593.8	0.11572	
192	194	0.48	0.48	0.2558	108.4	273.2	0.13883	
195	261	0.8	0.3	0.891	113.1	314.16	0.36501	
197	263	0.8	0.3	0.75	593.8	392.7	0.60672	
1267	197	0.48	0.8	0.1987	79.24	742	0.08958	
1267	263	0.48	0.3	0.1987	79.24	393	0.08355	
1267	242	0.48	0.3	0.4122	79.24	473.99	0.14112	
1267	265	0.48	0.8	0.044	79.24	197.9	0.02301	
1267	199	0.48	0.48	0.044	79.24	100.5	0.02231	
200	300	0.9	0.9	1	530.9	530.9	3.01648	
204	304	0.9	0.9	1	720.89	755.32	4.11301	
210	310	0.9	0.9	1	1530.14	1546.52	8.70236	
220	320	0.9	0.9	1	1530.14	1546.52	8.70236	
230	330	0.9	0.9	1	1530.14	1546.52	8.70236	
240	340	0.9	0.8	1	557.63	563.6	3.17141	
242	342	0.9	0.9	1	473.99	478	2.69568	
250	344	0.3	0.9	1	263.25	263.25	0.53075	
250	350	0.3	0.8	1	60.87	61.45	0.12276	
250	366	0.3	0.3	1	60.87	61.45	0.07489	
266	366	0.3	0.3	1	179.63	180.7	0.22082	

See Nomenclature List For Definition Of The Terms & Equations Used In These Calculations

FILE: PTSRLTR.007; p1/3 04/26/94

TABLE 3.6.2.1-3 RADIATION INTERCHANGE VALUES FOR RTG TRANSPORT THERMAL MODEL (Continued)

NODE 1	NODE 2	EMISS-1	EMISS-2	VIEW FACTOR	AREA1	AREA2	RADIATION FACTOR	REMARKS
400	401	0.48	0.48	1	1336.4	1336.4	2.93070	
360	400	0.3	0.48	1	314.2	314.2	0.49403	
362	400	0.3	0.48	1	392.7	392.7	0.61745	
364	400	0.3	0.48	1	495.7	495.7	0.77940	
368	402	0.3	0.48	1	394.8	394.8	0.62075	
368	404	0.3	0.48	1	585.5	585.5	0.92060	
369	404	0.3	0.48	1	401.5	401.5	0.63129	
345	404	0.8	0.48	1	439.1	439.1	1.30685	
300	Ambient	0.8	1	0.5532	530.93	1	1.79184	
300	301	0.8	0.48	0.4	530.93	319	0.80979	
300	305	0.8	1	0.0468	530.93	3164.6	0.17056	
301	Ambient	0.48	1	1	319	1	1.06333	
304	Ambient	0.8	1	0.4273	782.99	1	2.04555	
305	304	0.8	0.8	0.1289	66.02	31.79	0.05377	Multiply By 48 For Total
305	Ambient	0.8	1	0.47772	3169	1	9.39153	
305	315/316	0.8	0.8	0.010797	65.93	17.58	0.00488	Multiply By 48 For Total
315/316	Ambient	0.8	1	0.96432	750.2	1	4.11533	
325/326	Ambient	0.8	1	0.958	750.2	1	4.02655	
335/336	Ambient	0.8	1	0.7689	1079.7	1	4.83662	
346	Ambient	0.8	1	0.6749	885.98	1	3.55295	Surface Area Minus Area For Bolt Access Tubes
1033	346	0.8	0.8	0.1298	539.94	885.98	0.46254	
335/336	346	0.8	0.8	0.1298	1079.7	885.98	0.90787	
1023	346	0.8	0.8	0.007824	375.13	885.98	0.02033	
325/326	346	0.8	0.8	0.007824	750.2	885.98	0.04061	
1013	346	0.8	0.8	0.002395	375.13	885.98	0.00623	
315/316	346	0.8	0.8	0.002395	750.2	885.98	0.01246	
351	Ambient	0.8	1	0.09829	99	1	0.06595	(24) 1.25" Cap Head Screws
349	Ambient	0.8	1	0.15676	678	1	0.71024	24 OCV & 8 Impact Limiter Bolt Access Tubes
351	349	0.8	0.8	0.90171	99	554	0.48978	
371	Ambient	0.8	1	0.09829	12	1	0.00799	(8) 0.75" Cap Head Screws
371	349	0.8	0.8	0.90171	12	124	0.06025	
1348	Ambient	0.8	1	0.5184	77	1	0.24458	

See Nomenclature List For Definition Of The Terms & Equations Used In These Calculations

FILE: PTSRLTR.007; p2/3 04/28/94

TABLE 3.6.2.1-3 RADIATION INTERCHANGE VALUES FOR RTG TRANSPORT THERMAL MODEL (Concluded)

NODE 1	NODE 2	EMISS-1	EMISS-2	VIEW FACTOR	AREA1	AREA2	RADIATION FACTOR	REMARKS
1346	406	0.8	0.8	0.4636	77	1583	0.22950	
1033	406	0.8	0.8	0.1013	539.94	1583	0.36736	
335/336	406	0.8	0.8	0.1013	1079.7	1583	0.72851	
1023	406	0.8	0.8	0.03564	375.13	1583	0.09183	
325/326	406	0.8	0.8	0.03564	750.2	1583	0.18327	
1013	406	0.8	0.8	0.01329	375.13	1583	0.03448	
315/316	406	0.8	0.8	0.01329	750.2	1583	0.06890	
356	404	0.3	0.48	0.9	75.8	84.43	0.11917	
356	369/347	0.3	0.3	0.43	43.96	394.8	0.06206	
369/347	404	0.3	0.48	0.0635	394.8	84.43	0.14150	
347	369	0.3	0.3	0.8686	394.8	394.8	0.47124	
352	369	0.3	0.3	1	171.3	171.5	0.21003	
356	369	0.3	0.3	1	197.1	197.3	0.24184	
406	Ambient	0.8	1	0.8754	1583	1	7.89541	
406	Ambient	0.8	1	1	3958	1	21.98889	
1013	Ambient	0.8	1	0.98432	375.13	1	2.05783	
1023	Ambient	0.8	1	0.958	375.13	1	2.01344	
1033	Ambient	0.8	1	0.7689	539.94	1	2.41821	
	THE FOLLOWING CONDUCTORS ARE USED ONLY FOR THE "NO COOLANT" CONDITION							
1011/1012	315/316	0.3	0.48	0.61805	706.8	745	0.98579	
1011/1012	313	0.3	0.48	0.38195	706.8	725.9	0.81720	
1021/1022	325/326	0.3	0.48	0.61805	706.8	745	0.98579	
1021/1022	323	0.3	0.48	0.38195	706.8	725.9	0.81720	
1031/1032	335/336	0.3	0.48	0.61805	706.8	745	0.98579	
1031/1032	333	0.3	0.48	0.38195	706.8	725.9	0.81720	
1041/1042	335/336	0.3	0.48	0.61805	257.3	271.2	0.35886	
1041/1042	333	0.3	0.48	0.38195	257.3	264.2	0.29748	
1043/1044	335/336	0.3	0.48	0.61805	53.7	56.6	0.07490	
1043/1044	333	0.3	0.48	0.38195	53.7	55.2	0.06210	
313	315/316	0.3	0.48	0.38195	725.9	745	0.83918	
323	325/326	0.3	0.48	0.38195	725.9	745	0.83918	
333	335/336	0.3	0.48	0.38195	1045.3	1072.8	1.20842	

See Nomenclature List For Definition Of The Terms & Equations Used In These Calculations

FILE: PTSRLTR.007; p3/3 04/28/94

TABLE 3.6.2.1-4 THERMAL CAPACITANCE VALUES FOR GPHS RTG SHIPPING RACK

NODE	ELEMENT	MEDIUM	DENSITY	GEOMETRIC DATA X1	X2	X3	SPEC. HEAT MULTIPLIER	REMARKS
	SHIPPING RACK FOR GPHS RTG							
190	PARALLEL	17-4PH S.Std	0.276	2	0.94	0.5	1.03776	Portion of Handling Bkt; Multiplied by 4 for total.
	PARALLEL	17-4PH S.Std	0.276	2	0.6	2	2.64960	" " "
	PARALLEL	17-4PH S.Std	0.276	2	1.06	0.976	2.28431	" " "
	CYLINDER	6061 Al	0.103	6.25	7.25	1	4.36838	Portion of Mid Ring Assembly
	PARALLEL	6061 Al	0.103	0.993	1.97	1.62	1.30585	Portion of Mid Ring Assy. - dimensions adjusted
						Total Wt. =	11.64571	Combined Node Mass
191	CYLINDER	6061 Al	0.103	7.5	10.65	0.75	13.87508	Converter Support Ring Assembly
192	CYLINDER	S.Std 304	0.29	0.07	1.5	5.25	42.95393	Support Leg & Bolt; Multiplied by 4 for total.
193	CYLINDER	S.Std 304	0.29	16.0625	16.25	5	27.59877	Rubble Dam On Barrier Plate
194	CYLINDER	S.Std 304	0.29	15.125	15.5	4.725	49.43758	Barrier Plate Outer Suppport
195	CYLINDER	Kaowool	0.00463	0	6	4.725	2.47420	Inner insulation blanket
197	CYLINDER	Kaowool	0.00463	6	15.125	4.725	13.24836	Outer insulation blanket
196	CYLINDER	S.Std 304	0.29	0	6	0.375	12.29934	Inner Portion of Barrier Plate
198	CYLINDER	S.Std 304	0.29	6	16.5	0.375	80.71439	Outer Portion of Barrier Plate
199								Arithmetic node at base of rubble dam
1001								Arithmetic node between 196 & 198
1002								Arithmetic node between 194 & 198
1003								Arithmetic node at top of support legs
1004								Arithmetic node at bottom of support legs
1005								Arithmetic node for contact from 192 to ICV base
1006								Arithmetic node between 261 & 263
1007								Arithmetic node between GPHS RTG (#175) & 190
1008								Arithmetic node between 1007 & 190
1000								Arithmetic node representing inner gas volume
1009								Arithmetic node representing outer gas volume

See Nomenclature List For Definition Of Terms & Equations Used In This Table — Total Wt. = 254.2473329 — FILE: SHIPTM.004; p1/1 2/28/94

TABLE 3.6.2.1-5 CONDUCTANCE VALUES FOR GPHS RTG SHIPPING RACK

				GEOMETRIC DATA			CONDUCTOR	
NODE 1	NODE 2	ELEMENT	MEDIUM	X1	X2	X3	MULTIPLIER	REMARKS
175	1007	SPECIAL	Contact	11.62			11.620000	4 Legs w/ 3.32 Sq-In. Total Area x 3.5 Btu/Sq-In
1007	1008	RECTANGLE	6061 Al	2	0.5	1.7	0.016340	Multiplied By 4 for Four Legs
1008	190	RECTANGLE	6061 Al	1	1	2.66	0.020666	Multiplied by 8 for 4 legs & 2 paths per leg
1008	1009	RECTANGLE	6061 Al	1.5	0.993	2.6	0.015913	Multiplied By 4 for Four Legs
1009	191	RECTANGLE	6061 Al	0.75	3.15	3.62	0.036257	Multiplied by 8 for 4 legs & 2 paths per leg
191	198	SPECIAL	Contact	270			270.000000	180 Sq-In. Total Area x 1.5 Btu/Sq-In
190	ICV	CONVECTIVE	Helium	225	1		1.562500	Approx. Total Area; Use Annuli Correlation
191	ICV	CONVECTIVE	Helium	280	1		1.944444	Approx. Total Area; Use Annuli Correlation
198	1001	CYLINDER	S. Stl 304	4.25	9	0.375	0.021808	
1001	198	CYLINDER	S. Stl 304	9	12.41	0.375	0.050929	
198	1002	CYLINDER	S. Stl 304	12.41	15.3125	0.375	0.077855	
1002	194	CIRCLE	S. Stl 304	15.125	15.5	2.55	0.098255	
1002	199	CYLINDER	S. Stl 304	15.3125	16.15625	0.375	0.305056	
199	193	CIRCLE	S. Stl 304	16.0625	16.25	2.6875	0.049183	
1001	1003	RECTANGLE	S. Stl 304	3	0.375	3.534	0.017685	Multiplied by 8 for 4 legs & 2 paths per leg
1003/192	192/1004	CIRCLE	S. Stl 304	0.07	1.5	2.53125	0.077401	Multiplied by 4 for four legs
1004	1005	SPECIAL	Contact	70.75			70.750000	4 Legs w/ 28.3 Sq-In. Total Area x 2.5 Btu/Sq-In
1004	1005	CIRCLE	S. Stl 304	0	0.375	1	0.012272	Multiplied by 4 for four legs
1005	1006	RECTANGLE	S. Stl 304	3	0.5	3.534	0.023580	Multiplied by 8 for 4 legs & 2 paths per leg
261	1006	CYLINDER	S. Stl 304	7	9	1.72	0.298627	
1006	263	CYLINDER	S. Stl 304	9	12.75	1.72	0.215469	
196	195	CIRCLE	Kaowool	0	6	2	0.392699	Two one inch layers of 8#/cu.-ft insulation
198	197	CIRCLE	Kaowool	6	15.125	2	2.102747	Two one inch layers of 8#/cu.-ft insulation
193	240	CYLINDER	Helium	16.25	17	5	4.835196	
196	193	CONVECTIVE	Helium	113	1	0	0.784722	Use annuli correlation
198	193	CONVECTIVE	Helium	742.2	1	0	5.154167	Use annuli correlation
195	1000	CONVECTIVE	Helium	113	1	30	0.784722	Use Horizontal Plate Correlation
192	1000	CONVECTIVE	Helium	217	1	3	1.506944	Use Vertical Plate Correlation
194	1000	CONVECTIVE	Helium	265.4	1	3	1.843056	Use Vertical Plate Correlation
197	1000	CONVECTIVE	Helium	605.8	1	30	4.206556	Use Horizontal Plate Correlation
194	1010	CONVECTIVE	Helium	460.2	1	3	3.195833	Use Vertical Plate Correlation
1002	1010	CONVECTIVE	Helium	100.5	1	1	0.697917	Use Horizontal Plate Correlation

See Nomenclature List For Definition Of The Terms & Equations Used In These Calculations

FILE: SHIPTC.004; p1/2 01/24/94

TABLE 3.6.2.1-5 CONDUCTANCE VALUES FOR GPHS RTG SHIPPING RACK

NODE 1	NODE 2	ELEMENT	MEDIUM	GEOMETRIC DATA X1	X2	X3	CONDUCTOR MULTIPLIER	REMARKS
242	1010	CONVECTIVE	Helium	534	1	5	3.708333	Use Vertical Plate Correlation
261	1000	CONVECTIVE	Helium	314.1	1	30	2.181250	Use Horizontal Plate Correlation
263	1000	CONVECTIVE	Helium	392.7	1	30	2.727083	Use Horizontal Plate Correlation
265	1010	CONVECTIVE	Helium	126.6	1	1	0.879167	Use Vertical Plate Correlation
Feed-thru Plug Assembly								
267	1266	CYLINDER	Helium	1.875	1.94	3.12	3.994672	
1266	1267	CYLINDER	Kaowool	2.045	3.05	3.875	0.422966	
198	1268	CIRCLE	Kaowool	0	1.875	1	0.076699	
1266	1266	CIRCLE	Std S 304	1.94	2.045	1.9375	0.004712	
1266	1267	CIRCLE	Std S 304	3.05	3.155	1.9375	0.007338	
1267	1000	CONVECTIVE	Helium	38.41	1	3.875	0.266736	Use Vertical Plate Correlation
1267	1010	CONVECTIVE	Helium	38.41	1	3.875	0.266736	Use Vertical Plate Correlation
1268	1269	CONVECTIVE	Helium	11.824	1	3.88	0.082111	Use Horizontal Plate Correlation
1269	268	CONVECTIVE	Helium	16.84	1	2.5	0.116944	Use Vertical Plate Correlation
1269	269	CONVECTIVE	Helium	3.6	1	2	0.025000	Use Horizontal Plate Correlation
1268	1269	CONVECTIVE	Helium	9.222	1	0.755	0.064042	Use Horizontal Plate Correlation
198	1000	CONVECTIVE	Helium	3.6	1	2	0.025000	Barrier Plate Plug Hole; Horiz Plate Correlation

See Nomenclature List For Definition Of The Terms & Equations Used In These Calculations FILE: SHIPTC.004; p2/2 01/24/94

TABLE 3.6.2.1-6 THERMAL CAPACITANCE VALUES FOR GPHS RTG THERMAL MODEL

NODE	ELEMENT	MEDIUM	DENSITY	GEOMETRIC DATA X1	X2	X3	SPEC. HEAT MULTIPLIER	REMARKS
50	SPECIAL	HEAT SOURCE	1	2.7738	0	7.54	2.77380	See Note 1; Q = 879.016 Watts
52	SPECIAL	HEAT SOURCE	1	8.6524	0	23.52	8.65240	See Note 2; Q = 2741.968 Watts
54	SPECIAL	HEAT SOURCE	1	2.7738	0	7.54	2.77380	See Note 1; Q = 879.016 Watts
51	SPECIAL	UNICOUPLE	1	1.172	0	7.54	1.17200	See Note 3
53	SPECIAL	UNICOUPLE	1	3.656	0	23.52	3.65600	See Note 3
55	SPECIAL	UNICOUPLE	1	1.172	0	7.54	1.17200	See Note 3
60	SPECIAL	END SUPPORT	1	1.11	0	0	1.11000	From GE's Node 12
62	SPECIAL	END SUPPORT	1	0.8	0	0	0.80000	From GE's Node 2
100	SPECIAL	OUTB'RD DOME	1	0.073	0	0	0.07300	From GE's Node 13
105	SPECIAL	FLANGE	1	0.094	0	0	0.09400	From GE's Node 14
107	SPECIAL	FLANGE	1	0.12	0	0	0.12000	From GE'S Node 15
110	CYLINDER	AL2219-T6	0.103	4.23	4.285	1.635	0.24777	Multiply By 0.4797 For Effective Area. See Note 4
112 & 113	PARALLEL	AL2219-T6	0.103	0.89	0.065	1.635	0.00974	Multiply By 8.0 For Total
120	CYLINDER	AL2219-T6	0.103	4.23	4.285	7.54	1.14263	Multiply By 0.4797 For Effective Area
122 & 123	PARALLEL	SHELL FLAT	0.103	0.89	0.065	7.54	0.04493	Multiply By 8.0 For Total
124 & 125	PARALLEL	AL2219-T87	0.103	1.07	0.055	7.54	0.04570	Multiply by 4 for the total
126 & 127	PARALLEL	AL2219-T87	0.103	3.03	0.035	7.48	0.08171	Multiply by 4 for the total
130	CYLINDER	AL2219-T6	0.103	4.23	4.285	7.54	1.14263	Multiply By 0.4797 For Effective Area
132 & 133	PARALLEL	SHELL FLAT	0.103	0.89	0.065	7.54	0.04493	Multiply By 8.0 For Total
134 & 135	PARALLEL	AL2219-T87	0.103	1.07	0.055	7.54	0.04570	Multiply by 4 for the total
136 & 137	PARALLEL	AL2219-T87	0.103	3.03	0.035	7.48	0.08171	Multiply by 4 for the total
140	CYLINDER	AL2219-T6	0.103	4.23	4.285	8.44	1.27902	Multiply By 0.4797 For Effective Area
141	CYLINDER	AL2219-T87	0.103	4.3	6	0.235	1.33150	Mid Span Ring
142 & 143	PARALLEL	SHELL FLAT	0.103	0.89	0.065	8.44	0.05029	Multiply By 8.0 For Total
144	PARALLEL	AL2219-T87	0.103	1.07	0.055	7.52	0.04558	Multiply by 4 for the total
146	PARALLEL	AL2219-T87	0.103	3.03	0.035	7.52	0.08214	Multiple by 4 for the total
145	PARALLEL	AL2219-T87	0.103	1.07	0.055	6.04	0.03661	Multiply by 4 for the total
147	PARALLEL	AL2219-T87	0.103	3.03	0.035	5.96	0.06510	Multiple by 4 for the total
150	CYLINDER	AL2219-T6	0.103	4.23	4.285	7.54	1.14263	Multiply By 0.4797 For Effective Area
152 & 153	PARALLEL	SHELL FLAT	0.103	0.89	0.065	7.54	0.04493	Multiply By 8.0 For Total
154	PARALLEL	AL2219-T87	0.103	1.07	0.055	7.54	0.04570	Multiply by 4 for the total
156	PARALLEL	AL2219-T87	0.103	3.03	0.035	7.48	0.08171	Multiply by 4 for the total

See Nomenclature List For Definition Of Terms & Equations Used In This Table

FILE: GPHSTM.XLS p1/2 11/22/91

BEST COPY AVAILABLE

TABLE 3.6.2.1-6 THERMAL CAPACITANCE VALUES FOR GPHS RTG THERMAL MODEL

NODE	ELEMENT	MATERIAL	DENSITY	GEOMETRIC DATA X1	X2	X3	SPEC. HEAT (BTU/LB-°F)	REMARKS
155	PARALLEL	AL2219-T87	0.103	1.252	0.055	7.54	0.05348	Multiply by 4 for the total
157	PARALLEL	AL2219-T87	0.103	2.85	0.035	7.48	0.07685	Multiply by 4 for the total
160	CYLINDER	AL2219-T6	0.103	4.23	4.285	7.54	1.14293	Multiply By 0.4797 For Effective Area
161	CYLINDER	AL2219-T6	0.103	4.3	5.27	0.115	0.34544	Lower Span Ring - RTD Mounting
162 & 163	PARALLEL	SHELL FLAT	0.103	0.89	0.045	7.54	0.04493	Multiply By 8.0 For Total
164	PARALLEL	AL2219-T87	0.103	1.07	0.055	7.54	0.04570	Multiply by 4 for the total
166	PARALLEL	AL2219-T87	0.103	3.03	0.035	7.48	0.08171	Multiply by 4 for the total
165	PARALLEL	AL2219-T87	0.103	1.8	0.055	7.54	0.08834	Multiply by 4 for the total
167	PARALLEL	AL2219-T87	0.103	2.5	0.035	7.48	0.06741	Multiply by 4 for the total
170	CYLINDER	AL2219-T6	0.103	4.23	4.285	1.647	0.24959	Multiply By 0.4797 For Effective Area.. See Note 4
172 & 173	PARALLEL	AL2219-T6	0.103	0.89	0.045	1.647	0.00981	Multiply By 8 For Total.. See Note 6
177	SPECIAL	FLANGE	1	0.48	0	0	0.49000	From GF's Node 5
175	SPECIAL	FLANGE	1	0.17	0	0	0.17000	From GF's Node 4
180	SPECIAL	INBOARD DOME	1	0.08	0	0	0.09000	From GF's Node 3
185	SPECIAL	SHORTING MOD.	1	0	0	0	0.00000	Arithmetic Node For Shorting Module Simulation
158	SPECIAL		1	0	0	0	0	Arithmetic Node At Joint Between Fin & RTD Rib
159	SPECIAL		1	0	0	0	0	Arithmetic Node At Joint Between Fin & RTD Rib
168	SPECIAL		1	0	0	0	0	Arithmetic Node At Inner Radius Of RTD Rib
169	SPECIAL		1	0	0	0	0	Arithmetic Node At Inner Radius Of RTD Rib

See Nomenclature List For Definition Of Terms & Equations Used In This Table

FILE: GPHSTM.XLS p2/2 11/22/91

BEST COPY AVAILABLE

Radiation heat transfer is calculated assuming standard gray-body equations. The shape factors between the various package components were computed using either pre-defined relationships or the string method for nonstandard geometric configurations.

Heat transfer across the ICV-to-OCV gap (1/4-in. maximum at the sides and 1/2-in. maximum at the heads) is assumed to be via radiation and conduction through the 19 $\pm$ 1 psia helium gas medium. The emittance of both surfaces is assumed to be 0.90, based on the use of the Carboline 4674-C900 high emissivity coating. Subsequent testing[32] on three sample coupons with Carboline coating yielded a measured normal emittance of 0.875 on all three sample coupons. While the measured values are slightly less than the assumed value of 0.90 used in the SARP analysis, the impact on the predicted temperatures is slight. This conclusion is based on the close match between the results for the qualification testing (see Reference 14) and the temperatures predicted by an analytical model that used a surface emittance value of 0.90. In addition, further analysis with an assumed emittance value of 0.70 to simulate possible wear-and-tear of the surface coating showed that the surface temperatures of the RTG increased by 4 °F or less. The temperature of the ICV sidewall increased about 2 °F. Therefore, the temperature levels presented in the SARP analysis herein are considered accurate despite the differences in assumed and measured emittance values for the Carboline coating. Because of the narrowness of the gap, convection heat transfer across the gap reduces to straight conduction (i.e., Nu = 1.0).

Thermal conductance between surfaces in direct contact with each other was determined using the data in Figure 8, page 4-19 of Reference 2. The specific value used depended on the surface materials, surface finish, gap material, and contact pressure. Table 3.6.2.1-2 provides the contact area and heat transfer coefficient assumed for each contact surface pair.

3.6.2.2 RTG-to-ICV Thermal Interface Models. The convection coefficients for the GPHS RTG to ICV heat transfer are computed using equation 22 from the Reference 11 paper by Khan and Kumar. This correlation was developed for the case of convective heat transfer across vertical annuli with a constant heat flux on the inner wall, adiabatic end surfaces, and smooth inner and outer walls. As such, the correlation predicted coefficients needed to be adjusted to account for the fact that the GPHS RTG is a finned cylinder, the end walls are not adiabatic, and the fact that a straight application of the correlation with the GPHS RTG would imply a larger ICV wall area than exists. A comparison of implied annuli areas with the actual geometry indicated that the calculated heat transfer coefficient needed to be multiplied by 0.75 to correct for these factors. Furthermore, because the correlation only provides the average coefficient, a second adjustment based on Figure 3 in the paper was made to account for temperature rise between the top and bottom of the package.

The general applicability of the Khan and Kumar correlation to the GPHS RTG-ICV geometry and the specific modifications made to the correlation were verified in the Reference 12 thermal development test and the Reference 14 thermal qualification tests. The results from both sets of tests showed that the adjusted correlation resulted in an accurate prediction of the convective coefficients and, hence, the RTG temperatures. Because of the good match-up with test results, only modest refinement to the correlation adjustments have been needed to those derived before testing.

For a detailed discussion of the test setup, results, and the adjustment procedure used to apply the correlation to this payload, the reader is directed to the referenced test reports.

Because a significant fraction of the heat transfer between the GPHS RTG and the ICV is via radiation, the shape factors between the various surfaces were determined by computer analysis using the University of Washington's VIEW program. The computed shape factors were validated by results from the GPHS development and qualification tests (References 12 and 14). The interchange factors between individual nodes of the GPHS RTG and other GPHS RTG nodes or the

ICV are not documented herein because of the sheer number of factors involved (more than 600). Instead, these radiation interchange factors may be found in the SINDA listing at the end of this section.

The shipping rack assembly for the GPHS RTG is modeled using 21 nodes. Heat transfer via conduction, convection, and radiation are addressed for the interfaces between the shipping rack assembly and the various RTG/ICV surfaces. Because the existing RTG support structure is used, the direct conduction between the GPHS RTG and the shipping rack assembly is essentially the same as it now exists with the current shipping method.

3.6.2.3 Package Model for Regulatory Normal Conditions of Transport. The package thermal model for the regulatory normal conditions of transport (NCT) used a slightly modified version of the normal operational condition model discussed in Sections 3.6.2.1 and 3.6.2.2. The model modifications assume an inoperative chiller system and that the coolant jacket is drained and dry. The damage from the NCT free drop will cause a negligible effect on the remaining aspects of the package thermal model.

Thermal modeling of an inoperative chiller system simply involved setting the conductors between the boundary node representing the chiller output and fluid nodes in the coolant jacket to zero. Modeling of a drained coolant jacket involved the following modifications:

- The thermal capacitance at the fluid nodes in the coolant jacket (i.e., nodes 311, 312, 321, etc.) were replaced by the thermal capacitance of an equivalent volume of air
- The forced convection conductors between the coolant jacket fluid nodes and the various surfaces of the coolant jacket were replaced with conductance across an equivalent air gap
- Radiation conductors were added to the model of the coolant jacket to simulate radiative interchange between the various coolant jacket surfaces.

All other aspects of the thermal model are the same as those described above for the normal operational conditions.

3.6.2.4 Package Model for Hypothetical Accident Conditions Fire. The thermal performance of the Package under the 10 CFR 71.73 hypothetical accident conditions (HAC) is evaluated analytically. The thermal model is based on the NCT model with modifications made to simulate the damage sustained from the HAC 30-ft free drops and the HAC 40-in. puncture drops. The results from a series of drop tests conducted on the two Certification Test Articles are presented in Sections 2.7.6 and 2.10.15. The following table summarizes the results from both test series and the logic for the selection of the worst case damage to the package that would occur under the HAC.

Test No.	Test description	Thermal impact
CTA-2 No.2	30-ft. free drop, bottom-down, near vertical	No significant damage to Packaging. RTG assumed to be damaged (typical for all HAC drops).
CTA-2 No.5	30-ft free drop, c.g. over corner	No ICV or OCV damage. Extrapolated impact limiter crush of 6.1 in. will leave 4.9 in. of foam at minimum distance.
CTA-2 No.12	30-ft free drop, side-slapdown	Minimal damage to ICV or OCV shells, possible local contact between ICV and OCV shells over 13 wide by 2-in.-long segment near the torispherical heads. Extrapolated 5.9 in. of foam crush at the top of the impact limiter will leave 1.75 in. of foam minimum.
CTA-2 No.8	30-ft free drop, bottom end down	No significant damage to Packaging.
CTA-2 No.13	30-ft free drop, top end down	No damage to the impact limiter. ICV and OCV contact over 15-in. diameter at the torispherical head. Crushing of all fins will reduce convective/radiative heat transfer between ambient and the OCV head.
CTA-2 No.6	40-in. puncture drop, c.g. over corner	The puncture bar increased previous c.g. over corner foam crush by 1.7 in. This left 4.9 - 1.7 = 3.2 in. of foam at the minimum distance.
CTA-1 No.12	40-in. puncture drop, bottom-down, over low density foam	The local foam crush of 2.5 in. leaves 5.8 in. of foam depth.
CTA-1 No.13	40-in. puncture drop, over OCV vent port	Maximum local foam crush of 3 in., leaving 4.6 in. at minimum distance.
CTA-2 No.14	40-in. puncture drop, normal impact to OCV sidewall	Localized deformation of ICV and OCV sidewalls over a 9-in. diameter area. Possible contact between ICV and OCV shells over 8-in. diameter area.
CTA-1 No.15	40-in. puncture drop, oblique impact to OCV sidewall	Localized deformation of ICV and OCV sidewalls less than CTA-1 test No. 14. No contact assumed between ICV and OCV shells because ICV deformed more than OCV.
CTA-2 No.15	40-in. puncture drop, top end impact	Maximum denting of ICV and OCV torispherical heads was 1.25 in.
CTA-2 No.3	40-in. puncture drop, impact limiter top edge	Denting of impact limiter top surface by 5/16 in. will cause no significant thermal effects.
CTA-1 No.18	40-in. puncture drop, top surface of thermal shield	Thermal shield dented by 1.3 in. at center and less elsewhere over a total dimple diameter of 7 in. The damage reduced the underlying fiberglass to approximately 1/2 of its original thickness.
CTA-1 No.19	40-in. puncture drop, over impact limiter bolt access tube.	Crushing of impact limiter top surface by 3/4 in. will cause no significant thermal effect. The buckling of the access tubes will reduce the convective and radiative heat transfer between the tube and bolt heads with the ambient.
CTA-2 No.9	40-in. puncture drop on side of impact limiter at lower corner weld.	The puncture dent depth was approximately 3.5 in. No evidence of incipient ripping of either impact limiter shell or weld was noted.

Test No.	Test description	Thermal impact
CTA-2 No.16	40-in. puncture drop on to impact limiter side wall plastic melt plug.	The melt plug holder weld failed and allowed the impact limiter side wall to tear, exposing about 12.7 sq. in. of foam.

Of the various combinations of 30-ft free drops and 40-in. puncture drops, the worst combination of the two events from a thermal point of view is represented by the 30-ft free drop with side-slapdown followed by the 40-in. puncture drop on the thermal shield (i.e., test Nos. 8 and 18). The damage caused by these test events maximizes the Package damage adjacent to the temperature sensitive Butyl O-rings. The amount of foam exposed by the puncture bar in CTA-2 test no. 16 was approximately 12.7 in^2. This area is quite small relative to the area of the impact limiter, and due to the intumescent behavior of the polyurethane foam material (see Reference 10), the opening will be effectively closed during the fire event.

Other combinations of free drop and puncture events exhibited lesser damage to the impact limiter and damage to the ICV/OCV shells that is more remote from the O-rings. While the top end down drops will cause an increase in the peak ICV temperature due to contact between the ICV and OCV heads, the increase will be less than 200 °F, and the same head contact will result in lower ICV temperatures following the fire because of the reduced thermal resistance between the ICV head and the ambient environment. Localized contact between the ICV and OCV shells due to the free and/or puncture drops will produce a similar effect on the peak and long-term ICV temperatures.

A 3-D analytical thermal model is used to evaluate the package performance under the 10 CFR 71.73 HAC fire. This level of modeling permits the simulation of the non-axisymmetric damage caused by the HAC free and puncture drops. The 3-D model is created using a SINDA program feature that permits a thermal model to be broken into submodels. Each submodel can be independently scaled and modified as necessary to represent their contribution to the overall thermal model. Conductors are used to complete the 3-D model by providing thermal communication between the various 2-D circumferential segments of the package. Table 3.6.2.4-1 presents the circumferential conductances used to tie the various 2-D submodels together. The values presented in the table are based on a 15° angle of separation. These conductances were scaled up or down to match the actual angle of separation between the 2-D submodels.

For this application, each circumferential segment of the package is represented by a different 2-D submodel. A total of four 2-D submodels represent one-half of the packaging and its payload about a line of symmetry. The plane of symmetry passes through the vertical axis of the package and the centerline of the HAC side drop damage. Symmetry conditions are assumed for the temperatures in the other half of the package. The first submodel (i.e., segment A) simulates the damaged section of the package, while the other three segments (i.e., segments B, C, and D) provide circumferential temperature resolution within the package components. The 3-D models for the circumferential heat source distribution (i.e., HAC thermal load case Nos. 1 amd 2) and the ungula rubble pile (i.e., HAC thermal load case Nos. 5 and 6) assumptions use submodel segments with subtended angles of 22.5, 45, 67.5, and 45 degrees for segments A through D, respectively. For the axial alignment of the aeroshells (i.e., HAC thermal load case Nos. 3 and 4), the subtended angles used are 15, 30, 90, and 45 degrees, respectively. The subtended angles used for each 3-D model were selected based on extent of the internal and external damage and the requirements of the associated thermal stress model.

Heat transfer within each of the 2-D submodel segments that make up the 3-D model is based on the same data for thermal capacitance, conductance, and radiation as used for the axisymmetric regulatory model for NCT (see Appendix 3.6.1 to 3.6.3). Modifications to this model data were made to reflect the presence of package damage and the payload reconfiguration. Additional general model modifications made for the HAC fire included the 10 CFR 71.73(c)(3) requirements for a package external surface absorptivity of 0.8 or greater and exposure of the entire package (including the impact limiter bottom) to the HAC fire environment. Although the credible post-accident orientation for thermal load case Nos. 1 and 2 is for the package to be resting on the impact limiter's bottom surface (thus

shielding the bottom), for conservatism the bottom surface was exposed to the fire environment for these load cases as well.

Because all of the HAC scenarios assume breakup of the RTG, the Khan and Kumar relationship for convective heat transfer between the RTG and the ICV is no longer applicable for the damaged configurations and was abandoned for the 3-D models. Instead, the convective heat transfer from each surface was treated as a free surface with a mean ICV gas temperature node serving as the appropriate boundary node. This approach is known to be conservative because it does not account for temperature stratification in the ICV, and the strength of a convective heat transfer flow is stronger in an enclosure for a given delta temperature.

Specific model modifications are made to each submodel of the 3-D model to account for the HAC free and puncture drop induced damage to the package exterior and the payload. As discussed above, several impact orientations were evaluated to determine the worst case thermal damage to the package. The following paragraphs describe the modifications made for each type of damage.

The impact limiter model for the 2-D segment that encompasses the crush zone of impact limiter damage (i.e., segment A) was modified to reflect a 4-in.-inward crush of the exterior shell of the impact limiter. This crush depth represents the maximum crush seen from the side-slapdown drop test. Although extrapolation of the foam structural properties for the warm foam conditions indicates a worst case crush depth of 5.9 in., using a 4-in. crush depth provides sufficient conservatism since it is applied across the entire 2-D segment. Under actual conditions the 5.9 in. of crush will only occur a single radial location and only at the top of the impact limiter. Further analysis of both configurations showed that the use of the 5.9-in. crush depth causes no increase in the predicted O-ring temperatures. This occurs because the conservative foam modeling assumptions used results in all foam in the damaged segment being ablated away at the start of the HAC fire under either crush depth scenario.

Additional conservatism lies in the fact that credit is not taken for the higher equivalent foam density that will result from the impact limiter crush (see Appendix 3.6.3 for the effect of foam density on the fire protection qualities of the foam). The impact limiter thermal model also assumes that the remaining foam in the damaged zone will be ablated away during the fire, exposing the inner shell of the limiter (i.e., thermal model node No. 404) to direct radiation and conduction exposure to the outer shell of the impact limiter (node No. 408). This is a conservative assumption because prior tests (see Reference 10) have shown that a char layer will form and act as a radiative shield.

The impact limiter at the undamaged sections of the 3-D model assumes the loss of the outer 2.5 in. of the impact limiter foam, because of ablation during the HAC fire, and this foam loss occurs immediately upon the initiation of the HAC fire.

Again, this assumption is conservative because the Reference 10 fire tests showed that the foam will actually expand slightly when exposed to the fire. The presence of an expanded foam will limit, at a greater rate than assumed by the 3-D model, radiative heat transfer to the interior foam nodes. The remaining foam is assumed to remain in place, either as a char layer or as virgin foam according to the modeling rules provided in Appendix 3.6.3.

The payload reconfiguration described in Section 3.5 is modeled as a combination of an empty GPHS RTG shell and 18 GPHS aeroshells. For the circumferential distribution assumption of HAC thermal load case Nos. 1 and 2, heat transfer between the aeroshells and the shipping rack assembly are modeled by a combination of radiation and conduction. Convection and radiation interchange with the ICV interior is also included.

TABLE 3.6.2.4-1 CIRCUMFERENTIAL CONDUCTOR VALUES FOR RTG PACKAGE: Based On 15 Degree Segments

				GEOMETRIC DATA			CONDUCTOR	
NODE 1	NODE 2	ELEMENT	MEDIUM	X1	X2	X3	MULTIPLIER	REMARKS
200b	200a/200c	RECTANGLE	S.Stl 304	0.375	13	2.40855	0.014056	
204b	204a/204c	RECTANGLE	S.Stl 304	0.375	4.5625	4.2412	0.002801	
204b	204a/204c	RECTANGLE	S.Stl 304	0.375	2.563	4.5488	0.001467	
210b	210a/210c	RECTANGLE	S.Stl 304	0.75	13.72	4.5488	0.015709	Repeat For 220 & 230
240b	240a/240c	RECTANGLE	S.Stl 304	0.75	5	4.5488	0.005725	
242b	242a/242c	RECTANGLE	S.Stl 304	0.75	5.25	4.5488	0.006011	
250b	250a/250c	RECTANGLE	S.Stl 304	2.375	1.8293	4.7615	0.006338	
261b	261a/261c	RECTANGLE	S.Stl 304	1.72	10	1.8328	0.065178	
263b	263a/263c	RECTANGLE	S.Stl 304	1.72	5	3.3379	0.017892	
265b	265a/265c	RECTANGLE	S.Stl 304	1.72	4.969	4.1888	0.014189	
280b	280a/280c	RECTANGLE	S.Stl 304	1.75	10	1.8328	0.066314	
282b	282a/282c	RECTANGLE	S.Stl 304	1.75	5	3.3379	0.018204	
284b	284a/284c	RECTANGLE	S.Stl 304	1.75	4.969	4.1888	0.014416	
286b	286a/286c	RECTANGLE	S.Stl 304	1.47	2.501	4.7778	0.005344	
300b	300a/300c	RECTANGLE	S.Stl 304	0.5	13	2.4066	0.018741	
304b	304a/304c	RECTANGLE	S.Stl 304	0.5	4.94	4.3459	0.003947	
304b	304a/304c	RECTANGLE	S.Stl 304	0.5	2.441	4.7621	0.00178	

See Nomenclature List For Definition Of The Terms & Equations Used In These Calculations

FILE: PTSDAMTC.007; p1/2 02/11/94

TABLE 3.6.2.4-1 CIRCUMFERENTIAL CONDUCTOR VALUES FOR RTG PACKAGE: Based On 15 Degree Segments

				GEOMETRIC DATA			CONDUCTOR	
NODE 1	NODE 2	ELEMENT	MEDIUM	X1	X2	X3	MULTIPLIER	REMARKS
310b	310a/310c	RECTANGLE	S.Std 304	0.5	13.72	4.7621	0.010004	Repeat For 320 & 330
340b	340a/340c	RECTANGLE	S.Std 304	0.5	5	4.7621	0.003646	
342b	342a/342c	RECTANGLE	S.Std 304	0.5	4.25	4.7621	0.003099	
344b	344a/344c	RECTANGLE	S.Std 304	1.7	1.2	4.9742	0.002848	
345b	345a/345c	RECTANGLE	S.Std 304	0.375	2.625	6.9213	0.000988	
346b	346a/346c	RECTANGLE	S.Std 304	6.185	0.375	5.9952	0.003555	
350b	350a/350c	RECTANGLE	S.Std 304	2.565	1	5.4664	0.003259	
352b	352a/352c	RECTANGLE	S.Std 304	2	1	6.0607	0.002292	
354b	354a/354c	RECTANGLE	S.Std 304	2.565	1.69	5.4664	0.005507	
356b	356a/356c	RECTANGLE	S.Std 304	2	1.69	6.0607	0.003873	
360b	360a/360c	RECTANGLE	S.Std 304	1.5	10	1.8326	0.056841	
362b	362a/362c	RECTANGLE	S.Std 304	1.5	5	3.3379	0.015604	
364b	364a/364c	RECTANGLE	S.Std 304	1.5	4.565	4.5553	0.010439	
366b	366a/366c	RECTANGLE	S.Std 304	2.56	3.5	5.4716	0.011372	
367b	367a/367c	RECTANGLE	S.Std 304	2.025	3.5	6.0633	0.008117	
368b	368a/368c	RECTANGLE	S.Std 304	2.475	3.5	6.3225	0.009515	
369b	369a/369c	RECTANGLE	S.Std 304	2.475	2.4	6.3225	0.006524	
198b	198a/198c	RECTANGLE	S.Std 304	10.5	0.375	3.2489	0.008416	
196b	196a/196c	RECTANGLE	S.Std 304	6	0.375	1.1125	0.014044	
193b	193a/193c	RECTANGLE	S.Std 304	5	0.1875	4.2297	0.001539	

See Nomenclature List For Definition Of The Terms & Equations Used In These Calculations FILE: PTSDAMTC.007; p2/2 02/11/94

The HAC thermal load case Nos. 3 and 4 model the axial alignment of the aeroshells on the ICV wall by a combination of radiation and conduction. For conservatism, the centerline of the aeroshells is assumed to be aligned with the package HAC side drop damage. The shell of the GPHS RTG is assumed to end up lying directly on top of the aeroshells, thereby blocking direct convection and radiation interchange between the aeroshells and the interior of the ICV cavity. Instead, all decay heat from the aeroshells must first pass into the ICV wall or the GPHS RTG shell of segment A and be conducted to the neighboring submodel segments before being convected or radiated to other portions of the 3-D model.

The HAC thermal load case Nos. 5 and 6 rely on radiation and conduction interchange between a lumped rubble pile of aeroshells and the shipping rack assembly. The rubble pile is assumed to be in the shape of an "ungula" with a total subtended angle of 135° arc. As such, the rubble pile is distributed across submodel segments A and B. The RTG shell is assumed to have come to rest at an angle across the rubble pile, providing a partial blockage of radiative heat loss between the rubble pile and the ICV wall. Because of the substantial void fraction of the rubble pile, free convection from within the rubble pile is assumed to be possible. The convection heat transfer rate is based on 50% of the total surface area of the aeroshells being directly exposed to helium gas. Additional details on the modeling of the rubble pile, conduction and radiation between the aeroshells and the shipping rack assembly/ICV wall is provided in Section 3.6.6.

3.6.2.5 Nomenclature Used In Spreadsheets, Tables 3.6.2.1-1 Through -5, and Table 3.6.2.4-1.

Area1: area, in square in., associated with node 1.

Area2: area, in square in., associated with node 2.

Conductor multiplier: the factor to be multiplied by the thermal conductivity of the material (i.e. in terms of Btu-in./ft^{2}hr-°F) listed under 'Medium' and the temperature difference between nodes 1 and 2 to yield the heat transferred by conduction between nodes 1 and 2. If the Element type equals 'Special,' this value is in terms of Btu/hr-°F (i.e., kA/L); if the Element type is 'Convective,' this value is in terms of square feet since it is to be multiplied by a calculated h_c. For all other Element types, the value listed is in terms of ft^2/in. (i.e., A/L).

Density: the mass per unit volume, pounds-mass/in.^{3}. A value of "1" indicates that this variable is unused for this calculation.

Element: geometric shape used to calculate the volume or conduction area for the associated node(s). These shape definitions are as follows:

Circle--a circular conduction element with Conductor Multiplier = pi*(X2^2 - X1^2)/X3/144.

Convective--surface heat transfer via convection. Conductor Multiplier = X1*X2/144 (i.e., Area). The h_c from correlation listed in the 'REMARKS' column using X3/12 as the characteristic length.

Cylinder--a right cylinder solid. Volume = pi*(X2^2 - X1^2)*X3. Conductor multiplier = 2*pi*X3/144/ln(X2/X1).

Parallel--a solid whose surfaces are parallelograms. Volume = X1*X2*X3.

Rectangle--an element with a rectangular-shaped heat transfer path. Conductor multiplier = X1*X2/X3/144.

Special--indicates an element whose thermal capacitance or conductance is obtained from other sources and is included as a direct input. See the "Remarks" column for specific details. A node with zero mass is known as an Arithmetic node. A heat balance is performed at the node, but it cannot store thermal energy.

Sphere--a solid of spherical shape. X2 = outer radius, X1 = inner radius, X3 = height of spherical segment. Volume = pi*X3**2 * (X2-X3/3) minus pi*(X3-X2+X1)**2 * (X1 - (X3-X2+X1)/3).

Emiss-1: Thermal emissivity of the surface area for node 1.

Emiss-2: Thermal emissivity of the surface area for node 2.

Medium: The material, component, or condition for which the thermal capacitance or conductance is being calculated.

Node: Number of the node in the thermal model. See Figures 1 and 2.

Radiation: Factor to be multiplied by the Stefan-Botzmann constant (i.e., 1.7141E-09 Btu/hr-ft^2-°R^4) and the difference of (T_1^4 - T_2^4) to yield the heat transferred factor by radiation.

Shape factor: The fraction of diffusely distributed radiation leaving surface at node 1 that reaches the surface at node 2.

Specific heat multiplier: The factor, when multiplied by the specific heat of the material listed under Medium, yields the thermal capacitance, in terms of Btu/°F.
If the Element type equals Special, this value is already in terms of Btu/°F and X3 indicates the height/length of the node section involved. Otherwise, the multiplier is equivalent to density times volume, or the weight of the node being modeled. A node with zero weight is known as an Arithmetic node. Heat balances are performed about these nodes, but because heat energy is not stored at these nodes, they have no effect on the transient behavior of the model.

X1,X2,X3 Geometric lengths (in in.) for the volume or conductor calculation. See 'Element' above.

3.6.3 Performance Of Rigid Polyurethane Foam Under Fire Accident Conditions

The General Plastic's LAST-A-FOAM® FR-3700 (see Reference 10) selected for the impact limiter has been used in a number of similar applications over the last 12 years. A special thermal feature of this proprietary rigid polyurethane foam is that exposure to fire causes the foam to degrade into an intumescent char that swells and tends to fill voids or gaps created by impact on a puncture bar or other damage. The char is structurally strong and will shield the underlying undamaged foam from direct exposure to external high temperatures. In addition, the foam will not support a flame once the external fire is removed.

The mechanisms behind variations in the thermal properties of FR-3700 foam at elevated temperatures are varied and complex. Because only a limited amount of research has been done on the thermal properties of foam during a fire, no definitive analytical model of the foam properties exists. Instead, a combination of empirical data and modeling conservatism is used for this application.

The Reference 10 product brochure describes the setup and results of a series of fire tests conducted on the foam. The test articles consisted of six 5 gallon paint cans filled with FR-3700 foam at densities of 8, 16, and 24 lb/ft^3. One end of the test articles (i.e., the "hot face (HF)" surface) was subjected to an open burner flame for 45 minutes. This flame duration is 15 minutes longer than called for by the 10 CFR 71.73 requirements. A thermal shield prevented direct exposure to the flame by any surface of the test article other than the HF. Each test article was instrumented with nine thermocouples: one on the HF of the can and then at distances of 1, 2, 3, 4, 5, 6, 9, and 12 in. in from the HF.

In addition, foam samples were subjected to thermal decomposition testing in a radiant oven. The exposure temperatures for the tests varied from 70 to 1500 °F and were conducted in air and nitrogen atmospheres. A thermogravimetric analysis (TGA) was conducted to evaluate the sample weight loss as a function of temperature.

Test results, together with visual observations during these and the TRUPACT II HAC fire testing, indicate the following steps in the thermal breakdown of the foam during a HAC fire.

- Below 500 °F, the variation in foam thermal properties with temperature are slight and reversible. As such, fixed values for specific heat and thermal conductivity are appropriate.

- Irreversible thermal degradation of the foam begins as the temperature rises above 500 °F. This degradation is accompanied by a vigorous outgassing from the foam and indeterminate amount of internal heat generation. Although the outgassing removes a significant amount of heat through mass transport processes, quantifying this heat removal as a function of temperature and time would require a complex analysis and series of benchmark tests.

- The weight loss due to outgassing not only has direct affect on the heat flux into the remaining virgin foam, but it changes the composition of the resulting foam char because the foam constituents are lost at different rates. This change in composition affects both the specific heat and the thermal conductivity of the foam char layer.

- As the temperature continues to rise, the developing char layer begins to take on the characteristics of a gas-filled cellular structure where radiative interchange from one cell surface to another becomes a significant portion of the overall heat transfer mechanism. This change in the dominant heat transfer mechanism causes the apparent heat conductivity to take on a highly nonlinear relationship with temperature.

- Finally, at temperatures near 1250 °F, the thermal breakdown of the foam is essentially completed. In the absence of direct exposure to the flame, the char layer will be the same or slightly thicker than the original foam depth. This char layer will continue to provide radiative

shielding to the underlying foam material.

Because of this complex variation in thermal properties, and in absence of a community consensus in the modeling approach necessary, a simplified and conservative modeling approach has been taken for this application. The approach used is the same as that in the HAC fire modeling for the 125B rail packaging SARP. The three main elements of the approach are described below.

1. For foam temperatures below 400 °F, a fixed specific heat of 0.30 Btu/lbm-°F and a fixed thermal conductivity of 0.278 Btu-in./hr-ft^2-°F is used for the 12 lb/ft^3 foam. The same fixed specific heat and a fixed thermal conductivity of 0.181 Btu-inch/hr-ft^2-°F is used for the 3 lb/ft^3 foam.

2. Once the temperature at any foam model node exceeds 400 °F, it is assumed to have been reduced to a char in an instantaneous process. The thermal conductance from the node to the surrounding nodes is replaced by that for an equivalent volume of air. The thermal mass of the node is left unchanged.

3. At the initiation of the HAC fire, the foam nodes adjacent to the exterior surfaces of the impact limiter are assumed to instantaneously ablate away. Heat transfer via conduction across an equivalent air gap and radiation assuming an emissivity of 0.9 is used to compute the heat flux from the impact limiter shell to the next set of interior foam nodes of the impact limiter model.

Figures 3.6.3-1 and 3.6.3-2 illustrate a comparison between the Reference 10 fire test data and the thermal model of the test setup using the above three modeling assumptions. Test data for 8 and 16 lb/ft^3 foam is used because it brackets the 12 lb/ft^3 foam data used in this application. The HF and the 12-in. T/C temperatures from the test are used as boundary node inputs in the model.

As expected, the simplified modeling assumptions over estimates the foam temperatures near the HF surface for the 8 lb/ft^3 foam and at all depths for the 16 lb/ft^3 foam. The higher density of the 16 lb/ft^3 foam provides a greater amount of material to outgas and, thus, to transport heat away from the underlying foam. In addition, despite flame temperatures up to 700 °F hotter than specified by 10 CFR 71.73, the test data indicates that undisturbed foam depths of 5 in. for 8 lb/ft^3 foam or 3 in. for 16 lb/ft^3 foam will prevent a rise in the cold face temperature because of the fire accident condition. Direct scaling of these results would yield a requirement for 4 in. of 12 lb/ft^3 foam to provide the same level of thermal protection. However, given the significantly lower 10 CFR 71 HAC fire temperatures, as little as 3 in. of 12 lb/ft^3 foam is expected to provide thermal protection to the package.

While no equivalent test data exists for the 3 lb/ft^3 foam, its performance during the HAC fire can be implied from that seen for the 8, 16, and 24 lb/ft^3 foam data. Assuming the required depth varies in proportion with foam thermal conductivity (i.e., greater depth needed for higher conductivity) and inversely with foam density (i.e., less depth needed as more mass is available for outgassing), then a curve fit of the ratio of k/density versus the required depth of undisturbed foam can be developed. The resulting relationship indicates a need for 8.7 in. of undisturbed 3 lb/ft^3 foam to provide an equivalent level of thermal protection. This conclusion is supported by tests conducted by SANDIA National Laboratory on the SST trailers for Rocky Flats. In these tests, a 1-ft-thick panel of 2 lb/ft^3 foam showed no temperature rise on the cold face 30 minutes after HAC fire initiation.

In conclusion, while it does not provide an accurate representation of the thermal properties of the foam, the thermal assumptions used for the foam are shown by Figures 3.6.3-1 and 3.6.3-2 to provide a conservative estimate of the internal foam temperatures. The test data indicates that the 8.3 in. of 3 lb/ft^3 foam installed at the bottom of the impact limiter is adequate to protect the center of the OCV base plate against the HAC fire temperatures, while depths of 3 in. or greater in the 12 lb/ft^3 foam will provide thermal protection at edges of the OCV base plate.

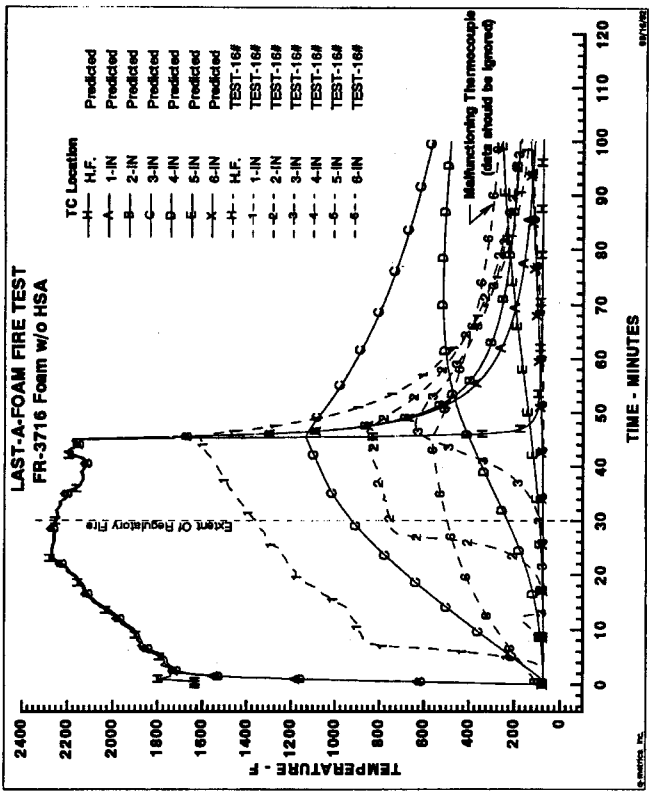


FIGURE 3.6.3-1. Simplified Foam Model Versus Test Data For 16 lb/ft^3 Foam.

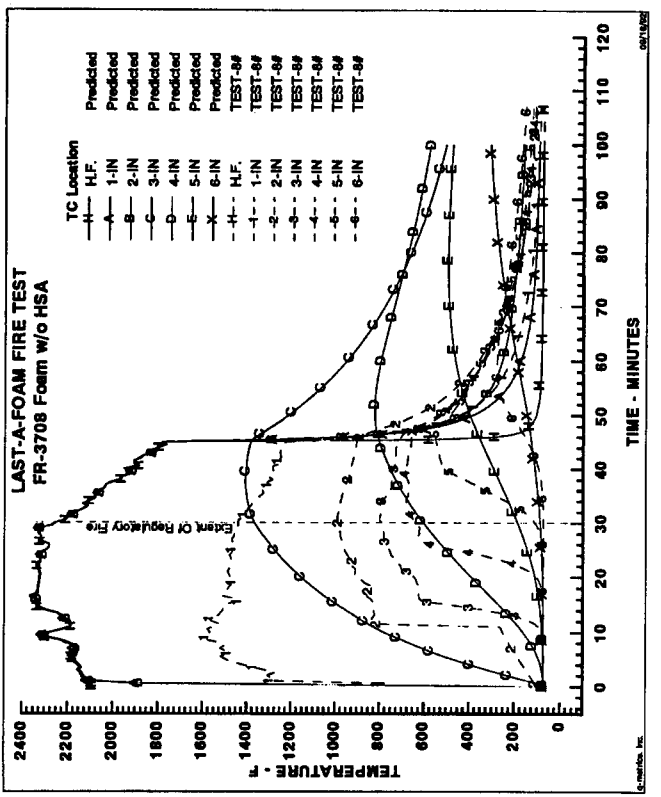


FIGURE 3.6.3-2. Simplified Foam Model Versus Test Data For 8 lb/ft^3 Foam.

3.6.4 SINDA Output For Normal Conditions Of Transport

```
                    SYSTEMS IMPROVED NUMERICAL DIFFERENCING ANALYZER '85 (SINDA '85)

MODEL = GPHS4              NORMAL TRANSPORT CONDITIONS: 100F AMB.,  FULL SOLAR,  GPHS RTG
  STDSTL          SARP Normal Condition Case #1  --  Max. Temperatures For Regulatory Conditions   4/27/94, 10am

 SUBMODEL NAME = PTS7

                                                CALCULATED                                ALLOWED
      MAX DIFF DELTA T PER ITER                 DRLXCC(PTS7       198)=-1.831055E-04 VS. DRLXCA= 2.000000E-03
      MAX ARITH DELTA T PER ITER                ARLXCC(PTS7      1001)=-1.831055E-04 VS. ARLXCA= 5.000000E-02
      MAX SYSTEM ENERGY BALANCE                 EBALSC              = 0.102099       VS. EBALSA * ESUMIS      = 2.00793
                                                                                        EBALSA= 1.000000E-04
      ENERGY INTO AND OUT OF SYS                ESUMIS              =  20079.3       ESUMOS=  20078.8
      MAX NODAL ENERGY BALANCE                  EBALNC(PTS7       366)= 2.629039E-02 VS. EBALNA= 1.000000E-03
      NUMBER OF ITERATIONS                      LOOPCT              =    1201        VS. NLOOPS=    1200
      PROBLEM TIME                              TIMEN               =       0.       VS. TIMEND=       0.

                                                DIFFUSION NODES IN ASCENDING NODE NUMBER ORDER
T   50= 1791.9   T   51= 1169.4   T   52= 1914.1   T   53= 1236.1   T   54= 1804.5   T   55= 1159.0
T   60=  973.41  T   62= 1216.9   T  100=  464.35  T  105=  481.34  T  107=  489.91  T  110=  484.24
T  112=  485.74  T  113=  485.75  T  120=  534.21  T  122=  548.08  T  123=  548.08  T  124=  513.22
T  125=  513.18  T  126=  435.52  T  127=  435.36  T  130=  546.90  T  132=  562.66  T  133=  562.53
T  134=  526.35  T  135=  525.97  T  136=  446.00  T  137=  445.52  T  140=  548.27  T  141=  549.21
T  142=  561.34  T  143=  563.15  T  144=  527.56  T  145=  526.74  T  146=  445.94  T  147=  442.80
T  150=  536.53  T  152=  552.23  T  153=  553.28  T  154=  515.92  T  155=  514.48  T  156=  435.04
T  157=  424.30  T  160=  500.98  T  161=  498.00  T  162=  514.99  T  163=  514.55  T  164=  481.67
T  165=  468.84  T  166=  397.51  T  167=  393.11  T  170=  392.53  T  172=  393.87  T  173=  393.86
T  175=  369.75  T  177=  380.93  T  180=  387.25  T  190=  326.07  T  191=  308.25  T  192=  251.07
T  193=  290.80  T  194=  257.58  T  195=  240.10  T  196=  316.12  T  197=  246.30  T  198=  307.55
T  200=  338.33  T  204=  307.57  T  210=  330.42  T  220=  329.47  T  230=  295.92  T  240=  251.95
T  242=  230.44  T  250=  218.91  T  260=  221.34  T  261=  221.84  T  262=  220.08  T  263=  220.79
T  264=  218.37  T  265=  219.40  T  266=  216.83  T  267=  223.53  T  268=  223.53  T  269=  222.87
T  300=  267.45  T  301=  174.20  T  304=  236.61  T  305=  158.19  T  310=  283.84  T  313=  262.42
T  315=  237.06  T  316=  237.06  T  320=  284.07  T  323=  262.78  T  325=  237.65  T  326=  237.65
T  330=  251.20  T  333=  229.93  T  335=  211.47  T  336=  211.47  T  340=  235.37  T  342=  220.96
T  343=  192.55  T  344=  212.54  T  345=  190.09  T  346=  182.85  T  347=  201.61  T  349=  190.81
T  350=  209.80  T  351=  206.87  T  352=  209.30  T  353=  207.99  T  354=  209.57  T  355=  210.16
T  356=  208.59  T  360=  220.18  T  362=  218.74  T  364=  215.78  T  366=  210.59  T  367=  209.99
T  368=  209.21  T  369=  208.57  T  371=  206.95  T  373=  207.85  T  375=  209.00  T  377=  209.67
T  400=  216.85  T  401=  216.43  T  402=  209.79  T  404=  194.98  T  406=  153.47  T  408=  122.99
T  410=  132.28  T  412=  137.30  T  414=  142.44  T  421=  203.28  T  422=  178.10  T  423=  154.06
T  424=  193.07  T  425=  167.76  T  426=  146.83  T  431=  172.64  T  432=  178.63  T  433=  176.53
T  434=  162.09  T  435=  149.44  T  436=  138.09  T  441=  154.16  T  442=  154.10  T  443=  151.62
T  444=  145.18  T  445=  138.91  T  446=  133.84  T  451=  138.45  T  452=  133.54  T  453=  131.94
```

```
 T   454= 130.05     T   455= 128.45     T   456= 128.46
                ARITHMETIC NODES IN ASCENDING NODE NUMBER ORDER
 T   158= 494.98     T   159= 491.84     T   168= 499.65     T   169= 502.91     T   199= 279.71     T   238= 276.76
 T   311= 260.62     T   312= 260.62     T   321= 261.02     T   322= 261.02     T   331= 228.47     T   332= 228.47
 T   337= 213.14     T   341= 219.45     T   357= 208.60     T   358= 207.05     T   359= 209.54     T   379= 210.26
 T   403= 209.71     T  1000= 244.23     T  1001= 300.51     T  1002= 279.05     T  1003= 260.38     T  1004= 244.59
 T  1005= 243.83     T  1006= 222.37     T  1007= 343.63     T  1008= 327.96     T  1009= 314.27     T  1010= 243.20
 T  1011= 283.30     T  1012= 283.30     T  1013= 246.20     T  1021= 283.53     T  1022= 283.53     T  1023= 246.67
 T  1031= 250.74     T  1032= 250.74     T  1033= 218.09     T  1041= 235.18     T  1042= 235.18     T  1043= 220.99
 T  1044= 220.99     T  1266= 224.79     T  1267= 237.73     T  1268= 233.63     T  1269= 225.52     T  1346= 184.58
 T  1347= 204.76
                   HEATER NODES IN ASCENDING NODE NUMBER ORDER
                                  ++NONE++
                  BOUNDARY NODES IN ASCENDING NODE NUMBER ORDER
 T     1= 100.00     T     2= 100.00     T   901= -999.00     T   902= -999.00

MEAN ICV GAS TEMP= 353.6 F   MEAN ICV GAS PRESSURE= 24.41 PSIA

MEAN ICV-OCV GAS TEMP= 284.6 F   MEAN ICV-OCV GAS PRESSURE= 26.27 PSIA
```

SYSTEMS IMPROVED NUMERICAL DIFFERENCING ANALYZER '85 (SINDA '85)

MODEL = GPHS4 NORMAL TRANSPORT CONDITIONS: -40F AMB., NO SOLAR, GPHS RTG, NO COOLING
STDSTL SARP Normal Condition Case #2 -- Maximum Temperature Gradients 4/28/94, 4pm

SUBMODEL NAME = PTS7

		CALCULATED			ALLOWED	
MAX DIFF DELTA T PER ITER	DRLXCC(PTS7	164)=-1.220703E-04	VS.	DRLXCA=	2.000000E-03	
MAX ARITH DELTA T PER ITER	ARLXCC(PTS7	169)=-1.220703E-04	VS.	ARLXCA=	5.000000E-02	
MAX SYSTEM ENERGY BALANCE	EBALSC	=-0.100992	VS.	EBALSA * ESUMIS	=	1.53585
				EBALSA=	1.000000E-04	
ENERGY INTO AND OUT OF SYS	ESUMIS	= 15358.5		ESUMOS=	15358.9	
MAX NODAL ENERGY BALANCE	EBALNC(PTS7	367)=-2.506668E-02	VS.	EBALNA=	1.000000E-03	
NUMBER OF ITERATIONS	LOOPCT	= 1201	VS.	NLOOPS=	1200	
PROBLEM TIME	TIMEN	= 0.	VS.	TIMEND=	0.	

DIFFUSION NODES IN ASCENDING NODE NUMBER ORDER

T 50=	1727.3	T 51=	1105.1	T 52=	1845.9	T 53=	1168.4	T 54=	1723.3	T 55=	1076.8
T 60=	911.29	T 62=	1125.4	T 100=	404.77	T 105=	420.80	T 107=	428.85	T 110=	422.31
T 112=	423.82	T 113=	423.83	T 120=	470.26	T 122=	484.08	T 123=	484.07	T 124=	447.58
T 125=	447.53	T 126=	361.79	T 127=	361.64	T 130=	481.56	T 132=	497.22	T 133=	497.10
T 134=	459.32	T 135=	458.94	T 136=	370.51	T 137=	370.01	T 140=	482.52	T 141=	484.00
T 142=	495.51	T 143=	497.38	T 144=	459.94	T 145=	458.74	T 146=	369.17	T 147=	364.51
T 150=	465.78	T 152=	481.48	T 153=	482.79	T 154=	443.18	T 155=	442.26	T 156=	352.83
T 157=	339.79	T 160=	417.88	T 161=	417.71	T 162=	431.60	T 163=	431.32	T 164=	395.91
T 165=	382.79	T 166=	298.92	T 167=	293.98	T 170=	288.63	T 172=	289.98	T 173=	289.99
T 175=	260.05	T 177=	273.21	T 180=	281.65	T 190=	205.36	T 191=	184.06	T 192=	114.65
T 193=	160.89	T 194=	123.68	T 195=	103.71	T 196=	189.55	T 197=	110.49	T 198=	183.19
T 200=	244.68	T 204=	203.42	T 210=	228.74	T 220=	220.17	T 230=	172.54	T 240=	116.79
T 242=	89.097	T 250=	73.094	T 260=	75.642	T 261=	76.277	T 262=	73.913	T 263=	74.725
T 264=	71.928	T 265=	73.261	T 266=	70.132	T 267=	78.432	T 268=	78.443	T 269=	77.605
T 300=	147.57	T 301=	-15.935	T 304=	104.81	T 305=	12.079	T 310=	170.76	T 313=	146.94
T 315=	118.48	T 316=	118.48	T 320=	165.30	T 323=	142.23	T 325=	114.73	T 326=	114.73
T 330=	117.43	T 333=	94.005	T 335=	74.430	T 336=	74.430	T 340=	98.262	T 342=	76.850
T 343=	35.294	T 344=	64.665	T 345=	36.235	T 346=	24.359	T 347=	50.443	T 349=	29.793
T 350=	60.819	T 351=	56.913	T 352=	60.183	T 353=	58.378	T 354=	60.511	T 355=	61.312
T 356=	59.221	T 360=	74.322	T 362=	72.396	T 364=	68.676	T 366=	61.869	T 367=	61.118
T 368=	60.230	T 369=	59.493	T 371=	56.899	T 373=	58.073	T 375=	59.661	T 377=	60.642
T 400=	69.881	T 401=	69.280	T 402=	60.846	T 404=	39.732	T 406=	-13.151	T 408=	-34.411
T 410=	-23.433	T 412=	-17.382	T 414=	-11.150	T 421=	54.894	T 422=	27.477	T 423=	1.4094
T 424=	42.564	T 425=	15.210	T 426=	-7.2255	T 431=	12.518	T 432=	21.742	T 433=	20.699
T 434=	7.2220	T 435=	-5.5573	T 436=	-17.306	T 441=	-8.0586	T 442=	-4.2694	T 443=	-5.2707
T 444=	-11.026	T 445=	-17.122	T 446=	-22.065	T 451=	-22.431	T 452=	-24.596	T 453=	-25.408
T 454=	-27.010	T 455=	-28.464	T 456=	-28.099						

ARITHMETIC NODES IN ASCENDING NODE NUMBER ORDER

T	158=	413.78	T	159=	410.60	T	168=	419.26	T	169=	422.46	T	199=	150.05
T	238=	148.32	T	311=	144.99	T	312=	144.99	T	321=	140.36	T	322=	140.36
T	331=	92.385	T	332=	92.385	T	337=	66.337	T	341=	75.005	T	357=	59.147
T	358=	56.842	T	359=	60.489	T	379=	61.447	T	403=	60.705	T	1000=	105.98
T	1001=	173.69	T	1002=	149.11	T	1003=	125.82	T	1004=	106.15	T	1005=	105.24
T	1006=	76.917	T	1007=	228.21	T	1008=	208.28	T	1009=	191.48	T	1010=	105.05
T	1011=	170.32	T	1012=	170.32	T	1013=	128.83	T	1021=	164.88	T	1022=	164.88
T	1023=	124.70	T	1031=	117.09	T	1032=	117.09	T	1033=	81.520	T	1041=	98.145
T	1042=	98.145	T	1043=	76.967	T	1044=	76.967	T	1266=	80.194	T	1267=	98.459
T	1268=	92.145	T	1269=	81.244	T	1346=	29.821	T	1347=	54.501			

HEATER NODES IN ASCENDING NODE NUMBER ORDER
++NONE++
BOUNDARY NODES IN ASCENDING NODE NUMBER ORDER

T	1=	-40.000	T	2=	-40.000	T	901=	-999.00	T	902=	-999.00

MEAN ICV GAS TEMP= 255.9 F MEAN ICV GAS PRESSURE= 21.48 PSIA

MEAN ICV-OCV GAS TEMP= 165.1 F MEAN ICV-OCV GAS PRESSURE= 22.05 PSIA

SYSTEMS IMPROVED NUMERICAL DIFFERENCING ANALYZER '85 (SINDA '85)

MODEL = GPHS4
STDSTL

NORMAL TRANSPORT CONDITIONS: 100F AMB., FULL SOLAR, GPHS RTG, ACTIVE COOLING
SARP Normal Condition Case #3 -- Simulated Conditions In Vented Trailer 4/28/94, 10am

SUBMODEL NAME = PTS7

		CALCULATED		ALLOWED	
MAX DIFF DELTA T PER ITER	DRLXCC(PTS7	143)= 1.831055E-04	VS.	DRLXCA= 2.000000E-03	
MAX ARITH DELTA T PER ITER	ARLXCC(PTS7	1010)=-6.103516E-05	VS.	ARLXCA= 5.000000E-02	
MAX SYSTEM ENERGY BALANCE	EBALSC	=-2.504925E-02	VS.	EBALSA * ESUMIS = 2.00793	
				EBALSA= 1.000000E-04	
ENERGY INTO AND OUT OF SYS	ESUMIS	= 20079.3		ESUMOS= 20079.3	
MAX NODAL ENERGY BALANCE	EBALNC(PTS7	330)=-4.555769E-02	VS.	EBALNA= 1.000000E-03	
NUMBER OF ITERATIONS	LOOPCT	= 1201	VS.	NLOOPS= 1200	
PROBLEM TIME	TIMEN	= 0.	VS.	TIMEND= 0.	

DIFFUSION NODES IN ASCENDING NODE NUMBER ORDER

T 50= 1714.6	T 51= 1094.9	T 52= 1813.0	T 53= 1134.5	T 54= 1688.5	T 55= 1042.0
T 60= 907.85	T 62= 1087.4	T 100= 410.06	T 105= 422.68	T 107= 429.52	T 110= 421.67
T 112= 423.18	T 113= 423.18	T 120= 462.60	T 122= 476.31	T 123= 476.30	T 124= 439.46
T 125= 439.40	T 126= 353.93	T 127= 353.75	T 130= 449.16	T 132= 464.74	T 133= 464.62
T 134= 425.78	T 135= 425.40	T 136= 331.55	T 137= 331.08	T 140= 447.36	T 141= 449.28
T 142= 460.34	T 143= 462.25	T 144= 423.54	T 145= 422.09	T 146= 326.95	T 147= 321.28
T 150= 428.75	T 152= 444.50	T 153= 445.99	T 154= 405.08	T 155= 404.53	T 156= 308.60
T 157= 294.08	T 160= 382.53	T 161= 382.99	T 162= 396.82	T 163= 396.61	T 164= 360.67
T 165= 347.61	T 166= 260.61	T 167= 255.73	T 170= 246.19	T 172= 247.59	T 173= 247.59
T 175= 216.09	T 177= 229.62	T 180= 239.68	T 190= 156.36	T 191= 137.52	T 192= 104.43
T 193= 121.61	T 194= 104.68	T 195= 98.882	T 196= 141.89	T 197= 102.52	T 198= 136.89
T 200= 274.80	T 204= 230.97	T 210= 150.93	T 220= 134.32	T 230= 117.85	T 240= 77.742
T 242= 76.929	T 250= 83.473	T 260= 87.221	T 261= 87.423	T 262= 86.323	T 263= 86.514
T 264= 85.332	T 265= 85.328	T 266= 84.770	T 267= 87.577	T 268= 87.576	T 269= 87.328
T 300= 222.44	T 301= 167.43	T 304= 177.88	T 305= 135.36	T 310= 64.166	T 311= 44.469
T 312= 44.469	T 313= 51.090	T 315= 49.894	T 316= 49.894	T 320= 58.601	T 321= 42.929
T 322= 42.929	T 323= 48.418	T 325= 48.075	T 326= 48.075	T 330= 54.465	T 331= 41.640
T 332= 41.640	T 333= 46.137	T 335= 46.779	T 336= 46.779	T 340= 49.230	T 342= 61.983
T 343= 95.152	T 344= 79.513	T 345= 92.439	T 346= 96.169	T 347= 88.019	T 349= 101.29
T 350= 84.744	T 351= 86.361	T 352= 85.135	T 353= 86.026	T 354= 84.123	T 355= 85.531
T 356= 85.149	T 360= 86.901	T 362= 86.175	T 364= 85.408	T 366= 85.434	T 367= 85.567
T 368= 85.905	T 369= 86.078	T 371= 86.409	T 373= 86.107	T 375= 85.932	T 377= 85.866
T 400= 86.189	T 401= 86.370	T 402= 85.853	T 404= 95.096	T 406= 122.08	T 408= 119.23
T 410= 115.85	T 412= 113.99	T 414= 112.14	T 421= 90.844	T 422= 99.602	T 423= 108.05
T 424= 92.589	T 425= 102.43	T 426= 110.39	T 431= 108.02	T 432= 102.12	T 433= 101.59
T 434= 105.50	T 435= 109.72	T 436= 113.75	T 441= 116.22	T 442= 111.33	T 443= 110.33
T 444= 111.73	T 445= 113.63	T 446= 115.32	T 451= 119.13	T 452= 117.08	T 453= 116.60

```
 T   454=  116.90     T   455=  117.33     T   456=  117.26
                    ARITHMETIC NODES IN ASCENDING NODE NUMBER ORDER
 T   158=  378.76     T   159=  375.61     T   168=  384.37     T   169=  387.65     T   199=  117.90     T   238=  100.38
 T   337=  56.396     T   341=  58.892     T   357=  85.052     T   358=  86.372     T   359=  84.946     T   379=  85.508
 T   403=  85.862     T  1000=  98.657     T  1001=  132.84     T  1002=  117.75     T  1003=  109.76     T  1004=  100.62
 T  1005=  100.21     T  1006=  87.613     T  1007=  182.47     T  1008=  160.95     T  1009=  144.70     T  1010=  91.060
 T  1011=  58.790     T  1012=  58.790     T  1013=  51.070     T  1021=  54.311     T  1022=  54.311     T  1023=  48.926
 T  1031=  50.948     T  1032=  50.948     T  1033=  47.275     T  1041=  47.143     T  1042=  47.143     T  1043=  56.424
 T  1044=  56.424     T  1266=  88.091     T  1267=  93.113     T  1268=  91.698     T  1269=  88.380     T  1346=  94.223
 T  1347=  87.233
                          HEATER NODES IN ASCENDING NODE NUMBER ORDER
                                          ++NONE++
                          BOUNDARY NODES IN ASCENDING NODE NUMBER ORDER
 T     1=  100.00     T     2=  100.00     T   901=  40.000     T   902=  40.000

MEAN ICV GAS TEMP= 212.8 F   MEAN ICV GAS PRESSURE= 20.18 PSIA

MEAN ICV-OCV GAS TEMP= 115.1 F   MEAN ICV-OCV GAS PRESSURE= 20.27 PSIA
```

SYSTEMS IMPROVED NUMERICAL DIFFERENCING ANALYZER '85 (SINDA '85)

MODEL = GPHS4 NORMAL TRANSPORT CONDITIONS: 100F AMB., NO SOLAR, GPHS RTG, NO COOLING
STDSTL SARP Normal Condition Case #4 -- Pre-HAC Steady-State Condition 4/27/94, 11am

SUBMODEL NAME = PTS7

		CALCULATED			ALLOWED	
MAX DIFF DELTA T PER ITER	DRLXCC(PTS7	266)=	1.220703E-04	VS.	DRLXCA=	2.000000E-03
MAX ARITH DELTA T PER ITER	ARLXCC(PTS7	332)=	-1.220703E-04	VS.	ARLXCA=	5.000000E-02
MAX SYSTEM ENERGY BALANCE	EBALSC		-2.956656E-02	VS.	EBALSA * ESUMIS =	1.53585
					EBALSA=	1.000000E-04
ENERGY INTO AND OUT OF SYS	ESUMIS	=	15358.5		ESUMOS=	15359.2
MAX NODAL ENERGY BALANCE	EBALNC(PTS7	320)=	2.964434E-02	VS.	EBALNA=	1.000000E-03
NUMBER OF ITERATIONS	LOOPCT	=	1201	VS.	NLOOPS=	1200
PROBLEM TIME	TIMEN	=	0.	VS.	TIMEND=	0.

DIFFUSION NODES IN ASCENDING NODE NUMBER ORDER

T	50=	1784.1	T	51=	1161.6	T	52=	1906.2	T	53=	1228.3	T	54=	1794.8	T	55=	1149.2
T	60=	965.66	T	62=	1205.9	T	100=	456.68	T	105=	473.64	T	107=	482.18	T	110=	476.45
T	112=	477.96	T	113=	477.97	T	120=	526.41	T	122=	540.27	T	123=	540.27	T	124=	505.22
T	125=	505.17	T	126=	426.55	T	127=	426.39	T	130=	539.37	T	132=	555.11	T	133=	554.99
T	134=	518.63	T	135=	518.25	T	136=	437.36	T	137=	436.88	T	140=	540.69	T	141=	541.68
T	142=	553.75	T	143=	555.57	T	144=	519.77	T	145=	518.91	T	146=	437.15	T	147=	433.87
T	150=	528.30	T	152=	544.00	T	153=	545.07	T	154=	507.45	T	155=	506.06	T	156=	425.53
T	157=	414.54	T	160=	491.06	T	161=	488.42	T	162=	505.02	T	163=	504.59	T	164=	471.41
T	165=	458.54	T	166=	385.75	T	167=	381.28	T	170=	380.03	T	172=	381.37	T	173=	381.37
T	175=	356.51	T	177=	367.96	T	180=	374.45	T	190=	311.58	T	191=	293.15	T	192=	232.57
T	193=	274.73	T	194=	239.80	T	195=	221.17	T	196=	300.87	T	197=	227.71	T	198=	292.42
T	200=	326.59	T	204=	294.26	T	210=	319.47	T	220=	317.83	T	230=	281.23	T	240=	235.01
T	242=	211.22	T	250=	198.13	T	260=	200.58	T	261=	201.12	T	262=	199.22	T	263=	199.97
T	264=	197.41	T	265=	198.54	T	266=	195.77	T	267=	202.97	T	268=	202.97	T	269=	202.25
T	300=	252.66	T	301=	130.46	T	304=	219.55	T	305=	145.52	T	310=	272.10	T	313=	250.65
T	315=	225.25	T	316=	225.25	T	320=	271.83	T	323=	250.54	T	325=	225.39	T	326=	225.39
T	330=	235.36	T	333=	213.80	T	335=	195.49	T	336=	195.49	T	340=	218.59	T	342=	201.28
T	343=	166.88	T	344=	191.16	T	345=	167.59	T	346=	157.83	T	347=	179.40	T	349=	162.29
T	350=	187.94	T	351=	184.48	T	352=	187.39	T	353=	185.80	T	354=	187.66	T	355=	188.38
T	356=	186.57	T	360=	199.36	T	362=	197.79	T	364=	194.58	T	366=	188.86	T	367=	188.21
T	368=	187.40	T	369=	186.71	T	371=	184.46	T	373=	185.56	T	375=	187.00	T	377=	187.86
T	400=	195.76	T	401=	195.33	T	402=	188.03	T	404=	172.19	T	406=	127.92	T	408=	103.95
T	410=	113.04	T	412=	117.97	T	414=	123.06	T	421=	182.44	T	422=	157.84	T	423=	134.39
T	424=	171.82	T	425=	147.36	T	426=	127.17	T	431=	148.96	T	432=	156.11	T	433=	154.61
T	434=	141.35	T	435=	129.42	T	436=	118.61	T	441=	130.70	T	442=	132.49	T	443=	130.85
T	444=	125.07	T	445=	119.23	T	446=	114.48	T	451=	116.68	T	452=	113.43	T	453=	112.30
T	454=	110.65	T	455=	109.19	T	456=	109.27									

ARITHMETIC NODES IN ASCENDING NODE NUMBER ORDER

T	158=	485.30	T	159=	482.14	T	168=	490.07	T	169=	493.31	T	199=	263.19	T	238=	261.10
T	311=	248.85	T	312=	248.85	T	321=	248.78	T	322=	248.78	T	331=	212.30	T	332=	212.30
T	337=	192.49	T	341=	199.68	T	357=	186.50	T	358=	184.52	T	359=	187.65	T	379=	188.50
T	403=	187.92	T	1000=	225.33	T	1001=	284.82	T	1002=	262.45	T	1003=	242.42	T	1004=	225.60
T	1005=	224.80	T	1006=	201.69	T	1007=	329.68	T	1008=	313.51	T	1009=	299.38	T	1010=	224.57
T	1011=	271.57	T	1012=	271.57	T	1013=	234.41	T	1021=	271.30	T	1022=	271.30	T	1023=	234.43
T	1031=	234.91	T	1032=	234.91	T	1033=	202.07	T	1041=	218.41	T	1042=	218.41	T	1043=	201.37
T	1044=	201.37	T	1266=	204.34	T	1267=	218.57	T	1268=	213.98	T	1269=	205.15	T	1346=	162.03
T	1347=	182.70															

HEATER NODES IN ASCENDING NODE NUMBER ORDER
++NONE++

BOUNDARY NODES IN ASCENDING NODE NUMBER ORDER

T	1=	100.00	T	2=	100.00	T	901=	-999.00	T	902=	-999.00

MEAN ICV GAS TEMP= 342.3 F MEAN ICV GAS PRESSURE= 24.07 PSIA

MEAN ICV-OCV GAS TEMP= 270.7 F MEAN ICV-OCV GAS PRESSURE= 25.78 PSIA

SYSTEMS IMPROVED NUMERICAL DIFFERENCING ANALYZER '85 (SINDA '85)

MODEL = GPHS4 NORMAL TRANSPORT CONDITIONS: -20F AMB., NO SOLAR, GPHS RTG, NO COOLING
STDSTL SARP Normal Condition Case #5 -- Alternative Pre-HAC Steady-State Condition 4/28/94, 3pm

SUBMODEL NAME = PTS7

		CALCULATED			ALLOWED	
MAX DIFF DELTA T PER ITER	DRLXCC(PTS7	269)= 6.103516E-05	VS.	DRLXCA= 2.000000E-03		
MAX ARITH DELTA T PER ITER	ARLXCC(PTS7	1010)= 1.220703E-04	VS.	ARLXCA= 5.000000E-02		
MAX SYSTEM ENERGY BALANCE	EBALSC	=-0.184330	VS.	EBALSA * ESUMIS	=	1.53585
				EBALSA= 1.000000E-04		
ENERGY INTO AND OUT OF SYS	ESUMIS	= 15358.5		ESUMOS= 15359.0		
MAX NODAL ENERGY BALANCE	EBALNC(PTS7	379)=-3.368918E-02	VS.	EBALNA= 1.000000E-03		
NUMBER OF ITERATIONS	LOOPCT	= 1201	VS.	NLOOPS= 1200		
PROBLEM TIME	TIMEN	= 0.	VS.	TIMEND= 0.		

DIFFUSION NODES IN ASCENDING NODE NUMBER ORDER

T	50=	1735.3	T	51=	1113.1	T	52=	1854.5	T	53=	1177.0	T	54=	1733.7	T	55=	1087.4						
T	60=	918.88	T	62=	1137.2	T	100=	411.94	T	105=	428.12	T	107=	436.26	T	110=	429.85						
T	112=	431.36	T	113=	431.37	T	120=	478.19	T	122=	492.02	T	123=	492.01	T	124=	455.72						
T	125=	455.67	T	126=	370.97	T	127=	370.81	T	130=	489.81	T	132=	505.49	T	133=	505.36						
T	134=	467.78	T	135=	467.40	T	136=	380.08	T	137=	379.59	T	140=	490.83	T	141=	492.22						
T	142=	503.83	T	143=	505.69	T	144=	468.48	T	145=	467.33	T	146=	378.90	T	147=	374.47						
T	150=	474.77	T	152=	490.47	T	153=	491.74	T	154=	452.43	T	155=	451.43	T	156=	363.33						
T	157=	350.61	T	160=	428.56	T	161=	427.99	T	162=	442.31	T	163=	442.01	T	164=	406.94						
T	165=	393.85	T	166=	311.69	T	167=	306.82	T	170=	302.11	T	172=	303.46	T	173=	303.47						
T	175=	274.30	T	177=	287.21	T	180=	295.33	T	190=	221.13	T	191=	200.27	T	192=	132.17						
T	193=	177.89	T	194=	140.98	T	195=	121.05	T	196=	206.17	T	197=	127.83	T	198=	199.42						
T	200=	256.50	T	204=	216.54	T	210=	242.00	T	220=	234.60	T	230=	188.64	T	240=	134.36						
T	242=	107.21	T	250=	91.611	T	260=	94.141	T	261=	94.762	T	262=	92.469	T	263=	93.272						
T	264=	90.510	T	265=	91.813	T	266=	88.737	T	267=	96.879	T	268=	96.888	T	269=	96.064						
T	300=	163.24	T	301=	5.6490	T	304=	121.89	T	305=	31.927	T	310=	185.75	T	313=	162.31						
T	315=	134.34	T	316=	134.34	T	320=	181.16	T	323=	158.38	T	325=	131.25	T	326=	131.25						
T	330=	134.99	T	333=	111.84	T	335=	92.454	T	336=	92.454	T	340=	116.17	T	342=	95.329						
T	343=	54.821	T	344=	83.413	T	345=	55.691	T	346=	44.196	T	347=	69.542	T	349=	49.439						
T	350=	79.646	T	351=	75.807	T	352=	79.022	T	353=	77.250	T	354=	79.346	T	355=	80.128						
T	356=	78.083	T	360=	92.833	T	362=	90.961	T	364=	87.317	T	366=	80.674	T	367=	79.935						
T	368=	79.054	T	369=	78.321	T	371=	75.793	T	373=	76.956	T	375=	78.519	T	377=	79.477						
T	400=	88.521	T	401=	87.946	T	402=	79.674	T	404=	59.299	T	406=	7.3215	T	408=	-14.560						
T	410=	-3.8032	T	412=	2.1109	T	414=	8.2007	T	421=	73.691	T	422=	46.514	T	423=	20.661						
T	424=	61.576	T	425=	34.461	T	426=	12.198	T	431=	32.480	T	432=	41.453	T	433=	40.324						
T	434=	26.746	T	435=	13.987	T	436=	2.2859	T	441=	12.090	T	442=	15.593	T	443=	14.478						
T	444=	8.6613	T	445=	2.5501	T	446=	-2.4088	T	451=	-2.3523	T	452=	-4.7113	T	453=	-5.5817						
T	454=	-7.2080	T	455=	-8.6772	T	456=	-8.3575																

ARITHMETIC NODES IN ASCENDING NODE NUMBER ORDER

```
T  158= 424.18   T  159= 421.00   T  168= 429.55   T  169= 432.76   T  199= 166.90   T  238= 165.05
T  311= 160.38   T  312= 160.38   T  321= 156.52   T  322= 156.52   T  331= 110.24   T  332= 110.24
T  337= 85.077   T  341= 93.526   T  357= 78.011   T  358= 75.754   T  359= 79.322   T  379= 80.260
T  403= 79.538   T 1000= 123.73   T 1001= 190.22   T 1002= 165.99   T 1003= 143.14   T 1004= 123.88
T 1005= 122.98   T 1006= 95.394   T 1007= 243.22   T 1008= 223.88   T 1009= 207.50   T 1010= 122.81
T 1011= 185.30   T 1012= 185.30   T 1013= 144.50   T 1021= 180.73   T 1022= 180.73   T 1023= 141.07
T 1031= 134.64   T 1032= 134.64   T 1033= 99.467   T 1041= 116.05   T 1042= 116.05   T 1043= 95.445
T 1044= 95.445   T 1266= 98.584   T 1267= 116.27   T 1268= 110.21   T 1269= 99.597   T 1346= 49.414
T 1347= 73.480

                          HEATER NODES IN ASCENDING NODE NUMBER ORDER
                                        ++NONE++
                        BOUNDARY NODES IN ASCENDING NODE NUMBER ORDER
T    1= -20.000   T    2= -20.000   T  901= -999.00   T  902= -999.00

MEAN ICV GAS TEMP= 268.6 F   MEAN ICV GAS PRESSURE= 21.86 PSIA

MEAN ICV-OCV GAS TEMP= 180.7 F   MEAN ICV-OCV GAS PRESSURE= 22.60 PSIA
```

SYSTEMS IMPROVED NUMERICAL DIFFERENCING ANALYZER '85 (SINDA '85)

MODEL = GPHS4 NORMAL TRANSPORT CONDITIONS: 100F AMB., NO SOLAR, GPHS RTG, ACTIVE COOLING
STDSTL SARP Normal Condition Case #6 -- Compliance w/ 10 CFR 71.43(g) 4/27/94, 10am

SUBMODEL NAME = PTS7

		CALCULATED			ALLOWED	
MAX DIFF DELTA T PER ITER	DRLXCC(PTS7	197)=-1.220703E-04	VS.	DRLXCA=	2.000000E-03	
MAX ARITH DELTA T PER ITER	ARLXCC(PTS7	199)= 1.831055E-04	VS.	ARLXCA=	5.000000E-02	
MAX SYSTEM ENERGY BALANCE	EBALSC	=-0.102929	VS.	EBALSA * ESUMIS	= 1.76592	
				EBALSA=	1.000000E-04	
ENERGY INTO AND OUT OF SYS	ESUMIS	= 17659.2		ESUMOS=	17659.6	
MAX NODAL ENERGY BALANCE	EBALNC(PTS7	379)=-3.663889E-02	VS.	EBALNA=	1.000000E-03	
NUMBER OF ITERATIONS	LOOPCT	= 1201	VS.	NLOOPS=	1200	
PROBLEM TIME	TIMEN	= 0.	VS.	TIMEND=	0.	

DIFFUSION NODES IN ASCENDING NODE NUMBER ORDER

T 50=	1711.1	T 51=	1091.1	T 52=	1811.0	T 53=	1132.6	T 54=	1686.6	T 55=	1040.1
T 60=	903.69	T 62=	1085.3	T 100=	405.32	T 105=	418.17	T 107=	425.09	T 110=	417.29
T 112=	418.80	T 113=	418.80	T 120=	458.62	T 122=	472.34	T 123=	472.33	T 124=	435.41
T 125=	435.35	T 126=	349.24	T 127=	349.06	T 130=	447.08	T 132=	462.67	T 133=	462.55
T 134=	423.66	T 135=	423.29	T 136=	329.16	T 137=	328.69	T 140=	445.62	T 141=	447.56
T 142=	458.61	T 143=	460.52	T 144=	421.79	T 145=	420.31	T 146=	324.94	T 147=	319.19
T 150=	427.11	T 152=	442.86	T 153=	444.36	T 154=	403.42	T 155=	402.89	T 156=	306.75
T 157=	292.17	T 160=	380.64	T 161=	381.16	T 162=	394.92	T 163=	394.72	T 164=	358.71
T 165=	345.65	T 166=	258.28	T 167=	253.37	T 170=	244.04	T 172=	245.44	T 173=	245.44
T 175=	213.79	T 177=	227.38	T 180=	237.44	T 190=	153.95	T 191=	134.60	T 192=	95.695
T 193=	117.84	T 194=	97.840	T 195=	89.304	T 196=	138.70	T 197=	92.950	T 198=	133.92
T 200=	265.59	T 204=	220.57	T 210=	148.99	T 220=	133.16	T 230=	116.23	T 240=	74.444
T 242=	69.333	T 250=	71.349	T 260=	74.760	T 261=	75.032	T 262=	73.721	T 263=	74.013
T 264=	72.577	T 265=	72.814	T 266=	71.810	T 267=	75.552	T 268=	75.553	T 269=	75.197
T 300=	208.38	T 301=	121.12	T 304=	162.13	T 305=	122.71	T 310=	63.139	T 311=	44.007
T 312=	44.007	T 313=	50.192	T 315=	48.357	T 316=	48.357	T 320=	57.987	T 321=	42.582
T 322=	42.582	T 323=	47.714	T 325=	46.655	T 326=	46.655	T 330=	53.791	T 331=	41.391
T 332=	41.391	T 333=	45.315	T 335=	45.226	T 336=	45.226	T 340=	48.034	T 342=	55.811
T 343=	71.741	T 344=	66.681	T 345=	72.147	T 346=	71.450	T 347=	70.853	T 349=	73.874
T 350=	69.973	T 351=	70.309	T 352=	70.160	T 353=	70.409	T 354=	69.389	T 355=	70.748
T 356=	69.944	T 360=	74.280	T 362=	73.341	T 364=	72.044	T 366=	70.784	T 367=	70.754
T 368=	70.885	T 369=	70.890	T 371=	70.256	T 373=	70.359	T 375=	70.688	T 377=	70.941
T 400=	72.981	T 401=	73.119	T 402=	70.993	T 404=	75.576	T 406=	88.721	T 408=	98.461
T 410=	95.665	T 412=	94.161	T 414=	92.719	T 421=	76.443	T 422=	83.087	T 423=	89.568
T 424=	76.473	T 425=	84.582	T 426=	91.176	T 431=	82.659	T 432=	80.775	T 433=	81.466
T 434=	86.149	T 435=	90.214	T 436=	93.828	T 441=	88.525	T 442=	88.571	T 443=	89.382
T 444=	91.468	T 445=	93.497	T 446=	95.141	T 451=	93.528	T 452=	95.104	T 453=	95.623

```
 T  454= 96.237    T  455= 96.762    T  456= 96.795
                ARITHMETIC NODES IN ASCENDING NODE NUMBER ORDER
 T  158= 376.91    T  159= 373.76    T  168= 382.54    T  169= 385.82    T  199= 113.02    T  238= 98.039
 T  337= 50.732    T  341= 53.331    T  357= 69.795    T  358= 70.200    T  359= 70.069    T  379= 70.763
 T  403= 70.957    T 1000= 89.781    T 1001= 128.88    T 1002= 112.72    T 1003= 101.93    T 1004= 91.074
 T 1005= 90.587    T 1006= 75.298    T 1007= 180.05    T 1008= 158.43    T 1009= 141.90    T 1010= 83.561
 T 1011= 57.916    T 1012= 57.916    T 1013= 49.621    T 1021= 53.770    T 1022= 53.770    T 1023= 47.618
 T 1031= 50.390    T 1032= 50.390    T 1033= 45.807    T 1041= 46.207    T 1042= 46.207    T 1043= 51.860
 T 1044= 51.860    T 1266= 76.296    T 1267= 83.787    T 1268= 81.436    T 1269= 76.720    T 1346= 72.551
 T 1347= 70.946
                HEATER NODES IN ASCENDING NODE NUMBER ORDER
                                ++NONE++
                BOUNDARY NODES IN ASCENDING NODE NUMBER ORDER
 T    1= 100.00    T    2= 100.00    T  901= 40.000    T  902= 40.000

MEAN ICV GAS TEMP= 209.8 F   MEAN ICV GAS PRESSURE= 20.10 PSIA

MEAN ICV-OCV GAS TEMP= 111.4 F   MEAN ICV-OCV GAS PRESSURE= 20.14 PSIA
```

SYSTEMS IMPROVED NUMERICAL DIFFERENCING ANALYZER '85 (SINDA '85)

MODEL = GPHS4
STDSTL

NORMAL OPERATIONAL CONDITIONS, AMB. TEMP: 70F, NO SOLAR, GPHS RTG, ACTIVE COOLING
SARP Normal Condition Case #7 -- Simulated Conditions At Facility 4/27/94, 9am

SUBMODEL NAME = PTS7

		CALCULATED			ALLOWED	
MAX DIFF DELTA T PER ITER	DRLXCC(PTS7	125)=	1.220703E-04	VS. DRLXCA=	2.000000E-03	
MAX ARITH DELTA T PER ITER	ARLXCC(PTS7	1003)=	6.103516E-05	VS. ARLXCA=	5.000000E-02	
MAX SYSTEM ENERGY BALANCE	EBALSC		=-6.303066E-02	VS. EBALSA * ESUMIS		= 1.54335
				EBALSA=	1.000000E-04	
ENERGY INTO AND OUT OF SYS	ESUMIS		= 15433.5	ESUMOS=	15434.1	
MAX NODAL ENERGY BALANCE	EBALNC(PTS7	332)=	3.486323E-02	VS. EBALNA=	1.000000E-03	
NUMBER OF ITERATIONS	LOOPCT		= 1201	VS. NLOOPS=	1200	
PROBLEM TIME	TIMEN		= 0.	VS. TIMEND=	0.	

DIFFUSION NODES IN ASCENDING NODE NUMBER ORDER

T 50= 1707.0	T 51= 1086.8	T 52= 1808.8	T 53= 1130.5	T 54= 1684.5	T 55= 1038.1
T 60= 898.97	T 62= 1083.4	T 100= 399.98	T 105= 413.08	T 107= 420.07	T 110= 412.32
T 112= 413.83	T 113= 413.84	T 120= 454.08	T 122= 467.81	T 123= 467.80	T 124= 430.78
T 125= 430.72	T 126= 343.88	T 127= 343.70	T 130= 444.69	T 132= 460.29	T 133= 460.17
T 134= 421.24	T 135= 420.87	T 136= 326.43	T 137= 325.96	T 140= 443.65	T 141= 445.60
T 142= 456.63	T 143= 458.54	T 144= 419.78	T 145= 418.28	T 146= 322.65	T 147= 316.80
T 150= 425.30	T 152= 441.04	T 153= 442.54	T 154= 401.58	T 155= 401.08	T 156= 304.69
T 157= 290.05	T 160= 378.70	T 161= 379.27	T 162= 392.97	T 163= 392.78	T 164= 356.70
T 165= 343.64	T 166= 255.88	T 167= 250.96	T 170= 242.12	T 172= 243.52	T 173= 243.52
T 175= 211.83	T 177= 225.43	T 180= 235.54	T 190= 151.94	T 191= 132.31	T 192= 90.221
T 193= 115.11	T 194= 93.445	T 195= 83.442	T 196= 136.17	T 197= 87.424	T 198= 131.61
T 200= 255.02	T 204= 208.71	T 210= 146.72	T 220= 131.82	T 230= 114.79	T 240= 72.194
T 242= 64.675	T 250= 64.084	T 260= 67.236	T 261= 67.550	T 262= 66.136	T 263= 66.488
T 264= 64.923	T 265= 65.301	T 266= 64.048	T 267= 68.280	T 268= 68.282	T 269= 67.871
T 300= 191.87	T 301= 92.096	T 304= 143.86	T 305= 97.247	T 310= 61.853	T 311= 43.416
T 312= 43.416	T 313= 48.951	T 315= 46.016	T 316= 46.016	T 320= 57.217	T 321= 42.164
T 322= 42.164	T 323= 46.743	T 325= 44.520	T 326= 44.520	T 330= 53.108	T 331= 41.125
T 332= 41.125	T 333= 44.410	T 335= 43.209	T 336= 43.209	T 340= 47.089	T 342= 52.087
T 343= 59.315	T 344= 59.141	T 345= 59.994	T 346= 57.818	T 347= 60.681	T 349= 60.180
T 350= 61.271	T 351= 61.027	T 352= 61.336	T 353= 61.300	T 354= 60.761	T 355= 61.957
T 356= 61.036	T 360= 66.659	T 362= 65.615	T 364= 64.035	T 366= 62.062	T 367= 61.932
T 368= 61.906	T 369= 61.806	T 371= 60.964	T 373= 61.205	T 375= 61.680	T 377= 62.011
T 400= 64.959	T 401= 64.977	T 402= 62.080	T 404= 62.680	T 406= 65.221	T 408= 69.348
T 410= 68.686	T 412= 68.349	T 414= 68.092	T 421= 65.397	T 422= 66.435	T 423= 67.541
T 424= 63.615	T 425= 65.819	T 426= 67.565	T 431= 64.209	T 432= 64.050	T 433= 64.395
T 434= 65.950	T 435= 67.162	T 436= 68.183	T 441= 65.721	T 442= 66.226	T 443= 66.660
T 444= 67.382	T 445= 68.016	T 446= 68.515	T 451= 67.409	T 452= 68.236	T 453= 68.494

T 454= 68.717 T 455= 68.892 T 456= 68.937

ARITHMETIC NODES IN ASCENDING NODE NUMBER ORDER

T	158=	374.99	T	159=	371.84	T	168=	380.64	T	169=	383.92	T	199=	109.69	T	238=	96.249
T	337=	47.447	T	341=	50.004	T	357=	60.905	T	358=	60.919	T	359=	61.303	T	379=	61.987
T	403=	62.032	T	1000=	84.154	T	1001=	126.00	T	1002=	109.31	T	1003=	96.946	T	1004=	85.158
T	1005=	84.627	T	1006=	67.865	T	1007=	178.03	T	1008=	156.35	T	1009=	139.67	T	1010=	78.860
T	1011=	56.819	T	1012=	56.819	T	1013=	47.448	T	1021=	53.098	T	1022=	53.098	T	1023=	45.669
T	1031=	49.822	T	1032=	49.822	T	1033=	43.948	T	1041=	45.449	T	1042=	45.449	T	1043=	49.080
T	1044=	49.080	T	1266=	69.147	T	1267=	77.952	T	1268=	75.101	T	1269=	69.645	T	1346=	59.571
T	1347=	61.235															

HEATER NODES IN ASCENDING NODE NUMBER ORDER

++NONE++

BOUNDARY NODES IN ASCENDING NODE NUMBER ORDER

T 1= 70.000 T 2= 70.000 T 901= 40.000 T 902= 40.000

MEAN ICV GAS TEMP= 206.6 F MEAN ICV GAS PRESSURE= 20.00 PSIA

MEAN ICV-OCV GAS TEMP= 107.4 F MEAN ICV-OCV GAS PRESSURE= 20.00 PSIA

SYSTEMS IMPROVED NUMERICAL DIFFERENCING ANALYZER '85 (SINDA '85) PAGE 1/1

MODEL = GPHS4
FWDBCK

LOAD TRANSIENT W/ GPHS RTG, Worst Case Load Procedure Timing Used
Normal Condition Case #8 -- Peak ICV Sidewall Temperature

SUBMODEL NAME = PTS7

		CALCULATED			ALLOWED	
MAX DIFF DELTA T PER ITER	DRLXCC(	0)=	0.	VS. DRLXCA=	2.000000E-03	
MAX ARITH DELTA T PER ITER	ARLXCC(PTS7	1004)=	2.563477E-03	VS. ARLXCA=	5.000000E-02	
MAX DIFF DEL T PER TIME STEP	DTMPCC(PTS7	62)=	3.295898E-03	VS. DTMPCA=	20.0000	
MAX ARITH DEL T PER TIME STEP	ATMPCC(PTS7	1004)=	2.563477E-03	VS. ATMPCA=	50.0000	
MIN STABILITY CRITERIA	CSGMIN(PTS7	161)=	1.522156E-03			
MAX STABILITY CRITERIA	CSGMAX(PTS7	434)=	4.61424			
NUMBER OF ITERATIONS	LOOPCT	=	1	VS. NLOOPT=	800	
PROBLEM TIME	TIMEN	=	8.50000	VS. TIMEND=	8.50000	
TIME STEP USED	DTIMEU	=	8.258820E-04	VS. DTIMEI=	0.	

DIFFUSION NODES IN ASCENDING NODE NUMBER ORDER

T	50=	1743.5	T	51=	1123.9	T	52=	1855.8	T	53=	1179.7	T	54=	1735.7	T	55=	1091.6
T	60=	929.47	T	62=	1137.9	T	100=	428.60	T	105=	444.03	T	107=	451.83	T	110=	445.31
T	112=	446.82	T	113=	446.83	T	120=	492.24	T	122=	505.98	T	123=	505.97	T	124=	470.10
T	125=	470.05	T	126=	388.01	T	127=	387.85	T	130=	495.44	T	132=	511.04	T	133=	510.91
T	134=	473.53	T	135=	473.14	T	136=	386.75	T	137=	386.24	T	140=	495.11	T	141=	496.49
T	142=	508.07	T	143=	509.94	T	144=	472.85	T	145=	471.77	T	146=	384.14	T	147=	379.95
T	150=	478.93	T	152=	494.60	T	153=	495.86	T	154=	456.73	T	155=	455.71	T	156=	368.26
T	157=	355.70	T	160=	435.60	T	161=	434.63	T	162=	449.55	T	163=	449.23	T	164=	414.75
T	165=	401.76	T	166=	322.20	T	167=	317.51	T	170=	310.99	T	172=	312.35	T	173=	312.35
T	175=	283.61	T	177=	296.36	T	180=	303.96	T	190=	231.91	T	191=	210.92	T	192=	127.57
T	193=	179.85	T	194=	154.04	T	195=	112.15	T	196=	215.88	T	197=	129.91	T	198=	210.04
T	200=	290.31	T	204=	260.44	T	210=	246.43	T	220=	234.14	T	230=	201.82	T	240=	127.13
T	242=	94.285	T	250=	77.074	T	260=	77.160	T	261=	77.683	T	262=	76.664	T	263=	77.400
T	264=	75.584	T	265=	76.503	T	266=	74.624	T	267=	81.261	T	268=	81.214	T	269=	80.202
T	300=	172.22	T	301=	88.003	T	304=	135.69	T	305=	94.186	T	310=	61.969	T	311=	43.337
T	312=	43.337	T	313=	48.927	T	315=	45.951	T	316=	45.951	T	320=	56.236	T	321=	42.074
T	322=	42.074	T	323=	46.402	T	325=	44.370	T	326=	44.370	T	330=	52.097	T	331=	41.091
T	332=	41.091	T	333=	44.244	T	335=	43.155	T	336=	43.155	T	340=	47.382	T	342=	54.284
T	343=	63.206	T	344=	65.189	T	345=	64.381	T	346=	60.424	T	347=	66.360	T	349=	64.029
T	350=	68.069	T	351=	67.357	T	352=	68.066	T	353=	67.879	T	354=	67.245	T	355=	69.133
T	356=	67.533	T	360=	76.199	T	362=	75.445	T	364=	73.402	T	366=	69.391	T	367=	69.038
T	368=	68.812	T	369=	68.540	T	371=	67.248	T	373=	67.675	T	375=	68.489	T	377=	69.064
T	400=	73.847	T	401=	73.721	T	402=	69.188	T	404=	67.959	T	406=	66.388	T	408=	69.684
T	410=	69.912	T	412=	69.972	T	414=	70.000	T	421=	72.150	T	422=	70.780	T	423=	70.186
T	424=	69.383	T	425=	69.822	T	426=	69.988	T	431=	68.039	T	432=	68.910	T	433=	69.136
T	434=	69.790	T	435=	69.990	T	436=	70.000	T	441=	67.988	T	442=	69.263	T	443=	69.604
T	444=	69.814	T	445=	69.928	T	446=	69.949	T	451=	68.529	T	452=	69.504	T	453=	69.694
T	454=	69.765	T	455=	69.806	T	456=	69.842									

ARITHMETIC NODES IN ASCENDING NODE NUMBER ORDER

T	158=	430.98	T	159=	427.82	T	168=	436.17	T	169=	439.41	T	199=	176.85	T	205=	164.10
T	238=	169.49	T	337=	48.557	T	341=	51.650	T	357=	67.344	T	358=	67.188	T	359=	68.066
T	379=	69.194	T	403=	69.102	T	1000=	127.97	T	1001=	198.20	T	1002=	177.41	T	1003=	140.97
T	1004=	116.68	T	1005=	115.52	T	1006=	79.223	T	1007=	253.20	T	1008=	234.36	T	1009=	218.09
T	1010=	120.53	T	1011=	56.884	T	1012=	56.884	T	1013=	47.401	T	1021=	52.359	T	1022=	52.359
T	1023=	45.441	T	1031=	49.078	T	1032=	49.078	T	1033=	43.850	T	1041=	45.653	T	1042=	45.653
T	1043=	50.669	T	1044=	50.669	T	1266=	83.385	T	1267=	104.83	T	1268=	98.137	T	1269=	83.631
T	1346=	63.375	T	1347=	67.397												

HEATER NODES IN ASCENDING NODE NUMBER ORDER
++NONE++

BOUNDARY NODES IN ASCENDING NODE NUMBER ORDER

T	1=	70.000	T	2=	70.000	T	901=	40.000	T	902=	40.000

MEAN ICV GAS TEMP= F MEAN ICV GAS PRESSURE= 20.00 PSIA

MEAN ICV-OCV GAS TEMP= 145.3 F MEAN ICV-OCV GAS PRESSURE= 14.70 PSIA

3.6.5 SINDA Output For Hypothetical Accident Conditions Of Transport

The following pages present output from the SINDA computer program for the six HAC load cases (see Table 3.5-1 for a description of each). Because a transient analysis is used to evaluate each HAC load case, it is impractical to present the entire output in this document. Instead, the following pages present output at three significant time points in the HAC fire for each load case. These time points are: (1) time of maximum OCV sidewall temperature (typically at the end of the HAC fire), (2) time of maximum ICV sidewall temperature (typically 40 to 50 minutes into the HAC fire), and (3) the final steady-state package temperatures following the HAC fire.

The printouts are arranged in order of the HAC load case number. Within each HAC load case grouping, printouts are arranged by time point within the HAC fire. Finally, within the printout for each time point, four pages of output are used to present the thermal model node temperatures for each of the four submodel segments (A through D). As such, a total of 12 pages of output are presented for each HAC load case.

Temperatures on each printout are arranged by thermal model node number. All temperatures are in terms of °F, time is listed in hours, and energy is presented as of Btu/hour.

SYSTEMS IMPROVED NUMERICAL DIFFERENCING ANALYZER '85 (SINDA '85) PAGE 1/4

MODEL = DAMAGE1 HAC LOAD CASE NO. 1 CONDITIONS - Circumferential Distribution, 100F 5/2/94
FWDBCK ***** Peak OCV Sidewall Temperature Time Point *****

SUBMODEL NAME = MAIN
PROBLEM TIME TIMEN = 0.500000 VS. TIMEND= 0.500000

DIFFUSION NODES IN ASCENDING NODE NUMBER ORDER

T	267=	218.65	T	268=	218.46	T	269=	214.35			

ARITHMETIC NODES IN ASCENDING NODE NUMBER ORDER

T	201=	780.84	T	1266=	229.11	T	1267=	331.08	T	1268=	299.15	T	1269=	235.85

HEATER NODES IN ASCENDING NODE NUMBER ORDER
++NONE++

BOUNDARY NODES IN ASCENDING NODE NUMBER ORDER
++NONE++

MEAN ICV GAS TEMP= 780.8 F MEAN ICV GAS PRESSURE= 37.19 PSIA
MEAN ICV-OCV GAS TEMP= 841.3 F MEAN ICV-OCV GAS PRESSURE= 45.89 PSIA

SUBMODEL NAME = PTSA

	CALCULATED			ALLOWED	
MAX DIFF DELTA T PER ITER	DRLXCC(PTSA	161)=	1.757812E-02	VS. DRLXCA=	5.000000E-02
MAX ARITH DELTA T PER ITER	ARLXCC(PTSA	1004)=	2.838135E-02	VS. ARLXCA=	0.500000
MAX DIFF DEL T PER TIME STEP	DTMPCC(PTSA	100)=	3.01590	VS. DTMPCA=	10.0000
MAX ARITH DEL T PER TIME STEP	ATMPCC(PTSA	238)=	2.26358	VS. ATMPCA=	100.000
MIN STABILITY CRITERIA	CSGMIN(PTSA	431)=	3.004479E-05		
MAX STABILITY CRITERIA	CSGMAX(PTSA	424)=	1.95845		
NUMBER OF ITERATIONS	LOOPCT	=	5	VS. NLOOPT=	600
PROBLEM TIME	TIMEN	=	0.500000	VS. TIMEND=	0.500000
MEAN PROBLEM TIME	TIMEM	=	0.498793		
AVERAGE TIME STEP USED	DTIMEU	=	9.259260E-04	VS. DTIMEI=	0.

DIFFUSION NODES IN ASCENDING NODE NUMBER ORDER

T	51=	708.54	T	53=	720.70	T	55=	762.31	T	60=	858.68	T	62=	1029.5	T	100=	1016.4
T	105=	913.91	T	107=	868.37	T	110=	823.95	T	112=	823.60	T	113=	826.34	T	120=	716.97
T	122=	714.16	T	123=	721.82	T	124=	711.41	T	125=	716.82	T	126=	709.05	T	127=	710.55
T	130=	696.04	T	132=	695.32	T	133=	699.59	T	134=	694.23	T	135=	697.07	T	136=	694.83
T	137=	695.33	T	140=	684.19	T	141=	682.53	T	142=	684.55	T	143=	686.83	T	144=	684.19
T	145=	686.01	T	146=	686.43	T	147=	687.54	T	150=	695.28	T	152=	695.59	T	153=	696.44
T	154=	694.90	T	155=	695.36	T	156=	695.39	T	157=	695.62	T	160=	709.28	T	161=	704.49
T	162=	710.57	T	163=	709.97	T	164=	709.25	T	165=	708.47	T	166=	709.27	T	167=	709.77
T	170=	690.63	T	172=	690.27	T	173=	690.08	T	175=	682.67	T	177=	682.66	T	180=	670.64
T	190=	677.41	T	191=	788.61	T	192=	294.95	T	193=	703.75	T	194=	387.74	T	196=	594.39
T	198=	794.12	T	200=	1093.5	T	204=	1115.4	T	210=	725.40	T	220=	710.06	T	230=	672.49
T	240=	622.90	T	242=	370.75	T	250=	224.77	T	260=	202.98	T	261=	205.17	T	262=	204.88
T	263=	210.00	T	264=	204.69	T	265=	209.99	T	266=	206.35	T	300=	1229.9	T	304=	1238.3
T	305=	1376.7	T	310=	934.12	T	313=	1106.8	T	315=	1281.3	T	316=	1281.3	T	320=	921.23
T	323=	1097.8	T	325=	1274.7	T	326=	1274.7	T	330=	880.12	T	333=	1053.4	T	335=	1247.2
T	336=	1247.2	T	340=	854.77	T	342=	579.37	T	343=	1035.5	T	344=	332.33	T	345=	965.43
T	346=	1260.0	T	347=	543.93	T	349=	1044.0	T	350=	258.87	T	351=	425.43	T	352=	263.11
T	353=	341.74	T	354=	296.08	T	355=	224.81	T	356=	306.40	T	360=	200.33	T	362=	200.01
T	364=	200.20	T	366=	217.19	T	367=	222.86	T	368=	248.23	T	369=	267.71	T	371=	435.40
T	373=	347.02	T	375=	258.26	T	377=	225.43	T	400=	199.71	T	401=	209.05	T	402=	221.70
T	404=	1202.2	T	406=	1371.8	T	408=	1363.1	T	410=	1411.5	T	412=	1411.0	T	414=	1419.3
T	421=	471.47	T	422=	1414.7	T	423=	1417.5	T	424=	264.28	T	425=	1401.7	T	426=	1404.2

T 431= 1361.8 T 432= 1361.6 T 433= 1348.6 T 434= 1347.3 T 435= 1382.1 T 436= 1363.6
T 950= 903.86

ARITHMETIC NODES IN ASCENDING NODE NUMBER ORDER

T 50= 723.30 T 52= 723.72 T 54= 779.89 T 158= 705.15 T 159= 704.99 T 168= 704.91
T 169= 705.18 T 195= 300.14 T 197= 348.89 T 199= 564.37 T 238= 650.87 T 311= 1123.1
T 312= 1123.1 T 321= 1113.8 T 322= 1113.8 T 331= 1068.0 T 332= 1068.0 T 337= 796.75
T 341= 683.78 T 357= 327.06 T 358= 407.31 T 359= 261.54 T 379= 221.16 T 403= 224.20
T 1000= 333.38 T 1001= 669.84 T 1002= 563.31 T 1003= 370.86 T 1004= 275.89 T 1005= 273.64
T 1006= 210.12 T 1007= 700.42 T 1008= 710.60 T 1009= 764.75 T 1010= 359.26 T 1011= 956.37
T 1012= 956.37 T 1013= 1230.4 T 1021= 943.65 T 1022= 943.65 T 1023= 1223.6 T 1031= 901.96
T 1032= 901.96 T 1033= 1191.1 T 1041= 878.37 T 1042= 878.37 T 1043= 620.10 T 1044= 620.10
T 1346= 1135.0 T 1347= 448.07

HEATER NODES IN ASCENDING NODE NUMBER ORDER
++NONE++

BOUNDARY NODES IN ASCENDING NODE NUMBER ORDER
T 1= 1475.0 T 2= 1424.7

SYSTEMS IMPROVED NUMERICAL DIFFERENCING ANALYZER '85 (SINDA '85) PAGE 2/4

MODEL = DAMAGE1 HAC LOAD CASE NO. 1 CONDITIONS - Circumferential Distribution, 100F 5/2/94
FWDBCK ***** Peak OCV Sidewall Temperature Time Point *****

SUBMODEL NAME = PTSB

	CALCULATED			ALLOWED	
MAX DIFF DELTA T PER ITER	DRLXCC(PTSB	161)=	-2.441406E-03	VS. DRLXCA=	5.000000E-02
MAX ARITH DELTA T PER ITER	ARLXCC(PTSB	1004)=	-7.568359E-03	VS. ARLXCA=	0.500000
MAX DIFF DEL T PER TIME STEP	DTMPCC(PTSB	100)=	2.99857	VS. DTMPCA=	10.0000
MAX ARITH DEL T PER TIME STEP	ATMPCC(PTSB	238)=	2.25650	VS. ATMPCA=	100.000
MIN STABILITY CRITERIA	CSGMIN(PTSB	446)=	3.008679E-05		
MAX STABILITY CRITERIA	CSGMAX(PTSB	434)=	3.26587		
NUMBER OF ITERATIONS	LOOPCT	=	5	VS. NLOOPT=	600
PROBLEM TIME	TIMEN	=	0.500000	VS. TIMEND=	0.500000
MEAN PROBLEM TIME	TIMEM	=	0.498793		
AVERAGE TIME STEP USED	DTIMEU	=	9.259260E-04	VS. DTIMEI=	0.

DIFFUSION NODES IN ASCENDING NODE NUMBER ORDER

T	51=	719.72	T	53=	721.05	T	55=	755.56	T	60=	860.04	T	62=	1027.9	T	100=	1019.4
T	105=	921.45	T	107=	877.87	T	110=	835.48	T	112=	832.67	T	113=	844.45	T	120=	739.21
T	122=	727.75	T	123=	759.86	T	124=	722.99	T	125=	745.54	T	126=	717.04	T	127=	722.72
T	130=	707.88	T	132=	702.91	T	133=	718.38	T	134=	701.33	T	135=	711.96	T	136=	701.06
T	137=	703.37	T	140=	690.20	T	141=	688.45	T	142=	689.17	T	143=	694.94	T	144=	688.89
T	145=	693.14	T	146=	691.25	T	147=	692.94	T	150=	696.72	T	152=	697.14	T	153=	697.19
T	154=	696.91	T	155=	696.86	T	156=	698.39	T	157=	698.62	T	160=	707.03	T	161=	703.09
T	162=	709.52	T	163=	704.92	T	164=	709.05	T	165=	706.38	T	166=	710.86	T	167=	710.82
T	170=	689.87	T	172=	689.85	T	173=	688.09	T	175=	682.42	T	177=	681.87	T	180=	669.44
T	190=	678.59	T	191=	796.23	T	192=	291.58	T	193=	707.14	T	194=	394.09	T	196=	588.44
T	198=	802.12	T	200=	1093.4	T	204=	1115.5	T	210=	725.94	T	220=	710.81	T	230=	679.34
T	240=	623.35	T	242=	372.46	T	250=	224.02	T	260=	202.59	T	261=	204.55	T	262=	202.75
T	263=	205.93	T	264=	203.58	T	265=	208.39	T	266=	205.31	T	300=	1229.8	T	304=	1238.3
T	305=	1376.7	T	310=	934.12	T	313=	1106.7	T	315=	1281.1	T	316=	1281.1	T	320=	920.99
T	323=	1097.3	T	325=	1274.2	T	326=	1274.2	T	330=	881.42	T	333=	1052.8	T	335=	1245.9
T	336=	1245.9	T	340=	854.12	T	342=	578.23	T	343=	1023.7	T	344=	328.47	T	345=	824.62
T	346=	1256.9	T	347=	468.64	T	349=	1040.6	T	350=	252.46	T	351=	418.29	T	352=	253.52
T	353=	336.21	T	354=	288.59	T	355=	217.58	T	356=	292.52	T	360=	200.18	T	362=	199.32
T	364=	199.27	T	366=	211.33	T	367=	213.05	T	368=	219.98	T	369=	229.85	T	371=	427.73
T	373=	341.45	T	375=	252.76	T	377=	216.24	T	400=	199.32	T	401=	208.80	T	402=	211.29
T	404=	934.27	T	406=	1360.3	T	408=	1380.5	T	410=	1406.3	T	412=	1410.4	T	414=	1419.2
T	421=	471.36	T	422=	1414.7	T	423=	1417.5	T	424=	245.79	T	425=	1400.9	T	426=	1406.5
T	431=	1230.5	T	432=	1323.1	T	433=	246.10	T	434=	222.10	T	435=	1386.4	T	436=	1396.6
T	441=	1379.9	T	442=	1370.0	T	443=	1373.2	T	444=	1373.2	T	445=	1391.4	T	446=	1380.9
T	451=	1372.2	T	452=	1360.6	T	453=	1376.5	T	454=	1381.2	T	455=	1405.8	T	456=	1391.9
T	950=	908.53															

ARITHMETIC NODES IN ASCENDING NODE NUMBER ORDER

T	50=	732.23	T	52=	724.21	T	54=	774.54	T	158=	704.21	T	159=	703.56	T	168=	703.47

T	169=	703.58	T	195=	291.75	T	197=	350.35	T	199=	587.91	T	238=	654.94	T	311=	1123.0
T	312=	1123.0	T	321=	1113.4	T	322=	1113.4	T	331=	1067.5	T	332=	1067.5	T	337=	795.10
T	341=	682.50	T	357=	316.94	T	358=	398.82	T	359=	253.56	T	379=	213.47	T	403=	214.60
T	1000=	317.91	T	1001=	672.92	T	1002=	581.01	T	1003=	368.92	T	1004=	272.98	T	1005=	270.76
T	1006=	208.02	T	1007=	702.12	T	1008=	713.42	T	1009=	770.89	T	1010=	379.72	T	1011=	956.36
T	1012=	956.36	T	1013=	1230.3	T	1021=	943.37	T	1022=	943.37	T	1023=	1223.1	T	1031=	903.08
T	1032=	903.08	T	1033=	1189.9	T	1041=	877.66	T	1042=	877.66	T	1043=	618.91	T	1044=	618.91
T	1346=	1057.4	T	1347=	381.55												

HEATER NODES IN ASCENDING NODE NUMBER ORDER
++NONE++

BOUNDARY NODES IN ASCENDING NODE NUMBER ORDER

T	1=	1475.0	T	2=	1424.7

SYSTEMS IMPROVED NUMERICAL DIFFERENCING ANALYZER '85 (SINDA '85) PAGE 3/4

MODEL = DAMAGE1
FWDBCK

HAC LOAD CASE NO. 1 CONDITIONS - Circumferential Distribution, 100F
***** Peak OCV Sidewall Temperature Time Point *****

5/2/94

SUBMODEL NAME = PTSC

		CALCULATED		ALLOWED
MAX DIFF DELTA T PER ITER	DRLXCC(PTSC	161)=-3.051758E-03	VS. DRLXCA=	5.000000E-02
MAX ARITH DELTA T PER ITER	ARLXCC(PTSC	1004)=-4.394531E-03	VS. ARLXCA=	0.500000
MAX DIFF DEL T PER TIME STEP	DTMPCC(PTSC	100)= 2.78018	VS. DTMPCA=	10.0000
MAX ARITH DEL T PER TIME STEP	ATMPCC(PTSC	238)= 2.29459	VS. ATMPCA=	100.000
MIN STABILITY CRITERIA	CSGMIN(PTSC	446)= 3.008758E-05		
MAX STABILITY CRITERIA	CSGMAX(PTSC	434)= 3.26588		
NUMBER OF ITERATIONS	LOOPCT	= 5	VS. NLOOPT=	600
PROBLEM TIME	TIMEN	= 0.500000	VS. TIMEND=	0.500000
MEAN PROBLEM TIME	TIMEM	= 0.498793		
AVERAGE TIME STEP USED	DTIMEU	= 9.259260E-04	VS. DTIMEI=	0.

DIFFUSION NODES IN ASCENDING NODE NUMBER ORDER

T	51=	755.27	T	53=	720.64	T	55=	732.40	T	60=	866.26	T	62=	1025.6	T	100=	1021.6
T	105=	955.45	T	107=	928.07	T	110=	911.39	T	112=	906.03	T	113=	913.26	T	120=	830.01
T	122=	815.18	T	123=	834.80	T	124=	830.48	T	125=	843.38	T	126=	857.08	T	127=	859.27
T	130=	751.43	T	132=	744.28	T	133=	753.94	T	134=	751.90	T	135=	758.30	T	136=	766.20
T	137=	767.35	T	140=	709.70	T	141=	709.65	T	142=	707.67	T	143=	711.18	T	144=	710.48
T	145=	713.31	T	146=	719.51	T	147=	720.97	T	150=	696.18	T	152=	697.00	T	153=	696.84
T	154=	697.12	T	155=	696.40	T	156=	699.82	T	157=	699.13	T	160=	693.11	T	161=	694.59
T	162=	696.28	T	163=	693.27	T	164=	694.41	T	165=	691.95	T	166=	694.08	T	167=	693.64
T	170=	678.18	T	172=	678.95	T	173=	677.70	T	175=	679.11	T	177=	674.76	T	180=	681.65
T	190=	672.45	T	191=	795.67	T	192=	291.55	T	193=	709.23	T	194=	394.58	T	196=	584.36
T	198=	801.69	T	200=	1076.2	T	204=	1082.4	T	210=	735.62	T	220=	714.26	T	230=	654.19
T	240=	621.29	T	242=	372.08	T	250=	223.96	T	260=	202.52	T	261=	204.46	T	262=	202.66
T	263=	205.81	T	264=	203.52	T	265=	208.31	T	266=	205.27	T	300=	1225.2	T	304=	1229.6
T	305=	1375.5	T	310=	937.55	T	313=	1108.6	T	315=	1281.8	T	316=	1281.8	T	320=	922.26
T	323=	1098.0	T	325=	1274.5	T	326=	1274.5	T	330=	871.39	T	333=	1048.3	T	335=	1244.1
T	336=	1244.1	T	340=	851.15	T	342=	577.04	T	343=	1023.4	T	344=	328.14	T	345=	823.75
T	346=	1256.4	T	347=	468.32	T	349=	1040.4	T	350=	252.35	T	351=	418.17	T	352=	253.40
T	353=	336.13	T	354=	288.44	T	355=	217.50	T	356=	292.37	T	360=	200.14	T	362=	199.28
T	364=	199.25	T	366=	211.26	T	367=	212.95	T	368=	219.78	T	369=	229.57	T	371=	427.60
T	373=	341.37	T	375=	252.74	T	377=	216.21	T	400=	199.31	T	401=	208.79	T	402=	211.26
T	404=	934.19	T	406=	1360.1	T	408=	1380.5	T	410=	1406.3	T	412=	1410.4	T	414=	1419.2
T	421=	471.36	T	422=	1414.7	T	423=	1417.5	T	424=	245.79	T	425=	1400.9	T	426=	1406.5
T	431=	1230.3	T	432=	1322.9	T	433=	246.10	T	434=	222.10	T	435=	1386.4	T	436=	1396.6
T	441=	1379.9	T	442=	1369.9	T	443=	1373.2	T	444=	1373.2	T	445=	1391.4	T	446=	1380.9
T	451=	1372.2	T	452=	1360.5	T	453=	1376.5	T	454=	1381.2	T	455=	1405.8	T	456=	1391.9
T	950=	908.86															

ARITHMETIC NODES IN ASCENDING NODE NUMBER ORDER

T	50=	760.60	T	52=	724.33	T	54=	756.23	T	158=	694.67	T	159=	694.04	T	168=	694.42		

T	169=	694.70	T	195=	291.52	T	197=	350.38	T	199=	588.51	T	238=	639.81	T	311=	1124.8
T	312=	1124.8	T	321=	1114.1	T	322=	1114.1	T	331=	1063.1	T	332=	1063.1	T	337=	793.90
T	341=	681.14	T	357=	316.80	T	358=	398.68	T	359=	253.45	T	379=	213.39	T	403=	214.57
T	1000=	318.05	T	1001=	671.67	T	1002=	581.39	T	1003=	368.62	T	1004=	272.93	T	1005=	270.71
T	1006=	207.92	T	1007=	698.33	T	1008=	709.35	T	1009=	769.26	T	1010=	379.78	T	1011=	959.66
T	1012=	959.66	T	1013=	1231.4	T	1021=	944.60	T	1022=	944.60	T	1023=	1223.5	T	1031=	893.45
T	1032=	893.45	T	1033=	1187.3	T	1041=	874.60	T	1042=	874.60	T	1043=	617.45	T	1044=	617.45
T	1346=	1056.7	T	1347=	381.26												

HEATER NODES IN ASCENDING NODE NUMBER ORDER
++NONE++
BOUNDARY NODES IN ASCENDING NODE NUMBER ORDER

T	1=	1475.0	T	2=	1424.7

SYSTEMS IMPROVED NUMERICAL DIFFERENCING ANALYZER '85 (SINDA '85) PAGE 4/4

MODEL = DAMAGE1 HAC LOAD CASE NO. 1 CONDITIONS - Circumferential Distribution, 100F 5/2/94
FWDBCK ***** Peak OCV Sidewall Temperature Time Point *****

SUBMODEL NAME = PTSD

	CALCULATED		ALLOWED
MAX DIFF DELTA T PER ITER	DRLXCC(PTSD	161)=-2.929688E-03	VS. DRLXCA= 5.000000E-02
MAX ARITH DELTA T PER ITER	ARLXCC(PTSD	1004)=-6.408691E-03	VS. ARLXCA= 0.500000
MAX DIFF DEL T PER TIME STEP	DTMPCC(PTSD	100)= 2.77335	VS. DTMPCA= 10.0000
MAX ARITH DEL T PER TIME STEP	ATMPCC(PTSD	238)= 2.28043	VS. ATMPCA= 100.000
MIN STABILITY CRITERIA	CSGMIN(PTSD	446)= 3.008726E-05	
MAX STABILITY CRITERIA	CSGMAX(PTSD	434)= 3.26587	
NUMBER OF ITERATIONS	LOOPCT	= 5	VS. NLOOPT= 600
PROBLEM TIME	TIMEN	= 0.500000	VS. TIMEND= 0.500000
MEAN PROBLEM TIME	TIMEM	= 0.498793	
AVERAGE TIME STEP USED	DTIMEU	= 9.259260E-04	VS. DTIMEI= 0.

DIFFUSION NODES IN ASCENDING NODE NUMBER ORDER

T	51=	763.23	T	53=	720.66	T	55=	726.89	T	60=	867.25	T	62=	1024.2	T	100=	1024.0
T	105=	961.12	T	107=	935.15	T	110=	919.76	T	112=	919.41	T	113=	920.06	T	120=	845.16
T	122=	842.07	T	123=	844.29	T	124=	849.80	T	125=	851.09	T	126=	864.05	T	127=	864.01
T	130=	759.89	T	132=	758.17	T	133=	759.40	T	134=	762.51	T	135=	763.18	T	136=	771.25
T	137=	771.23	T	140=	714.34	T	141=	714.27	T	142=	714.15	T	143=	714.78	T	144=	715.96
T	145=	716.78	T	146=	723.16	T	147=	724.16	T	150=	698.12	T	152=	698.51	T	153=	698.64
T	154=	699.16	T	155=	698.79	T	156=	702.99	T	157=	702.59	T	160=	692.15	T	161=	694.12
T	162=	693.22	T	163=	693.02	T	164=	693.14	T	165=	693.02	T	166=	696.20	T	167=	696.36
T	170=	676.73	T	172=	676.67	T	173=	676.44	T	175=	676.92	T	177=	672.65	T	180=	679.46
T	190=	670.80	T	191=	792.22	T	192=	291.08	T	193=	708.30	T	194=	393.54	T	196=	583.16
T	198=	798.38	T	200=	1076.4	T	204=	1083.0	T	210=	736.38	T	220=	714.78	T	230=	666.77
T	240=	622.70	T	242=	372.27	T	250=	223.97	T	260=	202.50	T	261=	204.43	T	262=	202.63
T	263=	205.77	T	264=	203.51	T	265=	208.29	T	266=	205.27	T	300=	1225.3	T	304=	1229.7
T	305=	1375.5	T	310=	937.75	T	313=	1108.7	T	315=	1281.9	T	316=	1281.9	T	320=	922.41
T	323=	1098.1	T	325=	1274.5	T	326=	1274.5	T	330=	876.24	T	333=	1050.5	T	335=	1244.9
T	336=	1244.9	T	340=	852.70	T	342=	577.62	T	343=	1023.5	T	344=	328.27	T	345=	823.81
T	346=	1256.6	T	347=	468.34	T	349=	1040.5	T	350=	252.37	T	351=	418.20	T	352=	253.42
T	353=	336.15	T	354=	288.48	T	355=	217.50	T	356=	292.39	T	360=	200.14	T	362=	199.27
T	364=	199.25	T	366=	211.26	T	367=	212.96	T	368=	219.78	T	369=	229.57	T	371=	427.64
T	373=	341.39	T	375=	252.74	T	377=	216.21	T	400=	199.31	T	401=	208.79	T	402=	211.26
T	404=	934.20	T	406=	1360.2	T	408=	1380.5	T	410=	1406.3	T	412=	1410.4	T	414=	1419.2
T	421=	471.36	T	422=	1414.7	T	423=	1417.5	T	424=	245.79	T	425=	1400.9	T	426=	1406.5
T	431=	1230.4	T	432=	1323.0	T	433=	246.10	T	434=	222.10	T	435=	1386.4	T	436=	1396.6
T	441=	1379.9	T	442=	1370.0	T	443=	1373.2	T	444=	1373.2	T	445=	1391.4	T	446=	1380.9
T	451=	1372.2	T	452=	1360.6	T	453=	1376.5	T	454=	1381.2	T	455=	1405.8	T	456=	1391.9
T	950=	905.90															

ARITHMETIC NODES IN ASCENDING NODE NUMBER ORDER

T	50=	766.93	T	52=	724.45	T	54=	751.81	T	158=	694.14	T	159=	694.10	T	168=	693.96

```
T  169= 694.11    T  195= 291.07    T  197= 349.51    T  199= 587.00    T  238= 647.54    T  311= 1124.9
T  312= 1124.9    T  321= 1114.2    T  322= 1114.2    T  331= 1065.2    T  332= 1065.2    T  337= 794.48
T  341= 681.81    T  357= 316.83    T  358= 398.72    T  359= 253.46    T  379= 213.39    T  403= 214.58
T 1000= 317.41    T 1001= 669.26    T 1002= 579.69    T 1003= 367.73    T 1004= 272.55    T 1005= 270.34
T 1006= 207.87    T 1007= 696.10    T 1008= 707.09    T 1009= 766.17    T 1010= 379.29    T 1011= 959.85
T 1012= 959.85    T 1013= 1231.4    T 1021= 944.74    T 1022= 944.74    T 1023= 1223.5    T 1031= 898.10
T 1032= 898.10    T 1033= 1188.6    T 1041= 876.18    T 1042= 876.18    T 1043= 618.16    T 1044= 618.16
T 1346= 1056.8    T 1347= 381.27
                  HEATER NODES IN ASCENDING NODE NUMBER ORDER
                                    ++NONE++
                  BOUNDARY NODES IN ASCENDING NODE NUMBER ORDER
T    1= 1475.0    T    2= 1424.7

RESTART RECORD NUMBER       5852 WRITTEN FOR TIMEN =  0.500000
```

```
                    SYSTEMS IMPROVED NUMERICAL DIFFERENCING ANALYZER '85 (SINDA '85)                PAGE   1/4

MODEL = DAMAGE1          HAC LOAD CASE NO. 1 CONDITIONS - Circumferential Distribution, 100F              5/2/94
  FWDBCK                 *****      Peak ICV Sidewall Temperature Time Point      *****

 SUBMODEL NAME = MAIN

       PROBLEM TIME                    TIMEN                  = 0.700000     VS. TIMEND=  12.0000
                                  DIFFUSION NODES IN ASCENDING NODE NUMBER ORDER
  T   267=  228.80     T   268=  228.57     T   269=  223.25
                                  ARITHMETIC NODES IN ASCENDING NODE NUMBER ORDER
  T   201=  835.47     T  1266=  241.81     T  1267=  370.34     T  1268=  327.36     T  1269=  249.95
                                  HEATER NODES IN ASCENDING NODE NUMBER ORDER
                                        ++NONE++
                                  BOUNDARY NODES IN ASCENDING NODE NUMBER ORDER
                                        ++NONE++
MEAN ICV GAS TEMP= 835.5 F   MEAN ICV GAS PRESSURE= 38.88 PSIA
MEAN ICV-OCV GAS TEMP= 790.8 F   MEAN ICV-OCV GAS PRESSURE= 44.11 PSIA


 SUBMODEL NAME = PTSA
                                  CALCULATED                                  ALLOWED
       MAX DIFF DELTA T PER ITER  DRLXCC(PTSA      161)= 2.197266E-02 VS. DRLXCA= 5.000000E-02
       MAX ARITH DELTA T PER ITER ARLXCC(PTSA      337)=-0.121582     VS. ARLXCA= 0.500000
       MAX DIFF DEL T PER TIME STEP DTMPCC(PTSA    423)= -2.65891     VS. DTMPCA=  10.0000
       MAX ARITH DEL T PER TIME STEP ATMPCC(PTSA  1346)= -1.74936     VS. ATMPCA=  100.000
       MIN STABILITY CRITERIA     CSGMIN(PTSA      431)= 1.479723E-04
       MAX STABILITY CRITERIA     CSGMAX(PTSA      424)=  2.06472
       NUMBER OF ITERATIONS       LOOPCT              =  3           VS. NLOOPT=  600
       PROBLEM TIME               TIMEN               = 0.700000     VS. TIMEND=  12.0000
       MEAN PROBLEM TIME          TIMEM               = 0.699196
       AVERAGE TIME STEP USED     DTIMEU              = 8.771930E-04 VS. DTIMEI=  0.

                                  DIFFUSION NODES IN ASCENDING NODE NUMBER ORDER
  T    51=  751.50     T    53=  737.60     T    55=  765.44     T    60=  860.20     T    62=  978.56     T   100=  966.60
  T   105=  918.62     T   107=  895.74     T   110=  869.19     T   112=  869.15     T   113=  870.65     T   120=  801.07
  T   122=  798.54     T   123=  802.95     T   124=  798.42     T   125=  801.46     T   126=  798.39     T   127=  799.15
  T   130=  782.12     T   132=  780.29     T   133=  783.25     T   134=  781.82     T   135=  783.74     T   136=  784.85
  T   137=  785.09     T   140=  773.05     T   141=  773.09     T   142=  771.88     T   143=  774.01     T   144=  772.94
  T   145=  774.58     T   146=  775.87     T   147=  776.54     T   150=  772.35     T   152=  771.10     T   153=  772.76
  T   154=  772.54     T   155=  773.72     T   156=  775.61     T   157=  776.08     T   160=  776.42     T   161=  775.28
  T   162=  775.98     T   163=  776.74     T   164=  776.90     T   165=  777.73     T   166=  779.78     T   167=  780.38
  T   170=  761.11     T   172=  760.58     T   173=  761.05     T   175=  752.87     T   177=  753.67     T   180=  743.05
  T   190=  752.61     T   191=  824.23     T   192=  321.59     T   193=  776.88     T   194=  431.07     T   196=  697.37
  T   198=  829.20     T   200=  997.75     T   204=  992.32     T   210=  812.97     T   220=  793.93     T   230=  765.22
  T   240=  703.60     T   242=  439.65     T   250=  251.76     T   260=  205.39     T   261=  208.29     T   262=  210.61
  T   263=  217.62     T   264=  215.64     T   265=  222.96     T   266=  222.67     T   300=  897.55     T   304=  902.07
  T   305=  622.74     T   310=  802.45     T   313=  732.43     T   315=  620.26     T   316=  620.26     T   320=  788.38
  T   323=  723.03     T   325=  615.88     T   326=  615.88     T   330=  765.69     T   333=  704.38     T   335=  623.92
  T   336=  623.92     T   340=  730.71     T   342=  542.45     T   343=  664.08     T   344=  368.67     T   345=  821.36
  T   346=  735.82     T   347=  562.89     T   349=  573.84     T   350=  296.89     T   351=  357.36     T   352=  301.43
  T   353=  329.21     T   354=  328.04     T   355=  254.06     T   356=  336.09     T   360=  202.06     T   362=  203.75
  T   364=  210.91     T   366=  247.45     T   367=  255.19     T   368=  279.35     T   369=  307.65     T   371=  361.36
  T   373=  334.87     T   375=  280.23     T   377=  250.21     T   400=  205.93     T   401=  218.15     T   402=  246.46
  T   404=  848.82     T   406=  716.35     T   408=  746.83     T   410=  733.05     T   412=  783.00     T   414=  723.80
```

T	421=	494.30	T	422=	754.86	T	423=	744.72	T	424=	304.83	T	425=	891.13	T	426=	821.27
T	431=	750.19	T	432=	848.12	T	433=	921.74	T	434=	919.88	T	435=	851.12	T	436=	748.56
T	950=	932.01															

ARITHMETIC NODES IN ASCENDING NODE NUMBER ORDER

T	50=	759.30	T	52=	740.75	T	54=	780.27	T	158=	775.53	T	159=	775.79	T	168=	775.36
T	169=	775.34	T	195=	325.43	T	197=	379.88	T	199=	609.87	T	238=	738.38	T	311=	714.51
T	312=	714.51	T	321=	705.26	T	322=	705.26	T	331=	686.91	T	332=	686.91	T	337=	612.15
T	341=	584.42	T	357=	338.29	T	358=	358.32	T	359=	299.37	T	379=	251.96	T	403=	248.95
T	1000=	363.62	T	1001=	720.21	T	1002=	606.62	T	1003=	402.58	T	1004=	297.96	T	1005=	295.12
T	1006=	215.88	T	1007=	765.90	T	1008=	773.46	T	1009=	808.71	T	1010=	405.66	T	1011=	796.90
T	1012=	796.90	T	1013=	657.21	T	1021=	783.24	T	1022=	783.24	T	1023=	651.06	T	1031=	761.33
T	1032=	761.33	T	1033=	649.37	T	1041=	727.94	T	1042=	727.94	T	1043=	547.17	T	1044=	547.17
T	1346=	758.10	T	1347=	462.48														

HEATER NODES IN ASCENDING NODE NUMBER ORDER

++NONE++

BOUNDARY NODES IN ASCENDING NODE NUMBER ORDER

T	1=	100.00	T	2=	100.00

SYSTEMS IMPROVED NUMERICAL DIFFERENCING ANALYZER '85 (SINDA '85) PAGE 2/4

MODEL = DAMAGE1 HAC LOAD CASE NO. 1 CONDITIONS - Circumferential Distribution, 100F 5/2/94
FWDBCK ***** Peak ICV Sidewall Temperature Time Point *****

SUBMODEL NAME = PTSB

	CALCULATED			ALLOWED	
MAX DIFF DELTA T PER ITER	DRLXCC(PTSB	161)=	2.124023E-02	VS. DRLXCA=	5.000000E-02
MAX ARITH DELTA T PER ITER	ARLXCC(PTSB	337)=	-0.120361	VS. ARLXCA=	0.500000
MAX DIFF DEL T PER TIME STEP	DTMPCC(PTSB	423)=	-2.65829	VS. DTMPCA=	10.0000
MAX ARITH DEL T PER TIME STEP	ATMPCC(PTSB	1346)=	-1.40927	VS. ATMPCA=	100.000
MIN STABILITY CRITERIA	CSGMIN(PTSB	455)=	1.701538E-04		
MAX STABILITY CRITERIA	CSGMAX(PTSB	434)=	3.55931		
NUMBER OF ITERATIONS	LOOPCT	=	3	VS. NLOOPT=	600
PROBLEM TIME	TIMEN	=	0.700000	VS. TIMEND=	12.0000
MEAN PROBLEM TIME	TINEM	=	0.699196		
AVERAGE TIME STEP USED	DTIMEU	=	8.771930E-04	VS. DTIMEI=	0.

DIFFUSION NODES IN ASCENDING NODE NUMBER ORDER

T	51=	765.93	T	53=	741.58	T	55=	762.74	T	60=	862.90	T	62=	976.91	T	100=	967.85
T	105=	922.72	T	107=	900.95	T	110=	875.38	T	112=	874.07	T	113=	879.76	T	120=	813.21
T	122=	806.38	T	123=	823.01	T	124=	805.26	T	125=	816.68	T	126=	803.39	T	127=	805.93
T	130=	790.00	T	132=	785.56	T	133=	795.20	T	134=	786.94	T	135=	793.39	T	136=	789.58
T	137=	790.75	T	140=	778.76	T	141=	778.83	T	142=	776.34	T	143=	781.27	T	144=	777.53
T	145=	781.08	T	146=	780.56	T	147=	781.62	T	150=	775.81	T	152=	774.09	T	153=	776.10
T	154=	775.99	T	155=	777.47	T	156=	779.82	T	157=	780.41	T	160=	777.49	T	161=	776.99
T	162=	777.37	T	163=	776.00	T	164=	779.11	T	165=	779.17	T	166=	783.43	T	167=	783.83
T	170=	762.95	T	172=	762.40	T	173=	761.95	T	175=	754.75	T	177=	755.37	T	180=	743.43
T	190=	755.50	T	191=	833.75	T	192=	316.60	T	193=	781.95	T	194=	439.38	T	196=	692.69
T	198=	839.10	T	200=	996.85	T	204=	992.13	T	210=	813.98	T	220=	795.44	T	230=	770.59
T	240=	705.41	T	242=	446.47	T	250=	250.38	T	260=	204.71	T	261=	207.28	T	262=	206.98
T	263=	211.21	T	264=	213.35	T	265=	220.22	T	266=	219.98	T	300=	896.85	T	304=	901.87
T	305=	622.69	T	310=	802.95	T	313=	732.83	T	315=	620.65	T	316=	620.65	T	320=	789.07
T	323=	723.64	T	325=	616.61	T	326=	616.61	T	330=	768.39	T	333=	706.14	T	335=	625.71
T	336=	625.71	T	340=	731.64	T	342=	541.83	T	343=	660.80	T	344=	360.53	T	345=	737.02
T	346=	729.54	T	347=	502.77	T	349=	567.64	T	350=	283.74	T	351=	344.06	T	352=	284.96
T	353=	316.83	T	354=	314.70	T	355=	239.97	T	356=	317.36	T	360=	201.72	T	362=	202.25
T	364=	208.16	T	366=	235.07	T	367=	238.57	T	368=	248.42	T	369=	265.39	T	371=	347.78
T	373=	323.00	T	375=	269.17	T	377=	236.72	T	400=	204.95	T	401=	217.43	T	402=	232.23
T	404=	793.80	T	406=	740.80	T	408=	688.12	T	410=	765.83	T	412=	784.33	T	414=	723.82
T	421=	494.09	T	422=	754.88	T	423=	744.88	T	424=	277.90	T	425=	891.88	T	426=	829.24
T	431=	794.80	T	432=	952.46	T	433=	292.39	T	434=	258.48	T	435=	965.14	T	436=	817.34
T	441=	691.85	T	442=	775.21	T	443=	796.39	T	444=	796.17	T	445=	785.91	T	446=	693.36
T	451=	713.95	T	452=	739.71	T	453=	734.47	T	454=	737.73	T	455=	763.64	T	456=	727.46
T	950=	938.32															

ARITHMETIC NODES IN ASCENDING NODE NUMBER ORDER

T	50=	771.37	T	52=	744.84	T	54=	778.55	T	158=	777.45	T	159=	777.54	T	168=	777.02		

T	169=	776.86	T	195=	315.31	T	197=	376.89	T	199=	637.63	T	238=	742.21	T	311=	714.94
T	312=	714.94	T	321=	705.95	T	322=	705.95	T	331=	688.77	T	332=	688.77	T	337=	610.23
T	341=	583.47	T	357=	322.71	T	358=	344.12	T	359=	284.57	T	379=	237.56	T	403=	235.22
T	1000=	344.53	T	1001=	724.48	T	1002=	627.78	T	1003=	399.64	T	1004=	293.33	T	1005=	290.55
T	1006=	212.54	T	1007=	769.54	T	1008=	778.11	T	1009=	816.73	T	1010=	430.99	T	1011=	797.40
T	1012=	797.40	T	1013=	657.61	T	1021=	783.92	T	1022=	783.92	T	1023=	651.75	T	1031=	763.96
T	1032=	763.96	T	1033=	651.16	T	1041=	728.90	T	1042=	728.90	T	1043=	546.65	T	1044=	546.65
T	1346=	703.69	T	1347=	410.32												

HEATER NODES IN ASCENDING NODE NUMBER ORDER
++NONE++

BOUNDARY NODES IN ASCENDING NODE NUMBER ORDER

T	1=	100.00	T	2=	100.00

SYSTEMS IMPROVED NUMERICAL DIFFERENCING ANALYZER '85 (SINDA '85) PAGE 3/4

MODEL = DAMAGE1 HAC LOAD CASE NO. 1 CONDITIONS - Circumferential Distribution, 100F 5/2/94
FWDBCK ***** Peak ICV Sidewall Temperature Time Point *****

SUBMODEL NAME = PTSC

		CALCULATED		ALLOWED
MAX DIFF DELTA T PER ITER	DRLXCC(PTSC	161)= 1.623535E-02	VS. DRLXCA=	5.000000E-02
MAX ARITH DELTA T PER ITER	ARLXCC(PTSC	337)=-0.121460	VS. ARLXCA=	0.500000
MAX DIFF DEL T PER TIME STEP	DTMPCC(PTSC	423)= -2.65817	VS. DTMPCA=	10.0000
MAX ARITH DEL T PER TIME STEP	ATMPCC(PTSC	1346)= -1.41000	VS. ATMPCA=	100.000
MIN STABILITY CRITERIA	CSGMIN(PTSC	455)= 1.701556E-04		
MAX STABILITY CRITERIA	CSGMAX(PTSC	434)= 3.55934		
NUMBER OF ITERATIONS	LOOPCT	= 3	VS. NLOOPT=	600
PROBLEM TIME	TIMEN	= 0.700000	VS. TIMEND=	12.0000
MEAN PROBLEM TIME	TIMEM	= 0.699196		
AVERAGE TIME STEP USED	DTIMEU	= 8.771930E-04	VS. DTIMEI=	0.

DIFFUSION NODES IN ASCENDING NODE NUMBER ORDER

T	51=	811.50	T	53=	751.47	T	55=	751.03	T	60=	873.77	T	62=	974.29	T	100=	960.59
T	105=	934.92	T	107=	922.86	T	110=	909.90	T	112=	907.54	T	113=	911.11	T	120=	859.21
T	122=	851.18	T	123=	861.63	T	124=	857.77	T	125=	864.71	T	126=	867.66	T	127=	868.95
T	130=	816.49	T	132=	810.97	T	133=	817.07	T	134=	816.59	T	135=	820.60	T	136=	825.46
T	137=	826.12	T	140=	794.63	T	141=	795.50	T	142=	791.70	T	143=	794.71	T	144=	794.55
T	145=	796.80	T	146=	800.44	T	147=	801.22	T	150=	779.64	T	152=	778.40	T	153=	779.58
T	154=	780.32	T	155=	780.94	T	156=	784.22	T	157=	784.23	T	160=	771.68	T	161=	774.73
T	162=	772.16	T	163=	771.27	T	164=	773.00	T	165=	772.91	T	166=	775.64	T	167=	775.77
T	170=	758.03	T	172=	758.13	T	173=	757.72	T	175=	754.65	T	177=	753.59	T	180=	753.67
T	190=	750.65	T	191=	832.45	T	192=	316.46	T	193=	780.37	T	194=	439.31	T	196=	688.49
T	198=	837.85	T	200=	975.48	T	204=	956.74	T	210=	823.65	T	220=	798.50	T	230=	753.17
T	240=	701.73	T	242=	445.50	T	250=	250.15	T	260=	204.55	T	261=	207.09	T	262=	206.77
T	263=	210.96	T	264=	213.17	T	265=	220.01	T	266=	219.84	T	300=	885.09	T	304=	882.96
T	305=	616.67	T	310=	808.66	T	313=	737.03	T	315=	623.48	T	316=	623.48	T	320=	790.96
T	323=	725.05	T	325=	617.60	T	326=	617.60	T	330=	757.62	T	333=	699.45	T	335=	621.11
T	336=	621.11	T	340=	727.11	T	342=	540.00	T	343=	660.26	T	344=	359.87	T	345=	735.89
T	346=	728.67	T	347=	502.16	T	349=	567.21	T	350=	283.40	T	351=	343.74	T	352=	284.62
T	353=	316.58	T	354=	314.29	T	355=	239.71	T	356=	316.97	T	360=	201.63	T	362=	202.14
T	364=	208.05	T	366=	234.82	T	367=	238.27	T	368=	247.94	T	369=	264.74	T	371=	347.44
T	373=	322.78	T	375=	269.04	T	377=	236.60	T	400=	204.92	T	401=	217.41	T	402=	232.10
T	404=	793.63	T	406=	740.47	T	408=	688.09	T	410=	765.83	T	412=	784.33	T	414=	723.82
T	421=	494.08	T	422=	754.88	T	423=	744.88	T	424=	277.89	T	425=	891.88	T	426=	829.24
T	431=	794.60	T	432=	952.29	T	433=	292.38	T	434=	258.48	T	435=	965.14	T	436=	817.33
T	441=	691.81	T	442=	775.08	T	443=	796.37	T	444=	796.15	T	445=	785.89	T	446=	693.33
T	451=	713.80	T	452=	739.40	T	453=	734.41	T	454=	737.70	T	455=	763.63	T	456=	727.44
T	950=	937.73															

ARITHMETIC NODES IN ASCENDING NODE NUMBER ORDER

T	50=	809.34	T	52=	755.23	T	54=	770.54	T	158=	774.60	T	159=	774.61	T	168=	774.44

T	169=	774.37	T	195=	314.87	T	197=	376.58	T	199=	636.79	T	238=	730.74	T	311=	719.18
T	312=	719.18	T	321=	707.38	T	322=	707.38	T	331=	682.16	T	332=	682.16	T	337=	608.34
T	341=	581.37	T	357=	322.32	T	358=	343.76	T	359=	284.23	T	379=	237.29	T	403=	235.10
T	1000=	344.35	T	1001=	722.66	T	1002=	627.01	T	1003=	399.13	T	1004=	293.18	T	1005=	290.40
T	1006=	212.33	T	1007=	767.55	T	1008=	775.04	T	1009=	814.89	T	1010=	430.43	T	1011=	802.97
T	1012=	802.97	T	1013=	660.92	T	1021=	785.77	T	1022=	785.77	T	1023=	652.89	T	1031=	753.47
T	1032=	753.47	T	1033=	645.85	T	1041=	724.34	T	1042=	724.34	T	1043=	544.64	T	1044=	544.64
T	1346=	702.73	T	1347=	409.72												

HEATER NODES IN ASCENDING NODE NUMBER ORDER
++NONE++
BOUNDARY NODES IN ASCENDING NODE NUMBER ORDER

T	1=	100.00	T	2=	100.00

SYSTEMS IMPROVED NUMERICAL DIFFERENCING ANALYZER '85 (SINDA '85) PAGE 4/4

MODEL = DAMAGE1 HAC LOAD CASE NO. 1 CONDITIONS - Circumferential Distribution, 100F 5/2/94
FWDBCK ***** Peak ICV Sidewall Temperature Time Point *****

SUBMODEL NAME = PTSD

	CALCULATED			ALLOWED	
MAX DIFF DELTA T PER ITER	DRLXCC(PTSD	161)=	1.538086E-02	VS. DRLXCA=	5.000000E-02
MAX ARITH DELTA T PER ITER	ARLXCC(PTSD	337)=	-0.120605	VS. ARLXCA=	0.500000
MAX DIFF DEL T PER TIME STEP	DTMPCC(PTSD	423)=	-2.65829	VS. DTMPCA=	10.0000
MAX ARITH DEL T PER TIME STEP	ATMPCC(PTSD	1346)=	-1.40939	VS. ATMPCA=	100.000
MIN STABILITY CRITERIA	CSGMIN(PTSD	455)=	1.701547E-04		
MAX STABILITY CRITERIA	CSGMAX(PTSD	434)=	3.55933		
NUMBER OF ITERATIONS	LOOPCT	=	3	VS. NLOOPT=	600
PROBLEM TIME	TIMEN	=	0.700000	VS. TIMEND=	12.0000
MEAN PROBLEM TIME	TIMEM	=	0.699196		
AVERAGE TIME STEP USED	DTIMEU	=	8.771930E-04	VS. DTIMEI=	0.

DIFFUSION NODES IN ASCENDING NODE NUMBER ORDER

T	51=	821.90	T	53=	754.60	T	55=	749.26	T	60=	875.78	T	62=	972.77	T	100=	962.14
T	105=	938.52	T	107=	927.23	T	110=	914.91	T	112=	914.83	T	113=	915.35	T	120=	868.20
T	122=	866.14	T	123=	867.76	T	124=	868.82	T	125=	869.83	T	126=	872.22	T	127=	872.38
T	130=	822.45	T	132=	820.17	T	133=	821.26	T	134=	823.81	T	135=	824.44	T	136=	829.32
T	137=	829.34	T	140=	799.35	T	141=	800.29	T	142=	797.84	T	143=	798.57	T	144=	799.83
T	145=	800.51	T	146=	804.11	T	147=	804.55	T	150=	783.10	T	152=	781.95	T	153=	782.62
T	154=	783.99	T	155=	784.33	T	156=	788.06	T	157=	788.11	T	160=	773.27	T	161=	776.68
T	162=	772.56	T	163=	773.00	T	164=	774.50	T	165=	775.54	T	166=	778.95	T	167=	779.32
T	170=	759.04	T	172=	758.67	T	173=	758.74	T	175=	754.87	T	177=	754.10	T	180=	753.54
T	190=	750.92	T	191=	831.47	T	192=	315.97	T	193=	780.80	T	194=	438.62	T	196=	688.10
T	198=	836.94	T	200=	975.44	T	204=	957.57	T	210=	825.04	T	220=	799.71	T	230=	762.53
T	240=	703.63	T	242=	445.96	T	250=	250.21	T	260=	204.52	T	261=	207.05	T	262=	206.74
T	263=	210.90	T	264=	213.16	T	265=	219.99	T	266=	219.85	T	300=	884.89	T	304=	883.28
T	305=	616.77	T	310=	809.39	T	313=	737.53	T	315=	623.81	T	316=	623.81	T	320=	791.59
T	323=	725.48	T	325=	617.88	T	326=	617.88	T	330=	763.20	T	333=	702.87	T	335=	623.45
T	336=	623.45	T	340=	729.42	T	342=	540.89	T	343=	660.46	T	344=	360.10	T	345=	735.97
T	346=	729.05	T	347=	502.21	T	349=	567.38	T	350=	283.45	T	351=	343.80	T	352=	284.65
T	353=	316.62	T	354=	314.37	T	355=	239.72	T	356=	317.01	T	360=	201.62	T	362=	202.13
T	364=	208.05	T	366=	234.83	T	367=	238.27	T	368=	247.94	T	369=	264.74	T	371=	347.51
T	373=	322.82	T	375=	269.06	T	377=	236.61	T	400=	204.92	T	401=	217.41	T	402=	232.10
T	404=	793.65	T	406=	740.65	T	408=	688.10	T	410=	765.83	T	412=	784.33	T	414=	723.82
T	421=	494.08	T	422=	754.88	T	423=	744.88	T	424=	277.89	T	425=	891.88	T	426=	829.24
T	431=	794.68	T	432=	952.38	T	433=	292.38	T	434=	258.48	T	435=	965.14	T	436=	817.33
T	441=	691.82	T	442=	775.15	T	443=	796.37	T	444=	796.16	T	445=	785.90	T	446=	693.34
T	451=	713.88	T	452=	739.57	T	453=	734.44	T	454=	737.71	T	455=	763.63	T	456=	727.45
T	950=	936.36															

ARITHMETIC NODES IN ASCENDING NODE NUMBER ORDER

T	50=	818.08	T	52=	758.43	T	54=	769.45	T	158=	776.52	T	159=	776.79	T	168=	776.37

T	169=	776.21	T	195=	314.57	T	197=	376.13	T	199=	636.46	T	238=	736.87	T	311=	719.70
T	312=	719.70	T	321=	707.82	T	322=	707.82	T	331=	685.55	T	332=	685.55	T	337=	609.26
T	341=	582.40	T	357=	322.38	T	358=	343.83	T	359=	284.27	T	379=	237.30	T	403=	235.10
T	1000=	343.92	T	1001=	721.93	T	1002=	626.52	T	1003=	398.59	T	1004=	292.92	T	1005=	290.14
T	1006=	212.27	T	1007=	767.57	T	1008=	774.94	T	1009=	814.18	T	1010=	430.37	T	1011=	803.68
T	1012=	803.68	T	1013=	661.32	T	1021=	786.38	T	1022=	786.38	T	1023=	653.22	T	1031=	758.91
T	1032=	758.91	T	1033=	648.55	T	1041=	726.67	T	1042=	726.67	T	1043=	545.62	T	1044=	545.62
T	1346=	702.89	T	1347=	409.75												

HEATER NODES IN ASCENDING NODE NUMBER ORDER

++NONE++

BOUNDARY NODES IN ASCENDING NODE NUMBER ORDER

T	1=	100.00	T	2=	100.00

SYSTEMS IMPROVED NUMERICAL DIFFERENCING ANALYZER '85 (SINDA '85) PAGE 4/4

MODEL = DAMAGE1 HAC LOAD CASE NO. 1 CONDITIONS - Circumferential Distribution, 100F
STDSTL *** Steady-state Conditions After The Fire *** 5/2/94 9am

SUBMODEL NAME = MAIN

PROBLEM TIME TIMEN = 999.000 VS. TIMEND= 999.000

DIFFUSION NODES IN ASCENDING NODE NUMBER ORDER

T	267=	291.07	T	268=	291.07	T	269=	289.19			

ARITHMETIC NODES IN ASCENDING NODE NUMBER ORDER

T	201=	390.85	T	1266=	294.23	T	1267=	323.05	T	1268=	317.14

T	1269=	296.35	

HEATER NODES IN ASCENDING NODE NUMBER ORDER

++NONE++

BOUNDARY NODES IN ASCENDING NODE NUMBER ORDER

++NONE++

MEAN ICV GAS TEMP= 390.9 F MEAN ICV GAS PRESSURE= 25.53 PSIA
MEAN ICV-OCV GAS TEMP= 263.7 F MEAN ICV-OCV GAS PRESSURE= 25.52 PSIA

SUBMODEL NAME = PTSA

	CALCULATED			ALLOWED		
MAX DIFF DELTA T PER ITER	DRLXCC(PTSA	406)= -1.95154	VS.	DRLXCA=	5.000000E-02	
MAX ARITH DELTA T PER ITER	ARLXCC(PTSA	1346)=-1.647949E-02	VS.	ARLXCA=	5.000000E-02	
MAX SYSTEM ENERGY BALANCE	EBALSC	= 1.000000E+30	VS.	EBALSA * ESUMIS =	0.	
				EBALSA=	1.000000E-03	
ENERGY INTO AND OUT OF SYS	ESUMIS	= 0.		ESUMOS=	0.	
MAX NODAL ENERGY BALANCE	EBALNC(	0)= 0.	VS.	EBALNA=	1.000000E-03	
NUMBER OF ITERATIONS	LOOPCT	= 1001	VS.	NLOOPS=	1000	
PROBLEM TIME	TIMEN	= 999.000	VS.	TIMEND=	999.000	

DIFFUSION NODES IN ASCENDING NODE NUMBER ORDER

T	51=	306.95	T	53=	356.70	T	55=	438.06	T	60=	297.59	T	62=	459.53	T	100=	285.21
T	105=	288.46	T	107=	289.77	T	110=	291.21	T	112=	291.33	T	113=	291.04	T	120=	301.03
T	122=	301.35	T	123=	300.59	T	124=	300.82	T	125=	300.15	T	126=	300.13	T	127=	299.67
T	130=	327.46	T	132=	328.63	T	133=	327.00	T	134=	327.07	T	135=	325.66	T	136=	323.98
T	137=	323.11	T	140=	350.50	T	141=	350.72	T	142=	351.17	T	143=	349.11	T	144=	351.34
T	145=	349.83	T	146=	352.34	T	147=	351.79	T	150=	389.70	T	152=	390.05	T	153=	386.84
T	154=	393.08	T	155=	391.24	T	156=	397.91	T	157=	398.42	T	160=	447.85	T	161=	438.07
T	162=	448.24	T	163=	445.20	T	164=	448.74	T	165=	447.35	T	166=	449.99	T	167=	449.32
T	170=	493.61	T	172=	493.68	T	173=	493.42	T	175=	509.34	T	177=	501.87	T	180=	502.47
T	190=	515.48	T	191=	595.63	T	192=	369.01	T	193=	458.73	T	194=	379.83	T	196=	470.05
T	198=	599.31	T	200=	264.52	T	204=	258.21	T	210=	271.97	T	220=	280.58	T	230=	309.22
T	240=	319.12	T	242=	292.39	T	250=	269.86	T	260=	281.58	T	261=	283.32	T	262=	279.70
T	263=	283.32	T	264=	271.79	T	265=	275.44	T	266=	265.46	T	300=	208.71	T	304=	195.31
T	305=	136.27	T	310=	234.52	T	313=	218.19	T	315=	198.88	T	316=	198.88	T	320=	243.35
T	323=	225.97	T	325=	205.45	T	326=	205.45	T	330=	265.93	T	333=	245.71	T	335=	221.73
T	336=	221.73	T	340=	267.81	T	342=	259.03	T	343=	205.56	T	344=	247.96	T	345=	204.45
T	346=	187.81	T	347=	227.01	T	349=	197.82	T	350=	243.81	T	351=	237.22	T	352=	242.64
T	353=	239.88	T	354=	242.79	T	355=	245.19	T	356=	240.88	T	360=	277.31	T	362=	273.74
T	364=	262.95	T	366=	246.44	T	367=	244.56	T	368=	241.99	T	369=	240.03	T	371=	237.11
T	373=	239.25	T	375=	242.06	T	377=	243.58	T	400=	266.23	T	401=	264.06	T	402=	243.85
T	404=	193.87	T	406=	132.81	T	408=	114.08	T	410=	104.44	T	412=	105.62	T	414=	106.81

T	421=	214.04	T	422=	115.39	T	423=	110.36	T	424=	194.81	T	425=	113.13	T	426=	109.47
T	431=	128.66	T	432=	127.54	T	433=	124.16	T	434=	117.30	T	435=	110.40	T	436=	112.90
T	950=	707.83															

ARITHMETIC NODES IN ASCENDING NODE NUMBER ORDER

T	50=	312.93	T	52=	358.11	T	54=	429.30	T	158=	438.37	T	159=	437.94	T	168=	438.01
T	169=	437.76	T	195=	328.36	T	197=	346.57	T	199=	448.68	T	238=	313.58	T	311=	216.81
T	312=	216.81	T	321=	224.52	T	322=	224.52	T	331=	244.03	T	332=	244.03	T	337=	242.57
T	341=	253.96	T	357=	240.75	T	358=	237.27	T	359=	243.21	T	379=	245.43	T	403=	243.67
T	1000=	343.28	T	1001=	531.01	T	1002=	457.34	T	1003=	400.28	T	1004=	350.57	T	1005=	348.27
T	1006=	286.17	T	1007=	527.49	T	1008=	537.95	T	1009=	578.06	T	1010=	332.59	T	1011=	234.15
T	1012=	234.15	T	1013=	205.86	T	1021=	242.95	T	1022=	242.95	T	1023=	212.83	T	1031=	265.44
T	1032=	265.44	T	1033=	230.33	T	1041=	267.29	T	1042=	267.29	T	1043=	258.65	T	1044=	258.65
T	1346=	195.39	T	1347=	232.53												

HEATER NODES IN ASCENDING NODE NUMBER ORDER

++NONE++

BOUNDARY NODES IN ASCENDING NODE NUMBER ORDER

T	1=	100.00	T	2=	100.00

SYSTEMS IMPROVED NUMERICAL DIFFERENCING ANALYZER '85 (SINDA '85) PAGE 2/4

MODEL = DAMAGE1 HAC LOAD CASE NO. 1 CONDITIONS - Circumferential Distribution, 100F
STDSTL *** Steady-state Conditions After The Fire *** 5/2/94 9am

SUBMODEL NAME = PTSB

		CALCULATED			ALLOWED	
MAX DIFF DELTA T PER ITER	DRLXCC(PTSB	406)= -1.36334	VS.	DRLXCA= 5.000000E-02		
MAX ARITH DELTA T PER ITER	ARLXCC(PTSB	1346)=-1.202393E-02	VS.	ARLXCA= 5.000000E-02		
MAX SYSTEM ENERGY BALANCE	EBALSC	= 1.000000E+30	VS.	EBALSA * ESUMIS	=	0.
				EBALSA= 1.000000E-03		
ENERGY INTO AND OUT OF SYS	ESUMIS	= 0.		ESUMOS= 0.		
MAX NODAL ENERGY BALANCE	EBALNC(	0)= 0.	VS.	EBALNA= 1.000000E-03		
NUMBER OF ITERATIONS	LOOPCT	= 1001	VS.	NLOOPS= 1000		
PROBLEM TIME	TIMEN	= 999.000	VS.	TIMEND= 999.000		

DIFFUSION NODES IN ASCENDING NODE NUMBER ORDER

T 51= 304.55	T 53= 350.25	T 55= 429.14	T 60= 295.95	T 62= 455.75	T 100= 284.48
T 105= 287.55	T 107= 288.80	T 110= 290.15	T 112= 290.44	T 113= 289.75	T 120= 299.18
T 122= 300.10	T 123= 297.93	T 124= 299.81	T 125= 297.99	T 126= 299.65	T 127= 298.63
T 130= 323.56	T 132= 325.94	T 133= 321.31	T 134= 324.88	T 135= 321.07	T 136= 322.92
T 137= 320.95	T 140= 344.89	T 141= 345.09	T 142= 347.09	T 143= 341.22	T 144= 348.01
T 145= 343.50	T 146= 350.78	T 147= 348.90	T 150= 380.87	T 152= 384.48	T 153= 373.09
T 154= 388.44	T 155= 380.48	T 156= 395.37	T 157= 394.10	T 160= 439.12	T 161= 429.88
T 162= 442.66	T 163= 431.25	T 164= 444.13	T 165= 437.78	T 166= 447.91	T 167= 445.03
T 170= 492.64	T 172= 493.34	T 173= 490.36	T 175= 511.89	T 177= 502.74	T 180= 505.47
T 190= 523.00	T 191= 602.83	T 192= 372.89	T 193= 460.70	T 194= 387.42	T 196= 474.53
T 198= 606.30	T 200= 264.89	T 204= 258.51	T 210= 272.12	T 220= 280.94	T 230= 314.99
T 240= 320.62	T 242= 290.62	T 250= 268.16	T 260= 280.85	T 261= 282.63	T 262= 276.47
T 263= 279.02	T 264= 269.62	T 265= 272.86	T 266= 263.86	T 300= 209.00	T 304= 195.54
T 305= 136.35	T 310= 234.68	T 313= 218.33	T 315= 199.00	T 316= 199.00	T 320= 243.72
T 323= 226.29	T 325= 205.72	T 326= 205.72	T 330= 269.20	T 333= 248.05	T 335= 223.61
T 336= 223.61	T 340= 269.63	T 342= 258.84	T 343= 204.91	T 344= 247.47	T 345= 204.55
T 346= 187.72	T 347= 226.80	T 349= 197.57	T 350= 243.29	T 351= 236.77	T 352= 242.16
T 353= 239.39	T 354= 242.33	T 355= 244.60	T 356= 240.44	T 360= 276.59	T 362= 271.68
T 364= 261.51	T 366= 245.80	T 367= 244.01	T 368= 241.58	T 369= 239.71	T 371= 236.67
T 373= 238.79	T 375= 241.56	T 377= 243.08	T 400= 264.86	T 401= 262.70	T 402= 243.36
T 404= 196.40	T 406= 133.28	T 408= 112.65	T 410= 104.96	T 412= 105.73	T 414= 106.78
T 421= 213.14	T 422= 115.30	T 423= 110.29	T 424= 196.05	T 425= 113.22	T 426= 108.83
T 431= 157.28	T 432= 143.48	T 433= 159.61	T 434= 138.14	T 435= 108.20	T 436= 108.12
T 441= 118.27	T 442= 122.91	T 443= 116.69	T 444= 114.38	T 445= 109.26	T 446= 111.29
T 451= 121.56	T 452= 128.56	T 453= 116.56	T 454= 112.64	T 455= 106.96	T 456= 109.28
T 950= 712.41					

ARITHMETIC NODES IN ASCENDING NODE NUMBER ORDER

T 50= 310.07	T 52= 351.75	T 54= 421.16	T 158= 431.23	T 159= 429.29	T 168= 429.73
T 169= 429.25	T 195= 331.56	T 197= 361.96	T 199= 462.33	T 238= 317.46	T 311= 216.95

T	312=	216.95	T	321=	224.84	T	322=	224.84	T	331=	246.30	T	332=	246.30	T	337=	242.62
T	341=	254.04	T	357=	240.30	T	358=	236.83	T	359=	242.70	T	379=	244.84	T	403=	243.18
T	1000=	350.12	T	1001=	536.92	T	1002=	468.51	T	1003=	404.56	T	1004=	353.17	T	1005=	350.70
T	1006=	284.18	T	1007=	532.64	T	1008=	544.59	T	1009=	585.09	T	1010=	338.58	T	1011=	234.31
T	1012=	234.31	T	1013=	205.98	T	1021=	243.32	T	1022=	243.32	T	1023=	213.12	T	1031=	268.69
T	1032=	268.69	T	1033=	232.37	T	1041=	269.11	T	1042=	269.11	T	1043=	258.51	T	1044=	258.51
T	1346=	195.43	T	1347=	232.32												

HEATER NODES IN ASCENDING NODE NUMBER ORDER
++NONE++

BOUNDARY NODES IN ASCENDING NODE NUMBER ORDER

T	1=	100.00	T	2=	100.00

SYSTEMS IMPROVED NUMERICAL DIFFERENCING ANALYZER '85 (SINDA '85) PAGE 3/4

MODEL = DAMAGE1
STDSTL

HAC LOAD CASE NO. 1 CONDITIONS - Circumferential Distribution, 100F
*** Steady-state Conditions After The Fire *** 5/2/94 9am

SUBMODEL NAME = PTSC

		CALCULATED		ALLOWED	
MAX DIFF DELTA T PER ITER	DRLXCC(PTSC	451)= 0.240601	VS. DRLXCA=	5.000000E-02	
MAX ARITH DELTA T PER ITER	ARLXCC(PTSC	1004)= 3.533936E-02	VS. ARLXCA=	5.000000E-02	
MAX SYSTEM ENERGY BALANCE	EBALSC	= 3.77577	VS. EBALSA * ESUMIS	=	2.87972
			EBALSA=	1.000000E-03	
ENERGY INTO AND OUT OF SYS	ESUMIS	= 2879.72	ESUMOS=	2857.42	
MAX NODAL ENERGY BALANCE	EBALNC(PTSC	367)= 1.02580	VS. EBALNA=	1.000000E-03	
NUMBER OF ITERATIONS	LOOPCT	= 1001	VS. NLOOPS=	1000	
PROBLEM TIME	TIMEN	= 999.000	VS. TIMEND=	999.000	

DIFFUSION NODES IN ASCENDING NODE NUMBER ORDER

T	51=	298.30	T	53=	332.25	T	55=	401.62	T	60=	291.34	T	62=	440.37	T	100=	282.38
T	105=	284.74	T	107=	285.70	T	110=	286.70	T	112=	287.05	T	113=	286.57	T	120=	294.03
T	122=	294.97	T	123=	293.42	T	124=	293.82	T	125=	292.52	T	126=	291.97	T	127=	291.24
T	130=	312.45	T	132=	314.83	T	133=	311.55	T	134=	312.28	T	135=	309.55	T	136=	307.49
T	137=	305.98	T	140=	326.89	T	141=	327.17	T	142=	329.38	T	143=	325.55	T	144=	326.78
T	145=	323.69	T	146=	321.60	T	147=	320.59	T	150=	351.11	T	152=	355.64	T	153=	347.72
T	154=	353.52	T	155=	347.09	T	156=	347.85	T	157=	344.21	T	160=	406.77	T	161=	397.72
T	162=	411.41	T	163=	403.27	T	164=	406.62	T	165=	399.57	T	166=	396.97	T	167=	394.21
T	170=	473.41	T	172=	475.39	T	173=	472.96	T	175=	504.31	T	177=	490.33	T	180=	508.22
T	190=	518.85	T	191=	604.27	T	192=	372.69	T	193=	477.16	T	194=	388.92	T	196=	474.93
T	198=	608.07	T	200=	267.13	T	204=	262.79	T	210=	274.74	T	220=	282.97	T	230=	298.57
T	240=	320.88	T	242=	289.52	T	250=	266.71	T	260=	279.99	T	261=	281.79	T	262=	275.12
T	263=	277.69	T	264=	268.18	T	265=	271.45	T	266=	262.39	T	300=	210.36	T	304=	197.84
T	305=	137.18	T	310=	236.71	T	313=	220.09	T	315=	200.43	T	316=	200.43	T	320=	244.99
T	323=	227.39	T	325=	206.61	T	326=	206.61	T	330=	259.38	T	333=	241.08	T	335=	217.98
T	336=	217.98	T	340=	265.13	T	342=	256.11	T	343=	203.31	T	344=	245.59	T	345=	203.11
T	346=	186.07	T	347=	225.24	T	349=	196.13	T	350=	241.64	T	351=	235.13	T	352=	240.52
T	353=	237.75	T	354=	240.64	T	355=	242.99	T	356=	238.80	T	360=	275.65	T	362=	270.32
T	364=	260.05	T	366=	244.20	T	367=	242.42	T	368=	240.04	T	369=	238.19	T	371=	235.03
T	373=	237.15	T	375=	239.94	T	377=	241.48	T	400=	263.51	T	401=	261.37	T	402=	241.79
T	404=	195.22	T	406=	133.32	T	408=	112.51	T	410=	104.90	T	412=	105.67	T	414=	106.72
T	421=	212.21	T	422=	115.17	T	423=	110.20	T	424=	195.01	T	425=	113.08	T	426=	108.74
T	431=	156.74	T	432=	143.28	T	433=	158.98	T	434=	137.72	T	435=	108.10	T	436=	108.02
T	441=	118.10	T	442=	122.83	T	443=	116.52	T	444=	114.21	T	445=	109.15	T	446=	111.15
T	451=	121.44	T	452=	128.55	T	453=	116.43	T	454=	112.51	T	455=	106.88	T	456=	109.17
T	950=	714.95															

ARITHMETIC NODES IN ASCENDING NODE NUMBER ORDER

T	50=	302.42	T	52=	333.91	T	54=	395.95	T	158=	397.63	T	159=	395.61	T	168=	397.61
T	169=	397.71	T	195=	331.33	T	197=	362.20	T	199=	467.68	T	238=	308.40	T	311=	218.69

T	312=	218.69	T	321=	225.93	T	322=	225.93	T	331=	239.47	T	332=	239.47	T	337=	239.93
T	341=	251.17	T	357=	238.64	T	358=	235.19	T	359=	241.06	T	379=	243.24	T	403=	241.58
T	1000=	350.36	T	1001=	538.05	T	1002=	472.39	T	1003=	404.62	T	1004=	352.59	T	1005=	350.11
T	1006=	283.15	T	1007=	527.93	T	1008=	541.54	T	1009=	585.16	T	1010=	338.78	T	1011=	236.33
T	1012=	236.33	T	1013=	207.54	T	1021=	244.59	T	1022=	244.59	T	1023=	214.09	T	1031=	258.93
T	1032=	258.93	T	1033=	226.26	T	1041=	264.58	T	1042=	264.58	T	1043=	255.72	T	1044=	255.72
T	1346=	194.01	T	1347=	230.79												

HEATER NODES IN ASCENDING NODE NUMBER ORDER
++NONE++
BOUNDARY NODES IN ASCENDING NODE NUMBER ORDER

T	1=	100.00	T	2=	100.00

SYSTEMS IMPROVED NUMERICAL DIFFERENCING ANALYZER '85 (SINDA '85) PAGE 4/4

MODEL = DAMAGE1
STDSTL

HAC LOAD CASE NO. 1 CONDITIONS - Circumferential Distribution, 100F
*** Steady-state Conditions After The Fire *** 5/2/94 9am

SUBMODEL NAME = PTSD

		CALCULATED			ALLOWED	
MAX DIFF DELTA T PER ITER	DRLXCC(PTSD	406)= -1.34656	VS.	DRLXCA=	5.000000E-02	
MAX ARITH DELTA T PER ITER	ARLXCC(PTSD	1346)=-1.324463E-02	VS.	ARLXCA=	5.000000E-02	
MAX SYSTEM ENERGY BALANCE	EBALSC	= 1.000000E+30	VS.	EBALSA * ESUMIS	=	0.
				EBALSA=	1.000000E-03	
ENERGY INTO AND OUT OF SYS	ESUMIS	= 0.		ESUMOS=	0.	
MAX NODAL ENERGY BALANCE	EBALNC(	0)= 0.	VS.	EBALNA=	1.000000E-03	
NUMBER OF ITERATIONS	LOOPCT	= 1001	VS.	NLOOPS=	1000	
PROBLEM TIME	TIMEN	= 999.000	VS.	TIMEND=	999.000	

DIFFUSION NODES IN ASCENDING NODE NUMBER ORDER

T	51=	295.60	T	53=	325.54	T	55=	391.74	T	60=	289.25	T	62=	431.88	T	100=	281.12
T	105=	283.30	T	107=	284.19	T	110=	285.14	T	112=	285.32	T	113=	285.14	T	120=	291.86
T	122=	292.23	T	123=	291.70	T	124=	291.39	T	125=	290.92	T	126=	290.25	T	127=	289.93
T	130=	308.10	T	132=	309.17	T	133=	308.11	T	134=	307.37	T	135=	306.44	T	136=	304.24
T	137=	303.61	T	140=	320.67	T	141=	320.92	T	142=	321.51	T	143=	320.45	T	144=	319.96
T	145=	319.16	T	146=	317.27	T	147=	317.37	T	150=	342.33	T	152=	343.24	T	153=	341.35
T	154=	343.11	T	155=	341.51	T	156=	341.75	T	157=	340.66	T	160=	396.96	T	161=	388.32
T	162=	397.85	T	163=	395.88	T	164=	395.31	T	165=	393.22	T	166=	390.40	T	167=	389.69
T	170=	466.00	T	172=	466.94	T	173=	466.17	T	175=	496.88	T	177=	482.93	T	180=	500.97
T	190=	511.90	T	191=	593.85	T	192=	370.02	T	193=	473.51	T	194=	385.91	T	196=	471.93
T	198=	597.51	T	200=	266.95	T	204=	262.33	T	210=	274.24	T	220=	282.48	T	230=	306.93
T	240=	322.10	T	242=	289.70	T	250=	266.68	T	260=	279.37	T	261=	281.13	T	262=	274.61
T	263=	277.12	T	264=	267.94	T	265=	271.13	T	266=	262.33	T	300=	210.36	T	304=	197.63
T	305=	137.10	T	310=	236.34	T	313=	219.77	T	315=	200.17	T	316=	200.17	T	320=	244.78
T	323=	227.20	T	325=	206.46	T	326=	206.46	T	330=	264.47	T	333=	244.77	T	335=	220.96
T	336=	220.96	T	340=	267.90	T	342=	257.31	T	343=	203.88	T	344=	246.13	T	345=	203.57
T	346=	186.78	T	347=	225.65	T	349=	196.63	T	350=	242.01	T	351=	235.54	T	352=	240.89
T	353=	238.14	T	354=	241.05	T	355=	243.31	T	356=	239.19	T	360=	275.14	T	362=	269.95
T	364=	259.97	T	366=	244.49	T	367=	242.73	T	368=	240.34	T	369=	238.49	T	371=	235.44
T	373=	237.55	T	375=	240.30	T	377=	241.80	T	400=	263.32	T	401=	261.18	T	402=	242.08
T	404=	195.41	T	406=	132.17	T	408=	112.51	T	410=	104.90	T	412=	105.68	T	414=	106.72
T	421=	212.08	T	422=	115.16	T	423=	110.19	T	424=	195.19	T	425=	113.10	T	426=	108.75
T	431=	156.67	T	432=	142.58	T	433=	159.02	T	434=	137.78	T	435=	108.12	T	436=	108.04
T	441=	118.05	T	442=	122.37	T	443=	116.51	T	444=	114.23	T	445=	109.16	T	446=	111.17
T	451=	121.22	T	452=	127.69	T	453=	116.29	T	454=	112.49	T	455=	106.89	T	456=	109.18
T	950=	707.97															

ARITHMETIC NODES IN ASCENDING NODE NUMBER ORDER

T	50=	299.25	T	52=	327.24	T	54=	386.61	T	158=	387.72	T	159=	387.14	T	168=	388.17
T	169=	388.13	T	195=	329.65	T	197=	359.43	T	199=	462.67	T	238=	313.61	T	311=	218.37

T	312=	218.37	T	321=	225.74	T	322=	225.74	T	331=	243.09	T	332=	243.09	T	337=	241.20
T	341=	252.53	T	357=	239.05	T	358=	235.60	T	359=	241.43	T	379=	243.54	T	403=	241.90
T	1000=	348.12	T	1001=	530.53	T	1002=	466.91	T	1003=	400.99	T	1004=	350.56	T	1005=	348.12
T	1006=	282.48	T	1007=	520.11	T	1008=	533.50	T	1009=	575.47	T	1010=	337.32	T	1011=	235.96
T	1012=	235.96	T	1013=	207.25	T	1021=	244.37	T	1022=	244.37	T	1023=	213.92	T	1031=	263.99
T	1032=	263.99	T	1033=	229.50	T	1041=	267.36	T	1042=	267.36	T	1043=	256.95	T	1044=	256.95
T	1346=	194.51	T	1347=	231.14												

HEATER NODES IN ASCENDING NODE NUMBER ORDER

++NONE++

BOUNDARY NODES IN ASCENDING NODE NUMBER ORDER

T	1=	100.00	T	2=	100.00

SYSTEMS IMPROVED NUMERICAL DIFFERENCING ANALYZER '85 (SINDA '85) PAGE 1/4

MODEL = DAMAGE2 HAC LOAD CASE NO. 2 CONDITIONS - Circumferential Distribution, -20F 5/2/94
FWDBCK ***** Peak OCV Sidewall Temperature Time Point *****

SUBMODEL NAME = MAIN

MEAN PROBLEM TIME TIMEM = 0.500000

DIFFUSION NODES IN ASCENDING NODE NUMBER ORDER

T 267= 113.13 T 268= 113.01 T 269= 108.77

ARITHMETIC NODES IN ASCENDING NODE NUMBER ORDER

T 201= 713.53 T 1266= 124.44 T 1267= 233.55 T 1268= 198.28 T 1269= 131.59

HEATER NODES IN ASCENDING NODE NUMBER ORDER

++NONE++

BOUNDARY NODES IN ASCENDING NODE NUMBER ORDER

++NONE++

MEAN ICV GAS TEMP= 713.5 F MEAN ICV GAS PRESSURE= 35.22 PSIA
MEAN ICV-OCV GAS TEMP= 786.9 F MEAN ICV-OCV GAS PRESSURE= 43.94 PSIA

SUBMODEL NAME = PTSA

	CALCULATED			ALLOWED	
MAX DIFF DELTA T PER ITER	DRLXCC(PTSA	105)=	3.662109E-04	VS. DRLXCA=	5.000000E-02
MAX ARITH DELTA T PER ITER	ARLXCC(PTSA	1346)=	-0.122803	VS. ARLXCA=	0.500000
MAX DIFF DEL T PER TIME STEP	DTMPCC(PTSA	105)=	3.967285E-04	VS. DTMPCA=	10.0000
MAX ARITH DEL T PER TIME STEP	ATMPCC(PTSA	1346)=	-0.122772	VS. ATMPCA=	100.000
MIN STABILITY CRITERIA	CSGMIN(PTSA	431)=	3.041521E-05		
MAX STABILITY CRITERIA	CSGMAX(PTSA	424)=	1.96051		
NUMBER OF ITERATIONS	LOOPCT	=	1	VS. NLOOPT=	600
PROBLEM TIME	TIMEN	=	0.500000	VS. TIMEND=	0.500000
MEAN PROBLEM TIME	TIMEM	=	0.500000		
AVERAGE TIME STEP USED	DTIMEU	=	1.666667E-02	VS. DTIMEI=	0.

DIFFUSION NODES IN ASCENDING NODE NUMBER ORDER

T	51=	648.69	T	53=	658.69	T	55=	696.20	T	60=	807.16	T	62=	961.21	T	100=	963.05
T	105=	855.87	T	107=	809.98	T	110=	764.69	T	112=	764.18	T	113=	767.31	T	120=	649.03
T	122=	645.92	T	123=	654.73	T	124=	642.07	T	125=	648.44	T	126=	637.72	T	127=	639.69
T	130=	623.80	T	132=	623.08	T	133=	628.09	T	134=	621.13	T	135=	624.55	T	136=	620.28
T	137=	620.98	T	140=	610.08	T	141=	608.39	T	142=	610.59	T	143=	613.24	T	144=	609.39
T	145=	611.51	T	146=	610.08	T	147=	611.48	T	150=	622.46	T	152=	623.01	T	153=	623.91
T	154=	621.64	T	155=	622.08	T	156=	620.89	T	157=	621.03	T	160=	638.07	T	161=	632.85
T	162=	639.58	T	163=	638.73	T	164=	637.99	T	165=	636.92	T	166=	637.56	T	167=	638.04
T	170=	620.09	T	172=	619.81	T	173=	619.56	T	175=	613.73	T	177=	612.98	T	180=	601.47
T	190=	607.83	T	191=	726.72	T	192=	197.27	T	193=	630.17	T	194=	298.17	T	196=	505.18
T	198=	732.41	T	200=	1052.4	T	204=	1075.6	T	210=	657.01	T	220=	637.52	T	230=	588.79
T	240=	530.67	T	242=	266.63	T	250=	117.67	T	260=	97.248	T	261=	99.661	T	262=	98.183
T	263=	103.16	T	264=	97.641	T	265=	102.97	T	266=	98.919	T	300=	1210.1	T	304=	1218.2
T	305=	1372.4	T	310=	899.00	T	313=	1085.5	T	315=	1272.5	T	316=	1272.5	T	320=	883.69
T	323=	1074.9	T	325=	1265.2	T	326=	1265.2	T	330=	834.80	T	333=	1024.4	T	335=	1234.5
T	336=	1234.5	T	340=	807.28	T	342=	510.69	T	343=	1011.9	T	344=	235.74	T	345=	906.03
T	346=	1246.1	T	347=	455.36	T	349=	1018.3	T	350=	152.36	T	351=	330.25	T	352=	156.13
T	353=	242.26	T	354=	192.93	T	355=	116.37	T	356=	202.90	T	360=	94.402	T	362=	93.449
T	364=	92.889	T	366=	108.35	T	367=	113.25	T	368=	136.12	T	369=	153.39	T	371=	341.30
T	373=	249.17	T	375=	154.80	T	377=	118.00	T	400=	92.753	T	401=	100.71	T	402=	113.17
T	404=	1185.5	T	406=	1367.5	T	408=	1357.4	T	410=	1409.8	T	412=	1408.4	T	414=	1418.6

T	421=	393.60	T	422=	1413.7	T	423=	1416.6	T	424=	159.20	T	425=	1397.7	T	426=	1400.9
T	431=	1356.0	T	432=	1355.5	T	433=	1339.2	T	434=	1337.7	T	435=	1377.5	T	436=	1358.0
T	950=	848.23															

ARITHMETIC NODES IN ASCENDING NODE NUMBER ORDER

T	50=	663.86	T	52=	661.65	T	54=	714.13	T	158=	633.52	T	159=	633.28	T	168=	633.30
T	169=	633.59	T	195=	212.93	T	197=	260.41	T	199=	492.70	T	238=	563.48	T	311=	1102.7
T	312=	1102.7	T	321=	1091.9	T	322=	1091.9	T	331=	1040.1	T	332=	1040.1	T	337=	747.70
T	341=	624.62	T	357=	226.55	T	358=	315.04	T	359=	154.83	T	379=	112.20	T	403=	116.47
T	1000=	237.92	T	1001=	597.09	T	1002=	489.22	T	1003=	279.16	T	1004=	176.64	T	1005=	174.32
T	1006=	104.37	T	1007=	632.62	T	1008=	643.44	T	1009=	701.29	T	1010=	262.65	T	1011=	922.38
T	1012=	922.38	T	1013=	1217.8	T	1021=	907.25	T	1022=	907.25	T	1023=	1210.0	T	1031=	857.80
T	1032=	857.80	T	1033=	1173.3	T	1041=	832.09	T	1042=	832.09	T	1043=	552.99	T	1044=	552.99
T	1346=	1099.1	T	1347=	356.55												

HEATER NODES IN ASCENDING NODE NUMBER ORDER

++NONE++

BOUNDARY NODES IN ASCENDING NODE NUMBER ORDER

T	1=	1475.0	T	2=	1424.7

SYSTEMS IMPROVED NUMERICAL DIFFERENCING ANALYZER '85 (SINDA '85) PAGE 2/4

MODEL = DAMAGE2 HAC LOAD CASE NO. 2 CONDITIONS - Circumferential Distribution, -20F 5/2/94
FWDBCK ***** Peak OCV Sidewall Temperature Time Point *****

SUBMODEL NAME = PTSB

	CALCULATED		ALLOWED
MAX DIFF DELTA T PER ITER	DRLXCC(PTSB	404)= 2.441406E-04	VS. DRLXCA= 5.000000E-02
MAX ARITH DELTA T PER ITER	ARLXCC(PTSB	1346)=-0.139648	VS. ARLXCA= 0.500000
MAX DIFF DEL T PER TIME STEP	DTMPCC(PTSB	404)= 2.746582E-04	VS. DTMPCA= 10.0000
MAX ARITH DEL T PER TIME STEP	ATMPCC(PTSB	1346)=-0.139618	VS. ATMPCA= 100.000
MIN STABILITY CRITERIA	CSGMIN(PTSB	446)= 3.012901E-05	
MAX STABILITY CRITERIA	CSGMAX(PTSB	424)= 2.05948	
NUMBER OF ITERATIONS	LOOPCT	= 1	VS. NLOOPT= 600
PROBLEM TIME	TIMEN	= 0.500000	VS. TIMEND= 0.500000
MEAN PROBLEM TIME	TIMEM	= 0.500000	
AVERAGE TIME STEP USED	DTIMEU.	= 1.666667E-02	VS. DTIMEI= 0.

DIFFUSION NODES IN ASCENDING NODE NUMBER ORDER

T	51=	660.28	T	53=	659.24	T	55=	689.29	T	60=	808.55	T	62=	959.70	T	100=	966.67
T	105=	864.42	T	107=	820.58	T	110=	777.60	T	112=	774.45	T	113=	787.00	T	120=	673.97
T	122=	661.39	T	123=	696.18	T	124=	655.46	T	125=	680.46	T	126=	647.21	T	127=	654.30
T	130=	637.37	T	132=	631.90	T	133=	648.96	T	134=	629.49	T	135=	641.49	T	136=	627.75
T	137=	630.74	T	140=	616.89	T	141=	615.07	T	142=	615.88	T	143=	622.23	T	144=	614.83
T	145=	619.61	T	146=	615.83	T	147=	617.95	T	150=	623.90	T	152=	624.63	T	153=	624.57
T	154=	623.79	T	155=	623.58	T	156=	624.23	T	157=	624.35	T	160=	635.17	T	161=	630.89
T	162=	638.10	T	163=	632.81	T	164=	637.41	T	165=	634.12	T	166=	638.97	T	167=	638.71
T	170=	619.03	T	172=	619.15	T	173=	617.20	T	175=	613.39	T	177=	612.01	T	180=	600.18
T	190=	609.11	T	191=	734.68	T	192=	193.06	T	193=	633.67	T	194=	303.21	T	196=	497.76
T	198=	740.78	T	200=	1052.4	T	204=	1075.6	T	210=	657.63	T	220=	638.54	T	230=	598.23
T	240=	531.94	T	242=	267.94	T	250=	117.06	T	260=	96.837	T	261=	98.998	T	262=	96.172
T	263=	99.305	T	264=	96.681	T	265=	101.64	T	266=	98.051	T	300=	1210.1	T	304=	1218.2
T	305=	1372.4	T	310=	899.15	T	313=	1085.6	T	315=	1272.5	T	316=	1272.5	T	320=	883.87
T	323=	1074.9	T	325=	1265.2	T	326=	1265.2	T	330=	837.71	T	333=	1025.4	T	335=	1234.6
T	336=	1234.6	T	340=	807.97	T	342=	510.24	T	343=	1000.2	T	344=	232.55	T	345=	763.50
T	346=	1244.0	T	347=	380.56	T	349=	1015.5	T	350=	146.76	T	351=	323.88	T	352=	147.49
T	353=	237.39	T	354=	186.21	T	355=	109.93	T	356=	189.80	T	360=	94.202	T	362=	92.730
T	364=	92.068	T	366=	103.20	T	367=	104.32	T	368=	108.59	T	369=	116.71	T	371=	334.42
T	373=	244.20	T	375=	149.71	T	377=	109.22	T	400=	92.046	T	401=	100.10	T	402=	103.12
T	404=	888.81	T	406=	1365.4	T	408=	1379.8	T	410=	1413.0	T	412=	1408.5	T	414=	1418.6
T	421=	393.35	T	422=	1413.7	T	423=	1416.7	T	424=	140.67	T	425=	1397.8	T	426=	1404.7
T	431=	1224.1	T	432=	1350.2	T	433=	244.45	T	434=	213.27	T	435=	1405.6	T	436=	1404.6
T	441=	1379.2	T	442=	1372.3	T	443=	1372.5	T	444=	1372.5	T	445=	1394.6	T	446=	1380.2
T	451=	1373.9	T	452=	1365.7	T	453=	1376.5	T	454=	1381.5	T	455=	1412.4	T	456=	1394.5
T	950=	852.96															

ARITHMETIC NODES IN ASCENDING NODE NUMBER ORDER

T	50=	673.14	T	52=	662.34	T	54=	708.69	T	158=	632.10	T	159=	631.30	T	168=	631.31		

T	169=	631.45	T	195=	202.62	T	197=	262.42	T	199=	514.03	T	238=	569.40	T	311=	1102.7
T	312=	1102.7	T	321=	1092.0	T	322=	1092.0	T	331=	1041.1	T	332=	1041.1	T	337=	746.89
T	341=	624.15	T	357=	217.23	T	358=	307.37	T	359=	147.72	T	379=	105.31	T	403=	107.30
T	1000=	221.24	T	1001=	600.00	T	1002=	505.41	T	1003=	276.56	T	1004=	172.89	T	1005=	170.63
T	1006=	102.29	T	1007=	634.38	T	1008=	646.41	T	1009=	707.71	T	1010=	282.19	T	1011=	922.51
T	1012=	922.51	T	1013=	1217.9	T	1021=	907.42	T	1022=	907.42	T	1023=	1210.0	T	1031=	860.57
T	1032=	860.57	T	1033=	1173.7	T	1041=	832.78	T	1042=	832.78	T	1043=	552.63	T	1044=	552.63
T	1346=	1022.3	T	1347=	288.60												

HEATER NODES IN ASCENDING NODE NUMBER ORDER

++NONE++

BOUNDARY NODES IN ASCENDING NODE NUMBER ORDER

T	1=	1475.0	T	2=	1424.7

SYSTEMS IMPROVED NUMERICAL DIFFERENCING ANALYZER '85 (SINDA '85) PAGE 3/4

MODEL = DAMAGE2 HAC LOAD CASE NO. 2 CONDITIONS - Circumferential Distribution, -20F 5/2/94
FWDBCK ***** Peak OCV Sidewall Temperature Time Point *****

SUBMODEL NAME = PTSC

	CALCULATED		ALLOWED
MAX DIFF DELTA T PER ITER	DRLXCC(PTSC	320)= 2.441406E-04	VS. DRLXCA= 5.000000E-02
MAX ARITH DELTA T PER ITER	ARLXCC(PTSC	1346)=-0.139404	VS. ARLXCA= 0.500000
MAX DIFF DEL T PER TIME STEP	DTMPCC(PTSC	320)= 2.746582E-04	VS. DTMPCA= 10.0000
MAX ARITH DEL T PER TIME STEP	ATMPCC(PTSC	1346)=-0.139374	VS. ATMPCA= 100.000
MIN STABILITY CRITERIA	CSGMIN(PTSC	446)= 3.012980E-05	
MAX STABILITY CRITERIA	CSGMAX(PTSC	424)= 2.05948	
NUMBER OF ITERATIONS	LOOPCT	= 1	VS. NLOOPT= 600
PROBLEM TIME	TIMEN	= 0.500000	VS. TIMEND= 0.500000
MEAN PROBLEM TIME	TIMEM	= 0.500000	
AVERAGE TIME STEP USED	DTIMEU	= 1.666667E-02	VS. DTIMEI= 0.

DIFFUSION NODES IN ASCENDING NODE NUMBER ORDER

T	51=	696.00	T	53=	659.45	T	55=	666.46	T	60=	814.71	T	62=	957.55	T	100=	972.29
T	105=	902.10	T	107=	874.03	T	110=	856.92	T	112=	851.17	T	113=	858.84	T	120=	770.08
T	122=	754.46	T	123=	775.59	T	124=	770.82	T	125=	785.00	T	126=	800.43	T	127=	803.13
T	130=	684.18	T	132=	676.66	T	133=	687.27	T	134=	684.54	T	135=	691.74	T	136=	700.06
T	137=	701.55	T	140=	637.81	T	141=	637.60	T	142=	635.84	T	143=	639.68	T	144=	638.42
T	145=	641.56	T	146=	647.47	T	147=	649.20	T	150=	623.04	T	152=	624.21	T	153=	623.96
T	154=	623.63	T	155=	622.70	T	156=	625.23	T	157=	624.24	T	160=	619.60	T	161=	620.91
T	162=	623.23	T	163=	619.76	T	164=	620.69	T	165=	617.56	T	166=	619.08	T	167=	618.41
T	170=	606.44	T	172=	607.38	T	173=	605.99	T	175=	609.51	T	177=	604.27	T	180=	611.31
T	190=	603.00	T	191=	733.97	T	192=	192.97	T	193=	634.66	T	194=	303.41	T	196=	492.58
T	198=	740.18	T	200=	1036.3	T	204=	1044.4	T	210=	666.93	T	220=	641.72	T	230=	567.31
T	240=	528.51	T	242=	267.28	T	250=	116.96	T	260=	96.754	T	261=	98.896	T	262=	96.076
T	263=	99.182	T	264=	96.616	T	265=	101.55	T	266=	98.007	T	300=	1206.2	T	304=	1210.8
T	305=	1371.5	T	310=	902.18	T	313=	1087.2	T	315=	1273.1	T	316=	1273.1	T	320=	884.93
T	323=	1075.5	T	325=	1265.4	T	326=	1265.4	T	330=	826.87	T	333=	1020.6	T	335=	1232.7
T	336=	1232.7	T	340=	804.55	T	342=	508.90	T	343=	999.86	T	344=	232.18	T	345=	762.68
T	346=	1243.4	T	347=	380.27	T	349=	1015.3	T	350=	146.66	T	351=	323.77	T	352=	147.39
T	353=	237.32	T	354=	186.07	T	355=	109.86	T	356=	189.67	T	360=	94.157	T	362=	92.686
T	364=	92.043	T	366=	103.15	T	367=	104.24	T	368=	108.42	T	369=	116.47	T	371=	334.29
T	373=	244.13	T	375=	149.68	T	377=	109.20	T	400=	92.041	T	401=	100.09	T	402=	103.10
T	404=	888.75	T	406=	1365.2	T	408=	1379.8	T	410=	1413.0	T	412=	1408.5	T	414=	1418.6
T	421=	393.35	T	422=	1413.7	T	423=	1416.7	T	424=	140.67	T	425=	1397.8	T	426=	1404.7
T	431=	1224.0	T	432=	1350.0	T	433=	244.44	T	434=	213.27	T	435=	1405.6	T	436=	1404.6
T	441=	1379.2	T	442=	1372.3	T	443=	1372.5	T	444=	1372.5	T	445=	1394.6	T	446=	1380.2
T	451=	1373.8	T	452=	1365.5	T	453=	1376.5	T	454=	1381.5	T	455=	1412.4	T	456=	1394.5
T	950=	853.04															

ARITHMETIC NODES IN ASCENDING NODE NUMBER ORDER

T	50=	701.72	T	52=	663.04	T	54=	690.73	T	158=	620.99	T	159=	620.19	T	168=	620.78

T	169=	621.13	T	195=	202.23	T	197=	262.24	T	199=	514.17	T	238=	550.37	T	311=	1104.4
T	312=	1104.4	T	321=	1092.6	T	322=	1092.6	T	331=	1036.5	T	332=	1036.5	T	337=	745.56
T	341=	622.61	T	357=	217.09	T	358=	307.24	T	359=	147.63	T	379=	105.24	T	403=	107.28
T	1000=	221.25	T	1001=	598.38	T	1002=	505.42	T	1003=	276.13	T	1004=	172.80	T	1005=	170.54
T	1006=	102.18	T	1007=	630.31	T	1008=	642.22	T	1009=	705.95	T	1010=	281.98	T	1011=	925.43
T	1012=	925.43	T	1013=	1218.8	T	1021=	908.45	T	1022=	908.45	T	1023=	1210.3	T	1031=	850.14
T	1032=	850.14	T	1033=	1170.9	T	1041=	829.28	T	1042=	829.28	T	1043=	551.00	T	1044=	551.00
T	1346=	1021.7	T	1347=	288.34												

HEATER NODES IN ASCENDING NODE NUMBER ORDER
++NONE++
BOUNDARY NODES IN ASCENDING NODE NUMBER ORDER

T	1=	1475.0	T	2=	1424.7

SYSTEMS IMPROVED NUMERICAL DIFFERENCING ANALYZER '85 (SINDA '85) PAGE 4/4

MODEL = DAMAGE2 HAC LOAD CASE NO. 2 CONDITIONS - Circumferential Distribution, -20F 5/2/94
FWDBCK ***** Peak OCV Sidewall Temperature Time Point *****

SUBMODEL NAME = PTSD

	CALCULATED		ALLOWED
MAX DIFF DELTA T PER ITER	DRLXCC(PTSD	345)= 2.441406E-04	VS. DRLXCA= 5.000000E-02
MAX ARITH DELTA T PER ITER	ARLXCC(PTSD	1346)=-0.139526	VS. ARLXCA= 0.500000
MAX DIFF DEL T PER TIME STEP	DTMPCC(PTSD	345)= 2.746582E-04	VS. DTMPCA= 10.0000
MAX ARITH DEL T PER TIME STEP	ATMPCC(PTSD	1346)=-0.139496	VS. ATMPCA= 100.000
MIN STABILITY CRITERIA	CSGMIN(PTSD	446)= 3.012940E-05	
MAX STABILITY CRITERIA	CSGMAX(PTSD	424)= 2.05948	
NUMBER OF ITERATIONS	LOOPCT	= 1	VS. NLOOPT= 600
PROBLEM TIME	TIMEN	= 0.500000	VS. TIMEND= 0.500000
MEAN PROBLEM TIME	TIMEM	= 0.500000	
AVERAGE TIME STEP USED	DTIMEU	= 1.666667E-02	VS. DTIMEI= 0.

DIFFUSION NODES IN ASCENDING NODE NUMBER ORDER

T	51=	704.29	T	53=	659.63	T	55=	660.77	T	60=	815.72	T	62=	956.11	T	100=	975.13
T	105=	908.50	T	107=	881.93	T	110=	866.27	T	112=	865.79	T	113=	866.50	T	120=	787.03
T	122=	783.80	T	123=	786.30	T	124=	792.26	T	125=	793.76	T	126=	808.50	T	127=	808.52
T	130=	693.83	T	132=	692.13	T	133=	693.55	T	134=	696.56	T	135=	697.39	T	136=	706.00
T	137=	706.03	T	140=	643.03	T	141=	642.79	T	142=	643.03	T	143=	643.75	T	144=	644.59
T	145=	645.51	T	146=	651.69	T	147=	652.86	T	150=	625.06	T	152=	625.76	T	153=	625.87
T	154=	625.80	T	155=	625.29	T	156=	628.78	T	157=	628.18	T	160=	618.22	T	161=	620.12
T	162=	619.57	T	163=	619.25	T	164=	619.00	T	165=	618.55	T	166=	621.27	T	167=	621.37
T	170=	604.52	T	172=	604.58	T	173=	604.30	T	175=	606.81	T	177=	601.66	T	180=	608.63
T	190=	600.90	T	191=	729.98	T	192=	192.44	T	193=	633.56	T	194=	302.26	T	196=	490.95
T	198=	736.33	T	200=	1036.5	T	204=	1045.0	T	210=	667.66	T	220=	642.32	T	230=	583.31
T	240=	530.27	T	242=	267.50	T	250=	116.98	T	260=	96.736	T	261=	98.866	T	262=	96.054
T	263=	99.140	T	264=	96.604	T	265=	101.53	T	266=	98.008	T	300=	1206.3	T	304=	1210.9
T	305=	1371.5	T	310=	902.35	T	313=	1087.3	T	315=	1273.2	T	316=	1273.2	T	320=	885.11
T	323=	1075.6	T	325=	1265.4	T	326=	1265.4	T	330=	832.30	T	333=	1023.0	T	335=	1233.6
T	336=	1233.6	T	340=	806.26	T	342=	509.54	T	343=	1000.0	T	344=	232.34	T	345=	762.73
T	346=	1243.7	T	347=	380.29	T	349=	1015.4	T	350=	146.68	T	351=	323.81	T	352=	147.41
T	353=	237.34	T	354=	186.11	T	355=	109.87	T	356=	189.69	T	360=	94.150	T	362=	92.680
T	364=	92.041	T	366=	103.15	T	367=	104.24	T	368=	108.42	T	369=	116.47	T	371=	334.34
T	373=	244.15	T	375=	149.69	T	377=	109.20	T	400=	92.038	T	401=	100.09	T	402=	103.10
T	404=	888.76	T	406=	1365.3	T	408=	1379.8	T	410=	1413.0	T	412=	1408.5	T	414=	1418.6
T	421=	393.35	T	422=	1413.7	T	423=	1416.7	T	424=	140.67	T	425=	1397.8	T	426=	1404.7
T	431=	1224.1	T	432=	1350.1	T	433=	244.45	T	434=	213.27	T	435=	1405.6	T	436=	1404.6
T	441=	1379.2	T	442=	1372.3	T	443=	1372.5	T	444=	1372.5	T	445=	1394.6	T	446=	1380.2
T	451=	1373.8	T	452=	1365.6	T	453=	1376.5	T	454=	1381.5	T	455=	1412.4	T	456=	1394.5
T	950=	849.81															

ARITHMETIC NODES IN ASCENDING NODE NUMBER ORDER

T	50=	708.33	T	52=	663.31	T	54=	686.18	T	158=	620.14	T	159=	620.01	T	168=	620.00

T	169=	620.21	T	195=	201.66	T	197=	261.20	T	199=	512.40	T	238=	560.20	T	311=	1104.5
T	312=	1104.5	T	321=	1092.7	T	322=	1092.7	T	331=	1038.8	T	332=	1038.8	T	337=	746.20
T	341=	623.36	T	357=	217.12	T	358=	307.28	T	359=	147.64	T	379=	105.24	T	403=	107.28
T	1000=	220.53	T	1001=	595.52	T	1002=	503.44	T	1003=	275.08	T	1004=	172.37	T	1005=	170.12
T	1006=	102.12	T	1007=	627.59	T	1008=	639.49	T	1009=	702.34	T	1010=	281.47	T	1011=	925.59
T	1012=	925.59	T	1013=	1218.8	T	1021=	908.62	T	1022=	908.62	T	1023=	1210.4	T	1031=	855.36
T	1032=	855.36	T	1033=	1172.3	T	1041=	831.03	T	1042=	831.03	T	1043=	551.79	T	1044=	551.79
T	1346=	1021.8	T	1347=	288.36												

HEATER NODES IN ASCENDING NODE NUMBER ORDER
++NONE++
BOUNDARY NODES IN ASCENDING NODE NUMBER ORDER

T	1=	1475.0	T	2=	1424.7

```
                    SYSTEMS IMPROVED NUMERICAL DIFFERENCING ANALYZER '85 (SINDA '85)                PAGE   1/4

MODEL = DAMAGE2          HAC LOAD CASE NO. 2 CONDITIONS - Circumferential Distribution, -20F              5/2/94
  FWDBCK                 *****      Peak ICV Sidewall Temperature Time Point     *****

 SUBMODEL NAME = MAIN

       PROBLEM TIME                    TIMEN                  = 0.766666     VS. TIMEND=  12.0000
                                  DIFFUSION NODES IN ASCENDING NODE NUMBER ORDER
  T  267=  126.52     T  268=  126.40     T  269=  120.62
                                  ARITHMETIC NODES IN ASCENDING NODE NUMBER ORDER
  T  201=  776.77     T 1266=  141.18     T 1267=  284.47     T 1268=  234.94     T 1269=  150.10
                                  HEATER NODES IN ASCENDING NODE NUMBER ORDER
                                            ++NONE++
                                  BOUNDARY NODES IN ASCENDING NODE NUMBER ORDER
                                            ++NONE++
MEAN ICV GAS TEMP= 776.8 F   MEAN ICV GAS PRESSURE= 37.12 PSIA
MEAN ICV-OCV GAS TEMP= 715.6 F   MEAN ICV-OCV GAS PRESSURE= 41.43 PSIA


 SUBMODEL NAME = PTSA
                                  CALCULATED                                    ALLOWED
       MAX DIFF DELTA T PER ITER  DRLXCC(PTSA      161)= 5.126953E-03 VS. DRLXCA= 5.000000E-02
       MAX ARITH DELTA T PER ITER ARLXCC(PTSA      337)=-6.451416E-02 VS. ARLXCA= 0.500000
       MAX DIFF DEL T PER TIME STEP DTMPCC(PTSA    423)= -1.27573     VS. DTMPCA=  10.0000
       MAX ARITH DEL T PER TIME STEP ATMPCC(PTSA  1346)=-0.953827     VS. ATMPCA=  100.000
       MIN STABILITY CRITERIA     CSGMIN(PTSA      431)= 2.095422E-04
       MAX STABILITY CRITERIA     CSGMAX(PTSA      424)=  2.15480
       NUMBER OF ITERATIONS       LOOPCT                =     3     VS. NLOOPT=     600
       PROBLEM TIME               TIMEN                 = 0.766666  VS. TIMEND=  12.0000
       MEAN PROBLEM TIME          TIMEM                 = 0.766172
       AVERAGE TIME STEP USED     DTIMEU                = 7.936509E-04 VS. DTIMEI=      0.
                                  DIFFUSION NODES IN ASCENDING NODE NUMBER ORDER
  T   51=  704.31     T   53=  682.10     T   55=  704.48     T   60=  808.24     T   62=  896.88     T  100=  888.50
  T  105=  847.24     T  107=  828.97     T  110=  806.51     T  112=  806.42     T  113=  807.85     T  120=  744.58
  T  122=  742.27     T  123=  746.54     T  124=  741.76     T  125=  744.76     T  126=  740.86     T  127=  741.69
  T  130=  723.80     T  132=  721.99     T  133=  725.07     T  134=  723.30     T  135=  725.32     T  136=  725.86
  T  137=  726.15     T  140=  715.00     T  141=  715.29     T  142=  713.81     T  143=  716.11     T  144=  714.49
  T  145=  716.26     T  146=  716.60     T  147=  717.35     T  150=  714.51     T  152=  713.27     T  153=  715.08
  T  154=  714.54     T  155=  715.84     T  156=  717.24     T  157=  717.76     T  160=  719.83     T  161=  718.66
  T  162=  719.29     T  163=  720.06     T  164=  720.29     T  165=  721.18     T  166=  723.21     T  167=  723.84
  T  170=  708.63     T  172=  708.16     T  173=  708.71     T  175=  702.57     T  177=  702.78     T  180=  692.32
  T  190=  703.51     T  191=  773.83     T  192=  234.97     T  193=  719.59     T  194=  357.33     T  196=  640.30
  T  198=  778.60     T  200=  919.42     T  204=  902.74     T  210=  756.68     T  220=  734.57     T  230=  701.24
  T  240=  629.96     T  242=  356.52     T  250=  153.99     T  260=  100.56     T  261=  103.97     T  262=  105.71
  T  263=  112.98     T  264=  112.43     T  265=  120.20     T  266=  121.01     T  300=  815.55     T  304=  804.48
  T  305=  503.98     T  310=  728.13     T  313=  654.51     T  315=  543.57     T  316=  543.57     T  320=  711.13
  T  323=  642.24     T  325=  536.59     T  326=  536.59     T  330=  681.88     T  333=  613.43     T  335=  531.51
  T  336=  531.51     T  340=  642.17     T  342=  454.17     T  343=  550.05     T  344=  278.11     T  345=  710.44
  T  346=  616.61     T  347=  466.49     T  349=  454.34     T  350=  200.83     T  351=  252.05     T  352=  204.59
  T  353=  224.21     T  354=  232.78     T  355=  154.48     T  356=  239.39     T  360=  96.774     T  362=  98.593
  T  364=  107.72     T  366=  148.27     T  367=  155.31     T  368=  175.24     T  369=  202.25     T  371=  257.12
  T  373=  231.52     T  375=  180.03     T  377=  150.19     T  400=  101.12     T  401=  115.89     T  402=  146.08
  T  404=  745.04     T  406=  603.03     T  408=  640.91     T  410=  620.50     T  412=  673.44     T  414=  608.35
```

T	421=	416.18	T	422=	641.06	T	423=	629.49	T	424=	212.77	T	425=	783.42	T	426=	711.20
T	431=	645.09	T	432=	742.51	T	433=	819.98	T	434=	817.82	T	435=	745.19	T	436=	642.83
T	950=	886.15															

ARITHMETIC NODES IN ASCENDING NODE NUMBER ORDER

T	50=	710.62	T	52=	685.26	T	54=	718.28	T	158=	718.84	T	159=	719.12	T	168=	718.70
T	169=	718.67	T	195=	249.10	T	197=	301.35	T	199=	551.42	T	238=	670.24	T	311=	638.98
T	312=	638.98	T	321=	626.93	T	322=	626.93	T	331=	597.94	T	332=	597.94	T	337=	515.83
T	341=	493.26	T	357=	240.93	T	358=	256.72	T	359=	202.85	T	379=	152.46	T	403=	148.87
T	1000=	278.36	T	1001=	663.51	T	1002=	545.91	T	1003=	323.05	T	1004=	207.69	T	1005=	204.59
T	1006=	112.07	T	1007=	716.07	T	1008=	723.83	T	1009=	758.56	T	1010=	323.03	T	1011=	723.21
T	1012=	723.21	T	1013=	581.01	T	1021=	706.59	T	1022=	706.59	T	1023=	572.11	T	1031=	677.91
T	1032=	677.91	T	1033=	558.30	T	1041=	639.76	T	1042=	639.76	T	1043=	458.07	T	1044=	458.07
T	1346=	648.19	T	1347=	364.53												

HEATER NODES IN ASCENDING NODE NUMBER ORDER

++NONE++

BOUNDARY NODES IN ASCENDING NODE NUMBER ORDER

T	1=	-20.000	T	2=	-20.000									

SYSTEMS IMPROVED NUMERICAL DIFFERENCING ANALYZER '85 (SINDA '85) PAGE 2/4

MODEL = DAMAGE2 HAC LOAD CASE NO. 2 CONDITIONS - Circumferential Distribution, -20F 5/2/94
FWDBCK ***** Peak ICV Sidewall Temperature Time Point *****

SUBMODEL NAME = PTSB

		CALCULATED			ALLOWED	
MAX DIFF DELTA T PER ITER	DRLXCC(PTSB	161)=	4.882812E-03	VS. DRLXCA=	5.000000E-02
MAX ARITH DELTA T PER ITER	ARLXCC(PTSB	337)=	-6.402588E-02	VS. ARLXCA=	0.500000
MAX DIFF DEL T PER TIME STEP	DTMPCC(PTSB	435)=	-1.29636	VS. DTMPCA=	10.0000
MAX ARITH DEL T PER TIME STEP	ATMPCC(PTSB	1346)=	-0.780609	VS. ATMPCA=	100.000
MIN STABILITY CRITERIA	CSGMIN(PTSB	455)=	2.661042E-04		
MAX STABILITY CRITERIA	CSGMAX(PTSB	424)=	2.22717		
NUMBER OF ITERATIONS	LOOPCT	=	3	VS. NLOOPT=	600
PROBLEM TIME	TIMEN	=	0.766666	VS. TIMEND=	12.0000
MEAN PROBLEM TIME	TIMEM	=	0.766172		
AVERAGE TIME STEP USED	DTIMEU	=	7.936509E-04	VS. DTIMEI=	0.

DIFFUSION NODES IN ASCENDING NODE NUMBER ORDER

T	51=	719.43	T	53=	687.23	T	55=	702.58	T	60=	811.51	T	62=	895.36	T	100=	889.79
T	105=	851.09	T	107=	833.78	T	110=	812.23	T	112=	811.05	T	113=	815.81	T	120=	755.88
T	122=	749.81	T	123=	764.37	T	124=	748.49	T	125=	758.69	T	126=	746.04	T	127=	748.53
T	130=	731.69	T	132=	727.45	T	133=	736.47	T	134=	728.71	T	135=	734.85	T	136=	731.06
T	137=	732.29	T	140=	720.96	T	141=	721.27	T	142=	718.56	T	143=	723.35	T	144=	719.49
T	145=	723.01	T	146=	721.94	T	147=	723.08	T	150=	718.10	T	152=	716.49	T	153=	718.27
T	154=	718.32	T	155=	719.68	T	156=	721.99	T	157=	722.62	T	160=	720.76	T	161=	720.33
T	162=	720.68	T	163=	718.89	T	164=	722.61	T	165=	722.50	T	166=	727.22	T	167=	727.55
T	170=	710.71	T	172=	710.24	T	173=	709.67	T	175=	704.98	T	177=	704.88	T	180=	693.18
T	190=	707.25	T	191=	784.41	T	192=	228.47	T	193=	725.28	T	194=	365.62	T	196=	635.18
T	198=	789.55	T	200=	918.39	T	204=	902.54	T	210=	757.85	T	220=	736.52	T	230=	708.16
T	240=	632.89	T	242=	363.45	T	250=	152.61	T	260=	99.765	T	261=	102.80	T	262=	101.88
T	263=	106.39	T	264=	110.03	T	265=	117.59	T	266=	118.07	T	300=	814.71	T	304=	804.24
T	305=	503.92	T	310=	728.81	T	313=	655.02	T	315=	543.95	T	316=	543.95	T	320=	712.24
T	323=	643.10	T	325=	537.26	T	326=	537.26	T	330=	685.86	T	333=	615.89	T	335=	533.15
T	336=	533.15	T	340=	644.10	T	342=	453.62	T	343=	546.63	T	344=	269.43	T	345=	637.49
T	346=	609.66	T	347=	412.32	T	349=	447.46	T	350=	186.83	T	351=	237.90	T	352=	187.53
T	353=	210.70	T	354=	218.78	T	355=	139.50	T	356=	220.51	T	360=	96.337	T	362=	96.838
T	364=	104.55	T	366=	134.95	T	367=	138.01	T	368=	144.98	T	369=	161.06	T	371=	242.78
T	373=	218.62	T	375=	167.92	T	377=	136.16	T	400=	99.768	T	401=	114.82	T	402=	131.40
T	404=	704.72	T	406=	608.84	T	408=	575.67	T	410=	630.58	T	412=	674.20	T	414=	608.38
T	421=	415.69	T	422=	641.10	T	423=	629.60	T	424=	184.17	T	425=	783.69	T	426=	715.66
T	431=	662.35	T	432=	736.68	T	433=	348.86	T	434=	294.54	T	435=	747.28	T	436=	663.41
T	441=	579.45	T	442=	658.61	T	443=	688.66	T	444=	688.15	T	445=	667.08	T	446=	580.75
T	451=	593.62	T	452=	608.89	T	453=	619.91	T	454=	622.40	T	455=	629.23	T	456=	604.67
T	950=	893.17															

ARITHMETIC NODES IN ASCENDING NODE NUMBER ORDER

T	50=	723.42	T	52=	690.47	T	54=	717.35	T	158=	720.78	T	159=	720.82	T	168=	720.33

T	169=	720.13	T	195=	237.08	T	197=	299.73	T	199=	578.40	T	238=	675.44	T	311=	639.51
T	312=	639.51	T	321=	627.81	T	322=	627.81	T	331=	600.34	T	332=	600.34	T	337=	513.90
T	341=	492.45	T	357=	224.89	T	358=	241.92	T	359=	187.33	T	379=	137.23	T	403=	134.64
T	1000=	258.04	T	1001=	668.17	T	1002=	566.84	T	1003=	319.08	T	1004=	201.83	T	1005=	198.81
T	1006=	108.51	T	1007=	720.45	T	1008=	729.35	T	1009=	767.59	T	1010=	349.73	T	1011=	723.88
T	1012=	723.88	T	1013=	581.44	T	1021=	707.68	T	1022=	707.68	T	1023=	572.84	T	1031=	681.79
T	1032=	681.79	T	1033=	560.22	T	1041=	641.68	T	1042=	641.68	T	1043=	457.62	T	1044=	457.62
T	1346=	598.97	T	1347=	316.70												

HEATER NODES IN ASCENDING NODE NUMBER ORDER
++NONE++

BOUNDARY NODES IN ASCENDING NODE NUMBER ORDER

T	1=	-20.000	T	2=	-20.000

SYSTEMS IMPROVED NUMERICAL DIFFERENCING ANALYZER '85 (SINDA '85) PAGE 3/4

MODEL = DAMAGE2 HAC LOAD CASE NO. 2 CONDITIONS - Circumferential Distribution, -20F 5/2/94
FWDBCK ***** Peak ICV Sidewall Temperature Time Point *****

SUBMODEL NAME = PTSC

	CALCULATED		ALLOWED
MAX DIFF DELTA T PER ITER	DRLXCC(PTSC	120)=-4.516602E-03	VS. DRLXCA= 5.000000E-02
MAX ARITH DELTA T PER ITER	ARLXCC(PTSC	337)=-6.494141E-02	VS. ARLXCA= 0.500000
MAX DIFF DEL T PER TIME STEP	DTMPCC(PTSC	435)= -1.29623	VS. DTMPCA= 10.0000
MAX ARITH DEL T PER TIME STEP	ATMPCC(PTSC	1346)=-0.781219	VS. ATMPCA= 100.000
MIN STABILITY CRITERIA	CSGMIN(PTSC	455)= 2.661084E-04	
MAX STABILITY CRITERIA	CSGMAX(PTSC	424)= 2.22717	
NUMBER OF ITERATIONS	LOOPCT	= 3	VS. NLOOPT= 600
PROBLEM TIME	TIMEN	= 0.766666	VS. TIMEND= 12.0000
MEAN PROBLEM TIME	TIMEM	= 0.766172	
AVERAGE TIME STEP USED	DTIMEU	= 7.936509E-04	VS. DTIMEI= 0.

DIFFUSION NODES IN ASCENDING NODE NUMBER ORDER

T	51=	764.98	T	53=	699.50	T	55=	693.03	T	60=	823.74	T	62=	892.86	T	100=	883.29
T	105=	860.97	T	107=	851.41	T	110=	839.84	T	112=	837.90	T	113=	840.88	T	120=	794.85
T	122=	788.15	T	123=	797.33	T	124=	793.17	T	125=	799.42	T	126=	800.89	T	127=	802.23
T	130=	755.63	T	132=	750.63	T	133=	756.34	T	134=	755.59	T	135=	759.43	T	136=	763.69
T	137=	764.42	T	140=	735.69	T	141=	736.51	T	142=	733.00	T	143=	735.91	T	144=	735.41
T	145=	737.60	T	146=	740.42	T	147=	741.23	T	150=	720.84	T	152=	719.88	T	153=	720.92
T	154=	721.29	T	155=	721.79	T	156=	724.28	T	157=	724.21	T	160=	713.44	T	161=	716.33
T	162=	714.11	T	163=	712.95	T	164=	714.63	T	165=	714.23	T	166=	716.50	T	167=	716.57
T	170=	704.62	T	172=	704.90	T	173=	704.40	T	175=	704.01	T	177=	702.14	T	180=	702.10
T	190=	702.11	T	191=	782.63	T	192=	228.16	T	193=	722.88	T	194=	365.09	T	196=	630.05
T	198=	787.82	T	200=	897.78	T	204=	870.06	T	210=	766.53	T	220=	738.91	T	230=	688.20
T	240=	627.69	T	242=	361.92	T	250=	152.25	T	260=	99.560	T	261=	102.56	T	262=	101.63
T	263=	106.08	T	264=	109.81	T	265=	117.32	T	266=	117.87	T	300=	802.51	T	304=	785.33
T	305=	497.09	T	310=	734.41	T	313=	659.34	T	315=	547.02	T	316=	547.02	T	320=	713.88
T	323=	644.39	T	325=	538.21	T	326=	538.21	T	330=	673.17	T	333=	607.62	T	335=	527.21
T	336=	527.21	T	340=	638.12	T	342=	451.19	T	343=	545.97	T	344=	268.57	T	345=	636.29
T	346=	608.57	T	347=	411.64	T	349=	446.91	T	350=	186.42	T	351=	237.51	T	352=	187.12
T	353=	210.39	T	354=	218.28	T	355=	139.19	T	356=	220.04	T	360=	96.210	T	362=	96.696
T	364=	104.41	T	366=	134.65	T	367=	137.67	T	368=	144.45	T	369=	160.34	T	371=	242.37
T	373=	218.33	T	375=	167.75	T	377=	136.01	T	400=	99.733	T	401=	114.80	T	402=	131.24
T	404=	704.54	T	406=	608.42	T	408=	575.63	T	410=	630.58	T	412=	674.20	T	414=	608.38
T	421=	415.68	T	422=	641.10	T	423=	629.60	T	424=	184.16	T	425=	783.69	T	426=	715.65
T	431=	662.11	T	432=	736.43	T	433=	348.83	T	434=	294.54	T	435=	747.28	T	436=	663.40
T	441=	579.40	T	442=	658.45	T	443=	688.64	T	444=	688.13	T	445=	667.06	T	446=	580.72
T	451=	593.43	T	452=	608.50	T	453=	619.83	T	454=	622.37	T	455=	629.23	T	456=	604.65
T	950=	892.09															

ARITHMETIC NODES IN ASCENDING NODE NUMBER ORDER

T	50=	761.78	T	52=	703.12	T	54=	711.33	T	158=	716.17	T	159=	716.10	T	168=	716.04		

T	169=	716.00	T	195=	236.38	T	197=	299.07	T	199=	577.00	T	238=	661.85	T	311=	643.83
T	312=	643.83	T	321=	629.10	T	322=	629.10	T	331=	592.18	T	332=	592.18	T	337=	511.40
T	341=	489.66	T	357=	224.42	T	358=	241.47	T	359=	186.92	T	379=	136.91	T	403=	134.49
T	1000=	257.61	T	1001=	665.80	T	1002=	565.55	T	1003=	318.32	T	1004=	201.54	T	1005=	198.52
T	1006=	108.24	T	1007=	717.87	T	1008=	725.84	T	1009=	765.27	T	1010=	348.75	T	1011=	729.36
T	1012=	729.36	T	1013=	584.95	T	1021=	709.29	T	1022=	709.29	T	1023=	573.91	T	1031=	669.37
T	1032=	669.37	T	1033=	553.47	T	1041=	635.68	T	1042=	635.68	T	1043=	454.98	T	1044=	454.98
T	1346=	597.90	T	1347=	316.04												

HEATER NODES IN ASCENDING NODE NUMBER ORDER
++NONE++

BOUNDARY NODES IN ASCENDING NODE NUMBER ORDER

T	1=	-20.000	T	2=	-20.000

SYSTEMS IMPROVED NUMERICAL DIFFERENCING ANALYZER '85 (SINDA '85) PAGE 4/4

MODEL = DAMAGE2 HAC LOAD CASE NO. 2 CONDITIONS - Circumferential Distribution, -20F 5/2/94
FWDBCK ***** Peak ICV Sidewall Temperature Time Point *****

SUBMODEL NAME = PTSD

	CALCULATED		ALLOWED
MAX DIFF DELTA T PER ITER	DRLXCC(PTSD	120)=-4.394531E-03	VS. DRLXCA= 5.000000E-02
MAX ARITH DELTA T PER ITER	ARLXCC(PTSD	337)=-6.396484E-02	VS. ARLXCA= 0.500000
MAX DIFF DEL T PER TIME STEP	DTMPCC(PTSD	435)= -1.29623	VS. DTMPCA= 10.0000
MAX ARITH DEL T PER TIME STEP	ATMPCC(PTSD	1346)=-0.780853	VS. ATMPCA= 100.000
MIN STABILITY CRITERIA	CSGMIN(PTSD	455)= 2.661075E-04	
MAX STABILITY CRITERIA	CSGMAX(PTSD	424)= 2.22717	
NUMBER OF ITERATIONS	LOOPCT	= 3	VS. NLOOPT= 600
PROBLEM TIME	TIMEN	= 0.766666	VS. TIMEND= 12.0000
MEAN PROBLEM TIME	TIMEM	= 0.766172	
AVERAGE TIME STEP USED	DTIMEU	= 7.936509E-04	VS. DTIMEI= 0.

DIFFUSION NODES IN ASCENDING NODE NUMBER ORDER

T	51=	775.98	T	53=	703.63	T	55=	692.10	T	60=	826.19	T	62=	891.38	T	100=	884.91
T	105=	864.45	T	107=	855.57	T	110=	844.59	T	112=	844.46	T	113=	844.97	T	120=	803.37
T	122=	801.70	T	123=	803.32	T	124=	803.44	T	125=	804.51	T	126=	805.48	T	127=	805.71
T	130=	761.63	T	132=	759.52	T	133=	760.68	T	134=	762.74	T	135=	763.45	T	136=	767.76
T	137=	767.82	T	140=	740.66	T	141=	741.54	T	142=	739.23	T	143=	740.05	T	144=	740.90
T	145=	741.62	T	146=	744.46	T	147=	744.91	T	150=	724.52	T	152=	723.48	T	153=	724.26
T	154=	725.15	T	155=	725.54	T	156=	728.56	T	157=	728.58	T	160=	715.08	T	161=	718.39
T	162=	714.35	T	163=	714.85	T	164=	716.14	T	165=	717.15	T	166=	720.18	T	167=	720.57
T	170=	705.80	T	172=	705.51	T	173=	705.61	T	175=	704.46	T	177=	702.86	T	180=	702.16
T	190=	702.68	T	191=	781.90	T	192=	227.62	T	193=	723.58	T	194=	364.44	T	196=	629.54
T	198=	787.13	T	200=	897.68	T	204=	870.91	T	210=	768.04	T	220=	740.38	T	230=	699.20
T	240=	630.18	T	242=	362.57	T	250=	152.35	T	260=	99.518	T	261=	102.51	T	262=	101.59
T	263=	106.02	T	264=	109.80	T	265=	117.31	T	266=	117.89	T	300=	802.25	T	304=	785.67
T	305=	497.21	T	310=	735.27	T	313=	659.96	T	315=	547.45	T	316=	547.45	T	320=	714.72
T	323=	644.99	T	325=	538.62	T	326=	538.62	T	330=	679.97	T	333=	611.98	T	335=	530.33
T	336=	530.33	T	340=	641.16	T	342=	452.36	T	343=	546.23	T	344=	268.88	T	345=	636.40
T	346=	609.06	T	347=	411.70	T	349=	447.13	T	350=	186.48	T	351=	237.59	T	352=	187.16
T	353=	210.44	T	354=	218.38	T	355=	139.21	T	356=	220.10	T	360=	96.187	T	362=	96.677
T	364=	104.41	T	366=	134.67	T	367=	137.68	T	368=	144.45	T	369=	160.35	T	371=	242.45
T	373=	218.39	T	375=	167.77	T	377=	136.02	T	400=	99.728	T	401=	114.79	T	402=	131.25
T	404=	704.57	T	406=	608.65	T	408=	575.64	T	410=	630.58	T	412=	674.20	T	414=	608.38
T	421=	415.68	T	422=	641.10	T	423=	629.60	T	424=	184.16	T	425=	783.69	T	426=	715.65
T	431=	662.22	T	432=	736.57	T	433=	348.84	T	434=	294.54	T	435=	747.28	T	436=	663.41
T	441=	579.42	T	442=	658.53	T	443=	688.65	T	444=	688.13	T	445=	667.07	T	446=	580.73
T	451=	593.53	T	452=	608.72	T	453=	619.87	T	454=	622.38	T	455=	629.23	T	456=	604.66
T	950=	890.95															

ARITHMETIC NODES IN ASCENDING NODE NUMBER ORDER

T	50=	771.15	T	52=	707.29	T	54=	711.03	T	158=	718.19	T	159=	718.46	T	168=	718.09		

T	169=	717.94	T	195=	236.05	T	197=	298.64	T	199=	576.82	T	238=	669.18	T	311=	644.47
T	312=	644.47	T	321=	629.72	T	322=	629.72	T	331=	596.49	T	332=	596.49	T	337=	512.62
T	341=	491.02	T	357=	224.50	T	358=	241.56	T	359=	186.97	T	379=	136.92	T	403=	134.50
T	1000=	257.18	T	1001=	665.17	T	1002=	565.21	T	1003=	317.76	T	1004=	201.22	T	1005=	198.21
T	1006=	108.18	T	1007=	718.14	T	1008=	726.01	T	1009=	764.82	T	1010=	348.76	T	1011=	730.20
T	1012=	730.20	T	1013=	585.45	T	1021=	710.12	T	1022=	710.12	T	1023=	574.39	T	1031=	676.03
T	1032=	676.03	T	1033=	557.02	T	1041=	638.74	T	1042=	638.74	T	1043=	456.27	T	1044=	456.27
T	1346=	598.10	T	1347=	316.08												

HEATER NODES IN ASCENDING NODE NUMBER ORDER
++NONE++
BOUNDARY NODES IN ASCENDING NODE NUMBER ORDER

T	1=	-20.000	T	2=	-20.000

SYSTEMS IMPROVED NUMERICAL DIFFERENCING ANALYZER '85 (SINDA '85) PAGE 1/4

MODEL = DAMAGE2
STDSTL

HAC LOAD CASE NO. 2 CONDITIONS - Circumferential Distribution, -20F
*** Steady-state Conditions After The Fire ***

5/2/94 10am

SUBMODEL NAME = MAIN

PROBLEM TIME TIMEN = 999.000 VS. TIMEND= 999.000

DIFFUSION NODES IN ASCENDING NODE NUMBER ORDER

T	267=	181.10	T	268=	181.13	T	269=	178.84			

ARITHMETIC NODES IN ASCENDING NODE NUMBER ORDER

T	201=	312.85	T	1266=	185.46	T	1267=	226.68	T	1268=	215.95	T	1269=	188.32

HEATER NODES IN ASCENDING NODE NUMBER ORDER

++NONE++

BOUNDARY NODES IN ASCENDING NODE NUMBER ORDER

++NONE++

MEAN ICV GAS TEMP= 312.8 F MEAN ICV GAS PRESSURE= 23.20 PSIA
MEAN ICV-OCV GAS TEMP= 172.2 F MEAN ICV-OCV GAS PRESSURE= 22.27 PSIA

SUBMODEL NAME = PTSA

	CALCULATED		ALLOWED	
MAX DIFF DELTA T PER ITER	DRLXCC(PTSA	368)= 0.639160	VS. DRLXCA=	5.000000E-02
MAX ARITH DELTA T PER ITER	ARLXCC(PTSA	1005)= 4.38379	VS. ARLXCA=	0.500000
MAX SYSTEM ENERGY BALANCE	EBALSC	= 6.75369	VS. EBALSA * ESUMIS	= 0.959906
			EBALSA=	1.000000E-03
ENERGY INTO AND OUT OF SYS	ESUMIS	= 959.906	ESUMOS=	948.226
MAX NODAL ENERGY BALANCE	EBALNC(PTSA	350)= 0.801862	VS. EBALNA=	1.000000E-02
NUMBER OF ITERATIONS	LOOPCT	= 140	VS. NLOOPS=	1200
PROBLEM TIME	TIMEN	= 999.000	VS. TIMEND=	999.000

DIFFUSION NODES IN ASCENDING NODE NUMBER ORDER

T	51=	228.84	T	53=	280.40	T	55=	367.64	T	60=	219.87	T	62=	393.46	T	100=	208.11
T	105=	210.80	T	107=	211.92	T	110=	213.20	T	112=	213.32	T	113=	213.07	T	120=	222.62
T	122=	222.89	T	123=	222.23	T	124=	222.17	T	125=	221.56	T	126=	221.03	T	127=	220.57
T	130=	250.76	T	132=	251.92	T	133=	250.36	T	134=	250.20	T	135=	248.76	T	136=	246.66
T	137=	245.49	T	140=	273.52	T	141=	273.70	T	142=	274.17	T	143=	272.22	T	144=	274.21
T	145=	272.74	T	146=	274.89	T	147=	274.31	T	150=	313.69	T	152=	314.05	T	153=	310.88
T	154=	317.29	T	155=	315.40	T	156=	322.46	T	157=	322.95	T	160=	377.90	T	161=	367.09
T	162=	378.80	T	163=	375.22	T	164=	378.60	T	165=	377.14	T	166=	379.77	T	167=	378.91
T	170=	431.77	T	172=	431.76	T	173=	431.76	T	175=	449.87	T	177=	441.54	T	180=	443.40
T	190=	458.42	T	191=	537.33	T	192=	287.28	T	193=	388.74	T	194=	300.11	T	196=	408.58
T	198=	541.04	T	200=	182.42	T	204=	174.81	T	210=	188.29	T	220=	195.34	T	230=	221.16
T	240=	228.87	T	242=	197.49	T	250=	172.48	T	260=	186.02	T	261=	187.85	T	262=	180.45
T	263=	182.90	T	264=	173.58	T	265=	177.06	T	266=	167.67	T	300=	112.55	T	304=	94.798
T	305=	22.078	T	310=	143.03	T	313=	124.96	T	315=	103.45	T	316=	103.45	T	320=	151.10
T	323=	132.10	T	325=	109.52	T	326=	109.52	T	330=	170.54	T	333=	148.69	T	335=	123.39
T	336=	123.39	T	340=	171.73	T	342=	160.12	T	343=	100.55	T	344=	149.02	T	345=	101.79
T	346=	80.315	T	347=	127.15	T	349=	91.125	T	350=	145.08	T	351=	137.64	T	352=	144.28
T	353=	140.65	T	354=	143.93	T	355=	146.79	T	356=	142.18	T	360=	181.91	T	362=	175.97
T	364=	165.16	T	366=	148.08	T	367=	146.28	T	368=	144.84	T	369=	142.63	T	371=	138.11
T	373=	140.22	T	375=	143.27	T	377=	145.24	T	400=	169.11	T	401=	167.14	T	402=	145.66
T	404=	100.58	T	406=	16.236	T	408=	-8.2607	T	410=	-15.168	T	412=	-12.849	T	414=	-12.285

T	421=	110.73	T	422=	0.46304	T	423=	-7.5431	T	424=	86.014	T	425=	1.4922	T	426=	-6.5927
T	431=	21.232	T	432=	20.090	T	433=	19.882	T	434=	2.1944	T	435=	-8.9075	T	436=	-8.8851
T	950=	653.54																	

ARITHMETIC NODES IN ASCENDING NODE NUMBER ORDER

T	50=	235.12	T	52=	282.00	T	54=	358.50	T	158=	367.35	T	159=	366.90	T	168=	367.03
T	169=	366.77	T	195=	243.69	T	197=	260.95	T	199=	379.49	T	238=	224.55	T	311=	123.46
T	312=	123.46	T	321=	130.54	T	322=	130.54	T	331=	146.90	T	332=	146.90	T	337=	142.03
T	341=	154.67	T	357=	141.92	T	358=	137.53	T	359=	144.56	T	379=	147.08	T	403=	145.37
T	1000=	253.94	T	1001=	468.53	T	1002=	387.33	T	1003=	322.50	T	1004=	265.89	T	1005=	267.15
T	1006=	189.18	T	1007=	469.01	T	1008=	480.16	T	1009=	519.94	T	1010=	242.59	T	1011=	142.72
T	1012=	142.72	T	1013=	111.27	T	1021=	150.77	T	1022=	150.77	T	1023=	117.71	T	1031=	170.15
T	1032=	170.15	T	1033=	132.43	T	1041=	171.31	T	1042=	171.31	T	1043=	159.86	T	1044=	159.86
T	1346=	90.917	T	1347=	133.90														

HEATER NODES IN ASCENDING NODE NUMBER ORDER

++NONE++

BOUNDARY NODES IN ASCENDING NODE NUMBER ORDER

T	1=	-20.000	T	2=	-20.000														

SYSTEMS IMPROVED NUMERICAL DIFFERENCING ANALYZER '85 (SINDA '85) PAGE 2/4

MODEL = DAMAGE2
STDSTL

HAC LOAD CASE NO. 2 CONDITIONS - Circumferential Distribution, -20
*** Steady-state Conditions After The Fire ***

5/2/94 10am

SUBMODEL NAME = PTSB

		CALCULATED		ALLOWED	
MAX DIFF DELTA T PER ITER	DRLXCC(PTSB	194)=-3.686523E-02	VS.	DRLXCA= 5.000000E-02	
MAX ARITH DELTA T PER ITER	ARLXCC(PTSB	197)=-0.109863	VS.	ARLXCA= 0.500000	
MAX SYSTEM ENERGY BALANCE	EBALSC	= 1.76287	VS.	EBALSA * ESUMIS	= 1.91981
				EBALSA= 1.000000E-03	
ENERGY INTO AND OUT OF SYS	ESUMIS	= 1919.81		ESUMOS= 1908.60	
MAX NODAL ENERGY BALANCE	EBALNC(PTSB	367)= 0.549181	VS.	EBALNA= 1.000000E-02	
NUMBER OF ITERATIONS	LOOPCT	= 140	VS.	NLOOPS= 1200	
PROBLEM TIME	TIMEN	= 999.000	VS.	TIMEND= 999.000	

DIFFUSION NODES IN ASCENDING NODE NUMBER ORDER

T	51=	226.69	T	53=	274.13	T	55=	359.01	T	60=	218.38	T	62=	390.49	T	100=	207.30
T	105=	209.98	T	107=	211.06	T	110=	212.27	T	112=	212.54	T	113=	211.93	T	120=	221.03
T	122=	221.82	T	123=	219.95	T	124=	221.34	T	125=	219.73	T	126=	220.78	T	127=	219.75
T	130=	247.05	T	132=	249.36	T	133=	245.01	T	134=	248.16	T	135=	244.45	T	136=	245.82
T	137=	243.62	T	140=	268.11	T	141=	268.28	T	142=	270.25	T	143=	264.67	T	144=	271.08
T	145=	266.66	T	146=	273.65	T	147=	271.59	T	150=	305.01	T	152=	308.59	T	153=	297.47
T	154=	312.80	T	155=	304.78	T	156=	320.29	T	157=	318.74	T	160=	369.32	T	161=	359.06
T	162=	372.78	T	163=	361.58	T	164=	374.24	T	165=	367.74	T	166=	378.23	T	167=	374.81
T	170=	431.85	T	172=	432.43	T	173=	429.69	T	175=	454.08	T	177=	443.83	T	180=	448.00
T	190=	468.76	T	191=	546.74	T	192=	296.45	T	193=	392.35	T	194=	313.86	T	196=	414.65
T	198=	550.20	T	200=	182.80	T	204=	175.22	T	210=	188.71	T	220=	196.10	T	230=	229.56
T	240=	232.69	T	242=	200.33	T	250=	174.55	T	260=	186.85	T	261=	188.84	T	262=	182.10
T	263=	184.75	T	264=	175.32	T	265=	178.76	T	266=	169.68	T	300=	112.84	T	304=	95.088
T	305=	22.181	T	310=	143.40	T	313=	125.29	T	315=	103.72	T	316=	103.72	T	320=	151.81
T	323=	132.74	T	325=	110.06	T	326=	110.06	T	330=	175.72	T	333=	152.83	T	335=	126.64
T	336=	126.64	T	340=	175.00	T	342=	163.01	T	343=	102.01	T	344=	151.71	T	345=	104.63
T	346=	81.863	T	347=	129.59	T	349=	92.972	T	350=	147.85	T	351=	140.49	T	352=	146.76
T	353=	143.51	T	354=	146.59	T	355=	149.66	T	356=	144.69	T	360=	182.61	T	362=	177.42
T	364=	167.11	T	366=	150.89	T	367=	149.19	T	368=	147.27	T	369=	145.63	T	371=	140.40
T	373=	142.86	T	375=	146.27	T	377=	148.33	T	400=	170.65	T	401=	168.68	T	402=	148.76
T	404=	110.90	T	406=	17.606	T	408=	-12.453	T	410=	-15.287	T	412=	-12.538	T	414=	-12.156
T	421=	112.04	T	422=	0.72690	T	423=	-7.3487	T	424=	94.051	T	425=	3.0269	T	426=	-5.9913
T	431=	56.762	T	432=	40.788	T	433=	58.508	T	434=	25.701	T	435=	-8.5984	T	436=	-11.369
T	441=	1.1814	T	442=	4.7527	T	443=	-1.6142	T	444=	-6.9062	T	445=	-12.856	T	446=	-12.804
T	451=	1.6645	T	452=	8.2599	T	453=	-4.9319	T	454=	-9.7356	T	455=	-13.796	T	456=	-13.496
T	950=	659.56															

ARITHMETIC NODES IN ASCENDING NODE NUMBER ORDER

T	50=	232.49	T	52=	275.84	T	54=	350.68	T	158=	360.39	T	159=	358.41	T	168=	358.90
T	169=	358.43	T	195=	252.49	T	197=	285.65	T	199=	396.37	T	238=	230.93	T	311=	123.78

T	312=	123.78	T	321=	131.17	T	322=	131.17	T	331=	150.98	T	332=	150.98	T	337=	144.56
T	341=	157.53	T	357=	144.39	T	358=	140.36	T	359=	147.28	T	379=	149.95	T	403=	148.47
T	1000=	269.58	T	1001=	476.94	T	1002=	402.28	T	1003=	331.50	T	1004=	273.01	T	1005=	270.22
T	1006=	190.80	T	1007=	476.34	T	1008=	489.26	T	1009=	529.25	T	1010=	255.86	T	1011=	143.09
T	1012=	143.09	T	1013=	111.56	T	1021=	151.48	T	1022=	151.48	T	1023=	118.28	T	1031=	175.30
T	1032=	175.30	T	1033=	136.10	T	1041=	174.59	T	1042=	174.59	T	1043=	162.76	T	1044=	162.76
T	1346=	93.279	T	1347=	136.80												

HEATER NODES IN ASCENDING NODE NUMBER ORDER
++NONE++

BOUNDARY NODES IN ASCENDING NODE NUMBER ORDER

T	1=	-20.000	T	2=	-20.000

SYSTEMS IMPROVED NUMERICAL DIFFERENCING ANALYZER '85 (SINDA '85) PAGE 3/4

MODEL = DAMAGE2 HAC LOAD CASE NO. 2 CONDITIONS - Circumferential Distribution, -20
STDSTL *** Steady-state Conditions After The Fire *** 5/2/94 10am

SUBMODEL NAME = PTSC

		CALCULATED			ALLOWED	
MAX DIFF DELTA T PER ITER	DRLXCC(PTSC	250)=	4.962158E-02	VS. DRLXCA=	5.000000E-02	
MAX ARITH DELTA T PER ITER	ARLXCC(PTSC	1044)=	3.637695E-02	VS. ARLXCA=	0.500000	
MAX SYSTEM ENERGY BALANCE	EBALSC	=	25.1190	VS. EBALSA * ESUMIS	=	2.87972
				EBALSA=	1.000000E-03	
ENERGY INTO AND OUT OF SYS	ESUMIS	=	2879.72	ESUMOS=	2807.14	
MAX NODAL ENERGY BALANCE	EBALNC(PTSC	367)=	3.11621	VS. EBALNA=	1.000000E-02	
NUMBER OF ITERATIONS	LOOPCT	=	140	VS. NLOOPS=	1200	
PROBLEM TIME	TIMEN	=	999.000	VS. TIMEND=	999.000	

DIFFUSION NODES IN ASCENDING NODE NUMBER ORDER

T	51=	221.16	T	53=	257.09	T	55=	332.21	T	60=	214.19	T	62=	375.24	T	100=	205.22
T	105=	207.42	T	107=	208.29	T	110=	209.28	T	112=	209.59	T	113=	209.16	T	120=	216.65
T	122=	217.45	T	123=	216.08	T	124=	216.28	T	125=	215.09	T	126=	214.33	T	127=	213.57
T	130=	236.87	T	132=	239.11	T	133=	236.01	T	134=	236.57	T	135=	233.90	T	136=	231.64
T	137=	229.96	T	140=	251.32	T	141=	251.56	T	142=	253.62	T	143=	250.02	T	144=	251.03
T	145=	248.06	T	146=	245.68	T	147=	244.57	T	150=	276.47	T	152=	280.80	T	153=	273.00
T	154=	278.83	T	155=	272.29	T	156=	273.08	T	157=	268.85	T	160=	337.91	T	161=	327.70
T	162=	342.35	T	163=	334.24	T	164=	337.39	T	165=	330.10	T	166=	327.17	T	167=	323.96
T	170=	413.58	T	172=	415.48	T	173=	413.06	T	175=	446.54	T	177=	431.93	T	180=	449.63
T	190=	464.38	T	191=	547.71	T	192=	296.98	T	193=	407.36	T	194=	315.27	T	196=	415.53
T	198=	551.49	T	200=	184.80	T	204=	179.10	T	210=	191.27	T	220=	197.49	T	230=	206.84
T	240=	230.54	T	242=	198.61	T	250=	173.48	T	260=	186.89	T	261=	188.93	T	262=	181.68
T	263=	184.38	T	264=	174.60	T	265=	178.11	T	266=	168.72	T	300=	114.06	T	304=	97.138
T	305=	22.893	T	310=	145.35	T	313=	126.99	T	315=	105.13	T	316=	105.13	T	320=	152.45
T	323=	133.29	T	325=	110.51	T	326=	110.51	T	330=	162.01	T	333=	142.74	T	335=	118.33
T	336=	118.33	T	340=	167.66	T	342=	159.07	T	343=	100.17	T	344=	149.58	T	345=	103.00
T	346=	79.851	T	347=	127.96	T	349=	91.367	T	350=	146.24	T	351=	138.84	T	352=	145.17
T	353=	141.91	T	354=	144.87	T	355=	148.22	T	356=	143.05	T	360=	182.59	T	362=	176.98
T	364=	166.24	T	366=	149.49	T	367=	147.76	T	368=	145.90	T	369=	144.28	T	371=	138.74
T	373=	141.24	T	375=	144.77	T	377=	146.91	T	400=	170.06	T	401=	168.09	T	402=	147.37
T	404=	109.59	T	406=	16.655	T	408=	-12.600	T	410=	-15.347	T	412=	-12.598	T	414=	-12.188
T	421=	111.60	T	422=	0.65460	T	423=	-7.3983	T	424=	93.126	T	425=	2.8482	T	426=	-6.1036
T	431=	55.809	T	432=	39.887	T	433=	57.650	T	434=	25.237	T	435=	-8.7229	T	436=	-11.474
T	441=	0.80661	T	442=	4.2047	T	443=	-1.8882	T	444=	-7.0978	T	445=	-12.970	T	446=	-12.929
T	451=	1.1726	T	452=	7.5487	T	453=	-5.2288	T	454=	-9.9146	T	455=	-13.893	T	456=	-13.606
T	950=	661.60															

ARITHMETIC NODES IN ASCENDING NODE NUMBER ORDER

T	50=	225.57	T	52=	258.92	T	54=	326.17	T	158=	327.57	T	159=	325.48	T	168=	327.63
T	169=	327.70	T	195=	252.92	T	197=	286.26	T	199=	401.24	T	238=	217.29	T	311=	125.47

T	312=	125.47	T	321=	131.72	T	322=	131.72	T	331=	141.07	T	332=	141.07	T	337=	140.67
T	341=	153.31	T	357=	142.71	T	358=	138.70	T	359=	145.68	T	379=	148.53	T	403=	147.06
T	1000=	270.23	T	1001=	478.00	T	1002=	405.75	T	1003=	332.13	T	1004=	273.46	T	1005=	270.64
T	1006=	190.73	T	1007=	471.47	T	1008=	485.94	T	1009=	528.92	T	1010=	255.76	T	1011=	145.03
T	1012=	145.03	T	1013=	113.08	T	1021=	152.12	T	1022=	152.12	T	1023=	118.77	T	1031=	161.66
T	1032=	161.66	T	1033=	127.15	T	1041=	167.23	T	1042=	167.23	T	1043=	158.76	T	1044=	158.76
T	1346=	91.628	T	1347=	135.31														

HEATER NODES IN ASCENDING NODE NUMBER ORDER
++NONE++
BOUNDARY NODES IN ASCENDING NODE NUMBER ORDER

T	1=	-20.000	T	2=	-20.000

SYSTEMS IMPROVED NUMERICAL DIFFERENCING ANALYZER '85 (SINDA '85) PAGE 4/4

MODEL = DAMAGE2
STDSTL

HAC LOAD CASE NO. 2 CONDITIONS - Circumferential Distribution, -20
*** Steady-state Conditions After The Fire ***

5/2/94 10am

SUBMODEL NAME = PTSD

	CALCULATED			ALLOWED		
MAX DIFF DELTA T PER ITER	DRLXCC(PTSD	351)=	4.907227E-02	VS. DRLXCA=	5.000000E-02	
MAX ARITH DELTA T PER ITER	ARLXCC(PTSD	1346)=	3.527832E-02	VS. ARLXCA=	0.500000	
MAX SYSTEM ENERGY BALANCE	EBALSC	=	13.0745	VS. EBALSA * ESUMIS	=	1.91981
				EBALSA=	1.000000E-03	
ENERGY INTO AND OUT OF SYS	ESUMIS	=	1919.81	ESUMOS=	1899.10	
MAX NODAL ENERGY BALANCE	EBALNC(PTSD	367)=	2.11134	VS. EBALNA=	1.000000E-02	
NUMBER OF ITERATIONS	LOOPCT	=	140	VS. NLOOPS=	1200	
PROBLEM TIME	TIMEN	=	999.000	VS. TIMEND=	999.000	

DIFFUSION NODES IN ASCENDING NODE NUMBER ORDER

T	51=	218.62	T	53=	250.44	T	55=	322.10	T	60=	212.13	T	62=	366.21	T	100=	203.86
T	105=	205.95	T	107=	206.79	T	110=	207.73	T	112=	207.91	T	113=	207.74	T	120=	214.64
T	122=	214.97	T	123=	214.47	T	124=	214.05	T	125=	213.59	T	126=	212.69	T	127=	212.34
T	130=	232.60	T	132=	233.67	T	133=	232.62	T	134=	231.78	T	135=	230.81	T	136=	228.33
T	137=	227.60	T	140=	245.20	T	141=	245.42	T	142=	246.03	T	143=	244.98	T	144=	244.36
T	145=	243.56	T	146=	241.29	T	147=	241.38	T	150=	267.57	T	152=	268.47	T	153=	266.51
T	154=	268.29	T	155=	266.58	T	156=	266.58	T	157=	265.23	T	160=	327.77	T	161=	317.96
T	162=	328.62	T	163=	326.54	T	164=	325.73	T	165=	323.39	T	166=	320.02	T	167=	319.10
T	170=	405.42	T	172=	406.40	T	173=	405.56	T	175=	438.10	T	177=	423.66	T	180=	441.34
T	190=	456.17	T	191=	535.68	T	192=	294.17	T	193=	403.40	T	194=	312.12	T	196=	412.32
T	198=	539.29	T	200=	184.61	T	204=	178.63	T	210=	190.78	T	220=	197.61	T	230=	219.31
T	240=	233.01	T	242=	199.62	T	250=	174.31	T	260=	187.47	T	261=	189.43	T	262=	182.23
T	263=	184.85	T	264=	175.29	T	265=	178.74	T	266=	169.52	T	300=	114.05	T	304=	96.930
T	305=	22.820	T	310=	145.03	T	313=	126.71	T	315=	104.91	T	316=	104.91	T	320=	152.79
T	323=	133.59	T	325=	110.76	T	326=	110.76	T	330=	169.65	T	333=	148.44	T	335=	123.01
T	336=	123.01	T	340=	172.11	T	342=	161.40	T	343=	101.26	T	344=	150.93	T	345=	104.01
T	346=	81.033	T	347=	129.00	T	349=	92.324	T	350=	147.29	T	351=	139.84	T	352=	146.21
T	353=	142.91	T	354=	145.97	T	355=	149.18	T	356=	144.11	T	360=	183.16	T	362=	177.61
T	364=	167.02	T	366=	150.45	T	367=	148.73	T	368=	146.86	T	369=	145.25	T	371=	139.75
T	373=	142.25	T	375=	145.75	T	377=	147.86	T	400=	170.76	T	401=	168.79	T	402=	148.32
T	404=	110.48	T	406=	17.225	T	408=	-12.510	T	410=	-15.309	T	412=	-12.557	T	414=	-12.159
T	421=	112.10	T	422=	0.72974	T	423=	-7.3506	T	424=	93.763	T	425=	2.9713	T	426=	-6.0265
T	431=	56.425	T	432=	40.452	T	433=	58.216	T	434=	25.545	T	435=	-8.6420	T	436=	-11.407
T	441=	1.0368	T	442=	4.5359	T	443=	-1.7168	T	444=	-6.9780	T	445=	-12.900	T	446=	-12.852
T	451=	1.4691	T	452=	7.9757	T	453=	-5.0479	T	454=	-9.8047	T	455=	-13.833	T	456=	-13.538
T	950=	653.64															

ARITHMETIC NODES IN ASCENDING NODE NUMBER ORDER

T	50=	222.53	T	52=	252.31	T	54=	316.61	T	158=	317.33	T	159=	316.67	T	168=	317.85
T	169=	317.79	T	195=	251.58	T	197=	283.50	T	199=	395.54	T	238=	225.34	T	311=	125.19

T	312=	125.19	T	321=	132.01	T	322=	132.01	T	331=	146.66	T	332=	146.66	T	337=	142.97
T	341=	155.82	T	357=	143.78	T	358=	139.74	T	359=	146.73	T	379=	149.49	T	403=	148.01
T	1000=	268.24	T	1001=	469.41	T	1002=	399.55	T	1003=	328.16	T	1004=	271.38	T	1005=	268.65
T	1006=	191.10	T	1007=	462.43	T	1008=	476.58	T	1009=	517.70	T	1010=	254.68	T	1011=	144.71
T	1012=	144.71	T	1013=	112.83	T	1021=	152.46	T	1022=	152.46	T	1023=	119.03	T	1031=	169.26
T	1032=	169.26	T	1033=	132.20	T	1041=	171.69	T	1042=	171.69	T	1043=	161.12	T	1044=	161.12
T	1346=	92.634	T	1347=	136.31												

HEATER NODES IN ASCENDING NODE NUMBER ORDER
++NONE++
BOUNDARY NODES IN ASCENDING NODE NUMBER ORDER

T	1=	-20.000	T	2=	-20.000

```
                    SYSTEMS IMPROVED NUMERICAL DIFFERENCING ANALYZER '85 (SINDA '85)                PAGE  1/4

MODEL = DAMAGE3                  LOAD CASE NO. 3 CONDITIONS - Axial Distribution, 100F                  5/2/94
  FWDBCK                 *****      Peak OCV Sidewall Temperature Time Point    *****

 SUBMODEL NAME = MAIN
       PROBLEM TIME                    TIMEN                  = 0.500000     VS. TIMEND= 0.500000

                                 DIFFUSION NODES IN ASCENDING NODE NUMBER ORDER
  T  267= 207.90     T  268= 207.85     T  269= 206.53
                                 ARITHMETIC NODES IN ASCENDING NODE NUMBER ORDER
  T  201= 693.88     T 1266= 213.12     T 1267= 269.94     T 1268= 245.54     T 1269= 219.11
                                 HEATER NODES IN ASCENDING NODE NUMBER ORDER
                                          ++NONE++
                                 BOUNDARY NODES IN ASCENDING NODE NUMBER ORDER
                                          ++NONE++
MEAN ICV GAS TEMP= 693.9 F   MEAN ICV GAS PRESSURE= 34.46 PSIA
MEAN ICV-OCV GAS TEMP= 836.1 F   MEAN ICV-OCV GAS PRESSURE= 45.67 PSIA


 SUBMODEL NAME = PTSA
                                      CALCULATED                                  ALLOWED
       MAX DIFF DELTA T PER ITER      DRLXCC(PTSA      161)= 4.064941E-02 VS. DRLXCA= 5.000000E-02
       MAX ARITH DELTA T PER ITER     ARLXCC(PTSA      168)= 3.491211E-02 VS. ARLXCA= 0.500000
       MAX DIFF DEL T PER TIME STEP   DTMPCC(PTSA      200)=  7.16336     VS. DTMPCA=  10.0000
       MAX ARITH DEL T PER TIME STEP  ATMPCC(PTSA      238)=  5.17447     VS. ATMPCA=  100.000
       MIN STABILITY CRITERIA         CSGMIN(PTSA      431)= 3.001466E-05
       MAX STABILITY CRITERIA         CSGMAX(PTSA      424)=  1.95861
       NUMBER OF ITERATIONS           LOOPCT             =       11     VS. NLOOPT=      600
       PROBLEM TIME                   TIMEN              = 0.500000     VS. TIMEND= 0.500000
       MEAN PROBLEM TIME              TIMEM              = 0.496871
       AVERAGE TIME STEP USED         DTIMEU             = 5.555552E-03 VS. DTIMEI=      0.

                                 DIFFUSION NODES IN ASCENDING NODE NUMBER ORDER
  T   51= 993.11     T   53= 985.74     T   55= 940.07     T   60= 923.22     T   62= 1044.3     T  100= 911.06
  T  105= 919.81     T  107= 925.78     T  110= 940.48     T  112= 945.54     T  113= 931.97     T  120= 1057.3
  T  122= 1095.1     T  123= 967.75     T  124= 1091.7     T  125= 962.63     T  126= 1085.2     T  127= 952.26
  T  130= 1034.3     T  132= 1081.1     T  133= 924.29     T  134= 1078.6     T  135= 920.01     T  136= 1073.7
  T  137= 911.41     T  140= 984.50     T  141= 967.45     T  142= 1019.0     T  143= 893.14     T  144= 1016.4
  T  145= 889.17     T  146= 1010.9     T  147= 881.34     T  150= 1000.0     T  152= 1053.4     T  153= 875.73
  T  154= 1049.6     T  155= 872.18     T  156= 1045.5     T  157= 863.19     T  160= 934.78     T  161= 922.45
  T  162= 983.92     T  163= 819.81     T  164= 979.26     T  165= 823.02     T  166= 975.65     T  167= 818.24
  T  170= 579.36     T  172= 588.01     T  173= 558.50     T  175= 488.93     T  177= 523.83     T  180= 509.15
  T  190= 365.03     T  191= 357.50     T  192= 235.84     T  193= 468.69     T  194= 264.64     T  196= 329.23
  T  198= 359.96     T  200= 1074.1     T  204= 1129.0     T  210= 1166.6     T  220= 1158.6     T  230= 1090.3
  T  240= 626.11     T  242= 357.80     T  250= 222.54     T  260= 201.16     T  261= 202.13     T  262= 201.52
  T  263= 204.06     T  264= 202.33     T  265= 205.28     T  266= 205.56     T  300= 1222.6     T  304= 1248.6
  T  305= 1380.3     T  310= 1177.4     T  313= 1253.4     T  315= 1343.1     T  316= 1343.1     T  320= 1169.5
  T  323= 1247.5     T  325= 1338.9     T  326= 1338.9     T  330= 1089.0     T  333= 1150.2     T  335= 1287.9
  T  336= 1287.9     T  340= 908.93     T  342= 602.20     T  343= 1058.6     T  344= 344.88     T  345= 971.07
  T  346= 1277.5     T  347= 551.95     T  349= 1075.2     T  350= 267.63     T  351= 465.21     T  352= 271.69
  T  353= 368.38     T  354= 308.73     T  355= 228.94     T  356= 318.79     T  360= 199.74     T  362= 199.06
  T  364= 200.23     T  366= 220.19     T  367= 225.71     T  368= 249.34     T  369= 268.90     T  371= 461.68
  T  373= 365.32     T  375= 266.57     T  377= 227.96     T  400= 199.65     T  401= 209.01     T  402= 223.26
  T  404= 1203.3     T  406= 1380.2     T  408= 1363.7     T  410= 1411.6     T  412= 1411.0     T  414= 1419.3
```

T 421= 471.48 T 422= 1414.7 T 423= 1417.5 T 424= 264.34 T 425= 1401.7 T 426= 1404.3

T 431= 1362.5 T 432= 1365.5 T 433= 1349.2 T 434= 1347.9 T 435= 1382.4 T 436= 1364.2

T 950= 1476.9 T 952= 1467.4 T 954= 1445.5

ARITHMETIC NODES IN ASCENDING NODE NUMBER ORDER

T 50= 986.00 T 52= 984.23 T 54= 954.76 T 158= 942.74 T 159= 896.03 T 168= 926.71

T 169= 920.56 T 195= 236.06 T 197= 258.89 T 199= 347.22 T 238= 897.84 T 311= 1265.6

T 312= 1265.6 T 321= 1259.7 T 322= 1259.7 T 331= 1161.3 T 332= 1161.3 T 337= 821.55

T 341= 710.27 T 357= 342.69 T 358= 432.13 T 359= 270.35 T 379= 224.37 T 403= 226.40

T 1000= 252.36 T 1001= 332.35 T 1002= 332.01 T 1003= 254.23 T 1004= 228.66 T 1005= 227.83

T 1006= 204.02 T 1007= 422.10 T 1008= 382.72 T 1009= 365.21 T 1010= 288.51 T 1011= 1189.7

T 1012= 1189.7 T 1013= 1317.8 T 1021= 1182.0 T 1022= 1182.0 T 1023= 1313.3 T 1031= 1101.2

T 1032= 1101.2 T 1033= 1248.6 T 1041= 935.43 T 1042= 935.43 T 1043= 649.41 T 1044= 649.41

T 1346= 1143.4 T 1347= 453.43

HEATER NODES IN ASCENDING NODE NUMBER ORDER

++NONE++

BOUNDARY NODES IN ASCENDING NODE NUMBER ORDER

T 1= 1475.0 T 2= 1424.7

SYSTEMS IMPROVED NUMERICAL DIFFERENCING ANALYZER '85 (SINDA '85) PAGE 2/4

MODEL = DAMAGE3 LOAD CASE NO. 3 CONDITIONS - Axial Distribution, 100F 5/2/94
FWDBCK ***** Peak OCV Sidewall Temperature Time Point *****

SUBMODEL NAME = PTSB

	CALCULATED			ALLOWED	
MAX DIFF DELTA T PER ITER	DRLXCC(PTSB	132)=	2.209473E-02	VS. DRLXCA=	5.000000E-02
MAX ARITH DELTA T PER ITER	ARLXCC(PTSB	168)=	1.110840E-02	VS. ARLXCA=	0.500000
MAX DIFF DEL T PER TIME STEP	DTMPCC(PTSB	100)=	7.19913	VS. DTMPCA=	10.0000
MAX ARITH DEL T PER TIME STEP	ATMPCC(PTSB	238)=	6.23135	VS. ATMPCA=	100.000
MIN STABILITY CRITERIA	CSGMIN(PTSB	446)=	3.008285E-05		
MAX STABILITY CRITERIA	CSGMAX(PTSB	434)=	3.26613		
NUMBER OF ITERATIONS	LOOPCT	=	11	VS. NLOOPT=	600
PROBLEM TIME	TIMEN	=	0.500000	VS. TIMEND=	0.500000
MEAN PROBLEM TIME	TIMEN	=	0.496871		
AVERAGE TIME STEP USED	DTIMEU	=	5.555552E-03	VS. DTIMEI=	0.

DIFFUSION NODES IN ASCENDING NODE NUMBER ORDER

T	51=	831.24	T	53=	800.91	T	55=	759.09	T	60=	880.57	T	62=	1005.2	T	100=	1005.6
T	105=	955.02	T	107=	933.69	T	110=	923.31	T	112=	928.73	T	113=	918.19	T	120=	889.27
T	122=	931.01	T	123=	861.23	T	124=	912.89	T	125=	866.62	T	126=	883.59	T	127=	875.11
T	130=	826.29	T	132=	879.42	T	133=	790.26	T	134=	853.65	T	135=	793.48	T	136=	810.95
T	137=	798.76	T	140=	789.40	T	141=	789.54	T	142=	838.74	T	143=	758.05	T	144=	813.08
T	145=	756.95	T	146=	767.92	T	147=	755.62	T	150=	759.31	T	152=	823.17	T	153=	717.83
T	154=	789.27	T	155=	716.22	T	156=	733.29	T	157=	715.44	T	160=	702.73	T	161=	707.44
T	162=	765.42	T	163=	664.18	T	164=	733.59	T	165=	663.30	T	166=	680.34	T	167=	661.23
T	170=	528.76	T	172=	539.69	T	173=	519.26	T	175=	454.81	T	177=	485.47	T	180=	448.32
T	190=	380.36	T	191=	373.21	T	192=	234.59	T	193=	471.49	T	194=	268.46	T	196=	343.41
T	198=	376.60	T	200=	1058.5	T	204=	1072.8	T	210=	762.59	T	220=	743.33	T	230=	673.14
T	240=	553.81	T	242=	347.90	T	250=	220.73	T	260=	200.98	T	261=	201.75	T	262=	200.23
T	263=	201.38	T	264=	201.61	T	265=	204.30	T	266=	204.46	T	300=	1218.7	T	304=	1227.5
T	305=	1375.2	T	310=	951.75	T	313=	1116.3	T	315=	1284.9	T	316=	1284.9	T	320=	937.36
T	323=	1106.2	T	325=	1277.7	T	326=	1277.7	T	330=	879.77	T	333=	1049.2	T	335=	1244.4
T	336=	1244.4	T	340=	836.07	T	342=	573.42	T	343=	1039.6	T	344=	334.11	T	345=	830.78
T	346=	1262.3	T	347=	476.32	T	349=	1067.8	T	350=	260.03	T	351=	456.22	T	352=	261.23
T	353=	361.79	T	354=	298.81	T	355=	221.67	T	356=	303.34	T	360=	199.68	T	362=	198.63
T	364=	199.39	T	366=	214.28	T	367=	215.99	T	368=	221.71	T	369=	231.85	T	371=	451.84
T	373=	358.51	T	375=	260.71	T	377=	218.72	T	400=	199.30	T	401=	208.78	T	402=	212.85
T	404=	935.63	T	406=	1361.3	T	408=	1380.7	T	410=	1406.4	T	412=	1410.4	T	414=	1419.2
T	421=	471.36	T	422=	1414.7	T	423=	1417.5	T	424=	245.83	T	425=	1400.9	T	426=	1406.5
T	431=	1231.7	T	432=	1325.1	T	433=	246.42	T	434=	222.11	T	435=	1386.4	T	436=	1396.7
T	441=	1380.1	T	442=	1370.6	T	443=	1373.3	T	444=	1373.3	T	445=	1391.5	T	446=	1381.0
T	451=	1372.7	T	452=	1361.7	T	453=	1376.7	T	454=	1381.4	T	455=	1405.9	T	456=	1392.0

ARITHMETIC NODES IN ASCENDING NODE NUMBER ORDER

T	50=	831.51	T	52=	801.65	T	54=	785.62	T	158=	717.98	T	159=	697.29	T	168=	708.38
T	169=	711.09	T	195=	225.64	T	197=	241.69	T	199=	359.90	T	238=	621.61	T	311=	1132.7

T	312=	1132.7	T	321=	1122.4	T	322=	1122.4	T	331=	1064.1	T	332=	1064.1	T	337=	792.05
T	341=	677.12	T	357=	330.57	T	358=	421.59	T	359=	261.33	T	379=	216.69	T	403=	216.78
T	1000=	227.24	T	1001=	345.59	T	1002=	343.42	T	1003=	255.82	T	1004=	227.39	T	1005=	226.56
T	1006=	202.68	T	1007=	414.16	T	1008=	390.20	T	1009=	378.40	T	1010=	301.02	T	1011=	973.33
T	1012=	973.33	T	1013=	1235.8	T	1021=	959.15	T	1022=	959.15	T	1023=	1228.2	T	1031=	901.33
T	1032=	901.33	T	1033=	1187.8	T	1041=	860.62	T	1042=	860.62	T	1043=	614.13	T	1044=	614.13
T	1346=	1062.3	T	1347=	386.93												

HEATER NODES IN ASCENDING NODE NUMBER ORDER
++NONE++

BOUNDARY NODES IN ASCENDING NODE NUMBER ORDER

T	1=	1475.0	T	2=	1424.7

SYSTEMS IMPROVED NUMERICAL DIFFERENCING ANALYZER '85 (SINDA '85) PAGE 3/4

MODEL = DAMAGE3 LOAD CASE NO. 3 CONDITIONS - Axial Distribution, 100F 5/2/94
FWDBCK ***** Peak OCV Sidewall Temperature Time Point *****

SUBMODEL NAME = PTSC

		CALCULATED		ALLOWED
MAX DIFF DELTA T PER ITER	DRLXCC(PTSC	161)=-1.953125E-03	VS. DRLXCA=	5.000000E-02
MAX ARITH DELTA T PER ITER	ARLXCC(PTSC	168)=-1.708984E-03	VS. ARLXCA=	0.500000
MAX DIFF DEL T PER TIME STEP	DTMPCC(PTSC	100)= 7.23074	VS. DTMPCA=	10.0000
MAX ARITH DEL T PER TIME STEP	ATMPCC(PTSC	238)= 5.90115	VS. ATMPCA=	100.000
MIN STABILITY CRITERIA	CSGMIN(PTSC	446)= 3.008490E-05		
MAX STABILITY CRITERIA	CSGMAX(PTSC	434)= 3.26601		
NUMBER OF ITERATIONS	LOOPCT	= 11	VS. NLOOPT=	600
PROBLEM TIME	TIMEN	= 0.500000	VS. TIMEND=	0.500000
MEAN PROBLEM TIME	TIMEN	= 0.496871		
AVERAGE TIME STEP USED	DTIMEU	= 5.555552E-03	VS. DTIMEI=	0.

DIFFUSION NODES IN ASCENDING NODE NUMBER ORDER

T	51=	752.69	T	53=	702.66	T	55=	663.70	T	60=	860.81	T	62=	987.74	T	100=	989.24
T	105=	930.66	T	107=	906.69	T	110=	892.73	T	112=	894.35	T	113=	892.43	T	120=	825.19
T	122=	828.79	T	123=	821.78	T	124=	831.80	T	125=	826.92	T	126=	837.69	T	127=	836.50
T	130=	741.00	T	132=	746.76	T	133=	737.10	T	134=	746.03	T	135=	739.23	T	136=	745.67
T	137=	744.03	T	140=	692.02	T	141=	691.47	T	142=	699.03	T	143=	689.71	T	144=	695.76
T	145=	689.31	T	146=	692.45	T	147=	691.45	T	150=	657.54	T	152=	666.35	T	153=	654.63
T	154=	660.48	T	155=	651.48	T	156=	653.53	T	157=	650.64	T	160=	603.26	T	161=	610.96
T	162=	612.46	T	163=	601.47	T	164=	608.32	T	165=	599.89	T	166=	604.03	T	167=	601.62
T	170=	488.75	T	172=	489.96	T	173=	487.20	T	175=	443.00	T	177=	459.12	T	180=	446.23
T	190=	407.53	T	191=	396.28	T	192=	235.62	T	193=	486.11	T	194=	270.15	T	196=	403.16
T	198=	400.68	T	200=	1045.8	T	204=	1055.6	T	210=	712.81	T	220=	688.07	T	230=	620.24
T	240=	546.10	T	242=	346.26	T	250=	220.49	T	260=	200.92	T	261=	201.69	T	262=	200.09
T	263=	201.21	T	264=	201.49	T	265=	204.16	T	266=	204.36	T	300=	1214.5	T	304=	1221.3
T	305=	1374.1	T	310=	927.68	T	313=	1102.9	T	315=	1279.5	T	316=	1279.5	T	320=	911.32
T	323=	1091.7	T	325=	1271.9	T	326=	1271.9	T	330=	858.04	T	333=	1039.8	T	335=	1240.7
T	336=	1240.7	T	340=	828.55	T	342=	570.43	T	343=	1038.9	T	344=	333.25	T	345=	828.84
T	346=	1261.1	T	347=	475.61	T	349=	1067.4	T	350=	259.76	T	351=	455.95	T	352=	260.95
T	353=	361.62	T	354=	298.43	T	355=	221.50	T	356=	302.98	T	360=	199.65	T	362=	198.56
T	364=	199.33	T	366=	214.12	T	367=	215.77	T	368=	221.25	T	369=	231.22	T	371=	451.54
T	373=	358.35	T	375=	260.65	T	377=	218.67	T	400=	199.29	T	401=	208.77	T	402=	212.79
T	404=	935.48	T	406=	1360.7	T	408=	1380.7	T	410=	1406.4	T	412=	1410.4	T	414=	1419.2
T	421=	471.37	T	422=	1414.7	T	423=	1417.5	T	424=	245.84	T	425=	1400.9	T	426=	1406.5
T	431=	1231.3	T	432=	1324.6	T	433=	246.42	T	434=	222.12	T	435=	1386.4	T	436=	1396.7
T	441=	1380.0	T	442=	1370.3	T	443=	1373.3	T	444=	1373.3	T	445=	1391.4	T	446=	1381.0
T	451=	1372.5	T	452=	1361.1	T	453=	1376.7	T	454=	1381.3	T	455=	1405.9	T	456=	1392.0

ARITHMETIC NODES IN ASCENDING NODE NUMBER ORDER

T	50=	755.55	T	52=	704.96	T	54=	696.67	T	158=	612.88	T	159=	610.38	T	168=	611.30
T	169=	612.10	T	195=	230.73	T	197=	244.34	T	199=	371.20	T	238=	588.03	T	311=	1119.3

T	312=	1119.3	T	321=	1107.9	T	322=	1107.9	T	331=	1054.7	T	332=	1054.7	T	337=	789.10
T	341=	673.72	T	357=	330.21	T	358=	421.26	T	359=	261.05	T	379=	216.50	T	403=	216.72
T	1000=	228.48	T	1001=	375.12	T	1002=	354.67	T	1003=	262.48	T	1004=	228.18	T	1005=	227.32
T	1006=	202.61	T	1007=	422.16	T	1008=	409.92	T	1009=	400.44	T	1010=	301.81	T	1011=	950.16
T	1012=	950.16	T	1013=	1228.0	T	1021=	934.05	T	1022=	934.05	T	1023=	1219.7	T	1031=	880.50
T	1032=	880.50	T	1033=	1182.3	T	1041=	852.99	T	1042=	852.99	T	1043=	610.61	T	1044=	610.61
T	1346=	1060.8	T	1347=	386.29												

HEATER NODES IN ASCENDING NODE NUMBER ORDER
++NONE++

BOUNDARY NODES IN ASCENDING NODE NUMBER ORDER

T	1=	1475.0	T	2=	1424.7

SYSTEMS IMPROVED NUMERICAL DIFFERENCING ANALYZER '85 (SINDA '85) PAGE 4/4

MODEL = DAMAGE3 LOAD CASE NO. 3 CONDITIONS - Axial Distribution, 100F 5/2/94
FWDBCK ***** Peak OCV Sidewall Temperature Time Point *****

SUBMODEL NAME = PTSD

	CALCULATED		ALLOWED
MAX DIFF DELTA T PER ITER	DRLXCC(PTSD	161)=-1.708984E-03	VS. DRLXCA= 5.000000E-02
MAX ARITH DELTA T PER ITER	ARLXCC(PTSD	169)=-1.464844E-03	VS. ARLXCA= 0.500000
MAX DIFF DEL T PER TIME STEP	DTMPCC(PTSD	100)= 7.26126	VS. DTMPCA= 10.0000
MAX ARITH DEL T PER TIME STEP	ATMPCC(PTSD	238)= 5.89102	VS. ATMPCA= 100.000
MIN STABILITY CRITERIA	CSGMIN(PTSD	446)= 3.008492E-05	
MAX STABILITY CRITERIA	CSGMAX(PTSD	434)= 3.26601	
NUMBER OF ITERATIONS	LOOPCT	= 11	VS. NLOOPT= 600
PROBLEM TIME	TIMEN	= 0.500000	VS. TIMEND= 0.500000
MEAN PROBLEM TIME	TIMEM	= 0.496871	
AVERAGE TIME STEP USED	DTIMEU	= 5.5555552E-03	VS. DTIMEI= 0.

DIFFUSION NODES IN ASCENDING NODE NUMBER ORDER

T	51=	744.30	T	53=	690.71	T	55=	652.06	T	60=	858.85	T	62=	985.73	T	100=	988.63
T	105=	928.87	T	107=	904.45	T	110=	890.04	T	112=	890.54	T	113=	890.07	T	120=	818.77
T	122=	818.59	T	123=	817.02	T	124=	824.16	T	125=	822.91	T	126=	834.48	T	127=	833.99
T	130=	731.07	T	132=	731.80	T	133=	729.58	T	134=	734.43	T	135=	732.76	T	136=	740.00
T	137=	739.52	T	140=	678.97	T	141=	678.28	T	142=	681.12	T	143=	678.89	T	144=	681.35
T	145=	680.02	T	146=	684.86	T	147=	685.19	T	150=	644.68	T	152=	647.69	T	153=	644.81
T	154=	645.62	T	155=	642.97	T	156=	645.60	T	157=	644.66	T	160=	590.26	T	161=	598.64
T	162=	594.07	T	163=	591.38	T	164=	593.52	T	165=	591.39	T	166=	595.91	T	167=	595.32
T	170=	481.90	T	172=	481.79	T	173=	480.98	T	175=	438.86	T	177=	453.65	T	180=	443.47
T	190=	405.42	T	191=	395.35	T	192=	235.62	T	193=	483.56	T	194=	269.86	T	196=	407.70
T	198=	399.80	T	200=	1045.0	T	204=	1054.8	T	210=	711.19	T	220=	686.13	T	230=	620.36
T	240=	545.72	T	242=	346.19	T	250=	220.49	T	260=	200.92	T	261=	201.69	T	262=	200.08
T	263=	201.20	T	264=	201.49	T	265=	204.16	T	266=	204.35	T	300=	1214.2	T	304=	1221.0
T	305=	1374.0	T	310=	927.03	T	313=	1102.6	T	315=	1279.4	T	316=	1279.4	T	320=	910.58
T	323=	1091.3	T	325=	1271.7	T	326=	1271.7	T	330=	858.03	T	333=	1039.8	T	335=	1240.7
T	336=	1240.7	T	340=	828.46	T	342=	570.41	T	343=	1038.9	T	344=	333.25	T	345=	828.84
T	346=	1261.1	T	347=	475.61	T	349=	1067.4	T	350=	259.76	T	351=	455.95	T	352=	260.95
T	353=	361.62	T	354=	298.43	T	355=	221.50	T	356=	302.99	T	360=	199.65	T	362=	198.56
T	364=	199.33	T	366=	214.12	T	367=	215.77	T	368=	221.25	T	369=	231.22	T	371=	451.54
T	373=	358.35	T	375=	260.65	T	377=	218.67	T	400=	199.29	T	401=	208.77	T	402=	212.79
T	404=	935.48	T	406=	1360.7	T	408=	1380.7	T	410=	1406.4	T	412=	1410.4	T	414=	1419.2
T	421=	471.37	T	422=	1414.7	T	423=	1417.5	T	424=	245.84	T	425=	1400.9	T	426=	1406.5
T	431=	1231.3	T	432=	1324.6	T	433=	246.42	T	434=	222.12	T	435=	1386.4	T	436=	1396.7
T	441=	1380.0	T	442=	1370.3	T	443=	1373.3	T	444=	1373.3	T	445=	1391.4	T	446=	1381.0
T	451=	1372.5	T	452=	1361.1	T	453=	1376.7	T	454=	1381.3	T	455=	1405.9	T	456=	1392.0

ARITHMETIC NODES IN ASCENDING NODE NUMBER ORDER

T	50=	747.27	T	52=	693.24	T	54=	685.84	T	158=	599.83	T	159=	599.18	T	168=	598.86
T	169=	599.38	T	195=	231.03	T	197=	243.95	T	199=	370.11	T	238=	587.93	T	311=	1118.9

```
T  312= 1118.9    T  321= 1107.5    T  322= 1107.5    T  331= 1054.7    T  332= 1054.7    T  337= 789.08
T  341= 673.70    T  357= 330.21    T  358= 421.26    T  359= 261.05    T  379= 216.50    T  403= 216.72
T 1000= 228.45    T 1001= 375.76    T 1002= 353.79    T 1003= 262.60    T 1004= 228.17    T 1005= 227.31
T 1006= 202.61    T 1007= 419.32    T 1008= 407.83    T 1009= 399.16    T 1010= 301.61    T 1011= 949.54
T 1012= 949.54    T 1013= 1227.8    T 1021= 933.34    T 1022= 933.34    T 1023= 1219.5    T 1031= 880.48
T 1032= 880.48    T 1033= 1182.3    T 1041= 852.90    T 1042= 852.90    T 1043= 610.59    T 1044= 610.59
T 1346= 1060.8    T 1347= 386.29
                    HEATER NODES IN ASCENDING NODE NUMBER ORDER
                                          ++NONE++
                    BOUNDARY NODES IN ASCENDING NODE NUMBER ORDER
T    1= 1475.0    T    2= 1424.7
```

```
                    SYSTEMS IMPROVED NUMERICAL DIFFERENCING ANALYZER '85 (SINDA '85)          PAGE  1/4

MODEL = DAMAGE3                    LOAD CASE NO. 3 CONDITIONS - Axial Distribution, 100F          5/2/94
  FWDBCK                  *****      Peak ICV Sidewall Temperature Time Point   *****

 SUBMODEL NAME = MAIN

       MEAN PROBLEM TIME                TIMEM                  = 0.832405
                                  DIFFUSION NODES IN ASCENDING NODE NUMBER ORDER
  T  267= 220.25     T  268= 220.18     T  269= 217.69
                                  ARITHMETIC NODES IN ASCENDING NODE NUMBER ORDER
  T  201= 728.76     T 1266= 229.14     T 1267= 324.60     T 1268= 283.13     T 1269= 239.07
                                  HEATER NODES IN ASCENDING NODE NUMBER ORDER
                                          ++NONE++
                                  BOUNDARY NODES IN ASCENDING NODE NUMBER ORDER
                                          ++NONE++
MEAN ICV GAS TEMP= 728.8 F   MEAN ICV GAS PRESSURE= 35.68 PSIA
MEAN ICV-OCV GAS TEMP= 746.5 F   MEAN ICV-OCV GAS PRESSURE= 42.51 PSIA


 SUBMODEL NAME = PTSA
                                          CALCULATED                          ALLOWED
       MAX DIFF DELTA T PER ITER    DRLXCC(PTSA      123)=-4.052734E-02 VS. DRLXCA= 5.000000E-02
       MAX ARITH DELTA T PER ITER   ARLXCC(PTSA     1007)= 9.338379E-02 VS. ARLXCA= 0.500000
       MAX DIFF DEL T PER TIME STEP DTMPCC(PTSA      425)= -1.85397     VS. DTMPCA=  10.0000
       MAX ARITH DEL T PER TIME STEP ATMPCC(PTSA     1346)= -1.43478    VS. ATMPCA=  100.000
       MIN STABILITY CRITERIA       CSGMIN(PTSA      431)= 2.399240E-04
       MAX STABILITY CRITERIA       CSGMAX(PTSA      424)= 2.20153
       NUMBER OF ITERATIONS         LOOPCT                =     3      VS. NLOOPT=     600
       PROBLEM TIME                 TIMEN                 = 0.833333   VS. TIMEND=  12.0000
       MEAN PROBLEM TIME            TIMEM                 = 0.832405
       AVERAGE TIME STEP USED       DTIMEU                = 9.259260E-04 VS. DTIMEI=     0.
                                  DIFFUSION NODES IN ASCENDING NODE NUMBER ORDER
  T   51= 1035.2     T   53= 1014.5     T   55= 961.06     T   60= 943.57     T   62= 972.38     T  100= 968.90
  T  105= 967.46     T  107= 966.07     T  110= 969.79     T  112= 981.43     T  113= 934.61     T  120= 1080.7
  T  122= 1125.4     T  123= 977.67     T  124= 1126.1     T  125= 979.03     T  126= 1127.4     T  127= 981.70
  T  130= 1080.4     T  132= 1127.5     T  133= 969.52     T  134= 1127.6     T  135= 970.20     T  136= 1128.0
  T  137= 971.49     T  140= 1053.0     T  141= 1038.2     T  142= 1086.2     T  143= 962.11     T  144= 1086.2
  T  145= 962.42     T  146= 1086.1     T  147= 962.97     T  150= 1067.3     T  152= 1117.8     T  153= 947.52
  T  154= 1116.0     T  155= 948.02     T  156= 1115.4     T  157= 948.09     T  160= 1006.1     T  161= 996.24
  T  162= 1051.4     T  163= 896.78     T  164= 1048.4     T  165= 903.38     T  166= 1047.4     T  167= 902.94
  T  170= 665.63     T  172= 672.22     T  173= 651.97     T  175= 571.83     T  177= 609.34     T  180= 585.51
  T  190= 438.08     T  191= 454.59     T  192= 252.31     T  193= 663.31     T  194= 335.23     T  196= 419.62
  T  198= 456.83     T  200= 877.60     T  204= 886.90     T  210= 1190.0     T  220= 1185.1     T  230= 1118.9
  T  240= 731.60     T  242= 447.99     T  250= 264.25     T  260= 203.29     T  261= 205.03     T  262= 209.22
  T  263= 214.16     T  264= 220.38     T  265= 225.24     T  266= 233.32     T  300= 781.94     T  304= 781.88
  T  305= 505.52     T  310= 1058.0     T  313= 923.76     T  315= 755.60     T  316= 755.60     T  320= 1055.2
  T  323= 922.91     T  325= 758.40     T  326= 758.40     T  330= 968.90     T  333= 806.37     T  335= 683.39
  T  336= 683.39     T  340= 771.77     T  342= 547.85     T  343= 546.54     T  344= 381.90     T  345= 699.56
  T  346= 620.05     T  347= 516.56     T  349= 448.60     T  350= 313.29     T  351= 342.45     T  352= 316.03
  T  353= 323.27     T  354= 339.71     T  355= 271.64     T  356= 343.15     T  360= 201.80     T  362= 204.87
  T  364= 219.72     T  366= 266.41     T  367= 273.25     T  368= 290.53     T  369= 316.38     T  371= 348.41
  T  373= 330.06     T  375= 289.35     T  377= 265.82     T  400= 210.28     T  401= 221.46     T  402= 263.02
  T  404= 698.51     T  406= 599.18     T  408= 601.29     T  410= 574.01     T  412= 622.54     T  414= 559.64
```

T	421=	472.16	T	422=	588.89	T	423=	578.00	T	424=	318.03	T	425=	722.45	T	426=	656.53
T	431=	606.24	T	432=	697.92	T	433=	762.13	T	434=	760.34	T	435=	689.14	T	436=	602.72
T	950=	1517.5	T	952=	1507.1	T	954=	1473.0									

ARITHMETIC NODES IN ASCENDING NODE NUMBER ORDER

T	50=	1024.4	T	52=	1012.8	T	54=	968.87	T	158=	1015.0	T	159=	971.47	T	168=	999.93
T	169=	993.85	T	195=	263.68	T	197=	306.75	T	199=	454.19	T	238=	956.45	T	311=	908.04
T	312=	908.04	T	321=	907.81	T	322=	907.81	T	331=	791.05	T	332=	791.05	T	337=	590.91
T	341=	583.62	T	357=	343.04	T	358=	348.58	T	359=	314.72	T	379=	270.25	T	403=	264.87
T	1000=	293.37	T	1001=	415.26	T	1002=	429.57	T	1003=	283.87	T	1004=	242.71	T	1005=	241.61
T	1006=	210.29	T	1007=	503.62	T	1008=	464.11	T	1009=	457.49	T	1010=	353.26	T	1011=	1044.8
T	1012=	1044.8	T	1013=	811.66	T	1021=	1042.2	T	1022=	1042.2	T	1023=	812.83	T	1031=	957.01
T	1032=	957.01	T	1033=	724.17	T	1041=	770.72	T	1042=	770.72	T	1043=	556.45	T	1044=	556.45
T	1346=	646.45	T	1347=	434.68									

HEATER NODES IN ASCENDING NODE NUMBER ORDER

++NONE++

BOUNDARY NODES IN ASCENDING NODE NUMBER ORDER

T	1=	100.00	T	2=	100.00

SYSTEMS IMPROVED NUMERICAL DIFFERENCING ANALYZER '85 (SINDA '85) PAGE 2/4

MODEL = DAMAGE3
FWDBCK

***** LOAD CASE NO. 3 CONDITIONS - Axial Distribution, 100F
Peak ICV Sidewall Temperature Time Point *****

5/2/94

SUBMODEL NAME = PTSB

		CALCULATED			ALLOWED
MAX DIFF DELTA T PER ITER	DRLXCC(PTSB	123)=	-2.490234E-02	VS. DRLXCA=	5.000000E-02
MAX ARITH DELTA T PER ITER	ARLXCC(PTSB	1007)=	0.110229	VS. ARLXCA=	0.500000
MAX DIFF DEL T PER TIME STEP	DTMPCC(PTSB	435)=	-1.90427	VS. DTMPCA=	10.0000
MAX ARITH DEL T PER TIME STEP	ATMPCC(PTSB	1346)=	-1.23557	VS. ATMPCA=	100.000
MIN STABILITY CRITERIA	CSGMIN(PTSB	455)=	2.891161E-04		
MAX STABILITY CRITERIA	CSGMAX(PTSB	434)=	3.89842		
NUMBER OF ITERATIONS	LOOPCT	=	3	VS. NLOOPT=	600
PROBLEM TIME	TIMEN	=	0.833333	VS. TIMEND=	12.0000
MEAN PROBLEM TIME	TIMEM	=	0.832405		
AVERAGE TIME STEP USED	DTIMEU	=	9.259260E-04	VS. DTIMEI=	0.

DIFFUSION NODES IN ASCENDING NODE NUMBER ORDER

T	51=	887.93	T	53=	843.86	T	55=	790.49	T	60=	891.14	T	62=	912.13	T	100=	872.14
T	105=	875.23	T	107=	877.05	T	110=	875.95	T	112=	893.67	T	113=	866.47	T	120=	884.16
T	122=	934.07	T	123=	852.48	T	124=	906.53	T	125=	852.43	T	126=	860.10	T	127=	850.21
T	130=	870.54	T	132=	923.58	T	133=	834.38	T	134=	896.30	T	135=	837.37	T	136=	851.10
T	137=	840.33	T	140=	861.07	T	141=	861.59	T	142=	908.07	T	143=	830.47	T	144=	882.90
T	145=	830.20	T	146=	837.49	T	147=	826.80	T	150=	837.48	T	152=	896.60	T	153=	798.51
T	154=	865.01	T	155=	799.67	T	156=	813.26	T	157=	799.91	T	160=	788.80	T	161=	792.47
T	162=	845.07	T	163=	753.56	T	164=	816.39	T	165=	755.98	T	166=	768.96	T	167=	755.02
T	170=	636.92	T	172=	643.02	T	173=	631.38	T	175=	560.51	T	177=	594.82	T	180=	541.61
T	190=	483.57	T	191=	485.60	T	192=	246.90	T	193=	638.98	T	194=	337.21	T	196=	445.11
T	198=	488.21	T	200=	867.57	T	204=	841.83	T	210=	843.44	T	220=	825.56	T	230=	775.30
T	240=	645.59	T	242=	434.25	T	250=	258.54	T	260=	202.74	T	261=	204.03	T	262=	205.70
T	263=	207.80	T	264=	217.44	T	265=	221.99	T	266=	228.72	T	300=	774.45	T	304=	747.34
T	305=	486.96	T	310=	789.50	T	313=	707.13	T	315=	595.68	T	316=	595.68	T	320=	775.12
T	323=	696.76	T	325=	590.65	T	326=	590.65	T	330=	726.51	T	333=	645.67	T	335=	566.82
T	336=	566.82	T	340=	659.89	T	342=	502.21	T	343=	527.79	T	344=	360.23	T	345=	649.84
T	346=	589.66	T	347=	475.82	T	349=	431.27	T	350=	296.31	T	351=	324.60	T	352=	297.32
T	353=	306.56	T	354=	321.19	T	355=	255.76	T	356=	322.71	T	360=	201.54	T	362=	203.31
T	364=	215.81	T	366=	251.93	T	367=	255.82	T	368=	264.52	T	369=	281.98	T	371=	330.11
T	373=	313.56	T	375=	274.90	T	377=	250.83	T	400=	208.89	T	401=	220.38	T	402=	247.74
T	404=	685.62	T	406=	606.16	T	408=	540.67	T	410=	607.87	T	412=	624.92	T	414=	559.71
T	421=	471.82	T	422=	588.96	T	423=	578.22	T	424=	288.57	T	425=	723.93	T	426=	664.05
T	431=	659.88	T	432=	796.31	T	433=	310.27	T	434=	271.29	T	435=	793.86	T	436=	652.98
T	441=	546.27	T	442=	625.73	T	443=	635.79	T	444=	635.34	T	445=	627.48	T	446=	546.84
T	451=	570.77	T	452=	603.47	T	453=	582.76	T	454=	583.46	T	455=	605.26	T	456=	574.41

ARITHMETIC NODES IN ASCENDING NODE NUMBER ORDER

T	50=	882.39	T	52=	843.99	T	54=	807.90	T	158=	801.98	T	159=	784.06	T	168=	793.34
T	169=	795.71	T	195=	246.13	T	197=	275.61	T	199=	468.34	T	238=	719.32	T	311=	694.56

T	312=	694.56	T	321=	684.72	T	322=	684.72	T	331=	633.45	T	332=	633.45	T	337=	541.27
T	341=	530.34	T	357=	323.77	T	358=	329.91	T	359=	296.88	T	379=	254.32	T	403=	249.79
T	1000=	252.38	T	1001=	439.66	T	1002=	443.95	T	1003=	284.49	T	1004=	237.79	T	1005=	236.75
T	1006=	206.97	T	1007=	519.78	T	1008=	496.30	T	1009=	488.87	T	1010=	373.07	T	1011=	783.66
T	1012=	783.66	T	1013=	633.57	T	1021=	769.66	T	1022=	769.66	T	1023=	626.58	T	1031=	721.81
T	1032=	721.81	T	1033=	593.06	T	1041=	657.95	T	1042=	657.95	T	1043=	505.92	T	1044=	505.92
T	1346=	606.62	T	1347=	397.73												

HEATER NODES IN ASCENDING NODE NUMBER ORDER
++NONE++

BOUNDARY NODES IN ASCENDING NODE NUMBER ORDER

T	1=	100.00	T	2=	100.00

SYSTEMS IMPROVED NUMERICAL DIFFERENCING ANALYZER '85 (SINDA '85) PAGE 3/4

MODEL = DAMAGE3 LOAD CASE NO. 3 CONDITIONS - Axial Distribution, 100F 5/2/94
FWDBCK ***** Peak ICV Sidewall Temperature Time Point *****

SUBMODEL NAME = PTSC

	CALCULATED			ALLOWED	
MAX DIFF DELTA T PER ITER	DRLXCC(PTSC	120)=	-2.319336E-02	VS. DRLXCA=	5.000000E-02
MAX ARITH DELTA T PER ITER	ARLXCC(PTSC	1007)=	0.125488	VS. ARLXCA=	0.500000
MAX DIFF DEL T PER TIME STEP	DTMPCC(PTSC	435)=	-1.90427	VS. DTMPCA=	10.0000
MAX ARITH DEL T PER TIME STEP	ATMPCC(PTSC	1346)=	-1.24252	VS. ATMPCA=	100.000
MIN STABILITY CRITERIA	CSGMIN(PTSC	455)=	2.891498E-04		
MAX STABILITY CRITERIA	CSGMAX(PTSC	434)=	3.89842		
NUMBER OF ITERATIONS	LOOPCT	=	3	VS. NLOOPT=	600
PROBLEM TIME	TIMEN	=	0.833333	VS. TIMEND=	12.0000
MEAN PROBLEM TIME	TIMEM	=	0.832405		
AVERAGE TIME STEP USED	DTIMEU	=	9.259260E-04	VS. DTIMEI=	0.

DIFFUSION NODES IN ASCENDING NODE NUMBER ORDER

T	51=	812.82	T	53=	747.71	T	55=	697.74	T	60=	863.15	T	62=	886.86	T	100=	846.38
T	105=	837.35	T	107=	834.07	T	110=	827.38	T	112=	829.60	T	113=	826.98	T	120=	807.94
T	122=	813.63	T	123=	805.60	T	124=	809.33	T	125=	803.91	T	126=	800.68	T	127=	799.68
T	130=	782.60	T	132=	788.48	T	133=	778.78	T	134=	785.49	T	135=	778.88	T	136=	779.50
T	137=	778.11	T	140=	766.74	T	141=	767.20	T	142=	772.63	T	143=	763.84	T	144=	768.57
T	145=	762.38	T	146=	760.31	T	147=	758.91	T	150=	740.99	T	152=	748.36	T	153=	737.69
T	154=	743.21	T	155=	735.54	T	156=	734.84	T	157=	732.76	T	160=	699.80	T	161=	706.06
T	162=	706.41	T	163=	697.04	T	164=	703.63	T	165=	697.16	T	166=	699.18	T	167=	697.68
T	170=	625.20	T	172=	625.32	T	173=	624.14	T	175=	589.71	T	177=	604.30	T	180=	583.28
T	190=	567.11	T	191=	549.39	T	192=	252.87	T	193=	627.34	T	194=	344.93	T	196=	544.99
T	198=	551.59	T	200=	850.69	T	204=	819.05	T	210=	786.11	T	220=	760.00	T	230=	709.21
T	240=	627.55	T	242=	429.29	T	250=	257.34	T	260=	202.53	T	261=	203.85	T	262=	205.33
T	263=	207.50	T	264=	216.89	T	265=	221.42	T	266=	228.06	T	300=	764.18	T	304=	733.67
T	305=	481.64	T	310=	742.67	T	313=	670.74	T	315=	569.26	T	316=	569.26	T	320=	722.84
T	323=	656.29	T	325=	561.21	T	326=	561.21	T	330=	681.43	T	333=	617.44	T	335=	546.91
T	336=	546.91	T	340=	638.47	T	342=	493.44	T	343=	525.45	T	344=	357.19	T	345=	647.19
T	346=	585.43	T	347=	474.10	T	349=	429.39	T	350=	294.97	T	351=	323.32	T	352=	296.01
T	353=	305.53	T	354=	319.54	T	355=	254.80	T	356=	321.24	T	360=	201.39	T	362=	203.04
T	364=	215.37	T	366=	250.99	T	367=	254.77	T	368=	263.10	T	369=	280.13	T	371=	328.76
T	373=	312.59	T	375=	274.33	T	377=	250.30	T	400=	208.80	T	401=	220.32	T	402=	247.18
T	404=	685.06	T	406=	603.89	T	408=	540.50	T	410=	607.84	T	412=	624.91	T	414=	559.70
T	421=	471.82	T	422=	588.95	T	423=	578.21	T	424=	288.55	T	425=	723.92	T	426=	664.03
T	431=	658.82	T	432=	795.36	T	433=	310.24	T	434=	271.29	T	435=	793.84	T	436=	652.92
T	441=	546.01	T	442=	624.85	T	443=	635.68	T	444=	635.24	T	445=	627.40	T	446=	546.69
T	451=	569.76	T	452=	601.34	T	453=	582.34	T	454=	583.29	T	455=	605.22	T	456=	574.31

ARITHMETIC NODES IN ASCENDING NODE NUMBER ORDER

T	50=	808.69	T	52=	749.37	T	54=	720.63	T	158=	707.38	T	159=	705.43	T	168=	706.24
T	169=	706.67	T	195=	255.68	T	197=	292.55	T	199=	484.21	T	238=	673.75	T	311=	658.09

T	312=	658.09	T	321=	644.05	T	322=	644.05	T	331=	605.15	T	332=	605.15	T	337=	532.19
T	341=	520.29	T	357=	322.23	T	358=	328.45	T	359=	295.56	T	379=	253.33	T	403=	249.25
T	1000=	255.08	T	1001=	503.86	T	1002=	465.65	T	1003=	302.47	T	1004=	242.40	T	1005=	241.20
T	1006=	206.94	T	1007=	574.27	T	1008=	565.47	T	1009=	554.30	T	1010=	375.36	T	1011=	737.82
T	1012=	737.82	T	1013=	603.73	T	1021=	718.45	T	1022=	718.45	T	1023=	593.35	T	1031=	677.78
T	1032=	677.78	T	1033=	570.25	T	1041=	636.50	T	1042=	636.50	T	1043=	496.48	T	1044=	496.48
T	1346=	603.75	T	1347=	396.02												

HEATER NODES IN ASCENDING NODE NUMBER ORDER

++NONE++

BOUNDARY NODES IN ASCENDING NODE NUMBER ORDER

T	1=	100.00	T	2=	100.00

SYSTEMS IMPROVED NUMERICAL DIFFERENCING ANALYZER '85 (SINDA '85) PAGE 4/4

MODEL = DAMAGE3 LOAD CASE NO. 3 CONDITIONS - Axial Distribution, 100F 5/2/94
FWDBCK ***** Peak ICV Sidewall Temperature Time Point *****

SUBMODEL NAME = PTSD

	CALCULATED			ALLOWED	
MAX DIFF DELTA T PER ITER	DRLXCC(PTSD	120)=	-2.233887E-02	VS. DRLXCA=	5.000000E-02
MAX ARITH DELTA T PER ITER	ARLXCC(PTSD	1007)=	0.123413	VS. ARLXCA=	0.500000
MAX DIFF DEL T PER TIME STEP	DTMPCC(PTSD	435)=	-1.90427	VS. DTMPCA=	10.0000
MAX ARITH DEL T PER TIME STEP	ATMPCC(PTSD	1346)=	-1.24252	VS. ATMPCA=	100.000
MIN STABILITY CRITERIA	CSGMIN(PTSD	455)=	2.891499E-04		
MAX STABILITY CRITERIA	CSGMAX(PTSD	434)=	3.89842		
NUMBER OF ITERATIONS	LOOPCT	=	3	VS. NLOOPT=	600
PROBLEM TIME	TIMEN	=	0.833333	VS. TIMEND=	12.0000
MEAN PROBLEM TIME	TIMEN	=	0.832405		
AVERAGE TIME STEP USED	DTIMEU	=	9.259260E-04	VS. DTIMEI=	0.

DIFFUSION NODES IN ASCENDING NODE NUMBER ORDER

T 51=	804.70	T 53=	735.85	T 55=	686.32	T 60=	860.38	T 62=	883.39	T 100=	844.28
T 105=	834.06	T 107=	830.24	T 110=	823.01	T 112=	823.51	T 113=	823.16	T 120=	800.11
T 122=	801.22	T 123=	799.91	T 124=	799.90	T 125=	799.04	T 126=	796.31	T 127=	796.24
T 130=	772.69	T 132=	773.16	T 133=	771.40	T 134=	773.71	T 135=	772.49	T 136=	773.73
T 137=	773.46	T 140=	755.08	T 141=	755.46	T 142=	756.01	T 143=	754.25	T 144=	755.39
T 145=	754.15	T 146=	753.53	T 147=	753.25	T 150=	729.71	T 152=	731.30	T 153=	729.21
T 154=	729.90	T 155=	728.21	T 156=	728.06	T 157=	727.53	T 160=	689.30	T 161=	696.09
T 162=	690.85	T 163=	688.99	T 164=	691.40	T 165=	690.43	T 166=	692.94	T 167=	692.81
T 170=	621.53	T 172=	621.21	T 173=	620.79	T 175=	588.29	T 177=	601.77	T 180=	584.13
T 190=	565.04	T 191=	548.81	T 192=	253.09	T 193=	625.09	T 194=	344.49	T 196=	558.72
T 198=	551.07	T 200=	849.43	T 204=	817.83	T 210=	784.79	T 220=	757.48	T 230=	707.91
T 240=	626.74	T 242=	429.06	T 250=	257.29	T 260=	202.52	T 261=	203.85	T 262=	205.31
T 263=	207.48	T 264=	216.87	T 265=	221.39	T 266=	228.04	T 300=	763.33	T 304=	732.99
T 305=	481.39	T 310=	741.47	T 313=	669.79	T 315=	568.56	T 316=	568.56	T 320=	721.00
T 323=	654.88	T 325=	560.19	T 326=	560.19	T 330=	680.72	T 333=	617.03	T 335=	546.64
T 336=	546.64	T 340=	637.99	T 342=	493.26	T 343=	525.43	T 344=	357.14	T 345=	647.17
T 346=	585.38	T 347=	474.09	T 349=	429.37	T 350=	294.96	T 351=	323.31	T 352=	296.00
T 353=	305.52	T 354=	319.52	T 355=	254.79	T 356=	321.23	T 360=	201.38	T 362=	203.04
T 364=	215.36	T 366=	250.98	T 367=	254.77	T 368=	263.09	T 369=	280.12	T 371=	328.75
T 373=	312.59	T 375=	274.32	T 377=	250.30	T 400=	208.79	T 401=	220.32	T 402=	247.18
T 404=	685.06	T 406=	603.85	T 408=	540.50	T 410=	607.84	T 412=	624.91	T 414=	559.70
T 421=	471.82	T 422=	588.95	T 423=	578.21	T 424=	288.55	T 425=	723.92	T 426=	664.03
T 431=	658.80	T 432=	795.35	T 433=	310.23	T 434=	271.29	T 435=	793.84	T 436=	652.92
T 441=	546.01	T 442=	624.84	T 443=	635.67	T 444=	635.24	T 445=	627.40	T 446=	546.69
T 451=	569.74	T 452=	601.31	T 453=	582.33	T 454=	583.29	T 455=	605.22	T 456=	574.31

ARITHMETIC NODES IN ASCENDING NODE NUMBER ORDER

T 50=	800.56	T 52=	737.74	T 54=	709.86	T 158=	696.69	T 159=	696.37	T 168=	696.14
T 169=	696.28	T 195=	257.12	T 197=	289.77	T 199=	483.26	T 238=	672.66	T 311=	657.14

T	312=	657.14	T	321=	642.63	T	322=	642.63	T	331=	604.71	T	332=	604.71	T	337=	532.02
T	341=	520.08	T	357=	322.22	T	358=	328.44	T	359=	295.55	T	379=	253.32	T	403=	249.25
T	1000=	255.62	T	1001=	507.10	T	1002=	464.89	T	1003=	303.31	T	1004=	242.69	T	1005=	241.48
T	1006=	206.95	T	1007=	572.78	T	1008=	563.94	T	1009=	553.42	T	1010=	375.04	T	1011=	736.64
T	1012=	736.64	T	1013=	602.94	T	1021=	716.64	T	1022=	716.64	T	1023=	592.20	T	1031=	677.08
T	1032=	677.08	T	1033=	569.93	T	1041=	636.03	T	1042=	636.03	T	1043=	496.30	T	1044=	496.30
T	1346=	603.72	T	1347=	396.01												

HEATER NODES IN ASCENDING NODE NUMBER ORDER
++NONE++

BOUNDARY NODES IN ASCENDING NODE NUMBER ORDER

T	1=	100.00	T	2=	100.00

```
                    SYSTEMS IMPROVED NUMERICAL DIFFERENCING ANALYZER '85 (SINDA '85)          PAGE  1/4

MODEL = DAMAGE3          LOAD CASE NO. 3 CONDITIONS - Axial Distribution, 100F
  STDSTL                   ***  Steady-state Conditions After The Fire  ***                  5/2/94  11am

 SUBMODEL NAME = MAIN

      PROBLEM TIME                    TIMEN                  =  999.000     VS. TIMEND=  999.000
                                DIFFUSION NODES IN ASCENDING NODE NUMBER ORDER
 T  267=  230.87     T  268=  230.92     T  269=  229.67
                                ARITHMETIC NODES IN ASCENDING NODE NUMBER ORDER
 T  201=  238.58     T 1266=  233.72     T 1267=  265.76     T 1268=  252.01     T 1269=  236.97
                                HEATER NODES IN ASCENDING NODE NUMBER ORDER
                                          ++NONE++
                                BOUNDARY NODES IN ASCENDING NODE NUMBER ORDER
                                          ++NONE++

MEAN ICV GAS TEMP= 238.6 F   MEAN ICV GAS PRESSURE= 20.96 PSIA
MEAN ICV-OCV GAS TEMP= 247.0 F   MEAN ICV-OCV GAS PRESSURE= 24.91 PSIA


 SUBMODEL NAME = PTSA

                                    CALCULATED                          ALLOWED
      MAX DIFF DELTA T PER ITER     DRLXCC(PTSA      261)= -3.30078     VS. DRLXCA= 5.000000E-02
      MAX ARITH DELTA T PER ITER    ARLXCC(PTSA     1044)=-0.628784     VS. ARLXCA= 0.500000
      MAX SYSTEM ENERGY BALANCE     EBALSC               = -2.95446     VS. EBALSA * ESUMIS      =  7.67925
                                                                        EBALSA= 1.000000E-03
      ENERGY INTO AND OUT OF SYS    ESUMIS               =  7679.25     ESUMOS=  3394.01
      MAX NODAL ENERGY BALANCE      EBALNC(PTSA      350)=-0.244710     VS. EBALNA= 1.000000E-02
      NUMBER OF ITERATIONS          LOOPCT               =     156     VS. NLOOPS=    1000
      PROBLEM TIME                  TIMEN                =  999.000     VS. TIMEND=  999.000

                                DIFFUSION NODES IN ASCENDING NODE NUMBER ORDER
 T   51=  686.15     T   53=  716.88     T   55=  686.16     T   60=  590.26     T   62=  563.85     T  100=  537.46
 T  105=  535.19     T  107=  534.57     T  110=  541.59     T  112=  559.41     T  113=  486.39     T  120=  727.21
 T  122=  788.08     T  123=  586.90     T  124=  788.07     T  125=  586.93     T  126=  788.07     T  127=  586.93
 T  130=  760.82     T  132=  823.50     T  133=  615.10     T  134=  823.50     T  135=  615.10     T  136=  823.50
 T  137=  615.10     T  140=  739.86     T  141=  720.88     T  142=  783.46     T  143=  621.62     T  144=  783.46
 T  145=  621.63     T  146=  783.46     T  147=  621.63     T  150=  775.09     T  152=  838.21     T  153=  624.71
 T  154=  836.60     T  155=  625.74     T  156=  836.60     T  157=  625.74     T  160=  729.94     T  161=  712.81
 T  162=  785.35     T  163=  594.08     T  164=  781.88     T  165=  602.31     T  166=  781.88     T  167=  602.31
 T  170=  447.12     T  172=  459.27     T  173=  412.86     T  175=  389.24     T  177=  410.84     T  180=  396.35
 T  190=  324.12     T  191=  287.55     T  192=  244.92     T  193=  370.21     T  194=  286.51     T  196=  256.34
 T  198=  285.77     T  200=  217.27     T  204=  336.62     T  210=  944.57     T  220=  964.21     T  230=  868.24
 T  240=  469.42     T  242=  319.93     T  250=  243.22     T  260=  203.86     T  261=  201.83     T  262=  220.15
 T  263=  223.12     T  264=  225.43     T  265=  227.82     T  266=  229.91     T  300=  186.39     T  304=  266.27
 T  305=  174.92     T  310=  790.39     T  313=  692.77     T  315=  575.68     T  316=  575.68     T  320=  814.84
 T  323=  714.49     T  325=  594.70     T  326=  594.70     T  330=  683.70     T  333=  553.87     T  335=  470.40
 T  336=  470.40     T  340=  504.48     T  342=  351.04     T  343=  237.83     T  344=  260.66     T  345=  225.23
 T  346=  253.13     T  347=  228.39     T  349=  214.73     T  350=  231.53     T  351=  228.41     T  352=  229.50
 T  353=  227.78     T  354=  236.09     T  355=  225.15     T  356=  231.48     T  360=  203.78     T  362=  216.40
 T  364=  222.80     T  366=  225.34     T  367=  224.66     T  368=  222.34     T  369=  221.72     T  371=  229.74
 T  373=  229.10     T  375=  226.11     T  377=  223.95     T  400=  215.04     T  401=  213.44     T  402=  223.54
 T  404=  197.64     T  406=  209.94     T  408=  121.81     T  410=  106.11     T  412=  105.58     T  414=  105.13
```

T	421=	179.41	T	422=	111.19	T	423=	107.74	T	424=	181.96	T	425=	112.24	T	426=	110.12
T	431=	140.45	T	432=	163.86	T	433=	132.33	T	434=	124.10	T	435=	115.56	T	436=	119.72
T	950=	1355.5	T	952=	1355.6	T	954=	1298.7									

ARITHMETIC NODES IN ASCENDING NODE NUMBER ORDER

T	50=	681.60	T	52=	713.33	T	54=	679.35	T	158=	735.97	T	159=	682.02	T	168=	717.33
T	169=	709.80	T	195=	233.91	T	197=	257.90	T	199=	307.97	T	238=	702.42	T	311=	684.26
T	312=	684.26	T	321=	705.86	T	322=	705.86	T	331=	546.07	T	332=	546.07	T	337=	345.42
T	341=	363.46	T	357=	233.04	T	358=	230.48	T	359=	230.30	T	379=	225.04	T	403=	223.80
T	1000=	251.97	T	1001=	271.82	T	1002=	299.78	T	1003=	249.96	T	1004=	237.93	T	1005=	237.11
T	1006=	213.32	T	1007=	348.53	T	1008=	324.11	T	1009=	298.61	T	1010=	281.85	T	1011=	783.93
T	1012=	783.93	T	1013=	616.45	T	1021=	807.94	T	1022=	807.94	T	1023=	635.95	T	1031=	677.89
T	1032=	677.89	T	1033=	499.61	T	1041=	504.90	T	1042=	504.90	T	1043=	355.87	T	1044=	355.87
T	1346=	227.72	T	1347=	224.85												

HEATER NODES IN ASCENDING NODE NUMBER ORDER

++NONE++

BOUNDARY NODES IN ASCENDING NODE NUMBER ORDER

T	1=	100.00	T	2=	100.00

SYSTEMS IMPROVED NUMERICAL DIFFERENCING ANALYZER '85 (SINDA '85) PAGE 2/4

MODEL = DAMAGE3
STDSTL

LOAD CASE NO. 3 CONDITIONS - Axial Distribution, 100F
*** Steady-state Conditions After The Fire *** 5/2/94 11am

SUBMODEL NAME = PTSB

		CALCULATED			ALLOWED	
MAX DIFF DELTA T PER ITER	DRLXCC(PTSB	401)= 3.741455E-02	VS.	DRLXCA=	5.000000E-02	
MAX ARITH DELTA T PER ITER	ARLXCC(PTSB	1004)=-3.680420E-02	VS.	ARLXCA=	0.500000	
MAX SYSTEM ENERGY BALANCE	EBALSC	=-0.708162	VS.	EBALSA * ESUMIS =	0.	
				EBALSA=	1.000000E-03	
ENERGY INTO AND OUT OF SYS	ESUMIS	= 0.		ESUMOS=	1856.94	
MAX NODAL ENERGY BALANCE	EBALNC(PTSB	367)=-0.506099	VS.	EBALNA=	1.000000E-02	
NUMBER OF ITERATIONS	LOOPCT	= 156	VS.	NLOOPS=	1000	
PROBLEM TIME	TIMEN	= 999.000	VS.	TIMEND=	999.000	

DIFFUSION NODES IN ASCENDING NODE NUMBER ORDER

T	51=	448.82	T	53=	476.71	T	55=	453.83	T	60=	396.17	T	62=	399.28	T	100=	341.36
T	105=	366.56	T	107=	375.77	T	110=	386.60	T	112=	419.49	T	113=	362.29	T	120=	443.69
T	122=	527.05	T	123=	373.94	T	124=	493.51	T	125=	373.63	T	126=	419.74	T	127=	370.09
T	130=	467.65	T	132=	553.93	T	133=	394.61	T	134=	519.30	T	135=	396.47	T	136=	444.87
T	137=	396.92	T	140=	479.07	T	141=	479.88	T	142=	550.31	T	143=	420.63	T	144=	520.23
T	145=	418.40	T	146=	450.38	T	147=	408.53	T	150=	471.92	T	152=	560.23	T	153=	398.30
T	154=	523.60	T	155=	400.03	T	156=	446.38	T	157=	396.43	T	160=	448.37	T	161=	449.43
T	162=	529.59	T	163=	383.26	T	164=	495.33	T	165=	385.76	T	166=	424.28	T	167=	377.15
T	170=	354.61	T	172=	375.68	T	173=	336.04	T	175=	325.81	T	177=	338.07	T	180=	319.72
T	190=	303.14	T	191=	277.74	T	192=	227.68	T	193=	292.06	T	194=	251.99	T	196=	254.46
T	198=	276.69	T	200=	216.72	T	204=	255.19	T	210=	389.60	T	220=	405.06	T	230=	363.69
T	240=	298.37	T	242=	250.82	T	250=	217.93	T	260=	199.74	T	261=	199.85	T	262=	208.23
T	263=	209.03	T	264=	210.99	T	265=	212.33	T	266=	211.86	T	300=	180.03	T	304=	202.04
T	305=	140.33	T	310=	353.55	T	313=	322.27	T	315=	285.10	T	316=	285.10	T	320=	369.60
T	323=	336.55	T	325=	297.37	T	326=	297.37	T	330=	319.15	T	333=	283.21	T	335=	254.26
T	336=	254.26	T	340=	288.69	T	342=	245.69	T	343=	186.23	T	344=	216.62	T	345=	186.54
T	346=	183.51	T	347=	197.99	T	349=	175.05	T	350=	206.67	T	351=	201.42	T	352=	205.68
T	353=	202.87	T	354=	207.62	T	355=	205.24	T	356=	205.40	T	360=	199.61	T	362=	206.43
T	364=	208.27	T	366=	205.70	T	367=	205.03	T	368=	203.71	T	369=	202.94	T	371=	202.29
T	373=	203.22	T	375=	203.87	T	377=	204.08	T	400=	203.95	T	401=	202.46	T	402=	204.08
T	404=	173.62	T	406=	137.67	T	408=	110.94	T	410=	104.13	T	412=	104.31	T	414=	104.52
T	421=	171.59	T	422=	110.00	T	423=	106.80	T	424=	169.66	T	425=	109.79	T	426=	106.62
T	431=	148.50	T	432=	142.46	T	433=	147.53	T	434=	129.57	T	435=	106.64	T	436=	106.71
T	441=	116.84	T	442=	123.88	T	443=	114.48	T	444=	112.23	T	445=	107.92	T	446=	109.71
T	451=	122.17	T	452=	131.57	T	453=	115.64	T	454=	111.13	T	455=	105.92	T	456=	107.96

ARITHMETIC NODES IN ASCENDING NODE NUMBER ORDER

T	50=	447.69	T	52=	474.08	T	54=	451.88	T	158=	464.40	T	159=	431.69	T	168=	449.98
T	169=	451.95	T	195=	216.32	T	197=	228.51	T	199=	270.16	T	238=	335.32	T	311=	319.65
T	312=	319.65	T	321=	333.82	T	322=	333.82	T	331=	280.71	T	332=	280.71	T	337=	235.19

T	341=	245.76	T	357=	205.54	T	358=	202.47	T	359=	206.16	T	379=	205.33	T	403=	204.08
T	1000=	222.81	T	1001=	263.14	T	1002=	267.20	T	1003=	234.33	T	1004=	222.68	T	1005=	222.07
T	1006=	204.50	T	1007=	309.41	T	1008=	299.47	T	1009=	284.39	T	1010=	247.03	T	1011=	352.62
T	1012=	352.62	T	1013=	298.48	T	1021=	368.58	T	1022=	368.58	T	1023=	311.39	T	1031=	318.27
T	1032=	318.27	T	1033=	264.65	T	1041=	288.38	T	1042=	288.38	T	1043=	246.15	T	1044=	246.15
T	1346=	182.09	T	1347=	199.90												

HEATER NODES IN ASCENDING NODE NUMBER ORDER
++NONE++

BOUNDARY NODES IN ASCENDING NODE NUMBER ORDER

T	1=	100.00	T	2=	100.00

SYSTEMS IMPROVED NUMERICAL DIFFERENCING ANALYZER '85 (SINDA '85) PAGE 3/4

MODEL = DAMAGE3
STDSTL

LOAD CASE NO. 3 CONDITIONS - Axial Distribution, 100F
*** Steady-state Conditions After The Fire *** 5/2/94 11am

SUBMODEL NAME = PTSC

		CALCULATED		ALLOWED	
MAX DIFF DELTA T PER ITER	DRLXCC(PTSC	173)=-2.874756E-02	VS.	DRLXCA=	5.000000E-02
MAX ARITH DELTA T PER ITER	ARLXCC(PTSC	1004)=-2.905273E-02	VS.	ARLXCA=	0.500000
MAX SYSTEM ENERGY BALANCE	EBALSC	= -23.1527	VS.	EBALSA * ESUMIS =	0.
				EBALSA=	1.000000E-03
ENERGY INTO AND OUT OF SYS	ESUMIS	= 0.		ESUMOS=	1750.97
MAX NODAL ENERGY BALANCE	EBALNC(PTSC	367)= -2.94931	VS.	EBALNA=	1.000000E-02
NUMBER OF ITERATIONS	LOOPCT	= 156	VS.	NLOOPS=	1000
PROBLEM TIME	TIMEN	= 999.000	VS.	TIMEND=	999.000

DIFFUSION NODES IN ASCENDING NODE NUMBER ORDER

T	51=	271.82	T	53=	286.73	T	55=	277.23	T	60=	255.72	T	62=	262.14	T	100=	239.37
T	105=	246.07	T	107=	248.61	T	110=	251.63	T	112=	258.00	T	113=	248.85	T	120=	269.04
T	122=	283.94	T	123=	259.19	T	124=	274.48	T	125=	253.89	T	126=	252.92	T	127=	241.76
T	130=	281.34	T	132=	297.65	T	133=	270.73	T	134=	287.26	T	135=	264.99	T	136=	263.80
T	137=	251.90	T	140=	290.24	T	141=	290.58	T	142=	304.01	T	143=	282.29	T	144=	293.93
T	145=	275.47	T	146=	269.43	T	147=	259.47	T	150=	283.60	T	152=	299.75	T	153=	273.19
T	154=	289.35	T	155=	267.24	T	156=	266.22	T	157=	252.28	T	160=	274.85	T	161=	274.77
T	162=	289.17	T	163=	266.07	T	164=	280.21	T	165=	260.12	T	166=	260.01	T	167=	249.94
T	170=	248.95	T	172=	253.94	T	173=	246.74	T	175=	240.48	T	177=	244.11	T	180=	239.85
T	190=	231.04	T	191=	225.98	T	192=	196.87	T	193=	212.13	T	194=	200.08	T	196=	231.15
T	198=	225.69	T	200=	187.88	T	204=	185.05	T	210=	199.72	T	220=	205.62	T	230=	198.60
T	240=	186.05	T	242=	178.68	T	250=	176.52	T	260=	185.42	T	261=	185.74	T	262=	181.40
T	263=	181.84	T	264=	178.40	T	265=	179.26	T	266=	175.85	T	300=	159.04	T	304=	150.95
T	305=	119.94	T	310=	180.23	T	313=	171.40	T	315=	160.99	T	316=	160.99	T	320=	185.89
T	323=	176.51	T	325=	165.47	T	326=	165.47	T	330=	178.24	T	333=	168.60	T	335=	159.12
T	336=	159.12	T	340=	173.75	T	342=	169.88	T	343=	147.66	T	344=	167.90	T	345=	149.63
T	346=	141.35	T	347=	159.63	T	349=	142.60	T	350=	167.21	T	351=	163.18	T	352=	166.80
T	353=	164.85	T	354=	166.46	T	355=	168.17	T	356=	165.78	T	360=	184.19	T	362=	180.27
T	364=	175.52	T	366=	168.70	T	367=	168.00	T	368=	167.13	T	369=	166.37	T	371=	163.50
T	373=	164.75	T	375=	166.47	T	377=	167.48	T	400=	177.34	T	401=	176.18	T	402=	167.64
T	404=	145.16	T	406=	115.92	T	408=	105.82	T	410=	102.38	T	412=	102.80	T	414=	103.34
T	421=	153.07	T	422=	107.43	T	423=	105.03	T	424=	145.36	T	425=	106.41	T	426=	104.29
T	431=	127.11	T	432=	120.95	T	433=	128.07	T	434=	118.00	T	435=	103.91	T	436=	103.84
T	441=	108.61	T	442=	110.80	T	443=	107.81	T	444=	106.68	T	445=	104.30	T	446=	105.20
T	451=	110.16	T	452=	113.48	T	453=	107.73	T	454=	105.87	T	455=	103.28	T	456=	104.31

ARITHMETIC NODES IN ASCENDING NODE NUMBER ORDER

T	50=	272.27	T	52=	285.55	T	54=	277.05	T	158=	276.83	T	159=	270.86	T	168=	275.06
T	169=	275.70	T	195=	192.40	T	197=	193.64	T	199=	210.01	T	238=	193.10	T	311=	170.64
T	312=	170.64	T	321=	175.72	T	322=	175.72	T	331=	167.87	T	332=	167.87	T	337=	163.26

T	341=	167.86	T	357=	165.49	T	358=	163.48	T	359=	166.99	T	379=	168.30	T	403=	167.53
T	1000=	190.98	T	1001=	222.34	T	1002=	210.19	T	1003=	201.64	T	1004=	194.27	T	1005=	193.95
T	1006=	184.53	T	1007=	234.73	T	1008=	231.13	T	1009=	227.55	T	1010=	189.60	T	1011=	180.06
T	1012=	180.06	T	1013=	164.76	T	1021=	185.71	T	1022=	185.71	T	1023=	169.46	T	1031=	178.06
T	1032=	178.06	T	1033=	162.54	T	1041=	173.63	T	1042=	173.63	T	1043=	169.81	T	1044=	169.81
T	1346=	145.42	T	1347=	162.51												

HEATER NODES IN ASCENDING NODE NUMBER ORDER

++NONE++

BOUNDARY NODES IN ASCENDING NODE NUMBER ORDER

T	1=	100.00	T	2=	100.00

SYSTEMS IMPROVED NUMERICAL DIFFERENCING ANALYZER '85 (SINDA '85) PAGE 4/4

MODEL = DAMAGE3
STDSTL

LOAD CASE NO. 3 CONDITIONS - Axial Distribution, 100F
*** Steady-state Conditions After The Fire ***

5/2/94 11am

SUBMODEL NAME = PTSD

		CALCULATED		ALLOWED
MAX DIFF DELTA T PER ITER	DRLXCC(PTSD	196)=-4.418945E-02	VS. DRLXCA=	5.000000E-02
MAX ARITH DELTA T PER ITER	ARLXCC(PTSD	1033)=-2.380371E-02	VS. ARLXCA=	0.500000
MAX SYSTEM ENERGY BALANCE	EBALSC	= 3.52679	VS. EBALSA * ESUMIS =	0.
			EBALSA=	1.000000E-03
ENERGY INTO AND OUT OF SYS	ESUMIS	= 0.	ESUMOS=	731.116
MAX NODAL ENERGY BALANCE	EBALNC(PTSD	367)= 1.37608	VS. EBALNA=	1.000000E-02
NUMBER OF ITERATIONS	LOOPCT	= 156	VS. NLOOPS=	1000
PROBLEM TIME	TIMEN	= 999.000	VS. TIMEND=	999.000

DIFFUSION NODES IN ASCENDING NODE NUMBER ORDER

T	51=	232.29	T	53=	243.02	T	55=	238.25	T	60=	222.96	T	62=	231.72	T	100=	213.46
T	105=	217.19	T	107=	218.61	T	110=	220.32	T	112=	222.82	T	113=	219.68	T	120=	230.56
T	122=	236.20	T	123=	227.51	T	124=	231.44	T	125=	224.09	T	126=	220.64	T	127=	216.36
T	130=	239.39	T	132=	245.67	T	133=	236.10	T	134=	240.38	T	135=	232.30	T	136=	228.49
T	137=	223.78	T	140=	245.75	T	141=	245.91	T	142=	251.19	T	143=	243.45	T	144=	245.88
T	145=	239.14	T	146=	233.04	T	147=	229.22	T	150=	241.51	T	152=	247.70	T	153=	238.29
T	154=	242.46	T	155=	234.33	T	156=	230.82	T	157=	224.69	T	160=	236.98	T	161=	236.81
T	162=	242.38	T	163=	234.36	T	164=	237.97	T	165=	230.37	T	166=	227.92	T	167=	224.17
T	170=	225.51	T	172=	227.39	T	173=	225.01	T	175=	222.15	T	177=	223.59	T	180=	222.08
T	190=	218.25	T	191=	215.65	T	192=	185.43	T	193=	201.59	T	194=	188.82	T	196=	220.68
T	198=	215.44	T	200=	180.74	T	204=	177.64	T	210=	187.63	T	220=	191.17	T	230=	186.86
T	240=	173.35	T	242=	165.87	T	250=	163.80	T	260=	175.31	T	261=	175.64	T	262=	169.39
T	263=	169.82	T	264=	165.85	T	265=	166.71	T	266=	163.21	T	300=	153.43	T	304=	145.60
T	305=	117.90	T	310=	168.83	T	313=	161.35	T	315=	152.53	T	316=	152.53	T	320=	172.47
T	323=	164.67	T	325=	155.49	T	326=	155.49	T	330=	167.03	T	333=	158.64	T	335=	150.68
T	336=	150.68	T	340=	162.38	T	342=	158.08	T	343=	139.21	T	344=	155.59	T	345=	140.63
T	346=	134.26	T	347=	148.60	T	349=	135.13	T	350=	154.75	T	351=	151.50	T	352=	154.37
T	353=	152.85	T	354=	154.15	T	355=	155.57	T	356=	153.55	T	360=	173.93	T	362=	168.33
T	364=	163.04	T	366=	156.09	T	367=	155.41	T	368=	154.64	T	369=	153.99	T	371=	151.75
T	373=	152.78	T	375=	154.23	T	377=	155.09	T	400=	165.68	T	401=	164.67	T	402=	155.21
T	404=	136.80	T	406=	113.26	T	408=	104.77	T	410=	101.96	T	412=	102.33	T	414=	102.85
T	421=	145.02	T	422=	106.32	T	423=	104.28	T	424=	137.10	T	425=	105.29	T	426=	103.55
T	431=	122.21	T	432=	117.33	T	433=	122.93	T	434=	114.72	T	435=	103.22	T	436=	103.16
T	441=	107.09	T	442=	108.95	T	443=	106.41	T	444=	105.48	T	445=	103.53	T	446=	104.26
T	451=	108.41	T	452=	111.19	T	453=	106.37	T	454=	104.82	T	455=	102.71	T	456=	103.54

ARITHMETIC NODES IN ASCENDING NODE NUMBER ORDER

T	50=	232.82	T	52=	242.29	T	54=	238.23	T	158=	237.38	T	159=	235.13	T	168=	236.99
T	169=	237.31	T	195=	181.66	T	197=	182.23	T	199=	199.23	T	238=	180.94	T	311=	160.71
T	312=	160.71	T	321=	164.01	T	322=	164.01	T	331=	157.99	T	332=	157.99	T	337=	152.66

T	341=	156.53	T	357=	153.35	T	358=	151.74	T	359=	154.55	T	379=	155.70	T	403=	155.13
T	1000=	179.70	T	1001=	211.84	T	1002=	199.37	T	1003=	190.38	T	1004=	182.61	T	1005=	182.32
T	1006=	173.60	T	1007=	219.70	T	1008=	218.15	T	1009=	216.41	T	1010=	177.58	T	1011=	168.69
T	1012=	168.69	T	1013=	155.73	T	1021=	172.32	T	1022=	172.32	T	1023=	158.81	T	1031=	166.88
T	1032=	166.88	T	1033=	153.55	T	1041=	162.30	T	1042=	162.30	T	1043=	158.05	T	1044=	158.05
T	1346=	137.33	T	1347=	150.90												

HEATER NODES IN ASCENDING NODE NUMBER ORDER

++NONE++

BOUNDARY NODES IN ASCENDING NODE NUMBER ORDER

T	1=	100.00	T	2=	100.00

```
                    SYSTEMS IMPROVED NUMERICAL DIFFERENCING ANALYZER '85 (SINDA '85)                PAGE   1/4

MODEL = DAMAGE4                HAC LOAD CASE NO. 4 CONDITIONS - Axial Distribution, -20F                 5/2/94
  FWDBCK                *****      Peak OCV Sidewall Temperature Time Point     *****

 SUBMODEL NAME = MAIN

       PROBLEM TIME                    TIMEN                  = 0.500000     VS. TIMEND= 0.500000
                                  DIFFUSION NODES IN ASCENDING NODE NUMBER ORDER
  T   267=  100.68     T   268=  100.66     T   269=  99.476
                                  ARITHMETIC NODES IN ASCENDING NODE NUMBER ORDER
  T   201=  620.52     T  1266=  105.89     T  1267=  161.78     T  1268=  137.59     T  1269=  111.78
                                  HEATER NODES IN ASCENDING NODE NUMBER ORDER
                                            ++NONE++
                                  BOUNDARY NODES IN ASCENDING NODE NUMBER ORDER
                                            ++NONE++
MEAN ICV GAS TEMP= 620.5 F   MEAN ICV GAS PRESSURE= 32.43 PSIA
MEAN ICV-OCV GAS TEMP= 786.1 F   MEAN ICV-OCV GAS PRESSURE= 43.95 PSIA


 SUBMODEL NAME = PTSA
                                  CALCULATED                                  ALLOWED
       MAX DIFF DELTA T PER ITER     DRLXCC(PTSA      304)= 2.441406E-04 VS. DRLXCA= 5.000000E-02
       MAX ARITH DELTA T PER ITER    ARLXCC(PTSA     1346)=-0.269775     VS. ARLXCA= 0.500000
       MAX DIFF DEL T PER TIME STEP  DTMPCC(PTSA      304)= 2.746582E-04 VS. DTMPCA=  10.0000
       MAX ARITH DEL T PER TIME STEP ATMPCC(PTSA     1346)=-0.269745     VS. ATMPCA=  100.000
       MIN STABILITY CRITERIA        CSGMIN(PTSA      431)= 3.037313E-05
       MAX STABILITY CRITERIA        CSGMAX(PTSA      424)=  1.96050
       NUMBER OF ITERATIONS          LOOPCT              =       1     VS. NLOOPT=     600
       PROBLEM TIME                  TIMEN               = 0.500000    VS. TIMEND= 0.500000
       MEAN PROBLEM TIME             TIMEM               = 0.500000
       AVERAGE TIME STEP USED        DTIMEU              = 1.666667E-02 VS. DTIMEI=      0.
                                  DIFFUSION NODES IN ASCENDING NODE NUMBER ORDER
  T    51=  941.30     T    53=  934.14     T    55=  883.50     T    60=  874.56     T    62=  976.45     T   100=  854.08
  T   105=  863.00     T   107=  869.23     T   110=  884.44     T   112=  889.48     T   113=  876.27     T   120=  1003.9
  T   122=  1042.1     T   123=  913.54     T   124=  1038.6     T   125=  908.08     T   126=  1031.8     T   127=  897.16
  T   130=  979.59     T   132=  1027.4     T   133=  867.61     T   134=  1024.9     T   135=  863.25     T   136=  1020.1
  T   137=  854.60     T   140=  928.11     T   141=  910.84     T   142=  963.57     T   143=  834.59     T   144=  961.04
  T   145=  830.68     T   146=  955.82     T   147=  823.09     T   150=  944.12     T   152=  998.91     T   153=  816.96
  T   154=  995.15     T   155=  813.53     T   156=  991.38     T   157=  805.03     T   160=  875.47     T   161=  863.56
  T   162=  925.92     T   163=  757.69     T   164=  921.37     T   165=  761.37     T   166=  918.08     T   167=  756.94
  T   170=  503.19     T   172=  512.41     T   173=  480.66     T   175=  408.35     T   177=  444.58     T   180=  429.19
  T   190=  278.54     T   191=  268.74     T   192=  134.50     T   193=  363.72     T   194=  163.62     T   196=  232.97
  T   198=  271.20     T   200=  1030.4     T   204=  1087.9     T   210=  1114.3     T   220=  1103.7     T   230=  1029.4
  T   240=  535.26     T   242=  253.99     T   250=  115.54     T   260=  95.381     T   261=  96.464     T   262=  94.806
  T   263=  97.065     T   264=  95.316     T   265=  98.153     T   266=  98.231     T   300=  1202.5     T   304=  1228.1
  T   305=  1375.8     T   310=  1136.4     T   313=  1226.7     T   315=  1331.1     T   316=  1331.1     T   320=  1126.2
  T   323=  1219.2     T   325=  1325.9     T   326=  1325.9     T   330=  1040.1     T   333=  1118.2     T   335=  1273.2
  T   336=  1273.2     T   340=  861.27     T   342=  534.47     T   343=  1036.7     T   344=  249.64     T   345=  912.83
  T   346=  1263.6     T   347=  464.82     T   349=  1052.0     T   350=  162.36     T   351=  375.24     T   352=  165.98
  T   353=  272.67     T   354=  207.31     T   355=  121.19     T   356=  217.09     T   360=  93.786     T   362=  92.457
  T   364=  92.985     T   366=  111.83     T   367=  116.57     T   368=  137.46     T   369=  154.79     T   371=  371.27
  T   373=  270.33     T   375=  164.60     T   377=  121.02     T   400=  92.709     T   401=  100.68     T   402=  114.96
  T   404=  1186.7     T   406=  1375.4     T   408=  1358.0     T   410=  1409.9     T   412=  1408.4     T   414=  1418.6
```

T	421=	393.61	T	422=	1413.7	T	423=	1416.6	T	424=	159.27	T	425=	1397.7	T	426=	1401.0
T	431=	1356.7	T	432=	1359.2	T	433=	1339.8	T	434=	1338.3	T	435=	1377.8	T	436=	1358.5
T	950=	1437.0	T	952=	1426.4	T	954=	1403.1											

ARITHMETIC NODES IN ASCENDING NODE NUMBER ORDER

T	50=	934.45	T	52=	932.38	T	54=	897.86	T	158=	884.33	T	159=	836.52	T	168=	867.86
T	169=	861.58	T	195=	136.27	T	197=	154.21	T	199=	250.25	T	238=	825.71	T	311=	1240.3
T	312=	1240.3	T	321=	1232.8	T	322=	1232.8	T	331=	1130.8	T	332=	1130.8	T	337=	772.92
T	341=	651.77	T	357=	244.43	T	358=	343.41	T	359=	164.91	T	379=	115.95	T	403=	119.10
T	1000=	146.60	T	1001=	239.82	T	1002=	235.32	T	1003=	154.66	T	1004=	126.22	T	1005=	125.33
T	1006=	97.962	T	1007=	338.80	T	1008=	296.84	T	1009=	277.34	T	1010=	183.10	T	1011=	1150.5
T	1012=	1150.5	T	1013=	1301.5	T	1021=	1140.5	T	1022=	1140.5	T	1023=	1295.9	T	1031=	1054.1
T	1032=	1054.1	T	1033=	1228.7	T	1041=	888.79	T	1042=	888.79	T	1043=	582.91	T	1044=	582.91
T	1346=	1108.0	T	1347=	363.05														

HEATER NODES IN ASCENDING NODE NUMBER ORDER

++NONE++

BOUNDARY NODES IN ASCENDING NODE NUMBER ORDER

T	1=	1475.0	T	2=	1424.7

SYSTEMS IMPROVED NUMERICAL DIFFERENCING ANALYZER '85 (SINDA '85) PAGE 2/4

MODEL = DAMAGE4
FWDBCK

HAC LOAD CASE NO. 4 CONDITIONS - Axial Distribution, -20F
***** Peak OCV Sidewall Temperature Time Point *****

5/2/94

SUBMODEL NAME = PTSB

		CALCULATED		ALLOWED	
MAX DIFF DELTA T PER ITER	DRLXCC(PTSB	404)= 2.441406E-04	VS. DRLXCA=	5.000000E-02	
MAX ARITH DELTA T PER ITER	ARLXCC(PTSB	1346)=-0.304932	VS. ARLXCA=	0.500000	
MAX DIFF DEL T PER TIME STEP	DTMPCC(PTSB	404)= 2.746582E-04	VS. DTMPCA=	10.0000	
MAX ARITH DEL T PER TIME STEP	ATMPCC(PTSB	1346)=-0.304901	VS. ATMPCA=	100.000	
MIN STABILITY CRITERIA	CSGMIN(PTSB	446)= 3.012037E-05			
MAX STABILITY CRITERIA	CSGMAX(PTSB	424)= 2.05956			
NUMBER OF ITERATIONS	LOOPCT	= 1	VS. NLOOPT=	600	
PROBLEM TIME	TIMEN	= 0.500000	VS. TIMEND=	0.500000	
MEAN PROBLEM TIME	TIMEM	= 0.500000			
AVERAGE TIME STEP USED	DTIMEU	= 1.666667E-02	VS. DTIMEI=	0.	

DIFFUSION NODES IN ASCENDING NODE NUMBER ORDER

T	51=	776.45	T	53=	746.34	T	55=	699.47	T	60=	829.89	T	62=	937.63	T	100=	953.49
T	105=	900.27	T	107=	878.67	T	110=	868.29	T	112=	873.69	T	113=	862.90	T	120=	833.36
T	122=	876.50	T	123=	803.91	T	124=	858.35	T	125=	809.24	T	126=	827.88	T	127=	817.95
T	130=	766.34	T	132=	821.88	T	133=	727.97	T	134=	795.28	T	135=	730.44	T	136=	749.31
T	137=	734.59	T	140=	727.16	T	141=	727.36	T	142=	778.77	T	143=	693.70	T	144=	752.02
T	145=	691.41	T	146=	702.78	T	147=	687.77	T	150=	695.93	T	152=	763.05	T	153=	651.32
T	154=	727.74	T	155=	648.23	T	156=	666.76	T	157=	644.59	T	160=	635.87	T	161=	641.46
T	162=	701.83	T	163=	594.26	T	164=	669.02	T	165=	592.19	T	166=	611.50	T	167=	588.00
T	170=	447.49	T	172=	459.77	T	173=	437.16	T	175=	372.09	T	177=	402.78	T	180=	370.01
T	190=	290.63	T	191=	283.15	T	192=	133.31	T	193=	369.86	T	194=	167.87	T	196=	246.20
T	198=	286.51	T	200=	1015.4	T	204=	1032.2	T	210=	693.37	T	220=	670.81	T	230=	590.50
T	240=	461.59	T	242=	243.56	T	250=	113.94	T	260=	95.240	T	261=	96.138	T	262=	93.883
T	263=	95.082	T	264=	94.829	T	265=	97.614	T	266=	97.344	T	300=	1199.1	T	304=	1208.4
T	305=	1371.2	T	310=	915.19	T	313=	1094.2	T	315=	1275.8	T	316=	1275.8	T	320=	898.89
T	323=	1082.9	T	325=	1268.2	T	326=	1268.2	T	330=	836.20	T	333=	1022.3	T	335=	1233.4
T	336=	1233.4	T	340=	792.25	T	342=	507.06	T	343=	1018.2	T	344=	239.60	T	345=	770.86
T	346=	1250.3	T	347=	389.68	T	349=	1045.5	T	350=	155.57	T	351=	367.09	T	352=	156.45
T	353=	266.79	T	354=	198.18	T	355=	114.68	T	356=	202.42	T	360=	93.713	T	362=	92.105
T	364=	92.270	T	366=	106.62	T	367=	107.69	T	368=	110.46	T	369=	118.80	T	371=	362.31
T	373=	264.17	T	375=	159.16	T	377=	112.19	T	400=	92.046	T	401=	100.10	T	402=	104.91
T	404=	890.54	T	406=	1366.2	T	408=	1379.9	T	410=	1413.0	T	412=	1408.5	T	414=	1418.6
T	421=	393.34	T	422=	1413.7	T	423=	1416.7	T	424=	140.73	T	425=	1397.8	T	426=	1404.7
T	431=	1225.1	T	432=	1351.1	T	433=	245.22	T	434=	213.32	T	435=	1405.6	T	436=	1404.7
T	441=	1379.3	T	442=	1372.8	T	443=	1372.7	T	444=	1372.6	T	445=	1394.7	T	446=	1380.3
T	451=	1374.3	T	452=	1366.4	T	453=	1376.7	T	454=	1381.6	T	455=	1412.4	T	456=	1394.6

ARITHMETIC NODES IN ASCENDING NODE NUMBER ORDER

T	50=	777.07	T	52=	746.84	T	54=	725.96	T	158=	652.58	T	159=	629.98	T	168=	642.35
T	169=	645.09	T	195=	124.98	T	197=	139.91	T	199=	262.79	T	238=	534.97	T	311=	1111.5

T	312=	1111.5	T	321=	1100.1	T	322=	1100.1	T	331=	1038.2	T	332=	1038.2
T	337=	745.37	T	341=	620.41	T	357=	233.12	T	358=	333.76	T	359=	156.76
T	379=	109.04	T	403=	109.90	T	1000=	123.64	T	1001=	252.07	T	1002=	246.57
T	1003=	156.13	T	1004=	125.11	T	1005=	124.22	T	1006=	96.938	T	1007=	328.19
T	1008=	301.69	T	1009=	288.82	T	1010=	198.07	T	1011=	937.96	T	1012=	937.96
T	1013=	1222.8	T	1021=	921.90	T	1022=	921.90	T	1023=	1214.5	T	1031=	858.97
T	1032=	858.97	T	1033=	1171.9	T	1041=	817.88	T	1042=	817.88	T	1043=	549.40
T	1044=	549.40	T	1346=	1027.9	T	1347=	295.09						

HEATER NODES IN ASCENDING NODE NUMBER ORDER

++NONE++

BOUNDARY NODES IN ASCENDING NODE NUMBER ORDER

T	1=	1475.0	T	2=	1424.7

SYSTEMS IMPROVED NUMERICAL DIFFERENCING ANALYZER '85 (SINDA '85) PAGE 3/4

MODEL = DAMAGE4 HAC LOAD CASE NO. 4 CONDITIONS - Axial Distribution, -20F 5/2/94
FWDBCK ***** Peak OCV Sidewall Temperature Time Point *****

SUBMODEL NAME = PTSC

		CALCULATED			ALLOWED
MAX DIFF DELTA T PER ITER	DRLXCC(PTSC	127)= 2.441406E-04	VS.	DRLXCA=	5.000000E-02
MAX ARITH DELTA T PER ITER	ARLXCC(PTSC	1346)=-0.303467	VS.	ARLXCA=	0.500000
MAX DIFF DEL T PER TIME STEP	DTMPCC(PTSC	127)= 2.746582E-04	VS.	DTMPCA=	10.0000
MAX ARITH DEL T PER TIME STEP	ATMPCC(PTSC	1346)=-0.303436	VS.	ATMPCA=	100.000
MIN STABILITY CRITERIA	CSGMIN(PTSC	446)= 3.012212E-05			
MAX STABILITY CRITERIA	CSGMAX(PTSC	424)= 2.05948			
NUMBER OF ITERATIONS	LOOPCT	= 1	VS.	NLOOPT=	600
PROBLEM TIME	TIMEN	= 0.500000	VS.	TIMEND=	0.500000
MEAN PROBLEM TIME	TIMEN	= 0.500000			
AVERAGE TIME STEP USED	DTIMEU	= 1.666667E-02	VS.	DTIMEI=	0.

DIFFUSION NODES IN ASCENDING NODE NUMBER ORDER

T	51=	693.75	T	53=	643.26	T	55=	599.06	T	60=	808.82	T	62=	919.21	T	100=	936.60
T	105=	875.05	T	107=	850.79	T	110=	836.81	T	112=	838.41	T	113=	836.37	T	120=	766.23
T	122=	770.16	T	123=	762.67	T	124=	773.58	T	125=	768.23	T	126=	780.36	T	127=	778.96
T	130=	675.77	T	132=	682.14	T	133=	671.66	T	134=	681.06	T	135=	673.49	T	136=	680.06
T	137=	678.02	T	140=	623.14	T	141=	622.52	T	142=	630.84	T	143=	620.71	T	144=	626.86
T	145=	619.61	T	146=	621.94	T	147=	620.55	T	150=	586.73	T	152=	596.45	T	153=	583.59
T	154=	589.52	T	155=	579.34	T	156=	580.34	T	157=	576.45	T	160=	528.40	T	161=	536.85
T	162=	538.59	T	163=	526.44	T	164=	533.68	T	165=	523.83	T	166=	527.39	T	167=	524.25
T	170=	402.54	T	172=	404.14	T	173=	401.03	T	175=	355.21	T	177=	371.85	T	180=	360.94
T	190=	313.68	T	191=	303.26	T	192=	134.25	T	193=	392.15	T	194=	169.77	T	196=	304.47
T	198=	307.38	T	200=	1003.4	T	204=	1015.7	T	210=	642.68	T	220=	614.62	T	230=	537.03
T	240=	454.48	T	242=	242.10	T	250=	113.75	T	260=	95.195	T	261=	96.098	T	262=	93.793
T	263=	94.980	T	264=	94.758	T	265=	97.536	T	266=	97.271	T	300=	1195.4	T	304=	1202.8
T	305=	1370.2	T	310=	892.64	T	313=	1081.8	T	315=	1271.0	T	316=	1271.0	T	320=	874.62
T	323=	1069.7	T	325=	1262.9	T	326=	1262.9	T	330=	816.24	T	333=	1013.8	T	335=	1230.1
T	336=	1230.1	T	340=	785.47	T	342=	504.35	T	343=	1017.6	T	344=	238.82	T	345=	769.05
T	346=	1249.2	T	347=	389.04	T	349=	1045.2	T	350=	155.34	T	351=	366.86	T	352=	156.21
T	353=	266.65	T	354=	197.85	T	355=	114.54	T	356=	202.12	T	360=	93.678	T	362=	92.057
T	364=	92.228	T	366=	106.48	T	367=	107.51	T	368=	110.07	T	369=	118.27	T	371=	362.05
T	373=	264.03	T	375=	159.11	T	377=	112.15	T	400=	92.037	T	401=	100.10	T	402=	104.86
T	404=	890.43	T	406=	1365.7	T	408=	1379.9	T	410=	1413.0	T	412=	1408.5	T	414=	1418.6
T	421=	393.35	T	422=	1413.7	T	423=	1416.7	T	424=	140.73	T	425=	1397.8	T	426=	1404.7
T	431=	1224.8	T	432=	1350.6	T	433=	245.21	T	434=	213.32	T	435=	1405.6	T	436=	1404.7
T	441=	1379.3	T	442=	1372.5	T	443=	1372.6	T	444=	1372.6	T	445=	1394.7	T	446=	1380.3
T	451=	1374.0	T	452=	1365.9	T	453=	1376.6	T	454=	1381.6	T	455=	1412.4	T	456=	1394.6

ARITHMETIC NODES IN ASCENDING NODE NUMBER ORDER

T	50=	697.11	T	52=	645.36	T	54=	632.37	T	158=	538.80	T	159=	535.90	T	168=	537.18
T	169=	538.06	T	195=	129.97	T	197=	140.26	T	199=	275.80	T	238=	501.23	T	311=	1099.1

T	312=	1099.1	T	321=	1086.8	T	322=	1086.8	T	331=	1029.7	T	332=	1029.7	T	337=	742.72
T	341=	617.34	T	357=	232.82	T	358=	333.48	T	359=	156.53	T	379=	108.88	T	403=	109.86
T	1000=	125.15	T	1001=	279.33	T	1002=	258.40	T	1003=	162.32	T	1004=	125.83	T	1005=	124.92
T	1006=	96.906	T	1007=	331.59	T	1008=	317.38	T	1009=	307.57	T	1010=	199.10	T	1011=	916.21
T	1012=	916.21	T	1013=	1215.6	T	1021=	898.47	T	1022=	898.47	T	1023=	1206.8	T	1031=	839.79
T	1032=	839.79	T	1033=	1166.9	T	1041=	811.00	T	1042=	811.00	T	1043=	546.20	T	1044=	546.20
T	1346=	1026.6	T	1347=	294.53												

HEATER NODES IN ASCENDING NODE NUMBER ORDER
++NONE++
BOUNDARY NODES IN ASCENDING NODE NUMBER ORDER

T	1=	1475.0	T	2=	1424.7

SYSTEMS IMPROVED NUMERICAL DIFFERENCING ANALYZER '85 (SINDA '85) PAGE 4/4

MODEL = DAMAGE4 HAC LOAD CASE NO. 4 CONDITIONS - Axial Distribution, -20F 5/2/94
FWDBCK ***** Peak OCV Sidewall Temperature Time Point *****

SUBMODEL NAME = PTSD

	CALCULATED		ALLOWED
MAX DIFF DELTA T PER ITER	DRLXCC(PTSD	107)= 2.441406E-04	VS. DRLXCA= 5.000000E-02
MAX ARITH DELTA T PER ITER	ARLXCC(PTSD	1346)=-0.303467	VS. ARLXCA= 0.500000
MAX DIFF DEL T PER TIME STEP	DTMPCC(PTSD	107)= 2.746582E-04	VS. DTMPCA= 10.0000
MAX ARITH DEL T PER TIME STEP	ATMPCC(PTSD	1346)=-0.303436	VS. ATMPCA= 100.000
MIN STABILITY CRITERIA	CSGMIN(PTSD	446)= 3.012212E-05	
MAX STABILITY CRITERIA	CSGMAX(PTSD	424)= 2.05948	
NUMBER OF ITERATIONS	LOOPCT	= 1	VS. NLOOPT= 600
PROBLEM TIME	TIMEN	= 0.500000	VS. TIMEND= 0.500000
MEAN PROBLEM TIME	TIMEM	= 0.500000	
AVERAGE TIME STEP USED	DTIMEU	= 1.666667E-02	VS. DTIMEI= 0.

DIFFUSION NODES IN ASCENDING NODE NUMBER ORDER

T 51= 684.33	T 53= 629.96	T 55= 586.11	T 60= 806.58	T 62= 916.99	T 100= 935.62
T 105= 872.78	T 107= 848.05	T 110= 833.59	T 112= 834.06	T 113= 833.51	T 120= 758.98
T 122= 759.03	T 123= 757.22	T 124= 765.10	T 125= 763.64	T 126= 776.69	T 127= 776.12
T 130= 664.47	T 132= 665.58	T 133= 663.02	T 134= 668.00	T 135= 666.03	T 136= 673.47
T 137= 672.86	T 140= 608.19	T 141= 607.42	T 142= 610.82	T 143= 608.26	T 144= 610.47
T 145= 608.85	T 146= 613.01	T 147= 613.28	T 150= 571.99	T 152= 575.58	T 153= 572.26
T 154= 572.59	T 155= 569.44	T 156= 570.96	T 157= 569.53	T 160= 513.51	T 161= 522.62
T 162= 517.93	T 163= 514.80	T 164= 516.72	T 165= 513.92	T 166= 517.71	T 167= 516.87
T 170= 394.79	T 172= 394.91	T 173= 394.00	T 175= 350.47	T 177= 365.71	T 180= 357.43
T 190= 311.49	T 191= 302.35	T 192= 134.25	T 193= 389.49	T 194= 169.48	T 196= 309.00
T 198= 306.52	T 200= 1002.5	T 204= 1014.8	T 210= 641.03	T 220= 612.71	T 230= 537.62
T 240= 454.20	T 242= 242.06	T 250= 113.74	T 260= 95.191	T 261= 96.094	T 262= 93.789
T 263= 94.975	T 264= 94.755	T 265= 97.529	T 266= 97.270	T 300= 1195.1	T 304= 1202.4
T 305= 1370.1	T 310= 892.03	T 313= 1081.5	T 315= 1270.9	T 316= 1270.9	T 320= 873.97
T 323= 1069.3	T 325= 1262.8	T 326= 1262.8	T 330= 816.37	T 333= 1013.9	T 335= 1230.1
T 336= 1230.1	T 340= 785.44	T 342= 504.35	T 343= 1017.6	T 344= 238.83	T 345= 769.05
T 346= 1249.2	T 347= 389.05	T 349= 1045.2	T 350= 155.35	T 351= 366.87	T 352= 156.22
T 353= 266.65	T 354= 197.85	T 355= 114.54	T 356= 202.12	T 360= 93.676	T 362= 92.056
T 364= 92.228	T 366= 106.48	T 367= 107.51	T 368= 110.07	T 369= 118.27	T 371= 362.05
T 373= 264.04	T 375= 159.11	T 377= 112.15	T 400= 92.037	T 401= 100.10	T 402= 104.86
T 404= 890.43	T 406= 1365.6	T 408= 1379.9	T 410= 1413.0	T 412= 1408.5	T 414= 1418.6
T 421= 393.35	T 422= 1413.7	T 423= 1416.7	T 424= 140.73	T 425= 1397.8	T 426= 1404.7
T 431= 1224.8	T 432= 1350.6	T 433= 245.21	T 434= 213.32	T 435= 1405.6	T 436= 1404.7
T 441= 1379.3	T 442= 1372.5	T 443= 1372.6	T 444= 1372.6	T 445= 1394.7	T 446= 1380.3
T 451= 1374.0	T 452= 1365.9	T 453= 1376.6	T 454= 1381.6	T 455= 1412.4	T 456= 1394.6

ARITHMETIC NODES IN ASCENDING NODE NUMBER ORDER

T 50= 687.83	T 52= 632.32	T 54= 620.32	T 158= 523.78	T 159= 522.94	T 168= 522.84
T 169= 523.44	T 195= 130.25	T 197= 139.96	T 199= 274.67	T 238= 501.45	T 311= 1098.7

T	312=	1098.7	T	321=	1086.4	T	322=	1086.4	T	331=	1029.8	T	332=	1029.8	T	337=	742.72
T	341=	617.34	T	357=	232.82	T	358=	333.48	T	359=	156.53	T	379=	108.88	T	403=	109.86
T	1000=	125.10	T	1001=	279.97	T	1002=	257.50	T	1003=	162.45	T	1004=	125.83	T	1005=	124.92
T	1006=	96.901	T	1007=	328.43	T	1008=	315.15	T	1009=	306.26	T	1010=	198.90	T	1011=	915.63
T	1012=	915.63	T	1013=	1215.5	T	1021=	897.84	T	1022=	897.84	T	1023=	1206.6	T	1031=	839.91
T	1032=	839.91	T	1033=	1167.0	T	1041=	810.98	T	1042=	810.98	T	1043=	546.21	T	1044=	546.21
T	1346=	1026.6	T	1347=	294.53												

HEATER NODES IN ASCENDING NODE NUMBER ORDER

++NONE++

BOUNDARY NODES IN ASCENDING NODE NUMBER ORDER

T	1=	1475.0	T	2=	1424.7

SYSTEMS IMPROVED NUMERICAL DIFFERENCING ANALYZER '85 (SINDA '85) PAGE 1/4

MODEL = DAMAGE4
FWDBCK

HAC LOAD CASE NO. 4 CONDITIONS - Axial Distribution, -20F 5/2/94
***** Peak ICV Sidewall Temperature Time Point *****

SUBMODEL NAME = MAIN

MEAN PROBLEM TIME TIMEM = 0.833234

DIFFUSION NODES IN ASCENDING NODE NUMBER ORDER

T 267= 112.43 T 268= 112.43 T 269= 110.13

ARITHMETIC NODES IN ASCENDING NODE NUMBER ORDER

T 201= 671.87 T 1266= 121.74 T 1267= 220.61 T 1268= 177.07 T 1269= 131.97

HEATER NODES IN ASCENDING NODE NUMBER ORDER

++NONE++

BOUNDARY NODES IN ASCENDING NODE NUMBER ORDER

++NONE++

MEAN ICV GAS TEMP= 671.9 F MEAN ICV GAS PRESSURE= 33.97 PSIA
MEAN ICV-OCV GAS TEMP= 696.0 F MEAN ICV-OCV GAS PRESSURE= 40.77 PSIA

SUBMODEL NAME = PTSA

	CALCULATED		ALLOWED
MAX DIFF DELTA T PER ITER	DRLXCC(PTSA	123)=-3.784180E-03 VS. DRLXCA=	5.000000E-02
MAX ARITH DELTA T PER ITER	ARLXCC(PTSA	337)=-3.088379E-02 VS. ARLXCA=	0.500000
MAX DIFF DEL T PER TIME STEP	DTMPCC(PTSA	425)=-0.205658 VS. DTMPCA=	10.0000
MAX ARITH DEL T PER TIME STEP	ATMPCC(PTSA	1346)=-0.162201 VS. ATMPCA=	100.000
MIN STABILITY CRITERIA	CSGMIN(PTSA	431)= 2.645104E-04	
MAX STABILITY CRITERIA	CSGMAX(PTSA	424)= 2.22072	
NUMBER OF ITERATIONS	LOOPCT	= 2 VS. NLOOPT=	600
PROBLEM TIME	TIMEN	= 0.833333 VS. TIMEND=	12.0000
MEAN PROBLEM TIME	TIMEM	= 0.833234	
AVERAGE TIME STEP USED	DTIMEU	= 2.487562E-04 VS. DTIMEI=	0.

DIFFUSION NODES IN ASCENDING NODE NUMBER ORDER

T	51=	986.83	T	53=	962.85	T	55=	903.87	T	60=	894.78	T	62=	904.78	T	100=	925.41
T	105=	924.43	T	107=	923.25	T	110=	927.36	T	112=	938.69	T	113=	893.35	T	120=	1037.2
T	122=	1081.4	T	123=	934.98	T	124=	1081.9	T	125=	936.19	T	126=	1082.9	T	127=	938.55
T	130=	1034.4	T	132=	1081.2	T	133=	923.47	T	134=	1081.2	T	135=	923.95	T	136=	1081.1
T	137=	924.84	T	140=	1005.4	T	141=	990.41	T	142=	1038.7	T	143=	914.16	T	144=	1038.4
T	145=	914.23	T	146=	1037.8	T	147=	914.31	T	150=	1019.1	T	152=	1069.8	T	153=	898.32
T	154=	1067.7	T	155=	898.49	T	156=	1066.7	T	157=	897.93	T	160=	952.84	T	161=	943.44
T	162=	998.69	T	163=	842.20	T	164=	995.49	T	165=	848.65	T	166=	994.08	T	167=	847.84
T	170=	592.61	T	172=	599.52	T	173=	578.08	T	175=	493.89	T	177=	532.61	T	180=	507.72
T	190=	355.04	T	191=	373.04	T	192=	150.48	T	193=	579.95	T	194=	233.94	T	196=	321.22
T	198=	375.48	T	200=	848.11	T	204=	856.17	T	210=	1151.4	T	220=	1144.4	T	230=	1073.8
T	240=	663.18	T	242=	359.14	T	250=	159.28	T	260=	97.288	T	261=	99.195	T	262=	101.59
T	263=	106.04	T	264=	112.53	T	265=	117.22	T	266=	125.73	T	300=	751.94	T	304=	748.14
T	305=	451.68	T	310=	1017.9	T	313=	885.86	T	315=	719.18	T	316=	719.18	T	320=	1013.0
T	323=	883.27	T	325=	720.65	T	326=	720.65	T	330=	920.95	T	333=	759.74	T	335=	639.32
T	336=	639.32	T	340=	718.31	T	342=	479.19	T	343=	495.08	T	344=	292.16	T	345=	655.92
T	346=	578.48	T	347=	446.38	T	349=	376.00	T	350=	212.31	T	351=	244.61	T	352=	214.88
T	353=	222.64	T	354=	242.50	T	355=	165.20	T	356=	246.06	T	360=	95.574	T	362=	97.738
T	364=	112.10	T	366=	159.74	T	367=	166.29	T	368=	182.32	T	369=	207.77	T	371=	251.85
T	373=	231.27	T	375=	186.67	T	377=	159.92	T	400=	103.28	T	401=	117.53	T	402=	156.31
T	404=	676.40	T	406=	568.76	T	408=	573.92	T	410=	547.42	T	412=	599.32	T	414=	532.99

T 421= 404.66 T 422= 565.57 T 423= 553.33 T 424= 219.61 T 425= 706.97 T 426= 635.71

T 431= 579.50 T 432= 679.77 T 433= 748.02 T 434= 745.86 T 435= 672.22 T 436= 575.74

T 950= 1482.4 T 952= 1470.7 T 954= 1434.7

ARITHMETIC NODES IN ASCENDING NODE NUMBER ORDER

T 50= 975.59 T 52= 960.96 T 54= 911.51 T 158= 962.42 T 159= 918.39 T 168= 947.21

T 169= 941.07 T 195= 168.23 T 197= 204.31 T 199= 367.98 T 238= 902.29 T 311= 870.32

T 312= 870.32 T 321= 868.39 T 322= 868.39 T 331= 744.34 T 332= 744.34 T 337= 530.92

T 341= 519.57 T 357= 246.15 T 358= 252.56 T 359= 213.66 T 379= 163.55 T 403= 158.76

T 1000= 189.40 T 1001= 326.70 T 1002= 340.89 T 1003= 184.83 T 1004= 139.91 T 1005= 138.76

T 1006= 103.67 T 1007= 423.81 T 1008= 382.55 T 1009= 375.95 T 1010= 253.59 T 1011= 1005.7

T 1012= 1005.7 T 1013= 775.18 T 1021= 1001.1 T 1022= 1001.1 T 1023= 774.90 T 1031= 910.05

T 1032= 910.05 T 1033= 679.53 T 1041= 717.73 T 1042= 717.73 T 1043= 487.93 T 1044= 487.93

T 1346= 601.83 T 1347= 352.43

HEATER NODES IN ASCENDING NODE NUMBER ORDER

++NONE++

BOUNDARY NODES IN ASCENDING NODE NUMBER ORDER

T 1= -20.000 T 2= -20.000

SYSTEMS IMPROVED NUMERICAL DIFFERENCING ANALYZER '85 (SINDA '85) PAGE 2/4

MODEL = DAMAGE4 HAC LOAD CASE NO. 4 CONDITIONS - Axial Distribution, -20F 5/2/94
FWDBCK ***** Peak ICV Sidewall Temperature Time Point *****

SUBMODEL NAME = PTSB

	CALCULATED		ALLOWED
MAX DIFF DELTA T PER ITER	DRLXCC(PTSB	110)=-2.685547E-03	VS. DRLXCA= 5.000000E-02
MAX ARITH DELTA T PER ITER	ARLXCC(PTSB	337)=-3.826904E-02	VS. ARLXCA= 0.500000
MAX DIFF DEL T PER TIME STEP	DTMPCC(PTSB	435)=-0.207489	VS. DTMPCA= 10.0000
MAX ARITH DEL T PER TIME STEP	ATMPCC(PTSB	1346)=-0.139435	VS. ATMPCA= 100.000
MIN STABILITY CRITERIA	CSGMIN(PTSB	455)= 3.487125E-04	
MAX STABILITY CRITERIA	CSGMAX(PTSB	424)= 2.28145	
NUMBER OF ITERATIONS	LOOPCT	= 2	VS. NLOOPT= 600
PROBLEM TIME	TIMEN	= 0.833333	VS. TIMEND= 12.0000
MEAN PROBLEM TIME	TIMEM	= 0.833234	
AVERAGE TIME STEP USED	DTIMEU	= 2.487562E-04	VS. DTIMEI= 0.

DIFFUSION NODES IN ASCENDING NODE NUMBER ORDER

T	51=	838.70	T	53=	789.37	T	55=	729.34	T	60=	842.04	T	62=	844.16	T	100=	837.57
T	105=	837.82	T	107=	838.45	T	110=	836.61	T	112=	854.03	T	113=	827.06	T	120=	841.63
T	122=	891.79	T	123=	808.92	T	124=	864.76	T	125=	808.97	T	126=	817.65	T	127=	806.67
T	130=	823.81	T	132=	877.61	T	133=	786.01	T	134=	850.72	T	135=	789.15	T	136=	804.57
T	137=	792.35	T	140=	812.18	T	141=	812.75	T	142=	859.93	T	143=	780.15	T	144=	834.95
T	145=	779.80	T	146=	788.35	T	147=	776.18	T	150=	786.37	T	152=	847.02	T	153=	745.23
T	154=	815.34	T	155=	746.22	T	156=	761.76	T	157=	746.27	T	160=	731.73	T	161=	736.91
T	162=	789.85	T	163=	694.21	T	164=	761.53	T	165=	697.29	T	166=	713.16	T	167=	696.85
T	170=	561.32	T	172=	568.08	T	173=	555.07	T	175=	480.43	T	177=	515.66	T	180=	464.58
T	190=	394.50	T	191=	401.67	T	192=	144.93	T	193=	558.73	T	194=	236.68	T	196=	346.64
T	198=	404.58	T	200=	836.93	T	204=	808.13	T	210=	795.86	T	220=	774.98	T	230=	717.74
T	240=	573.96	T	242=	342.37	T	250=	153.61	T	260=	96.781	T	261=	98.196	T	262=	98.814
T	263=	100.89	T	264=	110.14	T	265=	114.86	T	266=	121.50	T	300=	744.15	T	304=	712.38
T	305=	432.76	T	310=	745.38	T	313=	664.72	T	315=	553.66	T	316=	553.66	T	320=	728.72
T	323=	652.42	T	325=	546.96	T	326=	546.96	T	330=	674.35	T	333=	595.09	T	335=	517.68
T	336=	517.68	T	340=	604.26	T	342=	431.74	T	343=	477.21	T	344=	270.15	T	345=	598.06
T	346=	548.37	T	347=	400.91	T	349=	358.86	T	350=	195.45	T	351=	226.82	T	352=	196.10
T	353=	206.12	T	354=	223.96	T	355=	149.46	T	356=	225.23	T	360=	95.341	T	362=	96.449
T	364=	108.50	T	366=	145.49	T	367=	148.85	T	368=	155.21	T	369=	171.49	T	371=	233.56
T	373=	214.97	T	375=	172.49	T	377=	145.14	T	400=	101.85	T	401=	116.39	T	402=	141.19
T	404=	654.28	T	406=	554.32	T	408=	507.38	T	410=	555.76	T	412=	600.08	T	414=	533.04
T	421=	404.09	T	422=	565.63	T	423=	553.46	T	424=	189.98	T	425=	707.20	T	426=	639.40
T	431=	604.55	T	432=	672.12	T	433=	361.86	T	434=	303.08	T	435=	669.69	T	436=	587.85
T	441=	512.46	T	442=	592.78	T	443=	616.47	T	444=	615.73	T	445=	593.77	T	446=	512.76
T	451=	530.49	T	452=	553.09	T	453=	551.26	T	454=	551.39	T	455=	554.53	T	456=	533.11

ARITHMETIC NODES IN ASCENDING NODE NUMBER ORDER

T	50=	832.46	T	52=	789.41	T	54=	747.04	T	158=	746.90	T	159=	727.86	T	168=	737.70
T	169=	740.02	T	195=	146.48	T	197=	180.17	T	199=	380.94	T	238=	655.85	T	311=	651.91

T	312=	651.91	T	321=	640.09	T	322=	640.09	T	331=	582.25	T	332=	582.25	T	337=	479.95
T	341=	464.56	T	357=	226.70	T	358=	233.83	T	359=	195.85	T	379=	147.74	T	403=	143.87
T	1000=	147.19	T	1001=	349.77	T	1002=	354.37	T	1003=	185.15	T	1004=	134.97	T	1005=	133.89
T	1006=	100.84	T	1007=	436.20	T	1008=	410.29	T	1009=	404.30	T	1010=	275.93	T	1011=	740.06
T	1012=	740.06	T	1013=	591.62	T	1021=	723.80	T	1022=	723.80	T	1023=	582.86	T	1031=	670.16
T	1032=	670.16	T	1033=	543.51	T	1041=	602.72	T	1042=	602.72	T	1043=	435.70	T	1044=	435.70
T	1346=	555.73	T	1347=	311.92												

HEATER NODES IN ASCENDING NODE NUMBER ORDER

++NONE++

BOUNDARY NODES IN ASCENDING NODE NUMBER ORDER

T	1=	-20.000	T	2= -20.000

SYSTEMS IMPROVED NUMERICAL DIFFERENCING ANALYZER '85 (SINDA '85) PAGE 3/4

MODEL = DAMAGE4 HAC LOAD CASE NO. 4 CONDITIONS - Axial Distribution, -20F 5/2/94
FWDBCK ***** Peak ICV Sidewall Temperature Time Point *****

SUBMODEL NAME = PTSC

	CALCULATED		ALLOWED
MAX DIFF DELTA T PER ITER	DRLXCC(PTSC	110)=-3.173828E-03	VS. DRLXCA= 5.000000E-02
MAX ARITH DELTA T PER ITER	ARLXCC(PTSC	337)=-4.132080E-02	VS. ARLXCA= 0.500000
MAX DIFF DEL T PER TIME STEP	DTMPCC(PTSC	435)=-0.207489	VS. DTMPCA= 10.0000
MAX ARITH DEL T PER TIME STEP	ATMPCC(PTSC	1346)=-0.140045	VS. ATMPCA= 100.000
MIN STABILITY CRITERIA	CSGMIN(PTSC	455)= 3.487503E-04	
MAX STABILITY CRITERIA	CSGMAX(PTSC	424)= 2.28137	
NUMBER OF ITERATIONS	LOOPCT	= 2	VS. NLOOPT= 600
PROBLEM TIME	TIMEN	= 0.833333	VS. TIMEND= 12.0000
MEAN PROBLEM TIME	TIMEM	= 0.833234	
AVERAGE TIME STEP USED	DTIMEU	= 2.487562E-04	VS. DTIMEI= 0.

DIFFUSION NODES IN ASCENDING NODE NUMBER ORDER

T	51=	761.20	T	53=	688.81	T	55=	631.03	T	60=	812.80	T	62=	816.46	T	100=	811.36
T	105=	799.66	T	107=	795.30	T	110=	787.77	T	112=	790.03	T	113=	787.34	T	120=	763.60
T	122=	769.32	T	123=	760.94	T	124=	765.29	T	125=	759.55	T	126=	756.74	T	127=	755.58
T	130=	732.69	T	132=	738.67	T	133=	728.42	T	134=	736.01	T	135=	728.90	T	136=	730.35
T	137=	728.73	T	140=	714.00	T	141=	714.46	T	142=	720.08	T	143=	710.76	T	144=	716.17
T	145=	709.49	T	146=	707.98	T	147=	706.32	T	150=	685.16	T	152=	692.90	T	153=	681.46
T	154=	687.70	T	155=	679.35	T	156=	679.21	T	157=	676.76	T	160=	636.97	T	161=	644.68
T	162=	644.10	T	163=	633.89	T	164=	641.73	T	165=	634.73	T	166=	638.03	T	167=	636.21
T	170=	545.70	T	172=	545.94	T	173=	544.48	T	175=	504.79	T	177=	520.92	T	180=	499.22
T	190=	475.52	T	191=	461.89	T	192=	150.66	T	193=	554.45	T	194=	244.74	T	196=	450.97
T	198=	464.41	T	200=	820.14	T	204=	785.59	T	210=	737.40	T	220=	708.04	T	230=	650.11
T	240=	557.50	T	242=	337.71	T	250=	152.54	T	260=	96.640	T	261=	98.137	T	262=	98.553
T	263=	100.69	T	264=	109.73	T	265=	114.46	T	266=	120.95	T	300=	734.06	T	304=	698.99
T	305=	427.60	T	310=	698.74	T	313=	628.49	T	315=	527.09	T	316=	527.09	T	320=	676.85
T	323=	612.29	T	325=	517.50	T	326=	517.50	T	330=	630.16	T	333=	567.61	T	335=	498.12
T	336=	498.12	T	340=	583.91	T	342=	423.31	T	343=	475.10	T	344=	267.25	T	345=	595.29
T	346=	544.49	T	347=	399.20	T	349=	357.12	T	350=	194.21	T	351=	225.65	T	352=	194.90
T	353=	205.18	T	354=	222.42	T	355=	148.59	T	356=	223.87	T	360=	95.219	T	362=	96.252
T	364=	108.15	T	366=	144.64	T	367=	147.90	T	368=	153.86	T	369=	169.70	T	371=	232.32
T	373=	214.10	T	375=	171.99	T	377=	144.68	T	400=	101.78	T	401=	116.34	T	402=	140.70
T	404=	653.79	T	406=	552.22	T	408=	507.24	T	410=	555.74	T	412=	600.06	T	414=	533.02
T	421=	404.09	T	422=	565.62	T	423=	553.45	T	424=	189.97	T	425=	707.19	T	426=	639.39
T	431=	603.56	T	432=	671.00	T	433=	361.79	T	434=	303.08	T	435=	669.67	T	436=	587.81
T	441=	512.23	T	442=	592.02	T	443=	616.37	T	444=	615.64	T	445=	593.70	T	446=	512.63
T	451=	529.57	T	452=	551.15	T	453=	550.88	T	454=	551.25	T	455=	554.50	T	456=	533.02

ARITHMETIC NODES IN ASCENDING NODE NUMBER ORDER

T	50=	756.21	T	52=	690.43	T	54=	654.63	T	158=	646.18	T	159=	644.07	T	168=	644.82
T	169=	645.27	T	195=	158.54	T	197=	182.80	T	199=	398.40	T	238=	609.97	T	311=	615.44

```
T  312= 615.44    T  321= 599.60    T  322= 599.60    T  331= 554.55    T  332= 554.55    T  337= 471.30
T  341= 454.94    T  357= 225.28    T  358= 232.48    T  359= 194.63    T  379= 146.84    T  403= 143.40
T 1000= 152.58    T 1001= 413.01    T 1002= 376.56    T 1003= 202.89    T 1004= 139.44    T 1005= 138.22
T 1006= 100.91    T 1007= 486.67    T 1008= 476.17    T 1009= 466.25    T 1010= 278.53    T 1011= 694.33
T 1012= 694.33    T 1013= 561.68    T 1021= 672.89    T 1022= 672.89    T 1023= 549.67    T 1031= 626.91
T 1032= 626.91    T 1033= 521.13    T 1041= 582.31    T 1042= 582.31    T 1043= 426.65    T 1044= 426.65
T 1346= 552.86    T 1347= 310.25
                        HEATER NODES IN ASCENDING NODE NUMBER ORDER
                                                ++NONE++
                        BOUNDARY NODES IN ASCENDING NODE NUMBER ORDER
T    1= -20.000   T    2= -20.000
```

SYSTEMS IMPROVED NUMERICAL DIFFERENCING ANALYZER '85 (SINDA '85) PAGE 4/4

MODEL = DAMAGE4
FWDBCK

HAC LOAD CASE NO. 4 CONDITIONS - Axial Distribution, -20F
***** Peak ICV Sidewall Temperature Time Point *****

5/2/94

SUBMODEL NAME = PTSD

	CALCULATED		ALLOWED
MAX DIFF DELTA T PER ITER	DRLXCC(PTSD	110)=-3.173828E-03 VS.	DRLXCA= 5.000000E-02
MAX ARITH DELTA T PER ITER	ARLXCC(PTSD	337)=-4.150391E-02 VS.	ARLXCA= 0.500000
MAX DIFF DEL T PER TIME STEP	DTMPCC(PTSD	435)=-0.207489 VS.	DTMPCA= 10.0000
MAX ARITH DEL T PER TIME STEP	ATMPCC(PTSD	1346)=-0.140167 VS.	ATMPCA= 100.000
MIN STABILITY CRITERIA	CSGMIN(PTSD	455)= 3.487192E-04	
MAX STABILITY CRITERIA	CSGMAX(PTSD	424)= 2.28137	
NUMBER OF ITERATIONS	LOOPCT	= 2 VS.	NLOOPT= 600
PROBLEM TIME	TIMEN	= 0.833333 VS.	TIMEND= 12.0000
MEAN PROBLEM TIME	TIMEM	= 0.833234	
AVERAGE TIME STEP USED	DTIMEU	= 2.487562E-04 VS.	DTIMEI= 0.

DIFFUSION NODES IN ASCENDING NODE NUMBER ORDER

T	51=	752.40	T	53=	675.68	T	55=	618.17	T	60=	809.71	T	62=	812.51	T	100=	809.17
T	105=	796.22	T	107=	791.31	T	110=	783.20	T	112=	783.74	T	113=	783.33	T	120=	755.27
T	122=	756.33	T	123=	754.86	T	124=	755.34	T	125=	754.35	T	126=	752.11	T	127=	751.99
T	130=	721.90	T	132=	722.31	T	133=	720.32	T	134=	723.31	T	135=	721.92	T	136=	724.09
T	137=	723.76	T	140=	701.18	T	141=	701.56	T	142=	702.16	T	143=	700.17	T	144=	701.82
T	145=	700.40	T	146=	700.51	T	147=	700.16	T	150=	672.67	T	152=	674.38	T	153=	671.99
T	154=	673.08	T	155=	671.17	T	156=	671.64	T	157=	671.04	T	160=	625.08	T	161=	633.37
T	162=	626.85	T	163=	624.70	T	164=	628.00	T	165=	627.05	T	166=	630.86	T	167=	630.72
T	170=	541.06	T	172=	540.75	T	173=	540.24	T	175=	502.52	T	177=	517.49	T	180=	499.09
T	190=	473.19	T	191=	461.24	T	192=	150.85	T	193=	552.08	T	194=	244.29	T	196=	465.52
T	198=	463.83	T	200=	818.88	T	204=	784.38	T	210=	736.25	T	220=	705.59	T	230=	649.10
T	240=	556.80	T	242=	337.53	T	250=	152.51	T	260=	96.632	T	261=	98.132	T	262=	98.542
T	263=	100.68	T	264=	109.72	T	265=	114.43	T	266=	120.94	T	300=	733.23	T	304=	698.32
T	305=	427.35	T	310=	697.63	T	313=	627.60	T	315=	526.42	T	316=	526.42	T	320=	675.10
T	323=	610.95	T	325=	516.53	T	326=	516.53	T	330=	629.68	T	333=	567.35	T	335=	497.97
T	336=	497.97	T	340=	583.58	T	342=	423.19	T	343=	475.09	T	344=	267.22	T	345=	595.28
T	346=	544.46	T	347=	399.20	T	349=	357.11	T	350=	194.21	T	351=	225.64	T	352=	194.89
T	353=	205.18	T	354=	222.41	T	355=	148.58	T	356=	223.86	T	360=	95.211	T	362=	96.245
T	364=	108.14	T	366=	144.64	T	367=	147.89	T	368=	153.86	T	369=	169.69	T	371=	232.31
T	373=	214.09	T	375=	171.99	T	377=	144.68	T	400=	101.78	T	401=	116.34	T	402=	140.70
T	404=	653.79	T	406=	552.20	T	408=	507.24	T	410=	555.74	T	412=	600.06	T	414=	533.02
T	421=	404.09	T	422=	565.62	T	423=	553.45	T	424=	189.97	T	425=	707.19	T	426=	639.39
T	431=	603.55	T	432=	670.99	T	433=	361.79	T	434=	303.08	T	435=	669.67	T	436=	587.81
T	441=	512.23	T	442=	592.02	T	443=	616.37	T	444=	615.64	T	445=	593.70	T	446=	512.63
T	451=	529.56	T	452=	551.13	T	453=	550.87	T	454=	551.25	T	455=	554.50	T	456=	533.02

ARITHMETIC NODES IN ASCENDING NODE NUMBER ORDER

T	50=	747.36	T	52=	677.56	T	54=	642.53	T	158=	634.12	T	159=	633.79	T	168=	633.39
T	169=	633.53	T	195=	159.70	T	197=	181.95	T	199=	397.37	T	238=	609.10	T	311=	614.55

T	312=	614.55	T	321=	598.24	T	322=	598.24	T	331=	554.28	T	332=	554.28	T	337=	471.18
T	341=	454.80	T	357=	225.27	T	358=	232.48	T	359=	194.62	T	379=	146.84	T	403=	143.40
T	1000=	152.63	T	1001=	416.42	T	1002=	375.74	T	1003=	203.76	T	1004=	139.59	T	1005=	138.36
T	1006=	100.91	T	1007=	484.68	T	1008=	474.34	T	1009=	465.24	T	1010=	278.23	T	1011=	693.24
T	1012=	693.24	T	1013=	560.94	T	1021=	671.18	T	1022=	671.18	T	1023=	548.57	T	1031=	626.45
T	1032=	626.45	T	1033=	520.94	T	1041=	581.99	T	1042=	581.99	T	1043=	426.54	T	1044=	426.54
T	1346=	552.84	T	1347=	310.25												

HEATER NODES IN ASCENDING NODE NUMBER ORDER
++NONE++

BOUNDARY NODES IN ASCENDING NODE NUMBER ORDER

T	1=	-20.000	T	2=	-20.000

```
                    SYSTEMS IMPROVED NUMERICAL DIFFERENCING ANALYZER '85 (SINDA '85)                PAGE   1/4

MODEL = DAMAGE4          HAC LOAD CASE NO. 4 CONDITIONS - Axial Distribution, -20F
  STDSTL                    ***  Steady-state Conditions After The Fire  ***                      5/9/94  9am

 SUBMODEL NAME = MAIN

       PROBLEM TIME                    TIMEN                  =  999.000     VS. TIMEND=  999.000
                                  DIFFUSION NODES IN ASCENDING NODE NUMBER ORDER
  T   267=  137.57     T   268=  137.53     T   269=  135.71
                                  ARITHMETIC NODES IN ASCENDING NODE NUMBER ORDER
  T   201=  151.64     T  1266=  140.30     T  1267=  173.00     T  1268=  158.97     T  1269=  143.66
                                  HEATER NODES IN ASCENDING NODE NUMBER ORDER
                                        ++NONE++
                                  BOUNDARY NODES IN ASCENDING NODE NUMBER ORDER
                                        ++NONE++
MEAN ICV GAS TEMP= 151.6 F   MEAN ICV GAS PRESSURE= 18.35 PSIA
MEAN ICV-OCV GAS TEMP= 157.1 F   MEAN ICV-OCV GAS PRESSURE= 21.76 PSIA


 SUBMODEL NAME = PTSA

                                        CALCULATED                          ALLOWED
       MAX DIFF DELTA T PER ITER        DRLXCC(PTSA      373)= 0.144958     VS. DRLXCA= 5.000000E-02
       MAX ARITH DELTA T PER ITER       ARLXCC(PTSA     1009)= 5.487061E-02 VS. ARLXCA= 0.500000
       MAX SYSTEM ENERGY BALANCE        EBALSC             = 0.662816     VS. EBALSA * ESUMIS      =  7.67925
                                                                           EBALSA= 1.000000E-03
       ENERGY INTO AND OUT OF SYS       ESUMIS             =  7679.25          ESUMOS=  3273.24
       MAX NODAL ENERGY BALANCE         EBALNC(PTSA      367)= 0.278587     VS. EBALNA= 1.000000E-02
       NUMBER OF ITERATIONS             LOOPCT             =  203          VS. NLOOPS=  800
       PROBLEM TIME                     TIMEN              =  999.000      VS. TIMEND=  999.000

                                  DIFFUSION NODES IN ASCENDING NODE NUMBER ORDER
  T    51=  637.45     T    53=  669.68     T    55=  635.14     T    60=  538.67     T    62=  503.15     T   100=  484.21
  T   105=  481.90     T   107=  481.24     T   110=  488.46     T   112=  506.89     T   113=  431.28     T   120=  679.72
  T   122=  742.10     T   123=  535.51     T   124=  742.10     T   125=  535.51     T   126=  742.10     T   127=  535.51
  T   130=  714.86     T   132=  779.08     T   133=  565.20     T   134=  779.08     T   135=  565.20     T   136=  779.08
  T   137=  565.20     T   140=  693.72     T   141=  674.24     T   142=  738.46     T   143=  572.13     T   144=  738.46
  T   145=  572.13     T   146=  738.46     T   147=  572.13     T   150=  729.76     T   152=  794.45     T   153=  575.25
  T   154=  792.77     T   155=  576.25     T   156=  792.77     T   157=  576.25     T   160=  680.40     T   161=  663.39
  T   162=  737.33     T   163=  540.60     T   164=  733.81     T   165=  549.12     T   166=  733.81     T   167=  549.12
  T   170=  377.68     T   172=  390.34     T   173=  342.01     T   175=  314.43     T   177=  337.80     T   180=  322.12
  T   190=  243.35     T   191=  202.63     T   192=  152.82     T   193=  286.43     T   194=  198.99     T   196=  168.44
  T   198=  200.74     T   200=  126.41     T   204=  258.43     T   210=  908.12     T   220=  929.43     T   230=  826.63
  T   240=  402.88     T   242=  237.82     T   250=  150.85     T   260=  107.41     T   261=  108.40     T   262=  124.68
  T   263=  127.89     T   264=  130.47     T   265=  133.01     T   266=  135.48     T   300=  86.023     T   304=  171.25
  T   305=  62.403     T   310=  747.14     T   313=  649.68     T   315=  532.11     T   316=  532.11     T   320=  773.81
  T   323=  673.43     T   325=  552.88     T   326=  552.88     T   330=  630.42     T   333=  497.83     T   335=  413.86
  T   336=  413.86     T   340=  443.66     T   342=  273.24     T   343=  137.33     T   344=  169.85     T   345=  126.82
  T   346=  152.30     T   347=  131.90     T   349=  109.39     T   350=  136.29     T   351=  131.62     T   352=  134.09
  T   353=  131.35     T   354=  141.76     T   355=  129.38     T   356=  136.20     T   360=  106.80     T   362=  120.63
  T   364=  127.59     T   366=  129.68     T   367=  128.89     T   368=  126.45     T   369=  125.72     T   371=  133.63
  T   373=  132.90     T   375=  130.15     T   377=  128.11     T   400=  118.78     T   401=  116.63     T   402=  127.70
  T   404=  99.078     T   406=  104.16     T   408=  4.8943     T   410= -12.195     T   412= -11.878     T   414= -11.936
```

T	421=	78.101	T	422=	0.90146	T	423=	-5.9585	T	424=	80.240	T	425=	1.7430	T	426=	-4.3240
T	431=	36.514	T	432=	54.843	T	433=	24.943	T	434=	10.323	T	435=	-0.84778	T	436=	1.9902
T	950=	1330.4	T	952=	1331.0	T	954=	1271.0									

ARITHMETIC NODES IN ASCENDING NODE NUMBER ORDER

T	50=	632.82	T	52=	665.84	T	54=	627.99	T	158=	687.18	T	159=	631.71	T	168=	668.00
T	169=	660.26	T	195=	144.15	T	197=	165.07	T	199=	222.84	T	238=	651.39	T	311=	641.26
T	312=	641.26	T	321=	664.86	T	322=	664.86	T	331=	489.96	T	332=	489.96	T	337=	263.78
T	341=	285.47	T	357=	137.78	T	358=	134.01	T	359=	135.17	T	379=	129.31	T	403=	127.98
T	1000=	158.92	T	1001=	184.87	T	1002=	214.08	T	1003=	158.83	T	1004=	144.93	T	1005=	144.06
T	1006=	117.80	T	1007=	270.46	T	1008=	243.31	T	1009=	215.11	T	1010=	193.28	T	1011=	741.18
T	1012=	741.18	T	1013=	573.34	T	1021=	767.40	T	1022=	767.40	T	1023=	594.71	T	1031=	625.12
T	1032=	625.12	T	1033=	443.49	T	1041=	444.18	T	1042=	444.18	T	1043=	277.80	T	1044=	277.80
T	1346=	127.84	T	1347=	128.57												

HEATER NODES IN ASCENDING NODE NUMBER ORDER

++NONE++

BOUNDARY NODES IN ASCENDING NODE NUMBER ORDER

T	1=	-20.000	T	2=	-20.000

SYSTEMS IMPROVED NUMERICAL DIFFERENCING ANALYZER '85 (SINDA '85) PAGE 2/4

MODEL = DAMAGE4
STDSTL

HAC LOAD CASE NO. 4 CONDITIONS - Axial Distribution, -20F
*** Steady-state Conditions After The Fire ***

5/9/94 9am

SUBMODEL NAME = PTSB

		CALCULATED			ALLOWED
MAX DIFF DELTA T PER ITER	DRLXCC(PTSB	263)=-0.105835	VS.	DRLXCA=	5.000000E-02
MAX ARITH DELTA T PER ITER	ARLXCC(PTSB	1006)=-9.716797E-02	VS.	ARLXCA=	0.500000
MAX SYSTEM ENERGY BALANCE	EBALSC	=-0.236677	VS.	EBALSA * ESUMIS =	0.
				EBALSA=	1.000000E-03
ENERGY INTO AND OUT OF SYS	ESUMIS	= 0.		ESUMOS=	1830.55
MAX NODAL ENERGY BALANCE	EBALNC(PTSB	260)= 0.299775	VS.	EBALNA=	1.000000E-02
NUMBER OF ITERATIONS	LOOPCT	= 203	VS.	NLOOPS=	800
PROBLEM TIME	TIMEN	= 999.000	VS.	TIMEND=	999.000

DIFFUSION NODES IN ASCENDING NODE NUMBER ORDER

T	51=	391.40	T	53=	420.91	T	55=	394.02	T	60=	337.59	T	62=	332.81	T	100=	282.73
T	105=	307.17	T	107=	316.12	T	110=	327.07	T	112=	361.71	T	113=	301.15	T	120=	386.42
T	122=	473.82	T	123=	312.15	T	124=	439.89	T	125=	310.33	T	126=	362.51	T	127=	302.84
T	130=	411.89	T	132=	502.22	T	133=	334.33	T	134=	467.05	T	135=	334.56	T	136=	388.58
T	137=	331.01	T	140=	424.34	T	141=	425.32	T	142=	498.60	T	143=	362.57	T	144=	467.90
T	145=	358.56	T	146=	393.92	T	147=	343.93	T	150=	416.34	T	152=	508.81	T	153=	338.06
T	154=	471.52	T	155=	338.12	T	156=	390.18	T	157=	329.69	T	160=	388.74	T	161=	390.79
T	162=	474.00	T	163=	319.38	T	164=	439.36	T	165=	320.52	T	166=	365.10	T	167=	308.53
T	170=	281.10	T	172=	303.32	T	173=	261.48	T	175=	248.50	T	177=	262.00	T	180=	244.03
T	190=	220.00	T	191=	191.74	T	192=	135.13	T	193=	205.77	T	194=	163.73	T	196=	166.43
T	198=	190.60	T	200=	124.52	T	204=	166.69	T	210=	319.76	T	220=	337.12	T	230=	289.54
T	240=	216.51	T	242=	161.66	T	250=	123.45	T	260=	103.42	T	261=	103.99	T	262=	112.33
T	263=	113.17	T	264=	115.30	T	265=	116.76	T	266=	116.27	T	300=	78.485	T	304=	100.28
T	305=	25.620	T	310=	281.10	T	313=	248.71	T	315=	209.96	T	316=	209.96	T	320=	299.53
T	323=	265.26	T	325=	224.33	T	326=	224.33	T	330=	239.97	T	333=	201.73	T	335=	171.35
T	336=	171.35	T	340=	206.58	T	342=	155.43	T	343=	82.429	T	344=	121.39	T	345=	85.114
T	346=	78.638	T	347=	99.201	T	349=	67.864	T	350=	109.79	T	351=	103.09	T	352=	108.65
T	353=	104.99	T	354=	110.79	T	355=	108.27	T	356=	108.19	T	360=	102.68	T	362=	110.24
T	364=	112.19	T	366=	108.83	T	367=	108.07	T	368=	106.68	T	369=	105.85	T	371=	104.24
T	373=	105.44	T	375=	106.46	T	377=	106.94	T	400=	107.20	T	401=	105.17	T	402=	107.01
T	404=	72.207	T	406=	23.281	T	408=	-7.6417	T	410=	-14.467	T	412=	-13.428	T	414=	-12.741
T	421=	69.736	T	422=	-0.92831	T	423=	-7.3216	T	424=	67.033	T	425=	-1.7798	T	426=	-8.3174
T	431=	41.098	T	432=	33.801	T	433=	40.182	T	434=	17.979	T	435=	-9.0433	T	436=	-10.563
T	441=	3.5054	T	442=	8.6180	T	443=	-0.13501	T	444=	-4.3262	T	445=	-10.212	T	446=	-9.2725
T	451=	6.0761	T	452=	13.496	T	453=	-1.2693	T	454=	-6.3633	T	455=	-11.684	T	456=	-10.520

ARITHMETIC NODES IN ASCENDING NODE NUMBER ORDER

T	50=	390.35	T	52=	418.00	T	54=	392.00	T	158=	406.77	T	159=	371.34	T	168=	391.29
T	169=	393.27	T	195=	124.46	T	197=	136.14	T	199=	183.28	T	238=	257.89	T	311=	246.03
T	312=	246.03	T	321=	262.46	T	322=	262.46	T	331=	199.06	T	332=	199.06	T	337=	142.38

T	341=	155.34	T	357=	108.24	T	358=	104.28	T	359=	109.20	T	379=	108.40	T	403=	106.96
T	1000=	129.61	T	1001=	175.53	T	1002=	180.11	T	1003=	142.73	T	1004=	129.21	T	1005=	128.57
T	1006=	108.74	T	1007=	228.85	T	1008=	216.57	T	1009=	199.34	T	1010=	157.37	T	1011=	280.30
T	1012=	280.30	T	1013=	224.00	T	1021=	298.65	T	1022=	298.65	T	1023=	239.09	T	1031=	239.22
T	1032=	239.22	T	1033=	182.34	T	1041=	206.35	T	1042=	206.35	T	1043=	155.92	T	1044=	155.92
T	1346=	79.098	T	1347=	101.86												

HEATER NODES IN ASCENDING NODE NUMBER ORDER
++NONE++
BOUNDARY NODES IN ASCENDING NODE NUMBER ORDER

T	1=	-20.000	T	2=	-20.000

SYSTEMS IMPROVED NUMERICAL DIFFERENCING ANALYZER '85 (SINDA '85) PAGE 3/4

MODEL = DAMAGE4
STDSTL

HAC LOAD CASE NO. 4 CONDITIONS - Axial Distribution, -20F
*** Steady-state Conditions After The Fire *** 5/9/94 9am

SUBMODEL NAME = PTSC

		CALCULATED			ALLOWED	
MAX DIFF DELTA T PER ITER	DRLXCC(PTSC	360)=	-3.057861E-02	VS. DRLXCA=	5.000000E-02	
MAX ARITH DELTA T PER ITER	ARLXCC(PTSC	1006)=	-2.264404E-02	VS. ARLXCA=	0.500000	
MAX SYSTEM ENERGY BALANCE	EBALSC	=	-16.6823	VS. EBALSA * ESUMIS =	0.	
				EBALSA=	1.000000E-03	
ENERGY INTO AND OUT OF SYS	ESUMIS	=	0.	ESUMOS=	1829.34	
MAX NODAL ENERGY BALANCE	EBALNC(PTSC	367)=	-1.96507	VS. EBALNA=	1.000000E-02	
NUMBER OF ITERATIONS	LOOPCT	=	203	VS. NLOOPS=	800	
PROBLEM TIME	TIMEN	=	999.000	VS. TIMEND=	999.000	

DIFFUSION NODES IN ASCENDING NODE NUMBER ORDER

T	51=	204.25	T	53=	220.83	T	55=	207.23	T	60=	187.00	T	62=	187.70	T	100=	169.65
T	105=	176.64	T	107=	179.27	T	110=	182.55	T	112=	189.44	T	113=	179.49	T	120=	201.37
T	122=	217.29	T	123=	190.57	T	124=	207.35	T	125=	184.53	T	126=	183.82	T	127=	170.13
T	130=	215.38	T	132=	232.70	T	133=	203.78	T	134=	221.84	T	135=	197.26	T	136=	196.32
T	137=	181.78	T	140=	225.52	T	141=	225.95	T	142=	240.08	T	143=	216.82	T	144=	229.49
T	145=	209.14	T	146=	202.72	T	147=	190.36	T	150=	217.26	T	152=	234.46	T	153=	205.87
T	154=	223.52	T	155=	199.09	T	156=	198.29	T	157=	181.04	T	160=	204.61	T	161=	205.30
T	162=	219.97	T	163=	195.05	T	164=	210.71	T	165=	188.55	T	166=	188.99	T	167=	176.69
T	170=	170.23	T	172=	175.52	T	173=	167.86	T	175=	159.15	T	177=	163.71	T	180=	158.77
T	190=	146.80	T	191=	139.72	T	192=	101.59	T	193=	122.87	T	194=	107.83	T	196=	144.40
T	198=	139.36	T	200=	95.209	T	204=	91.463	T	210=	108.91	T	220=	115.44	T	230=	105.99
T	240=	89.936	T	242=	79.994	T	250=	76.237	T	260=	86.472	T	261=	86.871	T	262=	81.681
T	263=	82.210	T	264=	78.164	T	265=	79.246	T	266=	75.208	T	300=	56.209	T	304=	44.595
T	305=	4.4653	T	310=	84.809	T	313=	74.951	T	315=	63.251	T	316=	63.251	T	320=	91.460
T	323=	81.007	T	325=	68.622	T	326=	68.622	T	330=	80.605	T	333=	69.609	T	335=	59.007
T	336=	59.007	T	340=	74.976	T	342=	68.748	T	343=	39.605	T	344=	65.616	T	345=	43.121
T	346=	32.274	T	347=	55.338	T	349=	32.427	T	350=	64.627	T	351=	59.531	T	352=	64.141
T	353=	61.601	T	354=	63.710	T	355=	65.779	T	356=	62.875	T	360=	85.067	T	362=	80.359
T	364=	74.678	T	366=	66.425	T	367=	65.620	T	368=	64.763	T	369=	63.976	T	371=	60.012
T	373=	61.534	T	375=	63.680	T	377=	64.999	T	400=	76.587	T	401=	74.952	T	402=	65.207
T	404=	38.929	T	406=	0.64728E-01	T	408=	-13.042	T	410=	-16.530	T	412=	-15.464	T	414=	-14.464
T	421=	47.933	T	422=	-5.4011	T	423=	-10.328	T	424=	38.592	T	425=	-7.4922	T	426=	-11.994
T	431=	16.583	T	432=	10.308	T	433=	17.540	T	434=	4.2817	T	435=	-13.020	T	436=	-14.116
T	441=	-7.0929	T	442=	-5.6643	T	443=	-8.4557	T	444=	-10.753	T	445=	-14.259	T	446=	-13.832
T	451=	-6.9471	T	452=	-4.2463	T	453=	-9.9417	T	454=	-12.263	T	455=	-15.070	T	456=	-14.495

ARITHMETIC NODES IN ASCENDING NODE NUMBER ORDER

T	50=	204.79	T	52=	219.38	T	54=	207.18	T	158=	207.54	T	159=	200.95	T	168=	205.57
T	169=	206.23	T	195=	96.533	T	197=	98.263	T	199=	120.35	T	238=	98.961	T	311=	74.109
T	312=	74.109	T	321=	80.126	T	322=	80.126	T	331=	68.759	T	332=	68.759	T	337=	60.465

T	341=	66.354	T	357=	62.483	T	358=	59.867	T	359=	64.369	T	379=	65.960	T	403=	65.063
T	1000=	94.492	T	1001=	134.46	T	1002=	120.39	T	1003=	107.76	T	1004=	97.979	T	1005=	97.591
T	1006=	85.469	T	1007=	151.67	T	1008=	146.83	T	1009=	141.89	T	1010=	93.968	T	1011=	84.665
T	1012=	84.665	T	1013=	67.519	T	1021=	91.305	T	1022=	91.305	T	1023=	73.126	T	1031=	80.455
T	1032=	80.455	T	1033=	62.862	T	1041=	74.886	T	1042=	74.886	T	1043=	68.722	T	1044=	68.722
T	1346=	37.786	T	1347=	59.076												

HEATER NODES IN ASCENDING NODE NUMBER ORDER

++NONE++

BOUNDARY NODES IN ASCENDING NODE NUMBER ORDER

T	1=	-20.000	T	2= -20.000

SYSTEMS IMPROVED NUMERICAL DIFFERENCING ANALYZER '85 (SINDA '85) PAGE 4/4

MODEL = DAMAGE4
STDSTL

HAC LOAD CASE NO. 4 CONDITIONS - Axial Distribution, -20F
*** Steady-state Conditions After The Fire *** 5/9/94 9am

SUBMODEL NAME = PTSD

		CALCULATED		ALLOWED	
MAX DIFF DELTA T PER ITER	DRLXCC(PTSD	351)=	-4.537964E-02	VS. DRLXCA=	5.000000E-02
MAX ARITH DELTA T PER ITER	ARLXCC(PTSD	358)=	-3.338623E-02	VS. ARLXCA=	0.500000
MAX SYSTEM ENERGY BALANCE	EBALSC	=	-6.77970	VS. EBALSA * ESUMIS =	0.
				EBALSA=	1.000000E-03
ENERGY INTO AND OUT OF SYS	ESUMIS	=	0.	ESUMOS=	787.950
MAX NODAL ENERGY BALANCE	EBALNC(PTSD	350)=	-1.09441	VS. EBALNA=	1.000000E-02
NUMBER OF ITERATIONS	LOOPCT	=	203	VS. NLOOPS=	800
PROBLEM TIME	TIMEN	=	999.000	VS. TIMEND=	999.000

DIFFUSION NODES IN ASCENDING NODE NUMBER ORDER

T	51=	161.18	T	53=	173.38	T	55=	164.88	T	60=	150.87	T	62=	154.85	T	100=	140.48
T	105=	144.49	T	107=	146.01	T	110=	147.92	T	112=	150.70	T	113=	147.20	T	120=	159.32
T	122=	165.49	T	123=	155.85	T	124=	160.24	T	125=	151.84	T	126=	147.94	T	127=	142.49
T	130=	169.71	T	132=	176.56	T	133=	165.99	T	134=	170.80	T	135=	161.61	T	136=	157.43
T	137=	151.47	T	140=	177.07	T	141=	177.29	T	142=	182.99	T	143=	174.47	T	144=	177.22
T	145=	169.56	T	146=	162.80	T	147=	157.89	T	150=	171.37	T	152=	178.15	T	153=	167.74
T	154=	172.40	T	155=	163.15	T	156=	159.31	T	157=	151.46	T	160=	163.34	T	161=	163.79
T	162=	169.27	T	163=	160.43	T	164=	164.60	T	165=	156.05	T	166=	153.54	T	167=	148.86
T	170=	145.32	T	172=	147.33	T	173=	144.77	T	175=	139.85	T	177=	142.09	T	180=	139.82
T	190=	133.86	T	191=	129.57	T	192=	90.417	T	193=	112.74	T	194=	96.514	T	196=	134.55
T	198=	129.31	T	200=	88.348	T	204=	84.324	T	210=	96.634	T	220=	100.60	T	230=	94.472
T	240=	76.716	T	242=	66.763	T	250=	63.266	T	260=	75.870	T	261=	76.273	T	262=	69.255
T	263=	69.785	T	264=	65.296	T	265=	66.351	T	266=	62.384	T	300=	50.553	T	304=	39.235
T	305=	2.5259	T	310=	72.576	T	313=	63.993	T	315=	53.813	T	316=	53.813	T	320=	77.000
T	323=	68.053	T	325=	57.457	T	326=	57.457	T	330=	68.958	T	333=	59.073	T	335=	49.866
T	336=	49.866	T	340=	63.143	T	342=	56.750	T	343=	31.413	T	344=	53.539	T	345=	34.258
T	346=	25.202	T	347=	44.634	T	349=	25.344	T	350=	52.563	T	351=	48.308	T	352=	52.122
T	353=	50.029	T	354=	51.795	T	355=	53.513	T	356=	51.058	T	360=	74.344	T	362=	68.049
T	364=	62.045	T	366=	54.108	T	367=	53.346	T	368=	52.528	T	369=	51.814	T	371=	48.703
T	373=	49.966	T	375=	51.748	T	377=	52.854	T	400=	64.683	T	401=	63.218	T	402=	53.057
T	404=	30.429	T	406=	-2.6155	T	408=	-14.004	T	410=	-16.972	T	412=	-16.032	T	414=	-15.095
T	421=	39.542	T	422=	-7.1129	T	423=	-11.453	T	424=	30.314	T	425=	-9.1562	T	426=	-13.034
T	431=	11.425	T	432=	6.1744	T	433=	12.197	T	434=	0.86621	T	435=	-13.951	T	436=	-14.896
T	441=	-8.8477	T	442=	-7.6067	T	443=	-10.044	T	444=	-12.026	T	445=	-15.034	T	446=	-14.675
T	451=	-8.7189	T	452=	-6.3938	T	453=	-11.320	T	454=	-13.322	T	455=	-15.725	T	456=	-15.239

ARITHMETIC NODES IN ASCENDING NODE NUMBER ORDER

T	50=	161.79	T	52=	172.41	T	54=	165.02	T	158=	164.42	T	159=	161.89	T	168=	163.96
T	169=	164.31	T	195=	85.524	T	197=	86.705	T	199=	109.72	T	238=	86.704	T	311=	63.258
T	312=	63.258	T	321=	67.295	T	322=	67.295	T	331=	58.316	T	332=	58.316	T	337=	49.690

T	341=	54.803	T	357=	50.753	T	358=	48.560	T	359=	52.329
T	379=	53.672	T	403=	52.916	T	1000=	83.020	T	1001=	124.28
T	1002=	109.67	T	1003=	96.777	T	1004=	86.747	T	1005=	86.358
T	1006=	74.112	T	1007=	136.09	T	1008=	133.63	T	1009=	130.81
T	1010=	81.710	T	1011=	72.456	T	1012=	72.456	T	1013=	57.528
T	1021=	76.873	T	1022=	76.873	T	1023=	61.312	T	1031=	68.828
T	1032=	68.828	T	1033=	53.215	T	1041=	63.073	T	1042=	63.073
T	1043=	56.745	T	1044=	56.745	T	1346=	29.786	T	1347=	47.730

HEATER NODES IN ASCENDING NODE NUMBER ORDER
++NONE++
BOUNDARY NODES IN ASCENDING NODE NUMBER ORDER

T	1=	-20.000	T	2= -20.000

SYSTEMS IMPROVED NUMERICAL DIFFERENCING ANALYZER '85 (SINDA '85) PAGE 1/4

MODEL = DAMAGE5 HAC LOAD CASE NO. 5 -- Ungula Distribution, 100F 4/30/94
FWDBCK ***** Peak OCV Sidewall Temperature Time Point *****

SUBMODEL NAME = MAIN

MEAN PROBLEM TIME TIMEM = 0.500000

DIFFUSION NODES IN ASCENDING NODE NUMBER ORDER

T 267= 233.32 T 268= 233.07 T 269= 226.43

ARITHMETIC NODES IN ASCENDING NODE NUMBER ORDER

T 201= 782.68 T 1266= 249.50 T 1267= 400.38 T 1268= 356.43 T 1269= 259.69

HEATER NODES IN ASCENDING NODE NUMBER ORDER

++NONE++

BOUNDARY NODES IN ASCENDING NODE NUMBER ORDER

++NONE++

MEAN ICV GAS TEMP= 782.7 F MEAN ICV GAS PRESSURE= 37.30 PSIA
MEAN ICV-OCV GAS TEMP= 845.2 F MEAN ICV-OCV GAS PRESSURE= 46.03 PSIA

SUBMODEL NAME = PTSA

	CALCULATED		ALLOWED
MAX DIFF DELTA T PER ITER	DRLXCC(PTSA	264)=-1.831055E-04	VS. DRLXCA= 5.000000E-02
MAX ARITH DELTA T PER ITER	ARLXCC(PTSA	1346)=-5.541992E-02	VS. ARLXCA= 0.500000
MAX DIFF DEL T PER TIME STEP	DTMPCC(PTSA	264)=-1.831055E-04	VS. DTMPCA= 10.0000
MAX ARITH DEL T PER TIME STEP	ATMPCC(PTSA	1346)=-5.538940E-02	VS. ATMPCA= 100.000
MIN STABILITY CRITERIA	CSGMIN(PTSA	431)= 3.003038E-05	
MAX STABILITY CRITERIA	CSGMAX(PTSA	424)= 1.95834	
NUMBER OF ITERATIONS	LOOPCT	= 1	VS. NLOOPT= 600
PROBLEM TIME	TIMEN	= 0.500000	VS. TIMEND= 0.500000
MEAN PROBLEM TIME	TIMEM	= 0.500000	
AVERAGE TIME STEP USED	DTIMEU	= 1.666667E-02	VS. DTIMEI= 0.

DIFFUSION NODES IN ASCENDING NODE NUMBER ORDER

T 51= 751.24	T 53= 869.75	T 55= 1019.2	T 60= 870.61	T 62= 1114.8	T 100= 1025.1
T 105= 929.30	T 107= 886.45	T 110= 843.84	T 112= 844.08	T 113= 844.34	T 120= 753.32
T 122= 753.16	T 123= 752.61	T 124= 752.12	T 125= 751.67	T 126= 752.38	T 127= 752.10
T 130= 777.55	T 132= 783.34	T 133= 770.09	T 134= 782.97	T 135= 773.64	T 136= 782.93
T 137= 780.50	T 140= 824.31	T 141= 824.72	T 142= 830.40	T 143= 808.15	T 144= 835.80
T 145= 821.58	T 146= 847.77	T 147= 844.56	T 150= 915.56	T 152= 924.36	T 153= 884.13
T 154= 932.92	T 155= 911.49	T 156= 945.01	T 157= 945.54	T 160= 981.40	T 161= 968.76
T 162= 993.43	T 163= 944.32	T 164= 1000.2	T 165= 980.11	T 166= 1011.4	T 167= 1007.8
T 170= 958.65	T 172= 962.37	T 173= 932.45	T 175= 926.83	T 177= 937.95	T 180= 877.66
T 190= 950.02	T 191= 1071.0	T 192= 348.92	T 193= 962.51	T 194= 494.17	T 196= 707.73
T 198= 1074.2	T 200= 1097.3	T 204= 1119.8	T 210= 732.95	T 220= 732.91	T 230= 775.58
T 240= 817.12	T 242= 431.79	T 250= 235.13	T 260= 204.98	T 261= 208.51	T 262= 209.96
T 263= 218.92	T 264= 209.04	T 265= 217.66	T 266= 210.01	T 300= 1230.7	T 304= 1239.4
T 305= 1376.9	T 310= 937.22	T 313= 1108.6	T 315= 1282.0	T 316= 1282.0	T 320= 931.09
T 323= 1103.4	T 325= 1277.1	T 326= 1277.1	T 330= 931.38	T 333= 1086.9	T 335= 1260.9
T 336= 1260.9	T 340= 933.90	T 342= 609.06	T 343= 1039.0	T 344= 340.31	T 345= 966.54
T 346= 1265.0	T 347= 544.61	T 349= 1046.0	T 350= 259.99	T 351= 426.74	T 352= 263.83
T 353= 342.52	T 354= 298.13	T 355= 225.13	T 356= 307.45	T 360= 201.01	T 362= 201.62
T 364= 201.31	T 366= 217.61	T 367= 223.10	T 368= 248.31	T 369= 267.79	T 371= 436.84
T 373= 347.83	T 375= 258.52	T 377= 225.55	T 400= 199.97	T 401= 209.20	T 402= 221.81
T 404= 1202.3	T 406= 1373.5	T 408= 1363.2	T 410= 1411.5	T 412= 1411.0	T 414= 1419.3

T 421= 471.50 T 422= 1414.7 T 423= 1417.5 T 424= 264.28 T 425= 1401.7 T 426= 1404.2

T 431= 1362.0 T 432= 1362.4 T 433= 1348.7 T 434= 1347.4 T 435= 1382.1 T 436= 1363.7

T 950= 1064.1 T 952= 1104.8

ARITHMETIC NODES IN ASCENDING NODE NUMBER ORDER

T 50= 777.36 T 52= 871.98 T 54= 1007.8 T 158= 974.54 T 159= 968.58 T 168= 968.97

T 169= 966.44 T 195= 348.43 T 197= 430.17 T 199= 733.98 T 238= 976.45 T 311= 1124.8

T 312= 1124.8 T 321= 1119.4 T 322= 1119.4 T 331= 1100.5 T 332= 1100.5 T 337= 824.03

T 341= 717.20 T 357= 328.59 T 358= 408.78 T 359= 262.47 T 379= 221.48 T 403= 224.31

T 1000= 405.01 T 1001= 879.06 T 1002= 738.49 T 1003= 459.17 T 1004= 319.78 T 1005= 316.22

T 1006= 217.48 T 1007= 960.60 T 1008= 980.90 T 1009= 1043.2 T 1010= 438.29 T 1011= 959.35

T 1012= 959.35 T 1013= 1231.5 T 1021= 953.15 T 1022= 953.15 T 1023= 1227.0 T 1031= 951.74

T 1032= 951.74 T 1033= 1210.8 T 1041= 954.08 T 1042= 954.08 T 1043= 650.58 T 1044= 650.58

T 1346= 1137.0 T 1347= 448.55

HEATER NODES IN ASCENDING NODE NUMBER ORDER

++NONE++

BOUNDARY NODES IN ASCENDING NODE NUMBER ORDER

T 1= 1475.0 T 2= 1424.7

SYSTEMS IMPROVED NUMERICAL DIFFERENCING ANALYZER '85 (SINDA '85) PAGE 2/4

MODEL = DAMAGE5 HAC LOAD CASE NO. 5 -- Ungula Distribution, 100F 4/30/94
FWDBCK ***** Peak OCV Sidewall Temperature Time Point *****

SUBMODEL NAME = PTSB

		CALCULATED			ALLOWED
MAX DIFF DELTA T PER ITER	DRLXCC(PTSB	455)=	-1.220703E-04	VS. DRLXCA=	5.000000E-02
MAX ARITH DELTA T PER ITER	ARLXCC(PTSB	1346)=	-6.933594E-02	VS. ARLXCA=	0.500000
MAX DIFF DEL T PER TIME STEP	DTMPCC(PTSB	443)=	1.525879E-04	VS. DTMPCA=	10.0000
MAX ARITH DEL T PER TIME STEP	ATMPCC(PTSB	1346)=	-6.930542E-02	VS. ATMPCA=	100.000
MIN STABILITY CRITERIA	CSGMIN(PTSB	446)=	3.008141E-05		
MAX STABILITY CRITERIA	CSGMAX(PTSB	434)=	3.26578		
NUMBER OF ITERATIONS	LOOPCT	=	1	VS. NLOOPT=	600
PROBLEM TIME	TIMEN	=	0.500000	VS. TIMEND=	0.500000
MEAN PROBLEM TIME	TIMEM	=	0.500000		
AVERAGE TIME STEP USED	DTIMEU	=	1.666667E-02	VS. DTIMEI=	0.

DIFFUSION NODES IN ASCENDING NODE NUMBER ORDER

T	51=	746.24	T	53=	816.09	T	55=	917.50	T	60=	867.71	T	62=	1082.4	T	100=	1025.3
T	105=	930.59	T	107=	888.22	T	110=	846.66	T	112=	845.22	T	113=	854.02	T	120=	759.00
T	122=	752.35	T	123=	774.62	T	124=	746.52	T	125=	761.99	T	126=	738.33	T	127=	742.12
T	130=	753.84	T	132=	759.88	T	133=	754.23	T	134=	754.23	T	135=	749.92	T	136=	745.74
T	137=	744.22	T	140=	771.71	T	141=	771.45	T	142=	784.23	T	143=	760.48	T	144=	780.77
T	145=	764.71	T	146=	777.06	T	147=	773.60	T	150=	825.04	T	152=	849.60	T	153=	793.37
T	154=	845.64	T	155=	810.83	T	156=	839.57	T	157=	835.81	T	160=	865.11	T	161=	856.44
T	162=	898.47	T	163=	820.83	T	164=	892.48	T	165=	851.25	T	166=	886.22	T	167=	878.07
T	170=	833.85	T	172=	851.49	T	173=	802.71	T	175=	807.78	T	177=	816.63	T	180=	774.64
T	190=	813.63	T	191=	908.66	T	192=	313.95	T	193=	821.20	T	194=	443.46	T	196=	633.82
T	198=	912.05	T	200=	1096.7	T	204=	1119.5	T	210=	729.91	T	220=	722.14	T	230=	713.69
T	240=	697.62	T	242=	396.40	T	250=	227.93	T	260=	203.39	T	261=	205.87	T	262=	204.25
T	263=	208.45	T	264=	205.10	T	265=	211.07	T	266=	206.65	T	300=	1230.6	T	304=	1239.2
T	305=	1376.8	T	310=	935.79	T	313=	1107.7	T	315=	1281.5	T	316=	1281.5	T	320=	925.91
T	323=	1100.2	T	325=	1275.4	T	326=	1275.4	T	330=	898.28	T	333=	1064.0	T	335=	1250.4
T	336=	1250.4	T	340=	881.94	T	342=	589.06	T	343=	1024.9	T	344=	331.37	T	345=	825.06
T	346=	1258.6	T	347=	468.87	T	349=	1041.3	T	350=	252.86	T	351=	418.76	T	352=	253.78
T	353=	336.49	T	354=	289.33	T	355=	217.69	T	356=	292.89	T	360=	200.45	T	362=	199.81
T	364=	199.67	T	366=	211.48	T	367=	213.13	T	368=	220.00	T	369=	229.87	T	371=	428.25
T	373=	341.74	T	375=	252.86	T	377=	216.28	T	400=	199.41	T	401=	208.84	T	402=	211.32
T	404=	934.35	T	406=	1360.8	T	408=	1380.6	T	410=	1406.3	T	412=	1410.4	T	414=	1419.2
T	421=	471.38	T	422=	1414.7	T	423=	1417.5	T	424=	245.78	T	425=	1400.9	T	426=	1406.5
T	431=	1230.8	T	432=	1323.6	T	433=	246.10	T	434=	222.10	T	435=	1386.4	T	436=	1396.6
T	441=	1380.0	T	442=	1370.3	T	443=	1373.2	T	444=	1373.2	T	445=	1391.4	T	446=	1380.9
T	451=	1372.5	T	452=	1361.2	T	453=	1376.6	T	454=	1381.3	T	455=	1405.8	T	456=	1391.9
T	954=	945.37															

ARITHMETIC NODES IN ASCENDING NODE NUMBER ORDER

T	50=	766.14	T	52=	818.65	T	54=	918.41	T	158=	864.61	T	159=	852.86	T	168=	856.74

T 169= 855.75	T 195= 311.66	T 197= 386.28	T 199= 666.58	T 238= 742.74	T 311= 1123.9
T 312= 1123.9	T 321= 1116.2	T 322= 1116.2	T 331= 1078.4	T 332= 1078.4	T 337= 804.86
T 341= 694.51	T 357= 317.49	T 358= 399.34	T 359= 253.89	T 379= 213.59	T 403= 214.64
T 1000= 347.13	T 1001= 755.21	T 1002= 658.59	T 1003= 404.40	T 1004= 290.88	T 1005= 288.11
T 1006= 210.54	T 1007= 828.29	T 1008= 840.22	T 1009= 887.68	T 1010= 415.35	T 1011= 957.96
T 1012= 957.96	T 1013= 1230.9	T 1021= 948.12	T 1022= 948.12	T 1023= 1224.8	T 1031= 919.47
T 1032= 919.47	T 1033= 1196.5	T 1041= 904.28	T 1042= 904.28	T 1043= 629.93	T 1044= 629.93
T 1346= 1058.0	T 1347= 381.74				

HEATER NODES IN ASCENDING NODE NUMBER ORDER
++NONE++

BOUNDARY NODES IN ASCENDING NODE NUMBER ORDER

T 1= 1475.0 T 2= 1424.7

SYSTEMS IMPROVED NUMERICAL DIFFERENCING ANALYZER '85 (SINDA '85) PAGE 3/4

MODEL = DAMAGE5
FWDBCK

HAC LOAD CASE NO. 5 -- Ungula Distribution, 100F
***** Peak OCV Sidewall Temperature Time Point *****

4/30/94

SUBMODEL NAME = PTSC

	CALCULATED			ALLOWED	
MAX DIFF DELTA T PER ITER	DRLXCC(PTSC	456)= 1.220703E-04	VS. DRLXCA=	5.000000E-02	
MAX ARITH DELTA T PER ITER	ARLXCC(PTSC	1346)=-6.896973E-02	VS. ARLXCA=	0.500000	
MAX DIFF DEL T PER TIME STEP	DTMPCC(PTSC	456)= 1.525879E-04	VS. DTMPCA=	10.0000	
MAX ARITH DEL T PER TIME STEP	ATMPCC(PTSC	1346)=-6.893921E-02	VS. ATMPCA=	100.000	
MIN STABILITY CRITERIA	CSGMIN(PTSC	446)= 3.008508E-05			
MAX STABILITY CRITERIA	CSGMAX(PTSC	434)= 3.26579			
NUMBER OF ITERATIONS	LOOPCT	= 1	VS. NLOOPT=	600	
PROBLEM TIME	TIMEN	= 0.500000	VS. TIMEND=	0.500000	
MEAN PROBLEM TIME	TIMEM	= 0.500000			
AVERAGE TIME STEP USED	DTIMEU	= 1.666667E-02	VS. DTIMEI=	0.	

DIFFUSION NODES IN ASCENDING NODE NUMBER ORDER

T	51=	759.92	T	53=	736.97	T	55=	736.51	T	60=	867.22	T	62=	1006.7	T	100=	1019.2
T	105=	953.76	T	107=	926.74	T	110=	910.51	T	112=	906.06	T	113=	912.01	T	120=	831.39
T	122=	819.37	T	123=	834.77	T	124=	832.66	T	125=	842.75	T	126=	855.89	T	127=	857.61
T	130=	757.77	T	132=	756.99	T	133=	757.15	T	134=	760.17	T	135=	760.05	T	136=	766.80
T	137=	766.54	T	140=	719.48	T	141=	719.10	T	142=	726.80	T	143=	716.77	T	144=	722.98
T	145=	716.06	T	146=	718.93	T	147=	718.06	T	150=	701.95	T	152=	721.74	T	153=	693.10
T	154=	709.08	T	155=	687.96	T	156=	689.52	T	157=	683.14	T	160=	674.29	T	161=	675.74
T	162=	705.17	T	163=	661.31	T	164=	686.37	T	165=	653.28	T	166=	656.26	T	167=	647.45
T	170=	559.21	T	172=	578.85	T	173=	551.55	T	175=	501.88	T	177=	524.90	T	180=	500.60
T	190=	448.99	T	191=	435.36	T	192=	242.42	T	193=	550.14	T	194=	284.46	T	196=	470.12
T	198=	439.12	T	200=	1073.5	T	204=	1079.9	T	210=	735.15	T	220=	711.62	T	230=	633.03
T	240=	563.34	T	242=	348.85	T	250=	220.17	T	260=	201.16	T	261=	202.05	T	262=	200.27
T	263=	201.56	T	264=	201.50	T	265=	204.53	T	266=	203.87	T	300=	1224.2	T	304=	1228.6
T	305=	1375.3	T	310=	937.46	T	313=	1108.6	T	315=	1281.8	T	316=	1281.8	T	320=	921.44
T	323=	1097.6	T	325=	1274.3	T	326=	1274.3	T	330=	863.07	T	333=	1042.5	T	335=	1241.8
T	336=	1241.8	T	340=	833.74	T	342=	569.30	T	343=	1022.9	T	344=	326.13	T	345=	823.67
T	346=	1255.6	T	347=	468.19	T	349=	1040.1	T	350=	252.07	T	351=	417.92	T	352=	253.23
T	353=	335.98	T	354=	287.95	T	355=	217.40	T	356=	292.13	T	360=	199.73	T	362=	198.55
T	364=	198.79	T	366=	211.12	T	367=	212.88	T	368=	219.75	T	369=	229.55	T	371=	427.33
T	373=	341.23	T	375=	252.68	T	377=	216.18	T	400=	199.20	T	401=	208.72	T	402=	211.22
T	404=	934.18	T	406=	1359.8	T	408=	1380.5	T	410=	1406.3	T	412=	1410.4	T	414=	1419.2
T	421=	471.37	T	422=	1414.7	T	423=	1417.5	T	424=	245.78	T	425=	1400.9	T	426=	1406.5
T	431=	1230.2	T	432=	1322.7	T	433=	246.08	T	434=	222.10	T	435=	1386.4	T	436=	1396.6
T	441=	1379.9	T	442=	1369.8	T	443=	1373.2	T	444=	1373.2	T	445=	1391.4	T	446=	1380.8
T	451=	1372.1	T	452=	1360.2	T	453=	1376.4	T	454=	1381.2	T	455=	1405.8	T	456=	1391.9

ARITHMETIC NODES IN ASCENDING NODE NUMBER ORDER

T	50=	766.34	T	52=	739.53	T	54=	759.85	T	158=	680.02	T	159=	670.96	T	168=	676.35
T	169=	678.21	T	195=	245.75	T	197=	261.55	T	199=	405.47	T	238=	602.73	T	311=	1124.8

T	312=	1124.8	T	321=	1113.6	T	322=	1113.6	T	331=	1057.2	T	332=	1057.2	T	337=	787.30
T	341=	672.93	T	357=	316.45	T	358=	398.37	T	359=	253.22	T	379=	213.28	T	403=	214.54
T	1000=	250.92	T	1001=	416.09	T	1002=	385.13	T	1003=	276.15	T	1004=	233.53	T	1005=	232.51
T	1006=	203.18	T	1007=	471.24	T	1008=	453.41	T	1009=	440.87	T	1010=	313.16	T	1011=	959.56
T	1012=	959.56	T	1013=	1231.3	T	1021=	943.80	T	1022=	943.80	T	1023=	1223.3	T	1031=	885.32
T	1032=	885.32	T	1033=	1183.9	T	1041=	857.97	T	1042=	857.97	T	1043=	609.70	T	1044=	609.70
T	1346=	1056.4	T	1347=	381.21												

HEATER NODES IN ASCENDING NODE NUMBER ORDER
++NONE++

BOUNDARY NODES IN ASCENDING NODE NUMBER ORDER

T	1=	1475.0	T	2=	1424.7

SYSTEMS IMPROVED NUMERICAL DIFFERENCING ANALYZER '85 (SINDA '85) PAGE 4/4

MODEL = DAMAGE5 HAC LOAD CASE NO. 5 -- Ungula Distribution, 100F 4/30/94
FWDBCK ***** Peak OCV Sidewall Temperature Time Point *****

SUBMODEL NAME = PTSD

		CALCULATED			ALLOWED
MAX DIFF DELTA T PER ITER	DRLXCC(PTSD	456)=-1.220703E-04	VS.	DRLXCA=	5.000000E-02
MAX ARITH DELTA T PER ITER	ARLXCC(PTSD	1346)=-6.884766E-02	VS.	ARLXCA=	0.500000
MAX DIFF DEL T PER TIME STEP	DTMPCC(PTSD	453)= 1.525879E-04	VS.	DTMPCA=	10.0000
MAX ARITH DEL T PER TIME STEP	ATMPCC(PTSD	1346)=-6.881714E-02	VS.	ATMPCA=	100.000
MIN STABILITY CRITERIA	CSGMIN(PTSD	446)= 3.008491E-05			
MAX STABILITY CRITERIA	CSGMAX(PTSD	434)= 3.26579			
NUMBER OF ITERATIONS	LOOPCT	= 1	VS.	NLOOPT=	600
PROBLEM TIME	TIMEN	= 0.500000	VS.	TIMEND=	0.500000
MEAN PROBLEM TIME	TIMEM	= 0.500000			
AVERAGE TIME STEP USED	DTIMEU	= 1.666667E-02	VS.	DTIMEI=	0.

DIFFUSION NODES IN ASCENDING NODE NUMBER ORDER

T	51=	761.32	T	53=	713.79	T	55=	685.05	T	60=	866.51	T	62=	993.22	T	100=	1020.2
T	105=	957.26	T	107=	931.35	T	110=	916.12	T	112=	915.98	T	113=	916.35	T	120=	841.68
T	122=	839.31	T	123=	840.54	T	124=	846.43	T	125=	847.05	T	126=	859.62	T	127=	859.49
T	130=	755.23	T	132=	755.10	T	133=	754.02	T	134=	758.27	T	135=	757.35	T	136=	765.01
T	137=	764.67	T	140=	705.33	T	141=	704.76	T	142=	707.61	T	143=	705.10	T	144=	707.54
T	145=	706.06	T	146=	710.90	T	147=	711.40	T	150=	674.77	T	152=	679.50	T	153=	673.96
T	154=	676.26	T	155=	671.62	T	156=	674.33	T	157=	672.84	T	160=	629.33	T	161=	635.75
T	162=	637.34	T	163=	628.61	T	164=	633.97	T	165=	627.16	T	166=	632.53	T	167=	631.17
T	170=	515.88	T	172=	518.32	T	173=	514.18	T	175=	466.34	T	177=	484.50	T	180=	467.06
T	190=	429.34	T	191=	412.20	T	192=	240.09	T	193=	541.54	T	194=	280.14	T	196=	421.32
T	198=	415.65	T	200=	1072.9	T	204=	1079.5	T	210=	734.03	T	220=	707.95	T	230=	641.22
T	240=	560.91	T	242=	347.75	T	250=	219.97	T	260=	200.91	T	261=	201.69	T	262=	200.10
T	263=	201.29	T	264=	201.35	T	265=	204.27	T	266=	203.78	T	300=	1224.0	T	304=	1228.4
T	305=	1375.3	T	310=	936.91	T	313=	1108.2	T	315=	1281.7	T	316=	1281.7	T	320=	919.89
T	323=	1096.7	T	325=	1274.0	T	326=	1274.0	T	330=	865.98	T	333=	1043.7	T	335=	1242.2
T	336=	1242.2	T	340=	833.72	T	342=	569.24	T	343=	1022.9	T	344=	326.10	T	345=	823.69
T	346=	1255.7	T	347=	468.20	T	349=	1040.2	T	350=	252.06	T	351=	417.93	T	352=	253.22
T	353=	335.98	T	354=	287.94	T	355=	217.40	T	356=	292.13	T	360=	199.63	T	362=	198.49
T	364=	198.76	T	366=	211.12	T	367=	212.88	T	368=	219.75	T	369=	229.55	T	371=	427.34
T	373=	341.23	T	375=	252.68	T	377=	216.18	T	400=	199.19	T	401=	208.71	T	402=	211.22
T	404=	934.19	T	406=	1359.9	T	408=	1380.5	T	410=	1406.3	T	412=	1410.4	T	414=	1419.2
T	421=	471.37	T	422=	1414.7	T	423=	1417.5	T	424=	245.78	T	425=	1400.9	T	426=	1406.5
T	431=	1230.2	T	432=	1322.8	T	433=	246.08	T	434=	222.10	T	435=	1386.4	T	436=	1396.6
T	441=	1379.9	T	442=	1369.8	T	443=	1373.2	T	444=	1373.2	T	445=	1391.4	T	446=	1380.9
T	451=	1372.1	T	452=	1360.3	T	453=	1376.4	T	454=	1381.2	T	455=	1405.8	T	456=	1391.9

ARITHMETIC NODES IN ASCENDING NODE NUMBER ORDER

T	50=	764.29	T	52=	716.34	T	54=	715.36	T	158=	637.41	T	159=	635.52	T	168=	636.04
T	169=	636.78	T	195=	240.62	T	197=	256.55	T	199=	395.08	T	238=	606.35	T	311=	1124.5

T	312=	1124.5	T	321=	1112.8	T	322=	1112.8	T	331=	1058.4	T	332=	1058.4	T	337=	787.30
T	341=	672.90	T	357=	316.45	T	358=	398.38	T	359=	253.22	T	379=	213.28	T	403=	214.54
T	1000=	247.94	T	1001=	389.32	T	1002=	374.00	T	1003=	268.91	T	1004=	231.67	T	1005=	230.70
T	1006=	202.80	T	1007=	443.55	T	1008=	430.24	T	1009=	417.71	T	1010=	310.27	T	1011=	959.03
T	1012=	959.03	T	1013=	1231.1	T	1021=	942.31	T	1022=	942.31	T	1023=	1222.7	T	1031=	888.11
T	1032=	888.11	T	1033=	1184.6	T	1041=	858.03	T	1042=	858.03	T	1043=	609.73	T	1044=	609.73
T	1346=	1056.4	T	1347=	381.22												

HEATER NODES IN ASCENDING NODE NUMBER ORDER
++NONE++

BOUNDARY NODES IN ASCENDING NODE NUMBER ORDER

T	1=	1475.0	T	2=	1424.7

```
                    SYSTEMS IMPROVED NUMERICAL DIFFERENCING ANALYZER '85 (SINDA '85)                PAGE   1/4

MODEL = DAMAGE5                      HAC LOAD CASE NO. 5 -- Ungula Distribution, 100F                    4/30/94
  FWDBCK                  *****        Peak ICV Sidewall Temperature Time Point     *****

 SUBMODEL NAME = MAIN

       MEAN PROBLEM TIME                    TIMEM                  = 0.632697
                                    DIFFUSION NODES IN ASCENDING NODE NUMBER ORDER
  T   267= 242.77     T   268= 242.52     T   269= 235.05
                                    ARITHMETIC NODES IN ASCENDING NODE NUMBER ORDER
  T   201= 836.93     T  1266= 260.64     T  1267= 429.51     T  1268= 377.23     T  1269= 271.65
                                    HEATER NODES IN ASCENDING NODE NUMBER ORDER
                                                ++NONE++
                                    BOUNDARY NODES IN ASCENDING NODE NUMBER ORDER
                                                ++NONE++
MEAN ICV GAS TEMP= 836.9 F   MEAN ICV GAS PRESSURE= 38.92 PSIA
MEAN ICV-OCV GAS TEMP= 818.3 F   MEAN ICV-OCV GAS PRESSURE= 45.08 PSIA


 SUBMODEL NAME = PTSA
                                                CALCULATED                          ALLOWED
       MAX DIFF DELTA T PER ITER        DRLXCC(PTSA      161)= 7.324219E-04 VS. DRLXCA= 5.000000E-02
       MAX ARITH DELTA T PER ITER       ARLXCC(PTSA     1004)= 2.978516E-02 VS. ARLXCA= 0.500000
       MAX DIFF DEL T PER TIME STEP     DTMPCC(PTSA      423)= -3.04379     VS. DTMPCA=  10.0000
       MAX ARITH DEL T PER TIME STEP    ATMPCC(PTSA     1346)= -1.59128     VS. ATMPCA=  100.000
       MIN STABILITY CRITERIA           CSGMIN(PTSA      431)= 1.061729E-04
       MAX STABILITY CRITERIA           CSGMAX(PTSA      424)= 1.98920
       NUMBER OF ITERATIONS             LOOPCT                =       5     VS. NLOOPT=      600
       PROBLEM TIME                     TIMEN                 = 0.633334     VS. TIMEND=  6.00000
       MEAN PROBLEM TIME                TIMEM                 = 0.632697
       AVERAGE TIME STEP USED           DTIMEU                = 8.130082E-04 VS. DTIMEI=       0.
                                    DIFFUSION NODES IN ASCENDING NODE NUMBER ORDER
  T    51= 779.33     T    53= 868.97     T    55= 1000.6     T    60= 874.32     T    62= 1095.4     T   100= 1022.7
  T   105= 964.23     T   107= 934.89     T   110= 901.60     T   112= 902.05     T   113= 901.57     T   120= 828.08
  T   122= 827.44     T   123= 825.31     T   124= 828.60     T   125= 827.12     T   126= 830.91     T   127= 830.47
  T   130= 844.55     T   132= 848.51     T   133= 836.03     T   134= 850.32     T   135= 841.83     T   136= 852.80
  T   137= 850.92     T   140= 880.81     T   141= 881.73     T   142= 885.05     T   143= 865.18     T   144= 890.95
  T   145= 878.52     T   146= 902.48     T   147= 899.85     T   150= 950.39     T   152= 957.19     T   153= 921.16
  T   154= 965.99     T   155= 947.18     T   156= 978.22     T   157= 978.79     T   160= 1002.5     T   161= 992.80
  T   162= 1012.6     T   163= 967.67     T   164= 1020.0     T   165= 1002.3     T   166= 1031.9     T   167= 1029.1
  T   170= 980.32     T   172= 983.60     T   173= 955.74     T   175= 948.28     T   177= 959.45     T   180= 902.08
  T   190= 976.30     T   191= 1071.4     T   192= 373.94     T   193= 986.06     T   194= 523.20     T   196= 750.69
  T   198= 1075.7     T   200= 1058.5     T   204= 1066.6     T   210= 816.65     T   220= 813.00     T   230= 850.82
  T   240= 863.72     T   242= 489.24     T   250= 256.91     T   260= 207.30     T   261= 211.48     T   262= 215.42
  T   263= 226.14     T   264= 217.85     T   265= 228.54     T   266= 222.31     T   300= 968.16     T   304= 990.03
  T   305= 730.47     T   310= 848.64     T   313= 790.45     T   315= 675.32     T   316= 675.32     T   320= 843.92
  T   323= 788.23     T   325= 676.26     T   326= 676.26     T   330= 864.75     T   333= 809.13     T   335= 717.89
  T   336= 717.89     T   340= 858.55     T   342= 598.82     T   343= 764.51     T   344= 374.85     T   345= 893.74
  T   346= 854.43     T   347= 582.51     T   349= 663.71     T   350= 289.71     T   351= 372.59     T   352= 294.18
  T   353= 338.05     T   354= 325.33     T   355= 245.85     T   356= 333.71     T   360= 202.50     T   362= 204.83
  T   364= 208.75     T   366= 238.58     T   367= 246.09     T   368= 272.72     T   369= 300.14     T   371= 376.48
  T   373= 343.32     T   375= 277.00     T   377= 243.24     T   400= 204.21     T   401= 216.13     T   402= 239.01
  T   404= 955.51     T   406= 837.66     T   408= 856.10     T   410= 858.06     T   412= 903.63     T   414= 853.53
```

T	421=	499.35	T	422=	885.92	T	423=	876.43	T	424=	294.83	T	425=	1017.4	T	426=	944.85
T	431=	859.04	T	432=	970.37	T	433=	1038.2	T	434=	1036.5	T	435=	975.06	T	436=	858.06
T	950=	1087.9	T	952=	1111.8												

ARITHMETIC NODES IN ASCENDING NODE NUMBER ORDER

T	50=	799.60	T	52=	871.58	T	54=	991.54	T	158=	998.01	T	159=	992.77	T	168=	992.91
T	169=	990.39	T	195=	365.14	T	197=	450.60	T	199=	752.33	T	238=	1013.9	T	311=	766.37
T	312=	766.37	T	321=	764.41	T	322=	764.41	T	331=	786.60	T	332=	786.60	T	337=	692.78
T	341=	656.27	T	357=	339.14	T	358=	369.73	T	359=	292.26	T	379=	243.16	T	403=	241.82
T	1000=	426.36	T	1001=	893.23	T	1002=	756.07	T	1003=	481.53	T	1004=	340.69	T	1005=	336.57
T	1006=	222.96	T	1007=	979.90	T	1008=	999.03	T	1009=	1049.1	T	1010=	470.96	T	1011=	843.05
T	1012=	843.05	T	1013=	711.72	T	1021=	838.54	T	1022=	838.54	T	1023=	711.64	T	1031=	859.58
T	1032=	859.58	T	1033=	745.57	T	1041=	853.72	T	1042=	853.72	T	1043=	606.22	T	1044=	606.22
T	1346=	838.73	T	1347=	474.59												

HEATER NODES IN ASCENDING NODE NUMBER ORDER

++NONE++

BOUNDARY NODES IN ASCENDING NODE NUMBER ORDER

T	1=	100.00	T	2=	100.00									

SYSTEMS IMPROVED NUMERICAL DIFFERENCING ANALYZER '85 (SINDA '85) PAGE 2/4

MODEL = DAMAGE5
FWDBCK

HAC LOAD CASE NO. 5 -- Ungula Distribution, 100F
***** Peak ICV Sidewall Temperature Time Point *****

4/30/94

SUBMODEL NAME = PTSB

	CALCULATED			ALLOWED	
MAX DIFF DELTA T PER ITER	DRLXCC(PTSB	161)=	9.765625E-04	VS. DRLXCA=	5.000000E-02
MAX ARITH DELTA T PER ITER	ARLXCC(PTSB	1004)=	2.166748E-02	VS. ARLXCA=	0.500000
MAX DIFF DEL T PER TIME STEP	DTMPCC(PTSB	423)=	-3.04343	VS. DTMPCA=	10.0000
MAX ARITH DEL T PER TIME STEP	ATMPCC(PTSB	1033)=	-1.41501	VS. ATMPCA=	100.000
MIN STABILITY CRITERIA	CSGMIN(PTSB	455)=	1.183057E-04		
MAX STABILITY CRITERIA	CSGMAX(PTSB	434)=	3.40049		
NUMBER OF ITERATIONS	LOOPCT	=	5	VS. NLOOPT=	600
PROBLEM TIME	TIMEN	=	0.633334	VS. TIMEND=	6.00000
MEAN PROBLEM TIME	TIMEM	=	0.632697		
AVERAGE TIME STEP USED	DTIMEU	=	8.130082E-04	VS. DTIMEI=	0.

DIFFUSION NODES IN ASCENDING NODE NUMBER ORDER

T	51=	776.83	T	53=	818.16	T	55=	902.82	T	60=	871.37	T	62=	1055.0	T	100=	1021.6
T	105=	963.40	T	107=	934.01	T	110=	901.04	T	112=	900.57	T	113=	905.57	T	120=	828.24
T	122=	823.71	T	123=	837.01	T	124=	820.98	T	125=	830.11	T	126=	816.78	T	127=	818.80
T	130=	821.46	T	132=	826.11	T	133=	819.40	T	134=	823.46	T	135=	818.75	T	136=	819.24
T	137=	817.96	T	140=	833.91	T	141=	834.40	T	142=	843.60	T	143=	823.41	T	144=	841.67
T	145=	828.41	T	146=	839.86	T	147=	837.29	T	150=	869.75	T	152=	889.85	T	153=	842.41
T	154=	887.19	T	155=	858.49	T	156=	883.22	T	157=	880.50	T	160=	896.81	T	161=	891.02
T	162=	925.38	T	163=	858.03	T	164=	920.72	T	165=	885.81	T	166=	916.30	T	167=	909.84
T	170=	864.10	T	172=	879.89	T	173=	836.77	T	175=	835.77	T	177=	845.78	T	180=	803.59
T	190=	843.28	T	191=	918.94	T	192=	333.06	T	193=	857.98	T	194=	472.31	T	196=	682.14
T	198=	923.49	T	200=	1057.2	T	204=	1066.0	T	210=	813.62	T	220=	802.26	T	230=	795.55
T	240=	761.01	T	242=	455.43	T	250=	247.15	T	260=	205.02	T	261=	207.97	T	262=	207.42
T	263=	212.42	T	264=	211.87	T	265=	219.53	T	266=	216.66	T	300=	967.31	T	304=	989.61
T	305=	730.35	T	310=	846.93	T	313=	789.24	T	315=	674.59	T	316=	674.59	T	320=	837.59
T	323=	783.74	T	325=	673.45	T	326=	673.45	T	330=	828.50	T	333=	780.02	T	335=	699.24
T	336=	699.24	T	340=	804.37	T	342=	575.52	T	343=	759.14	T	344=	361.25	T	345=	782.76
T	346=	844.48	T	347=	509.91	T	349=	656.56	T	350=	277.09	T	351=	359.52	T	352=	278.25
T	353=	326.75	T	354=	311.35	T	355=	233.13	T	356=	314.26	T	360=	201.56	T	362=	201.85
T	364=	205.39	T	366=	227.56	T	367=	230.62	T	368=	240.45	T	369=	256.00	T	371=	362.88
T	373=	332.34	T	375=	267.30	T	377=	230.66	T	400=	203.09	T	401=	215.35	T	402=	225.51
T	404=	857.72	T	406=	854.99	T	408=	806.05	T	410=	886.10	T	412=	904.26	T	414=	853.53
T	421=	499.16	T	422=	885.92	T	423=	876.57	T	424=	269.95	T	425=	1017.6	T	426=	952.99
T	431=	894.83	T	432=	1068.3	T	433=	280.31	T	434=	249.32	T	435=	1088.9	T	436=	939.10
T	441=	808.88	T	442=	896.70	T	443=	923.97	T	444=	923.82	T	445=	909.26	T	446=	810.43
T	451=	831.25	T	452=	854.45	T	453=	856.59	T	454=	860.28	T	455=	884.38	T	456=	847.20
T	954=	964.66															

ARITHMETIC NODES IN ASCENDING NODE NUMBER ORDER

T	50=	790.71	T	52=	821.06	T	54=	904.92	T	158=	898.00	T	159=	888.10	T	168=	891.21		

T	169=	890.24	T	195=	326.12	T	197=	402.12	T	199=	692.29	T	238=	808.94	T	311=	765.15
T	312=	765.15	T	321=	759.88	T	322=	759.88	T	331=	757.54	T	332=	757.54	T	337=	669.71
T	341=	630.14	T	357=	322.99	T	358=	355.27	T	359=	278.00	T	379=	230.04	T	403=	228.95
T	1000=	364.52	T	1001=	776.35	T	1002=	682.66	T	1003=	423.85	T	1004=	306.65	T	1005=	303.45
T	1006=	213.99	T	1007=	853.59	T	1008=	864.00	T	1009=	902.11	T	1010=	451.74	T	1011=	841.39
T	1012=	841.39	T	1013=	710.83	T	1021=	832.38	T	1022=	832.38	T	1023=	708.26	T	1031=	824.15
T	1032=	824.15	T	1033=	723.39	T	1041=	801.25	T	1042=	801.25	T	1043=	582.56	T	1044=	582.56
T	1346=	767.72	T	1347=	413.07												

HEATER NODES IN ASCENDING NODE NUMBER ORDER
++NONE++

BOUNDARY NODES IN ASCENDING NODE NUMBER ORDER

T	1=	100.00	T	2=	100.00

SYSTEMS IMPROVED NUMERICAL DIFFERENCING ANALYZER '85 (SINDA '85) PAGE 3/4

MODEL = DAMAGE5
FWDBCK

HAC LOAD CASE NO. 5 -- Ungula Distribution, 100F
***** Peak ICV Sidewall Temperature Time Point *****

4/30/94

SUBMODEL NAME = PTSC

		CALCULATED			ALLOWED	
MAX DIFF DELTA T PER ITER	DRLXCC(PTSC	175)=	1.953125E-03	VS. DRLXCA=	5.000000E-02
MAX ARITH DELTA T PER ITER	ARLXCC(PTSC	199)=	2.673340E-02	VS. ARLXCA=	0.500000
MAX DIFF DEL T PER TIME STEP	DTMPCC(PTSC	423)=	-3.04343	VS. DTMPCA=	10.0000
MAX ARITH DEL T PER TIME STEP	ATMPCC(PTSC	1033)=	-1.50632	VS. ATMPCA=	100.000
MIN STABILITY CRITERIA	CSGMIN(PTSC	455)=	1.183103E-04		
MAX STABILITY CRITERIA	CSGMAX(PTSC	434)=	3.40055		
NUMBER OF ITERATIONS	LOOPCT	=	5	VS. NLOOPT=	600
PROBLEM TIME	TIMEN	=	0.633334	VS. TIMEND=	6.00000
MEAN PROBLEM TIME	TIMEM	=	0.632697		
AVERAGE TIME STEP USED	DTIMEU	=	8.130082E-04	VS. DTIMEI=	0.

DIFFUSION NODES IN ASCENDING NODE NUMBER ORDER

T	51=	801.22	T	53=	751.07	T	55=	737.69	T	60=	872.89	T	62=	964.08	T	100=	1006.0
T	105=	971.19	T	107=	954.01	T	110=	938.35	T	112=	935.90	T	113=	939.55	T	120=	873.64
T	122=	865.27	T	123=	875.24	T	124=	873.30	T	125=	879.88	T	126=	885.50	T	127=	886.68
T	130=	819.68	T	132=	818.50	T	133=	817.78	T	134=	821.88	T	135=	821.31	T	136=	827.29
T	137=	827.05	T	140=	790.45	T	141=	790.75	T	142=	795.26	T	143=	787.20	T	144=	793.38
T	145=	787.99	T	146=	791.22	T	147=	790.57	T	150=	767.83	T	152=	782.81	T	153=	760.02
T	154=	774.16	T	155=	758.03	T	156=	761.34	T	157=	757.38	T	160=	734.38	T	161=	738.03
T	162=	759.18	T	163=	723.01	T	164=	745.56	T	165=	719.99	T	166=	725.00	T	167=	719.01
T	170=	626.43	T	172=	642.75	T	173=	619.59	T	175=	568.22	T	177=	591.67	T	180=	562.59
T	190=	520.37	T	191=	501.90	T	192=	250.11	T	193=	635.71	T	194=	315.69	T	196=	543.18
T	198=	505.98	T	200=	1027.0	T	204=	1018.4	T	210=	818.73	T	220=	789.99	T	230=	718.60
T	240=	640.33	T	242=	402.13	T	250=	236.15	T	260=	201.76	T	261=	202.87	T	262=	201.74
T	263=	203.47	T	264=	206.43	T	265=	210.64	T	266=	212.13	T	300=	953.35	T	304=	968.27
T	305=	724.75	T	310=	849.35	T	313=	790.90	T	315=	675.58	T	316=	675.58	T	320=	831.15
T	323=	779.27	T	325=	670.45	T	326=	670.45	T	330=	785.36	T	333=	748.02	T	335=	678.74
T	336=	678.74	T	340=	748.33	T	342=	549.88	T	343=	756.42	T	344=	353.71	T	345=	780.84
T	346=	840.19	T	347=	508.68	T	349=	654.54	T	350=	275.56	T	351=	358.01	T	352=	277.09
T	353=	325.71	T	354=	308.96	T	355=	232.47	T	356=	312.77	T	360=	200.28	T	362=	199.71
T	364=	203.72	T	366=	226.79	T	367=	230.03	T	368=	239.92	T	369=	255.34	T	371=	361.26
T	373=	331.30	T	375=	266.87	T	377=	230.38	T	400=	202.63	T	401=	215.05	T	402=	225.23
T	404=	857.43	T	406=	853.48	T	408=	805.95	T	410=	886.09	T	412=	904.26	T	414=	853.53
T	421=	499.12	T	422=	885.92	T	423=	876.57	T	424=	269.94	T	425=	1017.6	T	426=	952.99
T	431=	894.08	T	432=	1067.5	T	433=	280.28	T	434=	249.31	T	435=	1088.9	T	436=	939.08
T	441=	808.74	T	442=	896.11	T	443=	923.90	T	444=	923.75	T	445=	909.22	T	446=	810.33
T	451=	830.59	T	452=	853.01	T	453=	856.34	T	454=	860.19	T	455=	884.36	T	456=	847.15

ARITHMETIC NODES IN ASCENDING NODE NUMBER ORDER

T	50=	801.05	T	52=	753.90	T	54=	759.06	T	158=	741.70	T	159=	734.71	T	168=	738.43
T	169=	739.79	T	195=	259.81	T	197=	281.56	T	199=	462.42	T	238=	684.59	T	311=	766.84

T	312=	766.84	T	321=	755.24	T	322=	755.24	T	331=	725.09	T	332=	725.09	T	337=	646.58
T	341=	602.57	T	357=	321.10	T	358=	353.51	T	359=	276.66	T	379=	229.37	T	403=	228.67
T	1000=	267.67	T	1001=	475.77	T	1002=	438.43	T	1003=	294.45	T	1004=	239.82	T	1005=	238.63
T	1006=	204.67	T	1007=	539.23	T	1008=	522.53	T	1009=	508.20	T	1010=	353.40	T	1011=	843.73
T	1012=	843.73	T	1013=	712.06	T	1021=	826.10	T	1022=	826.10	T	1023=	704.74	T	1031=	782.00
T	1032=	782.00	T	1033=	698.91	T	1041=	746.73	T	1042=	746.73	T	1043=	556.53	T	1044=	556.53
T	1346=	765.34	T	1347=	412.08												

HEATER NODES IN ASCENDING NODE NUMBER ORDER

++NONE++

BOUNDARY NODES IN ASCENDING NODE NUMBER ORDER

T	1=	100.00	T	2=	100.00

SYSTEMS IMPROVED NUMERICAL DIFFERENCING ANALYZER '85 (SINDA '85) PAGE 4/4

MODEL = DAMAGES
FWDBCK

***** HAC LOAD CASE NO. 5 -- Ungula Distribution, 100F
Peak ICV Sidewall Temperature Time Point ***** 4/30/94

SUBMODEL NAME = PTSD

	CALCULATED		ALLOWED
MAX DIFF DELTA T PER ITER	DRLXCC(PTSD	175)=-7.019043E-03	VS. DRLXCA= 5.000000E-02
MAX ARITH DELTA T PER ITER	ARLXCC(PTSD	1007)=-3.198242E-02	VS. ARLXCA= 0.500000
MAX DIFF DEL T PER TIME STEP	DTMPCC(PTSD	423)= -3.04343	VS. DTMPCA= 10.0000
MAX ARITH DEL T PER TIME STEP	ATMPCC(PTSD	1033)= -1.50449	VS. ATMPCA= 100.000
MIN STABILITY CRITERIA	CSGMIN(PTSD	455)= 1.181964E-04	
MAX STABILITY CRITERIA	CSGMAX(PTSD	434)= 3.40055	
NUMBER OF ITERATIONS	LOOPCT	= 5	VS. NLOOPT= 600
PROBLEM TIME	TIMEN	= 0.633334	VS. TIMEND= 6.00000
MEAN PROBLEM TIME	TIMEM	= 0.632697	
AVERAGE TIME STEP USED	DTIMEU	= 8.130082E-04	VS. DTIMEI= 0.

DIFFUSION NODES IN ASCENDING NODE NUMBER ORDER

T	51=	805.04	T	53=	731.68	T	55=	691.74	T	60=	872.52	T	62=	947.40	T	100=	1006.4
T	105=	973.51	T	107=	957.06	T	110=	941.95	T	112=	942.05	T	113=	942.40	T	120=	880.38
T	122=	878.18	T	123=	879.18	T	124=	882.18	T	125=	882.76	T	126=	887.74	T	127=	887.78
T	130=	817.16	T	132=	815.82	T	133=	815.06	T	134=	819.60	T	135=	818.99	T	136=	825.58
T	137=	825.36	T	140=	779.99	T	141=	780.25	T	142=	780.45	T	143=	778.61	T	144=	781.73
T	145=	780.69	T	146=	785.36	T	147=	785.64	T	150=	747.39	T	152=	749.79	T	153=	745.82
T	154=	749.14	T	155=	746.07	T	156=	750.43	T	157=	749.86	T	160=	698.68	T	161=	706.76
T	162=	703.85	T	163=	697.18	T	164=	703.76	T	165=	699.75	T	166=	707.12	T	167=	706.59
T	170=	588.80	T	172=	590.44	T	173=	586.93	T	175=	534.94	T	177=	555.13	T	180=	530.08
T	190=	499.50	T	191=	478.07	T	192=	246.75	T	193=	627.93	T	194=	310.41	T	196=	495.18
T	198=	481.98	T	200=	1026.2	T	204=	1018.1	T	210=	817.94	T	220=	786.68	T	230=	724.58
T	240=	637.71	T	242=	400.60	T	250=	235.80	T	260=	201.32	T	261=	202.29	T	262=	201.44
T	263=	203.04	T	264=	206.16	T	265=	210.22	T	266=	211.96	T	300=	952.74	T	304=	968.00
T	305=	724.66	T	310=	848.81	T	313=	790.48	T	315=	675.29	T	316=	675.29	T	320=	829.29
T	323=	777.92	T	325=	669.55	T	326=	669.55	T	330=	788.29	T	333=	749.51	T	335=	679.71
T	336=	679.71	T	340=	748.15	T	342=	549.64	T	343=	756.48	T	344=	353.63	T	345=	780.87
T	346=	840.31	T	347=	508.69	T	349=	654.60	T	350=	275.54	T	351=	358.01	T	352=	277.08
T	353=	325.71	T	354=	308.93	T	355=	232.46	T	356=	312.76	T	360=	200.08	T	362=	199.59
T	364=	203.65	T	366=	226.77	T	367=	230.02	T	368=	239.92	T	369=	255.34	T	371=	361.26
T	373=	331.30	T	375=	266.86	T	377=	230.38	T	400=	202.61	T	401=	215.03	T	402=	225.22
T	404=	857.44	T	406=	853.54	T	408=	805.95	T	410=	886.09	T	412=	904.26	T	414=	853.53
T	421=	499.12	T	422=	885.92	T	423=	876.57	T	424=	269.94	T	425=	1017.6	T	426=	952.99
T	431=	894.11	T	432=	1067.5	T	433=	280.28	T	434=	249.31	T	435=	1088.9	T	436=	939.08
T	441=	808.75	T	442=	896.13	T	443=	923.90	T	444=	923.76	T	445=	909.22	T	446=	810.34
T	451=	830.62	T	452=	853.06	T	453=	856.35	T	454=	860.19	T	455=	884.36	T	456=	847.15

ARITHMETIC NODES IN ASCENDING NODE NUMBER ORDER

T	50=	801.43	T	52=	734.47	T	54=	719.10	T	158=	708.21	T	159=	707.09	T	168=	706.85
T	169=	707.19	T	195=	254.12	T	197=	275.91	T	199=	451.89	T	238=	686.88	T	311=	766.43

T	312=	766.43	T	321=	753.87	T	322=	753.87	T	331=	726.56	T	332=	726.56	T	337=	646.46
T	341=	602.38	T	357=	321.08	T	358=	353.51	T	359=	276.64	T	379=	229.36	T	403=	228.66
T	1000=	263.97	T	1001=	448.62	T	1002=	426.89	T	1003=	286.20	T	1004=	237.17	T	1005=	236.05
T	1006=	204.06	T	1007=	512.09	T	1008=	498.87	T	1009=	484.42	T	1010=	349.94	T	1011=	843.20
T	1012=	843.20	T	1013=	711.73	T	1021=	824.29	T	1022=	824.29	T	1023=	703.69	T	1031=	784.84
T	1032=	784.84	T	1033=	700.06	T	1041=	746.62	T	1042=	746.62	T	1043=	556.37	T	1044=	556.37
T	1346=	765.39	T	1347=	412.09												

HEATER NODES IN ASCENDING NODE NUMBER ORDER

++NONE++

BOUNDARY NODES IN ASCENDING NODE NUMBER ORDER

T	1=	100.00	T	2=	100.00

SYSTEMS IMPROVED NUMERICAL DIFFERENCING ANALYZER '85 ($INDA '85) PAGE 1/4

MODEL = DAMAGE5
STDSTL

HAC LOAD CASE NO. 5 -- Ungula Distribution, 100F
*** Steady-state Conditions After The Fire ***

4/30/94 9am

SUBMODEL NAME = MAIN

PROBLEM TIME TIMEN = 999.000 VS. TIMEND= 999.000

DIFFUSION NODES IN ASCENDING NODE NUMBER ORDER

T 267= 342.07 T 268= 342.30 T 269= 338.82

ARITHMETIC NODES IN ASCENDING NODE NUMBER ORDER

T 201= 389.52 T 1266= 347.61 T 1267= 412.88 T 1268= 397.16 T 1269= 352.26

HEATER NODES IN ASCENDING NODE NUMBER ORDER

++NONE++

BOUNDARY NODES IN ASCENDING NODE NUMBER ORDER

++NONE++

MEAN ICV GAS TEMP= 389.5 F MEAN ICV GAS PRESSURE= 25.50 PSIA
MEAN ICV-OCV GAS TEMP= 263.4 F MEAN ICV-OCV GAS PRESSURE= 25.50 PSIA

SUBMODEL NAME = PTSA

		CALCULATED		ALLOWED	
MAX DIFF DELTA T PER ITER	DRLXCC(PTSA	375)=-0.705322	VS. DRLXCA=	5.000000E-02	
MAX ARITH DELTA T PER ITER	ARLXCC(PTSA	1000)=-0.498962	VS. ARLXCA=	0.500000	
MAX SYSTEM ENERGY BALANCE	EBALSC	= -6.56009	VS. EBALSA * ESUMIS	=	4.07869
			EBALSA=	1.000000E-03	
ENERGY INTO AND OUT OF SYS	ESUMIS	= 4078.69	ESUMOS=	1331.31	
MAX NODAL ENERGY BALANCE	EBALNC(PTSA	367)=-0.778349	VS. EBALNA=	1.000000E-02	
NUMBER OF ITERATIONS	LOOPCT	= 133	VS. NLOOPS=	1000	
PROBLEM TIME	TIMEN	= 999.000	VS. TIMEND=	999.000	

DIFFUSION NODES IN ASCENDING NODE NUMBER ORDER

T 51= 365.10	T 53= 508.26	T 55= 676.82	T 60= 342.22	T 62= 686.73	T 100= 310.07
T 105= 318.49	T 107= 321.77	T 110= 324.58	T 112= 325.50	T 113= 321.94	T 120= 349.09
T 122= 352.46	T 123= 343.24	T 124= 353.74	T 125= 346.26	T 126= 356.77	T 127= 352.95
T 130= 423.70	T 132= 431.63	T 133= 413.82	T 134= 431.91	T 135= 417.80	T 136= 431.00
T 137= 424.87	T 140= 500.11	T 141= 501.55	T 142= 506.25	T 143= 483.62	T 144= 514.19
T 145= 497.84	T 146= 531.11	T 147= 524.60	T 150= 614.27	T 152= 622.31	T 153= 585.77
T 154= 636.84	T 155= 615.24	T 156= 659.73	T 157= 660.04	T 160= 707.86	T 161= 694.74
T 162= 717.70	T 163= 676.86	T 164= 728.14	T 165= 710.76	T 166= 745.57	T 167= 739.21
T 170= 738.94	T 172= 742.62	T 173= 719.77	T 175= 747.80	T 177= 741.05	T 180= 727.25
T 190= 788.07	T 191= 842.70	T 192= 467.97	T 193= 733.27	T 194= 503.56	T 196= 636.40
T 198= 844.97	T 200= 259.04	T 204= 253.86	T 210= 279.30	T 220= 307.33	T 230= 422.55
T 240= 518.35	T 242= 391.97	T 250= 323.32	T 260= 304.74	T 261= 307.72	T 262= 320.85
T 263= 327.95	T 264= 315.88	T 265= 322.32	T 266= 310.96	T 300= 205.12	T 304= 193.34
T 305= 135.64	T 310= 240.51	T 313= 223.41	T 315= 203.15	T 316= 203.15	T 320= 266.23
T 323= 245.82	T 325= 221.70	T 326= 221.70	T 330= 363.53	T 333= 335.22	T 335= 293.74
T 336= 293.74	T 340= 394.79	T 342= 340.90	T 343= 244.12	T 344= 300.63	T 345= 238.92
T 346= 224.13	T 347= 266.28	T 349= 231.99	T 350= 286.17	T 351= 278.94	T 352= 284.65
T 353= 281.44	T 354= 287.13	T 355= 285.93	T 356= 283.40	T 360= 299.71	T 362= 310.13
T 364= 303.42	T 366= 287.32	T 367= 284.99	T 368= 281.21	T 369= 278.72	T 371= 279.03
T 373= 280.63	T 375= 282.22	T 377= 283.73	T 400= 300.82	T 401= 298.35	T 402= 283.82
T 404= 221.90	T 406= 146.63	T 408= 118.95	T 410= 105.82	T 412= 107.09	T 414= 108.19

T	421=	237.99	T	422=	118.48	T	423=	112.46	T	424=	220.98	T	425=	116.59	T	426=	112.08
T	431=	137.60	T	432=	137.53	T	433=	131.70	T	434=	122.90	T	435=	113.87	T	436=	117.33
T	950=	798.86	T	952=	868.06												

ARITHMETIC NODES IN ASCENDING NODE NUMBER ORDER

T	50=	382.25	T	52=	509.29	T	54=	655.15	T	158=	699.90	T	159=	694.59	T	168=	694.19
T	169=	691.92	T	195=	398.30	T	197=	443.38	T	199=	628.61	T	238=	671.56	T	311=	221.95
T	312=	221.95	T	321=	244.12	T	322=	244.12	T	331=	332.23	T	332=	332.23	T	337=	318.52
T	341=	337.76	T	357=	283.88	T	358=	279.43	T	359=	285.62	T	379=	286.10	T	403=	283.76
T	1000=	437.55	T	1001=	735.43	T	1002=	636.15	T	1003=	520.78	T	1004=	435.85	T	1005=	431.60
T	1006=	321.37	T	1007=	779.36	T	1008=	797.59	T	1009=	828.90	T	1010=	436.49	T	1011=	240.12
T	1012=	240.12	T	1013=	210.44	T	1021=	265.73	T	1022=	265.73	T	1023=	230.37	T	1031=	362.60
T	1032=	362.60	T	1033=	308.53	T	1041=	393.16	T	1042=	393.16	T	1043=	340.45	T	1044=	340.45
T	1346=	228.68	T	1347=	271.39												

HEATER NODES IN ASCENDING NODE NUMBER ORDER

++NONE++

BOUNDARY NODES IN ASCENDING NODE NUMBER ORDER

T	1=	100.00	T	2=	100.00

SYSTEMS IMPROVED NUMERICAL DIFFERENCING ANALYZER '85 (SINDA '85) PAGE 2/4

MODEL = DAMAGE5
STDSTL

HAC LOAD CASE NO. 5 -- Ungula Distribution, 100F
*** Steady-state Conditions After The Fire ***

4/30/94 9am

SUBMODEL NAME = PTSB

		CALCULATED			ALLOWED	
MAX DIFF DELTA T PER ITER	DRLXCC(PTSB	353)= 0.302795	VS.	DRLXCA= 5.000000E-02		
MAX ARITH DELTA T PER ITER	ARLXCC(PTSB	1004)= 0.249817	VS.	ARLXCA= 0.500000		
MAX SYSTEM ENERGY BALANCE	EBALSC	= -1.02327	VS.	EBALSA * ESUMIS	=	3.60058
				EBALSA= 1.000000E-03		
ENERGY INTO AND OUT OF SYS	ESUMIS	= 3600.58		ESUMOS= 2234.74		
MAX NODAL ENERGY BALANCE	EBALNC(PTSB	330)=-0.586719	VS.	EBALNA= 1.000000E-02		
NUMBER OF ITERATIONS	LOOPCT	= 133	VS.	NLOOPS= 1000		
PROBLEM TIME	TIMEN	= 999.000	VS.	TIMEND= 999.000		

DIFFUSION NODES IN ASCENDING NODE NUMBER ORDER

T	51=	343.28	T	53=	452.72	T	55=	586.47	T	60=	325.48	T	62=	601.25	T	100=	300.43
T	105=	307.14	T	107=	309.77	T	110=	312.14	T	112=	314.34	T	113=	309.50	T	120=	330.69
T	122=	337.00	T	123=	323.30	T	124=	336.10	T	125=	324.99	T	126=	334.46	T	127=	329.06
T	130=	387.77	T	132=	401.36	T	133=	373.68	T	134=	398.19	T	135=	376.18	T	136=	390.82
T	137=	380.94	T	140=	446.28	T	141=	447.41	T	142=	460.97	T	143=	425.92	T	144=	462.87
T	145=	436.39	T	146=	467.54	T	147=	457.18	T	150=	531.60	T	152=	557.29	T	153=	491.13
T	154=	563.81	T	155=	519.19	T	156=	573.90	T	157=	566.53	T	160=	610.81	T	161=	600.31
T	162=	641.47	T	163=	562.66	T	164=	644.45	T	165=	601.11	T	166=	651.71	T	167=	637.37
T	170=	645.72	T	172=	660.81	T	173=	617.37	T	175=	656.60	T	177=	649.50	T	180=	643.59
T	190=	688.26	T	191=	727.34	T	192=	425.37	T	193=	630.98	T	194=	457.28	T	196=	578.68
T	198=	728.97	T	200=	259.01	T	204=	253.23	T	210=	275.20	T	220=	292.82	T	230=	355.43
T	240=	417.10	T	242=	342.55	T	250=	296.56	T	260=	293.40	T	261=	295.80	T	262=	297.85
T	263=	301.60	T	264=	293.15	T	265=	297.60	T	266=	288.28	T	300=	205.24	T	304=	192.88
T	305=	135.44	T	310=	237.25	T	313=	220.56	T	315=	200.83	T	316=	200.83	T	320=	254.05
T	323=	235.26	T	325=	213.06	T	326=	213.06	T	330=	308.42	T	333=	285.74	T	335=	254.14
T	336=	254.14	T	340=	326.97	T	342=	298.89	T	343=	224.29	T	344=	274.74	T	345=	222.41
T	346=	205.54	T	347=	247.52	T	349=	214.93	T	350=	266.13	T	351=	258.91	T	352=	264.61
T	353=	261.79	T	354=	266.06	T	355=	266.55	T	356=	263.14	T	360=	288.91	T	362=	291.21
T	364=	283.42	T	366=	267.84	T	367=	265.83	T	368=	262.88	T	369=	260.76	T	371=	258.85
T	373=	260.96	T	375=	263.42	T	377=	264.70	T	400=	283.54	T	401=	281.22	T	402=	264.93
T	404=	211.46	T	406=	138.84	T	408=	114.84	T	410=	105.73	T	412=	106.52	T	414=	107.52
T	421=	226.08	T	422=	116.97	T	423=	111.42	T	424=	210.40	T	425=	115.07	T	426=	110.06
T	431=	166.35	T	432=	150.29	T	433=	169.02	T	434=	144.07	T	435=	109.44	T	436=	109.42
T	441=	121.30	T	442=	126.78	T	443=	119.47	T	444=	116.80	T	445=	110.83	T	446=	113.24
T	451=	125.21	T	452=	133.44	T	453=	119.38	T	454=	114.80	T	455=	108.10	T	456=	110.86
T	954=	750.75															

ARITHMETIC NODES IN ASCENDING NODE NUMBER ORDER

T	50=	356.41	T	52=	453.75	T	54=	570.16	T	158=	609.16	T	159=	596.40	T	168=	599.73
T	169=	597.87	T	195=	369.51	T	197=	415.17	T	199=	570.17	T	238=	429.65	T	311=	219.15

T	312=	219.15	T	321=	233.68	T	322=	233.68	T	331=	283.59	T	332=	283.59	T	337=	279.27
T	341=	294.32	T	357=	263.22	T	358=	259.17	T	359=	265.34	T	379=	266.77	T	403=	264.78
T	1000=	399.74	T	1001=	644.44	T	1002=	570.56	T	1003=	468.10	T	1004=	398.25	T	1005=	394.74
T	1006=	302.51	T	1007=	680.82	T	1008=	694.69	T	1009=	717.38	T	1010=	398.60	T	1011=	236.87
T	1012=	236.87	T	1013=	207.96	T	1021=	253.61	T	1022=	253.61	T	1023=	221.05	T	1031=	307.78
T	1032=	307.78	T	1033=	265.44	T	1041=	325.97	T	1042=	325.97	T	1043=	298.47	T	1044=	298.47
T	1346=	212.37	T	1347=	253.12												

HEATER NODES IN ASCENDING NODE NUMBER ORDER
++NONE++

BOUNDARY NODES IN ASCENDING NODE NUMBER ORDER

T	1=	100.00	T	2=	100.00

SYSTEMS IMPROVED NUMERICAL DIFFERENCING ANALYZER '85 (SINDA '85) PAGE 3/4

MODEL = DAMAGE5
STDSTL

HAC LOAD CASE NO. 5 -- Ungula Distribution, 100F
*** Steady-state Conditions After The Fire *** 4/30/94 9am

SUBMODEL NAME = PTSC

		CALCULATED			ALLOWED	
MAX DIFF DELTA T PER ITER	DRLXCC(PTSC	192)=	-0.275635	VS. DRLXCA=	5.000000E-02	
MAX ARITH DELTA T PER ITER	ARLXCC(PTSC	1347)=	0.276428	VS. ARLXCA=	0.500000	
MAX SYSTEM ENERGY BALANCE	EBALSC	=	-12.5452	VS. EBALSA * ESUMIS	=	0.
				EBALSA=	1.000000E-03	
ENERGY INTO AND OUT OF SYS	ESUMIS	=	0.	ESUMOS=	2538.85	
MAX NODAL ENERGY BALANCE	EBALNC(PTSC	330)=	-1.20876	VS. EBALNA=	1.000000E-02	
NUMBER OF ITERATIONS	LOOPCT	=	133	VS. NLOOPS=	1000	
PROBLEM TIME	TIMEN	=	999.000	VS. TIMEND=	999.000	

DIFFUSION NODES IN ASCENDING NODE NUMBER ORDER

T	51=	309.17	T	53=	356.34	T	55=	406.47	T	60=	298.46	T	62=	392.66	T	100=	285.35
T	105=	288.95	T	107=	290.34	T	110=	292.02	T	112=	293.82	T	113=	291.11	T	120=	303.20
T	122=	307.91	T	123=	299.84	T	124=	304.36	T	125=	297.77	T	126=	297.13	T	127=	293.81
T	130=	331.17	T	132=	341.45	T	133=	324.87	T	134=	334.15	T	135=	320.67	T	136=	318.91
T	137=	312.20	T	140=	353.02	T	141=	353.19	T	142=	365.81	T	143=	345.49	T	144=	356.38
T	145=	339.71	T	146=	334.97	T	147=	327.48	T	150=	376.62	T	152=	401.80	T	153=	360.02
T	154=	387.10	T	155=	353.43	T	156=	355.21	T	157=	337.35	T	160=	408.50	T	161=	400.07
T	162=	441.03	T	163=	388.51	T	164=	420.41	T	165=	376.96	T	166=	378.14	T	167=	359.72
T	170=	392.55	T	172=	412.27	T	173=	384.84	T	175=	381.47	T	177=	387.12	T	180=	383.01
T	190=	360.35	T	191=	358.54	T	192=	295.48	T	193=	325.01	T	194=	290.76	T	196=	412.17
T	198=	358.23	T	200=	262.30	T	204=	258.92	T	210=	273.54	T	220=	277.23	T	230=	262.16
T	240=	256.81	T	242=	246.63	T	250=	244.12	T	260=	266.09	T	261=	266.94	T	262=	255.99
T	263=	256.98	T	264=	248.84	T	265=	250.64	T	266=	243.17	T	300=	207.08	T	304=	195.54
T	305=	136.35	T	310=	235.56	T	313=	219.12	T	315=	199.66	T	316=	199.66	T	320=	239.86
T	323=	222.93	T	325=	202.94	T	326=	202.94	T	330=	228.97	T	333=	213.07	T	335=	195.16
T	336=	195.16	T	340=	226.73	T	342=	226.37	T	343=	189.67	T	344=	225.99	T	345=	190.65
T	346=	173.59	T	347=	210.67	T	349=	183.92	T	350=	225.49	T	351=	219.56	T	352=	224.70
T	353=	222.13	T	354=	224.01	T	355=	227.42	T	356=	222.83	T	360=	262.81	T	362=	253.41
T	364=	242.80	T	366=	228.43	T	367=	226.96	T	368=	225.08	T	369=	223.47	T	371=	219.40
T	373=	221.49	T	375=	224.44	T	377=	226.11	T	400=	247.74	T	401=	245.75	T	402=	226.40
T	404=	184.53	T	406=	128.65	T	408=	110.95	T	410=	104.34	T	412=	105.09	T	414=	106.11
T	421=	201.35	T	422=	113.77	T	423=	109.26	T	424=	184.77	T	425=	111.72	T	426=	107.82
T	431=	150.12	T	432=	137.85	T	433=	152.27	T	434=	133.51	T	435=	107.18	T	436=	107.10
T	441=	115.87	T	442=	119.75	T	443=	114.52	T	444=	112.50	T	445=	108.04	T	446=	109.77
T	451=	118.60	T	452=	124.54	T	453=	114.33	T	454=	110.97	T	455=	106.07	T	456=	108.05

ARITHMETIC NODES IN ASCENDING NODE NUMBER ORDER

T	50=	314.50	T	52=	356.36	T	54=	398.66	T	158=	404.33	T	159=	392.14	T	168=	400.59
T	169=	401.93	T	195=	286.26	T	197=	284.49	T	199=	317.13	T	238=	259.81	T	311=	217.72
T	312=	217.72	T	321=	221.51	T	322=	221.51	T	331=	211.83	T	332=	211.83	T	337=	213.49

T	341=	221.83	T	357=	222.48	T	358=	219.45	T	359=	225.07	T	379=	227.63	T	403=	226.21
T	1000=	281.73	T	1001=	361.81	T	1002=	317.50	T	1003=	308.02	T	1004=	288.25	T	1005=	287.40
T	1006=	263.84	T	1007=	370.04	T	1008=	363.21	T	1009=	359.97	T	1010=	268.79	T	1011=	235.19
T	1012=	235.19	T	1013=	206.69	T	1021=	239.47	T	1022=	239.47	T	1023=	210.13	T	1031=	228.62
T	1032=	228.62	T	1033=	201.59	T	1041=	226.42	T	1042=	226.42	T	1043=	226.06	T	1044=	226.06
T	1346=	182.16	T	1347=	216.20												

HEATER NODES IN ASCENDING NODE NUMBER ORDER

++NONE++

BOUNDARY NODES IN ASCENDING NODE NUMBER ORDER

T	1=	100.00	T	2=	100.00

SYSTEMS IMPROVED NUMERICAL DIFFERENCING ANALYZER '85 (SINDA '85) PAGE 4/4

MODEL = DAMAGE5
STDSTL

HAC LOAD CASE NO. 5 -- Ungula Distribution, 100F
*** Steady-state Conditions After The Fire ***

4/30/94 9am

SUBMODEL NAME = PTSD

		CALCULATED		ALLOWED	
MAX DIFF DELTA T PER ITER	DRLXCC(PTSD	62)=	-0.125122	VS. DRLXCA=	5.000000E-02
MAX ARITH DELTA T PER ITER	ARLXCC(PTSD	54)=	-9.307861E-02	VS. ARLXCA=	0.500000
MAX SYSTEM ENERGY BALANCE	EBALSC	=	-8.51626	VS. EBALSA * ESUMIS =	0.
				EBALSA=	1.000000E-03
ENERGY INTO AND OUT OF SYS	ESUMIS	=	0.	ESUMOS=	1608.57
MAX NODAL ENERGY BALANCE	EBALNC(PTSD	367)=	-1.56687	VS. EBALNA=	1.000000E-02
NUMBER OF ITERATIONS	LOOPCT	=	133	VS. NLOOPS=	1000
PROBLEM TIME	TIMEN	=	999.000	VS. TIMEND=	999.000

DIFFUSION NODES IN ASCENDING NODE NUMBER ORDER

T	51=	294.22	T	53=	318.29	T	55=	340.36	T	60=	286.77	T	62=	334.79	T	100=	278.22
T	105=	280.86	T	107=	281.89	T	110=	283.20	T	112=	284.01	T	113=	283.02	T	120=	291.28
T	122=	293.15	T	123=	290.28	T	124=	291.10	T	125=	288.73	T	126=	287.30	T	127=	286.07
T	130=	307.49	T	132=	311.50	T	133=	305.79	T	134=	307.73	T	135=	303.01	T	136=	300.34
T	137=	297.83	T	140=	318.20	T	141=	318.24	T	142=	322.78	T	143=	316.45	T	144=	318.17
T	145=	312.97	T	146=	308.19	T	147=	306.19	T	150=	325.51	T	152=	332.85	T	153=	321.63
T	154=	327.20	T	155=	317.79	T	156=	315.27	T	157=	309.58	T	160=	341.27	T	161=	337.15
T	162=	351.02	T	163=	336.77	T	164=	343.54	T	165=	330.73	T	166=	328.81	T	167=	323.81
T	170=	333.49	T	172=	338.23	T	173=	332.32	T	175=	330.25	T	177=	331.87	T	180=	331.50
T	190=	323.36	T	191=	321.24	T	192=	270.36	T	193=	308.03	T	194=	268.57	T	196=	349.63
T	198=	320.88	T	200=	260.77	T	204=	256.30	T	210=	269.79	T	220=	269.66	T	230=	263.77
T	240=	244.19	T	242=	230.56	T	250=	226.95	T	260=	249.00	T	261=	249.67	T	262=	237.60
T	263=	238.41	T	264=	230.91	T	265=	232.47	T	266=	225.96	T	300=	206.28	T	304=	194.03
T	305=	135.78	T	310=	232.60	T	313=	216.52	T	315=	197.50	T	316=	197.50	T	320=	233.92
T	323=	217.76	T	325=	198.70	T	326=	198.70	T	330=	226.13	T	333=	209.08	T	335=	191.80
T	336=	191.80	T	340=	219.15	T	342=	214.16	T	343=	180.16	T	344=	211.66	T	345=	180.71
T	346=	166.66	T	347=	197.92	T	349=	175.02	T	350=	210.66	T	351=	205.68	T	352=	209.96
T	353=	207.82	T	354=	209.53	T	355=	212.17	T	356=	208.44	T	360=	246.13	T	362=	235.55
T	364=	225.76	T	366=	213.07	T	367=	211.76	T	368=	210.07	T	369=	208.69	T	371=	205.52
T	373=	207.29	T	375=	209.78	T	377=	211.18	T	400=	230.88	T	401=	229.07	T	402=	211.31
T	404=	174.55	T	406=	126.32	T	408=	109.72	T	410=	103.87	T	412=	104.53	T	414=	105.45
T	421=	189.76	T	422=	112.27	T	423=	108.26	T	424=	174.70	T	425=	110.39	T	426=	106.95
T	431=	144.64	T	432=	134.27	T	433=	146.29	T	434=	129.63	T	435=	106.38	T	436=	106.31
T	441=	114.23	T	442=	117.93	T	443=	112.93	T	444=	111.10	T	445=	107.14	T	446=	108.68
T	451=	116.87	T	452=	122.44	T	453=	112.86	T	454=	109.77	T	455=	105.40	T	456=	107.16

ARITHMETIC NODES IN ASCENDING NODE NUMBER ORDER

T	50=	296.76	T	52=	318.15	T	54=	336.94	T	158=	338.19	T	159=	334.62	T	168=	337.40
T	169=	337.96	T	195=	263.32	T	197=	262.12	T	199=	292.58	T	238=	255.20	T	311=	215.16
T	312=	215.16	T	321=	216.42	T	322=	216.42	T	331=	207.80	T	332=	207.80	T	337=	203.06

T	341=	210.66	T	357=	208.18	T	358=	205.58	T	359=	210.29	T	379=	212.35	T	403=	211.22		
T	1000=	260.25	T	1001=	319.93	T	1002=	291.46	T	1003=	279.69	T	1004=	264.71	T	1005=	264.06		
T	1006=	245.79	T	1007=	326.26	T	1008=	323.86	T	1009=	322.04	T	1010=	249.52	T	1011=	232.24		
T	1012=	232.24	T	1013=	204.38	T	1021=	233.55	T	1022=	233.55	T	1023=	205.56	T	1031=	225.77		
T	1032=	225.77	T	1033=	198.00	T	1041=	218.90	T	1042=	218.90	T	1043=	213.98	T	1044=	213.98		
T	1346=	173.51	T	1347=	202.54														

HEATER NODES IN ASCENDING NODE NUMBER ORDER

++NONE++

BOUNDARY NODES IN ASCENDING NODE NUMBER ORDER

T	1=	100.00	T	2=	100.00														

SYSTEMS IMPROVED NUMERICAL DIFFERENCING ANALYZER '85 (SINDA '85) PAGE 1/4

MODEL = DAMAGE6 LOAD CASE NO. 6 CONDITIONS - Ungula Distributions, -20F 4/30/94
FWDBCK ***** PEAK OCV SIDEWALL TEMPERATURE TIME POINT *****

SUBMODEL NAME = MAIN

MEAN PROBLEM TIME TIMEM = 0.500000

DIFFUSION NODES IN ASCENDING NODE NUMBER ORDER

T 267= 127.13 T 268= 126.98 T 269= 120.10

ARITHMETIC NODES IN ASCENDING NODE NUMBER ORDER

T 201= 714.43 T 1266= 144.84 T 1267= 308.34 T 1268= 258.70 T 1269= 155.64

HEATER NODES IN ASCENDING NODE NUMBER ORDER

++NONE++

BOUNDARY NODES IN ASCENDING NODE NUMBER ORDER

++NONE++

MEAN ICV GAS TEMP= 714.4 F MEAN ICV GAS PRESSURE= 35.24 PSIA
MEAN ICV-OCV GAS TEMP= 790.2 F MEAN ICV-OCV GAS PRESSURE= 44.06 PSIA

SUBMODEL NAME = PTSA

	CALCULATED			ALLOWED
MAX DIFF DELTA T PER ITER	DRLXCC(PTSA	240)=	2.441406E-04 VS. DRLXCA=	5.000000E-02
MAX ARITH DELTA T PER ITER	ARLXCC(PTSA	1346)=	-0.108032 VS. ARLXCA=	0.500000
MAX DIFF DEL T PER TIME STEP	DTMPCC(PTSA	240)=	2.746582E-04 VS. DTMPCA=	10.0000
MAX ARITH DEL T PER TIME STEP	ATMPCC(PTSA	1346)=	-0.108002 VS. ATMPCA=	100.000
MIN STABILITY CRITERIA	CSGMIN(PTSA	431)=	3.040860E-05	
MAX STABILITY CRITERIA	CSGMAX(PTSA	424)=	1.96050	
NUMBER OF ITERATIONS	LOOPCT	=	1 VS. NLOOPT=	600
PROBLEM TIME	TIMEM	=	0.500000 VS. TIMEND=	0.500000
MEAN PROBLEM TIME	TIMEM	=	0.500000	
AVERAGE TIME STEP USED	DTIMEU	=	1.666667E-02 VS. DTIMEI=	0.

DIFFUSION NODES IN ASCENDING NODE NUMBER ORDER

T 51= 691.41	T 53= 810.51	T 55= 959.38	T 60= 819.11	T 62= 1048.6	T 100= 971.94
T 105= 871.05	T 107= 827.62	T 110= 784.09	T 112= 784.17	T 113= 784.91	T 120= 685.18
T 122= 684.77	T 123= 685.48	T 124= 682.71	T 125= 683.11	T 126= 681.25	T 127= 681.21
T 130= 707.75	T 132= 713.73	T 133= 701.09	T 134= 712.70	T 135= 703.48	T 136= 711.58
T 137= 708.80	T 140= 755.04	T 141= 755.42	T 142= 761.47	T 143= 739.44	T 144= 766.78
T 145= 752.35	T 146= 779.08	T 147= 775.50	T 150= 850.74	T 152= 860.13	T 153= 819.44
T 154= 869.29	T 155= 846.94	T 156= 882.73	T 157= 883.11	T 160= 919.45	T 161= 906.85
T 162= 932.07	T 163= 882.25	T 164= 939.65	T 165= 918.78	T 166= 952.48	T 167= 948.31
T 170= 895.81	T 172= 899.79	T 173= 869.22	T 175= 866.63	T 177= 876.32	T 180= 816.80
T 190= 889.41	T 191= 1017.7	T 192= 253.65	T 193= 902.11	T 194= 412.58	T 196= 618.90
T 198= 1021.1	T 200= 1056.0	T 204= 1079.6	T 210= 663.82	T 220= 658.93	T 230= 694.80
T 240= 737.03	T 242= 329.90	T 250= 127.96	T 260= 99.195	T 261= 103.03	T 262= 102.62
T 263= 111.20	T 264= 101.57	T 265= 110.12	T 266= 102.33	T 300= 1210.9	T 304= 1219.1
T 305= 1372.6	T 310= 901.58	T 313= 1087.0	T 315= 1273.1	T 316= 1273.1	T 320= 892.16
T 323= 1079.7	T 325= 1267.2	T 326= 1267.2	T 330= 882.74	T 333= 1055.3	T 335= 1246.9
T 336= 1246.9	T 340= 882.55	T 342= 538.16	T 343= 1015.0	T 344= 243.17	T 345= 907.05
T 346= 1250.5	T 347= 455.98	T 349= 1020.1	T 350= 153.35	T 351= 331.40	T 352= 156.76
T 353= 242.93	T 354= 194.77	T 355= 116.65	T 356= 203.81	T 360= 95.051	T 362= 94.837
T 364= 93.893	T 366= 108.71	T 367= 113.45	T 368= 136.18	T 369= 153.45	T 371= 342.56
T 373= 249.87	T 375= 155.03	T 377= 118.10	T 400= 92.955	T 401= 100.82	T 402= 113.27
T 404= 1185.7	T 406= 1369.0	T 408= 1357.4	T 410= 1409.8	T 412= 1408.4	T 414= 1418.6

T	421=	393.61	T	422=	1413.7	T	423=	1416.6	T	424=	159.20	T	425=	1397.7	T	426=	1400.9
T	431=	1356.1	T	432=	1356.2	T	433=	1339.3	T	434=	1337.8	T	435=	1377.5	T	436=	1358.0
T	950=	1005.2	T	952=	1053.2														

ARITHMETIC NODES IN ASCENDING NODE NUMBER ORDER

T	50=	718.31	T	52=	812.70	T	54=	947.55	T	158=	912.87	T	159=	906.68	T	168=	906.96
T	169=	904.47	T	195=	267.91	T	197=	349.07	T	199=	674.21	T	238=	907.01	T	311=	1104.1
T	312=	1104.1	T	321=	1096.7	T	322=	1096.7	T	331=	1070.3	T	332=	1070.3	T	337=	772.95
T	341=	655.77	T	357=	227.91	T	358=	316.33	T	359=	155.64	T	379=	112.47	T	403=	116.57
T	1000=	314.12	T	1001=	813.02	T	1002=	675.08	T	1003=	371.46	T	1004=	222.48	T	1005=	218.86
T	1006=	111.49	T	1007=	901.80	T	1008=	922.61	T	1009=	988.38	T	1010=	346.79	T	1011=	924.87
T	1012=	924.87	T	1013=	1218.7	T	1021=	915.45	T	1022=	915.45	T	1023=	1212.8	T	1031=	904.45
T	1032=	904.45	T	1033=	1191.4	T	1041=	904.28	T	1042=	904.28	T	1043=	581.29	T	1044=	581.29
T	1346=	1100.9	T	1347=	356.97														

HEATER NODES IN ASCENDING NODE NUMBER ORDER

++NONE++

BOUNDARY NODES IN ASCENDING NODE NUMBER ORDER

T	1=	1475.0	T	2=	1424.7

SYSTEMS IMPROVED NUMERICAL DIFFERENCING ANALYZER '85 (SINDA '85) PAGE 2/4

MODEL = DAMAGE6 LOAD CASE NO. 6 CONDITIONS - Ungula Distributions, -20F 4/30/94
FWDBCK ***** PEAK OCV SIDEWALL TEMPERATURE TIME POINT *****

SUBMODEL NAME = PTSB

	CALCULATED			ALLOWED	
MAX DIFF DELTA T PER ITER	DRLXCC(PTSB	200)=	2.441406E-04	VS. DRLXCA=	5.000000E-02
MAX ARITH DELTA T PER ITER	ARLXCC(PTSB	1346)=	-0.122803	VS. ARLXCA=	0.500000
MAX DIFF DEL T PER TIME STEP	DTMPCC(PTSB	200)=	2.746582E-04	VS. DTMPCA=	10.0000
MAX ARITH DEL T PER TIME STEP	ATMPCC(PTSB	1346)=	-0.122772	VS. ATMPCA=	100.000
MIN STABILITY CRITERIA	CSGMIN(PTSB	446)=	3.012734E-05		
MAX STABILITY CRITERIA	CSGMAX(PTSB	424)=	2.05948		
NUMBER OF ITERATIONS	LOOPCT	=	1	VS. NLOOPT=	600
PROBLEM TIME	TIMEN	=	0.500000	VS. TIMEND=	0.500000
MEAN PROBLEM TIME	TIMEM	=	0.500000		
AVERAGE TIME STEP USED	DTIMEU	=	1.666667E-02	VS. DTIMEI=	0.

DIFFUSION NODES IN ASCENDING NODE NUMBER ORDER

T	51=	687.30	T	53=	757.62	T	55=	857.71	T	60=	816.35	T	62=	1016.0	T	100=	972.72
T	105=	873.55	T	107=	830.88	T	110=	788.72	T	112=	786.91	T	113=	796.58	T	120=	694.05
T	122=	686.22	T	123=	711.31	T	124=	679.30	T	125=	697.15	T	126=	668.94	T	127=	673.87
T	130=	685.93	T	132=	691.64	T	133=	687.22	T	134=	685.26	T	135=	681.68	T	136=	675.21
T	137=	673.65	T	140=	703.47	T	141=	703.14	T	142=	716.15	T	143=	692.50	T	144=	712.45
T	145=	696.04	T	146=	708.07	T	147=	704.12	T	150=	760.02	T	152=	785.37	T	153=	727.71
T	154=	781.84	T	155=	745.17	T	156=	776.16	T	157=	771.55	T	160=	802.17	T	161=	793.47
T	162=	836.66	T	163=	756.55	T	164=	831.49	T	165=	787.94	T	166=	826.43	T	167=	816.78
T	170=	769.06	T	172=	787.46	T	173=	736.22	T	175=	744.88	T	177=	752.63	T	180=	711.54
T	190=	750.16	T	191=	852.64	T	192=	216.56	T	193=	757.00	T	194=	356.81	T	196=	543.26
T	198=	856.20	T	200=	1055.6	T	204=	1079.4	T	210=	661.23	T	220=	649.23	T	230=	632.52
T	240=	610.26	T	242=	292.41	T	250=	120.92	T	260=	97.629	T	261=	100.36	T	262=	97.538
T	263=	101.66	T	264=	98.093	T	265=	104.21	T	266=	99.312	T	300=	1210.8	T	304=	1219.0
T	305=	1372.5	T	310=	900.56	T	313=	1086.4	T	315=	1272.8	T	316=	1272.8	T	320=	888.13
T	323=	1077.4	T	325=	1266.2	T	326=	1266.2	T	330=	853.03	T	333=	1035.5	T	335=	1238.6
T	336=	1238.6	T	340=	833.79	T	342=	520.02	T	343=	1001.2	T	344=	235.18	T	345=	763.87
T	346=	1245.5	T	347=	380.75	T	349=	1016.1	T	350=	147.10	T	351=	324.28	T	352=	147.71
T	353=	237.62	T	354=	186.86	T	355=	110.02	T	356=	190.11	T	360=	94.471	T	362=	93.176
T	364=	92.431	T	366=	103.33	T	367=	104.38	T	368=	108.60	T	369=	116.71	T	371=	334.86
T	373=	244.44	T	375=	149.78	T	377=	109.25	T	400=	92.117	T	401=	100.14	T	402=	103.15
T	404=	888.83	T	406=	1365.9	T	408=	1379.8	T	410=	1413.0	T	412=	1408.5	T	414=	1418.6
T	421=	393.35	T	422=	1413.7	T	423=	1416.7	T	424=	140.67	T	425=	1397.8	T	426=	1404.7
T	431=	1224.4	T	432=	1350.7	T	433=	244.45	T	434=	213.27	T	435=	1405.6	T	436=	1404.6
T	441=	1379.2	T	442=	1372.6	T	443=	1372.5	T	444=	1372.5	T	445=	1394.6	T	446=	1380.2
T	451=	1374.1	T	452=	1366.2	T	453=	1376.6	T	454=	1381.5	T	455=	1412.4	T	456=	1394.5
T	954=	891.43															

ARITHMETIC NODES IN ASCENDING NODE NUMBER ORDER

T	50=	707.89	T	52=	760.10	T	54=	858.24	T	158=	802.08	T	159=	789.68	T	168=	793.71
T	169=	792.70	T	195=	225.64	T	197=	301.86	T	199=	599.37	T	238=	661.51	T	311=	1103.5

T	312=	1103.5	T	321=	1094.4	T	322=	1094.4	T	331=	1051.0	T	332=	1051.0	T	337=	755.72
T	341=	635.07	T	357=	217.70	T	358=	307.82	T	359=	148.00	T	379=	105.40	T	403=	107.33
T	1000=	252.76	T	1001=	686.27	T	1002=	588.96	T	1003=	314.04	T	1004=	191.61	T	1005=	188.81
T	1006=	104.81	T	1007=	766.57	T	1008=	779.07	T	1009=	830.11	T	1010=	319.83	T	1011=	923.87
T	1012=	923.87	T	1013=	1218.3	T	1021=	911.55	T	1022=	911.55	T	1023=	1211.4	T	1031=	875.50
T	1032=	875.50	T	1033=	1179.6	T	1041=	857.55	T	1042=	857.55	T	1043=	562.62	T	1044=	562.62
T	1346=	1022.9	T	1347=	288.72												

HEATER NODES IN ASCENDING NODE NUMBER ORDER
++NONE++

BOUNDARY NODES IN ASCENDING NODE NUMBER ORDER

T	1=	1475.0	T	2=	1424.7

SYSTEMS IMPROVED NUMERICAL DIFFERENCING ANALYZER '85 (SINDA '85) PAGE 3/4

MODEL = DAMAGE6 LOAD CASE NO. 6 CONDITIONS - Ungula Distributions, -20F 4/30/94
FWDBCK ***** PEAK OCV SIDEWALL TEMPERATURE TIME POINT *****

SUBMODEL NAME = PTSC

	CALCULATED			ALLOWED	
MAX DIFF DELTA T PER ITER	DRLXCC(PTSC	408)=	2.441406E-04	VS. DRLXCA=	5.000000E-02
MAX ARITH DELTA T PER ITER	ARLXCC(PTSC	1346)=	-0.122437	VS. ARLXCA=	0.500000
MAX DIFF DEL T PER TIME STEP	DTMPCC(PTSC	408)=	2.746582E-04	VS. DTMPCA=	10.0000
MAX ARITH DEL T PER TIME STEP	ATMPCC(PTSC	1346)=	-0.122406	VS. ATMPCA=	100.000
MIN STABILITY CRITERIA	CSGMIN(PTSC	446)=	3.013040E-05		
MAX STABILITY CRITERIA	CSGMAX(PTSC	424)=	2.05948		
NUMBER OF ITERATIONS	LOOPCT	=	1	VS. NLOOPT=	600
PROBLEM TIME	TIMEN	=	0.500000	VS. TIMEND=	0.500000
MEAN PROBLEM TIME	TIMEM	=	0.500000		
AVERAGE TIME STEP USED	DTIMEU	=	1.666667E-02	VS. DTIMEI=	0.

DIFFUSION NODES IN ASCENDING NODE NUMBER ORDER

T	51=	701.59	T	53=	679.27	T	55=	676.27	T	60=	815.95	T	62=	938.99	T	100=	970.33
T	105=	900.95	T	107=	873.25	T	110=	856.59	T	112=	851.73	T	113=	858.15	T	120=	772.28
T	122=	759.40	T	123=	776.36	T	124=	773.77	T	125=	785.11	T	126=	799.93	T	127=	802.10
T	130=	692.85	T	132=	691.82	T	133=	692.63	T	134=	695.13	T	135=	695.45	T	136=	702.41
T	137=	702.22	T	140=	651.83	T	141=	651.38	T	142=	659.36	T	143=	649.21	T	144=	655.15
T	145=	647.96	T	146=	650.18	T	147=	649.10	T	150=	634.62	T	152=	655.22	T	153=	625.27
T	154=	641.70	T	155=	619.00	T	156=	619.70	T	157=	611.75	T	160=	606.05	T	161=	607.72
T	162=	638.39	T	163=	592.09	T	164=	618.77	T	165=	582.79	T	166=	585.69	T	167=	574.92
T	170=	477.85	T	172=	499.10	T	173=	469.63	T	175=	416.68	T	177=	441.18	T	180=	417.15
T	190=	355.76	T	191=	342.95	T	192=	141.46	T	193=	465.82	T	194=	184.64	T	196=	370.09
T	198=	346.40	T	200=	1033.9	T	204=	1042.3	T	210=	666.77	T	220=	640.04	T	230=	548.95
T	240=	471.85	T	242=	244.58	T	250=	113.37	T	260=	95.390	T	261=	96.385	T	262=	93.922
T	263=	95.258	T	264=	94.742	T	265=	97.893	T	266=	96.721	T	300=	1205.4	T	304=	1210.0
T	305=	1371.4	T	310=	902.21	T	313=	1087.3	T	315=	1273.2	T	316=	1273.2	T	320=	884.55
T	323=	1075.4	T	325=	1265.3	T	326=	1265.3	T	330=	820.48	T	333=	1016.0	T	335=	1230.9
T	336=	1230.9	T	340=	789.90	T	342=	502.44	T	343=	999.48	T	344=	230.49	T	345=	762.59
T	346=	1242.8	T	347=	380.16	T	349=	1015.1	T	350=	146.43	T	351=	323.57	T	352=	147.25
T	353=	237.20	T	354=	185.66	T	355=	109.78	T	356=	189.47	T	360=	93.741	T	362=	92.031
T	364=	91.621	T	366=	103.03	T	367=	104.18	T	368=	108.39	T	369=	116.44	T	371=	334.08
T	373=	244.01	T	375=	149.64	T	377=	109.17	T	400=	91.947	T	401=	100.04	T	402=	103.06
T	404=	888.70	T	406=	1365.0	T	408=	1379.7	T	410=	1413.0	T	412=	1408.5	T	414=	1418.6
T	421=	393.35	T	422=	1413.7	T	423=	1416.7	T	424=	140.67	T	425=	1397.8	T	426=	1404.7
T	431=	1223.9	T	432=	1349.8	T	433=	244.42	T	434=	213.27	T	435=	1405.6	T	436=	1404.6
T	441=	1379.2	T	442=	1372.2	T	443=	1372.5	T	444=	1372.5	T	445=	1394.6	T	446=	1380.2
T	451=	1373.7	T	452=	1365.3	T	453=	1376.4	T	454=	1381.5	T	455=	1412.4	T	456=	1394.5

ARITHMETIC NODES IN ASCENDING NODE NUMBER ORDER

T	50=	708.66	T	52=	681.69	T	54=	699.29	T	158=	612.14	T	159=	602.30	T	168=	608.32
T	169=	610.22	T	195=	148.12	T	197=	171.17	T	199=	313.88	T	238=	515.48	T	311=	1104.4

T	312=	1104.4	T	321=	1092.4	T	322=	1092.4	T	331=	1031.9	T	332=	1031.9	T	337=	740.13
T	341=	615.78	T	357=	216.81	T	358=	307.00	T	359=	147.44	T	379=	105.15	T	403=	107.25
T	1000=	147.56	T	1001=	320.39	T	1002=	291.38	T	1003=	176.37	T	1004=	131.55	T	1005=	130.47
T	1006=	97.421	T	1007=	382.26	T	1008=	361.83	T	1009=	348.72	T	1010=	210.77	T	1011=	925.46
T	1012=	925.46	T	1013=	1218.8	T	1021=	908.08	T	1022=	908.08	T	1023=	1210.2	T	1031=	843.89
T	1032=	843.89	T	1033=	1168.3	T	1041=	815.28	T	1042=	815.28	T	1043=	544.57	T	1044=	544.57
T	1346=	1021.5	T	1347=	288.26												

HEATER NODES IN ASCENDING NODE NUMBER ORDER
++NONE++

BOUNDARY NODES IN ASCENDING NODE NUMBER ORDER

T	1=	1475.0	T	2=	1424.7

SYSTEMS IMPROVED NUMERICAL DIFFERENCING ANALYZER '85 (SINDA '85) PAGE 4/4

MODEL = DAMAGE6 LOAD CASE NO. 6 CONDITIONS - Ungula Distributions, -20F 4/30/94
FWDBCK ***** PEAK OCV SIDEWALL TEMPERATURE TIME POINT *****

SUBMODEL NAME = PTSD

	CALCULATED			ALLOWED	
MAX DIFF DELTA T PER ITER	DRLXCC(PTSD	127)=	2.441406E-04	VS. DRLXCA=	5.000000E-02
MAX ARITH DELTA T PER ITER	ARLXCC(PTSD	1346)=	-0.122314	VS. ARLXCA=	0.500000
MAX DIFF DEL T PER TIME STEP	DTMPCC(PTSD	127)=	2.746582E-04	VS. DTMPCA=	10.0000
MAX ARITH DEL T PER TIME STEP	ATMPCC(PTSD	1346)=	-0.122284	VS. ATMPCA=	100.000
MIN STABILITY CRITERIA	CSGMIN(PTSD	446)=	3.013021E-05		
MAX STABILITY CRITERIA	CSGMAX(PTSD	424)=	2.05948		
NUMBER OF ITERATIONS	LOOPCT	=	1	VS. NLOOPT=	600
PROBLEM TIME	TIMEN	=	0.500000	VS. TIMEND=	0.500000
MEAN PROBLEM TIME	TIMEM	=	0.500000		
AVERAGE TIME STEP USED	DTIMEU	=	1.666667E-02	VS. DTIMEI=	0.

DIFFUSION NODES IN ASCENDING NODE NUMBER ORDER

T	51=	703.19	T	53=	655.25	T	55=	622.18	T	60=	815.23	T	62=	924.90	T	100=	971.76
T	105=	905.16	T	107=	878.67	T	110=	863.17	T	112=	862.90	T	113=	863.33	T	120=	784.28
T	122=	781.79	T	123=	783.28	T	124=	789.61	T	125=	790.42	T	126=	804.72	T	127=	804.63
T	130=	690.78	T	132=	690.81	T	133=	689.74	T	134=	693.93	T	135=	693.00	T	136=	701.03
T	137=	700.65	T	140=	636.85	T	141=	636.19	T	142=	639.51	T	143=	636.80	T	144=	638.96
T	145=	637.32	T	146=	641.62	T	147=	642.13	T	150=	605.05	T	152=	610.46	T	153=	604.30
T	154=	606.30	T	155=	601.01	T	156=	602.69	T	157=	600.61	T	160=	556.68	T	161=	563.69
T	162=	565.75	T	163=	555.93	T	164=	561.66	T	165=	553.63	T	166=	558.61	T	167=	556.69
T	170=	430.01	T	172=	432.96	T	173=	428.33	T	175=	377.99	T	177=	397.04	T	180=	381.03
T	190=	334.08	T	191=	317.58	T	192=	139.07	T	193=	457.11	T	194=	180.03	T	196=	318.21
T	198=	320.68	T	200=	1033.5	T	204=	1041.9	T	210=	665.73	T	220=	636.63	T	230=	560.66
T	240=	469.91	T	242=	243.57	T	250=	113.18	T	260=	95.151	T	261=	96.045	T	262=	93.767
T	263=	95.001	T	264=	94.602	T	265=	97.652	T	266=	96.644	T	300=	1205.2	T	304=	1209.8
T	305=	1371.3	T	310=	901.74	T	313=	1087.0	T	315=	1273.0	T	316=	1273.0	T	320=	883.24
T	323=	1074.6	T	325=	1265.0	T	326=	1265.0	T	330=	824.19	T	333=	1017.6	T	335=	1231.5
T	336=	1231.5	T	340=	790.26	T	342=	502.54	T	343=	999.57	T	344=	230.50	T	345=	762.63
T	346=	1243.0	T	347=	380.17	T	349=	1015.2	T	350=	146.43	T	351=	323.59	T	352=	147.25
T	353=	237.21	T	354=	185.67	T	355=	109.78	T	356=	189.48	T	360=	93.649	T	362=	91.978
T	364=	91.593	T	366=	103.03	T	367=	104.17	T	368=	108.39	T	369=	116.44	T	371=	334.10
T	373=	244.02	T	375=	149.64	T	377=	109.17	T	400=	91.938	T	401=	100.04	T	402=	103.06
T	404=	888.70	T	406=	1365.1	T	408=	1379.7	T	410=	1413.0	T	412=	1408.5	T	414=	1418.6
T	421=	393.35	T	422=	1413.7	T	423=	1416.7	T	424=	140.67	T	425=	1397.8	T	426=	1404.7
T	431=	1223.9	T	432=	1349.9	T	433=	244.42	T	434=	213.27	T	435=	1405.6	T	436=	1404.6
T	441=	1379.2	T	442=	1372.2	T	443=	1372.5	T	444=	1372.5	T	445=	1394.6	T	446=	1380.2
T	451=	1373.7	T	452=	1365.4	T	453=	1376.5	T	454=	1381.5	T	455=	1412.4	T	456=	1394.5

ARITHMETIC NODES IN ASCENDING NODE NUMBER ORDER

T	50=	706.67	T	52=	657.64	T	54=	652.58	T	158=	565.39	T	159=	563.19	T	168=	563.96
T	169=	564.81	T	195=	142.22	T	197=	157.32	T	199=	302.61	T	238=	521.35	T	311=	1104.1

T	312=	1104.1	T	321=	1091.7	T	322=	1091.7	T	331=	1033.4	T	332=	1033.4	T	337=	740.27
T	341=	615.92	T	357=	216.81	T	358=	307.01	T	359=	147.44	T	379=	105.15	T	403=	107.25
T	1000=	145.77	T	1001=	291.46	T	1002=	279.28	T	1003=	168.60	T	1004=	129.61	T	1005=	128.58
T	1006=	97.046	T	1007=	351.95	T	1008=	336.37	T	1009=	323.32	T	1010=	207.74	T	1011=	925.00
T	1012=	925.00	T	1013=	1218.7	T	1021=	906.82	T	1022=	906.82	T	1023=	1209.8	T	1031=	847.45
T	1032=	847.45	T	1033=	1169.2	T	1041=	815.71	T	1042=	815.71	T	1043=	544.77	T	1044=	544.77
T	1346=	1021.5	T	1347=	288.27												

HEATER NODES IN ASCENDING NODE NUMBER ORDER
++NONE++

BOUNDARY NODES IN ASCENDING NODE NUMBER ORDER

T	1=	1475.0	T	2=	1424.7

```
                    SYSTEMS IMPROVED NUMERICAL DIFFERENCING ANALYZER '85 (SINDA '85)                PAGE   1/4

MODEL = DAMAGE6                    LOAD CASE NO. 6 CONDITIONS - Ungula Distributions, -20F                4/30/94
  FWDBCK                  *****      PEAK ICV SIDEWALL TEMPERATURE TIME POINT    *****

 SUBMODEL NAME = MAIN

       MEAN PROBLEM TIME                TIMEM                = 0.666118
                                  DIFFUSION NODES IN ASCENDING NODE NUMBER ORDER
  T  267= 139.05     T  268= 138.92     T  269= 131.00
                                  ARITHMETIC NODES IN ASCENDING NODE NUMBER ORDER
  T  201= 780.29     T 1266= 158.93     T 1267= 345.05     T 1268= 284.96     T 1269= 170.75
                                    HEATER NODES IN ASCENDING NODE NUMBER ORDER
                                                ++NONE++
                                  BOUNDARY NODES IN ASCENDING NODE NUMBER ORDER
                                                ++NONE++
MEAN ICV GAS TEMP= 780.3 F    MEAN ICV GAS PRESSURE= 37.22 PSIA
MEAN ICV-OCV GAS TEMP= 754.5 F    MEAN ICV-OCV GAS PRESSURE= 42.80 PSIA


 SUBMODEL NAME = PTSA
                                    CALCULATED                                  ALLOWED
       MAX DIFF DELTA T PER ITER    DRLXCC(PTSA      161)= 8.178711E-03 VS. DRLXCA= 5.000000E-02
       MAX ARITH DELTA T PER ITER   ARLXCC(PTSA      337)=-9.033203E-02 VS. ARLXCA= 0.500000
       MAX DIFF DEL T PER TIME STEP DTMPCC(PTSA      423)= -2.22836     VS. DTMPCA=  10.0000
       MAX ARITH DEL T PER TIME STEP ATMPCC(PTSA    1346)= -1.29770     VS. ATMPCA=  100.000
       MIN STABILITY CRITERIA       CSGMIN(PTSA      431)= 1.337324E-04
       MAX STABILITY CRITERIA       CSGMAX(PTSA      424)=  2.03348
       NUMBER OF ITERATIONS         LOOPCT              =         3     VS. NLOOPT=      600
       PROBLEM TIME                 TIMEN               = 0.666667     VS. TIMEND=  6.00000
       MEAN PROBLEM TIME            TIMEM               = 0.666118
       AVERAGE TIME STEP USED       DTIMEU              = 9.259260E-04 VS. DTIMEI=       0.

                                  DIFFUSION NODES IN ASCENDING NODE NUMBER ORDER
  T   51= 726.56     T   53= 809.55     T   55= 937.89     T   60= 823.55     T   62= 1025.6     T  100= 964.54
  T  105= 908.33     T  107= 881.29     T  110= 849.65     T  112= 850.01     T  113= 849.73     T  120= 774.53
  T  122= 773.71     T  123= 772.19     T  124= 774.61     T  125= 773.53     T  126= 776.41     T  127= 776.04
  T  130= 788.17     T  132= 791.98     T  133= 780.09     T  134= 793.84     T  135= 785.56     T  136= 796.41
  T  137= 794.36     T  140= 823.35     T  141= 824.38     T  142= 827.54     T  143= 808.26     T  144= 833.61
  T  145= 821.31     T  146= 845.74     T  147= 842.93     T  150= 893.33     T  152= 900.27     T  153= 864.51
  T  154= 909.74     T  155= 890.60     T  156= 923.41     T  157= 923.92     T  160= 946.00     T  161= 936.80
  T  162= 956.30     T  163= 911.31     T  164= 964.63     T  165= 946.68     T  166= 978.41     T  167= 975.12
  T  170= 923.68     T  172= 927.13     T  173= 898.94     T  175= 894.18     T  177= 904.00     T  180= 847.48
  T  190= 923.91     T  191= 1019.9     T  192= 286.68     T  193= 931.32     T  194= 450.82     T  196= 675.96
  T  198= 1024.5     T  200= 1002.9     T  204= 1004.9     T  210= 765.00     T  220= 756.71     T  230= 788.90
  T  240= 795.93     T  242= 404.66     T  250= 155.89     T  260= 102.08     T  261= 106.79     T  262= 109.13
  T  263= 119.85     T  264= 112.37     T  265= 123.46     T  266= 117.68     T  300= 906.20     T  304= 919.35
  T  305= 635.71     T  310= 785.25     T  313= 721.97     T  315= 607.01     T  316= 607.01     T  320= 777.46
  T  323= 717.30     T  325= 606.09     T  326= 606.09     T  330= 793.63     T  333= 732.22     T  335= 640.41
  T  336= 640.41     T  340= 783.63     T  342= 520.13     T  343= 676.63     T  344= 285.52     T  345= 814.65
  T  346= 764.80     T  347= 501.65     T  349= 565.57     T  350= 190.84     T  351= 268.25     T  352= 194.89
  T  353= 233.61     T  354= 228.83     T  355= 142.38     T  356= 236.58     T  360= 96.883     T  362= 98.742
  T  364= 103.22     T  366= 135.16     T  367= 142.23     T  368= 166.04     T  369= 192.76     T  371= 273.36
  T  373= 241.12     T  375= 176.25     T  377= 140.03     T  400= 98.037     T  401= 112.49     T  402= 134.87
  T  404= 883.18     T  406= 751.85     T  408= 779.26     T  410= 774.19     T  412= 824.49     T  414= 767.42
```

T	421=	427.58	T	422=	800.68	T	423=	790.35	T	424=	199.01	T	425=	939.55	T	426=	865.64
T	431=	782.64	T	432=	892.32	T	433=	965.85	T	434=	963.72	T	435=	897.06	T	436=	781.34
T	950=	1035.9	T	952=	1062.8												

ARITHMETIC NODES IN ASCENDING NODE NUMBER ORDER

T	50=	746.14	T	52=	812.28	T	54=	928.72	T	158=	942.14	T	159=	936.83	T	168=	936.80
T	169=	934.31	T	195=	290.54	T	197=	374.66	T	199=	697.35	T	238=	955.21	T	311=	700.36
T	312=	700.36	T	321=	695.93	T	322=	695.93	T	331=	711.50	T	332=	711.50	T	337=	611.81
T	341=	577.19	T	357=	241.53	T	358=	269.71	T	359=	193.13	T	379=	139.61	T	403=	138.38
T	1000=	341.60	T	1001=	832.44	T	1002=	697.77	T	1003=	401.03	T	1004=	249.76	T	1005=	245.43
T	1006=	118.28	T	1007=	927.12	T	1008=	946.75	T	1009=	997.42	T	1010=	388.93	T	1011=	780.07
T	1012=	780.07	T	1013=	644.34	T	1021=	772.53	T	1022=	772.53	T	1023=	642.12	T	1031=	788.82
T	1032=	788.82	T	1033=	669.13	T	1041=	779.31	T	1042=	779.31	T	1043=	526.66	T	1044=	526.66
T	1346=	758.13	T	1347=	387.12												

HEATER NODES IN ASCENDING NODE NUMBER ORDER

++NONE++

BOUNDARY NODES IN ASCENDING NODE NUMBER ORDER

T	1=	-20.000	T	2=	-20.000

SYSTEMS IMPROVED NUMERICAL DIFFERENCING ANALYZER '85 (SINDA '85) PAGE 2/4

MODEL = DAMAGE6
FWDBCK

LOAD CASE NO. 6 CONDITIONS - Ungula Distributions, -20F
***** PEAK ICV SIDEWALL TEMPERATURE TIME POINT *****

4/30/94

SUBMODEL NAME = PTSB

	CALCULATED		ALLOWED
MAX DIFF DELTA T PER ITER	DRLXCC(PTSB	161)= 1.025391E-02	VS. DRLXCA= 5.000000E-02
MAX ARITH DELTA T PER ITER	ARLXCC(PTSB	337)=-9.606934E-02	VS. ARLXCA= 0.500000
MAX DIFF DEL T PER TIME STEP	DTMPCC(PTSB	423)= -2.22836	VS. DTMPCA= 10.0000
MAX ARITH DEL T PER TIME STEP	ATMPCC(PTSB	1346)= -1.06271	VS. ATMPCA= 100.000
MIN STABILITY CRITERIA	CSGMIN(PTSB	455)= 1.589451E-04	
MAX STABILITY CRITERIA	CSGMAX(PTSB	424)= 2.12500	
NUMBER OF ITERATIONS	LOOPCT	= 3	VS. NLOOPT= 600
PROBLEM TIME	TIMEN	= 0.666667	VS. TIMEND= 6.00000
MEAN PROBLEM TIME	TIMEM	= 0.666118	
AVERAGE TIME STEP USED	DTIMEU	= 9.259260E-04	VS. DTIMEI= 0.

DIFFUSION NODES IN ASCENDING NODE NUMBER ORDER

T	51=	725.83	T	53=	760.30	T	55=	840.84	T	60=	820.89	T	62=	983.26	T	100=	963.58
T	105=	907.95	T	107=	880.98	T	110=	849.76	T	112=	849.20	T	113=	854.00	T	120=	775.85
T	122=	771.09	T	123=	784.35	T	124=	768.26	T	125=	777.54	T	126=	763.57	T	127=	765.82
T	130=	766.57	T	132=	770.85	T	133=	764.61	T	134=	768.38	T	135=	763.89	T	136=	764.20
T	137=	762.84	T	140=	778.28	T	141=	778.88	T	142=	787.63	T	143=	767.98	T	144=	785.94
T	145=	772.79	T	146=	784.33	T	147=	781.54	T	150=	814.05	T	152=	834.10	T	153=	786.65
T	154=	832.14	T	155=	802.80	T	156=	829.07	T	157=	825.96	T	160=	840.86	T	161=	835.56
T	162=	869.74	T	163=	801.43	T	164=	866.11	T	165=	830.12	T	166=	863.24	T	167=	855.86
T	170=	806.73	T	172=	822.99	T	173=	778.26	T	175=	779.96	T	177=	789.05	T	180=	747.29
T	190=	788.73	T	191=	866.38	T	192=	241.88	T	193=	801.92	T	194=	394.87	T	196=	606.31
T	198=	871.15	T	200=	1001.5	T	204=	1004.3	T	210=	762.47	T	220=	747.10	T	230=	734.92
T	240=	691.09	T	242=	368.19	T	250=	145.57	T	260=	99.669	T	261=	103.03	T	262=	101.36
T	263=	106.48	T	264=	106.47	T	265=	114.73	T	266=	111.88	T	300=	905.31	T	304=	918.93
T	305=	635.59	T	310=	783.86	T	313=	720.98	T	315=	606.35	T	316=	606.35	T	320=	771.91
T	323=	713.31	T	325=	603.41	T	326=	603.41	T	330=	758.63	T	333=	703.33	T	335=	620.88
T	336=	620.88	T	340=	730.15	T	342=	496.97	T	343=	671.56	T	344=	271.75	T	345=	707.22
T	346=	754.43	T	347=	429.62	T	349=	558.25	T	350=	177.86	T	351=	254.80	T	352=	178.60
T	353=	221.81	T	354=	214.56	T	355=	129.26	T	356=	216.83	T	360=	95.833	T	362=	95.699
T	364=	99.705	T	366=	123.76	T	367=	126.40	T	368=	133.66	T	369=	148.34	T	371=	259.42
T	373=	229.68	T	375=	166.10	T	377=	127.29	T	400=	96.643	T	401=	111.44	T	402=	121.24
T	404=	794.25	T	406=	757.58	T	408=	721.96	T	410=	787.10	T	412=	825.16	T	414=	767.44
T	421=	427.17	T	422=	800.70	T	423=	790.47	T	424=	172.81	T	425=	939.83	T	426=	871.52
T	431=	793.69	T	432=	891.99	T	433=	323.29	T	434=	275.88	T	435=	909.35	T	436=	822.04
T	441=	724.79	T	442=	810.61	T	443=	843.14	T	444=	842.82	T	445=	821.97	T	446=	726.32
T	451=	741.79	T	452=	757.71	T	453=	771.19	T	454=	774.49	T	455=	785.80	T	456=	756.39
T	954=	915.25															

ARITHMETIC NODES IN ASCENDING NODE NUMBER ORDER

T	50=	738.86	T	52=	763.28	T	54=	842.67	T	158=	842.77	T	159=	832.58	T	168=	835.67		

T	169=	834.67	T	195=	245.67	T	197=	322.74	T	199=	631.72	T	238=	745.36	T	311=	699.34
T	312=	699.34	T	321=	691.85	T	322=	691.85	T	331=	682.47	T	332=	682.47	T	337=	588.77
T	341=	551.19	T	357=	225.08	T	358=	254.96	T	359=	178.51	T	379=	126.12	T	403=	125.37
T	1000=	275.57	T	1001=	713.74	T	1002=	619.71	T	1003=	339.66	T	1004=	212.52	T	1005=	209.16
T	1006=	109.15	T	1007=	798.89	T	1008=	809.87	T	1009=	849.08	T	1010=	367.67	T	1011=	778.72
T	1012=	778.72	T	1013=	643.56	T	1021=	767.11	T	1022=	767.11	T	1023=	638.97	T	1031=	754.49
T	1032=	754.49	T	1033=	646.36	T	1041=	727.31	T	1042=	727.31	T	1043=	503.15	T	1044=	503.15
T	1346=	687.27	T	1347=	325.86												

HEATER NODES IN ASCENDING NODE NUMBER ORDER
++NONE++

BOUNDARY NODES IN ASCENDING NODE NUMBER ORDER

T	1=	-20.000	T	2=	-20.000

SYSTEMS IMPROVED NUMERICAL DIFFERENCING ANALYZER '85 (SINDA '85) PAGE 3/4

MODEL = DAMAGE6 LOAD CASE NO. 6 CONDITIONS - Ungula Distributions, -20F 4/30/94
FWDBCK ***** PEAK ICV SIDEWALL TEMPERATURE TIME POINT *****

SUBMODEL NAME = PTSC

	CALCULATED			ALLOWED	
MAX DIFF DELTA T PER ITER	DRLXCC(PTSC	161)=	1.245117E-02	VS. DRLXCA=	5.000000E-02
MAX ARITH DELTA T PER ITER	ARLXCC(PTSC	1007)=	0.119934	VS. ARLXCA=	0.500000
MAX DIFF DEL T PER TIME STEP	DTMPCC(PTSC	423)=	-2.22836	VS. DTMPCA=	10.0000
MAX ARITH DEL T PER TIME STEP	ATMPCC(PTSC	1033)=	-1.11984	VS. ATMPCA=	100.000
MIN STABILITY CRITERIA	CSGMIN(PTSC	455)=	1.589517E-04		
MAX STABILITY CRITERIA	CSGMAX(PTSC	424)=	2.12500		
NUMBER OF ITERATIONS	LOOPCT	=	3	VS. NLOOPT=	600
PROBLEM TIME	TIMEN	=	0.666667	VS. TIMEND=	6.00000
MEAN PROBLEM TIME	TIMEM	=	0.666118		
AVERAGE TIME STEP USED	DTIMEU	=	9.259260E-04	VS. DTIMEI=	0.

DIFFUSION NODES IN ASCENDING NODE NUMBER ORDER

T	51=	753.37	T	53=	696.51	T	55=	677.43	T	60=	823.30	T	62=	886.54	T	100=	949.14
T	105=	915.61	T	107=	899.72	T	110=	884.30	T	112=	881.96	T	113=	885.44	T	120=	819.51
T	122=	811.43	T	123=	821.28	T	124=	819.00	T	125=	825.63	T	126=	830.81	T	127=	832.16
T	130=	765.30	T	132=	764.03	T	133=	763.45	T	134=	767.49	T	135=	767.02	T	136=	773.17
T	137=	772.95	T	140=	736.18	T	141=	736.51	T	142=	740.83	T	143=	732.92	T	144=	739.02
T	145=	733.62	T	146=	736.68	T	147=	735.92	T	150=	712.78	T	152=	727.79	T	153=	704.77
T	154=	719.10	T	155=	702.48	T	156=	705.65	T	157=	701.13	T	160=	676.94	T	161=	681.24
T	162=	702.21	T	163=	664.99	T	164=	688.78	T	165=	661.98	T	166=	667.59	T	167=	660.70
T	170=	558.02	T	172=	575.36	T	173=	550.79	T	175=	496.16	T	177=	520.98	T	180=	490.91
T	190=	442.34	T	191=	425.36	T	192=	151.10	T	193=	572.78	T	194=	223.74	T	196=	460.98
T	198=	429.14	T	200=	971.55	T	204=	957.45	T	210=	767.68	T	220=	735.62	T	230=	656.51
T	240=	568.72	T	242=	312.67	T	250=	133.84	T	260=	96.095	T	261=	97.380	T	262=	95.701
T	263=	97.543	T	264=	100.87	T	265=	105.49	T	266=	107.12	T	300=	890.91	T	304=	897.12
T	305=	629.45	T	310=	786.45	T	313=	722.82	T	315=	607.52	T	316=	607.52	T	320=	765.98
T	323=	709.14	T	325=	600.54	T	326=	600.54	T	330=	715.28	T	333=	670.78	T	335=	599.30
T	336=	599.30	T	340=	674.94	T	342=	471.90	T	343=	668.95	T	344=	264.26	T	345=	705.27
T	346=	750.21	T	347=	428.36	T	349=	556.24	T	350=	176.32	T	351=	253.30	T	352=	177.44
T	353=	220.76	T	354=	212.17	T	355=	128.59	T	356=	215.35	T	360=	94.389	T	362=	93.483
T	364=	97.917	T	366=	122.98	T	367=	125.80	T	368=	133.12	T	369=	147.67	T	371=	257.82
T	373=	228.64	T	375=	165.65	T	377=	127.00	T	400=	96.186	T	401=	111.15	T	402=	120.95
T	404=	793.98	T	406=	756.11	T	408=	721.87	T	410=	787.09	T	412=	825.16	T	414=	767.44
T	421=	427.14	T	422=	800.70	T	423=	790.47	T	424=	172.80	T	425=	939.83	T	426=	871.51
T	431=	792.96	T	432=	891.09	T	433=	323.22	T	434=	275.88	T	435=	909.34	T	436=	822.02
T	441=	724.65	T	442=	810.06	T	443=	843.08	T	444=	842.76	T	445=	821.93	T	446=	726.23
T	451=	741.16	T	452=	756.32	T	453=	770.94	T	454=	774.40	T	455=	785.79	T	456=	756.34

ARITHMETIC NODES IN ASCENDING NODE NUMBER ORDER

T	50=	752.15	T	52=	699.30	T	54=	698.08	T	158=	685.01	T	159=	677.69	T	168=	681.60
T	169=	682.94	T	195=	167.74	T	197=	191.27	T	199=	385.43	T	238=	618.43	T	311=	701.21

T	312=	701.21	T	321=	687.52	T	322=	687.52	T	331=	649.45	T	332=	649.45	T	337=	566.08
T	341=	524.16	T	357=	223.20	T	358=	253.22	T	359=	177.16	T	379=	125.43	T	403=	125.08
T	1000=	169.43	T	1001=	394.53	T	1002=	358.14	T	1003=	199.33	T	1004=	139.35	T	1005=	138.08
T	1006=	99.225	T	1007=	464.38	T	1008=	445.93	T	1009=	431.64	T	1010=	261.65	T	1011=	781.24
T	1012=	781.24	T	1013=	644.98	T	1021=	761.32	T	1022=	761.32	T	1023=	635.65	T	1031=	712.02
T	1032=	712.02	T	1033=	620.92	T	1041=	673.39	T	1042=	673.39	T	1043=	477.67	T	1044=	477.67
T	1346=	684.87	T	1347=	324.85												

HEATER NODES IN ASCENDING NODE NUMBER ORDER
++NONE++

BOUNDARY NODES IN ASCENDING NODE NUMBER ORDER

T	1=	-20.000	T	2=	-20.000

SYSTEMS IMPROVED NUMERICAL DIFFERENCING ANALYZER '85 (SINDA '85) PAGE 4/4

MODEL = DAMAGE6 LOAD CASE NO. 6 CONDITIONS - Ungula Distributions, -20F 4/30/94
FWDBCK ***** PEAK ICV SIDEWALL TEMPERATURE TIME POINT *****

SUBMODEL NAME = PTSD

	CALCULATED		ALLOWED
MAX DIFF DELTA T PER ITER	DRLXCC(PTSD	161)= 1.354980E-02	VS. DRLXCA= 5.000000E-02
MAX ARITH DELTA T PER ITER	ARLXCC(PTSD	1007)= 0.116882	VS. ARLXCA= 0.500000
MAX DIFF DEL T PER TIME STEP	DTMPCC(PTSD	423)= -2.22836	VS. DTMPCA= 10.0000
MAX ARITH DEL T PER TIME STEP	ATMPCC(PTSD	1033)= -1.11667	VS. ATMPCA= 100.000
MIN STABILITY CRITERIA	CSGMIN(PTSD	455)= 1.589508E-04	
MAX STABILITY CRITERIA	CSGMAX(PTSD	424)= 2.12500	
NUMBER OF ITERATIONS	LOOPCT	= 3	VS. NLOOPT= 600
PROBLEM TIME	TIMEN	= 0.666667	VS. TIMEND= 6.00000
MEAN PROBLEM TIME	TIMEM	= 0.666118	
AVERAGE TIME STEP USED	DTIMEU	= 9.259260E-04	VS. DTIMEI= 0.

DIFFUSION NODES IN ASCENDING NODE NUMBER ORDER

T	51=	758.15	T	53=	677.34	T	55=	630.09	T	60=	823.10	T	62=	868.25	T	100=	949.77
T	105=	918.16	T	107=	902.99	T	110=	888.15	T	112=	888.17	T	113=	888.55	T	120=	826.65
T	122=	824.49	T	123=	825.63	T	124=	828.22	T	125=	828.92	T	126=	833.47	T	127=	833.58
T	130=	763.02	T	132=	761.63	T	133=	760.92	T	134=	765.48	T	135=	764.91	T	136=	771.74
T	137=	771.53	T	140=	725.78	T	141=	726.09	T	142=	726.22	T	143=	724.38	T	144=	727.49
T	145=	726.42	T	146=	730.99	T	147=	731.23	T	150=	691.73	T	152=	694.26	T	153=	690.13
T	154=	693.47	T	155=	690.22	T	156=	694.48	T	157=	693.79	T	160=	639.18	T	161=	648.25
T	162=	644.74	T	163=	637.58	T	164=	644.89	T	165=	640.55	T	166=	648.53	T	167=	647.83
T	170=	517.22	T	172=	519.17	T	173=	515.34	T	175=	460.25	T	177=	481.54	T	180=	456.04
T	190=	419.16	T	191=	399.13	T	192=	147.42	T	193=	565.21	T	194=	217.92	T	196=	408.74
T	198=	402.74	T	200=	970.70	T	204=	957.24	T	210=	767.07	T	220=	732.67	T	230=	664.98
T	240=	566.64	T	242=	311.17	T	250=	133.47	T	260=	95.624	T	261=	96.759	T	262=	95.379
T	263=	97.075	T	264=	100.58	T	265=	105.04	T	266=	106.94	T	300=	890.29	T	304=	896.89
T	305=	629.37	T	310=	786.00	T	313=	722.47	T	315=	607.26	T	316=	607.26	T	320=	764.32
T	323=	707.91	T	325=	599.69	T	326=	599.69	T	330=	719.41	T	333=	673.02	T	335=	600.81
T	336=	600.81	T	340=	675.32	T	342=	471.88	T	343=	669.05	T	344=	264.23	T	345=	705.31
T	346=	750.40	T	347=	428.38	T	349=	556.32	T	350=	176.31	T	351=	253.31	T	352=	177.43
T	353=	220.77	T	354=	212.16	T	355=	128.58	T	356=	215.35	T	360=	94.166	T	362=	93.347
T	364=	97.837	T	366=	122.97	T	367=	125.79	T	368=	133.12	T	369=	147.67	T	371=	257.83
T	373=	228.65	T	375=	165.66	T	377=	126.99	T	400=	96.157	T	401=	111.13	T	402=	120.95
T	404=	793.99	T	406=	756.20	T	408=	721.88	T	410=	787.09	T	412=	825.16	T	414=	767.44
T	421=	427.14	T	422=	800.70	T	423=	790.47	T	424=	172.80	T	425=	939.83	T	426=	871.51
T	431=	793.00	T	432=	891.14	T	433=	323.23	T	434=	275.88	T	435=	909.34	T	436=	822.02
T	441=	724.66	T	442=	810.09	T	443=	843.08	T	444=	842.76	T	445=	821.93	T	446=	726.24
T	451=	741.20	T	452=	756.41	T	453=	770.96	T	454=	774.40	T	455=	785.79	T	456=	756.34

ARITHMETIC NODES IN ASCENDING NODE NUMBER ORDER

T	50=	753.33	T	52=	680.06	T	54=	656.92	T	158=	649.77	T	159=	648.55	T	168=	648.28
T	169=	648.65	T	195=	160.87	T	197=	182.35	T	199=	373.99	T	238=	622.39	T	311=	700.86

T	312=	700.86	T	321=	686.27	T	322=	686.27	T	331=	651.66	T	332=	651.66	T	337=	566.17
T	341=	524.21	T	357=	223.20	T	358=	253.23	T	359=	177.15	T	379=	125.42	T	403=	125.07
T	1000=	165.72	T	1001=	364.75	T	1002=	345.55	T	1003=	190.22	T	1004=	136.42	T	1005=	135.22
T	1006=	98.567	T	1007=	434.75	T	1008=	419.86	T	1009=	405.46	T	1010=	257.93	T	1011=	780.80
T	1012=	780.80	T	1013=	644.69	T	1021=	759.70	T	1022=	759.70	T	1023=	634.66	T	1031=	716.05
T	1032=	716.05	T	1033=	622.68	T	1041=	673.82	T	1042=	673.82	T	1043=	477.73	T	1044=	477.73
T	1346=	684.94	T	1347=	324.86												

HEATER NODES IN ASCENDING NODE NUMBER ORDER
++NONE++

BOUNDARY NODES IN ASCENDING NODE NUMBER ORDER

T	1=	-20.000	T	2=	-20.000

```
                    SYSTEMS IMPROVED NUMERICAL DIFFERENCING ANALYZER '85 (SINDA '85)          PAGE   1/4

MODEL = DAMAGE6          LOAD CASE NO. 6 CONDITIONS - Ungula Distributions, -20F
  STDSTL                   *** Steady-state Conditions After The Fire ***                    5/2/94  2pm

 SUBMODEL NAME = MAIN

        PROBLEM TIME                    TIMEN                  =  999.000     VS. TIMEND=  999.000
                                  DIFFUSION NODES IN ASCENDING NODE NUMBER ORDER
 T   267=  267.73     T   268=  267.85     T   269=  261.91
                                ARITHMETIC NODES IN ASCENDING NODE NUMBER ORDER
 T   201=  312.00     T  1266=  275.33     T  1267=  343.66     T  1268=  326.63     T  1269=  279.91
                                  HEATER NODES IN ASCENDING NODE NUMBER ORDER
                                                ++NONE++
                                  BOUNDARY NODES IN ASCENDING NODE NUMBER ORDER
                                                ++NONE++
MEAN ICV GAS TEMP= 312.0 F   MEAN ICV GAS PRESSURE= 23.20 PSIA
MEAN ICV-OCV GAS TEMP= 174.9 F   MEAN ICV-OCV GAS PRESSURE= 22.37 PSIA


 SUBMODEL NAME = PTSA
                                          CALCULATED                          ALLOWED
       MAX DIFF DELTA T PER ITER          DRLXCC(PTSA          371)= 3.753662E-02 VS. DRLXCA= 5.000000E-02
       MAX ARITH DELTA T PER ITER         ARLXCC(PTSA          358)= 1.739502E-02 VS. ARLXCA= 0.500000
       MAX SYSTEM ENERGY BALANCE          EBALSC                 =  1.53377       VS. EBALSA * ESUMIS      =  4.07869
                                                                                     EBALSA= 1.000000E-03
       ENERGY INTO AND OUT OF SYS         ESUMIS                 =  4078.69       ESUMOS=  1303.94
       MAX NODAL ENERGY BALANCE           EBALNC(PTSA          354)= 0.209371     VS. EBALNA= 1.000000E-02
       NUMBER OF ITERATIONS               LOOPCT                 =  128           VS. NLOOPS=  1000
       PROBLEM TIME                       TIMEN                  =  999.000       VS. TIMEND=  999.000
                                  DIFFUSION NODES IN ASCENDING NODE NUMBER ORDER
 T    51=  291.59     T    53=  439.41     T    55=  613.05     T    60=  269.68     T    62=  626.76     T   100=  238.89
 T   105=  246.07     T   107=  248.86     T   110=  251.26     T   112=  252.19     T   113=  248.69     T   120=  274.83
 T   122=  278.16     T   123=  269.15     T   124=  279.21     T   125=  271.66     T   126=  281.70     T   127=  277.44
 T   130=  353.99     T   132=  361.77     T   133=  344.02     T   134=  361.88     T   135=  347.46     T   136=  360.68
 T   137=  353.63     T   140=  430.44     T   141=  431.79     T   142=  436.69     T   143=  414.35     T   144=  445.03
 T   145=  428.47     T   146=  463.17     T   147=  455.82     T   150=  546.66     T   152=  555.09     T   153=  518.51
 T   154=  570.80     T   155=  548.56     T   156=  596.52     T   157=  596.63     T   160=  644.15     T   161=  630.96
 T   162=  654.38     T   163=  613.42     T   164=  665.56     T   165=  647.71     T   166=  684.90     T   167=  677.49
 T   170=  680.91     T   172=  684.77     T   173=  661.72     T   175=  693.49     T   177=  685.19     T   180=  673.57
 T   190=  736.45     T   191=  790.88     T   192=  401.82     T   193=  678.59     T   194=  442.26     T   196=  574.59
 T   198=  793.18     T   200=  177.68     T   204=  171.11     T   210=  195.26     T   220=  221.61     T   230=  341.15
 T   240=  443.46     T   242=  311.30     T   250=  236.63     T   260=  216.81     T   261=  220.23     T   262=  235.50
 T   263=  244.00     T   264=  228.75     T   265=  235.95     T   266=  222.94     T   300=  109.46     T   304=  93.240
 T   305=  21.598     T   310=  148.84     T   313=  130.06     T   315=  107.70     T   316=  107.70     T   320=  174.09
 T   323=  152.28     T   325=  126.30     T   326=  126.30     T   330=  275.24     T   333=  246.07     T   335=  203.13
 T   336=  203.13     T   340=  306.78     T   342=  250.83     T   343=  143.54     T   344=  208.93     T   345=  140.43
 T   346=  120.35     T   347=  171.44     T   349=  129.24     T   350=  194.41     T   351=  185.66     T   352=  192.31
 T   353=  188.59     T   354=  194.68     T   355=  194.11     T   356=  190.71     T   360=  211.32     T   362=  223.31
 T   364=  214.83     T   366=  195.72     T   367=  193.16     T   368=  189.39     T   369=  186.85     T   371=  185.77
 T   373=  188.03     T   375=  190.53     T   377=  191.76     T   400=  211.88     T   401=  208.75     T   402=  191.97
 T   404=  124.13     T   406=  30.231     T   408=  0.91711     T   410= -12.529     T   412= -9.9413     T   414= -7.9076
```

T	421=	142.87	T	422=	12.658	T	423=	1.4421	T	424=	122.60	T	425=	8.7026	T	426=	-1.1861		
T	431=	33.137	T	432=	27.524	T	433=	24.857	T	434=	9.5292	T	435=	-2.9236	T	436=	-0.91998		
T	950=	738.82	T	952=	817.04														

ARITHMETIC NODES IN ASCENDING NODE NUMBER ORDER

T	50=	309.44	T	52=	440.49	T	54=	591.38	T	158=	636.29	T	159=	630.84	T	168=	630.30		
T	169=	628.08	T	195=	330.00	T	197=	378.03	T	199=	575.48	T	238=	599.83	T	311=	128.50		
T	312=	128.50	T	321=	150.49	T	322=	150.49	T	331=	243.02	T	332=	243.02	T	337=	225.45		
T	341=	246.83	T	357=	191.09	T	358=	185.97	T	359=	193.33	T	379=	194.36	T	403=	191.83		
T	1000=	368.34	T	1001=	679.35	T	1002=	581.33	T	1003=	456.64	T	1004=	365.61	T	1005=	361.03		
T	1006=	236.10	T	1007=	726.54	T	1008=	745.53	T	1009=	777.02	T	1010=	365.30	T	1011=	148.51		
T	1012=	148.51	T	1013=	115.83	T	1021=	173.69	T	1022=	173.69	T	1023=	135.71	T	1031=	274.49		
T	1032=	274.49	T	1033=	218.58	T	1041=	305.46	T	1042=	305.46	T	1043=	250.49	T	1044=	250.49		
T	1346=	128.05	T	1347=	177.90														

HEATER NODES IN ASCENDING NODE NUMBER ORDER

++NONE++

BOUNDARY NODES IN ASCENDING NODE NUMBER ORDER

T	1=	-20.000	T	2=	-20.000														

SYSTEMS IMPROVED NUMERICAL DIFFERENCING ANALYZER '85 (SINDA '85) PAGE 2/4

MODEL = DAMAGE6
STDSTL

LOAD CASE NO. 6 CONDITIONS - Ungula Distributions, -20F
*** Steady-state Conditions After The Fire ***

5/2/94 2pm

SUBMODEL NAME = PTSB

		CALCULATED		ALLOWED	
MAX DIFF DELTA T PER ITER	DRLXCC(PTSB	351)=-3.198242E-02	VS.	DRLXCA=	5.000000E-02
MAX ARITH DELTA T PER ITER	ARLXCC(PTSB	358)=-2.655029E-02	VS.	ARLXCA=	0.500000
MAX SYSTEM ENERGY BALANCE	EBALSC	= -11.5250	VS.	EBALSA * ESUMIS =	3.60058
				EBALSA=	1.000000E-03
ENERGY INTO AND OUT OF SYS	ESUMIS	= 3600.58		ESUMOS=	2223.82
MAX NODAL ENERGY BALANCE	EBALNC(PTSB	367)= -1.17477	VS.	EBALNA=	1.000000E-02
NUMBER OF ITERATIONS	LOOPCT	= 128	VS.	NLOOPS=	1000
PROBLEM TIME	TIMEN	= 999.000	VS.	TIMEND=	999.000

DIFFUSION NODES IN ASCENDING NODE NUMBER ORDER

T	51=	270.31	T	53=	384.53	T	55=	523.05	T	60=	253.11	T	62=	540.93	T	100=	228.85
T	105=	234.72	T	107=	236.99	T	110=	239.07	T	112=	241.25	T	113=	236.44	T	120=	257.03
T	122=	263.19	T	123=	249.77	T	124=	262.16	T	125=	250.98	T	126=	260.20	T	127=	254.09
T	130=	318.33	T	132=	331.92	T	133=	304.41	T	134=	328.80	T	135=	306.33	T	136=	321.33
T	137=	309.97	T	140=	377.67	T	141=	378.74	T	142=	392.33	T	143=	357.62	T	144=	394.69
T	145=	367.81	T	146=	400.35	T	147=	388.56	T	150=	464.69	T	152=	490.61	T	153=	424.47
T	154=	498.39	T	155=	452.65	T	156=	511.05	T	157=	502.35	T	160=	547.58	T	161=	536.87
T	162=	578.59	T	163=	499.48	T	164=	582.52	T	165=	537.87	T	166=	591.77	T	167=	575.17
T	170=	587.40	T	172=	602.85	T	173=	558.38	T	175=	601.32	T	177=	592.98	T	180=	588.59
T	190=	635.75	T	191=	675.19	T	192=	355.52	T	193=	575.31	T	194=	391.55	T	196=	516.59
T	198=	676.89	T	200=	177.71	T	204=	170.62	T	210=	191.78	T	220=	208.01	T	230=	271.80
T	240=	336.86	T	242=	257.89	T	250=	207.50	T	260=	204.17	T	261=	206.86	T	262=	208.50
T	263=	212.43	T	264=	203.46	T	265=	208.29	T	266=	198.27	T	300=	109.62	T	304=	92.879
T	305=	21.450	T	310=	146.02	T	313=	127.59	T	315=	105.65	T	316=	105.65	T	320=	162.46
T	323=	142.09	T	325=	117.86	T	326=	117.86	T	330=	217.78	T	333=	193.83	T	335=	160.43
T	336=	160.43	T	340=	236.11	T	342=	206.83	T	343=	123.28	T	344=	182.18	T	345=	123.40
T	346=	101.06	T	347=	152.32	T	349=	112.00	T	350=	173.54	T	351=	165.38	T	352=	171.95
T	353=	168.40	T	354=	172.97	T	355=	174.30	T	356=	170.08	T	360=	199.34	T	362=	201.63
T	364=	193.00	T	366=	175.70	T	367=	173.58	T	368=	170.64	T	369=	168.48	T	371=	165.38
T	373=	167.76	T	375=	170.71	T	377=	172.32	T	400=	192.80	T	401=	189.83	T	402=	172.61
T	404=	114.25	T	406=	23.095	T	408=	-3.9888	T	410=	-12.645	T	412=	-10.568	T	414=	-8.7712
T	421=	129.50	T	422=	10.248	T	423=	-0.13248	T	424=	111.84	T	425=	6.6447	T	426=	-3.0859
T	431=	61.572	T	432=	45.027	T	433=	64.612	T	434=	34.497	T	435=	-4.9106	T	436=	-7.1834
T	441=	8.2619	T	442=	11.340	T	443=	5.6451	T	444=	0.76740	T	445=	-7.1516	T	446=	-5.9670
T	451=	8.7225	T	452=	14.790	T	453=	2.4964	T	454=	-2.5789	T	455=	-9.1470	T	456=	-7.6217
T	954=	699.99															

ARITHMETIC NODES IN ASCENDING NODE NUMBER ORDER

T	50=	284.10	T	52=	385.58	T	54=	506.37	T	158=	546.00	T	159=	532.86	T	168=	536.22
T	169=	534.43	T	195=	297.46	T	197=	345.87	T	199=	512.90	T	238=	349.46	T	311=	126.06

```
T  312= 126.06    T  321= 140.42    T  322= 140.42    T  331= 191.51    T  332= 191.51    T  337= 184.38
T  341= 201.47    T  357= 170.08    T  358= 165.43    T  359= 172.72    T  379= 174.56    T  403= 172.41
T 1000= 325.82    T 1001= 587.44    T 1002= 512.10    T 1003= 400.98    T 1004= 324.49    T 1005= 320.66
T 1006= 214.17    T 1007= 627.10    T 1008= 641.86    T 1009= 665.02    T 1010= 322.22    T 1011= 145.70
T 1012= 145.70    T 1013= 113.63    T 1021= 162.09    T 1022= 162.09    T 1023= 126.64    T 1031= 217.26
T 1032= 217.26    T 1033= 172.48    T 1041= 235.30    T 1042= 235.30    T 1043= 206.47    T 1044= 206.47
T 1346= 111.26    T 1347= 159.27
                    HEATER NODES IN ASCENDING NODE NUMBER ORDER
                                      ++NONE++
                    BOUNDARY NODES IN ASCENDING NODE NUMBER ORDER
T    1= -20.000    T    2= -20.000
```

SYSTEMS IMPROVED NUMERICAL DIFFERENCING ANALYZER '85 (SINDA '85) PAGE 3/4

MODEL = DAMAGE6
STDSTL

LOAD CASE NO. 6 CONDITIONS - Ungula Distributions, -20F
*** Steady-state Conditions After The Fire *** 5/2/94 2pm

SUBMODEL NAME = PTSC

		CALCULATED		ALLOWED	
MAX DIFF DELTA T PER ITER	DRLXCC(PTSC	55)= 2.655029E-02	VS.	DRLXCA= 5.000000E-02	
MAX ARITH DELTA T PER ITER	ARLXCC(PTSC	54)= 2.331543E-02	VS.	ARLXCA= 0.500000	
MAX SYSTEM ENERGY BALANCE	EBALSC	= 3.47679	VS.	EBALSA * ESUMIS =	0.
				EBALSA= 1.000000E-03	
ENERGY INTO AND OUT OF SYS	ESUMIS	= 0.		ESUMOS= 2570.22	
MAX NODAL ENERGY BALANCE	EBALNC(PTSC	320)=-0.787053	VS.	EBALNA= 1.000000E-02	
NUMBER OF ITERATIONS	LOOPCT	= 128	VS.	NLOOPS= 1000	
PROBLEM TIME	TIMEN	= 999.000	VS.	TIMEND= 999.000	

DIFFUSION NODES IN ASCENDING NODE NUMBER ORDER

T	51=	236.84	T	53=	289.14	T	55=	343.22	T	60=	225.86	T	62=	327.27	T	100=	212.28
T	105=	215.80	T	107=	217.16	T	110=	218.82	T	112=	220.64	T	113=	217.88	T	120=	230.31
T	122=	234.92	T	123=	226.86	T	124=	231.29	T	125=	224.51	T	126=	223.63	T	127=	219.78
T	130=	262.41	T	132=	272.72	T	133=	255.91	T	134=	265.40	T	135=	251.33	T	136=	249.57
T	137=	241.68	T	140=	286.11	T	141=	286.27	T	142=	298.74	T	143=	278.35	T	144=	289.41
T	145=	272.22	T	146=	267.53	T	147=	258.76	T	150=	311.54	T	152=	336.64	T	153=	294.30
T	154=	322.39	T	155=	287.38	T	156=	290.38	T	157=	269.51	T	160=	346.28	T	161=	337.51
T	162=	378.99	T	163=	325.48	T	164=	358.75	T	165=	313.47	T	166=	316.02	T	167=	294.75
T	170=	327.08	T	172=	347.51	T	173=	318.90	T	175=	313.95	T	177=	320.36	T	180=	315.38
T	190=	290.84	T	191=	287.15	T	192=	212.07	T	193=	246.90	T	194=	207.57	T	196=	347.14
T	198=	286.77	T	200=	180.81	T	204=	176.02	T	210=	190.88	T	220=	193.20	T	230=	170.81
T	240=	164.79	T	242=	153.31	T	250=	149.44	T	260=	173.97	T	261=	174.97	T	262=	162.42
T	263=	163.57	T	264=	154.45	T	265=	156.59	T	266=	148.12	T	300=	111.32	T	304=	95.343
T	305=	22.272	T	310=	144.85	T	313=	126.55	T	315=	104.75	T	316=	104.75	T	320=	148.39
T	323=	129.71	T	325=	107.51	T	326=	107.51	T	330=	131.63	T	333=	114.31	T	335=	94.741
T	336=	94.741	T	340=	129.06	T	342=	128.19	T	343=	85.013	T	344=	127.92	T	345=	87.434
T	346=	66.402	T	347=	110.51	T	349=	77.816	T	350=	127.58	T	351=	120.83	T	352=	126.74
T	353=	123.78	T	354=	125.86	T	355=	129.92	T	356=	124.58	T	360=	170.51	T	362=	159.65
T	364=	147.57	T	366=	131.11	T	367=	129.50	T	368=	127.71	T	369=	126.12	T	371=	120.67
T	373=	123.02	T	375=	126.43	T	377=	128.48	T	400=	152.90	T	401=	150.32	T	402=	128.91
T	404=	82.613	T	406=	11.009	T	408=	-8.2278	T	410=	-14.330	T	412=	-12.499	T	414=	-10.728
T	421=	101.37	T	422=	4.9738	T	423=	-3.5980	T	424=	82.203	T	425=	1.0713	T	426=	-6.6029
T	431=	41.945	T	432=	29.319	T	433=	44.560	T	434=	21.811	T	435=	-8.3393	T	436=	-10.180
T	441=	1.0903	T	442=	2.9052	T	443=	-0.71378	T	444=	-4.4100	T	445=	-10.385	T	446=	-9.6001
T	451=	0.92978	T	452=	4.9564	T	453=	-3.4265	T	454=	-7.0576	T	455=	-11.820	T	456=	-10.775

ARITHMETIC NODES IN ASCENDING NODE NUMBER ORDER

T	50=	242.82	T	52=	289.10	T	54=	334.70	T	158=	341.88	T	159=	329.19	T	168=	338.00
T	169=	339.28	T	195=	201.78	T	197=	200.39	T	199=	238.85	T	238=	168.17	T	311=	125.03
T	312=	125.03	T	321=	128.18	T	322=	128.18	T	331=	112.96	T	332=	112.96	T	337=	113.20

T	341=	122.96	T	357=	124.12	T	358=	120.58	T	359=	127.14	T	379=	130.21	T	403=	128.62
T	1000=	195.38	T	1001=	290.11	T	1002=	239.04	T	1003=	226.88	T	1004=	202.91	T	1005=	201.87
T	1006=	171.58	T	1007=	301.24	T	1008=	293.52	T	1009=	289.09	T	1010=	180.31	T	1011=	144.54
T	1012=	144.54	T	1013=	112.68	T	1021=	148.06	T	1022=	148.06	T	1023=	115.55	T	1031=	131.35
T	1032=	131.35	T	1033=	101.82	T	1041=	128.81	T	1042=	128.81	T	1043=	127.95	T	1044=	127.95
T	1346=	77.355	T	1347=	117.33												

HEATER NODES IN ASCENDING NODE NUMBER ORDER
++NONE++

BOUNDARY NODES IN ASCENDING NODE NUMBER ORDER

T	1=	-20.000	T	2=	-20.000

SYSTEMS IMPROVED NUMERICAL DIFFERENCING ANALYZER '85 (SINDA '85) PAGE 4/4

MODEL = DAMAGE6 LOAD CASE NO. 6 CONDITIONS - Ungula Distributions, -20F
STDSTL *** Steady-state Conditions After The Fire *** 5/2/94 2pm

SUBMODEL NAME = PTSD

		CALCULATED		ALLOWED	
MAX DIFF DELTA T PER ITER	DRLXCC(PTSD	351)=	-1.953125E-02	VS. DRLXCA=	5.000000E-02
MAX ARITH DELTA T PER ITER	ARLXCC(PTSD	197)=	-2.551270E-02	VS. ARLXCA=	0.500000
MAX SYSTEM ENERGY BALANCE	EBALSC	=	-7.97927	VS. EBALSA * ESUMIS =	0.
				EBALSA=	1.000000E-03
ENERGY INTO AND OUT OF SYS	ESUMIS	=	0.	ESUMOS=	1653.44
MAX NODAL ENERGY BALANCE	EBALNC(PTSD	367)=	-1.01213	VS. EBALNA=	1.000000E-02
NUMBER OF ITERATIONS	LOOPCT	=	128	VS. NLOOPS=	1000
PROBLEM TIME	TIMEN	=	999.000	VS. TIMEND=	999.000

DIFFUSION NODES IN ASCENDING NODE NUMBER ORDER

T	51=	221.52	T	53=	249.81	T	55=	274.11	T	60=	213.58	T	62=	265.95	T	100=	204.34
T	105=	207.07	T	107=	208.13	T	110=	209.49	T	112=	210.35	T	113=	209.30	T	120=	218.11
T	122=	220.02	T	123=	217.02	T	124=	217.78	T	125=	215.23	T	126=	213.41	T	127=	211.91
T	130=	237.78	T	132=	241.98	T	133=	235.92	T	134=	237.92	T	135=	232.77	T	136=	229.60
T	137=	226.53	T	140=	250.04	T	141=	250.10	T	142=	254.78	T	143=	248.14	T	144=	249.89
T	145=	244.25	T	146=	238.84	T	147=	236.29	T	150=	258.20	T	152=	265.90	T	153=	253.94
T	154=	259.96	T	155=	249.68	T	156=	246.92	T	157=	239.85	T	160=	275.56	T	161=	271.21
T	162=	285.91	T	163=	270.62	T	164=	278.04	T	165=	264.01	T	166=	261.92	T	167=	255.75
T	170=	263.56	T	172=	268.66	T	173=	262.25	T	175=	258.49	T	177=	260.85	T	180=	259.65
T	190=	249.89	T	191=	245.94	T	192=	184.74	T	193=	230.01	T	194=	183.72	T	196=	280.60
T	198=	245.54	T	200=	179.50	T	204=	173.76	T	210=	187.65	T	220=	186.84	T	230=	178.09
T	240=	153.23	T	242=	136.94	T	250=	131.53	T	260=	155.60	T	261=	156.38	T	262=	142.95
T	263=	143.87	T	264=	135.58	T	265=	137.41	T	266=	130.16	T	300=	110.67	T	304=	94.068
T	305=	21.817	T	310=	142.30	T	313=	124.32	T	315=	102.91	T	316=	102.91	T	320=	143.42
T	323=	125.36	T	325=	103.90	T	326=	103.90	T	330=	131.89	T	333=	112.60	T	335=	93.235
T	336=	93.235	T	340=	123.34	T	342=	116.57	T	343=	75.456	T	344=	113.55	T	345=	77.216
T	346=	59.442	T	347=	97.478	T	349=	68.893	T	350=	112.51	T	351=	106.69	T	352=	111.73
T	353=	109.19	T	354=	111.14	T	355=	114.36	T	356=	109.91	T	360=	152.57	T	362=	140.73
T	364=	129.72	T	366=	115.37	T	367=	113.95	T	368=	112.29	T	369=	110.86	T	371=	106.56
T	373=	108.55	T	375=	111.40	T	377=	113.10	T	400=	135.07	T	401=	132.69	T	402=	113.42
T	404=	72.024	T	406=	8.8451	T	408=	-9.3730	T	410=	-14.844	T	412=	-13.195	T	414=	-11.586
T	421=	88.870	T	422=	2.6016	T	423=	-5.1375	T	424=	71.638	T	425=	-0.95508	T	426=	-7.8722
T	431=	35.991	T	432=	25.071	T	433=	38.093	T	434=	17.605	T	435=	-9.4430	T	436=	-11.108
T	441=	-0.75497	T	442=	1.0695	T	443=	-2.5211	T	444=	-5.9105	T	445=	-11.302	T	446=	-10.605
T	451=	-0.76688	T	452=	3.0516	T	453=	-4.9065	T	454=	-8.2765	T	455=	-12.584	T	456=	-11.656

ARITHMETIC NODES IN ASCENDING NODE NUMBER ORDER

T	50=	224.56	T	52=	249.57	T	54=	270.17	T	158=	272.29	T	159=	268.38	T	168=	271.45
T	169=	272.02	T	195=	176.49	T	197=	176.10	T	199=	212.55	T	238=	167.22	T	311=	122.83
T	312=	122.83	T	321=	123.88	T	322=	123.88	T	331=	111.18	T	332=	111.18	T	337=	103.35

T	341=	112.48	T	357=	109.56	T	358=	106.46	T	359=	112.10	T	379=	114.59	T	403=	113.21
T	1000=	172.23	T	1001=	244.56	T	1002=	210.94	T	1003=	196.05	T	1004=	177.45	T	1005=	176.62
T	1006=	152.26	T	1007=	253.34	T	1008=	250.15	T	1009=	247.22	T	1010=	160.06	T	1011=	141.99
T	1012=	141.99	T	1013=	110.70	T	1021=	143.11	T	1022=	143.11	T	1023=	111.68	T	1031=	131.59
T	1032=	131.59	T	1033=	100.24	T	1041=	123.14	T	1042=	123.14	T	1043=	116.45	T	1044=	116.45
T	1346=	68.486	T	1347=	103.30												

HEATER NODES IN ASCENDING NODE NUMBER ORDER
++NONE++
BOUNDARY NODES IN ASCENDING NODE NUMBER ORDER

T	1=	-20.000	T	2=	-20.000

3.6.6 Miscellaneous Calculations

The following pages present miscellaneous hand calculations that support various parameters used in the package thermal model.

"Ungula" Rubble Pile Thermal Data

Objective: Determine heat transfer parameters for an ungula-shaped pile of GPHS heat source modules (aeroshells).

Basis of Analysis:

1) Conservatively assume that all 18 aeroshells escape from the RTG shell.

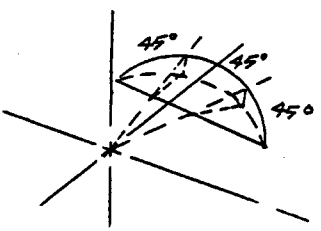
2) Worst case package orientation would be a 45° tip angle with aeroshells grouped in a ungula shaped pile.

3) Model testing and analytical calculations indicate the pile would be 50% void space and subtend at a 136° angle.

Analysis:

Use three 45° model segments to simulate the rubble pile (ungula-shaped pile of aeroshells.

Per analytical calculations, the various dimensions of the rubble pile are as follows:



	Total	Side 45°	Middle 45°	Side 45°
Bottom area ($in.^2$)	241.2	72.1	97.0	72.1
Side area ($in.^2$)	277.2	70.5	136.2	70.5
Volume ($in.^3$)	1048.9	245.9	557.1	245.9

Side Area of Shipping Rack Assembly Barrier Plate: $= \frac{45°}{360°} \times 2\pi \times 16.0625\ in. \times 5\ in.$

$= 63.08\ in.^2\ per\ 45°\ segment$

$$\textit{Bottom Area of Barrier Plate} = \frac{45°}{360°} \times \pi \times 16.0625^2$$

$$= 101.318\ in^2\ per\ 45°\ segment$$

Because side area of barrier plate is less than side area of ungula pile, some of the pile will extend above the edge of the barrier plate and lie against the ICV wall.

Because the bottom area of the ungula pile at each 45° segment is less than the bottom area of the barrier plate, the rubble pile will not extend past the centerline of the barrier plate. Therefore, the appropriate distribution of rubble pile area and model nodes is:

	Side 45°	Middle 45°	Side 45°
ICV wall at #238	7.42 in.^{2}	73.2 in.^{2}	7.42 in.^{2}
Barrier plate at #193	63.08	63.08	63.08
Barrier plate at #198	72.1	87.2	72.1
Barrier plate at #193	0	9.8*	0

*Combine area with that at #198 under the assumption that RTG support legs will keep aeroshells from center.

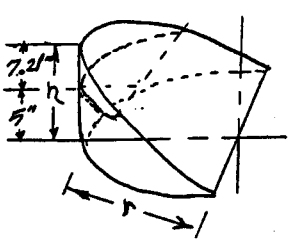
Model rubble pile as homogenous mass with one node representing side segment pile and two at center segment, one for portion of pile above barrier plate vertical wall and one for portion below the barrier plate vertical wall.

This approach is valid because pile will be a porous and open assembly of aeroshells. Therefore, radiation and convection can and will occur from deep within the pile. Using the bulk average temperatures will be appropriate given the conservative assumption that all 18 aeroshells spill out during an accident.

Peak height, h, and average depth, r, of pile is:

$$r \approx 11.35\ in.$$

$$h \approx 12.21\ in.$$



$\therefore$ *peak height above barrier plate is*

$$12.21\ in. - 5\ in. = 7.21\ in. = h'$$

Depth of pile above barrier plate is

$$r' \approx 73.2\ in^2 + 2 + 7.21\ in.$$

$$\approx 5.08\ in.$$

Now volume of pile above barrier plate is

$$V' \approx \frac{2}{3} r'^2 \times h'$$

$$\approx \frac{2}{3} \times (5.08)^2 \times 7.21$$

$$\approx 124.0\ in.^3$$

Surface Area of pile above barrier plate is

$$A' \approx \frac{\pi}{2} \times 5.08\ in. \sqrt{5.08^2 + 7.21^2}$$

$$\approx 70.4\ in.^2$$

Surface area of aeroshells is:

$$A_{modules} = 18 \times [(3.83\ in. \times 3.64\ in. \times 2) +$$

$$(3.64\ in. \times 2.09\ in. \times 2) + (2.09\ in. \times 3.83\ in. \times 2)]$$

$$= 1063.93\ in.^3$$

Assume 50% of surface area of each aeroshell is sufficiently exposed to participate in convective heat transfer.

Radiation from the pile will be based on the plane area of the rubble pile. Radiation from rubble pile will be to the RTG shell only, because of assumed blockage by shell and for reasons of conservatism.

Therefore, a summary of thermal properties assumed for each model node is as follows:

	Node #954 side segment	Center segment top #950	Center segment bottom #952
Rubble volume	245.9 in.^{3}	124.0 in.^{3}	433.1 in.^{3}
Thermal mass	3.33 Btu/°F	1.68 Btu/°F	5.86 Btu/°F
Heat dissipation	1054.96 W	531.99 W	1858.09 W
Pile surface area	75.6 in.^{2}	70.4 in.^{2}	75.6 in.^{2}
Convection area	124.7 in.^{2}	62.9 in.^{2}	219.7 in.^{2}

Further Assumptions

- Emissivity of graphite aeroshells approximately 0.5
- Nominal gap between aeroshells and ICV/barrier plate walls is approximately 0.25 in.; assume full area contact
- Nominal gap between aeroshells and barrier plate bottom is assumed to be 0.05 in.; use full area contact

$$\textit{Radiation from } 954 \textit{ to } 193 = \frac{63.08 \text{ in.}^2/144 \times \sigma}{\left(\frac{1}{0.5} - 1\right) + \frac{1}{1} + \left(\frac{1}{0.48} - 1\right)}$$

$$= 0.324 \times \frac{63.08}{144} \times \sigma$$

$$954 \textit{ to } 238 = \frac{7.42 \text{ in.}^2/144 \times \sigma}{\left(\frac{1}{0.5} - 1\right) + \frac{1}{1} + \left(\frac{1}{0.9} - 1\right)}$$

$$= 0.474 \times 7.42/144 \times \sigma$$

$$954 \textit{ to } 198 = \frac{72.1/144 \times \sigma}{\left(\frac{1}{0.5} - 1\right) + \frac{1}{1} + \left(\frac{1}{0.48} - 1\right)}$$

$$= 0.324 \times 72.1/144 \times \sigma$$

$$950 \text{ to } 238 = 0.474 \times \frac{73.2}{2^*}/144 \times \sigma$$

$* \frac{1}{2}$ *factor for symmetry condition*

$$952 \text{ to } 193 = 0.324 \times \frac{63.08}{2}/144 \times \sigma$$

$$952 \text{ to } 198 = 0.324 \times \frac{97.0}{2}/144 \times \sigma$$

Conduction

$$954 \text{ to } 193 = \frac{63.08/144}{0.25 \text{ in. gap}} \times K_{He}$$

$$= 1.7522 \times K_{He}$$

$$954 \text{ to } 238 = \frac{7.42/144}{0.25 \text{ in.}} \times K_{He}$$

$$= 0.2061 \times K_{He}$$

$$954 \text{ to } 198 = \frac{72.1/144}{0.05 \text{ in.}} \times K_{He}$$

$$= 10.0139 \times K_{He}$$

$$950 \text{ to } 238 = \frac{73.2/144}{0.25 \text{ in.}} \times K_{He} \times \frac{1}{2}$$

$$= 1.0167 \times K_{He}$$

$$952 \text{ to } 193 = \frac{63.08/144}{0.25 \text{ in.}} \times K_{He} \times \frac{1}{2}$$

$$= 0.8761 \times K_{He}$$

$$952 \text{ to } 198 = \frac{97.0/144}{0.25 \text{ in.}} \times K_{He} \times \frac{1}{2}$$

$$= 6.7361 \times K_{He}$$

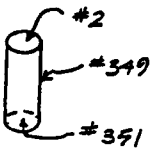
Radiation View Factors

Objective: Determine miscellaneous view factors for RTG transport package.

Analysis:

OCV Bolt Tubes →

Tube diameter = 2.26 in.
Tube Length = 3¼ in.



$$F_{2\text{-}349_a} = 2H[(1+H^2)^{\frac{1}{2}} - H] \qquad H = \frac{\text{length}}{\text{diameter}}$$

Reference: Table 6.2, Item O, Handbook of Applied Thermal Design, Eric C. Guyer

$$H = \frac{3.25}{2.26}$$

$$= 1.43805$$

$$\therefore F_{2-349_a} = 0.90171$$

$$F_{2-351} = 1.0 - F_{2-349_a}$$

$$= 1.0 - 0.90171$$

$$= 0.09829$$

$$F_{349_a-2} = A_2 \times F_{2-349_a}/A_{349_a}$$

$$= (\frac{\pi}{4} \times 2.26^2 \times 0.90171)/(\pi \times 2.26 \times 3.25)$$

$$= 0.15676$$

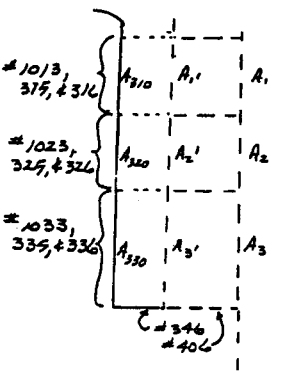
Impact Limiter Tubes → tube diameter = 1.51 in.

$$F_{2-349_b} = 0.95117 \text{ with } H = 2.15232$$

$$F_{349_0 - 2} = (\frac{\pi}{4} \times 1.51^2 \times 0.95117)/(\pi \times 1.51 \times 3.25)$$

$$= 0.11048$$

OCV Cooling Jacket and Impact Limiter



Computer shape factor via equations for configuration #5, page 14-41, Handbook of Heat Transfer Fundamentals, Rohsenow, et al.

$$F_{1033/335/336 - A_3'} = (A_{3'} \times F_{A_3' - 1033/335/336})/(A_{1033/335/336})$$

$$= \frac{2\pi \times 26.625 \text{ in.} \times 19.76 \text{ in.} \times 0.544390}{2\pi \times 19.575 \text{ in.} \times 19.76 \text{ in.}}$$

$$= 0.74045$$

$$\therefore F_{330 - 346} = \frac{1}{2}(1.0 - 0.74045)$$

$$= 0.129775$$

$$F_{A_{330} - A_3} = A_3 \times F_{A_3 - 1033/335/336} / A_{1033/335/336}$$

$$= \frac{2\pi \times 35 \text{ in.} \times 19.76 \text{ in.} \times 0.300816}{2\pi \times 19.575 \times 19.76 \text{ in.}}$$

$$= 0.53786$$

$$F_{330 - 346/406} = \frac{1}{2} \times (1.0 - 0.53786)$$

$$= 0.23107$$

$$F_{330 - 406} = F_{330/ - 346/406} - F_{330 - 346}$$

$$= 0.23107 - 0.129775$$

$$= 0.101295$$

$$F_{330 - \infty} = 0.53786 + 0.23107$$

$$= 0.76893$$

$$F_{320/330 - A_{2' \& 3'}} = \frac{A_{2' \& 3'} \times F_{A_{2' \& 3'} - 1023/325/326/1033/335/336}}{A_{1023/325/326/1033/336/336}}$$

$$= \frac{2\pi \times 26.625 \text{ in.} \times 33.48 \text{ in.} \times 0.617842}{2\pi \times 19.575 \text{ in.} \times 33.48 \text{ in.}}$$

$$= 0.84036$$

$$\therefore F_{320/330 - 346} = \frac{1}{2}(1.0 - 0.84036)$$

$$= 0.0798$$

$$A_{320} F_{320 - 346} = A_{320/330} F_{320/330 - 346} - A_{330} F_{330 - 346}$$

$$2\pi \times 19.575 \text{ in.} \times 13.72 \text{ in.} \times F_{320 - 346} = (2\pi \times 19.575 \text{ in.} \times 33.48 \text{ in.} \times 0.0798 \text{ in.}) -$$

$$(2\pi \times 19.575 \text{ in.} \times 19.76 \text{ in.} \times 0.129775)$$

$$F_{320 - 346} = 0.007824$$

$$F_{320/330 - A_{2/3}} = A_{2/3} \times F_{A_{2/3} - 320/330} / A_{320/330}$$

$$= \frac{35\ in.}{19.575\ in.} \times 0.386812$$

$$= 0.691618$$

$$F_{320/330-346/406} = \frac{1}{2}(1.0 - 0.691618)$$

$$= 0.154191$$

$$F_{320/330 - 406} = F_{320/330 - 346/406} - F_{320/330 - 346}$$

$$= 0.154191 - 0.0798$$

$$= 0.07439$$

$$A_{320} F_{320 - 406} = A_{320/330} F_{320/330 - 406} - A_{330} F_{330 - 406}$$

$$2\pi \times 19.575\ in. \times 13.72\ in. \times F_{320 - 406} = (2\pi \times 19.575\ in. \times 33.48\ in. \times 0.07439) -$$

$$(2\pi \times 19.575\ in. \times 19.76\ in. \times 0.101295)$$

$$F_{320 - 406} = 0.035641$$

$$F_{320 - -} = 1.0 - F_{320 - 406} - F_{320 - 346}$$

$$= 0.957999$$

$$F_{310/320/330 - A_{1/2/3/}} = \frac{A_{1/2/3/} \times F_{A_{1/2/3/} - 310/320/330}}{A_{310/320/330}}$$

$$= \frac{2\pi \times 26.625\ in. \times 47.2\ in. \times 0.650953}{2\pi \times 19.575\ in. \times 47.2\ in.}$$

$$= 0.88540$$

$$F_{310/320/330 - 346} = \frac{1}{2}(1.0 - 0.88540)$$

$$= 0.0573$$

$$A_{310} F_{310-346} = (A_{310/320/330} \times F_{310/320/330-346}) - (A_{320/330} \times F_{320/330-346})$$

$$13.72 \text{ in.} \times F_{310-346} = (47.2 \text{ in.} \times 0.0573) - (33.48 \text{ in.} \times 0.0798)$$

$$F_{310-346} = 0.002395$$

$$F_{310/320/330} - A_{1/2/3} = \frac{A_{1/2/3} \times F_{A_{1/2/3}-310/320/330}}{A_{310/320/330}}$$

$$= \frac{2\pi \times 35 \text{ in.} \times 47.2 \text{ in.} \times 0.431849}{2\pi \times 19.575 \text{ in.} \times 47.2 \text{ in.}}$$

$$= 0.77214$$

$$\therefore F_{310/320/330-346/406} = \frac{1}{2}(1.0 - 0.77214)$$

$$= 0.11393$$

$$F_{310/320/330-406} = F_{310/320/330-346/406} - F_{310/320/330-346}$$

$$= 0.11393 - 0.0573$$

$$= 0.05663$$

$$A_{310} \times F_{310-346} = A_{310/320/330} \times F_{310/320/330-406} - A_{320/330} \times F_{320/330-406}$$

$$13.72 \text{ in.} \times F_{310-406} = (47.2 \text{ in.} \times 0.05663) - (33.48 \text{ in.} \times 0.07439)$$

$$F_{310-406} = 0.01329$$

$$F_{310-\infty} = (1.0 - F_{310-346}) - F_{310-406}$$

$$= (1.0 - 0.002395) - 0.01329$$

$$= 0.984315$$

$$F_{406\text{ - }310/320/330} = \frac{A_{310/320/330} \times F_{310/320/330\text{ - }406}}{A_{406}}$$

$$= \frac{2\pi \times 19.575 \text{ in.} \times 47.2 \text{ in.} \times 0.05663}{\pi\,(35^2 - 19.625^2)\text{ in.}^2}$$

$$= 0.124599$$

$$\therefore F_{406\text{ - }\infty} = 1.0 - 0.124599$$

$$= 0.8754$$

$$F_{346\text{ - }310/320/330} = \frac{A_{310/320/330} \times F_{310/320/330\text{ - }346}}{A_{346}}$$

$$= \frac{2\pi \times 19.575 \text{ in.} \times 47.2 \text{ in.} \times 0.0573}{\pi\,(26.625^2 - 19.575^2)\text{ in.}^2}$$

$$= 0.32509$$

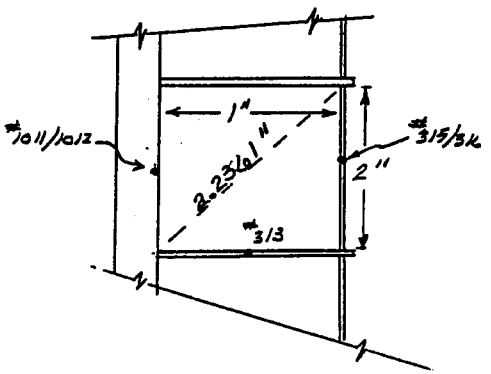
$$F_{346\text{ - }\infty} = 1.0 - F_{346\text{ - }310/320/330}$$

$$= 1.0 - 0.32509$$

$$= 0.6749$$

Coolant Channels:

- ignore curvature of shell
- use string method



$$F_{1011-313} = 2 \times \frac{(2\ in. + 1\ in.) - (2.2361\ in. + 0\ in.)}{2 \times 2\ in.}$$

$$= 0.38195$$

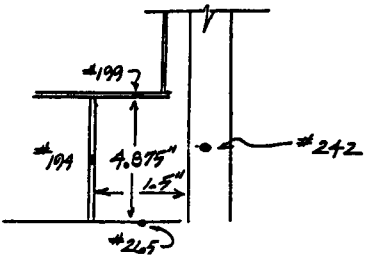
$$F_{1011-315} = \frac{(2.2361\ in. + 2.2361\ in.) - (1\ in. + 1\ in.)}{2 \times 2\ in.}$$

$$= 0.61805$$

$$F_{313-315} = \frac{(1\ in. + 2\ in.) - (2.2361\ in. + 0\ in.)}{2 \times 1\ in.}$$

$$= 0.38195$$

Shipping Rack



Use string method:

$$F_{265-242} = \frac{(1.5\ in. + 4.875\ in.) - (0\ in. + 5.1006\ in.)}{2 \times 1.5\ in.}$$

$$= 0.4248$$

$$F_{199-242} = F_{265-242}$$

$$= 0.4248$$

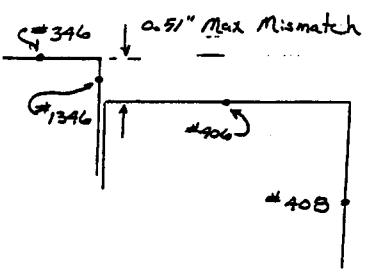
$$F_{194-242} = \frac{(2 \times 5.1006\ in.) - (2 \times 1.5\ in.)}{2 \times 4.875\ in.}$$

$$= 0.73858$$

$$F_{194-265} = F_{194-199} = \frac{1.0 - 0.7386}{2}$$

$$= 0.1307$$

Bolt Circle



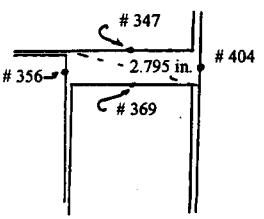
Gap Below Bolt Circle:

$$F_{1346-amb} = \frac{35\ in. \times 0.024935}{26.625\ in.} + \frac{1}{2} \times \left[1 - \frac{35\ in. \times 0.024935}{26.625\ in.}\right]$$

$$= 0.5164$$

$$F_{1346-406} = \frac{1}{2}\left[1 - \frac{35\ in. \times 0.024935}{26.625\ in.}\right]$$

$$= 0.4836$$



$$F_{356-404} = \frac{(2 \times 2.795\ in.) - (2 \times 2.750\ in.)}{2 \times 0.50\ in.}$$

$$= 0.09$$

$$F_{356-\frac{369}{347}} = \frac{0.50\ in. + 2.5\ in. - 2.55\ in.}{2 \times 0.50\ in.}$$

$$= 0.45$$

$$F_{\frac{369}{347}-404} = \frac{0.50\ in. + 2.750\ in. - 2.795\ in.}{2 \times 2.750\ in.}$$

$$= 0.0827$$

3.6.7 Listing of 2-D Computer Model

The following pages list the input file for the SINDA 2-D model of the RTG Transportation System Package and its GPHS RTG payload. The model is valid for the Normal Condtions of Transport (NCT) load case No. 1 (i.e., an undamaged Package, 100 °F, regulatory solar).

```
HEADER OPTIONS DATA
TITLE NORMAL CONDITION OF TRANSPORT - CASE 1: 100F,
SOLAR, GPHS RTG
      MODEL= GPHS4
      OUTPUT= ptsgphs.nc7.ss
      PPOUT= ALL1
      USER1= ptsgphs.007.dat
      USER2= nicas1.thm
C*****************************************************
*******************
HEADER NODE DATA, PTS7
C*****************************************************
*******************
C INCLUDE gphstm.002
C *** RTG PAYLOAD ***
C  GPHS FUEL SOURCE
      50,  1779.6,   2.7738
      52,  1915.3,   8.6524
      54,  1809.4,   2.7738
C  GPHS THERMOPILE
      51,  1156.2,   1.172
      53,  1237.8,   3.656
      55,  1165.8,   1.172
      60,   948.,    1.11
      62,  1210.,    0.8

C  GPHS OUTER SHELL AND FINS
     100,   428.1,  0.073
     105,   449.3,  0.094
     107,   459.0,  0.120
     SPV 110,  455.,  A6, 0.24777*.4797
     SPV 112,  457.,  A6, 0.00974 * 8.
     SPV 113,  457.,  A6, 0.00974 * 8.

     SPV 120,  520.,  A6, 1.14263*.4797
     SPV 122,  534.,  A6, 0.04493 *8.
     SPV 123,  534.,  A6, 0.04493 *8.
     SPM 124, 2,1,  498.,  A6, 0.04570 * 4.
     SPM 126, 2,1,  422.,  A6, 0.08171 * 4.

     SPV 130,  547.,  A6, 1.14263*.4797
     SPV 132,  562.,  A6, 0.04493 *8.
     SPV 133,  562.,  A6, 0.04493 *8.
     SPM 134, 2,1,  524.,  A6, 0.04570 * 4.
     SPM 136, 2,1,  441.,  A6, 0.08171 * 4.

     SPV 140,  549.,  A6, 1.27902*.4797
     SPV 141,  547.,  A6, 1.33150
     SPV 142,  562.,  A6, 0.05029 *8.
     SPV 143,  564.,  A6, 0.05029 *8.
     SPV 144,  527.,  A6, 0.04558 * 4.
     SPV 145,  528.,  A6, 0.03661 * 4.
     SPV 146,  445.,  A6, 0.08214 * 4.
     SPV 147,  445.,  A6, 0.06510 * 4.

     SPV 150,  545.,  A6, 1.14263*.4797
     SPV 152,  560.,  A6, 0.04493 *8.
     SPV 153,  561.,  A6, 0.04493 *8.
     SPV 154,  522.,  A6, 0.04570 * 4.
     SPV 155,  521.,  A6, 0.05348 * 4.
     SPV 156,  439.,  A6, 0.08171 * 4.
     SPV 157,  429.,  A6, 0.07685 * 4.

     SPV 160,  509.,  A6, 1.14263*.4797
     SPV 161,  503.,  A6, 0.34544
     SPV 162,  524.,  A6, 0.04493 *8.
     SPV 163,  523.,  A6, 0.04493 *8.
     SPV 164,  490.,  A6, 0.04570 * 4.
     SPV 165,  478.,  A6, 0.06834 * 4.
     SPV 166,  410.,  A6, 0.08171 * 4.
     SPV 167,  406.,  A6, 0.06741 * 4.

     SPV 170,  386.,  A6, 0.24959*.4797
     SPV 172,  387.,  A6, 0.00981 * 8.
     SPV 173,  387.,  A6, 0.00981 * 8.
     177,   370.2,  0.48
     175,   355.2,  0.17

     180,   361.8,  0.08

C  ARITHMETIC NODES
       158,    501.,    -1.0
       159,    498.,    -1.0
       168,    506.,    -1.0
       169,    509.,    -1.0


C INCLUDE icvtm.007
C  INTER-CONTAINMENT SHELL - SARP MODEL, 2/28/94
     SPV  200, 276.,  A2,  71.06255
     SPV  204, 283.,  A2,  78.06855
     SPV  210,        317.,  A2,  325.77523
     SPV  220,        335.,  A2,  325.77523
     SPV  230,        312.,  A2,  325.77523
     SPV  240,        236.,  A2,  118.72275
     SPV  242,        213.,  A2,  124.65889
     SPV  250,        200.,  A2,  143.97909
     SPV  260,        204.,  A2,  159.43583
     SPV  261,        204.,  A2,  156.70264
     SPV  262,        201.,  A2,  199.29478
     SPV  263,        201.,  A2,  195.87830
     SPV  264,        200.,  A2,  100.41412
     SPV  265,        200.,  A2,   98.69273
     SPV  266,        198.,  A2,  122.52831

     SPV  267,   201.,  A2,    5.37235  $Feed Thru
Plug Housing
     SPV  268,   201.,  A2,    1.07365  $Feed Thru
Plug Sleeve
     SPV  269,   201.,  A2,    0.50000  $Feed Thru
Plug

       238,   274.,    -1.   $ Arithmetic Node
Between #230 & #240
       1266,  157.,    -1.   $ Metal Housing @ Inside
Of Feedthru Insulation
       1267,  157.,    -1.   $ Metal Housing @
Outside Of Feedthru Insulation
       1268,  157.,    -1.   $ Arith. Node @
Underside Of Barrier Insulation
       1269,  157.,    -1.   $ Arith. Gas Node w/i
Feedthru Cavity
C INCLUDE ocvtm.nc7
C  OUTER-CONTAINMENT SHELL w/ Drained Coolant Jacket -
SARP MODEL, 4/28/94
     SPV  300, 252.,  A2,  99.26473
     SPV  301, 131.,  A2,  29.20000
     SPV  304, 220.,  A2,  129.99777
     SPV  305, 146.,  A2,  118.17610
     SPV  310,        272.,  A2,  227.37080
     SPV  320,        272.,  A2,  227.37080
     SPV  330,        236.,  A2,  227.37080
     SPV  340,        220.,  A2,   82.86108
     SPV  342,        203.,  A2,   70.43192
          343,        170.,  3.10147 *0.20
     SPV  344,        193.,  A2,   70.62521
     SPV  345,        171.,  A2,   47.41970
     SPV  346,        162.,  A2,  126.01934
     SPV  347,        182.,  A2,   28.47068
     SPV  349, 165.,  A2,   24.95726
     SPV  350, 190.,  A2,  110.07622
     SPV  352, 190.,  A2,   95.22874
     SPV  354, 190.,  A2,  164.62726
     SPV  356, 189.,  A2,  142.42175

     SPV  351, 187.,  A70,  20.88000  $ OCV Cap Head
Screw
     SPV  353, 188.,  A70,  22.97584  $ OCV Cap Head
Screw - Shank Portion
     SPV  355, 190.,  A70,  28.27139  $ OCV Cap Head
Screw - Thread End
```

```
      SPV  360, 201.,  A2,   136.65928
      SPV  362, 200.,  A2,   170.82410
      SPV  364, 197.,  A2,   214.56467
      SPV  366, 191.,  A2,   342.81445
      SPV  367, 190.,  A2,   298.80466
      SPV  368, 189.,  A2,   400.72003
      SPV  369, 189.,  A2,   278.21419

      SPV  371, 187.,  A70,   1.74000  $ Cap Head
Screw - Impact Limiter
      SPV  373, 188.,  A70,   1.61140  $ Cap Head
Screw - Shank Portion
      SPV  375, 189.,  A70,   1.99996  $ Cap Head
Screw - Shank Portion
      SPV  377, 190.,  A70,   1.22319  $ Cap Head
Screw - Thread End

C     SIM  311, 2, 1,    40.,  A20,  26.21303
C     SIM  321, 2, 1,    40.,  A20,  26.21303
      GEN  311, 2, 1,   249.,  -1.
      GEN  321, 2, 1,   249.,  -1.

      SPV  313,         251.,  A2,   66.54918
      SPV  323,         251.,  A2,   66.54918
      SPM  315, 2, 1,   225.,  A2,   29.27137
      SPM  325, 2, 1,   226.,  A2,   29.27137
C     SIM  331, 2, 1,    40.,  A20,  37.72957
      GEN  331, 2, 1,   214.,  -1.
      SPV  333,         215.,  A2,   96.32118
      SPM  335, 2, 1,   197.,  A2,   42.13158

C  ARITHMETIC NODES
      337,   195.,   -1.   $ Arithmetic Node On Bolt
Shield Ring
      341,   201.,   -1.   $ Arithmetic Node At Joint
w/ Thermal Shield
      357,   189.,   -1.   $ Arithmetic Node; Midway
Between #354 & #356
      358,   187.,   -1.   $ Arithmetic Node; @ Base
of OCV Bolt Heads
      359,   190.,   -1.   $ Arithmetic Node; Midway
Between #350 & #352
      379,   191.,   -1.   $ Arithmetic Node; Midway
Between #366 & #367
     1011,   272.,  -1.0  $  Outer Surface Of OCV
Wall @ 310; Channel #1
     1012,   272.,  -1.0  $  Outer Surface Of OCV
Wall @ 310;   "     #2
     1013,   235.,  -1.0  $  End Of Coolant Jacket
Bar @ 310
     1021,   272.,  -1.0  $  Outer Surface Of OCV
Wall @ 320; Channel #1
     1022,   272.,  -1.0  $  Outer Surface Of OCV
Wall @ 320;   "     #2
     1023,   235.,  -1.0  $  End Of Coolant Jacket
Bar @ 320
     1031,   236.,  -1.0  $  Outer Surface Of OCV
Wall @ 330; Channel #1
     1032,   236.,  -1.0  $  Outer Surface Of OCV
Wall @ 330;   "     #2
     1033,   203.,  -1.0  $  End Of Coolant Jacket
Bar @ 330
     1041,   219.,  -1.0  $  Outer Surface Of OCV
Wall @ 340; Channel #1
     1042,   219.,  -1.0  $  Outer Surface Of OCV
Wall @ 340;   "     #2
     1043,   203.,  -1.0  $  Outer Surface Of OCV
Wall @ 342; Channel #1
     1044,   203.,  -1.0  $  Outer Surface Of OCV
Wall @ 342;   "     #2
     1346,   166.,  -1.0  $  Junction Between 346 &
345
     1347,   185.,  -1.0  $  Air Gap Between 347 &
369

C INCLUDE standgtm.008
```

```
C   ** SUPPORT STAND FOR GPHS RTG **
C  GE'S GPHS RTG ADAPTOR RING & QUICK CONNECT ASSEMBLY
      SPV 190,  312.,  A4,   11.64571
      SPV 191,  294.,  A4,   13.87508

C  RTG SUPPORT STAND
      SPV 192,  234.,  A2, 42.95393
      SPV 193,  276.,  A2, 27.59877  $ RUBBLE DAM
      SPV 194,  241.,  A2, 49.43756  $ OUTER PLATE
SUPPORT
      SPV 196,  301.,  A2, 12.29934  $ INNER BARRIER
PLATE
      SPV 198,  293.,  A2, 80.71439  $ OUTER BARRIER
PLATE

C        195,  223.,       -1.   $ INNER INSULATION
C        197,  229.,       -1.   $ OUTER INSULATION
         195,  223.,   2.47420 *0.20  $ INNER
INSULATION
         197,  229.,  13.24836 *0.20  $ OUTER
INSULATION
         199,  264.,       -1.   $ NODE AT BASE OF
#193
        1000,  227.,       -1.   $ INNER GAS VOLUME
        1010,  226.,       -1.   $ OUTER GAS VOLUME
        1001,  286.,       -1.   $ NODE BETWEEN 196 &
198
        1002,  263.,       -1.   $ NODE BETWEEN 194 &
198
        1003,  244.,       -1.   $ NODE BETWEEN 192 &
1001
        1004,  227.,       -1.   $ NODE BETWEEN 192 &
1005
        1005,  226.,       -1.   $ NODE AT ICV BASE
        1006,  203.,       -1.   $ NODE BETWEEN 261 &
263
        1007,  330.,       -1.   $ NODE BETWEEN 175 &
1008
        1008,  314.,       -1.   $ NODE BETWEEN 1007
& 190
        1009,  300.,       -1.   $ NODE BETWEEN 190 &
191

C INCLUDE foamtm.007
C  IMPACT LIMITER MODEL NODES - SARP Model, 4/28/94
      SPV  400, 196.,  A2,   143.57766
      SPV  401, 195.,  A2,    22.89585
      SPV  402, 188.,  A2,   284.60309
      SPV  404, 172.,  A2,   142.60810
      SPV  406, 128.,  A2,   147.30904
      SPV  408, 104.,  A2,   300.35622
      SPV  410, 113.,  A2,   138.16734
      SPV  412, 118.,  A2,    85.98591
      SPV  414, 123.,  A2,   119.64805

          421,       182.,    6.34914* .3
          422,       158.,    6.34914* .3
          423,       134.,    6.34914* .3
          424,       172.,   19.06724* .3
          425,       147.,   19.06724* .3
          426,       127.,   19.06724* .3
          431,       149.,    9.90174* .3*2.1
          432,       156.,    9.90174* .3*2.1
          433,       155.,    9.90174* .3*2.1
          434,       142.,    9.02231* .3*2.1
          435,       129.,    9.02231* .3*2.1
          436,       119.,    9.02231* .3*2.1

          441,       131.,   10.27998* .3
          442,       133.,   10.27998* .3
          443,       131.,   10.27998* .3
          444,       125.,    9.36696* .3
          445,       119.,    9.36696* .3
          446,       115.,    9.36696* .3
          451,       117.,   11.10901* .3
          452,       113.,   11.10901* .3
```

```
          453,       112.,   11.10901* .3
          454,       111.,   10.12236* .3
          455,       109.,   10.12236* .3
          456,       109.,   10.12236* .3

      403,   188.,    -1.   $ Arithmetic Node On
Bolt Ring

C  EXTERNAL NODES
      -901,    40.,   1.0    $ ENTERING COOLANT TEMP
FOR LOOP 1
      -902,    40.,   1.0    $ ENTERING COOLANT TEMP
FOR LOOP 2
        -1,   100.,   1.0    $ CONVECTION SINK NODE
        -2,   100.,   1.0    $ RADIATIVE SINK NODE

C*****************************************************
*******************
HEADER CONDUCTOR DATA, PTS7
C*****************************************************
*******************
C INCLUDE gphstc.004
C
C  *** CONDUCTION WITHIN UNDAMAGED GPHS RTG IN SHORTED
CONDITION***
C       Updated RTG-ICV Convection Linkage Based on
GPHS QUAL Test REsults
C
C  CONDUCTION FROM FUEL SOURCE TO SHELL
      50,     50,51,   54,55,       4.344   $ W/ ARGON
      52,     52,53,                13.552  $ W/ ARGON
C     50,     50,51,   54,55,       3.702   $ W/ VACUUM
C     52,     52,53,                11.546  $ W/ VACUUM
      54,     52,50,   52,54,       0.7345
      56,     50,60,   54,62,       0.4712
C  CONDUCTION FROM FUEL SOURCE TO SHELL
      51,  51,120, 53,130, 53,150, 55,160, 0.3475 $ W/
ARGON
      53,  51,122, 51,123, 53,132, 53,133,
           53,152, 53,153, 55,162, 55,163, 1.9984 $ W/
ARGON
      55,  53,140,                          0.3890 $ W/
ARGON
      57,  53,142, 53,143,                  2.2369 $ W/
ARGON
C     51,  51,120, 53,130, 53,150, 55,160, 0.2961 $ W/
VACUUM
CC    521, 51,110,                 55,170, 0.0321 $ W/
VACUUM
CC    522, 51,112, 51,113, 55,172, 55,173, 0.0161 $ W/
VACUUM
C     53,  51,122, 51,123, 53,132, 53,133,
C          53,152, 53,153, 55,162, 55,163, 1.7027 $ W/
VACUUM
C     55,  53,140,                          0.3315 $ W/
VACUUM
C     57,  53,142, 53,143,                  1.9061 $ W/
VACUUM
      60,  60,100,  62,180,     0.2400
      61,  60,107,              0.545    $ W/ ARGON
      62,  62,177,              0.093    $ W/ ARGON
C     61,  60,107,              0.045    $ W/ VACUUM
C     62,  62,177,              0.02     $ W/ VACUUM
C  CONDUCTION WITHIN GPHS OUTER SHELL
         100,    100,105,  175,180,   5.65
         101,    105,107,  177,175,   20.0
      SPV 102,   107,110,  A5,       0.0124982 *
.4797
      SPM 103, 2,1, 107,0,  112,1, A5,    0.000454 *8.
      SPV 105, 110,112,             A5,    0.00053135 *
8.
      SPV 106,          110,113,    A5,    0.00053135 *
8.
      SPV 110,    110,120,  A5,       0.002169 *.4797
      SPM 111, 2,1, 112,1,  122,1, A5,    0.000087572
*8.
      SPV 120, 120,122,             A5,    0.00245038 *
8.
      SPV 121,          120,123,    A5,    0.00245038 *
8.
      SPV 122, 122,124,             A5,    0.003697 * 4.
      SPV 123,          123,125,    A5,    0.003697 * 4.
      SPV 124, 124,126,             A5,    0.001206 * 4.
      SPV 125,          125,127,    A5,    0.001206 * 4.

      SPV 130,    120,130,  A5,       0.0013551 *
.4797
      SPM 131, 2,1, 122,1,  132,1, A5,    0.000053281
*8.
      SPV 133, 130,132,             A5,    0.00245038 *
8.
      SPV 134,          130,133,    A5,    0.00245038 *
8.
      SPV 135, 132,134,             A5,    0.003697 * 4.
      SPV 136,          133,135,    A5,    0.003697 * 4.
      SPV 137, 134,136,             A5,    0.001206 * 4.
      SPV 138,          135,137,    A5,    0.001206 * 4.

      SPV 140,    130,140,  A5,       0.001279 * .4797
      SPM 141, 2,1, 132,1,  142,1, A5,    0.000050280
*8.
      SPV 143, 140,142,             A5,    0.002743 * 8.
      SPV 1431,         140,143,    A5,    0.002743 * 8.
      SPV 144, 142,144,             A5,    0.003842 * 4.
      SPV 145, 144,146,             A5,    0.001168 * 4.
      SPV 146, 143,145,             A5,    0.002961 * 4.
      SPV 147, 145,147,             A5,    0.000961 * 4.
      SPV 148, 140,141,             A5,    0.053911
*.4797
      SPV 149, 142,141,             A5,    0.053911
*.2601
      SPV 1491          143,141,    A5,    0.053911
*.2601

      SPV 150,    140,150,  A5,       0.001279 *.4797
      SPM 151, 2,1, 142,1,  152,1, A5,    0.000050280
*8.
      SPV 153, 150,152,             A5,    0.002450 * 8.
      SPV 1531,         150,153,    A5,    0.002450 * 8.
      SPV 154, 152,154,             A5,    0.003697 * 4.
      SPV 155, 154,156,             A5,    0.001206 * 4.
      SPV 156, 153,155,             A5,    0.003310 * 4.
      SPV 157, 155,157,             A5,    0.000876 * 4.
      SPV 158, 150,168,             A5,    0.001643
*.4797
      SPM 1581,2,1, 152,1,  169,0, A5,    0.000064588
*8.
      SPV 159, 154,158,             A5,    0.00005956 *
4.
      SPV 1591,         155,159,    A5,    0.00005956 *
4.

      SPV 161, 160,162,             A5,    0.002450 * 8.
      SPV 1611,         160,163,    A5,    0.002450 * 8.
      SPV 162, 162,164,             A5,    0.003697 * 4.
      SPV 163, 164,166,             A5,    0.001206 * 4.
      SPV 164, 163,165,             A5,    0.002762 * 4.
      SPV 165, 165,167,             A5,    0.001239 * 4.
      SPV 166, 160,168,             A5,    0.007740
*.4797
      SPM 167, 2,1, 162,1,  169,0, A5,    0.000304 * 8.
      SPV 169, 164,158,             A5,    0.000281 * 4.
      SPV 1691,         165,159,    A5,    0.000281 * 4.

      SPV 1601, 168,161,            A5,    0.043003
*.4797
      SPV 1602, 169,161,            A5,    0.043003
*.5203
      SPV 1603, 158,161,            A5,    0.000412 * 8.
      SPV 1604,         159,161,    A5,    0.000412 * 8.

      SPV 170,    160,170,  A5,       0.002166 *.4797
```

```
      SPM 171, 2,1, 162,1,  172,1, A5,   0.000087 * 8.
      SPV 173, 170,172,            A5,   0.000535 * 8.
      SPV 1731,        170,173,    A5,   0.000535 * 8.
      SPV 174,    170,177,  A5,        0.012407 *.4797
      SPM 175, 2,1, 172,1,  177,0, A5,   0.000488 * 8.

C
C  RADIATION BETWEEN RTG & ICV SURFACES w/ ICV e= 0.90
C    #193/196/198 e= 0.48, & #190 e= 0.20
C
      -100200,   100, 200,    0.3861        $ Hand
Calculations
      -105200,   105, 204,    0.0988125     $ Hand
Calculations
      -107210,   107,210,       0.01684
      -107220,   107,220,       0.00740
      -107230,   107,230,       0.00272
      -107193,   107,193,       0.00034
      -107198,   107,198,       0.00119
      -107190,   107,190,       0.00011
      -110200,   110,200,       0.01288
      -110204,   110,204,       0.03885
      -110210,   110,210,       0.04873
      -110220,   110,220,       0.00663
      -110230,   110,230,       0.00055
      -112200,   112,200,       0.00791
      -112204,   112,204,       0.02156
      -112210,   112,210,       0.02456
      -112220,   112,220,       0.00333
      -112230,   112,230,       0.00028
      -112193,   112,193,       0.00005
      -113200,   113,200,       0.00807
      -113204,   113,204,       0.02135
      -113210,   113,210,       0.02456
      -113220,   113,220,       0.00333
      -113230,   113,230,       0.00026
      -113193,   113,193,       0.00004
      -120200,   120,200,       0.04121
      -120204,   120,204,       0.09999
      -120210,   120,210,       0.22526
      -120220,   120,220,       0.05779
      -120230,   120,230,       0.00791
      -120193,   120,193,       0.00091
      -120198,   120,198,       0.00171
      -122200,   122,200,       0.01634
      -122204,   122,204,       0.04049
      -122210,   122,210,       0.09406
      -122220,   122,220,       0.02429
      -122230,   122,230,       0.00340
      -122193,   122,193,       0.00040
      -122198,   122,198,       0.00071
      -123200,   123,200,       0.01633
      -123204,   123,204,       0.04055
      -123210,   123,210,       0.09346
      -123220,   123,220,       0.02452
      -123230,   123,230,       0.00339
      -123193,   123,193,       0.00040
      -123198,   123,198,       0.00079
      -124200,   124,200,       0.02186
      -124204,   124,204,       0.04018
      -124210,   124,210,       0.07888
      -124220,   124,220,       0.02262
      -124230,   124,230,       0.00334
      -124193,   124,193,       0.00046
      -124198,   124,198,       0.00080
      -125200,   125,200,       0.02181
      -125204,   125,204,       0.03988
      -125210,   125,210,       0.08138
      -125220,   125,220,       0.02370
      -125230,   125,230,       0.00330
      -125193,   125,193,       0.00045
      -125198,   125,198,       0.00073
      -126200,   126,200,       0.10503
      -126204,   126,204,       0.17223
      -126210,   126,210,       0.36442
      -126220,   126,220,       0.10236
      -126230,   126,230,       0.01472
      -126193,   126,193,       0.00182
      -126198,   126,198,       0.00367
      -127200,   127,200,       0.10497
      -127204,   127,204,       0.17131
      -127210,   127,210,       0.37696
      -127220,   127,220,       0.09775
      -127230,   127,230,       0.01466
      -127193,   127,193,       0.00188
      -127198,   127,198,       0.00354
      -130200,   130,200,       0.01060
      -130204,   130,204,       0.03700
      -130210,   130,210,       0.20413
      -130220,   130,220,       0.16796
      -130230,   130,230,       0.02761
      -130193,   130,193,       0.00251
      -130198,   130,198,       0.00259
      -132200,   132,200,       0.00423
      -132204,   132,204,       0.01526
      -132210,   132,210,       0.08498
      -132220,   132,220,       0.06992
      -132230,   132,230,       0.01149
      -132193,   132,193,       0.00102
      -132198,   132,198,       0.00108
      -133200,   133,200,       0.00423
      -133204,   133,204,       0.01530
      -133210,   133,210,       0.08513
      -133220,   133,220,       0.06956
      -133230,   133,230,       0.01150
      -133193,   133,193,       0.00104
      -133198,   133,198,       0.00108
      -134200,   134,200,       0.00517
      -134204,   134,204,       0.01420
      -134210,   134,210,       0.07073
      -134220,   134,220,       0.05380
      -134230,   134,230,       0.01152
      -134193,   134,193,       0.00107
      -134198,   134,198,       0.00119
      -135200,   135,200,       0.00525
      -135204,   135,204,       0.01406
      -135210,   135,210,       0.07070
      -135220,   135,220,       0.06199
      -135230,   135,230,       0.01089
      -135193,   135,193,       0.00102
      -135198,   135,198,       0.00111
      -136200,   136,200,       0.02107
      -136204,   136,204,       0.05886
      -136210,   136,210,       0.31903
      -136220,   136,220,       0.24133
      -136230,   136,230,       0.04195
      -136193,   136,193,       0.00404
      -136198,   136,198,       0.00579
      -137200,   137,200,       0.02109
      -137204,   137,204,       0.05795
      -137210,   137,210,       0.31899
      -137220,   137,220,       0.26065
      -137230,   137,230,       0.04099
      -137193,   137,193,       0.00419
      -137198,   137,198,       0.00575
      -140200,   140,200,       0.00247
      -140204,   140,204,       0.00969
      -140210,   140,210,       0.08379
      -140220,   140,220,       0.27625
      -140230,   140,230,       0.08088
      -140193,   140,193,       0.00522
      -140198,   140,198,       0.00476
      -140190,   140,190,       0.00060
      -141200,   141,200,       0.01416
      -141204,   141,204,       0.02250
      -141210,   141,210,       0.05648
      -141220,   141,220,       0.05418
      -141230,   141,230,       0.05509
      -141193,   141,193,       0.00784
      -141198,   141,198,       0.01252
      -141196,   141,196,       0.00062
      -141190,   141,190,       0.00344
```

-142200,	142,200,	0.00130
-142204,	142,204,	0.00441
-142210,	142,210,	0.03454
-142220,	142,220,	0.11332
-142230,	142,230,	0.03387
-142193,	142,193,	0.00226
-142198,	142,198,	0.00198
-142190,	142,190,	0.00025
-143200,	143,200,	0.00136
-143204,	143,204,	0.00489
-143210,	143,210,	0.03709
-143220,	143,220,	0.12377
-143230,	143,230,	0.03610
-143193,	143,193,	0.00232
-143198,	143,198,	0.00210
-143190,	143,190,	0.00026
-144200,	144,200,	0.00110
-144204,	144,204,	0.00361
-144210,	144,210,	0.02869
-144220,	144,220,	0.09141
-144230,	144,230,	0.02835
-144193,	144,193,	0.00185
-144198,	144,198,	0.00182
-144190,	144,190,	0.00030
-145200,	145,200,	0.00097
-145204,	145,204,	0.00299
-145210,	145,210,	0.02366
-145220,	145,220,	0.06872
-145230,	145,230,	0.02458
-145193,	145,193,	0.00158
-145198,	145,198,	0.00140
-145190,	145,190,	0.00024
-146200,	146,200,	0.00618
-146204,	146,204,	0.02139
-146210,	146,210,	0.12902
-146220,	146,220,	0.36697
-146230,	146,230,	0.12606
-146193,	146,193,	0.01010
-146198,	146,198,	0.01081
-146190,	146,190,	0.00153
-147200,	147,200,	0.00521
-147204,	147,204,	0.01768
-147210,	147,210,	0.10758
-147220,	147,220,	0.30347
-147230,	147,230,	0.10464
-147193,	147,193,	0.00890
-147198,	147,198,	0.00906
-147190,	147,190,	0.00128
-150200,	150,200,	0.00055
-150204,	150,204,	0.00551
-150210,	150,210,	0.02833
-150220,	150,220,	0.17062
-150230,	150,230,	0.20204
-150193,	150,193,	0.02216
-150198,	150,198,	0.01586
-150190,	150,190,	0.00238
-152200,	152,200,	0.00022
-152204,	152,204,	0.00220
-152210,	152,210,	0.01184
-152220,	152,220,	0.07130
-152230,	152,230,	0.08406
-152193,	152,193,	0.00944
-152198,	152,198,	0.00658
-152190,	152,190,	0.00096
-153200,	153,200,	0.00020
-153204,	153,204,	0.00223
-153210,	153,210,	0.01180
-153220,	153,220,	0.07129
-153230,	153,230,	0.08399
-153193,	153,193,	0.00943
-153198,	153,198,	0.00656
-153190,	153,190,	0.00096
-154200,	154,200,	0.00022
-154204,	154,204,	0.00279
-154210,	154,210,	0.01169
-154220,	154,220,	0.05924
-154230,	154,230,	0.06408
-154193,	154,193,	0.00822
-154198,	154,198,	0.00614
-154190,	154,190,	0.00131
-155200,	155,200,	0.00031
-155204,	155,204,	0.00304
-155210,	155,210,	0.01378
-155220,	155,220,	0.07608
-155230,	155,230,	0.09390
-155193,	155,193,	0.01206
-155198,	155,198,	0.00796
-155190,	155,190,	0.00178
-156200,	156,200,	0.00272
-156204,	156,204,	0.01147
-156210,	156,210,	0.04282
-156220,	156,220,	0.26364
-156230,	156,230,	0.28503
-156193,	156,193,	0.03332
-156198,	156,198,	0.02677
-156196,	156,196,	0.00118
-156190,	156,190,	0.00602
-157200,	157,200,	0.00274
-157204,	157,204,	0.00967
-157210,	157,210,	0.03937
-157220,	157,220,	0.24599
-157230,	157,230,	0.28802
-157193,	157,193,	0.03195
-157198,	157,198,	0.02494
-157196,	157,196,	0.00115
-157190,	157,190,	0.00556
-160204,	160,204,	0.00144
-160210,	160,210,	0.00621
-160220,	160,220,	0.05208
-160230,	160,230,	0.22855
-160193,	160,193,	0.06369
-160198,	160,198,	0.03387
-160190,	160,190,	0.01787
-161200,	161,200,	0.00225
-161204,	161,204,	0.00455
-161210,	161,210,	0.00749
-161220,	161,220,	0.02498
-161230,	161,230,	0.02426
-161193,	161,193,	0.01221
-161198,	161,198,	0.01512
-161196,	161,196,	0.00674
-161190,	161,190,	0.00937
-162204,	162,204,	0.00059
-162210,	162,210,	0.00271
-162220,	162,220,	0.02178
-162230,	162,230,	0.09528
-162193,	162,193,	0.02618
-162198,	162,198,	0.01388
-162190,	162,190,	0.00698
-163204,	163,204,	0.00059
-163210,	163,210,	0.00268
-163220,	163,220,	0.02189
-163230,	163,230,	0.09532
-163193,	163,193,	0.02599
-163198,	163,198,	0.01373
-163190,	163,190,	0.00700
-164204,	164,204,	0.00087
-164210,	164,210,	0.00266
-164220,	164,220,	0.02029
-164230,	164,230,	0.08115
-164193,	164,193,	0.02260
-164198,	164,198,	0.01383
-164196,	164,196,	0.00054
-164190,	164,190,	0.01088
-165200,	165,200,	0.00043
-165204,	165,204,	0.00168
-165210,	165,210,	0.00514
-165220,	165,220,	0.03607
-165230,	165,230,	0.13851
-165193,	165,193,	0.04031
-165198,	165,198,	0.02471
-165196,	165,196,	0.00164

```
      -165190,   165,190,      0.01742
      -166200,   166,200,      0.00156
      -166204,   166,204,      0.00605
      -166210,   166,210,      0.01495
      -166220,   166,220,      0.10140
      -166230,   166,230,      0.38269
      -166193,   166,193,      0.09213
      -166198,   166,198,      0.06540
      -166196,   166,196,      0.00877
      -166190,   166,190,      0.03736
      -167200,   167,200,      0.00122
      -167204,   167,204,      0.00455
      -167210,   167,210,      0.01275
      -167220,   167,220,      0.08689
      -167230,   167,230,      0.32675
      -167193,   167,193,      0.08382
      -167198,   167,198,      0.05559
      -167196,   167,196,      0.00760
      -167190,   167,190,      0.03013
      -170204,   170,204,      0.00036
      -170210,   170,210,      0.00086
      -170220,   170,220,      0.00667
      -170230,   170,230,      0.05057
      -170193,   170,193,      0.02795
      -170198,   170,198,      0.00693
      -170190,   170,190,      0.01036
      -172204,   172,204,      0.00020
      -172210,   172,210,      0.00041
      -172220,   172,220,      0.00336
      -172230,   172,230,      0.02499
      -172193,   172,193,      0.01372
      -172198,   172,198,      0.00344
      -172196,   172,196,      0.00004
      -172190,   172,190,      0.00576
      -173204,   173,204,      0.00015
      -173210,   173,210,      0.00041
      -173220,   173,220,      0.00337
      -173230,   173,230,      0.02533
      -173193,   173,193,      0.01343
      -173198,   173,198,      0.00334
      -173196,   173,196,      0.00004
      -173190,   173,190,      0.00559
      -177200,   177,200,      0.00103
      -177204,   177,204,      0.00202
      -177210,   177,210,      0.00263
      -177220,   177,220,      0.00759
      -177230,   177,230,      0.01591
      -175196,   175, 196,     0.098831    $ Hand
Calculations
      -180190,   180, 190,     0.096525    $ Hand
Calculations
      -180196,   180, 196,     0.19305     $ Hand
Calculations
      -180198,   180, 198,     0.096525    $ Hand
Calculations

C
C  RADIATION BETWEEN RTG SURFACES
C
      -107110,   107,110,      0.01826
      -107112,   107,112,      0.00795
      -107113,   107,113,      0.00791
      -107120,   107,120,      0.00074
      -107122,   107,122,      0.00019
      -107123,   107,123,      0.00019
      -107124,   107,124,      0.00164
      -107125,   107,125,      0.00163
      -107126,   107,126,      0.00490
      -107127,   107,127,      0.00492
      -107136,   107,136,      0.00033
      -107137,   107,137,      0.00033
      -110124,   110,124,      0.00059
      -110125,   110,125,      0.00060
      -110126,   110,126,      0.00628
      -110127,   110,127,      0.00638
      -112124,   112,124,      0.00152
      -112126,   112,126,      0.00261
      -112127,   112,127,      0.00046
      -113125,   113,125,      0.00152
      -113126,   113,126,      0.00044
      -113127,   113,127,      0.00261
      -120124,   120,124,      0.01065
      -120125,   120,125,      0.01040
      -120126,   120,126,      0.06552
      -120127,   120,127,      0.06550
      -120134,   120,134,      0.00093
      -120135,   120,135,      0.00090
      -120136,   120,136,      0.01029
      -120137,   120,137,      0.01025
      -122124,   122,124,      0.09680
      -122126,   122,126,      0.03642
      -122127,   122,127,      0.00332
      -122134,   122,134,      0.00113
      -122136,   122,136,      0.00341
      -122137,   122,137,      0.00099
      -123125,   123,125,      0.09645
      -123126,   123,126,      0.00333
      -123127,   123,127,      0.03603
      -123135,   123,135,      0.00113
      -123136,   123,136,      0.00097
      -123137,   123,137,      0.00341
      -124125,   124,125,      0.01477
      -124127,   124,127,      0.05721
      -124130,   124,130,      0.00094
      -124132,   124,132,      0.00114
      -124135,   124,135,      0.00321
      -124137,   124,137,      0.01428
      -124141,   124,141,      0.00036
      -124147,   124,147,      0.00072
      -125126,   125,126,      0.05396
      -125130,   125,130,      0.00093
      -125133,   125,133,      0.00114
      -125134,   125,134,      0.00321
      -125136,   125,136,      0.01121
      -125141,   125,141,      0.00037
      -125146,   125,146,      0.00084
      -126127,   126,127,      0.17566
      -126130,   126,130,      0.01064
      -126132,   126,132,      0.00341
      -126133,   126,133,      0.00103
      -126135,   126,135,      0.01461
      -126137,   126,137,      0.05021
      -126141,   126,141,      0.00129
      -126145,   126,145,      0.00064
      -126147,   126,147,      0.00326
      -127130,   127,130,      0.01067
      -127132,   127,132,      0.00104
      -127133,   127,133,      0.00341
      -127134,   127,134,      0.01456
      -127136,   127,136,      0.04246
      -127141,   127,141,      0.00128
      -127144,   127,144,      0.00072
      -127146,   127,146,      0.00377
      -130134,   130,134,      0.01199
      -130135,   130,135,      0.01169
      -130136,   130,136,      0.07201
      -130137,   130,137,      0.07213
      -130141,   130,141,      0.00301
      -130144,   130,144,      0.00093
      -130145,   130,145,      0.00089
      -130146,   130,146,      0.00969
      -130147,   130,147,      0.00892
      -132134,   132,134,      0.10445
      -132136,   132,136,      0.03905
      -132137,   132,137,      0.00375
      -132141,   132,141,      0.00096
      -132144,   132,144,      0.00151
      -132146,   132,146,      0.00319
      -132147,   132,147,      0.00084
      -133135,   133,135,      0.10445
      -133136,   133,136,      0.00376
      -133137,   133,137,      0.03905
```

-133141,	133,141,	0.00096
-133145,	133,145,	0.00160
-133146,	133,146,	0.00093
-133147,	133,147,	0.00306
-134135,	134,135,	0.01707
-134137,	134,137,	0.06062
-134140,	134,140,	0.00095
-134141,	134,141,	0.00339
-134142,	134,142,	0.00145
-134145,	134,145,	0.00259
-134147,	134,147,	0.01132
-135136,	135,136,	0.05766
-135140,	135,140,	0.00093
-135141,	135,141,	0.00339
-135143,	135,143,	0.00145
-135144,	135,144,	0.00280
-135146,	135,146,	0.00963
-136137,	136,137,	0.17594
-136140,	136,140,	0.00982
-136141,	136,141,	0.00920
-136142,	136,142,	0.00337
-136143,	136,143,	0.00083
-136145,	136,145,	0.01088
-136147,	136,147,	0.03933
-136157,	136,157,	0.00242
-137140,	137,140,	0.00995
-137141,	137,141,	0.00920
-137142,	137,142,	0.00085
-137143,	137,143,	0.00337
-137144,	137,144,	0.01203
-137146,	137,146,	0.03725
-137156,	137,156,	0.00246
-140141,	140,141,	0.10344
-140144,	140,144,	0.01062
-140145,	140,145,	0.00878
-140146,	140,146,	0.06007
-140147,	140,147,	0.04955
-140154,	140,154,	0.00098
-140155,	140,155,	0.00152
-140156,	140,156,	0.01008
-140157,	140,157,	0.00952
-141142,	141,142,	0.04094
-141143,	141,143,	0.04103
-141144,	141,144,	0.04274
-141145,	141,145,	0.02488
-141146,	141,146,	0.06050
-141147,	141,147,	0.04382
-141150,	141,150,	0.00312
-141152,	141,152,	0.00097
-141153,	141,153,	0.00097
-141154,	141,154,	0.00345
-141155,	141,155,	0.00430
-141156,	141,156,	0.00951
-141157,	141,157,	0.00878
-141161,	141,161,	0.00204
-141165,	141,165,	0.00040
-141166,	141,166,	0.00132
-141167,	141,167,	0.00107
-142144,	142,144,	0.10468
-142146,	142,146,	0.03496
-142147,	142,147,	0.00230
-142154,	142,154,	0.00150
-142156,	142,156,	0.00352
-142157,	142,157,	0.00094
-143145,	143,145,	0.08460
-143146,	143,146,	0.00291
-143147,	143,147,	0.02896
-143155,	143,155,	0.00188
-143156,	143,156,	0.00088
-143157,	143,157,	0.00326
-144145,	144,145,	0.01030
-144147,	144,147,	0.03544
-144150,	144,150,	0.00099
-144152,	144,152,	0.00159
-144155,	144,155,	0.00397
-144157,	144,157,	0.01167
-144167,	144,167,	0.00068
-145146,	145,146,	0.03417
-145150,	145,150,	0.00089
-145153,	145,153,	0.00160
-145154,	145,154,	0.00259
-145156,	145,156,	0.00890
-145166,	145,166,	0.00063
-146147,	146,147,	0.11238
-146150,	146,150,	0.00974
-146152,	146,152,	0.00316
-146153,	146,153,	0.00093
-146155,	146,155,	0.01575
-146157,	146,157,	0.04256
-146161,	146,161,	0.00076
-146165,	146,165,	0.00097
-146167,	146,167,	0.00328
-147150,	147,150,	0.00902
-147152,	147,152,	0.00080
-147153,	147,153,	0.00306
-147154,	147,154,	0.01152
-147156,	147,156,	0.03744
-147161,	147,161,	0.00065
-147166,	147,166,	0.00326
-150154,	150,154,	0.01199
-150155,	150,155,	0.02148
-150156,	150,156,	0.07199
-150157,	150,157,	0.06344
-150161,	150,161,	0.00239
-150164,	150,164,	0.00078
-150165,	150,165,	0.00216
-150166,	150,166,	0.01033
-150167,	150,167,	0.00884
-152154,	152,154,	0.10445
-152156,	152,156,	0.03906
-152157,	152,157,	0.00463
-152161,	152,161,	0.00067
-152164,	152,164,	0.00104
-152166,	152,166,	0.00342
-152167,	152,167,	0.00110
-153155,	153,155,	0.11392
-153156,	153,156,	0.00375
-153157,	153,157,	0.02962
-153161,	153,161,	0.00067
-153165,	153,165,	0.00182
-153166,	153,166,	0.00102
-153167,	153,167,	0.00270
-154155,	154,155,	0.02281
-154157,	154,157,	0.05340
-154160,	154,160,	0.00075
-154161,	154,161,	0.00356
-154162,	154,162,	0.00103
-154165,	154,165,	0.00405
-154167,	154,167,	0.01172
-155156,	155,156,	0.07367
-155160,	155,160,	0.00157
-155161,	155,161,	0.00475
-155163,	155,163,	0.00147
-155164,	155,164,	0.00304
-155166,	155,166,	0.01435
-156157,	156,157,	0.16448
-156160,	156,160,	0.00804
-156161,	156,161,	0.00798
-156162,	156,162,	0.00281
-156163,	156,163,	0.00065
-156165,	156,165,	0.01794
-156167,	156,167,	0.04226
-157160,	157,160,	0.00706
-157161,	157,161,	0.00682
-157162,	157,162,	0.00079
-157163,	157,163,	0.00227
-157164,	157,164,	0.00852
-157166,	157,166,	0.04538
-160161,	160,161,	0.06853
-160164,	160,164,	0.01006
-160165,	160,165,	0.02716
-160166,	160,166,	0.06358

```
      -160167,   160,167,        0.04708
      -160177,   160,177,        0.00116
      -161162,   161,162,        0.02929
      -161163,   161,163,        0.02937
      -161164,   161,164,        0.03894
      -161165,   161,165,        0.05122
      -161166,   161,166,        0.02371
      -161167,   161,167,        0.01401
      -161170,   161,170,        0.00034
      -161177,   161,177,        0.00223
      -162164,   162,164,        0.09926
      -162166,   162,166,        0.03557
      -162167,   162,167,        0.00364
      -162177,   162,177,        0.00030
      -163165,   163,165,        0.11443
      -163166,   163,166,        0.00326
      -163167,   163,167,        0.01978
      -163177,   163,177,        0.00030
      -164165,   164,165,        0.02283
      -164167,   164,167,        0.04010
      -164170,   164,170,        0.00076
      -164172,   164,172,        0.00162
      -164177,   164,177,        0.00240
      -165166,   165,166,        0.08196
      -165170,   165,170,        0.00238
      -165173,   165,173,        0.00255
      -165177,   165,177,        0.00367
      -166167,   166,167,        0.14420
      -166170,   166,170,        0.00673
      -166172,   166,172,        0.00261
      -166177,   166,177,        0.00490
      -167170,   167,170,        0.00506
      -167172,   167,172,        0.00053
      -167173,   167,173,        0.00158
      -167177,   167,177,        0.00341
      -170177,   170,177,        0.01788
      -172177,   172,177,        0.00789
      -173177,   173,177,        0.00779

C  CONVECTIVE HEAT TRANSFER WITH INNER VESSEL
          500,   100, 200,    1.                  $ DUMMY
VALUE
          501,   105, 200,    1.                  $ DUMMY
VALUE
          502,   107, 200,    1.                  $ DUMMY
VALUE
          503,   110, 200,    1.                  $ DUMMY
VALUE
          504,   112, 200,  113, 200,  1.         $ DUMMY
VALUE
          506,   120, 204,    1.                  $ DUMMY
VALUE
          508,   122, 204,  123, 204,  1.         $ DUMMY
VALUE
          510,   126, 204,  127, 204,  1.         $ DUMMY
VALUE
          512,   130, 210,    1.                  $ DUMMY
VALUE
          514,   132, 210,  133, 210,  1.         $ DUMMY
VALUE
          516,   136, 210,  137, 210,  1.         $ DUMMY
VALUE
          518,   140, 210,    1.                  $ DUMMY
VALUE
          520,   142, 210,  143, 210,  1.         $ DUMMY
VALUE
          522,   146, 210,  147, 210,  1.         $ DUMMY
VALUE
          524,   150, 220,    1.                  $ DUMMY
VALUE
          526,   152, 220,  153, 220,  1.         $ DUMMY
VALUE
          528,   156, 220,  157, 220,  1.         $ DUMMY
VALUE
          530,   160, 220,    1.                  $ DUMMY
VALUE
C         531,   161, 220,    1.                  $ DUMMY
VALUE
          532,   162, 230,  163, 230,  1.         $ DUMMY
VALUE
          534,   166, 230,  167, 230,  1.         $ DUMMY
VALUE
          536,   170, 230,                 1.     $ DUMMY
VALUE
          538,   172, 230,  173, 230,  1.         $ DUMMY
VALUE
C         540,   175, 1000,                1.
          541,   177, 230,                 1.
C         542,   180, 1000,                1.

          5061,   120, 200,    1.                 $ DUMMY
VALUE
          5081,   122, 200,  123, 200,  1.        $ DUMMY
VALUE
          5101,   126, 200,  127, 200,  1.        $ DUMMY
VALUE
          5121,   130, 200,    1.                 $ DUMMY
VALUE
          5141,   132, 200,  133, 200,  1.        $ DUMMY
VALUE
          5161,   136, 200,  137, 200,  1.        $ DUMMY
VALUE
          5181,   140, 200,    1.                 $ DUMMY
VALUE
          5201,   142, 200,  143, 200,  1.        $ DUMMY
VALUE
          5221,   146, 200,  147, 200,  1.        $ DUMMY
VALUE
          5241,   150, 200,    1.                 $ DUMMY
VALUE
          5261,   152, 200,  153, 200,  1.        $ DUMMY
VALUE
          5281,   156, 200,  157, 200,  1.        $ DUMMY
VALUE
          5301,   160, 200,    1.                 $ DUMMY
VALUE
          5321,   162, 200,  163, 200,  1.        $ DUMMY
VALUE
          5341,   166, 200,  167, 200,  1.        $ DUMMY
VALUE


C INCLUDE icvtc.007
C  ICV CONDUCTORS - Version 007, SARP Model, 4/28/94
C This File Seperates The RTG to ICV Radiation
Interchange
C And Convection From The Remaining Conductors

C  CONDUCTANCE WITHIN INTER-CONTAINMENT SHELL
       SPV 14,  200, 204,  A1,  0.028919
       SPV 15,  204, 210,  A1,  0.039433
       SPM 16,  2,1, 210,10,  220,10,    A1,  0.041443
       SPV 18,        230,        238,        A1,  0.138344
       SPV 19,        238,        240,        A1,  0.108304
       SPV 20,        240,        242,        A1,  0.110945
       DPV 21,  242,  250,  A1,  0.216608,  A1,  0.674411
C  SEE SUPPORT RACK MODEL FOR NODES 261 TO 263
C      SPM 22,        261,        263,        A1,  0.125161
       SPV 23,        263,        265,        A1,  0.330529
       SPV 24,        260,        262,        A1,  0.127344
       SPV 25,        262,        264,        A1,  0.336294
       SPV 26,        264,        266,        A1,  0.487480

       SPV 27,  260,  261,  A1,  1.257442
       SPV 28,  262,  263,  A1,  1.571802
       SPV 29,  264,  265,  A1,  0.791948

C  FEED THRU PLUG
       SPV 1,   263,  267,  A1,  0.020720
       SPV 2,   267,  268,  A1,  0.004784
       SPV 3,   267,  268,  A9,  9.910562
       SPV 4,   268,  269,  A1,  0.005772
```

```
      SPV 5,   263, 269,  A9,  0.180640

C  ICV BASE TO ICV FLANGE
      DPV 6,   265, 250,  A1,  0.570385,  A9,
42.490320
      DPV 7,   264, 250,  A1,  0.092853,  A9,
6.917029
      DPV 8,   266, 250,  A1,  0.420356,  2.75, 113.
      DPV 9,   266, 250,  A1,  0.721917,  A9,
17.354681

      -25065,  250, 265,  0.23237
      -25064,  250, 264,  0.03662
      -25066,  250, 266,  0.10973

      -265242, 265, 242,  0.19797

C INCLUDE ocvtc.nc7
C  CONDUCTANCE WITHIN OUTER-CONTAINMENT SHELL W/
DRAINED COOLANT JACKET
C    OCV BOLT NODES ARE INCLUDED  - Version 007, -
SARP Model, 4/28/94
C This File Seperates The Convection Conductances From
The Remaining Conductors

C  CONDUCTANCE WITHIN OUTER-CONTAINMENT SHELL
      SPV 30,  300, 304,  A1,  0.036965
      DPV 31,  304, 310,  A1,  0.238513,  A1, 0.042667
      DPV 32,  304, 305,  A1,  0.906667,  A1, 0.125000
      SPM 33,  2,1, 310,10,  320,10,   A1,  0.028925
      SPV 35,  330, 340,  A1,  0.042398
      SPV 36,  340, 341,  A1,  0.099211
      SPV 37,  341, 337,  A1,  0.404970
      SPV 38,  337, 346,  A1,  0.086181
      SPV 39,  341, 342,  A1,  0.634951
      DPV 40,  342, 344,  A1,  0.264563,  A1,
1.624183
      SPV 41,  344, 354,  A1,  0.799354
      SPV 42,  354, 356,  A1,  0.428709
      SPV 43,  350, 352,  A1,  0.286652
      SPV 44,  354, 350,  A1,  1.654381
      SPV 45,  356, 352,  A1,  1.431232

      SPV 46,  346, 1346, A1,  0.113908
      SPV 47, 1346, 345,  A1,  0.288388
      DPV 48,  345, 347,  A1,  0.364280,  A1,
0.195113
      DPV 49,  347, 356,  A1,  0.251778,  A1,
0.783353
      SPV 70,  346, 349,  A1,  0.156388

      SPV 71,  349, 358,  A1,  0.127543
          72,  351, 358,        96.6 $ CONTACT
RESISTANCE
      SPV 73,  358, 357,  A1,  1.445375
      SPV 74,  351, 353,  A69, 0.116211
      SPV 75,  353, 355,  A69, 0.052356
      DPV 76,  353, 357,  A7, 12.077918,  A1, 2.232816
      DPV 77,  353, 359,  A7,  9.544089,  A1, 1.764393
      SPV 771, 357, 354,  A1,  2.327259
      SPV 772, 357, 356,  A1,  2.327259
      SPV 773, 359, 350,  A1,  1.685771
      SPV 774, 359, 352,  A1,  1.685771

          78,  355, 379,       338.64
      DPV 79,  355, 379,  A7, 19.792404,  A1, 2.919837
      SPV 92,  379, 366,  A1,  5.221414
      SPV 93,  379, 367,  A1,  5.221414
          94,  371, 358,        12.90
      SPV 95,  371, 373,  A69, 0.007674
      SPV 96,  373, 375,  A69, 0.004265
      SPV 97,  375, 377,  A69, 0.005280
      DPV 98,  373, 357,  A7,  1.370597,  A1, 0.358112
      DPV 982, 373, 359,  A7,  1.018931,  A1, 0.266228
      DPV 983, 375, 379,  A7,  1.559351,  A1, 0.824600
          99,  377, 403,        24.80

      SPV 80,  360, 362,  A1,  0.109152
      SPV 81,  362, 364,  A1,  0.210491
      SPV 82,  364, 366,  A1,  0.357105
      SPV 83,  366, 367,  A1,  0.892404
      SPV 84,  367, 368,  A1,  1.654161
      SPV 85,  368, 369,  A1,  0.929374
      DPV 86,  366, 350,  A1,  1.013164,  243.8,  2.75

      DPV 87,  367, 352,  A1,  0.894566,  289.8,  2.00


      DPV 88,  356, 369,  A1,  0.606396,  A7,
54.766245
      DPV 89,  352, 369,  A1,  0.527098,  A7,
47.604506

C  ***  COOLANT JACKET - BOTH LOOPS ACTIVE  ***
C     31101,  311,1011, 321,1021, 331,1031,  1. $
DUMMY VALUE
C     31201,  312,1012, 322,1022, 332,1032,  1. $
DUMMY VALUE
C     33101,  331,1041,                      1. $
DUMMY VALUE
C     33202,          332,1042,              1. $
DUMMY VALUE
C     33103,  331,1043,                      1. $
DUMMY VALUE
C     33204,          332,1044,              1. $
DUMMY VALUE
C     31115,      311,315,   321,325,    1.  $ DUMMY
VALUE
C     31216,      312,316,   322,326,    1.  $ DUMMY
VALUE
C     31113,      311,313,   321,323,    1.  $ DUMMY
VALUE
C     31213,      312,313,   322,323,    1.  $ DUMMY
VALUE
C     33133,      331,333,               1.  $ DUMMY
VALUE
C     33233,      332,333,               1.  $ DUMMY
VALUE
C     33135,      331,335,               1.  $ DUMMY
VALUE
C     33236,      332,336,               1.  $ DUMMY
VALUE
C     33732,      337,331,   337,332,    1.  $ DUMMY
VALUE

C       380,   -901,331, -331,321, -321,311, -311,901,
  37.4*64.43*0.911
C       381,   -902,332, -332,322, -322,312, -312,902,
  37.4*64.43*0.911

C  BEGIN MODIFICATIONS FOR DRY COOLANT JACKET
SIMULATION
      SPM 31101, 3,1, 311,10, 1011,10,  A7,  9.948569
      SPM 31201, 3,1, 312,10, 1012,10,  A7,  9.948569
      SPV 33101,      331,    1041,     A7,  3.623888
      SPV 33202,      332,    1042,     A7,  3.623888
      SPV 33103,      331,    1043,     A7,  0.753482
      SPV 33204,      332,    1044,     A7,  0.753482
      SPM 31113, 2,1, 311,10, 313,10,   A7,  5.040972
      SPM 31213, 2,1, 312,10, 313,10,   A7,  5.040972
      SPM 31115, 2,1, 311,10, 315,10,   A7, 10.214747
      SPM 31216, 2,1, 312,10, 316,10,   A7, 10.214747
      SPV 33133,      331,    333,      A7,
5.040972*1.44
      SPV 33233,      332,    333,      A7,
5.040972*1.44
      SPV 33135,      331,    335,      A7,
10.214747*1.44
      SPV 33236,      332,    336,      A7,
10.214747*1.44
      SPM 33732, 2,1, 337,0,  331,1,    A7,
0.826389*0.5
```

```
C  DRAINED COOLANT JACKET RADIATION - w/ e= 0.3 @ OCV
Shell & e= 0.48 @ Jacket
      -101115,  1011,315, 1012,316,      0.98579
      -101113,  1011,313, 1012,313,      0.81720
      -102125,  1021,325, 1022,326,      0.98579
      -102123,  1021,323, 1022,323,      0.81720
      -103135,  1031,335, 1032,336,      0.98579
      -103133,  1031,333, 1032,333,      0.81720
      -104135,  1041,335, 1042,336,      0.35886
      -104133,  1041,333, 1042,333,      0.29748
      -104335,  1043,335, 1044,336,      0.07490
      -104333,  1043,333, 1044,333,      0.06210

      -313315,  313,315,  313,316,       0.83918
      -323325,  323,325,  323,326,       0.83918
      -333335,  333,335,  333,336,       1.20842

C  DRAINED COOLANT JACKET RADIATION - w/ e= 0.5
C     -101115,  1011,315, 1012,316,      1.37615
C     -101113,  1011,313, 1012,313,      1.06893
C     -102125,  1021,325, 1022,326,      1.37615
C     -102123,  1021,323, 1022,323,      1.06893
C     -103135,  1031,335, 1032,336,      1.37615
C     -103133,  1031,333, 1032,333,      1.06893
C     -104135,  1041,335, 1042,336,      0.50096
C     -104133,  1041,333, 1042,333,      0.38911
C     -104335,  1043,335, 1044,336,      0.10455
C     -104333,  1043,333, 1044,333,      0.08123

C     -313315,  313,315,  313,316,       1.09765
C     -323325,  323,325,  323,326,       1.09765
C     -333335,  333,335,  333,336,       1.58062

C  DRAINED COOLANT JACKET RADIATION - w/ e= 0.3
C     -101115,  1011,315, 1012,316,      0.79616
C     -101113,  1011,313, 1012,313,      0.67950
C     -102125,  1021,325, 1022,326,      0.79616
C     -102123,  1021,323, 1022,323,      0.67950
C     -103135,  1031,335, 1032,336,      0.79616
C     -103133,  1031,333, 1032,333,      0.67950
C     -104135,  1041,335, 1042,336,      0.28983
C     -104133,  1041,333, 1042,333,      0.24735
C     -104335,  1043,335, 1044,336,      0.06049
C     -104333,  1043,333, 1044,333,      0.05164

C     -313315,  313,315,  313,316,       0.69771
C     -323325,  323,325,  323,326,       0.69771
C     -333335,  333,335,  333,336,       1.00471

C  END OF DRY COOLANT JACKET SIMULATION REVISIONS

      SPM 31011,  2,1, 310,0, 1011,1,    A1, 3.525455
      SPM 32011,  2,1, 320,0, 1021,1,    A1, 3.525455
      SPM 33011,  2,1, 330,0, 1031,1,    A1, 3.525455
      SPM 34011,  2,1, 340,0, 1041,1,    A1,
3.525455*0.364
      SPM 34211,  2,1, 342,0, 1043,1,    A1,
3.525455*0.076

      SPM 31013,  3,1, 310,10, 313,10,   A1, 1.378570
      SPV 34013,       340,    333,      A1,
1.378570*0.364
      SPV 34213,       342,    333,      A1,
1.378570*0.076

      SPM 31315,  2,1, 1013,0,  315,1,   A1, 1.246121
      SPM 31325,  2,1, 1023,0,  325,1,   A1, 1.246121
      SPV 31313,       1013,    313,      A1, 1.833891
      SPV 31323,       1023,    323,      A1, 1.833891
      SPM 33315,  2,1, 1033,0,  335,1,   A1,
1.246121*1.44
      SPV 33313,       1033,    333,      A1,
1.833891*1.44

C  FIBERGLASS INSULATION WITHIN BOLT CIRCLE CAVITY
      SPV 401, 342, 343,  A63,  0.528760
      SPV 402, 346, 343,  A63,  5.797259
      SPV 403, 345, 343,  A63,  0.760085
      SPV 404, 354, 343,  A63,  1.777278
      SPV 405, 356, 343,  A63,  1.537552
      SPV 407, 349, 343,  A63,  7.798219

      DPV 90,  369, 1347,  A1,  2.284711,  A7,
9.752900
      DPV 91,  356, 1347,  A1,  1.787473,  A7,
0.393590
      SPV 911,  347, 1347,  A7,  10.966613
      SPV 912,  404, 1347,  A7,  0.422906

C INCLUDE standgtc.006
C
C  CONDUCTION FROM RTG TO SUPPORT STAND & ICV BASE
PLATE
C
      175107,  175, 1007,   11.62
      SPV 107108,  1007,1008,  A3, 0.016340
      SPV 108190,  1008, 190,  A3, 0.020886
      SPV 108109,  1008,1009,  A3, 0.015913
      SPV 109191,  1009, 191,  A3, 0.036257
      191198,  191,  198,  270.

      SPV 196101,  196, 1001,  A1,   0.021808
      SPV 198101,  198, 1001,  A1,   0.050929
      SPV 198102,  198, 1002,  A1,   0.077855
      SPV 194102,  194, 1002,  A1,   0.098255
      SPV 199102,  199, 1002,  A1,   0.305056
      SPV 199193,  199,  193,  A1,   0.049183
      SPV 101103, 1001, 1003,  A1,   0.017685
      SPV 192103,  192, 1003,  A1,   0.077401
      SPV 192104,  192, 1004,  A1,   0.077401
      104105,     1004, 1005,         70.75  $ CONTACT

      SPV 105104, 1004, 1005,  A1,   0.012272
      SPV 105106, 1005, 1006,  A1,   0.023580
      SPV 106261,  261, 1006,  A1,   0.303835
      SPV 106263, 1006,  263,  A1,   0.219227

      SPV 196195,  196, 195,   A64,   0.392699
      SPV 198197,  198, 197,   A64,   2.102747

      SPV 193240,  193, 240,  A9,   4.83196
      195100,  195, 1000,   1.0    $ DUMMY VALUES
      192100,  192, 1000,   1.0
      194100,  194, 1000,   1.0
      197100,  197, 1000,   1.0
      194110,  194, 1010,   1.0
      102110, 1002, 1010,   1.0
      242110,  242, 1010,   1.0
      261100,  261, 1000,   1.0
      263100,  263, 1000,   1.0
      265110,  265, 1010,   1.0

     -19924,  199, 242,  0.20178
     -19324,  193, 240,  1.63179
     -19424,  194, 242,  0.73428
     -19465,  194, 265,  0.20298
     -19499,  194, 199,  0.23334
     -19463,  194, 263,  0.34930
     -19497,  194, 197,  0.48360
     -19261,  192, 261,  0.10362
     -19263,  192, 263,  0.10597
     -19295,  192, 195,  0.11237
     -19297,  192, 197,  0.11572
     -19294,  192, 194,  0.13883

     -19561,  195, 261,  0.35501
     -19763,  197, 263,  0.80672
C
C  RADIATION BETWEEN ICV & RTG STAND SURFACES
C
     -200193,   200,193,       0.01239
     -200198,   200,198,       0.04436
```

```
      -200196,   200,196,        0.01605
      -200190,   200,190,        0.01056
      -204193,   204,193,        0.01453
      -204198,   204,198,        0.06412
      -204196,   204,196,        0.01839
      -204190,   204,190,        0.01489
      -210193,   210,193,        0.00895
      -210198,   210,198,        0.05003
      -210196,   210,196,        0.01737
      -210190,   210,190,        0.01929
      -220193,   220,193,        0.03405
      -220198,   220,198,        0.14957
      -220196,   220,196,        0.05279
      -220190,   220,190,        0.06285
      -230193,   230,193,        0.15374
      -230198,   230,198,        0.71510
      -230196,   230,196,        0.11887
      -230190,   230,190,        0.25007
      -193198,   193,198,        0.73848
      -193196,   193,196,        0.01450
      -193190,   193,190,        0.06321


        544,   190, 230,             1.
        546,   191, 230,             1.
        547,   196, 230,             1.
        548,   198, 230,             1.

C  FEEDTHRU PLUG
      SPV 2266,   267,   1266,   A9, 3.994672
      SPV 2267,  1266,   1267,  A64, 0.422968
      SPV 1988,   198,   1268,  A64, 0.076699
      SPV 2268,  1268,   1266,   A1, 0.004712
      SPV 2269,  1268,   1267,   A1, 0.007336

      267100,  1267, 1000,    1.0   $ DUMMY VALUE
      267110,  1267, 1010,    1.0

      268269,  1268, 1269,    1.0   $ DUMMY VALUE
      269268,  1269,  268,    1.0
      269269,  1269,  269,    1.0
      266269,  1266, 1269,    1.0

      198100,   198, 1000,    1.0

     -26763, 1267, 263,  0.03118
     -26742, 1267, 242,  0.02859
     -26797, 1267, 197,  0.04801

C INCLUDE foamtc.007
C  FOAM IMPACT LIMITER CONDUCTORS - Version 007 - SARP
Model, 2/28/94

C  CONDUCTANCE WITHIN IMPACT LIMITER SHELL
      SPV 921,  400, 402,  A1,    0.032471
      SPV 922,  403, 402,  A1,    0.115207
      DPV 931,  402, 404,  A1, 0.138920,  A1, 0.062774
      DPV 941,  404, 406,  A1, 0.062774,  A1, 0.078960
      DPV 951,  406, 408,  A1, 0.092614,  A1, 0.042865
      DPV 961,  408, 410,  A1, 0.042865,  A1, 0.115767
      SPV 971,  410, 412,  A1, 0.053277
      SPV 981,  412, 414,  A1, 0.027059

C  MODEL FOAM AT NON-DAMAGED SECTIONS
      SPV 4100, 400, 401, A7,  148.489340
      4109, 401, 421,          6.700783 * 0.181
      4103, 421,422,           3.350391 * 0.181
      4104, 422,423,           3.350391 * 0.181
      4105, 423,414,           6.700783 * 0.181

      4200, 402, 424,          4.867695 * 0.278
      4201, 424,425,           2.433847 * 0.278
      4202, 425,426,           2.433847 * 0.278
      4203, 426, 412,          4.867695 * 0.278

      4106, 421,424,           0.239855* 0.278
      4107, 422,425,           0.239855* 0.278
      4108, 423,426,           0.239855* 0.278

      4301, 406,431,           2.162321 * 0.278
      4302, 431,432,           1.081160 * 0.278
      4303, 432,433,           1.081160 * 0.278
      4304, 433,434,           1.131404 * 0.278
      4305, 434,435,           1.186544 * 0.278
      4306, 435,436,           1.186544 * 0.278
      4307, 436, 410,          2.373089 * 0.278

      4308, 404, 431,          2.830943 * 0.278
      4309, 404, 432,          2.830943 * 0.278
      4310, 404, 433,          2.830943 * 0.278

      4208, 424, 434,          0.717996 * 0.278
      4209, 425, 435,          0.717996 * 0.278
      4210, 426, 436,          0.717996 * 0.278

      4401, 406,441,           2.224721 * 0.278
      4402, 441,442,           1.112360 * 0.278
      4403, 442,443,           1.112360 * 0.278
      4404, 443,444,           1.164054 * 0.278
      4405, 444,445,           1.220785 * 0.278
      4406, 445,446,           1.220785 * 0.278
      4407, 446, 410,          2.441571 * 0.278

      4408, 441, 431,          1.531170 * 0.278
      4409, 442, 432,          1.531170 * 0.278
      4410, 443, 433,          1.531170 * 0.278
      4411, 444, 434,          1.395178 * 0.278
      4412, 445, 435,          1.395178 * 0.278
      4413, 446, 436,          1.395178 * 0.278

      4501, 406,451,           2.404134 * 0.278
      4502, 451,452,           1.202067 * 0.278
      4503, 452,453,           1.202067 * 0.278
      4504, 453,454,           1.257929 * 0.278
      4505, 454,455,           1.319236 * 0.278
      4506, 455,456,           1.319236 * 0.278
      4507, 456, 410,          2.638472 * 0.278

      4508, 441, 451,          1.697203 * 0.278
      4509, 442, 452,          1.697203 * 0.278
      4510, 443, 453,          1.697203 * 0.278
      4511, 444, 454,          1.546465 * 0.278
      4512, 445, 455,          1.546465 * 0.278
      4513, 446, 456,          1.546465 * 0.278

      4608, 408, 451,          3.680771 * 0.278
      4609, 408, 452,          3.680771 * 0.278
      4610, 408, 453,          3.680771 * 0.278
      4611, 408, 454,          3.352860 * 0.278
      4612, 408, 455,          3.352860 * 0.278
      4613, 408, 456,          3.352860 * 0.278

C  RADIATION WITHIN IMPACT LIMITER
      -4101, 400, 401,        2.930700
C INCLUDE icvocvtc.max
C  CONDUCTORS BETWEEN CONTAINMENT SHELLS - Version
007; 2/28/94
C  ICV to OCV Conductance w/ Maximum Gaps
      SPV 200, 200, 300,  A9,   7.374016   $ w/
Maximum 1/2" Gap
      SPV 201, 204, 304,  A9,  10.412879   $ w/
Maximum 1/2" Gap At Top &
C                                          1/4"
Gap At Side
      SPM 202, 3,1, 210,10, 310,10, A9,  42.80263  $
w/ Maximum 1/4" Gap
      SPV 206, 240, 340,  A9,   15.598626  $ w/
Maximum 1/4" Gap
      SPV 207, 242, 342,  A9,   13.258832  $ w/
Maximum 1/4" Gap

C  ICV to OCV Conductance w/ Nominal Gaps
```

```
C     SPV 200, 200, 300,  A9,  11.798426    $ w/
Nominal 5/16" Gap
C     SPV 201, 204, 304,  A9,  14.776072    $ w/
Nominal 5/16" Gap At Top &
C                                                    3/16"
Gap At Side
C     SPM 202, 3,1, 210,10, 310,10, A9,  56.970804 $
w/ Nominal 3/16" Gap
C     SPV 206, 240, 340,  A9,    20.761955   $ w/
Nominal 3/16" Gap
C     SPV 207, 242, 342,  A9,    17.647662   $ w/
Nominal 3/16" Gap

C  ICV to OCV Conductance w/ Minimum Gaps
C     SPV 200, 200, 300,  A9,  29.496064    $ w/
Minimum 1/8" Gap
C     SPV 201, 204, 304,  A9,  31.872483    $ w/
Minimum 1/8" Gap At Top &
C                                                    1/16"
Gap At Side
C     SPM 202, 3,1, 210,10, 310,10, A9, 170.315162 $
w/ Minimum 1/16" Gap
C     SPV 206, 240, 340,  A9,    62.068208   $ w/
Minimum 1/16" Gap
C     SPV 207, 242, 342,  A9,    52.757976   $ w/
Minimum 1/16" Gap


      SPV 208, 250, 344,  A9,   5.223214
      SPV 209, 250, 350,  A9,   2.295739
      SPV 210, 250, 366,  A9,   2.295739

      DPV 211, 260, 360,  A1,  1.342561,  314.2,  0.2
      DPV 212, 262, 362,  A1,  1.678201,  392.7,  0.2
      DPV 213, 264, 364,  A1,  0.845101,  197.8,  0.2
      DPV 214, 266, 364,  A1,  1.223529,  286.3,  0.2
      DPV 215, 266, 366,  A1,  0.473071,  A9,
38.457365

      DPV 216, 360, 400,  A1,  2.908882,  A7,
43.633231
      DPV 217, 362, 400,  A1,  3.636103,  A7,
54.541539
      DPV 218, 364, 400,  A1,  4.589903,  A7,
68.848538
      DPV 219, 366, 402,  A1,  1.330519,  202.,  0.8
      DPV 220, 367, 402,  A1,  1.168210,  216.,  0.8
      DPV 221, 368, 402,  A1,  1.566659,  A7,
54.833064
      DPV 222, 368, 404,  A1,  3.242285,  A7,
18.147681
      DPV 223, 369, 404,  A1,  2.223281,  A7,
12.444124
      SPV 224, 345, 404,  A7,  0.099998


        -2030, 200, 300,  3.01648
        -2034, 204, 304,  4.11301
        -2131, 210, 310,  8.70236
        -2231, 220, 320,  8.70236
        -2331, 230, 330,  8.70236
        -2431, 240, 340,  3.17141
        -2432, 242, 342,  2.69569
        -2433, 250, 344,  0.53075
        -2434, 250, 350,  0.12276
        -2435, 250, 366,  0.07489

        -2636, 266, 366,  0.22082

        -4030, 400, 360,  0.49403
        -4032, 400, 362,  0.61745
        -4034, 400, 364,  0.77940
        -4238, 402, 368,  0.62075
        -4438, 404, 368,  0.92060
        -4439, 404, 369,  0.63129
        -4434, 404, 345,  1.30685
```

```
C INCLUDE exttc.007
C  EXTERIOR CONDUCTORS - Undamaged Package, Upright
Position - Ver. 007, 4/28/94
      300,    300,   1,  1.0     $ DUMMY VALUE
      301,    301,   1,  1.0     $ DUMMY VALUE
      304,    304,   1,  1.0     $ DUMMY VALUE
      305,    305,   1,  1.0     $ DUMMY VALUE
      315,    315,   1,  1.0     $ DUMMY VALUE
      316,    316,   1,  1.0     $ DUMMY VALUE
      325,    325,   1,  1.0     $ DUMMY VALUE
      326,    326,   1,  1.0     $ DUMMY VALUE
      335,    335,   1,  1.0     $ DUMMY VALUE
      336,    336,   1,  1.0     $ DUMMY VALUE
     1013,   1013,   1,  1.0     $ DUMMY VALUE
     1023,   1023,   1,  1.0     $ DUMMY VALUE
     1033,   1033,   1,  1.0     $ DUMMY VALUE

      346,    346,   1,  1.0     $ DUMMY VALUE
      349,    349,   1,  1.0     $ DUMMY VALUE
      351,    351,   1,  1.0     $ DUMMY VALUE
      371,    351,   1,  1.0     $ DUMMY VALUE
     1346,   1346,   1,  1.0     $ DUMMY VALUE

      406,    406,   1,  1.0     $ DUMMY VALUE
      408,    408,   1,  1.0     $ DUMMY VALUE

C  EXTERIOR RADIATION
      -303,    300,   2,  1.79184
      -3031,   300, 301,  0.80979
      -3035,   300, 305,  0.17056
      -3015,   301,   2,  1.06333
      -3041,   304,   2,  2.04555
      -3045    305, 304,  0.05370 * 48.
      -3051,   305,   2,  9.39153
      -3058    305,315,  305,316,  0.00488 * 48.
      -3152,   315,2, 316,2,   4.11533
      -3252,   325,2, 326,2,   4.02655
      -3352,   335,2, 336,2,   4.83562

      -3462,   346,   2,  3.55295
      -34633,  346,1033,  0.46254
      -34335,  346,335,  346,336,   0.90787
      -34623,  346,1023,  0.02033
      -34325,  346,325,  346,326,   0.04061
      -34613,  346,1013,  0.00623
      -34315,  346,315,  346,316,   0.01246

      -3512,   351,   2,  0.06595
      -3492,   349,   2,  0.71024
      -3519,   351, 349,  0.48978
      -3712,   371,   2,  0.00799
      -3719,   371, 349,  0.06025

      -1348,  1346,   2,  0.27098
      -1347,  1346, 406,  0.25415

      -1336,  1033, 406,  0.36736
      -3356,   335,406, 336,406,  0.72851
      -1236,  1023, 406,  0.09183
      -3256,   325,406, 326,406,  0.18327
      -1136,  1013, 406,  0.03448
      -3156,   315,406, 316,406,  0.06890

      -35604,  356,  404,   0.11917
      -35647,  356,347, 356,369,   0.06206
      -36904,  369,404, 347,404,   0.14150
      -34769,  347,  369,   0.47124
      -35269,  352,  369,   0.21003
      -35669,  356,  369,   0.24164


      -4062,   406,   2,  7.89541
      -4082,   408,   2, 21.98889

      -1014,  1013,   2,  2.05783
      -1024,  1023,   2,  2.01344
```

```
      -1034,  1033,   2,  2.41821

C  RADITION LINKS USED ONLY WITH PACKAGE ON ITS SIDE
C     -4102,   410,   2,  8.23333
C     -4122,   412,   2,  5.50556
C     -4142,   414,   2,  7.33333


C*****************************************************
******************
HEADER SOURCE DATA, PTS7
C*****************************************************
******************
      50,     879.016 * 3.413  $ DESIGN HEAT LOAD
      52,    2741.968 * 3.413  $ DESIGN HEAT LOAD
      54,     879.016 * 3.413  $ DESIGN HEAT LOAD

     300,      3.6870 * 245.83333 *0.25 *0.5 $ SOLAR
LOAD
     301,      2.2153 * 245.83333 *0.70 $ SOLAR LOAD

     304,      5.2985 * 245.83333 *0.25 $ SOLAR LOAD

     305,     22.0069 *  61.41667 *0.25 $ SOLAR LOAD

     315,      5.2097 * 122.91667 *0.25 $ SOLAR LOAD

     316,      5.2097 * 122.91667 *0.25 $ SOLAR LOAD

    1013,      2.6051 * 122.91667 *0.25 $ SOLAR LOAD

     325,      5.2097 * 122.91667 *0.25 $ SOLAR LOAD

     326,      5.2097 * 122.91667 *0.25 $ SOLAR LOAD

    1023,      2.6051 * 122.91667 *0.25 $ SOLAR LOAD

     335,      7.4979 * 122.91667 *0.25 $ SOLAR LOAD

     336,      7.4979 * 122.91667 *0.25 $ SOLAR LOAD

    1033,      3.7496 * 122.91667 *0.25 $ SOLAR LOAD

     346,      6.1526 * 245.83333 *0.25 $ SOLAR LOAD

     349,      4.7083 * 122.91667 *0.50 $ SOLAR LOAD

    1346,      0.5344 * 122.91667 *0.25 $ SOLAR LOAD

     406,     10.7014 * 245.83333 *0.25 $ SOLAR LOAD

     408,     27.4861 * 122.91667 *0.25 $ SOLAR LOAD

C*****************************************************
******************
HEADER CONTROL DATA, GLOBAL
C*****************************************************
******************
      SIGMA= 1.7141E-09
      NLOOPS= 1200
      EXTLIM= 25.
      ITERXT= 4
      ITEROT= 1200
      ARLXCA=.05
      DRLXCA= .002
      ATMPCA= 50.
      DTMPCA= 20.
      EBALSA=.0001
      EBALNA=.001
      NLOOPT= 800
      OUTPUT= 1./60.
      DTIMEH = 0.02
C*****************************************************
******************
HEADER USER DATA, PTS7
C*****************************************************
******************
      10 = 32.174          $ GC IN FT/SEC**2
      11 = 20.0            $ ICV Gas Pressure
C     1  = 58.88           $ mdot*cp For Coolant, w/
p=64.63 & cp=.911 @ 40F
      2  = 0.
      3  = 0.
      4  = 0.
      5  = 0.
      6  = 0.
      7  = 0.              $ Model Scale Factor
      8  = 0.
      9  = 0.
      12 = 0.
C*****************************************************
*******
HEADER ARRAY DATA, PTS7
C*****************************************************
*******
C INCLUDE array
      1 =  $304 STAINLESS STEEL CONDUCTIVITY -
BTU-IN/HR-SF-F
      91.346,      7.1499E-2,   -3.9267E-6
      2 =  $304 STAINLESS STEEL SPECIFIC HEAT -
BTU/LB-F
      0.1155,      3.3294E-5,   -1.1252E-9
      3 =  $AL6061-T6 CONDUCTIVITY - BTU-IN/HR-SF-F
      1000.5,      0.7437,      -5.7268E-4
      4 =  $AL6061-T6 SPECIFIC HEAT - BTU/LB-F
      0.2022,      9.8729E-5,   -3.4089E-8
      5 =  $AL2219-T6 CONDUCTIVITY - BTU-IN/HR-SF-F
      804.70,      0.5831,      -2.2709E-4
      6 =  $AL2219-T6 SPECIFIC HEAT - BTU/LB-F
      0.1986,      8.0573E-5,   -2.1537E-8
      7 =  $AIR CONDUCTIVITY - BTU-IN/HR-SF-F
      0.1574,      2.6254E-4,   -3.2429E-8
      8 =  $AIR SPECIFIC HEAT - BTU/LB-F
      0.2362,      2.7871E-5,   -2.2971E-9
      9 =  $HELIUM CONDUCTIVITY - BTU-IN/HR-SF-F
      0.9412,      1.2361E-3,   -5.1711E-8
      10=  $HELIUM SPECIFIC HEAT - BTU/LB-F
      1.2404       0.,          0.
      11 =  $HELIUM CONDUCTIVITY - BTU/HR-FT-F
      0., .078, 98.33,.08846, 206.33,.09875,
404.33,.1183
      548.33,.1347, 800.33,.1607, 1160.33,.1937,
1520.33,.2249
      12 =  $HELIUM SPECIFIC HEAT - BTU/LB-F
      0., 1.240, 4000.,1.240
      13 =  $HELIUM ABSOLUTE VISCOSITY - LB/FT-HR
      0.,.04104,  116.33,.05034, 224.33,.0567,
404.33,.06653
      566.33,.0747, 890.33,.0899, 1160.33,.1016,
1520.33,.1161
      14=  $AIR CONDUCTIVITY - BTU/HR-FT-F
      0., .0133, 100.,.0154, 200.,.0174, 400.,.02212,
1000.,.03828
      1500.,.04, 2000.,.0471, 2500.,.051, 3000.,.054
      15 =  $AIR SPECIFIC HEAT - BTU/LB-F
      0., .2398, 100.,.2404, 200.,.2410,  400.,.2450,
1000.,.2620
      1500.,.276, 2000.,.286, 2500.,.292, 3000.,.297
      16 =  $AIR ABSOLUTE VISCOSITY - LB/FT-HR
      0., .03960, 100.,.04626, 200.,.05184,
400.,.0630, 1000.,.08892
      1500.,.108, 2000.,.1242, 2500.,.1328, 3000.,.139
      17=  $TI-6AL-4V CONDUCTIVITY - BTU-IN/HR-SF-F
      47.478,      2.4914E-2,    1.4798E-5
      18=  $TI-6AL-4V SPECIFIC HEAT - BTU/LB-F
      0.1277,      3.8124E-5,   -8.0366E-9
      19 =  $30% ETHYLENE GLYCOL/WATER CONDUCTIVITY -
BTU/HR-FT-F
      0., 0.234, 20.,0.243 , 40.,0.251, 60.,0.259
      80.,0.266, 100.,0.272, 120.,0.277, 140.,0.282
      180.,0.288, 200.,0.290, 240.,0.292
      20 =  $30% ETHYLENE GLYCOL/WATER SPECIFIC HEAT -
```

```
BTU/LB-F
      0., 0.847,  20.,0.854,  40.,0.861,  60.,0.869
      80.,0.876, 100.,0.884, 120.,0.891, 140.,0.899
      180.,0.914, 200.,0.921, 240.,0.936
      21 = $30% ETHYLENE GLYCOL/WATER ABSOLUTE
VISCOSITY - LB/FT-HR
      0., 20.36,  20.,12.99,  40., 8.57 , 60.,6.02
      80.,4.44,  100.,3.41,  120.,2.69,  140.,2.18
      180.,1.52 , 200.,1.29 , 240.,0.98
      22 = $30% ETHYLENE GLYCOL/WATER DENSITY -
LB/FT**3
      0., 65.98,  20.,65.84,  40.,65.65,  60.,65.43
      80.,65.16, 100.,64.86, 120.,64.52, 140.,64.14
      180.,63.28, 200.,62.79, 240.,61.70
      23= $EBP GRAPHITE SPECIFIC HEAT - BTU/LB-F
      0.2350,      1.7610E-4,   -3.0710E-8
      24= $PUO2 FUEL SPECIFIC HEAT - BTU/LB-F
      7.746E-2,    3.9860E-6,   -6.1330E-10
      25= $MIN-K INSULATION SPECIFIC HEAT - BTU/LB-F
      0.1950,      9.7500E-5,   -3.1300E-8
      26= $BERYLLIUM-COPPER SPECIFIC HEAT - BTU/LB-F
      0.097,       3.7000E-5,    0.0000
      27= $BERYLLIUM-COPPER CONDUCTIVITY -
BTU/IN-HR-F
      5.2830,      5.1640E-3,   -2.1450E-6
      28= $T/E MODULE CONDUCTIVITY - BTU/IN-HR-F
      0.1319,     -1.9160E-4,    4.7320E-7
      48= $CARBON STEEL CONDUCTIVITY - BTU-IN/HR-SF-F
      316.4315,    5.90354E-2,   -6.607106E-6
      49= $CARBON STEEL SPECIFIC HEAT - BTU/LB-F
      0.1155,      3.3294E-5,   -1.1252E-9
      53 = $DERIVATIVE OF HUMIDITY RATIO W/ TEMP
-LB/LB-F
      24.,.000125, 28.,.000145, 30.,.0001475,
35.,.0001775
      40.,.000205, 45.,.0002525, 50.,.00029,
55.,.00035
      60.,.0004, 65.,.00046, 70.,.00056, 75.,.00065
      80.,.0007625
      54 = $ENTHALPLY OF LIQUID TO VAPOR (WATER) -
BTU/LBM
      32.02,1075.4, 101.70,1036., 126.04,1022.1
      141.43,1013.1, 152.93,1006.4, 193.19,982.1
      61= $MIN-K INSULATION SPECIFIC HEAT - BTU/LB-F
      0.1950,      9.7500E-5,   -3.1300E-8
      62 = $MIN-K CONDUCTIVITY - BTU-IN/HR-SF-F
      0.1685,      8.3040E-5,    4.1324E-8
      63 = $FIBERGLASS INSULATION - BTU-IN/HR-SF-F
      0.2217,      1.6504E-4,    8.9412E-7
      64 = $8#/CU-FT KAOWOOL  - BTU-IN/HR-SF-F
      0.1893,      3.5879E-4,    2.5900E-7
      65 =  $30% PROPOLYENE GLYCOL/WATER CONDUCTIVITY
- BTU/HR-FT-F
      10., 0.236, 20.,0.241 , 40.,0.249, 60.,0.256
      80.,0.262, 100.,0.268, 120.,0.272, 140.,0.276
      180.,0.281, 200.,0.282, 240.,0.282
      66 = $30% PROPOLYENE GLYCOL/WATER SPECIFIC HEAT
- BTU/LB-F
      10., 0.901,  20.,0.904,  40.,0.911,  60.,0.919
      80.,0.926, 100.,0.933, 120.,0.940, 140.,0.948
      180.,0.962, 200.,0.969, 240.,0.984
      67 = $30% PROPOLYENE GLYCOL/WATER ABSOLUTE
VISCOSITY - LB/FT-HR
      10., 30.31,  20.,22.62,  40.,13.37,  60.,8.50
      80.,5.76,  100.,4.12,  120.,3.09,  140.,2.42
      180.,1.62 , 200.,1.38 , 240.,1.06
      68 = $30% PROPOLYENE GLYCOL/WATER DENSITY -
LB/FT**3
      10., 64.96,  20.,64.86,  40.,64.63,  60.,64.36
      80.,64.05, 100.,63.70, 120.,63.31, 140.,62.88
      180.,61.90, 200.,61.35, 240.,60.14
      69= $AISI4130/ASTM A320 CRO-MOLY STEEL
CONDUCTIVITY - BTU-IN/HR-SF-F
      303.50,     -4.5162E-2,   -9.2092E-6
      70= $AISI4130/ASTM A320 CRO-MOLY STEEL SPECIFIC
HEAT - BTU/LB-F
      0.1116,      1.3016E-5,    3.8778E-8
C*****************************************************
******************
HEADER OUTPUT CALLS, PTS7
C*****************************************************
******************
C     CALL GPRINT('PTS7')
C     CALL QPRINT('PTS7')
C     CALL QMAP('PTS7','QD',1)
      CALL SORTPR('PTS7',0)
C     CALL TECPLOT
      CALL PNOSS
C     CALL NODTRN('PTS7' ,  9101 , K2)
C     WRITE(6,50) K2
C 50  FORMAT(' NODE 9101= ', I6)
      WRITE(6,50) XK6, XK11
      WRITE(6,52) XK8, XK9
  50  FORMAT(/,' MEAN ICV GAS TEMP= ', F5.1, ' F',
     * '   MEAN ICV GAS PRESSURE= ', F5.2, ' PSIA' )
  52  FORMAT(/,' MEAN ICV-OCV GAS TEMP= ', F5.1, ' F',
     * '   MEAN ICV-OCV GAS PRESSURE= ', F5.2, ' PSIA'
)
C     WRITE(6,55) XK8, XK9
C 55  FORMAT(/,' HEAT TRANSFER W/O CONDENSATION= ',
F8.2, ' BTU/HR',
C    * ' HEAT TRANSFER W/ CONDENSATION= ', F8.2, '
BTU/HR')
C*****************************************************
******************
HEADER OPERATION DATA
C*****************************************************
******************
BUILD GPHS4, PTS7
C     CALL RESTAR(1035)
      CALL STDSTL
C     CALL TECPLOT
C     CALL PNOSS
C     TIMEND= 20.
C     CALL FORWRD
C     CALL RESAVE('T')
C     CALL TECPLOT
C*****************************************************
******************
HEADER VARIABLES 1, PTS7
C*****************************************************
******************
C  SET MODEL SCALE FACTOR
       XK7 = 1.0

C  SET COOLANT LOOP TEMPERATURES FOR LOOPS 1 & 2,
RESPECTIVELY
       T901 =  -999.
C      T901 =    40.

       T902 =  -999.
C      T902 =    40.

C  COMPUTE COOLANT DENSITY & SPECIFIC HEAT: 30%
PROPOLYENE GLYCOL SOLUTION
C       CALL D1D1WM(T321, A66, 37.4,  K2 )
C       CALL D1D1WM(T321, A68, K2,   G380)
C       G380 = 0.

C       CALL D1D1WM(T322, A66, 37.4,  K2 )
C       CALL D1D1WM(T322, A68, K2,   G381)
C       G381 = 0.

C  SET AMBIENT BOUNDARY TEMPERATURES
      IF(TIMEN .LE.  0.0) THEN
        T1 =  100.
        T2 =  100.
      ELSEIF(TIMEN .GT. .501) THEN
        T1 =  100.
        T2 =  100.
      ELSEIF(TIMEN .GT. 0. .AND. TIMEN .LE. .500) THEN
        T1 = 1475.
```

```
        T2 = 1424.7
       END IF

       IF(TIMEN .LE.  0.75) THEN
         OUTPUT = 1./60.
       ELSEIF(TIMEN .GT. .751) THEN
         OUTPUT = 5./60.
       ELSEIF(TIMEN .GT. 5.001) THEN
         OUTPUT = 20./60.
       ELSEIF(TIMEN .GT. 10.001) THEN
         OUTPUT = 1.
       ELSEIF(TIMEN .GT. 25.001) THEN
         OUTPUT = 5.
       END IF

C INCLUDE extvar.nc7
C  VARIABLE BLOCK FOR OCV EXTERIOR CONDUCTORS -
Drained Jacket - SARP Model, 4/28/94
C      SUBROUTINE FRCVHD(HA,ST,AT,AREA,CL,G,B,CP,K,U,
C     +                  RHO, PRESS, R)
C      SUBROUTINE FRCVHU(HA,ST,AT,AREA,CL,G,B,CP,K,U,
C     +                  RHO, PRESS, R)
C      SUBROUTINE FRCONDES(HA, ST1, ST2, AREA, CL, G,
CP, K,
C     +      U, RHO, PRESS, R, HLG, DWDT, HA1 )
C      SUBROUTINE FRCVV(HA,ST,AT,AREA,CL,G,B,CP,K,U,
C     +                  RHO, PRESS, R)
C      SUBROUTINE
FOREXCV(HA,ST,AT,AREA,CL,G,VEL,CP,K,U,
C     +                  RHO, PRESS, R)

       XK6 = 0.5*(T304 + T1)
        IF(TIMEN .GT. 0. .OR. TIMEN .LE. 0.5) XK6 = T1
       CALL FRCVHU(G300, T300, XK6, 3.687, 3.240,
      +     XK10, 0., A15, A14, A16, 0., 14.69, 53.35)
       G300 = G300*0.85
       XK6 = 0.20*T301 + 0.80*T1
        IF(TIMEN .GT. 0. .OR. TIMEN .LE. 0.5) XK6 = T1
       CALL FRCVV(G301, T301, XK6, 3.6806, 0.1,
      +     XK10, 0., A15, A14, A16, 0., 14.69, 53.35)

       CALL FRCVHU(G304, T304, T1, 5.2985, 3.240,
      +     XK10, 0., A15, A14, A16, 0., 14.69, 53.35)
        G304 = G304 * 0.75
       CALL FRCVV( G305, T305, T1, 22.007, 1.0,
      +     XK10, 0., A15, A14, A16, 0., 14.69, 53.35)

       CALL FRCVV( G315, T315, T1, 5.20972, 4.00,
      +     XK10, 0., A15, A14, A16, 0., 14.69, 53.35)
       CALL FRCVV( G316, T316, T1, 5.20972, 4.00,
      +     XK10, 0., A15, A14, A16, 0., 14.69, 53.35)
       CALL FRCVV( G325, T325, T1, 5.20972, 3.00,
      +     XK10, 0., A15, A14, A16, 0., 14.69, 53.35)
       CALL FRCVV( G326, T326, T1, 5.20972, 3.00,
      +     XK10, 0., A15, A14, A16, 0., 14.69, 53.35)
       CALL FRCVV( G335, T335, T1, 7.4979, 1.75,
      +     XK10, 0., A15, A14, A16, 0., 14.69, 53.35)
       CALL FRCVV( G336, T336, T1, 7.4979, 1.75,
      +     XK10, 0., A15, A14, A16, 0., 14.69, 53.35)

       CALL FRCVV( G1013, T1013, T1, 2.6051, 4.00,
      +     XK10, 0., A15, A14, A16, 0., 14.69, 53.35)
       CALL FRCVV( G1023, T1023, T1, 2.6051, 2.67,
      +     XK10, 0., A15, A14, A16, 0., 14.69, 53.35)
       CALL FRCVV( G1033, T1033, T1, 3.7496, 1.33,
      +     XK10, 0., A15, A14, A16, 0., 14.69, 53.35)

       CALL FRCVHU( G346, T346, T1, 6.1526, 3.0000,
      +     XK10, 0., A15, A14, A16, 0., 14.69, 53.35)
C  CONVECTION AT BOLT TUBES
       CALL FRCVV( G349, T349, T1, 4.70833, 0.16,
      +     XK10, 0., A15, A14, A16, 0., 14.69, 53.35)
       G349 = G349*.5
       CALL FRCVHU( G351, T351, T1, 0.6875, 0.156,
      +     XK10, 0., A15, A14, A16, 0., 14.69, 53.35)
       G351 = G351*.25

       CALL FRCVHU( G371, T371, T1, 0.0833, 0.094,
      +     XK10, 0., A15, A14, A16, 0., 14.69, 53.35)
       G371 = G371*.25

       CALL FRCVV(G1346, T1346, T1, 0.5344, 0.04,
      +     XK10, 0., A15, A14, A16, 0., 14.69, 53.35)
       CALL FRCVHU(G406, T406, T1, 10.701, 3.0000,
      +     XK10, 0., A15, A14, A16, 0., 14.69, 53.35)
       CALL FRCVV( G408, T408, T1, 27.486, 1.33,
      +     XK10, 0., A15, A14, A16, 0., 14.69, 53.35)

C INCLUDE standgvar.006
C  COMPUTE CONVECTIVE HEAT TRANSFER W/I FALSE FLOOR
SECTION
C   BELOW SUPPORT RACK
C
       CALL FRCVHD(G195100, T195, T1000, 0.7847, 2.50,

      +     XK10, 0., A12, A11, A13, 0., XK11, 384.04)
       CALL FRCVHD(G192100, T192, T1000, 1.5069, 0.25,

      +     XK10, 0., A12, A11, A13, 0., XK11, 384.04)
       CALL FRCVV (G194100, T194, T1000, 1.8431, 0.25,
      +     XK10, 0., A12, A11, A13, 0., XK11, 384.04)
        G197100 = G195100*4.2056/0.7847
       CALL FRCVV (G194110, T194, T1010, 3.1958, 0.5,
      +     XK10, 0., A12, A11, A13, 0., XK11, 384.04)
       CALL FRCVHD(G102110, T1002, T1010, 0.6979, 0.08,

      +     XK10, 0., A12, A11, A13, 0., XK11, 384.04)

       CALL FRCVV (G242110, T242, T1010, 3.7083,
0.41667,
      +     XK10, 0., A12, A11, A13, 0., XK11, 384.04)
       CALL FRCVHU(G263100, T263, T1000, 2.7271, 2.50,

      +     XK10, 0., A12, A11, A13, 0., XK11, 384.04)
        G261100 = G263100 * 2.1813/2.7271
       CALL FRCVHU(G265110, T265, T1010, 0.8792, 0.08,

      +     XK10, 0., A12, A11, A13, 0., XK11, 384.04)


C  CONVECTION FROM FEED THRU PLUG ASSEMBLY
       CALL FRCVV (G267100, T1267, T1000, 0.2667,
0.323,
      +     XK10, 0., A12, A11, A13, 0., XK11, 384.04)
       CALL FRCVV (G267110, T1267, T1010, 0.2667,
0.323,
      +     XK10, 0., A12, A11, A13, 0., XK11, 384.04)

       CALL FRCVHD(G268269, T1268, T1269, 0.0821,
0.323,
      +     XK10, 0., A12, A11, A13, 0., XK11, 384.04)
       CALL FRCVV (G269268, T268, T1269, 0.1169,
0.2083,
      +     XK10, 0., A12, A11, A13, 0., XK11, 384.04)
       CALL FRCVHU(G269269, T269, T1269, 0.0250,
0.1667,
      +     XK10, 0., A12, A11, A13, 0., XK11, 384.04)
       CALL FRCVHD(G266269, T1266, T1269, 0.0649,
0.063,
      +     XK10, 0., A12, A11, A13, 0., XK11, 384.04)

       CALL FRCVHD (G198100, T198, T1000, 0.025,
0.1667,
      +     XK10, 0., A12, A11, A13, 0., XK11, 384.04)
C INCLUDE gphsvar.004
C
C       Updated RTG-ICV Convection Linkage Based on
GPHS QUAL Test Results
C  COMPUTE VARIABLE CONDUCTION BETWEEN THE RTG &
PACKAGE
       XK2  = ((T120 + T130 + T140 + T150 + T160
)*97.378 +
      * ( T126 +  T127 +  T136 + T137 +  T146 + T147 +
```

```
     * T156 +  T157 +  T166 + T167 )*181.315 +
     * ( T122 +  T123 +  T132 + T133 +  T142 + T143 +
     * T152 +  T153 +  T162 + T163 )*52.026)/2820.3
      XK3  = (T200*0.371 + T204*0.431 + T210 + T220 +
     *  T230 + T240*0.444)/4.426

C  COMPUTE ICV GAS TEMPERATURE & PRESSURE
      XK6 = (XK2*2820.3 + XK3*6051.6)/8871.9
      XK11 = 20. * (XK6 + 460.)/666.6
C
C     SUBROUTINE FRCVANU(HA,ST1,ST2, AREA, H,   DR,
CL,
C          G,   B,   CP,   K,   U, RHO, PRESS, R)
      CALL FRCVANU(G518, XK2, XK3,   0.7570, 3.5000,
3.505,
     +  1.01,  XK10, 0., A12, A11, A13, 0., XK11,
384.04)
      G518 = G518 * 0.75
      G520 = G518 * 58.51/109.001
      XK5  = ( T126 +  T127 +  T136 + T137 +  T146 +
T147 +
     * T156 +  T157 +  T166 + T167 )/10.
      CALL FRCVANU(G522, XK5, XK3,   1.219,  3.5000,
1.669,
     +  0.568, XK10, 0., A12, A11, A13, 0., XK11,
384.04)
      G522 = G522 * 0.75
      G503 = G518 * 0.70 * 21.1158/109.001
      G504 = G518 * 0.70 * 11.2815/109.001
      G506 = G518 * 0.75 * 97.378/109.001
      G508 = G518 * 0.75 * 52.026/109.001
      G510 = G522 * 0.75 * 181.315/175.498
      G512 = G518 * 0.95 * 97.378/109.001
      G514 = G518 * 0.95 * 52.026/109.001
      G516 = G522 * 0.95 * 181.315/175.498
      G524 = G518 * 1.10 * 97.378/109.001
      G526 = G518 * 1.10 * 52.026/109.001
      G528 = G522 * 1.10 * 181.315/175.498
      G530 = G518 * 1.10 * 97.378/109.001
C     G531 = G518 * 1.10 * 0.75 * 58.336/109.001
C     G531 = G518 * 1.10 * 58.336/109.001 *.25
      G532 = G518 * 1.10 * 52.026/109.001
      G534 = G522 * 1.85 * 181.315/175.498
      G536 = G518 * 1.10 * 21.271/109.001
      G538 = G518 * 1.10 * 11.364/109.001

      G500 = G518 * 0.05 * 61.100/109.001
      G501 = G518 * 0.05 * 15.813/109.001
      G502 = G518 * 0.05 * 15.813/109.001

C     G542 = G518 * 1.65 * 61.100/109.001
      G541 = G518 * 1.65 * 15.813/109.001
C     G540 = G518 * 1.65 * 15.813/109.001

      G544 = G518 * 1.85 * 225./109.001
      G546 = G518 * 1.85 * 280./109.001
      G547 = G518 * 1.25 * 113.0/109.001
      G548 = G518 * 1.25 * 742.2/109.001

C       Updated RTG-ICV Convection Linkage Based on
GPHS QUAL Test REsults
C           Adjustment For Heat To ICV Dome
        G5061 = G506*.25
        G5081 = G508*.25
        G5101 = G510*.25
        G5121 = G512*.25
        G5141 = G514*.25
        G5161 = G516*.25
        G5181 = G518*.25
        G5201 = G520*.25
        G5221 = G522*.25
        G5241 = G524*.25
        G5261 = G526*.25
        G5281 = G528*.25
        G5301 = G530*.25
        G5321 = G532*.25
        G5341 = G534*.25


C
C  COMPUTE OCV GAS TEMPERATURE & PRESSURE
       XK8 = (T200*530.9 + T204*720.9 + T210*1530.1 +
      I T220*1530.1 + T230*1530.1 + T240*557.6 +
T242*474.0 +
      I T300*530.9 + T304*755.3 + T310*1546.5 +
T320*1546.5 +
      I T330*1546.5 + T340*563.6 + T342*479.0)/13842.0
       XK9 = 20.0* (XK8 + 460.)/566.97
C*************************************************
******************
HEADER SUBROUTINES
C*************************************************
******************
C INCLUDE frcvhd.f
F     SUBROUTINE FRCVHD(HA,ST,AT,AREA,CL,G,B,CP,K,U,
F    +                  RHO, PRESS, R)
C
C    HA = FREE CONVECTION HEAT TRANSFER CONDUCTANCE
FROM
C          A HEATED PLATE FACING DOWN OR A COOLED
PLATE
C          FACING UP - BTU/HR-F
C    ST = SURFACE TEMP - F
C    AT = AMBIENT TEMP - F
C    AREA= SURFACE AREA - FT**2
C    CL = CHARACTERISTIC LENGTH - FT
C    G = GRAVITATIONAL CONSTANT - FT/SEC**2
C    B = COEFF. OF THERMAL EXPANSION ARRAY - 1/F
C    CP = SPECIFIC HEAT VS. TEMPERATURE ARRAY -
BTU/LB-F
C    K = THERMAL CONDUCTANCE VS. TEMPERATURE ARRAY
C    U = ABSOLUTE VISCOSITY VS. TEMPERATURE ARRAY -
LB/FT-HR
C    RHO = FLUID DENSITY ARRAY OR 0. FOR IDEAL GAS
C    PRESS = FLUID PRESSURE - LBS/IN**2
C    R = GAS CONSTANT
C
F     REAL HA, ST, AT, AREA, CL, G, RHO, PRESS, R, GR,
F    +  PR, BAVE, UAVE, TDIFF, KAVE, CPAVE, RHOX
C
C    COMPUTE MEAN FLUID TEMPERATURE
C
F     TAVE = .5*(ST + AT)
F     TDIFF = ABS(ST - AT)
F     IF(TDIFF .EQ. 0.) TDIFF = 1.0E-10
C
C    COMPUTE FLUID DENSITY FROM TABLE LOOKUP OR IDEAL
C    GAS EQUATIONS
C
F     IF(RHO .EQ. 0.) THEN
F       RHOX = PRESS*144./(R*(TAVE+459.67))
F     ELSE
F       CALL D1DEG1(TAVE, RHO, RHOX)
F     END IF
C
C    COMPUTE GRASHOF NUMBER
C
F     IF(B .EQ. 0.) THEN
F       BAVE = 1./(TAVE+459.67)
F     ELSE
F       CALL D1DEG1(TAVE, B, BAVE)
F     END IF
F     CALL D1DEG1(TAVE, U, UAVE)
F     GR = RHOX**2 * G*(3600.**2) *BAVE *TDIFF
*CL**3/UAVE**2
C
C    COMPUTE PRANDTL NUMBER
C
F     CALL D1DEG1(TAVE, K, KAVE)
F     CALL D1DEG1(TAVE, CP, CPAVE)
F     PR = CPAVE * UAVE/KAVE
C
```

```
C     COMPUTE CONVECTION HEAT TRANSFER COEFF. USING
C     EQUATIONS 7-21, 7-22, & 7-23; FROM PRINCIPLES OF
HEAT
C     TRANSFER, 3RD EDITION, FRANK KREITH
C
F      RA = PR * GR
F      IF(ST .GE. AT .AND. RA .LE. 1E+09) THEN
C
C     HOT SURFACE FACING DOWN  ; LAMINAR FLOW
C
F        HA = AREA * 0.27 * KAVE * (GR*PR)**.25/CL
F      ELSE IF(ST .GE. AT .AND. RA .GT. 1E+09) THEN
C
C     HOT SURFACE FACING DOWN  ; TURBULENT FLOW
C
F        HA = AREA * 0.07 * KAVE * (GR*PR)**.33/CL
F      ELSE IF(ST .LT. AT .AND. RA .LE. 1E+09) THEN
C
C     COLD SURFACE FACING DOWN  ; LAMINAR FLOW
C
F        HA = AREA * 0.54 * KAVE * (GR*PR)**.25/CL
F      ELSE IF(ST .LT. AT .AND. RA .GT. 1E+09) THEN
C
C     COLD SURFACE FACING DOWN  ; TURBULENT FLOW
C
F        HA = AREA * 0.14 * KAVE * (GR*PR)**.33/CL
F      END IF
F      RETURN
F      END
C INCLUDE frcvhu.f
F      SUBROUTINE FRCVHU(HA,ST,AT,AREA,CL,G,B,CP,K,U,
F     +                  RHO, PRESS, R)
C
C     HA = FREE CONVECTION HEAT TRANSFER CONDUCTANCE
FROM
C          A HEATED PLATE FACING UP OR A COOLED PLATE
C          FACING DOWN - BTU/HR-F
C     ST = SURFACE TEMP - F
C     AT = AMBIENT TEMP - F
C     AREA= SURFACE AREA - SQ.-FT.
C     CL = CHARACTERISTIC LENGTH - FEET
C     G = GRAVITATIONAL CONSTANT - FT/SEC**2
C     B = COEFF. OF THERMAL EXPANSION ARRAY - 1/F
C     CP = SPECIFIC HEAT VS. TEMPERATURE ARRAY -
BTU/LBM-F
C     K = THERMAL CONDUCTANCE VS.TEMPERATURE ARRAY -
BTUH/F-SF
C     U = ABSOLUTE VISCOSITY VS. TEMPERATURE ARRAY
C     RHO = FLUID DENSITY ARRAY OR 0. FOR IDEAL GAS
C     PRESS = FLUID PRESSURE - LBS/SQ.-INCH
C     R = GAS CONSTANT
C
F      REAL HA, ST, AT, AREA, CL, G, RHO, PRESS, R, GR,
F     +  PR, BAVE, UAVE, TDIFF, KAVE, CPAVE, RHOX
C
C     COMPUTE MEAN FLUID TEMPERATURE
C
F      TAVE = .5*(ST + AT)
F      TDIFF = ABS(ST - AT)
F      IF(TDIFF .EQ. 0.) TDIFF = 1.0E-10
C
C     COMPUTE FLUID DENSITY FROM TABLE LOOKUP OR IDEAL
C     GAS EQUATIONS
C
F      IF(RHO .EQ. 0.) THEN
F        RHOX = PRESS*144./(R*(TAVE+459.67))
F      ELSE
F        CALL D1DEG1(TAVE, RHO, RHOX)
F      END IF
C
C     COMPUTE GRASHOF NUMBER
C
F      IF(B .EQ. 0.) THEN
F        BAVE = 1./(TAVE+459.67)
F      ELSE
F        CALL D1DEG1(TAVE, B, BAVE)
F      END IF
F      CALL D1DEG1(TAVE, U, UAVE)
F      GR = RHOX**2 *G*(3600.**2)* BAVE *TDIFF
*CL**3/UAVE**2
C
C     COMPUTE PRANDTL NUMBER
C
F      CALL D1DEG1(TAVE, K, KAVE)
F      CALL D1DEG1(TAVE, CP, CPAVE)
F      PR = CPAVE * UAVE/KAVE
C
C     COMPUTE CONVECTION HEAT TRANSFER COEFF. USING
C     EQUATIONS 7-21, 7-22, & 7-23; FROM PRINCIPLES OF
HEAT
C     TRANSFER, 3RD EDITION, FRANK KREITH
C
F      RA = PR * GR
F      IF(ST .GE. AT .AND. RA .LE. 1E+09) THEN
C
C     HOT SURFACE FACING UPWARD; LAMINAR FLOW
C
F        HA = AREA * 0.54 * KAVE * (GR*PR)**.25/CL
F      ELSE IF(ST .GE. AT .AND. RA .GT. 1E+09) THEN
C
C     HOT SURFACE FACING UPWARD; TURBULENT FLOW
C
F        HA = AREA * 0.14 * KAVE * (GR*PR)**.33/CL
F      ELSE IF(ST .LT. AT .AND. RA .LE. 1E+09) THEN
C
C     COLD SURFACE FACING UPWARD; LAMINAR FLOW
C
F        HA = AREA * 0.27 * KAVE * (GR*PR)**.25/CL
F      ELSE IF(ST .LT. AT .AND. RA .GT. 1E+09) THEN
C
C     COLD SURFACE FACING UPWARD; TURBULENT FLOW
C
F        HA = AREA * 0.07 * KAVE * (GR*PR)**.33/CL
F      END IF
F      RETURN
F      END
C INCLUDE frcvv.f
F      SUBROUTINE FRCVV(HA,ST,AT,AREA,CL,G,B,CP,K,U,
F     +                 RHO, PRESS, R)
C
C     HA = FREE CONVECTION HEAT TRANSFER CONDUCTANCE
FROM
C          A VERTICAL FLAT PLATE - BTU/HR-F
C     ST = SURFACE TEMP - F
C     AT = AMBIENT TEMP - F
C     AREA= SURFACE AREA - FT**2
C     CL = CHARACTERISTIC LENGTH - FT
C     G = GRAVITATIONAL CONSTANT - FT/SEC**2
C     B = COEFF. OF THERMAL EXPANSION ARRAY - 1/F
C     CP = SPECIFIC HEAT VS. TEMPERATURE ARRAY -
BTU/LB-F
C     K = THERMAL CONDUCTANCE VS. TEMPERATURE ARRAY
-BTUH/FT-F
C     U = ABSOLUTE VISCOSITY VS. TEMPERATURE ARRAY -
LB/FT-HR
C     RHO = FLUID DENSITY ARRAY OR 0. FOR IDEAL GAS
C     PRESS = FLUID PRESSURE - LBF/SQ.-INCH
C     R = GAS CONSTANT
C
F      REAL HA, ST, AT, AREA, CL, G, RHO, PRESS, R, GR,
F     + PR, BAVE, UAVE, TDIFF, KAVE, CPAVE, RHOX, NU,
NUL, NUT
C
C     COMPUTE MEAN FLUID TEMPERATURE
C
F      TAVE = .5*(ST + AT)
F      TDIFF = ABS(ST - AT)
F      IF(TDIFF .EQ. 0.) TDIFF = 1.0E-10
C
C     COMPUTE FLUID DENSITY FROM TABLE LOOKUP OR IDEAL
C     GAS EQUATIONS
C
```

```
F      IF(RHO .EQ. 0.) THEN
F        RHOX = PRESS*144./(R*(TAVE+459.67))
F      ELSE
F        CALL D1DEG1(TAVE, RHO, RHOX)
F      END IF
C
C     COMPUTE GRASHOF NUMBER
C
F      IF(B .EQ. 0.) THEN
F        BAVE = 1./(TAVE+459.67)
F      ELSE
F        CALL D1DEG1(TAVE, B, BAVE)
F      END IF
F      CALL D1DEG1(TAVE, U, UAVE)
F      GR = RHOX**2
*G*(3600.**2)*BAVE*TDIFF*CL**3/UAVE**2
C
C     COMPUTE PRANDTL NUMBER
C
F      CALL D1DEG1(TAVE, K, KAVE)
F      CALL D1DEG1(TAVE, CP, CPAVE)
F      PR = CPAVE * UAVE/KAVE
C
C     COMPUTE CONVECTION HEAT TRANSFER COEFF. USING
C     EQUATIONS 6-39 TO 6-42; HANDBOOK OF HEAT TRANSFER
C     FUNDAMENTALS, 2ND EDITION, ROHSENOW, HARTNETT, &
GANIC
C
F      RA = PR * GR
C
F      CLAM = 1.33333*.503/(1. +
(0.492/PR)**0.5625)**0.44444444
F      CTURB = 0.13*PR**0.22/(1. + 0.61*PR**0.81)**0.42
C
F      NUT = CLAM * RA**0.25
F      NUL = 2.8/(LOG(1. + 2.8/NUT))
F      NUT = CTURB * RA**.3333333
F      NU = (NUL**6. + NUT**6.)**0.16666666667
C
F        HA = AREA * KAVE * NU/CL
C
F      RETURN
F      END
C INCLUDE frcvanu.f
F      SUBROUTINE FRCVANU(HA,ST1,ST2,AREA,H,DR,
CL,G,B,CP,K,U,
F     +                   RHO, PRESS, R)
C
C     HA = FREE CONVECTION HEAT TRANSFER CONDUCTANCE
WITHIN
C          A VERTICAL ENCLOSURE WITH ONE SIDE HEATED,
ONE
C          COOLED, AND THE TOP/BOTTOM ADIABATIC  -
BTU/HR-F
C     ST1= FIRST SURFACE TEMP - F
C     ST2= SECOND SURFACE TEMP - F
C     AREA= SURFACE AREA - SQ.-FT.
C     H  = CAVITY HEIGHT - FEET
C     DR = RAIO OF OUTER TO INNER DIAMETERS
C     CL = CHARACTERISTIC LENGHT (GAP) - FT
C     G = GRAVITATIONAL CONSTANT - FT/SEC**2
C     B = COEFF. OF THERMAL EXPANSION ARRAY - 1/F
C     CP = SPECIFIC HEAT VS. TEMPERATURE ARRAY -
BTU/LBM-F
C     K = THERMAL CONDUCTANCE VS.TEMPERATURE ARRAY -
BTUH/F-SF
C     U = ABSOLUTE VISCOSITY VS. TEMPERATURE ARRAY
C     RHO = FLUID DENSITY ARRAY OR 0. FOR IDEAL GAS
C     PRESS = FLUID PRESSURE - LBS/SQ.-INCH
C     R = GAS CONSTANT
C
F      REAL HA, ST1, ST2, AREA, H, CL, G, RHO, PRESS,
R, GR,
F     +  PR, BAVE, UAVE, TDIFF, KAVE, CPAVE, RHOX
C
F      REAL NU, NUCRIT, NUL, NUT
C
C     COMPUTE MEAN FLUID TEMPERATURE
C
F      TAVE = .5*(ST1 + ST2)
F      TDIFF = ABS(ST1 - ST2)
F      IF(TDIFF .EQ. 0.) TDIFF = 1.0E-10
C
C     COMPUTE FLUID DENSITY FROM TABLE LOOKUP OR IDEAL
C     GAS EQUATIONS
C
F      IF(RHO .EQ. 0.) THEN
F        RHOX = PRESS*144./(R*(TAVE+459.67))
F      ELSE
F        CALL D1DEG1(TAVE, RHO, RHOX)
F      END IF
C
F      IF(B .EQ. 0.) THEN
F        BAVE = 1./(TAVE+459.67)
F      ELSE
F        CALL D1DEG1(TAVE, B, BAVE)
F      END IF
F      CALL D1DEG1(TAVE, U, UAVE)
C
C     COMPUTE GRASHOF, PRANDTL, & RAYLEIGH NUMBERS
C
F      CALL D1DEG1(TAVE, K, KAVE)
F      CALL D1DEG1(TAVE, CP, CPAVE)
F      PR = CPAVE * UAVE/KAVE
C
F      GR = RHOX**2 *G*(3600.**2)* BAVE *TDIFF
*CL**3/UAVE**2
C
F      RA = PR * GR
C
F      RACRIT = 62.5*DR + 750
F      IF(RA .LE. 1.1*RACRIT) GO TO 99
C
C     COMPUTE CONVECTION HEAT TRANSFER COEFF. USING
C     EQUATIONS 22 FROM "NATURAL CONVECTION IN VERTICAL

C     ANNULI", JOURNAL OF HEAT TRANSFER, NOV. 1989,
PAGES 909
C     TO 915.  NOTE: THE EQN. AS PUBLISHED CONTAINS
ERRORS,
C     SEE THE EQN. FORMAT BELOW FOR CORRECT EXPONENTS.
C
F      ASPECT = H/CL
F      X1 = DR**(0.39087/DR + 0.40764)
C
F      NUL = 0.158*(RA**0.29)*X1/(ASPECT**0.0645)
C
C
F        HA = AREA * NUL* KAVE/CL
F      RETURN
F  99 CONTINUE
F        NUL = 1.
F        HA = AREA * NUL* KAVE/CL
F      RETURN
F      END
END OF DATA
```

*** RMIS View/Print Document Cover Sheet ***

This document was retrieved from the Documentation and Records Management (DRM) ISEARCH System. It is intended for Information only and may not be the most recent or updated version. Contact a Document Service Center (see Hanford Info for locations) if you need additional retrieval information.

Accession #: D196080893

Document #: SD-RTG-SARP-001

Title/Desc:
RTG TRANSPORTATION SYSTEM SARP DOCKET NO 94-6-9904 [VOL II] [SEC 4 OF 4]

Pages: 194

This document was too large to scan as a whole document, therefore it required breaking into smaller sections.

Document number: SD-RTG-SARP-001

Section 4 **of** 4

Title: RADIOISOTOPE THERMOELECTRIC GENERATOR TRANSPORTATION SYSTEM SAFETY ANALYSIS REPORT FOR PACKAGING

Date: 4/18/96 **Revision:** 0

Originator: FERRELL PC
Co: WHC

Recipient:
Co:

References: EDT-613639

4.0 CONTAINMENT

The Radioisotope Thermoelectric Generator (RTG) Transportation System Package possesses two levels of leaktight containment: the inner containment vessel (ICV), which acts as the secondary containment boundary, and the outer containment vessel (OCV), which acts as the primary containment boundary. Two levels of containment are required per 10 CFR 71.63[1] for packages transporting quantities of plutonium greater than 20 curies (Ci). Both the OCV and ICV containment boundaries are leaktight per the requirements of Paragraph 5.4 of ANSI standards N14.5[2].

Although the entire containment boundary is addressed herein, this section will concentrate on the butyl rubber elastomer O-ring seals used for maintaining closure between metallic components. The use of circular cross-section elastomer O-rings has been proven as a reliable method of sealing the containment system(s) of transportation packages subject to the requirements of 10 CFR 71. Of particular concern are the maximum temperatures and minimum compression experienced by the containment O-ring seals over the course of the normal conditions of transport (NCT) and hypothetical accident condition (HAC) test requirements. This section will demonstrate that temperature and compression limits are met under all NCT and HAC events for both containment vessels of the RTG Transportation System Package.

4.1 CONTAINMENT BOUNDARY

Each of the two packaging vessels is an independent containment boundary, which consists of a bell, a base, two elastomer O-ring seals (one of which is the containment seal), an electrical feed-through connector, and one (for the OCV) or two (for the ICV) vent port plugs with elastomer O-ring seals. Both vessels are sealed between their flange and base by a pair of face-type O-rings, of which the inner O-ring is the containment seal and the outer O-ring is used for leakage rate testing purposes.

4.1.1 Containment Vessel

As described in Section 2.1.1.1, the OCV consists of a stainless steel base, to which a stainless steel bell is attached by 24, 1-1/4-in. diameter, high-strength steel alloy closure bolts. The bell is made of a cylindrical shell, welded to an American Society of Mechanical Engineers (ASME) torispherical head and a bolting flange. The bell flange fits within a counterbore in the base, which limits radial motion in an accident such that the closure bolts cannot be loaded in direct shear. The seal between the bell flange and the base is effected by two concentrically arranged butyl rubber O-ring face seals. The inner containment seal has a nominal diameter of 0.393 in., and the outer test seal has a nominal diameter of 0.275 in. Figure 4.1.1-1 illustrates an exploded view of the OCV containment boundary components.

As described in Section 2.1.1.2, the ICV consists of a stainless steel base to which a stainless steel bell is attached by 24, 3/4-in. diameter, high-strength steel alloy closure bolts. The bell is made of a cylindrical shell welded to an ASME torispherical head and a bolting flange. The bell fits closely over the base, which limits radial motion in an accident such that the closure bolts cannot be loaded in direct shear. The seal between the bell flange and the base is effected by two concentrically arranged butyl rubber O-ring face seals. Both the inner containment seal and the outer test seal have a nominal diameter of 0.275 in. Figure 4.1.1-2 illustrates an exploded view of the ICV containment boundary components.

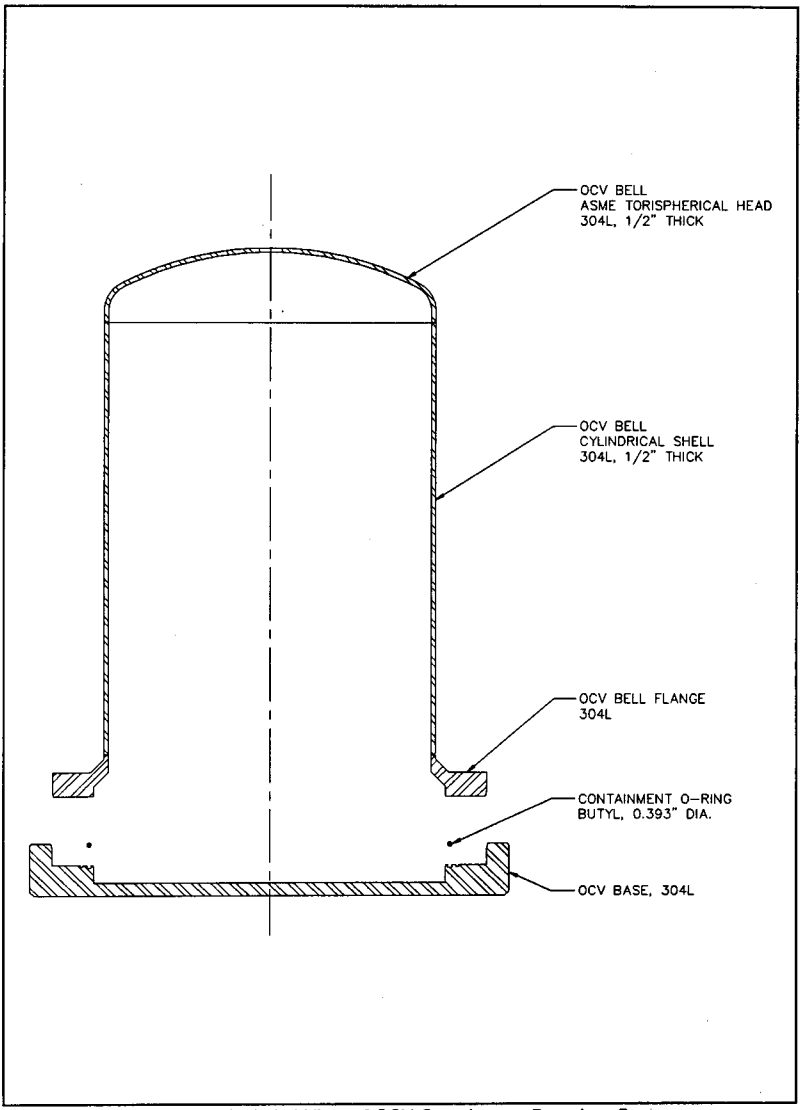


FIGURE 4.1.1-1. Exploded View of OCV Containment Boundary Components.

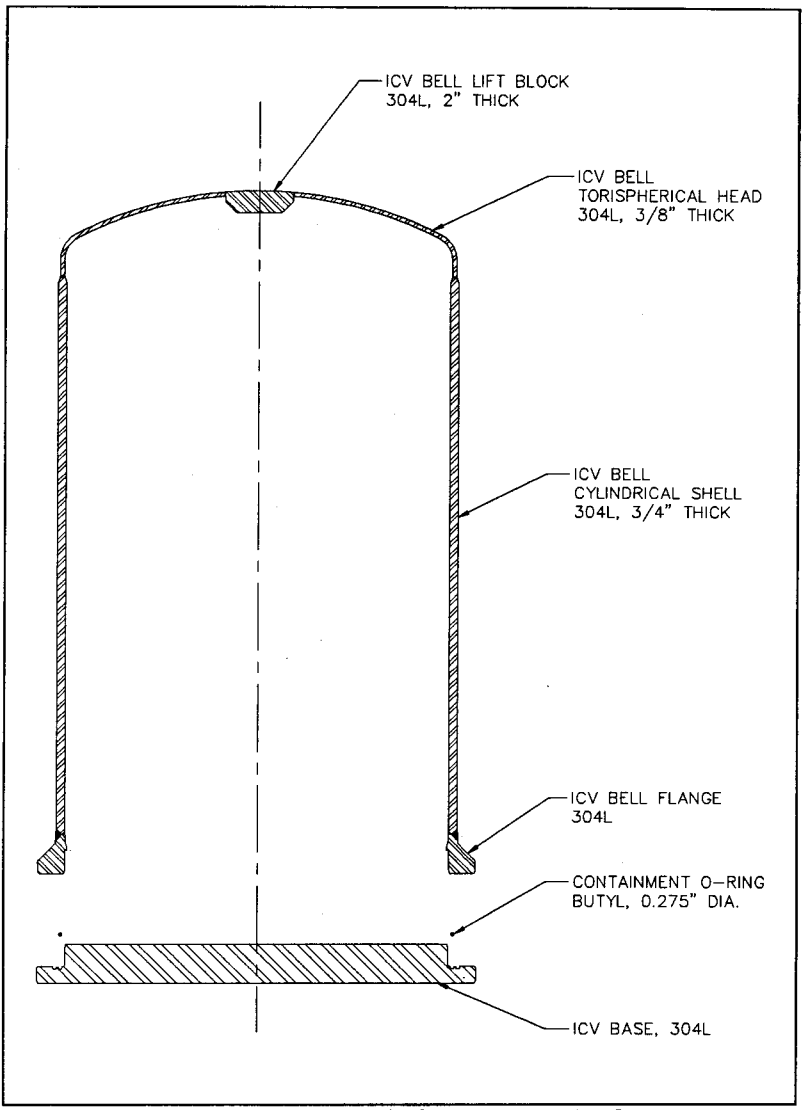


FIGURE 4.1.1-2. Exploded View of ICV Containment Boundary Components.

Two additional design features are used to help protect the integrity of the ICV containment boundary. The GPHS RTG payload requires a specific shipping rack assembly that has an integral barrier plate. The shipping rack assembly is securely fastened to the ICV base, and is designed to remain in place during a HAC drop to prevent heat generating payload debris from reaching the proximity of the ICV O-ring seal area. To further protect the ICV O-ring seals from smaller, nonheat generating debris, a stainless steel debris shield is located at the internal junction of the ICV bell and base.

Demonstration of containment vessel integrity under NCT and HAC free drops and HAC puncture drops has been primarily demonstrated by an extensive certification test program (see Appendices 2.10.9 and 2.10.10, and Section 2.7.6 for details).

4.1.2 Containment Penetrations

The containment vessels include two types of penetrations: (1) those that are periodically made and broken through the life of the package, and (2) those that are permanently installed during initial fabrication. The only OCV containment make-and-break type of boundary penetration is one vent port, through which air is evacuated from the annulus between the ICV and OCV, and through which helium is backfilled. One seal test port is also provided, but does not penetrate the OCV containment boundary because the port only accesses a region outboard of the containment O-ring. Vent and test port plugs are made of brass and sealed using butyl Parker Stat-O-Seals®. Each plug is protected by a brass cap sealed with a Teflon® weather gasket. An exploded view of the OCV vent port and cover design is shown in Figure 4.1.2-1.

A primary and secondary vent port, which are used during the helium purge process, are the only ICV make-and-break type of containment penetrations. One seal test port is also provided, but does not penetrate the ICV containment boundary because the port accesses a region outboard of the containment O-ring. Vent and test port plugs are made of brass and sealed using butyl Parker Stat-O-Seals®. An exploded view of the ICV vent port and cover design is shown in Figure 4.1.2-2.

One permanently installed electrical feed-through connector is installed in each containment boundary base plate. The electrical feed-through connector consists of an AISI Type 316L stainless steel body and sleeve, electrical conductor pins, and a glass sealing material between the body and the pins. Each electrical feed-through connector assembly fits closely within its surrounding base plate, and is sealed to the base plate material with a 3/16-in. fillet weld. Inside the ICV containment and outside the OCV containment, removable connectors are used to connect the electrical feed-through devices to the RTG-mounted thermocouples and to the recording devices, respectively. Permanent wire connections are used in conjunction with a spring-loaded pin contact assembly to complete the electrical feed-through circuit between the two vessels. See Figure 4.1.2-3 for a schematic of the electrical feed-through components. Details of the electrical feed-through components are shown in the drawings in Section 1.3.2. The containment boundary portions of the ICV and OCV electrical feed-through penetrations are shown in Figures 4.1.2-4 and 4.1.2-5, respectively.

The electrical feed-through assemblies are manufactured by D. G. O'Brien, part No. 1070019-112 (receptacle, containing the sealed pins). The connector used inside the ICV and outside the OCV is part No. 1071003-119 (straight plug). This design was tested by Teledyne Energy Systems to determine the peak temperature at which a leaktight seal can be ensured. Two reports, HPG5-DST-236 and HPG3-DST-1000 (see Appendix 4.5.2,) conclude that an electrical feed-through device of this design can withstand temperatures of at least 475 °F before degradation of the seal can be expected. As shown in Section 2.10.7, the peak temperature of

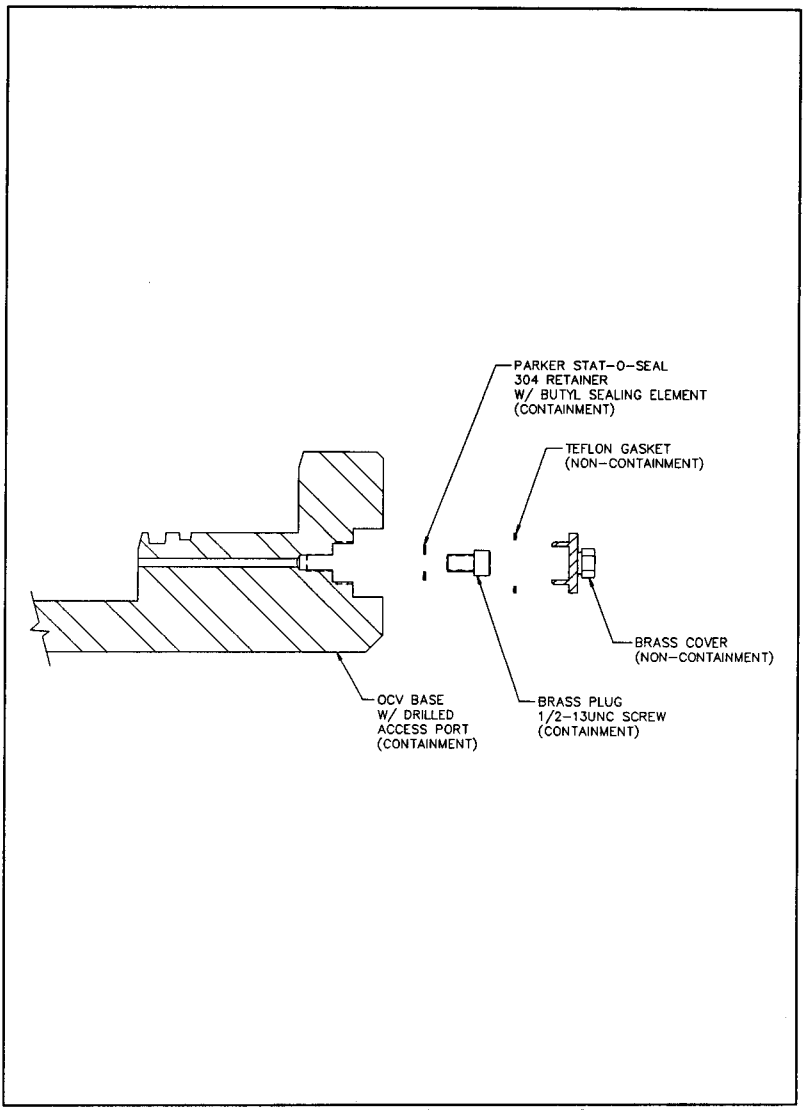


FIGURE 4.1.2-1. Exploded View of OCV Vent Port and Cover Design.

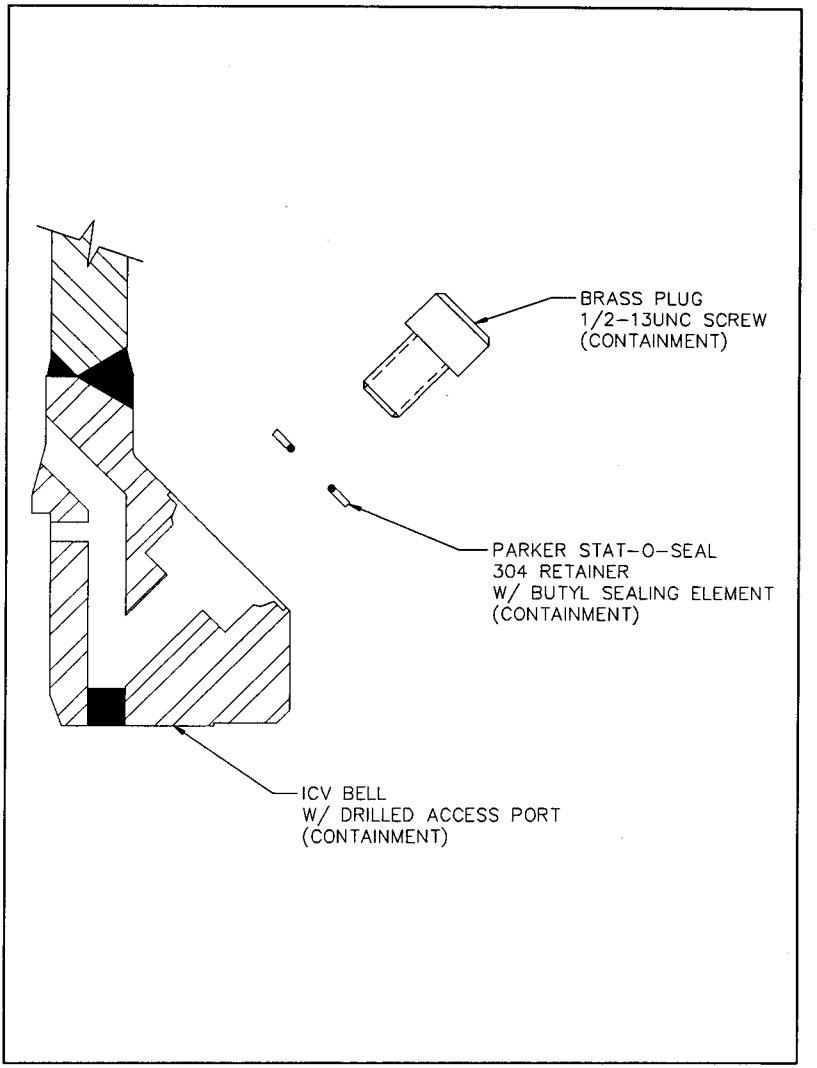


FIGURE 4.1.2-2. Exploded View of ICV Vent Port Design. (Primary and secondary vent ports are identical except for noncontainment primary vent port inner tube.)

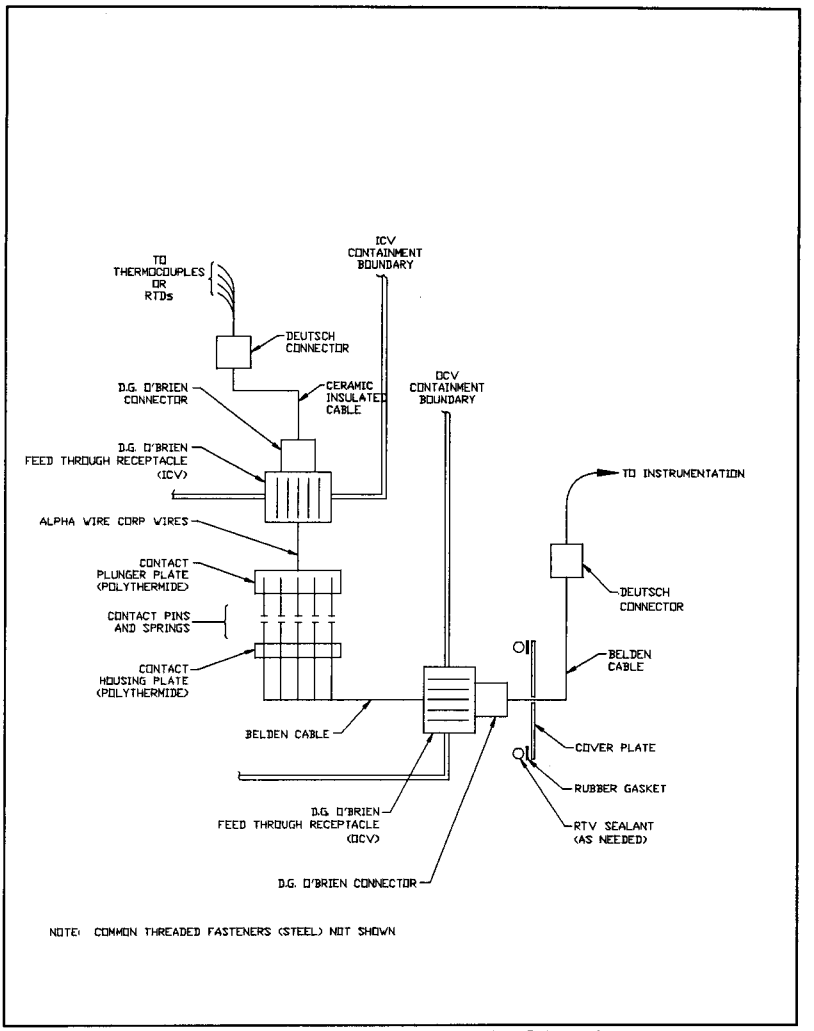


FIGURE 4.1.2-3. Feed-through Materials Schematic.

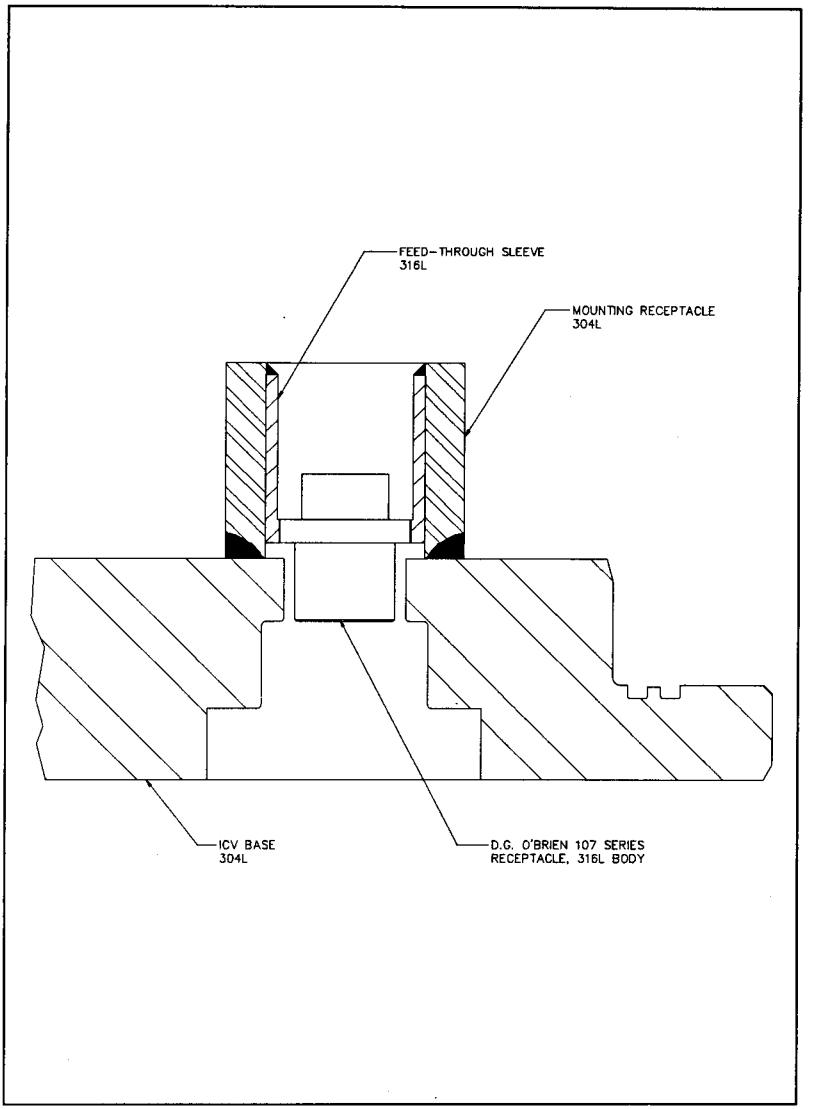


FIGURE 4.1.2-4. ICV Feed-through Containment Boundary Components and Welds.

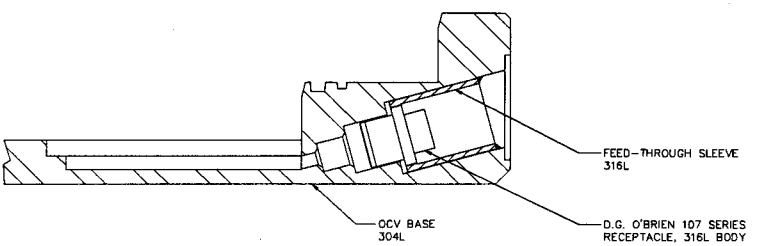


FIGURE 4.1.2-5. OCV Feed-through Containment Boundary Components and Welds.

thermal model node 269 (the ICV electrical feed-through) or node 368 (the OCV electrical feed-through) in the worst-case HAC event is 377 °F (for HAC load case No. 5). Thus, worst-case HAC electrical feed-through temperatures are well below those for which a leaktight seal has been demonstrated. The electrical feed-through connectors were also subjected to the full series of regulatory drop tests without loss of leaktight condition (see Section 2.7.6.).

4.1.3 Seals and Welds

4.1.3.1 Seals. The containment O-ring seals must possess the ability to maintain a leaktight seal (a leakage rate of less than 1×10^{-7} scc/sec air) when subjected to the compressions and temperatures associated with NCT and HAC events as defined by 10 CFR 71. Extreme conditions are addressed in the following sections. Emphasis is placed on the primary containment seals, because the vent and fill port seals do not experience any worst-case temperature or any loss of compression for the following reasons:

- The ICV vent port plugs, because of proximity to the main ICV seals, have virtually the same temperature as the main seals
- The OCV vent port is located on the side of the base, in a position that is somewhat cooler than the primary OCV seals
- The OCV and ICV vent ports are well protected within the impact limiter from free drop or puncture bar impacts. Consequently, once sealed, no change of seal compression is experienced by the vent and fill port seals.

The compound chosen for the primary containment O-ring seals is butyl, Rainier Rubber compound No. RR-0405-70. Butyl rubber has excellent impermeability under helium pressure, thus enhancing leakage rate test operations. Further, this particular compound has also been approved by the Nuclear Regulatory Commission (NRC) for the TRUPACT-II Package.

Section 2.10.6 contains a report of leakage rate testing of seals fabricated from this compound. The material was made into O-rings and leakage rate tested in a fixture at various low temperatures and after high temperature soaks. The test fixture simulated a face-type seal, and the O-ring compression values were controlled by shims and O-ring groove depth. The test commenced with a leakage rate test at a seal temperature of -40 °F followed by a soak for a specified time at high temperature and another leakage rate test. Subsequent to the high temperature soak, the fixture was returned to -20 °F and leakage rate tested again. Pertinent results are summarized in the following sections.

4.1.3.1.1 Cold Tests. Butyl rubber remained leaktight at -40 °F (before the high-temperature soak) and at -20 °F (subsequent to high temperature soak). The minimum compression in the test fixture was at least as low as 10%, as calculated in Section 2.10.6.

4.1.3.1.2 Elevated Temperature Tests. Elevated temperature tests were performed on the butyl rubber O-rings with compressions as low as 10%. The time/temperature test parameters were 380 °F for 24 hours followed by 350 °F for 144 hours for a total of 168 hours (1 week). At these high temperatures, rapid helium permeability of the O-rings occurs and helium leakage rate detection is not feasible. Therefore, after each of the high-temperature soak periods, a hard vacuum, less than 0.2 mbar, was pulled on the test O-rings. This indicated there were no leaks. At the end of the test sequence, the O-rings were stabilized at -20 °F and helium leakage rate tested. The O-rings were leaktight and showed no permanent degradation.

The data collected in the testing covers NCT cold and HAC fire temperatures. Normal regulatory warm conditions, however, are assumed to be experienced for up to 60 days. The test data can be conservatively extrapolated to 60 days as follows.

The high temperature capability of elastomer materials is commonly plotted on semilog scales, with temperature plotted on a linear ordinate and time on a logarithmic abscissa (see Figure A3-6 from the Parker O-ring Handbook[3]). Because of the direction of curvature of the elastomer time/temperature limit curves, the linear extrapolation from one time to a greater time is conservative, because it would result in a lower temperature limit than the one actually indicated by the curve itself. Therefore, linear extrapolation of time/temperature data to longer times is conservative, using a logarithmic scale for time. Linearly extrapolating the segment between the 380 °F/24-hour point and the 350 °F/144-hour point leads to

$$\frac{(380° - 350°)}{(ln144\ hr - ln24\ hr)} = \frac{x}{(ln1{,}440\ hr - ln144\ hr)}$$

where x is the reduction in temperature limit below 350 °F because of the extension of soak time from 144 hours to 1,440 hours (60 days). Solving the above equation yields x = 39 °F. The conservative limit at 60 days is therefore 350 °F - 39 °F = 311 °F. The full range of acceptable temperature/time results for the butyl material is shown in Table 4.1.3.1.2-1.

TABLE 4.1.3.1.2-1. Performance Capability of Rainier Rubber RR-0405-70 Butyl Rubber (compressed at 10%).

Seal temperature (°F)	Time at temperature	Leaktight	Related conditions
-40	Steady state	Yes	NCT cold
311	Steady state (60 days)	Yes	NCT warm
350	Steady state (144 hours)	Yes*	HAC post fire
380	24 hours	Yes*	HAC peak fire

*The O-rings were subjected to a hard vacuum (less than 0.2 mbar). This was used to infer they were leaktight.

4.1.3.1.3 Impermeability and Helium Retention. Heat rejection by the payload depends, in part, upon the convection currents within the ICV. For this purpose, a nominal charge of 19 psia of helium gas is used during shipment of the payloads. Butyl rubber has excellent helium gas retention capability, as is demonstrated in the following calculations.

The *Parker O-Ring Handbook*[3], page A2-4, gives this relation for permeation through an O-ring seal:

$$L = (0.7)\ FDPQ\ (1 - S)^2 \qquad [1]$$

where: L = approximate permeation rate, scc/sec
F = permeability rate, scc-cm/cm^2-sec-bar
D = O-ring inside diameter, in.
P = differential pressure across seal, psid
Q = permeability factor (Parker Table A2-2)
S = percent compression, expressed in decimal form

From Figure A2-2 of Reference 3, conservatively assume *Q* is equal to 1.52 for a dry O-ring. Then, using Table A2-4, *F* at temperature is as shown in Table 4.1.3.1.3-1.

Table 4.1.3.1.3-1. Permeability Rate Versus Temperature for Butyl Elastomer.

Temperature (°F)	*F* cc-cm/cm^2-sec-bar
176	$52(10)^{-8}$
302	$240(10)^{-8}$

Linearly interpolating for the maximum NCT seal temperature of approximately 220 °F, a value for *F* of $117.65(10)^{-8}$ results. Assuming a conservatively large diameter for the seals of 40 in., and a conservatively low value of minimum squeeze, *S*, of 0.15 (15%), the permeation rate as a function of internal pressure will then be the following:

$$L = 3.618(10)^{-5} (P) \text{ scc/sec} \quad [2]$$

The loss of pressure over time within the ICV will be what is known as a first order fall, that is, exponential. It can be determined by considering the perfect gas law given below:

$$PV = nRT \quad [3]$$

where: *P* = pressure, psia
V = void volume of ICV, 22.25 ft^3 (see Section 2.6.1.1.1)
n = the number of lb-moles
R = the gas constant, 10.74 psia-ft^3/lb-mole-°R (Handbook of Chemistry and Physics[4])
T = temperature, 460 + 220 = 680 °R

Differentiating this equation with respect to time, yields the following:

$$\frac{dP}{dt} = \left[\frac{RT}{V}\right]\frac{dn}{dt} \quad [4]$$

Because there are $3.53(10)^{-5}$ standard cubic feet in a standard cubic centimeter and 392 ft^3 in one lb-mole of any gas*, the permeation rate, L, is converted into lb-moles per second, which is identical to the quantity dn/dt above:

$$\frac{dn}{dt} = -3.26(10)^{-12} (P) \; lb\text{-}moles/\text{sec}$$

where the minus sign signifies a decreasing quantity of moles in the ICV. Substituting this into Equation 4, along with values for R, T, and V, and rearranging, yields the following:

$$\frac{dP}{P} = -1.07(10)^{-9} \, dt$$

This differential equation is solved to yield the following:

$$\ln P = -1.07(10)^{-9} (t) + C \qquad [5]$$

The constant of integration is evaluated by noting that, from Section 2.6.1.1, the ICV internal pressure differential is 10 psid. Taking $t = 0$, the constant C is determined to be 2.303. Substituting this value and performing the exponential on Equation 5, the pressure differential with respect to time is given below:

$$P = \exp\left[-107(10)^{-9} (t) + 2.303\right] psid \qquad [6]$$

Using Equation 6 with 86,400 seconds/day, the remaining differential pressure after 60 days (maximum assumed transport duration) is 9.949 psia, where 60 x 86,400 has been used for t. This is a drop of 10.0 - 9.949 = 0.051 psid, or the following:

$$\left[\frac{0.051}{10.0}\right] x \; 100 = 0.51\%$$

In one year (i.e., $3.1536(10)^7$ seconds), the pressure differential will fall to 9.672 psig, a decrease of 0.328 psi, or 3.28%.

*Obtainable from the perfect gas law for ambient pressure and 77 °F, which is the standard leak test temperature used in ANSI N14.5.

4.1.3.1.4 Temperature Conditions. 10 CFR 71 requires the package containment seals to successfully operate under the following conditions:

1. Ambient temperature of -40 °F, no insolation, internal heat load, or dynamic conditions

2. Ambient temperature of -20 °F, no insolation or internal heat load, with HAC free drop and puncture events

3. Ambient temperature of 100 °F, maximum insolation and internal heat load with and without active cooling

4. Ambient temperature of 100 °F, maximum insolation and internal heat load, with HAC free drop and puncture events

5. Ambient temperature of 1475 °F for 30 minutes, maximum internal heat load, subsequent to HAC free drop and puncture events.

To determine the temperature conditions and exposure times experienced by the O-ring seals, detailed thermal analyses were made for each of the above conditions. Two aspects of package configuration were taken into account to determine these relationships.

1. The redundant active cooling systems are assumed to be inoperative when maximum temperatures are calculated per 10 CFR 71.51(b).

2. For HAC, the possibility of payload structural failure and reconfiguration has been considered. Analysis of the GPHS RTG by its manufacturer (General Electric) established that the smallest heat-producing elements that could be released from the GPHS RTG would be the 18 heat source modules, which are brick-like rectangular aeroshells designed to survive atmospheric re-entry conditions. A worst-case configuration of the aeroshells was considered in the HAC thermal analyses.

The temperatures and times corresponding to the above five conditions are listed in Table 4.1.3.1.4-1. Maximums for either OCV or ICV containment seals are presented. Comparison with Table 4.1.3.1.2-1 indicates that seals will remain leaktight for all conditions.

TABLE 4.1.3.1.4-1. Package O-ring Seal Environments.

Seal temperature (°F)	Time at temperature	Condition (as defined in 4.1.3.1.4 above)	Case No. (from Secs. 2.6.1 and 2.7.3)
-40[a]	Steady state	(1) NCT cold	--
-20[a]	Steady state	(2) Initial cold condition for HAC free drop and puncture	--
83	Steady state	(3a) Normal operating steady state (with cooling)	NCT case 3
219	60 days (1,440 hours)	(3b) NCT regulatory steady state (without cooling)	NCT case 1
323[b]	1 week (168 hours)	(4) Post-HAC steady state with reconfigured payload	HAC case 5
360[c]	Instantaneous peak	(5) Reconfigured payload plus HAC fire	HAC case 5

[a]Because the minimum payloads heat load is assumed to be zero, the minimum temperatures are taken as identical to prescribed ambient.

[b]A post-HAC recovery time of 168 hours (1 week) is used, consistent with 10 CFR 71.51(a)(2).

[c]This is the maximum temperature that could result from a reconfigured payload plus 10 CFR 71 HAC fire conditions. The temperature duration above 350 °F is about 15 hours.

4.1.3.2 Welds. All containment welds, except the ICV vent port plug welds and those associated with the electrical feed-through connector, are full penetration, radiograph inspected, and in full accordance with NUREG/CR-3019[5]. The electrical feed-through weld (GTAW) and vent port plug welds are classified as nonstructural, seal-type welds. Per Subsection NB-5271, Section III of the ASME Boiler and Pressure Code, liquid penetrant inspection of this type of weld is sufficient to qualify the weld integrity. Containment weld integrity under NCT and HAC free drops and HAC puncture drops has been demonstrated by the certification test program (see Section 2.7.6.)

4.1.4 Closure

The OCV closure is effected by 24, 1-1/4-in. diameter bolts, torqued to 300 ±30 ft-lb. The ICV closure is via 24, 3/4-in. diameter bolts, torqued to 250 ±25 ft-lb. The OCV closure bolt material is ASTM-A320, Grade L43 and the ICV closure bolt material is ASTM-A540, Grade B23. All closure bolts are cadmium plated.

4.2 REQUIREMENTS FOR NORMAL CONDITIONS OF TRANSPORT

4.2.1 Containment of Radioactive Material

The release rate limits of 10 CFR 71.51 are satisfied by the leaktight sealing criterion (a leakage rate of less than 1×10^{-7} scc/sec air) imposed on the RTG Transportation System Package. All elastomeric sealing components are sized and dimensioned so that minimum seal compression during the NCT test sequence is never less than that demonstrated to be adequate for leaktight

sealing (see Section 4.1.3.1). Additionally, the maximum O-ring seal temperature for NCT is maintained below the allowable limit. This limit, as listed in Table 4.1.3.1.2-1, is 311 °F for 60 days. The maximum calculated seal temperature for NCT, from Table 4.1.3.1.4-1 is 219 °F. The structural and leaktight integrity of the remaining containment boundary is demonstrated by reference to Section 2.6.1.3 and the successful leakage rate testing of both ICV and OCV vessels at the end of the structural certification testing. Consequently, containment is maintained for the RTG Transportation System Package under NCT.

4.2.2 Pressurization of Containment Vessel

The maximum normal operational pressure (MNOP) for the ICV is 30 psia. This includes the nominal operational installed pressure of 19 psia, as well as a conservative allowance for thermal increase and gas pressure buildup, as detailed in Section 2.6.1.1.1. The analyses in Section 2.6.1 demonstrate that this pressure has negligible consequences on the ICV operation.

The MNOP for the OCV is also 30 psia. This value results from conservative upward adjustment of the nominal operational installed pressure of 19 psia to account for thermal increase. Again, as shown in Section 2.6.1, the consequences of this internal pressure have been shown to be insignificant.

4.2.3 Containment Criterion

Package containment for NCT is ensured by initially accepting packaging hardware that has been demonstrated to be leaktight, by maintaining O-rings and electrical feed-through connectors below their respective time-temperature limits, and by the maintenance of the minimum O-ring compression. A combination of certification testing and analysis helps establish minimum residual O-ring compression and maximum O-ring temperature for NCT. Electrical feed-through connector temperature limits are established by test as detailed in Appendix 4.5.2. All main containment seals and vent port plug seals are leakage rate tested at the time of package assembly.

Maximum O-ring seal temperatures for NCT are maintained below the temperature limit established for the 60-day maximum shipping period. The NCT seal area distortion does not control the minimum residual compression requirement. This is because temperatures and temperature gradients, as well as impact-induced seal area deformations, are worse for the HAC events, as detailed below. Similarly, maximum electrical feed-through temperatures are controlled by HAC.

4.3 CONTAINMENT REQUIREMENTS FOR HYPOTHETICAL ACCIDENT CONDITIONS

4.3.1 Fission Gas Products

As detailed in Section 2.6.1.1.1, the gas product developed by the GPHS RTG payload is a maximum of $2.06(10)^{-4}$ scc/sec of helium. The resulting pressure increase is insignificant, and is accounted for (in Section 2.6.1.1.1) by conservatively increasing the calculated ICV normal operating pressure.

4.3.2 Containment of Radioactive Materials

The release rate limits of 10 CFR 71.51 are satisfied by the leaktight sealing criterion imposed on the RTG Transportation System Package. Leak tightness is determined by the containment criteria set out below. These criteria depend in part on maintenance of a minimum residual containment O-ring seal compression during and after the HAC test sequence, including the fire event. An important aspect of the containment capability of the containment vessels is the maximum amount of relative differential thermal expansion between seal flange and base plate exhibited during and following the HAC fire event. Additionally, maximum allowable O-ring seal temperatures and times at temperature are imposed per Section 4.1.3.1.2, and all O-ring seal temperatures must be maintained below the allowable limits. Maximum electrical feed-through connector temperature is imposed per Section 4.1.2.

Thermal distortion values were determined from the ANSYS finite element models presented in Appendices 2.10.12 and 2.10.8. The ICV deflections were determined with a three-dimensional (3-D) finite element model. An axisymmetric model was used to evaluate OCV thermal expansions, because it exhibits much more uniform circumferential temperature distributions. This is because the OCV does not have concentrated heat sources (aeroshells) applied directly to its interior, and the HAC fire is applied uniformly to the OCV exterior. Temperatures used for both ICV and OCV models were derived from the 3-D SINDA thermal analysis code (see Section 3.4.1). The temperatures used for the axisymmetric OCV model are conservatively assumed to be those of the warmest segment of the 3-D thermal model. Appendix 2.10.13 demonstrates the conservatism of this approach.

The HAC load cases evaluated are detailed in Section 2.7.3.1.1.3. All HAC load cases combine maximum HAC free drop and puncture damage with the HAC fire. The thermal load cases evaluated comply with the load combination requirements of 10 CFR 71 and Regulatory Guide 7.8 by imposing minimum and maximum ambient temperature conditions (-20 and 100 °F, respectively) with package temperatures arising from minimum and maximum payload heat generation. The maximum heat is generated by the GPHS RTG payload. Minimum payload heat generation and minimum ambient temperature result in essentially uniform package component temperatures. The structural and containment effects of this load case are insignificant and are not included in the summary table. In addition to the regulatory load combinations, the nonregulatory combination of minimum ambient temperature and maximum payload heat generation is conservatively imposed. This latter load case is evaluated because of its greater potential for inducing maximum differential thermal expansions in the package components.

Relative differential thermal expansion results at the containment seal location for both vessels are summarized in Tables 4.3.2-1 and 4.3.2-2. The HAC load cases are defined in Section 2.7.3.1.1.3. The effect of thermal distortion of the vessel flanges is a rotation of the flange, which causes a slight separation of the flange and base in the area of the O-rings. The amount of rotation at the location of the containment O-ring seal can be converted directly into compression reduction, as shown below. To the thermal separation must also be added the separation resulting from distortions related to the free drop and puncture events. The measurements of the seal area taken after the full series of NCT free drops and HAC free drops and puncture events are given in Section 2.10.14. The conservative assumption is made that the maximum seal area separation from drop events is circumferentially coincident with the maximum thermal distortion separation.

For the OCV containment seal, the minimum O-ring diameter is 0.386 in. The maximum seal area groove depth is 0.285 in. From Table 4.3.2-1, the maximum thermally-induced separation for HAC load case 6 is 0.0263 in., and from Table 2.10.14-2, the HAC free drop event-induced separation is 0.005 in., for a total compression reduction of 0.0313 in. Minimum O-ring percent compression is given below.

$$\left[\frac{0.386 - 0.285 - 0.0313}{0.386}\right] x\ 100 = 18.1\% \quad [9]$$

For the ICV containment seal, the minimum O-ring diameter is 0.270 in. The maximum seal area groove depth is 0.203 in. From Table 4.3.2-2, the maximum thermally-induced separation for HAC load case 6 is 0.0099 in., and from Table 2.10.14-1, the HAC free drop event-induced separation is 0.001 in., for a total compression reduction of 0.0109 in. Minimum O-ring percent compression is given below:

$$\left[\frac{0.270 - 0.203 - 0.0109}{0.270}\right] x\ 100 = 20.8\%$$

Of the two containment vessels, the OCV possesses the least containment O-ring seal compression in the worst case HAC fire, having a value of 18.1%. This value results from the worst case tolerances on the O-ring and the O-ring mounting groove, as well as (1) measured distortions caused by the free drop and puncture events and (2) calculated thermal distortions resulting from worst case HAC fire and payload reconfiguration assumptions. In Appendix 2.10.6, Table 3 shows that the butyl material used for the RTG packaging containment seals was capable of maintaining a leaktight seal under conditions of 10% compression, while subjected to temperature conditions that were more severe than those predicted for the containment seals both during and after the HAC fire. Therefore, containment will be maintained in the HAC fire event.

TABLE 4.3.2-1. Maximum Seal Area Distortion and Residual Compression for the OCV.

HAC load case No.	Case 1	Case 2	Case 3	Case 4	Case 5	Case 6
Maximum thermal axial separation (in.)	0.0213	0.0255	0.0218	0.0260	0.0222	0.0263
Maximum permanent axial separation (in.)	0.006	0.006	0.006	0.006	0.006	0.006
Sum (in.)	0.0273	0.0315	0.0278	0.0320	0.0282	0.0323
Minimum residual O-ring compression (%)	19.1	18.0	19.0	17.9	18.9	17.8

TABLE 4.3.2-2. Maximum Seal Area Distortion and Residual Compression for the ICV.

HAC load case no.	Case 1	Case 2	Case 3	Case 4	Case 5	Case 6
Maximum thermal axial separation (in.)	0.0088	0.0091	0.0091	0.0094	0.0096	0.0099
Maximum permanent axial separation (in.)	0.001	0.001	0.001	0.001	0.001	0.001
Sum (in.)	0.0098	0.0101	0.0101	0.0104	0.0106	0.0109
Minimum residual O-ring compression (%)	21.2	21.1	21.1	21.0	20.9	20.8

According to reference 23, the preload force may vary by up to ±30% for a given applied torque value. The low end of this range (i.e., 70% of nominal preload force) could allow a greater thermal axial separation to occur. Therefore, the cases for each vessel having the largest thermal axial separation were rerun using a pre-stretch in the elements representing the bolts of 70% of the nominal preload force. For both vessels, the worst case is HAC load case 6. The results are given in Table 4.3.2-3. Minimum residual O-ring compression is calculated using the equations previously presented for each vessel. As shown, the minimum compression (again for the OCV) is well above the limit established by testing and discussed in Section 2.10.6.

TABLE 4.3.2-3. Maximum Seal Area Distortion for Low-limit Bolt Preload (70% of Nominal).

Vessel and HAC load case no.	ICV (Case 4)	OCV (Case 6)
Maximum thermal axial separation (in.)	0.0100	0.0303
Maximum permanent axial separation (in.)	0.001	0.005
Sum (in.)	0.0110	0.353
Minimum residual O-ring compression (%)	20.7	17.0

A summary of containment O-ring seal and electrical feed-through connector maximum HAC temperatures is summarized in Table 4.3.2-4. Time at temperature can be evaluated from Figures 3.5.3-1 to 3.5.3-6. As discussed in Sections 3.4.2 and 3.5.3, the OCV electrical feed-through connector temperatures are in each case lower than the ICV electrical feed-through temperatures, and are therefore not listed.

TABLE 4.3.2-4. Summary of Maximum O-ring Seal and Electrical Feed-through HAC Temperatures.

HAC load case No.	Case 1	Case 2	Case 3	Case 4	Case 5	Case 6
OCV peak seal temperature (°F)	317	218	320	222	325	229
ICV peak seal temperature (°F)	322	227	325	233	360	269
ICV peak feed-through (°F)	332	240	314	220	377	288

4.3.3 Containment Criterion

Package containment for HAC is ensured by maintaining O-rings and electrical feed-through connectors below their respective time-temperature limits, and by the maintenance of the minimum required O-ring compression. A combination of (1) certification testing and (2) analysis determines

minimum resultant O-ring compression and maximum O-ring temperature for HAC events. O-ring and electrical feed-through connector temperature limits are established by test as detailed in Section 2.10.6 and Appendix 4.5.2, respectively.

1. Certification testing has determined what seal area deformations may arise from the HAC free drop and puncture events, as well as to determine worst-case deformations of the thermally-insulating impact limiter. Seal area measurements are detailed in Section 2.10.14.

2. Worst-case temperatures are established by analysis, and are evaluated against the limits for temperature sensitive components such as containment O-ring seals and electrical feed-through connectors. Analytically derived temperatures are then used with structural analysis to establish maximum sealing surface deformations. Worst-case payload heat redistribution is assumed, and worst-case impact limiter deformations (extrapolated to maximum temperatures using certification test unit deformations) are used. Additionally, closure bolt stresses are limited to the yield strength of the bolting material to ensure that there will be no additional reduction in containment seal compression.

For a detailed summary of HAC thermal load cases used in evaluating seal area differential thermal expansions, see Sections 2.7.3.1.1.1 and 2.7.3.1.1.2. The load cases evaluated for the HAC fire event are given below.

1. Package in upright position, GPHS RTG aeroshells situated symmetrically around the perimeter of the payload shipping rack barrier plate in positions nearest the ICV containment seal.

2. Package lying on its side, GPHS RTG aeroshells situated linearly along the length of the ICV, from the payload shipping rack barrier plate to the ICV torispherical head.

3. Package conservatively balanced in an unstable position at a 45° angle, GPHS RTG aeroshells piled up in one corner (at the intersection of the shipping rack barrier plate and the ICV wall) in random orientations.

Summaries of relative differential thermal expansion values (relative expansion between seal flanges and base sealing surfaces) for all HAC load cases are presented in Tables 4.3.2-1 and 4.3.2-2. The worst-case impact limiter deformation was used for all HAC load cases, as discussed in Section 2.7.3.1.1.3.

Leak tightness for both vessels comprising the RTG Transportation System Package following the full-scale structural certification testing has been demonstrated (see Section 2.7.2.3). It has also been shown that the containment seals meet the temperature and residual compression requirements under the combined effects of the following:

- Maximum combinations of seal area deformations arising from the NCT and HAC free drops and HAC puncture tests

- Maximum seal area relative thermal differential expansion arising from worst-case assumptions regarding post-HAC impact package and payload reconfiguration.

Summaries of minimum residual O-ring seal compressions for the various HAC load cases are given in Tables 4.3.2-1 and 4.3.2-2. Maximum HAC O-ring seal temperatures are summarized in Table 4.3.2-4. The butyl O-ring material capabilities are given in Appendix 2.10.6. No loss of containment or leaktight capability is suffered by the package in any NCT or HAC event.

4.4 SPECIAL REQUIREMENTS

The special requirements of 10 CFR 71.63 apply to the RTG Transportation System Package. As detailed above, the secondary containment of the package consists of an ICV. This vessel and the primary containment, the OCV, both feature leaktight sealing capability, ensuring compliance with the regulatory release rate limits.

4.5 APPENDIX

The following is a list of appendices contained within this section:

4.5.1 References

4.5.2 Teledyne Test Reports

4.5.1 References

1. 10 CFR 71, 1993, "Packaging and Transportation of Radioactive Materials," *Code of Federal Regulations*, as amended.

2. ANSI 1987, *American National Standard for Radioactive Materials--Leakage Tests on Packages for Shipment*, ANSI Standard N14.5, American National Standards Institute, New York, New York.

3. *Parker O-Ring Handbook*, ORD 5700, Parker Seal O-Ring Division, Lexington, Kentucky.

4. *Handbook of Chemistry and Physics*, 66th Edition, Chemical Rubber Co., Boca Raton, Florida.

5. NUREG/CR-3019 1985, *Recommended Welding Criteria For Use in the Fabrication of Shipping Containers for Radioactive Materials*.

4.5.2 Teledyne Test Reports HPG5-DST-236 and HPG3-DST-1000

MEMORANDUM

TELEDYNE ENERGY SYSTEMS

20 February 1992

Refer to: HPG5-DST-236

To: T. Christenbury, W. Brittain, D. Anderson, M. McKittrick, T. Hammel, A. Lieberman, C. Heusler, E. Charyszyn, K. Campbell

From: D. Trimmer

Subject: Results of Five-Watt High Pressure Receptacle Thermal Margin Tests

---

Introduction

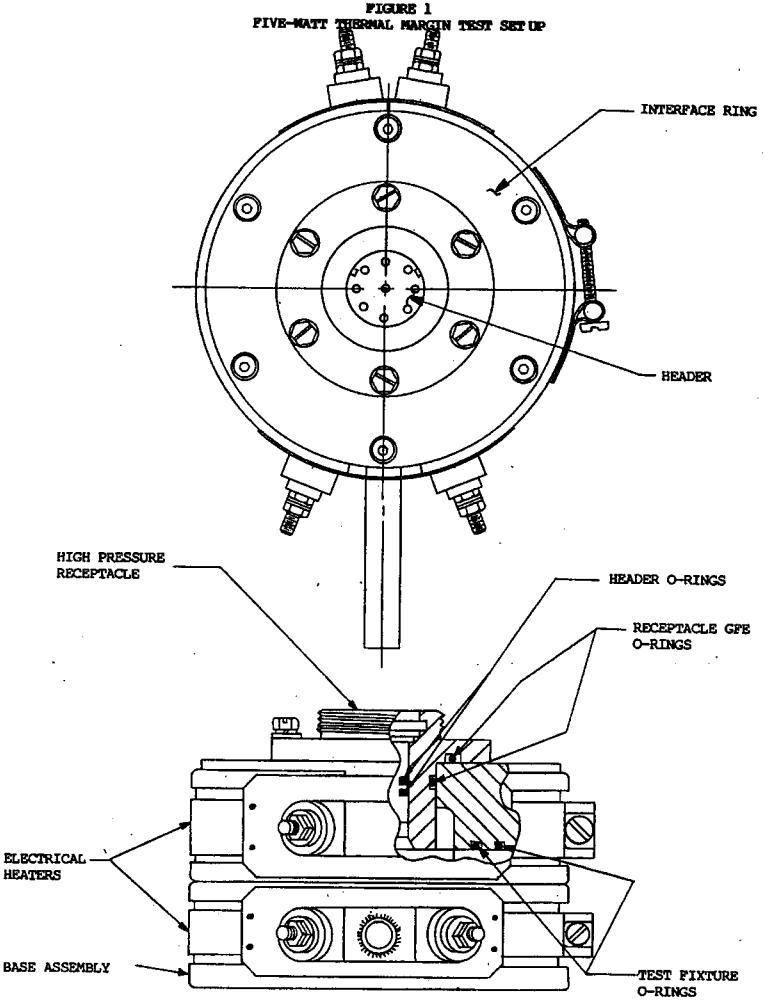
Two Five-Watt high pressure receptacles were selected to undergo thermal margin testing in accordance with the HPG MOD 3/Five-Watt RTG High Pressure Electrical Receptacle Elevated Temperature Qualification Test Procedure, HPGA3040303. Figure 1 shows the receptacle mounted in the test fixture. Receptacles S/N 5291AD and S/N 5296AD were chosen for the tests. Both receptacles underwent identical inspection, thermal testing and evaluation procedures. The part numbers of the two receptacles differed because the receptacle headers were fabricated using different materials. Receptacle S/N 5291AD had a monel header and the part number was C12CO072GO1. Receptacle S/N 5296AD had a stainless steel header and the part number was C12CO072GO6.

The thermal margin test is divided into two phases. The first is a thirty day soak of the receptacle at 400 °F followed by a test of the header only which basically consists of quickly heating the high pressure receptacle headers one at a time to a temperature high enough to cause a failure in the glass-to-metal hermetic seals. Ideally, the heating rate is sufficiently high that the glass-to-metal hermetic seal failure occurs before any failure can occur of O-rings used in the test configuration. Failure is indicated by a rapid increase in the measured helium leak rate for a small temperature increase. At failure, the measured leak rate typically increases 2 or 3 orders of magnitude with very little temperature increase.

Initial Inspection of Receptacles

The O-rings and O-ring grooves of both receptacles were inspected and measured. In addition, the headers were removed from their receptacle bodies and the header O-rings were discarded. The solder cups of all the pins for each header were filled with solder using the Five-Watt standard procedure to simulate attachment of wires. Eutectic lead-tin solder and Kester's type 1544 flux were used. The soldered pins were cleaned using the standard Five-Watt procedure.

FIGURE 1
FIVE-WATT THERMAL MARGIN TEST SET UP



A new set of header O-rings and the O-ring grooves were inspected and measured. After installing the new O-rings, the headers were inserted into the receptacle bodies. The percent fill for each of the O-rings (header and receptacle) in its O-ring groove was calculated and is recorded in Table 1. As noted in the table, each of the four O-rings had an approximate 70% fill in their respective O-ring groove.

TABLE 1

PERCENT FILL AND COMPRESSION SET

FOR O-RINGS USED IN FIVE-WATT THERMAL MARGIN TEST

O-Ring[1]	Location	Receptacle S/N 5291AD		Receptacle S/N 5296AD	
		% Fill	Compression Set (%)[2]	% Fill	Compression Set (%)
-224	Receptacle Flange	69.7	55.0	70.0	63.1
-218	Receptacle Gland	68.3	34.6	68.2	42.7
-118	Header #1	69.3	19.5	68.9	0
-118	Header #2	69.3	0	69.0	5.0
Predicted Compression Set for Thermal History Experienced			64		66

1. All O-rings are Viton** per M83248/1.
2. Measured after 30-day soak at 400 °F.

**_Viton_ is a registered trademark of the E.I. duPont de Nemours Company.

A helium leak test of the receptacles before and after soldering the pins was used to confirm that the thermal cycle of the soldering operation did not cause damage to the glass-to-metal hermetic seals.

Thermal Margin Test - Receptacle S/N 5291AD

High pressure receptacle S/N 5291AD was installed into the thermal margin test fixture first. Prior to beginning the test, an insulation resistance test and a dielectric strength test were conducted between the pins and the receptacle body in accordance with the test procedure. The results of both tests were negative, indicating no shorting problems existed.

The thermal margin test began by heating the receptacle in temperature increments to 400 °F. At each step, two helium leak tests were conducted, one on the "pins plus header O-rings" and another on the "total" receptacle (pins plus header O-rings plus receptacle O-rings). The "pins only" leak rate cannot be measured in this test fixture (except as an initial test conducted quickly after helium is introduced and before the helium has permeated the header O-ring seals). The measured leak rates for the two O-ring configurations were very similar with the "total" being generally higher than the "pins + header O-ring" measurements as expected (see Figure 2). The receptacle was maintained at 400 °F for 30 days and then the temperature was reduced to room temperature in the same increments used during the heat-up. The "total" leak rate versus temperature for the heat up and cooldown portion of this test is shown in Figure 3 and is representative of test results measured on other Five-Watt receptacles. These leak rates are representative of the permeation of helium through the O-rings and the fact that the leak rates during cooldown are essentially the same as those measured during heat-up indicate that the glass-to-metal and O-ring hermetic seals were unaffected by the operation at 400 °F. It was observed that the conformal coating in the receptacle header began to form cracks in its surface above 300 °F and some flaking of the coating occurred. No change in color was observed in the conformal coating as a result of the 400 °F operation. Solder had melted and dripped from the solder cups as expected because of the 400 °F operating temperature. The solder cups were still tinned with relatively clean looking solder. The insulation resistance and dielectric strength tests were repeated on the pins of the receptacle with the results again being negative.

The header O-rings were removed and compression set was measured on these as well as on the receptacle O-rings. The results are presented in Table 1. The predicted compression set of 64% is in fair agreement with the value measured on the receptacle flange (55%) but the comparison is poor with the values measured on the other three O-rings.

All of the O-rings were replaced and the header was installed in the Two-Watt thermal margin test fixture, STA4040007-009 as shown in Figure 4, and thermal margin testing was continued in accordance with the High Pressure Receptacle Header Qualification Test Procedure, STA4040400. With the receptacle header in this test fixture, the "pins only" leak rate measurement can be obtained at all operating temperatures. The "pins only" leak rate measurement was monitored as the receptacle header was heated rapidly from room temperature to 750 °F. The measured leak rate remained at the lowest detectable level (2×10^{-10} sccHe/sec) until the temperature reached 511 °F at which time the leak rate increased to 2.9×10^{-8} sccHe/sec indicating a failure of the glass-to-metal hermetic seal. The measured leak rate continued to increase as the temperature was increased from 511 °F to 750 °F. The temperature was then cooled rapidly to room temperature. Figure 5 presents the "pins only" helium leak rate measurement for the thermal cycle to 750 °F.

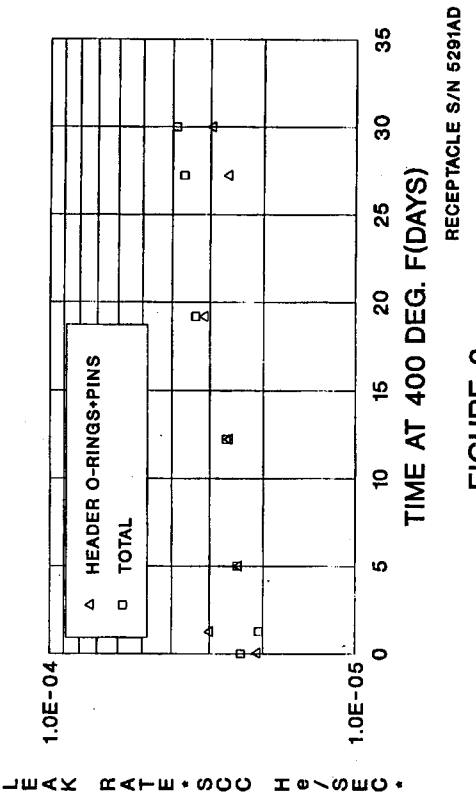

FIVE-WATT
HIGH PRESSURE RECEPTACLE
THERMAL MARGIN TEST
LEAK RATE • SCC He/SEC •
1.0E-04
1.0E-05
HEADER O-RINGS•PINS
TOTAL
0
5
10
15
20
25
30
35
TIME AT 400 DEG. F(DAYS)
RECEPTACLE S/N 5291AD

FIGURE 2

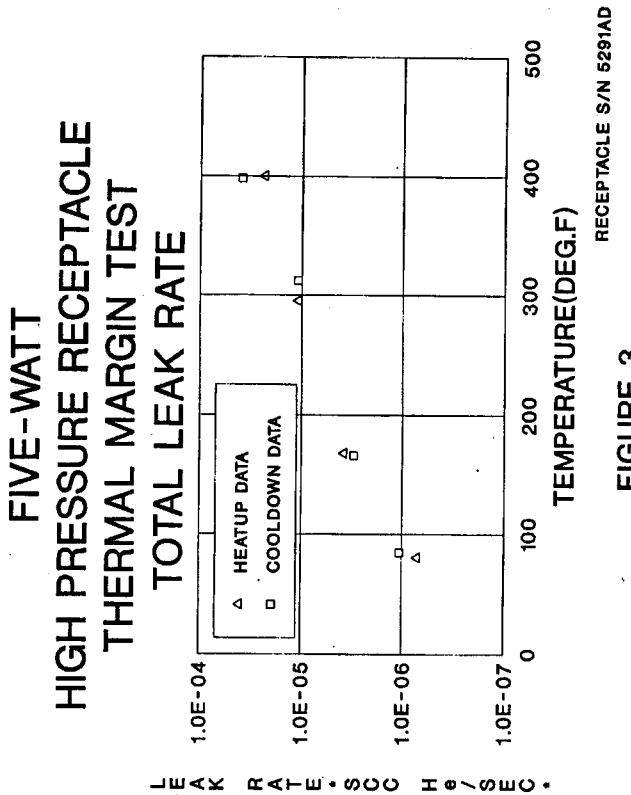
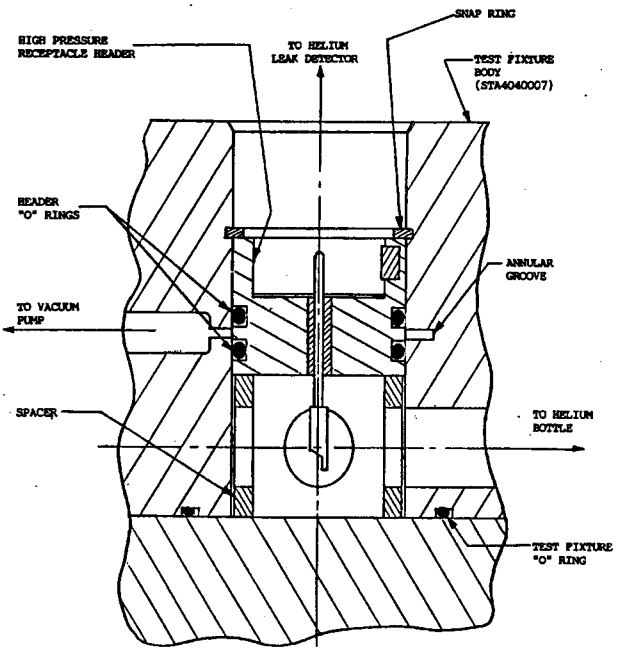

FIVE-WATT
HIGH PRESSURE RECEPTACLE
THERMAL MARGIN TEST
TOTAL LEAK RATE
HEATUP DATA
COOLDOWN DATA
LEAK RATE • SCC He/SEC •
1.0E-04
1.0E-05
1.0E-06
1.0E-07
0
100
200
300
400
500
TEMPERATURE(DEG.F)
RECEPTACLE S/N 5291AD

FIGURE 3

FIGURE 4

FIVE-WATT RECEPTACLE HEADER

THERMAL MARGIN TEST FIXTURE



To assure that the failure was in the hermetic seal and not in the header O-rings, the header O-rings were replaced and a final "pins only" room temperature leak rate measurement was made. This final leak rate measurement was in good agreement with the initial value measured at 511 °F confirming that the failure was in the glass-to-metal hermetic seal and not the viton O-rings. This test also confirmed that the leak in the glass-to-metal seal did not reseal after returning to room temperature. All of the helium leak rate measurements are presented in Appendix A.

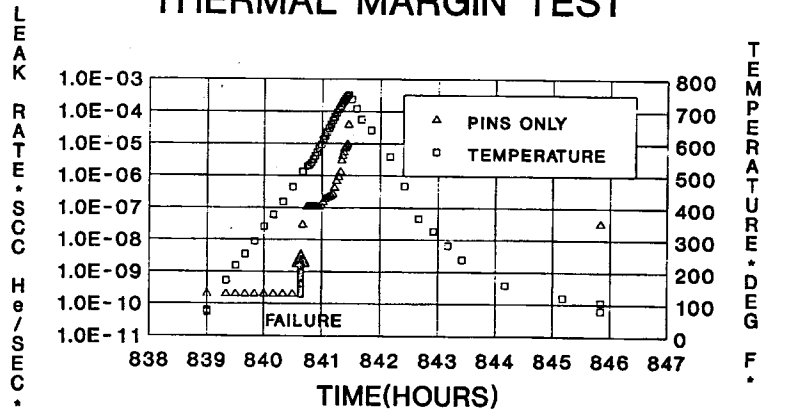
Thermal Margin Test - Receptacle S/N 5296AD

The thermal margin test with high pressure receptacle, S/N 5196AD, was performed using the same procedure as with the first receptacle. Before the thermal margin test was begun, insulation resistance and dielectric strength tests were conducted on the pins of this receptacle and the results were negative.

The "pins plus header O-rings" and "total" helium leak rate measurements were obtained as the receptacle was heated from room temperature to 400 °F. The receptacle was maintained at 400 °F for 30 days (see Figure 6 for test data) and then the temperature was reduced to room temperature. The "total" helium leak rate was always greater than the "pins plus header O-rings" leak rate as expected. Figure 7 shows the "total" leak rate measurements versus temperature for this receptacle for the heatup and cooldown portion of the 400 °F thermal cycle. The results agree well with those of receptacle S/N 5291AD and also of other Five-Watt receptacles previously tested in this manner. The results again confirm that the glass-to-metal hermetic seal of this receptacle has maintained its integrity during this 400 °F thermal cycle and that the helium leak rate measurements are representative of normal helium permeation through the viton O-rings.

The conformal coating in the receptacle header was also observed to have formed cracks as a result of operation at 400 °F and some flaking of the coating occurred. No change in color was observed. The solder cups on the back of the pins were still coated with clean solder but most of the solder had melted and dripped from the cups as expected. Insulation resistance and dielectric strength measurements were repeated on the pins of the receptacle with the results again being negative.

FIVE WATT
HIGH PRESSURE RECEPTACLE
THERMAL MARGIN TEST



RECEPTACLE S/N 5291AD
MONEL HEADER

FIGURE 5

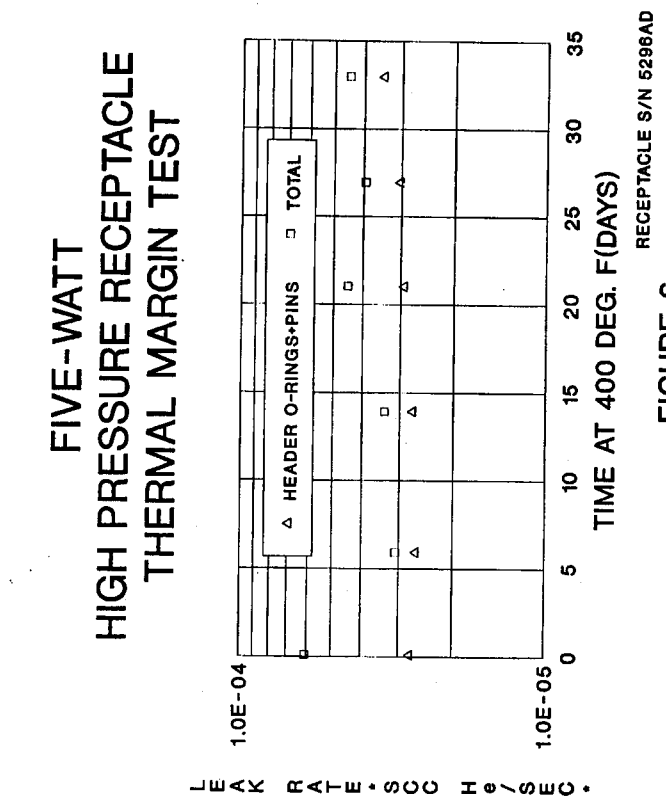

FIVE-WATT
HIGH PRESSURE RECEPTACLE
THERMAL MARGIN TEST
LEAK RATE*SCC He/SEC*
1.0E-04
1.0E-05
HEADER O-RINGS+PINS
TOTAL
0
5
10
15
20
25
30
35
TIME AT 400 DEG. F(DAYS)
RECEPTACLE S/N 5296AD

FIGURE 6

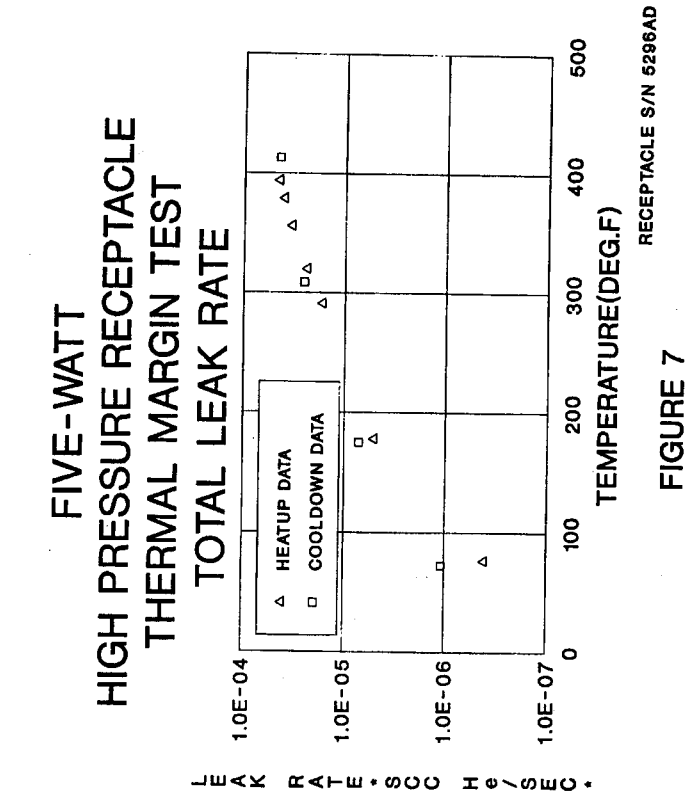

FIVE-WATT
HIGH PRESSURE RECEPTACLE
THERMAL MARGIN TEST
TOTAL LEAK RATE
LEAK RATE * SCC He/SEC *
1.0E-04
1.0E-05
1.0E-06
1.0E-07
HEATUP DATA
COOLDOWN DATA
0
100
200
300
400
500
TEMPERATURE(DEG.F)
RECEPTACLE S/N 5296AD

FIGURE 7

The header O-rings were removed to measure the compression set. The compression set measurements of these O-rings and those of the receptacle O-rings also are presented in Table 1. For this receptacle, the predicted compression set is 66% which is in fair agreement with the measurements on the receptacle O-rings (especially the receptacle flange O-ring) but does not agree with measurements made on the header O-rings.

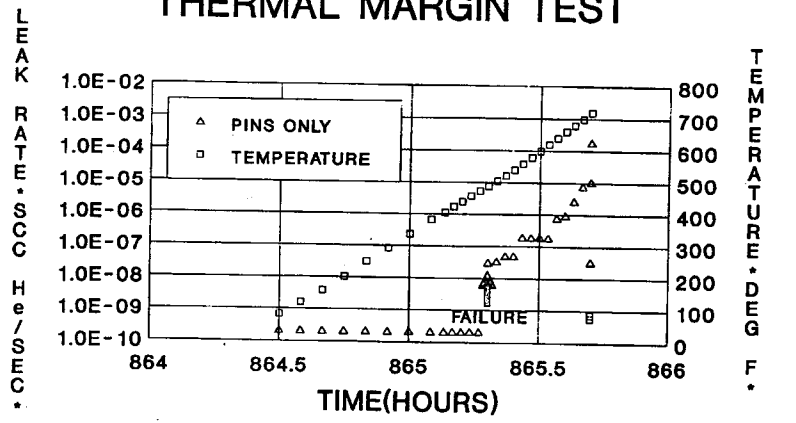
All of the O-rings were replaced and the receptacle header was assembled again into the Two-Watt thermal margin test fixture. Using the Two-Watt test procedure previously mentioned, the receptacle header was rapidly heated from room temperature to 718 °F while monitoring the "pins only" helium leak rate. At a temperature of 487 °F, the leak rate measurement changed from the lowest detectable level (2×10^{-10} sccHe/sec) to 2.89×10^{-8} sccHe/sec. This abrupt change indicates a failure of the glass-to-metal hermetic seal. As the temperature was increased above 487 °F the measured leak rate increased significantly as expected. The receptacle header temperature was then reduced to room temperature. Figure 8 presents the "pins only" leak rate measurement for the thermal cycle to 718 °F. At room temperature the "pins only" leak rate measurement was 1.71×10^{-4} sccHe/sec which would indicate a failure through the O-rings due to excessive compression set or a further deterioration of the hermetic seal. In order to confirm the hermetic seal failure, the header O-rings were replaced with new O-rings and the "pins only" room temperature helium leak rate measurement was repeated. This time the measure leak rate was nearly the same value as measured at 487 °F when the failure was first observed. This result indicates that the glass-to-metal hermetic seal failure did not change since it was first observed and the very large leak rate measured when the receptacle header was at room temperature was indeed a result of a failure of the header viton O-rings. The helium leak rate measurements for receptacle S/N 5296AD are presented in Appendix B.

Disassembly and Final Inspection

After completion of the thermal margin test, each header was removed from the Two-Watt test fixture and carefully inspected. More cracking was observed in the conformal coating than had initially been observed during the thermal soak at 400 °F. Small pieces of the coating continued to flake off the surface. But there was still no noticeable change in color of the conformal coating. The header O-rings were still compliant. Compression set measurements of the header O-rings were not made after the 700 °F thermal cycle, but visual observations indicated that permanent deformation was significant; approaching 100% compression set as expected.

The remaining solder coating the solder cups appeared very oxidized and burnt as expected from the very high operating temperature of 700 °F compared to the solder melting point of 361 °F. The headers of both receptacles only exhibited a slight amount of oxidation of their metallic surfaces. The monel header of receptacle S/N 5291AD had less oxidation of its surface than the stainless steel header of receptacle S/N 5296AD but the difference in amount of oxidation was small and may not be statistically significant. Therefore, the limiting consideration for elevated temperature operation should be the O-ring seals.

FIVE WATT
HIGH PRESSURE RECEPTACLE
THERMAL MARGIN TEST



RECEPTACLE S/N 5296AD
STAINLESS STEEL HEADER

FIGURE 8

Conclusions

The glass-to-metal hermetic seal of receptacle S/N 5291AD failed at 511 °F and failure of receptacle S/N 5296AD occurred at 487 °F. It can therefore be concluded that failure of the Five-Watt receptacle headers will occur at 500 ± 25 °F. There appears to be no noticeable advantage for either of the two header body materials (monel vs stainless steel) tested. The test results obtained and observations made were similar for both headers in all instances.

Two (2) Two-Watt receptacle headers were tested to failure in the same thermal margin test fixture in 1988. The criteria for determining failure was different for these headers. Therefore conclusions drawn in the earlier test must be reevaluated using the same failure criteria as used in this test. Using the present Five-Watt failure criteria (sudden large changes in "pins only" helium leak rate), the failure of the Two-Watt headers occurred 80 °F to 100 °F higher than the Five-Watt headers which is reasonable agreement when compared to the qualification temperature of 300 °F. However, a direct comparison of the hermetic seal failure temperatures for the two types of headers is questionable because of differences in the test programs and hermetic seal configurations. The Two-Watt headers were not exposed to a 400 °F thermal soak prior to the thermal margin test and they have eight pins compared to nine pins in the Five-Watt header design.

The receptacle and header O-ring seals survived the 400 °F thermal test although the compression set experienced by the receptacle O-rings was significant for the relatively short duration of the test. The compression set on the face seal O-rings was comparable to expectations. The compression set for the gland O-rings was much less than expected. Perhaps this is related to the geometry of the gland O-ring configuration. Compression set is probably related to the amount of squeeze or O-ring deformation. The TES data base is based on face type seals. None of the O-rings survived the 700 °F thermal cycle without excessive compression set. However, the O-rings were not expected to withstand these high temperatures for very long. They were only required to survive until the glass-to-metal hermetic seals failed which they did. Under normal operation of the receptacles, the temperature is not expected to exceed 300 °F which is within the normal range of operation for viton O-rings.

The conformal coating cracked and more pronounced flaking of the coating occurred for both receptacles at temperatures above 400 °F. The possibility of flaking at the expected maximum operating temperature of 300 °F is being investigated as a part of the 300 °F soak tests being conducted concurrently with this thermal margin test. It is not desirable to have the conformal coating experience any flaking during normal operation as it may interfere with proper mating/demoting operations and could cause poor electrical contact between mated pins and sockets. The conformal coating of both receptacles showed no evidence of a color change as a result of the 700 °F temperature extreme.

The insulation resistance and dielectric strength measurements all demonstrated good isolation between the receptacle pins and the receptacle body at the end of the 400 °F thermal soak test. This confirms that the conformal coating is not changing its insulating properties as a result of the 400 °F operating temperature.

APPENDIX A

RECEPTACLE S/N 5291AD HELIUM LEAK RATE MEASUREMENTS DURING THERMAL MARGIN TEST

HPG5-DST-236

20 February 1992

APPENDIX A
FIVE WATT RECEPTACLE THERMAL MARGIN TEST DATA

RECEPTACLE P/N C12C0072G01
RECEPTACLE S/N S291AD

			LEAK RATE MEASUREMENT				
TEST DATE	TEST TIME	SPECIMEN TEMP.(F)	"PINS ONLY" (scc He/sec)	"HEADER O-RINGS+PINS" (scc He/sec)	"TOTAL" (scc He/sec)	COMMENTS	ELAPSED HOURS
3/25/91	10:00	80	5.00E-10	3.05E-7	7.1E-7		0
3/25/91	14:00	172		3.30E-6			4
3/25/91	15:00	168			3.80E-6		5
3/26/91	09:20	272					23
3/26/91	12:00	296		1.05E-5			26
3/26/91	13:00	295			1.08E-5		27
3/27/91	09:00	400			2.36E-5		47
3/27/91	10:00	399		2.09E-5			48
3/28/91	18:00	404		2.99E-5	3.06E-5		77
4/1/91	09:00	396		2.41E-5	2.43E-5		167
4/8/91	14:30	400		2.89E-5	2.64E-5		341
4/15/91	13:30	413		3.12E-5	3.34E-5		508
4/22/91	14:30	413		2.41E-5	3.66E-5		701
4/26/91	09:00	398		2.96E-5	3.87E-5		767
4/26/91	12:30	312		1.17E-5			771
4/26/91	13:00	312			1.08E-5		771
4/29/91	09:00	166		2.59E-6	3.01E-6		839
4/30/91	08:30	84		5.74E-7	1.06E-6		839
						POTTING IS CRACKED INSIDE CONNECTOR AROUND PINS	
5/10/91		73	2.00E-10			STEP 6.3.4 *	839
5/24/91	08:20	78	2.00E-10			STEP 6.3.8 *	839
5/24/91	08:40	172	2.00E-10				839
5/24/91	08:50	218	2.00E-10				840
5/24/91	09:00	253	2.00E-10				840
5/24/91	09:10	294	2.00E-10				840
5/24/91	09:20	340	2.00E-10				840
5/24/91	09:30	377	2.00E-10				840
5/24/91	09:40	417	2.00E-10				840
5/24/91	09:50	464	2.00E-10				841
5/24/91	10:00	511	2.90E-8			FAILURE	841
5/24/91	10:05	529	1.08E-7				841
5/24/91	10:07	532	1.08E-7				841
5/24/91	10:09	539	1.08E-7				841
5/24/91	10:11	550	1.08E-7				841
5/24/91	10:13	561	1.08E-7				841
5/24/91	10:15	572	1.08E-7				841
5/24/91	10:17	585	1.08E-7				841
5/24/91	10:19	597	1.18E-7				841
5/24/91	10:21	612	1.49E-7				841
5/24/91	10:23	622	1.86E-7				841
5/24/91	10:25	635	1.99E-7				841

* STA4040400

BEST COPY AVAILABLE

APPENDIX A
FIVE WATT RECEPTACLE THERMAL MARGIN TEST DATA

RECEPTACLE P/N C12C0072G01
RECEPTACLE S/N 5291AD

			LEAK RATE MEASUREMENT				
TEST DATE	TEST TIME	SPECIMEN TEMP.(F)	"PINS ONLY" (scc He/sec)	"HEADER O-RINGS+PINS" (scc He/sec)	"TOTAL" (scc He/sec)	COMMENTS	ELAPSED HOURS
5/24/91	10:27	647	2.12E-7				841
5/24/91	10:29	659	2.34E-7				841
5/24/91	10:31	672	2.65E-7				841
5/24/91	10:33	682	4.12E-7				841
5/24/91	10:35	696	6.59E-7				841
5/24/91	10:37	706	9.00E-7				841
5/24/91	10:39	715	1.29E-6				841
5/24/91	10:40	722	2.94E-6				841
5/24/91	10:41	727	4.10E-6				841
5/24/91	10:42	731	5.38E-6				841
5/24/91	10:43	734	6.95E-6				841
5/24/91	10:44	739	7.31E-6				841
5/24/91	10:45	744	8.19E-6				841
5/24/91	10:46	748	9.55E-6				841
5/24/91	10:47	750	3.82E-5				841
5/24/91	10:50	737					842
5/24/91	10:55	708					842
5/24/91	11:00	674					842
5/24/91	11:10	641					842
5/24/91	11:30	558					842
5/24/91	11:45	467					842
5/24/91	12:00	366					843
5/24/91	12:15	326					843
5/24/91	12:30	281					843
5/24/91	12:45	238					843
5/24/91	13:30	159					844
5/24/91	14:30	119					845
5/24/91	15:10	105					846
5/31/91		79	3.19E-8			STEP 6.3.9 *	846

* STA4040400

BEST COPY AVAILABLE

APPENDIX B

RECEPTACLE S/N 5296AD HELIUM LEAK RATE MEASUREMENTS DURING THERMAL MARGIN TEST

HPG5-DST-236

20 February 1992

APPENDIX B

FIVE WATT RECEPTACLE THERMAL MARGIN TEST DATA

RECEPTACLE P/N C12C0072G06

RECEPTACLE S/N 5296AD

			LEAK RATE MEASUREMENT				
TEST DATE	TEST TIME	SPECIMEN TEMP.(F)	"PINS ONLY" (scc He/sec)	"HEADER O-RINGS+PINS" (scc He/sec)	"TOTAL" (scc He/sec)	COMMENTS	ELAPSED HOURS
7/30/91	10:00	76	2.00E-10	2.27E-7	4.04E-7		0
7/31/91	11:00	178		3.31E-6	5.09E-6		25
8/1/91	11:00	291		1.30E-5	1.67E-5		49
8/1/91	11:10	320			2.38E-5		49
8/1/91	11:20	356			3.37E-5		49
8/1/91	11:30	379			4.02E-5		50
8/1/91	11:40	394			4.53E-5		50
8/1/91	12:00	398			5.04E-5		50
8/1/91	13:00	402			5.65E-5		51
8/1/91	13:30	404			5.57E-5		52
8/1/91	14:00	402		2.75E-5	6.08E-5		52
8/7/91	10:00	390		2.64E-5	3.08E-5		192
8/15/91	10:00	394		2.72E-5	3.37E-5		384
8/22/91	12:30	401		2.93E-5	4.48E-5		555
8/28/91	10:30	407		3.03E-5	3.94E-5		697
9/3/91	11:00	413		3.46E-5	4.47E-5		841
9/3/91	14:30	309		1.65E-5	2.53E-5		845
9/4/91	10:30	175		3.43E-6	7.13E-6		865
9/6/91	10:00	72		4.12E-7	1.07E-6	POTTING IS CRACKED INSIDE CONNECTOR AROUND PINS	
10/21/91	08:00	82	2.00E-10			STEP 6.3.4 *	865
10/21/91	08:05	119	2.00E-10			STEP 6.3.5 *	865
10/21/91	08:10	158	2.00E-10				865
10/21/91	08:15	201	2.00E-10				865
10/21/91	08:20	249	2.00E-10				865
10/21/91	08:25	292	2.00E-10				865
10/21/91	08:30	336	2.00E-10				865
10/21/91	08:35	381	2.00E-10				865
10/21/91	08:38	404	2.00E-10				865
10/21/91	08:40	422	2.00E-10				865
10/21/91	08:42	438	2.00E-10				865
10/21/91	08:44	456	2.00E-10				865
10/21/91	08:46	472	2.00E-10				865
10/21/91	08:48	487	2.89E-8			FAILURE	865
10/21/91	08:50	504	3.19E-8				865
10/21/91	08:52	520	4.65E-8				865
10/21/91	08:54	539	4.65E-8				865
10/21/91	08:56	558	1.80E-7				865
10/21/91	08:58	578	1.80E-7				865
10/21/91	09:00	598	1.80E-7				866
10/21/91	09:02	618	1.75E-7				866
10/21/91	09:04	638	7.35E-7				866

APPENDIX B

FIVE WATT RECEPTACLE THERMAL MARGIN TEST DATA

RECEPTACLE P/N C12C0072G06

RECEPTACLE S/N 5296AD

			LEAK RATE MEASUREMENT				
TEST DATE	TEST TIME	SPECIMEN TEMP.(F)	"PINS ONLY" (scc He/sec)	"HEADER O-RINGS+PINS" (scc He/sec)	"TOTAL" (scc He/sec)	COMMENTS	ELAPSED HOURS
10/21/91	09:06	658	8.89E-7				866
10/21/91	09:08	678	2.48E-6				866
10/21/91	09:10	698	7.27E-6				866
10/21/91	09:12	718	1.01E-5				866
10/22/91	10:00	85	1.71E-4	1.71E-4			866
10/30/91	10:30	75	3.13E-8			STEP 6.3.9 *	866

MEMORANDUM

TELEDYNE ENERGY SYSTEMS

19 December 1991

Refer to: HPG3-DST-1000

To: T. Christenbury, W. Brittain, D. Anderson, M. McKittrick, T. Hammel, A. Lieberman, C. Heusler

From: D. Trimer

Subject: Results of HPG MOD 3 High Pressure Receptacle Thermal Margin Tests

---

Introduction

Two HPG MOD 3 high pressure receptacles (P/N NCM24217/4-206M) were selected to undergo thermal margin testing in accordance with the HPG MOD 3/Five-Watt RTG High Pressure Electrical Receptacle Elevated Temperature Qualification Test Procedure, HPGA3040303. Figure 1 shows the receptacle mounted in the test fixture. The thermal margin test basically consists of quickly heating the high pressure receptacles one at a time to a temperature high enough to cause a failure in the hermetic seals. Receptacles S/N 813 and S/N 814 were chosen for the tests.

Initial Inspection of Receptacles

Both receptacles were inspected and measurements were taken of the O-rings and O-ring grooves so that the percentage fill of the grooves could be determined. Table 1 lists the percent fill for the O-rings associated with each receptacle. Then the pins of each receptacle were soldered using the HPG MOD 3 standard procedure to simulate attachment of wires. The solder used was eutectic lead-tin solder and in the case of the thermocouple pins, type 817 flux was used to wet the pins with the solder. All pins were then cleaned by the HPG MOD 3 standard process depending on the type of flux used. A helium leak test of the hermetic seals before and after soldering the pins was used to confirm that the thermal cycle of the soldering operation did not cause damage to the hermetic seals.

Thermal Margin Test-Receptacle S/N 813

High pressure receptacle S/N 813 was installed into the thermal margin test fixture first. Prior to beginning the test, an insulation resistance test and a dielectric strength test were conducted between the pins and the receptacle body in accordance with the test procedure. The results of both tests were negative, indicating no shorting problems existed. The actual thermal test began by quickly heating the receptacle (S/N 813) in small temperature increments. At each step, two helium leak tests were conducted, one on the hermetic seals (pins only) and another on the entire receptacle (pins plus receptacle O-rings). The "pins only" helium leak rate measurement is the most

FIGURE 1

HPG MOD 3 THERMAL MARGIN TEST SET UP

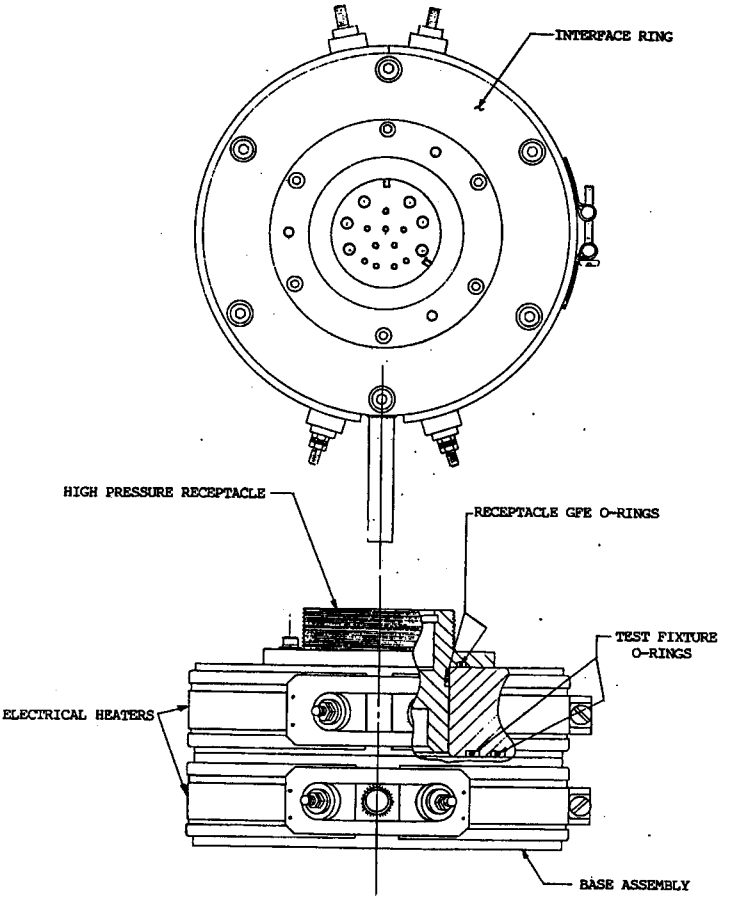


TABLE 1

PERCENT FILL AND COMPRESSION SET

FOR O-RINGS USED IN HPG MOD 3 THERMAL MARGIN TEST

O-Ring[1]	Location	Receptacle S/N 813		Receptacle S/N 814	
		% Fill	Compression Set (%)[2]	% Fill	Compression Set (%)[3]
-234	Receptacle Flange	69.3	68.9	70.0	NA
-230	Receptacle Gland	70.3	59.5	70.3	NA
-348	Interface Ring	NA	62.0	NA	NA
-340	Interface Ring	NA	56.8	NA	NA

1. All O-rings are Viton per M83248/1.
2. Measured at completion of test.
3. O-rings destroyed by high temperature operation.

reliable determination of the integrity of the receptacle glass-to-metal hermetic seals since this measurement should remain very small until a leak appears. Essentially, no helium should be detected greater than the sensitivity of the equipment as long as the hertstic seal is intact. This minimum measured leak rate is approximately 2×10^{-10} sccHe/sec. Figures 2 and 3 show the test data for the "pins only" and "total" helium leak rates respectively. As the temperature, was increased on receptacle S/N 813, the helium leak rate remained very low until a temperature of 487 °F was reached at which point the "pins only" leak rate increased to 1.9×10^{-6} sccHe/sec. This leak rate implied a failure of the hermetic seal. The total leak rate measurements indicated that the initial O-ring seal leakage increased as expected due to increased helium permeation through the O-rings. Figure 4 shows this increasing permeation of helium through the O-rings for the first 225 hours of the test. The temperature continued to be increased until it reached 600 °F without failure of the receptacle O-ring seals. In fact, the measured total leak rate decreased as the temperature was further increased. This effect has been observed before with other O-ring seals and has been attributed to formation of a metal-to-metal seal. Then the receptacle was cooled to room temperature. A final room temperature "pins only" helium leak check indicated that the leak had resealed; see Figure 2 at about 320 hours. This type behavior has been observed by TES on other receptacle O-ring designs. Also as seen in Figure 3 at the same time, the "total" leak rate returned to a value near the initial measurement. At the completion of the thermal margin test, the insulation resistance and dielectric strength tests were repeated with the results again being negative. The helium leak test results for this thermal margin test are presented in Appendix A.

Thermal Margin Test-Receptacle S/N 814

The thermal margin test with high pressure receptacle, S/N 814, was performed essentially the same as with the first receptacle except that Engineering Work Order HPGM3-719 was written to allow the thermal cycle to be repeated a second time. Before the thermal margin test was begun, the insulation resistance and dielectric strength tests were conducted on the pins of this receptacle and the results were negative.

The thermal margin test was begun by heating the receptacle in small temperature increments. Two helium leak tests were performed at each temperature step ("pins only" and "total"). Figures 5 and 6 show the results for each of the leak rate tests. The receptacle was heated in this manner to a temperature of 700 °F without observing any increase in the "pins only" helium leak rate measurement above the background value. At 700 °F, the insulation resistance and dielectric strength tests were repeated and the results were negative (no low impedance paths). The receptacle was then cooled to room temperature. The "total" helium leak rate measured during this temperature cycle showed normal expected variations with temperature during the heat-up until a metal-to-metal seal began appearing above a temperature of 450 °F. The initial heat-up of the receptacle is shown in Figure 7 and the results are very much like those seen in Figure 4 for receptacle S/N 813. At temperatures above 450 °F the leak rate of receptacle S/N 814 became unreliable, sometimes decreasing as the temperature was increasing and finally increasing as the temperature was being reduced. These changes can be explained by a combination of effects; first a metal-to-metal seal behavior at high temperature resulting in a decreased leak rate and second an O-ring failure as the receptacle was being cooled down from 700 °F due to excessive compression set of the O-rings. This type behavior has been observed on other O-ring seal configurations.

HPG MOD 3
HIGH PRESSURE RECEPTACLE
THERMAL MARGIN TEST

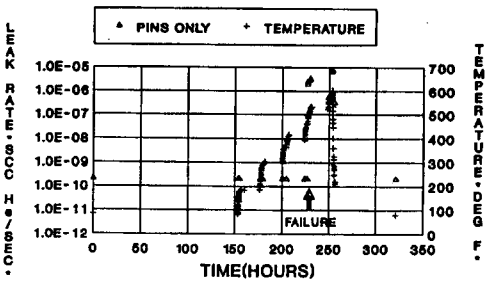


FIGURE 2

RECEPTACLE S/N 813

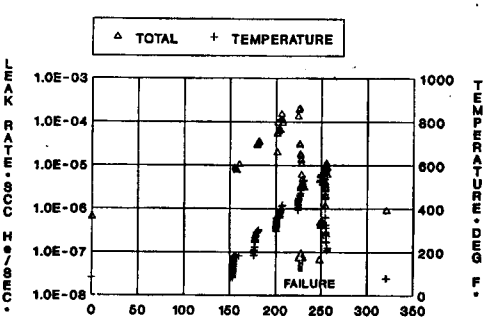


FIGURE 3

HPG MOD 3
HIGH PRESSURE RECEPTACLE
THERMAL MARGIN TEST

FIGURE 4

HPG MOD 3
HIGH PRESSURE RECEPTACLE
THERMAL MARGIN TEST

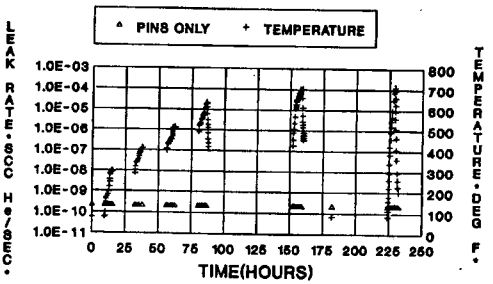


FIGURE 5

RECEPTACLE S/N 814

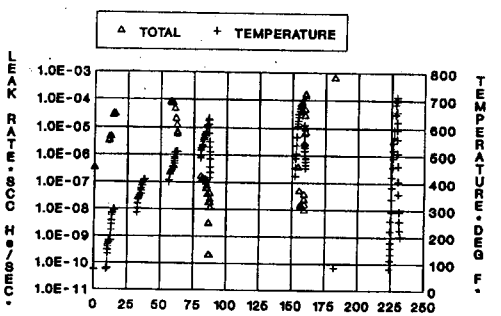


FIGURE 6

The receptacle was then reheated as specified in the Engineering Work Order. This time the receptacle temperature reached 711 °F and the "pins only" helium leak rate measurements still indicated no failure of the hermetic seals. Insulation resistance and dielectric strength tests were conducted again at the high temperature and again the results were negative. The receptacle was then cooled to room temperature. The insulation resistance and dielectric strength measurements were repeated with the results being negative. All of the helium leak test results taken on receptacle S/N 814 are presented in Appendix B.

Disassembly and Final Inspection

After completion of the thermal margin test, each receptacle was removed from the test fixture and inspected carefully. The bolts used to hold the receptacle to the interface ring were checked and it was confirmed that all bolts for each receptacle had maintained the original torque values. Three 8-32 screws placed in the tapped holes of the receptacle mounting flange were used to carefully force the receptacles from the interface ring.

The conformal coating in the hermetic seal area of each receptacle was very dark and much of the surface appeared as though it had melted, formed bubbles, and chips and flakes appeared when it was cooled. Comparing the coatings of both receptacles, the bubbling and melting was more extensive with receptacle S/N 814 than for receptacle S/N 813. This difference in appearance is likely the result of the higher maximum temperature of S/N 814 compared to S/N 813 rather than an indication of receptacle conformal coating variability. During heat up several observations were made concerning changes to the conformal coating. A small flake of conformal coating from receptacle S/N 813 had chipped off at a temperature of about 415 °F. The initial color change to brown began at about 300 °F for both receptacles. The color continued to darken at higher temperatures. At about 500 °F the coating began to melt and bubbles began forming.

The O-rings from receptacle S/N 813 appeared to have some permanent deformation. The flange O-ring was sticking to the flange but was easy to remove. Both O-rings were still quite pliable. The majority of the solder in the solder cups of the receptacle had dripped down to the bottom of the interface ring. This is expected because the test temperature of 600 °F exceeds the solder melting temperature of 361 °F. The solder remaining on the pins appeared oxidized and burned. The thermocouple pins were checked for residual acid flux using the HPG MOD 3 standard test but none was found. As expected, the receptacle body was noticeably oxidized. The interface ring was also removed to examine the O-rings sealing it to the rest of the fixture (see Figure 1). These O-rings also had some compression set but were quite pliable. All four O-rings (receptacle and interface ring) were measured to determine their compression set. Table 1 presents the results of these measurements. In all cases, the O-rings experienced a compression set of 57% or more.

HPG MOD 3
HIGH PRESSURE RECEPTACLE THERMAL MARGIN TEST

FIGURE 7

As expected, the O-rings from receptacle S/N 814 were destroyed by the 700 °F temperature. They fell apart as the receptacle was being removed. The O-rings were very hard and brittle; somewhat like graphite. This was also true of the O-rings in the interface ring. Therefore, no compression set measurements could be obtained for these O-rings as indicated in Table 1. The solder had dripped out of the solder cups in each receptacle pin and large drops had collected in the bottom of the interface ring. The solder remaining on the pins again appeared very oxidized and burned. This was undoubtedly due to the very high temperature of operation compared to the normal operating temperature of the solder (melting point of 361 °F). The thermocouple pins were-checked for residual Acid flux and none was detected. The surfaces of the receptacle shell were darkened from oxidation due to the high temperature operation.

Conclusions

The glass-to-metal hermetic seals of receptacle S/N 813 failed at a temperature of 487 °F whereas for receptacle S/N 814, the hermetic seals did not fail when cycled twice to 700 °F. It may have been that the conformal coating on receptacle S/N 814 masked a failure of this receptacle's hermetic seals. However, the conclusion must still be that temperatures in the range of 450-500 °F are sufficient to cause failure of the glass-to-metal hermetic seals of the HPG MOD 3 high pressure receptacles.

The receptacle-to-housing O-ring seals of receptacle S/N 813 survived the 600 °F thermal cycle although the measured compression set of 60% or more after about 300 hours of operation indicates that Viton O-rings would be unsatisfactory for long term use at these temperatures. Similar O-rings on receptacle S/N 814 were completely destroyed by the short term operation at temperatures up to 700 °F. However, none of these O-rings were expected to survive the 600-700 °F temperature extremes for very long. The thermal margin tests are short term high temperature tests where the temperature limit of the glass-to-metal hermetic seals is expected to be exceeded before the O-rings fail. During normal operation, the maximum service temperature of the receptacles is intended to be about 300 °F which is within the normal range of operation for these viton O-rings.

The conformal coating began to change color at about 300 °F and showed signs of melting at about 500 °F. The manufacturer of the high pressure receptacles has indicated that there are other coating materials which will maintain their original color to higher temperatures. If the coating material is changed, then further tests should be performed to assure the compatibility of the new coating at the expected operating temperature of the receptacle.

Insulation resistance and dielectric strength measurements all indicated good isolation of the receptacle pins for each other and the receptacle body at elevated temperatures as well as at room temperature after completing the thermal test.

APPENDIX A

RECEPTACLE S/N 813 HELIUM LEAK RATE

MEASUREMENTS DURING THERMAL MARGIN TEST

APPENDIX A
HPG MOD 3 RECEPTACLE THERMAL MARGIN TEST DATA

RECEPTACLE P/N MCM24317/4-206M
RECEPTACLE S/N 813

TEST DATE	TEST TIME	SPECIMEN TEMP.(F)	LEAK RATE MEASUREMENT "FINE ONLY" (scc He/sec)	LEAK RATE MEASUREMENT "TOTAL" (scc He/sec)	COMMENTS	ELAPSED HOURS
3/12/91		83	2.00E-10	6.67E-7		0
3/18/91	0830	82	2.00E-10			153
3/18/91	0835	91	2.00E-10			153
3/18/91	0840	99	2.00E-10			153
3/18/91	0845	108	2.00E-10			153
3/18/91	0850	116	2.00E-10			154
3/18/91	0855	124	2.00E-10			154
3/18/91	1000	134	2.00E-10			154
3/18/91	1005	140	2.00E-10			154
3/18/91	1010	147	2.00E-10			154
3/18/91	1015	154	2.00E-10			154
3/18/91	1020	159	2.00E-10			154
3/18/91	1025	163	2.00E-10			154
3/18/91	1030	166	2.00E-10			154
3/18/91	1035	170	2.00E-10			154
3/18/91	1040	173	2.00E-10			154
3/18/91	1045	175	2.00E-10			154
3/18/91	1050	177	2.00E-10			155
3/18/91	1100	178	2.00E-10			155
3/18/91	1115	178		6.67E-6		155
3/18/91	1215	184		7.09E-6		156
3/18/91	1315	186		7.69E-6		157
3/18/91	1615	182		1.03E-5		160
3/19/91	0825	184	2.00E-10			176
3/19/91	0830	185	2.00E-10			176
3/19/91	0835	186	2.00E-10			176
3/19/91	0845	197	2.00E-10			176
3/19/91	0850	204	2.00E-10			176
3/19/91	0855	211	2.00E-10			177
3/19/91	0905	222	2.00E-10			177
3/19/91	0925	245	2.00E-10			177
3/19/91	0930	251	2.00E-10			177
3/19/91	0940	257	2.00E-10			177
3/19/91	0950	266	2.00E-10			178
3/19/91	1000	272	2.00E-10			178
3/19/91	1010	278	2.00E-10			178
3/19/91	1020	278	2.00E-10			178
3/19/91	1050	286	2.00E-10			179
3/19/91	1110	288	2.00E-10			179
3/19/91	1130	292	2.00E-10			179
3/19/91	1139	292		2.93E-5		179
3/19/91	1200	293		3.18E-5		180
3/19/91	1300	297		3.39E-5		181
3/19/91	1335	302		3.55E-5		181
3/20/91	0815	298	2.00E-10			200
3/20/91	0825	307	2.00E-10			200

BEST COPY AVAILABLE

APPENDIX A

EPS MOD 3 RECEPTACLE THERMAL MARGIN TEST DATA

RECEPTACLE P/N MCH34217/4-2068
RECEPTACLE S/N 813

TEST DATE	TEST TIME	SPECIMEN TEMP.(F)	LEAK RATE MEASUREMENT "PINS ONLY" (scc He/sec)	LEAK RATE MEASUREMENT "TOTAL" (scc He/sec)	COMMENTS	ELAPSED HOURS
3/20/91	0830	316	2.00E-10			200
3/20/91	0835	323	2.00E-10			200
3/20/91	0840	329	2.00E-10			200
3/20/91	0845	334	2.00E-10			200
3/20/91	0850	339	2.00E-10			200
3/20/91	0855	343	2.00E-10			201
3/20/91	0900	355	2.00E-10			201
3/20/91	0905	357	2.00E-10			201
3/20/91	0910	351		1.97E-5		201
3/20/91	0930	356		5.27E-5		201
3/20/91	1000	363		9.47E-5		202
3/20/91	1030	363		6.01E-5		202
3/20/91	1110	364		6.93E-5		203
3/20/91	1245	358	2.00E-10	6.55E-5		204
3/20/91	1250	366	2.00E-10			205
3/20/91	1255	375	2.00E-10			205
3/20/91	1300	381	2.00E-10			205
3/20/91	1305	386	2.00E-10			205
3/20/91	1310	390	2.00E-10			205
3/20/91	1315	392	2.00E-10			205
3/20/91	1320	393	2.00E-10			205
3/20/91	1330	391		1.14E-4		205
3/20/91	1400	398		1.49E-4		206
3/20/91	1430	409		1.09E-4		206
3/20/91	1500	413		9.32E-5		207
3/20/91	1530	418		1.07E-4		207
3/21/91	0820	393	2.00E-10	1.33E-4	*PIECE OF POTTING	224
3/21/91	0825	398	2.00E-10		FLAKED OFF BOTTOM	224
3/21/91	0830	408	2.00E-10		OF RECEPTACLE	224
3/21/91	0835	416	2.00E-10			224
3/21/91	0840	421	2.00E-10			224
3/21/91	0845	429	2.00E-10			224
3/21/91	0850	434	2.00E-10			224
3/21/91	0855	439	2.00E-10			225
3/21/91	0900	441	2.00E-10			225
3/21/91	0905	444	2.00E-10			225
3/21/91	0910	447	2.00E-10			225
3/21/91	0915	444		1.89E-4		225
3/21/91	1000	457		2.01E-4		226
3/21/91	1030	461		3.10E-5	*INITIAL INDICATION	226
3/21/91	1045	462		2.93E-5	OF INTERMITTENT	226
3/21/91	1100	461		1.80E-5	METAL-TO-METAL SEAL	227
3/21/91	1115	461	2.00E-10	1.67E-5	BEHAVIOR FOR "TOTAL"	227
3/21/91	1120	472	2.00E-10			227
3/21/91	1125	487	1.91E-6		*"PINS ONLY" LEAK	227
3/21/91	1130	492	1.08E-6		STARTED AT 485 DEG.F	227

BEST COPY AVAILABLE

APPENDIX A
MPS MOD 3 RECEPTACLE THERMAL MARGIN TEST DATA

RECEPTACLE P/N MCM14217/4-206M
RECEPTACLE S/N 813

			LEAK RATE MEASUREMENT			
TEST DATE	TEST TIME	SPECIMEN TEMP.(F)	"PINS ONLY" (scc He/sec)	"TOTAL" (scc He/sec)	COMMENTS	ELAPSED HOURS
3/21/91	1135	488	2.96E-6			227
3/21/91	1140	499	2.35E-6			227
3/21/91	1145	488		1.32E-5		227
3/21/91	1200	490		1.08E-5		228
3/21/91	1230	505		6.01E-6		228
3/21/91	1300	510		4.65E-6		229
3/21/91	1345	513	2.07E-6	3.64E-6		229
3/21/91	1350	516	2.85E-6			230
3/21/91	1355	524	3.01E-6			230
3/21/91	1400	526	3.28E-6	3.56E-6		230
3/21/91	1415	528		3.25E-6		230
3/21/91	1430	531		3.19E-6		230
3/21/91	1500	531		3.06E-6		231
3/21/91	1530	533		3.05E-6		231
3/22/91	0830	523		6.54E-8		248
3/22/91	0900	531		4.75E-7		249
3/22/91	0905	548	9.01E-7			249
3/22/91	0910	551	9.01E-7			249
3/22/91	0915	553	9.01E-7			249
3/22/91	0920	553	9.54E-7			249
3/22/91	0930	545		4.05E-7		249
3/22/91	1000	558		4.75E-7		250
3/22/91	1030	558		4.63E-7		250
3/22/91	1100	560		4.75E-7		251
3/22/91	1130	560		4.75E-7		251
3/22/91	1300	570	9.05E-7			253
3/22/91	1305	575	6.59E-6			253
3/22/91	1310	582	7.58E-6			253
3/22/91	1315	588	7.41E-6			253
3/22/91	1320	591	7.41E-6			253
3/22/91	1325	596	7.41E-6			253
3/22/91	1330	601	7.41E-6	6.91E-6		253
3/22/91	1335	585		6.44E-6		253
3/22/91	1340	575		5.55E-6		253
3/22/91	1345	556		4.32E-6		253
3/22/91	1350	534		4.01E-6		254
3/22/91	1355	515		3.98E-6		254
3/22/91	1400	500		3.61E-6		254
3/22/91	1405	481		3.98E-6		254
3/22/91	1410	465		3.51E-6		254
3/22/91	1415	446		3.05E-6		254
3/22/91	1430	400		1.98E-6		254
3/22/91	1445	360		1.15E-6		254
3/22/91	1500	325		7.11E-6		255
3/22/91	1505	312		8.11E-6		255
3/22/91	1515	291		9.06E-6		255

BEST COPY AVAILABLE

APPENDIX A
EPG MOD 3 RECEPTACLE THERMAL MARGIN TEST DATA

RECEPTACLE P/N MCM24217/4-206N
RECEPTACLE S/N 013

			LEAK RATE MEASUREMENT			
TEST DATE	TEST TIME	SPECIMEN TEMP.(F)	"FINE ONLY" (scc He/sec)	"TOTAL" (scc He/sec)	COMMENTS	ELAPSED HOURS
3/22/91	1520	283		1.05E-5		255
3/22/91	1525	275		1.05E-5		255
3/22/91	1530	267	3.15E-7	1.09E-5		255
3/22/91	1540	248		1.10E-5		255
3/22/91	1545	245		1.08E-5		255
3/22/91	1600	219		8.64E-6		256
3/22/91	1615	209		6.05E-6		256
3/25/91	0915	79	2.00E-10	8.92E-7		321

BEST COPY AVAILABLE

APPENDIX B

RECEPTACLE S/N 814 HELIUM LEAK RATE

MEASUREMENTS DURING THERMAL MARGIN TEST

APPENDIX B
HPG MOD 3 RECEPTACLE THERMAL MARGIN TEST DATA

RECEPTACLE P/N MCH24217/4-20SN
RECEPTACLE S/N 814

TEST DATE	TEST TIME	SPECIMEN TEMP.(F)	LEAK RATE MEASUREMENT "PINS ONLY" (scc He/sec)	LEAK RATE MEASUREMENT "TOTAL" (scc He/sec)	COMMENTS	ELAPSED HOURS
6/4/91		76	2.00E-10	3.38E-7		0
6/4/91	0930	76	2.00E-10			9
6/4/91	0945	78	2.00E-10			9
6/4/91	1000	81	2.00E-10			10
6/4/91	1010	100	2.00E-10			10
6/4/91	1020	133	2.00E-10			10
6/4/91	1030	148	2.00E-10			10
6/4/91	1040	161	2.00E-10			10
6/4/91	1055	169	2.00E-10	2.02E-6		11
6/4/91	1115	176		3.37E-6		11
6/4/91	1130	183		4.32E-6		11
6/4/91	1245	183		4.50E-6		12
6/4/91	1250	199	2.00E-10			13
6/4/91	1308	222	2.00E-10			13
6/4/91	1316	243	2.00E-10			13
6/4/91	1328	257	2.00E-10			13
6/4/91	1340	277	2.00E-10			13
6/4/91	1350	285	2.00E-10			14
6/4/91	1400	287	2.00E-10	2.62E-5		14
6/4/91	1430	293		3.00E-5		14
6/4/91	1500	299		2.87E-5		15
6/4/91	1550	295	2.00E-10	2.93E-5		16
6/5/91	0830	287	2.00E-10			32
6/5/91	0840	303	2.00E-10			32
6/5/91	0850	320	2.00E-10			32
6/5/91	0900	336	2.00E-10			33
6/5/91	0915	339	2.00E-10			33
6/5/91	0930	343				33
6/5/91	1000	344				34
6/5/91	1030	351				34
6/5/91	1100	357	2.00E-10			35
6/5/91	1115	369	2.00E-10			35
6/5/91	1130	377	2.00E-10			35
6/5/91	1145	388	2.00E-10			35
6/5/91	1200	387				36
6/5/91	1230	394				36
6/5/91	1330	408				37
6/5/91	1345	408				37
6/5/91	1400	410	2.00E-10			38
6/6/91	0830	400	2.00E-10			56
6/6/91	0845	408	2.00E-10			56
6/6/91	0900	426	2.00E-10			57
6/6/91	0915	433	2.00E-10			57
6/6/91	0930	438	2.00E-10	7.85E-5		57
6/6/91	1000	442		7.00E-5		58
6/6/91	1030	447		7.86E-5		58

BEST COPY AVAILABLE

APPENDIX B
RPS MOD 3 RECEPTACLE THERMAL MARGIN TEST DATA

RECEPTACLE P/N MCM24217/4-206N
RECEPTACLE S/N 014

			LEAK RATE MEASUREMENT			
TEST DATE	TEST TIME	SPECIMEN TEMP.(F)	"FINE ONLY" (scc He/sec)	"TOTAL" (scc He/sec)	COMMENTS	ELAPSED HOURS
6/6/91	1100	455		7.40E-5		59
6/6/91	1120	459	2.00E-10	7.32E-5		59
6/6/91	1215	453	2.00E-10			60
6/6/91	1230	469	2.00E-10			60
6/6/91	1235	477	2.00E-10			60
6/6/91	1240	486	2.00E-10			60
6/6/91	1245	493	2.00E-10			60
6/6/91	1250	501	2.00E-10			61
6/6/91	1255	509		4.80E-5	*BEGINNING OF METAL-	61
6/6/91	1330	510		2.03E-5	TO-METAL SEAL	61
6/6/91	1400	512		1.19E-5	BEHAVIOR FOR "TOTAL"	62
6/6/91	1430	512		6.76E-6		62
6/6/91	1455	512	2.00E-10	5.69E-6		63
6/7/91	0815	490	2.00E-10			80
6/7/91	0830	497	2.00E-10			80
6/7/91	0845	510	2.00E-10			80
6/7/91	0850	525	2.00E-10	1.69E-7		80
6/7/91	0920	528		1.35E-7		81
6/7/91	0950	531	2.00E-10	1.39E-7		82
6/7/91	0955	536	2.00E-10			82
6/7/91	1000	550	2.00E-10	1.40E-7		82
6/7/91	1030	555		1.25E-7		82
6/7/91	1100	557	2.00E-10	1.33E-7		83
6/7/91	1105	563	2.00E-10			83
6/7/91	1110	570	2.00E-10			83
6/7/91	1115	575	2.00E-10	1.28E-7		83
6/7/91	1215	580		1.25E-7		84
6/7/91	1220	585	2.00E-10	1.01E-7		84
6/7/91	1230	601	2.00E-10	5.88E-8		84
6/7/91	1300	605		7.37E-8		85
6/7/91	1330	607	2.00E-10	5.89E-8		85
6/7/91	1335	610	2.00E-10			85
6/7/91	1340	625	2.00E-10	3.46E-8		85
6/7/91	1410	631		1.79E-8		86
6/7/91	1440	626	2.00E-10	3.08E-9		86
6/7/91	1445	612		2.92E-9		86
6/7/91	1450	599		2.92E-9		86
6/7/91	1455	579		2.00E-10		87
6/7/91	1500	548		2.00E-10		87
6/7/91	1505	528		2.00E-10		87
6/7/91	1510	512		2.00E-10		87
6/7/91	1515	501		2.00E-10		87
6/7/91	1520	486		3.79E-8	*BEGINNING OF LONG	87
6/7/91	1530	456		2.37E-8	OF METAL-TO-METAL	87
6/7/91	1540	437		1.76E-8	SEAL BEHAVIOR FOR	87
6/7/91	1550	417		1.13E-8	"TOTAL" DURING	88

BEST COPY AVAILABLE

APPENDIX B

EPG MOD 3 RECEPTACLE THERMAL MARGIN TEST DATA

RECEPTACLE P/N MCM14317/4-206M
RECEPTACLE S/N 814

			LEAK RATE MEASUREMENT			
TEST DATE	TEST TIME	SPECIMEN TEMP.(F)	"PINS ONLY" (scc He/sec)	"TOTAL" (scc He/sec)	COMMENTS	ELAPSED HOURS
6/10/91	0815	425	2.00E-10		COOLDOWN	152
6/10/91	0830	495	2.00E-10			152
6/10/91	0850	489	2.00E-10			152
6/10/91	0900	507	2.00E-10			153
6/10/91	0915	536	2.00E-10			153
6/10/91	0940	568	2.00E-10			153
6/10/91	1010	607	2.00E-10			154
6/10/91	1020	617	2.00E-10			154
6/10/91	1030	626	2.00E-10			154
6/10/91	1045	640	2.00E-10			154
6/10/91	1055	649	2.00E-10	3.77E-7		155
6/10/91	1155	650		5.05E-8		156
6/10/91	1200	660	2.00E-10			156
6/10/91	1215	670	2.00E-10			156
6/10/91	1230	680	2.00E-10	1.44E-8		156
6/10/91	1300	673		1.32E-8		157
6/10/91	1330	676	2.00E-10	1.19E-8		157
6/10/91	1335	682	2.00E-10			157
6/10/91	1340	687	2.00E-10			157
6/10/91	1345	697	2.00E-10			157
6/10/91	1350	700	2.00E-10	1.26E-8		158
6/10/91	1500	701	2.00E-10	3.67E-8		159
6/10/91	1510	657		2.33E-8		159
6/10/91	1520	611		9.45E-9		159
6/10/91	1530	573		1.54E-8		159
6/10/91	1540	543		2.69E-6	*INDICATION OF	159
6/10/91	1545	529		9.85E-6	O-RING FAILURE DUE	159
6/10/91	1550	517		2.76E-5	TO EXCESSIVE	160
6/10/91	1555	501		4.71E-5	COMPRESSION SET FOR	160
6/10/91	1600	490		6.68E-5	"TOTAL" LEAK RATE	160
6/10/91	1605	477		1.44E-4		160
6/10/91	1610	465		1.60E-4		160
6/10/91	1615	454				160
6/11/91	1400	85	2.00E-10	6.30E-4		182
6/13/91	0810	82	2.00E-10		*"TOTAL" LEAK RATE	224
6/13/91	0815	113	2.00E-10		NOT MEASURED DURING	224
6/13/91	0820	135	2.00E-10		2ND THERMAL CYCLE	224
6/13/91	0825	160	2.00E-10			224
6/13/91	0830	179	2.00E-10			224
6/13/91	0840	222	2.00E-10			224
6/13/91	0850	260	2.00E-10			224
6/13/91	0900	293	2.00E-10			225
6/13/91	0915	340	2.00E-10			225
6/13/91	0930	384	2.00E-10			225
6/13/91	0945	422	2.00E-10			225
6/13/91	1000	459	2.00E-10			226

BEST COPY AVAILABLE

APPENDIX B

EPG MOD 3 RECEPTACLE THERMAL MARGIN TEST DATA

RECEPTACLE P/N MCM24217/4-206M

RECEPTACLE S/N 614

			LEAK RATE MEASUREMENT			
TEST DATE	TEST TIME	SPECIMEN TEMP.(F)	"PINS ONLY" (scc He/sec)	"TOTAL" (scc He/sec)	COMMENTS	ELAPSED HOURS
6/13/91	1015	492	2.00E-10			226
6/13/91	1030	520	2.00E-10			226
6/13/91	1045	547	2.00E-10			226
6/13/91	1100	566	2.00E-10			227
6/13/91	1115	596	2.00E-10			227
6/13/91	1200	649	2.00E-10			228
6/13/91	1230	685	2.00E-10			228
6/13/91	1300	703	2.00E-10			229
6/13/91	1315	711	2.00E-10			229
6/13/91	1320	595	2.00E-10			229
6/13/91	1325	650	2.00E-10			229
6/13/91	1330	623	2.00E-10			229
6/13/91	1335	584	2.00E-10			229
6/13/91	1340	560	2.00E-10			229
6/13/91	1350	509	2.00E-10			230
6/13/91	1400	463	2.00E-10			230
6/13/91	1415	407	2.00E-10			230
6/13/91	1430	359	2.00E-10			230
6/13/91	1500	294	2.00E-10			231
6/13/91	1515	258	2.00E-10			231
6/13/91	1530	226	2.00E-10			231
6/13/91	1600	201	2.00E-10			232

BEST COPY AVAILABLE

5.0 SHIELDING EVALUATION

Adequate shielding in the Radioisotope Thermoelectric Generator (RTG) Transportation System Package ensures that the most radioactive payload will not cause external dose rates to exceed the requirements of 71.47 and 71.51 of 10 CFR 71.

5.1 DISCUSSION AND RESULTS

The primary payload configuration to be transported inside a single RTG Transportation System Package is a general purpose heat source (GPHS) RTG. Because of a 5,000-W thermal limit inside the semitrailer, only one GPHS RTG can be shipped in the RTG exclusive-use transportation system trailer.

Primary shielding for the payload is provided by self-shielding of the plutonia fuel, the RTG body, the inner containment vessel (ICV), the outer containment vessel (OCV), and, out the side of the package by the external coolant jacket. While the semitrailer provides little significance in the way of shielding, it defines the physical boundary for determining external dose rates by regulatory normal conditions of transport (NCT). Regulatory hypothetical accident condition (HAC) dose rates are determined relative to the package surface.

Regulatory NCT and HAC shielding requirements for the package are determined by the following criteria;

NCT: per the requirements of 10 CFR 71.47, maximum dose rates of 1,000 mrem/hr at any point in contact with the secured package within the closed transport vehicle; 200 mrem/hr at any point on the outer surface of the vehicle; 10 mrem/hr at any lateral point 2 m from the outer surface of the vehicle; and 2 mrem/hr in the normally occupied positions of the vehicle.

HAC: per the requirement of 10 CFR 71.51(a)(2), a maximum dose rate of 1,000 mrem/hr at any point 1 m from the package.

Tables 5-1 and 5-1a summarize the results of the radiation shielding analyses for the regulatory NCT and HAC events. The 2nd entry in the "Gamma" column of Tables 5-1 and 5-1a is the contribution from gamma rays produced by neutrons, the 3rd entry is the contribution from the gamma source and the 1st entry is the total contribution from gammas (sum of 2nd and 3rd entry). Adequate shielding is available to meet all regulatory requirements in all cases. Also, the dose rates for NCT are verified before releasing the package for shipment. The calculations summarized in Table 5-1 were made with coolant in the coolant jacket. To compensate for the presence of coolant, new dose rate limits were calculated to ensure the limits of 10 CFR 71.47 would be met if the coolant water was lost. These operational control dose limits are listed in Table 5-1 and are used when coolant is present in the package. For completeness, the shielding results without coolant in the package coolant jacket are listed in Table 5-1a. However, it is noted that water is included in the coolant jacket for the NCT model described in Section 5.3.1 and the NCT model input files listed in Appendices 5.5.2 and 5.5.3.

Even though the generic payload definition (see Chapter 1) allows a PuO_2 content per trailer that is higher than that for a single GPHS RTG, the potential increase in dose rates due to the larger total PuO_2 mass is offset by geometry effects. Specifically, the minimum required separation distance of 9.5 feet between package centerlines when shipping more than a single package is sufficient to ensure reduced dose rates for two-package shipments. The shielding analysis for two packages per trailer is documented in the RTG Transportation System SARP Addendum,

WHC-SD-RTG-SARP-002.

5.2 SOURCE SPECIFICATION

The GPHS RTG is comprised of 18 GPHS modules consisting of a graphite aeroshell which, in turn, houses two graphite impact shells. Each graphite impact shell contains two iridium-cladded fuel pellets. Each of the 72 fuel pellets contain a maximum of 157 g of plutonia for a maximum total fuel mass of 11,304 g. Figure 5-1 illustrates the GPHS RTG and internal subcomponents and Figure 5-2 depicts a GPHS fuel module.

Tables 5-2 and 5-3 delineate the fuel pellet and initial fuel properties for the GPHS RTG. Tables 5-4 and 5-5 present the gamma[1] and neutron[2] spectra respectively for a single 157-g fueled clad. The values in Tables 5-4 and 5-5 are multiplied by 72 in the shielding analyses to reflect the total number of fueled clads in a GPHS RTG. Further, the gamma spectrum used in Table 5-4 is for a fuel age of 17.5 years, at which time the maximum gamma flux occurs. The neutron spectrum used in Table 5-5 conservatively ignores flux reduction because of plutonium decay ($T_{\frac{1}{2}}$ for ^{238}Pu is 87.74 years) and is based on a maximum neutron emission rate of 6000 n/s-g ^{238}Pu for a GPHS fueled clad. The alpha-n source was determined by subtracting the spontaneous fission source from the maximum neutron emission rate of 6000 n/s-g ^{238}Pu. The neutron spectrum from the Monte Carlo Neutron Photon (MCNP)[3,4] calculation includes all subcritical multiplication from fissions of ^{238}Pu and ^{239}Pu. Additional source term data are provided in Tables 5-6 and 5-7.

TABLE 5-1. Summary of Maximum Dose Rates With Coolant in the Jacket (mrem/hr).

Normal conditions of transport location	Gamma	Neutron	Total	Regulatory Limit	Operational Control Limit[c]
Side, surface of package	68.32 (.16%)[a] 2.09 (.47%) 66.23 (.14%)	115.5 (.33%)	183.8 (.22%)	1,000	590
Side, surface of semitrailer	11.54 (.32%) 0.262 (.8%) 11.28 (.31%)	21.68 (.48%)	33.22 (.34%)	200	120
Two meters from side surface of semitrailer	1.83 (.17%) 0.041(.35%) 1.79 (.15%)	3.93 (.24%)	5.76 (.18%)	10	6.4
Top surface of package	53.56 (.82%) 0.76 (2.5%) 52.80 (.76%)	156.1 (1.2%)	209.7 (.92%)	1,000	1,000
Top surface of semitrailer	12.97 (.62%) 0.184 (1.6%) 12.78 (.56%)	34.90 (.8%)	47.87 (.61%)	200	200
Bottom surface of semitrailer	1.025 (1.3%) 0.052 (2.8%) 0.973 (1.2%)	13.32 (0.8%)	14.35 (.75%)	200	190
Tractor cab (operator's seat)	0.31 (.19%) 0.0068 (.39%) 0.294 (.15%)	0.705 (.26%)	1.01 (.19%)	2	1.2
Hypothetical accident conditions	Gamma	Neutron	Total	Regulatory Limit	
One meter from the top surface of the package[b]	20.64 (.36%) 0.40 (1.2%) 20.24 (.32%)	112.50 (1.0%)	133.1 (.85%)	1,000	

[a]( ) = One standard deviation statistical uncertainties.

[b]For the HAC analyses, the plutonia fuel is conservatively reconfigured as a sphere located at the package top where shielding is a minimum (see Section 5.3.2).

[c]Operational control limit used when coolant is present in package. This applies only to NCT.

TABLE 5-1a. Summary of Maximum Dose Rates Without Coolant in the Jacket (mrem/hr).

Normal conditions of transport location	Gamma	Neutron	Total	Regulatory Limit
Side, surface of package	74.92 (.16%)[a] 0.57 (.95%) 74.35 (.14%)	230.2 (.40%)	305.1 (.31%)	1,000
Side, surface of semitrailer	12.64 (.32%) 0.087 (2.2%) 12.55 (.31%)	39.46 (.67%)	52.10 (.52%)	200
Two meters from side surface of semitrailer	2.01 (.18%) 0.014 (.71%) 1.99 (.16%)	6.99 (.30%)	9.00 (.24%)	10
Top surface of package	53.65 (.80%) 0.39 (4.4%) 53.26 (.74%)	147.73 (1.8%)	201.4 (1.4%)	1,000
Top surface of semitrailer	12.88 (.64%) 0.090 (2.6%) 12.79 (.58%)	33.33 (1.1%)	46.21 (.82%)	200
Bottom surface of semitrailer	1.14 (1.3%) 0.023 (4.1%) 1.120 (1.2%)	13.82 (1.2%)	14.96 (1.1%)	200
Tractor cab (operator's seat)	0.332 (.14%) 0.0025 (.74%) 0.329 (.17%)	1.26 (.33%)	1.59 (.26%)	2
Hypothetical accident conditions	Gamma	Neutron	Total	Regulatory Limit
One meter from the top surface of the package[b]	20.64 (.36%) 0.40 (1.2%) 20.24 (.32%)	112.50 (1.0%)	133.1 (.85%)	1,000

[a]( ) = One standard deviation statistical uncertainties.

[b]For the HAC analyses, the plutonia fuel is conservatively reconfigured as a sphere located at the package top where shielding is a minimum (see Section 5.3.2).

TABLE 5-2. GPHS RTG Fuel Physical, Thermal, and Radiological Properties.

Fuel pellet property (excluding cladding)	GPHS fuel pellet
Diameter (cm)	2.7534 (±0.0254)
Length (cm)	2.7559 (±0.0381)
Volume (cm^3)	16.409
Density (g/cm^3)	9.6
Weight (g)	157
Thermal power (W)	62.5
Power density (W/cm^3)	3.81
Activity (Ci)	1,990
Specific activity (Ci/g)	12.6

TABLE 5-3. Plutonium-238 Initial Fuel Properties.

^{238}Pu content	80 to 86 mol-% of total plutonium
^{236}Pu content	<0.0001 mol-% of total plutonium
Sum of actinide impurities	<1.0 mol-% of total plutonium
Individual actinide impurities	<0.5 mol-% of total plutonium
^{18}O contained in PuO_2 (a)	>99.98 mol-% of total oxygen in PuO_2
Sum of nonactinide cationic impurities	<0.2250 wt-% of fuel
Individual nonactinide cationic impurities	<0.0800 wt-% of fuel
Specific thermal power at time of manufacture	0.40 W per gram PuO_2 fuel
Approximate reduction of thermal power	0.8% per year
Maximum neutron emission rate for GPHS fueled clad	6000 n/s-g ^{238}Pu

(a) Atoms of oxygen are exchanged until the oxygen in PuO_2 is 99.98 mol-% ^{18}O. See Reference 5.1.

TABLE 5-4. Total Gamma Ray Source from One 157-g Pellet[1] (17½-year plutonia fuel).

E_{min} (MeV)	E_{av} (MeV)	E_{max} (MeV)	1ppm ^{238}Pu Source (ph/sec)
0.15	0.20	0.25	6.82E+08
0.25	0.30	0.35	4.96E+07
0.35	0.40	0.45	4.03E+06
0.45	0.50	0.55	9.25E+06
0.55	0.60	0.65	7.33E+06
0.65	0.70	0.75	1.78E+07
0.75	0.80	0.85	6.76E+06
0.85	0.90	0.95	6.72E+06
0.95	1.00	1.05	1.37E+06
1.05	1.10	1.15	5.30E+05
1.15	1.20	1.25	1.97E+05
1.25	1.30	1.35	1.00E+05
1.35	1.40	1.45	2.20E+04
1.45	1.50	1.55	3.31E+05
1.55	1.60	1.65	1.42E+06
1.65	1.70	1.75	8.22E+04
1.75	1.80	1.85	1.17E+05
1.85	1.90	1.95	1.31E+04
1.95	2.00	2.05	1.11E+04
2.05	2.10	2.15	1.00E+04

TABLE 5-4. Total Gamma Ray Source from One 157-g Pellet[1] (17½-year plutonia fuel). (Cont.)

E_{min} (MeV)	E_{av} (MeV)	E_{max} (MeV)	1ppm ^{238}Pu Source (ph/sec)
2.15	2.20	2.25	8.95E+03
2.25	2.30	2.35	7.95E+03
2.35	2.40	2.45	7.08E+03
2.45	2.50	2.55	6.25E+03
2.55	2.60	2.65	3.33E+07
2.65	2.70	2.75	4.99E+03
2.75	2.80	2.85	4.50E+03
2.85	2.90	2.95	4.03E+03
2.95	3.00	3.05	3.64E+03
3.05	3.10	3.15	3.27E+03
3.15	3.20	3.25	2.98E+03
3.25	3.30	3.35	2.67E+03
3.35	3.40	3.45	2.42E+03
3.45	3.50	3.55	2.21E+03
3.55	3.60	3.65	2.01E+03
3.65	3.70	3.75	1.83E+03
3.75	3.80	3.85	1.66E+03
3.85	3.90	3.95	1.54E+03
3.95	4.00	4.05	1.42E+03
4.05	4.10	4.15	1.29E+03

TABLE 5-4. Total Gamma Ray Source from One 157-g Pellet[1] (17½-year plutonia fuel). (Cont.)

E_{min} (MeV)	E_{av} (MeV)	E_{max} (MeV)	1ppm ^{236}Pu Source (ph/sec)
4.15	4.20	4.25	1.20E+03
4.25	4.30	4.35	1.11E+03
4.35	4.40	4.45	1.01E+03
4.45	4.40	4.55	9.33E+02
4.55	4.50	4.65	8.59E+02
4.65	4.60	4.75	7.92E+02
4.75	4.70	4.85	7.37E+02
4.85	4.90	4.95	6.79E+02
4.95	5.00	5.05	6.34E+02
5.05	5.10	5.15	5.74E+02
5.15	5.20	5.25	5.25E+02
5.25	5.30	5.35	4.87E+02
5.35	5.40	5.45	4.53E+02
5.45	5.50	5.55	4.16E+02
5.55	5.60	5.65	3.83E+02
5.65	5.70	5.75	3.54E+02
5.75	5.80	5.85	3.22E+02
5.85	5.90	5.95	2.97E+02
5.95	6.00	6.05	2.72E+02
6.05	6.10	6.15	2.49E+02

TABLE 5-4. Total Gamma Ray Source from One 157-g Pellet[1] (17½-year plutonia fuel). (Cont.)

E_{min} (MeV)	E_{av} (MeV)	E_{max} (MeV)	1ppm ^{238}Pu Source (ph/sec)
6.15	6.20	6.25	2.30E+02
6.25	6.30	6.35	2.10E+02
6.35	6.40	6.45	1.92E+02
6.45	6.50	6.55	1.70E+02
6.55	6.60	6.65	1.56E+02
6.65	6.70	6.75	1.40E+02
6.75	6.80	6.85	1.26E+02
6.85	6.90	6.95	1.12E+02
6.95	7.00	7.05	1.02E+02
7.05	7.10	7.15	8.92E+01
7.15	7.20	7.25	7.68E+01
7.25	7.30	7.35	6.68E+01
7.35	7.40	7.45	5.70E+01
7.45	7.50	7.55	4.74E+01
7.55	7.60	7.65	3.76E+01
	Total		8.21E+08

TABLE 5-5. Neutron Spectrum for a Single Fueled Clad[2] (157 g maximum, new plutonia fuel).

Energy (MeV)	n/pellet-sec for (α,n)	n/pellet-sec for s.f.	n/pellet-sec total	Fraction of flux at E_i
0.1	4.63×10^{3}	5.60×10^{3}	1.02×10^{4}	1.43×10^{-2}
0.2	5.17×10^{3}	7.42×10^{3}	1.26×10^{4}	1.76×10^{-2}
0.3	5.03×10^{3}	8.51×10^{3}	1.35×10^{4}	1.90×10^{-2}
0.4	5.98×10^{3}	9.14×10^{3}	1.51×10^{4}	2.12×10^{-2}
0.5	8.16×10^{3}	9.56×10^{3}	1.77×10^{4}	2.49×10^{-2}
0.6	9.18×10^{3}	9.78×10^{3}	1.90×10^{4}	2.66×10^{-2}
0.7	1.01×10^{4}	9.86×10^{3}	2.00×10^{4}	2.79×10^{-2}
0.8	1.10×10^{4}	9.82×10^{3}	2.08×10^{4}	2.92×10^{-2}
0.9	1.06×10^{4}	9.74×10^{3}	2.03×10^{4}	2.84×10^{-2}
1.0	8.70×10^{3}	9.55×10^{3}	1.83×10^{4}	2.56×10^{-2}
1.1	9.11×10^{3}	9.34×10^{3}	1.84×10^{4}	2.59×10^{-2}
1.2	9.86×10^{3}	9.06×10^{3}	1.89×10^{4}	2.65×10^{-2}
1.3	1.11×10^{4}	8.81×10^{3}	1.99×10^{4}	2.79×10^{-2}
1.4	1.20×10^{4}	8.52×10^{3}	2.05×10^{4}	2.87×10^{-2}
1.5	1.22×10^{4}	8.20×10^{3}	2.04×10^{4}	2.87×10^{-2}
1.6	1.28×10^{4}	7.87×10^{3}	2.07×10^{4}	2.91×10^{-2}
1.7	1.40×10^{4}	7.54×10^{3}	2.15×10^{4}	3.01×10^{-2}
1.8	1.55×10^{4}	7.21×10^{3}	2.27×10^{4}	3.19×10^{-2}
1.9	1.61×10^{4}	6.90×10^{3}	2.30×10^{4}	3.23×10^{-2}
2.0	1.69×10^{4}	6.57×10^{3}	2.35×10^{4}	3.30×10^{-2}
2.1	1.70×10^{4}	6.28×10^{3}	2.33×10^{4}	3.26×10^{-2}

TABLE 5-5. Neutron Spectrum for a Single Fueled Clad[2] (157 g maximum, new plutonia fuel). (Cont.)

Energy (MeV)	n/pellet-sec for (α,n)	n/pellet-sec for s.f.	n/pellet-sec total	Fraction of flux at E_i
2.2	1.78×10^{4}	5.98×10^{3}	2.38×10^{4}	3.33×10^{-2}
2.3	1.81×10^{4}	5.68×10^{3}	2.38×10^{4}	3.32×10^{-2}
2.4	1.72×10^{4}	5.39×10^{3}	2.26×10^{4}	3.18×10^{-2}
2.5	1.65×10^{4}	5.10×10^{3}	2.16×10^{4}	3.03×10^{-2}
2.6	1.59×10^{4}	4.82×10^{3}	2.07×10^{4}	2.91×10^{-2}
2.7	1.52×10^{4}	4.58×10^{3}	1.98×10^{4}	2.77×10^{-2}
2.8	1.40×10^{4}	4.33×10^{3}	1.83×10^{4}	2.70×10^{-2}
2.9	1.36×10^{4}	4.08×10^{3}	1.77×10^{4}	2.48×10^{-2}
3.0	1.28×10^{4}	3.84×10^{3}	1.66×10^{4}	2.33×10^{-2}
3.1	1.13×10^{4}	3.63×10^{3}	1.49×10^{4}	2.09×10^{-2}
3.2	1.06×10^{4}	3.44×10^{3}	1.40×10^{4}	1.7×10^{-2}
3.3	9.11×10^{3}	3.42×10^{3}	1.24×10^{4}	1.73×10^{-2}
3.4	7.41×10^{3}	3.04×10^{3}	1.04×10^{4}	1.47×10^{-2}
3.5	6.26×10^{3}	2.84×10^{3}	9.10×10^{3}	1.28×10^{-2}
3.6	5.37×10^{3}	2.69×10^{3}	8.06×10^{3}	1.13×10^{-2}
3.7	4.35×10^{3}	2.53×10^{3}	6.88×10^{3}	9.66×10^{-3}
3.8	3.74×10^{3}	2.38×10^{3}	6.12×10^{3}	8.58×10^{-3}
3.9	3.26×10^{3}	2.23×10^{3}	5.49×10^{3}	7.70×10^{-3}
4.0	2.65×10^{3}	2.07×10^{3}	4.72×10^{3}	6.62×10^{-3}
4.1	2.38×10^{3}	1.96×10^{3}	4.34×10^{3}	6.08×10^{-3}
4.2	1.56×10^{3}	1.84×10^{3}	3.40×10^{3}	4.77×10^{-3}

TABLE 5-5. Neutron Spectrum for a Single Fueled Clad[2] (157 g maximum, new plutonia fuel). (Cont.)

Energy (MeV)	n/pellet-sec for (α,n)	n/pellet-sec for s.f.	n/pellet-sec total	Fraction of flux at E_i
4.3	1.22×10^{3}	1.72×10^{3}	2.94×10^{3}	4.13×10^{-3}
4.4	7.48×10^{2}	1.61×10^{3}	2.36×10^{3}	3.30×10^{-3}
4.5	4.76×10^{2}	4.47×10^{3}	4.95×10^{3}	6.94×10^{-3}
5.0		5.20×10^{3}	5.20×10^{3}	7.48×10^{-3}
5.5		3.79×10^{3}	3.79×10^{3}	5.30×10^{-3}
6.0		2.66×10^{3}	2.66×10^{3}	3.72×10^{-3}
6.5		1.85×10^{3}	1.85×10^{3}	2.60×10^{-3}
7.0		1.29×10^{3}	1.29×10^{3}	1.81×10^{-3}
7.5		8.92×10^{2}	8.92×10^{2}	1.25×10^{-3}
8.0		6.13×10^{2}	6.13×10^{2}	8.60×10^{-4}
8.5		4.21×10^{2}	4.21×10^{2}	5.90×10^{-4}
9.0		2.57×10^{2}	2.57×10^{2}	4.03×10^{-4}
9.5		1.97×10^{2}	1.97×10^{2}	2.76×10^{-4}
10.0		1.98×10^{2}	1.98×10^{2}	2.78×10^{-4}
11.0		1.21×10^{2}	1.21×10^{2}	1.70×10^{-4}
12.0		5.53×10^{1}	5.53×10^{1}	7.75×10^{-5}
13.0		2.48×10^{1}	2.48×10^{1}	3.48×10^{-5}
14.0		1.11×10^{1}	1.11×10^{1}	1.55×10^{-5}
15.0		4.90×10^{0}	4.90×10^{0}	6.88×10^{-6}
Total	4.36×10^{5}	2.77×10^{5}	7.13×10^{5}	

TABLE 5-6. Concentrations of Plutonium Isotopes and Actinide Impurities Used in Developing Tables 5-4 and 5-5.

Isotope	Wt-% Pu	Wt Fraction of PuO_2
^{236}Pu	1×10^{-4}	8.81×10^{-7}
^{238}Pu	86	7.58×10^{-1}
^{239}Pu	11.5	1.01×10^{-1}
^{240}Pu	2.0	1.76×10^{-2}
^{241}Pu	0.4	3.52×10^{-3}
^{242}Pu	0.1	8.81×10^{-4}
^{241}Am		2.5×10^{-4}
^{234}U		6.0×10^{-3}
^{232}Th		2.0×10^{-4}
^{237}Np		2.0×10^{-4}

TABLE 5-7. Limits on Impurities and Quantity of Oxygen and Their Contribution to the Neutron Spectrum.

Element	Max. concentration in fueled clad (wt%)	n/sec per fuel clad	% of total
B	1×10^{-6}	1.55×10^{3}	0.22
Mg	5×10^{-5}	4.94×10^{3}	0.69
Na	2.5×10^{-4}	4.07×10^{4}	5.70
Si	2×10^{-4}	1.72×10^{3}	0.24
O*	1.19×10^{-1}	3.88×10^{5}	54.34
(α,n) Total		4.36×10^{5}	61.20
Total neutrons		7.13×10^{5}	100.00

* Not an impurity; O is present as the oxide in PuO_2.

GPHS - RTG

FIGURE 5-1. GPHS RTG Assembly Detail.

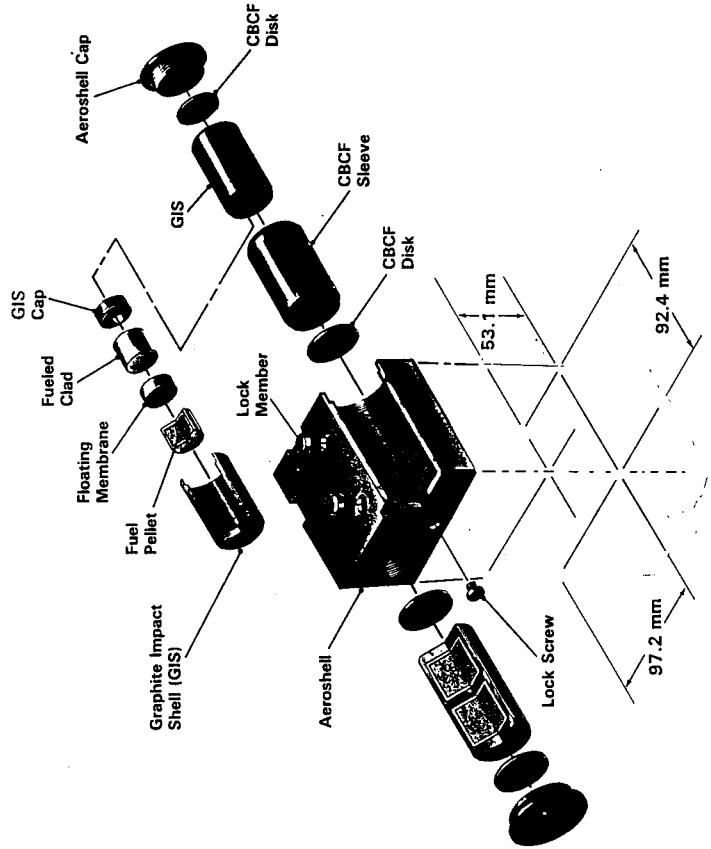


FIGURE 5-2. General Purpose Heat Source (GPHS) Assembly Detail.

5.3 MODEL SPECIFICATION

Two calculational models determine NCT and HAC dose rates. All gamma and neutron analyses are based on these two calculational models.

5.3.1 Regulatory Normal Conditions of Transport Model

Figure 5-3 shows an elevation view of the calculational model used for the NCT analyses. The NCT calculational model is comprised of a GPHS RTG payload model and RTG packaging model. The dimensions in Figure 5-3 are in centimeters. The central portion of the GPHS RTG payload model is identical to the central portion (without water reflector) of the calculational model for the criticality assessment (Chapter 6.0). The astroquartz insulation and thermopile and outer aluminum shell have been included beyond this central portion as shown in Figure 5-3.

Table 5-8 delineates the material compositions and densities used in this shielding calculational model. The neutron and gamma-ray sources are within the 72 small cylindrical cells of plutonia fuel.

Figure 5-4 shows an elevation view of the calculational model including the minimum width and height boundaries of the RTG Transportation System exclusive-use semitrailer. These boundaries were the locations for determining dose rates at the surfaces of the semitrailer.

The ground was treated in these calculations as Hanford soil. Only 11% of the neutron dose rate given in Table 5-1 at a distance of two meters from the side surface of the semitrailer was from scattering off the ground. Changing from Hanford soil to pure carbon for the ground reduces this dose rate from 0.43 (.50%) to 0.39 (.53%) mrem/hr; hence, the use of Hanford soil is conservative. The percentage contribution to the gamma ray portion of the dose rate is less than 2% from gamma rays scattering off the ground.

5.3.2 Regulatory Hypothetical Accident Condition Model

As shown in Figure 5-5, the HAC calculational model is conservatively configured into a spherical mass of homogenized plutonia fuel adjacent to the top center of the package model. The radius of this sphere is simply the radius to contain the 11,304 grams of plutonium oxide at a density of 9.60 g/cm^3, or r = 6.5508 cm. This spherical zone is summarized in Table 5-9, where the ICV and OCV are not changed for this HAC calculational model.

5.4 SHIELDING EVALUATION

This section discusses the basic methods used to determine the dose rates presented in the summary table for the NCT and HAC.

In all cases, NCT dose rates out the side of the package are determined at (1) r = 50.38 cm, which corresponds to the outside surface of the package, (2) 127.0 cm, which corresponds to the outside of a minimum width semitrailer (i.e., the semitrailer minimum width is 100 in.; thus, the trailer centerline-to-edge distance is 50 in.), (3) 327.0 cm, which corresponds to a distance 2 m from the side of the semitrailer, and (4) 847.09 cm, which corresponds to the tractor cab (estimated to be a minimum of 27.8 ft from the package centerline). All side detector distances are with reference to the source radial centerline.

TABLE 5-8. Summary of Material Compositions for the Normal Conditions of Transport Analysis Model.

Material description		Element name	Atomic No. (Z)	Partial density (g/cc)
RTG (3 different materials)	11,304 g Plutonium and Oxide	Plutonium	94	8.463
		Oxygen	8	1.137
	3370 g Clad	Iridium	77	22.50
	6732 g Carbon*	Carbon	6	1.950
Outer shell (0.1524 cm thick)		Aluminum	13	2.8523
ICV and OCV, Steel of Cooling Jacket; All Type 304L stainless steel*		Chromium	24	1.509
		Iron	26	5.509
		Nickel	28	0.852
		Manganese	25	0.159
		Carbon	6	0.0006
Cooling jacket coolant (water)		Hydrogen	1	0.1119
		Oxygen	8	0.8881
Dry air at 1.0 atmosphere		Nitrogen	7	0.0009333
		Oxygen	8	0.0002867

* The partial densities for the listed elements of Type 304L stainless steel are taken from the reference 4 data sets.

TABLE 5-9. Summary of the RTG Composition for the Hypothetical Accident Condition Analysis Model.

Material description	Element name	Atomic number(Z)	Partial density (g/cc)
RTG (11,304 g plutonia in sphere)	Plutonium	94	8.463
	Oxygen	8	1.137

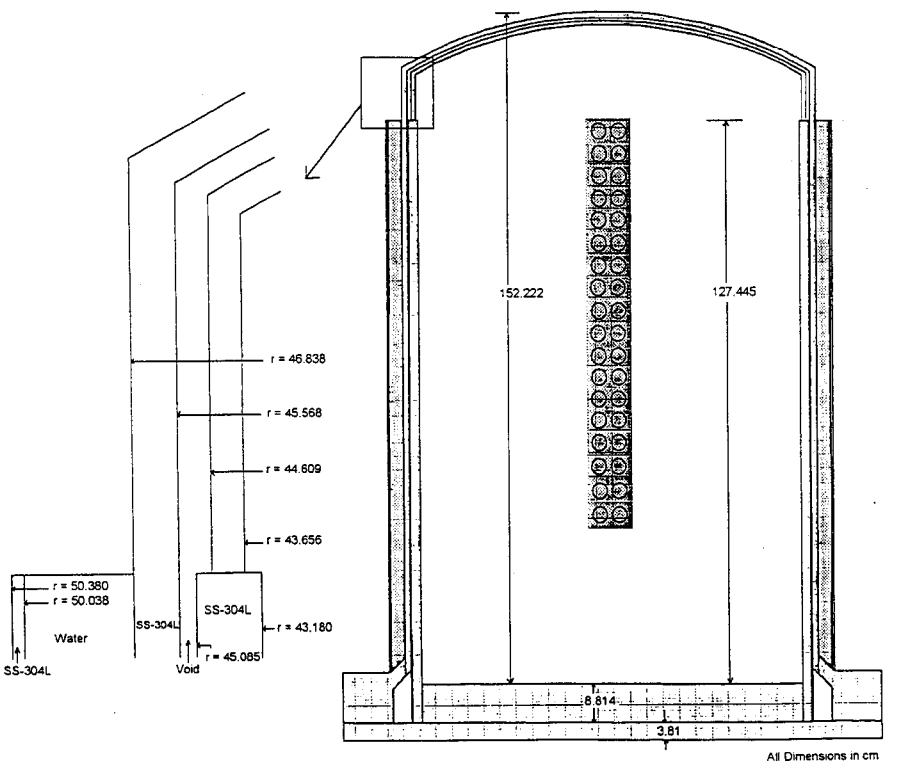


FIGURE 5-3. Elevation View of NCT Calculational Model Geometry Showing Dimensions.

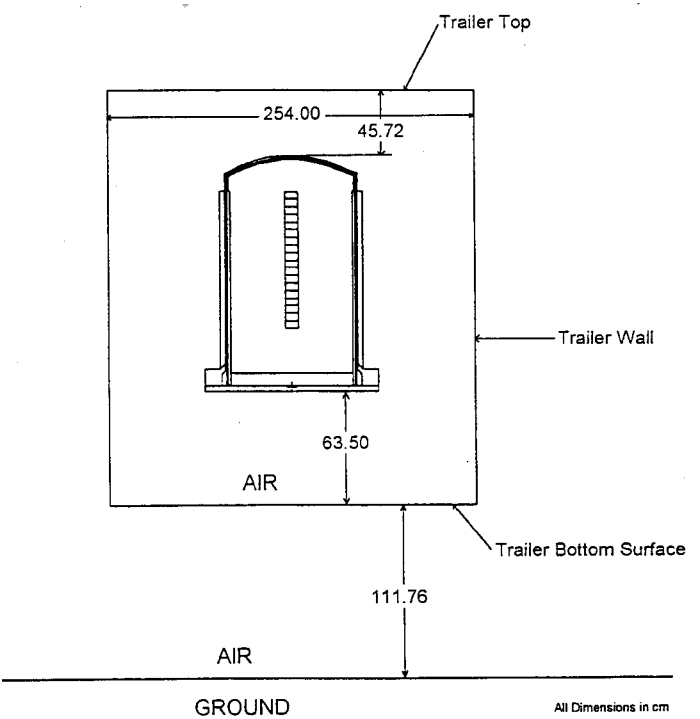


FIGURE 5-4. Elevation View of NCT Calculational Model Geometry Showing Outline of Semitrailer.

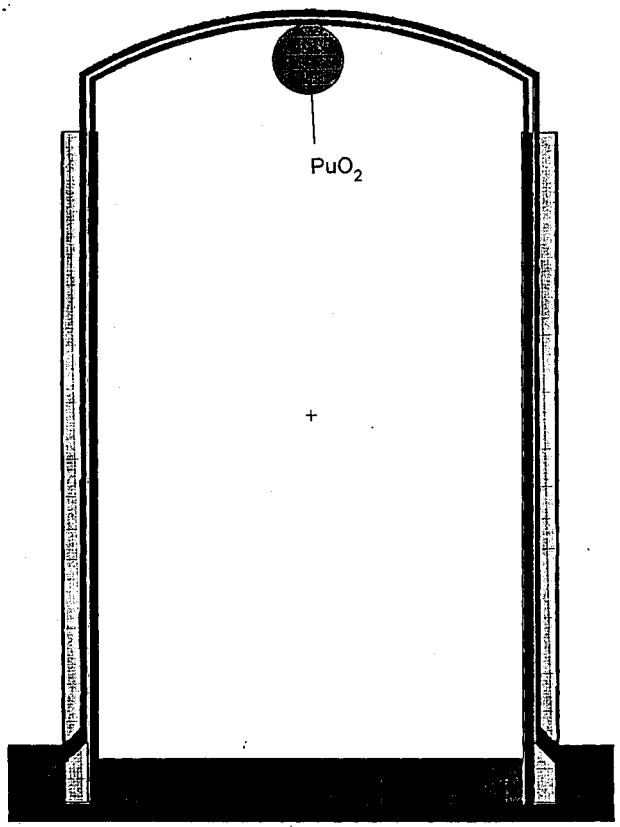


FIGURE 5-5. HAC Calculational Model Geometry.

Regulatory NCT dose rates out the package top are determined on the outer OCV surface, which corresponds to the outside surface of the package, and on the top of the semitrailer -- 45.78 cm (18 inches) above the top of the outer OCV surface.

Regulatory HAC dose rates are only determined out the package top where the minimum amount of gamma and neutron shielding exists. The HAC dose rates are determined at a distance of 1 m from the package top.

5.4.1 Gamma Shielding Analyses

All gamma shielding analyses are performed using the computer code MCNP[3,4]. There are two components to the gamma-rays, one from the gamma source in the RTG and the other from the gamma rays produced at neutron collisions. These latter gamma rays are included in the dose rate summary given in Table 5-1, but their contribution is typically only about one percent of that due to the gamma rays from the gamma source in the RTG. The MCNP analysis included Bremsstrahlung from the electrons produced during the photon transport, and the gamma source term included Bremsstrahlung from the electrons of the source. Gamma fluence-to-dose-rate (mrem/hr) conversion factors are based on ANSI/ANS 6.1.1[6]. The two MCNP input files for the NCT and HAC gamma shielding analysis are listed in Appendix 5.5.2.

5.4.2 Neutron Shielding Analyses

The neutron shielding analyses were also performed using the computer code MCNP[3,4]. The neutron input file was identical to that used for the gamma analysis except the neutron source of Table 5-5 was used rather than the gamma source of Table 5-4 and neutron tallies of dose rates were included. These analyses automatically included subcritical neutron multiplication.

Neutron fluence-to-dose-rate (mrem/hr) conversion factors, which include standard neutron quality factors, are based on ANSI/ANS 6.1.1[6].

The two MCNP input files for the NCT and HAC neutron shielding analysis are listed in Appendix 5.5.3.

5.4.3 Uncertainties in the Shielding Analysis Models

Components of uncertainties include sources, geometry description with the calculational models, attenuation (cross sections), and statistical in the Monte Carlo calculations. Because substantial detail has been included in the three-dimensional geometry calculational models, the uncertainty because of this is negligible compared to the other components of uncertainty. Similarly, neutron and photon cross sections are reasonably well known, especially for the rather small attenuations here, so their uncertainty is also assumed to be small. The statistical uncertainties shown in Table 5-1 are small -- a maximum of about 1.7% for the neutron portion of the dose rates, and about 1.4% for the gamma portion of the dose rates. Hence, the source is the dominant uncertainty. The neutron and gamma sources used in these calculations are conservative so that the dose rates given in Table 5-1 are really upper limit.

5.5 APPENDIX

The following is a list of appendices contained within this section:

5.5.1 References

5.5.2 Gamma Shielding Analyses MCNP Input Files

5.5.3 Neutron Shielding Analyses MCNP Input Files

5.5.1 References

1. Goldberg, H. J., 1995, *Neutron and Photon Spectrum and Abundances for an RTG Fuel Pellet and Comparison with Mound Document* (internal memo 8M730-HJG-95-020 to P. C. Ferrell, October 3, Table 2, Total Gamma Ray Source from one 157 g Pellet), Westinghouse Hanford Company, Richland, Washington.

2. Goldberg, H. J., 1995, *Neutron and Photon Spectrum and Abundances for an RTG Fuel Pellet and Comparison with Mound Document* (internal memo 8M730-HJG-95-020 to P. C. Ferrell, October 3, Table 1, Neutron Spectrum and Abundance, Westinghouse Hanford Company, Richland, Washington.

3. Breismeister, J.F., 1993, Editor, "MCNP - A General Monte Carlo Code N-Particle Transport Code, Version 4A," LA-12625, Los Alamos National Laboratory, Los Alamos, New Mexico.

4. Carter, L.L., 1994, "Certification of MCNP Version 4A for WHC Computer Platforms," ECN 186710, Westinghouse Hanford Company, Richland, Washington.

5. ANSI/ANS-1977 (N666), Neutron and Gamma Ray Flux-to-Dose Rate Factors, American Nuclear Society, and DOE 5480.11, *Radiation Protection for Occupational Workers*, 12-21-88.

6. General Electric, 1991, *Acceptance Specification for Fine Weave Pierced Fabric (FWPF) Graphite*, NS0060-01-20, Rev. C, 12/91, General Electric Astro Space Division.

5.5.2 Gamma Shielding Analyses MCNP Input Files

```
NCT GAMMA SHIELDING MCNP INPUT FILE

SHLD. CALC., GPHS-RTG, GAMMA, water, no q, p.det., rev mar 96 igdq
    1     0  -5 6 -1 3 -4 2  trcl=1 fill=1
    2     0  -7 8    u=1    lat=1
           fill=0:17 0:0 0:0   2 17r
    3     1  -1.9500  -9 (12 :-11 :20 )(14 :-13 :20 ) u=2
    4     1  -1.9500  -10 (12 :-11 :22 )(14 :-13 :22 ) u=2
    5     1  -1.9500  9 10  u=2
    6     2 -22.5  -12 11 -20 (-15 :16 :19 ) u=2
    7     2 -22.5  -14 13 -20 (-17 :18 :19 ) u=2
    8     3  -9.6000  -16 15 -19  u=2
    9     3  -9.6000  -18 17 -19  u=2
   10     2 -22.5  -12 11 -22 (-15 :16 :21 ) u=2
   11     2 -22.5  -14 13 -22 (-17 :18 :21 ) u=2
   12     3  -9.6000  -16 15 -21  u=2
   13     3  -9.6000  -18 17 -21  u=2
c       Astroquartz insulation and thermopile and Al shell
   14   231 -.00122  -121  134 -135   #1
   15     0          -122  133 -136  (121:-134:135)
   16   231 -.00122  -123  132 -137  (122:-133:136)
   17    12 -2.85    -124  131 -138  (123:-132:137)
c      inner containment
   21   231 -.00122 ((6 -52 -31 ):(52 -33 -53 )) (124:-131:138)
   22   201  -8.0300  51 -52 31 -32
   23   201  -8.0300  (52 -34 -54 )(33 :53 )
   24   201  -8.0300  51 -6 -31
c      outer containment
   41   231 -.00122 51 35 -64 -39
   42   231 -.00122 ((51 -35 -62 )(52 :32 ))(-52 :34 :54 )
   43   201  -8.0300  (-36 64 -63 )(62 :35 )
   44   237  -1.0 -52 65 36 -37
   45   201  -8.0300  -52 65 37 -38
   46   201  -8.0300  ((64 -65 36 51 -40 ):(-64 39 51 )):(65 38 -66 -40 )
   47   201  -8.0300  61 -51 -40
c       beyond outer containment and inside truck boundary
   71   231 -.00122 (((-52 :36 :63 ))(52 :38 :-66 ))(66 :40 :-61 )
              71 -72 73 -74 75 -76
c      beyond truck and inside large sphere, above ground
   72   231 -.00122  (-71:72:-73:74:-75:76)  77  -111
c     ground
   73   221 -1.67    -77 -111
c       outside world
   74     0  111

    1        py   4.659
    2        px  -4.859
    3        py  -4.659
    4        px   4.859
    5        pz  95.544
    6        pz  0.0000
```

```
    7        pz  5.30801
    8        pz  -0.00001
    9       c/y  -2.184  2.654  1.831
   10       c/y   2.184  2.654  1.831
   11        py  -3.1618
   12        py  -0.2941
   13        py  0.2941
   14        py  3.1618
   15        py  -3.1059
   16        py  -0.350
   17        py   0.350
   18        py  3.1059
   19       c/y  -2.1840 2.6540 1.3767
   20       c/y  -2.1840 2.6540 1.4326
   21       c/y  2.1840 2.6540 1.3767
   22       c/y  2.1840 2.6540 1.4326
c   radial surfaces for inner and outer containment
   31        cz  43.1800
   32        cz  45.0850
   33        cz  43.6562
   34        cz  44.6088
   35        cz  45.5676
   36        cz  46.8376
   37        cz  50.0380
   38        cz  50.3796
   39        cz  49.6443
   40        cz  61.3410
c   inner containment
   51        pz  -8.8138
   52        pz  127.4450
   53        sz  60.3377 88.9000
   54        sz  60.3377 89.8525
c   outer containment
   61        pz  -12.6238
   62        sz  60.1472 90.8050
   63        sz  60.1472 92.0750
   64        kz  48.7807 1.0000 -1.0000
   65        kz  53.0733 1.0000 -1.0000
   66        pz  2.6940
c     truck outside boundary
   71     px  -615.95
   72     px   603.25
   73     py  -127.00
   74     py   127.00
   75     pz  -72.3138
   76     pz   198.0
   77     pz  -184.0738
c      tally fs surfaces on outside of truck
   81     px   -90.0
   82     px   -30.0
   83     px    30.0
   84     px    90.0
   85     py   -90.0
   86     py   -30.0
```

```
   87      py    30.0
   88      py    90.0
   89      pz   -11.0
   90      pz    49.0
   91      pz   109.0
   92      pz   169.0
   93      pz    63.76
   94      pz    94.24
   95      cz    15.24
c      outside world.
  111        so  5000.0000
  121   cz  7.1165
  122   cz  8.8945
  123   cz 10.6426
  124   cz 10.7950
  131   pz  23.348
  132   pz  23.5004
  133   pz  29.6725
  134   pz  31.4505
  135   pz 127.0055
  136   pz 128.7835
  137   pz 134.9556
  138   pz 135.108

*tr1  0  0 31.4560
mode    p
m1    6000.01p  -1.950000
m2    77000.01p  -22.500000
m3    94000.01p -8.463     8000.01p -1.137
m11    8000.01p -.9631  14000.01p -.8452  42000.01p -.3391  $ ins.+therm.
m12   13000.01p -1.
m201  26000.01p 67.970001 24000.01p 20.000000 28000.01p 10.000000
      25000.01p 2.000000 6000.01p 0.030000
m221  8000.01p -0.511000 14000.01p -0.278200 20000.01p -0.071700
      26000.01p -0.109100 13000.01p -0.083260 12000.01p -0.031420
      19000.01p -0.011550 11000.01p -0.020220 22000.01p -0.016550
      25000.01p -0.001781 15000.01p -0.002400
m231  7000.01p -0.765000 8000.01p -0.235000
m236  1000.01p 0.666700 8000.01p 0.333300
imp:p  1          16r        4          3r         16         $ 1, 41
       8r  8         0          $ 42, 73
print   10 30 40 50 60 100 110 120 126 170
c       phys:p    j  1
cut:p    j j 0. 0.
sdef     cel d1  axs 0 1 0  rad d4  ext d5  erg=d9
           pos fcel d6    wgt=5.9118e10
c      source uniformly in all 72 lattice cells
sil  1 1:2(0 0 0):8  1:2(0 0 0):9  1:2(0 0 0):12  1:2(0 0 0):13
       1:2(1 0 0):8  1:2(1 0 0):9  1:2(1 0 0):12  1:2(1 0 0):13
       1:2(2 0 0):8  1:2(2 0 0):9  1:2(2 0 0):12  1:2(2 0 0):13
       1:2(3 0 0):8  1:2(3 0 0):9  1:2(3 0 0):12  1:2(3 0 0):13
       1:2(4 0 0):8  1:2(4 0 0):9  1:2(4 0 0):12  1:2(4 0 0):13
       1:2(5 0 0):8  1:2(5 0 0):9  1:2(5 0 0):12  1:2(5 0 0):13
       1:2(6 0 0):8  1:2(6 0 0):9  1:2(6 0 0):12  1:2(6 0 0):13
```

```
      1:2(7 0 0):8  1:2(7 0 0):9  1:2(7 0 0):12  1:2(7 0 0):13
      1:2(8 0 0):8  1:2(8 0 0):9  1:2(8 0 0):12  1:2(8 0 0):13
      1:2(9 0 0):8  1:2(9 0 0):9  1:2(9 0 0):12  1:2(9 0 0):13
     1:2(10 0 0):8 1:2(10 0 0):9 1:2(10 0 0):12 1:2(10 0 0):13
     1:2(11 0 0):8 1:2(11 0 0):9 1:2(11 0 0):12 1:2(11 0 0):13
     1:2(12 0 0):8 1:2(12 0 0):9 1:2(12 0 0):12 1:2(12 0 0):13
     1:2(13 0 0):8 1:2(13 0 0):9 1:2(13 0 0):12 1:2(13 0 0):13
     1:2(14 0 0):8 1:2(14 0 0):9 1:2(14 0 0):12 1:2(14 0 0):13
     1:2(15 0 0):8 1:2(15 0 0):9 1:2(15 0 0):12 1:2(15 0 0):13
     1:2(16 0 0):8 1:2(16 0 0):9 1:2(16 0 0):12 1:2(16 0 0):13
     1:2(17 0 0):8 1:2(17 0 0):9 1:2(17 0 0):12 1:2(17 0 0):13
sp1   1. 71r
si4   1.3767
sp4   -21 1
si5   0. 2.7559
sp5   -21 0
ds6   1  -2.184 -3.1059 2.654  -2.184 .35 2.654
              2.184 -3.1059 2.654  2.184 .35 2.654
            -2.184 -3.1059 2.654  -2.184 .35 2.654
              2.184 -3.1059 2.654  2.184 .35 2.654
            -2.184 -3.1059 2.654  -2.184 .35 2.654
              2.184 -3.1059 2.654  2.184 .35 2.654
            -2.184 -3.1059 2.654  -2.184 .35 2.654
              2.184 -3.1059 2.654  2.184 .35 2.654
            -2.184 -3.1059 2.654  -2.184 .35 2.654
              2.184 -3.1059 2.654  2.184 .35 2.654
            -2.184 -3.1059 2.654  -2.184 .35 2.654
              2.184 -3.1059 2.654  2.184 .35 2.654
            -2.184 -3.1059 2.654  -2.184 .35 2.654
              2.184 -3.1059 2.654  2.184 .35 2.654
            -2.184 -3.1059 2.654  -2.184 .35 2.654
              2.184 -3.1059 2.654  2.184 .35 2.654
            -2.184 -3.1059 2.654  -2.184 .35 2.654
              2.184 -3.1059 2.654  2.184 .35 2.654
            -2.184 -3.1059 2.654  -2.184 .35 2.654
              2.184 -3.1059 2.654  2.184 .35 2.654
            -2.184 -3.1059 2.654  -2.184 .35 2.654
              2.184 -3.1059 2.654  2.184 .35 2.654
            -2.184 -3.1059 2.654  -2.184 .35 2.654
              2.184 -3.1059 2.654  2.184 .35 2.654
            -2.184 -3.1059 2.654  -2.184 .35 2.654
              2.184 -3.1059 2.654  2.184 .35 2.654
            -2.184 -3.1059 2.654  -2.184 .35 2.654
              2.184 -3.1059 2.654  2.184 .35 2.654
            -2.184 -3.1059 2.654  -2.184 .35 2.654
              2.184 -3.1059 2.654  2.184 .35 2.654
            -2.184 -3.1059 2.654  -2.184 .35 2.654
              2.184 -3.1059 2.654  2.184 .35 2.654
c     final gamma spectrum from Harvey , 157 g fueled clad
#          si9       sp9       sb9
```

h	d	d
0.1500	0.0000E+00	0.0000E+00
0.2500	0.6820E+09	0.1066E+08
0.3500	0.4960E+08	0.2127E+07
0.4500	0.4030E+07	0.3672E+06
0.5500	0.9250E+07	0.3773E+07
0.6500	0.7330E+07	0.3841E+07
0.7500	0.1780E+08	0.1156E+08
0.8500	0.6760E+07	0.5298E+07
0.9500	0.6720E+07	0.6222E+07
1.0500	0.1370E+07	0.1474E+07
1.1500	0.5300E+06	0.6536E+06
1.2500	0.1970E+06	0.2753E+06
1.3500	0.1000E+06	0.1569E+06
1.4500	0.2200E+05	0.3841E+05
1.5500	0.3310E+06	0.6387E+06
1.6500	0.1420E+07	0.3010E+07
1.7500	0.8220E+05	0.1903E+06
1.8500	0.1170E+06	0.2944E+06
1.9500	0.1310E+05	0.3567E+05
2.0500	0.1110E+05	0.3258E+05
2.1500	0.1000E+05	0.3153E+05
2.2500	0.8950E+04	0.3021E+05
2.3500	0.7950E+04	0.2864E+05
2.4500	0.7080E+04	0.2715E+05
2.5500	0.6250E+04	0.2545E+05
2.6500	0.3330E+08	0.1437E+09
2.7500	0.4990E+04	0.2276E+05
2.8500	0.4500E+04	0.2165E+05
2.9500	0.4030E+04	0.2042E+05
3.0500	0.3640E+04	0.1939E+05
3.1500	0.3270E+04	0.1828E+05
3.2500	0.2980E+04	0.1746E+05
3.3500	0.2670E+04	0.1637E+05
3.4500	0.2420E+04	0.1551E+05
3.5500	0.2210E+04	0.1478E+05
3.6500	0.2010E+04	0.1402E+05
3.7500	0.1830E+04	0.1329E+05
3.8500	0.1660E+04	0.1254E+05
3.9500	0.1540E+04	0.1209E+05
4.0500	0.1420E+04	0.1157E+05
4.1500	0.1290E+04	0.1091E+05
4.2500	0.1200E+04	0.1051E+05
4.3500	0.1110E+04	0.1007E+05
4.4500	0.1010E+04	0.9481E+04
4.5500	0.9330E+03	0.9055E+04
4.6500	0.8590E+03	0.8613E+04
4.7500	0.7920E+03	0.8199E+04
4.8500	0.7370E+03	0.7872E+04
4.9500	0.6790E+03	0.7478E+04
5.0500	0.6340E+03	0.7195E+04
5.1500	0.5740E+03	0.6708E+04
5.2500	0.5250E+03	0.6315E+04
5.3500	0.4870E+03	0.6026E+04

```
            5.4500    0.4530E+03    0.5764E+04
            5.5500    0.4160E+03    0.5439E+04
            5.6500    0.3830E+03    0.5144E+04
            5.7500    0.3540E+03    0.4881E+04
            5.8500    0.3220E+03    0.4556E+04
            5.9500    0.2970E+03    0.4311E+04
            6.0500    0.2720E+03    0.4048E+04
            6.1500    0.2490E+03    0.3798E+04
            6.2500    0.2300E+03    0.3594E+04
            6.3500    0.2100E+03    0.3360E+04
            6.4500    0.1920E+03    0.3145E+04
            6.5500    0.1700E+03    0.2850E+04
            6.6500    0.1560E+03    0.2675E+04
            6.7500    0.1400E+03    0.2455E+04
            6.8500    0.1260E+03    0.2259E+04
            6.9500    0.1120E+03    0.2052E+04
            7.0500    0.1020E+03    0.1909E+04
            7.1500    0.8920E+02    0.1705E+04
            7.2500    0.7680E+02    0.1499E+04
            7.3500    0.6680E+02    0.1331E+04
            7.4500    0.5700E+02    0.1159E+04
            7.5500    0.4740E+02    0.9833E+03
            7.6500    0.3760E+02    0.7956E+03
c           total =   0.82108E+09
c           total =   8.2108E+08 x 72 =  5.9118E+10
ctme    2400
nps     5446924
c          nps        619115
prdmp    j -960  1
e0     .2 .6 .8 2. 20.
fc2   p dose rates (mrem/hr) on sides of truck, 7th entry = nearest
f2:p    73 74
fs2     -81 84 -82 83 -89 -90 -91 -92 t
sd2   142172 138738 16219 16219 3679 3600 2r 1740 329567
      142172 138738 16219 16219 3679 3600 2r 1740 329567
c      ansi/ans-6.1.1-1977 fluence-to-dose,photons(mrem/hr/(p/cm**2/s)
de2         0.01    0.03    0.05    0.07    0.10    0.15    0.20    0.25    0.30
            0.35    0.40    0.45    0.50    0.55    0.60    0.65    0.70    0.80
            1.00    1.40    1.80    2.20    2.60    2.80    3.25    3.75    4.25
            4.75    5.00    5.25    5.75    6.25    6.75    7.50    9.00   11.0
            13.0    15.0
df2         3.96-3 5.82-4 2.90-4 2.58-4 2.83-4 3.79-4 5.01-4 6.31-4 7.59-4
            8.78-4 9.85-4 1.08-3 1.17-3 1.27-3 1.36-3 1.44-3 1.52-3 1.68-3
            1.98-3 2.51-3 2.99-3 3.42-3 3.82-3 4.01-3 4.41-3 4.83-3 5.23-3
            5.60-3 5.80-3 6.01-3 6.37-3 6.74-3 7.11-3 7.66-3 8.77-3 1.03-2
            1.18-2 1.33-2
fc12  p dose rates (mrem/hr) on ends of truck, 7th entry = nearest
f12:p   71 72
fs12    -85 88 -86 87 -89 -90 -91 -92 t
sd12  10002 10002 16219 16219 3679 3600 2r 1740 68660
      10002 10002 16219 16219 3679 3600 2r 1740 68660
c      ansi/ans-6.1.1-1977 fluence-to-dose,photons(mrem/hr/(p/cm**2/s)
de12        0.01    0.03    0.05    0.07    0.10    0.15    0.20    0.25    0.30
            0.35    0.40    0.45    0.50    0.55    0.60    0.65    0.70    0.80
```

```
          1.00   1.40   1.80   2.20   2.60   2.80   3.25   3.75   4.25
          4.75   5.00   5.25   5.75   6.25   6.75   7.50   9.00   11.0
          13.0   15.0
df12      3.96-3 5.82-4 2.90-4 2.58-4 2.83-4 3.79-4 5.01-4 6.31-4 7.59-4
          8.78-4 9.85-4 1.08-3 1.17-3 1.27-3 1.36-3 1.44-3 1.52-3 1.68-3
          1.98-3 2.51-3 2.99-3 3.42-3 3.82-3 4.01-3 4.41-3 4.83-3 5.23-3
          5.60-3 5.80-3 6.01-3 6.37-3 6.74-3 7.11-3 7.66-3 8.77-3 1.03-2
          1.18-2 1.33-2
fc22   p dose rates (mrem/hr) on bottom and top, 7th entry = nearest
f22:p  75 76
fs22   -81 84 -82 83 -85 -86 -87 -88 t
sd22   133591 130366 15240 15240 2220 3600 2r 2220 309677
       133591 130366 15240 15240 2220 3600 2r 2220 309677
c      ansi/ans-6.1.1-1977 fluence-to-dose,photons(mrem/hr/(p/cm**2/s)
de22      0.01   0.03   0.05   0.07   0.10   0.15   0.20   0.25   0.30
          0.35   0.40   0.45   0.50   0.55   0.60   0.65   0.70   0.80
          1.00   1.40   1.80   2.20   2.60   2.80   3.25   3.75   4.25
          4.75   5.00   5.25   5.75   6.25   6.75   7.50   9.00   11.0
          13.0   15.0
df22      3.96-3 5.82-4 2.90-4 2.58-4 2.83-4 3.79-4 5.01-4 6.31-4 7.59-4
          8.78-4 9.85-4 1.08-3 1.17-3 1.27-3 1.36-3 1.44-3 1.52-3 1.68-3
          1.98-3 2.51-3 2.99-3 3.42-3 3.82-3 4.01-3 4.41-3 4.83-3 5.23-3
          5.60-3 5.80-3 6.01-3 6.37-3 6.74-3 7.11-3 7.66-3 8.77-3 1.03-2
          1.18-2 1.33-2
fc102   p dose rates (mrem/hr) on side of package, 2nd entry
f102:p     38
fs102   -132 -90 -93 -94 -91 -138 t
sd102   1 5j 1 1
c      ansi/ans-6.1.1-1977 fluence-to-dose,photons(mrem/hr/(p/cm**2/s)
de102     0.01   0.03   0.05   0.07   0.10   0.15   0.20   0.25   0.30
          0.35   0.40   0.45   0.50   0.55   0.60   0.65   0.70   0.80
          1.00   1.40   1.80   2.20   2.60   2.80   3.25   3.75   4.25
          4.75   5.00   5.25   5.75   6.25   6.75   7.50   9.00   11.0
          13.0   15.0
df102     3.96-3 5.82-4 2.90-4 2.58-4 2.83-4 3.79-4 5.01-4 6.31-4 7.59-4
          8.78-4 9.85-4 1.08-3 1.17-3 1.27-3 1.36-3 1.44-3 1.52-3 1.68-3
          1.98-3 2.51-3 2.99-3 3.42-3 3.82-3 4.01-3 4.41-3 4.83-3 5.23-3
          5.60-3 5.80-3 6.01-3 6.37-3 6.74-3 7.11-3 7.66-3 8.77-3 1.03-2
          1.18-2 1.33-2
fc122   p dose rates (mrem/hr) on top of package, 1st entry
f122:p     63
fs122    -95 t
c      ansi/ans-6.1.1-1977 fluence-to-dose,photons(mrem/hr/(p/cm**2/s)
de122     0.01   0.03   0.05   0.07   0.10   0.15   0.20   0.25   0.30
          0.35   0.40   0.45   0.50   0.55   0.60   0.65   0.70   0.80
          1.00   1.40   1.80   2.20   2.60   2.80   3.25   3.75   4.25
          4.75   5.00   5.25   5.75   6.25   6.75   7.50   9.00   11.0
          13.0   15.0
df122     3.96-3 5.82-4 2.90-4 2.58-4 2.83-4 3.79-4 5.01-4 6.31-4 7.59-4
          8.78-4 9.85-4 1.08-3 1.17-3 1.27-3 1.36-3 1.44-3 1.52-3 1.68-3
          1.98-3 2.51-3 2.99-3 3.42-3 3.82-3 4.01-3 4.41-3 4.83-3 5.23-3
          5.60-3 5.80-3 6.01-3 6.37-3 6.74-3 7.11-3 7.66-3 8.77-3 1.03-2
          1.18-2 1.33-2
fc5    p dose rates (mrem/hr) at detectors, 2 m, driver
```

```
f5:p    0. 327.00 79.  100.
        847.09  0. 79.  100.
        0. 327.00  0.0  100.
        0. 327.00 -79.0 100.
        0. 327.00 158.0 100.
c       ansi/ans-6.1.1-1977 fluence-to-dose,photons(mrem/hr/(p/cm**2/s)
de5         0.01   0.03   0.05   0.07   0.10   0.15   0.20   0.25   0.30
            0.35   0.40   0.45   0.50   0.55   0.60   0.65   0.70   0.80
            1.00   1.40   1.80   2.20   2.60   2.80   3.25   3.75   4.25
            4.75   5.00   5.25   5.75   6.25   6.75   7.50   9.00   11.0
            13.0   15.0
df5         3.96-3 5.82-4 2.90-4 2.58-4 2.83-4 3.79-4 5.01-4 6.31-4 7.59-4
            8.78-4 9.85-4 1.08-3 1.17-3 1.27-3 1.36-3 1.44-3 1.52-3 1.68-3
            1.98-3 2.51-3 2.99-3 3.42-3 3.82-3 4.01-3 4.41-3 4.83-3 5.23-3
            5.60-3 5.80-3 6.01-3 6.37-3 6.74-3 7.11-3 7.66-3 8.77-3 1.03-2
            1.18-2 1.33-2
ft5     icd
fu5      3 4 5 6 7 8 9 10 11 12 13 14 15 16 17  21 22 23 24
         41 42 43 44 45 46 47  71 72 73
```

HAC GAMMA SHIELDING MCNP INPUT FILE

```
SHLD. CALC., GPHS-RTG, GAMMA, , accident igaci
c       sphere of PuO2 for accident condition
    1    3  -9.60   -100
c      inner containment
   21    231 -.00122 ((6 -52 -31 ):(52 -33 -53 ))  100
   22    201  -8.0300  51 -52 31 -32
   23    201  -8.0300  (52 -34 -54 )(33 :53 )
   24    201  -8.0300  51 -6 -31
c      outer containment
   41    231 -.00122 51 35 -64 -39
   42    231 -.00122 ((51 -35 -62 )(52 :32 ))(-52 :34 :54 )
   43    201  -8.0300  (-36 64 -63 )(62 :35 )
   44      236  -1.0  -52 65 36 -37
   45    201  -8.0300  -52 65 37 -38
   46    201  -8.0300  ((64 -65 36 51 -40 ):(-64 39 51 )):(65 38 -66 -40 )
   47    201  -8.0300  61 -51 -40
c        beyond outer containment and inside truck boundary
   71    231 -.00122 (((-52 :36 :63 ))(52 :38 :-66 ))(66 :40 :-61 )
                71 -72 73 -74 75 -76
c      beyond truck and inside large sphere, above ground
   72    231 -.00122  (-71:72:-73:74:-75:76)  77  -111
c     ground
   73    221 -1.67    -77 -111
c       outside world
   74      0  111

    1         py   4.659
    2         px  -4.859
    3         py  -4.659
    4         px   4.859
    5         pz  95.544
    6         pz  0.0000
    7         pz  5.30801
    8         pz  -0.00001
    9        c/y  -2.184  2.654  1.831
   10        c/y   2.184  2.654  1.831
   11         py  -3.1618
   12         py  -0.2941
   13         py  0.2941
   14         py  3.1618
   15         py  -3.1059
   16         py  -0.350
   17         py   0.350
   18         py  3.1059
   19        c/y  -2.1840 2.6540 1.3767
   20        c/y  -2.1840 2.6540 1.4326
   21        c/y  2.1840 2.6540 1.3767
   22        c/y  2.1840 2.6540 1.4326
c   radial surfaces for inner and outer containment
   31         cz  43.1800
   32         cz  45.0850
   33         cz  43.6562
```

```
   34         cz  44.6088
   35         cz  45.5676
   36         cz  46.8376
   37         cz  50.0380
   38         cz  50.3796
   39         cz  49.6443
   40         cz  61.3410
c   inner containment
   51         pz  -8.8138
   52         pz  127.4450
   53         sz  60.3377 88.9000
   54         sz  60.3377 89.8525
c   outer containment
   61         pz  -12.6238
   62         sz  60.1472 90.8050
   63         sz  60.1472 92.0750
   64         kz  48.7807 1.0000 -1.0000
   65         kz  53.0733 1.0000 -1.0000
   66         pz  2.6940
c     truck outside boundary
   71      px  -615.95
   72      px   603.25
   73      py  -127.00
   74      py   127.00
   75      pz   -72.3138
   76      pz   198.0
   77      pz  -184.0738
c      tally fs surfaces on outside of truck
   81      px   -90.0
   82      px   -30.0
   83      px    30.0
   84      px    90.0
   85      py   -90.0
   86      py   -30.0
   87      py    30.0
   88      py    90.0
   89      pz   -11.0
   90      pz    49.0
   91      pz   109.0
   92      pz   169.0
   93      pz    63.76
   94      pz    94.24
   95      cz    15.24
  100      s     0. 0. 142.6  6.5508
c      outside world.
  111         so  5000.0000

*tr1  0  0 31.4560
mode    p
m1    6000.01p  -1.950000
m2    77000.01p  -22.500000
m3    94000.01p -8.463     8000.01p -1.137
m201  26000.01p 67.970001 24000.01p 20.000000 28000.01p 10.000000
      25000.01p 2.000000 6000.01p 0.030000
```

```
m221  8000.01p -0.511000 14000.01p -0.278200 20000.01p -0.071700
      26000.01p -0.109100 13000.01p -0.083260 12000.01p -0.031420
      19000.01p -0.011550 11000.01p -0.020220 22000.01p -0.016550
      25000.01p -0.001781 15000.01p -0.002400
m231  7000.01p -0.765000 8000.01p -0.235000
m236  1000.01p 0.666700 8000.01p 0.333300
imp:p  1                4          3r          16          $ 1, 41
       8r  8            0          $ 42, 73
print   10 30 40 50 60 100 110 120 126 170
phys:p    j  1
cut:p    j j 0. 0.
sdef         rad d4   erg=d9
           pos 0. 0. 142.6    wgt=5.9118e10
si4    6.5508
sp4     -21 2
c      gamma spectrum from Table 5-4, 157 g fueled clad
#           si9       sp9        sb9
             l         d          d
          0.1500    0.0000E+00    0.0000E+00
          0.2500    0.6820E+09    0.1066E+08
          0.3500    0.4960E+08    0.2127E+07
          0.4500    0.4030E+07    0.3672E+06
          0.5500    0.9250E+07    0.3773E+07
          0.6500    0.7330E+07    0.3841E+07
          0.7500    0.1780E+08    0.1156E+08
          0.8500    0.6760E+07    0.5298E+07
          0.9500    0.6720E+07    0.6222E+07
          1.0500    0.1370E+07    0.1474E+07
          1.1500    0.5300E+06    0.6536E+06
          1.2500    0.1970E+06    0.2753E+06
          1.3500    0.1000E+06    0.1569E+06
          1.4500    0.2200E+05    0.3841E+05
          1.5500    0.3310E+06    0.6387E+06
          1.6500    0.1420E+07    0.3010E+07
          1.7500    0.8220E+05    0.1903E+06
          1.8500    0.1170E+06    0.2944E+06
          1.9500    0.1310E+05    0.3567E+05
          2.0500    0.1110E+05    0.3258E+05
          2.1500    0.1000E+05    0.3153E+05
          2.2500    0.8950E+04    0.3021E+05
          2.3500    0.7950E+04    0.2864E+05
          2.4500    0.7080E+04    0.2715E+05
          2.5500    0.6250E+04    0.2545E+05
          2.6500    0.3330E+08    0.1437E+09
          2.7500    0.4990E+04    0.2276E+05
          2.8500    0.4500E+04    0.2165E+05
          2.9500    0.4030E+04    0.2042E+05
          3.0500    0.3640E+04    0.1939E+05
          3.1500    0.3270E+04    0.1828E+05
          3.2500    0.2980E+04    0.1746E+05
          3.3500    0.2670E+04    0.1637E+05
          3.4500    0.2420E+04    0.1551E+05
          3.5500    0.2210E+04    0.1478E+05
          3.6500    0.2010E+04    0.1402E+05
```

```
            3.7500    0.1830E+04    0.1329E+05
            3.8500    0.1660E+04    0.1254E+05
            3.9500    0.1540E+04    0.1209E+05
            4.0500    0.1420E+04    0.1157E+05
            4.1500    0.1290E+04    0.1091E+05
            4.2500    0.1200E+04    0.1051E+05
            4.3500    0.1110E+04    0.1007E+05
            4.4500    0.1010E+04    0.9481E+04
            4.5500    0.9330E+03    0.9055E+04
            4.6500    0.8590E+03    0.8613E+04
            4.7500    0.7920E+03    0.8199E+04
            4.8500    0.7370E+03    0.7872E+04
            4.9500    0.6790E+03    0.7478E+04
            5.0500    0.6340E+03    0.7195E+04
            5.1500    0.5740E+03    0.6708E+04
            5.2500    0.5250E+03    0.6315E+04
            5.3500    0.4870E+03    0.6026E+04
            5.4500    0.4530E+03    0.5764E+04
            5.5500    0.4160E+03    0.5439E+04
            5.6500    0.3830E+03    0.5144E+04
            5.7500    0.3540E+03    0.4881E+04
            5.8500    0.3220E+03    0.4556E+04
            5.9500    0.2970E+03    0.4311E+04
            6.0500    0.2720E+03    0.4048E+04
            6.1500    0.2490E+03    0.3798E+04
            6.2500    0.2300E+03    0.3594E+04
            6.3500    0.2100E+03    0.3360E+04
            6.4500    0.1920E+03    0.3145E+04
            6.5500    0.1700E+03    0.2850E+04
            6.6500    0.1560E+03    0.2675E+04
            6.7500    0.1400E+03    0.2455E+04
            6.8500    0.1260E+03    0.2259E+04
            6.9500    0.1120E+03    0.2052E+04
            7.0500    0.1020E+03    0.1909E+04
            7.1500    0.8920E+02    0.1705E+04
            7.2500    0.7680E+02    0.1499E+04
            7.3500    0.6680E+02    0.1331E+04
            7.4500    0.5700E+02    0.1159E+04
            7.5500    0.4740E+02    0.9833E+03
            7.6500    0.3760E+02    0.7956E+03
c          total =   0.82108E+09
c       total = .82108+9 * 72 = 5.9118+10
ctme    120
nps      1654422
prdmp    j -960
e0     .2 .6 .8 2. 20.
fc2   p dose rates (mrem/hr) on sides of truck, 7th entry = nearest
f2:p     73 74
fs2     -81 84 -82 83 -89 -90 -91 -92 t
sd2   142172 138738 16219 16219 3679 3600 2r 1740 329567
      142172 138738 16219 16219 3679 3600 2r 1740 329567
c      ansi/ans-6.1.1-1977 fluence-to-dose,photons(mrem/hr/(p/cm**2/s)
de2         0.01   0.03   0.05   0.07   0.10   0.15   0.20   0.25   0.30
            0.35   0.40   0.45   0.50   0.55   0.60   0.65   0.70   0.80
```

```
          1.00   1.40   1.80   2.20   2.60   2.80   3.25   3.75   4.25
          4.75   5.00   5.25   5.75   6.25   6.75   7.50   9.00   11.0
          13.0   15.0
df2       3.96-3 5.82-4 2.90-4 2.58-4 2.83-4 3.79-4 5.01-4 6.31-4 7.59-4
          8.78-4 9.85-4 1.08-3 1.17-3 1.27-3 1.36-3 1.44-3 1.52-3 1.68-3
          1.98-3 2.51-3 2.99-3 3.42-3 3.82-3 4.01-3 4.41-3 4.83-3 5.23-3
          5.60-3 5.80-3 6.01-3 6.37-3 6.74-3 7.11-3 7.66-3 8.77-3 1.03-2
          1.18-2 1.33-2
fc12  p dose rates (mrem/hr) on ends of truck, 7th entry = nearest
f12:p   71 72
fs12    -85 88 -86 87 -89 -90 -91 -92 t
sd12  10002 10002 16219 16219 3679 3600 2r 1740 68660
      10002 10002 16219 16219 3679 3600 2r 1740 68660
c      ansi/ans-6.1.1-1977 fluence-to-dose,photons(mrem/hr/(p/cm**2/s)
de12      0.01   0.03   0.05   0.07   0.10   0.15   0.20   0.25   0.30
          0.35   0.40   0.45   0.50   0.55   0.60   0.65   0.70   0.80
          1.00   1.40   1.80   2.20   2.60   2.80   3.25   3.75   4.25
          4.75   5.00   5.25   5.75   6.25   6.75   7.50   9.00   11.0
          13.0   15.0
df12      3.96-3 5.82-4 2.90-4 2.58-4 2.83-4 3.79-4 5.01-4 6.31-4 7.59-4
          8.78-4 9.85-4 1.08-3 1.17-3 1.27-3 1.36-3 1.44-3 1.52-3 1.68-3
          1.98-3 2.51-3 2.99-3 3.42-3 3.82-3 4.01-3 4.41-3 4.83-3 5.23-3
          5.60-3 5.80-3 6.01-3 6.37-3 6.74-3 7.11-3 7.66-3 8.77-3 1.03-2
          1.18-2 1.33-2
fc22   p dose rates (mrem/hr) on bottom and top, 7th entry = nearest
f22:p  75 76
fs22    -81 84 -82 83 -85 -86 -87 -88 t
sd22  133591 130366 15240 15240 2220 3600 2r 2220 309677
      133591 130366 15240 15240 2220 3600 2r 2220 309677
c      ansi/ans-6.1.1-1977 fluence-to-dose,photons(mrem/hr/(p/cm**2/s)
de22      0.01   0.03   0.05   0.07   0.10   0.15   0.20   0.25   0.30
          0.35   0.40   0.45   0.50   0.55   0.60   0.65   0.70   0.80
          1.00   1.40   1.80   2.20   2.60   2.80   3.25   3.75   4.25
          4.75   5.00   5.25   5.75   6.25   6.75   7.50   9.00   11.0
          13.0   15.0
df22      3.96-3 5.82-4 2.90-4 2.58-4 2.83-4 3.79-4 5.01-4 6.31-4 7.59-4
          8.78-4 9.85-4 1.08-3 1.17-3 1.27-3 1.36-3 1.44-3 1.52-3 1.68-3
          1.98-3 2.51-3 2.99-3 3.42-3 3.82-3 4.01-3 4.41-3 4.83-3 5.23-3
          5.60-3 5.80-3 6.01-3 6.37-3 6.74-3 7.11-3 7.66-3 8.77-3 1.03-2
          1.18-2 1.33-2
fc102   p dose rates (mrem/hr) on side of package, 2nd entry
f102:p     38
fs102    -93 -94 t
c      ansi/ans-6.1.1-1977 fluence-to-dose,photons(mrem/hr/(p/cm**2/s)
de102     0.01   0.03   0.05   0.07   0.10   0.15   0.20   0.25   0.30
          0.35   0.40   0.45   0.50   0.55   0.60   0.65   0.70   0.80
          1.00   1.40   1.80   2.20   2.60   2.80   3.25   3.75   4.25
          4.75   5.00   5.25   5.75   6.25   6.75   7.50   9.00   11.0
          13.0   15.0
df102     3.96-3 5.82-4 2.90-4 2.58-4 2.83-4 3.79-4 5.01-4 6.31-4 7.59-4
          8.78-4 9.85-4 1.08-3 1.17-3 1.27-3 1.36-3 1.44-3 1.52-3 1.68-3
          1.98-3 2.51-3 2.99-3 3.42-3 3.82-3 4.01-3 4.41-3 4.83-3 5.23-3
          5.60-3 5.80-3 6.01-3 6.37-3 6.74-3 7.11-3 7.66-3 8.77-3 1.03-2
          1.18-2 1.33-2
```

```
fc122   p dose rates (mrem/hr) on top of package, 1st entry
f122:p      63
fs122     -95 t
c       ansi/ans-6.1.1-1977 fluence-to-dose,photons(mrem/hr/(p/cm**2/s)
de122       0.01    0.03    0.05    0.07    0.10    0.15    0.20    0.25    0.30
            0.35    0.40    0.45    0.50    0.55    0.60    0.65    0.70    0.80
            1.00    1.40    1.80    2.20    2.60    2.80    3.25    3.75    4.25
            4.75    5.00    5.25    5.75    6.25    6.75    7.50    9.00    11.0
            13.0    15.0
df122       3.96-3 5.82-4 2.90-4 2.58-4 2.83-4 3.79-4 5.01-4 6.31-4 7.59-4
            8.78-4 9.85-4 1.08-3 1.17-3 1.27-3 1.36-3 1.44-3 1.52-3 1.68-3
            1.98-3 2.51-3 2.99-3 3.42-3 3.82-3 4.01-3 4.41-3 4.83-3 5.23-3
            5.60-3 5.80-3 6.01-3 6.37-3 6.74-3 7.11-3 7.66-3 8.77-3 1.03-2
            1.18-2 1.33-2
fc5     p dose rates (mrem/hr) at detectors, 1 m above top s
f5:p    0. 0. 252.22  50.
c       ansi/ans-6.1.1-1977 fluence-to-dose,photons(mrem/hr/(p/cm**2/s)
de5         0.01    0.03    0.05    0.07    0.10    0.15    0.20    0.25    0.30
            0.35    0.40    0.45    0.50    0.55    0.60    0.65    0.70    0.80
            1.00    1.40    1.80    2.20    2.60    2.80    3.25    3.75    4.25
            4.75    5.00    5.25    5.75    6.25    6.75    7.50    9.00    11.0
            13.0    15.0
df5         3.96-3 5.82-4 2.90-4 2.58-4 2.83-4 3.79-4 5.01-4 6.31-4 7.59-4
            8.78-4 9.85-4 1.08-3 1.17-3 1.27-3 1.36-3 1.44-3 1.52-3 1.68-3
            1.98-3 2.51-3 2.99-3 3.42-3 3.82-3 4.01-3 4.41-3 4.83-3 5.23-3
            5.60-3 5.80-3 6.01-3 6.37-3 6.74-3 7.11-3 7.66-3 8.77-3 1.03-2
            1.18-2 1.33-2
```

5.5.3 Neutron Shielding Analyses MCNP Input Files

NCT NEUTRON SHIELDING MCNP INPUT FILE

```
SHLD. CALC., GPHS-RTG, N-GAMMA, water, no q, p.det., rev Mar 96 ingdq
    1     0  -5 6 -1 3 -4 2  trcl=1 fill=1
    2     0  -7 8   u=1   lat=1
           fill=0:17 0:0 0:0   2 17r
    3     1  -1.9500  -9 (12 :-11 :20 )(14 :-13 :20 ) u=2
    4     1  -1.9500  -10 (12 :-11 :22 )(14 :-13 :22 ) u=2
    5     1  -1.9500  9 10  u=2
    6     2 -22.5  -12 11 -20 (-15 :16 :19 ) u=2
    7     2 -22.5  -14 13 -20 (-17 :18 :19 ) u=2
    8     3  -9.6000  -16 15 -19  u=2
    9     3  -9.6000  -18 17 -19  u=2
   10     2 -22.5  -12 11 -22 (-15 :16 :21 ) u=2
   11     2 -22.5  -14 13 -22 (-17 :18 :21 ) u=2
   12     3  -9.6000  -16 15 -21  u=2
   13     3  -9.6000  -18 17 -21  u=2
c       Astroquartz insulation and thermopile and Al shell
   14    231 -.00122  -121  134 -135   #1
   15      0          -122  133 -136  (121:-134:135)
   16    231 -.00122  -123  132 -137  (122:-133:136)
   17     12 -2.85    -124  131 -138  (123:-132:137)
c       inner containment
   21    231 -.00122 ((6 -52 -31 ):(52 -33 -53 )) (124:-131:138)
   22    201  -8.0300  51 -52 31 -32
   23    201  -8.0300  (52 -34 -54 )(33 :53 )
   24    201  -8.0300  51 -6 -31
c       outer containment
   41    231 -.00122 51 35 -64 -39
   42    231 -.00122 ((51 -35 -62 )(52 :32 ))(-52 :34 :54 )
   43    201  -8.0300  (-36 64 -63 )(62 :35 )
   44    236  -1.0 -52 65 36 -37
   45    201  -8.0300  -52 65 37 -38
   46    201  -8.0300  ((64 -65 36 51 -40 ):(-64 39 51 )):(65 38 -66 -40 )
   47    201  -8.0300  61 -51 -40
c        beyond outer containment and inside truck boundary
   71    231 -.00122 (((-52 :36 :63 ))(52 :38 :-66 ))(66 :40 :-61 )
               71 -72 73 -74 75 -76
c       beyond truck and inside large sphere, above ground
   72    231 -.00122  (-71:72:-73:74:-75:76)  77  -111
c      ground
   73    221 -1.67    -77 -111
c       outside world
   74      0  111

    1        py   4.659
    2        px  -4.859
    3        py  -4.659
    4        px   4.859
    5        pz  95.544
    6        pz  0.0000
```

```
    7        pz  5.30801
    8        pz  -0.00001
    9       c/y  -2.184  2.654  1.831
   10       c/y   2.184  2.654  1.831
   11        py  -3.1618
   12        py  -0.2941
   13        py  0.2941
   14        py  3.1618
   15        py  -3.1059
   16        py  -0.350
   17        py   0.350
   18        py  3.1059
   19       c/y  -2.1840 2.6540 1.3767
   20       c/y  -2.1840 2.6540 1.4326
   21       c/y  2.1840 2.6540 1.3767
   22       c/y  2.1840 2.6540 1.4326
c   radial surfaces for inner and outer containment
   31        cz  43.1800
   32        cz  45.0850
   33        cz  43.6562
   34        cz  44.6088
   35        cz  45.5676
   36        cz  46.8376
   37        cz  50.0380
   38        cz  50.3796
   39        cz  49.6443
   40        cz  61.3410
c   inner containment
   51        pz  -8.8138
   52        pz  127.4450
   53        sz  60.3377 88.9000
   54        sz  60.3377 89.8525
c   outer containment
   61        pz  -12.6238
   62        sz  60.1472 90.8050
   63        sz  60.1472 92.0750
   64        kz  48.7807 1.0000 -1.0000
   65        kz  53.0733 1.0000 -1.0000
   66        pz  2.6940
c     truck outside boundary
   71     px  -615.95
   72     px   603.25
   73     py  -127.00
   74     py   127.00
   75     pz   -72.3138
   76     pz   198.0
   77     pz  -184.0738
c      tally fs surfaces on outside of truck
   81     px   -90.0
   82     px   -30.0
   83     px    30.0
   84     px    90.0
   85     py   -90.0
```

```
   86      py   -30.0
   87      py    30.0
   88      py    90.0
   89      pz   -11.0
   90      pz    49.0
   91      pz   109.0
   92      pz   169.0
   93      pz    63.76
   94      pz    94.24
   95      cz    15.24
c      outside world.
  111         so  5000.0000
  121   cz  7.1165
  122   cz  8.8945
  123   cz 10.6426
  124   cz 10.7950
  131   pz  23.348
  132   pz  23.5004
  133   pz  29.6725
  134   pz  31.4505
  135   pz 127.0055
  136   pz 128.7835
  137   pz 134.9556
  138   pz 135.108

*trl  0  0 31.4560
mode  n p
m1    6000.50  -1.950000
m2    77000.55  -22.500000
m3    94238.50  -6.765000 94239.55  -1.698000 8016.50  -1.137000
m11    8016.50c -.9631  14000.50c -.8452  42000.50c -.3391  $ ins.+therm.
m12   13027.50c -1.
m201  26000.55c 67.970001 24000.50c 20.000000 28000.50c 10.000000
      25055.50c 2.000000 6000.50c 0.030000
c      Hanford hwvp soil
m221  8016.50c -0.511000 14000.50c -0.278200 20000.50c -0.071700
      26000.55c -0.109100 13027.50c -0.083260 12000.50c -0.031420
      19000.50c -0.011550 11023.50c -0.020220 22000.50c -0.016550
      25055.50c -0.001781 15031.50c -0.002400
m231  7014.50c -0.765000 8016.50c -0.235000
m236  1001.50c 0.666700 8016.50c 0.333300
imp:n  1          16r        4          3r         16         $ 1, 41
       8r  8        0          $ 42, 73
imp:p  1          16r        4          3r         16         $ 1, 41
       8r  8        0          $ 42, 73
print   10 30 40 50 60 100 110 120 126 170
c       phys:p    j  1
cut:p    j j 0. 0.
cut:n    j j 0. 0.
sdef     cel d1  axs 0 1 0  rad d4  ext d5  erg=d9
          pos fcel d6    wgt=5.13252e7
c      source uniformly in all 72 lattice cells
sil  1 1:2(0 0 0):8  1:2(0 0 0):9  1:2(0 0 0):12  1:2(0 0 0):13
```

```
      1:2(1 0 0):8  1:2(1 0 0):9  1:2(1 0 0):12  1:2(1 0 0):13
      1:2(2 0 0):8  1:2(2 0 0):9  1:2(2 0 0):12  1:2(2 0 0):13
      1:2(3 0 0):8  1:2(3 0 0):9  1:2(3 0 0):12  1:2(3 0 0):13
      1:2(4 0 0):8  1:2(4 0 0):9  1:2(4 0 0):12  1:2(4 0 0):13
      1:2(5 0 0):8  1:2(5 0 0):9  1:2(5 0 0):12  1:2(5 0 0):13
      1:2(6 0 0):8  1:2(6 0 0):9  1:2(6 0 0):12  1:2(6 0 0):13
      1:2(7 0 0):8  1:2(7 0 0):9  1:2(7 0 0):12  1:2(7 0 0):13
      1:2(8 0 0):8  1:2(8 0 0):9  1:2(8 0 0):12  1:2(8 0 0):13
      1:2(9 0 0):8  1:2(9 0 0):9  1:2(9 0 0):12  1:2(9 0 0):13
     1:2(10 0 0):8 1:2(10 0 0):9 1:2(10 0 0):12 1:2(10 0 0):13
     1:2(11 0 0):8 1:2(11 0 0):9 1:2(11 0 0):12 1:2(11 0 0):13
     1:2(12 0 0):8 1:2(12 0 0):9 1:2(12 0 0):12 1:2(12 0 0):13
     1:2(13 0 0):8 1:2(13 0 0):9 1:2(13 0 0):12 1:2(13 0 0):13
     1:2(14 0 0):8 1:2(14 0 0):9 1:2(14 0 0):12 1:2(14 0 0):13
     1:2(15 0 0):8 1:2(15 0 0):9 1:2(15 0 0):12 1:2(15 0 0):13
     1:2(16 0 0):8 1:2(16 0 0):9 1:2(16 0 0):12 1:2(16 0 0):13
     1:2(17 0 0):8 1:2(17 0 0):9 1:2(17 0 0):12 1:2(17 0 0):13
sp1    1. 71r
si4    1.3767
sp4    -21 1
si5   0. 2.7559
sp5    -21 0
ds6   1  -2.184 -3.1059 2.654  -2.184 .35 2.654
             2.184 -3.1059 2.654  2.184 .35 2.654
          -2.184 -3.1059 2.654  -2.184 .35 2.654
             2.184 -3.1059 2.654  2.184 .35 2.654
          -2.184 -3.1059 2.654  -2.184 .35 2.654
             2.184 -3.1059 2.654  2.184 .35 2.654
          -2.184 -3.1059 2.654  -2.184 .35 2.654
             2.184 -3.1059 2.654  2.184 .35 2.654
          -2.184 -3.1059 2.654  -2.184 .35 2.654
             2.184 -3.1059 2.654  2.184 .35 2.654
          -2.184 -3.1059 2.654  -2.184 .35 2.654
             2.184 -3.1059 2.654  2.184 .35 2.654
          -2.184 -3.1059 2.654  -2.184 .35 2.654
             2.184 -3.1059 2.654  2.184 .35 2.654
          -2.184 -3.1059 2.654  -2.184 .35 2.654
             2.184 -3.1059 2.654  2.184 .35 2.654
          -2.184 -3.1059 2.654  -2.184 .35 2.654
             2.184 -3.1059 2.654  2.184 .35 2.654
          -2.184 -3.1059 2.654  -2.184 .35 2.654
             2.184 -3.1059 2.654  2.184 .35 2.654
          -2.184 -3.1059 2.654  -2.184 .35 2.654
             2.184 -3.1059 2.654  2.184 .35 2.654
          -2.184 -3.1059 2.654  -2.184 .35 2.654
             2.184 -3.1059 2.654  2.184 .35 2.654
          -2.184 -3.1059 2.654  -2.184 .35 2.654
             2.184 -3.1059 2.654  2.184 .35 2.654
          -2.184 -3.1059 2.654  -2.184 .35 2.654
             2.184 -3.1059 2.654  2.184 .35 2.654
          -2.184 -3.1059 2.654  -2.184 .35 2.654
             2.184 -3.1059 2.654  2.184 .35 2.654
          -2.184 -3.1059 2.654  -2.184 .35 2.654
             2.184 -3.1059 2.654  2.184 .35 2.654
          -2.184 -3.1059 2.654  -2.184 .35 2.654
```

```
          2.184 -3.1059 2.654  2.184 .35 2.654
        -2.184 -3.1059 2.654  -2.184 .35 2.654
          2.184 -3.1059 2.654  2.184 .35 2.654
        -2.184 -3.1059 2.654  -2.184 .35 2.654
          2.184 -3.1059 2.654  2.184 .35 2.654
c     Harvey's new neutron spectrum , 157 g fueled clad
#         si9       sp9
           h         d
         0.00    0.0000E+00
          0.10000       0.1020E+05
          0.20000       0.1260E+05
          0.30000       0.1350E+05
          0.40000       0.1510E+05
          0.50000       0.1770E+05
          0.60000       0.1900E+05
          0.70000       0.2000E+05
          0.80000       0.2080E+05
          0.90000       0.2030E+05
          1.00000       0.1830E+05
          1.10000       0.1840E+05
          1.20000       0.1890E+05
          1.30000       0.1990E+05
          1.40000       0.2050E+05
          1.50000       0.2040E+05
          1.60000       0.2070E+05
          1.70000       0.2150E+05
          1.80000       0.2270E+05
          1.90000       0.2300E+05
          2.00000       0.2350E+05
          2.10000       0.2330E+05
          2.20000       0.2380E+05
          2.30000       0.2380E+05
          2.40000       0.2260E+05
          2.50000       0.2160E+05
          2.60000       0.2070E+05
          2.70000       0.1980E+05
          2.80000       0.1830E+05
          2.90000       0.1770E+05
          3.00000       0.1660E+05
          3.10000       0.1490E+05
          3.20000       0.1400E+05
          3.30000       0.1240E+05
          3.40000       0.1040E+05
          3.50000       0.9100E+04
          3.60000       0.8060E+04
          3.70000       0.6880E+04
          3.80000       0.6120E+04
          3.90000       0.5490E+04
          4.00000       0.4720E+04
          4.10000       0.4340E+04
          4.20000       0.3400E+04
          4.30000       0.2940E+04
          4.40000       0.2360E+04
```

```
            4.50000         0.4950E+04
            5.00000         0.5200E+04
            5.50000         0.3790E+04
            6.00000         0.2660E+04
            6.50000         0.1850E+04
            7.00000         0.1290E+04
            7.50000         0.8920E+03
            8.00000         0.6130E+03
            8.50000         0.4210E+03
            9.00000         0.2570E+03
            9.50000         0.1970E+03
           10.00000         0.1980E+03
           11.00000         0.1210E+03
           12.00000         0.5530E+02
           13.00000         0.2480E+02
           14.00000         0.1110E+02
           15.00000         0.4900E+01
c          total =    0.71285E+06 x 72 = 5.13252E+07
ctme    1200
nps      161911
prdmp    j -960
e0     .2 .6 .8 2. 20.
fc2   p dose rates (mrem/hr) on sides of truck, 7th entry = nearest
f2:p     73 74
fs2      -81 84 -82 83 -89 -90 -91 -92 t
sd2   142172 138738 16219 16219 3679 3600 2r 1740 329567
      142172 138738 16219 16219 3679 3600 2r 1740 329567
c      ansi/ans-6.1.1-1977 fluence-to-dose,photons(mrem/hr/(p/cm**2/s)
de2         0.01    0.03    0.05    0.07    0.10    0.15    0.20    0.25    0.30
            0.35    0.40    0.45    0.50    0.55    0.60    0.65    0.70    0.80
            1.00    1.40    1.80    2.20    2.60    2.80    3.25    3.75    4.25
            4.75    5.00    5.25    5.75    6.25    6.75    7.50    9.00    11.0
            13.0    15.0
df2         3.96-3 5.82-4 2.90-4 2.58-4 2.83-4 3.79-4 5.01-4 6.31-4 7.59-4
            8.78-4 9.85-4 1.08-3 1.17-3 1.27-3 1.36-3 1.44-3 1.52-3 1.68-3
            1.98-3 2.51-3 2.99-3 3.42-3 3.82-3 4.01-3 4.41-3 4.83-3 5.23-3
            5.60-3 5.80-3 6.01-3 6.37-3 6.74-3 7.11-3 7.66-3 8.77-3 1.03-2
            1.18-2 1.33-2
fc12  p dose rates (mrem/hr) on ends of truck, 7th entry = nearest
f12:p    71 72
fs12     -85 88 -86 87 -89 -90 -91 -92 t
sd12  10002 10002 16219 16219 3679 3600 2r 1740 68660
      10002 10002 16219 16219 3679 3600 2r 1740 68660
c      ansi/ans-6.1.1-1977 fluence-to-dose,photons(mrem/hr/(p/cm**2/s)
de12        0.01    0.03    0.05    0.07    0.10    0.15    0.20    0.25    0.30
            0.35    0.40    0.45    0.50    0.55    0.60    0.65    0.70    0.80
            1.00    1.40    1.80    2.20    2.60    2.80    3.25    3.75    4.25
            4.75    5.00    5.25    5.75    6.25    6.75    7.50    9.00    11.0
            13.0    15.0
df12        3.96-3 5.82-4 2.90-4 2.58-4 2.83-4 3.79-4 5.01-4 6.31-4 7.59-4
            8.78-4 9.85-4 1.08-3 1.17-3 1.27-3 1.36-3 1.44-3 1.52-3 1.68-3
            1.98-3 2.51-3 2.99-3 3.42-3 3.82-3 4.01-3 4.41-3 4.83-3 5.23-3
            5.60-3 5.80-3 6.01-3 6.37-3 6.74-3 7.11-3 7.66-3 8.77-3 1.03-2
```

```
          1.18-2 1.33-2
fc22   p dose rates (mrem/hr) on bottom and top, 7th entry = nearest
f22:p  75 76
fs22   -81 84 -82 83 -85 -86 -87 -88 t
sd22  133591 130366 15240 15240 2220 3600 2r 2220 309677
      133591 130366 15240 15240 2220 3600 2r 2220 309677
c      ansi/ans-6.1.1-1977 fluence-to-dose,photons(mrem/hr/(p/cm**2/s)
de22       0.01    0.03    0.05    0.07    0.10    0.15    0.20    0.25    0.30
           0.35    0.40    0.45    0.50    0.55    0.60    0.65    0.70    0.80
           1.00    1.40    1.80    2.20    2.60    2.80    3.25    3.75    4.25
           4.75    5.00    5.25    5.75    6.25    6.75    7.50    9.00   11.0
           13.0    15.0
df22       3.96-3 5.82-4 2.90-4 2.58-4 2.83-4 3.79-4 5.01-4 6.31-4 7.59-4
           8.78-4 9.85-4 1.08-3 1.17-3 1.27-3 1.36-3 1.44-3 1.52-3 1.68-3
           1.98-3 2.51-3 2.99-3 3.42-3 3.82-3 4.01-3 4.41-3 4.83-3 5.23-3
           5.60-3 5.80-3 6.01-3 6.37-3 6.74-3 7.11-3 7.66-3 8.77-3 1.03-2
           1.18-2 1.33-2
fc102   p dose rates (mrem/hr) on side of package, 2nd entry
f102:p      38
fs102    -132 -90 -93 -94 -91 -138 t
sd102    1 5j 1 1
c      ansi/ans-6.1.1-1977 fluence-to-dose,photons(mrem/hr/(p/cm**2/s)
de102      0.01    0.03    0.05    0.07    0.10    0.15    0.20    0.25    0.30
           0.35    0.40    0.45    0.50    0.55    0.60    0.65    0.70    0.80
           1.00    1.40    1.80    2.20    2.60    2.80    3.25    3.75    4.25
           4.75    5.00    5.25    5.75    6.25    6.75    7.50    9.00   11.0
           13.0    15.0
df102      3.96-3 5.82-4 2.90-4 2.58-4 2.83-4 3.79-4 5.01-4 6.31-4 7.59-4
           8.78-4 9.85-4 1.08-3 1.17-3 1.27-3 1.36-3 1.44-3 1.52-3 1.68-3
           1.98-3 2.51-3 2.99-3 3.42-3 3.82-3 4.01-3 4.41-3 4.83-3 5.23-3
           5.60-3 5.80-3 6.01-3 6.37-3 6.74-3 7.11-3 7.66-3 8.77-3 1.03-2
           1.18-2 1.33-2
fc122   p dose rates (mrem/hr) on top of package, 1st entry
f122:p      63
fs122     -95 t
c      ansi/ans-6.1.1-1977 fluence-to-dose,photons(mrem/hr/(p/cm**2/s)
de122      0.01    0.03    0.05    0.07    0.10    0.15    0.20    0.25    0.30
           0.35    0.40    0.45    0.50    0.55    0.60    0.65    0.70    0.80
           1.00    1.40    1.80    2.20    2.60    2.80    3.25    3.75    4.25
           4.75    5.00    5.25    5.75    6.25    6.75    7.50    9.00   11.0
           13.0    15.0
df122      3.96-3 5.82-4 2.90-4 2.58-4 2.83-4 3.79-4 5.01-4 6.31-4 7.59-4
           8.78-4 9.85-4 1.08-3 1.17-3 1.27-3 1.36-3 1.44-3 1.52-3 1.68-3
           1.98-3 2.51-3 2.99-3 3.42-3 3.82-3 4.01-3 4.41-3 4.83-3 5.23-3
           5.60-3 5.80-3 6.01-3 6.37-3 6.74-3 7.11-3 7.66-3 8.77-3 1.03-2
           1.18-2 1.33-2
fc32   n dose rates (mrem/hr) on sides of truck, 7th entry = nearest
f32:n    73 74
fs32     -81 84 -82 83 -89 -90 -91 -92 t
sd32  142172 138738 16219 16219 3679 3600 2r 1740 329567
      142172 138738 16219 16219 3679 3600 2r 1740 329567
c      ansi/ans-6.1.1-1977 fluence-to-dose,neutrons(mrem/hr/(n/cm**2/s)
de32    log   2.5e-08 1.0e-07 1.0e-06 1.0e-05 1.0e-04
```

```
             .001      .01      .1       .5       1.0
              2.5      5.0      7.0      10.0     14.0  20.0
df32    log   3.67e-3 3.67e-3 4.46e-3 4.54e-3  4.18e-3
             3.76e-3 3.56e-3 2.17e-2 9.26e-2  .132
              .125     .156     .147     .147     .208  .227
fc42  n dose rates (mrem/hr) on ends of truck, 7th entry = nearest
f42:n   71 72
fs42    -85 88 -86 87 -89 -90 -91 -92 t
sd42  10002 10002 16219 16219 3679 3600 2r 1740 68660
      10002 10002 16219 16219 3679 3600 2r 1740 68660
c      ansi/ans-6.1.1-1977 fluence-to-dose,neutrons(mrem/hr/(n/cm**2/s)
de42    log   2.5e-08 1.0e-07 1.0e-06 1.0e-05 1.0e-04
             .001      .01      .1       .5       1.0
              2.5      5.0      7.0      10.0     14.0  20.0
df42    log   3.67e-3 3.67e-3 4.46e-3 4.54e-3  4.18e-3
             3.76e-3 3.56e-3 2.17e-2 9.26e-2  .132
              .125     .156     .147     .147     .208  .227
fc52   n dose rates (mrem/hr) on bottom and top, 7th entry = nearest
f52:n  75 76
fs52   -81 84 -82 83 -85 -86 -87 -88 t
sd52  133591 130366 15240 15240 2220 3600 2r 2220 309677
      133591 130366 15240 15240 2220 3600 2r 2220 309677
c      ansi/ans-6.1.1-1977 fluence-to-dose,neutrons(mrem/hr/(n/cm**2/s)
de52    log   2.5e-08 1.0e-07 1.0e-06 1.0e-05 1.0e-04
             .001      .01      .1       .5       1.0
              2.5      5.0      7.0      10.0     14.0  20.0
df52    log   3.67e-3 3.67e-3 4.46e-3 4.54e-3  4.18e-3
             3.76e-3 3.56e-3 2.17e-2 9.26e-2  .132
              .125     .156     .147     .147     .208  .227
fc132  n dose rates (mrem/hr) on side of package, 2nd entry
f132:n     38
fs132   -132 -90 -93 -94 -91 -138 t
sd132    1 5j 1 1
c      ansi/ans-6.1.1-1977 fluence-to-dose,neutrons(mrem/hr/(n/cm**2/s)
de132    log   2.5e-08 1.0e-07 1.0e-06 1.0e-05 1.0e-04
             .001      .01      .1       .5       1.0
              2.5      5.0      7.0      10.0     14.0  20.0
df132    log   3.67e-3 3.67e-3 4.46e-3 4.54e-3  4.18e-3
             3.76e-3 3.56e-3 2.17e-2 9.26e-2  .132
              .125     .156     .147     .147     .208  .227
fc152  n dose rates (mrem/hr) on top of package, 1st entry
f152:n     63
fs152    -95 t
c      ansi/ans-6.1.1-1977 fluence-to-dose,neutrons(mrem/hr/(n/cm**2/s)
de152    log   2.5e-08 1.0e-07 1.0e-06 1.0e-05 1.0e-04
             .001      .01      .1       .5       1.0
              2.5      5.0      7.0      10.0     14.0  20.0
df152    log   3.67e-3 3.67e-3 4.46e-3 4.54e-3  4.18e-3
             3.76e-3 3.56e-3 2.17e-2 9.26e-2  .132
              .125     .156     .147     .147     .208  .227
fc5     p dose rates (mrem/hr) at detectors, 2 m, driver
f5:p    0. 327.00 79.  100.
        847.09  0. 79.  100.
```

```
        0. 327.00  0.0  100.
        0. 327.00 -79.0 100.
        0. 327.00 158.0 100.
c       ansi/ans-6.1.1-1977 fluence-to-dose,photons(mrem/hr/(p/cm**2/s)
de5        0.01   0.03   0.05   0.07   0.10   0.15   0.20   0.25   0.30
           0.35   0.40   0.45   0.50   0.55   0.60   0.65   0.70   0.80
           1.00   1.40   1.80   2.20   2.60   2.80   3.25   3.75   4.25
           4.75   5.00   5.25   5.75   6.25   6.75   7.50   9.00   11.0
           13.0   15.0
df5        3.96-3 5.82-4 2.90-4 2.58-4 2.83-4 3.79-4 5.01-4 6.31-4 7.59-4
           8.78-4 9.85-4 1.08-3 1.17-3 1.27-3 1.36-3 1.44-3 1.52-3 1.68-3
           1.98-3 2.51-3 2.99-3 3.42-3 3.82-3 4.01-3 4.41-3 4.83-3 5.23-3
           5.60-3 5.80-3 6.01-3 6.37-3 6.74-3 7.11-3 7.66-3 8.77-3 1.03-2
           1.18-2 1.33-2
ft5     icd
fu5     3 4 5 6 7 8 9 10 11 12 13 14 15 16 17  21 22 23 24
        41 42 43 44 45 46 47  71 72 73
fc15     n dose rates (mrem/hr) at detectors, 2 m, driver
f15:n    0. 327.00 79.  100.
        847.09  0. 79.  100.
        0. 327.00  0.0  100.
        0. 327.00 -79.0 100.
        0. 327.00 158.0 100.
c       ansi/ans-6.1.1-1977 fluence-to-dose,neutrons(mrem/hr/(n/cm**2/s)
de15    log   2.5e-08 1.0e-07 1.0e-06 1.0e-05 1.0e-04
             .001     .01     .1      .5      1.0
              2.5     5.0     7.0     10.0    14.0  20.0
df15    log   3.67e-3 3.67e-3 4.46e-3 4.54e-3  4.18e-3
             3.76e-3 3.56e-3 2.17e-2 9.26e-2  .132
              .125    .156    .147    .147    .208  .227
ft15     icd
fu15    3 4 5 6 7 8 9 10 11 12 13 14 15 16 17  21 22 23 24
        41 42 43 44 45 46 47  71 72 73
```

HAC GAMMA SHIELDING MCNP INPUT FILE

```
SHLD. CALC., GPHS-RTG, NEUTRON-GAMMA,  , accident ingaci
c       sphere of PuO2 for accident condition
    1    3  -9.60   -100
c      inner containment
   21    231 -.00122 ((6 -52 -31 ):(52 -33 -53 )) 100
   22    201  -8.0300  51 -52 31 -32
   23    201  -8.0300  (52 -34 -54 )(33 :53 )
   24    201  -8.0300  51 -6 -31
c      outer containment
   41    231 -.00122 51 35 -64 -39
   42    231 -.00122 ((51 -35 -62 )(52 :32 ))(-52 :34 :54 )
   43    201  -8.0300  (-36 64 -63 )(62 :35 )
   44      236  -1.0  -52 65 36 -37
   45    201  -8.0300  -52 65 37 -38
   46    201  -8.0300  ((64 -65 36 51 -40 ):(-64 39 51 )):(65 38 -66 -40 )
   47    201  -8.0300  61 -51 -40
c       beyond outer containment and inside truck boundary
   71    231 -.00122 (((-52 :36 :63 ))(52 :38 :-66 ))(66 :40 :-61 )
               71 -72 73 -74 75 -76
c      beyond truck and inside large sphere, above ground
   72    231 -.00122  (-71:72:-73:74:-75:76)  77  -111
c     ground
   73    221 -1.67    -77 -111
c       outside world
   74      0  111

    1        py   4.659
    2        px  -4.859
    3        py  -4.659
    4        px   4.859
    5        pz  95.544
    6        pz  0.0000
    7        pz  5.30801
    8        pz  -0.00001
    9       c/y  -2.184  2.654  1.831
   10       c/y   2.184  2.654  1.831
   11        py  -3.1618
   12        py  -0.2941
   13        py  0.2941
   14        py  3.1618
   15        py  -3.1059
   16        py  -0.350
   17        py   0.350
   18        py  3.1059
   19       c/y  -2.1840 2.6540 1.3767
   20       c/y  -2.1840 2.6540 1.4326
   21       c/y  2.1840 2.6540 1.3767
   22       c/y  2.1840 2.6540 1.4326
c   radial surfaces for inner and outer containment
   31        cz  43.1800
   32        cz  45.0850
```

```
   33         cz  43.6562
   34         cz  44.6088
   35         cz  45.5676
   36         cz  46.8376
   37         cz  50.0380
   38         cz  50.3796
   39         cz  49.6443
   40         cz  61.3410
c   inner containment
   51         pz  -8.8138
   52         pz  127.4450
   53         sz  60.3377 88.9000
   54         sz  60.3377 89.8525
c   outer containment
   61         pz  -12.6238
   62         sz  60.1472 90.8050
   63         sz  60.1472 92.0750
   64         kz  48.7807 1.0000 -1.0000
   65         kz  53.0733 1.0000 -1.0000
   66         pz  2.6940
c     truck outside boundary
   71      px  -615.95
   72      px   603.25
   73      py  -127.00
   74      py   127.00
   75      pz   -72.3138
   76      pz   198.0
   77      pz  -184.0738
c      tally fs surfaces on outside of truck
   81      px   -90.0
   82      px   -30.0
   83      px    30.0
   84      px    90.0
   85      py   -90.0
   86      py   -30.0
   87      py    30.0
   88      py    90.0
   89      pz   -11.0
   90      pz    49.0
   91      pz   109.0
   92      pz   169.0
   93      pz    63.76
   94      pz    94.24
   95      cz    15.24
  100      s     0. 0. 142.6  6.5508
c      outside world.
  111         so  5000.0000

*tr1  0  0 31.4560
mode  n p
m1    6000.50  -1.950000
m2    75187.50  -22.500000
m3    94238.50  -6.765000 94239.55  -1.698000 8016.50  -1.137000
```

```
m201  26000.55c 67.970001 24000.50c 20.000000 28000.50c 10.000000
      25055.50c 2.000000 6000.50c 0.030000
c      Hanford hwvp soil
m221  8016.50c -0.511000 14000.50c -0.278200 20000.50c -0.071700
      26000.55c -0.109100 13027.50c -0.083260 12000.50c -0.031420
      19000.50c -0.011550 11023.50c -0.020220 22000.50c -0.016550
      25055.50c -0.001781 15031.50c -0.002400
m231  7014.50c -0.765000 8016.50c -0.235000
m236  1001.50c 0.666700 8016.50c 0.333300
imp:n  1                  4          3r          16          $ 1, 41
       8r  8          0          $ 42, 73
imp:p  1                  4          3r          16          $ 1, 41
       8r  8          0          $ 42, 73
print   10 30 40 50 60 100 110 120 126 170
phys:p     j  1
cut:p    j j 0. 0.
cut:n    j j 0. 0.
sdef          rad d4    erg=d9
               pos 0. 0. 142.6   wgt=5.13252e7
si4    6.5508
sp4     -21 2
c      neutron spectrum from Harvey 10-3-95, 157 g fueled clad
#            si9       sp9
              h         d
            0.00    0.0000E+00
             0.10000       0.1020E+05
             0.20000       0.1260E+05
             0.30000       0.1350E+05
             0.40000       0.1510E+05
             0.50000       0.1770E+05
             0.60000       0.1900E+05
             0.70000       0.2000E+05
             0.80000       0.2080E+05
             0.90000       0.2030E+05
             1.00000       0.1830E+05
             1.10000       0.1840E+05
             1.20000       0.1890E+05
             1.30000       0.1990E+05
             1.40000       0.2050E+05
             1.50000       0.2040E+05
             1.60000       0.2070E+05
             1.70000       0.2150E+05
             1.80000       0.2270E+05
             1.90000       0.2300E+05
             2.00000       0.2350E+05
             2.10000       0.2330E+05
             2.20000       0.2380E+05
             2.30000       0.2380E+05
             2.40000       0.2260E+05
             2.50000       0.2160E+05
             2.60000       0.2070E+05
             2.70000       0.1980E+05
             2.80000       0.1830E+05
```

```
            2.90000         0.1770E+05
            3.00000         0.1660E+05
            3.10000         0.1490E+05
            3.20000         0.1400E+05
            3.30000         0.1240E+05
            3.40000         0.1040E+05
            3.50000         0.9100E+04
            3.60000         0.8060E+04
            3.70000         0.6880E+04
            3.80000         0.6120E+04
            3.90000         0.5490E+04
            4.00000         0.4720E+04
            4.10000         0.4340E+04
            4.20000         0.3400E+04
            4.30000         0.2940E+04
            4.40000         0.2360E+04
            4.50000         0.4950E+04
            5.00000         0.5200E+04
            5.50000         0.3790E+04
            6.00000         0.2660E+04
            6.50000         0.1850E+04
            7.00000         0.1290E+04
            7.50000         0.8920E+03
            8.00000         0.6130E+03
            8.50000         0.4210E+03
            9.00000         0.2570E+03
            9.50000         0.1970E+03
           10.00000         0.1980E+03
           11.00000         0.1210E+03
           12.00000         0.5530E+02
           13.00000         0.2480E+02
           14.00000         0.1110E+02
           15.00000         0.4900E+01
c          total =   0.71285E+06 x 72 = 5.13252E+07
ctme    200
nps        60000
prdmp     j -960
e0      .2 .6 .8 2. 20.
fc2    p dose rates (mrem/hr) on sides of truck, 7th entry = nearest
f2:p     73 74
fs2      -81 84 -82 83 -89 -90 -91 -92 t
sd2    142172 138738 16219 16219 3679 3600 2r 1740 329567
       142172 138738 16219 16219 3679 3600 2r 1740 329567
c       ansi/ans-6.1.1-1977 fluence-to-dose,photons(mrem/hr/(p/cm**2/s)
de2          0.01    0.03    0.05    0.07    0.10    0.15    0.20    0.25    0.30
             0.35    0.40    0.45    0.50    0.55    0.60    0.65    0.70    0.80
             1.00    1.40    1.80    2.20    2.60    2.80    3.25    3.75    4.25
             4.75    5.00    5.25    5.75    6.25    6.75    7.50    9.00    11.0
             13.0    15.0
df2          3.96-3 5.82-4 2.90-4 2.58-4 2.83-4 3.79-4 5.01-4 6.31-4 7.59-4
             8.78-4 9.85-4 1.08-3 1.17-3 1.27-3 1.36-3 1.44-3 1.52-3 1.68-3
             1.98-3 2.51-3 2.99-3 3.42-3 3.82-3 4.01-3 4.41-3 4.83-3 5.23-3
             5.60-3 5.80-3 6.01-3 6.37-3 6.74-3 7.11-3 7.66-3 8.77-3 1.03-2
```

```
          1.18-2 1.33-2
fc12  p dose rates (mrem/hr) on ends of truck, 7th entry = nearest
f12:p   71 72
fs12     -85 88 -86 87 -89 -90 -91 -92 t
sd12  10002 10002 16219 16219 3679 3600 2r 1740 68660
      10002 10002 16219 16219 3679 3600 2r 1740 68660
c      ansi/ans-6.1.1-1977 fluence-to-dose,photons(mrem/hr/(p/cm**2/s)
de12        0.01    0.03    0.05    0.07    0.10    0.15    0.20    0.25    0.30
            0.35    0.40    0.45    0.50    0.55    0.60    0.65    0.70    0.80
            1.00    1.40    1.80    2.20    2.60    2.80    3.25    3.75    4.25
            4.75    5.00    5.25    5.75    6.25    6.75    7.50    9.00   11.0
            13.0    15.0
df12        3.96-3 5.82-4 2.90-4 2.58-4 2.83-4 3.79-4 5.01-4 6.31-4 7.59-4
            8.78-4 9.85-4 1.08-3 1.17-3 1.27-3 1.36-3 1.44-3 1.52-3 1.68-3
            1.98-3 2.51-3 2.99-3 3.42-3 3.82-3 4.01-3 4.41-3 4.83-3 5.23-3
            5.60-3 5.80-3 6.01-3 6.37-3 6.74-3 7.11-3 7.66-3 8.77-3 1.03-2
            1.18-2 1.33-2
fc22   p dose rates (mrem/hr) on bottom and top, 7th entry = nearest
f22:p  75 76
fs22   -81 84 -82 83 -85 -86 -87 -88 t
sd22  133591 130366 15240 15240 2220 3600 2r 2220 309677
      133591 130366 15240 15240 2220 3600 2r 2220 309677
c      ansi/ans-6.1.1-1977 fluence-to-dose,photons(mrem/hr/(p/cm**2/s)
de22        0.01    0.03    0.05    0.07    0.10    0.15    0.20    0.25    0.30
            0.35    0.40    0.45    0.50    0.55    0.60    0.65    0.70    0.80
            1.00    1.40    1.80    2.20    2.60    2.80    3.25    3.75    4.25
            4.75    5.00    5.25    5.75    6.25    6.75    7.50    9.00   11.0
            13.0    15.0
df22        3.96-3 5.82-4 2.90-4 2.58-4 2.83-4 3.79-4 5.01-4 6.31-4 7.59-4
            8.78-4 9.85-4 1.08-3 1.17-3 1.27-3 1.36-3 1.44-3 1.52-3 1.68-3
            1.98-3 2.51-3 2.99-3 3.42-3 3.82-3 4.01-3 4.41-3 4.83-3 5.23-3
            5.60-3 5.80-3 6.01-3 6.37-3 6.74-3 7.11-3 7.66-3 8.77-3 1.03-2
            1.18-2 1.33-2
fc32   n dose rates (mrem/hr) on sides of truck, 7th entry = nearest
f32:n    73 74
fs32     -81 84 -82 83 -89 -90 -91 -92 t
sd32  142172 138738 16219 16219 3679 3600 2r 1740 329567
      142172 138738 16219 16219 3679 3600 2r 1740 329567
c      ansi/ans-6.1.1-1977 fluence-to-dose,neutrons(mrem/hr/(n/cm**2/s)
de32    log   2.5e-08 1.0e-07 1.0e-06 1.0e-05 1.0e-04
             .001     .01     .1      .5      1.0
              2.5     5.0     7.0     10.0    14.0  20.0
df32    log   3.67e-3 3.67e-3 4.46e-3 4.54e-3  4.18e-3
             3.76e-3 3.56e-3 2.17e-2 9.26e-2  .132
              .125    .156    .147    .147    .208  .227
fc42  n dose rates (mrem/hr) on ends of truck, 7th entry = nearest
f42:n   71 72
fs42     -85 88 -86 87 -89 -90 -91 -92 t
sd42  10002 10002 16219 16219 3679 3600 2r 1740 68660
      10002 10002 16219 16219 3679 3600 2r 1740 68660
c      ansi/ans-6.1.1-1977 fluence-to-dose,neutrons(mrem/hr/(n/cm**2/s)
de42    log   2.5e-08 1.0e-07 1.0e-06 1.0e-05 1.0e-04
             .001     .01     .1      .5      1.0
```

```
             2.5     5.0     7.0     10.0    14.0  20.0
df42    log  3.67e-3 3.67e-3 4.46e-3 4.54e-3  4.18e-3
            3.76e-3 3.56e-3 2.17e-2 9.26e-2  .132
             .125    .156    .147    .147    .208  .227
fc52   n dose rates (mrem/hr) on bottom and top, 7th entry = nearest
f52:n  75 76
fs52   -81 84 -82 83 -85 -86 -87 -88 t
sd52  133591 130366 15240 15240 2220 3600 2r 2220 309677
      133591 130366 15240 15240 2220 3600 2r 2220 309677
c      ansi/ans-6.1.1-1977 fluence-to-dose,neutrons(mrem/hr/(n/cm**2/s)
de52    log   2.5e-08 1.0e-07 1.0e-06 1.0e-05 1.0e-04
              .001    .01     .1      .5      1.0
               2.5     5.0     7.0     10.0    14.0  20.0
df52    log   3.67e-3 3.67e-3 4.46e-3 4.54e-3  4.18e-3
             3.76e-3 3.56e-3 2.17e-2 9.26e-2  .132
              .125    .156    .147    .147    .208  .227
fc102   p dose rates (mrem/hr) on side of package, 2nd entry
f102:p      38
fs102     -93 -94 t
c       ansi/ans-6.1.1-1977 fluence-to-dose,photons(mrem/hr/(p/cm**2/s)
de102       0.01    0.03    0.05    0.07    0.10    0.15    0.20    0.25    0.30
            0.35    0.40    0.45    0.50    0.55    0.60    0.65    0.70    0.80
            1.00    1.40    1.80    2.20    2.60    2.80    3.25    3.75    4.25
            4.75    5.00    5.25    5.75    6.25    6.75    7.50    9.00    11.0
            13.0    15.0
df102       3.96-3 5.82-4 2.90-4 2.58-4 2.83-4 3.79-4 5.01-4 6.31-4 7.59-4
            8.78-4 9.85-4 1.08-3 1.17-3 1.27-3 1.36-3 1.44-3 1.52-3 1.68-3
            1.98-3 2.51-3 2.99-3 3.42-3 3.82-3 4.01-3 4.41-3 4.83-3 5.23-3
            5.60-3 5.80-3 6.01-3 6.37-3 6.74-3 7.11-3 7.66-3 8.77-3 1.03-2
            1.18-2 1.33-2
fc122   p dose rates (mrem/hr) on top of package, 1st entry
f122:p      63
fs122     -95 t
c       ansi/ans-6.1.1-1977 fluence-to-dose,photons(mrem/hr/(p/cm**2/s)
de122       0.01    0.03    0.05    0.07    0.10    0.15    0.20    0.25    0.30
            0.35    0.40    0.45    0.50    0.55    0.60    0.65    0.70    0.80
            1.00    1.40    1.80    2.20    2.60    2.80    3.25    3.75    4.25
            4.75    5.00    5.25    5.75    6.25    6.75    7.50    9.00    11.0
            13.0    15.0
df122       3.96-3 5.82-4 2.90-4 2.58-4 2.83-4 3.79-4 5.01-4 6.31-4 7.59-4
            8.78-4 9.85-4 1.08-3 1.17-3 1.27-3 1.36-3 1.44-3 1.52-3 1.68-3
            1.98-3 2.51-3 2.99-3 3.42-3 3.82-3 4.01-3 4.41-3 4.83-3 5.23-3
            5.60-3 5.80-3 6.01-3 6.37-3 6.74-3 7.11-3 7.66-3 8.77-3 1.03-2
            1.18-2 1.33-2
fc132   n dose rates (mrem/hr) on side of package, 2nd entry
f132:n      38
fs132     -93 -94 t
c       ansi/ans-6.1.1-1977 fluence-to-dose,neutrons(mrem/hr/(n/cm**2/s)
de132    log   2.5e-08 1.0e-07 1.0e-06 1.0e-05 1.0e-04
               .001    .01     .1      .5      1.0
                2.5     5.0     7.0     10.0    14.0  20.0
df132    log   3.67e-3 3.67e-3 4.46e-3 4.54e-3  4.18e-3
              3.76e-3 3.56e-3 2.17e-2 9.26e-2  .132
```

```
              .125    .156    .147    .147    .208  .227
fc152   n dose rates (mrem/hr) on top of package, 1st entry
f152:n      63
fs152     -95 t
c       ansi/ans-6.1.1-1977 fluence-to-dose,neutrons(mrem/hr/(n/cm**2/s)
de152     log   2.5e-08 1.0e-07 1.0e-06 1.0e-05 1.0e-04
               .001     .01     .1      .5      1.0
                2.5     5.0     7.0     10.0    14.0  20.0
df152     log   3.67e-3 3.67e-3 4.46e-3 4.54e-3  4.18e-3
              3.76e-3 3.56e-3 2.17e-2 9.26e-2  .132
               .125    .156    .147    .147    .208  .227
fc5     p dose rates (mrem/hr) at detectors, 1 m above top s
f5:p    0. 0. 252.22  50.
c       ansi/ans-6.1.1-1977 fluence-to-dose,photons(mrem/hr/(p/cm**2/s)
de5        0.01   0.03   0.05   0.07   0.10   0.15   0.20   0.25   0.30
           0.35   0.40   0.45   0.50   0.55   0.60   0.65   0.70   0.80
           1.00   1.40   1.80   2.20   2.60   2.80   3.25   3.75   4.25
           4.75   5.00   5.25   5.75   6.25   6.75   7.50   9.00   11.0
           13.0   15.0
df5        3.96-3 5.82-4 2.90-4 2.58-4 2.83-4 3.79-4 5.01-4 6.31-4 7.59-4
           8.78-4 9.85-4 1.08-3 1.17-3 1.27-3 1.36-3 1.44-3 1.52-3 1.68-3
           1.98-3 2.51-3 2.99-3 3.42-3 3.82-3 4.01-3 4.41-3 4.83-3 5.23-3
           5.60-3 5.80-3 6.01-3 6.37-3 6.74-3 7.11-3 7.66-3 8.77-3 1.03-2
           1.18-2 1.33-2
fc15    n dose rates (mrem/hr) at detectors, 1 m above top s
f15:n   0. 0. 252.22  50.
c       ansi/ans-6.1.1-1977 fluence-to-dose,neutrons(mrem/hr/(n/cm**2/s)
de15    log   2.5e-08 1.0e-07 1.0e-06 1.0e-05 1.0e-04
              .001     .01     .1      .5      1.0
               2.5     5.0     7.0     10.0    14.0  20.0
df15    log   3.67e-3 3.67e-3 4.46e-3 4.54e-3  4.18e-3
              3.76e-3 3.56e-3 2.17e-2 9.26e-2  .132
               .125    .156    .147    .147    .208  .227
```

6.0 CRITICALITY EVALUATION

This chapter discusses the principal criticality engineering-physics design of the Radioisotope Thermoelectrical Generator (RTG) Transportation System Package and contents important to safety and necessary to comply with 10 CFR 71. A single package will be shipped as a fissile class III shipment. For normal conditions of transport (NCT), a one-package shipment is to remain subcritical when it is in contact with an identical one-package shipment and the two-package array is reflected on all sides by water. The single-package shipment must remain subcritical under hypothetical accident conditions (HAC) with optimum hydrogenous moderation and close reflection by water.

6.1 DISCUSSION AND RESULTS

The RTG Transportation System Package is a Type B(U) packaging system that is used to transport a RTG or similar payload. The primary payload for use in the package is one GPHS RTG. Because of the heat load limits, only one GPHS RTG can be shipped in the exclusive-use RTG Transportation System trailer. The GPHS RTG will be inside the package's two containment vessels when shipped. This will aid in preventing damage to the fueled portion of the RTG during HAC events. However, the main thrust of these analyses was to determine the maximum K_{eff} for the fuel involved in the most reactive configuration, assuming only that the fueled clads stay in their original shape and size.

The GPHS RTG criticality analyses were performed with the Monte Carlo Neutron Photon (MCNP)[1] code for both the actual configuration and the most reactive array of fueled clads. These results are summarized in Table 6-1 and show that the GPHS RTG will remain safely subcritical for all NCT and HAC events.

Although the total fuel quantity for the generic payload per trailer is greater (11.1%) than the GPHS RTG total fuel quantity (12,560 g PuO_2 vs. 11,304 g PuO_2), the maximum fuel quantity per package is only 55.6% of that for the GPHS. Consequently, the resultant k_{eff} value for the larger fuel quantity is slightly higher than the values summarized in Table 6-1. For the larger fuel mass, the k_{eff} for the HAC would increase from the GPHS RTG value of 0.745 to 0.780, which is a 4.7% increase. This result is documented in the RTG Transportation System SARP Addendum (WHC-SD-RTG-SARP-002). The higher value for the larger fuel quantity is still well below the k_{eff} limit of 0.95.

TABLE 6-1. Summary of Criticality Analyses (all cases reflected by 30 cm of water).

Case	Total mass of PuO_2 (Kg)	Moderator	$K_{eff} \pm 1\sigma$
GPHS RTGs (NCT)	--	--	--
One RTG	11.3	C	0.404 ± 0.003
Two RTGs	22.6	C	0.409 ± 0.002
GPHS RTG (HAC)	--	--	--
One RTG	12.6	H_2O	0.745 ± 0.004

6.2 PACKAGE FUEL LOADING

The maximum fuel loading for both NCT and HAC events is contained in Table 6.2-1.

TABLE 6.2-1. RTG Transportation System Package Payload Descriptions.

Payload description	Number of RTGs per package	Total mass of PuO_2 (kg)
GPHS-RTG	1	11.3

The material compositions used in the analyses are given in Table 6.2-2. The plutonium composition limits specified in Reference 2 are 80 to 86 molecular percent ^{238}Pu. Therefore, calculations were performed for both the 80 and 86 percent limits. The remainder of the plutonium was (conservatively) ^{239}Pu in all the calculations. The fuel loading is further defined in Table 6.3.2-1.

TABLE 6.2-2. MCNP Material Compositions Used.

Material	Weight %
PuO_2 (9.6 g/cm^3)[5]	
Plutonium	88.2
Oxygen	11.8
Graphite (1.95 g/cm^3)	100.0
Iridium (22.5 g/cm^3)	100.0
Water (1.0 g/cm^3, unless indicated otherwise)	
Oxygen	88.9
Hydrogen	11.1

6.3 MODEL SPECIFICATION

This section describes the computer models used for the analyses.

6.3.1 Description of Calculational Model

The design of the GPHS modules (also known as aeroshells) is shown in Figure 6.3.1-1. The MCNP computer geometries used for the GPHS RTG evaluation are shown in Figures 6.3.1-2 through 6.3.1-13. These figures show that the GPHS RTGs were evaluated in their normal fuel arrangement in an RTG. But, additional configurations of fuel were evaluated to be sure that the most reactive conditions were considered. Computer models were made for large spheres of fuel, arrays of GPHS aeroshells (which contain four fueled clads), and arrays of fueled clads. As detailed in Section 1.3.1, Reference 3, Chapter 1.0 of this SARP, the GPHS aeroshell is designed to survive atmospheric reentry and is the smallest size of heat-generating fragment that could arise from

break-up of the GPHS RTG during HAC events. The criticality evaluation is considered conservative because arrays of individual fueled clads are evaluated.

The GPHS RTG contains a vertical stack of 18 GPHS aeroshells; each one contains four fueled clads. Each fueled clad contains about 157 grams of PuO_2 (Reference 2).

All MCNP geometries were reflected by 30 cm of water, and water flooding was assumed for all HAC events.

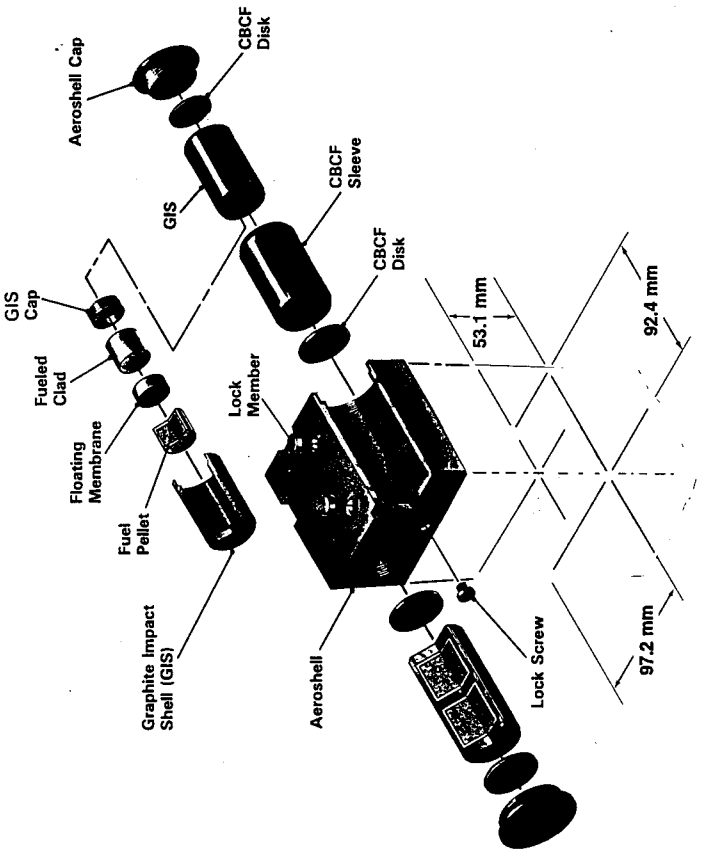


FIGURE 6.3.1-1. An Exploded View of a General Purpose Heat Source Module.

```
 11/24/93 08:18:38
CRIT CALCS, RTG FUEL IN SPHERE,
 9 CM RADIUS, 80 MOLECULARX
 PU-238
PROBID =  11/24/93 08:14:07
BASIS:
( 0.000000, 1.000000, 0.000000)
( 0.000000, 0.000000, 1.000000)
ORIGIN:
(    0.00,    0.20,   -0.80)
EXTENT = (   42.00,   42.00)
CELL LABELS ARE
 MASS DENSITIES

plot>
```

Material	Densities (g/cm^3)
PuO_2	9.6
C	1.95
Ir	22.5
H_2O	1.0

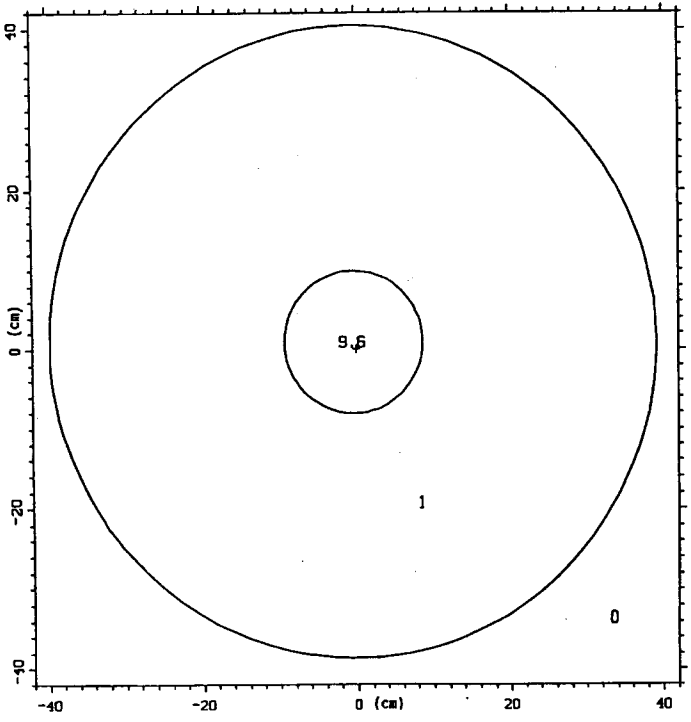


FIGURE 6.3.1-2. PuO_2 Sphere Water Reflector.

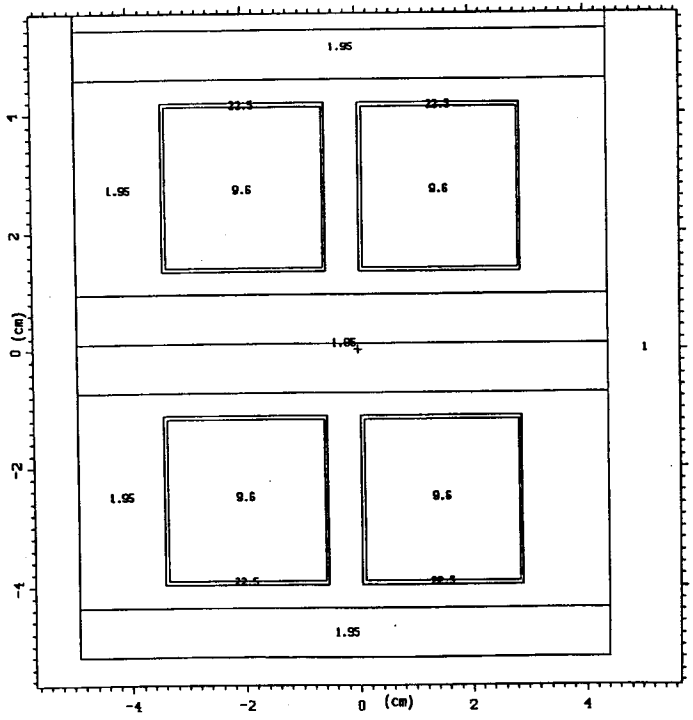
FIGURE 6.3.1-3. GPHS RTG with Water Reflector, Y-Z Plane.

FIGURE 6.3.1-4. GPHS RTG with Water Reflector, X-Z Plane.

```
 11/24/93 08:05:30
CRIT. CALC., GPHS-RTG, GRAPHITE,
 80% PU-238

PROBID =   11/24/93 08:01:17
BASIS:
( 0.000000, 1.000000, 0.000000)
( 0.000000, 0.000000, 1.000000)
ORIGIN:
(    2.00,     0.25,     5.20)
EXTENT = (    5.68,     5.68)
CELL LABELS ARE
 MASS DENSITIES

plot>
```



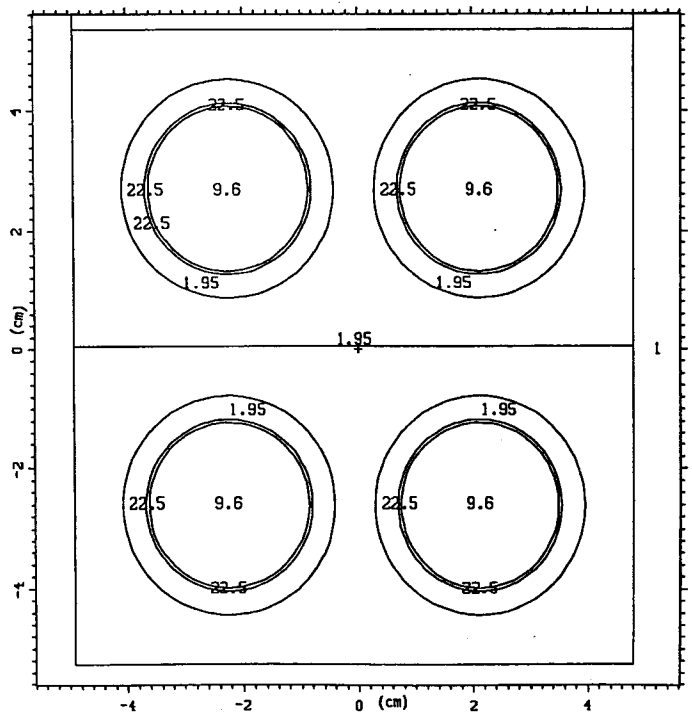
Material Densities (g/cm^3)	
PuO_2	9.6
C	1.95
Ir	22.5
H_2O	1.0

FIGURE 6.3.1-5. GPHS RTG with Water Reflector, Y-Z Plane.

```
11/24/93 08:07:05
CRIT. CALC., GPHS-RTG, GRAPHITE,
 BOX PU-238

PROBID =  11/24/93 08:03:17
BASIS:
( 1.000000, 0.000000, 0.000000)
( 0.000000, 0.000000, 1.000000)
ORIGIN=
(   0.07,     1.00,     5.261
EXTENT = (     5.61,     5.611
CELL LABELS ARE
 MASS DENSITIES

plot>
```



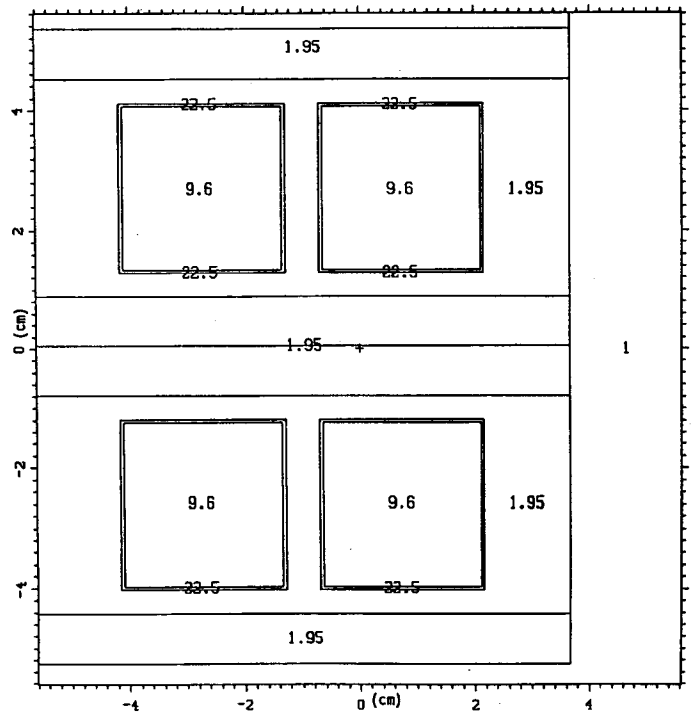
Material	Densities (g/cm^3)
PuO_2	9.6
C	1.95
Ir	22.5
H_2O	1.0

FIGURE 6.3.1-6. GPHS RTG with Water Reflector, X-Z Plane.

```
  11/24/93 08:08:33
CRIT. CALC., GPHS-RTG, GRAPHITE,
  BOX PU-238

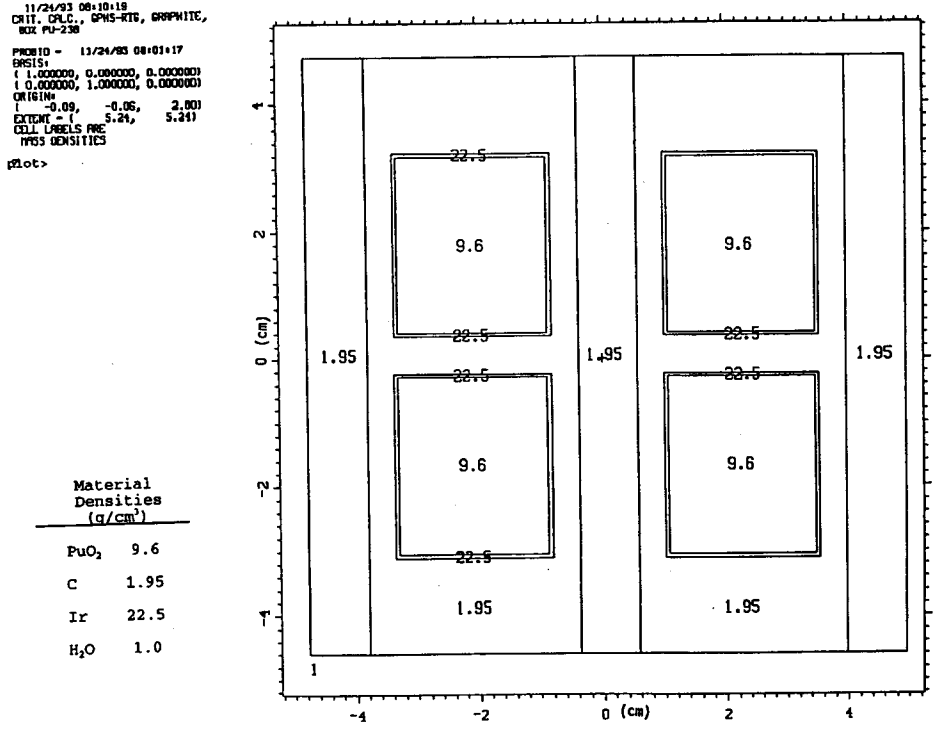
PROBID =  11/24/93 08:01:17
BASIS:
( 0.000000, 1.000000, 0.000000)
( 0.000000, 0.000000, 1.000000)
ORIGIN=
(  2.00,    1.00,    5.26)
EXTENT = (  5.61,    5.61)
CELL LABELS ARE
 MASS DENSITIES

plot>
```



Material	Densities (g/cm³)
PuO_2	9.6
C	1.95
Ir	22.5
H_2O	1.0

FIGURE 6.3.1-7. GPHS RTG with Water Reflector, Y-Z Plane.



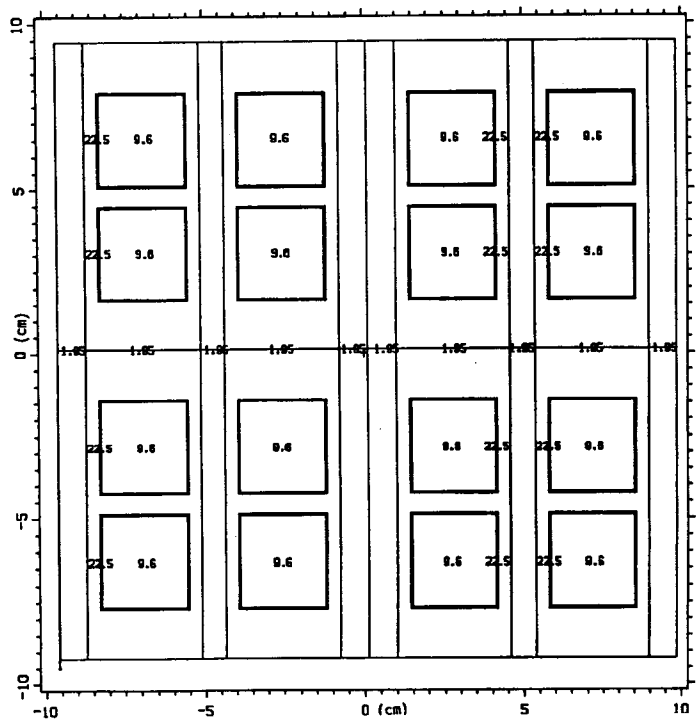
Material	Densities (g/cm^3)
PuO_2	9.6
C	1.95
Ir	22.5
H_2O	1.0

FIGURE 6.3.1-8. GPHS RTG with Water Reflector, X-Y Plane.

```
 11/24/93 08:44:02
CRIT. CALC, 3D GPHS - 4XS ARRAY,
 GRAPHITE, 95% PU-238

PROBID =   11/24/93 08:41:11
BASIS=
( 1.000000, 0.000000, 0.0000001
( 0.000000, 1.000000, 0.0000001
ORIGIN=
(    4.74,     4.55,     3.00)
EXTENT = (     10.20,    10.20)
CELL LABELS ARE
 MASS DENSITIES

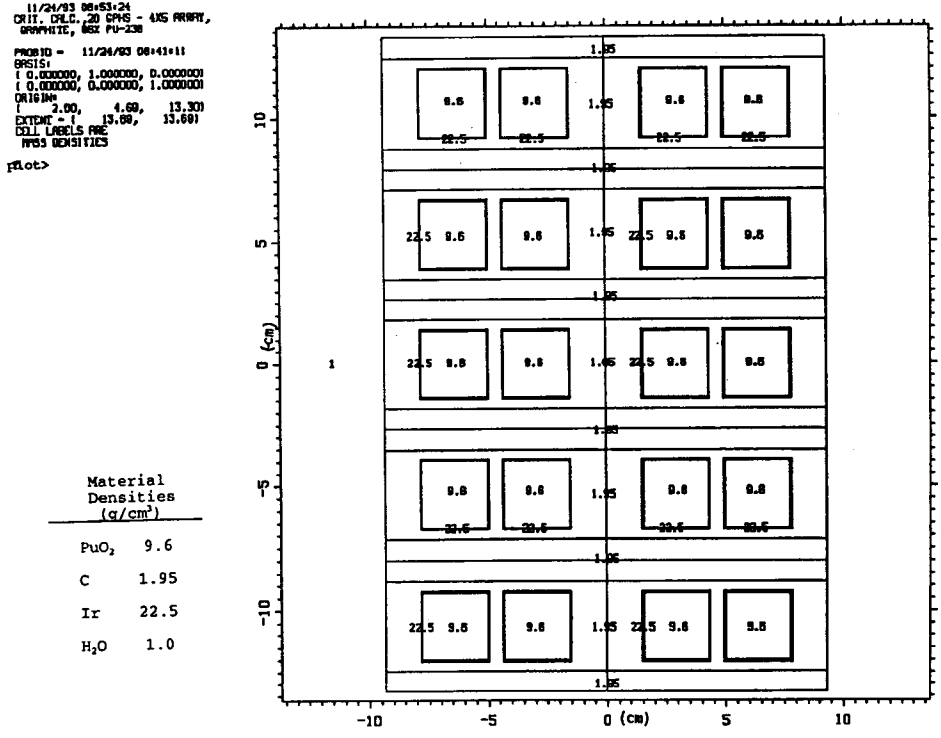
plot>
```



Material	Densities (g/cm^3)
PuO_2	9.6
C	1.95
Ir	22.5
H_2O	1.0

FIGURE 6.3.1-9. 2 x 2 x 5 Array of GPHS Water Reflected, X-Y Plane.

11/24/93 09:45:34
DRIVE PLC, 20 GPHS - 40S ARRAY,
GRAPHITE, 60% PU-238
PROBID - 11/24/93 08:41:11
BASIS: 0.000000, 0.000000, 0.000000
(0.000000, 0.000000, 1.000000)
ORIGIN:
(1.43, 2.00, 13.25)
EXTENT: 14.85, 14.85, 14.85
CELL LABELS ARE
MASS DENSITIES
plot>
Material
Densities
(g/cm³)
PuO2 9.6
C 1.95
Ir 22.5
H2O 1.0
10
5
0 (cm)
-5
-10
-10
-5
0
5
10
1.85
1.85
1.85



Material	Densities (g/cm^3)
PuO_2	9.6
C	1.95
Ir	22.5
H_2O	1.0

FIGURE 6.3.1-11. 2 x 2 x 5 Array of GPHS Water Reflected, Y-Z Plane.

```
 11/28/93 09:42:33
CLOSELY PACKED FUEL CLADS, 4X4X5
 ARRAY, CARBON MOD., 86% PU-238

PROBID =   11/28/93 09:37:46
BASIS:
( 1.000000, 0.000000, 0.0000001
( 0.000000, 1.000000, 0.0000001
ORIGIN:
(    4.26,     -4.31,      3.301
EXTENT = (     5.80,      5.901
CELL LABELS ARE
 MASS DENSITIES

plot>
```

Material	Densities (g/cm^3)
PuO_2	9.6
C	1.95
Ir	22.5
H_2O	1.0

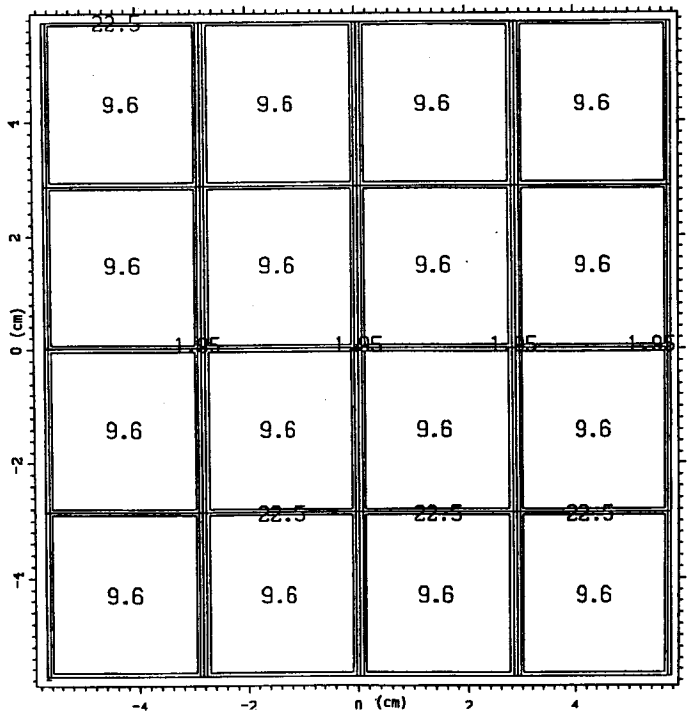
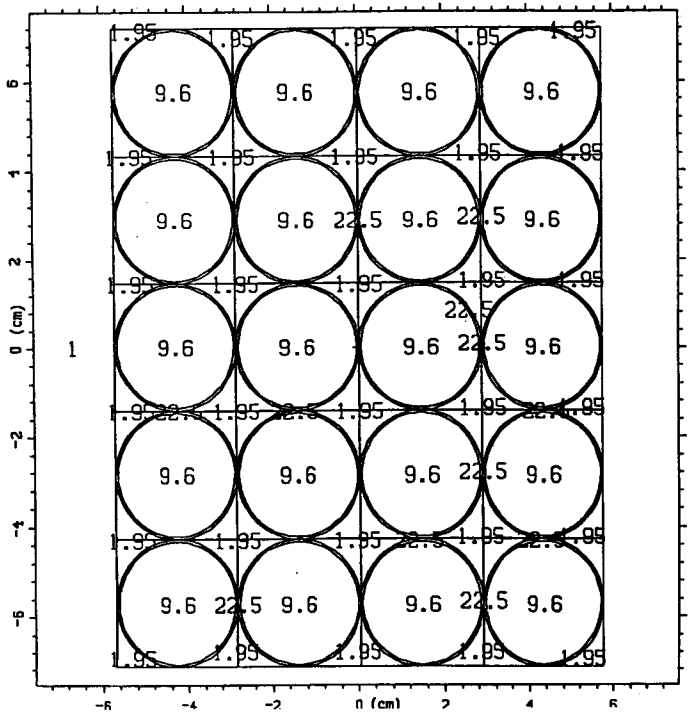


FIGURE 6.3.1-12. 4 x 4 x 5 Array of Fueled Clads Water Reflected, X-Y Plane.

```
11/29/93 09:47:51
CLOSELY PACKED FUEL CLADS, 4X4X5
 ARRAY, CARBON MOD., 86Z PU-238

PROBID =  11/29/93 09:37:46
BASIS:
( 1.000000, 0.000000, 0.000000)
( 0.000000, 0.000000, 1.000000)
ORIGIN:
(    4.26,      0.10,      5.70)
EXTENT = (      7.56,      7.56)
CELL LABELS ARE
 MASS DENSITIES

plot>
```



Material Densities (g/cm³)	
PuO_2	9.6
C	1.95
Ir	22.5
H_2O	1.0

FIGURE 6.3.1-13. 4 x 4 x 5 Array of Fueled Clads Water Reflected, X-Z Plane.

6.3.2 Package Regional Densities

The material densities used for these analyses are shown in Table 6.3.2-1. There was no change in material densities for the HAC event. The fuel densities and composition are given in Reference 2. This reference calls out a ^{238}Pu range of 80 to 86%. The remainder of the plutonium used was conservatively ^{239}Pu. The mass of a GPHS fuel pellet is 157 g.

TABLE 6.3.2-1. Material Densities Used for the GPHS RTG.

Material	Constituents	Mass density (g/cm^3)	Atom density (atoms/b-cm)
PuO_2(80%Pu238)	--	9.6	6.4199E-2
--	Pu238	6.765	1.7114E-2
--	Pu239	1.698	4.2776E-3
--	O16	1.137	4.2808E-2
PuO_2(86%Pu238)	--	9.6	6.4204E-2
--	Pu238	7.274	1.8402E-2
--	Pu239	1.189	2.9951E-3
--	O16	1.137	4.2807E-2
Graphite	C12	1.95	9.7768E-2
Ir(Re used)	Re187	22.5	7.2475E-2
Water	--	1.0	9.9858E-2
--	H	0.1111	6.6392E-2
--	O16	0.8889	3.3466E-2

6.4 CRITICALITY CALCULATIONS

This section describes the calculational methods used to determine the reactivity for the maximum fuel loadings of the RTG Transportation System Package.

6.4.1 Calculational Method

The MCNP code (References 1 and 3) was used for the reactivity evaluation of the package. The MCNP code was developed at the Los Alamos National Laboratory (LANL) and is now used extensively both in this country and throughout the world. The MCNP code is a general-purpose, continuous-energy, generalized-geometry neutron and photon transport code that calculates eigenvalues for criticality evaluations.

The MCNP code uses continuous energy cross-sections that are thoroughly documented in Appendix G of Reference 3. These cross-sections are defined with a high-energy resolution. All the cross-sections used in the RTG criticality analyses were generated from either Evaluated Nuclear Data Files (ENDF) or LANL evaluations. Processing this type of data is not required for different moderator-to-fuel ratio conditions.

These analyses help determine the maximum reactivity fueled clad arrays, assuming the fueled clads retained their original size and shape. The actual GPHS RTG geometry was also modeled and evaluated. It was substantially less reactive than equivalent numbers of tightly packed fueled clads.

6.4.2 Fuel/Moderator Loading Optimization

The fuel loadings used are maximum values from Reference 2. Evaluations were made for both the lower and upper limits of ^{238}Pu and ^{239}Pu. Evaluations were also made for maximum moderation even though no room for it existed in some cases. An evaluation was even made for abnormally high water densities (greater than 1 g/cm^3) with a square array of closely packed GPHS fueled clads (Table 6.4.3-1). Therefore, the reactivity increased with increasing water density, thus demonstrating that the square array was undermoderated. This shows that lower density water would decrease the reactivity.

Tighter fueled clad packing could be obtained than that from the square arrays used. But, the evaluation was made for much closer spacing than is possible with the graphite that surrounds the fuel in either NCT or HAC events. The analyses on the GPHS RTG showed that the closely packed fueled clads are more reactive than the larger normal spacing. All the calculations were made with a 30-cm-thick water reflector surrounding the model. All K_{eff} calculations were run to a 1-σ convergence criteria of 0.005 or less. Actual convergence values obtained are specified in Table 6.4.3-1. Continuous cross-sections were used in these evaluations; therefore, no cross-section adjustments were required for various geometric configurations and material compositions.

6.4.3 Criticality Results

The results of the MCNP calculations are contained in Table 6.4.3-1 for the GPHS RTG. It was determined that a sphere of PuO_2 with a mass of 11.3 kg (equivalent mass for one GPHS RTG) would remain safely subcritical. The reactivity increases as fueled clads become more tightly packed. Water moderation also increases reactivity for a tightly packed array of fueled clads. When the array expands, the K_{eff} decreases more from geometric expansion than it increases from increased moderation.

The analyses for the GPHS RTG showed that a single RTG in its normal configuration, except for full water reflection, would have a K_{eff} of 0.404. Two GPHS RTGs could only be brought to within a spacing of about 50 cm center-to-center, even if no credit is taken for the two containment vessels on each package. Two cases were run with this spacing. In the first, the water reflector was around and between both RTGs. In the second, a void channel was left directly between the two RTGs (for maximum neutron communication) with full water reflection around the rest. The maximum K_{eff} from these two calculations (with water reflection between RTGs) was 0.409.

A conservative model was generated for the HAC case. It consisted of a closely packed 4 by 4 by 5 array of fueled clads, water moderated, and no iridium cladding. The K_{eff} for this configuration was 0.745.

The remaining calculations reported in Table 6.4.3-1 show that increased spacing between fueled clads reduces the reactivity even with water moderation. The calculations with "nonreal" high density water show that a tightly packed array of fueled clads with normal water density will be undermoderated.

The cross-sections for iridium (the clad material of the fueled clads) were not available, so rhenium cross-sections were used in their place. This is conservative because the total cross-section for iridium in the thermal range is about five times that of rhenium and the cross sections at higher energies are nearly the same. Therefore, the substitution would be conservative. However, it was still necessary to see the effect of removing the iridium clad for a few MCNP runs. It can be seen in Table 6.4.3-1 that voiding out the iridium regions increased the k_{eff} by about 0.05. Even this unrealistic condition would not alter the conclusion that the package will be critically safe for both NCT and HAC events.

TABLE 6.4.3-1. Results of the MCNP Analyses for GPHS RTGs.

Case	Total mass of PuO_2 (Kg)	Moderator	$K_{eff} \pm 1\sigma$
Sphere, 80% ^{238}Pu, radius = 6 cm	8.68	None	0.753 ± 0.005
Sphere, 86% ^{238}Pu, radius = 6 cm	8.68	None	0.743 ± 0.004
Sphere, 80% ^{238}Pu, radius = 7 cm	13.8	None	0.869 ± 0.005
Sphere, 86% ^{238}Pu, radius = 7 cm	13.8	None	0.842 ± 0.005
Sphere, 80% ^{238}Pu, radius = 8 cm	20.6	None	0.954 ± 0.004
Sphere, 86% ^{238}Pu, radius = 8 cm	20.6	None	0.943 ± 0.005
Sphere, 80% ^{238}Pu, radius = 9 cm	29.3	None	1.053 ± 0.004
Sphere, 86% ^{238}Pu, radius = 9 cm	29.3	None	1.031 ± 0.004
GPHS RTG,80% ^{238}Pu, norm. config.	11.3	C	0.363 ± 0.002
GPHS RTG,80% ^{238}Pu, norm. config. no iridium clad	11.3	C	0.404 ± 0.003
GPHS RTG,86% ^{238}Pu, norm. config.	11.3	C	0.350 ± 0.002
GPHS RTG,80% ^{238}Pu, norm. config.	11.3	H_2O	0.369 ± 0.002
GPHS RTG,86% ^{238}Pu, norm. config.	11.3	H_2O	0.348 ± 0.002
Two GPHS RTGs,50 cm center-center spacing, 80% ^{238}Pu, water reflection around and between	22.6	C	0.409 ± 0.002
Two GPHS RTGs,50 cm center-center spacing, 80% ^{238}Pu, water reflection around, but void channel between RTGs	22.6	C	0.392 ± 0.003
2 by 2 by 5 array of GPHSs, 80% ^{238}Pu	12.6	C	0.473 ± 0.003
2 by 2 by 5 array of GPHSs, 86% ^{238}Pu	12.6	C	0.457 ± 0.003
2 by 2 by 5 array of GPHSs, 80% ^{238}Pu	12.6	H_2O	0.477 ± 0.002
2 by 2 by 5 array of GPHSs, 86% ^{238}Pu	12.6	H_2O	0.439 ± 0.003
4 by 4 by 5 array, close packed fueled clads, 80% ^{238}Pu	12.6	C	0.699 ± 0.004
4 by 4 by 5 array, close packed fueled clads, 80% ^{238}Pu no iridium clad	12.6	C	0.743 ± 0.004
4 by 4 by 5 array, close packed fueled clads, 86% ^{238}Pu	12.6	C	0.689 ± 0.003

TABLE 6.4.3-1. Results of the MCNP Analyses for GPHS RTGs. (Cont.)

Case	Total mass of PuO_2 (Kg)	Moderator	$K_{eff} \pm 1\sigma$
4 by 4 by 5 array, close packed fueled clads, 80% ^{238}Pu	12.6	H_2O	0.688 ± 0.003
4 by 4 by 5 array, close packed fueled clads, 80% ^{238}Pu no iridium clad	12.6	H_2O	0.745 ± 0.004
4 by 4 by 5 array, close packed fueled clads, 80% ^{238}Pu no iridium clad	12.6	Void	0.719 ± 0.004
4 by 4 by 5 array, close packed fueled clads, 86% ^{238}Pu	12.6	H_2O	0.671 ± 0.003
4 by 4 by 5 array, close packed fueled clads, 80% ^{238}Pu	12.6	H_2O,2 g/cm^3	0.700 ± 0.003
4 by 4 by 5 array, close packed fueled clads, 86% ^{238}Pu	12.6	H_2O,2 g/cm^3	0.674 ± 0.002
4 by 4 by 5 array, close packed fueled clads, 80% ^{238}Pu	12.6	H_2O,4 g/cm^3	0.713 ± 0.003
4 by 4 by 5 array, close packed fueled clads, 80% ^{238}Pu, no iridium clad	12.6	H_2O,4 g/cm^3	0.763 ± 0.003
4 by 4 by 5 array, close packed fueled clads, 86% ^{238}Pu	12.6	H_2O,4 g/cm^3	0.676 ± 0.003
4 by 4 by 5 array, close packed fueled clads, 80% ^{238}Pu	12.6	H_2O,8 g/cm^3	0.687 ± 0.003
4 by 4 by 5 array, close packed fueled clads, 86% ^{238}Pu	12.6	H_2O,8 g/cm^3	0.644 ± 0.002
4 by 4 by 5 array, 1 cm between fueled clads, 80% ^{238}Pu	12.6	H_2O	0.554 ± 0.002
4 by 4 by 5 array, 1 cm between fueled clads, 86% ^{238}Pu	12.6	H_2O	0.515 ± 0.002
4 by 4 by 5 array, 2 cm between fueled clads, 80% ^{238}Pu	12.6	C	0.467 ± 0.003
4 by 4 by 5 array, 2 cm between fueled clads, 86% ^{238}Pu	12.6	C	0.448 ± 0.002
4 by 4 by 5 array, 2 cm between fueled clads, 80% ^{238}Pu	12.6	H_2O	0.478 ± 0.002
4 by 4 by 5 array, 2 cm between fueled clads, 86% ^{238}Pu	12.6	H_2O	0.440 ± 0.002

Note: All calculations were performed with a 30.48 cm water reflector.

6.5 CRITICAL BENCHMARK EXPERIMENTS

This section justifies the validity of calculational methods and neutron cross-section values used by reporting the results of critical benchmark experiment analyses.

6.5.1 Benchmark Experiments and Applicability

The benchmark analyses were performed with the MCNP code[1] and associated cross-sections that are documented in Appendix G of Reference 3. Analyses were performed for both fast and thermalized benchmark problems (Reference 4).

The MCNP analyses were performed for two metal sphere benchmarks with different ^{239}Pu enrichments and for one moderated uranium array. A more comprehensive description of the experiments is contained in Section 6.5.2. These benchmarks contained both fast and thermal systems and two of them contained plutonium fuel. However, none of the three used ^{238}Pu. But, the ^{238}Pu cross-sections used were obtained from ENDF/B-V files, which are the most reliable sources available.

6.5.2 Details of Benchmark Calculations

The first critical experiment analyzed was Jezebel. It consisted of an unreflected plutonium metal sphere. It was 95.5% ^{239}Pu enriched. The remaining material was ^{240}Pu. The sphere had a mass of 17.02 kg, a density of 15.61 g/cm^3, and a radius of 6.385 cm.

The second critical experiment was also a bare sphere called Jezebel, but it had a ^{239}Pu enrichment of 80%; the remaining material was ^{240}Pu. It had a mass of 19.46 kg, a density of 15.73 g/cm^3, and a radius of 6.660 cm.

The third critical experiment consisted of three unreflected aluminum cylinders containing U(93.2)O_2F_2 water solutions. The inside cylinder diameter and critical height measured 20.3 and 41.4 cm, respectively. The aluminum container had a density of 2.71 g/cm^3 and was 0.15 cm thick. The three cylinders were set in an equilateral configuration with a surface separation of 0.38 cm. The MCNP model of this experiment is shown in Figure 6.5.2-1. Benchmark material densities used are contained in Table 6.5.2-1.

TABLE 6.5.2-1. Benchmark Material Densities.

Benchmark and material	Constituents	Mass density (g/cm^3)	Atom density (atoms/b-cm)
Jezebel (95.5% ^{239}Pu; 4.5% ^{240}Pu)	--	15.61	3.9316E-2
--	^{239}Pu	14.908	3.7554E-2
--	^{240}Pu	0.702	1.7621E-3
Jezebel (80% ^{239}Pu; 20% ^{240}Pu)	--	15.73	3.9593E-2
--	^{239}Pu	12.584	3.1701E-2
--	^{240}Pu	3.146	7.8921E-3
U(93.2)O_2F2 (cylinders) fuel solution	--	1.131	1.0274E-1
--	^{235}U	0.0856	2.1884E-4
--	^{238}U	0.0062	1.5411E-5
--	F19	0.0148	4.7055E-4
--	H2	0.1134	6.7736E-2
--	O16	0.9110	3.4298E-2
Aluminum	Al26	2.71	6.0485E-2

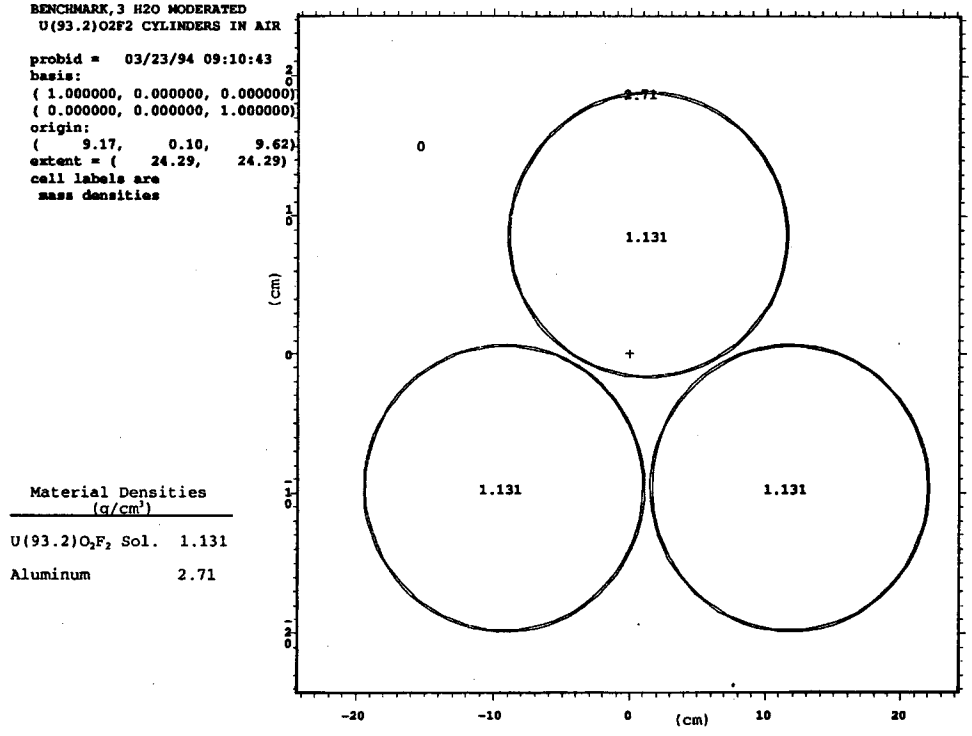


FIGURE 6.5.2-1. Benchmark Model $U(93.2)O_2F_2$ Water Moderated Canisters.

6.5.3 Results of Benchmark Calculations

The results of these three benchmark calculations are shown in Table 6.5.3-1. The MCNP accurately evaluated all critical experiments. Several other benchmark problems have also been evaluated by LANL personnel with MCNP (Reference 4). The results are shown in Table 6.5.3-2. These benchmark calculations do not produce a significant bias for MCNP.

Since the only experiments involving ^{238}Pu are at very low multiplication, an alternative to comparisons with experiments is to estimate conservative uncertainties in k from uncertainties in the microscopic cross-sections. To accomplish this, a ^{238}Pu-oxide sphere of 8-cm radius and a density of 9.6 g/cm^3 will be examined. ^{238}Pu is considered since the RTG fuel is at least 80% ^{238}Pu and has received less cross-section attention than ^{239}Pu. Also, oxide rather than water moderation will be used since water moderation would dramatically reduce k because of the partial fission threshhold below an MeV. The 8-cm radius was chosen since this gives a k of 0.823 which is greater than the relevant calculated k values in Chapter 6.

An MCNP calculation was made of the ^{238}Pu-oxide sphere to obtain the following k and one-group cross-sections:

k = .8237 (.23%)
One-group values:
total flux = 0.003213 (.28%)
total cross-section = 8.154
fission cross-section = 1.756
nu of fission = 3.181
capture cross-section = 0.208
elastic cross-section = 5.444
n,2n cross-section = 0.0036
inelastic, by subtraction = 8.154 - 7.412 = 0.742

It is first observed that these one-group cross-sections are similar in magnitude to values given [H.M. Fisher, "A Nuclear Cross-Section Data Handbook," LA-11711-M, Los Alamos National Laboratory, 1989 (page 234)] at 1 MeV from ENDF/B-V. They are also similar in magnitude to an average of the ENDF/B-V cross-sections over a fission spectrum.

Since

$$k = \upsilon f\phi/(a\phi + L)$$

with υ the number of neutrons per fission, f the fission cross-section, a the absorption cross-section, ϕ the total flux, and L the leakage, sensitivities of the one-group cross-sections can be examined. First look at the uncertainty in k due to the uncertainty in the fission cross-section.

$$dk/df = \upsilon\phi/(a\phi + L) - \upsilon f\phi\phi/(a\phi + L)^2 = (k/f)[1 - (k/\upsilon)]$$

where the absorption (removal) cross-section

$$a = f + c + i$$

is used under the assumption that inelastic scattering, i, reduces the neutron energy below the fission threshhold of Pu238 most of the time, so it is like an absorption event.

The fission cross-section is measured and has an estimated uncertainty of 0.035 barns, which results in

$dk = 0.035 * (.8237/1.756) * [1. - (.8237/3.181)] = 0.012$

i.e., a 1.2% change in k because of the uncertainty in the fission cross-section.

The uncertainty in k due to the uncertainty in the inelastic cross-section is given conservatively (assuming all inelastics reduce the neutron energy below the fission threshhold) by

$dk/di = -\upsilon f\phi\phi/(a\phi + L)^2 = k^2/(\upsilon f)$

Comparing the difference in i between the minimum fission spectrum average of four recent evaluations and that of ENDF/B-V gives a di of -0.11 barns; hence

$dk = 0.11 * 0.8237^2/(3.181*1.756) = 0.014$

Similarly, for the capture cross-section

$dk/dc = k^2/(\upsilon f)$

Comparing the difference in c between the minimum fission spectrum average of four recent evaluations and that of ENDF/B-V gives a dc of -0.072 barns; thus

$dk = 0.072 * 0.8237^2/(3.181*1.756) = 0.009$

Adding these results in quadrature gives a conservative, one-standard-deviation dk uncertainty of 0.021 or a three-standard-deviation dk uncertainty of 0.063.
This is conservative because the largest differences were used to estimate the uncertainty in a partical and because inelastic scattering was assumed to scatter neutrons below the inelastic threshhold of Pu-238.

TABLE 6.5.3-1. Results of MCNP analyses of Critical Experiments.

Critical experiment	Fuel composition and configuration	MCNP calculated K_{eff}
Jezebel (1)	95.5 wt% ^{239}Pu, ≈4.5% ^{240}Pu sphere, bare	0.9986 ± 0.0021
Jezebel (2)	80 wt% ^{239}Pu, ≈20% ^{240}Pu sphere, bare	1.0080 ± 0.0012
Three uranium cylinders	U(93.2 wt% ^{235}U)O_2F_2 water solution, 3 cylinders each at 20.3 cm in diameter and 41.4 cm in height, set in an equilateral triangular configuration with surface separation of 0.38 cm	1.0019 ± 0.0028

TABLE 6.5.3-2. MCNP Calculations of Critical Benchmark Experiments by LANL.

Critical experiment	Fuel composition and configuration	MCNP calculated K_{eff}
Jezebel (1)	95.5 wt% ^{239}Pu, ≈4.5% ^{240}Pu sphere, bare	0.9986 ± 0.0021
Jezebel (2)	80 wt% ^{239}Pu, ≈20% ^{240}Pu sphere, bare	1.0075 ± 0.0012
Uranium metal cylinder	10.9 wt% ^{235}U, ≈89.1% ^{238}U cylinder, bare	1.0024 ± 0.0013
Uranium metal cylinder	14.11 wt% ^{235}U, ≈85.89% ^{238}U cylinder, bare	1.0003 ± 0.0014
Reflected sphere	93.5 wt% ^{235}U, ≈6.5% ^{238}U sphere, graphite reflected	0.9981 ± 0.0010
Reflected sphere	97.67 wt% ^{235}U, ≈2.33% ^{238}U sphere, water reflected	0.9956 ± 0.0022
Three uranium cylinders	U(93.2 wt% ^{235}U)O_2F_2 water solution, 3 cylinders each at 20.3 cm in diameter and 41.4 cm in height, set in an equilateral triangular configuration with surface separation of 0.38 cm	0.9991 ± 0.0011
3 by 3 by 3 array of Pu fuel rods	Cylindrical cells containing 3 by 3 arrays of Pu (93.566 wt% ^{239}Pu) metal fuel rods, stacked on each other with spacers between	0.991 ± 0.005

6.6 APPENDIX

The following is a list of appendices contained within this section:

6.6.1 References

6.6.2 MCNP Code Input Listings

6.6.1 References

1. Carter, L. L., 1993, "Certification of MCNP Version 4xe for Westinghouse Hanford Company Computer Platforms," certified with ECN 186708.

2. WHC, 1994, *Specification for RTG Transportation System Package*, WHC-S-4025, Rev. 3, Westinghouse Hanford Company, Richland, Washington.

3. Briesmeister, J., 1993, "MCNP-4A, A General Monte Carlo N-Particle Transport Code," LA-12625.

4. Whalen, D. J., 1991, "MCNP: Neutron Benchmark Problems" LA-12212.

5. Los Alamos National Laboratory, "GPHS 238-Plutonium Dioxide Fuel Pellet Specification," 26Y-318181, Revision B, 11/3/94.

6.6.2 MCNP Code Input Listings

```
CRIT. CALC., GPHS RTG, GRAPHITE, 80% Pu-238
   1  0  -5 6 -1 3 -4 2  imp:n=1 fill=1  (0 0 0)
   2  0  -7 8           imp:n=1 lat=1  u=1  fill=2
   3  1 -1.95  -9 (12:-11:20) (14:-13:20) imp:n=1 u=2
   4  1 -1.95  -10 (12:-11:22) (14:-13:22) imp:n=1 u=2
   5  1 -1.95       9 10  imp:n=1 u=2
   6  2 -22.5  -12 11 -20 (-15:16:19) imp:n=1 u=2
   7  2 -22.5  -14 13 -20 (-17:18:19) imp:n=1 u=2
   8  3 -9.6   -16 15 -19  imp:n=1 u=2
   9  3 -9.6   -18 17 -19  imp:n=1 u=2
  10  2 -22.5  -12 11 -22 (-15:16:21)  imp:n=1 u=2
  11  2 -22.5  -14 13 -22 (-17:18:21)  imp:n=1 u=2
  12  3 -9.6   -16 15 -21  imp:n=1 u=2
  13  3 -9.6   -18 17 -21  imp:n=1 u=2
  14  4 -1.0   -24 -23 25 (5:-6:4:-2:1:-3)  imp:n=0.1
  15  0        (24:23:-25)                  imp:n=0

   1 py  4.659
   2 px  -4.859
   3 py  -4.659
   4 px  4.859
   5 pz  95.544
   6 pz  0.0
   7 pz  5.30801
   8 pz  -0.00001
   9 c/y  -2.184 2.654 1.831
  10 c/y   2.184 2.654 1.831
  11 py  -3.1618
  12 py -0.2941
  13 py  0.2941
  14 py  3.1618
  15 py  -3.1059
  16 py  -.35
  17 py   .35
  18 py  3.1059
  19 c/y -2.184 2.654 1.3767
  20 c/y -2.184 2.654 1.4326
  21 c/y 2.184  2.654 1.3767
  22 c/y 2.184  2.654 1.4326
  23 cz  35.0
  24 pz 126.
  25 pz -30.48

mode   n
  m1   6000.50  -1.95    $ carbon
  m2   75187.50 -22.5    $ Re for Ir
  m3   94238.50 -6.765  94239.55 -1.698  8016.50 -1.137  $ 80        molec % Pu-238 fuel
  m4   1001.50 -0.11111  8016.50 -0.88889                $ water
kcode  2000    0.4  3   50   $ n/cycle; k guess, skip, # cycles
ksrc
       -2.184  -1.5  2.654
        2.184   1.5  2.654
       -2.184   1.5  2.654
        2.184  -1.5  2.654
       -2.184  -1.5  92.89
```

```
        2.184   1.5  92.89
       -2.184   1.5  92.89
        2.184  -1.5  92.89
       -2.184  -1.5  39.81
        2.184   1.5  39.81
       -2.184   1.5  39.81
        2.184  -1.5  39.81
print  10 30 40 50 60 100 110 120 126 170
c       idum  4j 1
ctme   50
```

```
CRIT. CALC., GPHS RTG,H2O replaces GRAPHITE, 80% Pu-238
  1  0  -5 6 -1 3 -4 2  imp:n=1 fill=1  (0 0 0)
  2  0  -7 8           imp:n=1 lat=1  u=1  fill=2
  3  4 -1.0  -9 (12:-11:20) (14:-13:20) imp:n=1 u=2
  4  4 -1.0  -10 (12:-11:22) (14:-13:22) imp:n=1 u=2
  5  4 -1.0       9 10  imp:n=1 u=2
  6  2 -22.5  -12 11 -20 (-15:16:19) imp:n=1 u=2
  7  2 -22.5  -14 13 -20 (-17:18:19) imp:n=1 u=2
  8  3 -9.6   -16 15 -19  imp:n=1 u=2
  9  3 -9.6   -18 17 -19  imp:n=1 u=2
 10  2 -22.5  -12 11 -22 (-15:16:21)  imp:n=1 u=2
 11  2 -22.5  -14 13 -22 (-17:18:21)  imp:n=1 u=2
 12  3 -9.6   -16 15 -21  imp:n=1 u=2
 13  3 -9.6   -18 17 -21  imp:n=1 u=2
 14  4 -1.0   -24 -23 25 (5:-6:4:-2:1:-3)  imp:n=0.1
 15  0        (24:23:-25)                  imp:n=0

  1 py  4.659
  2 px  -4.859
  3 py  -4.659
  4 px  4.859
  5 pz  95.544
  6 pz  0.0
  7 pz  5.30801
  8 pz  -0.00001
  9 c/y  -2.184 2.654 1.831
 10 c/y   2.184 2.654 1.831
 11 py  -3.1618
 12 py -0.2941
 13 py  0.2941
 14 py  3.1618
 15 py  -3.1059
 16 py  -.35
 17 py  .35
 18 py  3.1059
 19 c/y -2.184 2.654 1.3767
 20 c/y -2.184 2.654 1.4326
 21 c/y 2.184  2.654 1.3767
 22 c/y 2.184  2.654 1.4326
 23 cz  35.0
 24 pz 126.
 25 pz -30.48

mode   n
  m1   6000.50  -1.95    $ carbon
  m2   75187.50 -22.5    $ Re for Ir
  m3   94238.50 -6.765  94239.55 -1.698  8016.50 -1.137  $ 80 molec % Pu-238 fuel
  m4   1001.50 -0.11111  8016.50 -0.88889              $ water
kcode  2000    0.4  3   50   $ n/cycle; k guess, skip, # cycles
c      ksrc
c      -2.184  -1.5  2.654
c       2.184   1.5  2.654
c      -2.184   1.5  2.654
c       2.184  -1.5  2.654
c      -2.184  -1.5  92.89
```

```
c        2.184   1.5  92.89
c       -2.184   1.5  92.89
c        2.184  -1.5  92.89
c       -2.184  -1.5  39.81
c        2.184   1.5  39.81
c       -2.184   1.5  39.81
c        2.184  -1.5  39.81
print   10 30 40 50 60 100 110 120 126 170
c       idum   4j 1
ctme    50
```

```
CRIT. CALC.,20 GPHS - 4x5 array, GRAPHITE, 86% Pu-238
  1  0  -5 6 -1 3 -4 2  imp:n=1 fill=1  (0 0 0)
  2  0   27 -29 -26 28 -7 8    imp:n=1 lat=1   u=1
       fill=0:0 0:1 0:4 2 2 2 2 2  2 2 2 2 2
  3  1 -1.95  -9 (12:-11:20) (14:-13:20) imp:n=1 u=2
  4  1 -1.95  -10 (12:-11:22) (14:-13:22) imp:n=1 u=2
  5  1 -1.95       9 10  imp:n=1 u=2
  6  2 -22.5  -12 11 -20 (-15:16:19) imp:n=1 u=2
  7  2 -22.5  -14 13 -20 (-17:18:19) imp:n=1 u=2
  8  3 -9.6   -16 15 -19  imp:n=1 u=2
  9  3 -9.6   -18 17 -19  imp:n=1 u=2
 10  2 -22.5  -12 11 -22 (-15:16:21)  imp:n=1 u=2
 11  2 -22.5  -14 13 -22 (-17:18:21)  imp:n=1 u=2
 12  3 -9.6   -16 15 -21  imp:n=1 u=2
 13  3 -9.6   -18 17 -21  imp:n=1 u=2
 14  4 -1.0   -24 -23 25 #1 #16  imp:n=0.1
 15  0        (24:23:-25)              imp:n=0
 16  0  -5 6 -1 3 -129 127  imp:n=1 fill=3  (9.719 0 0)
 17  0  227 -229   -26  28 -7 8  imp:n=1 lat=1   u=3
c        fill=0:0 0:1 0:4  4 4 4 4 4   4 4 4 4 4
        fill=4
103  1 -1.95  -109 (12:-11:120) (14:-13:120) imp:n=1 u=4
104  1 -1.95  -110 (12:-11:122) (14:-13:122) imp:n=1 u=4
105  1 -1.95      109 110  imp:n=1 u=4
106  2 -22.5  -12 11 -120 (-15:16:119) imp:n=1 u=4
107  2 -22.5  -14 13 -120 (-17:18:119) imp:n=1 u=4
108  3 -9.6   -16 15 -119  imp:n=1 u=4
109  3 -9.6   -18 17 -119  imp:n=1 u=4
110  2 -22.5  -12 11 -122 (-15:16:121)  imp:n=1 u=4
111  2 -22.5  -14 13 -122 (-17:18:121)  imp:n=1 u=4
112  3 -9.6   -16 15 -121  imp:n=1 u=4
113  3 -9.6   -18 17 -121  imp:n=1 u=4

  1 py  13.977
  2 px  -4.859
  3 py  -4.659
  4 px  4.859
  5 pz  26.54
  6 pz  0.0
  7 pz  5.30801
  8 pz  -0.00001
  9 c/y  -2.184 2.654 1.831
 10 c/y   2.184 2.654 1.831
 11 py  -3.1618
 12 py -0.2941
 13 py  0.2941
 14 py  3.1618
 15 py  -3.1059
 16 py  -.35
 17 py   .35
 18 py  3.1059
 19 c/y -2.184 2.654 1.3767
 20 c/y -2.184 2.654 1.4326
 21 c/y 2.184  2.654 1.3767
 22 c/y 2.184  2.654 1.4326
```

```
  23 c/z  4.859 4.659 40.
  24 pz 57.02
  25 pz -30.48
  26 py  4.65901
  27 px  -4.85901
  28 py  -4.65901
  29 px  4.85901
 109 c/y  7.534 2.654 1.831
 110 c/y  11.903 2.654 1.831
 119 c/y 7.534 2.654 1.3767
 120 c/y 7.534 2.654 1.4326
 121 c/y 11.903  2.654 1.3767
 122 c/y 11.903  2.654 1.4326
 127  px 4.8590002
 129  px 14.577
 227  px 4.859001
 229  px 14.577002

mode   n
  m1   6000.50  -1.95    $ carbon
  m2   75187.50 -22.5    $ Re for Ir
  m3   94238.50 -7.274  94239.55 -1.189  8016.50 -1.137  $86 mol% Pu-238 fuel
  m4   1001.50 -0.11111  8016.50 -0.88889              $ water
kcode  2000    0.4  3   80   $ n/cycle; k guess, skip, # cycles
ksrc
       -2.184  -1.5  2.654
        2.184   1.5  2.654
       -2.184   1.5  2.654
        2.184  -1.5  2.654
c      -2.184  -1.5  92.89
c       2.184   1.5  92.89
c      -2.184   1.5  92.89
c       2.184  -1.5  92.89
c      -2.184  -1.5  39.81
c       2.184   1.5  39.81
c      -2.184   1.5  39.81
c       2.184  -1.5  39.81
print  10 30 40 50 60 100 110 120 126 170
c      idum   4j 1
ctme   120
```

```
closely packed fuel clads, 4x4x5 array, carbon MOd., 80% Pu-238
  1  0 -14 13 -16 15 -18 17 imp:n=1 fill=1 (0 0 0)
  2  0 -2 1 -4 3 -12 7 imp:n=1 lat=1 u=1 fill=2
  3  1 -1.95    (6:-8:11) imp:n=1 u=2
  4  2 -22.5  -11 8 -6 (10:-9:5)  imp:n=1   u=2
  5  3 -9.6  -10 9 -5  imp:n=1   u=2
  6  4 -1.0  -22 21 -20 19 -24 23 (14:-13:16:-15:18:-17)              imp:n=0.1
  7  0  (20:-19:22:-21:24:-23)  imp:n=0

  1 px -1.4327
  2 px 1.4327
  3 pz -1.4327
  4 pz 1.4327
  5 cy 1.3767
  6 cy 1.4326
  7 py -1.43386
  8 py -1.43385
  9 py -1.37795
 10 py 1.37795
 11 py 1.43385
 12 py 1.43386
 13 px -1.4326
 14 px 10.0282
 15 py  -10.03695
 16 py 1.433855
 17 pz -1.4326
 18 pz 12.8934
 19 px -31.9
 20 px 40.5
 21 py -40.52
 22 py 31.92
 23 pz -31.92
 24 pz 43.37

 mode   n
  m1   6000.50  -1.95    $ carbon
  m2   75187.50 -22.5    $ Re for Ir
  m3   94238.50 -6.765  94239.55 -1.698  8016.50 -1.137  $ 80 molec % Pu-238 fuel
  m4   1001.50 -0.11111  8016.50 -0.88889              $ water
kcode  2000     0.6  3   80   $ n/cycle; k guess, skip, # cycles
ksrc
       0  0  0
print  10 30 40 50 60 100 110 120 126 170
c          idum     4j 1
ctme   120
```

```
closely packed fuel clads, 4x4x5 array, 8xden. H2O MOd., 80% Pu-238
  1  0 -14 13 -16 15 -18 17 imp:n=1 fill=1 (0 0 0)
  2  0 -2 1 -4 3 -12 7 imp:n=1 lat=1 u=1 fill=2
  3  4 -8.0    (6:-8:11) imp:n=1 u=2
  4  2 -22.5  -11 8 -6 (10:-9:5)  imp:n=1   u=2
  5  3 -9.6  -10 9 -5  imp:n=1   u=2
  6  4 -1.0  -22 21 -20 19 -24 23 (14:-13:16:-15:18:-17)        imp:n=0.1
  7  0  (20:-19:22:-21:24:-23)  imp:n=0

  1 px -1.4327
  2 px 1.4327
  3 pz -1.4327
  4 pz 1.4327
  5 cy 1.3767
  6 cy 1.4326
  7 py -1.43386
  8 py -1.43385
  9 py -1.37795
 10 py 1.37795
 11 py 1.43385
 12 py 1.43386
 13 px -1.4326
 14 px 10.0282
 15 py  -10.03695
 16 py 1.433855
 17 pz -1.4326
 18 pz 12.8934
 19 px -31.9
 20 px 40.5
 21 py -40.52
 22 py 31.92
 23 pz -31.92
 24 pz 43.37

 mode   n
  m1   6000.50  -1.95    $ carbon
  m2   75187.50 -22.5    $ Re for Ir
  m3   94238.50 -6.765  94239.55 -1.698  8016.50 -1.137  $ 80 molec % Pu-238 fuel
  m4   1001.50 -0.11111  8016.50 -0.88889              $ water
kcode  2000     0.6  3   80   $ n/cycle; k guess, skip, # cycles
ksrc
       0  0  0
print  10 30 40 50 60 100 110 120 126 170
c          idum     4j 1
ctme   120
```

BENCHMARK INPUT LISTINGS

```
BENCHMARK,3 H2O MODERATED U(93.2)O2F2 CYLINDERS IN AIR
   1    1 -1.131  -1 3 -4 imp:n=1 u=-1
   2    2 -2.71 1:-3:4  imp:n=1  u=1
   7    0  -2 8 -9  fill=1 imp:n=1
   5    0  -7 #7 #8 #9  imp:n=1
   6    0  7  imp:n=0
   8    like 7 but trcl=1
   9    like 7 but trcl=2

   1  cy 10.15
   2  cy 10.30
   3  py 0.0
   8  py -.15
   9  py 41.55
   4  py 41.40
   7  so  150.

  m1  92235.  .000383
      92238.  .0000276
      9019.   .000821
      1001.   .1183
      8016.   .05990
  m2  13027.  1.0
 tr1  20.98  0  0
 tr2  10.49  0  18.169
kcode   2000    .7  30  90
 sdef  axs 0 1 0 pos d1 rad d2 ext d3
  sp1  0.33  .33  .34
  si1  l  0 20.7 0  20.98 20.7 0  10.49 20.7 18.169
  si2  8
  si3  15
print
```

```
JEZEBEL, 95.5% Pu239, 4.5% Pu240, FAST CRITICAL
   1   1  -15.61  -1 imp:n=1
   2   0  1  imp:n=0

   1  so  6.385

   m1   94240.  -4.5  94239.  -95.5
kcode   3000  1.0  80  110
ksrc    0.  0.  0.
print
```

```
JEZEBEL, 80% Pu239, 20% Pu240, FAST CRITICAL
   1   1  -15.73  -1 imp:n=1
   2   0  1  imp:n=0

   1  so  6.660

  m1   94240. -20  94239. -80
kcode   3000  1.0  60  150
ksrc    0.  0.  0.
print
```

7.0 OPERATING PROCEDURES

7.1 PROCEDURES FOR LOADING THE PACKAGE

Loading the Radioisotope Thermoelectric Generator (RTG) Transportation System Package for shipment involves five steps: (1) open the empty packaging, (2) install the RTG payload, (3) close the inner containment vessel (ICV), purging with helium and leakage rate testing, (4) close the outer containment vessel (OCV), purging the OCV with helium and leakage rate testing, and (5) install the impact limiter and prepare for final shipment. The following sections detail the process of loading the RTG Transportation System Package for shipment.

7.1.1 General Information

The following general information establishes the planning, personnel qualifications, equipment, and Quality Assurance (QA) needed to conduct the specific operating procedures of Sections 7.1 through 7.3.

- Written, traceable and approved procedures shall be used throughout the operation.
- All applicable QA requirements of Chapter 9 shall be followed.
- Only trained and qualified (per Chapter 9) packaging and shipping personnel may load the package or direct its loading.
- Quality Assurance personnel shall observe and record the placement of the RTG payload into the packaging.
- Crane and forklift operations shall be performed by trained and qualified operators. A list of qualified operators shall be kept by the manager cognizant of lifting operations.
- Qualified Occupational Health Physics personnel shall survey the payload for smearable contamination before loading the package. Survey results must be recorded and maintained by the Occupational Health Physics personnel.
- The equipment and materials needed for operation of the package includes the following:
  - RTG Transportation System Packaging
  - Payload-specific shipping rack
  - Three-point lifting device (15,000 lb minimum capacity)
  - Vent port/test tool for helium leakage rate testing
  - Helium leakage rate detection system as specified in Chapter 8
  - Miscellaneous tools, including calibrated torque wrenches.
- The RTG Transportation System Packaging must be clean and undamaged before use.
- Personnel entering the equipment compartment of the semitrailer will be exposed to radiation dose rates of up to 267 mrem/hr (dose rate at top surface of package). All personnel entering the semitrailer shall comply with the cognizant facility organization's radiation protection program to minimize radiation exposure and comply with 10 CFR 19.12.

7.1.2 Opening the Empty Package

1. Remove the three 3/4-in. pins that secure the OCV head personnel barrier to the OCV. Remove the personnel barrier.

2. Attach a three-point lifting device to the three lift points (upper fins) on the OCV bell. Remove the eight 1-8 united national course (UNC) bolts that secure the impact limiter to the OCV base. Lift and remove the packaging from the impact limiter. Set the packaging down on to the disassembly area surface. Note: The packaging shall be in the upright position with the OCV base resting on the disassembly area surface.

3. Remove the OCV vent port cover. Install a vent/test port tool into the OCV vent port. If desired, plumb a gas sampling line to the vent/test port tool. Rotate the vent/test port tool stem to open the vent port; when the vent port plug is completely unthreaded, withdraw the tool stem to allow free flow of the OCV cavity atmosphere. Remove the vent/test port tool from the OCV vent port after completing any gas sampling operation.

4. Disconnect the feed-through connector from the thermal shield bulkhead connector. Remove the 24, 1¼-7 UNC bolts that secure the OCV bell to the OCV base. Lift the OCV bell to install the three spacer blocks. Install and hand tighten two 1¼-7 UNC bolts through the OCV bell flange into the top of each spacer block. Install and tighten with a wrench, one 1/2-13 UNC bolt through each spacer block into the ICV bell flange. Lower the OCV bell until it rests on the three spacer blocks. Tighten each of the 1¼-7 UNC bolts wrench tight.

5. Install a vent/test port tool into an ICV vent port (i.e., primary or secondary). If desired, plumb a gas sampling line to the vent/test port tool. Rotate the vent/test port tool stem to open the vent port; when the vent port plug is completely unthreaded, withdraw the tool stem to allow free flow of the ICV cavity atmosphere. Remove the vent/test port tool from the ICV vent port after completing any gas sampling operation.

6. Remove the 24, 3/4-10 UNC bolts that secure the ICV bell to the ICV base. Lift and remove the OCV/ICV bell assembly.

7. Alternately, using spacer blocks in steps 4 and 6 may be precluded and vessel bells removed individually. For this option, the lift point at the top center of the ICV bell would be used to remove the ICV bell.

7.1.3 Payload Installation

One general purpose heat source (GPHS) RTG may be installed within the RTG Transportation System Packaging. This section discusses the loading procedure for the payload shipping rack assembly and payload. At the time of payload installation, the ICV base will have been installed within the OCV base and secured with four 1/4-20 UNC bolts tightened to 120 ± 10 in.-lb.

1. Visually inspect the OCV and ICV O-ring seals for nicks, tears, or other damage and replace as necessary. Apply a thin coat of vacuum grease to each O-ring. Install each O-ring in its respective groove in the ICV or OCV base.

2. Install an electrical feed-through plug and cable assembly into the electrical feed-through connector located in the ICV base. With the plug in position, place the ICV electrical feed-through insulation cap over the plug/connector, ensuring that the cable is routed through the cable guide of the cap.

3. Install a GPHS shipping rack assembly onto the ICV base, aligning the eight holes in the shipping rack assembly base with the eight holes in the ICV base. Ensure the vent port tube cutout is aligned with the ICV base. Route the electrical feed-through cable and connector into the connector box located on the shipping rack assembly. Install four 3/4-10 UNC by 6-in.-long bolts through the shipping rack assembly (outermost holes) into the ICV base; tighten each to 75 ± 10 ft-lb torque.

4. Install a GPHS converter support ring onto the top of the GPHS shipping rack assembly, aligning the four holes in the converter support ring with the holes in the barrier plate. Install four 3/4-10 UNC by 8-in.-long bolts through the converter support ring and shipping rack assembly into the ICV base; tighten each bolt to 100 ± 10 ft-lb torque.

5. Lift and suspend the GPHS RTG over the GPHS shipping rack/converter support ring assembly, aligning the four quick-connect/disconnect mechanisms. Engage the four quick-connect devices to secure the GPHS RTG to the shipping rack/converter support ring assembly. Install the GPHS RTG shorting module connector cable, instrumentation connector cable, and the gas connector hose to their respective interface locations. Verify that any excess length of all RTG cables and/or hoses is coiled around the periphery of the shipping rack assembly within the 32.5-in. diameter cylinder and secured to minimize interference with the ICV bell during installation. Finally, connect the electrical feed-through instrumentation cables between the RTG payload and shipping rack assembly and establish temperature monitoring of the RTG payload.

7.1.4 Closure of the Inner Containment Vessel (ICV)

Before ICV closure, the ICV and OCV bells will be in a nested configuration with three spacer blocks installed (Section 7.1.1, Step 4).

1. Lift and install the OCV/ICV bell assembly, aligning the two guide pins in the ICV base with the two guide pin holes in the ICV bell flange. Prevent hitting or scraping against the RTG payload when installing the bell assembly. Install 24, 3/4-10 UNC by 2.0-in.-long bolts to secure the ICV bell to the ICV base; tighten each bolt to 250 ± 25 ft-lb torque.

2. Following the guidelines of Section 8.2.2.2, perform the helium purge and leakage rate testing of the main ICV closure seal. Following the guidelines of Sections 8.2.2.3 and 8.2.2.4, perform the leakage rate testing of the primary and secondary ICV vent port plug seals.

7.1.5 Closure of the Outer Containment Vessel (OCV)

1. Remove the two 1¼-7 UNC bolts that secure the OCV bell to each of the three spacer blocks. Lift the OCV bell to remove the three spacer blocks. Remove the 1/2-13 UNC bolt securing each spacer block to the ICV bell flange. Remove the three spacer blocks. Lower and install the OCV bell, aligning the two guide pins in the OCV base with the two guide pin holes in the OCV bell flange. Install 24 1¼-7 UNC by 6-in.-long bolts to secure the OCV bell to the OCV base; tighten each bolt to 300 ± 30 ft-lb torque.

2. Following the guidelines of Section 8.2.2.5, perform the helium purge and leakage rate testing of the main OCV closure seal. Following the guidelines of Section 8.2.2.6, perform the leakage rate testing of the OCV vent port plug seal.

3. Attach the electrical feed-through cable that protrudes from the OCV base, to the thermal shield bulkhead connector.

7.1.6 Installation of the Impact Limiter and Final Preparations for Shipment

1. Lift and install the package into the impact limiter ensuring the two alignment pins in the limiter mate with the two holes in the OCV base. Install eight 1-8 UNC by 8-in.-long modified bolts to secure the impact limiter to the OCV base; tighten each to 200 ± 20 ft-lb torque. Remove all lifting devices from the lift points on the OCV bell.

2. Install a tamper-indicating device over the top of an impact limiter attachment hole tube, thereby precluding inadvertent removal of the bolt.

3. Install the RTG Transportation System Package into the transport vehicle using the appropriate tiedown devices. Load a maximum of two RTG Transportation System Packages per transport vehicle, as limited by total wattage permitted within a single vehicle.

4. Install the OCV head personnel barrier. Secure the personnel barrier by inserting and securing the three 3/4-in. diameter pins through each of the three OCV lifting holes to preclude their use as a tiedown device.

5. Complete all necessary shipping papers in accordance with 49 CFR 172[1]; Subpart C, package marking will be in accordance with 49 CFR 172[1] Subpart D; labeling will be in accordance with 49 CFR 172[1] Subpart E; and placarding will be in accordance with Subpart F of 49 CFR 172[1]. Radiation monitor each RTG Transportation System Package per the requirements of Subpart I of 49 CFR 173.441[2] and determine that surface contamination levels meet the requirements of 49 CFR 173.443[2]. The measured dose rates for the normal conditions of transport shall not exceed the llimits specified in Table 7.1.6-1.

TABLE 7.1.6-1. Maximum Dose Rate Limits (mrem/hr).

Normal Conditions of Transport Location	Operational Control Limit(a)
Side, surface of package	590
Side, surface of semitrailer	120
Two meters from side surface of semitrailer	6.4
Top surface of package	1,000
Top surface of semitrailer	200
Bottom surface of semitrailer	190
Tractor cab (operator's seat)	1.2

(a)This limit is used when coolant is present in the package.

7.2 PROCEDURES FOR UNLOADING THE PACKAGE

Unloading the payload from the RTG Transportation System Package involves opening the package and removing the payload. The following sections detail the process of unloading the payload from the RTG Transportation System Package.

7.2.1 Opening the Package

1. Upon receipt, the conveyance and package shall be visually inspected for damage and surveyed for radiation level and smearable contamination. Smearable contamination levels on the external surfaces of each package shall not exceed the maximum permissible limits specified in 49 CFR 173.443. Each package shall be radiation monitored per Subpart I of 49 CFR 173.441.

2. Remove the three 3/4-in. pins that secure the OCV head personnel barrier to the OCV. Remove the personnel barrier.

3. Attach a three-point lifting device to the three lift points (upper fins) on the OCV bell. Remove the tamper indicating device from the top of the impact limiter attachment hole tube. Remove the eight 1-8 UNC bolts securing the impact limiter to the OCV base. Lift and remove the package from the impact limiter. Set the package down on the disassembly area surface. Note: The package will be in the upright position with the OCV base plate resting on the disassembly area surface.

4. Remove the OCV vent port cover. Install a vent/test port tool into the OCV vent port. If desired, plumb a gas sampling line to the vent/test port tool. Rotate the vent/test port tool stem to open the vent port; when vent port plug is completely unthreaded, withdraw the tool stem to allow free flow of the OCV cavity atmosphere. Upon completion of any gas sampling operations, remove the vent/test port tool from the OCV vent port.

5. Disconnect the electrical feed-through connector from the thermal shield bulk head connector. Remove the 24 1¼-7 UNC bolts securing the OCV bell to the OCV base. Lift the OCV bell to install the three spacer blocks. Install and hand tighten two 1¼-7 UNC bolts through the OCV bell flange into the top of each spacer. Install and tighten with a wrench one 1/2-13 UNC bolt through each spacer block into the ICV bell flange. Lower the OCV bell until it rests on the three spacer blocks. Tighten each of the 1¼-7 UNC bolts wrench tight.

6. Install a vent/test port tool into the ICV vent port (i.e., primary or secondary). If desired, plumb a gas sampling line to the vent/test port tool. Rotate the vent/test port tool stem to open the vent port; when the vent port plug is completely unthreaded, withdraw the tool stem to allow free flow of the OCV cavity atmosphere. Upon completion of any gas sampling operations, remove the vent/test port tool from the OCV vent port.

7. Remove the 24, 3/4-10 UNC bolts securing the ICV bell to the ICV base. Lift and remove the OCV/ICV bell assembly.

8. Alternately, using spacer blocks in Steps 5 and 7 may be precluded and vessel bells removed individually. For this option, the lift point at the top center of the ICV bell would be used to remove the ICV bell.

7.2.2 Payload Removal

1. Disconnect the electrical feed-through instrumentation cables between the RTG payload and the shipping rack assembly. Disconnect the GPHS RTG shorting module connector cable and gas connector hose from their respective interface locations.

2. Disengage the four quick-connect devices that secure the GPHS RTG to the shipping rack/converter support ring assembly. With an overhead crane or other suitable lifting device, lift the GPHS RTG from the shipping rack assembly and place it on the site holding stand.

3. The packaging can now be prepared for (1) storage, (2) shipment as an empty package, or (3) readied for shipment of another authorized payload.

7.3 PREPARATION OF AN EMPTY PACKAGE FOR TRANSPORT

Previously used and empty RTG Transportation System Packages shall be handled per Subpart I of 49 CFR 173.427[2].

7.4 REFERENCES

1. 49 CFR 172, "Hazardous Materials Tables and Hazardous Materials Communications Regulations," *Code of Federal Regulations*, as amended.

2. 49 CFR 173, "Shippers--General Requirements for Shipments and Packagings," *Code of Federal Regulations*, as amended.

8.0 ACCEPTANCE TESTS AND MAINTENANCE PROGRAM

8.1 ACCEPTANCE TESTS

This section discusses the tests to be performed before first use of the Radioisotope Thermoelectric Generator (RTG) Transportation System Package.

8.1.1 Visual Inspection

All packaging materials of construction and welds will be examined according to specifications delineated on the packaging drawings found in Appendix 1.3.2. Any items that are not in compliance with the packaging drawings will be identified on a discrepancy report for disposition per Section 9.3.15.

8.1.2 Structural and Pressure Tests

8.1.2.1 Lifting Device Load Testing. The maximum work load of the three outer containment vessel (OCV) lifting devices is 9,600 pounds, or 3,695 pounds per lifting point using a 60° minimum lift sling angle. However, a conservative value of 3,800 pounds will be used for the structural evaluation (see Section 2.5.1.2.1). Each set of OCV lifting devices will be load tested to at least 150% of their maximum total working load, that is, 5,700 pounds.

The maximum total working load of the inner containment vessel (ICV) bell provision for a lifting device is 1,600 pounds, as delineated in Section 2.5.1.1.1. The ICV provision for a lifting device will be load tested to at least 150% of its maximum total working load, that is, 2,400 pounds.

Per the requirements specified in the drawings in Appendix 1.3.2, accessible base material and welds directly related to the load testing of the lifting devices will be visually inspected for plastic deformation or cracking, and liquid penetrant inspected per Section V, Article 6, and Section III, Division 1, Subsection NB, Article NB-5000[1]. Crack indications will be recorded on a discrepancy report for disposition before repair and final acceptance per Section 9.3.15.

8.1.2.2 Containment Vessel Pressure Testing. The OCV and ICV will be pressure tested to at least 150% of the maximum normal operating pressure (MNOP) per the requirements of 10 CFR 71.85(b)[2] to verify structural integrity. The design pressure for the OCV and ICV is set at 50 psig, which conservatively exceeds the MNOP for either vessel (see Section 2.6.1.1). Thus, both the OCV and ICV will each be pressure tested to 150% of the design pressure, that is, 75 psig.

Per the requirements specified in the drawings in Appendix 1.3.2, accessible welds directly related to the pressure testing of the containment structures will be visually inspected for plastic deformation or cracking, and liquid penetrant inspected per Section V, Article 6, and Section III, Division 1, Subsection NB, Article NB-5000[1]. Indications of distortion or cracking will be recorded on a discrepancy report for disposition before repair and final acceptance per Section 9.3.15.

8.1.2.3 OCV Coolant Jacket Pressure Testing. The OCV coolant jacket will be pressure tested to at least 150% of its design pressure. The coolant jacket design pressure is set at 50 psig. Thus, each loop of the coolant jacket will be pressure tested to a minimum of 75 psig.

8.1.3 Leakage Rate Tests

Fabrication Verification Leakage Rate Testing will follow the guidelines of Section 6.3 of ANSI N14.5[3]. Fabrication Verification Leakage Rate Testing shall be performed, after the lifting device and pressure testing described in Section 8.1.2, above, to verify package configuration and performance to design criteria. Each containment vessel shall be thoroughly cleaned and leakage rate tested before installing ancillary components such as the shipping rack assemblies and OCV head personnel barrier.

Seven separate tests comprise the Fabrication Verification Leakage Rate Testing; four for the ICV and three for the OCV. The seven leakage rate tests are: (1) the main ICV closure seal, (2) the primary ICV vent port plug seal, (3) the secondary ICV vent port plug seal, (4) the ICV structure, (5) the OCV structure, (6) the main OCV closure seal, and (7) the OCV vent port plug seal. Each leakage rate test will meet the acceptance criteria delineated in Section 8.1.3.1.

8.1.3.1 Acceptance Criteria. To constitute acceptance, per Section 5.4(3) of ANSI N14.5-1987, each of the ICV and OCV containment vessels' indicated leakage rates shall be less than or equal to 1×10^{-7} standard cubic centimeters per second (scc/s), air. The sensitivity of the leakage rate test equipment shall be 5×10^{-8} scc/s, air, or less.

8.1.3.2 Leakage Rate Test of the Main ICV Closure Seal. This test uses helium at atmospheric pressure within the ICV cavity and an evacuated void outside the main ICV O-ring seal, thus following the guidelines of ANSI N14.5-1987, Section A3.10.1.

1. Assemble the RTG Transportation System Package ICV.

2. Install a test/vent port tool into the primary ICV vent port and ensure that the vent port is open.

3. Install a test/vent port tool into the secondary ICV vent port and open the vent port.

4. Install a test/vent port tool into the ICV seal test port and open the seal test port.

5. Establish a vacuum in the ICV seal test port sufficient to operate the helium mass spectrometer leak detector (MSLD) per the manufacturer's recommendations.

6. Plumb in a helium source to the primary vent port and flow helium through the ICV at a minimum flow rate of 5 cubic feet per minute for a minimum of 20 minutes.

7. Following the 20 minute purge, perform the leakage rate test. Record the indicated leakage rate. If the main ICV closure seal leakage rate exceeds the allowable specified in Section 8.1.3.1, disassemble the package, thoroughly clean all components, reassemble the package, and repeat the leakage rate test. If the system cannot pass the test, prepare a discrepancy report for disposition per Section 9.3.15.

8. Close primary and secondary ICV vent ports. Remove all plumbing and the test/vent port tool from the secondary ICV vent port.

9. Close the seal test port. Remove the test equipment, all plumbing, and the test/vent port tool from the ICV seal test port.

8.1.3.3 Leakage Rate Test of the Primary ICV Vent Port Plug Seal. This test uses helium at atmospheric pressure within the ICV cavity and an evacuated void outside the primary ICV vent port plug, thus following the guidelines of ANSI N14.5-1987, Section A3.10.1.

1. Install a test/vent port tool into the primary ICV vent port. Verify that the vent port is closed.

2. Plumb a calibrated helium MSLD to the test/vent port tool in the primary ICV vent port.

3. Establish a vacuum outboard of the closed primary ICV vent port sufficient to operate the MSLD per the manufacturer's recommendations.

4. Record the indicated leakage rate. If the leakage rate exceeds the allowable specified in Section 8.1.3.1, remove the vent port plug, thoroughly clean all components, replace the vent port plug seal (if necessary), replace the vent port plug, and repeat the leakage rate test. If the system cannot pass the test, prepare a discrepancy report for disposition per Section 9.3.15.

5. Remove the test equipment, all plumbing, and the test/vent port tool from the ICV seal test port.

8.1.3.4 Leakage Rate Test of the Secondary ICV Vent Port Plug Seal. This test uses helium at atmospheric pressure within the ICV cavity and an evacuated void outside the secondary ICV vent port plug, thus following the guidelines of ANSI N14.5-1987, Section A3.10.1.

1. Install a test/vent port tool into the secondary ICV vent port. Verify that the vent port is closed.

2. Plumb a calibrated helium MSLD to the test/vent port tool in the secondary ICV vent port.

3. Establish a vacuum outboard of the closed secondary ICV vent port sufficient to operate the MSLD per the manufacturer's recommendations.

4. Record the indicated leakage rate. If the indicated leakage rate exceeds the allowable specified in Section 8.1.3.1, remove the vent port plug, thoroughly clean all components, replace the vent port plug seal (if necessary), replace the vent port plug, and repeat the leakage rate test. If the system cannot pass the test, prepare a discrepancy report for disposition per Section 9.3.15.

5. Remove the test equipment, all plumbing, and the test/vent port tool from the ICV seal test port.

8.1.3.5 Leakage Rate Test of the ICV Structure. This test uses helium at atmospheric pressure within the ICV cavity and an evacuated void outside the ICV structure, thus following the guidelines of ANSI N14.5-1987, Section A3.10.1.

1. Assemble the RTG Transportation System Package ICV within the OCV. The ICV base will be shimmed a minimum of 0.030 in. up from the OCV base and the ICV-to-OCV base bolts (1/4-20 UNC) are not installed (this configuration allows helium to flow between the bases). Remove the ICV seal test port plug.

2. Install a test/vent port tool into the OCV vent port and open the vent port to allow flow into the OCV/ICV annulus.

3. Plumb a calibrated helium MSLD to the test/vent port tool in the OCV vent port.

4. Establish a vacuum in the OCV/ICV annulus sufficient to operate the MSLD per the manufacturer's recommendations.

Note: While evacuating the OCV/ICV annulus to test range, construct a tent of polyethylene plastic around the exterior of the OCV to prepare for Section 8.1.3.8. Use duct tape to seal all tent edges airtight. Seal a helium supply hose at the highest elevation in the tent and a small (1 in. diameter, or less) vent hole at the lowest elevation to ensure a complete helium purge. Ensure that all OCV coolant jacket connections are open and two helium supply hoses are placed into the upper pipe fittings in each of the two coolant loops to purge the coolant channels with helium.

5. Record the indicated leakage rate. If the indicated leakage rate exceeds the allowable specified in Section 8.1.3.1, disassemble the ICV, thoroughly clean all components, reassemble the ICV, and repeat the leakage rate test. If the system cannot pass the test, prepare a discrepancy report for disposition per Section 9.3.15.

8.1.3.6 Leakage Rate Test of the OCV Structure. This test uses helium at atmospheric pressure outside the OCV cavity and an evacuated void inside the OCV structure, thus following the guidelines of ANSI N14.5-1987, Section A3.10.2. This test immediately follows the ICV Structure Test (Section 8.1.3.5) and uses the test/hardware configuration existing at the end of that test, except that the OCV seal test port plug is removed.

1. Pressurize the polyethylene tent (see Paragraph 8.1.3.5, Item 4) with sufficient helium flow to cause the tent to bulge, but not burst. Continue to purge for 10 minutes to ensure a high concentration of helium within the tent.

   Note: To conservatively account for the less-than-pure concentration of helium within the tent, the measured leakage rate will be multiplied by a factor of two, assuming that the helium concentration inside the tent is 50% minimum.

2. Record the indicated leakage rate. When summed with the OCV vent port plug seal leakage rate from Section 8.1.3.8, if the total leakage rate exceeds the allowable specified in Section 8.1.3.1, disassemble the OCV, thoroughly clean all components, reassemble the OCV, and repeat the leakage rate test. If the system cannot pass the test, prepare a discrepancy report for disposition per Section 9.3.15.

3. Remove the polyurethane tent from around the OCV structure and the helium supply hoses from the two coolant loops.

4. Close the OCV vent port.

8.1.3.7 Leakage Rate Test of the Main OCV Closure Seal. This test uses helium at atmospheric pressure within the OCV cavity and an evacuated void outside the main OCV O-ring seal, thus following the guidelines of ANSI N14.5-1987, Section A3.10.1.

1. Install a test/vent port tool into the OCV seal test port. Open the seal test port.

2. Plumb a calibrated helium MSLD to the test/vent port tool in the OCV seal test port.

3. Install a test/vent port tool into the OCV vent port.

4. Establish a vacuum in the OCV seal test port sufficient to operate the MSLD per the manufacturer's recommendations.

5. Plumb a vacuum pump and helium gas source into the test/vent port tool in the OCV vent port as shown in Figure 8.1.3.7-1.

6. Open the OCV vent port and evacuate the OCV/ICV annulus to a pressure of 1 psia or less.

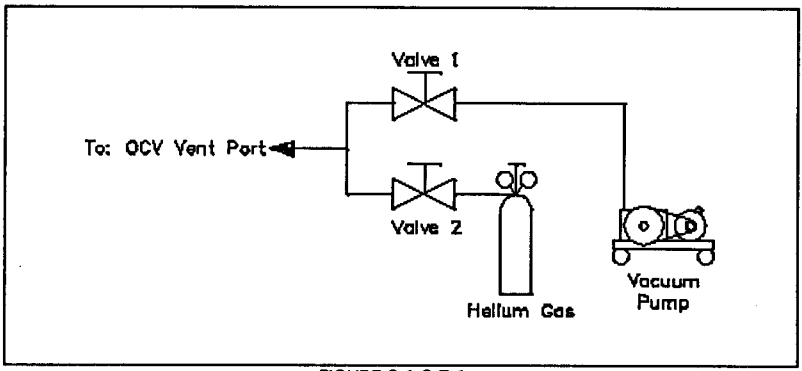


FIGURE 8.1.3.7-1.

7. Backfill the OCV/ICV annulus with helium gas to 15 ± 1 psia.

8. Close the OCV vent port. Remove all plumbing and the test/vent port tool from the OCV vent port.

9. Record the indicated leakage rate. If the indicated leakage rate exceeds the allowable specified in Section 8.1.3.1, disassemble the package, thoroughly clean all components, reassemble the package, and repeat the leakage rate test. If the system cannot pass the test, prepare a discrepancy report for disposition per Section 9.3.15.

10. Close the OCV seal test port. Remove all plumbing and the test/vent port tool from the OCV seal test port.

11. Install the OCV seal test port cover.

8.1.3.8 Leakage Rate Test of the OCV Vent Port Plug Seal. This test uses helium at atmospheric pressure within the OCV cavity and an evacuated void outside the vent port plug, thus following the guidelines of ANSI N14.5-1987, Section A3.10.1.

1. Install a test/vent port tool into the OCV vent port. Verify that the vent port is closed.

2. Plumb a calibrated helium MSLD to the test/vent port tool in the OCV vent port.

3. Establish a vacuum outboard of the closed OCV vent port sufficient to operate the MSLD per the manufacturer's recommendations.

4. Record the indicated leakage rate. When summed with the OCV Structure leakage rate from Section 8.1.3.6, if the total leakage rate exceeds the allowable specified in Section 8.1.3.1, remove the vent port plug, thoroughly clean all components, replace the vent port plug seal (if necessary), replace the vent port plug, and repeat the leakage rate test. If the system cannot pass the test, prepare a discrepancy report for disposition per

Section 9.3.15.

5. Remove all plumbing and the test/vent port tool from the OCV seal test port.

6. Install the OCV vent port cover.

8.1.4 Component Tests

8.1.4.1 Polyurethane Foam. Before polyurethane foam installation, the impact limiter cavity shall be cleaned of debris, scale, oil, and grease. The impact limiter cavity surfaces shall then be washed with a solvent or cleaner, compatible with the polyurethane foam, and coated with a foam bond release agent.

A cured foam disk with direction of rise parallel to the vertical (axial) axis of the packaging shall be installed into the center of the impact limiter cavity as specified in the drawings in Appendix 1.3.2. The cured foam shall have a density of about 3 pounds per cubic foot (lb/ft^3).

The remaining impact limiter cavity shall be foamed in place. Each foam pour shall be controlled to ensure that the liquid components react to form the rigid foam material and rise so that the entire void volume of the single foamed assembly is filled with expanded foam. The resultant foam density is about 12 lb/ft^3. The direction of foam rise shall be parallel to the vertical axis of the packaging.

Production records for each foam pouring operation shall be compiled during the operation. As a minimum, the record shall include pour dates, operator name, shell part number and serial number, Quality Assurance buy-off, and material traceability identified by batch number. This record shall be retained for the life of the container.

A certification referencing the production record data and testing data pertaining to each packaging shall be issued by the foam supplier after production. Test data relevant to the pouring operation shall be included with the certification. All Quality Assurance submittals shall be dated and signed by the foam supplier's designated Quality Assurance representative.

Each production pour made into the impact limiter assembly or used to make the low-density center disk, and each sample pour made during each production pour for test purposes shall be recorded. Test sample pours shall be foamed in test containers at the same time as the actual production pour they represent. Test coupons shall be taken from each test sample box prepared during production. If multiple pours into a single foamed assembly occur, test coupons from each pour shall be tested before installation of the next pour, and the level of each batch pour shall be recorded.

The coupons shall be tested for compressive strength per ASTM D1621[4]. Stress-strain plots, similar to that shown in Figure 2.3-2, shall be prepared for both the parallel-to-rise and perpendicular-to-rise orientations for both the 12 lb/ft^3 foam and the 3 lb/ft^3 foam. A minimum of three samples shall be tested for each pour and each direction of rise. The 3 lb/ft^3 foam shall be tested at room temperature (72 to 78 °F). The 12 lb/ft^3 foam shall be tested at cold and hot conditions: -20 to -25 °F and 160 to 165 °F. The test data shall be recorded and reviewed to ensure compliance with the foam structural acceptance criteria outlined in Section 2.3.

The coupons shall be tested for fire retardancy per Section 853(a) and Part I(d) of 14 CFR 25[6]. The testing shall satisfy the following criteria.

- The average burn length shall not exceed 6 in.

- The coupons shall self-extinguish in an average time not exceeding 15 seconds.
- After falling, drippings from test specimen shall self-extinguish in an average of 3 seconds.

Polyurethane foam not in compliance with the above requirements shall be documented on a discrepancy report for disposition before repair and final acceptance per Section 9.3.15.

8.1.4.2 O-Ring Seals. The containment O-ring seals and seal material, as appropriate, shall meet the following criteria. Any O-ring that does not satisfy these criteria shall be recorded on a discrepancy report for disposition before repair and final acceptance per Section 9.3.15.

- Compression set shall not exceed 25% after storage for 22 hours at 70 °C when tested per ASTM D395[6].
- Tensile strength and elongation shall be a minimum of 1,450 psi and 250% respectively, when tested per ASTM D412[7].
- Hardness shall be a minimum of 60 Durometer and a maximum of 80 Durometer when tested per ASTM D2240[8].
- All splices shall be subjected to the requirements of Class 3 per ASTM D2527[9].

8.1.5 Tests for Shielding Integrity

Both the ICV and OCV structures provide shielding for the payloads. Other than the monolithic configuration of these two components, no other materials of construction are singularly designated for shielding. Specific dimensional requirements specified in the drawings in Appendix 1.3.2 shall ensure shielding integrity of the ICV and OCV structures.

8.1.6 Thermal Acceptance Tests

Material properties established in Section 3.2 are consistently conservative for the analyses performed. As such, with the exception of the polyurethane foam fire retardancy test discussed in Section 8.1.4, acceptance tests for material thermal properties are not performed.

8.2 MAINTENANCE PROGRAM

This section describes the maintenance program used to ensure continued performance of the RTG Transportation System Package.

8.2.1 Structural and Pressure Tests

Other than the tests required for first use, no structural or pressure tests are necessary to ensure continued performance of the packaging.

8.2.2 Leakage Rate Tests

Maintenance Verification Leakage Rate Testing shall follow the guidelines of Section 6.4 of

ANSI N14.5-1987. Appropriate sections of the Maintenance Verification Leakage Rate Test shall be performed during routine maintenance to verify package configuration and performance to design criteria. Maintenance Verification Leakage Rate Tests of the main closure seals and vent port plug seals shall be performed upon seal replacement, but all seals need not necessarily be replaced at the same time (i.e., seals are replaced annually or when damaged). Maintenance Verification Leakage Rate Testing shall be used as Assembly Verification Leakage Rate Testing to determine leakage rates before a loaded shipment.

Five separate tests comprise the Maintenance Verification Leakage Rate Testing; two for the OCV and three for the ICV. The five leakage tests are: (1) the main ICV closure seal, (2) the primary ICV vent port plug seal, (3) the secondary ICV vent port plug seal, (4) the main OCV closure seal, and (5) the OCV vent port plug seal. Each leakage rate test shall meet the acceptance criteria delineated in Section 8.2.2.1, below.

8.2.2.1 Acceptance Criteria. To constitute acceptance per Section 5.4(3) of ANSI N14.5-1987, each of the ICV and OCV containment vessels' indicated leakage rates shall be less than or equal to 1×10^{-7} scc/s, air. To demonstrate that a containment vessel is leaktight per Section 7.3.2 of ANSI N14.5-1987, the sensitivity of the leakage rate test equipment shall be 5×10^{-8} scc/s, air, or less.

8.2.2.2 Leakage Rate Test of the Main ICV Closure Seal. This test uses helium at atmospheric pressure or above within the ICV cavity and an evacuated void outside the main ICV O-ring seal, thus following the guidelines of ANSI N14.5-1987, Section A3.10.1.

1. Assemble the RTG Transportation System Package ICV.

2. Install a test/vent port tool into the ICV seal test port and open the seal test port.

3. Plumb a calibrated helium MSLD to the test/vent port tool in the ICV seal test port.

4. Establish a vacuum in the ICV seal test port sufficient to operate the MSLD per the manufacturer's recommendations.

5. Install vent/test port tools into both the primary and secondary ICV vent ports.

6. Connect helium purge lines to the primary ICV vent port (helium purge inlet) and secondary ICV vent port (helium purge outlet). Open each vent port.

7. Flow helium through the ICV cavity at a minimum rate of 5 cubic feet per minute (cfm) for a minimum of 20 minutes.

8. Following the 20-minute purge, record the indicated leakage rate. If the leakage rate exceeds the allowable specified in Section 8.2.2.1, disassemble the package, thoroughly clean all components, reassemble the package, and repeat the leakage rate test. If the system cannot pass the test, prepare a discrepancy report for disposition per Section 9.3.15.

9. Close the seal test port. Remove all plumbing and the test/vent port tool from the ICV seal test port. Torque the seal test port plug to 110 ± 10 in.-lb.

10. Close the secondary ICV vent port. Remove all plumbing and the test/vent port tool from the secondary ICV vent port.

11. Charge the ICV cavity with helium gas to 19 ± 1 psia.

12. Close the primary ICV vent port. Remove all plumbing and the test/vent port tool from the primary ICV vent port. Torque the primary ICV vent port plug to 110 ± 10 in.-lb.

8.2.2.3 Leakage Rate Test of the Primary ICV Vent Port Plug Seal. This test uses helium at atmospheric pressure or above within the ICV cavity and an evacuated void outside the primary ICV vent port plug, thus following the guidelines of ANSI N14.5-1987, Section A3.10.1.

1. Install a test/vent port tool into the primary ICV vent port. Verify that the vent port is closed.

2. Plumb a calibrated helium MSLD to the test/vent port tool in the primary ICV vent port.

3. Establish a vacuum outboard of the closed primary ICV vent port sufficient to operate the MSLD per the manufacturer's recommendations.

4. Record the indicated leakage rate. When summed with the main ICV closure seal leakage rate from Section 8.2.2.2, if the total leakage rate exceeds the allowable specified in Section 8.2.2.1, remove the vent port plug, thoroughly clean all components, replace the vent port plug seal (if necessary), replace the vent port plug, and repeat the leakage rate test. If the system cannot pass the test, prepare a discrepancy report for disposition per Section 9.3.15.

5. Remove all plumbing and the test/vent port tool from the primary ICV vent port.

8.2.2.4 Leakage Rate Test of the Secondary ICV Vent Port Plug Seal. This test uses helium at atmospheric pressure or above within the ICV cavity and an evacuated void outside the secondary ICV vent port plug, thus following the guidelines of ANSI N14.5-1987, Section A3.10.1.

1. Install a test/vent port tool into the secondary ICV vent port. Verify that the port is closed.

2. Plumb a calibrated helium MSLD to the test/vent port tool in the secondary ICV vent port.

3. Establish a vacuum outboard of the closed secondary ICV vent port sufficient to operate the MSLD per the manufacturer's recommendations.

4. Record the indicated leakage rate. When summed with the main ICV closure seal and primary ICV vent port plug seal leakage rates from Sections 8.2.2.2 and 8.2.2.3, if the total leakage rate exceeds the allowable specified in Section 8.2.2.1, remove the vent port plug, thoroughly clean all components, replace the vent port plug seal (if necessary), replace the vent port plug, and repeat the leakage rate test. If the system cannot pass the test, prepare a discrepancy report for disposition per Section 9.3.15.

5. Remove all plumbing and the test/vent port tool from the secondary ICV vent port.

8.2.2.5 Leakage Rate Test of the Main OCV Closure Seal. This test uses helium at atmospheric pressure or above within the OCV cavity and an evacuated void outside the main OCV O-ring seal, thus following the guidelines of ANSI N14.5-1987, Section A3.10.1.

1. Assemble the RTG Transportation System Package OCV.

2. Install a test/vent port tool into the OCV seal test port and open the seal test port.

3. Plumb a calibrated helium MSLD to the test/vent port tool in the OCV seal test port.

4. Establish a vacuum in the OCV seal test port sufficient to operate the MSLD per the manufacturer's recommendations.

5. Install a vent/test port tool into the OCV vent port. Open the vent port.

6. As shown in Figure 8.2.2.5-1, plumb in parallel, with separate isolation valves, a vacuum pump and a source of helium gas to the test/vent port tool in the OCV vent port.

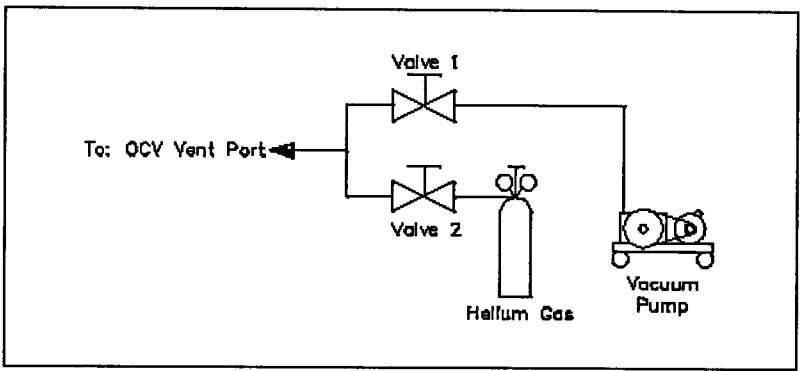


FIGURE 8.2.2.5-1.

7. Close valve 2 and open valve 1; operate the vacuum pump to achieve a vacuum in the OCV annulus equal to or below 25 torr (0.5 psia).

8. Close valve 1 and open valve 2 and pressurize the annulus to 19 ± 1 psia.

9. Record the indicated leakage rate. If the leakage rate exceeds the allowable specified in Section 8.2.2.1, disassemble the package, thoroughly clean all components, reassemble the package, and repeat the leakage rate test. If the system cannot pass the test, prepare a discrepancy report for disposition per Section 9.3.15.

10. Close the seal test port. Remove all plumbing and the test/vent port tool from the OCV seal test port. Torque the seal test port plug to 110 ± 10 in.-lb.

11. Close the OCV vent port. Remove the test/vent port tool from the OCV vent port. Torque the OCV vent port plug to 110 ± 10 in.-lb.

12. Install the OCV seal test port cover.

8.2.2.6 Leakage Rate Test of the OCV Vent Port Plug Seal. This test uses helium at atmospheric pressure or above within the OCV cavity and an evacuated void outside the vent port plug, thus following the guidelines of ANSI N14.5-1987, Section A3.10.1.

1. Install a test/vent port tool into the OCV vent port. Verify that the vent port is closed.

2. Plumb a calibrated helium MSLD to the test/vent port tool in the OCV vent port.

3. Establish a vacuum outboard of the closed OCV vent port plug sufficient to operate the MSLD per the manufacturer's recommendations.

4. Record the indicated leakage rate. When summed with the main OCV closure seal leakage rate from Section 8.2.2.5, if the total leakage rate exceeds the allowable specified in Section 8.2.2.1, remove the vent port plug, thoroughly clean all components, replace the vent port plug seal (if necessary), replace the vent port plug, and repeat the leakage rate test. If the system cannot pass the test, prepare a discrepancy report for disposition per Section 9.3.15.

5. Remove all plumbing and the test/vent port tool from the OCV vent port.

6. Install the OCV vent port cover.

8.2.3 Subsystems Maintenance

8.2.3.1 Fasteners. All threaded fasteners shall be inspected annually and before each use for deformed or stripped threads, or excessive damage to the cadmium-plated coating. Any damaged fasteners shall be replaced before further use. At a minimum, package containment boundary closure fasteners shall be replaced once every 5 years.

Test/vent port plugs and covers, all bolt thread inserts, and all noncontainment fasteners need not be replaced except when damaged.

8.2.3.2 Seal Areas and Grooves. Annually, at the time of seal replacement and before each use, inspect the O-ring seal grooves and mating sealing areas for damage that could impair the sealing capability of the packaging. Using fine emery cloth (e.g., 320 to 600 grit), smooth and polish the damaged areas to a surface finish as specified in the drawing in Appendix 1.3.2.

8.2.3.3 Painted Surfaces. Before each use, inspect the inner and outer surfaces of both the ICV and OCV, including the impact limiter for excessive damage to the coatings. The following criteria help determine if excessive damage is present.

1. Local damage: excessive localized damage is defined as bare metal exposure greater than 5% of any one square foot area (i.e., >7 $in.^2$) of coated surface. The five painted surfaces (ICV inner surface, ICV outer surface, OCV inner surface, OCV outer surface, and impact limiter outer surface) may each be assessed independently to determine local damage. Slight discolorations because of scuffing or rubbing-type abrasions are not considered localized damage unless bare metal is exposed.

2. Global damage: excessive global damage is defined as bare metal exposure greater than 2% of a total coated surface area. The five painted surfaces (ICV inner surface, ICV outer surface, OCV inner surface, OCV outer surface, and impact limiter outer surface) may each be assessed independently to determine global damage. Slight discolorations because of scuffing or rubbing-type abrasions are not considered global damage unless bare metal is exposed.

If either of the above criteria are not satisfied, prepare a discrepancy report for disposition per Section 9.3.15. Also inspect the package at the time of shipment to ensure that all external painted white surfaces are clean and free of dirt/debris.

8.2.4 Valves, Rupture Discs, and Gaskets on the Containment Vessel

This section describes the inspection and replacement schedule for these components.

8.2.4.1 Valves. There are no containment boundary valves on the RTG Transportation System Package. The relief valves used on the OCV coolant jacket require no routine maintenance.

8.2.4.2 Rupture Discs. There are no rupture discs on the RTG Transportation System Package.

8.2.4.3 Gaskets. All packaging containment O-ring seals and gaskets shall be replaced annually or when damaged, per the size and material specifications provided in Appendix 1.3.2. During payload loading, all containment seals including the replaced seal(s) shall be leakage rate tested to Section 8.2.2.

8.2.5 Shielding

No shielding inspections or tests are required to ensure continued performance of the RTG Transportation System Package.

8.2.6 Thermal

No thermal tests are required to ensure continued performance of the RTG Transportation System Package. The thermal insulation, located on the bottom of the payload shipping rack assembly and the ICV electrical feed-through insulation sleeve, should be inspected on a minimum of an annual basis for any significant shifting, deterioration, tears, and cuts. The existence of such deterioration shall require replacement of the damaged component.

8.3 REFERENCES

1. American Society of Mechanical Engineers (ASME) Boiler and Pressure Vessel Code.

2. 10 CFR 71, 1993, "Packaging and Transportation of Radioactive Materials," *Code of Federal Regulations*, as amended.

3. ANSI N14.5-1987, American National Standard for Radioactive Materials--Leakage Rate Tests on Packages for Shipment.

4. ASTM D1621, Method of Test for Compressive Properties of Rigid Cellular Plastics.

5. 14 CFR 25, 1986, "Airworthiness Standards; Transport Category Airplanes," *Code of Federal Regulations*, as amended.

6. ASTM D395, Test Methods for Rubber Property--Compression Set.

7. ASTM D412, Standard Test Methods for Rubber Properties in Tension.

8. ASTM D2240, Test Method for Rubber Property--Durometer Hardness.

9. ASTM D2527, Standard Specifications for Rubber Seals--Splice Strength.

9.0 QUALITY ASSURANCE

9.1 INTRODUCTION

The Radioisotope Thermoelectric Generator (RTG) Transportation System Package Quality Assurance Program (QAP) has been established to meet the quality assurance requirements of the U.S. Department of Energy (DOE) Orders, 5700.6C, Quality Assurance[1] and *5480.3, Safety Requirements for the Packaging and Transportation of Hazardous Materials, Hazardous Substances, and Hazardous Wastes*[2]. The QAP defines quality activities necessary to produce shipping containers that comply with 10 CFR 71, Subpart H, *Packaging and Transportation of Radioactive Material, Quality Assurance*[3]. The program was developed according to the guidance provided by U.S. Nuclear Regulatory Commission Regulatory Guide 7.10, Revision 1, *Establishing Quality Assurance Programs for Packaging Used in the Transport of Radioactive Material.*

The following describes the Westinghouse Hanford Company (WHC) Quality Assurance (QA) Program and its relationship to the RTG Transportation System Program. The RTG Transportation System Program is performed under the requirements of the current DOE-approved WHC QA Program as defined in WHC-CM-4-2, *Quality Assurance Manual*[4]. The requirements in the WHC QA manual apply to all WHC organizations and require that a Quality Assurance Program Plan (QAPP) be developed for each project. In response to this requirement, a QAPP (Document WHC-SD-RTG-QAPP-001) was developed for the RTG Transportation System Program. The QAPP lists the criteria from DOE Order 5700.6C and ASME NQA-1 and the existing implementation procedures that indicate how the criteria are to be met. The criteria listed in ASME NQA-1 not only cover all of the criteria in Title 10 of the Code of Federal Regulations Part 71 (10 CFR 71), Subpart H, but are also more rigorous. Therefore, all of the criteria in 10 CFR 71, Subpart H are met when the criteria of ASME NQA-1 are satisfied. The purpose of the QAPP is to ensure that the RTG Transportation System meets the requirements of the WHC QA manual and that the RTG packaging meets the requirements of 10 CFR 71, Subpart H. The purpose of the QAP described in Chapter 9 of the SARP is to define the quality activities necessary to produce packagings that comply with 10 CFR 71, Subpart H. The WHC QA Program and the RTG Transportation System QAPP comply with DOE Order 5700.6C and Title 10 of the Code of Federal Regulations, Parts 830.120, "Quality Assurance Requirements", and 71, Subpart H, "Quality Assurance".

9.2 SCOPE

The QAP applies to all aspects of packaging, including acquisition, inspection, handling, maintenance, utilization, and control for Type B nuclear shipping packages used for offsite transportation of radioactive material.

The QAP addresses the following quality elements: organization; quality assurance program; design control; procurement document control; instructions, procedures, and drawings; document control; control of purchased items and services; identification and control of items; control of processes; inspection; test control; control of measuring and test equipment; handling, storage, and shipping; inspection, test, and operating status; control of nonconforming items; corrective actions; quality assurance records; and audits. All elements of the QAP apply to subcontractors and subtier suppliers.

This QAP is not applicable to the Packaging System operational phase of the RTG Transportation System Package. Upon completion and acceptance of the packaging controlled under the QAP, the Certificate of Conformance holder (DOE) may designate the custodian for the Packaging System. The custodian will operate, maintain, repair, test, and store the RTG

packaging. The custodian will establish a QAP that meets the applicable requirements of DOE Order 5700.6C and 10 CFR 71, Subpart H. The custodian's QAP shall be approved by EH-332 before obtaining custodial control of operating, loading, or unloading the packaging.

9.3 QUALITY ASSURANCE PLAN

9.3.1 Quality Element 1.0, Organization

The Westinghouse Hanford Company (WHC) Quality Assurance manager has delegated the direct responsibility for quality of the RTG Transportation System Package to Engineering Applications and Support Quality Assurance (EA&SQA) and to Engineering Applications Quality Assurance (EAQA). The EA&SQA management hierarchy is independent of management responsible for conduct of the packaging development. The Quality Assurance (QA) personnel are independent from other personnel and organizations as shown in Figure 9.3.1-1.

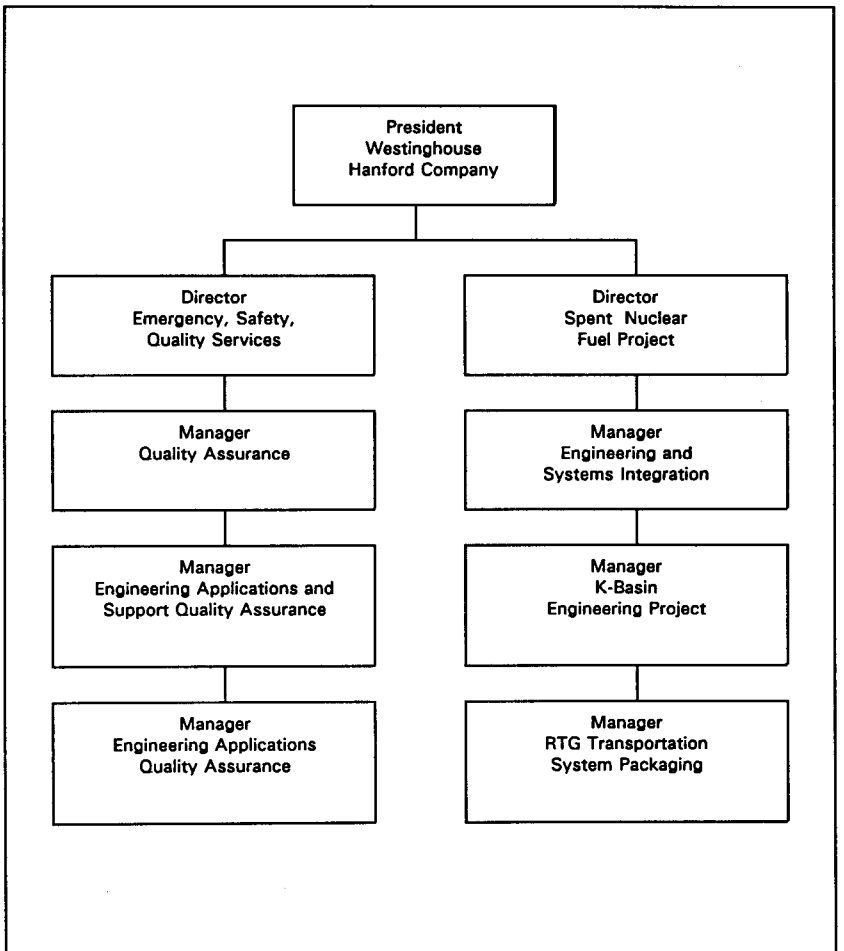


FIGURE 9.3.1-1. Reporting Independence of QA Organization.

9.3.2 Quality Element 2.0, Quality Assurance Program

All departments and service organizations that support the RTG Transportation System Package program shall comply with this QAP. If differences appear between this QAP and other documents, management shall provide resolution for all activities related to the RTG program.

Suppliers of services and equipment that affect the quality of the RTG Transportation System Package shall have a QA program in accordance with the applicable QA of this QAP. Audits of supplier's QA programs shall be per the requirements of this QAP applicable to the goods and services provided. A determination about invoking the contractual clauses that require a QAP, Quality Assurance Plan Index (QAPI), or Preaward Surveys shall be made before placing a Request for Quote (RFQ) and shall be approved by QA.

All systems and major equipment designed, fabricated, or procured for the RTG Transportation System Package shall be evaluated and the appropriate documents (procurement specifications) WHC-CM-3-5[6] shall be used to approve Environmental, Safety, and Quality Affecting Documents.

Quality levels shall be assigned to all RTG Transportation System Packaging components. Quality level assignment shall consider the impact to safety if the component were to fail or perform outside of design parameters. The three levels of QA categories from Appendix A, of NRC Regulatory Guide 7.10[6], are as follows:

QA Category A (Critical): This level includes those items with a critical impact to safety, such as structures, components, and systems whose failure or malfunction could result directly in a condition adversely affecting public health and safety. This includes such conditions as loss of primary or secondary containment with subsequent release of radioactive material, loss of shielding, or an unsafe geometry compromising criticality control.

QA Category B (Major): This level includes those items with a major impact to safety, such as structures, components, and systems whose failure or malfunction could result indirectly in a condition adversely affecting public health and safety. An unsafe condition could result only if the primary event occurs in conjunction with a secondary event or other failure or environmental occurrence.

QA Category C (Minor): This level includes those items with a minor impact to safety, such as structures, components, and systems whose failure or malfunction would not significantly reduce the packaging effectiveness and would be unlikely to create a condition adversely affecting public health and safety.

Adherence to appropriate design criteria (regulatory guides, safety, performance, maintainability, operability, lifetime) shall be the measure of quality and are to be evaluated in reviews of designs and related activities for the scope of this QAP. The graded approach assessment for the RTG Transportation System Package is listed in Table 9.3.2-1.

TABLE 9.3.2-1. Quality Assurance Levels for Design and Procurement of RTG Package Components.

Component	Subcomponent	QA level
Outer containment vessel	Bell flange	A
	Bell shell	A
	ASME torispherical head	A
	Fins and lifting doublers	B
	Tiedown doubler straps	B
	Coolant jacket structure	B
	Coolant jacket nipples and couplings	C
	Coolant jacket pressure relief valves	B
	Bell flange thermal shield structure	B
	Bell flange thermal shield insulation	C
	Base	A
	Closure bolts	B
	O-ring seals	B
	Vent and test port plugs	B
	Vent and test port plug seals	B
	Vent and test port covers	C
	Vent and test port cover gaskets	C
	Alignments pins	C
	Internal black paint coating	C
	External white paint coating	C
	Electrical feed-through	
	• Receptacle	B
	• OCV sleeve	A
	All other components	C
Inner containment vessel	Bell flange	A
	Bell shell	A
	ASME torispherical head	A
	Lifting plate	A
	Base	A
	Closure bolts	B
	O-ring seals	B
	Vent and test port plugs	B
	Vent and test port plug seals	B
	Alignment pins	C
	Purge tube	C
	Base (OCV-to-ICV) attachment bolts	C
	Debris shield	B
	Black painted coating	C
	Electrical feed-through	
	• Receptacle	B
	• ICV sleeve	A
	All other components	C

TABLE 9.3.2-1. Quality Assurance Levels for Design and Procurement of RTG Package Components. (cont.)

Component	Subcomponent	QA level
Impact limiter	Shells and plates	B
	Structural angles	B
	Polyurethane foam	B
	Bolting ring	B
	Thermal shield sheet	B
	Thermal shield wire	C
	Drain tubes	C
	Attachment bolts	B
	Blow-out plug coupling	C
	Blow-out plug	C
	Alignment pins	C
	White external paint coating	C
	All other components	C
GPHS shipping rack	Barrier plate	B
	Cylindrical shells	B
	Legs	C
	Ceramic fiber cloth	C
	Attachment bolts	B
	All other components	C

9.3.3 Quality Element 3.0, Package Design Control

The RTG Transportation System Package design is controlled by the Basic Requirement 3 and Supplement 3S-1 of ASME NQA-1[7]. The design is defined, controlled, and verified. Applicable design inputs are specified on a timely basis and translated into design documents. Design interfaces are identified and controlled. Design adequacy is verified by persons or organizations other than those who designed the item. Design changes, including field changes, are governed by control measures equal to those applied to the original design.

Design inputs consist of WHC-S-4025[8] specification, applicable DOE orders for the RTG Transportation System Package, national standards, specifications, and drawings. These are controlled by WHC through the Functions and Requirements for the RTG Transportation System Package (Sys. 100). Changes to the design input are formally controlled by a change control process.

9.3.4 Quality Element 4.0, Procurement Document Control

A graded approach shall be implemented for procurement of equipment and services for the RTG Transportation System Package based on safety, performance, and regulatory criteria. Quality Assurance shall ensure that procurement documents are adequate for their intended purpose per the assigned safety quality level described in Section 9.3.2.

Where extensive procurement detail is required, technical requirements and acceptance criteria shall normally be established by approved functions and specifications and/or design

drawings. Where the procurement does not require extensive detail, requirements and criteria may be specified in the body of the purchase order or data sheets referenced by and attached to the purchase order. Certain items, such as "off-the-shelf equipment" and "catalog items," may not require listing of the technical requirements and acceptance criteria and may be specified by model number or equivalent.

Supplier documentation requirements shall be included with the procurement documents identifying which items must be submitted by the supplier. A submittal list shall specify which documents shall be submitted for approval and which documents shall be submitted for information during the contract period. Examples of documents include fabrication and inspection procedures, equipment installation instructions, calibration procedures, operating and maintenance manuals, and spare parts lists.

For procurement involving vendor designs, vendor design control, document control, and change control shall be in accordance with WHC approved methods of document control or equivalent to the requirements of this QAP.

9.3.5 Quality Element 5.0, Instructions, Procedures, and Drawings

All instructions, procedures, and drawings used for the RTG Transportation System Package shall be approved according to the quality level and approval designation assigned by the cognizant design/project engineer and verified by QA as adequate for their intended purpose. Quality Assurance shall ensure that approved and correct documents are employed.

Quality Assurance shall approve witness points and hold points before the procurement, fabrication, or installation documentation approval. Witness and hold points, as a minimum, will be identified in inspection plans prepared per Section 9.3.10. Requirements for instructions, manuals, and equipment data shall be specified in the procurement document.

9.3.6 Quality Element 6.0, Document Control

All documents applicable to and used for the RTG Transportation System Package shall be reviewed and approved per the requirements of the assigned safety quality level, and applicable administrative, engineering, or technical document approval procedures. Changes to documents shall be controlled according to approved change control procedures applicable to each type of document, and are governed by control measures equal to those applied to the original documents.

9.3.7 Quality Element 7.0, Control of Purchased Material, Equipment and Services

This quality element applies to the purchase of items and services that affect quality. Procurement controls provide for source evaluation and selection, evaluation of objective evidence of quality furnished by the supplier, source inspection, audit, and examination of items or services upon delivery or completion.

Procurement activities are performed according to documented procedures to ensure a systematic approach and, as a minimum, address the following:

- Preparation, review, and release of procurement documents
- Selection of procurement sources
- Bid evaluation and award

- Supplier performance evaluation
- Control of supplier-generated documents
- Source and/or receiving inspections
- Control of changes to procurement documents for items and services
- Material identification and control
- Acceptance of items and services.

9.3.8 Quality Element 8.0, Identification and Control of Material, Parts and Components

Material control, where required, shall be specified in procurement documents, fabrication specifications, and construction specifications, so that only correct and accepted items are used and installed. These controls provide identification on items or in documents to ensure traceability. Each participant and subcontractor/supplier are responsible for implementing appropriate portions of the QAP program to identify and control items. The QAP complies with the requirements of DOE 5700.6C.

Items of production (i.e., batch, lot, component, or part) are identified from the initial receipt and fabrication through storage, installation, and use. This relates items to applicable design or other specifying documents.

Physical identification is the preferred method. Where physical identification is insufficient or not practical, control will be established by other approved and appropriate means, such as procedural control and physical separation. Markings, when used, shall be applied using materials and methods that provide clear and legible identification that will not affect the function or service life of the item. Markings will be transferred to each part of an item before subdividing. Caution shall be exercised to prevent obliteration by any surface treatment or coating.

Items that have limited calendar or operating life cycles or shelf life shall be controlled to preclude the use of expired items, and to replace installed items before failure or expiration.

9.3.9 Quality Element 9.0, Control of Special Processes

Processes affecting quality of items and services during fabrication and installation shall be controlled. The process control requirements shall be established in the design documents or in instructions, procedures, or drawings applicable to the process. Procedures that may be prepared to control and ensure the quality of processes shall have detail, based on the level of complexity or unique properties of the process. Stringency of review and approvals of process procedures that may be prepared shall be based on the safety quality level established in Section 9.3.2. Examples of processes that may require procedures are nondestructive examination, chemical analyses, metal finishing and coatings, heat treating, and cleaning. Personnel who perform special processes shall be qualified or certified as required to ensure quality.

All qualification records and support data are retained in the QA data file and maintained in a current status by QA personnel. These documents are controlled as delineated in Section 9.2.6, Document Control.

9.3.10 Quality Element 10.0, Inspection

Inspections shall be required to verify conformance of an item or activity to specified requirements. Inspection requirements shall be identified during the design and in the design documents. Inspection requirements shall be specified in procurement documents.

Inspections shall be performed with approved inspection plans and documented according to approved procedures. Inspectors shall be qualified or certified per the inspection requirements and shall be independent from the activity, process, or product being inspected.

9.3.11 Quality Element 11.0, Test Control

Tests are required when it is necessary to demonstrate that items or processes will perform satisfactorily. Test procedures shall specify the objectives of the tests, testing methods, required documentation, acceptance criteria, and shall be approved per the safety quality level established in Section 9.3.2.

Tests conducted by vendors at vendor plants shall be specified in the procurement documents. The Westinghouse Hanford Company (WHC) test approvals and required test observations shall be specified in test documents of vendor tests.

9.3.12 Quality Element 12.0, Control of Measuring and Test Equipment

All equipment used for measuring or testing shall be calibrated in accordance with the required test or measuring accuracy and repeatability and to approved standards of calibration. Calibrations and calibration records shall be traceable to the required calibration standard and the National Institute of Standards Technology, and the equipment shall be marked with calibration expiration dates.

Measuring and test equipment control shall be required for all suppliers that provide equipment or services that will be used to accept or test equipment or materials for the RTG Transportation System Package. Requirements to be invoked on suppliers in accordance with the QAP shall be specified in procurement documents.

9.3.13 Quality Element 13.0, Handling, Storage, and Shipping Control

All items that are part of the RTG Transportation System Package shall be controlled to prevent damage or loss, to protect against damage or deterioration, and to provide adequate safety of personnel involved in the material handling and storage operations.

Preshipment planning with suppliers shall be required for preservation, packaging, shipping, handling, and receiving in accordance with the complexity of equipment and systems for the RTG Transportation System Package. Requirements shall be specified in the procurement document. The planning will be dependent on whether an item will require special or unique handling, storage, or special planning because of vulnerability to damage by the environment or physical damage that could result from normal handling.

Information pertaining to shelf life, environment, packaging, temperature, cleaning, handling, and preservation is included as required to meet design, regulatory package approval, and/or U.S. Department of Transportation (DOT) shipping requirements.

9.3.14 Quality Element 14.0, Inspection, Test, and Operating Status

Work instructions, travelers, and similar documents will help maintain status during procurement and fabrication by the fabricator. In-process inspections, and inspection of incomplete items and activities shall be performed where necessary to verify quality and to ensure required inspections, verifications, and tests are performed.

Planning shall be performed before the turnover of the packaging to WHC upon completion of required assembly by the contractor. This planning will take into account the acceptance testing to be performed by the contractor to verify conformance to the specifications.

9.3.15 Quality Element 15.0, Nonconforming Materials, Parts, or Components

The control of nonconforming items, equipment, or conditions for the RTG Transportation System Package is accomplished by Nonconformance Reports (NCR). The NCR procedures promote consistency, timeliness of problem resolution, and processing of all necessary documentation. All RTG Transportation System Package participants can initiate an NCR.

Items or practices that do not meet specified requirements, or whose conformance is indeterminate, are documented on NCRs and controlled to prevent inadvertent installation or use. Controls are provided to notify affected organizations and for the identification, documentation, evaluation, segregation, and disposition of the items or conditions. The NCRs are tracked to completion and the verification of corrective action is documented. All personnel associated with the RTG Transportation System Package are responsible for documenting instances of nonconformance and for seeking resolution.

9.3.15.1 Identification. Nonconforming items are identified by marking, tagging, or other methods that do not adversely affect the item. When identification of nonconforming items is not practical, the container or package is marked, or segregated storage is provided.

9.3.15.2 Segregation. Nonconforming items are segregated by placing them in a designated and identified holding area until disposition is complete. When segregation is impossible or not practical because of size, weight, or access limitations, other precautions are used on a case by case basis.

9.3.15.3 Disposition. Documentation to identify, review, and disposition nonconforming items is controlled according to approved procedures that specify responsibilities and authority. Personnel who perform evaluations and approve dispositions must be competent in the specific areas they are evaluating, understand the requirements, and have access to the pertinent background information. Each organization identifies, in writing, the personnel by job title who are authorized to evaluate proposed NCR dispositions.

Control of further processing, delivery, installation, or use of nonconforming items is imposed pending resolution of NCRs.

9.3.16 Quality Element 16.0, Corrective Action

Conditions adverse to quality shall be identified and corrected as soon as practicable. An unsatisfactory condition or nonconformance may be revealed by an audit, an unusual occurrence, a random observation, during inspection, or from trend analyses of other reports. The controls shall

be implemented in accordance with this QAP. Corrective action requirements are described in approved WHC QA procedures.

9.3.17 Quality Element 17.0, Quality Assurance Records

Records that document evidence of quality are specified, prepared, and maintained. The quality records may be either the originals or copies. Copies must be capable of microfilming when used. Microfilm is acceptable, except for radiographs. Records shall be legible, identifiable, and retrievable. Records shall be protected from damage, deterioration, or loss. Lost or damaged records shall be replaced, restored, or substituted to the extent possible.

Requirements and responsibilities for record generation, transmittal, evaluation, distribution, retention, maintenance, and disposition are established and documented in Westinghouse Hanford Company (WHC) QA procedures. Each organization is responsible for generating records that furnish documentary evidence of quality, according to scoping statements appearing in work authorizing documents. The description of controls for records only applies to QA records that have been completed. Incomplete documentary evidence is not subject to the controls described.

Documents are considered valid records only if stamped, initialed, or signed, and dated by authorized personnel or otherwise authenticated.

9.3.17.1 Classification. Records are classified as "lifetime" or "nonpermanent." Lifetime records are required to be maintained by, or for, the owner for the life of the RTG Transportation System Package while it is installed or in service. Lifetime records are those that meet one or more of the following criteria:

- Those specified for lifetime retention by regulatory or contractual requirements
- Those that would be of significant value in demonstrating capability for safe operation
- Those that would be of significant value in maintaining, reworking, repairing, replacing, or modifying an item
- Those that would be of significant value in determining the cause of an accident or malfunction of an item
- Those that provide required baseline data for inservice inspections
- Those that substantiate development or major decisions involving safety and the environment
- Those that evidence conformance to codes and specifications.

Examples of lifetime records are as follows: calculations, drawings, results of design reviews, inspections, tests, and audits. Nonpermanent records are those required to show evidence that an activity was performed according to the applicable requirements, but need not be retained for the life of the item because they do not meet the criteria for lifetime.

9.3.18 Quality Element 18.0, Audits

Quality audits shall be conducted on RTG Transportation System Package activities (internal audits) and on the equipment suppliers (external audits) as required. Audits shall be conducted by qualified auditors and may be performed on a team basis as required by the audit scope.

9.4 REFERENCES

1. DOE, 1991, *Quality Assurance*, DOE Order 5700.6C, U.S. Department of Energy, Washington, D.C.

2. DOE, 1989, *Safety Requirements for the Packaging and Transportation of Hazardous Materials, Hazardous Substances, and Hazardous Wastes*, DOE Order 5480.3, U.S. Department of Energy, Washington, D.C.

3. 10 CFR 71, 1993, "Packaging and Transportation of Radioactive Materials," *Code of Federal Regulations*, as amended.

4. WHC, 1988, *Quality Assurance Manual*, WHC-CM-4-2, Westinghouse Hanford Company, Richland, Washington.

5. WHC, 1994, *Approval of Environmental, Safety, and Quality Effecting Documents*, WHC-CM-3-5, Westinghouse Hanford Company, Richland, Washington.

6. US NRC, 1986, "Establishing Quality Assurance Programs for Packaging Used in the Transport of Radioactive Materials," Regulatory Guide 7.10, Rev. 1.

7. ASME NQA-1, 1989, *Quality Assurance Requirements for Nuclear Facilities*.

8. WHC, 1992, *Specification for RTG Transportation System Package*, WHC-S-4025, Rev. 2, Westinghouse Hanford Company, Richland, Washington.

1 Packaging Technology, Inc.
4507 Pacific Highway East
Suite D
Tacoma, Washington 98424

A. A. Burns

1 Teledyne Brown Engineering
10707 Gilroy Road
Hunt Valley, Maryland 21031

S. T. Christenbury

ONSITE

2 U.S. Department of Energy,
Richland Operations Office

J. E. Mecca	R3-79
W. A. Ruhlman	N2-36

8 Westinghouse Hanford Company

D. L. Becker	G1-11
J. G. Field	G1-11
P. C. Ferrell (4)	G1-11
J. C. McCoy	G1-12
R. A. Stafford	G1-12
RTG Files	G1-11
DPC	A3-94

RTG SARP CONTROLLED DISTRIBUTION

Number of Copies

OFFSITE

2 U.S. Department of Energy-Headquarters
19901 Germantown Road
Germantown, Maryland 20874

A. K. Kapoor EM-76
E. F. Mastal NE-50

1 Eagle Research Group, Inc.
13241 Executive Park Terrace
Germantown, Maryland 20874

R. Towell

2 EG&G Mound Applied Technologies
Post Office Box 3000
Miamisburg, Ohio 45343

R. G. Miller (2)

7 Lawrence Livermore National Laboratory
7000 East Avenue
Building 543
Livermore, California 94551

M. Witte

1 Lockheed Martin
Post Office Box 8555
Building B
Philadelphia, Pennsylvania 19101

R. M. Reinstrom

1 Orbital Sciences Corporation
20301 Century Boulevard
Germantown, Maryland 20874

R. T. Carpenter